Into the Crucible

Methodological approaches to reconstructing crucible metallurgy, from New Kingdom Egypt to Late Roman Thrace

Frederik W. A. Rademakers

Thesis submitted to

University College London

for the degree of

DOCTOR OF PHILOSOPHY (PHD)

UCL Institute of Archaeology

31-34 Gordon Square

London, WC1H 0PY, United Kingdom

February 2015

I, Frederik Rademakers, confirm that the work presented in this thesis is my own. Where information has been derived from other sources, I confirm that this has been indicated in the thesis.

Date: 27 May 2015

Signed: 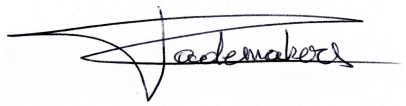

Abstract

The subject of this PhD thesis is the study of ancient metallurgical crucible assemblages, with a particular focus on the methodological framework for such studies. This is approached through three case studies from the eastern Mediterranean: Qantir – Pi-Ramesse (Ramesside Egypt, 13^{th} century BC), Gordion (Late Phrygian/Achaemenid Anatolia, 6^{th}-4^{th} century BC) and Nicopolis/Philippopolis/Serdica/Stara Zagora (Roman Thrace, 2^{nd}-5^{th} century AD).

For each of these three case studies, the metallurgical activities are reconstructed and contextualised. This involves determining the technical processes, material use and organisation of metal production both on the site and regional scale. No relation exists between these sites and each case study stands on its own: results from the technological reconstruction are interpreted within their particular archaeological and regional/historical context, to which they offer novel contributions.

The main research material consists of crucible remains, and to a lesser extent metal remains, which are investigated using optical microscopy and SEM(-EDS) to establish the technological processes and material use. The applicability of handheld XRF for such reconstructions is evaluated as well. Finally, lead isotope analysis (using MC-ICP-MS) of metal remains (scrap, spills, ingots, objects and prills extracted from crucible slag) and crucible ceramic and slag is performed.

The overarching goal of this research is to evaluate methodological approaches to the study of crucibles and crucible assemblages by comparing the results for these three examples, not in terms of technology, but by evaluating the influence of varying crucible typology, preservation, abundance, contextual information, and sample availability, as well as the use of various analytical techniques. These considerations are then combined to formulate more general recommendations for the sampling, examination and interpretation of ancient crucible assemblages.

Table of Contents

Part VII Conclusion

Bibliography

Methodology Appendices

Pi-Ramesse Appendices

Gordion Appendices

Roman Thrace Appendices

List of Figures

List of Tables

Acknowledgements

There are many people I would like to thank for making this PhD possible and turning it into the fantastic experience it has been for me.

I'll start with my supervisor, Thilo Rehren, who recognised my commitment and potential, and took me on as a student despite my less traditional background. Your guidance and mentorship has taught me not only about archaeological science, but scientific endeavour in general, and I hope to have become a better scholar for it. Our collaboration has been a privilege and a pleasure for me, and I hope it will continue beyond this PhD.
I'm very happy to have had Richard Bussmann appointed to me as my second supervisor. Though the more technical perspective of my research may have differed from your field of expertise, your interest in my project and broader reflections on its significance have greatly improved my education, and I am very grateful for your critical engagement.

Next, I would like to thank the European FP7 Marie Curie Initial Training Network, NARNIA, for providing me with the generous funding to undertake this research.

My work at the Institute would not have gone as smoothly as it has, had it not been for the help and companionship of all the people there. In particular, I want to thank all the "basement people" (past, present, and honorary): Siran Liu, P Venunan, Mainardo Gaudenzi Asinelli, Kristina Franke, Anastasya Cholakova, Loïc Boscher, Maninder Singh Gill, Matt Phelps, David Larreina Garcia, Rahil Alipour, Agnese Benzonelli, Vana Orfanou, Carmen Ting, Silvia Amicone, Ruth Fillery-Travis, Carlotta Gardner, Miljana Radivojević, Tere Plaza Calogne, Fernanda Kalazich, Edwinus Lyaya, Marianne Hem Eriksen, Géraldine Delley and Lou Iles-Bamforth. A special mention must be made here for my 2011 starting cohort in archaeometallurgy, who've accompanied me through this PhD almost every day: Siran, P, and Mainardo. Thank you so much for all the coffee, beers, dinners, trips, good times and enriching talks.
Next are my fellow 322b people, who've turned those long days at the office into a pleasant memory: Tessa Dickinson, Anke Marsh, Alice Hunt, Enrico Crema, Valentina Bernardi, Adi

Keinan-Schoonbaert, Alessio Palmisano, Eugenio Bortolini, Stuart Eve, Sophia Laparidou, Ying Zhang, Jennifer Tung, Eva Jobbova, Mariana Nabais, Stacy Hackner, Liz Farebrother, Joe Roe and Rob Kaleta. The graduate reps, for getting me out my shell and involved with IoA life: Hania Sosnowka, Oli Lown, Matilda Duncker, Tina Paphitis and Carl Walsh, and finally the MSc students I've met over the past years, particularly the '13-'14 bunch: Carlotta Farci, Lina María, Daniela Reggio, Ben Turkel, Erika Smith and Umberto Veronesi.
I have learned so much from all of you and, more importantly, had so much fun over these past few years. I'm fortunate to count you among my friends and look forward to being your colleague in the future!
I further want to thank the support staff at the Institute, in particular Stuart Laidlaw in the photography lab, Kevin Reeves in the SEM lab, Patrick Quinn and Harriet White in the sample preparation lab, Peter Schauer for IT support, Sandra Bond for various facilities, as well as Fiona McLean, Lisa Daniel and Thom Rynsaard on the ground floor. Your support has made my work here very easy! Special thanks are due to Harriet for introducing me to wall climbing this last year, which has had very beneficial effects on both my physical and mental health while writing up this thesis.
Finally, I would like to thank the academic staff at the Institute, in particular Ian Freestone, Marcos Martinón-Torres, John Merkel, Daniela Rosenow and Mike Charlton, and Myrto Georgakopoulou at UCL-Qatar, for their valuable support and insightful discussions.

The Garden Kiosk on Gordon Square and its staff are kindly acknowledged for providing daily caffeine and a good reason to walk in the park.

I must thank the London Surf Club and its members for contributing to my spiritual and physical balance over the years, through regular cold water therapy. It has been wonderful meeting so many different people from across the globe and sharing the British waves.

Next, I want to thank the "Narnians": Noemi Müller, Christina Makarona, Roberta Mentesana, Will Gilstrap, Artemi Chaviara, Andrea Ceglia, Andreas Charalambous, Lente Van Brempt, Demetrios Ioannides, Olivier Bonnerot, Lydia Avlonitou, Francesca Licenziati, Marta Tenconi, Elisavet Charalambous, Ioannis Christodoulakis, Evangelos Tsakalos, Ellery Frahm, and Sia and Mainardo. Being part of such a great project as NARNIA has been fantastic, and the various workshops throughout Europe have greatly enhanced my PhD experience. The true value of this project, however, lies in the people I met along the way. I'm very glad to know all of you, and to have learned so much from the different projects you are involved in. The many fun evenings across the world, at workshops and conferences, have been a privilege. I'm particularly grateful to Will and Artemi for helping me find my feet in Athens, when I was still so new to this strange world of archaeological scientists.

I further want to thank all the senior academic staff on the NARNIA project, who have taken their time to teach me about their various expertises at workshops and conferences, and for the pleasant times we shared: Lina Kassianidou, Peter Day, Vassilis Kilikoglou, Eleni Aloupi, Anno Hein, Roger Doonan, Karin Nys, Marcos, and all the others involved. A special thanks is reserved for Maria Dikomitou, who kept the project (and all those Narnians) on the rails and provided kind help at all times.
And finally, I'd like to thank Patrick Degryse for making me aware of NARNIA and encouraging me to apply, which has been crucial to beginning this adventure.

Several people have helped me with the acquisition and study of the three assemblages presented in this thesis, in each case facilitated by Thilo's support.
For the Pi-Ramesse crucibles, I am immensely indebted to Edgar Pusch, who excavated these crucibles all those years ago (and to Thilo, for not finding the time to analyse them before I arrived). Both in correspondence and during my time in Qantir and Doha in 2013, Edgar has provided me with more council and help than I could have wished for. Your hospitality, patience and gentility have turned the study of a daunting crucible mountain into a truly enjoyable experience. Thanks also to the spring 2013 excavation team for your help and good company, and to Ernst Pernicka for his feedback on my interpretation of the lead isotope data for the Pi-Ramesse metals.
The Gordion crucibles were kindly offered by Mary Voigt, who introduced me to the site and its archaeology. Your friendly welcome in Philadelphia, and the hospitality shown by you and Naomi Miller, have made this research trip yet another pleasant episode within this PhD. I would further like to thank Alison Fields for her help in gathering all the evidence related to the foundry at Gordion.
For the final assemblage, I have had great support from the excavator (and fellow Narnian) Sia Cholakova. Your knowledge and friendly help have not only made the examination of these little fragments more intelligible, but a pleasure to undertake.

Next, I want to thank my friends in Belgium. For not forgetting me while I've been on this island. For being there whenever I made it across. In particular, I'd like to thank Laurens Cerulus (for his help and the fun times during that first year in London), Sam Klein, Joris Wauters, Elise Goossens, Dieter Vander Velpen, Vincent Boeckx, Koen Hoornaert, Marijs Vrancken, Wouter Carmeliet, Patricia Goijens, Tim Mellaerts, Eline Jalon, Eline Van Eldere, Andries Brys, Chloé Vander Velpen, Hans Rymenams, Tinneke Vanwinkel, Annerose Allemon, Ide Smets, Ilse Peeters and Eline Mordijck.

Finally, I would like to thank my family. There are not that many of us, but your support has surely been the greatest.

My parents, Mama and Papa, have prepared me for independent life for as long as I can remember. Our many travels together and your guidance on the way towards responsibility and self-reliance have given me not only the ability, but indeed the eagerness to leave the comforts of the familiar and explore the world beyond. Your encouragement, love and support has brought me where I am today, and I am very happy to be here.
My sister, Emilie, has equally played a very important role. I may not have been around that much lately, but I feel we have grown much closer nonetheless. Our talks and times together have strengthened me over these past few years. I'm very fortunate to be your sibling and to count you among my dearest friends.
My grandparents: Bomma, Bompa, Oma and Opa. You have all been among my most important inspirations. It is such a great privilege to know you as parents, teachers and, most of all, good friends. Your open-mindedness and inquisitive spirits have made it so incredibly easy for me to sail off into the world. Losing three of you during the final year of my PhD has been difficult, particularly as I could not be with you as much as I would have liked. However, your unconditional support and love over all these years has allowed me to surpass the pain of your loss, and appreciate the role you have played in making me who I am today. This thesis is therefore dedicated to the four of you.
Finally, I want to thank Poety, Ef, Sarah, Tobia and Giuseppe. I love each one of you and am grateful for all the support you have given me these past years, each in your own way.

For several years now, my small family has grown a little and I therefore want to include Ann, Luc, Mirose, Dies and Sara and thank them for their support and friendship throughout this PhD and beyond.

This brings me to the final acknowledgement. Of course I haven't forgotten you. I just saved you for last. Like my favourite sweet from a richly filled box I can call my life. Thank you for understanding me. For knowing what I want, when I'm not really sure. For mentally evaporating this bit of water between us, and coming across with me. For generously taking care of me, my roots and my dreams.
You are my source of energy, inspiration and happiness.

Voor Bomma, Bompa, Oma en Opa

Watterson, 1992

Part I

Introduction

He bowed at the dark, straightened, tossed his hat over his shoulder, and, carrying the muleta *in his left hand and the sword in his right, walked out toward the bull.*

Hemingway, 1927

CHAPTER 1

Background, aims and layout of the thesis

Metals have played an important role for humans ever since their discovery, evolving from decorative personal objects and precious gifts to indispensable tools, shaping the world as we know it today. Their changing use across cultures and time therefore reflects human activity, innovation, creativity and value, from a societal to an individual level, making it an essential aspect of archaeological inquiry.

Archaeometallurgy focuses on the complete range of activities associated with the production, working and consumption of ancient metals. It has grown from the purely technical description of metals and production waste to the study of technological transfer and innovation, pre-modern economies, aspects of materiality, as well as the social contextualisation of technology (Killick and Fenn, 2012; Rehren and Pernicka, 2008). This has attracted scholars with highly variable backgrounds, ranging from archaeology, anthropology and history to geology, physics, chemistry and engineering, inevitably leading to different emphases being placed on the central aim within the discipline: understanding how and why people in the past made, viewed and consumed metals the way they did. Ideally, an integrated, holistic approach to archaeometallurgy should emerge, acknowledging the various aspects related to it. However, like so many other sub-disciplines of archaeology that have appeared over the last few decades (e.g., palaeobotany, archaeozoology, geoarchaeology), this one is still very much evolving. Both its theoretical and analytical approaches will continue to change in light of new discoveries through archaeological case studies, as well as experimental work and the integration of new theoretical concepts. Though steady development is an essential characteristic of any science, a formalised archaeometallurgical methodology still appears to be a while away.

This PhD thesis deals with crucibles employed for ancient metallurgical activities. Crucibles hold a high informative potential with regards to ancient human activity. They represent an integrative technology, drawing on both ceramic and metallurgical traditions. Furthermore, they bridge the gap between primary metal production and metal processing, and may inform and draw connections between these existing fields of research. They can provide way-points for metal trade routes, thus refining our understanding of a metal's journey from mine to deposited object, and the changes it undergoes along the way. Reconstructing crucible metallurgy within various workshop contexts further holds the potential to examine issues of technological (ex)change across different socio-cultural settings, regions and time, and offers a proxy for metal processing and consumption that have become archaeologically invisible.

This thesis contributes to the development of archaeometallurgy on two levels. Firstly, three case studies of metallurgical crucible activity from different east Mediterranean regions are presented, for which the study of metallurgical technology is currently limited. In doing so, a fundamental reference is established for future investigations of metallurgy in these particular areas and periods, and equally for studies of crucible technology in general. In their own right, these case studies provide technical reconstructions of a specific metallurgical activity, and a socio-cultural contextualisation of technology to the highest achievable degree for each particular historical region.

Secondly, an essential contribution to the methodology of crucible research is made. This encompasses primarily the more analytical aspects, such as sampling, analysis and data interpretation. However, more overarching issues related to the informative value of crucible research regarding reconstructions of not only technology, but its contextualisation on different scales (from a single crucible to an assemblage, workshop, site and eventually regional scale) are discussed as well. Given the current lack of explicit guidelines for crucible analysis and interpretation, this methodological perspective adds a timely contribution to a more formalised research methodology by providing some generalised practical recommendations for crucible analysis.

Section 1.1

Three case studies

This thesis is centred around the study of three crucible assemblages. Initially, each of these assemblages is studied in isolation. Through their analysis, a detailed reconstruction of metallurgical techniques and materials is offered. From this essentially technical

Figure 1.1: Map showing the location of the sites from which the three assemblages, studied in this thesis, were excavated: Qantir – Pi-Ramesse, Gordion and Roman Thrace (Google Earth 7.1.2, 2013)

foundation, the metallurgical activity reflected in the crucible remains is then considered in more detail within its particular archaeological context. This encompasses the interpretation of this metallurgical activity within a *chaîne opératoire* approach, both on the scale of an individual's use of a crucible, and the overarching scale of the broader organisation of metal production (see Chapter 2).

The three case studies cover assemblages from several sites in the eastern Mediterranean region, shown in Figure 1.1. The first case study is Qantir – Pi-Ramesse, the New Kingdom Egyptian capital, with metallurgical remains from the 13^{th} century BC royal workshops. This thesis presents the first full analytical study of metallurgical crucibles from ancient Egypt. The second case study is Late Phrygian (c. 540-330 BC) Gordion (Turkey), where crucibles from various dump contexts within the ancient citadel are examined. Again, no comparable studies exist for this area and period. The third and final case study involves crucibles from various rescue excavations in Thrace (modern Bulgaria), covering several Roman sites from the 2^{nd} - 5^{th} century AD (mainly 2^{nd} century). Though some comparable studies exist for the western Roman Empire, examples from the eastern Roman provinces are few.

For each case study, the crucibles relate mainly to copper-based, secondary metallurgical activity (e.g., refining, recycling, alloying and casting). Their analysis therefore provides a basis for a framework of metallurgical studies for each of their particular historical-

cultural settings, but equally contributes to secondary copper metallurgy studies in general. Surprisingly little research on secondary metallurgical activity currently exists, and the production of bronze, for example, is still poorly understood despite its apparently simple nature (Pigott *et al.*, 2003; Rovira, 2007).

All crucibles receive the same basic treatment, consisting of macroscopic description of the fragments and microscopic examination through the use of mounted samples for optical microscopy and scanning electron microscopy, as described in Chapter 3. The main case study, however, is Pi-Ramesse, where the most abundant and best-preserved material is available. While visiting Qantir (Egypt), the author has analysed the entire crucible assemblage by handheld XRF, which has not been possible for the Gordion and Roman assemblages as only a limited selection of those crucibles was available for study in London. In addition to this, lead isotope analysis has been conducted for the Pi-Ramesse crucibles and metal remains. Due to the high cost of lead isotope studies, this could only be performed for one assemblage. Furthermore, the expected utility of lead isotope analysis was highest for this assemblage: the existing framework for lead isotope studies in archaeology is strongly focused on the Late Bronze Age, and the analysis of bronze (at Pi-Ramesse), rather than leaded bronze (at Gordion) or various metals (Thrace), is expected to reveal patterns that may be interpreted less ambiguously. Therefore, the Pi-Ramesse chapter can be considered as a case study for which all the stops are pulled out, while Gordion and Roman Thrace represent a more common scale of analysis.

Going beyond their individual contributions to archaeology as case studies, the study of these assemblages is instrumental for exploring methodological issues for crucible research. This is achieved by assessing the effects of sampling on both the crucible and assemblage scale, as well as by evaluating the way by which crucible samples can then be analysed and interpreted. The archaeological contexts, as well as the crucible remains themselves, vary significantly among these three case studies, which further motivated their selection for this research. For Pi-Ramesse, there is an excellent conservation of the abundant remains, coming from a well-preserved workshop context, with high temporal resolution. The Gordion assemblage consists of fairly abundant, well-preserved material, but derives mainly from dump contexts, with less constrained dating and only inferred connections to production installations. Finally, the Roman material is far more limited, from various rescue excavation contexts, and covers a broad time period. Here sampling constraints allowed only small or tiny crucible fragments to be obtained. The comparison of these case studies therefore provides the opportunity to evaluate the influence of different crucible types and archaeological contexts on methodology.

Section 1.2

Archaeometallurgical methodology

There has been a slow but steady growth of interest in the study of ancient metallurgy over the past decades. Publications on various metallurgical waste products span the whole of Europe (e.g., from Scandinavia (Ling *et al.*, 2013) and England (Rohl and Needham, 1998) through France (König and Serneels, 2013), Germany (Brauns *et al.*, 2013) and the Alps (Doonan, 1999a) to Italy (Jung *et al.*, 2011), and from Portugal (Valério *et al.*, 2010) and Spain (Rovira, 2007) to Bulgaria (Gale *et al.*, 2003), Greece (Hein and Kilikoglou, 2011; Mangou and Ioannou, 2000) and beyond), the Near East (e.g., Allan, 1979; Davey and Edwards, 2007; Eliyahu-Behar *et al.*, 2012; Klein and Hauptmann, 1999; Levy *et al.*, 2012; Knapp, 2011; Nezafati *et al.*, 2011; Rothenberg, 1990 and Thornton and Rehren, 2009), Latin America (e.g., Guerra, 2004; Martinón-Torres *et al.*, 2007; Scott and Seeley, 1983 and Zori *et al.*, 2013), North America (e.g., Cooper *et al.*, 2008 and Wayman *et al.*, 1985), Asia (e.g., Li *et al.*, 2011; Murillo-Barroso *et al.*, 2010 and Pigott, 2011, 2012) and Africa (e.g., Chirikure *et al.*, 2010 and Iles and Martinón-Torres, 2009).

The field of archaeometallurgy, however, is still very much under development. This is evident from the range of approaches exemplified within the literature mentioned above. As recently noted by Rehren (2014), a few more decades of research are probably required before a formalised approach, in the shape of a textbook, can be generated. Though a few very important introductory publications already exist (e.g., Bachmann, 1982b; Bayley *et al.*, 2001, 2008 and Craddock, 1995), their lack of explicit guidelines for sampling, analysis and interpretation make them insufficient as practical tools for the archaeometallurgist. More case studies are needed, not only to develop a diachronic overview of metallurgical technology for various regions in the world, but equally to discover and agree on the best analytical procedures by which to study metallurgical production waste. Currently, most researchers already apply the same range of analytical techniques to investigate metal artefacts and their production waste. However, the methodological design by which these analytical techniques are employed usually does not follow any standard approach. It is mostly dictated by sample characteristics (availability, amounts, size etc.), regional and personal preference for particular analytical techniques, financial budgets and, of course, the research questions at hand. Unfortunately, the methodology section in publications is all too often limited to listing the applied techniques (methods), without actually stating the way in which they are used (methodology), or why they were selected. Most analysts have the same goals: to describe and characterise the structure, (micro-)

texture and chemical composition of metallurgical production waste, with the aim of reconstructing starting products, process parameters (e.g., temperature, redox-conditions) and the final (metal) product. There are, however, several ways to do this. While it is beyond the scope of this thesis to run through all branches of archaeometallurgy, the different ways by which crucibles can be analysed, and the effect this has on their interpretation, is discussed in depth. In doing so, this thesis advocates greater transparency in the research methodology for crucible studies, not only to enhance justification and comparability of published data, but to open the way for collective methodological improvements.

In comparison to other aspects of archaeometallurgy, crucible research is particularly in need of such a discussion. The study of iron smelting waste, for example, already has more developed analytical methodologies (e.g., Fluzin *et al.*, 2000) and entire conferences and books dedicated to it (Cech and Rehren, 2014; Humphris and Rehren, 2013). Similarly, the primary smelting of copper has received far more attention (e.g., Anguilano *et al.*, 2009; Artioli *et al.*, 2009; Bachmann, 1980, 1982a; Bamberger, 1985; Bassiakos and Catapotis, 2006; Bourgarit, 2007; Burger *et al.*, 2010; Chiarantini *et al.*, 2009; Doonan, 1994; Doonan *et al.*, 1996; Erb-Satullo *et al.*, 2014; Georgakopoulou *et al.*, 2011; Hauptmann, 2007; Hauptmann *et al.*, 1988, 2003; Kassianidou, 2013; Knapp *et al.*, 2001; Krismer *et al.*, 2013; Levy *et al.*, 2002; Maldonado and Rehren, 2009; Manasse *et al.*, 2001; Nocete *et al.*, 2008; Pryce *et al.*, 2007, 2011, 2010; Rostoker *et al.*, 1989; Rovira, 2002; Ryndina *et al.*, 1999; Schreiner *et al.*, 2003; Severin *et al.*, 2011; Zwicker and Goudarzloo, 1979 and Zwicker *et al.*, 1977, 1980, 1981), and benefits from the comparability to modern extractive metallurgy, for which many textbooks exist (e.g., Beeley, 2001; Davenport *et al.*, 2002 and Rosenqvist, 1974). The study of finished objects similarly benefits from modern metallography, and has been summarised for archaeological metals by Scott (1991, 2012, 2013). Though some more interest for crucibles existed in the earlier days of archaeometallurgy (e.g., Coghlan, 1975; Tylecote, 1982a; Zwicker, 1982 and Zwicker *et al.*, 1985), this has waned over the previous decades. It has, however, picked up again over the past few years (e.g., Angelini *et al.*, 2009; Davey and Edwards, 2007; Eniosova and Rehren, 2012; Evely *et al.*, 2012; König and Serneels, 2013; Lehner *et al.*, 2009; Martinón-Torres *et al.*, 2008; Masioli *et al.*, 2006; Rehren and Papachristou, 2003; Sahlén, 2013 and Thornton and Rehren, 2009), making this investigation all the more timely.

Important work for crucibles has already been undertaken in the past: Bayley and Rehren (2007) and Rehren (2003) provide essential introductions to the classification of crucibles, mainly from a typological perspective, but the practical framework for their analysis is beyond the scope of these and most other publications. Recent work by Martinón-Torres and Rehren (2014) offers an excellent overview of the range of metallurgical processes for

which crucibles are employed, and how some of these may be recognised macroscopically, microscopically and chemically. However, this text may only serve as a rough guide to crucible analysis, as a result of its broader focus on the study of technical ceramics in general. More detailed issues concerning sampling and analytical methodology (listed in section 1.3), which provide detailed practical guidelines for crucible analysis, were left for future discussion. Beyond some specific problems (e.g., Dungworth, 2000a), a general discussion of methodological approaches to crucible metallurgy is currently missing from the literature.

Through the comparison of the three case studies presented in this thesis, and drawing on existing literature, the influence of different crucible types, sampling strategies, analytical methods and archaeological contexts on the results of crucible research is evaluated. This raises several questions, relevant to the praxis of crucible research, which are elaborated in section 1.3.

Section 1.3

Research questions

The research aims of this thesis can be subdivided into two categories, related to the three case studies as such, and archaeometallurgical methodology more generally. Some of the terminology mentioned here is further explained in section 1.4.

For the three case studies, a range of questions are considered:

- How where the crucibles created? What materials were used, what was their design and how where they prepared for use?
- What metallurgical process is reflected in the crucible remains? More specifically, this involves establishing:
  - The raw materials employed in the process
  - The techniques used (e.g., simple metal melting, refining or alloying)
  - The process parameters characterising the process (e.g., temperature and redox-conditions)
- How do the crucibles relate to other metallurgical waste products, such as tuyères and moulds, and can these be used to create a more detailed reconstruction of the production sequence (*chaîne opératoire*) reflected in their archaeological context?

- Can the crucible technology be related to other (high-temperature) technologies attested on the site?
- How is this metallurgical activity more widely situated in the organisation of metal production for its particular socio-cultural setting?

Beyond this, more specific questions arise for each particular assemblage, which are formulated and addressed within their respective case studies.

In terms of broader methodological issues, many more questions arise, as already mentioned in the previous section:

- What are the effects of taking a sample of a certain size and from a particular crucible area in terms of its representativeness of that crucible?
- How can confidence be gained in having sufficiently large sample numbers to adequately represent the metallurgical activity reflected in an entire crucible assemblage?
- What is the effect of crucible abundance, preservation, typology and refractoriness on their potential for answering the questions formulated for the case studies above?
- Which techniques are most suitable in answering these questions, given limitations imposed by not only the crucible remains, but time, financial budget, export regulations and curatorial considerations as well?
- Under such limitations, how well can one expect to be able to answer those questions, and when does the cost of doing so outweigh the expected knowledge acquired?
- When confronted with a very limited, fragmented assemblage such as the Roman one (which is arguably the most common occurrence in archaeological projects), what may be expected from its study?
- Can some general recommendations for sampling, analysis and interpretation be defined?
- How do these methodological considerations influence the broader expectations that can be laid out for crucible studies? What is the expected informative value of crucible analysis with regards to ancient human behaviour?

A comparative approach is adopted to address these questions, drawing on the rich dataset presented within the three case studies and integrating the existing literature.

Section 1.4

Thesis layout and terminology

Following this introductory chapter, the analytical methodology applied for the analysis of crucibles throughout this research is detailed in Part II. Next, the three case studies are presented: Qantir – Pi-Ramesse (Part III), Gordion (Part IV), and Roman Thrace (Part V). Each of these case studies is similarly structured: after an introduction to the sites and the relevant historical and cultural background, the results of the crucible analysis are presented. This entails macroscopic and microscopic descriptions, chemical characterisation (bulk and micro-textural) of ceramic and slag, and the technical interpretation of these results. This interpretation aims to provide a purely technical reconstruction of the crucible processes, while broader contextualisation of these results is provided in the discussion at the end of each case study. There is some variability in the dimensions of these three case studies, reflecting the size of the assemblages and the range of analytical techniques applied to their study.
Finally, a broader discussion, transcending the individual case studies and focusing on broader methodological issues, is held in Part VI. This is further subdivided into a chapter on analytical methodology (Chapter 13) and a chapter on the contextualisation of crucible metallurgy (Chapter 14).
Concluding remarks are presented in Part VII.

The full analytical results are presented in the appendices, organised by case study, where a list of samples[1], bulk compositional data for ceramic and slag, as well as metallic prill compositions are compiled, along with other reference data.

Finally, a list of technical terminology used throughout this thesis is presented here. These terms are further elucidated through the overview of metallurgical processes in section 2.2.

- *Crucibles*: Free standing, movable ceramic vessels that are used for high-temperature metallurgical operations (Rehren, 2003). Crucibles may be used for both (primary) smelting and secondary metallurgical operations. An example, modelled after the Pi-Ramesse crucibles, is shown in Figure 1.2, with further associated terminology discussed below.

- *(Primary) smelting*: The metallurgical extraction process whereby metal is produced from an ore.

[1] Samples are labelled by excavation number and the date of sampling for this PhD.

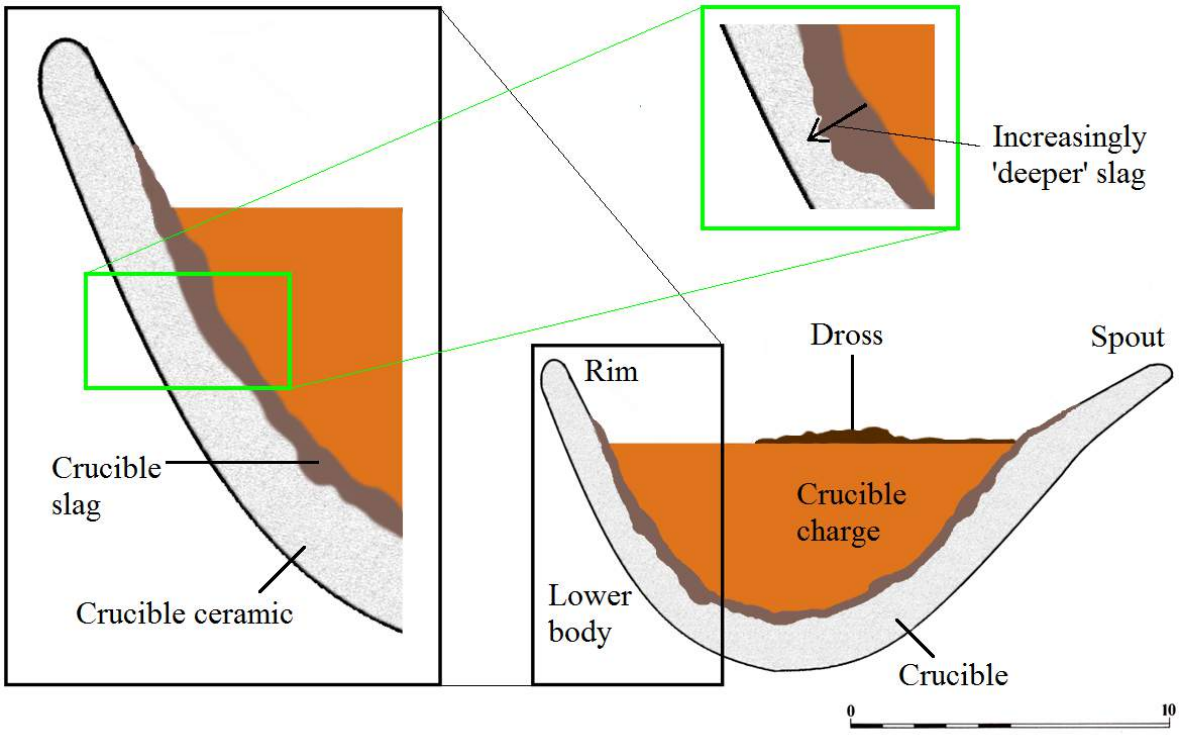

Figure 1.2: Crucible terminology overview

- *Secondary metallurgy*: High-temperature working of (raw) metal, such as refining, recycling and alloying (molten state) or hammering and annealing (solid-state).

- *Slag*: Generic term for metallurgical waste, typically referring to a "once molten silicate or silicate mixture, sometimes including oxides, phosphates, borates, sulphides, carbides, pure metals etc." (Bachmann, 1982b: 1). In the context of non-ferrous metallurgy, a distinction can be made between *smelting slag*, which is the waste product of primary smelting operations and therefore typically (though not exclusively) formed in furnaces (e.g., *furnace slag, tap slag*), and *crucible slag*, which is formed inside crucibles (see below) and usually associated with secondary metallurgy. Many process-specific slag types may be formed during particular metallurgical operations, which are not discussed in detail here (for an overview, see Craddock, 1995).

- *Crucible slag*: Slag that has developed at the interface of the crucible and its charge, through the combination of vitrified ceramic and various contributions from the crucible charge, such as fuel ash and metal oxides.
  When exposed to increasing temperatures, the crucible ceramic typically fuses and vitrifies to a certain extent. Depending on the heating mode, such vitrification may

occur in different areas. For internally heated crucibles, the interior surface of the crucible usually bloats and vitrifies to a certain depth into its ceramic body, away from the interior surface. It is, however, closer to this interior surface that actual *crucible slag* is formed, through the interaction between charge constituents and the vitrified ceramic. Though the vitrified crucible ceramic forms a continuum with the crucible slag, this slag is distinguished and defined by its various metallurgical waste products. As indicated in Figure 1.2, when 'deeper slag areas' are mentioned within this thesis, this refers to slag areas relatively further away from the crucible's interior surface. For externally heated crucibles, a thin vitrified layer may form on the exterior crucible surface (*glaze*), which is not considered 'slag', as it is not formed through interaction with the crucible charge.

- *Dross*: Crucible dross consists of various metal oxides that are not captured in the crucible slag and float on top of the crucible charge during the metallurgical process (see Figure 1.2). Such dross layers are sometimes referred to as crucible slag in the literature (e.g., Craddock, 2013 and Tylecote, 1986). In this thesis, however, the term crucible slag refers strictly to the slagged ceramic attached to the crucible interior, as defined above. Dross is a more generic term for what is sometimes called 'refining slag' in the literature (e.g., Craddock and Meeks, 1987; Karageorghis and Kassianidou, 1999; Merkel, 1990 and Pernicka, 1999).
  When the metal content is cast from the crucible, such dross layers may be removed manually beforehand, or left to settle within the crucible. It is thus sometimes deposited on top of the crucible slag, to which it may fuse and form a continuous layer. As illustrated for each assemblage, however, these dross layers may be distinguished from the crucible slag through microscopic and chemical analysis.

- *Tuyère*: A hollow pipe or tube through which air is blown into a furnace or crucible.

- *Bellow*: A device used to create a strong air blast, which is then directed through the tuyère into the furnace or crucible.

- *Mould*: Hollow container into which metal is cast into a particular shape.

- *Refractory*: In general, this term refers to materials that remain mechanically and chemically stable during high-temperature processes. In reference to archaeological materials, 'refractories' are commonly ceramics. Given the wide variety of ceramic types, as well as the different temperature and chemical requirements posed by various metallurgical processes, refractoriness should be considered a relative term in

archaeological context (Freestone, 1989; Freestone and Tite, 1986; Martinón-Torres and Rehren, 2014; Tite *et al.*, 1985).

- *Bronze*: Bronze in this thesis refers strictly to alloys of copper and tin. Different grades of bronze may be distinguished, with low- to intermediate-tin (±0-12 wt% Sn), intermediate- to high-tin (±12-20 wt% Sn) and high-tin (over ±20-25 wt% Sn) bronze. Clearly, these present rough ranges, rather than distinct categories.
  Leaded bronze refers to an alloy of copper, tin and lead, while *leaded copper* refers to an alloy of copper and lead.

CHAPTER 2

Theoretical framework

Archaeometallurgy is, first and foremost, an archaeological discipline (Rehren, 2000). As such, it shares the fundamental aim of archaeology, which is the study of human behaviour through the remains of material culture (Renfrew and Bahn, 2012: 12) in their particular context. This implies that certain fundamental theoretical concepts from archaeology apply to archaeometallurgical studies, though more specific concepts are equally needed. While this thesis leans strongly towards the analytical side of archaeometallurgy, focusing in particular on analytical methodology, theoretical considerations still play an important role. Not only is any scientific, laboratory observation inherently biased by theoretical preconceptions and expectations to some degree (Brewer and Lambert, 2001), but the archaeological interpretation of this generated data requires at least a minimal disclosure of the author's theoretical background. However, this is indeed kept to a minimum, as theoretical concepts applied in this thesis are primarily instrumental. This thesis does not intend to contribute significantly to interpretative theoretical frameworks, though some ideas concerning workshop interpretation are discussed further in the overall discussion (Part VI). This chapter therefore sets out the background against which research on ancient technology is undertaken, with particular focus on metallurgy. A more general discussion of archaeological theory (Johnson, 2010) and its fundamental concepts (Lyman, 2012) is omitted as it is not a focal point of this thesis, and such broad discussions would therefore be tedious and out of place here.

Section 2.1

Technology in archaeology

The study of technology has always been an integral part of archaeology, as most artefacts retrieved from the archaeological record were produced by humans in some way or another. Understanding how ancient people made things and manipulated the world around them has therefore become a core archaeological inquiry.
Rather than focusing only on the technical aspects of a certain technology, archaeologists are interested in the context within which technologies were developed and used. To do so, contextual evidence is combined with the material evidence to elucidate its meaning. A well known example is the variation in production contexts for pottery, proposed by Peacock (1982), which is mainly based on aspects such as standardisation (Roux, 2003), complexity and specialisation. Making use of parallels in contemporary pottery practice, Peacock took an ethnographic approach to understanding archaeological remains. The study of technology in archaeology in general has widely benefited from anthropological work, which provides theoretical frameworks for the discipline. It is beyond the scope of this thesis to discuss this in great detail, but some fundamental concepts used in this research are briefly presented here, while more specific ideas related to metallurgy are discussed in section 2.2.

Some basic concepts are defined here to avoid ambiguity of their use within this thesis, largely following terminology proposed by Miller (2007). *'Production'* refers to the processes, including both materials and techniques, involved in fabrication or creation of a certain material object, and the *'organisation of production'* is the way in which these production processes are organised socially. *'Technology'* is a broader term, encompassing both production and consumption, including the interaction between people and objects over this whole range of processes.
The reconstruction of production is the starting point for each case study presented in this thesis, and is covered in the technical interpretation of the analytical results. This aspect of technology is the most commonly investigated in archaeological research, and often relies on comparisons to modern production techniques. Here, researchers look at firing temperatures for ceramics, blowing techniques for glass, alloy compositions of metals, etc. While this is sometimes the end point, rather than just the starting point, of technological investigations, this thesis aims to include wider discussions of technology that go beyond mere descriptions of production processes.

As a first step, the organisation of production is considered. Four general parameters have

been suggested by Costin (1991) to describe the organisation of production. The first one is *'context'*, which represents the nature of control over production and distribution. A distinction can be made here between an attached production context, where production and consumption are largely elite-controlled, and independent production context, where independent specialists produce for a more general market. As *'context'* refers more generally to archaeological context, the term *'production context'* is used here. Within this thesis, Pi-Ramesse may be classified as an elite-controlled production context, while insufficient information is available to allocate confidently the other assemblages to a particular production context. Probably, they can be interpreted as more independent.

A second parameter is *'concentration'*, which reflects the relative regional concentration of production facilities. This parameter is particularly important when considering transport and trade issues, but cannot readily be assessed for these case studies: each represents the first regional example of (crucible) metallurgy.

'Scale' is the third parameter, which comprises both the size and make-up of production units. A simple correlation of, for example, workshop size to elite control is not necessarily valid, and can only be appreciated in light of other parameters, such as the ease by which a certain technical process can be conducted at various scales. Scale, then, does not equate size, but is rather concerned with the coordinated use of a production area of a certain size. The issue of production scale is considered in the final discussion of this thesis (Chapter 14).

Finally, *'intensity'* represents the degree to which producers are active on a part- to full-time basis. Costin (1991) argues, for example, that there is a greater tendency for attached specialists to work full-time in non-industrial economies for a variety of reasons, such as the elite control over highly desirable special goods. For the case studies considered here, it is difficult to substantiate any debate on the nature of production intensity on the basis of available evidence, though some remarks on the issue are made.

Overall, it is hard to assess the parameters listed here, and throughout this thesis only tentative suggestions can be made. While it is through the recognition of variation in these parameters within different environmental, social, cultural, economic and political contexts that the organisation of production may be understood, the isolated nature of the evidence presented here makes such discussions problematic. Furthermore, an understanding of the consumption-side of the market is essential to explain production. As mentioned in section 1.1, and detailed further for each case study, little comparative data is available to push the interpretation of production to the level of its organisation. Though some more evidence is available for New Kingdom Egypt (see section 4.5), almost nothing is known for Achaemenid Phrygia. Roman Thrace, in contrast, may draw on comparisons

to the broader Roman world, but the material and contextual limitations of this assemblage hinder such efforts. Therefore, discussions of the organisation of production in this thesis are mostly provisional, and aimed at illuminating where future studies may further our understanding of these issues.

The study of technology as a whole goes further than what has been discussed so far. Technology more broadly encompasses all human activity behind production and its organisation. This idea is perhaps best understood here through the concept of *'technological choice'* (Lemonnier, 1993). It refers to the selection of particular techniques and materials to achieve a certain goal, from the wider range of choices available to a person. Such choices are not considered in light of simply technical terms, as it is abundantly clear that influences from social, cultural, economic and ideological spheres can shape these choices, despite being 'non-technical'. Through the consideration of the many possible choices that were (consciously or unconsciously) forsaken in favour of the choice witnessed in archaeological remains, a wider view of technology, as embedded in a sociocultural context, becomes apparent.

The question of technological choice may be asked for each step of the production process, where the final objects represents a series of choices of techniques and materials, resulting in a particular outcome (Sillar and Tite, 2000). Such a sequence of steps was first described by Leroi-Gourhan (1964, 1965) in the context of Paleolithic stone technology (see further Audouze, 2002), who introduced the term *chaîne opératoire*. This is not limited to the listing of different production steps, but rather incorporates environmental factors, as well as economic, social and political organisation and the belief systems as fundamental factors influencing each of these steps.

The five most important areas for technological choice were defined by Sillar and Tite (2000) as the raw materials, tools, energy sources, techniques and the sequence (*chaîne opératoire*) in which they are applied. Sillar and Tite emphasise the need for researchers to consider the full scope of alternative techniques from which technological choices can be made, evaluating the influences from functional, environmental and cultural factors and the consequences, both immediate and longer-term, of these choices. The extent to which particular factors, such as environmental or cultural influences affect technological choice differ for each case study, but 'universals' such as chemical properties of materials and particular social contexts in which these materials were manipulated should be considered as embedded in technological choice.

Throughout this thesis, these opportunities for technological choice are considered, and an attempt is made to understand the broader factors underlying each production step, embedded within a wider technical and social practice. While material science offers the

baseline against which these choices are evaluated, socio-cultural factors are kept in mind throughout the analysis of the remains as these do not simply begin where purely technical, physical reasoning ends, but are deeply entwined (see Dobres, 2010, Doonan, 1999a and Lemonnier and Pfaffenberger, 1989). However, broader discussions of social and ritual meaning of technological activity (Pfaffenberger, 1988) as part of a 'sociotechnical system concept' (Pfaffenberger, 1992) are beyond what is intended here. Where needed, such issues are mentioned in the text, but they are not central to this research. Similarly, questions of materiality (e.g., Jones, 2004 and Martinón-Torres and Rehren, 2009) and technological style (e.g., Childs, 1991) are beyond the scope of this project.
This thesis is primarily concerned with the more technical interpretation of crucibles. While the entwined nature of technology in a much broader socio-cultural context must be kept in mind during such interpretations, the results presented throughout this thesis aim to show that current understanding of 'baseline material science' is often insufficient to address such questions for now. The study of ancient crucible metallurgy is still very much in its infancy, and requires thorough discussion of its analytical methodologies and many more case studies, before it becomes possible to make sense of these broader issues. Nonetheless, they should be kept in mind in the course of this ground-laying work, which is why some space has been allocated to the issue in this introduction. The contextual interpretation of crucible metallurgy within this thesis, then, aims to explore technological choices to the extent that the crucible and contextual evidence allow, without opening broader discussions for which the comparative evidence is currently lacking.

Section 2.2

Crucible metallurgy in a metallurgical chaîne opératoire

An overview of metallurgical production processes is given by Miller (2007) and shown in Figure 2.1 (a similar diagram is presented by Hauptmann (2014), Fig. 5.1, p. 92).

The main steps in the production of copper objects are:

1. Mining/collecting copper ores
2. Ore sorting, beneficiation and roasting, furnace and crucible manufacture, and other preliminary processes
3. Smelting: primary production of copper from its ore

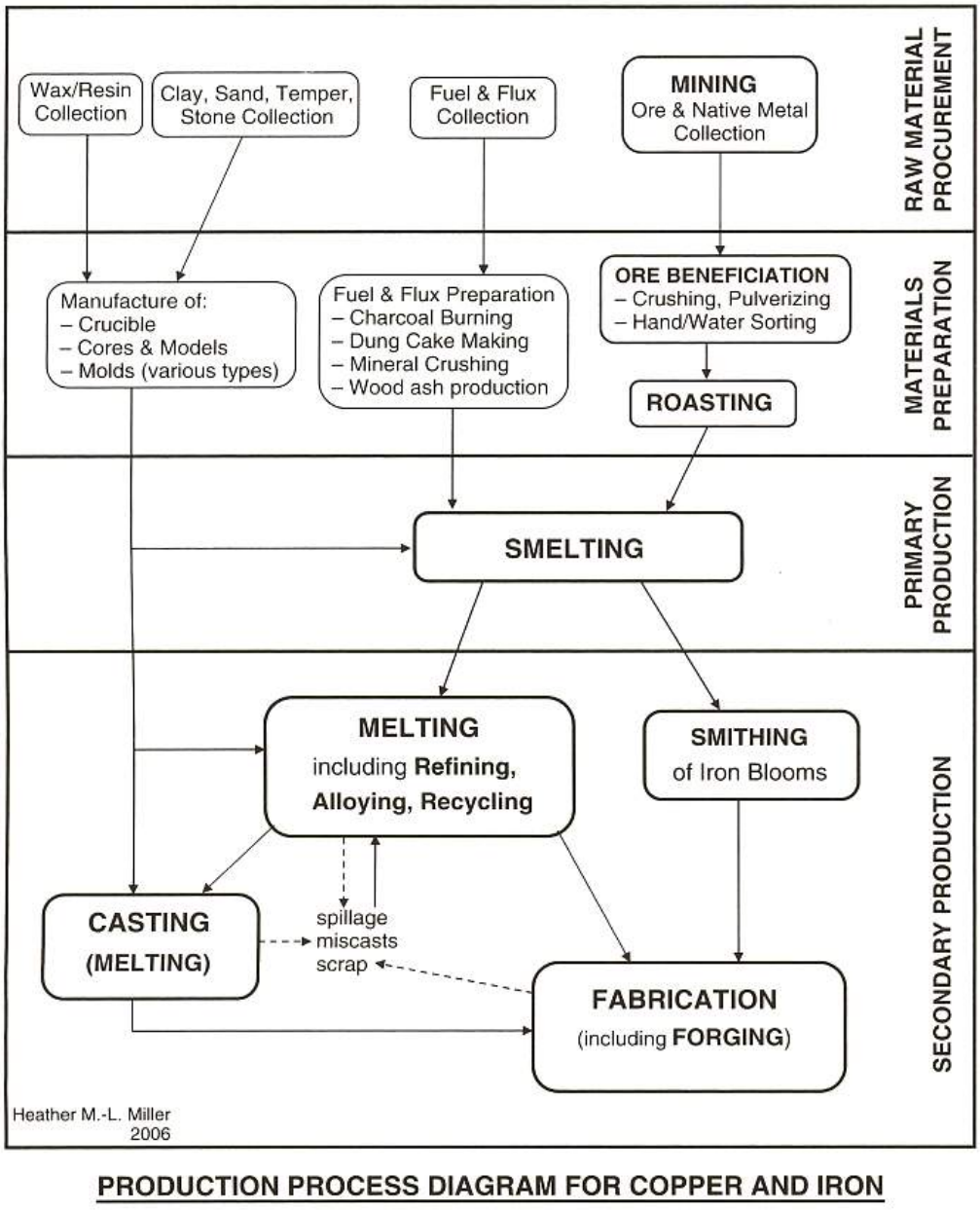

Figure 2.1: Stages in the production process of metals (from Miller, 2007, Figure 4.11, p. 146)

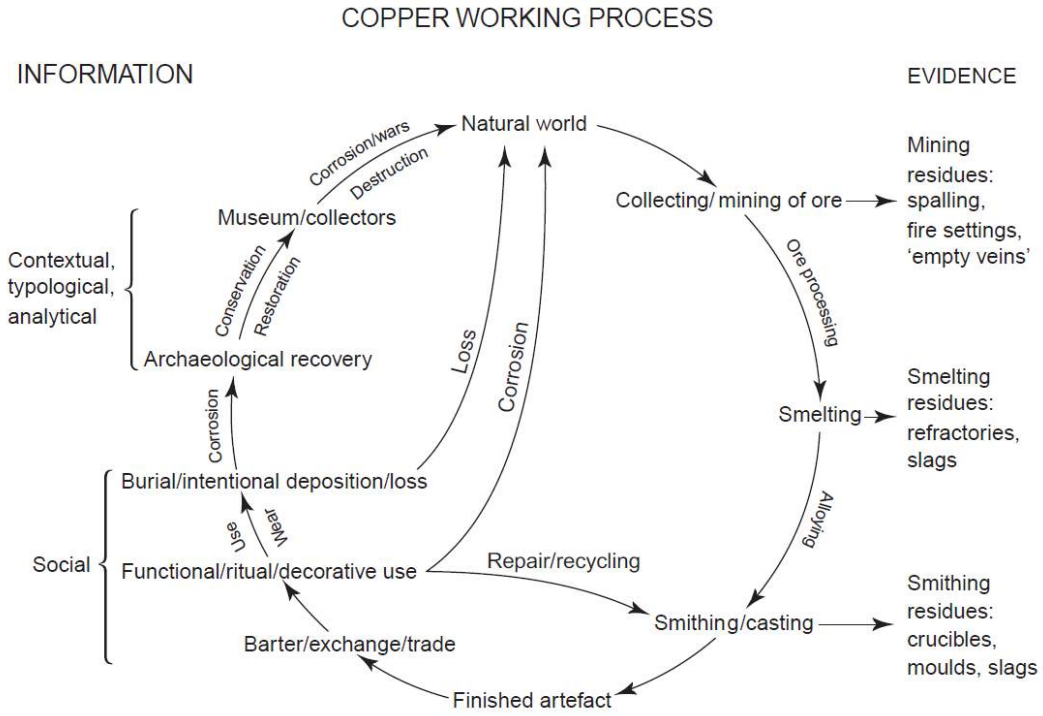

Figure 2.2: Metallurgical *chaîne opératoire* or 'Cycle of copper production and working' (from Ottaway, 2001, Figure 1, p. 88)

4. Secondary metallurgy: further high-temperature processes such as refining, recycling and alloying (molten state) or hammering and annealing (solid-state)

5. Creation of final objects by casting or other shaping methods

Figure 2.2 schematically shows the *chaîne opératoire* of copper production, as proposed by Ottaway (2001). The focus of a *chaîne opératoire* approach is wider and does not stop at artefact fabrication, but encompasses its use and ultimate destruction, which yields a 'life cycle'. It further incorporates social structure and historical context along each step, though Figure 2.2 only emphasises this for the finished artefacts. Much more detail could be added to the different steps shown here, but producing a state-of-the-art overview for each different step is beyond the scope of this research.

The value of the *chaîne opératoire* concept lies in its ability to integrate a wide variety of activities related to a particular technology, witnessed in archaeological contexts. It is a bottom-up approach, allowing archaeologists to refine or expand the *chaîne opératoire* as new data appears. As such, it is not so much an explanatory tool for understanding scientific results (like those produced in this thesis), but rather a framework that can be corroborated and improved by archaeologists studying ancient technology. In this way, others may familiarise themselves with the wide scope of technological choices ancient

people made and look at their particular case studies from a broader perspective.
In this thesis, the main focus lies on the secondary production processes, located in the bottom-right corner of Figure 2.2. Though crucibles are sometimes associated with primary smelting processes, they are most commonly (and in all the assemblages presented here) used for secondary metallurgy. They represent a transitional stage between raw metal and finished objects, and may be informative of both. For example, particular contaminants that are left behind in the crucible slag relate it to the melting of a particular raw copper that may no longer be present on site. Similarly, the prills embedded in it can infer the alloy composition of the finished object that is usually not found in archaeological association to the crucibles.
The crucibles themselves are ceramic vessels, which solicits comparisons to general ceramic technology. This may help in discovering overlaps between different technologies in technical, organisational and socio-cultural aspects. Such cross-craft comparisons are made, for example, in Pi-Ramesse to other contemporary high-temperature technologies like glass production.
The context in which these activities take place further informs the organisation of production. For example, the primary production of metal is commonly undertaken close to the mining areas, whereas secondary production is often encountered in urban environments, closer to the consumers. However, very few assemblages have hitherto been studied in detail, making such distinctions tentative at best, and in need of further testing. The existing bias for excavation of particular archaeological contexts, such as funerary and palatial environments in favour of rural settlements, further hinders such broad interpretations. While assemblages should be evaluated within their particular context, it is therefore important to keep in mind that a comparative approach is needed to evaluate the influence of contextual factors on a particular technology. As emphasised throughout this thesis, the absence of comparative data for all of the discussed assemblages imposes strong limitations on their contextualisation. Their presentation and discussion is therefore aimed at giving an overview of the existing knowledge of technology, and offer suggestions for future research in support of establishing a more complete *chaîne opératoire*.

Part II

Analytical Methodology

Get your facts first, and then you can distort them as much as you please.

Mark Twain in Kipling, 1899

CHAPTER 3

Methodology for the analysis of crucible remains

This chapter presents an overview of the methodology applied for analysing each assemblage. Sample selection and documentation is a first aspect of this methodology, but is covered for each case study separately. The next important step is macroscopic investigation, briefly discussed in section 3.1, followed by optical microscopy, detailed in section 3.2. The use of scanning electron microscopy (with energy dispersive spectrometry) is described in section 3.3, while lead isotope analysis is treated in section 3.4. Finally, section 3.5 discusses the application of handheld X-ray fluorescence spectrometry.

Section 3.1

Macroscopic investigation

Macroscopic investigation entails the analysis of an object's properties by eye. The recognition of an object as related to metallurgical activity often takes place already in the field, based on a number of observations related to its physical appearance. Bachmann (1982b) provides a reference for recognising metallurgical production waste and distinguishing it from other material such as rocks, ceramics and vitrified matter. This initial interpretation of the material allows it to be grouped in different categories for further study. Bachmann states that this initial stage of macroscopic sample description does not only serve as a prelude to further microscopic analysis, but may often render elaborate laboratory work unnecessary. Though this may sometimes be true, this research shows that elaborate laboratory work can often provide further details which allow a deeper understanding of cru-

cible technology. Nonetheless, crucible typology is often strongly reflective of its function, and macroscopically visible aspects of the crucible ceramic and slag can reveal much of the process.

For archaeometallurgists working on material excavated by others in the past, the ideal scenario is to receive an assemblage that has already been separated from non-metallurgical debris, without essential material having been left out. For each assemblage presented in this thesis, provisional identification of the metallurgical material by the excavators has yielded well-defined groups of crucible remains. An assessment of the representativeness of these crucibles for the ancient metallurgical activity they reflect, is made in the final discussion (Part VI). The macroscopic appearance differs significantly between these assemblages and is discussed separately for each case study.

Section 3.2

Reflected light microscopy

For the analysis of archaeological ceramics, thin section petrography is the technique of preference (e.g., Peterson, 2009 and Quinn, 2009), using transmitted light microscopy and drawing on the principles of mineralogy (e.g., MacKenzie and Guilford, 1980). Fabric descriptions are then commonly used to establish ceramic production technology and to provenance different wares (e.g., Arnold *et al.*, 1993; Day *et al.*, 1999; Hein *et al.*, 2008; Kilikoglou *et al.*, 1995; Müller *et al.*, 2010 and Tite *et al.*, 2001). This has been applied to the study of metallurgical ceramics to better understand the selection of raw materials used in their production (e.g., Hein *et al.*, 2007 and Katona *et al.*, 2007) and to evaluate their thermal and mechanical properties.

The study of metals using a reflected light microscope is a well established technique, commonly known as metallography, often applied to ancient metals (e.g., Chen *et al.*, 2009; Scott, 1991 and Yahalom-Mack *et al.*, 2014). In geology, reflected light microscopy is used for the study of opaque materials, such as ores (e.g., Ineson, 1989).

Metallurgical slag is often similar to ores in its composition and opacity, which makes microscopic study in mounted section (using reflected light) rather than thin section (using transmitted light) more sensible. However, the minerals and structures recognised in ore microscopy are not directly comparable to archaeometallurgical materials, which are not formed by natural processes. This means that the formation history is often very different and phases can be formed which naturally occur in different configurations or not at all.

Keeping this in mind, the microscopic study of metallurgical remains such as slag and technical ceramics can be very informative in understanding their formation history. Recognising different phases and structural features helps in achieving this understanding. The best (and only) systematic example of how to study these materials using reflected light microscopy is given by Bachmann (1982b). No real systematic methodology has been developed for studying (crucible) slag (see section 1.2); most publications are case studies in which a variety of approaches are used (e.g., Bassiakos and Catapotis, 2006; Georgakopoulou *et al.*, 2011; Stos and Gale, 2006; Thompson, 2006; Thornton and Rehren, 2009 and Zwicker *et al.*, 1981). This partially reflects the fact that methodological choices are strongly driven by specific research questions: it is often not very useful to recognise and quantify every single phase present in a sample. Rather, specific process markers and special features should be looked for, depending on the hypothesis one wants to test. This hypothesis is often already formed during macroscopic investigation, but can obviously change during further analysis. The overview by Martinón-Torres and Rehren (2014) of important process markers commonly encountered during crucible analysis, which are not reiterated here, is a good starting point for guiding crucible analysis. A more generalised analytical methodology, however, offering practical guidelines for consistent analysis, is currently still lacking. Such practical guidelines would consist of, e.g., how to best select a crucible sample, how many areas should be analysed, and which micro-phases are diagnostic of particular process parameters. Though some of this knowledge is often implicitly assumed, this thesis aims to highlight the need for more discussion of these practical matters and their effect on successful crucible analysis.

The study of metallurgical crucibles then is on the boundary between ceramic and slag analysis. For this project, a metallurgy-oriented approach is followed where the crucible contents rather than the ceramics themselves are the main object of interest. This means that, though adequate attention is given to the ceramic technology, the crucible slag receives the main focus. Therefore, crucible sections are mounted in resin for reflected light microscopic analysis of the opaque crucible slag (and ceramic) and subsequent chemical analysis using SEM-EDS (see section 3.3). Though the use of polished thin sections would allow both the use of transmitted light microscopy and chemical analysis using SEM-EDS (e.g., König and Serneels, 2013; Rehren, 1999, 2009 and Tite *et al.*, 1985), sample preparation for this approach is more time-consuming and does not present sufficient advantages for this research. The study of mounted sections is a common approach in crucible metallurgy reconstruction (e.g., Martinón-Torres *et al.*, 2008; Renzi *et al.*, 2009 and Thornton and Rehren, 2009).

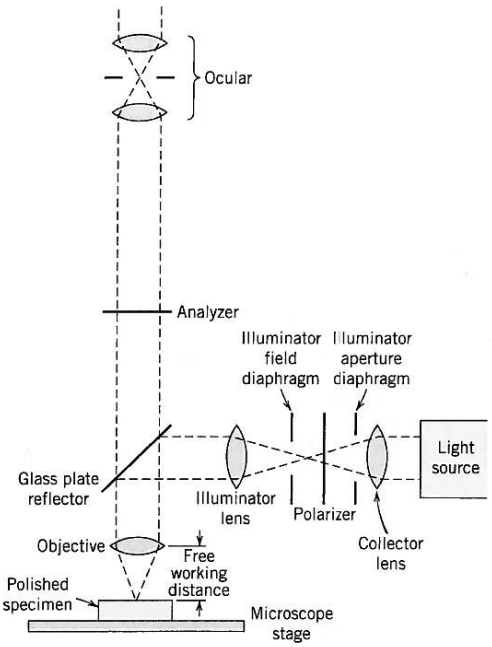

Figure 3.1: Schematic representation of reflected light microscopy (from Klein and Dutrow, 2007, Figure 13.27, p. 305)

3.2.1 The microscope

A Leica DM4500 P LED polarisation microscope, equipped with a Leica DFC 290 HD camera, has been used for microscopic analysis and image acquisition, using Leica Application Suite PC software.

Figure 3.1 shows the basic mechanism of a reflected light microscope: light (coming from the right) is first polarised ('polarizer') and then reflected down by the beam splitter ('glass plate reflector') onto the sample. The sample reflects this light, which then passes vertically upwards through the beam splitter to the ocular and/or camera. The 'analyzer' (which is oriented at a 90° angle from the 'polarizer') can be placed in the path between sample and ocular to polarise the light reflected from the sample. Viewing the sample with or without the use of this second polariser is respectively called cross- and plane-polarised reflected light microscopy.

This configuration allows analysts to make use of diagnostic optical properties of different materials, such as colour, reflectivity and bireflectance[1] (Klein and Dutrow, 2007). The main optical property used to distinguish between minerals is colour, typically a shade of grey or yellow. Isotropic crystal structures do not alter the state of polarisation of the light

[1] Bireflectance is a similar behaviour to pleochroism seen in transmitted-light microscopy of non-opaque minerals.

reflected from their surface[2] and therefore appear dark when viewed using crossed polarised light. Many nonisometric (i.e., non-cubic) minerals, however, show bireflectance and therefore change brightness or colour when rotated under plane-polarised light. Under cross-polarised light, these minerals exhibit extinction. These optical properties can be used to distinguish between different minerals present in the crucible samples.

3.2.2 Goals and objectives

The first objective of microscopic analysis is to get an overview of the crucible structure and texture. Observation at a low magnification (25-50X) is usually sufficient to get a good idea of the sample's different parts, such as ceramic fabric, slag and corrosion or dross layers, and structural relations between them.

After establishing this overview, a second objective is to study the different parts at a higher magnification and to investigate their mineralogical make-up.

Finally, specific phases, prills and other features can be identified under high magnification.

For each of these steps, both plane- and cross-polarised light is used and the sample stage is moved around to utilise the various phases' optical properties for identification.

Photomicrographs are taken using a digital camera. This documentation is a goal in itself, but is equally important as a reference while investigating the sample using SEM. Micrographs shown throughout this thesis are mostly SEM-BSE images (see below). Optical microscopy images are denoted as 'O.M. image'.

3.2.3 Sample preparation

The samples are cut[3] in such a way as to fit the 32 mm resin moulds. The location of where a sample is cut determines what is visible during microscopy. A section through the crucible wall, showing the changes from outside to inside, has been aimed at everywhere. The selection of a particular section of a crucible (fragment) is based on previous macroscopic investigation and greatly influences the information that can be gained from it. While it seems natural to go for 'juicy' areas –containing thicker, more developed slag– no guidelines exist for sample selection. Assessing the influence of taking samples from

[2] Isotropic minerals show neither bireflectance nor extinction positions.

[3] Samples are cut using a wet saw which is cleaned using de-ionised water after each sample, to avoid contamination.

particular areas within a crucible is one of the objectives of this research, further discussed in Chapter 13. Apart from considerations of 'information yield', a crucible's preference to fracture in certain areas and presenting itself as such in the archaeological record, after possible post-depositional effects, introduces inevitable restrictions. Furthermore, the researcher's personal habits and inclinations during sampling introduce an inherent bias, which are minimised by working in a consistent manner. Preservation of the artefact usually needs to be taken into account as well, by minimising disfigurement during sampling. Finally, the exclusion of large metal prills in a section is attempted, as these prills are candidates for lead isotope analysis (see section 3.4).

Once the samples have been cut, they are placed face-down into a clean resin mould. A label, containing sample ID, a brief description, researcher name and the date, is added to the mould, which is subsequently filled with epoxy resin. This is prepared as a 4:1 mixture of epoxy and resin hardener. Due to the often high porosity of crucible samples, it is necessary to place the moulds in a vacuum for a short period, to draw the air out of the pores and fill them with resin[4]. The samples are left to harden under a fume extraction vent for 24 hours at room temperature.

The hardened samples are then removed from the moulds and ground to create two flat parallel surfaces. Next, the surface exposing the sample is ground using abrasive paper, starting from a rough grit size (P120) and progressing to a finer grade (P320-P600-P1200-P2500-P4000)[5]. The sample is cleaned using running water between each paper grade, while a quick microscopic investigation shows whether the marks of the previous grade have been removed and the next grade can be started. After the P4000 grit, the sample is cleaned in acetone in an ultrasonic bath and dried. Finally, two polishing steps are performed, using cloths with consecutively 1 μm and 1/4 μm diamond paste (either by hand or on an automated polisher[6]). After each of these two steps, the samples are cleaned in the ultrasonic bath and dried. The finished samples are then stored in a dry environment to avoid hydration/oxidation at the sample surface.

Each finished sample is scanned using an ordinary office scanner. This image (see Figure 3.4b) is stored for future reference, while a print-out is used as a guide and note-taking paper when investigating the sample under the microscope and SEM.

[4]Large pores in the polished surface of the sample can lead to charge build-up during SEM-analysis, which suppresses the electron beam and disturbs analysis.

[5]The two last steps of grinding can be facilitated by the use of a Buehler MetaServ 3000 Variable Speed Grinder-Polisher with Vector LC Power head.

[6]Struers LaboPol-5 with Struers LaboForce-3.

3.2.4 Methodology

The samples are placed under the microscope for investigation by eye, while a camera attached to the microscope allows image acquisition and monitoring on a computer. The structure is first investigated at low magnification (50X). Further details of the different crystal phases are acquired at higher magnification (up to 500X), using both plane-polarised (PPL) and cross-polarised light (XPL). In this study, the main focus is given to the crucible slag, while only a basic description and abnormal features are recorded for the ceramic fabric (after a 'typical' ceramic description has been obtained). Throughout the analysis, photomicrographs are taken and mapped on the printout, for documentation purposes and as an aid during examination by SEM.

Sadly, references for phase identification are scarce. Bachmann (1982b) noted over thirty years ago that a general description of mineral content in ancient slags had not been compiled yet. Only through the collation of information from occasional papers dealing with particular sites and assemblages can such a list be generated. As the field of archaeometallurgy develops, such a list should be continuously expanded and updated. While Bachmann's publication was intended to serve as a first tentative guide, no concerted effort has taken place since 1982 to compile a list of phases encountered in ancient metallurgical (crucible) slag, and the investigator has to rely on his own resources and the case study oriented examples in the literature for their identification.

Section 3.3

Scanning electron microscopy - energy dispersive spectrometry

This section covers the principles of scanning electron microscopy, with energy dispersive spectrometry, and its specific application in the analysis of crucibles throughout this research.

3.3.1 The scanning electron microscope

An electron microscope uses an electron beam to illuminate the sample. This electron beam is focused onto the sample using a series of electromagnetic lenses, which control

(inter alia) the magnification, as shown by the diagram in Figure 3.2. The scanning electron microscope (SEM) moves this finely focused beam across the sample, sequentially building an image from the reflected electrons. Magnifications a thousand (or more) times greater can be obtained than for light microscopy and a better depth of field is achieved at the same resolution. Signals resulting from interaction between the electron beam and the sample are summarised in Figure 3.3.

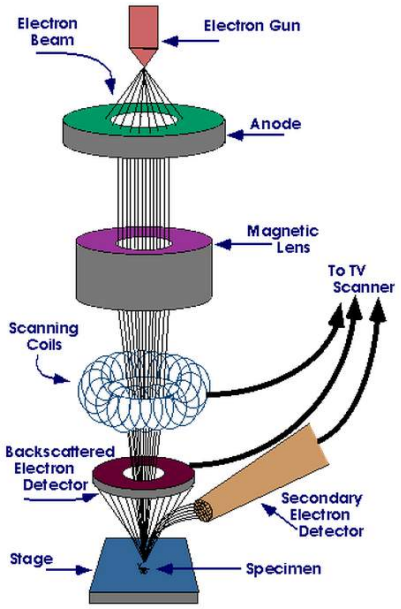

Figure 3.2: Diagram of scanning electron microscope (from *www.purdue.edu*)

Secondary electrons (SE) are low energy electrons detached from the surface atoms of a sample through inelastic collision and can be used for imaging surface topography. Backscattered electrons (BSE) are higher energy electrons which are reflected out of the sample interaction volume by elastic collisions with the nucleus of atoms in the sample. This backscatter is stronger for heavier elements, so BSE detection can produce images where light elements appear darker than heavy elements and thus highlight differences in chemical composition within samples. Micrographs shown in this thesis are SEM-BSE images, unless otherwise noted.

Elements under electron bombardment emit photons of X-radiation with specific energies and wavelengths. These X-rays are the result of inelastic collisions, during which electrons are ejected from one shell of the atom and an electron from a higher energy shell takes its place, thereby releasing energy in the form of X-radiation. Depending on which shell electrons are ejected from (typically K, L or M) and from which higher-energy shell another electron takes its place, X-rays have different energy-levels and wavelengths.

Therefore, each atom species produces a characteristic X-ray emission spectrum reflecting the likelihood of these different possible electron-jumps. It is possible to measure this X-radiation spectrum using either the energy-levels of these X-rays or their wavelengths, which is called energy (EDS) or wavelength dispersive spectrometry (WDS) respectively. These X-rays are representative of the surface atoms, as fluorescent photons cannot escape the sample from depths exceeding ±10 micron, even though the electron beam might penetrate deeper into the sample (Pollard *et al.*, 2007; Watt, 1997).
Besides this characteristic X-ray spectrum, *Bremsstrahlung* (a continuum background radiation) is emitted. The more discrete characteristic lines are superimposed onto this background radiation spectrum, the range of which is related to the maximum beam energy, rather than the atoms being excited.
Auger electrons and cathodoluminescence[7] are not discussed here.

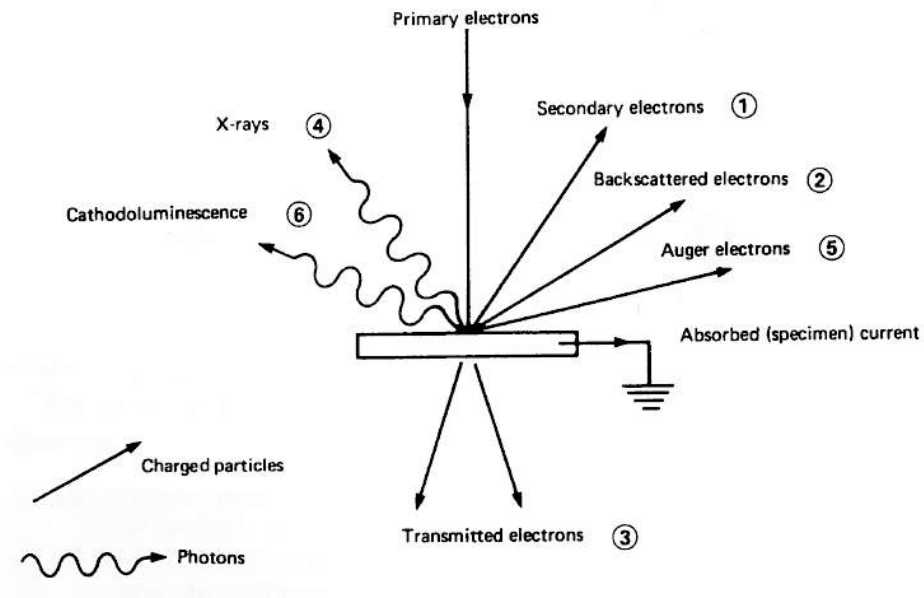

Figure 3.3: Schematic representation of electron beam and sample interaction in an electron microscope (from Watt, 1997, Figure 2.4, p. 34)

The main differences between EDS and WDS for chemical analysis are the range of elements that can be measured[8] and the higher quantitative precision that can be achieved by WDS[9]. The main disadvantage to WDS is the need for moving detectors with low (sequential) collection efficiency, resulting in a much slower method.

[7] For a recent application of CL in ceramic analysis, see Hunt (2013).

[8] EDS can detect elements from sodium (Z=11) upwards, while WDS can detect lighter elements from boron (Z=5) upwards.

[9] WDS is able to better resolve peaks (problems caused by proximity of characteristic X-rays emitted by different elements) than EDS and has lower detection limits (due to higher peak/background ratios).

EDS is considered more suited to the purposes of this research, as it is faster, more appropriate for the analysis of many large areas and discrete phases, and has sufficiently low detection limits to answer the questions at hand.
A JEOL 8600 Superprobe equipped with an Oxford Instruments EDS attachment is used with INCA software for data-processing.

Obviously, the above discussion is a strongly simplified and necessarily brief overview of SEM(-EDS) principles. For more detailed information on the workings and operation of scanning electron microscopes, the reader is referred to, e.g., Chescoe and Goodhew (1990); Goldstein *et al.* (2007) and Watt (1997).

3.3.2 Goals and objectives

In the first instance, SEM can be used for further microscopic investigation of the crucible structure and different crystal phases, similarly to optical microscopy (see section 3.2.2). Though this can be done at a much higher magnification than achievable by optical microscopy, SEM is much more time-consuming for this type of analysis and only produces greyscale images, which are indicative of elemental composition but do not allow the use of optical properties for mineral identification. For this reason, it is complementary to optical microscopy and cannot replace it (Photos and Salter, 1986).

The SEM is equipped with an EDS-system, which allows for chemical analysis of different phases at high spatial resolution. This feature is used to identify the chemical composition of phases and features that have been identified during microscopic analysis.

Finally, the chemical analysis of larger areas ('bulk analysis') within the sample is undertaken to look at chemical changes within each sample between the ceramic part and the slag part.

No analysis of fresh fracture surfaces to estimate firing temperatures (Hein *et al.*, 2007; Tite *et al.*, 1982) is performed.

3.3.3 Sample preparation

The mounted section prepared for optical microscopy can be used for SEM(-EDS). The only additionally required preparation step is to apply a carbon coating to the sample. This makes the surface conductive, which is necessary to avoid charge build-up on the sample surface. The carbon layer has a default thickness of approximately 15 nm.

The coated samples are placed in a holder and secured using carbon tape. This tape holds the samples in place and acts as a conduct for current between the sample face and the holder. The holder is then put into a vacuum lock before being introduced into the actual SEM chamber. This allows the JEOL 8600 Superprobe to maintain a permanent vacuum, contributing to the stability of the electron beam. The sample stage can be operated either by introducing the desired coordinates into a computer or by using a joystick.

3.3.4 Methodology

A PC equipped with INCA[10] software is attached to the JEOL 8600 Superprobe, which is used for data-acquisition during analysis. An accelerating voltage of 20 kV is used, with a working distance of 10 mm and a live time of 50 seconds. At the start of each session, a cobalt standard (loaded in the holder) is analysed for quantitative optimisation.

After optimisation, the actual sample analysis begins. As each archaeological sample is slightly different, the exact procedure differs for each case. However, a general methodology for analysing crucible sections has been followed and is detailed here. A visual example is shown in Figure 3.4.

- For the steps described here, a 100X magnification is used.
- The chemical composition of the entire area visible in the frame (± 1 mm^2) is measured[11]. Quartz grains and any other inclusions are included in these frames and not avoided, as their omission would bias any comparison in bulk chemical composition between different crucible parts. On average, five bulk measurements are taken for each part of the crucible. These are usually the ceramic and slag part, but the composition of other areas areas noted during microscopy (e.g., corrosion layers) is sometimes measured too[12].

[10] INCA Microanalysis Suite - Issue 16. Oxford Instruments INCA 4.06.

[11] INCA can automatically measure the bulk composition for the viewed area, but the author was initially unaware of this function. For this reason, the frame of analysis was selected manually during examination of the Pi-Ramesse material. This resulted in the analysis of areas of 75-80% of the field of view, the maximum frame size for which INCA software allows manual analysis. For the remaining two assemblages, the full frame was analysed.

[12] At the start of this study, bulk compositions of the bloated transition zone between ceramic and slag were measured. These are interesting for showing intermediate changes, but are omitted here as they do not contribute much in the interpretation stage: the real information (relevant to questions asked here) lies in the comparison of ceramic to slag composition.

(a) Crucible sample

(b) Mounted crucible sample

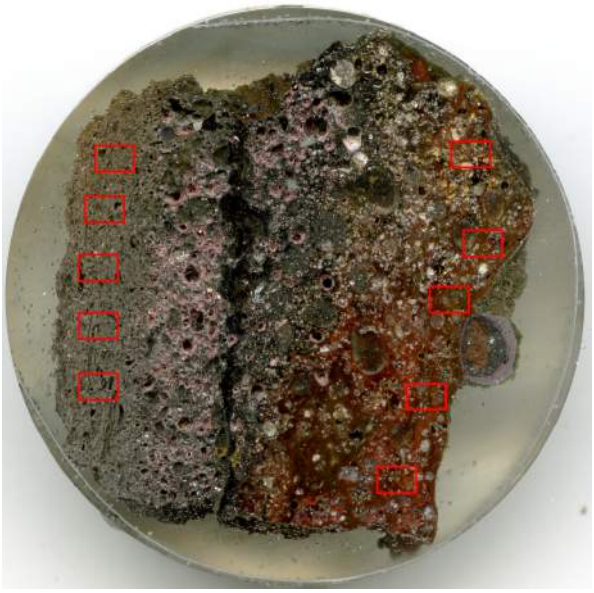

(c) Areas of chemical analysis

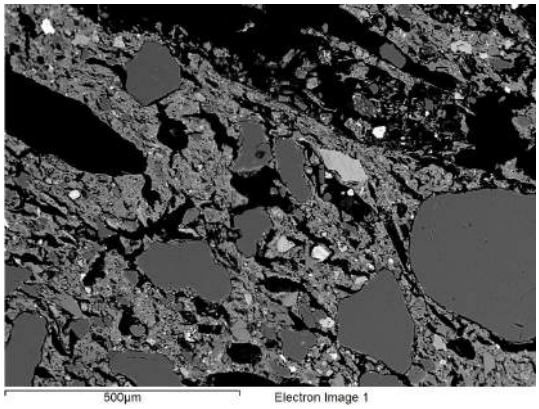

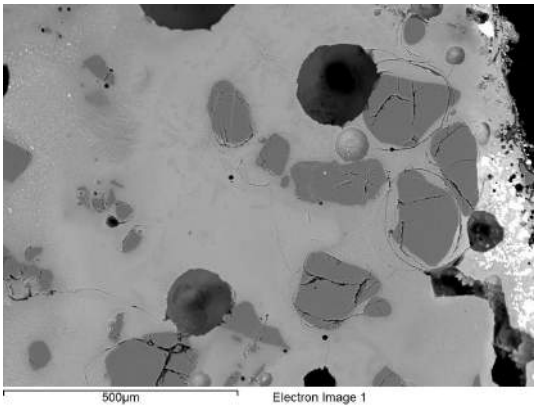

(d) Example of differences between ceramic and slag

Figure 3.4: An example of the applied SEM-EDS methodology

- For each frame of analysis, a number of set elements[13] are measured for their abundance. For each measurement, the spectrum is checked to see if any other elements are present, in which case they are incorporated into the analysis. Sometimes, the INCA software suggests the presence of elements that are absent or, inversely, neglects to suggest elements that are actually present. It is up to the operator to inspect spectra and decide whether or not to include a certain element in the analysis. Some further discussion on the use of a set list is given in section 3.3.6.

- The element abundances are then processed by stoichiometry, combining them with oxygen. This means that the actual measured oxygen is ignored and oxygen is added to the other measured elements according to their stoichiometry (e.g., Ca as CaO and Si as SiO_2). The oxidation state for each element is fixed by the INCA software (e.g., FeO and not Fe_2O_3), without regard for the actual oxidation state that each element is in[14]. This should be kept in mind during further analysis of the results.

- The bulk chemical compositions for each part (ceramic and slag) are calculated by averaging the measurements[15] and calculating a standard deviation[16] for each element (as oxide).

- Alumina is rarely a significant part of the crucible charge, and by looking at the changing ratios of oxides to Al_2O_3, the relative enrichment of these oxides in the slag (with respect to the ceramic) can be judged. This normalisation removes possible distorting effects from the inclusion of quartz grains and base metal(oxide)s (Cu, Sn and Pb), which vary greatly throughout crucibles and can distort absolute changes of other oxides between ceramic and slag. The (relative) change in ratio (in %) is calculated for each oxide as $\Delta^{oxide/Al_2O_3} = \frac{oxide_{slag}/Al_2O_{3slag} - oxide_{ceramic}/Al_2O_{3ceramic}}{oxide_{ceramic}/Al_2O_{3ceramic}}$.

The procedure outlined here is comparable to that used by Freestone and Tite (1986), who

[13] Set list of elements (as oxides) checked: Na_2O, MgO, Al_2O_3, SiO_2, P_2O_5, K_2O, CaO, TiO_2, MnO, FeO, CuO, As_2O_3 and SnO_2

[14] To get a better idea of the oxidation state of elements in a particular phase, the analysis of this phase is processed using the 'all elements' rather than 'elements by stoichiometry' option in INCA. However, the measurement of oxygen (Z=8) by EDS is not very precise and treated accordingly.

[15] The average here is an unweighed mean of the results, calculated as $\bar{x} = \frac{\sum x}{n}$, where x is one value out of the n values for a particular element and n is the number of values, corresponding to the number of frames analysed (typically five).

[16] To calculate the standard deviation, the function 'STDEV.S' in Microsoft Excel is used, which uses the following formula: $\sigma = \sqrt{\frac{\sum(x-\bar{x})^2}{(n-1)}}$, where x is one value out of the n values, $\bar{x}$ is the mean of the n values (i.e., the average) and n is the number of values, corresponding to the number of frames analysed.

similarly use a set list of elements, though no distinction is made here between 'bulk' and 'matrix' (omitting coarse grains) analysis. Here, five bulk measurements are averaged rather than only one to three. Other publications of metallurgical crucible analysis typically do not provide such detailed information on their analytical procedure, impeding any comparison. While SEM-EDS analysis does not offer the highest attainable accuracy and precision for bulk analysis, for which other methods (such as XRF, NAA) are often preferred, it is quite appropriate here. It avoids the often problematic physical separation of crucible ceramic and slag samples, and reduces the amount of sample needed as essential micro-textural information is obtained from the same mounted section. As discussed in more detail in section 13.3, it offers an adequate measurement of bulk composition for crucible studies.

The methodology described so far only concerns bulk chemical change occurring within the different parts in a sample. It is often very informative, however, to use the SEM-EDS to investigate different phases in the sample at a very high magnification to allow better understanding of their structure and chemical composition. This does not follow a set method, but rather is driven by the previous study by optical microscopy and what is discovered during the analysis described above. A good example is the study of metal prills: the composition of a single prill and (if present) the different phases within a prill can be measured, taking into account all elements (i.e., not processing oxygen by stoichiometry). Another example is the investigation of different oxide phases crystallised from the slag. This clarifies the distribution of the different elements measured during bulk analysis. Structural features like the presence of charcoal remains can equally be investigated. This stage cannot follow a set method, but rather is dictated by each sample's particular features and the specific research questions.

3.3.5 Note on detection limits

A number of certified reference materials (CRM's) have been analysed by SEM-EDS. These reference materials are selected to approximate as closely as possible the materials under study (i.e., ceramic, crucible slag and metal) and assess the accuracy and precision of the machine in measuring their composition. The results of this analysis are presented and discussed in full detail in Appendix A and only briefly summarised here.

The detection limit (i.e., the minimal concentration[17] for which an element or oxide can be accurately measured) for SEM-EDS analysis using the JEOL 8600 Superprobe is approximately 0.5 wt%, with the exception of a few elements/oxides which have detection limits

[17] Actually mass fractions are used here, expressed in wt%.

of ±1 wt%.
The measurement precision is generally high (coefficient of variation below 10%), though sometimes lower for elements/oxides present at low levels and for light elements/oxides. The accuracy is similarly good, typically showing a relative error of less than 10% when compared to certified reference values.
The presence of lead in metal can be problematic due to polishing effects, leading to poor precision and accuracy (consistent underestimation of ±30%) in its measurement and a lowered accuracy of the measurement of other alloy constituents, such as tin. In glass (and ceramic, not measured), PbO has a detection limit of ±1 wt%, due to lead's high-energy characteristic spectrum (Lα_1=10.551 keV and Lβ_1=12.619 keV).
No standards were available to assess precision and accuracy for measurements of silver, cobalt and bismuth, which are encountered in some crucibles. It is assumed that similar values apply for these elements.

For the measurement of SnO_2, it should be noted that standard SEM-EDS calibration provides wrong results: approximately SnO_3-Sn_3O_7. This problem is most likely due to an overlap between M-lines for tin and oxygen, and similarly affects the measurement of other tin-bearing oxides. A cassiterite-based standard has been developed to confirm the composition of such oxides.

3.3.6 Using a set list of elements in SEM-EDS

As mentioned above, a set list of elements is measured for each analysed area. Any other elements that show up are added into the analysis where appropriate.

The use of a set list has as a consequence that sometimes elements are measured that are not present. The software, however, still provides a result, often differing from zero and sometimes negative concentrations are reported, which obviously is not realistic. This results from the INCA software procedure to account for all elements checked by the user.

By performing multiple measurements for the same part of a sample (see section 3.3.4), the results can be averaged to get a better idea of the composition of this part. In doing so, a better estimate is achieved for elements that are not present, as any random variation introduced by the software is damped. For this reason, negative results are not initially zeroed by default, but rather taken along in the calculations, to get a more realistic estimate (with standard error) of the elements (not) present.

A side note should be made here: when processing elements by stoichiometry, the INCA software invariably sets Cl-oxide to zero. The reason for this is unknown, but it is an in-

herent and recurring problem. There appears to be a constant chlorine background of 0.1-0.2 wt% (measured as 'all elements') which can be attributed to epoxy resin (noted by Freestone and Tite, 1986). The omission of chlorine in the bulk chemical measurements is therefore not an issue as long as this background level is not exceeded. Where this is the case, a note is made.

Section 3.4

Lead isotope analysis

As mentioned in the introduction, lead isotope analysis is only performed for the Pi-Ramesse assemblage. This section briefly discusses the principles behind the technique, its application in archaeological science and specific use within this project.

3.4.1 The technique

Lead has four stable isotopes: ^{204}Pb, ^{206}Pb, ^{207}Pb and ^{208}Pb. The last three are the end members of radioactive decay series (uranium and thorium series), though each one equally occurs as primordial isotope. This means that, when the earth was formed, the ratios of ^{204}Pb to primordial ^{206}Pb, ^{207}Pb and ^{208}Pb within the earth's mantle were fixed. However, fresh ^{206}Pb, ^{207}Pb and ^{208}Pb has continued to form over time through radioactive decay, while ^{204}Pb has remained constant at its primordial level. This has caused the ratio of ^{204}Pb to ^{206}Pb, ^{207}Pb and ^{208}Pb in the earth's mantle to change through time accordingly (Stacey and Kramers, 1975; Vollmer, 1977).

When an ore body mineralises at a certain point in geological time, its lead content has an isotopic composition that reflects the lead isotope ratios as present in the earth's mantle at that time. While lead's isotopic composition within the mantle continues to change thereafter, it is 'frozen' in the mineralised ore body (Pernicka, 2014). As such, the ore body's lead isotope composition can be used as a time indicator for its formation in geological history. This is of course a crude simplification of reality, where lead isotope ratios within the earth's mantle present a far more complex issue (Cumming and Richards, 1975; Elliott *et al.*, 1999; Kramers and Tolstikhin, 1997) and the further geological history of ore deposits, involving for example hydrothermal and metamorphic processes, as well as the presence of U and/or Th, can alter lead isotope compositions after primary ore formation. Usually, then, an ore deposit encompasses a range of lead isotope compositions throughout its expanse, reflecting its formation history.

The technique used in archaeology is based on the premise that when copper ore formations are deposited, varying amounts of lead are chemically incorporated into the ore. This appears to be the case for most copper ore bodies encountered on earth. When smelting these ores, some of this lead partitions into the copper metal, without any noticeable fractionation[18] (Budd *et al.*, 1995a,c; Cui and Wu, 2011; Stos-Gale and Gale, 2009). Therefore, the isotopic composition of lead present in raw copper metal relates to the formation history of the copper ore from which it was smelted. When the lead isotope composition of archaeologically retrieved copper is determined, it can be compared to that of known ore bodies which have been exploited in ancient times, as discussed further in section 3.4.2.

A variety of techniques exist by which these isotopes can be measured, the most popular of which have been TIMS[19] and currently MC-ICP-MS[20] (see, e.g., Becker, 2002; Clayton *et al.*, 2002; Niederschlag *et al.*, 2003 and Pollard *et al.*, 2007). Both methods provide high accuracy (±0.1% or better) and precision which is needed for metal provenancing, while the accuracy of ICP-QMS[21] is too low and LA-ICP-MS[22] does not agree well with other methods when analysing low-lead (<100 ppm) samples (Stos-Gale and Gale, 2009).

3.4.2 Goals and objectives

The initial application of lead isotope analysis to archaeology has been to relate lead (Brill and Wampler, 1967) and copper (Gale and Stos-Gale, 1982) artefacts to the ore sources from which they were smelted. Following a period of great enthusiasm in the 1970's and 80's, particularly for its application to the study of Mediterranean Bronze Age metal trade (e.g., Gale, 1991; Muhly, 1977 and Stos-Gale *et al.*, 1997), methodological issues were raised and heavily discussed during the 90's. The literature generated by this debate is obscured by its scale and spread over a wide range of journals, rendering any overview here necessarily incomplete. The main (though not only) contributors to the debate are Budd *et al.* (1993, 1995b); Gale and Stos-Gale (1995); Hall (1995); Knapp (2000); Leese (1992); Muhly (1995); Pernicka (1995); Reedy and Reedy (1992); Rohl and Needham (1998); Sayre *et al.* (1992) and Tite (1996). A first major issue (mentioned in section 3.4.1) is the definition of lead isotope fields for ore bodies. Not only are sample numbers often insufficient to fully characterise internal variability of the isotope compositions within an ore body, but

[18] Isotope fractionation: change in isotope content between an original mixture (the ore) and the fractions that are separated from it (metal and slag).

[19] TIMS: Thermal Ionisation Mass Spectrometry.

[20] MC-ICP-MS: Multiple Collector - Inductively Coupled Plasma - Mass Spectrometry.

[21] ICP-QMS: Inductively Coupled Plasma - Quadrupole Mass Spectrometry.

[22] LA-ICP-MS: Laser Ablation - Inductively Coupled Plasma - Mass Spectrometry.

strong overlap can exist between different deposits (e.g., Timna and Feinan (Hauptmann, 2007)). A second point of contention is the possible distorting effect of mixing and recycling of copper objects: when two (or more) copper objects are mixed, their lead isotope composition becomes an intermediate product of their respective lead isotope compositions, depending on both their absolute lead contents and difference between isotope compositions. Especially for later historical periods, when more metal was (presumably) in circulation, mixing probably becomes a significant problem to the application of lead isotope studies as defined above.
The lead contribution from tin used for bronze alloying is often disregarded, but this is probably[23] a safe omission given the low natural lead content in cassiterite, the main tin ore (Begemann *et al.*, 1999; Galili *et al.*, 2013). When lead is added to produce leaded bronze, its isotope composition completely overshadows the much smaller contribution from lead in the copper.

Following some very fierce and sometimes personal discussions, the controversy has somewhat subsided into the background, without any real consensus having been achieved and applications often remaining controversial (see, e.g., Bray and Pollard, 2012; Gale, 2009 and Pollard, 2009, 2011). Nevertheless, careful use of the method continues steadily and the 'exclusion method', whereby potential ore sources are rejected based on their isotopic composition, appears a generally accepted application. While straightforward assignment of a copper object to a particular ore source should be avoided, the use of trace element chemistry can provide some further confidence in narrowing down the possible candidates[24] (Cooper *et al.*, 2008; Ling *et al.*, 2013, 2014; Pernicka, 1999; Rehren and Pernicka, 2008).

Finally, the way by which the actual isotope data should be analysed is still under discussion. For example, the traditional display of data using bivariate plots and point-by point comparison, using Euclidian distance, for the assignment of metals to ore sources, advocated by Stos-Gale and Gale (2010) and used by many others (see Stos-Gale and Gale, 2009), were recently contested by Albarède *et al.* (2012).

The primary aim of lead isotope analysis within this project, then, is not strictly to define potential ore sources for copper used in Pi-Ramesse. Rather, the identification of variation within copper sources used in the bronze workshops is a first aim in itself (see Chapter

[23] Convincing experimental evidence to confirm this assumption is, however, lacking.

[24] Stos-Gale and Gale (2009) note that most of this is a matter of semantics: following the exclusion of many sources based on comparison of their lead isotope compositions, trace element chemistry and historical information, only one potential source usually remains. One can then fairly say that *given the present state of knowledge* a copper object was smelted from that particular ore source.

1 and section 4.6). To this end, the lead isotope composition of prills embedded in the crucible slag, as well as metal artefacts from the workshop context, is analysed by MC-ICP-MS. These results are then compared to conclusions obtained from chemical analysis of the crucible slag, which provides further information on the use of particular copper sources through its bulk composition and that of metal prills embedded in it.
In addition to this, the lead isotope composition of actual crucible slag (without visible or 'extractable' prills) of selected crucibles is analysed and compared to the lead isotope composition of the crucible ceramic. This is a methodological exercise (similar to Lehner *et al.*, 2009) to determine the contribution of lead from the metal charge to the crucible slag and appraise the possible application of this method to reconstruct the lead isotope composition of the metal charge when no actual metal prills are present.

3.4.3 Sample selection and analytical methodology

The application of this method is limited to samples from Pi-Ramesse, where material and context are most suitable.

Three datasets are selected for lead isotope analysis. Firstly, small pieces of metal artefacts from the workshop contexts are analysed. All of these are additionally analysed by XRF[25] and some by NAA[26] to obtain their chemical composition. Secondly, metal prills are extracted from the crucible slag for lead isotope analysis. Finally, samples of both crucible ceramic and slag are analysed for their isotopic composition.

The selection of samples is dictated by the results from microscopy and SEM-EDS, as well as the spatial distribution of finds within the site. The aim is to select samples representative of different production contexts and from crucibles that indicate differing technology and material use (see section 5.5).

These samples are sent off to an external laboratory for MC-ICP-MS analysis following the protocol detailed by Niederschlag *et al.* (2003), which is not discussed further here. More general discussion on the use of lead isotope data for crucible analysis within this thesis is not concerned with the analytical procedure of obtaining these lead isotope data, but rather their interpretation towards understanding crucible metallurgy. This is in contrast to the other methods described in this chapter, for which both the practical aspects of data acquisition and their interpretation are discussed.

[25] XRF: X-Ray Fluorescence. This is performed by the same external lab performing the lead isotope analysis.

[26] NAA: Neutron Activation Analysis. Again by the same external lab performing the lead isotope analysis.

Section 3.5

Handheld X-ray fluorescence spectrometry

Handheld or portable X-ray fluorescence (pXRF) analysis is performed for the Pi-Ramesse assemblage, with the aims of testing the applicability of this technique for fast chemical characterisation of a complete crucible assemblage. The same procedure could not be repeated for the other two assemblages, as only a limited selection of those crucibles was available for study. This section briefly discusses the principles behind the technique, its application in archaeological science and specific use within this project.

3.5.1 X-ray fluorescence

The principles behind X-ray fluorescence are very similar to those explained for SEM-EDS (section 3.3.1). Rather than using an electron beam, the sample is exposed to X-rays[27] of a particular energy and wavelength. These primary X-rays hit the sample's atoms, creating inner shell vacancies (K-, L-, M-shells) to which electrons from outer shells fall back, producing secondary X-rays. These characteristic (secondary) X-rays can then be measured using energy- or wavelength-dispersive methods. Typical escape depths of a few micron (light elements) to several hundred microns (heavier elements) for fluorescent photons make this a surface-analysis technique (Pollard *et al.*, 2007).

Apart from the generation of secondary X-rays, the primary X-rays equally give rise to scattering (elastic, Rayleigh and inelastic, Compton scattering) and absorption processes, as well as Auger electron emission and the occurrence of sum and escape peaks in the spectrum. Scattered X-rays[28] produce peaks in the measured spectrum related to the primary X-ray source, rather than the sample under analysis, and need to be treated accordingly when converting spectra into quantitative compositional data for the sample. *Bremsstrahlung* occurs due to deceleration of electrons hitting the anode of the X-ray tube and, more importantly, due to primary X-rays decelerating within the matrix of the sample itself which produces non-characteristic secondary xrays, together creating background 'noise' in the spectrum (Shackley, 2011).

Matrix effects, caused by the absorption of X-rays and the generation of secondary fluorescence[29] are typically corrected for by either internal machine calibrations or software

[27] X-rays are generated using either an X-ray tube, a radioactive source or synchrotron radiation.

[28] Scattered X-rays do not occur for SEM-EDS, as there are no incident X-rays.

[29] When high-energy characteristic (secondary) X-rays of one element interact with another (lighter) element before escaping from the sample, this second element may be excited and generate characteristic

packages used for analysis of the raw data.

pXRF provides a portable alternative to the commonly laboratory-based application of XRF-analysis. The production of such compact devices necessarily results in analytical compromises relative to laboratory-based XRF-machines. These are overly complex to address in any detail here, but important to mention as they have sparked substantial debate in the archaeological literature. However, it is not so much the limitations of the analytical device itself that fuel the controversy,[30] but the way in which it can be used. The user-friendly nature of pXRF could lead to overconfidence (or overindulgence?) in its application and the seemingly simple output[31] belies very complex sample-beam interaction, measurement and calibration. Keeping all technical limitations of this surface-analysis technique in mind, however, the thoughtful use of pXRF in archaeology opens new methodological horizons, such as geochemical surveying (Derham *et al.*, 2013; Dungworth *et al.*, 2013), (*in situ*) stratigraphy characterisation (Davis *et al.*, 2012; Gauss *et al.*, 2013), rapid obsidian-sourcing in the field (Frahm *et al.*, 2014) or the non-invasive analysis of architectural glass (Dungworth, 2012a) and other objects that cannot be removed from sites or museums (Charalambous *et al.*, 2014). Frahm and Doonan (2013) present an overview of the application of pXRF in archaeology, while a good example of ongoing controversy is given by Frahm (2013a,b) and Speakman and Shackley (2013).

3.5.2 Goals and objectives

For this research project, pXRF is not used as a tool for quantitative chemical analysis. Rather, it is applied as a fast, on-site technique to qualitatively assess the presence and approximate abundance of certain elements in the (surface of) crucible slag.
Low acquisition times allow the analysis of an entire assemblage, which for practical reasons is not possible for microscopic and SEM-EDS analysis. Furthermore, multiple measurements at different areas within the same crucible fragment (further apart than the area covered by a polished sample) can be taken and compared.

The aim here is to look for broad (qualitative) trends obtained from the analysis of the entire Pi-Ramesse assemblage. This can then be related to results of the more detailed

X-rays. This results in an apparent absorption effect for the heavier element and a false enhancement for the lighter element (Shugar, 2009).

[30] Every analytical method has limitations, and any data generated using those methods is subject to interpretation within those limits.

[31] Many pXRF devices, originally conceived for quickly sorting through scrap or roughly assessing ore grade in a mining face, show only the calculated abundance of (selected) elements, with little opportunity (or encouragement) to manually inspect the actual spectra.

chemical analysis of polished samples. From this comparison, a discussion is held on the application of pXRF to the analysis of metallurgical crucible assemblages, which has hitherto not been addressed in the literature (though examples of the analysis of ceramics (Aimers *et al.*, 2012; Behrendt *et al.*, 2012; Forster *et al.*, 2011; Hunt and Speakman, 2014; Papadopoulou *et al.*, 2006) and primary production slag (Ben-Yosef and Levy, 2014; Eekelers *et al.*, 2014) already exist).

3.5.3 Sample preparation and methodology

±60% of the Pi-Ramesse assemblage (rather than the intended full assemblage, see section 5.3.1) is analysed in Qantir, Egypt, using an Innov-X Systems handheld XRF[32]. 3 measurements per sample are performed, with the following basic settings:

- Single Beam, suppress LE (MC=3, nS=2)
- Test time = 15s
- 40 kV

Though the device provides both spectral and elemental data output, only spectral data has been used in this analysis[33]. Spectral data output covers the 40 kV spectrum using 2048 intervals (i.e., 19.53V each). For each interval, or 'channel', the output presents the averaged intensity (in counts/second) at the centre of that interval. Results (section 5.3.2) are given as 'intensity', which corresponds to counts/second for a particular energy-level. Each different chemical element, when present and excited by the incident beam, produces X-rays with particular energy-levels (in keV):

- *Ca*: Kα_1 = 3.692 & Kβ_1 = 4.013
- *Ti*: Kα_1 = 4.512 & Kβ_1 = 4.932
- *Fe*: Kα_1 = 6.405 & Kβ_1 = 7.058
- *Co*: Kα_1 = 6.931 & Kβ_1 = 7.649
- *Cu*: Kα_1 = 8.046 & Kβ_1 = 8.905

[32] Delta Family XRF Handheld Analysers. Type: Premium. Model: DP 4000. Serial no.: 510240

[33] This spectral data represents the actual raw data generated by the instrument, while elemental data is the result of spectral interpretation using internal machine standards.

- *Pb*: Lα_1 = 10.551 & Lβ_1 = 12.619
- *As*: Kα_1 = 10.544 & Kβ_1 = 11.727
- *Sr*: Kα_1 = 14.165 & Kβ_1 = 15.836
- *Sn*: Kα_1 = 25.271 & Kβ_1 = 28.491

The intensity of the measured signal at these specific energy levels is calculated by interpolating between the two closest surrounding interval centres.

Analysis is performed directly on the clean surface of the crucible and no sample preparation is needed. Further details on sampling are discussed in section 5.3.1.

Part III

Qantir – Pi-Ramesse

Polish comes from the cities; wisdom from the desert.

Herbert, 1965

CHAPTER 4

Archaeological background

This chapter provides a background of both the archaeological context in Pi-Ramesse which included the bronze production remains and the wider historical and archaeological background against which these activities should be situated.
Section 4.1 presents a brief introduction to the site and its excavation. Section 4.2 offers an overview of the different production processes evidenced at Pi-Ramesse, while section 4.3 zooms in on the metallurgical context. Section 4.4 discusses the nature of such metallurgical workshop contexts. In section 4.5, the broad-scale organisation of ancient Egyptian metallurgy is discussed, setting out the interpretative framework for this case study and its particular research questions, outlined in section 4.6.

Section 4.1

Introduction

Ancient Pi-Ramesse is located largely underneath modern Qantir, in the eastern Nile Delta of Egypt (Figure 4.1). It lay on the (now silted up) Pelusiac branch of the Nile and was established as the capital under Pharaoh Ramses II (although there appears to have been continued habitation around Pi-Ramesse from the late Twelfth Dynasty onwards, initially centred around Avaris, and from the late Eighteenth Dynasty at Qantir (Bietak and Forstner-Müller, 2011). Under his reign, the city flourished as a Late Bronze Age trade centre, from where Ramses expanded his influence as one of the select rulers engaged in diplomatic exchange in the eastern Mediterranean (Van De Mieroop, 2007). During this period, Egypt

Figure 4.1: Location of Pi-Ramesse (Google Earth 7.1.2, 2013)

was at its largest territorial extent in history and actively involved in a complex and changing economic system (e.g., Bevan, 2010 and Sherratt, 1998, 2003) with associated politics and warfare in the Near East (e.g. the Battle of Qadesh), exposing it to an expanding cultural diversity. This highlights the importance of Pi-Ramesse as a strategic location, which served as the military basis for the pharaoh's chariot garrison. It is beyond the scope of this research to fully discuss the history and politics of Ramesside Egypt, but the international nature of Pi-Ramesse needs pointing out, as does its scale as an urban development project under Ramses the Great.

Pierre Montet discovered many of Pi-Ramesse's monuments at Tanis in the 1930s and the first excavations at Qantir took place already in 1929 (Hamza, 1930). However, it was only in the 1960s that its true location was discovered by Dr. Manfred Bietak, who mapped all branches of the ancient Nile Delta and firmly linked Qantir to Pi-Ramesse. Since the 1970s, the area has been investigated by the Austrian Archaeological Institute at Cairo, under direction of Dr. Bietak (Bietak, 1981). From 1980 onwards, this team has focused on the remains of ancient Avaris (modern Tell el-Dab'a), while Qantir was excavated by the Roemer-Pelizaeus Museum in Germany, led by Dr. Edgar B. Pusch (see Pusch, 1991 (early years), 1993 and Pusch and Herold, 1999).

A number of areas have since been excavated, the main ones labelled QI-QVII (Figure 4.2). Pi-Ramesse occupied islands in the Nile, which was vital to its harbour existence (Hodgkinson, 2007). An overview of the stratigraphy and dating is given in Table 4.1. Clearly, only a tiny fraction of the original city has been excavated, though all but the central area (believed to have held the pharaoh's palace, now underneath Qantir) has been mapped using magnetic and resistivity surveys (Abdallatif *et al.*, 2003; Forstner-Müller,

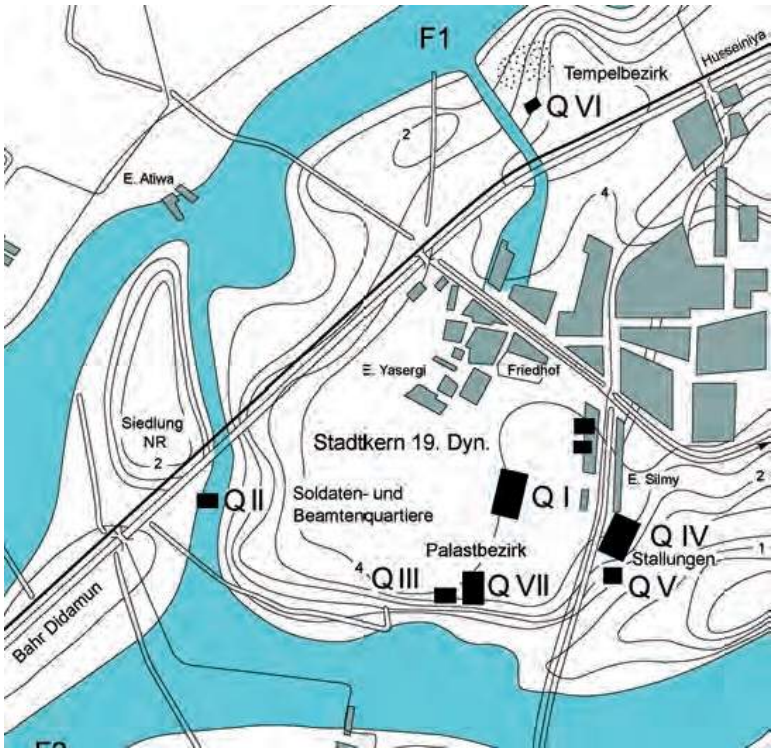

Figure 4.2: Excavated areas of Pi-Ramesse, showing (blue) ancient Nile (from Pusch and Rehren, 2007, Map 05, p. 53)

2009; Forstner-Müller *et al.*, 2009; Forstner-Müller and Müller, 2007; Pusch, 1998/99, 1999b; Pusch *et al.*, 1999). An artist's reconstruction of the city is given by Bietak (1996), Figure 2, p. 4.

Section 4.2

High-temperature processes in Pi-Ramesse

A number of high-temperature production processes, all of them centred around the use of copper, were carried out at Pi-Ramesse. All of these took place in the area surrounding sites QI, QIV and QV, which should probably be seen as one large high-temperature production centre. The degree to which these different processes depended on each other or interaction existed is unclear at this point. However, it seems likely that some resources, like copper, and knowledge would have been shared here, given their spatial and stratigraphic proximity.

The high-temperature process which has been most extensively studied so far (Rehren, 1997b; Rehren and Pusch, 1997, 1999, 2005; Rehren *et al.*, 1998, 2001), is the production

QI		QIV		QV		
Building level	Function	Building level	Function	Building level	Function	Dating
-	-	Aa'	Channel	-	-	Persian period
A/1	Disturbed	Aa	Squatter	-	-	Post 3^{rd} Intermediate Period
A/2	Cemetery	Ab	Cemetery	-	-	1^{st} millennium BC
		Ac	Burial	-	Disturbed?	$22^{nd}/21^{st}$ Dynasty
B/1	Demolition of previous layer	Ba	Living area	B/0	Fillings/pits/ disturbed	$21^{st}/20^{th}$ Dynasty
B/2a	Training court/ Multifunc. workshops	Bb	Horse stable	B/1	"Foreign Office"	$20^{th}/19^{th}$ Dynasty
B/2b	Training court/ Multifunc. workshops	Bc	Precursor to stable	B/2	Precursor to "Foreign Office"	19^{th} Dynasty
B/3a	Industrial bronze installations (N-S orientation)/ Multifunc. workshops	Bc/d	Glass industry	B/3	Glass industry	
B/3b	Industrial bronze installations (W-E orientation)/ Multifunc. workshops	Bd/e	Workshop			
C	? (contaminated sand)	Be/f	Residential buildings	-	-	$19^{th}/18^{th}$ Dynasty
D/1	Settlement area/pits	Bf/g	Settlement area/pits	-	-	18^{th} Dynasty

Table 4.1: Suggested correlation of strata and related dates at sites QI, QIV and QV (translated from Pusch and Rehren, 2007, Table 19, p. 130)

of glass, definitely published by Pusch and Rehren (2007). Production concerns almost exclusively copper-red glass, with some rare examples of Co-blue glass. Activities were mainly confined to area QIV and QV, though some remains occur at QI. The Hamza excavations (location shown in Figure 4.3) revealed additional production remains, though lacking contextual data, as well as a complete red glass ingot (now at the Museum of Egyptian Antiquities, Cairo).

Substantive evidence for the production of faience was first unearthed by Hamza (1930). An overview of faience moulds (mostly for small objects) from Pi-Ramesse is given by Hermann (1957), including a catalogue with drawings and some pictures. The production of architectural elements is discussed by Hayes (1937). More recent excavations furnished additional production remains, hitherto unpublished.

Excavation area QIV provided evidence for the production of Egyptian Blue, though this has not been thoroughly studied yet. Further material from Hamza (1930) again lacks contextual data.

Finally, there is evidence for the production of bronze (Prell, 2011; Pusch, 1990, 1994, 2000; Rehren and Pusch, 2012). The evidence for this production derives mainly from area QI (and QIV, to a lesser extent), which therefore receives more attention in the following section.

A note can be made here on the distinction between primary production (glass and Egyptian Blue) and secondary production (bronze) at Pi-Ramesse. Glass ingots for export were produced at Pi-Ramesse, while secondary glass workshops (where final objects were made, like at Malkata and Lisht (Mass *et al.*, 2002)) are absent or hitherto undiscovered. Bronze, on the other hand, was being recycled and alloyed (see section 5.4) to fabricate objects. Faience is a one-step product where this distinction is not really possible, though the thousands of moulds point to a large-scale production of usable objects.

Finally, Rehren *et al.* (2001) point out that, with copper abundant and central to technological activity in Pi-Ramesse, specialisation there appears to be governed by the virtuosity by which the material was worked under different conditions and in different compositions, rather than its availability. Of interest to this research is to appreciate that virtuosity in its application to bronze production, within a setting of cross-craft interaction.

Section 4.3

Site QI

Site QI is indicated in Figures 4.2 and 4.3. It is located to the south of modern Qantir, and presumably to the south of Ramses II's palace. As outlined in Table 4.1, there are two main phases (B/3 and B/2) of interest to the study of bronze production activity.

Phase B/3 contains industrial-scale facilities related to bronze-casting, shown in Figure 4.4, adjacent to small-scale workshops to the south (separated by a wall). The large installations encompass multiple melting batteries (with changing orientation: strata B/3a-b) and cross-furnaces, as well as many smaller finds related to metallurgical activity, such as tuyères, pot bellows, bronze objects, a piece of copper ingot, scrap metal, moulds for casting and cold working, and, importantly, hundreds to thousands of crucible fragments (Pusch, 1990). A detail of the melting batteries as found *in situ* is shown in Figure 4.5, while Figure 4.6 shows their reconstructed operation involving crucibles for melting bronze. Crucibles were placed inside the melting batteries, covered in charcoal and air was blown into them from above by tuyères powered by pot bellows. A detailed discussion of how these batteries were used is given by Pusch (1994) and further discussed in section 6.3. The function of the cross-furnaces is still not well understood (similar structures occur in Kerma (Bonnet, 1986, 2004)). In the smaller workshops, a number of different materials, including wood, bone, stone and metal, were being worked in a 'souk'-like environment and indications for ephemeral metallurgical activity are present.
Contemporary to these activities in QI, glass production was taking place at site QIV. As indicated earlier, however, some metallurgical activity took place at QIV (separate metal workshop context) and, conversely, some glass production remains were discovered at QI. As mentioned by Rehren *et al.* (1998), soundings have shown that the metallurgical activities must have extended over an area[1] of at least 10000 m^2, implying even more melting batteries in the surrounding area.

Phase B/2 records the closing down of the large scale metallurgical complex and the establishment of a chariot training court in its place, shown in Figure 4.7. This is mirrored by the termination of glass production at site QIV and the construction of horse stables there (Figure 4.3, right), with a capacity for holding hundreds of horses. At site QI, the multifunctional workshops remain in place though, and their expansion may point to an increased importance. A recent overview of these workshops, focusing mostly on stone and cold metal working, is given by Prell (2011).

[1] This probably covered the area bounded by areas QI-QIV and LH/MH (red dashed line in Figure 4.3).

These two phases seem indicative of a changing focus in activities. During the earliest phase, these were probably mostly concerned with the urban development of the new capital, such as the production of architectural features (e.g., faience decoration, bronze doors, statues, etc.), while phase B/2 seems focused on the establishment and maintenance of a chariot army that was stationed at Pi-Ramesse.

A detailed overview, including comparisons to Egyptological sources, of the installations is offered by Pusch (1990, 1994). Rehren *et al.* (1998) give an abbreviated overview.

Section 4.4

The nature of metallurgical workshop contexts

At this point, it is important to elaborate on the nature of the archaeological contexts at site QI and QIV.

To do so, it is necessary to establish what could reasonably be considered primary, secondary or tertiary archaeological contexts in a metallurgical workshop setting. The nature of such environments, with crucibles being very mobile items, makes the attribution of crucibles to particular contexts quite problematic.

Intuitively, a crucible found within a melting battery or furnace would appear to be in primary position. However, taking into consideration the role crucibles play in the *chaîne opératoire* for bronze production, this is not necessarily so. The crucibles would have been lifted from the melting battery after melting the metal inside and taken to another location for casting (possibly the cross furnaces). After casting, it seems unlikely that crucibles were reused (see section 6.3), so they would have been discarded. Whether an allocated depository for used crucibles existed is unclear, but is a distinct possibility, given the highly organised nature of the industrial area. In archaeological terms, such a deposit would be labelled a dump, which is usually not considered primary. From a *chaîne opératoire* point of view, however, it could be considered as such. In some locations, heaps of crucibles were recovered from pits which represent such dump contexts. During the second phase of production (B/2), the industrial area was shut down and levelled for the establishment of a training courtyard. At this point, any large piles of dumped crucibles would have probably been removed or at least moved. Possibly, these crucibles were spread out and mixed in the levelling layer. The majority of crucibles from the QI industrial area were, in fact, retrieved from stratum B/2. However, it is most likely that they were actually used in the preceding phase B/3 and migrated vertically in the archaeological stratigraphy, rather than having been used in the B/2 multifunctional workshops and moving horizontally across a

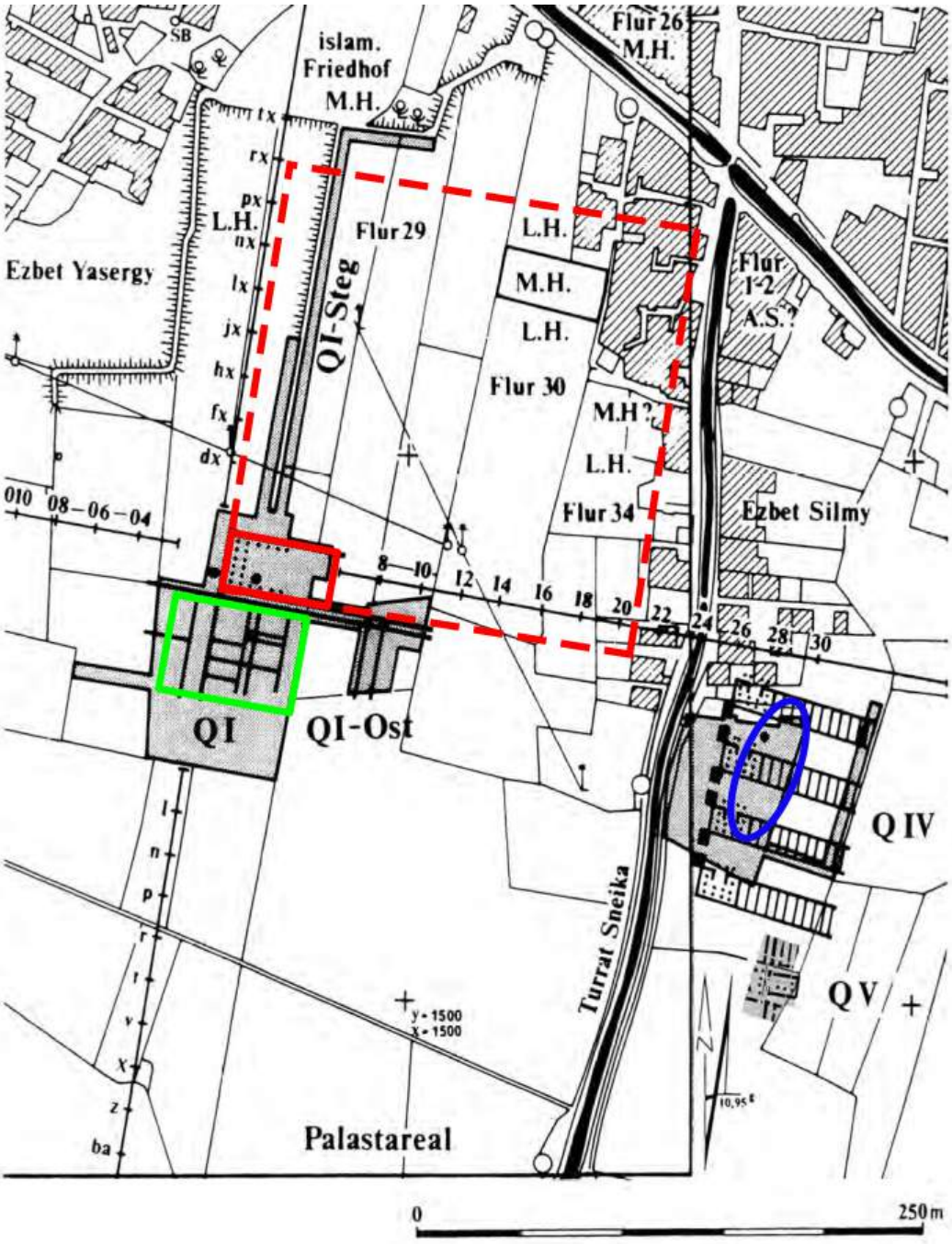

Figure 4.3: Map showing excavation areas QI, QIV and QV; LH and MH refer to excavations by Labib Habachi and Mahmoud Hamza respectively (from Pusch and Rehren, 2007, Map 01, p. 20). The industrial area is indicated in red, the multifunctional workshops in green, and the QIV workshop in blue

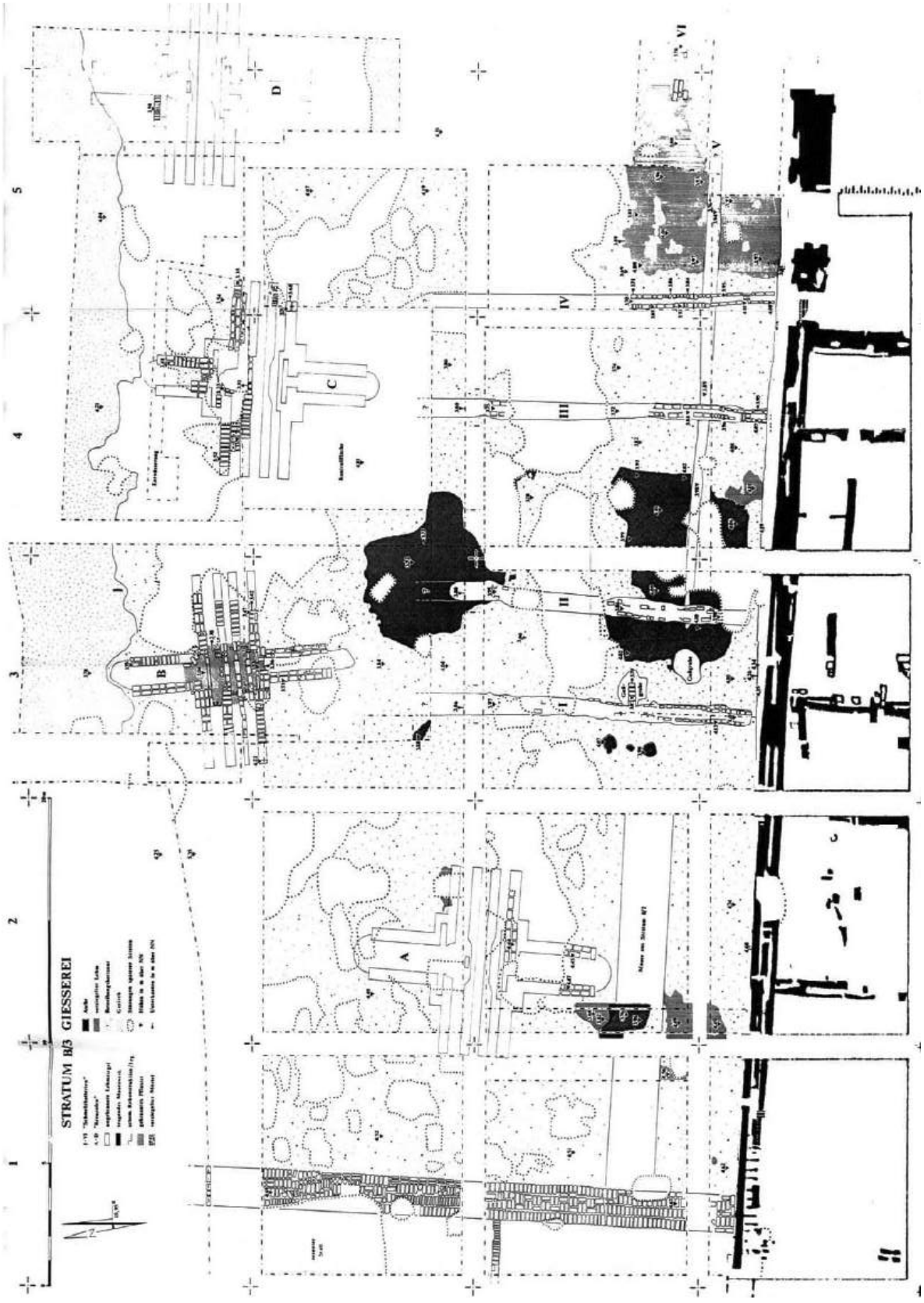

Figure 4.4: Map of industrial area within QI (red square in Figure 4.3)), stratum B/3, showing melting batteries (I-VI) and cross-furnaces (A-D); multifunctional workshops south of wall are not shown (from Pusch, 1990)

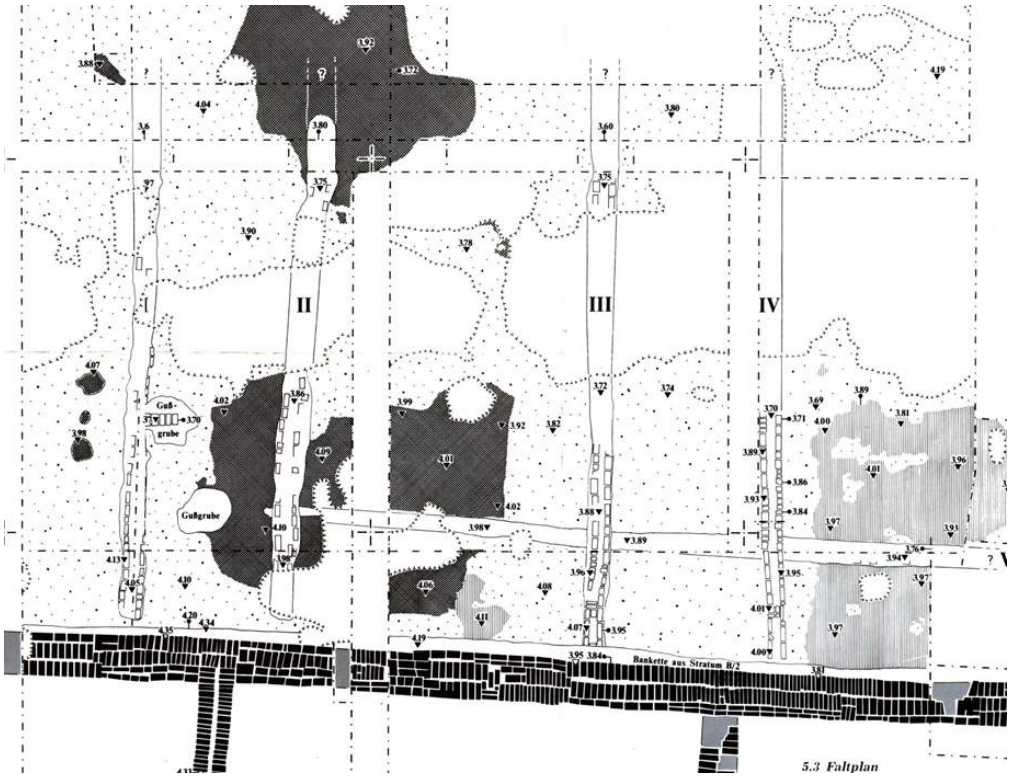

(a) Detail from Figure 4.4

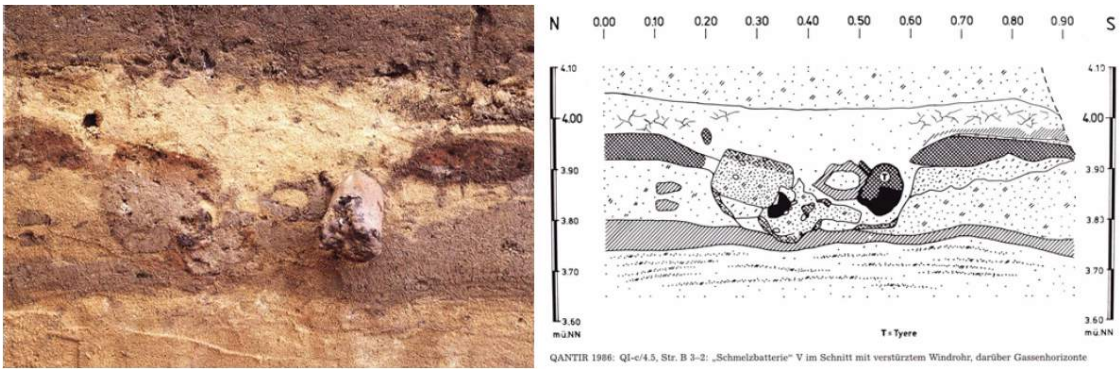

(b) Section of melting batteries with tuyères *in situ* (from Pusch, 1990, Table IV)

Figure 4.5: Detail of melting batteries

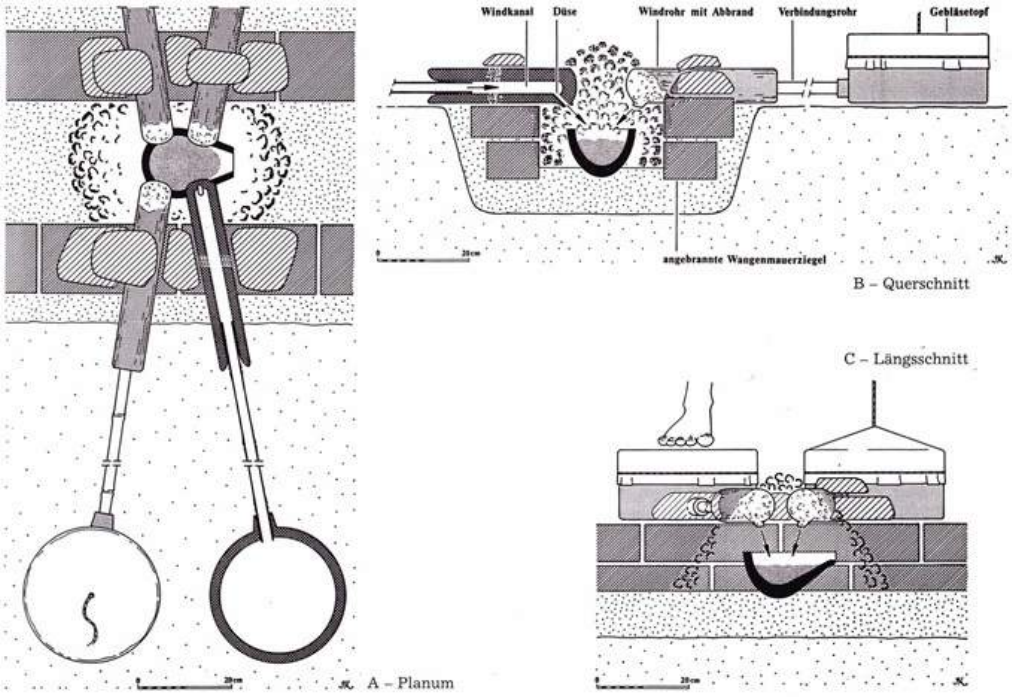

Figure 4.6: Operation of the B/3 melting batteries (from Pusch, 1994, Figure 1, p. 153)

double wall and alleyway to the industrial-area-turned-training-courtyard.
Nonetheless, in discussions of crucible distributions within Chapter 6, this uncertainty in relating crucibles to either the QI-B/3 industrial workshops or later QI-B/2 multifunctional workshops must be kept in mind. Furthermore, glass finds in QI might have moved there from QIV, without necessarily indicating glass production activity in QI, implying some crucibles may have moved between those areas as well. The metallurgical crucibles from QIV, however, are clearly associated to a 'smithy' (non-ferrous) there.
Full disclosure of contextual distributions of all excavated crucibles, including information on the exact deposit types (e.g., workshop floor, pit, levelling debris), will be included in the forthcoming Pi-Ramesse metallurgy volume (FoRa series, cfr. Pusch and Rehren, 2007). A summary for sampled crucibles is presented in Appendix B.

Section 4.5

The organisation of Egyptian metallurgy

Given Egyptian archaeology's dominant focus on architecture, inscriptions and artefacts, archaeometallurgy has hitherto received comparatively little attention (Killick, 2009). Though a pioneering work, Garland and Bannister's (1927) overview is largely outdated and fo-

Figure 4.7: Map of area QI, stratum B/2; multifunctional workshops in areas c-f (green) are separated by a double wall from the open courtyard (B/3 'industrial area' - red) in ax-b (from Prell, 2011, Figure 05, p. 23)

cuses mainly on metal artefacts. Scheel's (1989) summary of archaeological evidence remains concise, reflecting the scarcity of production waste studies in Egyptian archaeology. Lacking other overviews, a framework for studying (the organisation of) ancient Egyptian metallurgy is absent. A brief review of related studies is given here.

Much scholarly attention has been given to Egyptian presence in Timna (e.g., Bachmann, 1980; Ben-Yosef, 2012 and Rothenberg, 1988, 1990, 2003), and the debate on this subject is ongoing (e.g., Avner, 2013). An Egyptian presence in the region, influencing the mining and smelting of copper ore, can be inferred, though the extent of control remains unclear. The actual smelting was probably carried out by local people.

Garson (1977), Said (1990), and Abouzeid and Khalid (2011) present possible Egyptian metal ores from a geological perspective, while Beit-Arieh (1985), Chartier-Raymond *et al.* (1994), Stos-Gale *et al.* (1995), Hikade (1998, 2006, 2007), and Ogden (2000) discuss copper deposits exploited in ancient Egypt and particularly Sinai. Abd El-Rahman *et al.* (2013), Castel *et al.* (1996, 2008), Klemm and Klemm (2013), Rothenberg *et al.* (1998), Shaw (1994, 1998) and Shaw and Durucan (2008) discuss ancient mining and smelting of Eastern Desert copper, tin and gold. At the Middle Kingdom site of Ayn-Soukhna (Abd el Raziq *et al.*, 2011; Tallet, 2012), copper ore, probably from Sinai (Tallet *et al.*, 2011), arrived by ship, was smelted at the harbour and then transported further into Egypt.

Additional metal was traded into Egypt: a Late Bronze Age trade network of copper and tin ingots, seemingly coming from all over the known world (e.g., Budd *et al.*, 1995b; Gale, 2011; Kassianidou, 2003b; Knapp, 2000; Lo Schiavo, 2012; Muhly, 2003; Pulak, 1997; Sherratt, 2000; Stos, 2009 and Yahalom-Mack *et al.*, 2014), existed in which Egypt participated, as evidenced by tomb representations (e.g., Tomb of Rekhmire (Davies, 1935a), see Figure 4.8) and the find of a Cypriot oxhide ingot fragment at Pi-Ramesse (Gale, 1999). These different sources are summarized in Figure 4.9.

All the foregoing is concerned with procurement of raw metal, while its further trade and use within Egypt has received little attention. Though metal objects have attracted some interest (e.g., Cowell, 1986; Farag, 1981; James, 1972; Kallfass and Hörz, 1989; Pelleg *et al.*, 1979; Philip, 2007 and Scheel, 1985, 1986, 1987), research into the intermediate segment of the *chaîne opératoire* (secondary production processes) is lagging behind (noteworthy exceptions are Davey (1985), Eccleston and Kemp (2008), Pusch (1990, 1994), and Scheel (1988)). However, this gap in current knowledge merits filling, as it holds information on technological and material knowledge of ancient people in a variety of socio-cultural contexts. The study of bronze production at Pi-Ramesse aims to address this.

Rehren and Pusch (2012) have proposed a framework for understanding the consumption

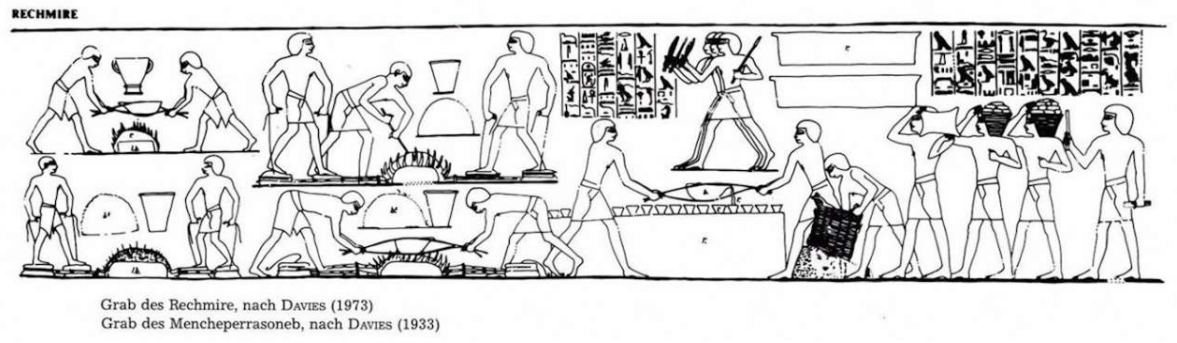

Figure 4.8: Wall decoration in Rekhmire Tomb (Theban Tomb 100), showing import of ingots on the right and crucible metallurgy (possibly similar to Pi-Ramesse) on the left (from Pusch, 1990, Figure 9, p. 94)

of copper in New Kingdom Egypt. They suggest a hierarchical system with three components:

1. *Scrap copper*: Metal accessible to most of the population through recycling, small-scale smelting and trickle-down from state-controlled metal.

2. *Mainstream copper*: State-controlled metal, produced through regular expeditions and projects, under a tightly controlled administration. Operations such as those at Timna should be seen in this context.

3. *Special project copper*: Exceptional projects requiring large amounts of copper on short notice, impossible to provide by regular expeditions, for political strategies (bribing?) or massive projects, such as the construction of a new capital at Pi-Ramesse.

The stratigraphic and contextual variation at Pi-Ramesse allows to test whether a distinction in technology and material use, which can be expected for this system, is discernible on site, though the resolution at which this variation can be discussed is moot (see section 4.4). As proposed by Rehren and Pusch (2012), scrap, mainstream and special project copper could all be expected in the production contexts at Pi-Ramesse. This provides some specific research questions for Pi-Ramesse, outlined in section 4.6.

Broadly speaking then, the study of bronze production at Pi-Ramesse aims to contribute in two main ways: on the one hand, it can clarify the organisation of metallurgical activity in ancient Egypt by considering the wide perspective elaborated here, while on the other hand it can inform on the much smaller workshop scale on the (organisation of) bronze-related activities within the Ramesside capital.

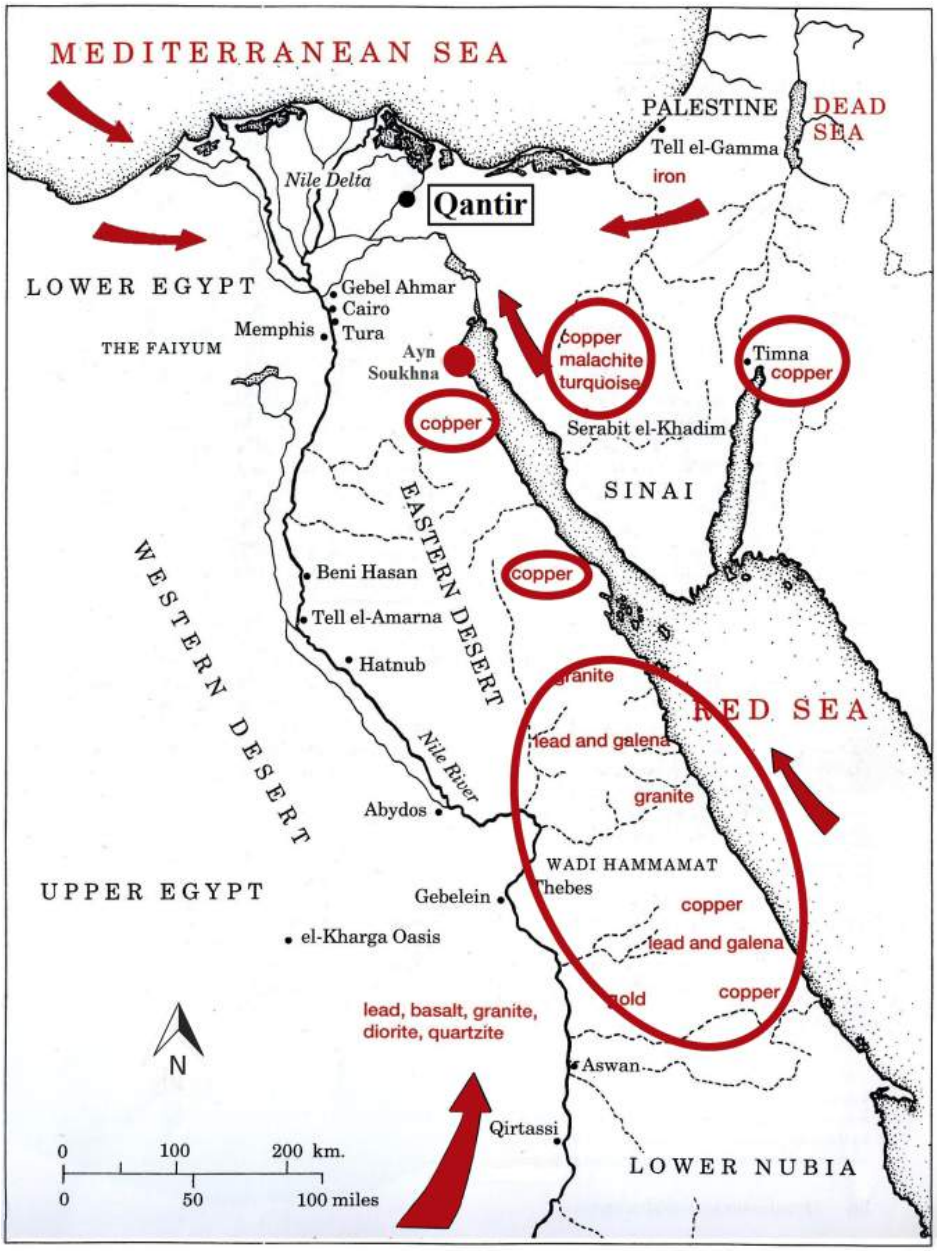

Figure 4.9: Map showing Qantir – Pi-Ramesse and possible sources of metal for ancient Egypt. Circled: 'Egyptian' mining, dot: Ayn-Soukhna, arrows: possible ingot/raw metal import (modified from Wilkinson, 1994)

Section 4.6

Specific questions

Some more detailed questions, flowing from the main research questions, are spelled out here. The aim of these questions is to maximise the use of contextual information to understand bronze metallurgy at Pi-Ramesse, elucidating this less studied segment of Egyptian metallurgical activity: the final productive stages and 'consumer-side' of metal trade.

- What techniques were used for bronze production?
- Is metal from multiple sources coming into Pi-Ramesse?
- How important is recycling?
- Do different production contexts ('industrial' vs. 'souk') show the use of different technologies and/or metal sources?
- Is production technology object specific? Is there, for example, differentiation between production technology for architectural materials (e.g., cast doors, sculptures etc.) and that used for producing military equipment?
- Who had access to particular materials and technologies?
- What are the relations to the glass, faience and Egyptian blue workshops? Are the material supplies and trade networks (for glass, see Jackson, 2005 and Rehren and Pusch, 2005) related[2]? Are there any technical relations (e.g., temperature ranges, fuel use, technical ceramics etc.) between the different production systems?
- How does metallurgical technology in Pi-Ramesse compare to other Egyptian metallurgical activity? How does it compare to contemporary bronze production elsewhere in the region?

To conclude, it is emphasised that through these specific questions, the research offers alternatives to an iconographic tradition of crafts-analysis in Egyptology, refining the understanding of metallurgical activity spatially within its context, as well as its social organisation. It thereby fits into a broader diachronic research of metallurgical practice in Egypt, which lags behind with respect to other eastern Mediterranean countries.

[2]This is focused on the specific materials produced in the Pi-Ramesse workshops. Broader discussions on the interconnected nature of various goods produced and traded throughout the eastern Mediterranean, as presented by Bevan (2010), are limited here.

CHAPTER 5

Analytical results

The excavations at Pi-Ramesse have yielded a total of 1042 collected crucible fragments: 814 in QI industrial area, 126 in QI workshop area and 97 in QIV area (and one in area QII, four in area QV). ±60% of these have been analysed by pXRF in Qantir, while forty-nine fragments were sampled[1] for further analysis using optical microscopy and SEM-EDS. A complete sample list, including contextual information, is presented in Appendix B. Section 5.1 gives an overview of the general crucible characteristics, while section 5.2 goes into more detail on the micro-structure and chemistry of the crucible slag, based on the microscopy and SEM-EDS data. Section 5.3 describes the results of the large-scale pXRF-study. These first sections are all meant to be purely descriptive, while section 5.4 offers a technical interpretation of all results combined. In section 5.5, the results of lead isotope analysis are presented separately. All analytical results are then integrated and further discussed in Chapter 6.

Section 5.1

General crucible characteristics

Rather than going into a detailed description of each crucible fragment that has been investigated, this section summarises the general characteristics of most samples. This is

[1] Sampling occurred prior to the start of this PhD project and samples were therefore not selected by the author. An attempt was made at that time to cover as well as possible the macroscopically visible variation within the assemblage. This is further discussed in section 5.4.3.

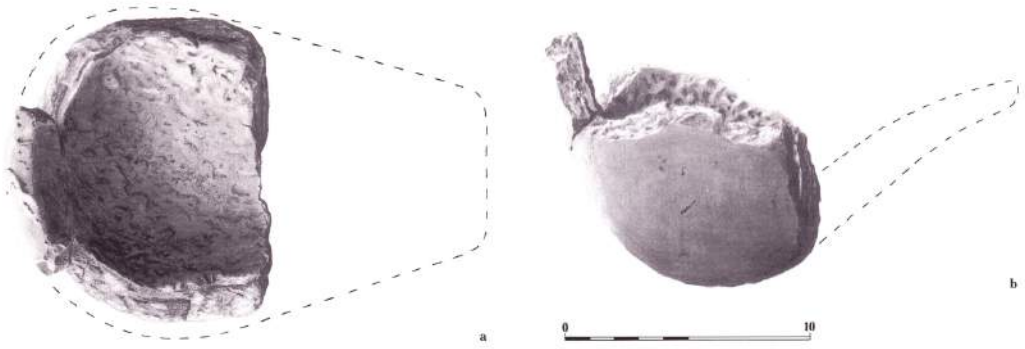

Figure 5.1: Reconstructed Pi-Ramesse crucible (left: top view; right: side view) (from Pusch, 1990, Figure 7, p. 89)

then used as a baseline against which samples can be compared, focusing on difference from the norm than rather describing each sample individually. Though no complete examples have been recovered, Figure 5.1 shows an outline of a reconstructed crucible. Typical dimensions are given by Pusch (1994) (see Appendix G.1): wall thickness ranges from 1-3 cm and volumes average around 350-400 ml (equivalent to 3-3.5 kg bronze).

5.1.1 Macroscopic investigation

The distinct industrial-like setting of melting batteries and cross-furnaces in which the crucibles were found at Pi-Ramesse, in association with tuyères, pot bellows, a piece of copper ingot, scrap bronze, moulds and bronze objects, immediately allowed them to be identified as part of a high-temperature bronze production facility. Macroscopic examination of the crucible fragments, for which some images are shown in Figure 5.2, reveals important information. For example, green corrosion products (Figure 5.2a) at the surface of the ceramic are indicative of the presence of copper/bronze.
Other striking features of the crucibles are their consistently thick walls, tempered with organic material (indicated by the high porosity and typical pore shapes). A comparison to contemporary ceramics from the site indicates the use of local Nile Silt as the basic raw material[2].

[2]Clay type Nilton I.C, as described by Aston *et al.* (2007: 518-519): *"While this material is represented by two sub-groups at Tell el-Dab'a, IC01 and IC02, in Qantir only subgroup IC01 is present. Both correspond with 'VS Nile C'. The I.C.01 material is characterized by an obvious and rich temper with significant coarse straw and chaff which are visible both in the fracture and on the surface. Also clearly visible are mica, quartz and sand grains, of variable quantities, that constitute the matrix. In its technical use as crucibles for bronze casting and the associated wind tubes for firing the furnaces, this material is sometimes exposed to extreme temperatures which leads to corresponding changes in its appearance."*

(a) Corroded prill stuck in slagged inner crucible surface (close-up)

(b) Largest recovered whole crucible fragment (Figure 5.1)

(c) Inside view of a fragment, showing slagged interior (left) and cross-section (right)

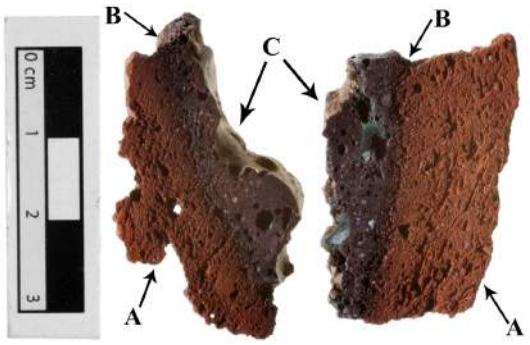

(d) Examples of crucible wall cross sections, with ceramic (A), bloated (B) and slag zone (C)

Figure 5.2: A few macroscopic observations

The gradient through the crucible wall - from a typically red fired ceramic on the outside to a dark grey slag on the inside - indicates a difference in temperature and redox-conditions outside and within the crucibles. This type of profile (Figure 5.2d) is indicative of the crucibles being heated from the inside. The slagged layer on most of the inner crucible surfaces, often trapping metallic prills, indicates exposure to high temperature.

Though no complete vessels remain, almost all fragments conform to a single type of crucible of standardised size (shown in Figure 5.1). This suggests a routine production, possibly (but not necessarily) involving the use of moulds. Finger imprints on some crucibles (see Figure 5.3) indicate that they were shaped and/or finished by hand, rather than using a wheel. The crucibles were then pre-fired, which can be inferred from the consistently red-fired outside of all fragments. Without pre-firing, the heating from above by tuyères would likely have resulted in a much more irregular firing of the ceramic during the (probably brief) metallurgical operation. Furthermore, pre-firing is a way of testing the crucible before use, which makes sense when producing large amounts of standard crucibles from fairly basic raw materials. Finally, using un-fired crucibles would probably mean significant loss of energy and time: metal remains solid while the ceramic is being fired, delaying the intended melting/alloying. The unexplained delay (up to 20 minutes) in reaching melting temperatures (1100-1200°C) when using unfired crucibles, noted by Davey and Edwards (2007), can most probably be attributed to a 'ceramic firing stage' at about 800°C (Th. Rehren, pers. comm.).

The tuyères are made of the same fabric as the crucibles, and their cross-sections are rounded to octagonal (exterior surface) with a circular opening through which the air flowed (see Pusch, 1990, Abb. 5, p. 87). They were most likely pre-fired at lower temperatures or for a shorter duration than the crucibles. The ends of the tuyères were exposed to high temperatures (see Figure 4.6) and their very ends are often vitrified and sometimes contaminated with copper and tin. All tuyère fragments are broken off at ±20-30 cm from this 'hot end', with the fragment connecting to the bellows consistently missing. This probably indicates that these tuyères were pushed aside and broken at the end of the operation: the fracture occurred at the point were the tuyères were not exposed to heat and remained low-fired. The 'cold ends' of these tuyères probably crumbled and disintegrated, leading to their archaeological absence. This discussion is further expanded in section 6.3.

Figure 5.3: Finger imprints on crucible exterior surface

5.1.2 Microscopic investigation

Looking at the samples under magnification allows some further general characteristics to be discerned.

1. Typically, three main parts are present in each section through a crucible wall:
   (a) On the outside, a fired ceramic part.
   (b) In the centre, a very porous part which marks the disintegration of the ceramic and the transition into a slagged part.
   (c) A slag part, consisting of vitrified ceramic and various charge components, such as metal prills.
2. The ceramic part is rich in silica. Almost invariably, there is a fine, angular quartz fraction which is part of the matrix and appears to occur naturally in the Nile Silt. In most samples, a coarser, sub-angular to (sub-)rounded quartz fraction is found, for which it is not clear whether it is natural or added as (sand) temper. Though a few samples argue in favour of tempering, many cases are dubious (see section 5.1.3).
3. The ceramic is porous due to the burning out of organic temper. This is evidenced by the characteristic shape of the voids (macroscopically visible) and the presence of phytoliths (microscopic siliceous plant secretions characteristic to each plant species and thus useful for their identification). No thorough analysis has been performed on these phytoliths, but they appear to indicate the use of rice husks or another grassy species, corroborating suggested use of straw or chaff (Aston *et al.*, 2007).

4. The ceramic part gradually becomes more porous towards the inside of the crucible wall, up to the point where it loses all its structurally bound water, disintegrates and bloats. Firing experiments performed with local Nile Silt indicate that this bloating takes place at temperatures of 1200°C upwards (Merkel and Rehren, 2007).

5. The inside of the crucible shows the continuation of this bloating into a (partly) vitrified zone, resulting from the further disintegration of the ceramic, and its interaction with the crucible charge to form crucible slag. Temperatures here did not necessarily exceed 1200°C; the occurrence of the bloated zone simply indicates how deep this temperature penetrated into the crucible wall.

6. 90% of all samples contain metallic prills. The size of metallic phases varies from tiny prills to quite large particles, and their abundance fluctuates between and within samples.

5.1.3 Sand tempering?

Generally, the crucible ceramic contains a fine, angular quartz fraction (natural component of Nile Silt) and a coarser, sub-angular to (sub-)rounded quartz fraction. In some cases, the abundance of this coarser fraction is too low to convincingly argue for this fraction being added as temper. The Nile silt may naturally have a bi-modal distribution, with a low abundance of this coarser quartz, or perhaps this variability existed in the available clay sources, from which a coarser mixture was selected for this fabric (see similar discussion for Amarna fabrics by Bourriau and Nicholson (1992)). While there are samples which might argue in favour of tempering (with quartz sand), in many cases both could be argued. Figure 5.4 shows some examples. Often, the ceramic is fused due to high-temperature exposure, making assessment of the quartz fraction distribution more difficult. Moreover, mounted sections are inferior to thin sections for addressing this question.

Section 5.2

Detailed description of crucible slag

The structural characteristics of the crucibles are quite consistent and do not allow for any meaningful distinction of groups. In this section, the chemical data obtained by SEM-EDS is used to look for broad trends in the bulk compositions of ceramic and slag. A description is given of all phases (oxides in section 5.2.3, metals in 5.2.4) that occur in minor or

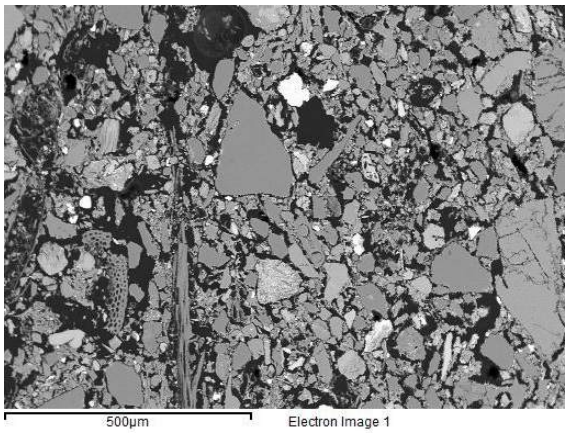

(a) 'Natural distribution', sample 84_1189b,0

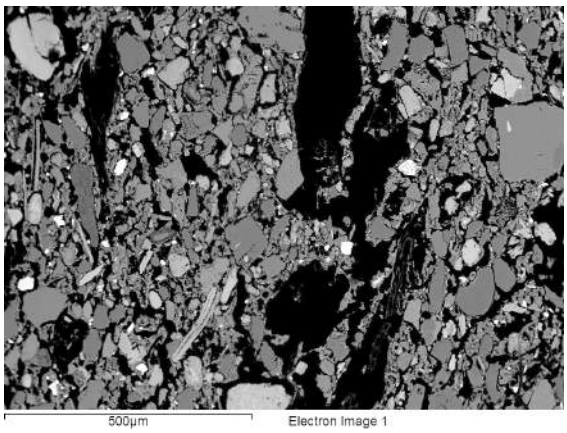

(b) 'Natural distribution', sample 86_0792b,04

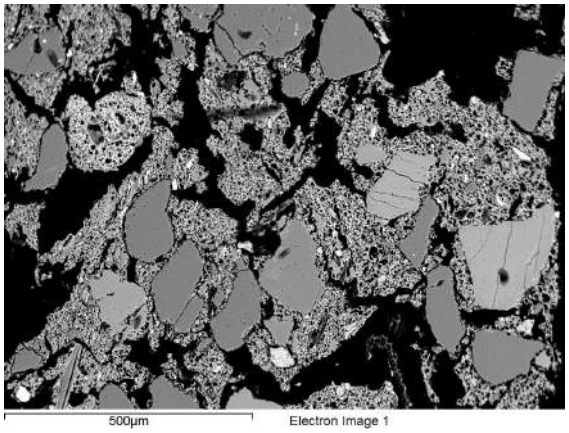

(c) 'Natural distribution'? Sample 86_0471b,01

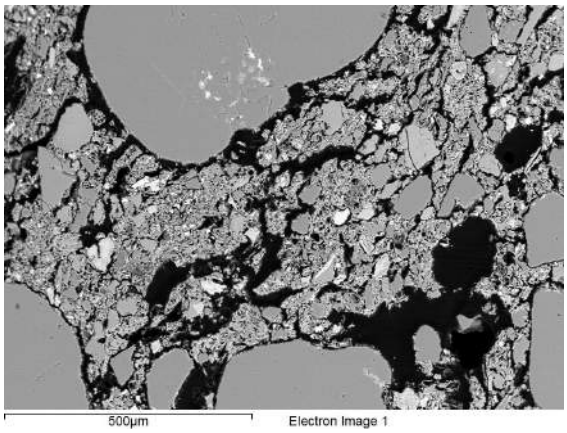

(d) 'Quartz temper', sample 82_0223b,01

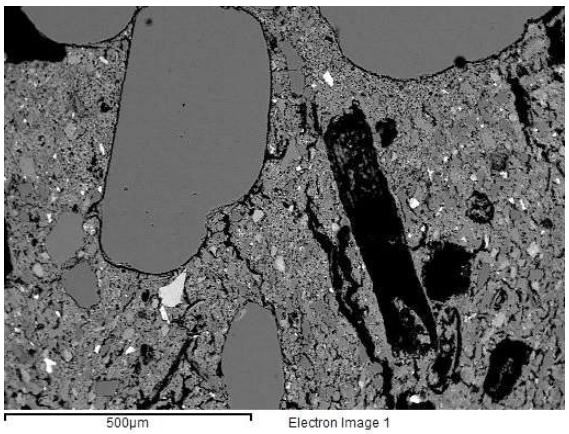

(e) 'Quartz temper', sample 87_0773,04

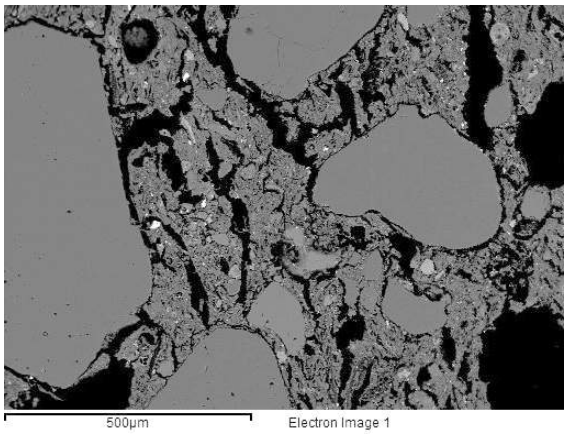

(f) 'Quartz temper', sample 92_0606

Figure 5.4: Examples of quartz fraction in crucible ceramic

major amounts in the crucible slag. This section aims to be purely descriptive, with interpretation and discussion reserved to section 5.4 and Chapter 13 respectively.

5.2.1 Some broad trends

Full results of the chemical analysis of crucible ceramic and slag are given in Appendix C. To process the large amounts of chemical data, the most abundant elements (adding up to ±91 wt% of ceramic and ±82 wt% of slag bulk composition) have been plotted in ternary diagrams to discern any broad patterns: SiO_2, Al_2O_3, FeO and CaO. Another way to simplify the data would be to calculate basicity and viscosity, as proposed by Bachmann (1980), though this method is aimed at liquid primary production slag (more specifically iron smelting slag) and not applicable here.

Figure 5.5 shows ternary plots of SiO_2 - Al_2O_3 - FeO and SiO_2 - Al_2O_3 - CaO for crucible ceramic and slag composition (in each case ignoring all other elements). The ceramic composition is quite uniform, except for some variability in silica content. This is either due to the natural variability in silica content of the Nile Silt or the (debatable) addition of sand temper. As discussed in Chapter 3, an effort has been made to minimise bias through inclusion/exclusion of large quartz grains in the area of analysis (a problem noted by Freestone and Tite (1986)). Therefore, this silica variability may be considered meaningful.

It should be stressed that melting temperatures shown for these compositions were not necessarily reached, as the crucible slag rarely became fully liquid: undissolved, fractured quartz grains are present in nearly all crucible slag. Moreover, true compositions are more complex than these ternary diagrams suggest, resulting in significantly lower melting temperatures (Hauptmann, 2007). Finally, redox-conditions during the metallurgical crucible process did not necessarily correspond to those at which these diagrams were constructed.

Another trend that can be noticed is that some of the slag compositions are not distinct from the ceramic composition, in terms of SiO_2 - Al_2O_3 - FeO. All slag, however, is at least somewhat enriched in CaO. Some slag compositions differ significantly, being enriched both in FeO and CaO. The overall impression from Figure 5.5 is that the slag compositions do not show any real grouping, but rather form a single group with a broad compositional spread. The impression that all variability witnessed in this crucible assemblage could be explained by the variability of a single process (i.e., a single process producing a variable waste product), rather than it being a reflection of multiple processes, is addressed in more detail in section 5.4.

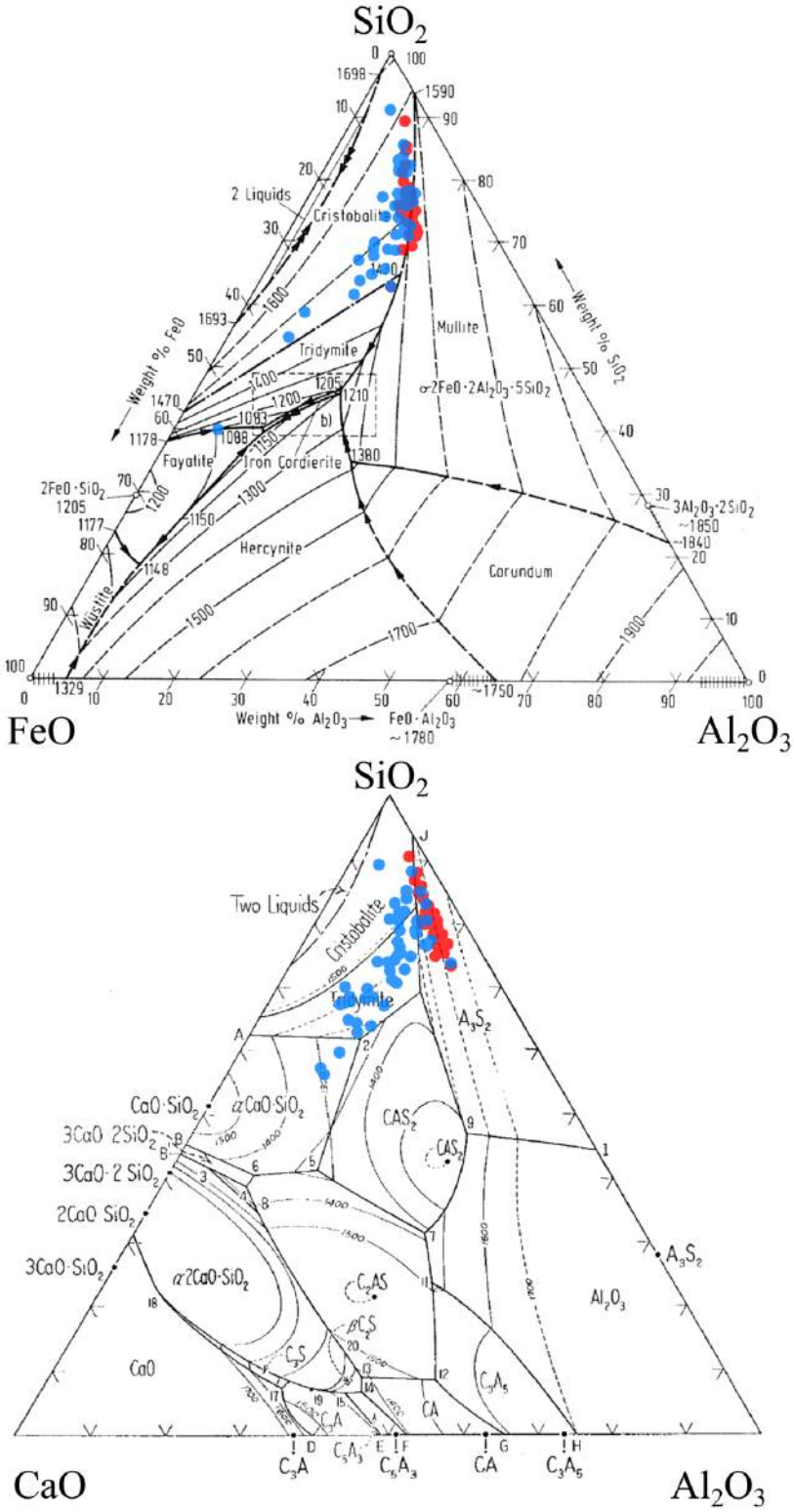

Figure 5.5: Ternary plots for ceramic (red) and slag (blue) composition (phase diagrams from Muan, 1957 (top) and Hall and Insley, 1933 (bottom))

Finally, the distinction between rim and body crucible fragments should be pointed out. Figure 5.6 again shows the slag compositions, distinguishing between rim and body samples (and body samples taken near rims). Body fragments tend to be more enriched in CaO and only body fragments are significantly enriched in FeO. Slag on rim fragments better resembles ceramic composition. Figure 5.7 shows a crucible fragment with visibly different slag types near the rim (reddish) and lower on the body (darker black/green). Both qualify as 'crucible slag', but the 'rim slag' is mainly ceramic fluxed by lime (with limited copper enrichment), while the 'body slag' (3 cm away) is enriched in iron, copper, tin and cobalt (measured by pXRF). The line demarcating the two slag types probably represents the level of liquid metal in the crucible during operation. This contrast introduces some important methodological issues, which are further discussed in Chapter 13.

5.2.2 Bulk analysis

'Bulk analysis', as defined in section 3.3.4, is conducted for all samples. The full compositional data for all crucibles is given in Appendix C and broken down into the ratios of oxides to alumina and changes of these ratios between ceramic and slag (ignoring base metal content[3]). The absolute Al_2O_3 content is slightly lower in slag than ceramic for most samples, as shown in Figure 5.8. This simply reflects dilution due to slag enrichment in other elements. The first part of this section is based on the changes in ratios of oxides to Al_2O_3. Base metal-oxide content is presented as wt% in slag (as ceramic base metal content is below detection limits, this metal content is equivalent to 'change in metal content').

Distributions have been tested for normality using the Shapiro-Wilk normality test. Correlation coefficients for two variables have been calculated using Pearson Product Moment Correlation[4]; R- and p-values are given in the text below.

- The change in SiO_2/Al_2O_3 between slag and ceramic (Figure 5.9) has a normal distribution (excluding two outliers) around a very minor increase.
- All samples show enrichment of CaO. The majority of samples show moderate enrichment and there is a decrease in incidence for higher enrichments (Figure 5.10).

[3] Base metals removed: copper, tin and lead. Arsenic is equally removed from calculations, while iron is not.

[4] *The pair(s) of variables with positive correlation coefficients (R) and p-values below 0.050 tend to increase together. For the pairs with negative correlation coefficients and p-values below 0.050, one variable tends to decrease while the other increases. For pairs with p-values greater than 0.050, there is no significant relationship between the two variables.* (SigmaPlot Version 12)

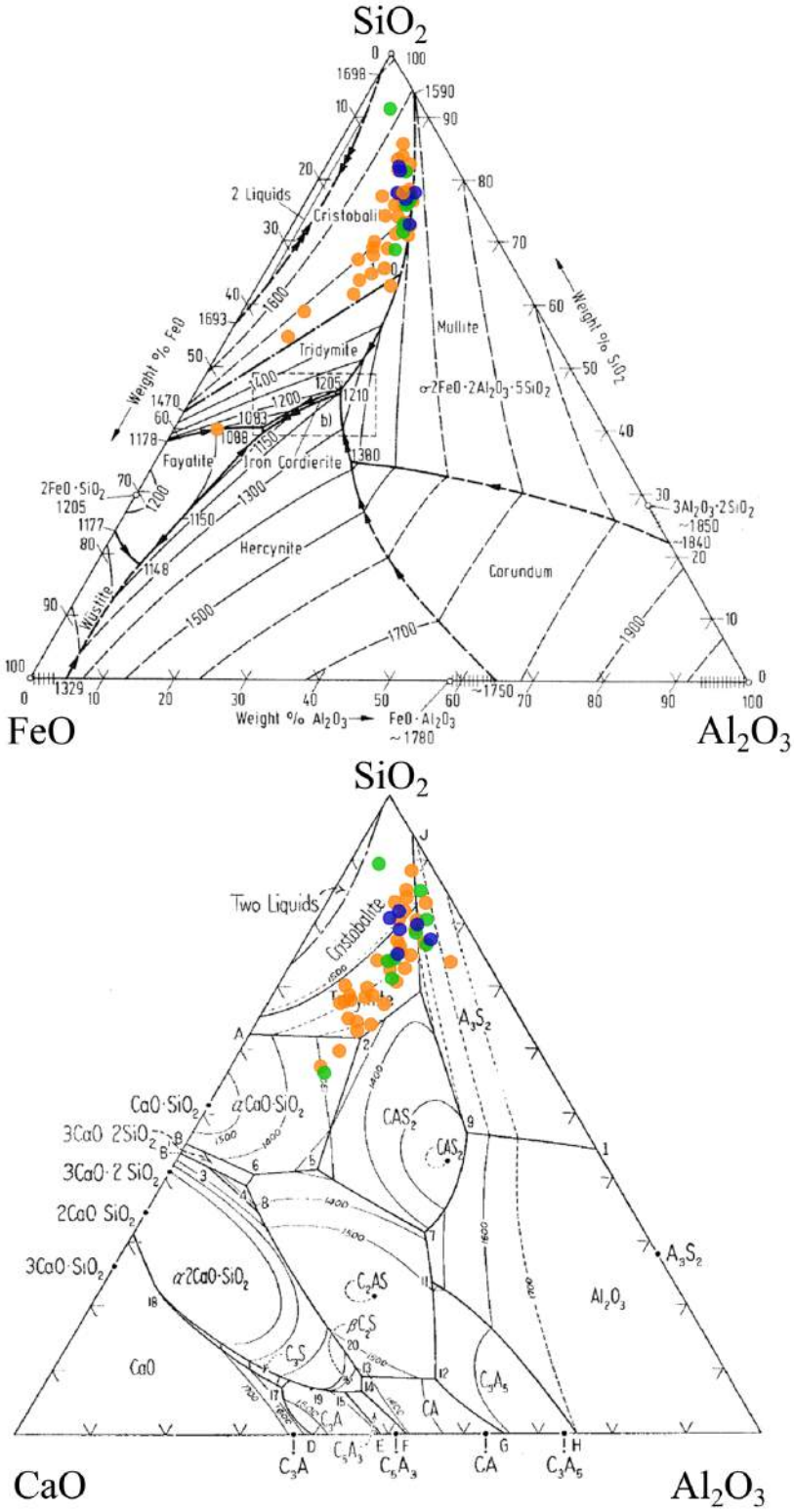

Figure 5.6: Ternary plots of slag composition, distinguishing between rim (green), body (orange) and body-near-rim (blue) samples

Figure 5.7: Crucible fragment showing reddish slag near rim and darker slag towards lower body (fragment 88_1374,0001)

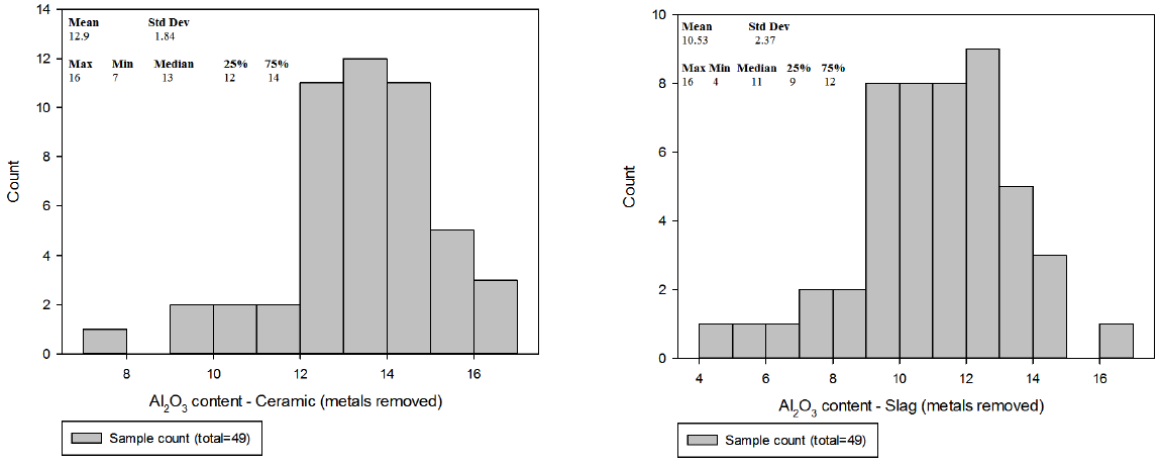

Figure 5.8: Absolute Al_2O_3 content (in wt%) in ceramic and slag (after removal of base metals)

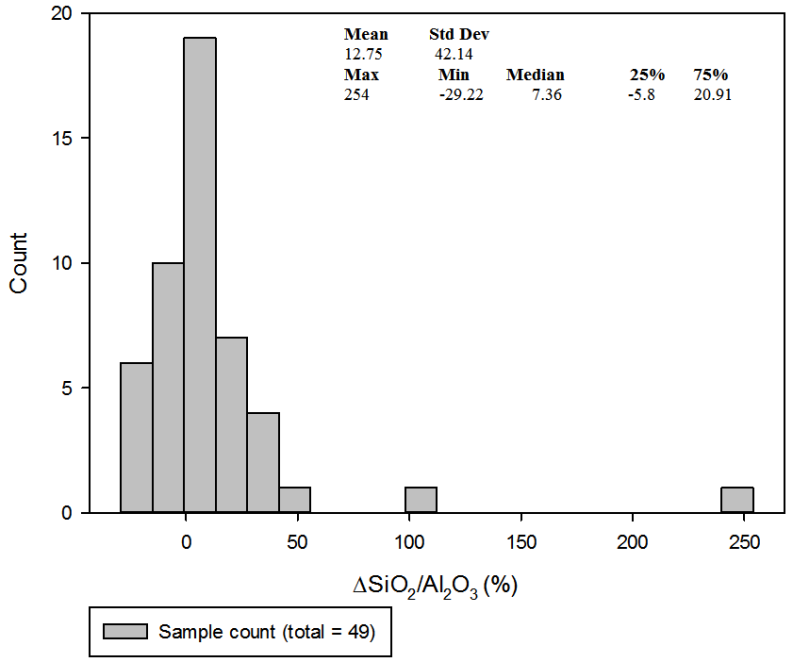

Figure 5.9: Change in the ratio $^{SiO_2}/_{Al_2O_3}$ between ceramic and slag (two outliers not shown)

The scatter plot shows the samples sorted by increasing enrichment, which appears to follow a step-wise increasing trend. Though some of this might be explained by insufficient sampling, it probably points to a bi-modal distribution (below and above ±400% change). Within these two, there are two further steps: ±0-200% change, ±200-400% change, ±400-600% change and ±600-1100% change. The main two groups are probably explained to some extent by the distinction between body and rim fragments. A second effect (which might explain the further division within each group) could then be the degree to which the ceramic was fluxed by CaO and slagged. This degree of slagging (indicated by higher lime enrichment), appears to be related to increased iron, copper and tin enrichment, as discussed further below and in more detail in section 5.4.9.

Figure 5.11 shows the increase in CaO plotted against MgO, P_2O_5, K_2O, Na_2O and SiO_2. There is a good correlation between the increase in CaO and MgO ($R = 0.802$, $p = 4.401 \times 10^{-12}$) and P_2O_5 ($R = 0.833$, $p = 1.089 \times 10^{-13}$). The correlation between CaO and Na_2O is weaker ($R = 0.525$, $p = 0.109 \times 10^{-3}$) and between CaO, K_2O ($R = 0.0859$, $p = 0.557$) and SiO_2 ($R = 0.0965$, $p = 0.509$), no significant correlation exists. These observations, most likely related to fuel ash contributions to the crucible slag, are discussed in section 5.2.5.

- The change in $^{TiO_2}/_{Al_2O_3}$-ratio, shown in Figure 5.12, has a normal distribution (ex-

cluding one outlier) around a very minor increase.

- The change in $^{FeO}/_{Al_2O_3}$-ratio, shown in Figure 5.13, has no normal distribution. The scatter plot shows the samples sorted by increasing enrichment. This trend shows an FeO enrichment with normal distribution around a low value, with an extended tail of higher enrichment. The low enrichment (normally distributed) occurs in both body and rim fragments. The tail of samples with higher enrichment (right of arrow) encompasses mainly body fragments.
  The data in Figure 5.13 probably presents two populations: one ($\pm^{31}/_{49}$ samples, 63% of population) normally distributed around a very low iron enrichment, and one group ($\pm^{18}/_{49}$ samples, 37% of population, starting at the bump indicated by the red arrow) more clearly enriched in iron (no normal distribution). The same histogram is shown with smaller bin size in Figure 5.14, visualising these two populations. Figure 5.15 shows that there is only moderate correlation ($R = 0.556$, $p = 0.34 \times 10^{-4}$) between CaO- and FeO-increase (the highest CaO enrichment occurs at moderate FeO-increase and vice-versa), indicating separate sources for these enrichments. However, they do tend to increase together.

- MnO content is very low (at detection limit), does not show any significant changes, and may be considered absent.

- As_2O_3 content is very low (at detection limit), does not show any significant changes, and may be considered absent.

- CuO content increases to varying degrees. 90% of all samples contain metallic prills, explaining the CuO increase in nearly all samples. However, due to the irregular occurrence of prills throughout the slag, their measurement is quite variable: it is sensitive to prills being present in the analysed frame. Figure 5.16 shows the distribution of CuO enrichment: the bulk of all samples has enrichment up to 6 wt%, with a few outliers showing higher enrichment.

- SnO_2 content increases to varying degrees. Due to the heterogeneous occurrence of SnO_2 aggregates (see Appendix D.4), their measurement is quite variable: it is sensitive to bronze prills and tin oxide clusters being present in the analysed frame. Figure 5.17 shows the distribution of SnO_2 enrichment: the bulk of all samples has enrichment up to 10 wt%, with a few outliers showing higher enrichment. Figure 5.18 shows a scatter plot of CuO vs SnO_2 enrichment, showing some correlation between both ($R = 0.711$, $p = 0.104 \times 10^{-7}$). The plot shows that there is actually one group of samples enriched in copper only (pure copper prills) and one group in which CuO

and SnO_2 increase together. In this second group, there is a higher average enrichment in SnO_2 than CuO ($\pm 2/1$), which does not match the ratio in bronze (usually $\pm 1/20 - 1/8$). Figure 5.19 shows there is a general trend for higher CuO and SnO_2 with higher Δ^{CaO/Al_2O_3} ($R = 0.495$, $p = 0.297 \times 10^{-3}$ and $R = 0.657, p = 0.296 \times 10^{-6}$).

- There is an increase in bulk CoO content (0.3-2.1 wt%) for six samples (and occurrence of Co-rich phases in an additional three samples, see Appendix D.5).
- There is a modest increase in bulk PbO content (up to 1.4 wt%) for seven samples.

It should be mentioned that with a beam voltage of 20 kV, Pb present in low quantities are not sufficiently excited to be picked up by SEM-EDS and remains below detection limits (± 1 wt%, see section 3.3.5), though pXRF-analysis, using a 40 kV-beam, could pick up lower concentrations (see section 5.3.2). The same problem exists for Sr.

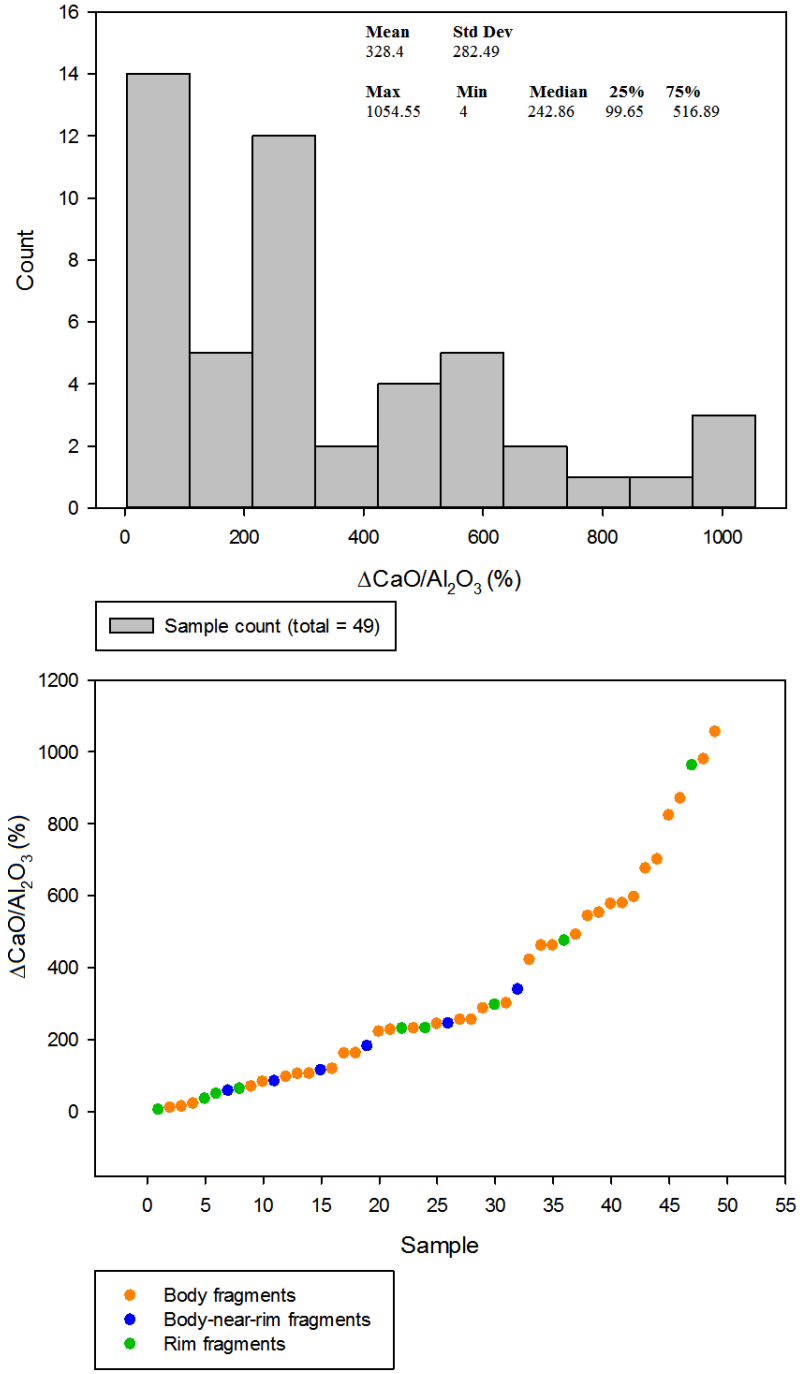

Figure 5.10: Change in the ratio $^{CaO}/_{Al_2O_3}$ between ceramic and slag

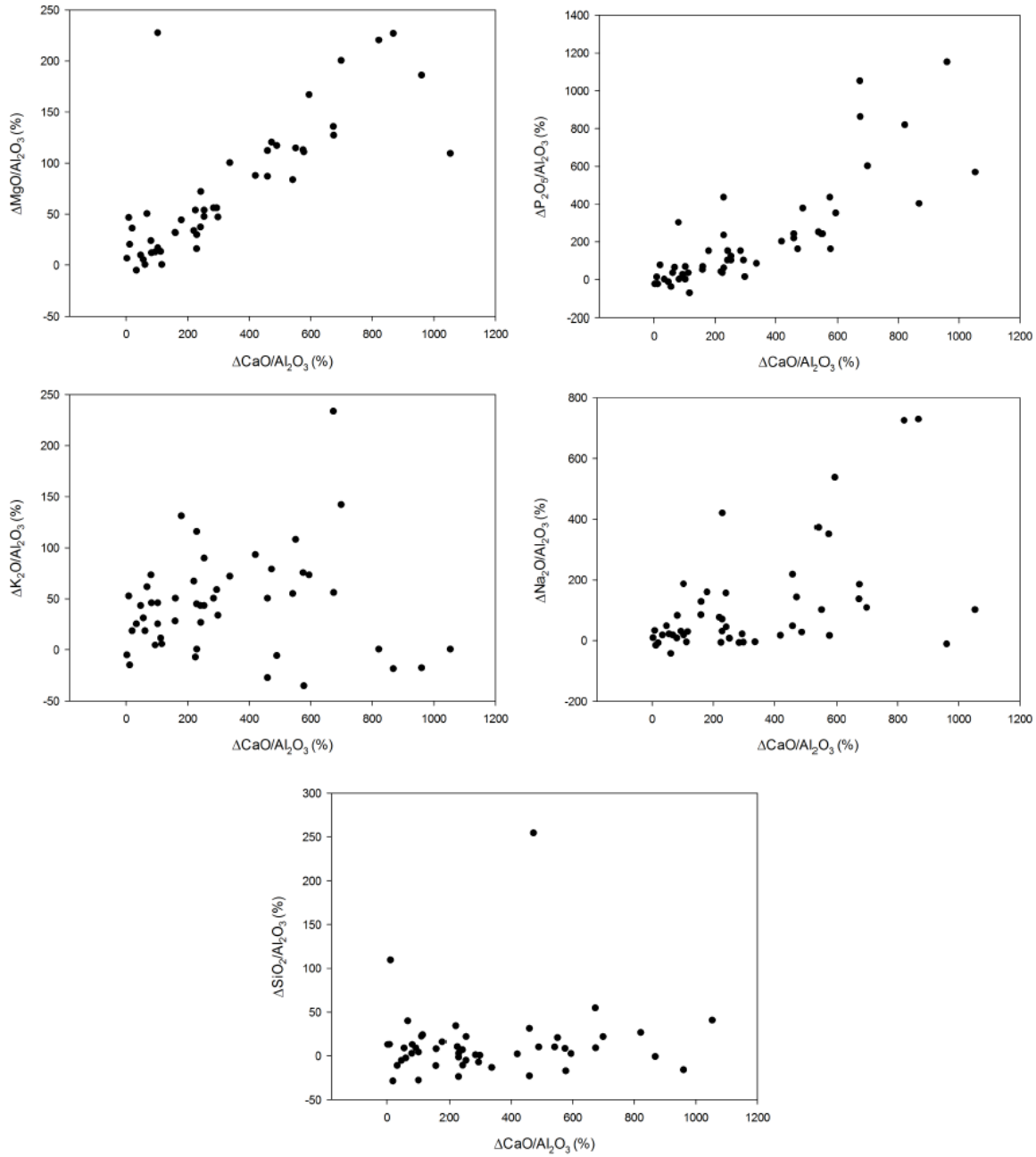

Figure 5.11: Change in the ratio CaO/Al_2O_3 vs MgO/Al_2O_3, P_2O_5/Al_2O_3, K_2O/Al_2O_3, Na_2O/Al_2O_3 and SiO_2/Al_2O_3, between ceramic and slag

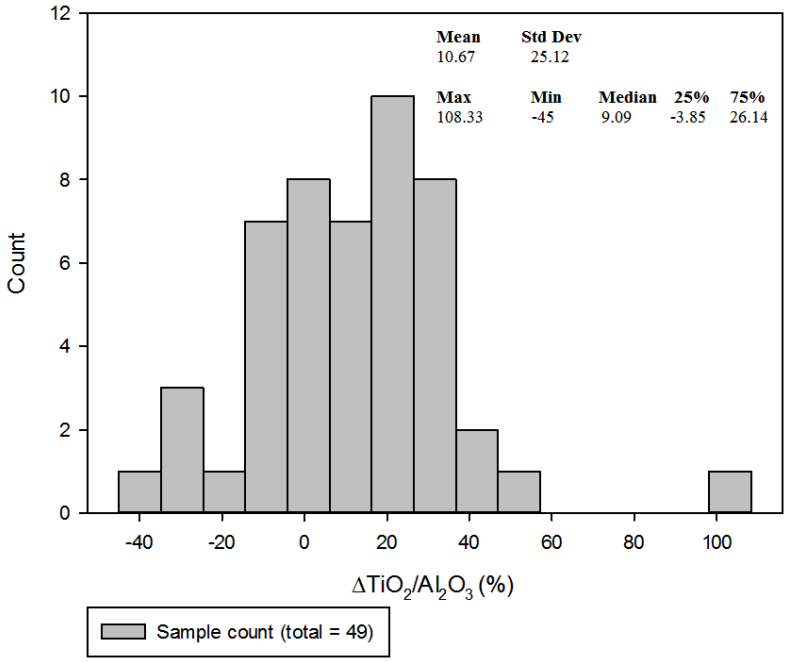

Figure 5.12: Change in the ratio TiO_2/Al_2O_3 between ceramic and slag

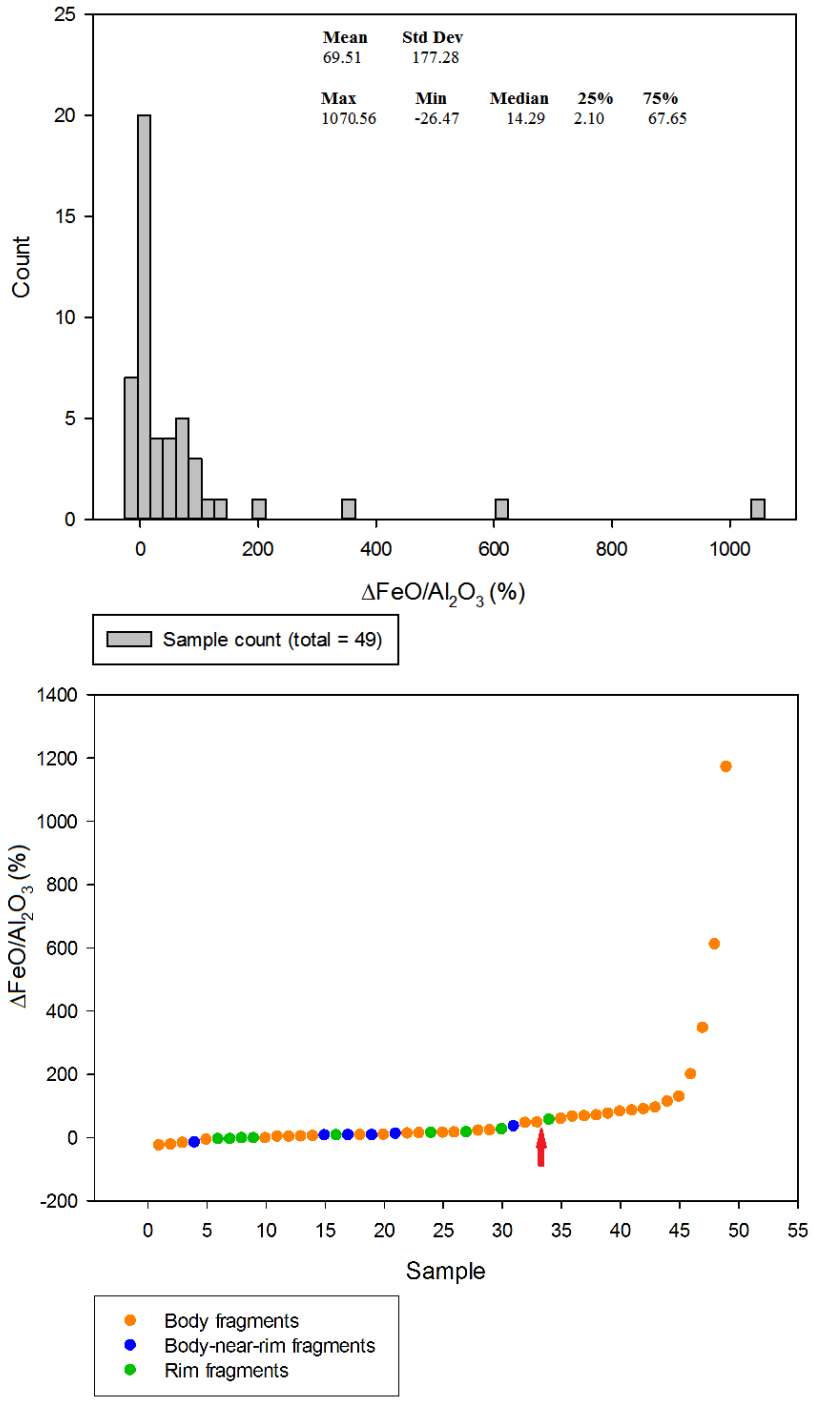

Figure 5.13: Change in the ratio $^{FeO}/_{Al_2O_3}$ between ceramic and slag

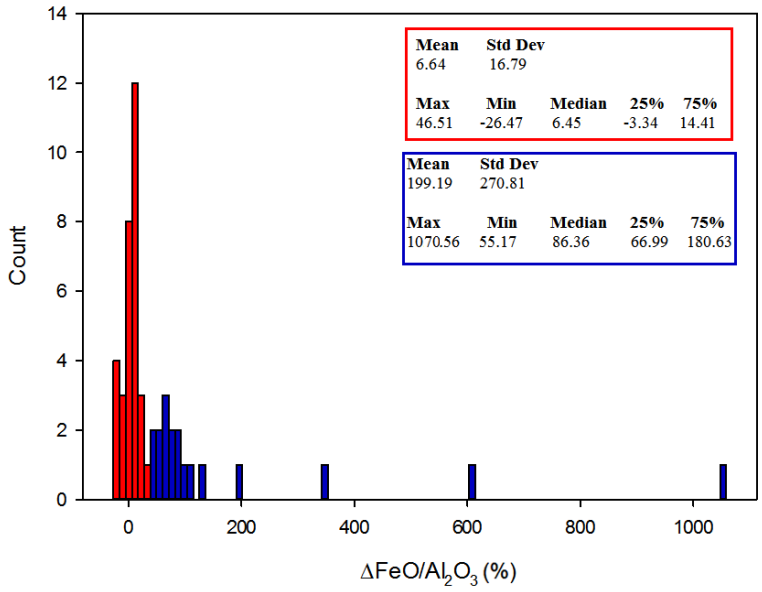

Figure 5.14: Change in the ratio $^{FeO}/_{Al_2O_3}$ between ceramic and slag: bi-modal distribution

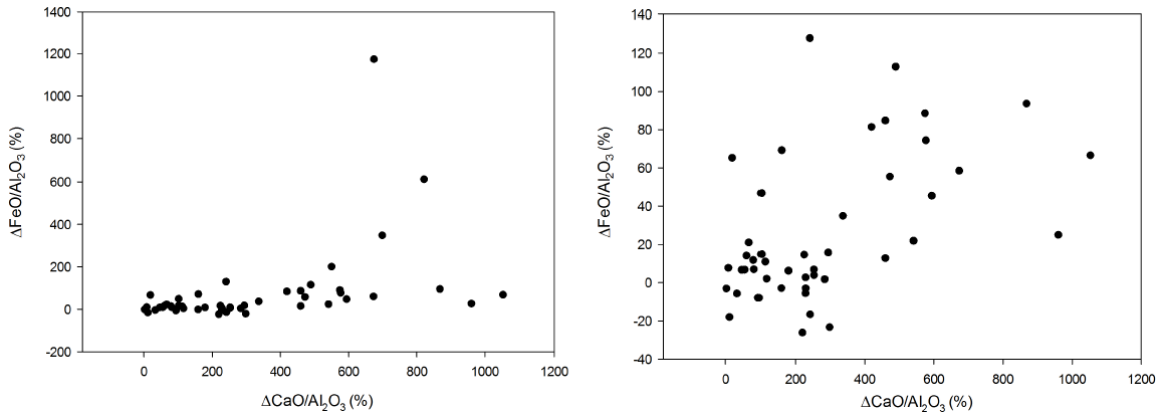

Figure 5.15: Change in the ratio $^{CaO}/_{Al_2O_3}$ vs $^{FeO}/_{Al_2O_3}$, with and without four high FeO-increase outliers, between ceramic and slag

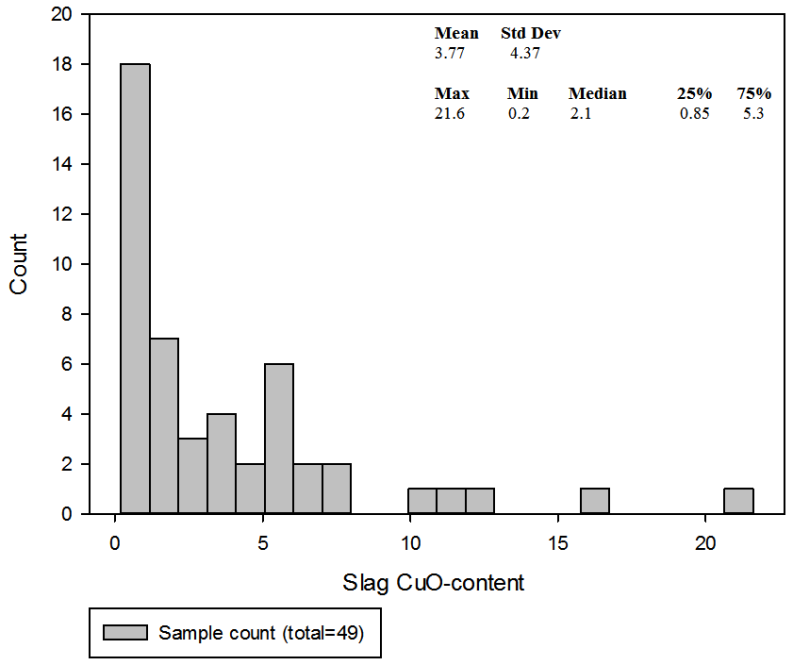

Figure 5.16: Bulk CuO content (in wt%) in slag

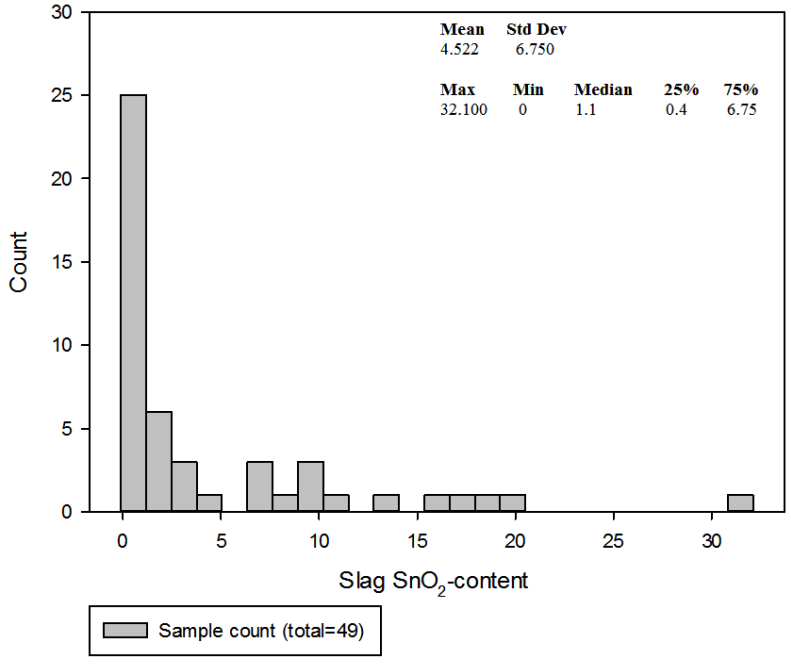

Figure 5.17: Bulk SnO_2 content (in wt%) in slag

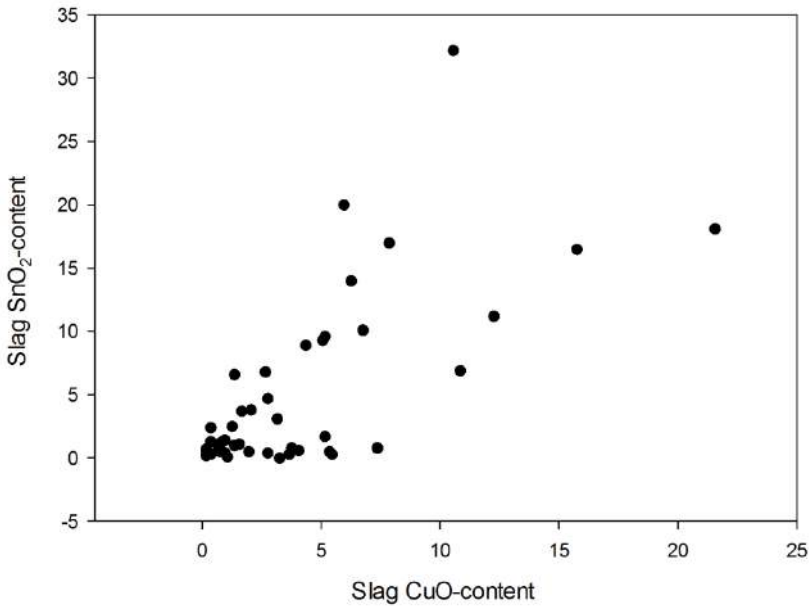

Figure 5.18: Bulk CuO vs SnO_2 content (in wt%) in slag

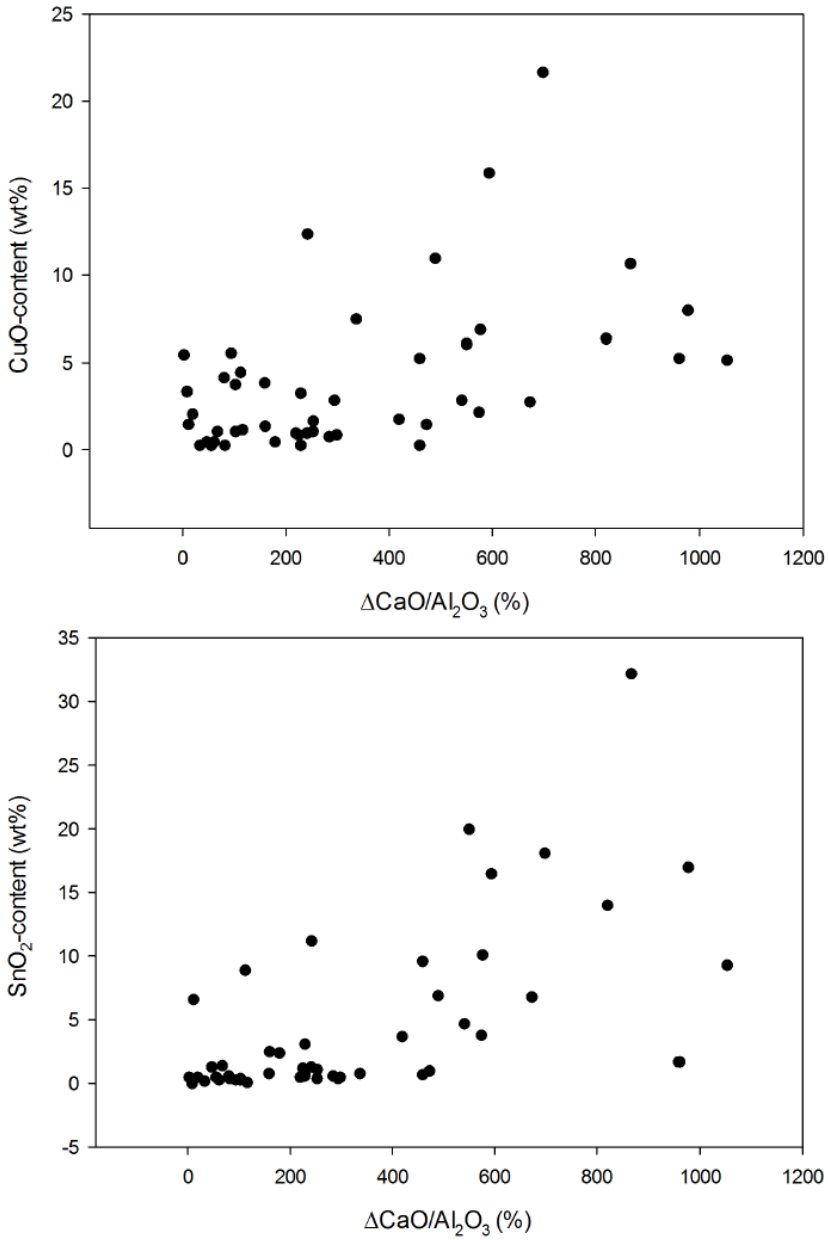

Figure 5.19: Bulk CuO and SnO_2 content vs $\Delta^{CaO}/_{Al_2O_3}$ between ceramic and slag

5.2.3 Oxide phases in crucible slag

A full list of oxides occurring in the crucible slag has been established, including details such as composition, shape, frequency of occurrence etc. Their varying occurrence is interpreted in section 5.4. The main oxides that occur are Fe-bearing, Ca-bearing, Cu-bearing, Sn-bearing and Co-bearing phases.
The recognition of these various phases is very time-consuming and their omission here to some extent misrepresents this crucible research. However, the majority of them do not offer diagnostic evidence for the technical reconstruction of metallurgical processes. Therefore, only more diagnostic phases are highlighted throughout this chapter, while the others are confined to Appendix D, to allow more space for relevant interpretation and discussion.

Terminology for the different oxides in the crucible slag is adapted from mineralogy (e.g., Klein and Dutrow, 2007). However, it should be emphasised that this terminology is used on the basis of compositional correspondence or similarity to natural minerals. Most slag crystals are formed during the high-temperature process, and are therefore essentially different from naturally occurring minerals. The importance of this distinction is especially crucial for the case of tin oxide and cassiterite, as argued in section 5.4.5.

5.2.4 Metallic prills

All prills are spherical (unless otherwise noted), indicative of a liquid state during the crucible process. Under the optical microscope, all copper-based prills have a yellowish colour, which varies with the Sn content (high-tin prills are lighter, more faded). Common alloy elements are Sn, Fe, Co, Ni, As and Pb. In a few samples, Cu_2S occurs. Here, a list is given of the main types of prills. A complete overview of all measured metallic prills is given in Appendix E. Often, prills are too small to measure by SEM-EDS, and noted as 'micro-prills'.

1. *Copper/bronze*: The main type of metallic phase found in the crucible slag is copper/bronze. A range of compositions is encountered, going from pure Cu to high-tin bronze, and less frequently other Cu-alloys. Figure 5.20 shows the phase diagram for Cu-Sn alloys.

   (a) Pure copper, sometimes with cuprite (Cu_2O) edge (e.g., Figure D.10a).

   (b) Low- to intermediate-tin bronze (0-12 wt% Sn). These prills are dominated by α-phase bronze (e.g., top left in Figure D.15d). Typical bronze artefacts from Pi-Ramesse (and most of contemporary Egypt[5]) have ±5-10 wt% Sn (Herold, 1998; Pusch and Rehren, 2007; Rehren *et al.*, 1998), and belong to this category.

   (c) High-tin bronze (over 20-25 wt% Sn). These prills are essential to the discussion of intentional alloying in section 5.4.4. Examples are shown in Figures D.1c, D.2a, 5.21 and 5.23. Prills consist of either δ-phase (±33 wt% Sn) dendrites in an $\alpha+\delta$ interdendritic (±25 wt% Sn) or a combination of δ-phase, ε-phase (±40 wt% Sn) and η-phase (±61 wt% Sn). δ-phase, ε-phase and η-phase are stable under normal casting conditions, while $\alpha+\delta$ does not form a stable solution (see Figure 5.20).

   (d) Bronze prills with variable composition, and minuscule dispersed Pb droplets (Pb is largely insoluble in copper) which do not show up in the bulk composition of the prill (below detection limit). An example is shown in Figures 5.22 and 5.24.

   (e) Cu or bronze prills enriched in other elements (Fe, As, Co, Ni and Pb). One example of Co-rich prills is shown in Figure 5.23. For its composition and more examples, see Appendix E.

   (f) Non-metallic prills:

[5] Occasionally higher levels occur, though rarely over 16 wt% (Ogden, 2000).

i. Chalcocite (Cu_2S) prills have been noted in six samples. One example is shown in Figure 5.24.

ii. Cuprite (Cu_2O). In many samples, prills entirely composed of cuprite occur (sometimes, prills of $Cu_4Cl_2O_5$). These are either indicative of (locally) very oxidising operating conditions or post-depositional alteration. Examples are shown in Appendix D.3.

These prills are sometimes composed of multiple phases (as indicated in Appendix E).

2. *Iron*: There are no pure Fe-prills occurring in any of the samples, though Fe-rich prills do occur. The example with highest Fe content occurs in sample 86_0749c. The two prills shown in Figure 5.25 have the following composition:

	Cu	Fe	As	Sn	Ni	S
Phase 1	7.3	89.4	2.8	-	0.5	-
Phase 2	91.3	6.7	1.0	1.0	-	-
Sulphidic edge (3)	67.8	8.1	-	-	-	24.1

(in wt%)

3. *Gold*: A single occurrence in sample 86_0749c: a prill with composition: 70 at% Au + 30 at% Cu, shown in Figure 5.26 (see section 5.4.11).

As shown in Figure D.12, dendritic structure in bronze prills is emphasised by differential corrosion. When a liquid bronze solidifies, the solid metal grows along a dendritic pattern. The first solidifying metal tends to be rather poor in tin, thereby increasing the tin content in the liquid phase. As solidification continues, the metal deposited towards the outside of the dendrites becomes richer in tin and thus harder. This is discussed more fully by Scott (1991). In a corrosive environment, the softer dendrite cores, low in tin, are removed first, resulting in a structure as shown in Figure D.12.

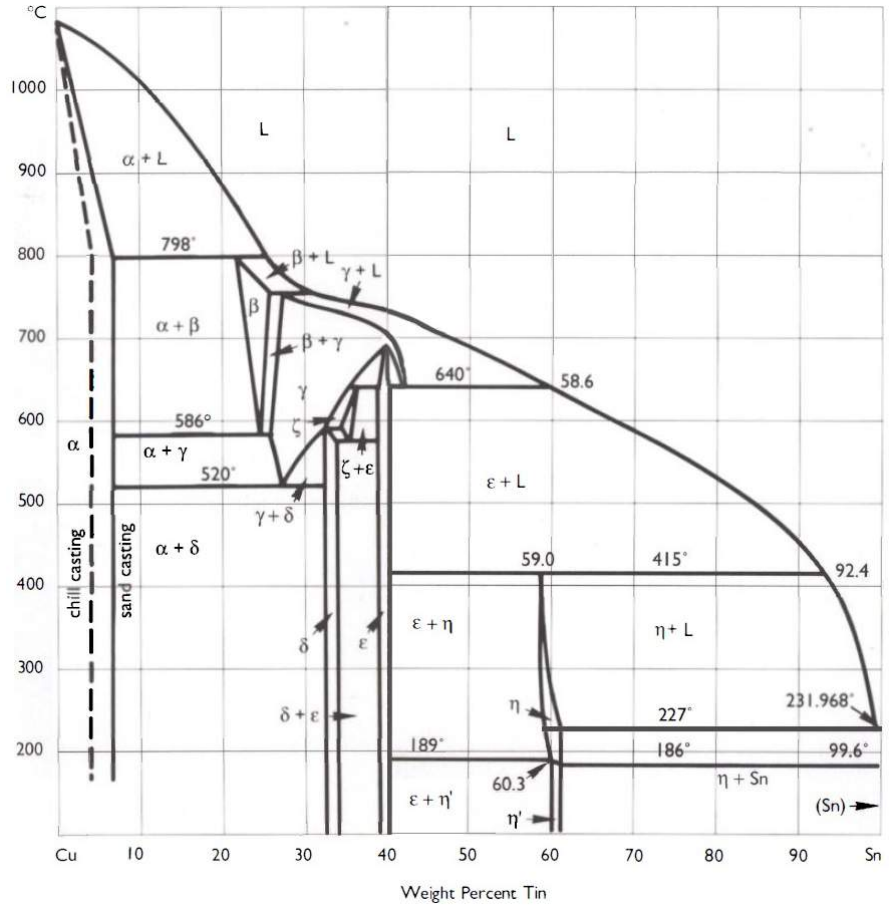

Figure 5.20: Cu-Sn phase diagram, casting conditions (modified from Scott, 1991; all phase compositional boundaries approximate)

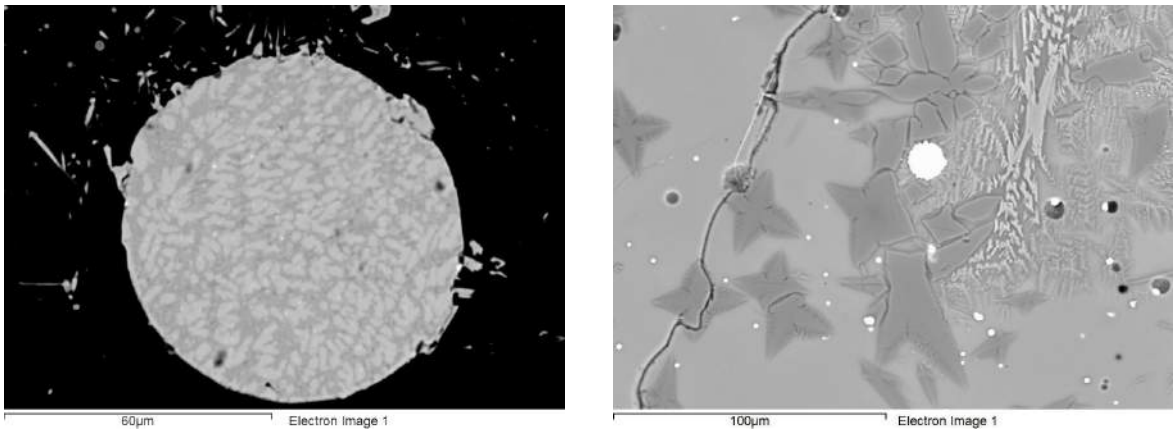

(a) Sample 87_0762,0Nv (1)

(b) Sample 94_0775,01

Figure 5.21: High-tin prills

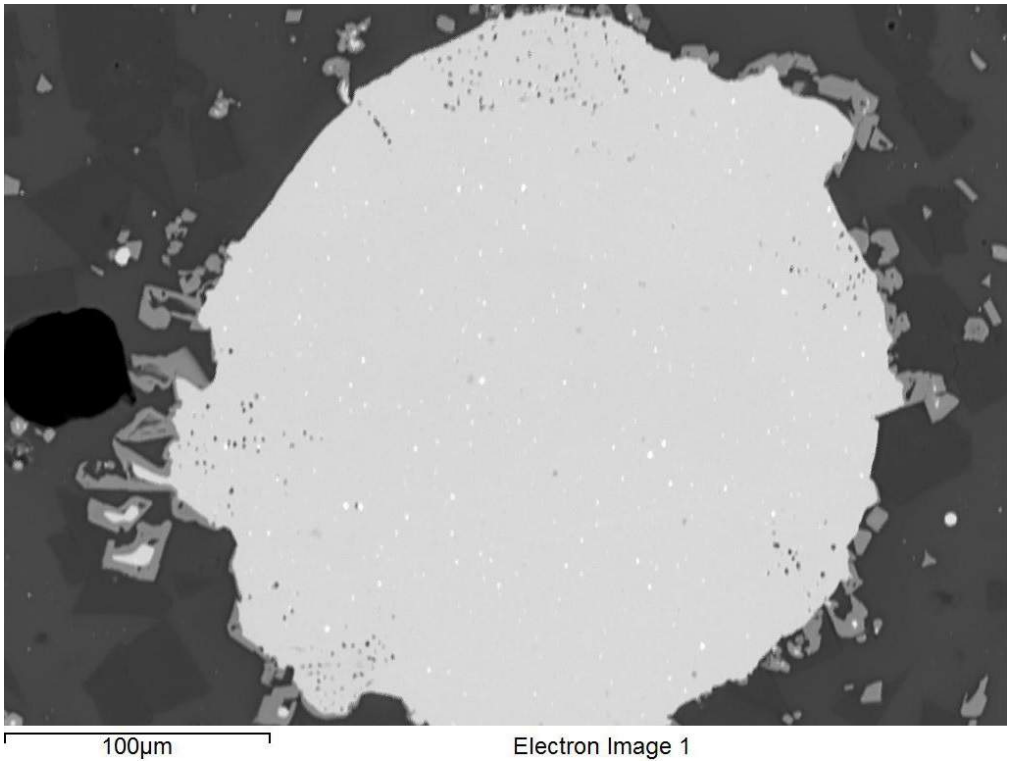

Figure 5.22: Prill with finely dispersed, undissolved Pb-droplets (and magnetite burnt out of prill), sample 87_0762

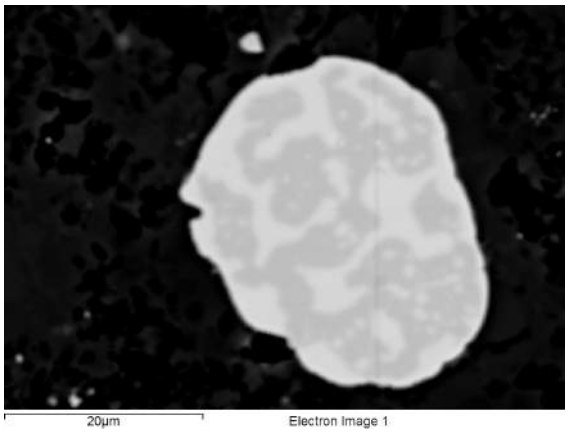

(a) Two phased (high-tin) prill

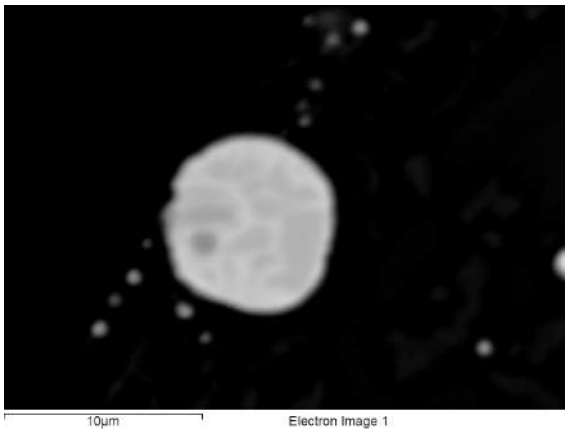

(b) Three-phased prill

Figure 5.23: Co-rich prills in sample 97_0690,02

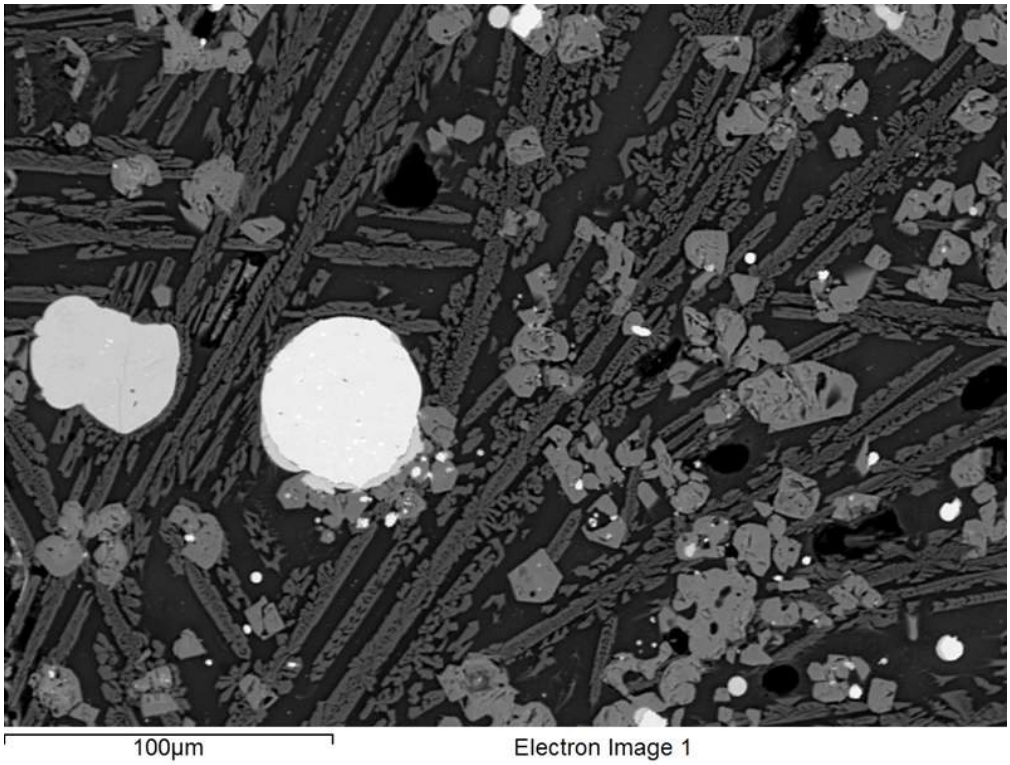

Figure 5.24: Cu_2S-prill on the far left and bronze prill (undissolved Pb-droplets) in the centre, fayalitic slag zone of sample 94_0560 (long chains, dark grey: fayalite; medium grey: magnetite)

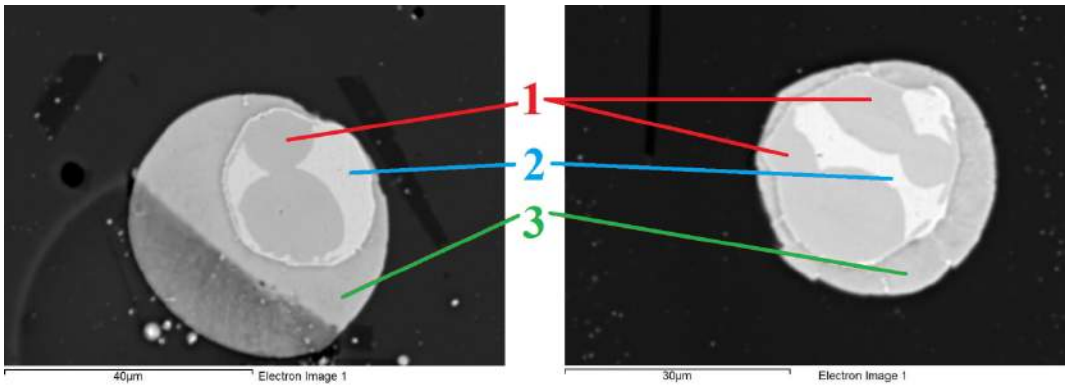

Figure 5.25: Two iron-rich prills in sample 86_0749c (three phases described on p. 130)

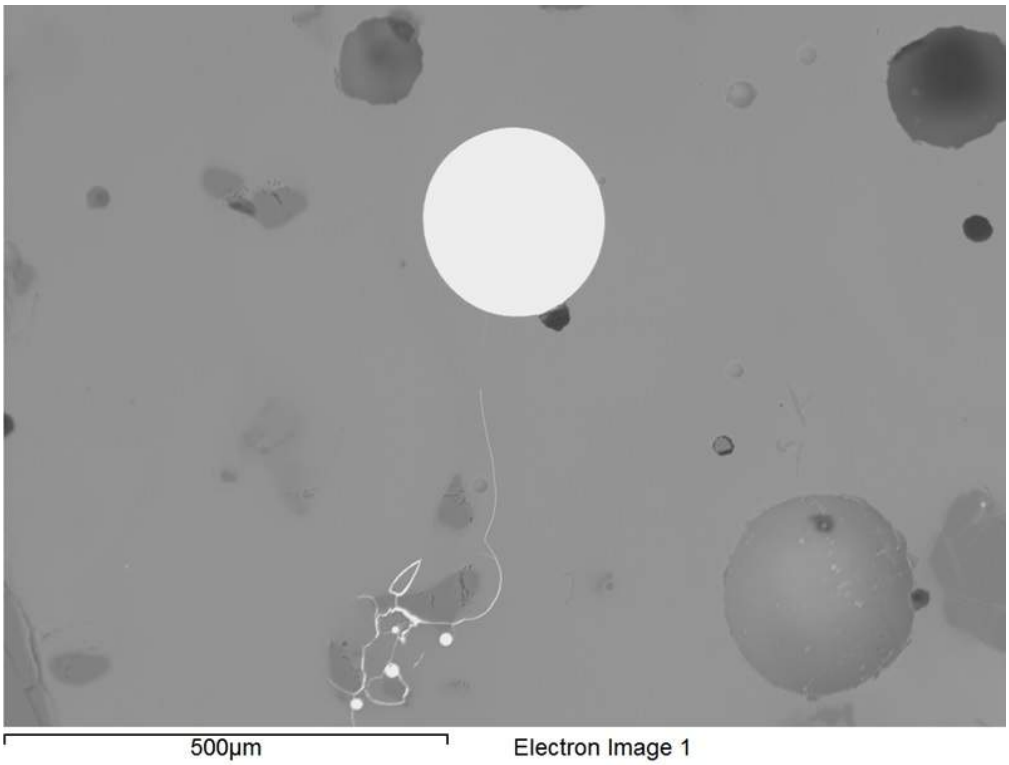

Figure 5.26: Gold-rich prill in sample 86_0749c

5.2.5 Charcoal and fuel ash

In situ production remains show that air was blown into the crucibles by tuyères from above, into a charcoal cover. This charcoal functioned both as fuel, producing heat to melt the charge, and as a reducing agent (Horne, 1982; Rehren, 1997a). A number of charcoal fragments from Pi-Ramesse have been analysed by M. Fischer (unpublished). Fragments from within the QI batteries are mainly acacia, and some fig sycamore[6]. Charcoal spread throughout the production levels is predominantly acacia, though some further species are represented. Charcoal remains are found embedded in the crucible slag in a number of samples, as shown in Figure 5.27. The pores of the charcoal in each of these examples shown are filled with Cu-(Fe-)silicate and light enrichment in CaO can be measured in some cases. During burning, this charcoal formed a fuel ash, which is typically enriched in lime (CaO), alkali (e.g., MgO and K_2O) and P_2O_5 (Evans and Tylecote, 1967; Misra *et al.*, 1993; Rovira, 2007; Tylecote, 1982b; Wood, 2009). This fuel ash acts as a flux for the ceramic, lowering its melting temperature and promoting slag formation, and enriching the slag in these elements. Figure 5.11 shows the change (between ceramic and slag) in the

[6]Charred fruit pits have been found within the batteries and larger area. These are most likely not intended as fuel, but might reflect workmen eating fruit and subsequently spitting pits into the fire.

ratios of CaO, MgO, P_2O_5, K_2O, Na_2O and SiO_2 to Al_2O_3 (correlation coefficients given in section 5.2.2).

Lime, potash and magnesia are the main constituents of fuel ash (Misra *et al.*, 1993, Table 4, p. 111) and should therefore be expected to show good correlation. This holds true for MgO, but not for K_2O. The reason for this is the dissociation of $K_2Ca(CO_3)_2$ and simultaneous volatilisation of K_2O formed after dissociation at about 900^0C (Misra *et al.*, 1993). As crucible temperatures reach around 1200^0C, potash is volatilised and does not contribute significantly to the fuel ash.

Phosphorus is a minor fuel ash component but, like magnesia, its abundance in fuel ash remains constant at higher temperatures and therefore is represented proportionally to lime in the crucible slag.

Silica and soda are usually only present in minor amounts, which could fit the minor increase seen here. Furthermore, SiO_2 is so abundantly (and variably) present in the ceramic, that any contributions can be expected to be small relative to background presence. Soda, however, does show some larger increases in a few samples.

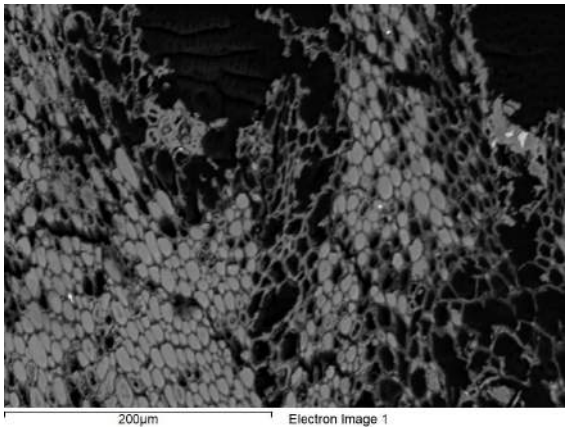

(a) Sample 83_0597l,01

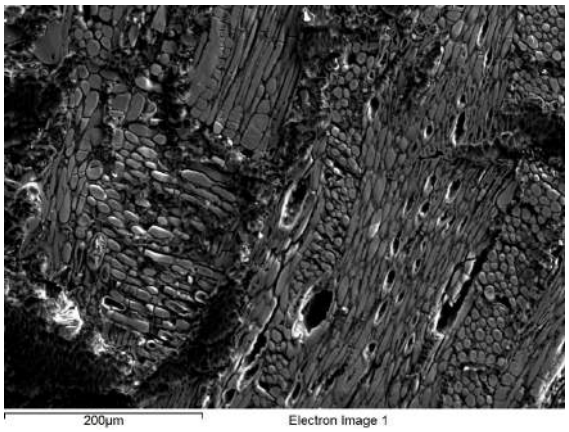

(b) Sample 87_0726,68-78b

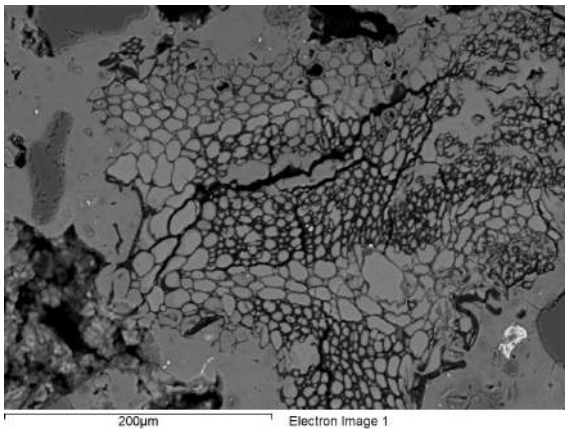

(c) Sample 97_0632D,01

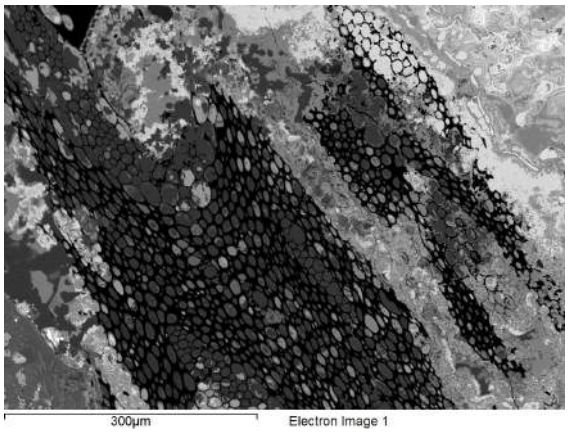

(d) Sample 94_0239,01

Figure 5.27: Charcoal

Section 5.3

Handheld XRF results

During the 2013 spring study season (May-June), the author took a handheld XRF-device (pXRF) to Qantir, Egypt, to study the full crucible assemblage in the excavation house. All crucible fragments were taken out of their find bags, visually inspected and described. Then, three measurements on the slag surface were taken with the pXRF. The goal of this study has been to acquire (qualitative) compositional data for the entire crucible assemblage. Given restrictions on sample export and the impracticality of studying 1042 samples by SEM-EDS, pXRF is the most appropriate method to chemically investigate a full assemblage within a reasonable time-frame[7], in a non-invasive manner. The main disadvantages to this method are that it provides surface analysis only, and does not produce quantitative data. Therefore, it can never provide the detailed information presented in section 5.2. However, under many circumstances, such detailed analysis is not possible due to sampling, budget, time, and other restrictions. It is therefore a useful exercise to compare the results from section 5.2 to those obtained by pXRF.

Apart from this methodological exercise, the analysis of the full crucible assemblage has another use. If the broad trends, such as iron and cobalt enrichment, can be similarly observed using pXRF, an analysis of the full assemblage could provide a more accurate view of the distribution of these particular trends within the different contexts on site.

Section 5.3.1 offers a brief overview of the methodological approach, while in section 5.3.2, the results for the entire assemblage are presented and broad trends are discussed. Details on sample preparation and analytical protocol are presented in section 3.5.3.

5.3.1 Approach

The goal at Qantir has been to analyse the slag on all crucible fragments. However, five find bags encountered by the end of the campaign contained such large numbers (>100-200), that a representative selection[8] had to be made.

The slagged surface of 615 crucible fragments was analysed, corresponding to 1834 measurements, out of a total of 1042 crucible fragments. The results for each crucible (three

[7] The description of all 1042 fragments, including three pXRF measurements per fragment, was performed in six days (including delays caused by daily power failures and machine overheating).

[8] Representative selection: the total number of rim, body and spout fragments in each bag was counted and a proportional selection of samples from that bag was analysed.

measurements[9]) were then averaged. For the five large bags which were 'sub-sampled', the results were proportionally multiplied to achieve the same number of measurements as there were fragments in the bags. This way, the results below represent a full sample of the assemblage (1042 fragments). Within this assemblage, 637 body fragments are present, 394 rim fragments and 11 spout fragments.

150 measurements of the ceramic fabric were made, which was expected to have fairly consistent chemical composition (see section 5.2), with exception of SiO_2 content, which is not measured by pXRF.

XRF typically does not allow reliable measurement of elements with atomic numbers lower than 11 (sodium) (Shackley, 2011). The three main chemical constituents of ceramic and slag, SiO_2, Al_2O_3 and CaO, are too light to be measured using a 40 kV beam intensity. To measure these elements, a method using two beams should be used (one 40 kV beam for heavy elements and a lower energy beam for lighter elements). As this doubles or triples measurement time, and metal content is the main interest for this research, this has been omitted. While the SEM-EDS provides fairly quantitative data on the chemical composition of ceramic and slag, pXRF clearly does not. Rather, the aim here is to focus on metal content.

The qualitative analysis of a full dataset, as proposed here, is intended to test groupings in composition that appeared in the analysis of forty-nine samples analysed by SEM-EDS, without requiring full quantitative data. The results are not translated into concentrations (wt%), as quantitative results cannot be expected here (Shugar, 2013). Comparison of peak intensities for different elements as a proxy for concentrations is dangerous for several reasons, such as element-dependent intensity, peak overlap etc. Therefore, each element is considered in isolation, taking into account overlap issues where relevant (see section 3.5).

For each element, intensities (in counts/second) are presented in tables (average, standard deviation, minimum, maximum, median, 25- and 75%-percentile) as well as histograms[10] for ceramic and slag. The slag data is additionally subdivided into body and rim fragments.

[9] Three measurements were taken on average; variation exists due to occasional failed measurements and tiny samples which received only one/two measurements

[10] For each element, the range of measured peak intensities was divided into 30 bins. For each of these bins, the number of samples with a peak intensity within that bin's range are shown. The range of the X-axis (intensity) shown in the figures in section 5.3.2, is kept constant for ceramic and slag. When the actual range for, e.g., ceramic is smaller than that occurring for slag, this results in narrower bins for ceramic. A note is made when more than 30 bins are used, which results in narrower bins.

The results for each separate fragment are not considered in isolation. Given the heterogeneity of crucible slag (see section 5.4.9), this approach is not useful. Rather, the strength of using pXRF lies in the analysis of large sample numbers, as argued in more depth in Chapter 13.

5.3.2 pXRF results

5.3.2.1 Titanium

The pXRF-results for titanium are given in Table 5.1 and shown in Figure 5.28.

	Ceramic	Slag	Slag - body	Slag - rim
Average	123	85	83	89
Std. dev.	21	21	21	21
Min	40	28	28	41
Max	197	162	162	152
Median	122	83	79	88
25%	114	70	68	72
75%	133	99	96	103

Table 5.1: Summary of pXRF results: titanium

Titanium content in the ceramic is higher than that in the slag; the content for body and rim fragments is similar. The full SEM-EDS data (Appendix C) equally show an average decrease of titanium content from ceramic (1.5 wt%) to slag (1.2 wt%), which points to a dilution effect as titanium is usually not a significant component of the crucible charge. When looking at the change in $^{TiO_2}/_{Al_2O_3}$ (see section section 5.2.2), a very small increase can be noted. This means that the dilution effect for titanium is slightly lower than for aluminium.

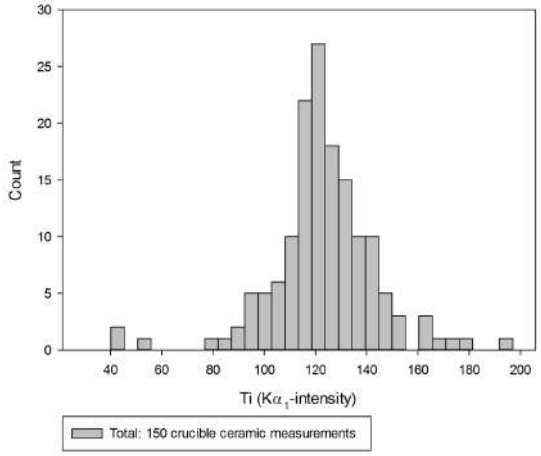

(a) Ceramic

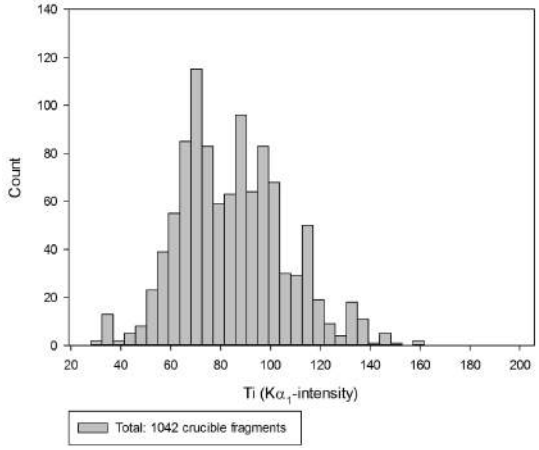

(b) Slag

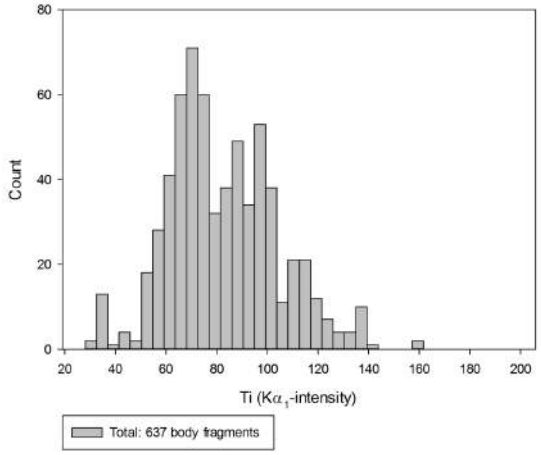

(c) Slag: body fragments

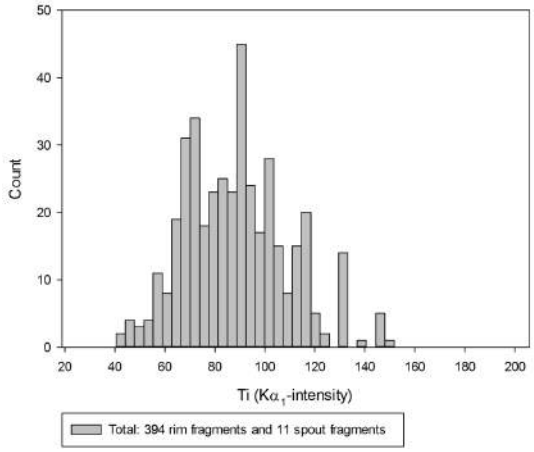

(d) Slag: rim fragments

Figure 5.28: pXRF: Titanium

5.3.2.2 Iron

The pXRF-results for iron are given in Table 5.2 and shown in Figure 5.29.

	Ceramic	Slag	Slag - body	Slag - rim
Average	5610	4689	4712	4653
Std. dev.	826	1444	1591	1178
Min	1990	1541	1541	1988
Max	7507	15705	15705	7937
Median	5600	4523	4553	4505
25%	5248	3793	3834	3769
75%	6016	5424	5434	5411

Table 5.2: Summary of pXRF results: iron

The iron content in the ceramic has a fairly normal distribution around an average of 5610 counts/s. This is higher than the average for slag (4689 counts/s), which however has a tail of high values. This lowered iron content in the slag is again a dilution effect, similar to that seen for titanium. To properly assess the change in iron content, the ratio $^{FeO}/_{Al_2O_3}$ (see section 5.2.2) should be evaluated. However, aluminium is not measured by pXRF. As an alternative, titanium, which undergoes a dilution effect similar to aluminium, can be used: the trends obtained for $^{FeO}/_{Al_2O_3}$ in section 5.2.2 have been identically reproduced by looking at the ratio $^{FeO}/_{TiO_2}$ for the SEM-EDS data (results omitted).

Table 5.3 and Figure 5.30 show the ratios of peak intensities measured for iron and titanium. From these results, the same trend seen in the SEM-EDS data emerges: there is an increase of iron relative to titanium in the slag compared to the ceramic. However, the increase is not a general trend for all crucible slag: there are two populations present in the crucible slag.

The ceramic shows a neatly, normally distributed Fe/Ti-ratio, with an average of 46 counts/s and a maximum of 56 counts/s. For the slag, $\pm^2/_3$ of the population (711/1042 fragments, 68%) have a value falling within the normal ceramic range (i.e., no significant iron enrichment). The other fragments (331/1042, 32%), however, have increased Fe/Ti-ratios. This observation corresponds very well with that made for the SEM-EDS data and verifies the trend seen there.

Figure 5.31 shows a scatter of Fe- vs Ti-intensity for both ceramic and slag, which illustrates the same trend: ceramic (red) has a normally distributed ratio of Fe to Ti, and $\pm^2/_3$ of the slag (blue) falls along that line, while $\pm^1/_3$ of the slag shows elevated Fe/Ti.

As Table 5.3 and Figure 5.32 show, iron enrichment occurs both in body and rim fragments,

but stronger enrichment tends to occur in body fragments. This again verifies trends seen in the SEM-EDS data.

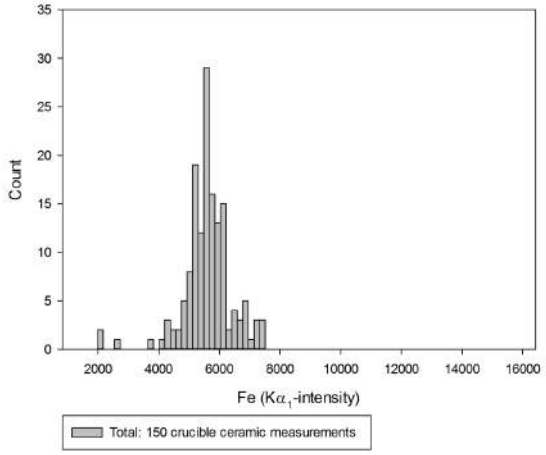

(a) Ceramic

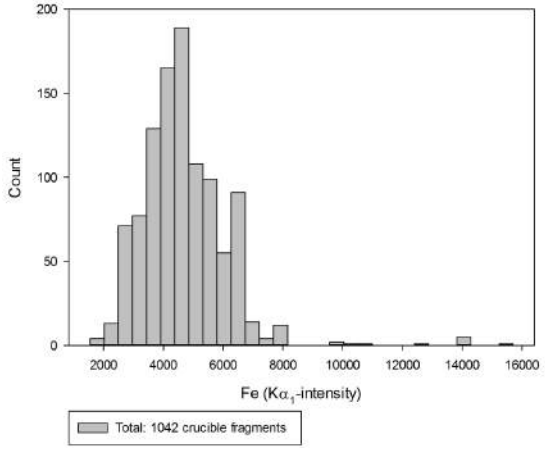

(b) Slag

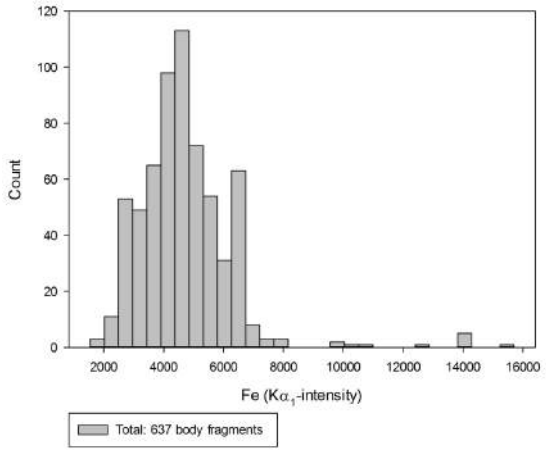

(c) Slag: body fragments

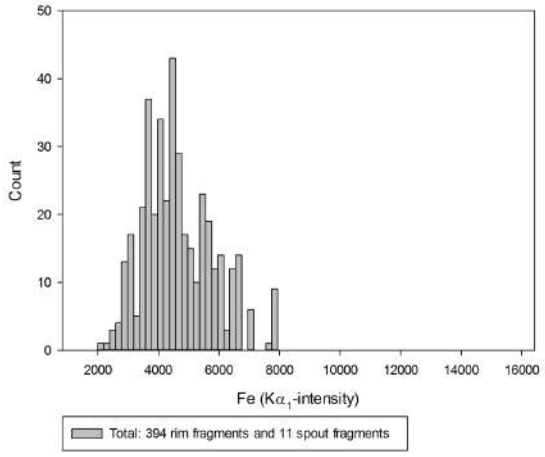

(d) Slag: rim fragments

Figure 5.29: pXRF: Iron

	Ceramic	Slag	Slag - body	Slag - rim
Average	46	56	59	53
Std. dev.	4	15	18	9
Min	36	26	26	33
Max	56	195	195	103
Median	46	52	53	51
25%	43	47	47	47
75%	48	60	64	56

Table 5.3: Summary of pXRF results: iron/titanium

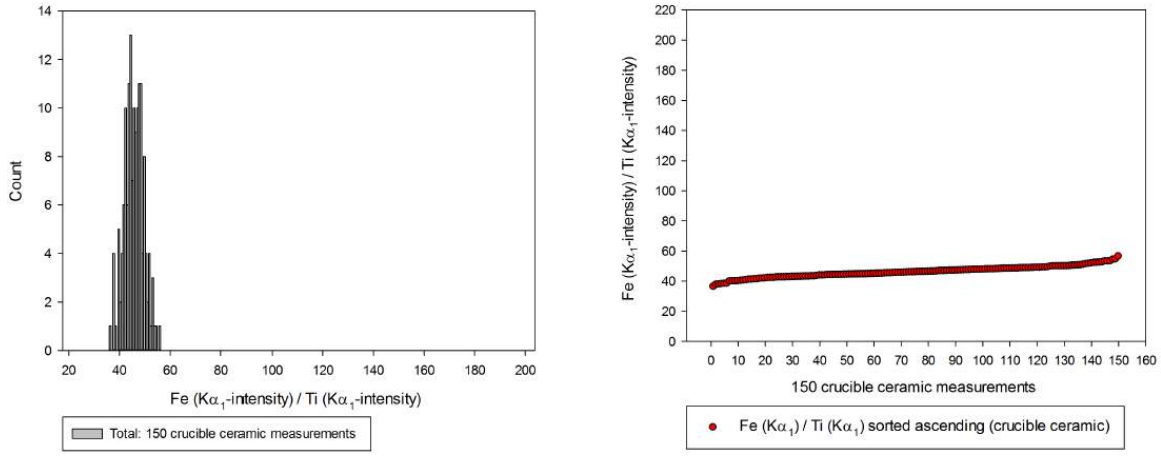

(a) Ceramic

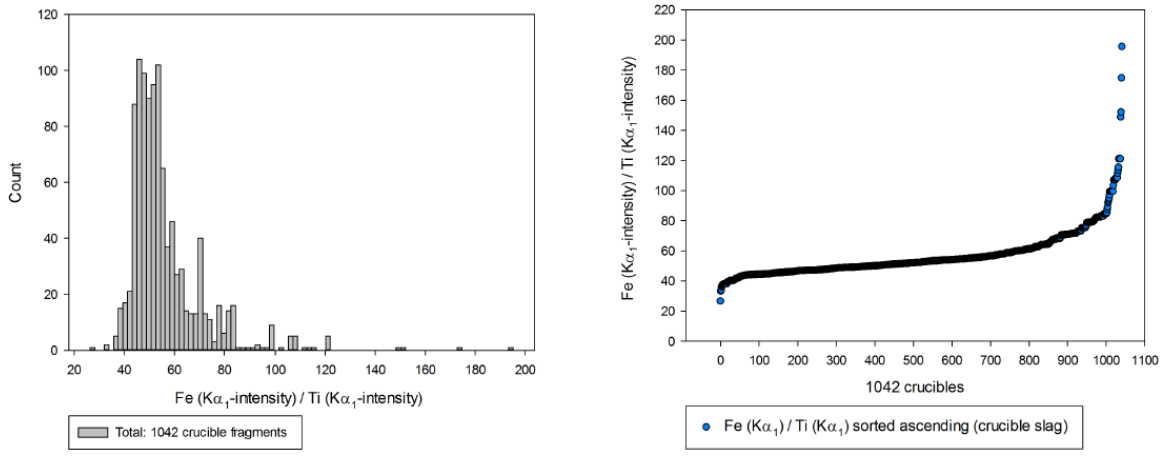

(b) Slag (narrow bins)

Figure 5.30: pXRF: Fe/Ti ratio ceramic and slag

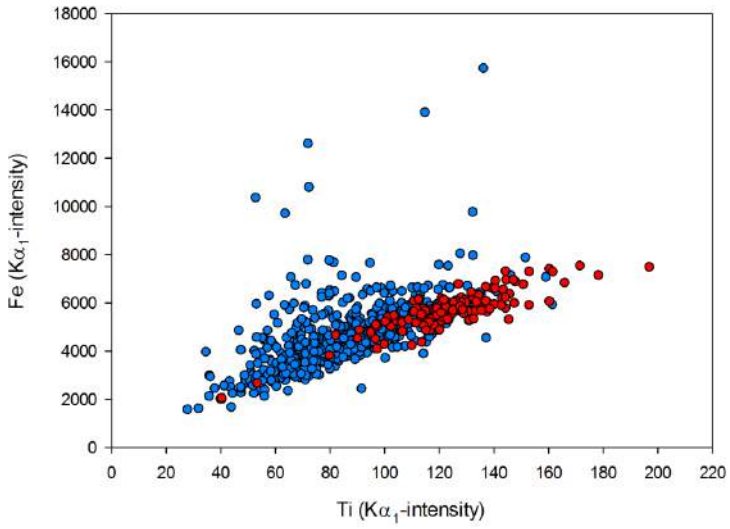

Figure 5.31: pXRF: Fe vs Ti, ceramic (red) and slag (blue)

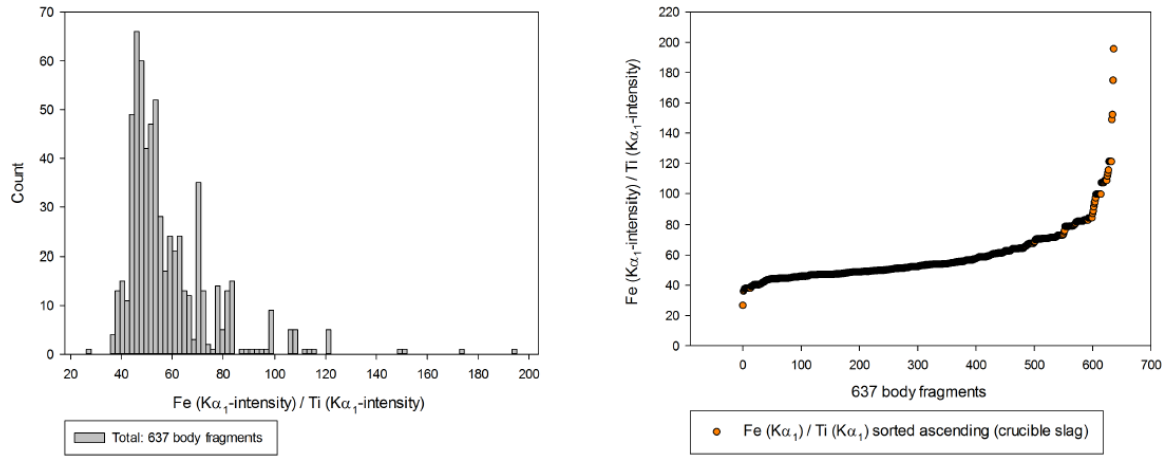

(a) Slag: body fragments

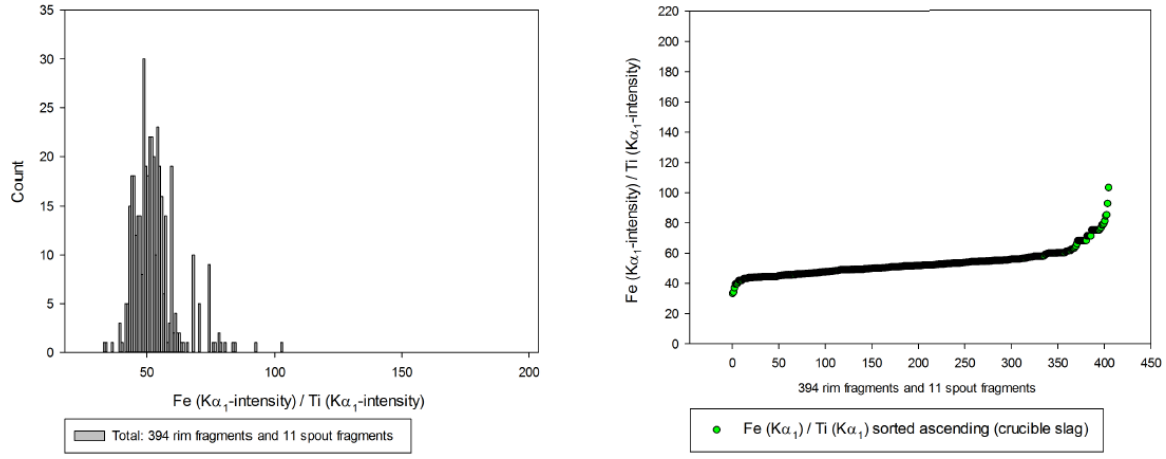

(b) Slag: rim fragments

Figure 5.32: pXRF: Fe/Ti ratio in slag (narrow bins)

5.3.2.3 Calcium

The pXRF-results for calcium are given in Table 5.4 and shown in Figure 5.33.

	Ceramic	Slag	Slag - body	Slag - rim
Average	173	303	304	301
Std. dev.	191	104	112	91
Min	87	67	67	117
Max	1597	806	806	771
Median	133	301	304	294
25%	117	228	224	235
75%	159	371	381	355

Table 5.4: Summary of pXRF results: calcium

Despite requiring a lower intensity beam to achieve more reliable results, the 40 kV beam generates some response in the calcium energy range which is worth examining (bearing in mind that this is less dependable than results for heavier elements). With the exception of three outliers (not visible in histogram), calcium content in ceramic is fairly low when compared to that in slag, corresponding to an average calcium enrichment of crucible slag.

Again, the ratio of calcium to titanium can be calculated to remove dilution effects. The results are shown in Table 5.5 and Figure 5.34, and show the relative increase of the crucible slag in lime more strongly. The effect is slightly higher in body fragments when compared to rim fragments.

This agrees well with SEM-EDS results, and reflects the increase in lime due to fuel ash contributions to the crucible slag.

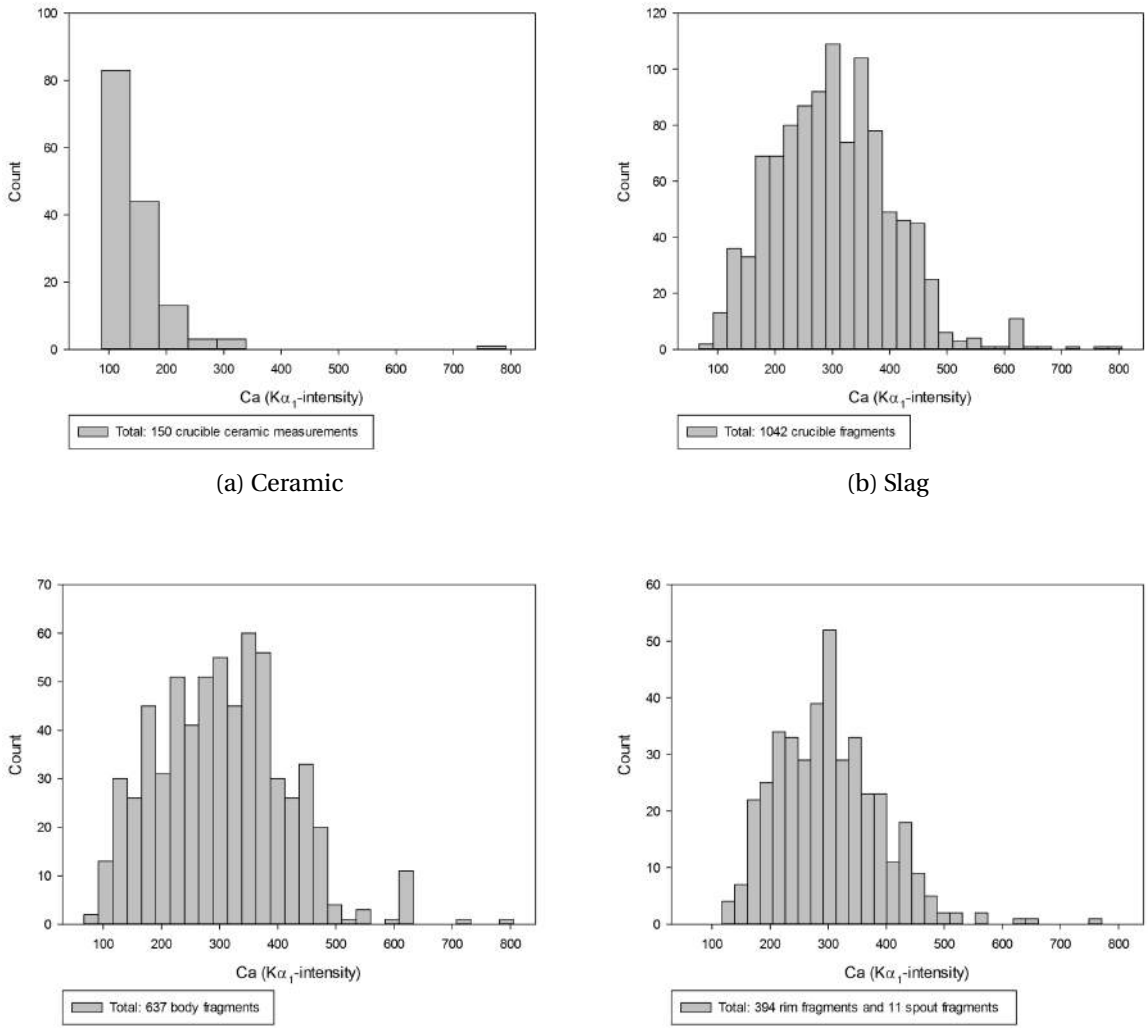

(a) Ceramic

(b) Slag

(c) Slag: body fragments

(d) Slag: rim fragments

Figure 5.33: pXRF: Calcium

	Ceramic	Slag	Slag - body	Slag - rim
Average	1.2	3.7	3.9	3.6
Std. dev.	0.6	1.5	1.6	1.3
Min	0.7	0.8	0.8	1.2
Max	6.5	14.5	14.3	14.5
Median	1.1	3.6	3.7	3.5
25%	0.9	2.7	2.8	2.7
75%	1.3	4.4	4.6	4.1

Table 5.5: Summary of pXRF results: Ca/Ti

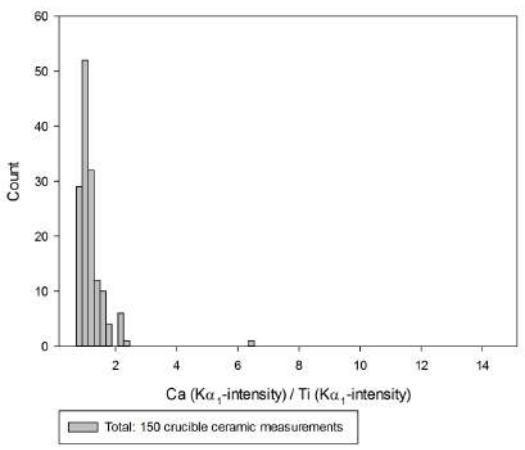

(a) Ceramic

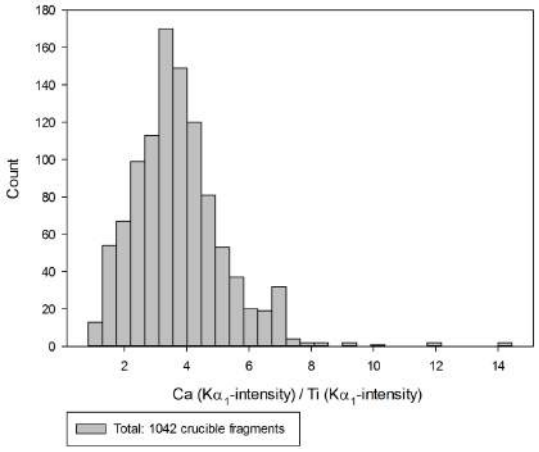

(b) Slag

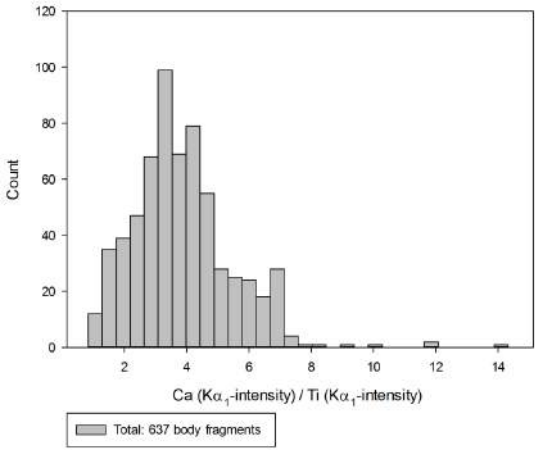

(c) Slag: body fragments

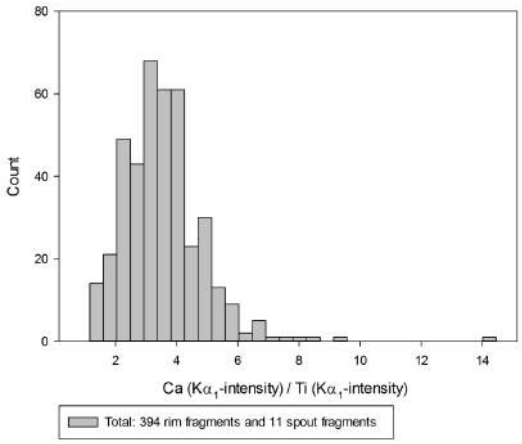

(d) Slag: rim fragments

Figure 5.34: pXRF: Ca/Ti

5.3.2.4 Strontium

The pXRF-results for strontium are given in Table 5.6 and shown in Figure 5.35.

	Ceramic	Slag	Slag - body	Slag - rim
Average	215	297	291	307
Std. dev.	53	105	110	96
Min	128	52	52	107
Max	417	651	651	622
Median	210	281	276	302
25%	179	225	208	237
75%	242	368	368	362

Table 5.6: Summary of pXRF results: strontium

Strontium content in the ceramic is lower than that in slag, both for body and rim fragments (slightly higher). Due to its high Kα_1 characteristic energy, strontium is not measured by SEM-EDS at 20 kV accelerating voltage, so results cannot be compared.
Again, the ratio of strontium to titanium is calculated to remove dilution effects. This better reveals the relative increase of the crucible slag in strontium (Table 5.7 and Figure 5.36). The effect is slightly higher in body fragments compared to rim fragments.
As Figure 5.37 shows, strontium- and calcium-increase in the crucible slag correlate well, indicating a similar origin: fuel ash (Freestone *et al.*, 2003; Pierce *et al.*, 1998; Wedepohl and Simon, 2010; Wedepohl *et al.*, 2011).

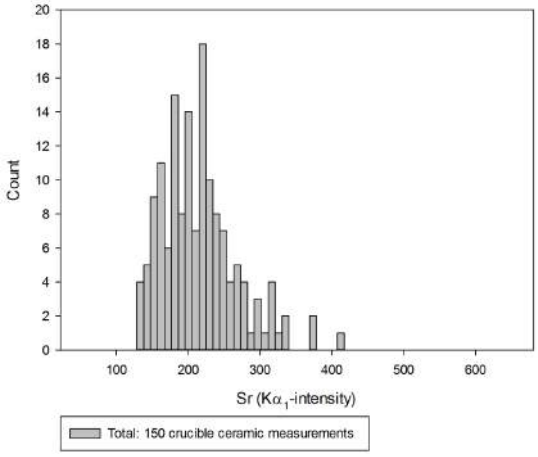

(a) Ceramic

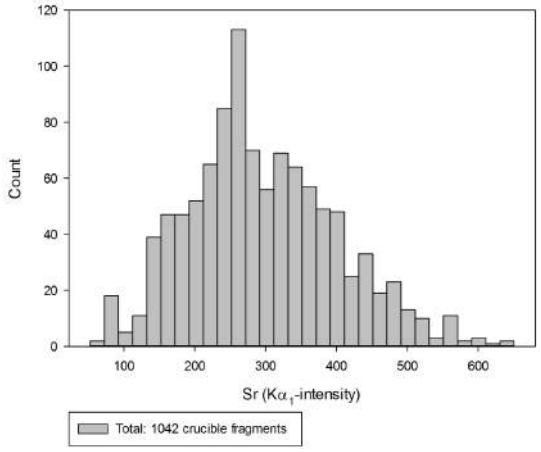

(b) Slag

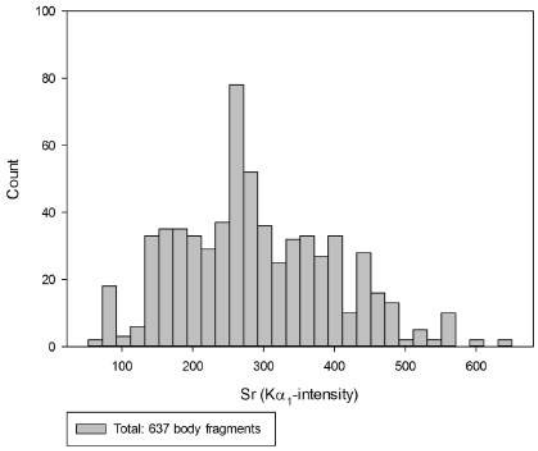

(c) Slag: body fragments

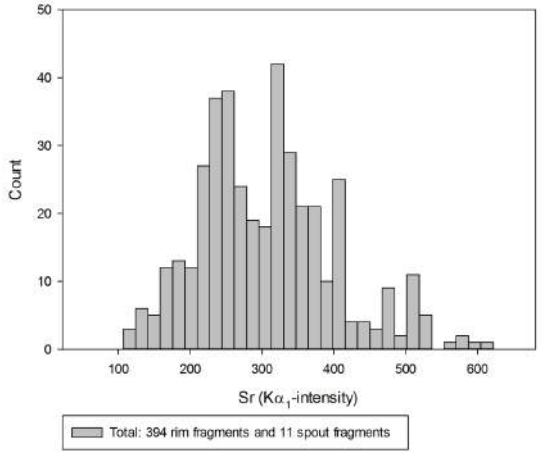

(d) Slag: rim fragments

Figure 5.35: pXRF: Strontium

	Ceramic	Slag	Slag - body	Slag - rim
Average	1.8	3.6	3.7	3.6
Std. dev.	1.0	1.3	1.4	1.3
Min.	1.0	1.0	1.0	1.2
Max.	9.4	8.6	8.6	8.2
Median	1.7	3.6	3.7	3.4
25%	1.4	2.5	2.5	2.6
75%	2.0	4.4	4.5	4.3

Table 5.7: Summary of pXRF results: Sr/Ti

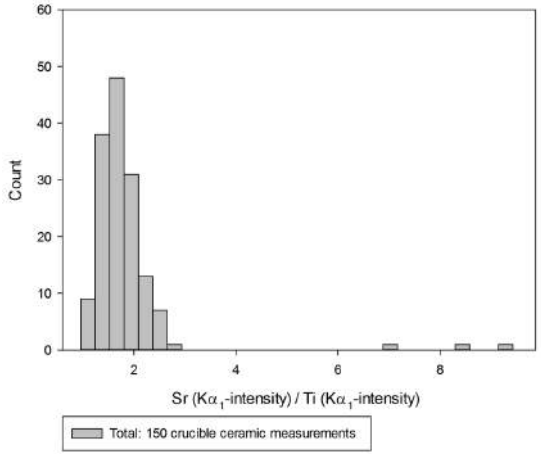

(a) Ceramic

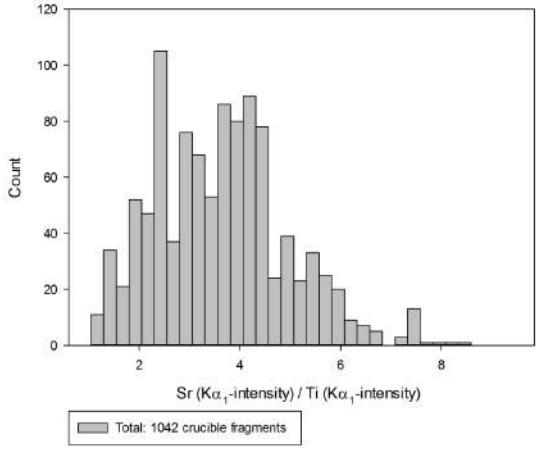

(b) Slag

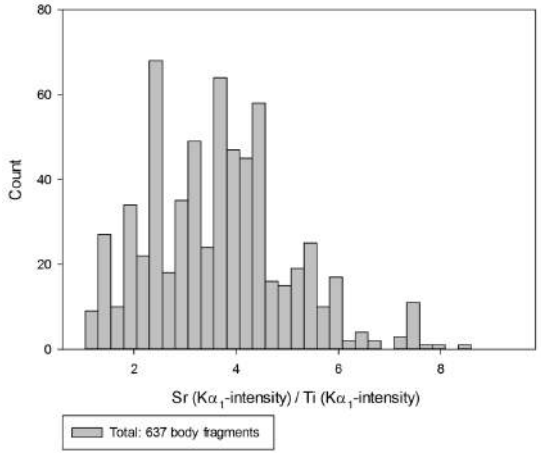

(c) Slag: body fragments

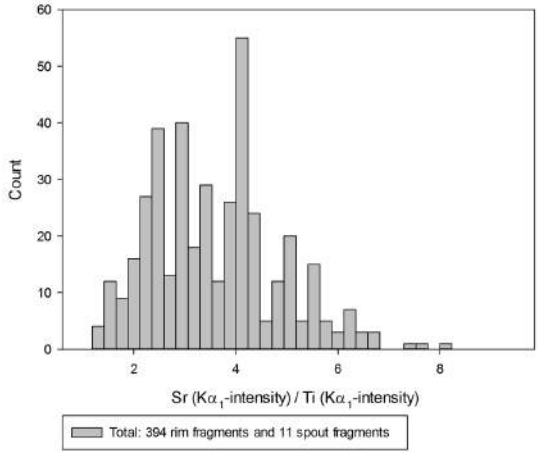

(d) Slag: rim fragments

Figure 5.36: pXRF: Sr/Ti

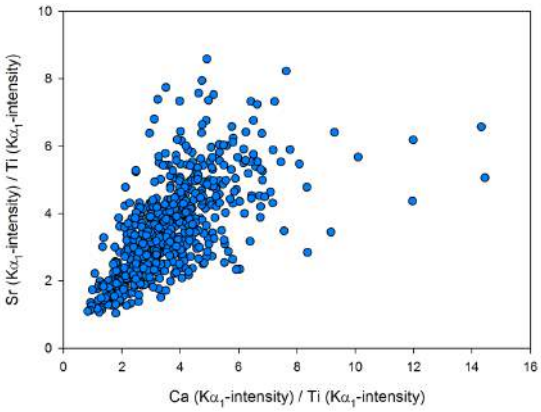

(a) Slag

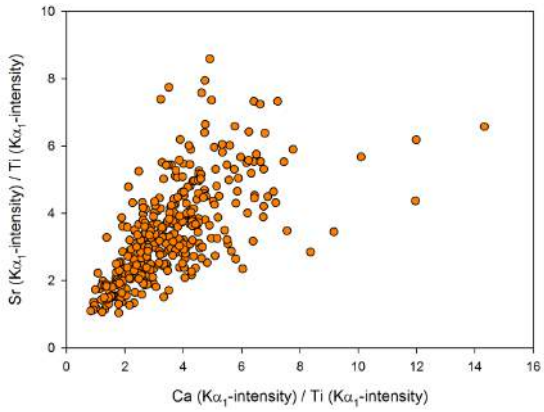

(b) Slag: body fragments

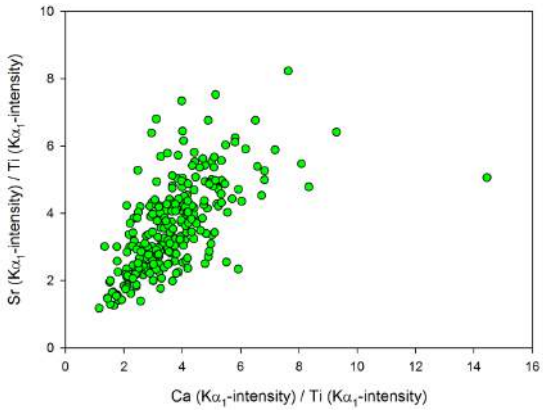

(c) Slag: rim fragments

Figure 5.37: pXRF: Strontium vs calcium

5.3.2.5 Copper

The pXRF-results for copper are given in Table 5.8 and shown in Figure 5.38.

	Ceramic	Slag	Slag - body	Slag - rim
Average	149	2207	2711	1414
Std. dev.	108	3022	3438	1971
Min	22	20	20	25
Max	656	27272	27272	13187
Median	135	1109	1487	626
25%	68	458	473	400
75%	191	2942	3720	1701

Table 5.8: Summary of pXRF results: copper

The copper measured in the ceramic is low, but present. Close inspection of the spectra shows that there is a very small peak for 8.046 keV, which cannot be attributed solely to the spectrum background. As copper is not expected to be naturally present in Nile Silt (Allen *et al.*, 1989; Bourriau *et al.*, 2006; Redmount and Morgenstein, 1996), this peak can probably be explained as a surface contamination from the sample bag, within which copper corrosion products are often visible as green dust.
Copper content in the crucible slag varies greatly. This is due to both the varying abundance of copper between different crucibles (trapping effect) and within crucibles (sampling effect). The trend seen here corresponds well to that seen in section 5.2.2. There is a markedly higher enrichment in copper noticeable for body fragments compared to rim fragments.

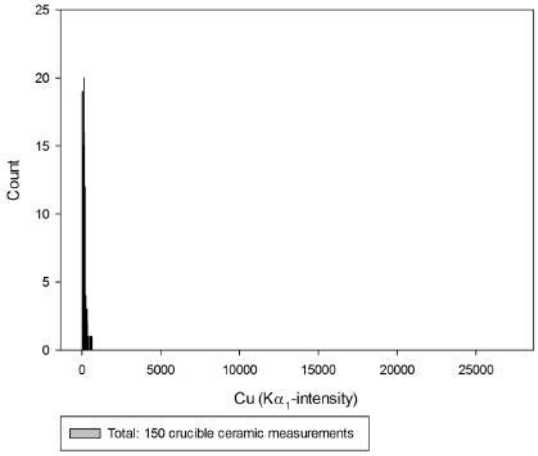

(a) Ceramic

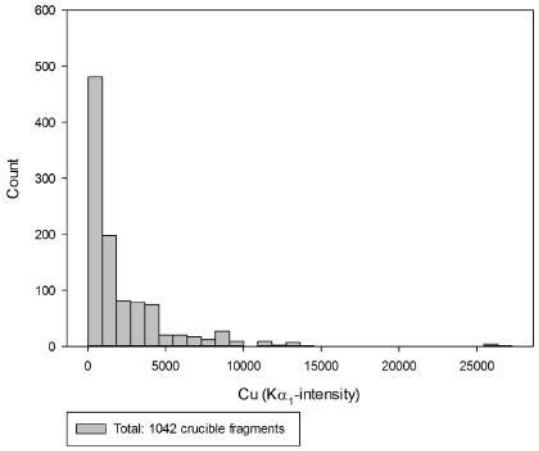

(b) Slag

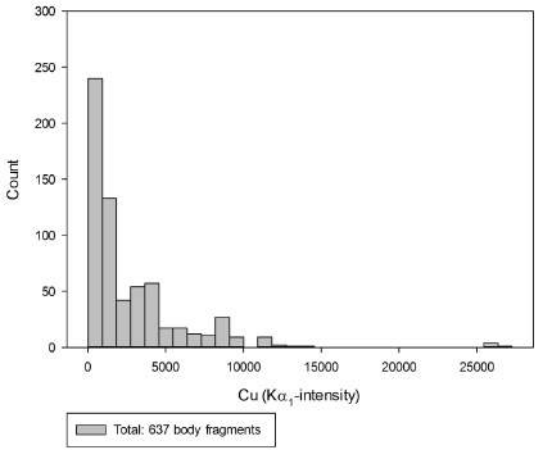

(c) Slag: body fragments

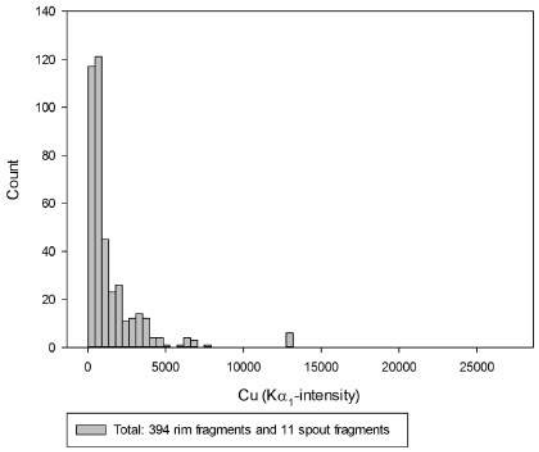

(d) Slag: rim fragments

Figure 5.38: pXRF: Copper

5.3.2.6 Tin

The pXRF-results for tin are given in Table 5.9 and shown in Figure 5.39.

	Ceramic	Slag	Slag - body	Slag - rim
Average	219	1280	1561	838
Std. dev.	33	1382	1578	828
Min	161	110	110	137
Max	315	7630	7630	5223
Median	215	676	930	538
25%	192	255	295	248
75%	239	1859	2492	1028

Table 5.9: Summary of pXRF results: tin

The tin measured in the ceramic is low, and closer inspection of the XRF-spectra shows that the background has an average value of ±200 counts/s in the 25 kV range. This means tin is practically absent in the spectrum, which is in agreement with Allen *et al.* (1989); Bourriau *et al.* (2006); Hancock *et al.* (1986); Redmount and Morgenstein (1996) and implies that tin contamination from the sample bag is not as important as copper contamination.

The amount of tin present in crucible slag varies greatly. This is due to both the varying abundance of tin between different crucibles (trapping effect) and within crucibles (sampling effect). The trend seen here corresponds well to that seen in section 5.2.2. There is a markedly higher enrichment in tin noticeable for body fragments compared to rim fragments.

As Figure 5.40 shows, most crucibles show limited copper and tin enrichment. For higher enrichments, there is little correlation between copper and tin: some crucibles are more enriched in copper, others more in tin and others yet in both. A similar trend is seen in Figure 5.18.

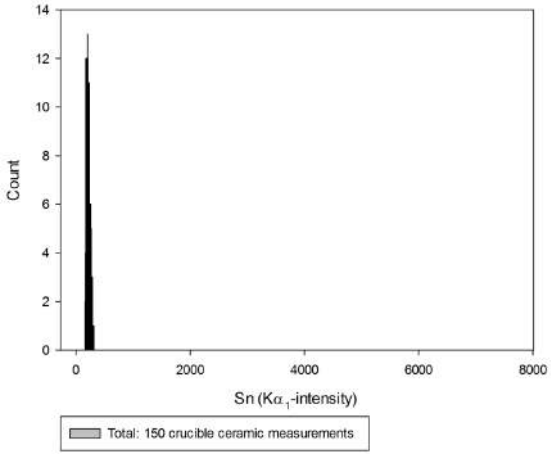

(a) Ceramic

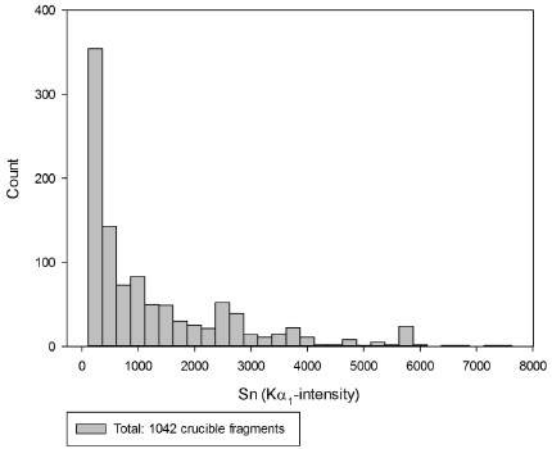

(b) Slag

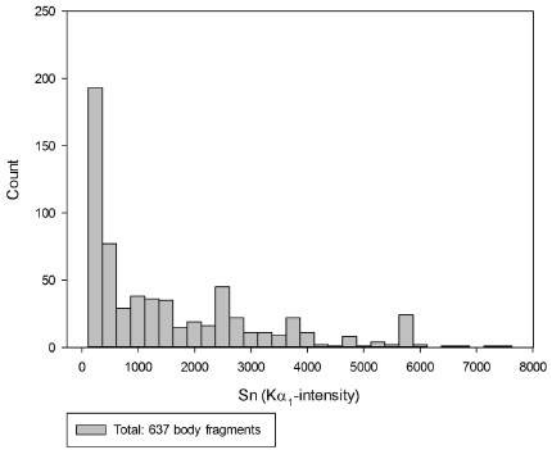

(c) Slag: body fragments

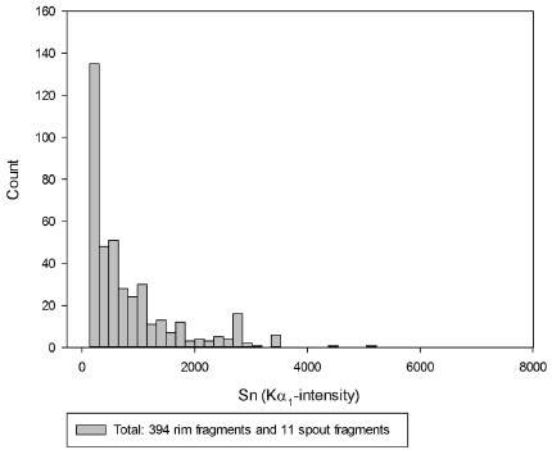

(d) Slag: rim fragments

Figure 5.39: pXRF: Tin

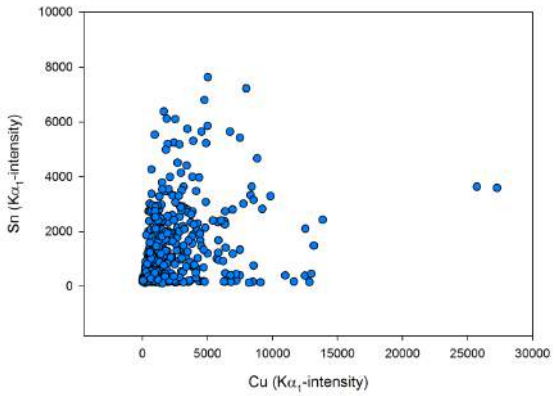

(a) Slag

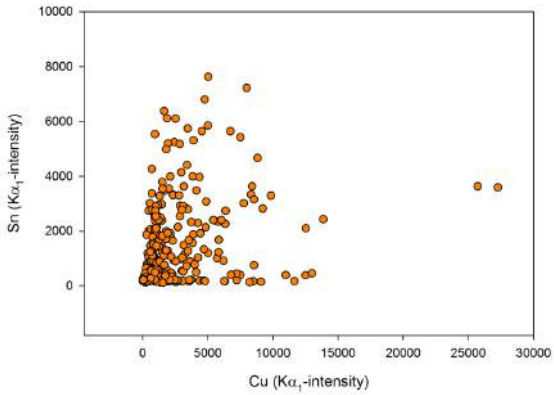

(b) Slag: body fragments

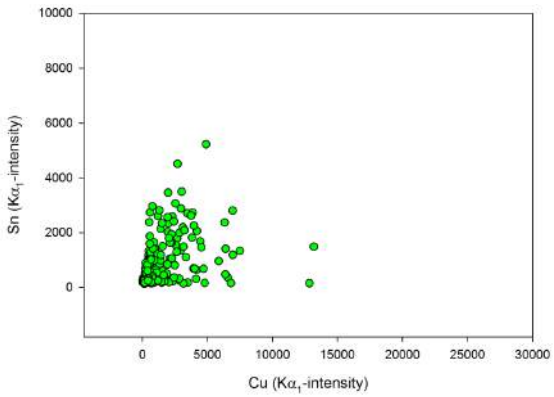

(c) Slag: rim fragments

Figure 5.40: pXRF: Copper vs tin

5.3.2.7 Cobalt

The pXRF-results for cobalt are given in Table 5.10 and shown in Figure 5.41.

	Ceramic	Slag	Slag - body	Slag - rim
Average	57	117	143	77
Std. dev.	12	162	193	78
Min	17	19	19	22
Max	89	2748	2748	906
Median	58	65	74	58
25%	51	48	51	46
75%	65	115	148	76

Table 5.10: Summary of pXRF results: cobalt

Cobalt is measured in very low values in the ceramic. Though Allen *et al.* (1989); Bourriau *et al.* (2006) report trace levels of Co naturally present in Nile Silt (±10-30 ppm), these are probably below the detection limit here as the Kα_1 line for cobalt (6.931 keV) is largely overshadowed by the Kβ_1 line of iron (7.058 keV). This influence of cobalt on the iron Kβ_1-peak is illustrated in Figure 5.42. It appears that, when no significant cobalt is present, the $K\alpha_1/K\beta_1$-ratio lies between 8 and 11. When significant cobalt is present, this ratio drops below 8. Using this rough cut-off value, 11.6% of the population (121/1042 fragments) shows elevated cobalt content in the slag.
This result compares fairly well to the SEM-EDS data (section 5.2.2), where (bulk) cobalt enrichment was measured in approximately 12.2% (6/49) of the samples.
As mentioned in Appendix D.5, cobalt actually occurs in nine samples (±18% of population), while only causing a noticeable increase of bulk CoO content in six. There is, then, a 'nugget-effect'[11] to detecting cobalt in crucible slag, as well as an attenuation effect effectively 'hiding' deeper-lying cobalt from detection by this surface-analysis. By looking at the non-averaged pXRF-measurements and counting single cobalt occurrences rather than bulk/averaged contents, an average of 13.8-17% of the fragments can be said to contain cobalt.

[11]This 'nugget"-effect is similarly important to the measurement of copper and tin in a sample, impeding direct comparison between pXRF and SEM-EDS results for a single crucible fragment, as further discussed in Chapter 13.

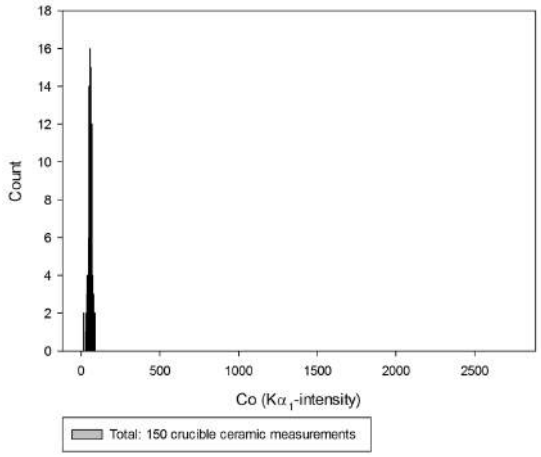

(a) Ceramic

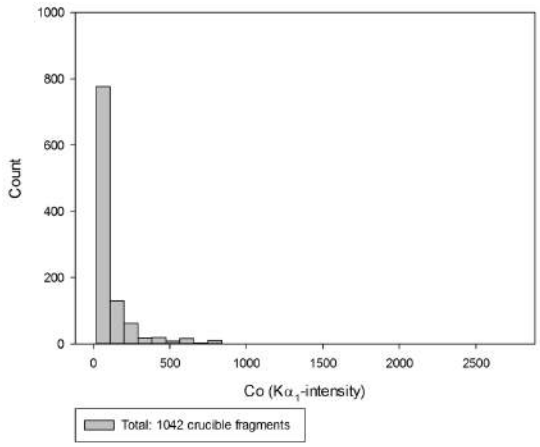

(b) Slag

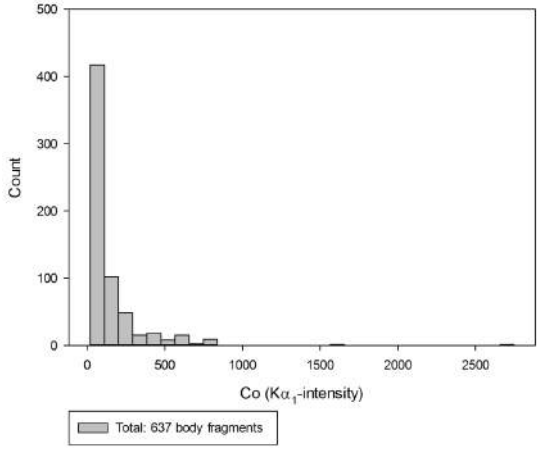

(c) Slag: body fragments

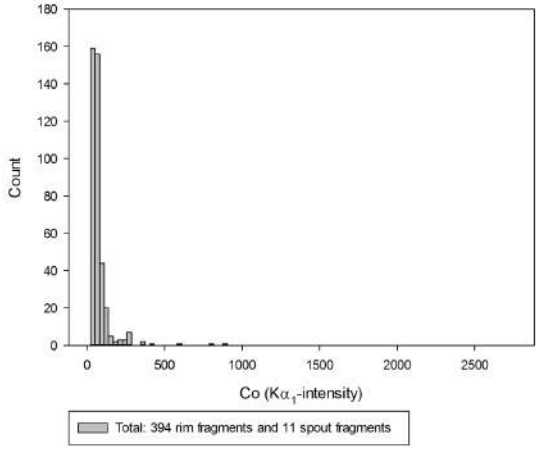

(d) Slag: rim fragments

Figure 5.41: pXRF: Cobalt

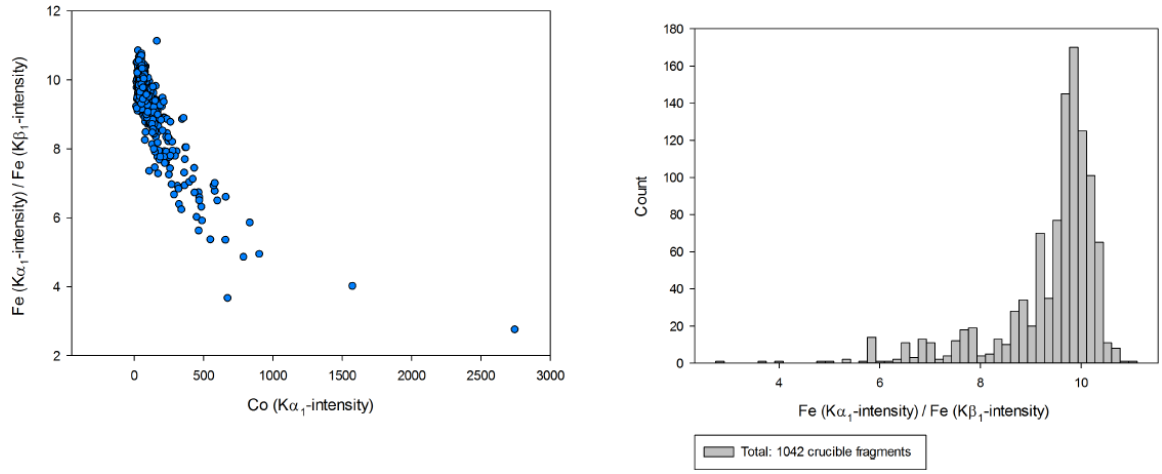

(a) Slag

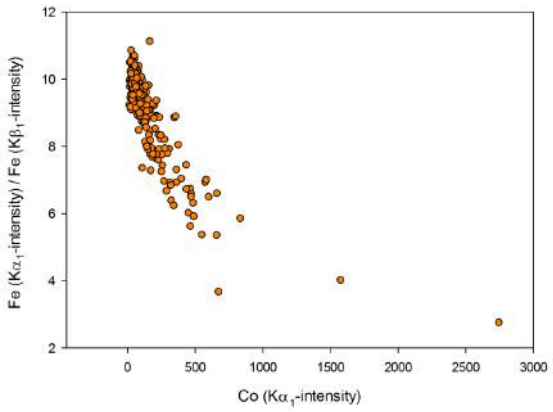

(b) Slag: body fragments

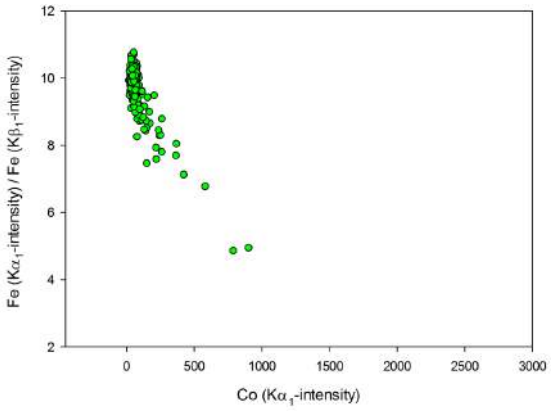

(c) Slag: rim fragments

Figure 5.42: Influence of cobalt on secondary iron peak

5.3.2.8 Lead and arsenic

The pXRF-results for lead are given in Table 5.11 and shown in Figure 5.43; for arsenic they are given in Table 5.12 and shown in Figure 5.44.
Given the very close proximity of the Pb-Lα_1 (10.551 keV) and As-Kα_1 (10.544 keV) lines, the presence of these two elements is difficult to disentangle. Evaluation of the secondary, lower-intensity lines (Pb-Lβ_1 (12.619 keV) and As-Kβ_1 (11.727 keV)) is necessary to interpret the actual presence of these elements. The problem here, though, is that while the Pb-Lβ_1-line has a similar characteristic intensity to the Pb-Lα_1-line, the As-Kβ_1-line has a much lower intensity (10% relative to As-Kα_1), resulting in lower sensitivity and more difficult quantification.
As Figure 5.45 shows, there are relative increases in both the Pb-Lβ_1 and As-Kβ_1 in the slag compared to the ceramic. The absolute increases are far more dramatic for lead and remain limited (not exceeding 70 counts/s) for arsenic. Furthermore, Figure 5.46 shows clearly that increases in Pb-Lα_1 are more tightly correlated to an increase in Pb-Lβ_1 than the increases between As-Kα_1 and As-Kβ_1. This suggests that the high counts/s measured at around 10.54-10.55 keV should be mainly attributed to lead. A minor presence of arsenic, however, cannot be excluded based on this data.

Lead content is not reported in the NAA results of Allen *et al.* (1989) and Bourriau *et al.* (2006). Based on the pXRF data shown here, it appears that there is lead naturally present in Nile Silt (trace levels).
For a number of fragments, an increased lead content is measured in the slag (though determining a cut-off value is difficult here). This was not revealed by SEM-EDS, which has fairly high detection limits for lead content when using an excitation voltage of 20 kV. It should be kept in mind here that even trace levels of lead in the metal charge can lead to elevated lead contents in the slag when measured by XRF (Dungworth, 2000a; Kearns *et al.*, 2010). Though some lead might have been present in the crucible charge of a number of crucibles (some prills analysed by SEM-EDS show undissolved lead), its limited contribution to the crucible slag suggest that it was probably present as a (copper) contaminant rather than being added as a separate alloying ingredient to produce leaded bronze. This is confirmed by object analysis presented in section 5.5. From these pXRF results, some lead presence can be suggested for ±15% of all crucibles, represented by the high-lead (>400-500 counts/second) tail in Figure 5.43. This matches the SEM-EDS results (section 5.2.2), where ±15% of all samples exhibited increased bulk lead content in the crucible slag.

Small amounts of arsenic have been noted in a few prills by SEM-EDS, but not in the bulk

	Ceramic	Slag	Slag - body	Slag - rim
Average	16	179	157	212
Std. dev.	12	270	142	393
Min	3	3	3	7
Max	86	2549	1091	2549
Median	13	115	115	118
25%	9	56	61	51
75%	18	202	204	194

Table 5.11: Summary of pXRF results: lead

	Ceramic	Slag	Slag - body	Slag - rim
Average	15	166	146	197
Std. dev.	11	250	13	364
Min	3	5	5	6
Max	75	2359	1008	2359
Median	13	107	107	108
25%	9	52	57	46
75%	18	188	192	184

Table 5.12: Summary of pXRF results: arsenic

analysis. Here too, it seems most likely that arsenic was introduced as a copper contaminant, rather than being deliberately added as an alloying ingredient.

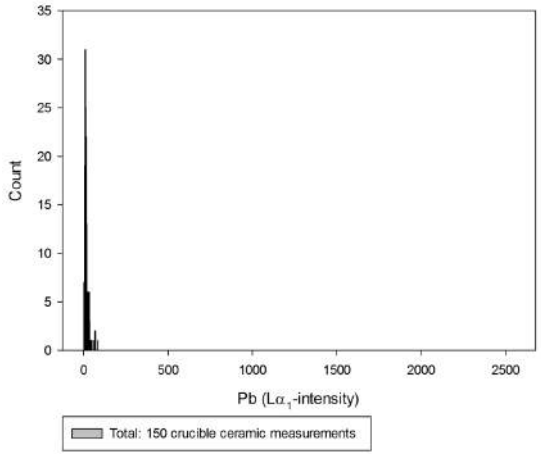

(a) Ceramic

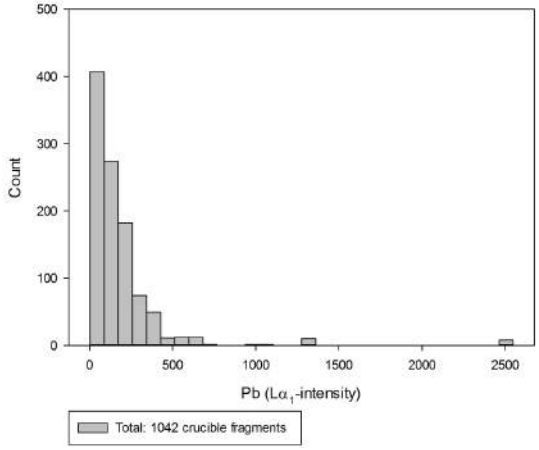

(b) Slag

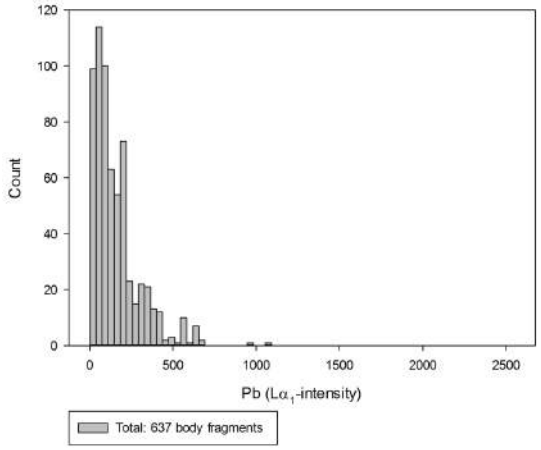

(c) Slag: body fragments

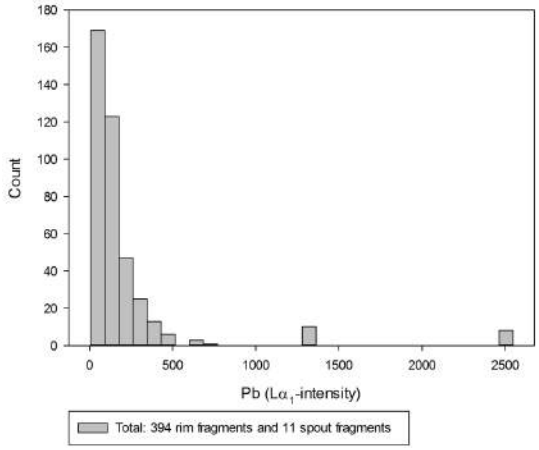

(d) Slag: rim fragments

Figure 5.43: pXRF: Lead

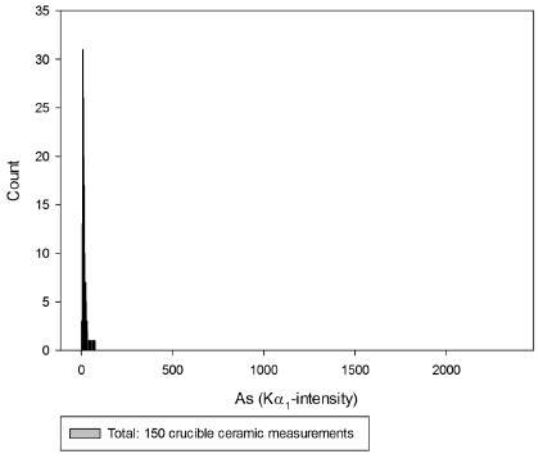

(a) Ceramic

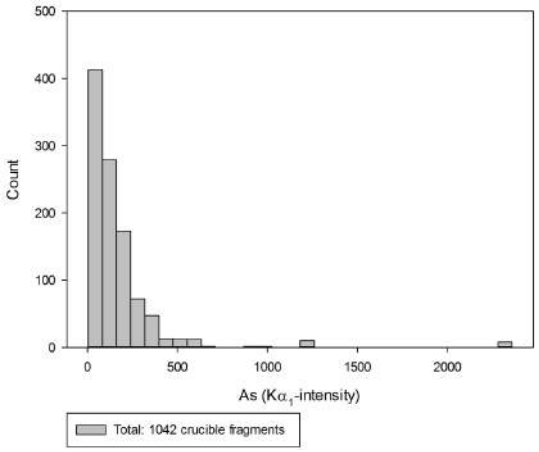

(b) Slag

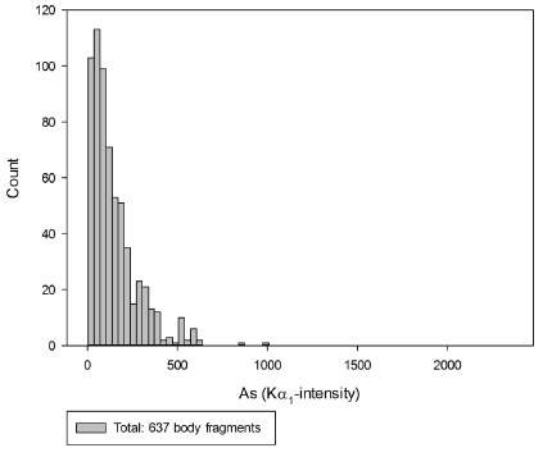

(c) Slag: body fragments

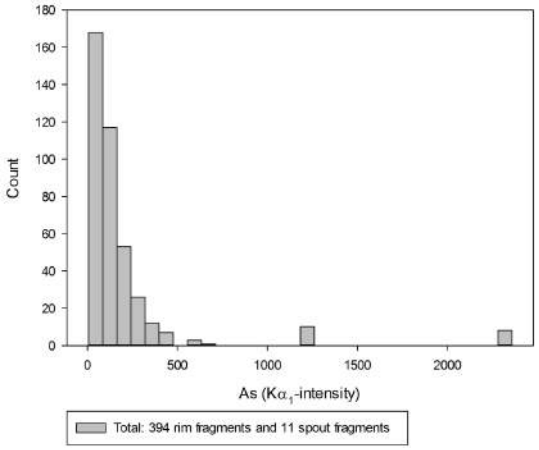

(d) Slag: rim fragments

Figure 5.44: pXRF: Arsenic

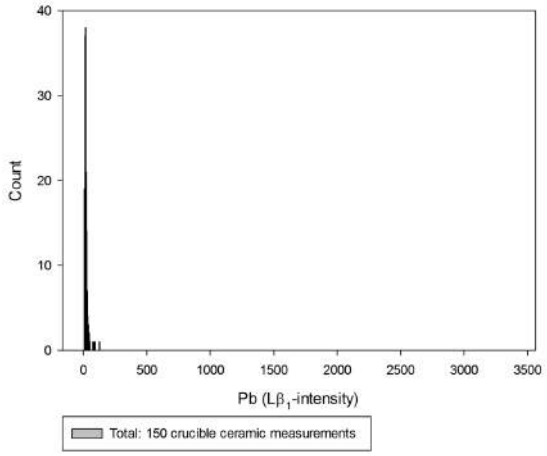

(a) Ceramic

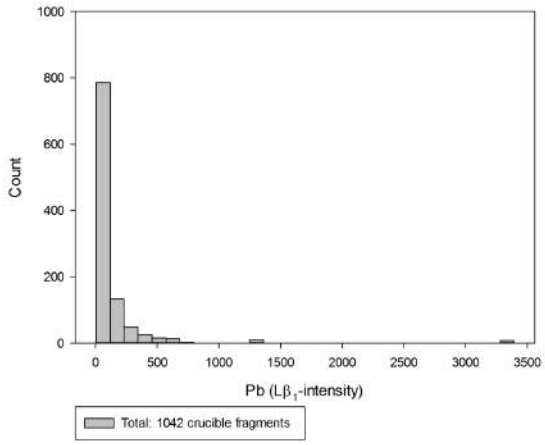

(b) Slag

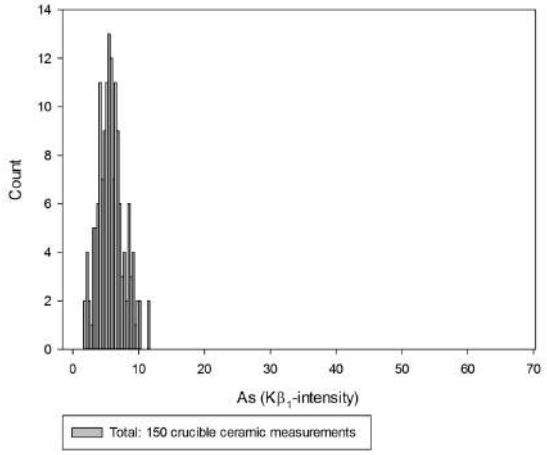

(c) Ceramic

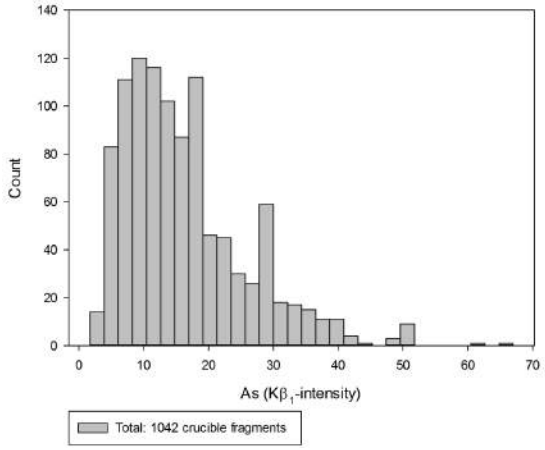

(d) Slag

Figure 5.45: pXRF: Secondary Pb and As peaks

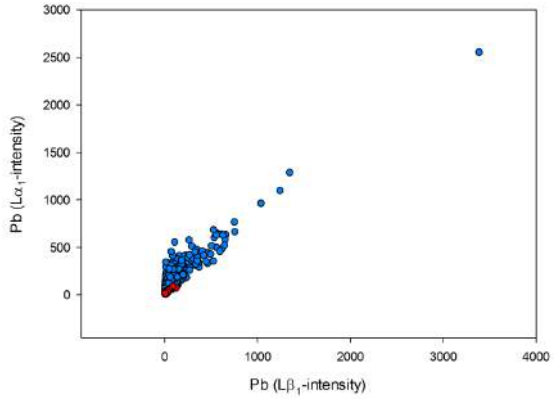

(a) Lead

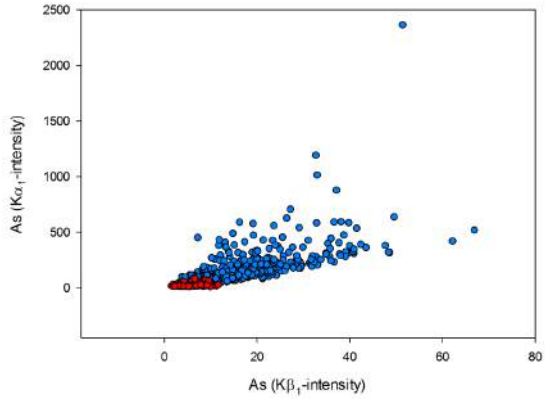

(b) Arsenic

Figure 5.46: pXRF: Primary vs secondary Pb and As peaks for ceramic (red) and slag (blue)

Section 5.4

Technical interpretation

5.4.1 Interpreting general crucible characteristics

General crucible characteristics, summarised in section 5.1, are further interpreted here.

Crucible wall thickness varies from 1 (rim) to 3 cm (lower body). Typically, three main parts are present in each section through a crucible wall: a fired ceramic part, a bloated transition zone and a slag part in which no ceramic structure remains. This structure is caused by internal heating of the crucible and occurs in all samples, though the extent of each zone varies between samples.

The ceramic zone is present in most samples, though sometimes the sample has lost all ceramic structure due to heating or, alternatively, the ceramic part has broken off along the bloated transition zone (acting as a perforated plane of weakness along which fractures can propagate easily). The thick, porous[12] ceramic acts as a thermal insulator (Hein and Kilikoglou, 2007; Hein *et al.*, 2007, 2013), allowing heat to be maintained inside the crucible. At the same time, its thickness and structure give the crucible mechanical strength: the temper-induced porosity impedes fracture propagation, while the quartz (which remains largely inert during the metallurgical process) reduces shrinkage, provides further strength and slows down disintegration at high temperatures (Freestone and Tite, 1986; Kilikoglou *et al.*, 1995, 1998).

The bloated transition zone is present in each analysed sample. The depth to which the slag zone penetrates the crucible wall varies, most likely due to changing operating conditions and duration, causing irregular slag zone thickness even within a crucible. In a few samples, barely any slag is present, which can reflect a lack of slag forming in some (areas of) crucibles or the slag breaking off from the crucible wall along the bloated zone.

Crucible edge fragments are often vitrified but, as they were most likely not in contact with the actual metal crucible charge, this 'slag' is mainly composed of ceramic and fuel ash contributions, and limited contamination from the charge. This contrasts with body fragments, where slag is composed of contributions from the ceramic, fuel ash and metal charge (and its contaminants). Clearly, rim fragments' slag reveals mainly fuel ash contributions, while body fragments are needed to reconstruct the metal charge.

[12] Porosity from burnt-out organic material and thermal expansion of silica

It should be emphasised here already that temperature and redox-conditions within crucibles often appear to be very heterogeneous. This can be highly problematic when only small crucible samples are available for study, as is the case here, because one fragment does not necessarily represent operating conditions throughout the crucible. This issue is less important when studying, for example, modern graphite crucibles or medieval mullite crucibles (Martinón-Torres *et al.*, 2006, 2008), which maintain more constant reducing conditions and barely participate in slag formation. In crucibles like those from Pi-Ramesse, however, operating conditions are far less homogeneous and the crucible interacts heavily with the charge. Therefore, the study of an assemblage of macroscopically similar crucible fragments (as is the case here) can yield variable results which should be interpreted as variations of the same process where possible. Some results, however, are not clearly related to variation of a single process and point to variations in technology and material use, as discussed further in the sections below.

Nearly all samples show evidence of metal being charged into the crucibles, with variable slag enrichment in copper and tin. It is therefore safe to say that these crucibles were primarily used to process bronze. Whether remelting, alloying or variations thereof were taking place, is discussed further below.

5.4.2 Aberrant crucible fragments

Before continuing the interpretation of the general assemblage, it should be noted that six fragments do not fit the general description given in section 5.4.1:

- Three fragments (1984_1171,0001 and 1987_1530a,0013-0014) are significantly thicker, larger and heavier than average, as shown in Figure 5.47. Though these fragments could represent the extreme end of the normal variation in crucible size, they are most likely outliers. Extrapolating from the fragments, these crucibles would have been very large ($\varnothing \approx \pm 30 - 40$ cm) and probably impossible to move when charged with metal. They may have been made for a particular purpose, though it is unclear which. The fragments are from the industrial area: fragment 1984_1171,0001 has unknown context, while fragments 1987_1530a,0013-0014 were found inside melting battery II (phase B/3a). These pieces show limited or no slagging, though a few copper prills are present on the interior surfaces.

- Two fragments (1992_0645b,0001-2), shown in Figure 5.48, seem to belong to a more shallow crucible type. Again, these could represent the extreme end of the normal

variation in crucible size, but are most likely outliers. Other fragments exhibiting a bent profile exist, but can reasonably be interpreted as variations of the 'normal' shape shown in Figure 5.1. These two fragments, however, exhibit a full profile, including a rim and an almost flat bottom, and therefore could represent a different crucible type. They belong to area QIV-i/28. Both fragments are slagged, but do not show deviant composition (measured by pXRF). Fragment 1992_0645b,0002 could be cobalt enriched.

- One fragment (1984_1264d) exhibits clear signs of repair and re-use. As Figure 5.49 shows, the original crucible had a typical profile, with a copper prill adhering to the rim (blue arrow). After its first use, a new layer of clay was applied over the rim (red arrow indicates boundary visible on exterior crucible surface, just below the original rim), extending the profile by 1-2 cm. The extent to which clay was applied to the interior surface of the crucible is unclear. The crucible was then re-used, creating a new slag layer and interior bloated zone. At the rim, this bloated zone does not completely overwrite the original profile and the two layers can be identified macroscopically. On the lower end of the fragment though, the two slag layers appear more fused. As the interior view shows, a clean fracture is needed to reveal this repair/re-use. No microscopic analysis of this fragment was performed, so it remains unknown whether the crucible slag from the first operation can be distinguished from that of the second operation.

The first five fragments discussed here represent either the extreme ends of the 'crucible shape spectrum' in the assemblage, or distinct crucible types. Either way, they constitute a marginal part of the assemblage and should not be attributed overly high importance.

The fragment demonstrating a practice of re-use, however, bears further contemplation. Clearly, signs of re-use are easy to miss, unless a fresh cut of the fragment is made. Even so, not all sections should be expected to show macroscopic signs of re-use, particularly those from body fragments. Therefore, re-use could easily go undetected.
Then again, the fact that no other examples of repair were found in the entire assemblage argues for a limited importance of this practice. Nonetheless, the possible ramifications should be taken into consideration when formulating a final interpretation of the assemblage, and are noted upon in section 6.1.5.

Figure 5.47: Exceptionally thick crucible fragments (top: 1984_1171,0001, bottom: 1987_1530a,0013-0014)

5.4.3 Rim vs. body fragments, crucible distributions and sample selection

A distinction needs to be made between rim and body fragments. Rim fragments are defined as fragments which include a rim in their section. These are mainly fragments with limited crucible wall remaining below that rim, but include more complete profiles. Body fragments have no rim attached and a curvature corresponding to a lower part of the crucible profile.
The complete assemblage (1042 fragments) is divided into:

QI (north) Industrial area (QI-Ia): 814 crucible fragments (78.1% of population)	
516 Body fragments	63.4%
294 Rim fragments	36.1%
4 Spout fragments	0.5%

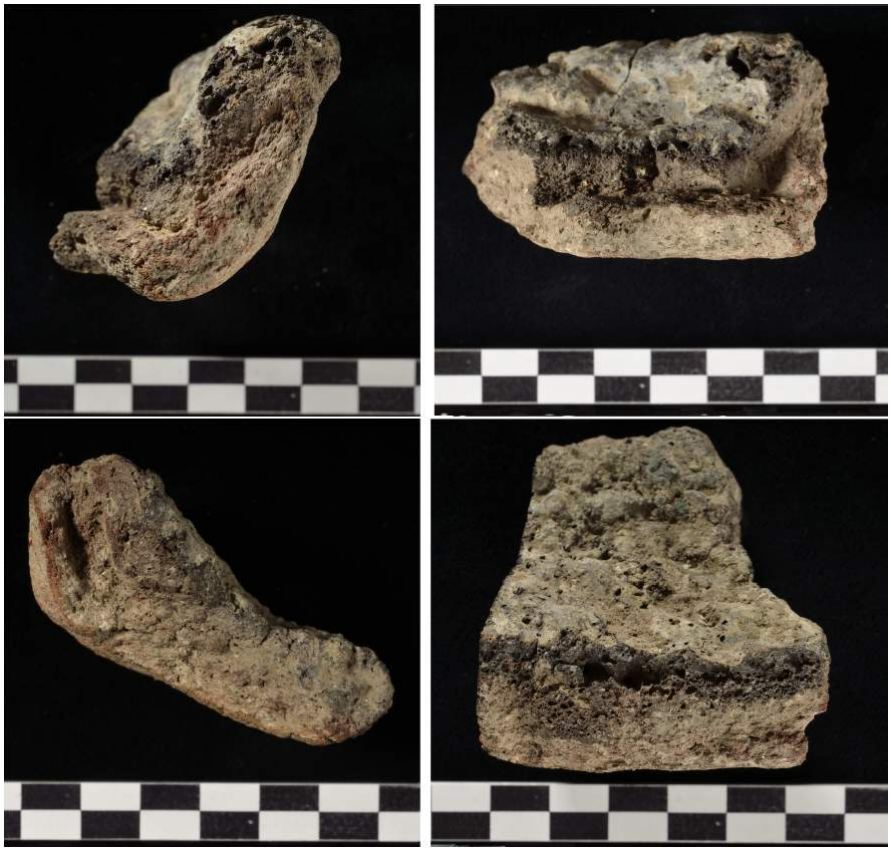

Figure 5.48: Exceptionally shallow crucible fragments, 1992_0645b,0001-2 (left: section through wall, right: section through bottom)

Figure 5.49: Crucible (1984_1264d) showing signs of repair and re-use. Top: section showing boundary between original rim and repair layer (red arrow) and a prill on top of original rim, beneath repair layer (blue arrow). Bottom: view of interior surface and section

QI (south) Workshop area (QI-Wa): 126 crucible fragments (12.1% of population)	
61 Body fragments	48.4%
59 Rim fragments	46.8%
6 Spout fragments	4.8%

QIV Workshop area (QIV-Wa): 97 crucible fragments (9.3% of population)	
57 Body fragments	58.8%
39 Rim fragments	40.2%
1 Spout fragment	1%

One rim fragment was found in area QIII and four fragments in area QV-b/9: three body fragments and one rim fragment.

Overall, body fragments make up 61.13%, rim fragments 37.81% and spout fragments 1.06% of the assemblage. The assemblage from QI-Wa deviates most strongly from this pattern, containing more rim fragments.

Table 5.13 summarises the distribution of the mounted samples across different areas and body vs. rim (see Appendix B). This selection deviates from the actual distributions: QI-Ia is under-represented, while QI-Wa and especially QIV-Wa are over-represented. The overall selection of body and rim fragments approximates the actual distribution, but within each area, the sample selection again deviates from the true pattern: body fragments are over-represented for QI-Ia and QIV-Wa, and under-represented for QI-Wa.
The selection of samples for detailed analysis was made prior to the start of this project, before detailed consideration of area and body-rim distributions, and is therefore a given for this study. However, it has some important implications for the interpretation of analytical results, as body and rim fragments have different characteristics and informative value (see section 5.2.1 and Chapter 13): relatively less information on the metal charge for crucibles from QI-Wa is available. Furthermore, overall trends are skewed due to the contextual distribution of selected samples. The effects of including both body and rim fragments is considered in the interpretation of tin, iron and cobalt in crucible slag (sections 5.4.5, 5.4.6 and 5.4.7). Finally, the results are contrasted for each area in section 6.3.

5.4.4 Alloying evidence

The abundant presence of copper and bronze prills in nearly all of the crucible fragments firmly places them in a context of bronze working. Some high-tin prills (defined as those

49 samples mounted for microscopy and SEM-EDS			
	# Samples	# Body fragments	# Rim + close to rim fragments
QI Industrial area	23 (47%)	20 (87%)	1 + 2 (13%)
QI Workshop area	11 (22%)	3 (27%)	5 + 3 (73%)
QIV Workshop area	15 (31%)	11 (73%)	2 + 2 (27%)
Total	49 (100%)	34 (69%)	8 + 7 (31%)

Table 5.13: Summary of mounted samples

with dominant δ-, ϵ- and/or η-phase, see section 5.2.4) give direct evidence for the alloying of copper (or recycled bronze) with fresh tin (or cassiterite) (Crew and Rehren, 2002; Rehren, 2001; Rehren and Pusch, 2012).

Re-melting of existing bronze can only result in prills with a tin content equal to or below that of the original bronze, as tin oxidises preferentially to copper, thereby lowering the tin content in trapped prills (Dungworth, 2000a; Kearns *et al.*, 2010). When alloying copper (or recycled bronze) with a fresh source of tin, however, any composition intermediate between pure copper and tin could occur. Prills of such intermediate composition, as shown in the phase diagram in Figure 5.50, can therefore be taken as very strong evidence for the use of a tin-rich material and indicate an active alloying process.

As the goal of alloying copper and tin in Pi-Ramesse would have been to form a manageable low- to intermediate-tin bronze (see section 5.2.4), such high-tin prills should be seen as an intermediate product of the alloying process and their trapping in the crucible slag incidental. Thus, there are two issues with this type of evidence: its absence cannot be interpreted as counter-evidence of active alloying (as these prills are only present when full reaction did not occur in the sampled crucible area) nor does its presence provide any information on the source of tin used in the alloying process.

Fragments in which low tin bronze prills, pure copper prills or no metallic prills occur, can therefore belong to a crucible that was used for re-melting or recycling bronze, but may equally have been used for active alloying.

5.4.5 Sources of tin

Active bronze alloying requires a source of tin to add to either pure copper or recycled bronze to control the final alloy. The two most common sources are tin metal and mineral cassiterite (the most common tin ore, SnO_2).

Though the presence of high-tin prills indicates the use of a fresh tin source, it does not

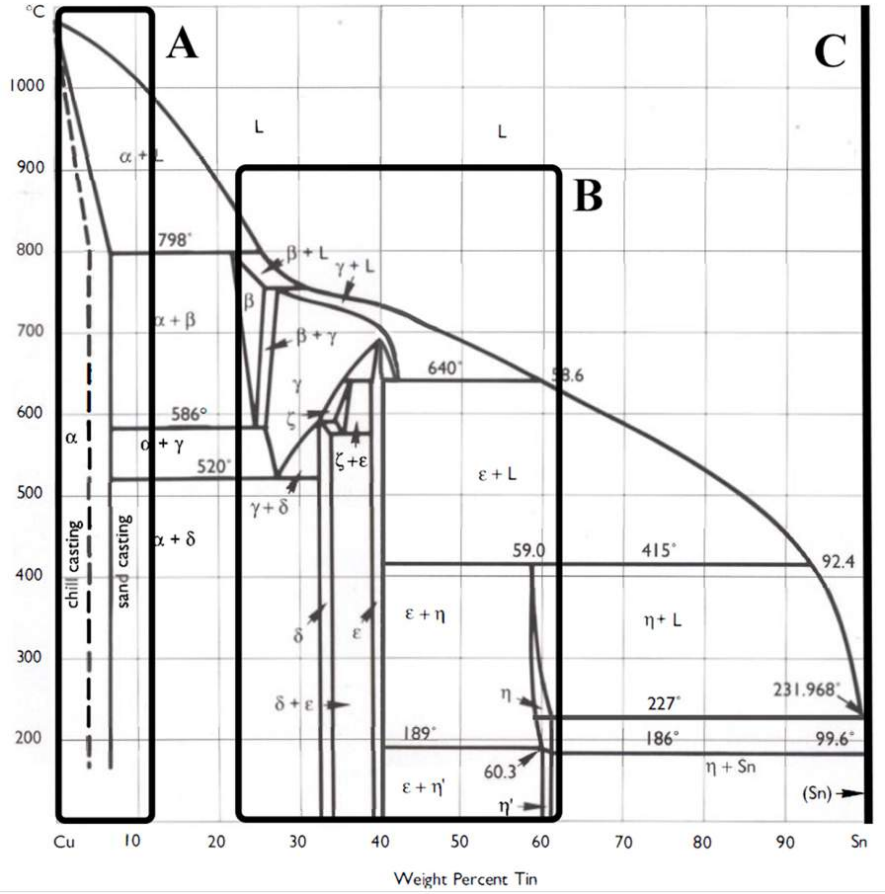

Figure 5.50: Cu-Sn phase diagram (casting conditions), showing typical Egyptian copper/bronze composition (A), high-tin prills of intermediate composition (B) and a source of fresh tin (C) (modified from Scott, 1991; all phase compositional boundaries approximate)

provide information on the nature of this tin. Here, it is argued that tin oxide crystals present in the crucible slag can, under some circumstances, provide further information on this tin source.

Tin oxide (SnO_2) is abundantly present in the crucible slag and in itself indicative of bronze-related activity. The varied shapes and forms in which this tin oxide occurs, however, have received relatively little attention in the archaeometallurgical literature, though some exceptions exist (Dungworth, 2000b; Eliyahu-Behar *et al.*, 2012; Figueiredo *et al.*, 2010b; Murillo-Barroso *et al.*, 2010; Rovira *et al.*, 2009; Schwab, 2011).

On the one hand, there are crystals which have shapes that clearly point to high-temperature formation, which are discussed in section 5.4.5.1. On the other hand, there are clusters of tin oxide which differ significantly from those crystallized at high temperature. It is argued in section 5.4.5.2 that these are residual cassiterite grains.

5.4.5.1 Burning out of SnO_2

As has been noted before, oxidising conditions can cause bronze to lose some of its tin content as it oxidises more readily than copper (Ellingham, 1944) and is thus 'burnt out' of the bronze. As explained in Appendix G, a limited loss of tin from the bronze charge can lead to significantly elevated tin content in the crucible slag. This occurs abundantly in Pi-Ramesse crucibles, as is shown for example in Figure 5.51, where crystals have formed all around the prill surface. Another example of burning out of bronze is shown in Figure 5.52. The orientation of the SnO_2 crystals (in a circle around the pore) indicates that these were burnt out from a prill (positioned at the location where now a pore is present). Further oxidation could have caused the copper to form the cuprite crystals in the pore (though cuprite formation might be post-depositional).

The tin oxide crystals formed in this way exhibit the shapes shown in Figure D.15, and occur in at least twenty-two of the analysed crucibles. Often, the core of such crystals contains copper or bronze, indicating that they formed by preferential oxidation of tin from a liquid melt (Cooke and Nielsen, 1978; Dungworth, 2000b; Hofmann and Klein, 1966; Klein and Hauptmann, 1999). Tin burning out of bronze in this way is indicative of locally oxidizing conditions in certain areas of the crucible. Tin oxide is then frequently found in a region rich in metallic copper rather than bronze. These crystals can form under locally oxidizing conditions in the context of any process involving bronze melting[13]. Tin could preferentially oxidise out of bronze that was either recycled (Rovira and Montero-Ruiz,

[13] Examples of similar crystals forming in Egyptian Blue are shown by Jaksch *et al.* (1983), Figure 8, p. 533, and with malayaite by El Goresy *et al.* (1996), Figure 3.a-c, p.327-329

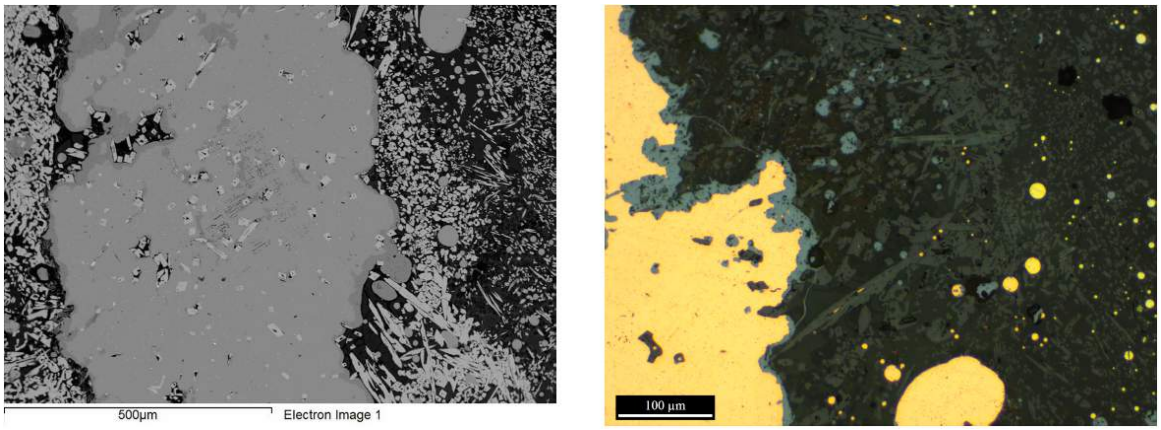

Figure 5.51: Clear example of tin oxidising out of a large prill (sample 97_0631E,04). Large clusters of tin oxide surround the prill, which is depleted of tin. More tin oxide occurs within the prill (shown section is close to prill surface). Cuprite formation, seen around the prill surface, occurs only after all tin has oxidized from the bronze (right: O.M. image)

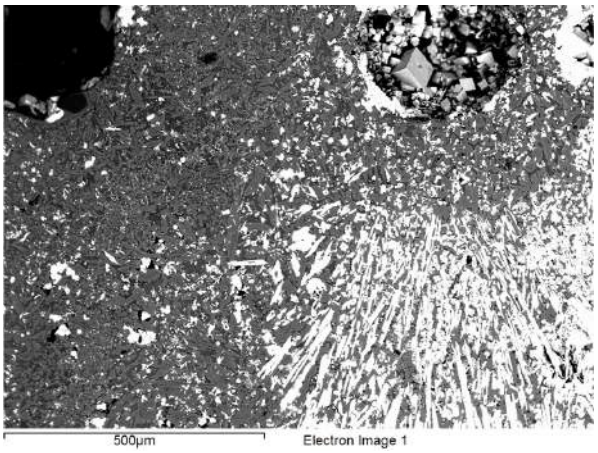

Figure 5.52: Copper-oxide crystals in a pore, with SnO_2 surrounding it, seemingly concentric - a completely burnt-out bronze prill? (sample 87_0884,01-56c)

2003) or freshly alloyed in the crucible. Alternatively, pure tin metal could oxidise directly. Finally, tin oxide could form directly from the re-crystallization of mineral cassiterite (e.g., Figure 5.53 (bottom right), Yener *et al.*, 2003, Figure 12.10, p. 189 and Murillo-Barroso *et al.*, 2010, Figure 14, p. 1170). Therefore, such high-temperature crystals provide no diagnostic information towards the source of tin for alloying.

5.4.5.2 Evidence for cassiterite?

Four examples, shown in Figure 5.53, occur in areas of crucible slag where reaction probably did not reach completion (e.g., deeper area of viscous slag or slag trapped in a crack). These clusters have the outline of mineral grains (composition: pure SnO_2): presumably, these were partly dissolved by the crucible slag and, when the reaction stopped, re-deposited in their macroscopic mineral shape (similar to residual ore fragments in primary production slag or partially reacted ilmenite shown in Figure D.4b). The adjacent metal prills are often bronze (though this is not always the case), indicating the formation of bronze rather than its oxidation. As Figure 5.53 shows, high-temperature SnO_2 crystals sometimes occur right next to re-deposited mineral grains (top right). This illustrates the highly heterogeneous conditions within a single crucible. Based mainly on their exceptional structural appearance, these partly dissolved grains are taken to be residual cassiterite, the most common tin ore. Such residual cassiterite has been identified in at least five crucibles.

5.4.5.3 Summary of tin sources for alloying

The few examples of possible residual cassiterite grains are insufficient to exclude the use of metallic tin at Pi-Ramesse. Firstly, there is no diagnostic evidence to be expected in the crucible slag for the use of metallic tin, so its absence does not argue against the use of metallic tin. Secondly, no tin ingots have been found at Pi-Ramesse, but this is to be expected for such a precious metal, as discussed further in section 6.1.2. Therefore, both cassiterite and metallic tin are likely to have been used for alloying at Pi-Ramesse.
Given that high-tin prills and residual cassiterite are intermediate products of an alloying process, it is impossible to estimate and compare the prevalence of each within separate contexts or the site as a whole.

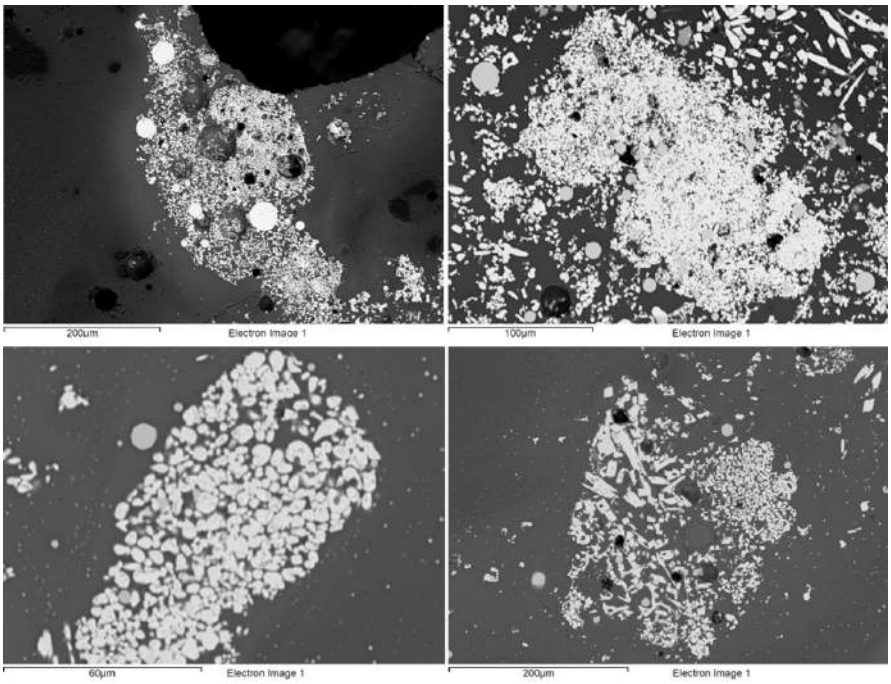

Figure 5.53: Residual cassiterite mineral grains in crucible slag. Bottom right example: left side partly re-crystallized

5.4.6 Iron enriched crucible slag

In approximately 1/3 of the crucible fragments, the crucible slag shows bulk chemical enrichment in iron compared to the ceramic. This trend is observed for both the 49 samples analysed by SEM-EDS and the larger sample analysed by pXRF. However, it should be kept in mind that this does not necessarily mean that 1/3 of all crucibles was enriched in iron, as counting both rim and body fragments skews the results: rim fragments are less likely to be enriched in iron, thereby lowering the overall incidence of iron enrichment. Out of 49 analysed fragments, ±18 are significantly enriched in iron (see section 5.2.1). Only one of these is a rim fragment and it shows lesser (though significant) enrichment. As 34 out of 49 analysed fragments are body fragments, it is likely that in reality about 50% of the crucibles are enriched in iron.

It should be noted that, out of this 50%, a fraction is enriched in both iron and cobalt. This is the case for ± 25-30% of the iron enriched fragments, or ±15% of the entire population (see section 5.4.7). This means that the fragments enriched in *iron only*, make up approximately 35% of the entire population.

A rough comparison between contexts, based on both SEM-EDS and pXRF data, indicates iron contamination to be approximately twice as prevalent in phase B/2 as it is in phase B/3. Cobalt enrichment, however, occurs more often in phase B/3 (industrial area) and

the B/2 multifunctional workshops than in QIV.

This iron increase is unlikely to derive from the fuel ash or an intentional iron addition. Instead, it probably originates from the use of a copper source enriched in iron, for example unrefined raw copper (Craddock, 2000; Craddock and Meeks, 1987) or copper ingots containing metallic iron (Rothenberg, 1990) or slag inclusions (Hauptmann *et al.*, 2002). Cassiterite used for cementation could be another source of iron (Murillo-Barroso *et al.*, 2010), as could metallic tin enriched in iron-tin inter-metallic phases ('hard head') formed during tin smelting (Chirikure *et al.*, 2010; Crew and Rehren, 2002; Miller and Hall, 2008; Tylecote *et al.*, 1989), but these are unlikely to be responsible for the high enrichment seen here as tin would have been added in comparatively low quantities. Moreover, there is evidence for iron-rich copper prills in the crucible slag (Figure 5.54), as well as iron oxidising out of copper and bronze prills and forming magnetite in the slag, as shown in Figure 5.55. Where locally oxidizing conditions prevail in the crucible, iron will preferentially oxidise out of metallic copper and bronze (or metallic tin) before any copper oxide is formed (Craddock and Meeks, 1987; Ellingham, 1944; Hauptmann *et al.*, 2002; Merkel, 1990), thereby effectively refining the copper. In this way, a copper used for melting or alloying which contained a few percent iron could produce strong iron enrichments in the crucible slag (similar to tin and cobalt enrichment, see Appendix G).

Though this appears to be the most likely scenario, others are possible. When iron-rich cassiterite is reduced in a cementation process, iron would inevitably be reduced with the tin, as their reducing conditions are very similar (Miller and Hall, 2008), and thus produce iron-rich bronze. Similarly, iron-rich bronze could be formed from alloying iron-rich tin metal with copper. Iron could then oxidise out of this iron-rich bronze in a more oxidising region of the crucible, as shown in the right-hand image in Figure 5.55. Here, iron in bronze could derive from either the copper or tin. This creates some ambiguity concerning the origin of iron in these prills. As the overview in Appendix E shows, most iron-rich prills have significant tin content. Though the left-hand image of Figure 5.55 shows iron-rich copper rather than bronze prills, the surrounding tin oxide crystals and tin-rich magnetite suggest that these prills were iron-rich bronze from which all the tin and most of the iron has oxidised.

This ambiguity concerning the source of iron largely disappears when considering that the iron-tin ratio in the iron-rich bronze prills greatly exceeds the levels which could reasonably be attributed to iron-rich tin or cassiterite. This suggests that the copper was iron-rich to begin with. More clarity exists for the samples discussed in section 5.4.7, where copper prills are enriched in iron, cobalt and sometimes nickel, with iron and cobalt oxidising

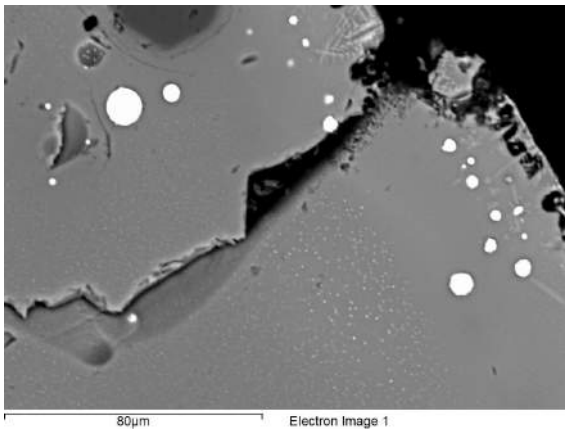

Figure 5.54: Iron-rich copper prills (98-99 wt% Cu with 1-2 wt% Fe), sample 83_1149b

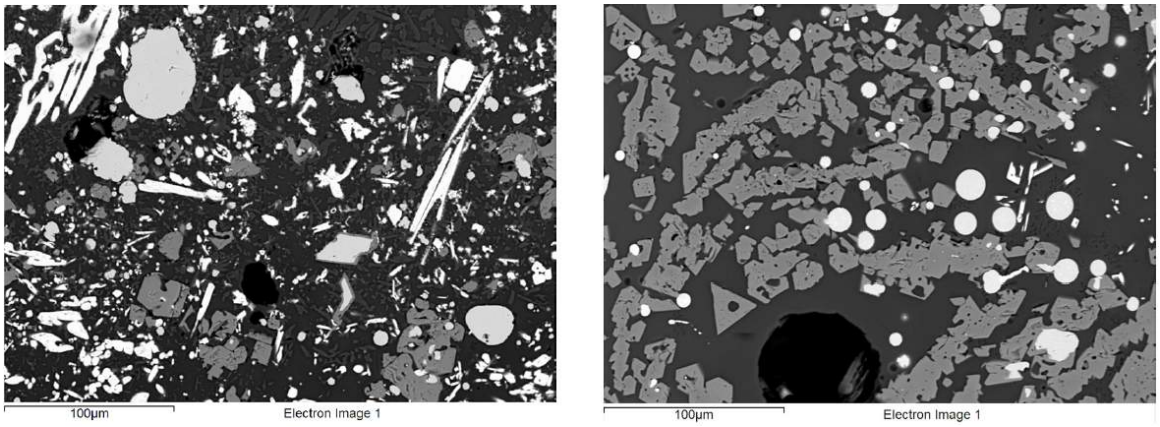

Figure 5.55: Iron-rich copper prills (left image, ±0-2 wt% Fe) and bronze prills (right image, ±3-6 wt% Sn and 1-3 wt% Fe) (light grey) from which iron and tin oxidised preferentially into the crucible slag, forming magnetite (mid grey crystals) and tin oxide (bright angular crystals). The magnetite is iron oxide incorporating ±1-8 wt% Sn, 1-2 wt% Al and 2-3 wt% Mg

into the slag from these prills.

5.4.7 Cobalt enriched crucible slag

In ±12% of the fragments, there is a significant increase (2-3 wt% of bulk composition) of CoO content in the slag, together with iron enrichment. This reflects cobalt contamination in ±15-18% of all crucibles (taking into account body/rim distributions and the occurrence of Co-bearing prills), revealed in both SEM-EDS and pXRF data. As described in Appendix D.5, this CoO is mostly found in a spinel-like, Fe-Al-oxide phase, and metallic cobalt only rarely occurs within copper prills.

This cobalt does not occur in the ceramic, so it must have been introduced into the crucible with the charge: either through the copper, tin or fuel ash (or an unknown charge constituent). Fuel ash has no significant cobalt content and is an unlikely source. Probably, metallic cobalt was introduced with the copper (as a contaminant) and oxidised into the slag: similarly to iron and tin, cobalt oxidises preferentially to copper (Ellingham, 1944) and is burned out into the slag in oxidising crucible environments[14]. A possible explanation is the use of raw copper which was enriched in cobalt and iron. Cobalt does not occur as a native metal and is (in modern times) produced as a by-product of nickel and copper mining. It occurs for example in hydrothermal vein deposits as carrollite ($CuCo_2S_4$), and could therefore have ended up in copper smelted from such ores, as a natural alloy. Using such an alloy at Pi-Ramesse would probably not have happened intentionally, given that there seems to be no conscious use of cobalt at the site[15] and low amounts (a few wt%) of cobalt in raw copper would not change its observable characteristics.

Another possibility is that the Co was already present as CoO in the copper. This could be due to it being part of the slag formed from smelting a Co-rich copper ore. If the copper from such a smelt was not properly separated from its slag, and this copper, with slag-inclusions, was melted in the crucibles, the CoO-rich slag could integrate with the crucible slag, as conditions do not appear to have been sufficiently reducing in the crucibles to warrant the formation of metallic cobalt.

However, the first explanation is most likely: the cobalt spinel appears to form by oxidation from cobalt- and iron-rich copper prills, similarly to iron (Figure 5.55). Figure 5.56 shows an example of the cobalt-rich spinel aggregates, and the process of oxidation from a prill into the the slag. In some cases, these prills are further enriched in nickel. Nickel, however, does not occur as an oxide in the crucible slag: cobalt is more easily oxidised into the slag than nickel (Hauptmann, 2007). Depending on the relative importance of nickel compared to cobalt as a contaminant in the copper, nickel could be expected in low concentrations in some of the bronze objects from Pi-Ramesse, which is indeed the case (see section 5.5.1). This combination of iron, cobalt and nickel is indicative of the geological origin of the ore from which the raw copper, used in these crucibles, was smelted under

[14] Merkel's 1990 refining experiments indicate that cobalt (at ppm level) burns off together with iron first, while tin (at ppm level) is retained in the copper.

[15] It is, however, interesting to note here that the glass-production industry at Pi-Ramesse was focused almost exclusively on Cu-coloured glass, while only three examples of Co-coloured glass occur (Pusch and Rehren, 2007), and one CoCu-coloured glass (Smirniou and Rehren, 2013). Importantly, cobalt-blue glass from New Kingdom Egypt was coloured using alum from the Western Oases of Egypt (Kaczmarczyk, 1986; Shortland *et al.*, 2006), for example in Amarna (Smirniou and Rehren, 2011; Tite and Shortland, 2003), rather than using scrap bronze, as has been suggested for the copper-red glas from Pi-Ramesse.

strongly reducing conditions.

There is no evidence to suggest that tin could be a source of cobalt here. The CoO enriched samples have 'average' SnO_2 enrichment (no correlation to CoO enrichment) and the ratio $^{\Delta CoO}/_{\Delta SnO_2}$ is 0.3-0.5(-1), which means the slag enrichment in tin is typically two or three times greater than that in cobalt. Given that the Gibbs-free energy of formation[16] for CoO (s) (at 25 ºC), is $\triangle G_f^0 = -214.22$ kJ/mol and for SnO_2 (s) (at 25 ºC), $\triangle G_f^0 = -519.6$ kJ/mol (for SnO (s) (at 25 ºC), $\triangle G_f^0 = -256.9$ kJ/mol), tin oxidises more readily than cobalt (Ellingham, 1944). In the hypothetical situation where cobalt came into the crucible charge with tin (metallic or mineral), the ratio of cobalt to tin would have to be very high ($\pm^1/_1$) to achieve the slag enrichments seen here. As typical Co-levels in tin minerals are in the ppm-range (Northover and Gillis, 1999), such a cobalt-tin alloy or mineral is unlikely to have existed and been used at Pi-Ramesse.

5.4.8 Lead (and arsenic) in crucible slag

Neither lead nor arsenic are important components of the crucible slag. Low levels of lead are measured as a bulk chemical component by SEM-EDS for seven out of forty-nine samples (though near detection limits for two or three of these), and in a similar portion of the larger sample when using pXRF: ±15% (taking into account body/rim distributions). It is rarely measured in metallic prills (two samples), though it can sometimes be seen as insoluble droplets. For the two cases were it is measured in appreciable levels in prills, it occurs together with arsenic and iron, and in one case with a sulphidic edge, within fayalitic slag.

Arsenic does not appear as a bulk component using SEM-EDS measurements and its presence cannot reliably be measured using pXRF. Low amounts of arsenic are measured in prills for seventeen out of forty-nine samples, accompanied by the presence of iron and cobalt in eight samples (and nickel in three).

Given the low levels at which both lead and arsenic occur, it seems unlikely that either were added intentionally to form a lead- or arsenic-rich copper alloy. Probably, both lead and arsenic were introduced into the crucibles with copper. This could point to the use of recycled arsenical copper or leaded bronze (though this is unlikely, given lead's association to iron and sulphide here and because leaded bronze was very uncommon in Egypt at this point in time). Another, more likely explanation is that these were contaminants of raw copper. Lead could be associated to raw copper smelted from ores like those at Feinan,

[16] Gibbs-free energy values from Oxtoby *et al.*, 2003, Appendix D

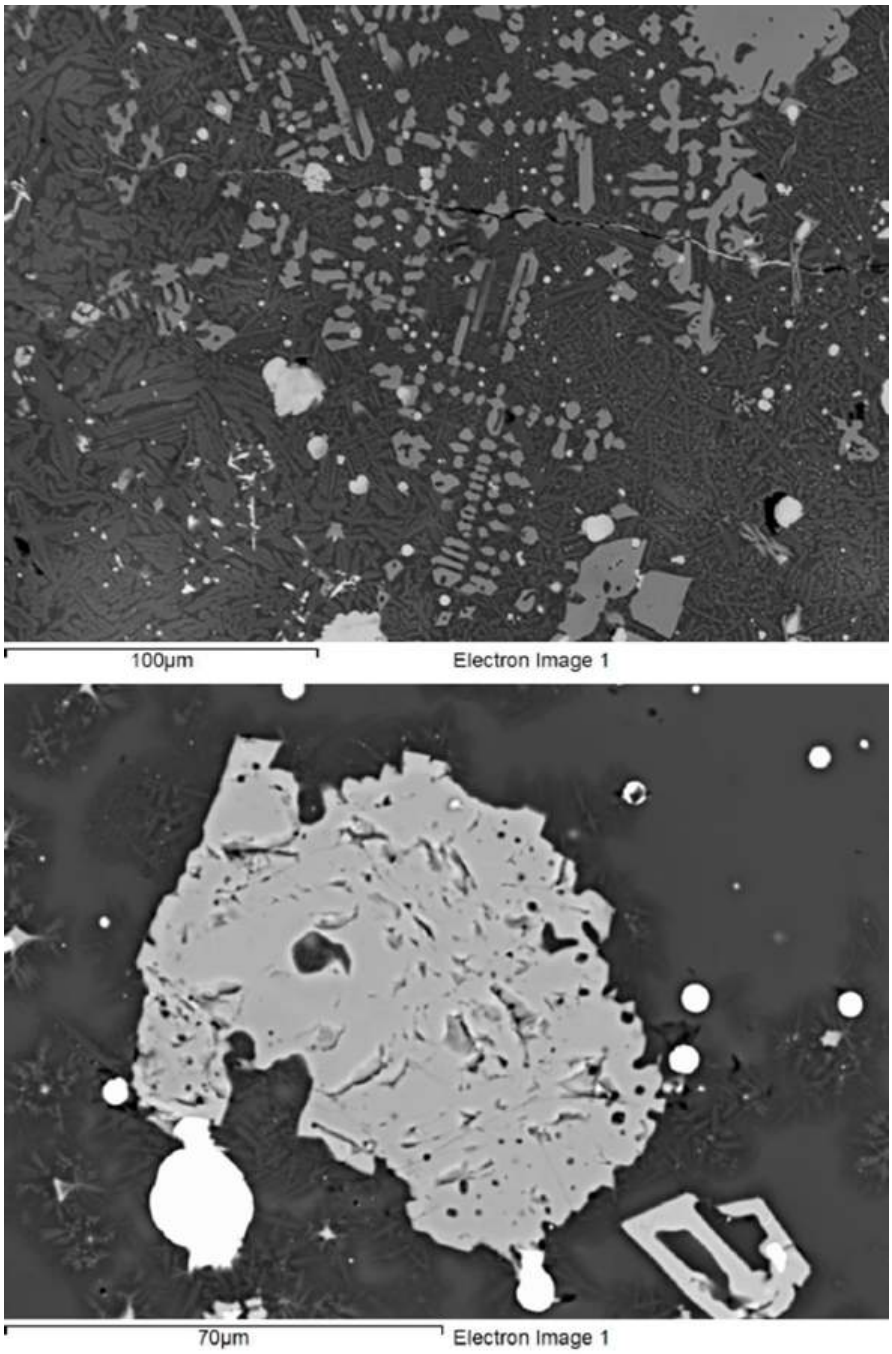

Figure 5.56: Cobalt spinel in crucible slag. Bottom micrograph shows a large spinel aggregate, probably oxidized out of cobalt/iron-rich copper prills (bright). The spinel has ±77 wt% FeO and 12 wt% CoO, as well as ±5-6 wt% Al2O3, 2-3 wt% TiO2 and 1 wt% SiO2, MgO and SnO2. The bronze prill contains ±5 wt% Sn, 2 wt% Fe and 0.5 wt% Co

which often incorporates copper sulphides and lead (e.g., EBA III Khirbet Hamra Ifdan ingot, see Hauptmann, 2007, Figure 7.16, p. 242), though no arsenic. Co-Ni-As-Fe ores appear in the rooting zones of massive sulphide deposits, for example in Limassol (Cyprus) where these were mined in Hellenistic-Roman times (Constantinou, 1980; Hauptmann, 2007). The use of copper smelted from such ores could explain the presence of prills with (some of) these elements in the crucible slag. For example, copper ingots smelted from ores in Oman are typically enriched in arsenic, cobalt and nickel (Begemann *et al.*, 2010), though not iron.
An issue with the identification of arsenic in crucible slag is its tendency to volatilise, especially under oxidising conditions. According to Pigott *et al.* (2003), the addition of tin or cassiterite to a crucible charged with Co-Ni-As-rich copper, would further increase the volatilisation of arsenic. Clearly, this complicates the evaluation of the importance of arsenic as a copper contaminant through the study of crucible slag.

5.4.9 Variation in crucible slag

Within the full crucible assemblage, there exists variability in the crucible slag composition, mineralogy and metal content. This variability is caused by several different interacting factors:

- **Variability in the composition of the crucible charge.** An example of this is the enrichment in iron and/or cobalt. Slag containing iron-rich phases usually shows bulk enrichment in iron-oxide (Figure D.5).

- **Variability in the cooling speed of the crucible slag.** As Figure D.6 shows, Ca-bearing phases occur in crucible slag with both low and high bulk lime enrichment. These phases are most likely formed at low cooling speed, while quick cooling results in more glassy slag. This effect appears less important for iron-rich phases, which precipitate whenever the slag bulk content is enriched in iron, due to iron oversaturation of the glassy matrix at these operating temperatures.

- **Variability in redox-conditions**. It appears that within a crucible, both reducing and more oxidising regions exist. This is exemplified by the occurrence of high-tin prills, created by alloying under relatively reducing conditions, as well as tin oxide crystals, formed by the oxidation of bronze, within a single crucible.

- **Variability in temperature**. This variability is most likely directly linked to variability in redox-conditions, and controlled through air supply (Hauptmann, 2007). Sud-

den variations in temperature can lead to slag solidification which traps liquid metal prills during the alloying process.

- **Variability of the process through time**. The oxidising regions, mentioned above, could exist in the crucible during the melting or alloying stage, but could equally reflect a more oxidising phase of the process, for example casting. The variability of the crucible process through time is thus reflected in the crucible slag.

- **Degree of slagging**. It appears that some crucibles (or areas of crucibles) are more slagged than others. This is probably due to differences in temperature and fluxing of the ceramic by fuel ash. The relative change in lime between ceramic and slag is indicative of the degree of fluxing and slagging of the crucible. This slagging has important implications:

  - More slagged crucibles tend to trap more metal prills, thereby elevating the bulk metal content.
  - Higher metal content due to prill trapping increases the likelihood of metal contaminants (e.g., iron[17] and cobalt) being elevated in the bulk content (though oxidising conditions are important here).

- **Location within a crucible**. The strong difference between body and rim fragments is caused by a combination of the above factors. The most important factor appears to be the contact with the metal charge, which does not occur close to the rim, as shown in Figure 5.7. This then again leads to variations in redox-conditions and slagging.

To summarise, it appears that the variability seen within this crucible assemblage is largely explained by two principal effects. The first effect is variability within the crucible due to changing oxygen supply, temperature, material presence and cooling rates. This causes the crucibles to slag to varying degrees, trap more or less metal prills and contaminants and exhibit more glassy or crystallised slag. The second effect is the variability in crucible charge, which introduces different materials, such as iron and cobalt or residual cassiterite. This second effect is of the highest interest from an archaeological perspective, but its visibility is impeded by the first effect.

[17] This probably explains the small (but existing) correlation between CaO- and FeO-increase (see Figure 5.15).

	Na_2O	MgO	Al_2O_3	SiO_2	P_2O_5	K_2O	CaO	TiO_2	MnO	FeO	CuO	As_2O_3	SnO_2	PbO
Normal slag	1.6	2.0	12	68	0.4	1.7	3.0	1.4	0.2	7.9	1.3	0	0.1	0.1
Fayalitic slag	1.7	1.5	5	30	1.5	1.1	8.2	0.5	0.5	38.9	5.8	0.2	4.9	0.5
Magnetite slag	1.4	1.6	4	23	1.3	0.8	9.0	0.3	0.2	31.6	10.7	0.3	15.4	1.1

Table 5.14: Bulk composition of normal slag layer, fayalite-dominated slag zone and magnetite-dominated slag zone in sample 94_0560 (in wt%, normalised to 100%)

5.4.10 Fayalitic slag in sample 94_560

For this particular crucible, two distinct slag areas are noted:

- A zone of slagged ceramic with increased amounts of fractured quartz but otherwise 'normal' crucible slag (relatively 'deeper').
- A second zone, partly infiltrating the first area, composed of highly crystallised slag with high metal content (towards interior surface).

A somewhat sharp, in places angular, boundary exists between these two zones, as shown in Figure 5.57. This second zone has a much higher FeO content than the typical crucible slag (outlier in Figure 5.5). It can be further sub-divided into two areas (shown in Figure 5.58):

- Area dominated by fayalitic slag (composition: $(Fe,Mg)_2SiO_4$, with $Mg/Fe \approx 1/8$) occurring mainly towards the border with the first zone, often with Fe_3O_4 (magnetite) interspersed.
- Further towards the inner surface of the crucible, magnetite dominates and less fayalite is present.

The bulk composition of the three slag areas is given in Table 5.14, and alumina ratios in Table 5.15. This shows the chemical similarity between the fayalite- and magnetite-dominated areas, and large difference between these and the normal slag zone. The two areas within the second zone are most likely explained by more oxidising conditions at the inner surface, producing magnetite.

Another remarkable feature of this second zone is the presence of iron-rich prills with a sulphidic edge, sometimes enriched in As and Pb (see Figure 5.24 and Appendix E).

The most likely explanation for these observations is that the interior zone represents normal crucible slag as observed in other crucibles, while the second zone represents a layer

	$\frac{Na_2O}{Al_2O_3}$	$\frac{MgO}{Al_2O_3}$	$\frac{SiO_2}{Al_2O_3}$	$\frac{P_2O_5}{Al_2O_3}$	$\frac{K_2O}{Al_2O_3}$	$\frac{CaO}{Al_2O_3}$	$\frac{TiO_2}{Al_2O_3}$	$\frac{MnO}{Al_2O_3}$	$\frac{FeO}{Al_2O_3}$
Normal slag	0.1	0.2	5.9	0	0.1	0.3	0.1	0	0.7
Fayalitic slag	0.4	0.3	6.1	0.3	0.2	1.7	0.1	0.1	8.1
Magnetite slag	0.4	0.4	6.3	0.3	0.2	2.5	0.1	0.1	8.7

Table 5.15: Alumina ratios for normal slag layer, fayalite-dominated slag zone and magnetite-dominated slag zone in sample 94_0560

formed on top of this after the formation of the first zone. The sharp boundary between the two zones argues in favour of this, rather than a segregation into two zones of one molten material. However, the two layers are fused, suggesting that the second layer came into contact with the first one while both were still hot and viscous.
The composition of the second layer is very different from that of all other crucible slag. It lies on a trough in the ternary diagram, indicating low melting temperatures, fairly close to the 'optimum 1' for iron bloomery smelting (as defined by Rehren *et al.*, 2007), and is similar to the composition of primary copper production slag (e.g., Maldonado and Rehren, 2009, Figure 8, p. 2003).

A likely explanation here is that a dross-like layer formed on top of the charge during melting. During casting, this layer stayed behind in the crucible and settled against the crucible wall, forming a second layer. As both the 'normal' crucible slag and the second layer were still very hot at this point, they fused and cooled down together.
The origin of this second layer is most likely a slag inclusion inside the copper that was charged into the crucible. This slag inclusion would be a remnant of the primary smelting process, poorly separated from the raw copper. Such poor separation has been attested for multiple ingots by Hauptmann *et al.* (2002); Tylecote and Bachmann (1990) and Zwicker *et al.* (1980). Upon remelting in the crucible, this slag would float to the surface of the liquid batch. During casting, it would then settle on the crucible wall. This process is presented schematically in Figure 5.59.
It is important to note that this fayalitic slag was not necessarily liquid inside the crucible, as its melting temperature (derived from the phase diagram shown in Figure 5.5) is ±1150-1200°C and exceeds the melting temperature of copper and bronze. Therefore, the fayalite and magnetite crystals could either be newly formed or residual from the original smelting process. The presence of iron-rich sulphidic prills[18] inside this 'primary slag', which did

[18]The iron and lead content in the prills points to reducing conditions (during primary smelting). The sulphide indicates that the copper was probably smelted from a sulphidic ore, though this is not necessarily the case (Balmuth and Tylecote, 1976).

not migrate from it into the metal batch, suggests that this slag may not have completely liquefied. Furthermore, the large fayalite crystals indicate a slow, homogeneous cooling, which does not correspond well to formation within an alloying/casting scenario. The magnetite crystals could have formed on top of the dross layer during the alloying/casting due to the more oxidising conditions at the surface of the batch, leading to a higher concentration of magnetite towards the exterior of the layer. However, a significant fraction of the magnetite could equally be residual.

Another possibility would be that the second layer was newly formed during the alloying process as an interaction between the (slagging) ceramic and the metal batch. This would imply a very high amount of iron migrating from the metal batch into the ceramic, in a way very different from what is seen in other crucibles (see section 5.4.6). It is unclear, however, how this would be possible, especially considering the (probably) short duration of the melting/alloying process.

Though giving a conclusive explanation for this fragment remains difficult, it appears that the second slag layer was formed through the introduction of a high amount of iron in the metal batch. This suggests the use of an 'iron-contaminated' copper source, probably with slag inclusions in the copper.

5.4.11 Sample 86_0749c: another peculiar case?

Macroscopically, this sample does not appear very different from other samples. No red ceramic zone is present (probably broken off), only a grey-black fired ceramic remains and the slag zone penetrates deep into it, but this occurs frequently. There are, however, some unusual features to this sample:

- A gold prill with composition 70-30 at% Au-Cu (Figure 5.26).
- Two iron-rich prills with bulk composition 87 wt% Fe, 10 wt% Cu and 1.5 wt% As, trace Ni and Sn. These prills contain two phases and a sulphidic edge (see Figure 5.25):

	Cu	Fe	As	Sn	Ni	S
Phase 1	7.3	89.4	2.8	-	0.5	-
Phase 2	91.3	6.7	1.0	1.0	-	-
Sulphidic edge (3)	67.8	8.1	-	-	-	24.1

(in wt%)

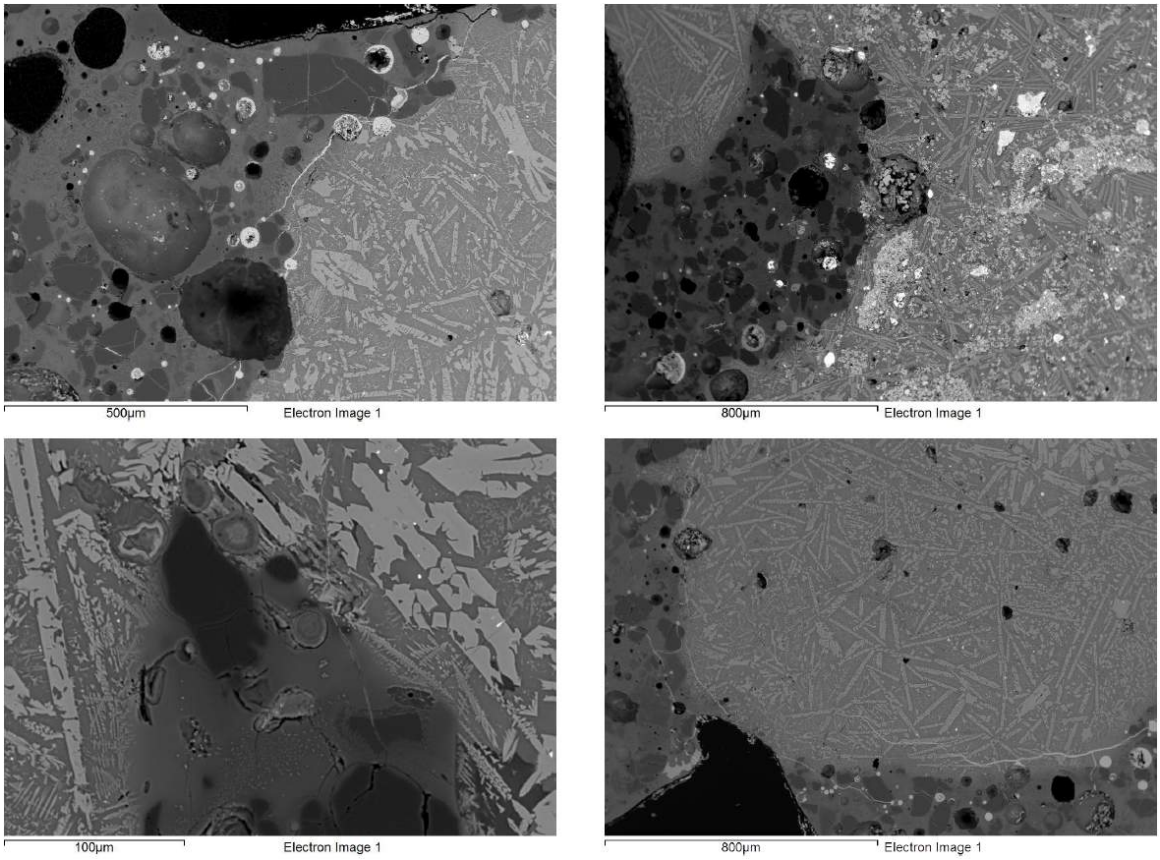

Figure 5.57: Sharp boundary between two slag layers in sample 94_560

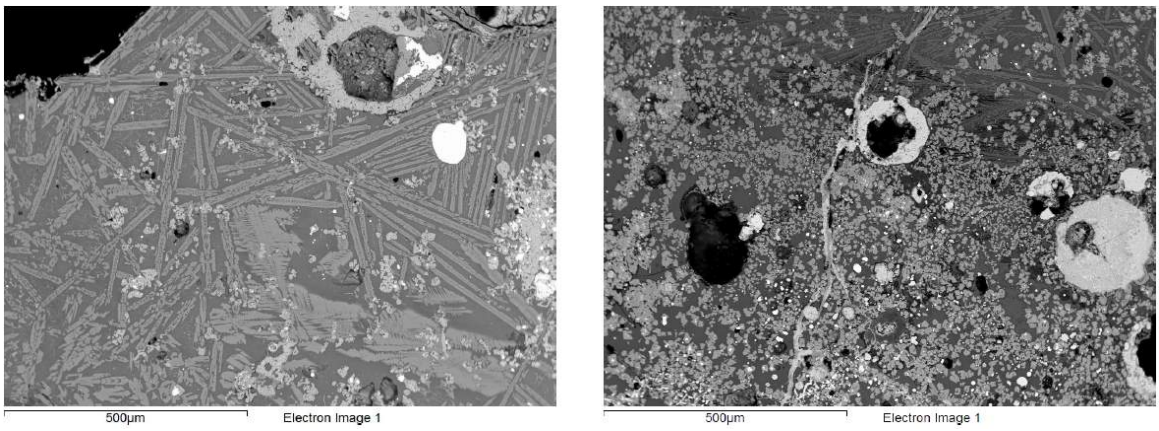

Figure 5.58: Fayalite-rich (left) and magnetite-rich (right) area in second slag zone of sample 94_560

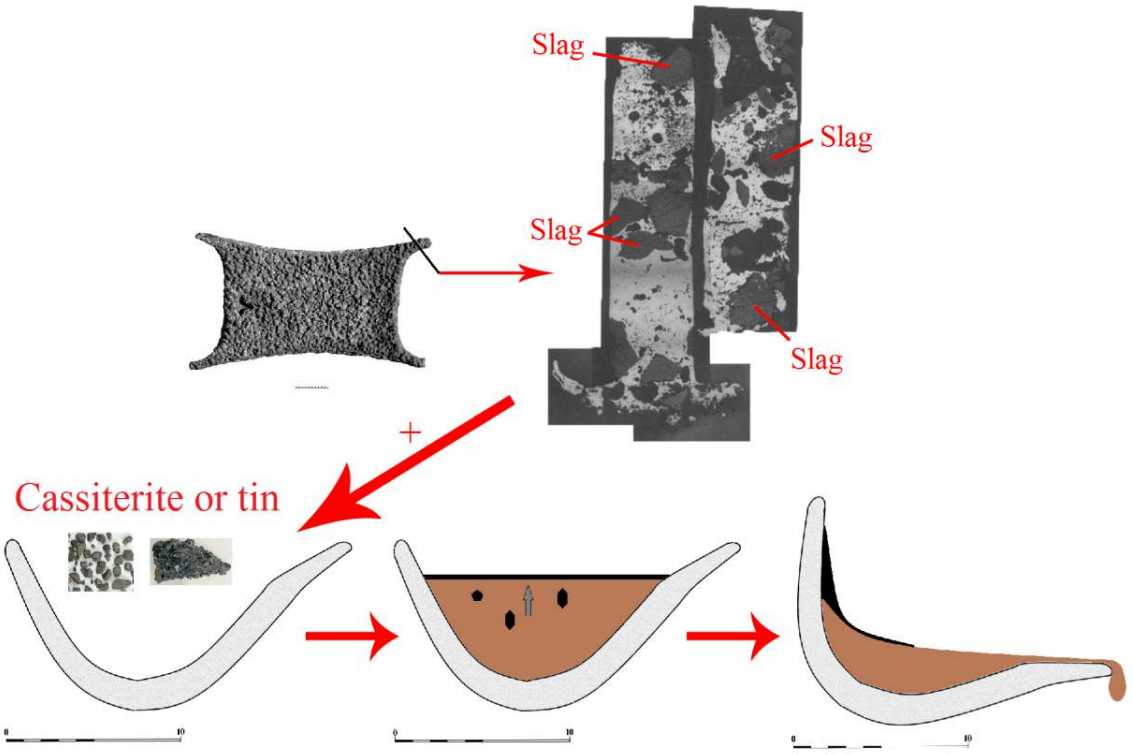

Figure 5.59: Top image: copper oxhide ingot (from Kassianidou, 2009) showing large slag inclusions in section (from Hauptmann *et al.*, 2002, not to scale). Bottom image: schematic representation of second slag layer formation: slag-rich ingot as part of crucible charge (left) - slag inclusions (black) rising to float on liquid bronze surface (central) - slag layer sticks to crucible wall during casting (right)

- A copper prill with 1.5 wt% As (not unique, other samples contain prills with higher As content, see Appendix 5.2.4).
- Copper occurs mostly as an oxide.
- Sample 86_0749c has low CuO (0.76±0.71 wt%) and SnO_2 (0.41±0.12 wt%) bulk content in the slag.

Disregarding the gold-rich prill, all of the features listed here are not unique and occur in other fragments within the assemblage. This particular sample could be interpreted as vitrified (fuel ash contaminated), probably from close to the crucible rim, with limited metal enrichment. The presence of two sulphidic prills is unusual, but not unique, and could point to the use of an impure copper source (see sections 5.4.6 and 5.4.10).

The occurrence of a gold-rich prill (though only a single one was found), is unique within the assemblage. If this is interpreted within the general setting of bronze production, it probably points to the recycling of a formerly gilded copper or bronze. Interesting to note here, is that Pusch and Rehren (2007) discovered microscopic gold prills in some glass fragments, which they tentatively relate to white quartz (basic glass constituent) being sourced from gold mining regions in the Eastern Desert or Nubia.

Viewed in isolation, the lack of significant copper and tin enrichment could point to this crucible being used for a non-bronze related process, e.g. remelting a gilded copper. However, the general characteristics of this crucible allow it to easily fit into the variability seen within the rest of the assemblage. Taking note of the occurrence of a single gold-rich prill, this crucible should probably be included as part of the 'normal' assemblage.

Section 5.5

Lead isotope analysis

Before starting an overall discussion of bronze metallurgy at Pi-Ramesse (Chapter 6), the results from lead isotope analysis are presented.
The lead isotope (LI) ratios have been analysed for two main material types: metal remains (26 copper alloys: some artefacts, some spills, drops etc.) and crucibles (both ceramic and slag parts of 12 crucibles and 1 further slag part). The sample information and raw data from these analyses are presented in Appendix F. These two datasets are discussed in sections 5.5.1 and 5.5.2, before attempting to reconcile all data in an overarching interpretation.

Some of this data (9 metal samples) was produced by the Oxford Isotrace Laboratory in 1996 within the Pi-Ramesse project, but has not been published or interpreted further since its mentioning by Gale (1999). The majority of the lead isotope data has been produced within the framework of this PhD by the Curt-Engelhorn-Centre Archaeometry Laboratory for Material Analysis (crucibles and metal spills). A selection of copper alloy materials has been made to get a representative spread across contexts and time, within the limited range of metal samples available in London, taking into account considerations of sample size and corrosion. The crucible samples were taken from the same crucible fragments previously sampled for analysis in mounted section. As such, an attempt has been made to reflect the different groups discussed earlier: 'clean', iron contaminated, iron-cobalt contaminated and (mildly) lead contaminated crucibles.
The sample numbers, both metal and crucible, are largely dictated by sample availability and budget considerations. As such, they are far from an ideal sample in statistical terms, but offer a qualitative assessment of the lead isotope compositional variability within the Pi-Ramesse bronzes.

5.5.1 Copper and bronze

The results for the LI analysis of all copper (alloys) are shown in Figure 5.60, distinguishing between the Isotrace and CEZ data. These samples and their contextual data are presented in Table F.1.
Most samples are (corroded) unidentified metal fragments, a few objects and two metal

prills extracted from crucibles. Lab-XRF analysis was performed for all samples[19], and NAA for seven of the samples (results summarised in Tables F.2, F.3 and F.4). Lead contents generally vary between <0.01 wt% to 1.1 wt% (average: ±0.5 wt%), with the exception of four samples that have higher lead content (three with ±2 wt%, one with ±5 wt%).

The lead isotope data is presented as ratios of ^{204}Pb, which provides a better means to distinguish between various lead sources and assess potential mixing more easily[20] (Ellam, 2010). The data shows a fairly wide spread, pointing to copper from various sources being used. No radiogenic lead appears to be present in any of the samples. Some samples, indicated in Figure 5.61, have very low lead contents, while others have unusually high lead contents. Rather than discussing the complete dataset straight away, the following sections address some particular patterns emerging from the data, before an overall interpretation is offered.

5.5.1.1 Apliki, Cyprus

The oxhide ingot fragment (1987_0803,0004) has previously been identified as coinciding with the LI range characteristic of Apliki ores by Gale (1999). Figure 5.62 shows a comparison between the LI composition of the copper (alloy) samples from Pi-Ramesse and Cypriot copper ores (Limassol, Solea and Apliki, data from Gale *et al.*, 1997), and copper ingots from the Uluburun wreck (ingot core data from Gale, 2005).
The oxhide ingot fragment indeed falls within the Apliki LI range (when considering both iron and copper ores), and matches the similarly identified Uluburun wreck ingots (as well as Apliki-consistent ingots identified by Yahalom-Mack *et al.* (2014)). Furthermore, samples 97_0390,02- and 87_0897a,01-45 (2) lie very close to the oxhide ingot and match the Apliki field as well. These are both metal prills, which were embedded in crucible slag and extracted for analysis. Unfortunately, no chemical compositional data is available for these two samples.
This result is particularly interesting, as it is the first evidence of a Late Bronze Age oxhide ingot (fragment) being molten down in a crucible.

Some close resemblance can be seen for two samples (1986_0720 and 1992_0905,0002) with the Limassol copper ores. However, exploitation of this copper source during the

[19] With the exception of 2 prills that were analysed together with the crucibles, for which no compositional data is available.

[20] It should be noted, however, that the same conclusions were reached during exploratory analysis of the data using the more common ratios found in archaeological literature (^{207}Pb/^{206}Pb vs ^{208}Pb/^{206}Pb and ^{208}Pb/^{204}Pb). The ratios of ^{204}Pb, however, provide even better distinction between groups. ^{207}Pb/^{204}Pb and ^{206}Pb/^{204}Pb are easily calculated from the other ratios presented in Appendix F.

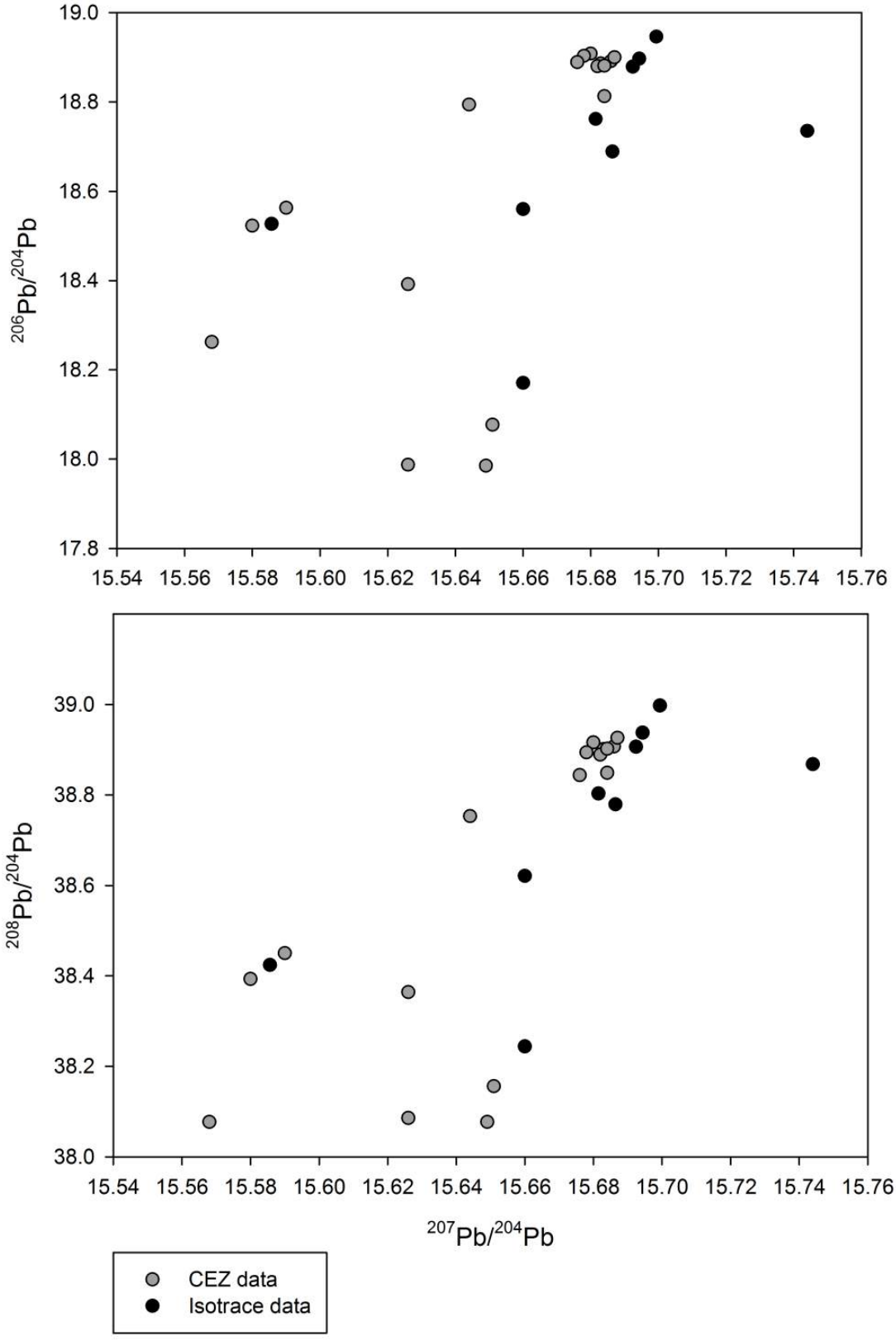

Figure 5.60: LI compositions for all analysed copper (alloys)

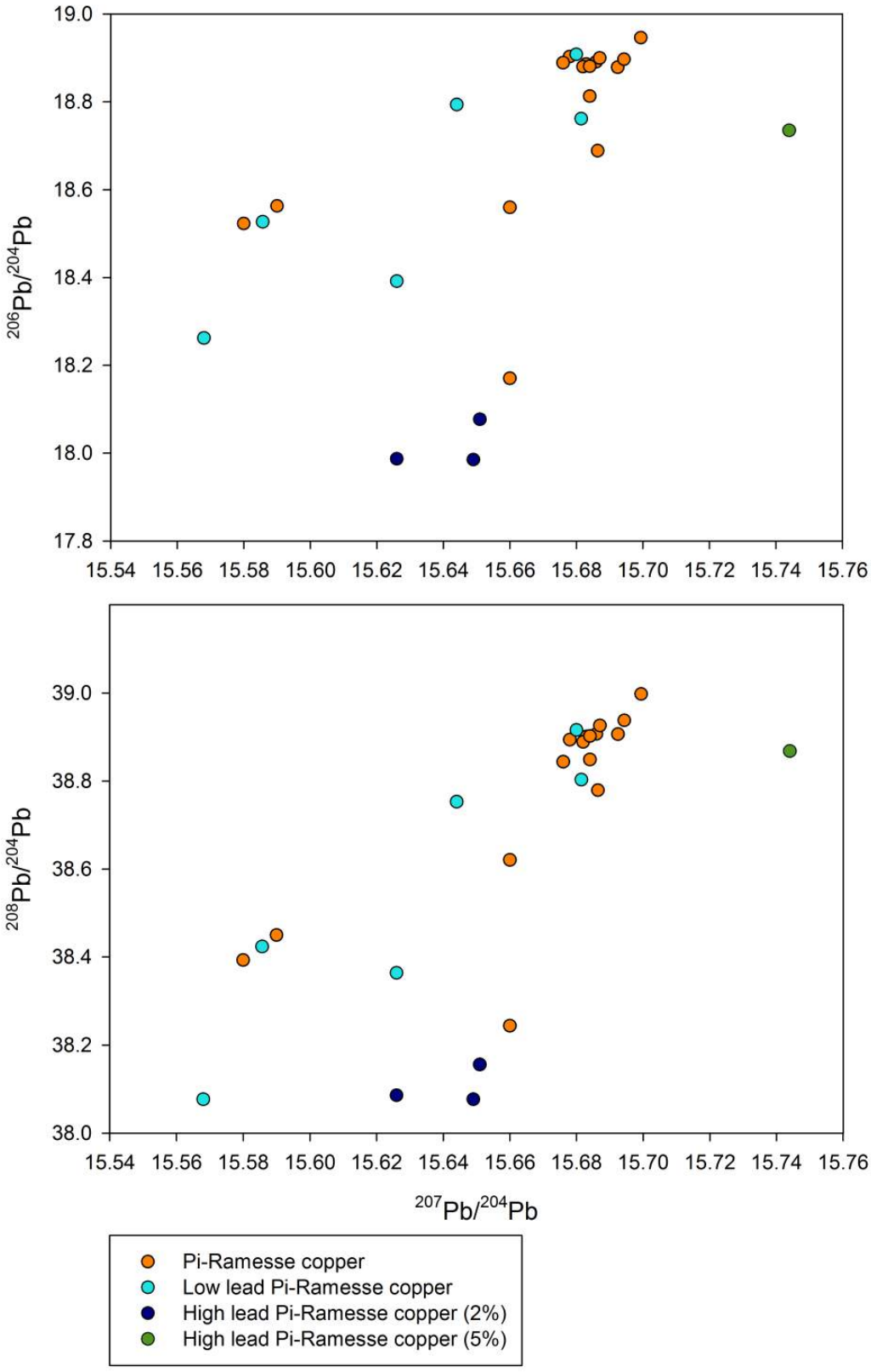

Figure 5.61: LI compositions for all analysed copper (alloys), showing high- and low-lead samples

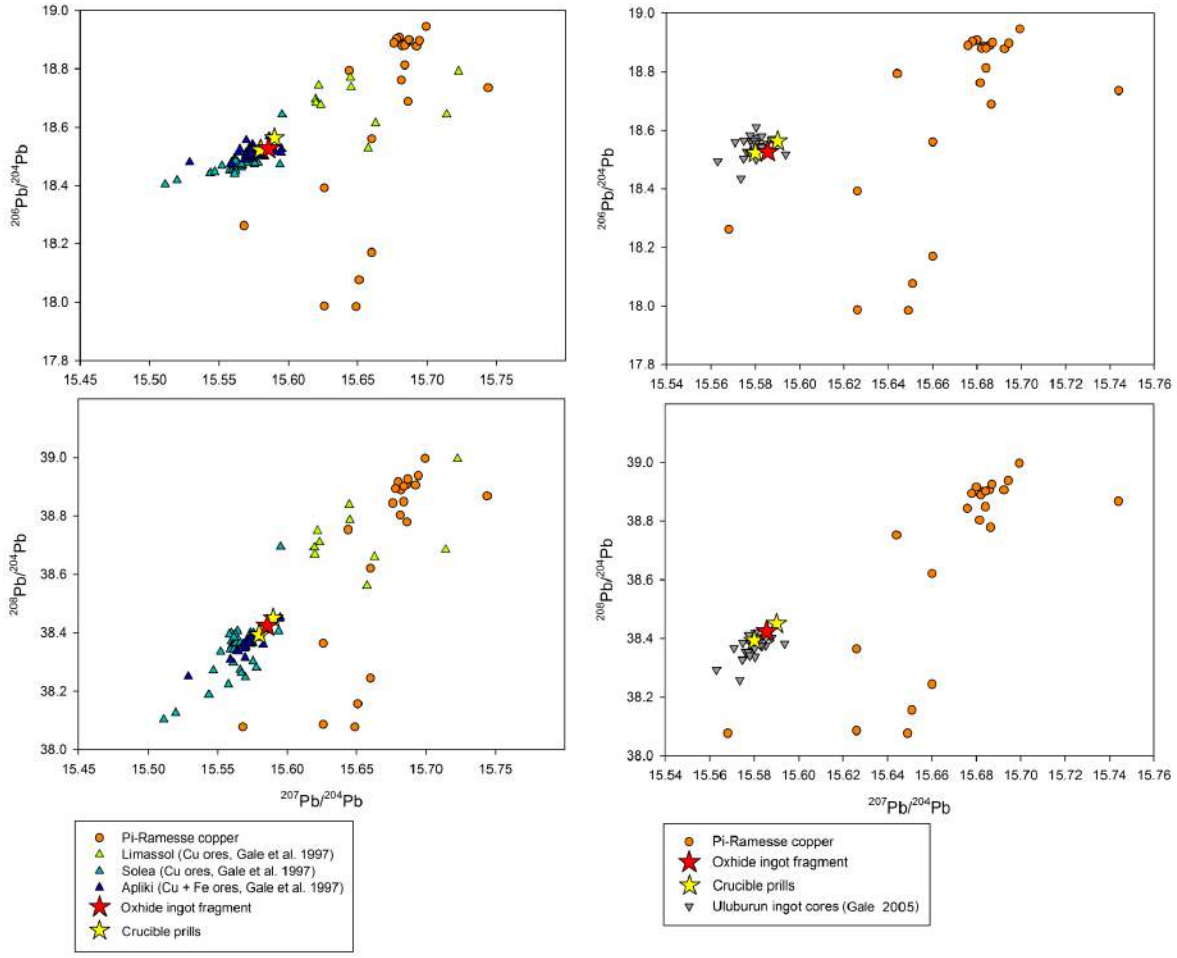

Figure 5.62: Comparison of Pi-Ramesse copper to Cyprus ores and Uluburun ingot cores LI compositions

Late Bronze Age is not well understood (Kassianidou, 2013) and is mainly confined to Hellenistic and Roman times (Constantinou, 1980; Hauptmann, 2007; Stos-Gale *et al.*, 1997). As discussed below, these samples more likely have a different provenance.

5.5.1.2 Moderately lead-rich samples - Timna/Feinan

Figure 5.63 shows a comparison of the LI composition of the Pi-Ramesse metal samples with Feinan (data from Hauptmann *et al.*, 1992) and Timna (data from Gale *et al.*, 1990) copper ores. The three samples with ±2 wt% lead content all fall within the isotopic range characteristic for both Feinan (DLS ores) and Timna, which are geologically very similar. Their moderate lead content is in line with an interpretation as copper smelted from either Feinan (DLS) or Timna ore, though lead contents for Timna tend to be lower (Hauptmann, 2007). The moderate iron content in these three samples does not contradict their

interpretation as raw copper (ingots). It must be noted that major mining activity for both Feinan (Ben-Yosef *et al.*, 2010; Levy *et al.*, 2012) and Timna (Ben-Yosef *et al.*, 2012) should be situated in the Iron Age, rather than Late Bronze Age. Given strong indications for cultural contact between Egypt and Timna during the Late Bronze Age (Rothenberg, 1987, 1988, 1990), and its geographical vicinity, it is more likely that these three samples represent Timna copper. Further correspondence to Timna copper can be found in comparison to ingots discussed by Yahalom-Mack *et al.* (2014). Feinan, however, cannot strictly be excluded.

The proximity of the 'tail' of the Feinan data (high $^{208-207-206}Pb/^{204}Pb$, representing MBS ores) to the largest cluster of Pi-Ramesse copper (see section 5.5.1.3) most likely holds little value.

Interestingly, these three samples all belong to the QIV context. Sample 1987_0512,0002 lies fairly close to them and could equally match Timna (or Feinan) but is not characterised by increased lead content (only 0.3 wt%).

5.5.1.3 Largest cluster

The largest cluster of data (around ±38.8-39 $^{208}Pb/^{204}Pb$, ±15.67-15.70 $^{207}Pb/^{204}Pb$ and ±18.7-18.9 $^{206}Pb/^{204}Pb$) shows strong likeness to one of the few available metal LI datasets available for Egypt: the bronzes from Amarna (Stos-Gale *et al.*, 1995), chronologically separated from Pi-Ramesse by only ±50 years. These are plotted alongside the Pi-Ramesse metal in Figure 5.64, together with contemporary Egyptian Blue samples from the Ramesside fortress at El Rakham (Shortland, 2006). Clearly, these three groups show very close resemblance in their LI composition.

At the time of publication, Stos-Gale *et al.* (1995) concluded that one of the Amarna samples might reflect Timna ores, while some overlapped with the Lavrion copper ores from Greece (Gale *et al.*, 2009), and the majority could not be assigned to any known ore source. More recently, a comparison was made to the Taurus 1A ores in Anatolia (Yener *et al.*, 1991), which appeared to coincide with the 'unknown' end of the Amarna data (Philip *et al.*, 2003). However, these are lead ores, and therefore not useful for comparison here.

The Pi-Ramesse, Amarna and El Rakham LI results are shown together with the Lavrion copper ore LI data (from Oxalid[21]) in Figure 5.65. This image shows that, though a few copper samples match the Lavrion copper ores, the majority does not coincide. In fact, the Lavrion copper ore lies on a different axis from this 'Egyptian group' (Lavrion sitting

[21] Oxalid: Oxford Archaeological Lead Isotope Database (http://oxalid.arch.ox.ac.uk/). LI data drawn from several publications is brought together there. Most of the Lavrion copper ore data is, however, unpublished.

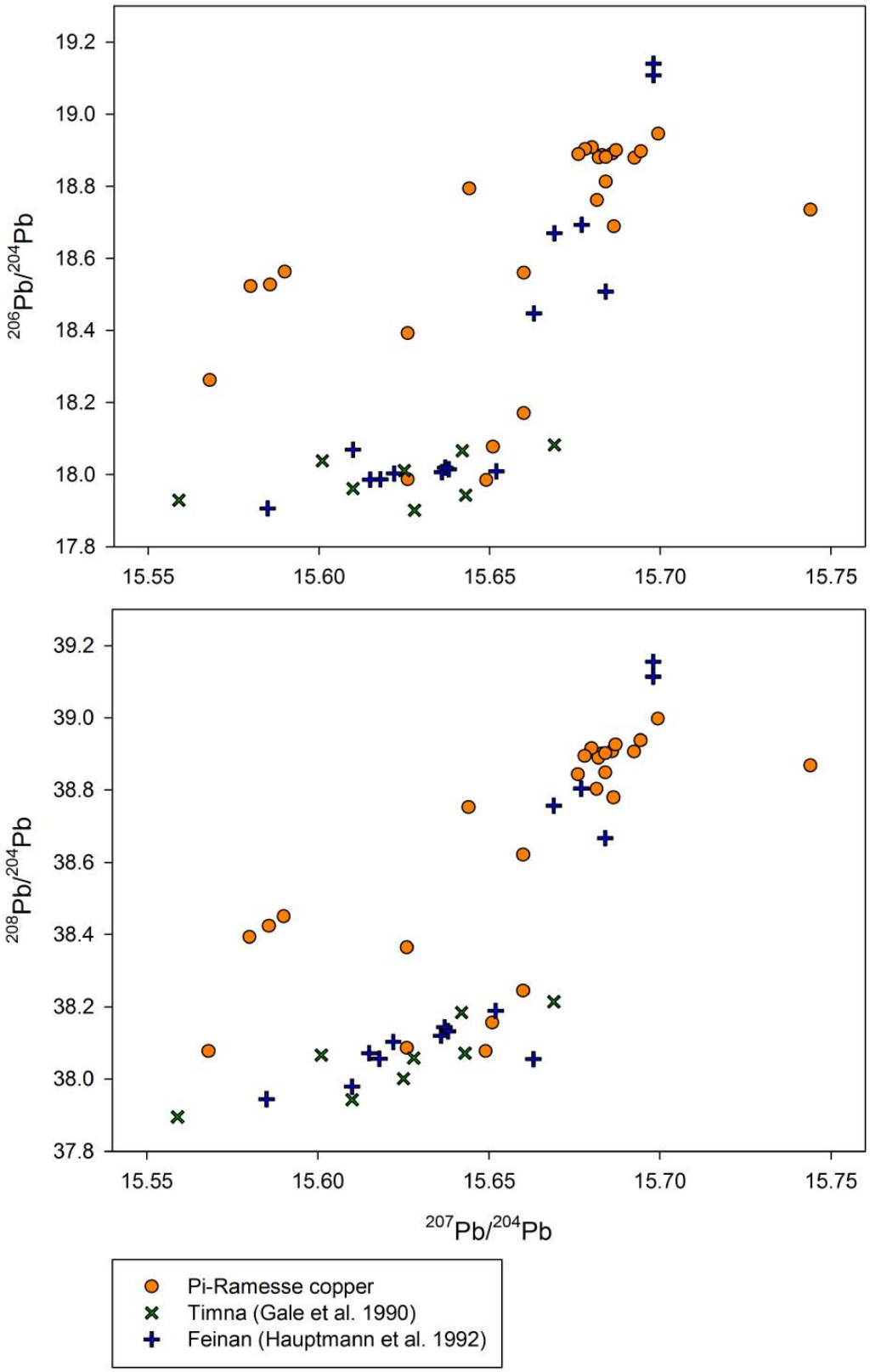

Figure 5.63: Comparison of Pi-Ramesse copper to Feinan and Timna LI compositions

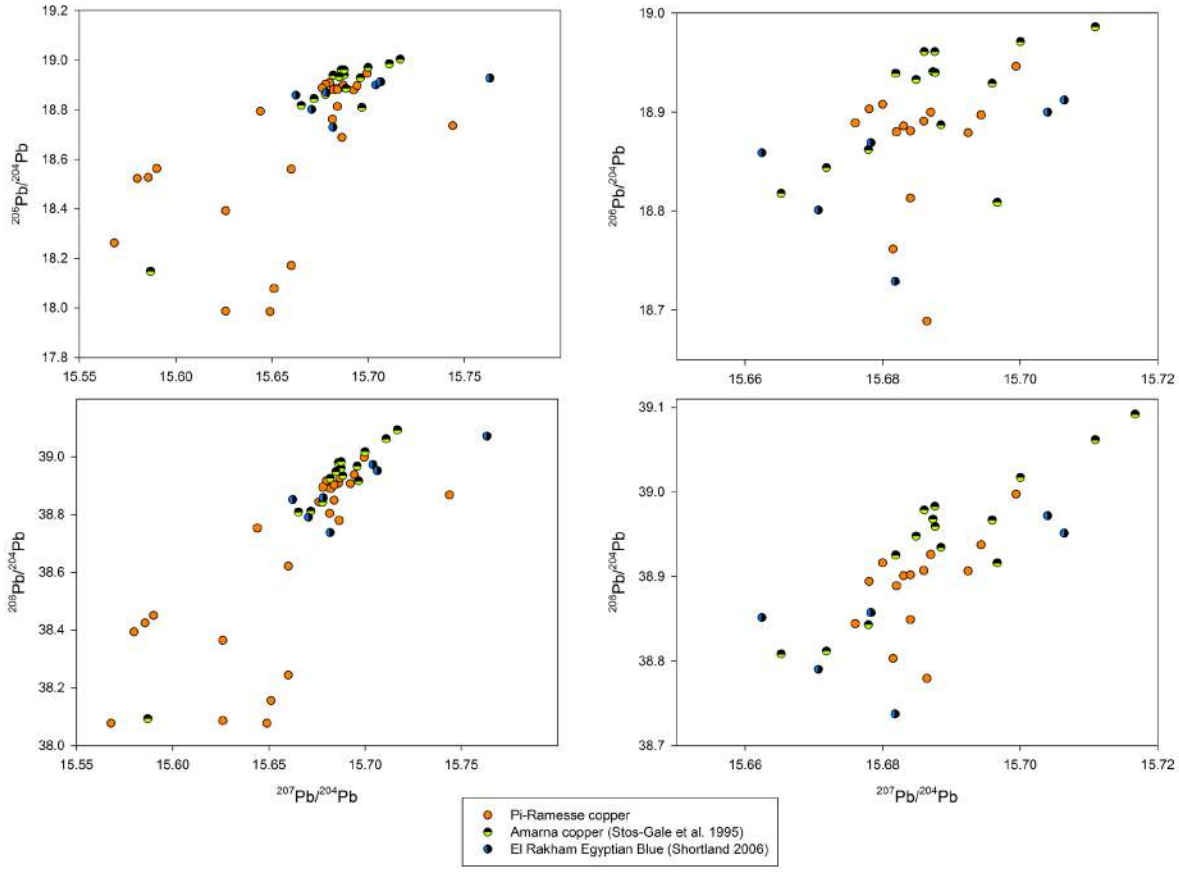

Figure 5.64: Comparison of Pi-Ramesse copper to Amarna copper and El Rakham Egyptian Blue LI compositions (left: all data, right: close-up)

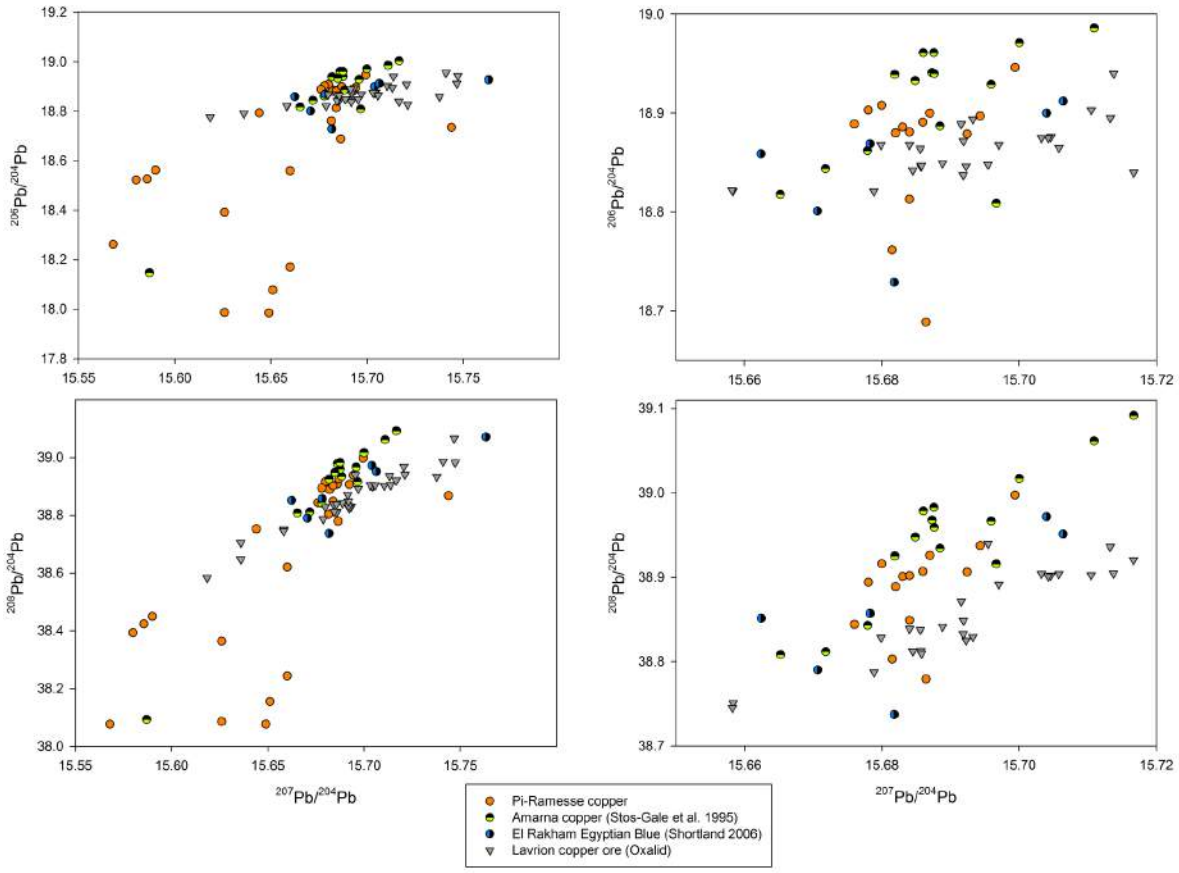

Figure 5.65: Comparison of Pi-Ramesse and Amarna copper and El Rakham Egyptian Blue to Lavrion copper ore LI compositions (left: all data, right: close-up)

below it in terms of $^{208}Pb/^{204}Pb$), and the proximity to some of the copper samples here is most likely incidental.

This group does not correspond to any of the other 'well-known Late Bronze Age copper suppliers[22]' (Stos, 2009), but appears to be a local, Egyptian metal group (not necessarily equating Egyptian ore sources). The contemporary material from Amarna and El Rakham offers particularly good support for such a statement.

Apart from Amarna, Maadi (Abdel-Motelib *et al.*, 2012) and Tell el-Farkha (Rehren and Pernicka, 2014), discussed below, the only known published LI analysis of Egyptian metals is by Fleming (1982), who examined Late Period Egyptian bronzes (8^{th}-5^{th} century BC) from Sanam abu Dom and Kawa (Upper Nile region) and Memphis (Lower Nile). It is important to note here that these are mainly leaded bronzes, such that their isotopic composition is dominated by that of the lead metal added to the alloy. Therefore, their comparison here is not very instructive.

Other materials have been analysed by Brill *et al.* (1974), El Goresy *et al.* (1998), Fleming

[22]Comparisons have been made to Cypriot, Arabah, Anatolian, Omani, Sardinian and Cretan ores

(1982) and Shortland (2006), including lead and silver objects, a few ores, *kohl* (majority of samples), glass, faience, Egyptian Blue and green frit. With the exception of Egyptian Blue, the LI composition of these materials mostly reflects their important lead content. The *kohl* (eye-paint produced from galena), for example, matches quite well to Egyptian lead ore bodies (Shortland, 2006) and indicates domestic production. This group of materials, however, offers no useful comparison for the Pi-Ramesse copper.
The Egyptian Blue samples from El Rakham, a coastal fortress-town from the reign of Ramses II at the western border of Egypt, offer more fruitful discussion. These appear to coincide quite well with the Pi-Ramesse and Amarna copper, which could indicate the use of similar copper for their production. In this context, the suggestion by Rehren *et al.* (2001) that Egyptian blue cakes were produced at Pi-Ramesse, and probably traded throughout Egypt, is particularly remarkable, and may shed further light on the interconnections existing between the different high-temperature technologies at Pi-Ramesse. Though Shortland (2006) concludes that the copper used to produce these pigments must have come from outside of Egypt, this must be revisited here in light of more recent investigations.

Abdel-Motelib *et al.* (2012) offer an overview of mining and smelting in the Eastern Desert of Egypt and in Sinai. It is important to note that all mineralisations there are very pure: very low concentrations of arsenic, nickel, cobalt, bismuth, lead, silver and gold occur, and should similarly be expected in any metal smelted from these ores. Though the majority of explored sites show evidence for Chalcolithic, Early and Middle Bronze Age exploitation, there is evidence for significant Late Bronze Age copper production as well. Specifically at Bir Nasib I, Abdel-Motelib *et al.* (2012) estimate that over 5000 ton of copper may have been produced during the New Kingdom, with ore probably coming from Wadi Umm Rinna, making it a major production area. It is therefore worth comparing LI data for these ore sources to copper from Pi-Ramesse, as was recently done by Rehren and Pernicka (2014) for metals from Tell el-Farkha. As discussed there, some of the Tell el-Farkha metal indicates radiogenic lead, which is most readily explained by a Sinai provenance, while other samples have higher $^{207}Pb/^{206}Pb$, which could equally point to Sinai, but are hard to distinguish from Feinan. In conjunction with the radiogenic lead samples, however, Sinai appears to be the most likely ore source for the majority of metals in Tell el-Farkha.
No radiogenic lead is attested for Pi-Ramesse (or Amarna), but a comparison to Sinai and Eastern Desert copper (ores) can still be made, and is shown in Figure 5.66. It is important to bear in mind, however, that ^{204}Pb-measurement was fairly imprecise for the Abdel-Motelib *et al.* assemblage (E. Pernicka, pers. comm., November 2014).
Again, there is no overlap with the large cluster from Pi-Ramesse (and Amarna) for any of the ore samples, though they fall within the broader LI range. The closest match is seen

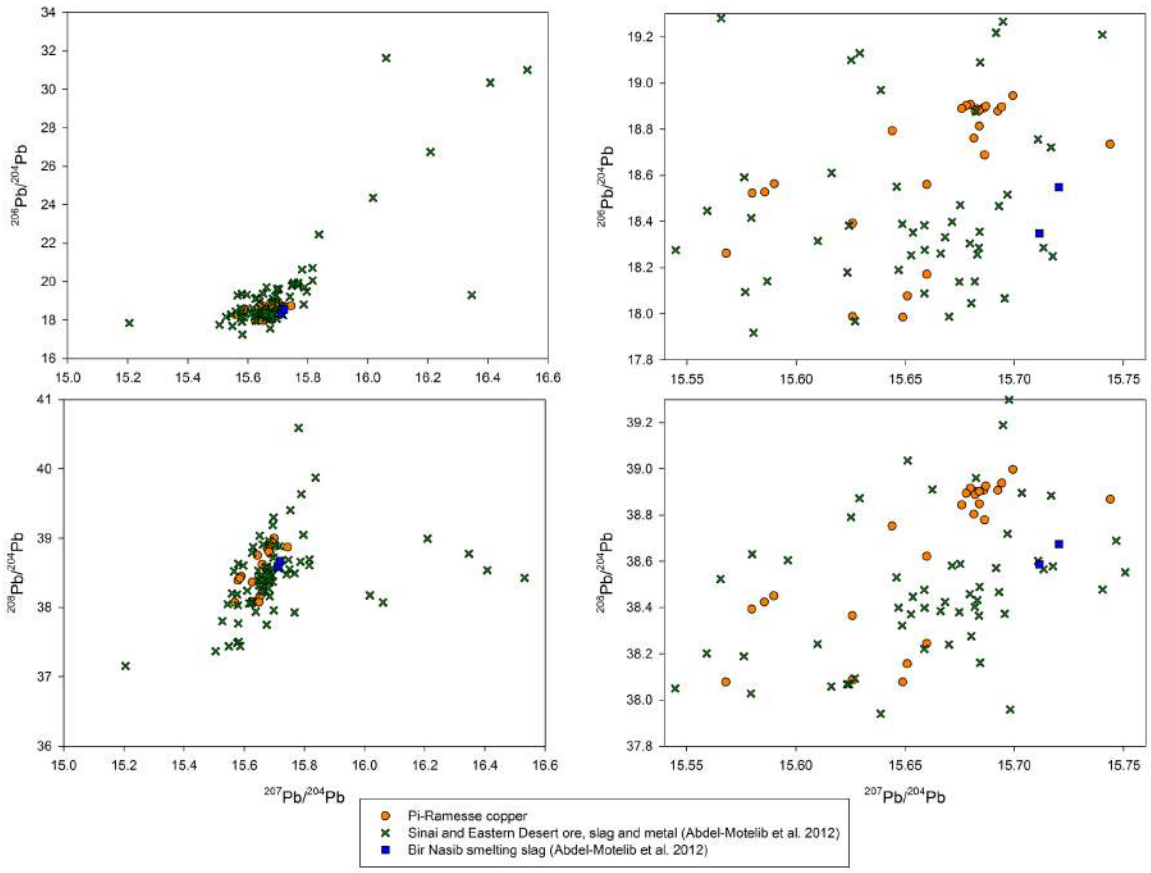

Figure 5.66: Comparison of Pi-Ramesse copper to Sinai and Eastern Desert copper ore, slag and metal LI compositions (left: all data, right: close-up)

for a copper ore fragment found in Maadi, most likely brought in from Sinai (Maadi H31 II 5/4), dating to the Naqadian period (4^{th} millennium BC). A copper fragment from Sheikh Muhsen overlaps with one of the moderately high-lead samples. Given the pure nature of these ores, Timna/Feinan is a more suitable candidate here. In general, the Sinai and Eastern Desert ores appear to sit both above and below the large Pi-Ramesse cluster in 'LI space'. It must be emphasised that this data reflects a very large range of deposits and exploitation evidence spanning several millennia. The most relevant site for this study, Bir Nasib I, is represented by only two (slag) samples, both of which have low to very low lead content.

The (admittedly limited) current evidence indicates that early Egyptians relied at least to some degree on local copper production from the Eastern Desert and Sinai in their provision of copper. Mining evidence further shows that there is continuity in production from this region at least up until Middle Kingdom times. Even during the New Kingdom, there was large scale production of copper from Bir Nasib I, South Sinai (Abdel-Motelib *et al.*, 2012; Rothenberg, 1987; Yahalom-Mack *et al.*, 2014), as well as the exploitation of

gold sources in the Eastern Desert (Klemm and Klemm, 2013). Altogether, there is fairly compelling evidence to suggest that 'domestic copper', coming from the Eastern Desert and/or Sinai, would have been in circulation in Egypt throughout its pharaonic history (see section 4.5). This copper, already attested early on in Maadi and Tell el-Farkha, would have probably been regularly replenished with freshly mined 'domestic copper', as well as (perhaps more occasional) copper from abroad. Here, the most likely candidates for long-time contribution are Timna (and Feinan), while sources from further away (Cyprus, Greece, Anatolia, etc.) are expectedly minor contributors, at least up until the Late Bronze Age.

For Pi-Ramesse (and Amarna), it would be highly likely that at least some of this 'Egyptian domestic copper' (the mainstream and scrap copper in circulation, as defined by Rehren and Pusch (2012)), was used. This could be both freshly mined copper and recycled circulating copper or bronze. In fact, there are good indications for the practice of recycling within the Pi-Ramesse workshops (see section 6.1). The presence of 'domestic copper' should therefore be reflected in the lead isotope field presented here.

It can therefore be suggested that this large LI cluster is in fact this 'domestic copper', representing both freshly smelted copper from various Sinai and Eastern Desert (extending into Nubia) copper ores, as well as recycled metal from these sources. Though no perfect match currently exists with the available data for these ores, this may be the most likely explanation for the clustering of the Pi-Ramesse, Amarna and El Rakham material. It is hoped that this hypothesis can be further tested in the future with more extensive data from various Sinai and Eastern Desert copper ores.

The notion of recycling should be expanded a bit further here. If circulating copper was indeed recycled and mixed within Egypt, with regular replenishment from its 'domestic ore sources' (Sinai and Eastern Desert), some clustering of LI composition would be expected, though a spread towards the end members of this mixing scenario would be maintained if regular replenishment took place. However, recycling does not necessarily imply mixing.

For the interpretation of such a scenario, more LI data is required from both Egyptian metal and 'domestic ores' to produce a diachronic picture for Egypt. This 19^{th} Dynasty 'snapshot' cannot elucidate this any further. It can be noted, however, that the Sinai and Eastern Desert show such a large LI compositional range, that, even though no exact overlap with the Pi-Ramesse metal exists for the current ore samples, copper ores probably exist which match the 'domestic metal group' seen here, and are yet to be analysed. Alternatively, a selection of ores (surrounding the 'domestic group') may have been mixed to arrive at this 'domestic group' composition, but it is currently impossible to validate this.

It is important to point out that this provisional interpretation differs from the (much

debated) *koine* proposed for the eastern Mediterranean trade as a whole by Budd *et al.* (1995b). The scale envisaged here is much smaller, and concerns a far more closed system, with metal input limited to internal sources (Eastern Desert and Sinai, perhaps Timna), with only the occasional influx of foreign metal[23] (compare to suggestions by Pinarelli (2004) for local Sardinian copper). This metal would have circulated internally in the Egyptian economy, where it could have been regularly recycled. This is suggested, for example, by the tight control over metal tools seen at Deir el-Medina (Eccleston and Kemp, 2008), and indications for the recycling of metal tools in the workshops (QI and QIV - B/2) at Pi-Ramesse (Prell, 2011). The general attitude of ancient Egyptians (especially the pharaonic state itself) towards (precious) resources seems to have been quite frugal, favouring a system of recycling.

5.5.1.4 Further information from chemical compositional data

Before continuing the discussion on LI composition for the remaining samples, some notes on chemical compositions are made.

Tin content averages at ±10-11% (see Figure 5.67). However, four samples (1984_1162,0001, 1985_0205,0001-0003, 1986_0909, and 1987_0803,0004) consist of unalloyed copper. Interestingly, these samples all have low (below detection limits) lead content as well, which does not occur for the alloyed samples. In terms of LI composition, they mainly plot intermediate to the clusters identified so far (see Figure 5.61). The two crucible prills which match the Apliki oxhide ingot are expected to have similarly low lead content, but this has not been measured. This coincidence of low lead and tin content is remarkable, as it concerns 15-20% of the samples.

Another interesting observation related to the unalloyed samples is that they have low gold contents as well. For samples 1984_1162,0001 and 1985_0205,0001-0003, gold content is <10 ppm, while the average gold content in the bronze samples is >100 ppm (no NAA data available for other two unalloyed samples). This could point to the presence of >100 ppm gold in most copper used at Pi-Ramesse, with the exception of these few instances. However, it is more likely that the tin used for alloying at Pi-Ramesse contained traces of gold, which is thus present in all bronzes. This would not be contrary to the proposed use of alluvial cassiterite from the Eastern Desert in a cementation process for bronze production (section 5.4.5). A similar argument was made for gold content noted in the Amarna

[23] Shaw (1998) notes that the quantities of copper acquired through Egyptian mining are cited by the ancient Egyptians in thousands [sic], while only small amounts came in through (military) expeditions abroad.

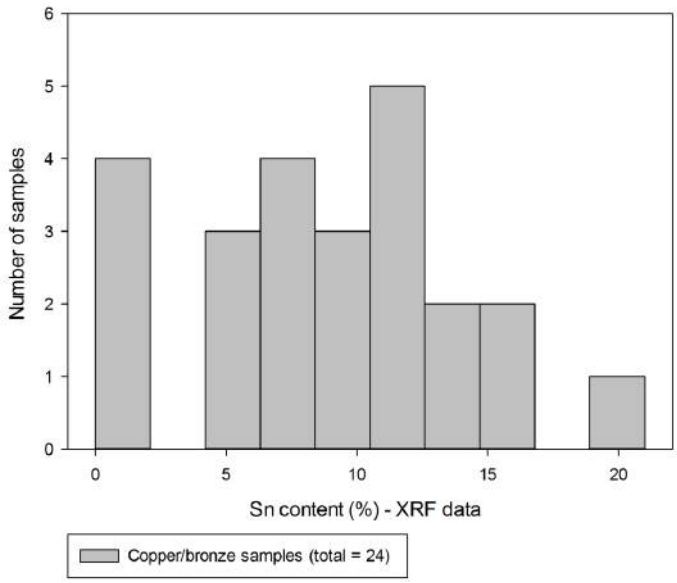

Figure 5.67: Histogram showing tin content for metal samples

bronzes by Stos-Gale *et al.* (1995) (referring to alluvial tin and gold deposits of Abu Dabbab).

0.2% gold was measured in one bronze object (1982_0219b,0002), described as possibly gilded. Such objects might have been indiscriminately remelted in the Pi-Ramesse crucibles, as indicated by copper-gold prills in crucible 86_0749c (section 5.4.11). The rarity of gold in both the bronze crucibles and objects suggests that it was not intentionally or actively processed in the bronze workshops at Pi-Ramesse (though it was probably worked elsewhere in the capital, see Pusch, 1999a). The LI composition for this sample sits below the 'domestic group'.

The lead content for all samples is summarised in Figure 5.68. With the exception of four samples with strongly elevated lead content (±5% and ±2%), all bronze samples have lead contents of ±0.5%. The four unalloyed copper samples have lead contents below detection limits. The lead content in the bronzes most likely indicates the presence of lead as an unintentional contaminant of copper, rather than its intentional alloying (in which case one would expect a normal distribution around a value exceeding 1%). Though values up to ±1% occur in four samples, this seems to be the normal range for limited remnant lead in copper (most likely from the smelting process (Pernicka *et al.*, 1990), though possibly from repeated recycling of (moderately) leaded copper).

High iron content (7.5% by NAA, 4.4% by XRF) is noted in sample 1985_0205,0001-0003, with moderately high iron content noted in another three or four. In at least two of these,

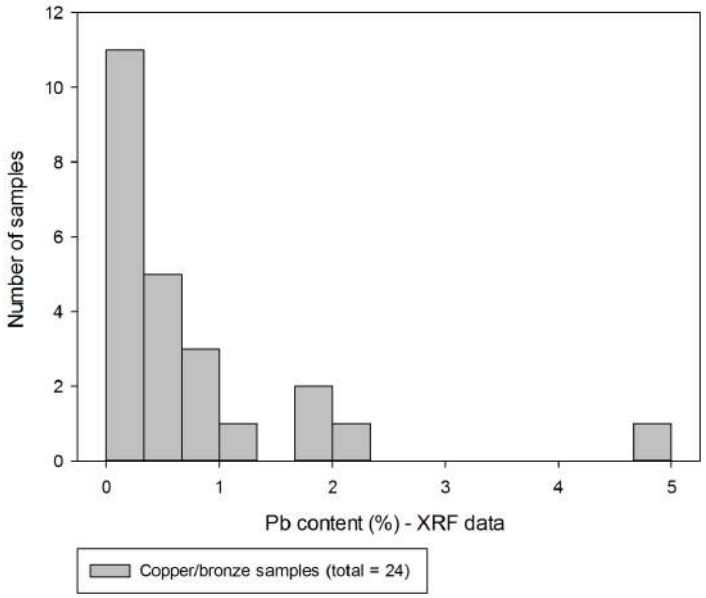

Figure 5.68: Histogram showing lead content for metal samples

there is significant cobalt enrichment as well. Moderate to low iron content (low<0.5%, 0.5%<moderate<1%) can be noted in most other samples (iron is below detection limits for the nine Isotrace samples).

This iron (and cobalt) content derives from a combination of several factors, including the ore composition, primary smelting process (redox-conditions etc.) and refining/recycling processes. The importance of these factors can vary for different samples, as they may have gone through different technological trajectories through time, and their absolute contents can therefore not be directly compared. Figures 5.69 and 5.70 show the iron and cobalt content in all analysed samples. This shows a similar pattern to that seen for lead, indicative of its presence as a contaminant in the copper (ore), diluted throughout metallurgical operations. This matches very well the results from crucible slag analysis concerning iron and cobalt (sections 5.4.6 and 5.4.7). As Figure 5.71 shows, iron and cobalt content do not fully correlate. Crucible analysis indicates that some iron-rich copper was used, which did not contain significant cobalt, while some copper had significant cobalt content, invariably accompanied by iron. This is mirrored by seven samples in Figure 5.71 with cobalt below detection limit, and eight samples with 0.01-0.06% Co. Cobalt content, when present, appears to have some correlation to iron content. Due to variable losses during smelting, remelting/recycling, alloying etc., a weak correlation is all that can be expected here.

The variable presence of cobalt (with iron) points to the use of copper smelted from cobalt-bearing ores. This provides further information on the geology of the copper ore sources

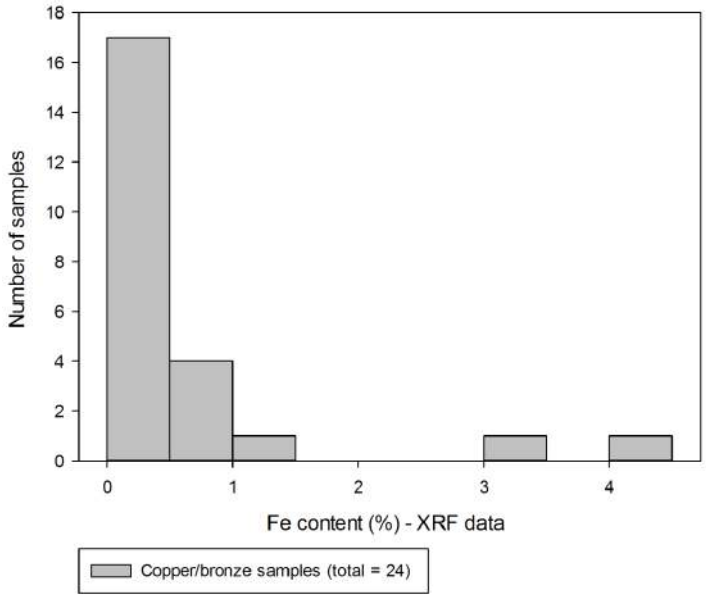

Figure 5.69: Histogram showing iron content for metal samples

for these samples, which could be useful in conjunction with the LI data. The absence of cobalt in other samples, however, could be due to losses during previous metallurgical operations, or indicative of the use of different ores.

Further plots of arsenic, nickel, cobalt, antimony, iron, lead, tin, zinc, silver and gold content are shown in Appendix F. Arsenic (average 0.5%), nickel (average 0.03%), antimony (average 0.042%), tin and gold (average 83 ppm) show fairly good correlation between each other, with correlation coefficients between arsenic and gold, antimony, and tin of 0.93, 0.72, and 0.64, respectively, and between gold and tin and antimony of 0.67. Gold and silver correlate quite well, with the exception of one sample. Cobalt and zinc are not very well correlated to any other element, with the exception of iron (correlation coefficients 0.73 and 0.86 respectively), which in turn does not correlate well to any of the above mentioned elements. Lead does not exhibit a linear correlation to any of these elements, though some correlation may exist between lead and arsenic, nickel and antimony at lower levels of lead.
The distributions of these elements (not plotted) suggest that arsenic, zinc and antimony are predominantly present as contaminants (i.e., patterns similar to iron and lead), while this is less clear for the other elements. It must be emphasised that this data represents mainly corroded metal and that the sensitivity of different elements to process-related changes (oxidation, volatilisation, siderophile/lithophile/chalcophile separation, etc.) in the course of their technological trajectory can obscure their initial relations from the ore. Furthermore, the number of samples analysed by NAA is very limited, and any conclu-

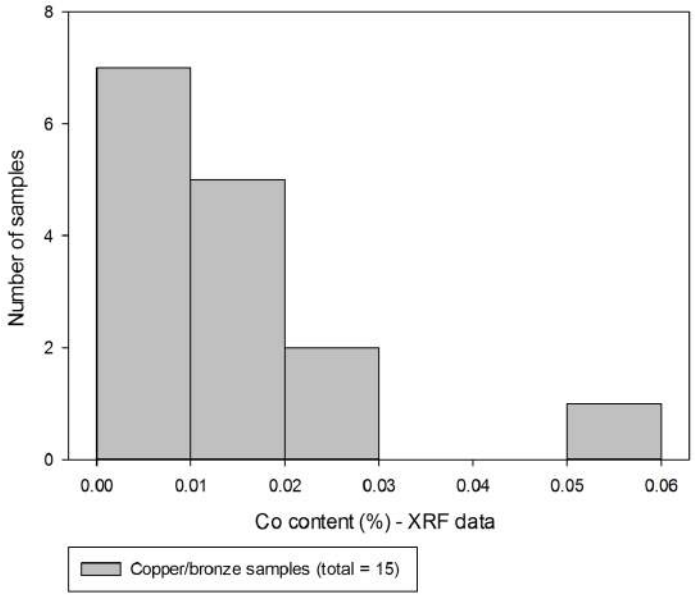

Figure 5.70: Histogram showing cobalt content for metal samples

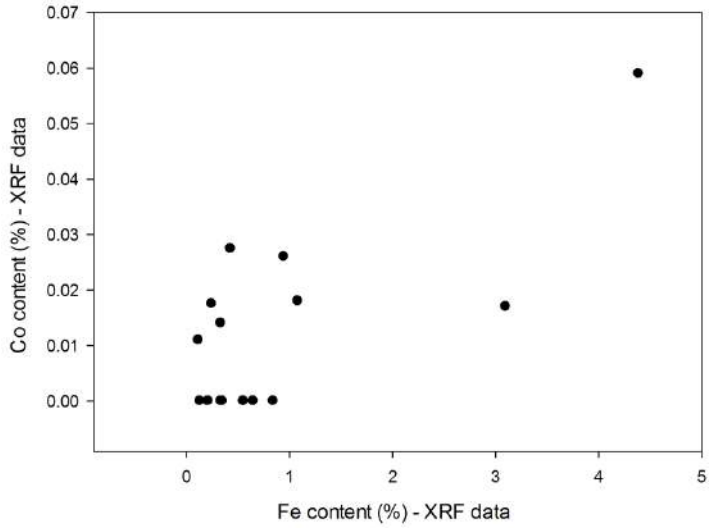

Figure 5.71: Iron vs cobalt content for metal samples

sions drawn here are therefore tentative at best.
Overall, most of these elements (arsenic, nickel, cobalt, antimony, iron, lead, zinc, silver and gold) are present at contaminant levels. Given that there appear to be several sources of metal introduced into these crucibles, the chemical relationships between elements may differ for these different sources.

5.5.1.5 Remaining samples and contextual distributions

With this information in mind, the remaining LI samples are considered. Figure 5.72 shows the samples tentatively assigned to particular groups so far: Apliki copper (ingot and two crucible prills), three moderately leaded samples of Timna copper (and one with lower lead content, close in composition), and a large group of 'domestic copper'. The high-lead (5%) and high-iron (7.5%) samples are both separate in terms of LI composition, while the remaining six samples are intermediate with respect to the three tentatively identified groups.

The high lead content in sample 1984_1381 may indicate intentional alloying to produce a leaded bronze (only 5% Sn) or the use of copper smelted from a lead-rich ore. Its identification as a 'round rod', provides no further clue as to why a leaded bronze would have been selected here. The lack of indications for intentional leaded bronze alloying in the Pi-Ramesse crucibles, coupled with the scarcity of leaded bronze use in Egypt as a whole for this period, suggests that its use as an intentional alloy is in fact doubtful. This leaves two plausible explanations for this sample:

1. It was produced as an intentionally leaded bronze elsewhere, and subsequently reused in Pi-Ramesse. At 5% lead, the lead content from the copper would provide only a limited contribution to the final LI composition of the leaded bronze. Therefore, this final composition is mostly reflective of the lead ore, rather than the copper ore.

2. Following primary smelting, the copper had an exceptionally high lead content. High lead contents have, for example, been noted for Feinan ingots (Hauptmann *et al.*, 1992, Table 6, p. 22). No further chemical data to support this interpretation as raw copper (e.g., increased iron) is available for this sample.

Whether this particular object was brought into Pi-Ramesse from abroad ready-made, or fabricated in the Ramesside workshops using foreign (lead-rich) metal remains unknown. It appears most likely, however, that the higher lead content is not intentional. No good ore match can be suggested for this sample at present.

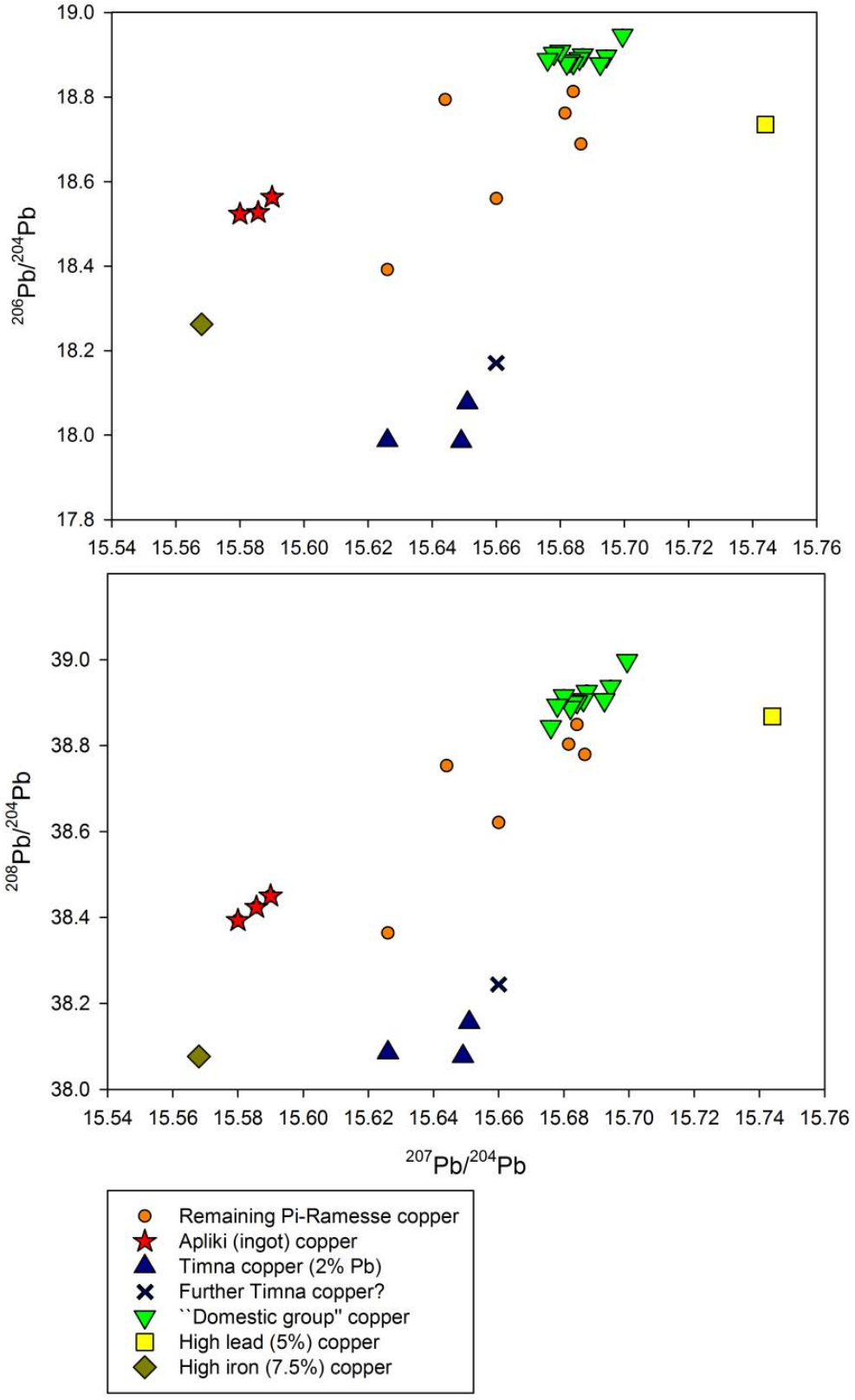

Figure 5.72: Interim overview of LI compositional groups

One sample (1985_0205,0001-0003) shows a particularly high iron content (7.5% by NAA, 4.4% by XRF), as well as fairly high cobalt content (620 ppm by NAA, 0.06% by XRF) and is an outlier for Pi-Ramesse in the LI field. It is not alloyed with tin and has a very low lead content. It has extremely low silver and gold content (7 ppm and 2 ppm by NAA respectively), as well as above average zinc content (263 ppm by NAA).
When copper with such a high iron content is melted in a crucible, it is more than likely that a significant and notable dross layer will form on top of the crucible charge (Merkel, 1990) and significant iron enrichment builds up in the crucible slag. This dross would have preferably been removed before adding any tin to the charge, perhaps through more than one refining operation.

At this point, it is worth including the contextual distribution of these samples in the discussion. In Figure 5.73, a distinction is made between the QI industrial workshops (phase B/3) and later finds from that area (phase B/2), the QI multifunctional workshops (phase B/2) and the QIV workshop. Possible stratigraphical mixing, discussed in section 4.4, has to be kept in mind though. Figure 5.74 highlights the most highly sampled excavation square (QI-c/4.5) and the five most iron-rich samples. These plots reveal some interesting patterns.
The QI industrial workshops appear to have mainly used 'domestic copper', while Apliki copper occurs in the same area only in phase B/2 and in QIV (contemporary). Timna copper appears exclusively in the QIV workshop. Perhaps most interestingly, the majority of remaining samples (with both intermediate and extreme LI compositions) belong to the QI multifunctional workshops, where some 'domestic copper' equally occurs. The five most iron-rich samples all belong to phase B/2, in particular the multifunctional workshops. This may not be a coincidence, and indicate more 'dirty copper' being used in this context, while the 'clean' Apliki and Timna copper was reserved to other workshops (though equally during phase B/2). Similarly, all samples with increased cobalt content belong to phase B/2 (multifunctional workshops and QIV workshop). Finally, the gilded bronze fragment belongs to the B/2 multifunctional workshops as well.

Of particular interest are the six QI-c/4.5 samples, which range from the 'dirtiest' (most iron-rich) copper to the 'domestic group'. It is noteworthy that three out of the four unalloyed samples belong to this group. Could this group of samples be indicative of refining activity in this particular workshop in area c/4.5, whereby successive remelting took place before the copper was considered clean enough to alloy? Could some of the more familiar domestic copper have been added to it, thus pulling the LI composition to this intermediate area? Or do these samples all represent different copper sources? Some could be identified as Limassol copper (see above), while the most iron rich might fall in the range

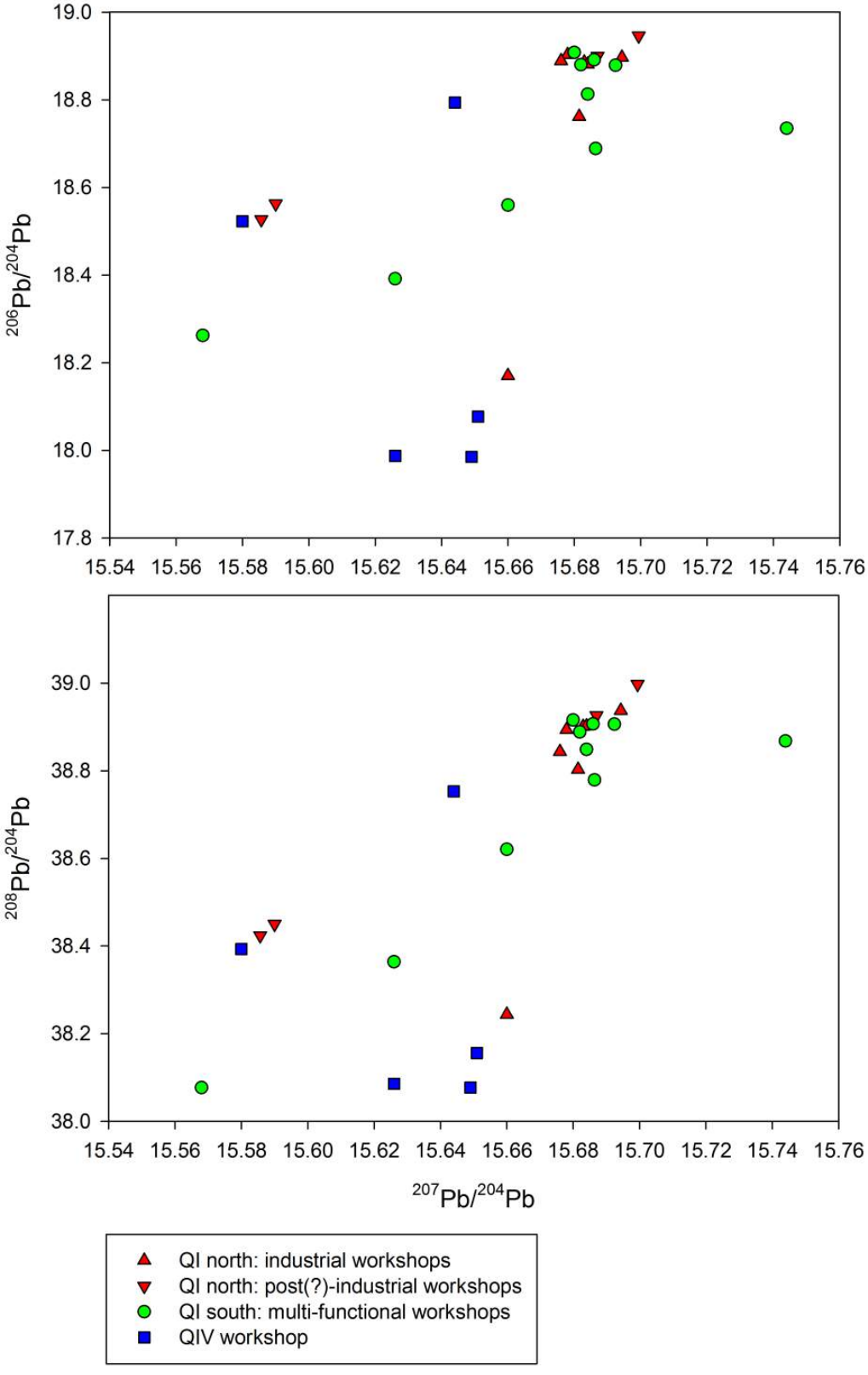

Figure 5.73: Overview of LI compositions by context

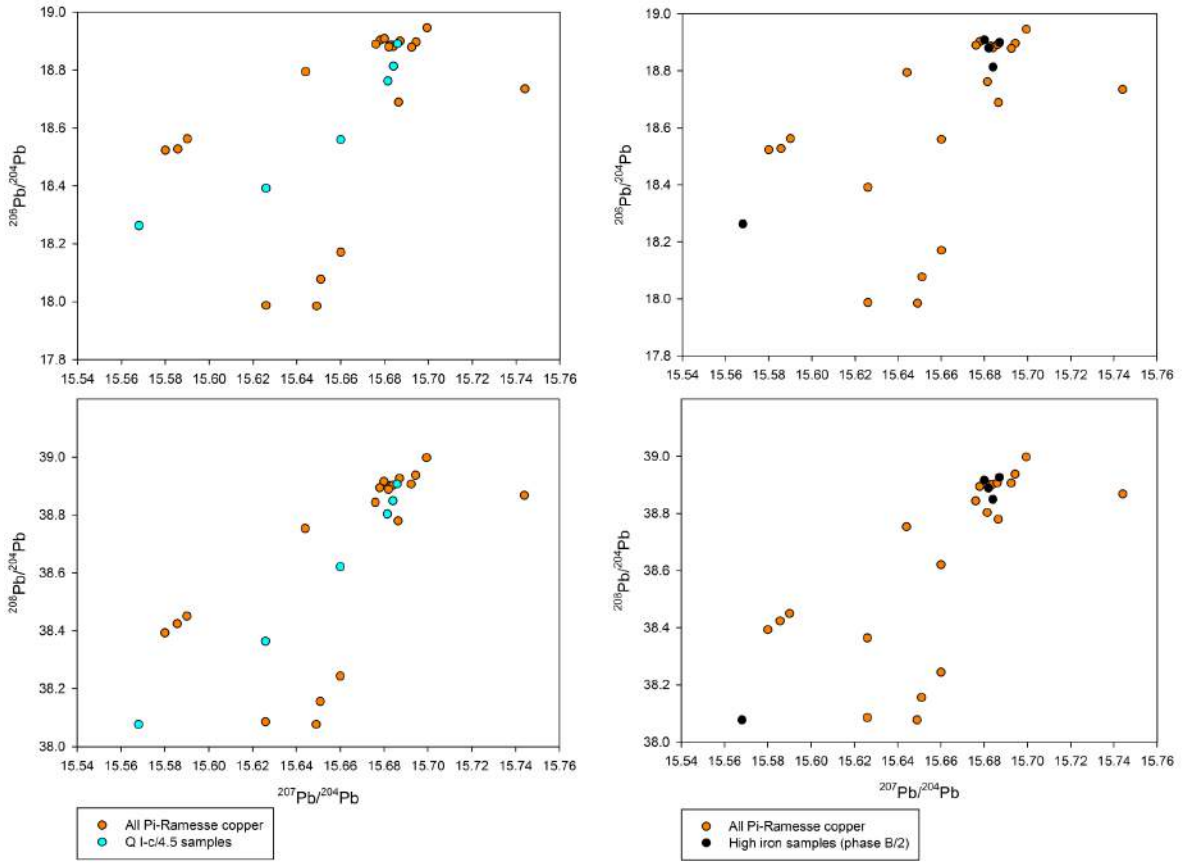

Figure 5.74: Overview of LI compositions, highlighting QI-c/4.5 samples (left) and most iron-rich samples (right)

of Timna copper. A final interesting comparison may be made to Omani copper ores and metals from Middle to Late Bronze Age Wadi Suq (data from Begemann *et al.*, 2010). As Figure 5.75 shows, these ore and metal samples (full range not shown) overlap to a reasonable degree with the 'QI-c/4.5' samples and some of the 'domestic copper'. Interestingly, this copper source has increased cobalt and nickel content, and 'dirty' export ingots produced from it could provide a match for these intermediate samples. It is difficult to push this interpretation any further here, but an interpretation as Omani copper may be a better explanation for these samples than any other available at this point.

5.5.1.6 Summary

Though overlap of Sinai and Eastern Desert ores exists with nearly the entire range of metals attested at Pi-Ramesse, this does not weaken the identification of certain materials as deriving from different sources. The integration of chemical (e.g., lead and iron content) and typological (e.g., oxhide ingot) information allows the distinction of at least three, and

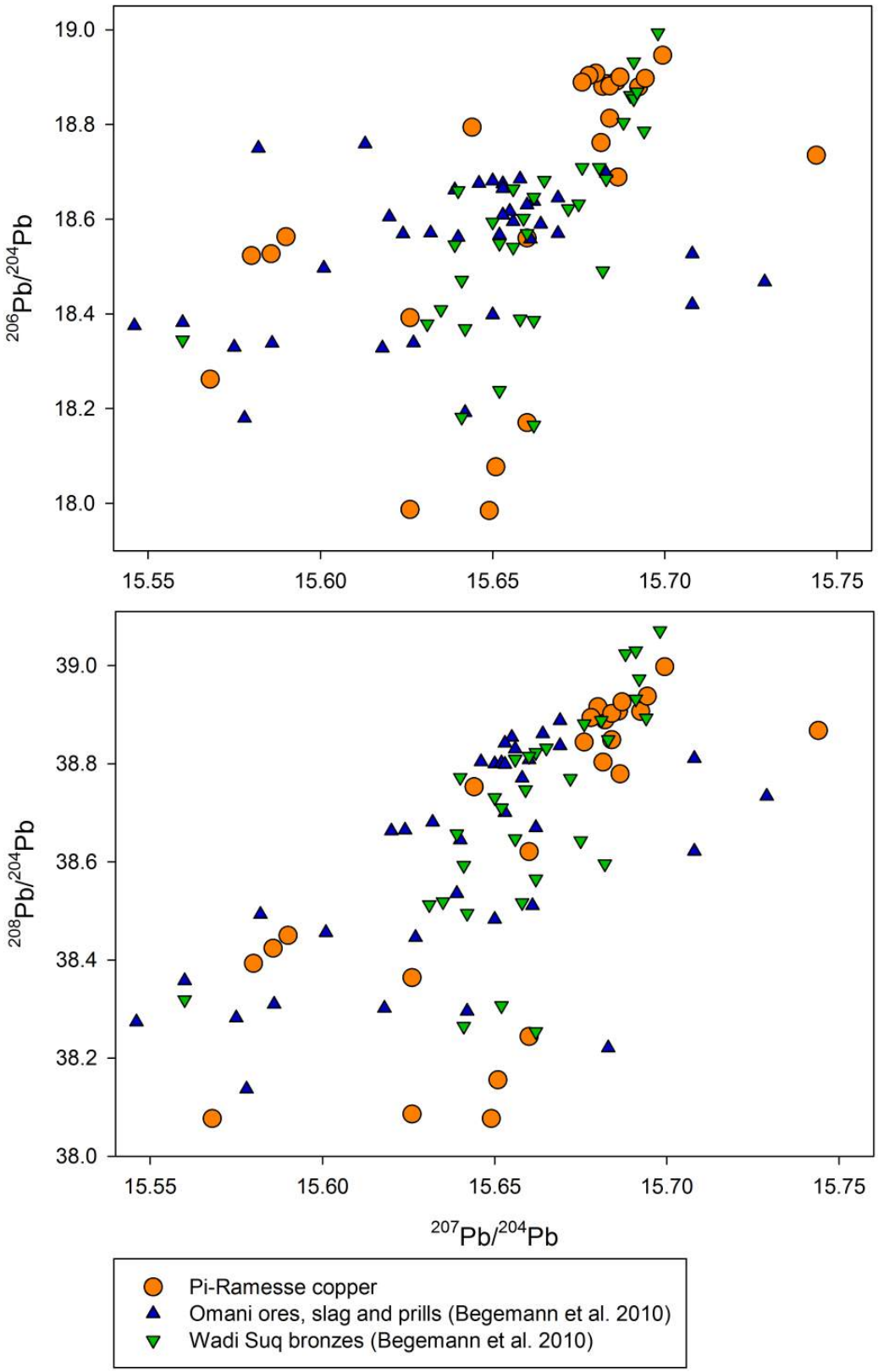

Figure 5.75: Comparison of Pi-Ramesse metal LI compositions to Omani ores and copper

most likely four, different metal sources within the Pi-Ramesse workshops, as shown in the final overview of Figure 5.76.

A 'domestic group', probably representing copper smelted from Sinai and Eastern Desert ores, forms the largest cluster, and represents copper used in QI, predominantly (though not exclusively) in the industrial workshop area. Secondly, the use of Cypriot oxhide ingot copper has been identified in both the QI and QIV area (phase B/2). Thirdly, the use of lead-rich copper, most likely from Timna, has been identified in area QIV.

One sample from QI may equally represent Timna copper, but its lower lead content and different dating (B/3 rather than B/2) suggests that it does not belong to the same 'batch' as the Timna copper attested in QIV. An Omani provenance may be suggested here, as an excellent match exists with a Wadi Suq bronze spearhead.
One sample from the QIV workshop is situated intermediately between the Apliki and domestic cluster. This could suggest the mixing of copper from these two sources in a crucible, resulting in an intermediate LI composition.
Finally, a varied group of samples from the multifunctional workshops remains. This consists of a very iron-rich copper, a leaded and a gilded bronze and two alloyed and two unalloyed samples with LI compositions intermediate to all other groups. This could suggest Omani copper being used in these workshops, or, alternatively, may indicate the refining and mixing of the raw, iron-rich copper (which may be Timna or Omani copper) with 'domestic copper'. If the three samples closest to the 'domestic group' (gilded bronze and copper/bronze from QI-c/4.5) may be included in that group (which seems reasonable), then the two remaining intermediate (QI-c/4.5) samples may indeed be interpreted as the result of mixing copper from different groups. This would not at all be surprising, given the clear archaeological evidence for metal recycling in these workshops.
It is, however, possible that these intermediate samples represent (unmixed) Sinai or Eastern Desert copper, or, more likely given the presence of cobalt, nickel and arsenic, Omani copper. If so, Figure 5.75 suggests that some of the 'domestic copper' may in fact be Omani copper as well.

Finally, some initial connections to the crucible slag analysis may be drawn here. The occurrence of limited lead enrichment of the crucible slag in ±15% of the assemblage may reflect the use of moderately leaded Timna copper. The use of 'clean copper' in approximately 50% of the assemblage may correspond to the 'domestic group' defined here. If this copper was indeed smelted from Sinai or Eastern Desert ores, few contaminants are to be expected indeed (Abdel-Motelib *et al.*, 2012). The more cobalt enriched crucibles, finally, could be related to the use of Omani copper. Such distinction is not tenable, however,

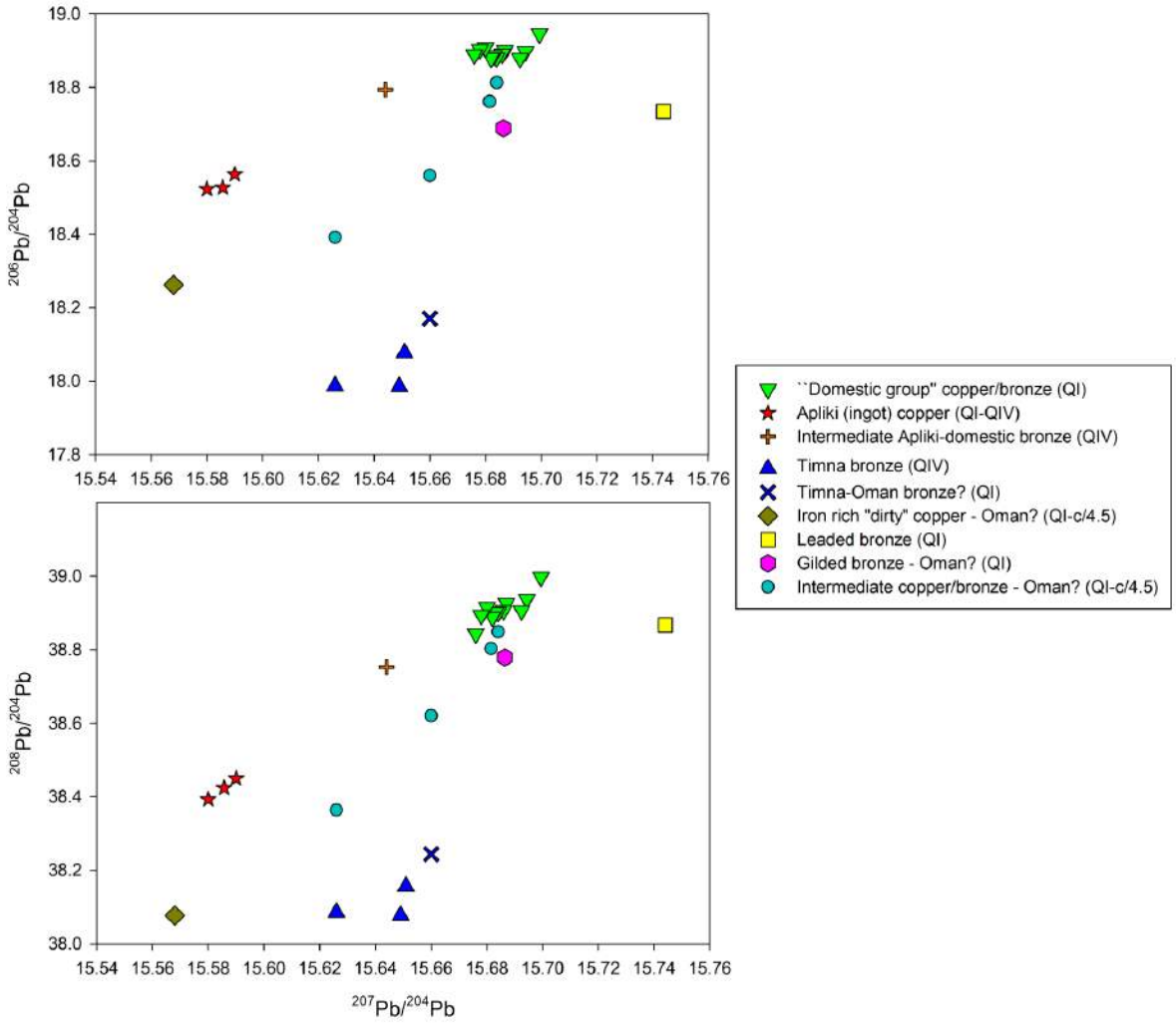

Figure 5.76: Final overview of LI compositions of Pi-Ramesse copper and bronze

based on the limited chemical data available, and certain samples identified as Timna and 'domestic' copper equally exhibit increased cobalt content (while cobalt is absent in others). The connection to iron contaminated crucible slag is discussed in section 6.2.
Further correspondence to crucible slag analysis may be found in the association of gold with tin. This further validates the tentatively identified use of alluvial cassiterite in a bronze cementation process.

5.5.2 Crucibles

5.5.2.1 Introduction

Figure 5.77 shows the LI compositions for ceramic and slag of the Pi-Ramesse crucibles (full data in Table F.5). These cover a very similar range to the metal samples, but the nature of the data is quite different here.

The ceramic part of the crucible, made of Nile silt, has a certain lead content[24] with strongly varying isotopic composition. This spread is assumed to be natural for the Egyptian Nile silt and reflective of the Nile basin geology, which draws on various upstream floodplains (see, e.g., Adamson *et al.*, 1980; Foucault and Stanley, 1989; Garzanti *et al.*, 2006; Krom *et al.*, 2002 and Stanley *et al.*, 1988) and therefore represents a broad geological time-scale. Publications on LI compositions for these sediments, however, do not exist.
In each crucible a slag layer is formed, which has a certain lead content too. This lead content is a mixture of lead from the molten ceramic and lead added into the slag from the molten charge. Therefore, the isotopic composition of lead in the crucible slag is a mixture of the isotopic composition of lead in the ceramic and copper/bronze charge respectively. In principle, these should both contribute to the slag proportionally to their absolute lead content. It can therefore be argued that, a line, drawn in the three dimensional space formed by the LI ratios going through the LI composition of the crucible ceramic and slag, should run through the LI composition of copper/bronze that was molten inside that crucible. The LI composition of the crucible slag would lie on this line intermediate to that of the ceramic and the metal. The distance between ceramic and slag and between slag and metal, would be determined by the relative contributions of both to the lead content in the slag.

[24] Lead content was not determined by NAA or labXRF and not detectable by SEM-EDS. pXRF analysis (see section 5.3) gives <75 ppm for the ceramic and an average of ±1600 ppm for the slag. These numbers should be treated with great caution, and provide a broad indication only: lead content in the slag is roughly 20 times higher than in the ceramic.

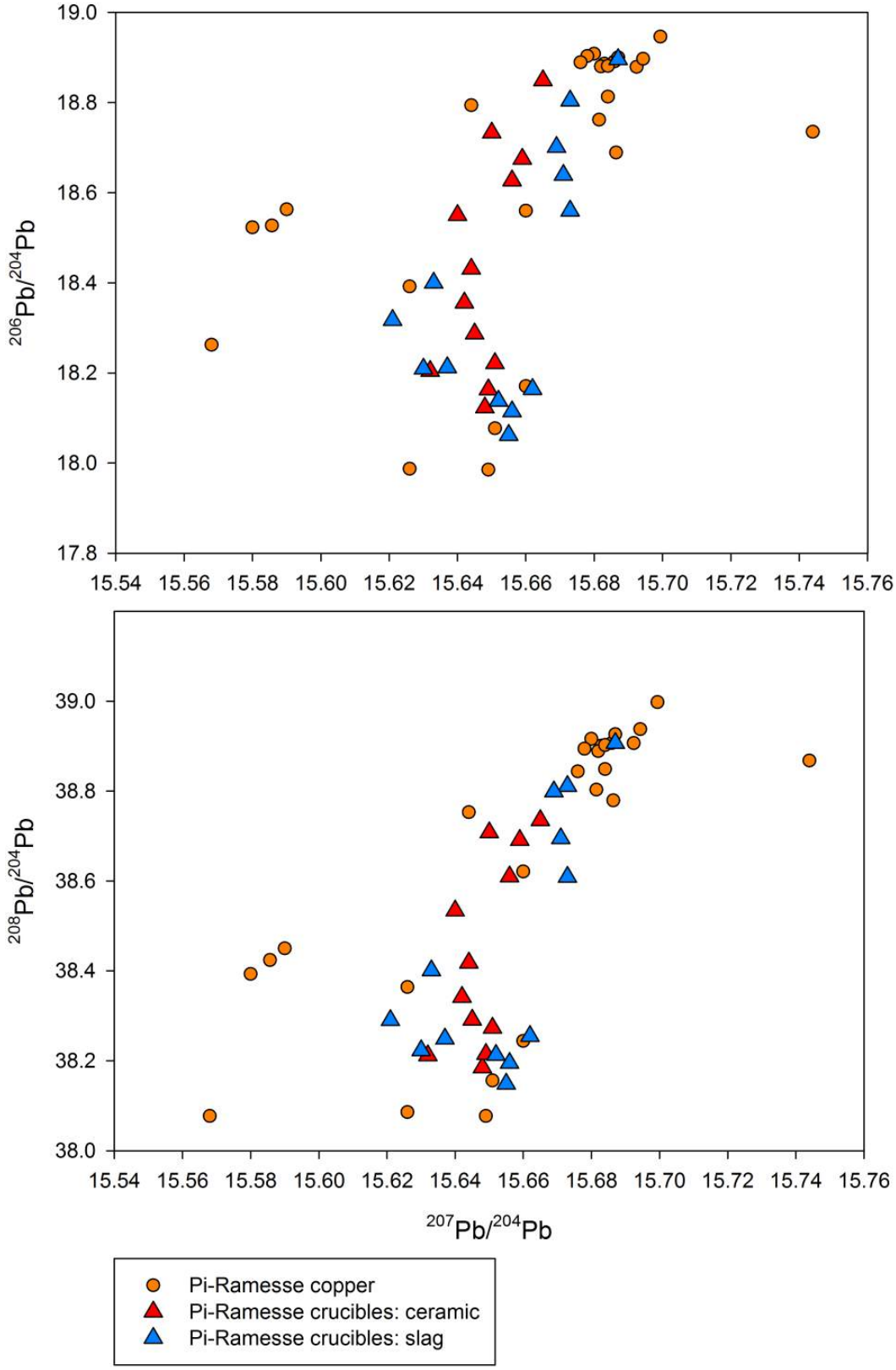

Figure 5.77: LI data for crucibles and copper/bronze from Pi-Ramesse

Some initial caveats:

- LI compositions for the Nile silt appear to vary; therefore, they might be variable within a single crucible, which complicates the principle outlined above.
- The relative contributions of lead to the slag by ceramic and metal are not just determined by absolute lead contents, but additionally influenced by the degree of slagging of the ceramic, contact with the metal batch etc. An example of high lead contributions from the ceramic to the slag (where the slag LI composition is dominated by that of the ceramic) is most likely seen in the Göltepe crucibles of Lehner *et al.* (2009), in the only known similar measurements of crucible lead isotope compositions.
- Other sources might contribute to the lead content in the crucible slag. Fuel ash deriving from charcoal made of trees grown in lead-rich soil could be an example. Such effects have hitherto not been studied, but are most likely marginal with respect to the two main contributors: ceramic and metal.

Theoretically, then, the results for these crucibles could be used to tentatively identify areas in the LI compositional space where metals molten in those crucibles are isotopically defined. Obviously, the stronger the contribution of the ceramic is, the more difficult it is to propose such an identification. The further away the slag LI composition is from the ceramic LI composition, the higher the confidence can be that it better reflects the metal LI composition. Nevertheless, any interpretations made from this kind of data should be considered tentative.

5.5.2.2 First example - Apliki

Figure 5.78 shows the only example of a crucible for which both ceramic and slag as well as a prill (manually extracted from its crucible slag) were analysed. This particular prill falls within the 'Apliki group', discussed in section 5.5.1.1. Interestingly, the slag LI composition is closer to that of the ceramic than to the metal prill. Though this can probably be mainly attributed to the typically low lead content of Apliki copper (Kassianidou, 2009), the relative contributions of copper and slag are further controlled by the crucible metallurgical process[25]. It should further be noted that the line connecting these three points in space is only approximately straight. This could be the result of other components contributing

[25] This crucible sample (97_0690,02-) shows no iron contamination and limited slagging.

to the slag LI composition or, perhaps more likely, the inhomogeneity in LI composition of the crucible ceramic. This example serves as a guide to interpreting the other samples, where these factors cannot always be assessed. As no prills are available for the other analysed crucibles, these have been studied by drawing a line between the ceramic and slag LI compositions. This appears to create a meaningful separation of three groups.

5.5.2.3 'Domestic group'-related crucibles

A first group of crucibles is shown in Figure 5.79. These all seem to have contained metal similar to the 'domestic group' defined in section 5.5.1. Such an interpretation seems especially appropriate for the sample with the highest $^{206}Pb/^{204}Pb$ (87_0634c,04), for which the crucible slag plots squarely in the middle of the 'domestic cluster'. Here, the slag LI composition is probably dominated by the copper contribution.
Copper from crucible 87_0897a,01-45 (2), with lower $^{208-207-206}Pb/^{204}Pb$, might similarly belong to this group. While more limited lead contribution from the copper may have led to the slag's intermediate position, it could equally point to the use of 'intermediate (QI-c/4.5-type) copper'. Interestingly, the SEM-EDS analysis of this particular crucible revealed significant iron and cobalt slag contamination, as well as the presence of Fe, Co, Ni, As and S in embedded prills. This is in contrast to the first crucible sample of this group, for which only iron enrichment is noted (possibly in line with Eastern Desert/Sinai ores), and may suggest the use of Omani copper (possible contributor to the 'domestic group') for this second crucible.
Finally, the third crucible (83_1149b) shows a very large distance between the ceramic and slag LI composition, indicative of a dominant lead contribution from the crucible charge. As a rim fragment, this crucible shows limited slag bulk enrichment, but several prills with very significant iron, cobalt and nickel content occur. Therefore, the copper melted in this crucible may be very similar to that noted in the second sample: Omani copper.

5.5.2.4 Timna-related crucibles

Five crucibles, shown in Figure 5.80, seem to have contained metal similar in LI composition to the Timna copper.

Some variability exists within this first group. Firstly, it can be noticed that there is a fairly large shift in LI composition between ceramic and slag for two crucibles, a medium shift for another two and a much smaller shift for one. While this may point to variable lead enrichment of the crucible slag for each sample, it may equally be explained by the inci-

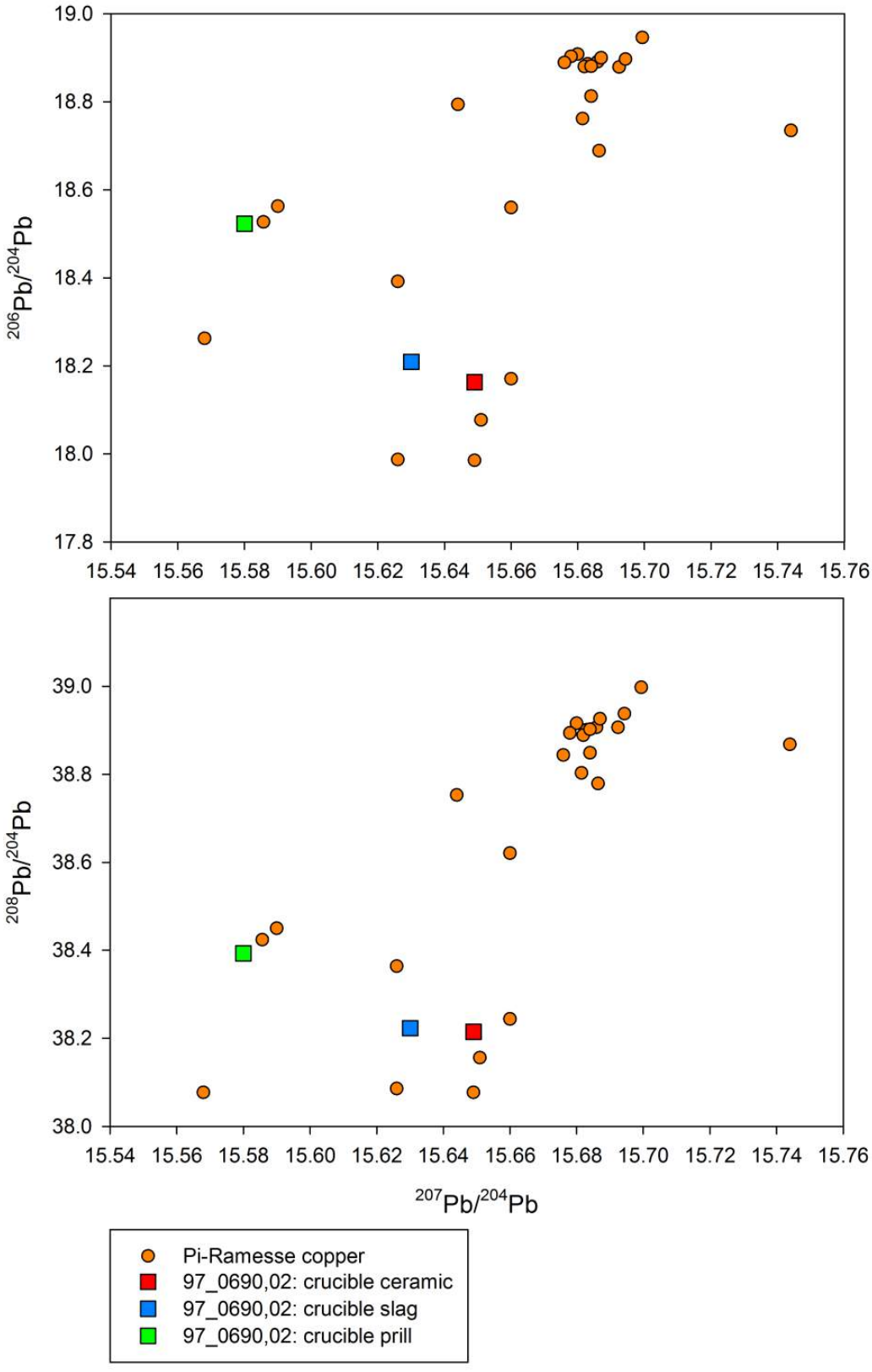

Figure 5.78: Example of ceramic, slag and prill of a single crucible

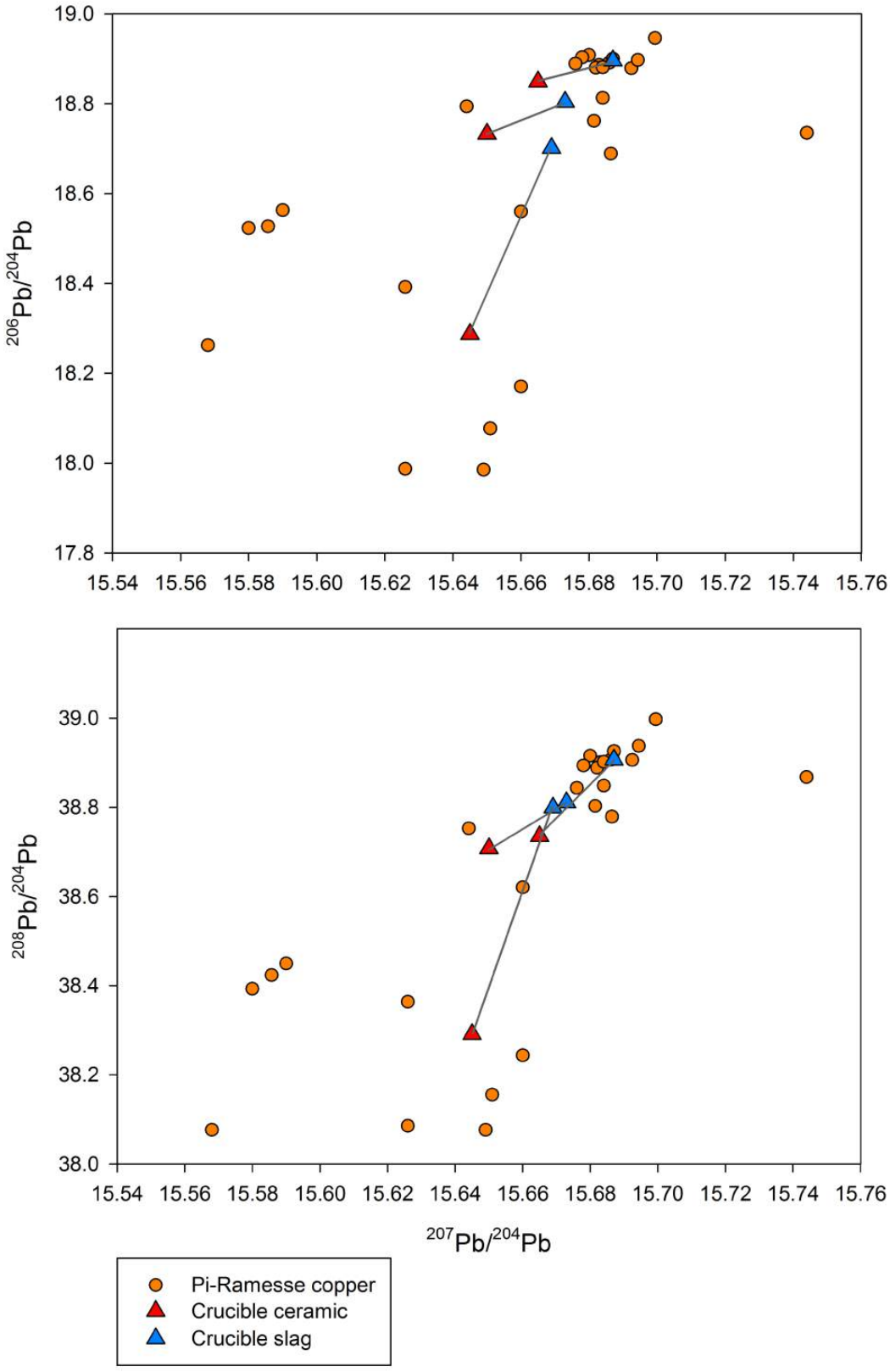

Figure 5.79: Crucible ceramic and slag - 'domestic' group; individual pairs of ceramic and slag are linked by lines

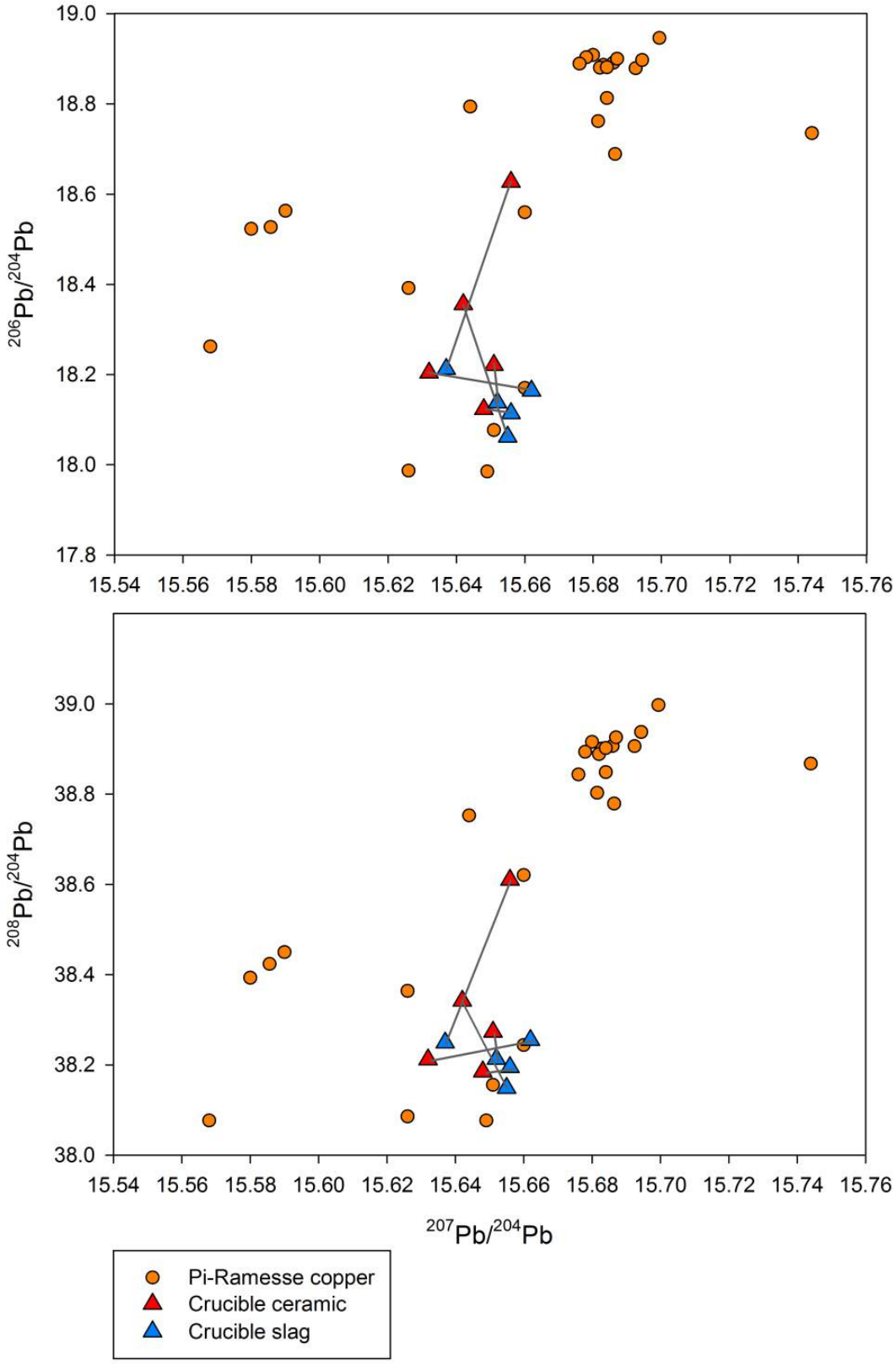

Figure 5.80: Crucible ceramic and slag - Timna group; individual pairs of ceramic and slag are linked by lines

dental proximity of ceramic and metal LI compositions in some samples. All slags show decreased $^{206}Pb/^{204}Pb$, indicative of a general 'pull' towards the Timna LI composition area.

One crucible slag plots clearly within the LI range seen in the three (tentatively identified) Timna samples, almost overlapping with one of the metal samples. This crucible (87_0762,0Nv) exhibited no bulk slag iron enrichment, but increased lead content, which further validates its association to this moderately leaded Timna copper.

The other two samples (97_0631E,01 and 97_0631E,04) with slag compositions very close to this first crucible slag both similarly exhibit minor lead bulk enrichments (and moderate iron enrichment in 97_0631E,04). For 97_0631E,04 there is barely any difference between ceramic and slag LI composition, which may be due to strong ceramic contribution or its incidental proximity. This illustrates the difficulty of this approach where no information from actual prills embedded in the crucible slag is available.

The crucible slag LI composition of a fourth sample (83_0597l,01) almost perfectly overlaps with the metal sample previously identified as 'Timna/Oman'. It exhibits minor bulk lead enrichment and no significant iron content.

The remaining sample (87_0942g,03) shows the largest jump in LI composition between ceramic and slag. No bulk lead enrichment of the crucible slag has been noted, while more significant iron and arsenic content was noted in embedded prills. Its slag LI composition does not plot squarely in the 'Timna range', but may have been influenced by it, explaining the large distance between ceramic and slag (in contrast to the Apliki example above). Alternatively, another 'intermediate' (Omani?) copper may have been charged in this crucible.

An interesting note can be made here: as mentioned earlier, the three lead-rich 'Timna copper samples' all come from area QIV. Crucible analysis confirms the use of this 'Timna copper' inside two crucibles found in QIV, but equally in a QI crucible dating to phase B/2. Therefore, the use of 'Timna copper' cannot be exclusively linked to the QIV workshop, though it may have been particularly important there, but evidence for its use is most strongly attested for phase B/2. The two remaining samples may be related either to Timna or Oman. Regardless, the lower lead content in both crucibles and metal samples indicates that this represents a batch of copper distinct from the other 'Timna copper'.

5.5.2.5 Intermediate group

The final group is shown in Figure 5.81. These three crucibles (83_0542b,01, 87_0762 and 98_0387,03) do not appear to be associated with any of the three above-mentioned groups,

but their slag LI compositions seem rather to fall in the intermediate copper LI range attested for the multifunctional workshop copper. They represent all workshop areas, but only phase B/2. The two samples with higher $^{208-206}Pb/^{204}Pb$ belong to area QI, while the sample with lower $^{208-206}Pb/^{204}Pb$ belongs to area QIV.
As mentioned earlier, the lack of data on the absolute lead content for ceramic and slag makes it very difficult to assess where (along the line from ceramic through slag) the LI composition representative of the crucible charge could be. This issue is particularly problematic for sample 87_0726,68-78b, for which no ceramic LI composition was measured. Its slag LI composition is similar to the other four discussed here. A tentative attribution to 'intermediate copper', possibly representing Omani copper, may be made here.

5.5.2.6 Conclusion

In conclusion, the analysis of crucibles can provide some further insight into the copper sources charged into them. However, when no data is available on the lead content of ceramic and slag, and no prills are available for analysis, this method is difficult to apply. Furthermore, the variability of the lead isotope composition of the clay, as well as the crucible process variability introduce possible problems for interpretation. These should be further clarified (through controlled experiments) before this method of analysis can be performed with great confidence. Nonetheless, the above examples could serve as an interesting starting point, and tie in quite well with the analysis of metals at Pi-Ramesse.

5.5.3 Overview of lead isotope analysis results

An overview of the analysed crucibles by context is presented in Figure 5.82. This offers contextual refinement to the use of different copper sources attested in the metal samples (Figure 5.73). It can be argued that copper from four different sources was used at Pi-Ramesse: Apliki, Timna, Sinai/Eastern Desert and Oman copper. However, these are only tentative identifications, and in particular Sinai/Eastern Desert and Oman are provisional: overlap exists between these sources, and some tentatively identified samples may belong to either of them, or represent (several) other sources altogether. The 'intermediate samples' could represent the mixing of copper, further complicating this provisional evaluation. This overview presents the best possible interpretation of the lead isotope data, taking into account the results from crucible analysis and the (limited) information available on ore sources.

It is worth mentioning here that about 30 to 50 different samples from a particular ore

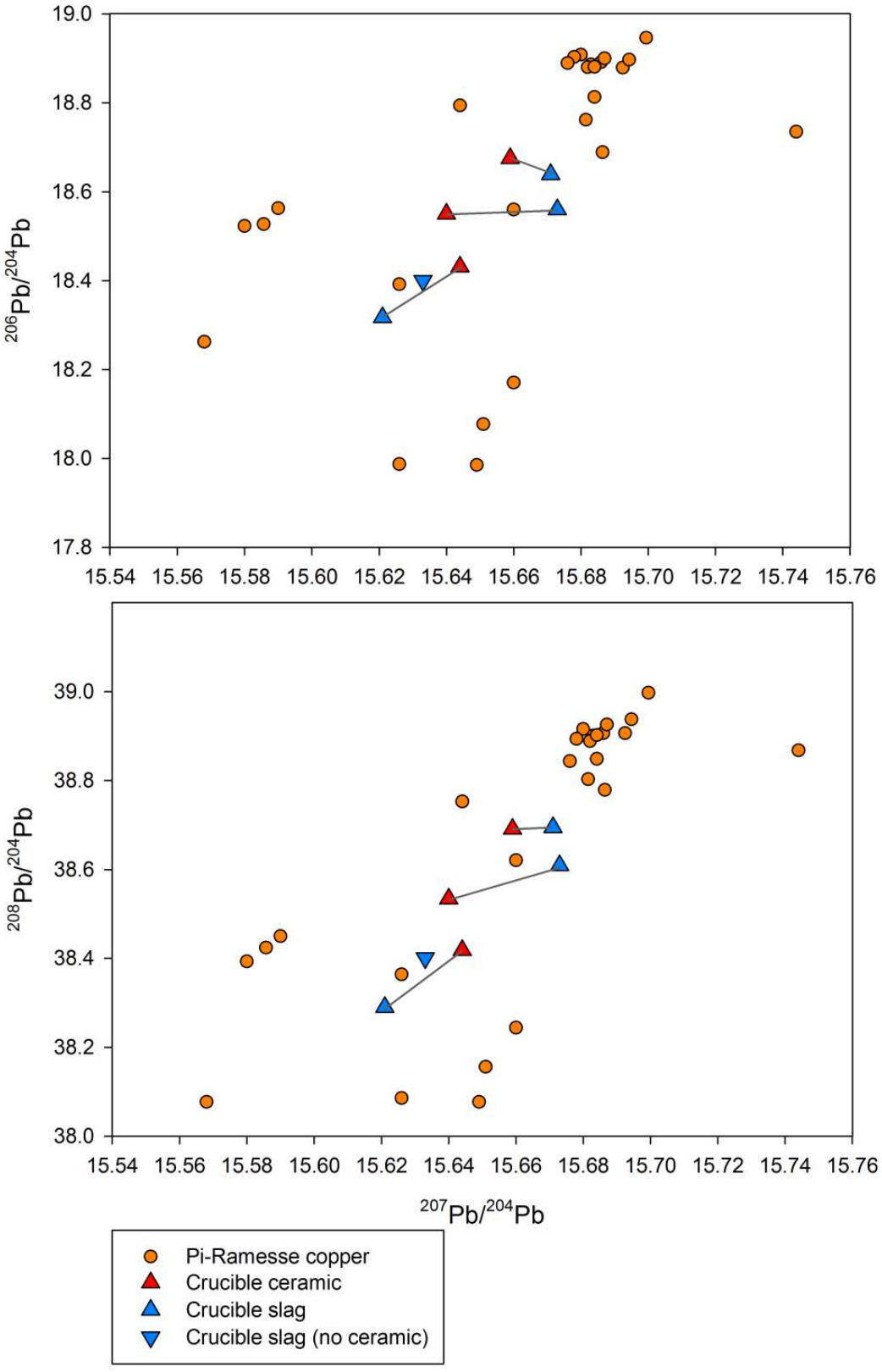

Figure 5.81: Crucible ceramic and slag - mixed group; individual pairs of ceramic and slag are linked by lines

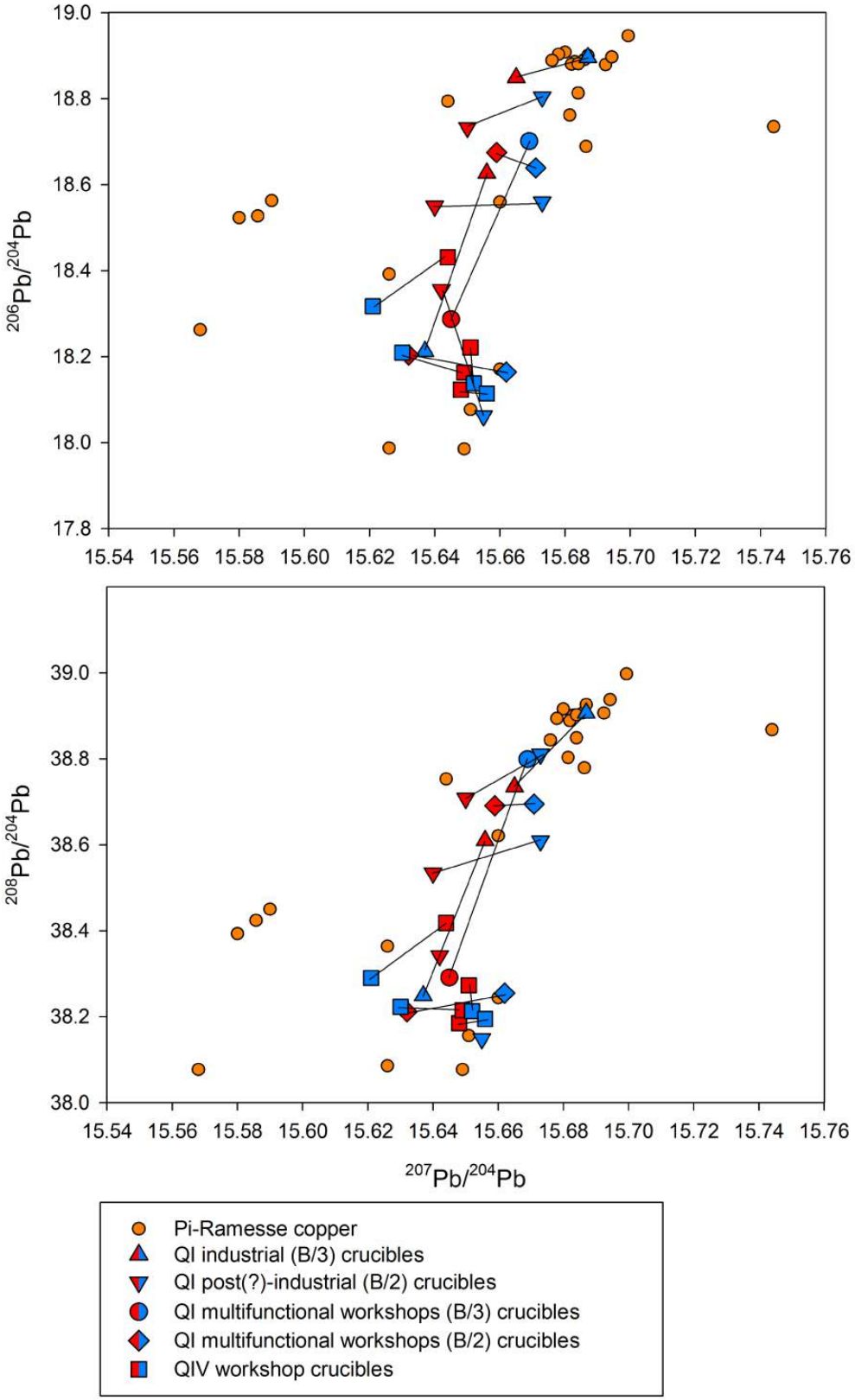

Figure 5.82: Crucible ceramic and slag - overview by context

deposit should ideally be analysed to establish its characteristic lead isotope field (Stos-Gale and Gale, 2009, see further Baxter, 1999; Baxter and Gale, 1998). Such sample sizes are rarely achieved, and this issue affects the discussion held here: many of the ore fields to which the Pi-Ramesse data is compared are under-sampled, while the Pi-Ramesse sample itself is equally limited. When considering the Sinai and Eastern Desert data, for example, far more data is clearly needed to achieve an understanding of several millennia of mining and metal smelting in this vast area, though Abdel-Motelib *et al.*'s 2012 publication is an important milestone along that way.

Differences between the various workshops at Pi-Ramesse appear to exist, nonetheless. 'Domestic copper' was predominantly used in area QI, during both phases and in both areas. 'Timna copper' was used during phase B/2 only, and predominantly (though not exclusively) in area QIV. It is possible though, that another batch of Timna copper, with lower lead content, was used in the (B/3) industrial QI workshops, but this sample may equally represent 'intermediate' or 'Omani' copper. This 'intermediate' or 'Omani' copper appears primarily in the QI multifunctional workshops, though its use may be assumed for all workshops. In general, however, the greatest variability in copper seems to have been gathered in the multifunctional workshops, where refining of 'dirty' (iron- and iron/cobalt-rich) copper took place alongside the recycling of existing bronzes (e.g., gilded and leaded bronze). This ties in with the finds of scrap copper and bronze during phase B/2, in both QI and QIV, and the identification of 'intermediate copper' in crucibles from both. Finally, the Apliki ingot copper appears during phase B/2, rather than B/3, in both area QI and QIV.

It is remarkable that Apliki copper has only been noted in its ingot form and as two prills trapped in crucible slag, but not in any objects. In fact, it has not been noted in any objects throughout the Late Bronze Age Mediterranean at all (with the exception of Cypriot artefacts: Gale and Stos-Gale, 2012), resulting in speculation that it was in fact never molten down, but (broken) ingots were used as currency or prestige objects. Its discovery in two crucibles is therefore a major one. However, its discovery embedded in the crucible slag begs a further question. Do these prills represent Apliki copper only *because* they did not interact further with the crucible charge? It may be that the low lead content in Apliki copper is overshadowed by the lead content of any tin added during alloying, even if that lead content is only minor, and Apliki copper therefore becomes invisible to archaeological scientists. When mixed with other copper, such a scenario seems especially likely. This may indeed explain the apparent dearth of Apliki copper in Late Bronze Age bronzes, despite its widespread trade (Gale, 2011). A similar argument for Apliki copper's disappearance in the crucible was made by Muhly (2003, 2009), though his suggested importance of 'Lavrion

lead contamination' appears unnecessary.

For the sample intermediate to Apliki and 'domestic' copper (Figure 5.76), it could be suggested that its LI composition is the result of mixing 'domestic copper' and Apliki copper. However, the resulting lead content in the bronze is only 0.02%, which would indicate a very minor contribution from the 'domestic copper', which typically has lead contents of ±0.5%. Alternatively, it may be suggested that adding 11% tin (with unknown lead content and isotopic composition) to Apliki copper was sufficient to pull it away from the Apliki LI range. Lead contents for Eastern Desert tin have never been measured, but typical lead contents for contemporary tin ingots are in the 10-100 ppm range (Galili *et al.*, 2013). Exceptions exist, however, with 600-1200 ppm Pb measured in some ingots (Begemann *et al.*, 1999; Molofsky *et al.*, 2014). Their addition to a virtually lead-free (Apliki) copper, would introduce lead in the 0.01% range (for ±10 wt% tin), which is sufficient to shift the resulting bronze LI composition away from that of Apliki copper. Several alternative interpretations may be suggested here, but without further data from both ancient materials (metals and ores) and, more importantly, experimental work on bronze alloying and recycling effects on resulting LI compositions, these difficult interpretations remain educated guesswork.

CHAPTER 6

Discussion

The analytical results, presented and interpreted in Chapter 5, are further discussed both from the perspective of a broader organisation of metallurgy in Late Bronze Age Egypt, and as a more contextual interpretation of metallurgical activities at Pi-Ramesse.

Section 6.1

Bronze production technology

There are four fundamental ways by which bronze can be produced: the alloying of two fresh metals (copper and tin), cementation (alloying copper metal with tin ore), co-smelting (smelting copper and tin ore together to directly form bronze) and recycling bronze (possibly adding a copper/tin source). Differentiating between these processes through the study of ancient production remains has received relatively little attention in archaeometallurgical studies (Pigott *et al.*, 2003; Rovira, 2007). However, it could provide valuable insights into technological choices and inform on technical ability, material availability and cultural preference of ancient metallurgists. In this section, the evidence at Pi-Ramesse in relation to each of these options is evaluated.

Before doing so, however, it is important to emphasize the complex nature of evidence derived from crucible analysis. It needs to be underscored that each sample covers only a flat, 2-3 cm section of a crucible, which in fact is a much larger, three-dimensional object. As conditions within a single open crucible are not in equilibrium and can vary rapidly

and over very short distances in terms of temperature, oxygen supply and material presence, it can hardly be expected that a single sample is representative of an entire crucible process. Even if conditions were homogeneous within a crucible, it can be expected that, contrary to primary production slag, crucible slag often presents different stages of the metallurgical process, thereby complicating its evaluation. Conversely, this theoretically allows the study of these different stages within each crucible. When studying an entire crucible assemblage, it is therefore important to realize that variability witnessed between samples should in the first instance be understood as different manifestations of a single process, before more complicated scenarios are considered. This principle is elaborated further in Chapter 13.

The three key parameters indicating the relevant process are the nature of metal prills trapped in the slag, the presence and shape of metal oxide crystals, and the slag composition compared to the composition of the crucible fabric.

6.1.1 Active alloying vs. recycling

The presence of high-tin prills (defined as those with dominant δ-, ε- or η-phase) in several Pi-Ramesse crucibles gives evidence for an active alloying process as opposed to recycling by remelting existing bronze without the addition of fresh tin (ore). However, these prills are intermediate products and can therefore not be expected to be found in each sample from a crucible used for active alloying: their absence does not rule out active alloying.
Another problem associated with these high-tin prills is that they do not provide any information on the nature of the tin source used for alloying. Here, the evidence provided by the morphology of tin oxide crystals in the crucible slag comes in.

6.1.2 Fresh metals or cementation?

It is a long-standing debate whether during the Late Bronze Age tin metal or mineral cassiterite was the tin source of choice for bronze production. The presence of tin-rich prills is inconclusive, since cassiterite has to be reduced to tin metal to facilitate alloying, and at this stage can form these prills in the same way as metallic tin added to copper. Thus, other indicators need to be found.

First it should be repeated that tin oxide crystals can be expected to form under locally oxidizing conditions in the context of any process involving bronze melting. Pure tin metal could oxidize (alloying of two metals), tin could preferentially oxidize out of bronze (recycled bronze or bronze produced by any method and then re-oxidized) or cassiterite

could directly re-crystallize to form new tin oxide crystals. Such high-temperature crystals provide no diagnostic information, though they are sometimes (questionably (Rehren, 2003)) taken as an indication for co-smelting or cementation using mineral cassiterite (e.g., Frisch and Thiele, 1985 and Valério *et al.*, 2013).
However, some Pi-Ramesse crucibles appear to contain residual cassiterite. This has been tentatively identified by its distinct structural appearance compared to newly-formed tin oxide crystals. Though more laboratory experiments are needed to verify this identification, comparison to geological cassiterite seems to confirm this assumption. Similar shapes have likewise been identified by Merideth (1998) in crucibles from Iberia, a region where cassiterite cementation has been reported repeatedly (e.g., Rovira, 2007 and Valério *et al.*, 2013).
The limited NAA data available for Pi-Ramesse copper and bronze indicates that tin was associated with gold, further corroborating the tentative identification of alluvial cassiterite as a tin source for alloying.

As discussed in section 5.4.5, the limited examples of tentatively identified residual cassiterite are inadequate for excluding the possible use of metallic tin at Pi-Ramesse. Metallic tin does not provide diagnostic evidence in the crucible slag and its possible use can therefore not be argued against. Given the precious nature of tin as a metal, likely acquired by long-distance trade (see section 6.2.3), it is not surprising that no ingots were found in Pi-Ramesse. The use of oxhide ingot copper in Pi-Ramesse corroborates the framework outlined earlier (Rehren and Pusch, 2012), suggesting Pi-Ramesse would have had access to the Late Bronze Age metal ingot trade and therefore to tin ingots. Tin ingot finds are exceptional though, and archaeological absence should be expected in a highly controlled workshop environment where important materials would have been under strict control. Therefore, the use of tin metal for alloying is not altogether unlikely, though proper evidence cannot be presented.

6.1.3 Co-smelting

Co-smelting, that is the smelting of mixed copper and tin ore, does not seem likely to have taken place in Pi-Ramesse. Though there are indications for the use of cassiterite, no remnant copper ore was found in the crucible slag. Furthermore, no slag resembling primary copper smelting slag was discerned (with the exception of sample 94_560, explained in section 5.4.10). The use of highly purified copper ore (e.g., malachite) is possible but unlikely as there is no evidence for ore (or its beneficiation) on site. As discussed in section 4.5, copper smelting during the Late Bronze Age typically took place at or close to copper

mines, rather than in urban centres. Typically, the smelting was performed in furnaces by this time, rather than crucibles. No evidence suggests that metallurgical practice at Pi-Ramesse deviated from this pattern.

6.1.4 Recycling

The evidence for recycling is even more difficult to obtain based on slag analysis. Very little (iron) contamination is to be expected, but the same holds true when alloying pure/refined metal. No high-tin prills would be formed but, as mentioned earlier, the absence of evidence cannot be used as the evidence for absence. In the case of Pi-Ramesse, however, scrap bronze present in the production area strongly suggests the practice of recycling. An example of such scrap material is shown in Figure 6.1. Hauptmann (2007) and Levy *et al.* (2002) use similar evidence (clustered metal prills, lumps and tools, with negative crucible base impressions) to argue for recycling and (re-)melting at Khirbat Hamra Ifdan (Jordan) and Shahdad (Iran).

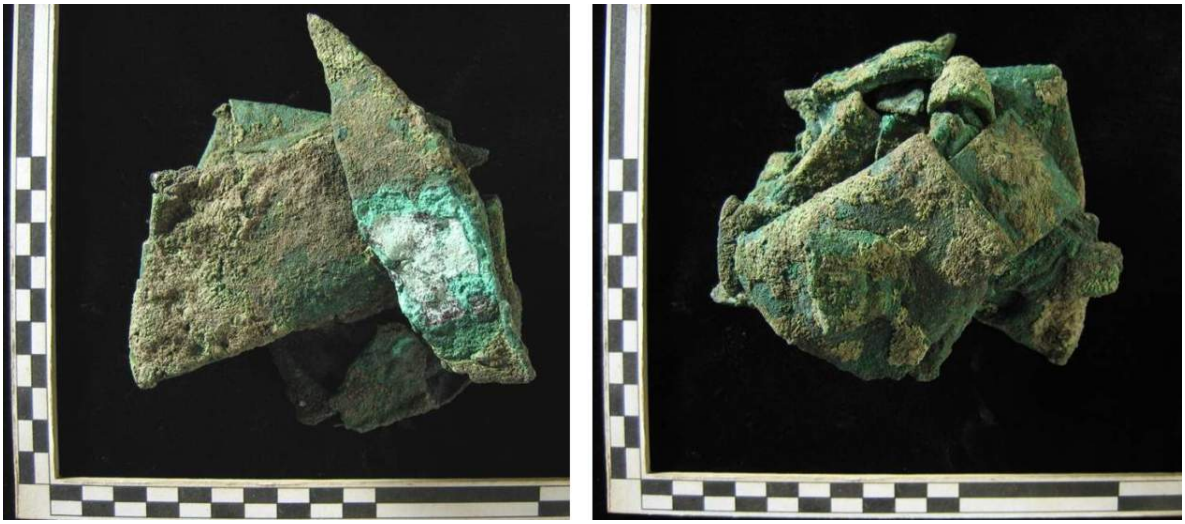

Figure 6.1: Scrap bronze found in the production area at Pi-Ramesse. FZN: 1997/1288, site: QIV-h/28, stratum Bd

6.1.5 Summary

The analytical results presented here demonstrate that active alloying took place at Pi-Ramesse, and there are indications that mineral cassiterite could have been used for bronze production by cementation. As mentioned before though, the production waste freezes a single moment of a process that is variable in time. As such, a sample cannot be taken as

representative for a heterogeneous crucible and should not be expected to reveal the variability that exists within a production technology. Samples lacking any residual cassiterite could therefore reflect the full reaction of cassiterite in a cementation process, or the use of an alternative technique. As the use of tin metal for alloying is not expected to produce diagnostic crucible slag, its prevalence in the various Pi-Ramesse workshops cannot be contrasted to that of cassiterite. Though the relative paucity (as attested by lead isotope data) of ingot copper relative to 'domestic copper' may similarly suggest that ingot tin was used to a lesser extent than 'domestic cassiterite' (discussed further below), this argument is insufficient to exclude the use of metallic tin for alloying.
In summary, it seems appropriate to suggest that fresh bronze alloying was accomplished at Pi-Ramesse through both the mixing of fresh metals and the cementation method. In addition to this, existing bronze was recycled, whereby both metallic tin or cassiterite may sometimes have been added to control the final alloy.

It can be noted that some copper may not have been alloyed with tin: while the crucibles within which no tin was detected most likely represent the 'clean end' (limited slag formation, reducing conditions) of the bronze alloying crucible spectrum, the possibility of pure copper melting cannot be excluded. If practised, it appears to have been of only minor importance at Pi-Ramesse: apart from casting waste and raw materials, all analysed objects in Pi-Ramesse are bronzes. Variability in tin content from five to twenty-one percent represents process variability to some degree, but most likely alloy composition was varied to suit the final object. While 5-10 wt% represented the 'normal range', special objects, such as a chariot wheel-hub (Table F.4), may have been deliberately made using a higher tin content, to achieve a more golden or silvery colour (Fang and McDonnell, 2011).

The possibility of crucible reuse, which appears not to have been widely practised in Pi-Ramesse (see section 6.3), does not affect this overall interpretation of technology. It is, e.g., possible that a crucible used for recycling was subsequently reused for active alloying, rendering the first recycling activity 'archaeologically invisible' when high-tin prills are discovered. Similarly, it may mix up signals of varying copper sources, discussed in section 6.2. However, the crucible remains are so variable anyway, that the variations in process may be expected to appear nonetheless if enough samples are investigated, and therefore assemblage-wide interpretations remain unchanged. The prevalence of each technique throughout the assemblage might be skewed if crucible reuse is involved, but assessments of this are approximate anyway. Broader issues related to reuse are explored in more depth in section 13.4.

Section 6.2

Sources of metal

6.2.1 Copper sources: the crucible evidence

The large scale of copper consumption at Pi-Ramesse and its distance from suitable ore deposits raises the question of where the copper came from. Several pieces of evidence indicate that multiple copper sources were used. In the first instance, the evidence derived from the crucible slag analysis is discussed, without considering the lead isotope results (section 6.2.2).

The crucible slag analysis indicates that, in approximately half of the crucibles, 'clean metal' (no iron contamination) was used. This implies the use of clean copper ingots (i.e., raw copper with few (natural) contaminants or previously refined) and/or recycling of fairly pure copper/bronze already in circulation.

Secondly, an iron-rich copper source can be inferred from the crucible slag analysis, which accounts for roughly 35% of the assemblage. This suggests the use of a raw copper, enriched in iron, such as:

- Unrefined copper from the primary smelting of sulphidic ores, e.g.,
  - Cypriot oxhide ingots (Knapp *et al.*, 2001; Stos-Gale, 2011)
  - 'Dirty' Uluburun ingots (Hauptmann *et al.*, 2002) (see section 5.4.10)

  Both of these examples often incorporate copper-sulphide inclusions.
- Raw copper smelted from oxidic ores (e.g., Timna and Faynan ingots) (Eliyahu-Behar *et al.*, 2012; Hauptmann, 2007; Rothenberg, 1990; Tylecote *et al.*, 1977)

In each case, the iron content reflects both ore composition and smelting conditions. Though tin and/or cassiterite could equally be responsible for iron contaminations, these high enrichments should be attributed to the copper source (see section 5.4.6).

The piece of oxhide ingot (Apliki copper) found in the production area could very well fall into either 'clean' or iron-rich copper sources discussed above. However, it does not necessarily constitute either of these groups and may represent a separate source.

Finally, a cobalt/nickel-rich copper source has been identified. This quite clearly points to a source different from Cyprus, as cobalt, nickel, arsenic and lead only occur in traces in

Cypriot ores exploited during this period in time (Constantinou, 1980; Hauptmann, 2007) and cobalt is generally absent from Late Bronze Age Mediterranean oxhide ingots[1], which are (presumably) predominantly Cypriot from 1400 BC onwards (Stos-Gale and Gale, 2009; Gale, 2011)[2]. Interesting to note is that cobalt occurs in ingots of Omani copper (Begemann *et al.*, 2010; Goy *et al.*, 2013; Weeks, 2003), though not always accompanied by significant iron content (Craddock *et al.*, 2003). Oman is known to have provided copper for Mesopotamia in earlier times (end of fourth to third millenium BC) and large-scale production of copper began again during the late second millenium BC (Begemann *et al.*, 2010), so its copper may well have reached Egypt at some point in time. Dayton (2003) suggests that copper ore from Kilembe (Uganda), rich in cobalt, could have been mined during the Middle Kingdom, together with the attested exploitation of *kohl* there. Interestingly, gold mining took place there as well, which raises the possibility of cassiterite exploitation (see section 6.2.3).

The 'Land of Punt', the location of which has been much debated in Egyptology (e.g., Fattovich, 2012; Manzo, 2012 and Meeks, 2003), should be mentioned here too. Its importance as an international trade partner for Egypt is attested from the Old Kingdom through to the Late Period, with strongest indications for trade during the Middle Kingdom period. Most likely, its core should be situated on the Arabian Peninsula towards or in Yemen, with trade posts along the Red Sea coast on both Arabian and African sides. The 'Mine of Punt' (Bia-Punt), a hinterland possibly encompassing parts of Sudan and Eritrea, is believed to have been the source of metals (particularly gold), ebony and other exotic materials imported to Egypt. Regardless of the exact position of Punt, it appears that the Egyptians were trading with people in the Red Sea basin who had access to raw materials from both the Eastern Desert of Sudan, the Eritrean-Sudanese lowlands and the Arabian Peninsula. This region is therefore another candidate metal supplier for the ancient Egyptian market, and may have provided access to Omani copper.

Though some of these options appear enticing, they are all speculative at this point. Furthermore, the cobalt and iron enrichment of this copper most likely points to a raw source of copper, but recycled material cannot be entirely excluded.

A further complication should be considered: the cobalt- and iron-rich source could be the same. Within the crucibles, it is possible that the slag is enriched in iron in one area,

[1] Though some more cobalt-(and iron-)rich Cretan (up to 0.8 wt% Co, Mangou and Ioannou, 2000, Table 3, p. 213) and Nuragic (up to 0.25 wt% Co, Begemann *et al.*, 2001) ingots exist. The highest level in Cypriot ingots (an oxhide ingot fragment from Mathiatis, Kassianidou, 2009, Table 9, p. 54) is 0.2 wt% Co.

[2] This issue of a Cypriot 'monopoly' in Late Bronze Age oxhide ingots has been hotly debated during the 1990's, without reaching any real consensus (see for example Sayre *et al.*, 1992 and comments, Budd *et al.*, 1995b and comments, and Pollard, 2009 and comments).

while it is enriched in both cobalt and iron in other areas. Sample 87_0897a,01-45 (1), for example, contains a prill with 1.1 wt% Co and its slag is enriched in bulk FeO content but exhibits no cobalt enrichment. Similar prills occur in sample 87_0897a,01-45 (2) (from the same find context), but additional cobalt-rich spinel is present in the crucible slag and a bulk enrichment in cobalt of ±1.5 wt% exists.
Though it can be said that it is likely that the iron-rich and cobalt/iron-rich fragments represent two different copper sources, some degree of overlap probably exists between the manifestation of these two sources in the crucible slag.
It is relevant to push this idea further still. If the iron- and cobalt/iron-rich fragments indeed represent varying crucible slag enrichment when using the same (iron/cobalt-rich) copper source, it could be argued that the 'clean crucible fragments' (without iron or cobalt slag enrichment) equally represent the use of this same copper. Under reducing circumstances, where limited copper burning takes place, the iron/cobalt-rich copper may not leave behind any trace of its contaminants, and thus such crucible fragments could represent the 'clean end of the spectrum'. The common attestation of oxidising conditions in many of these 'clean crucible fragments' (e.g., tin and copper oxides), and the recurring pattern of clean, iron-rich and cobalt/iron-rich copper from SEM-EDS, pXRF and NAA analysis, however, argues against such an interpretation.

A discussion of the importance of these three or four (or more) sources is necessarily qualitative. However, the good correspondence between the pXRF data and results from detailed SEM-EDS analysis provides some confidence in the measured distributions.
It appears that 'clean copper' accounts for approximately 50% of the copper used. This could represent a single or multiple raw sources, as well as recycled material.
Iron enriched copper makes up approximately 35% of the population, while cobalt/iron enriched copper covers the remaining 15%. These distributions are reconsidered in the next section, taking into account the results derived from lead isotope analysis.

6.2.2 Copper sources: connecting the lead isotope evidence

The results of lead isotope analysis can complement those obtained by crucible slag analysis to shed further light on the sources of metal used in the Pi-Ramesse bronze workshops. So far, this technique has rarely been applied for metals from ancient Egypt and Nubia (Killick, 2009), and these results may open the way to resolving ancient copper use for these areas.

Similarly to the crucible slag analysis, lead isotope data has tentatively identified three or four sources of copper used at Pi-Ramesse. Most securely identified are the use of oxhide

ingot copper from Cyprus and Timna copper. These appear to account for only a minor fraction of copper use, however, and are confined to phase B/2. The dominant group of copper was used everywhere, but predominantly in the industrial workshops (QI-B/3). It has been tentatively identified as a 'domestic copper', probably representing copper ores from Sinai and the Eastern Desert. Finally, a group of 'intermediate samples', with more strongly varying LI compositions, has been noted. It occurs primarily in the multifunctional workshops, and may represent copper from Oman, but further includes recycled and possibly mixed copper. Tentatively identified Oman copper may partially constitute the 'domestic group'.

It is difficult to propose a straightforward parallel between these groups and those defined by crucible slag analysis. One reason for this is the far more limited sample obtained for lead isotope analysis. Another is the fundamental difference between lead isotope and chemical groupings, as they are not altered by metallurgical processes in the same way. Nonetheless, a few correspondences may be noted.
The increased lead content for crucible slag in ±15% of the crucible population (as analysed by SEM-EDS), found across all different excavation areas, but all from phase B/2, may be related to the high lead content of 'Timna copper' in ±12.5% of the population (as analysed by LIA) and the single lead-rich (5% Pb) sample (±4% of population). In the crucible slag analysis, this lead content is never associated with any bulk cobalt enrichment, though two of the Timna copper samples identified by lead isotope analysis have notable cobalt content (±200 ppm).
For the Apliki copper (ingot and prills), no chemical data is available, making it impossible to relate to the crucible slag analysis. Its importance is equally difficult to assess based on lead isotope analysis, as it may be obscured there as a result of its low lead content (see section 5.5.3).
The 'domestic copper' group may largely represent copper from Sinai and the Eastern Desert. As such, it would be expected to have relatively low levels (<1 wt%) of contaminants such as arsenic, nickel, cobalt etc. (Abdel-Motelib *et al.*, 2012), and may largely coincide with the 'clean metal' defined in section 6.2.1. Too little chemical data is available to investigate this further, but some of the 'domestic copper' contains up to 600 ppm cobalt, while other samples (with almost identical LI composition) bear no detectable cobalt. Though it is very well possible that this may reflect the existence of hitherto undiscovered Sinai/Eastern Desert copper ores with a certain cobalt/nickel content, it may be argued that this 'domestic group' reflects the use of copper from a limited number of sources through time within Egypt, resulting in a mixed chemical composition, but fairly homogeneous LI composition. Such use would involve raw metal, as well as the recycling and

mixing of circulating metal (see section 5.5.1.3). A potential contributor to such a system could then be Omani copper. Raw Omani copper may be reflected in the most iron- and cobalt-rich sample identified, at the edge of the LI spectrum, as well as the 'intermediate LI group'. Omani copper may equally comprise some of the 'domestic group', or be mixed into it, thus creating a LI overlap. Its prevalence is very difficult to assess, but appears more limited than the Sinai/Eastern Desert copper. Overall, this discussion is quite tenuous given the analytical uncertainties and the limited samples.
Finally, it must be emphasised that, contrary to the lead isotope data, much of the crucible slag analysis data reflects mainly process, rather than provenance. This is especially true for iron enrichments, which are mainly the result of primary smelting conditions (controlling iron content in raw copper) and crucible conditions (controlling iron content in crucible slag). Obviously, the nature of the ore and previous refining operations do play a role in this as well. Still, it is difficult to correlate iron content to any of the provenance groups defined by lead isotope analysis. Nonetheless, these technological groupings are very relevant to the discussion of copper sources. They can reveal the existence of 'batches' of unrefined (and thus iron-rich) copper, for example, the characteristics of which probably often held more meaning to the ancient craftspeople than the distinction between particular ore sources. Given the nature of the crucible evidence, it is very difficult to trace such batches to particular contexts, but a very rough approximation can be gained from the pXRF data: iron-rich copper is roughly twice as prevalent in the B/2 crucibles (all workshops) compared to the B/3 crucibles. This reflects the more common use of 'clean copper' in the industrial area, while more raw copper is used in the later, smaller workshops. When iron enrichment occurs for the B/3 crucibles, it is more often connected to cobalt enrichment than elsewhere.

6.2.3 Tin sources

It is generally assumed that during the Late Bronze Age an international trade in tin ingots existed, in which Egypt would have participated (Dayton, 1971, 2003; Muhly, 1979; Penhallurick, 1986; Nezafati *et al.*, 2011), as mentioned in section 4.5. Although there is no conclusive evidence for this in the production context of Pi-Ramesse, the discussion of production technology (section 6.1) concludes that both tin metal and cassiterite could have been added to either fresh copper or recycled copper/bronze.

Tin metal would most likely have been imported to Pi-Ramesse in ingot form through international trade. Such ingots often moved together with copper ingots, as exemplified by the Uluburun, Cape Galedonya and Hishuley Carmel shipwrecks (Bass, 1967; Charles,

1979; Galili *et al.*, 1986, 2013; Pulak, 2000), and confirmed by other studies (e.g., Kassianidou, 2003b). It is therefore plausible that such tin ingots arrived in Pi-Ramesse, possibly together with (Cypriot) copper oxhide ingots.

The origin of tin for these Late Bronze Age ingots is one of the longest-standing unresolved debates in the study of ancient metallurgy. Geological tin sources exist throughout the world and appear to be concentrated in 'tin belts' (de Jesus, 1979). However, archaeological evidence for tin mining is largely absent. This is probably a result of the nature of tin deposits: primary deposits within granites were in all likelihood too hard to mine in ancient times, while secondary deposits (alluvial or placer concentrations of cassiterite, transported after weathering of the primary granite rock) require no invasive mining techniques and leave few visible traces. This is further exacerbated by the limited slag, and thus archaeological visibility, formed during tin smelting of such alluvial cassiterite. Some archaeological evidence exists in Cornwall and Iberia, but the role of these deposits in supplying the eastern Mediterranean is highly controversial (Eaton and McKerrel, 1976; Galili *et al.*, 2013; Haustein *et al.*, 2010; Tylecote, 1979). Similarly, Erzgebirge (Bartelheim *et al.*, 1998; Taylor, 1983), Aegean (Skarpelis, 2003) and Serbian tin (Durman, 1997) are unlikely to have been imported at Pi-Ramesse.

Another possible source of tin (again controversial: Hall and Steadman, 1991; Pernicka *et al.*, 1992; Sharp and Mittwede, 1994) is located in the Taurus Mountain range in south central Turkey. Evidence for tin mining at Kestel mine and tin smelting at Göltepe (Adriaens, 1996; Yener, 2000, 2009; Yener and Vandiver, 1993; Yener *et al.*, 1989, 2003), however, is mainly confined to the Early Bronze Age, and it does not seem to be a likely source of tin during the Late Bronze Age.

Ancient written accounts, discussed by Muhly (1979, 1985, 1999), offer further information. These tend to argue for a tin source in the east, perhaps Afghanistan, Uzbekistan, Kyrgyzstan or Tajikistan (ancient mining activity has been identified there: see Alimov *et al.*, 1999; Boroffka *et al.*, 2002; Cierny and Weisgerber, 2003; Parzinger and Boroffka, 2003), that could have reached the Mediterranean along various routes, possibly related to the trade in lapis lazuli. Muhly (1979) considers such a long-distance trade to be not only a possibility but a necessity. Work by Nezafati *et al.* (2006, 2009, 2011) suggests that mining activities at Deh Hosein (Iran) may have produced large amounts of tin during the early second to first millenium BC, which could imply an important supply role not only for ancient Iran and Mesopotamia (Helwing, 2009), but the wider Mediterranean world.

Perhaps even sources such as the Bauchi region in Nigeria (Taylor, 1982) should be considered for Egypt, even though exploitation evidence is absent there (Dayton, 2003) and the lack of interest in tin (and gold and lead) in central and southern Africa prior to their

contact with the Muslim world (Herbert, 1984; Killick, 2009) could perhaps argue against this option.
The role of Cyprus in the trade of tin (and obviously copper) is often cited and does not seem unlikely, based on ingots discussed by Muhly (1985) and finds such as the Uluburun shipwreck (Pulak, 1997; Pulak and Bass, 1997; Hauptmann *et al.*, 2002; Yalçin *et al.*, 2005). A good overview of the evidence related to ancient tin production and trade is given by Pigott (2011, 2012).

As mentioned earlier, the possibility to use either tin or cassiterite for alloying is of prime importance. While tin might make more sense as a trade commodity (higher value-to-weight), cassiterite appears to offer the technical advantage of higher tin-recovery when co-smelted directly with copper[3] (Charles, 1979). From a less technical point of view, it is a very different approach to alloying: in one case, copper is alloyed with another metal, while in the other case, a rock is used. This implies a different technological concept and understanding of material. Therefore, it is of high interest to elucidate the identification of tin oxide in crucible slag by experimental archaeometallurgy, to distinguish between non-diagnostic oxidation products and residual cassiterite.

The evidence presented here strongly indicates that cassiterite was indeed used for cementation at Pi-Ramesse. This cassiterite is likely to have had a more local origin than tin ingots discussed above. As Ogden (2000) equally notes that some, but not all tin was probably imported into Egypt, the possible use of cassiterite from Egyptian sources (see Dayton, 1971; Lucas, 1962; Muhly, 1985; Nibbi, 1976; Rothe and Rapp, 1995; Rothe *et al.*, 1996; Rothenberg *et al.*, 1998; Sabet *et al.*, 1976 and Wertime, 1979) gains particular importance in this context. Inscriptions in Egypt's (south) Eastern Desert indicate that tin mining took place there during the Old and Middle Kingdom (see, e.g., Rothe and Miller, 1999; Rothe *et al.*, 2008), secondary to gold mining activity. Although the co-occurrence of gold and cassiterite is rare (Penhallurick, 1986), it is possible (and not unlikely, given its obvious density (Killick, 2009)) that the Egyptian search for gold led to the discovery of cassiterite in alluvial deposits, for example at El Mueilha (Wertime, 1979). There are, however, no inscriptions related to tin mining dating to New Kingdom times. Though this has been interpreted to indicate a decline in exploitation of these tin sources, at least through state-organised expeditions, there is no plausible evidence to exclude the possibility that local (nomadic) people continued to (occasionally) exploit these sources and

[3] In the reaction $SnO_2 + C \longrightarrow Sn + CO_2$, the activity of Sn can be lowered by dissolving it into copper, assisting the reaction in the rightward direction. At the same time, the temperature at which reduction of cassiterite to tin takes place is lowered. Alloying copper with cassiterite would therefore lead to a higher overall recovery of tin.

that cassiterite made its way onto the Egyptian market in small quantities. The continued exploitation of alluvial gold deposits may indeed be reflected in second Intermediate Period gold-work (Troalen *et al.*, 2014). Abdel-Motelib *et al.* (2012) furthermore suggest much earlier ore/metal trade between the Naqadians and bedouins, and Rehren and Pusch (2012) equally indicate the importance of nomadic people's participation in the circulation of scrap metal throughout Egypt's history. The results from Pi-Ramesse should therefore renew interest for Egypt's potential domestic cassiterite/tin production and as such form an exciting contribution to the long-standing debate of tin supply in the Late Bronze Age. While a long-distance trade may have dominated the overall market system for tin during the Late Bronze Age, local use of domestic tin deposits (where available) may have been equally important, despite being less tangible in archaeological and historical evidence.

As far as provenance is concerned, the case of tin is even more difficult than that of copper. Lead content in tin is much lower than in copper, which dominates the lead isotope composition of bronzes, allowing their use for copper provenancing (Begemann *et al.*, 1999; Galili *et al.*, 2013). The use of trace elements, described by Rapp (1979), Rapp *et al.* (1999) and Grant (1999), becomes problematic once alloying has occurred. The use of tin isotopes (Begemann *et al.*, 1999; Budd *et al.*, 1995a; Clayton *et al.*, 2002; Yi *et al.*, 1999) is equally fraught with difficulty[4], but the further development of this technique holds some promise, as shown by Haustein *et al.* (2010) (method developed for cassiterite, not bronze), Nickel *et al.* (2012), Nowell *et al.* (2002) and Yamazaki *et al.* (2014). Gillis *et al.* (2003) measured tin isotopes of Wadi Mueilha cassiterite, which differed strongly from European and Central Asian tin. Their sample numbers are, however, very low and only increasing reference data will show whether or not this method is viable. As with lead isotope studies, increasing characterisation of ore sources will probably reveal more overlaps between them in terms of tin isotope composition.

As a final note, it should be pointed out that some of the tin did not necessarily end up in the Pi-Ramesse crucibles as a pure metal or as cassiterite, given that recycling of existing bronzes was part of the technological activity there.

[4]Tin has 10 natural isotopes. Contrary to lead isotope analysis though, which provides 3 independent variables, tin isotope analysis only yields one independent variable (Begemann *et al.*, 1999) and limited isotope fractionation (Gale, 1997; Northover and Gillis, 1999). Overlap between sources is therefore much more likely. Tin mixing, for example during ingot production, presents further possible issues.

6.2.4 Summary of metal use

The use of metal from a variety of sources has been identified in the Pi-Ramesse bronze workshops, which can be related to the broader framework introduced in section 4.5. The importance of 'special project copper' (Rehren and Pusch, 2012), as may be represented by Uluburun-type cargoes, appears minimal in Pi-Ramesse. Admittedly, the limited evidence for Apliki copper may in part be attributed to its weak lead isotope signal (low lead content). Nonetheless, it has been noted, but only in the phase B/2 workshops. This argues against large-scale use of such copper for the industrial-scale project, though it must be emphasised that this argument *in absentio* is not conclusive. It appears, however, that another group of metal dominates the supply for the industrial workshop. This has been tentatively identified as 'domestic copper', similarly occurring in Amarna metal and Ramesside Egyptian Blue objects, and cannot be equated to known ore sources. However, it may be argued that this group represents a domestic copper trade, representative for the 'scrap copper' and (to some extent) 'mainstream bronze' identified by Rehren and Pusch (2012), without necessarily equating this to a particular ore source. Most likely, it mainly reflects nearby ore sources that may be considered 'domestic' to ancient Egypt, such as Sinai and the Eastern Desert (for which massive Late Bronze Age exploitation is attested at Bir Nasib), and to a lesser extent imported copper from 'regular partners', such as the Land of Punt, or expeditions to Timna. It is important to emphasise that this may imply both the use of 'fresh domestic copper' and the remelting of 'circulating domestic copper' in Pi-Ramesse. Timna copper, probably furnished through state-organised mining expeditions, is again primarily attested for phase B/2, rather than the industrial workshops. Finally, the multifunctional workshops, for which some 'domestic copper' is attested, are dominated by copper with a more mixed lead isotope composition. This may indicate the mixing of above mentioned sources, or the use of more varied ore sources, probably including Omani copper. Overall, the industrial workshops are dominated by clean, domestic copper, the multifunctional workshops by mixed and 'dirtier' copper, and the QIV workshop by Timna and Apliki (and possibly mixed) copper.

The use of metallic tin, arriving at the Pi-Ramesse workshops as (parts of) trade ingots of unknown provenance cannot be excluded. It appears, however, that mineral cassiterite was used to some extent for the production of bronze by cementation. The nature of the evidence does not allow the attribution of this technique to a particular workshop context. It shows, however, that it was in use at Pi-Ramesse, which in turn suggests the use of a domestic cassiterite source. Domestic should be understood here in the same way as for the suggested 'domestic copper': cassiterite from the Eastern Desert, acquired through

both state-controlled mining expeditions and more informal trade and bartering. Some tin was further acquired through the remelting of existing bronze, most likely representing 'domestic bronze'.

Overall, this paints an interesting picture of ancient Egyptian metal provisioning systems. Rather than being heavily reliant on external sources, it suggests a strong self-reliance for the execution of large-scale projects, further supported by metal acquisition through international trade. The scope of this last category is difficult to quantify, but it seems likely that the domestic copper and bronze market in Egypt at this time constituted a large stock of metal, from which the state could draw in times of need. This only partially agrees with the hypothesis of Hikade (1998), who surmised that Ramses II may have increased independence of copper imports through increased domestic production. Rather, it leans more towards Warburton's (2010) suggestion that the state did not fully control copper production, but a freer market system existed which was sufficiently extensive to (quickly) supply the bulk of metal needed for the industrial workshops at Pi-Ramesse.

It is important to nuance the term 'sources', as discussed in the preceding sections. Lead isotope data is used to infer relations between copper metal and copper ore sources, and has been discussed as such. However, such relations were probably not always known to ancient people. As archaeologists, it is almost impossible to reconstruct how quickly copper travelled from mining districts to workshops, where it was stored along the way, how many times it was traded before it was molten down, etc. Pollard *et al.* (2014) have argued for the importance of 'time' in discussions of provenance. For example, was copper mined during the Middle Kingdom still available during the New Kingdom? If so, was any of it left as raw copper, or had it all been made into objects? How long did it take for copper to travel from Cyprus to Pi-Ramesse and how recently would that copper have been mined and smelted? The practice of recycling copper and bronze is very likely to have played a significant role throughout the Late Bronze Age (Gale, 2001; Knapp, 2000). It is therefore particularly significant to consider the 'domestic copper' as a palimpsest-type copper source, representing a dynamic pool, continuously replenished by both freshly mined and recycled 'old' copper, as presented in section 5.5.1.3. Probably, the 'intermediate' or Omani copper should equally be regarded as such, though its history from mine to Egyptian workshop may have been different, e.g., through the kingdoms of Punt and Sheba (Galili *et al.*, 2013). While its original source may have been foreign to the Egyptians (e.g., trade with the Land of Punt), it may have been part of the domestic copper trade by the time it arrived in Pi-Ramesse. When cast into an object, it would not have been identifiable in the way a raw ingot may be (through inscriptions or shape). The presence of scrap objects in the workshops illustrates the importance of this dual concept of source:

both the 'ultimate source' (reflecting an ore) and 'direct source' (reflecting where the workshops acquired its copper) are relevant to these discussions. The Timna and Apliki copper is more likely to represent 'fresh metal', arriving at Pi-Ramesse without a prior history of metallurgical use. Interestingly, this is the first evidence for oxhide ingot fragments effectively being molten down, rather than deposited as such (see, e.g., Lo Schiavo *et al.*, 2013 and Muhly, 2009). High iron contents and possible slag inclusions further argue for the existence of such raw copper in the workshops. However, the speed by which it travelled hence from the mines remains difficult to estimate, and it should be emphasised that such Timna (and possibly Sinai) copper were equally traded as scrap, together with 'fresh' Apliki ingots, as evidenced by the Kefar Samir shipwreck (Yahalom-Mack *et al.*, 2014), suggesting their presence in more 'informal' copper markets. Such trickling down of ingot copper into the scrap market over time should not be surprising (Rehren and Pusch, 2012).
Overall, it can be suggested that copper supply in Pi-Ramesse was largely supported through sources familiar to the ancient Egyptians: copper from Sinai, the Eastern Desert, Timna and the Land of Punt (Oman) represents the state's mining campaigns and trade with its close neighbours, and is probably representative of copper commonly available at the Ramesside Egyptian capital.

Section 6.3

Contextualising bronze production in Pi-Ramesse

As a final part of this discussion, all the preceding information is brought together to attempt a detailed reconstruction of the *chaîne opératoire* of bronze production, at Pi-Ramesse, expanding the work of Pusch (1990, 1994).
The onset of bronze production is situated in context QI-B/3, and appears to be a large-scale, state-controlled operation. Before actual bronze casting, a number of practical preparations were made: channel digging and construction with mud bricks, building of cross-furnaces, moulding and pre-firing (possibly in the cross-furnaces) of crucibles and tuyères, acquisition of charcoal, metal and cassiterite, construction of pot bellows, preparation of casting moulds etc. Considerations such as tuyère length and orientation, to avoid exposure of the bellow operators (Dungworth, 2013), and other 'health and safety' decisions related to large-scale operations may have been made at this point as well. The preparation of these large melting batteries must have required extensive planning and many hours of manual labour, before the actual bronze alloying could take place.
The preparation of crucibles and tuyères followed the same ceramic recipe, but the tuyères

did not go through the same pre-firing process as the crucibles. This suggests the involvement of the ancient 'metallurgists' in their production (as in Amarna, see Eccleston and Kemp, 2008), as a first technological choice for the metallurgical process was made there. The definition of 'metallurgist' is broad here: it simply refers to the people with the required skills and knowledge for bronze production, who may very well be involved with other high-temperature processes as well. While the Nile clay may not have been very refractory, it was well know to the craftspeople and customised to its particular function by tempering and ceramic design. This is exemplified in the use of the same clay for glass production crucibles, with a different design and heating mode (Rehren and Pusch, 1997). The choice not to pre-fire the tuyères to the same extent (thus saving fuel) is another example of how well material properties were understood for particular purposes.
When preparations were finished, several melting batteries may have been taken into operation at the same time to produce large quantities of bronze, though it is very well possible that single batteries may have been used individually as well. Nonetheless, the contemporary existence of several identical batteries next to each other suggests that simultaneous use did take place. Their changing orientation further suggests that multiple large-scale events took place, and infers a relation between these melting batteries and the similarly oriented cross-furnaces, which were possibly used for heating large moulds.

At the start of the process, the crucibles were set into the channels of the melting batteries. It is most likely that copper or bronze was placed inside the crucible, together with tin or cassiterite, and subsequently covered in charcoal, though some initial preheating with charcoal inside the crucible may have preceded this. Once covered, the tuyères were put in place, and the complete charcoal bed was quickly brought to combustion using a highly concentrated airflow directed at the crucible interior. It is possible that some of the charge was added to the crucible at this later point, as Charles (1980) and Merideth (1998) suggested for cassiterite, though this appears unlikely as the tuyère positions would have hindered easy access to the crucibles, once installed. The use of several (up to four) tuyères at once guaranteed quick attainment of necessary melting temperatures, probably resulting in a molten bronze batch of 3-3.5 kg in less than fifteen minutes (see experiments by Davey and Edwards (2007)). Other than speed, minimising fuel consumption may have been a consideration here. In this process, the ends of the tuyères were thoroughly fired and sometimes vitrified. Once the bronze in all the crucibles was molten, the tuyères were quickly pushed aside to lift the crucibles from their bed, perhaps leaving some charcoal on top of the crucibles until just before casting. This would have broken most of the tuyères at the transition of their fired and low-fired part, as reflected in the recurring fracture patterns of the tuyère remains. No 'cold ends' of the tuyères were preserved ar-

chaeologically, as these low-fired ends disintegrated more easily. Iconographic evidence indicates that strong sticks were used to carry the crucibles to the casting pits, which have been found scattered throughout the workshop (Pusch, 1991), or the large cross-furnaces, to pour the liquid metal into moulds. As shown through experiments by Schneider and Zimmer (1984) and Zwicker (1984), the exterior crucible surface temperatures would have been low enough to allow such handling (Rehren, 1996a). This heat concentration within the crucibles, due to their isolating properties and the concentrated heating set-up, further explains the limited burning of the mud bricks in the melting channels. A concerted effort must have been made to bring all crucibles to the large casting moulds (at the cross-furnaces) with as little time as possible in between, to attain an almost continuous pour. For the casting of smaller objects, this would not have been necessary. Casting moulds were probably made of unfired clay and disintegrated afterwards, leaving no archaeological remains. The only known clay moulds from Egypt were recently recovered in a Late Period tomb context in Qubbet el-Hawa (Fitzenreiter *et al.*, 2014). Further bronze working, attested in the multifunctional workshops for chariot production, is discussed by Prell (2011).

Following this casting, it is worth asking what happened to the crucibles. The exposure to high temperature, fluxing by fuel ash and interaction with the bronze produced a thick, irregular slag layer on their interior surfaces. It appears that very few crucibles were reused, though a single example of a repaired and reused crucible occurs in phase B/2. However, given the delicate planning and organisation of the B/3 operations, and the low cost of crucible production, it appears highly unlikely that the risk of crucible failure through repeated use would have been acceptable. Furthermore, the singular evidence for reuse in an assemblage of over one thousand fragments makes it difficult to believe this would have been a widespread practice. Most likely then, these crucibles were discarded after use.
Strikingly, not a single intact crucible was found in Pi-Ramesse. Considering that these vessels were quite solid and thick-walled, there must be a reason for their consistent disintegration. Without exception, the crucible fracturing occurred after solidification of the crucible slag, and thus not immediately after casting. This again argues against their failure during use, and thus makes it unlikely that they were repeatedly reused until the point of failure. Rather, the crucibles must have been broken when they were dumped or redeposited (incautiously) during later activities.

The duration over which these industrial installations were in use deserves further discussion. Stratigraphically, phase B/3 is constrained to approximately twenty years in time, which is a great archaeological resolution when looking at events taking place over three thousand years ago. However, it appears unlikely that these industrial activities lasted

twenty years. Considering the organisation needed to run such concerted castings, the large amounts of metal consumed and the (relatively) limited number of massive bronzes probably needed, a much shorter lifespan may be suggested for these workshops. Indeed, the changing orientations (B/3b to B/3a) may reflect two large casting events, each of which may have taken place in the course of days, or perhaps a week or two at most. It seems most appropriate to view the gathering of resources and people with the necessary knowledge into a large-scale operation like this as an 'event', rather than a standing operation, running for months or even years. Such an event, involving, for example, several batteries with twenty or forty crucibles each (Pusch, 1994), could have been performed a few times in the course of a single day, consuming over a hundred crucibles. It is therefore possible that the entire crucible assemblage, which is the biggest Late Bronze Age example hitherto recovered, was produced in the course of a week or two.
Of course, not all crucibles at Pi-Ramesse were recovered during excavation, and several other workshops are known to have existed in the wider vicinity of QI, but this does not change the argument: the majority of all remains were most likely produced in a series of fairly short-lived events.
In contrast, the 'multifunctional workshops' were presumably in use for longer, but produced far lower quantities of metal and crucibles. Metal production there was probably more an *ad hoc* operation, making it far more difficult to reconstruct in time. The dynamics of such workshops, with more ephemeral hearths, regular cleaning, outside dumping of waste and smaller scale casting are very different from the melting batteries, and a detailed reconstruction like that made for the industrial area is impossible. However, it appears that the general procedure was the same, with the exclusion of purpose-built structures, resulting in undistinguishable crucible evidence. In such a context, it is easier to imagine occasional crucible reuse.

Metal supply has been exhaustively discussed in section 6.2, but the foregoing remarks on workshop lifespan elicit some further thought. If the industrial workshops are indeed short-lived, it is not surprising to see less variation in metal sources there. It may not be surprising to see mainly 'domestic copper' in this context when a carefully orchestrated casting event was planned. While the timely delivery of such copper to Pi-Ramesse could probably be foreseen, either through organised mining expeditions or procurement of copper on the domestic market, oversea shipments were probably less reliable. Having a large workforce and specialised craftsmen on hold while awaiting delivery of raw resources may have been an expensive situation that the pharaonic institution wished to avoid.
The variability in copper sources detected within the multifunctional workshops can prob-

ably be attributed to the different supply chain to which these had access, but part of it may reflect different sources of metal arriving in Pi-Ramesse over time. Not only domestic copper, but other shipments of copper from, e.g., Cyprus, Timna and the land of Punt may have trickled into the local market and ended up in these workshops.
Of course, such discussions are difficult to substantiate, given the limited evidence available at this point. A much larger sample is needed for statistical evaluation of such variability across workshops and time, and these ideas must remain hypothetical.

Concerning the question who was active in these workshops, this research cannot offer many new insights. While the organisation of production in Pi-Ramesse, both for the industrial phase (state control) and the later workshops (state and/or private control), seems to differ clearly from domestic organisation in Amarna (Eccleston and Kemp, 2008), the identity of the metallurgist cannot be found inside the crucibles.
Comparisons to Amarna, Thebes (Pusch, 1994), Kerma (Bonnet, 1986) and Buhen (El Gayar and Jones, 1989a,b) are out of place here, as they cannot go beyond speculation as to the actual technology practised at these sites, or are too far separated in time to draw meaningful connections.
In the industrial workshops, it seems that a large group of people were employed for a short period in the execution of a major project. Apart from the overseers and, presumably, unskilled (or less skilled) manual labour, perhaps similarly employed in other projects such as mining expeditions, specialists of high-temperature processes were involved in the planning as well as execution of bronze production. These specialists may have been migrant, perhaps even international craftspeople, but could just as well have been local. Such considerations are beyond the scope of this research. However, it is likely that these people were well treated given their high skill, as suggested by Sapir-Hen and Ben-Yosef (2014), and may have enjoyed a higher degree of independence than suggested by Scheel (1989), despite their contractual engagements with the state. Indeed, following this large project, some may have remained active in the later multifunctional workshops on a (somewhat) more independent basis, which may explain the continuity in technology seen there. Whatever the case may be, it is difficult to elucidate such issues further without comparative data from different social contexts in ancient Egypt to contrast the very unique situation at Pi-Ramesse.

Finally, there must have been interaction between the different material workshops at Pi-Ramesse. Bronze filings were used for the production of Egyptian Blue (Jaksch *et al.*, 1983) and the colouring of glass (Mass *et al.*, 2002), as deduced from glass analysis in Pi-Ramesse (Pusch and Rehren, 2007). New lead isotope evidence presented in this thesis further established a link with Egyptian Blue production. Further research on the Egyp-

tian Blue production waste excavated at Pi-Ramesse may consolidate this connection to bronze production, and clarify the possible export of Egyptian Blue from Pi-Ramesse, perhaps drawing another parallel to glass production. While glass and Egyptian Blue were probably produced largely for export, as ingots and cakes, bronze and faience were presumably used at Pi-Ramesse for architectural purposes, as well as in objects. Contrary to faience, however, bronze could be recycled. This probably happened to many, if not most, Pi-Ramesse bronze objects. It is for example imaginable that large architectural bronzes were molten down by the time the Ramesside architecture was moved to Tanis (or earlier), and the bronze weaponry of Ramses II's army dispersed throughout Egypt and the Levant, despite the state's best efforts to control it. For these reasons, a diachronic approach is needed to fully understand the results presented here. While the crucible evidence is often ambiguous through its inherent variability, the Pi-Ramesse case study is simply the first of its kind, and many of the questions posed here require comparative data from Egypt and its neighbours. It is hoped that these questions can inspire future research into metallurgical activity in ancient Egypt.

Part IV

Gordion

I trust, that with your dispositions, even the acquisition of science is a pleasing employment. I can assure you, that the possession of it is what (next to an honest heart) will above all things render you dear to your friends, and give you fame and promotion in your own country. When your mind shall be well improved with science, nothing will be necessary to place you in the highest points of view, but to pursue the interests of your country, the interests of your friends, and your own interests also, with the purest integrity, the most chaste honor. ... If ever you find yourself environed with difficulties and perplexing circumstances, out of which you are at a loss how to extricate yourself, do what is right, and be assured that that will extricate you the best out of the worst situations. Though you cannot see, when you take one step, what will be the next, yet follow truth, justice, and plain dealing, and never fear their leading you out of the labyrinth, in the easiest manner possible. The knot which you thought a Gordian one, will untie itself before you.

Jefferson, 1785

CHAPTER 7

Archaeological background

Section 7.1

Introduction

Gordion is located on the ancient Sangarios river (modern Sakarya) in central Anatolia, near the modern town of Yassıhüyük, ±70-80 km southwest of Ankara, as shown in Figure 7.1. Its stratigraphic sequence was recently revised by Rose and Darbyshire (2012) (Table 7.1).

Gordion was the capital of the Phrygian kingdom, which reached its largest extent during the Early Phrygian period. It then bordered Lydia in the west and Assyria and Urartu in the east, and Gordion developed and expanded its monumental architecture. Following a destruction of the city[1], further construction and fortification of the citadel took place during the Middle Phrygian period, possibly under the influence of king Midas (whose touch, according to legend, could turn anything into gold) and his predecessor Gordios, who posthumously occupied the largest tumulus in the area (Tumulus MM). The citadel and surrounding tumuli are shown in Figure 7.2.

Phrygian independence ended when they were subjected to Persian rule by Cyrus the Great around 540 BC (probably following a period of Lydian control). Under Achaemenid government, Phrygia became a satrapy with Daskyleion as its capital. Gordion remained an important economic centre on the Royal Road (restored by Darius) and prospered: con-

[1] This destruction level was previously attributed to the Kimmerians (e.g., Sams, 1979 and Young, 1958), which is no longer tenable (Rose and Darbyshire, 2012).

tinuity in both size and monumentality can be seen between Middle and Late Phrygian Gordion. Though no longer a royal seat of power, Gordion retained much of its prestige, while escaping excessive cultural influence from the Persian rulers, as is attested more strongly in Lydia. By the late Achaemenid period, however, Gordion appears to have lost some of its glory, despite maintaining its commercial character and size.
In 333 BC, Gordion was visited by Alexander the Great, who (according to legend) cut the Gordian knot, a symbol of Gordion's strategic importance for trade and military east-west movement. The ensuing Hellenistic (and Roman) periods attested at Gordion indicate continued habitation, though the city never again achieved its former grandeur.
A brief historical overview of Gordion is given by Darbyshire and Pizzorno (2009).

Gordion was first discovered by A. Körte in 1893, who subsequently excavated there in 1900. Large scale excavations were undertaken by the University of Pennsylvania Museum, under the direction of R. S. Young, between 1950 and 1973. Following a period of post-excavation research led by K. DeVries, excavations (headed by M. M. Voigt) started anew in 1988-2006, under the directorship of K. Sams. The excavated areas of the citadel are shown in Figure 7.3. Kealhofer (2005) offers an overview of recent work at Gordion, while the Gordion project website[2] provides a historical overview as well as regularly updated news.

Though other Phrygian archaeological sites exist, such as Yazılıkaya ('Midas-City', Eskişehir Province) and Dorylaeum (near modern Eskişehir city), Gordion is the type-site for Phrygian culture, with the greatest wealth of archaeological evidence for this civilisation throughout its history.

Section 7.2

Metallurgy in Gordion

Metallurgical remains at Gordion were first encountered by Young during excavations in 1953. He noted a 'foundry' in the Late Phrygian level, but fairly little attention was given to this feature and the associated metallurgical products (although Young (1958: 228) mentions that "*ample evidence for a local bronzeworking industry operating as early as the middle of the seventh century*" exists in the form of "*deposits of bronze slag, and particularly fragments of coarse clay crucibles from which molten bronze has been poured*"). An overview of all excavation notes related to this foundry was compiled by A. Fields and

[2] Gordion Project website: http://sites.museum.upenn.edu/gordion/

Figure 7.1: Map showing location of Gordion (from Mellink, 1956, p. 370)

YHSS Phase	Period Name	Approximate Dates
0	Modern	1920s
1	Medieval	10th-15th centuries AD
3	Roman	1st-4th centuries AD
3A	Later Hellenistic	260?-100 BC
3B	Early Hellenistic	330-?260 BC
4	Late Phrygian	540s-333 BC
5	Middle Phrygian	after 800-540s BC
6A-B	Early Phrygian	900-800 BC
7A-B	Early Iron Age	?1100-900 BC
9-8	Late Bronze Age	1600-?1100 BC

Table 7.1: Stratigraphic sequence for Gordion (from Rose and Darbyshire, 2012, Table 0.1, p. 2)

Figure 7.2: Aerial overview of the site and its surroundings, showing the citadel mound, tumuli (dots) and Yassıhüyük village (from Rose and Darbyshire, 2012, Figure 0.1, p. xiv)

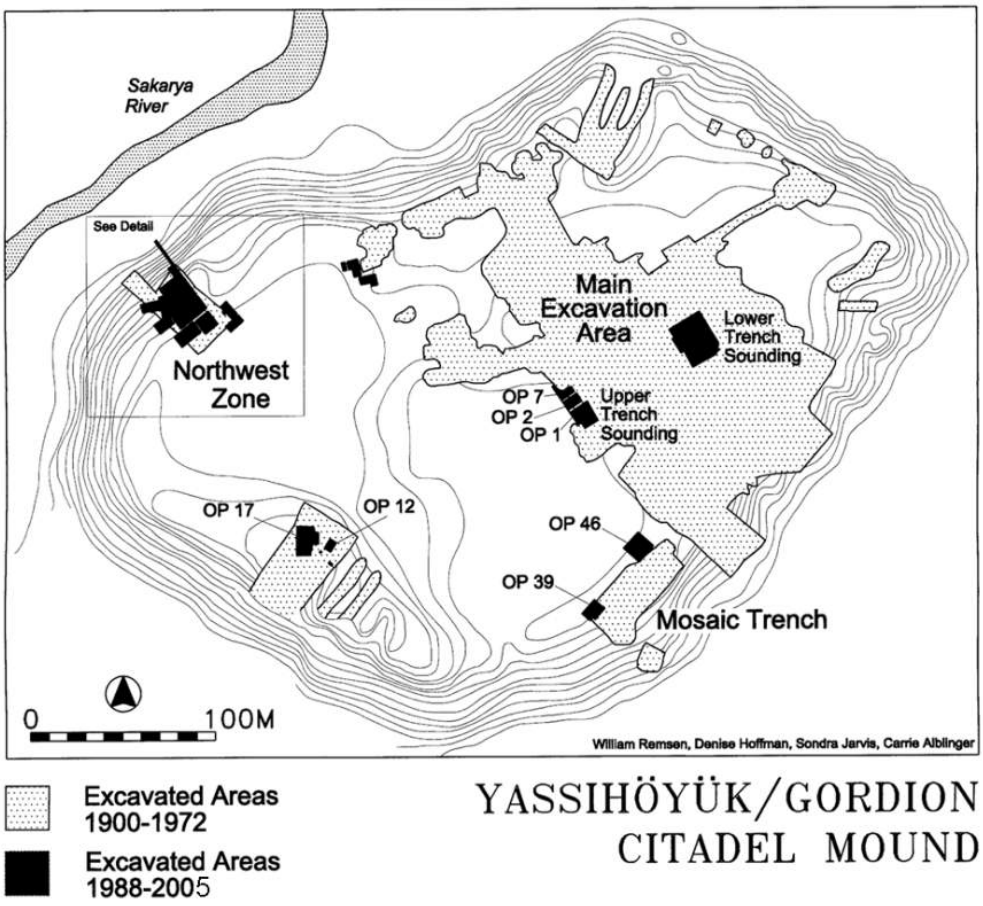

Figure 7.3: Overview of excavated areas within the Citadel Mound (from Voigt, 2012, Figure 1, p. 236)

is presented in Appendix H. Though no furnace remains could be identified, it appears that these 'foundry buildings' were associated with metallurgical activity comprising both bronze melting/alloying and possibly iron metallurgy, as indicated by crucible fragments, arrowheads, bronze and iron garments and 'iron slag clunkers'. The dating of this foundry is not straightforward, but it appears to have seen only a relatively short period of use during the Late Phrygian period (late 5th to early 4th century BC) and was out of use before the Hellenistic period. None of the crucibles discussed in this chapter were directly associated with this foundry, as the crucibles from this context were not preserved.
The location of the 'foundry' is over the Middle Phrygian 'Painted House' and 'Building C' on the Eastern Mound of the citadel, reconstructed by A. Fields as shown in Figure 7.4.

The metallurgical crucible assemblage under study in this chapter was unearthed in the more recent campaigns led by M. M. Voigt. They stem from various contexts in between several houses on the citadel, located in OP 1, 2 and 7 (see Figure 7.3). Only crucibles from Late Phrygian contexts are discussed here, which make up the majority of the assemblage (though crucibles from (mixed) Hellenistic contexts appear (macroscopically) to be part of the same assemblage).
None of the crucibles were excavated in an obvious metallurgical context associated with tuyères, bellows, furnaces or other structural features. Many of the contexts are pits that were dug and used as trash deposits for metallurgical debris as well as other (domestic) trash (pottery, bones, latrine waste etc.), while other find contexts are robber trenches, ash lenses, and few surfaces. More detailed descriptions of these contexts, spanning the entire Late Phrygian period, are given in Appendix I.
In addition to the crucibles, some bronze objects, spills and casting moulds have been identified within the same contexts (discussed in sections 8.4 and 8.5), as well as indications for iron metallurgy (not discussed in this thesis).

These deposits were strewn in between buildings in OP 1, 2 and 7, approximately 60 meters from the location of the presumed foundry. It is therefore possible that some crucibles are related to that foundry, and were discarded in the wider area. However, the amount of architecture separating crucible deposits and foundry, and the pre-dating of several crucible deposits to the foundry, indicates that other metallurgical workshops must have existed, most likely spread over a larger area.

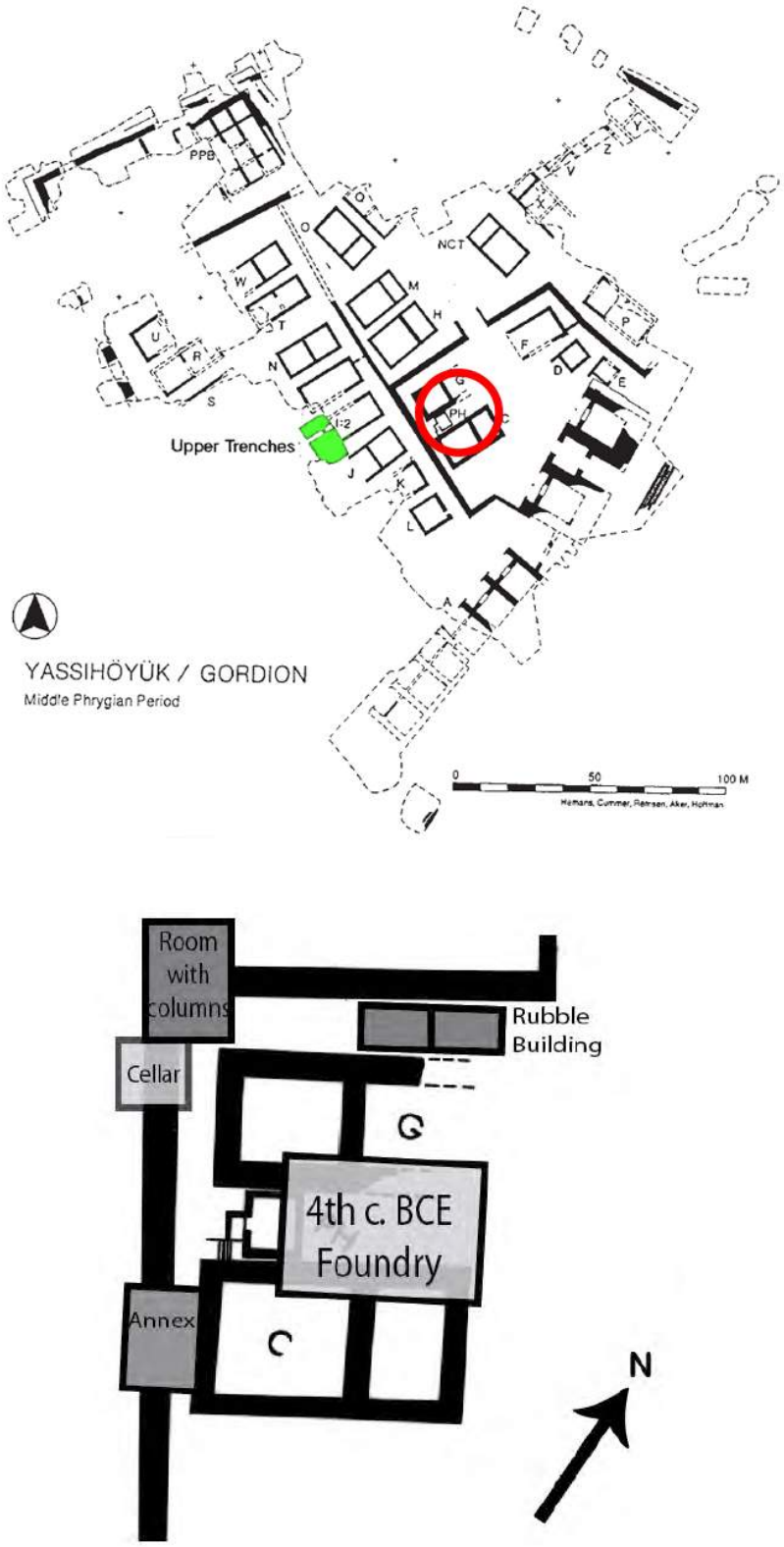

Figure 7.4: Top: Gordion, Middle Phrygian citadel: foundry area indicated in red, OP1 and OP2 (crucible excavation areas) in green (after Voigt and Young, 1999, Figure 8, p. 201). Bottom: Reconstructed location of 'foundry' within the Gordion citadel (from Fields, 2011, Figures 8 and 17)

CHAPTER 8

Analytical results

Section 8.1

General crucible characteristics

The general characteristics of most crucible samples are summarised here, offering an overview of the crucibles' design, ceramic fabric and the main zones occurring within each crucible. This serves as the basis for further examination of the crucible slag (section 8.2) and the interpretation of the metallurgical processes underlying its formation (section 8.3).

8.1.1 Macroscopic investigation

No complete crucible has been found in Gordion. The largest fragment, shown in Figure 8.1, indicates a crucible height of ±10 cm (±2 cm wall thickness, internal height ±8 cm) and a diameter of perhaps ±15-18 cm. The shape is unknown and is most probably circular to elliptical. No spout fragments have been encountered.
Most other fragments are smaller, usually around 5 cm in size. Wall thickness averages around 1.5-2 cm, sometimes tapering to 1 cm at the crucible rim. These fragments do not provide much information on the complete shape of the crucibles. They all conform to the shape deduced from the largest fragment, but might equally be fragments of smaller or larger crucibles. However, the average size appears to be roughly the same or slightly

Figure 8.1: Largest crucible fragment

larger than the Pi-Ramesse crucibles: $\varnothing \approx 10-15$ cm, volume $\approx 270-700$ ml. Reconstruction drawings are shown in Figure 8.2.

There are some macroscopic indications for the use of organic temper (see Figure 8.3), such as straw or chaff, though not in every fragment. Macroscopic indications are not as clear as for Pi-Ramesse and microscopically, the pores exhibit less characteristic shapes.

All crucibles were heated from the inside, as can be deduced from their wall profile: from fired ceramic on the outside, to bloated, slagged ceramic on the inside. The regularity by which the crucibles' external surface is fired, suggests pre-firing before use, similar to the Pi-Ramesse crucibles (section 5.1.1).
The internally slagged surface is typically dark grey to black in colour, and often contains green corrosion products, indicative of copper-related metallurgy. In fact, the amount of corrosion is markedly higher than that seen in the Pi-Ramesse crucibles, as shown in Figure 8.4.

It is difficult to say whether these crucibles were hand-shaped or wheel-turned. Though finger-imprints have not been noticed, the irregular rims, variable wall thickness and uneven exterior wall surface indicate that these crucibles were manually shaped.

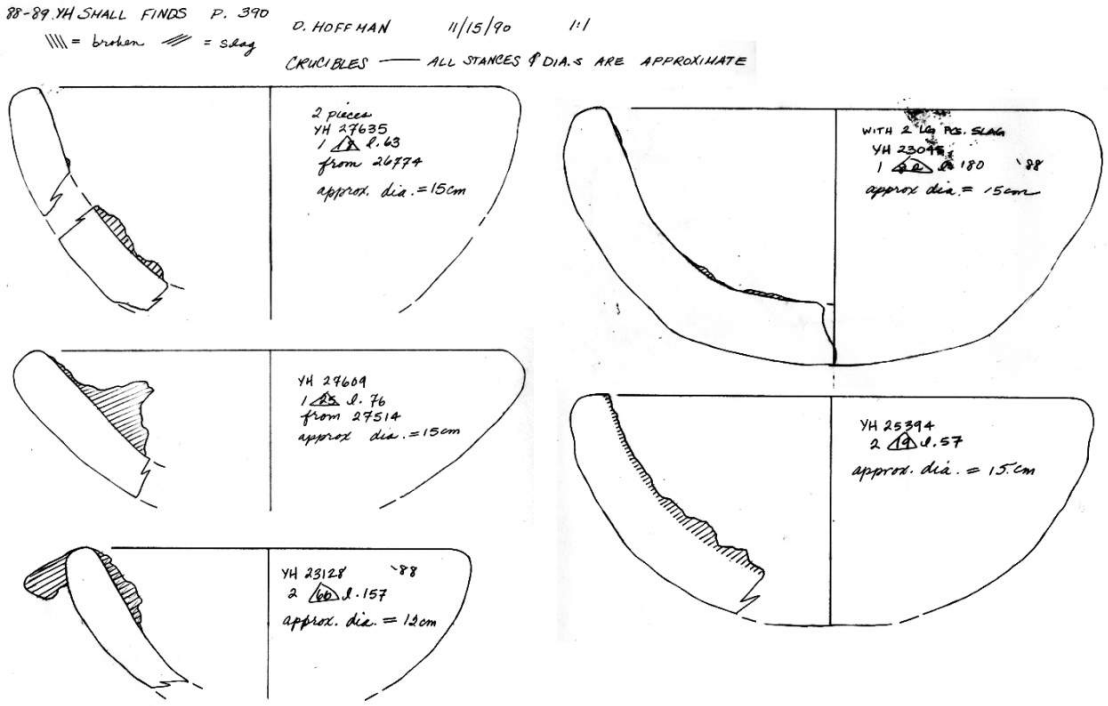

Figure 8.2: Crucible drawings

Figure 8.3: Indications for organic temper in crucibles: fibrous impressions on exterior surface and elongated porosity in cross-section

Figure 8.4: Corrosion products on interior crucible surfaces

8.1.2 Microscopic investigation

Microscopic investigation reveals some further general characteristics, listed here.

1. Typically, three main parts are present in each section through a crucible wall:
   (a) On the outside, a fired ceramic part.
   (b) In the centre, towards the interior surface, a porous, bloated part which marks the disintegration of the ceramic and the transition into a slagged part.
   (c) A slag part, consisting of vitrified ceramic (no original ceramic structure remaining) and varying quantities of charge contributions, such as fuel ash and metal oxides.
2. The ceramic part is made up of a fine clay fraction, with abundant small to medium angular quartz fragments and variable (from few to abundant) medium to (very) large coarse inclusions, further described in section 8.1.3.
3. The ceramic has a similar to slightly lower porosity than the Pi-Ramesse crucibles. Pore shapes are sometimes characteristic of burnt-out organic temper, though not

always. No phytoliths are encountered. In addition to porosity induced by organic temper, many pores appear due to expansion and shrinkage of the clay minerals and rock fragments (see section 8.1.3) upon firing.

4. The ceramic part gradually becomes more porous towards the inside of the crucible wall, up to the point where it loses all its structurally bound water, disintegrates and bloats, similar to the situation seen in the Pi-Ramesse crucibles.

5. The inside of the crucible shows the continuation of this bloated zone, which is a (partly) vitrified zone resulting from the further disintegration of the ceramic. Closer towards the crucible interior, this vitrified ceramic interacts with the crucible charge to form crucible slag. Important to note here is that this slag zone is not always well developed, resulting in a very thin or absent slag layer in 28% of all crucible samples.

6. In 30% of the crucible samples, an additional 'layer' exists, consisting primarily of copper and bronze corrosion products. The limited contribution of vitrified ceramic distinguishes this layer from the crucible slag, and 'dross' is a more appropriate term for it. This dross layer is difficult to see macroscopically, but can be noted as green areas embedded in the more glassy slag zone, sometimes with fibrous or powdery corrosion on the surface.

7. Metallic prills were noted in 74% of all samples.

Examples of the three to four main parts typically present in each crucible profile are shown in Figure 8.5.

8.1.3 Crucible ceramic fabric

In all samples (with three exceptions, see section 8.2.6), the ceramic fabric contains coarse inclusions. Some examples are shown in Figure 8.6. These inclusions typically consist of three main mineral[1] phases (colours refer to SEM images):

- *Pyroxene*: A light grey phase, with approximate composition of 70% diopside ($MgCaSi_2O_6$) - 30 % hedenbergite ($FeCaSi_2O_6$). These two minerals form a complete solid solution series at elevated temperatures. Typically, 0.4-0.5 at% Na and 0.8-1.0 at% Ti, i.e., minor augite ($(Ca,Na)(Mg,Fe,Al)(Si,Al)_2O_6$), is present (solid solution).

[1] Compositional, mineralogical and occurrence information from Klein and Dutrow (2007).

(a) Profiles through crucible walls

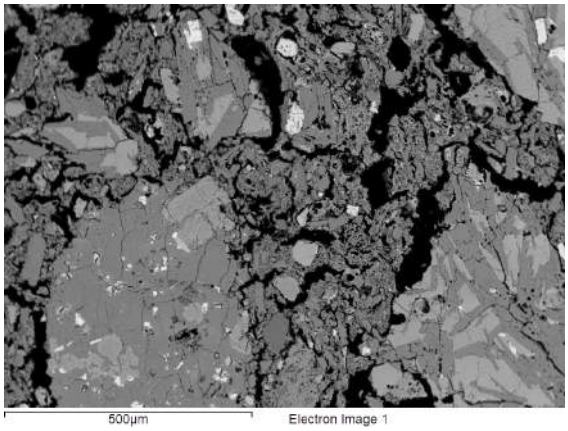

(b) Ceramic fabric

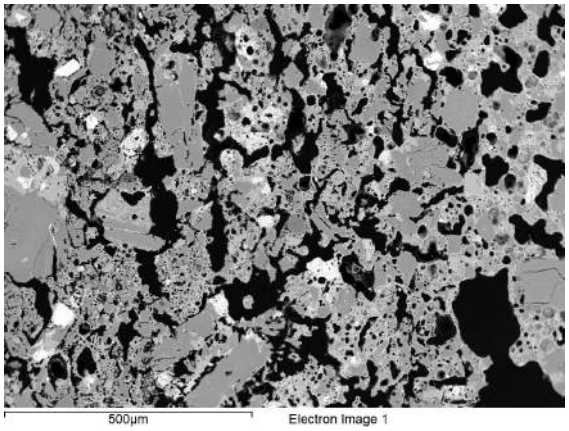

(c) Bloated ceramic

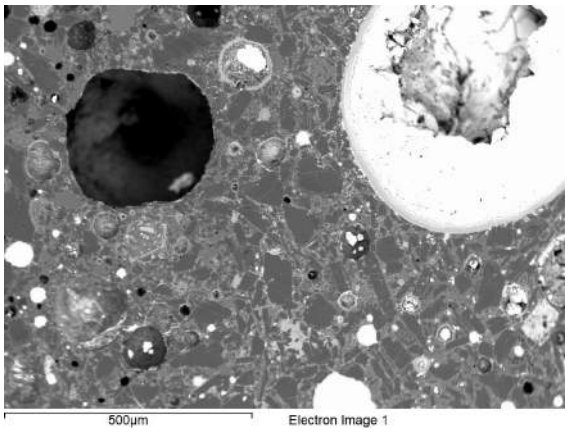

(d) Slag

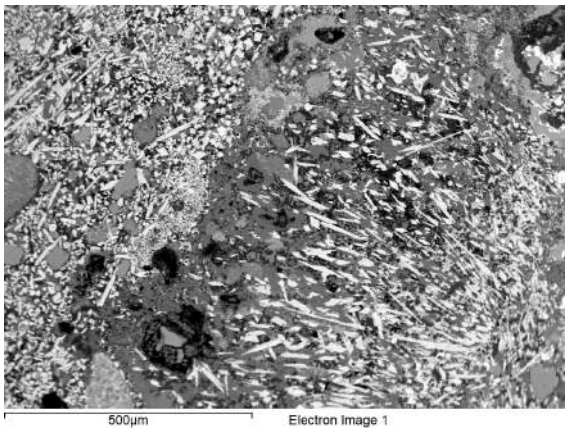

(e) Dross

Figure 8.5: Typical structural changes through crucible profile

	Na_2O	MgO	Al_2O_3	SiO_2	P_2O_5	K_2O	CaO	TiO_2	FeO
Average	4.5	3.7	20	52	0.7	1.2	10.2	1.8	6.9
St. dev. (12 measurements)	0.9	1.5	2	1	0.1	0.4	2.3	0.5	1.4

Table 8.1: Bulk composition of coarse inclusions in the ceramic fabric (in wt%, normalised to 100%)

- *Plagioclase*: A medium grey phase, with approximate labradorite composition, or 60% anorthite ($CaAl_2Si_2O_8$) - 40 % albite ($NaAlSi_3O_8$). Typically, 0.2 up to 0.6 at% potassium and 0.2 at% Fe are present. Some zoning can be seen in the bottom right example of Figure 8.6, with a lighter shade of grey in the central area of the plagioclase, darkening towards the edges.

- *Spinel*: A bright, almost white phase, with approximate composition of 65% ulvöspinel (Fe_2TiO_4) - 35% magnetite (Fe_3O_4). These two minerals form a solid solution at temperatures above 600°C.

Pyroxene and plagioclase make up the bulk of the inclusions, as more elongated crystals, while spinel is present in smaller quantities, with a characteristic isometric shape. Diopside and hedenbergite occur in metamorphic rocks, but are equally formed during igneous crystallisation. In gabbros and basalts, labradorite is the common feldspar. Ulvöspinel-magnetite is sometimes associated with metamorphic rocks, but often crystallises from mafic (basalt-gabbro) magmas. Therefore, these inclusions are most likely mafic (basalt-gabbro) rock fragments. These fragments could have been deliberately added to the clay as temper, or be present as residual fragments if the clay was weathered from this basalt-gabbro rock. The bulk composition of these coarse inclusions is given in Table 8.1. Based on chemical composition and following the system proposed by Le Bas *et al.* (1986), these rock fragments can be identified as (sodic) basaltic trachyandesite.
The bulk composition of the ceramic as a whole (see Appendix J, discussed in section 8.2.2) is very similar to this, but has slightly lower Na_2O and Al_2O_3 content and slightly higher FeO content. Smaller inclusions in the ceramic fabric include spinel (ulvöspinel-magnetite) and pyroxenes (diopside-hedenbergite, augite and ferrosilite[2]-magnetite), which are probably fragments from the coarse rock inclusions discussed above.

All of this agrees with the hypothesis that a clay weathered from a mafic mother rock, with some remaining rock inclusions, was used for fabricating these crucibles, without the deliberate addition of rock fragments. The presence of these rock fragments, however, might

[2]Ferrosilite is the iron-rich end-member of the orthopyroxene series, with an approximate $FeSiO_3$ composition.

have been the reason why this particular clay was (deliberately) selected for its purpose. This is discussed further in section 8.3.1.

Though no detailed mineralogical fabric description for (Late Phrygian) ceramics from Gordion exists (discussions by Grave *et al.* (2005, 2009); Henrickson (1994, 2005) and Henrickson and Blackman (1996) mention 'coarse inclusions', but not the nature of these inclusions[3]), the discussion of regional physical geography by Marsh (2000, 2005) sheds further light on the clay sources available for ceramic production. Two main soil types occur around Gordion, which reflect the major rock types upon which they developed: silty marl produced more calcareous, silty and pale clays, while basalt intrusions yielded less calcareous, red basalt-derived soils. These abundant basalt-derived soils from the eastern region surrounding Gordion, which would have been used for agricultural purposes, were most likely the source of sediment used to produce the metallurgical crucibles under investigation. Thin-section ceramic petrography could provide more conclusive evidence for this hypothesis.

Section 8.2

Detailed description of crucible slag

The structural characteristics of the forty-six analysed crucible samples (listed in Appendix I) are quite consistent and do not allow for any meaningful distinction of groups (exceptions are discussed in section 8.2.6). Here, the chemical data obtained by SEM-EDS is used to look for broad trends in the bulk compositions of ceramic and slag (dross layers are discussed separately in section 8.2.7). A description is given of all phases (oxides in section 8.2.3, metals in 8.2.4) that occur in minor or major amounts in the crucible slag. This section aims to be purely descriptive, with interpretation and discussion reserved to section 8.3 and Chapter 13.

8.2.1 Some broad trends

Full results of the chemical analysis of crucible ceramic and slag are given in Appendix J. The most abundant elements (SiO_2, Al_2O_3, FeO and CaO, adding up to ±89 wt% of ceramic and ±80 wt% of slag bulk composition) have been plotted in ternary diagrams to

[3]Furthermore, no full chemical compositional data is available - only trace element data and results of Principal Component Analysis are shown.

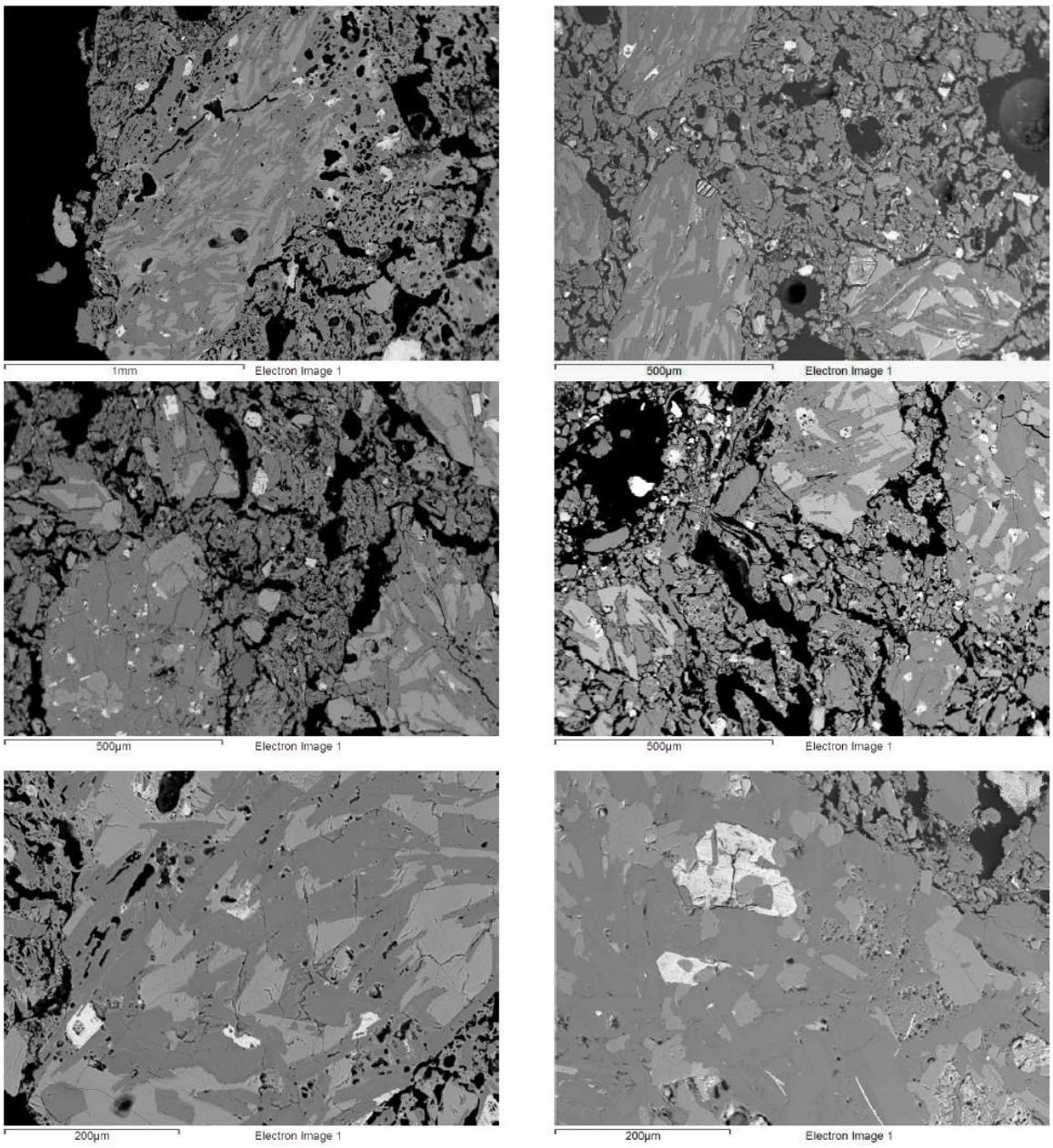

Figure 8.6: Coarse inclusions in the ceramic fabric

discern any broad patterns: Figure 8.7 shows these crucible ceramic and slag compositions, in each case ignoring all other elements. The ceramic composition (red) is very uniform, showing tight compositional clustering. As discussed in Chapter 3, an effort has been made to minimise bias through inclusion/exclusion of large inclusions in the area of analysis. The presence of coarse inclusions (discussed in section 8.1.3) therefore does not appear to cause variation in bulk composition in the way quartz does in the Pi-Ramesse crucibles (see section 5.2.2). This strengthens the hypothesis that the coarse ceramic inclusions are naturally present as residual mother rock in the clay used for making these crucibles.

The slag compositions (blue) almost completely overlap with the ceramic composition, both in SiO_2 - Al_2O_3 - FeO and SiO_2 - Al_2O_3 - CaO. Only a few samples show minor enrichment in FeO, while there is a general (small) enrichment in CaO. None of this is comparable to the extent of enrichment seen in the Pi-Ramesse crucibles.

Three crucible samples are clearly different from the rest of the assemblage. They are macroscopically identifiable due to their shape and the lighter colour of the ceramic fabric, which has a strongly different composition (orange) (excluded from average composition in Appendix J). Their slag composition (turquoise) shows a similar relation to the corresponding ceramic composition as for the other crucibles, and is included in section 8.2.2. These three samples are discussed in section 8.2.6.

The frequent presence of undissolved, fractured quartz grains in the crucible slag shows that it usually did not fully liquefy. Moreover, the actual chemical composition is more complex than these ternary diagrams suggest (Hauptmann, 2007). Therefore, the melting temperatures of 1400-1600°C, indicated by the ternary diagrams, were probably not reached. Additionally, redox-conditions during the metallurgical process did not necessarily correspond to those for which these diagrams were constructed.

Finally, Figure 8.8 shows the same slag compositions (ceramic compositions are omitted), distinguishing between crucible rim and body samples (and body samples near rims). Contrary to the Pi-Ramesse case (see Figure 5.6), there is no clear distinction between rim and body samples in terms of their bulk chemical composition. This is examined in more detail in section 8.3.2.

8.2.2 Bulk analysis

'Bulk analysis', as defined in section 3.3.4, is conducted for all samples. The full compositional data for all crucibles is given in Appendix J and broken down into the ratios of

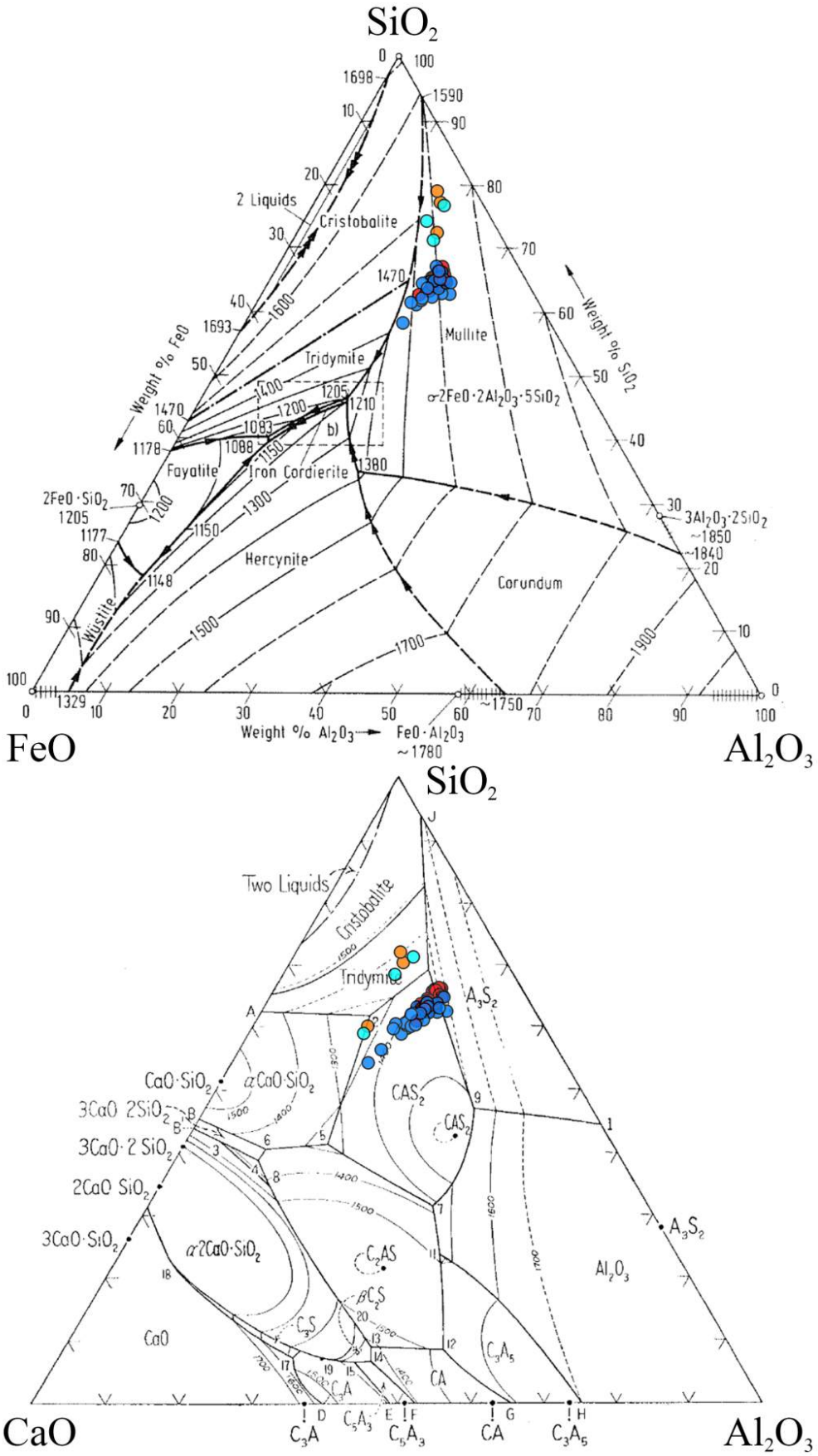

Figure 8.7: Ternary plots for ceramic (red+orange) and slag (blue+turquoise) composition

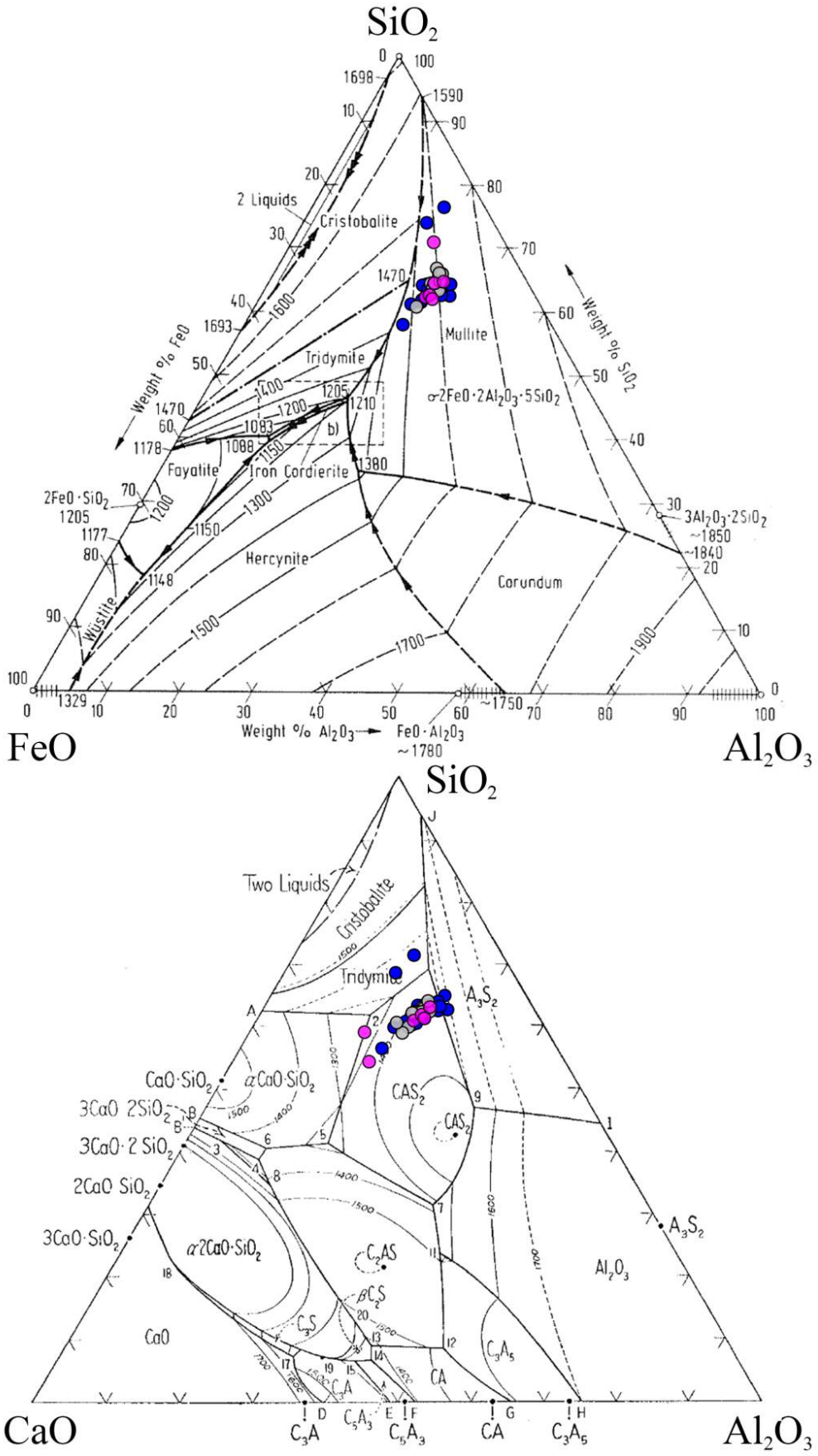

Figure 8.8: Ternary plots of slag composition, distinguishing between body (blue), rim (grey) and body-near-rim (pink) samples

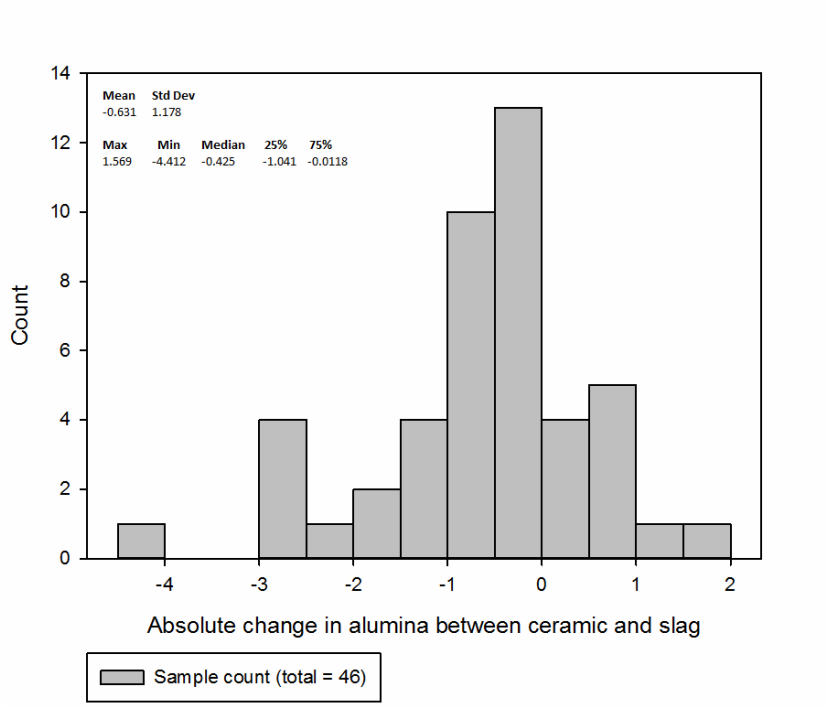

Figure 8.9: Absolute change in Al_2O_3 content (in wt%) between ceramic and slag (after removal of metals)

oxides to alumina and changes of these ratios between ceramic and slag (ignoring base metal content). Similar to the Pi-Ramesse crucibles, the absolute Al_2O_3 content is slightly lower in slag than ceramic, as shown in Figure 8.9, which simply reflects dilution due to slag enrichment in other elements.
First, the changes in ratios of oxides to Al_2O_3 are discussed to identify changes between crucible ceramic and slag. Next, base metal oxide content is presented as wt% in slag (as ceramic base metal content is below detection limits, this metal content is equivalent to 'change in metal content'). Distributions have again been tested for normality using the Shapiro-Wilk normality test and correlation coefficients for two variables have been calculated using Pearson Product Moment Correlation, as explained in section 5.2.2.

- Figure 8.10 shows that the change in SiO_2/Al_2O_3 between slag and ceramic has a normal distribution around a minor decrease. This reflects dilution of silica similar to that of alumina.

- ±90% of all samples show some enrichment in CaO. As the histogram in Figure 8.11 shows, the majority of samples show low enrichment and there is a decrease in incidence for higher enrichments. Compared to the Pi-Ramesse crucibles, the relative lime enrichment here is very low. The scatter plot shows the samples sorted by in-

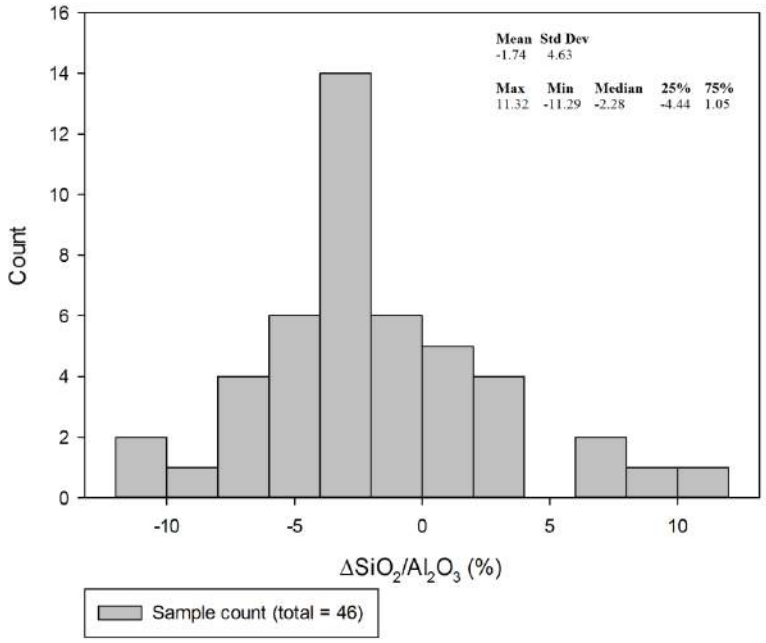

Figure 8.10: Change in the ratio $^{SiO_2}/_{Al_2O_3}$ between ceramic and slag

creasing enrichment, which again appears to follow a step-wise increasing trend. Though some of this might be explained by insufficient sampling, it probably points to a bi-modal distribution (below and above ±40% relative change) reflecting higher enrichments for body fragment slag. Compared to Pi-Ramesse, where there is a ±400% relative change, enrichments here are much lower (nearly ten times).
Figure 8.12 shows the relative increase in CaO plotted against MgO, P_2O_5, K_2O, Na_2O and SiO_2. There is a good correlation between the relative increase in CaO and P_2O_5 ($R = 0.757$, $p = 1.15 \times 10^{-9}$) and K_2O ($R = 0.856$, $p = 3.576 \times 10^{-14}$), and a weaker correlation between CaO and MgO ($R = 0.453$, $p = 1.58 \times 10^{-3}$) and SiO_2 ($R = 0.436$, $p = 0.244 \times 10^{-3}$). Between CaO and Na_2O, no significant correlation exists ($R = -0.0704$, $p = 0.642$). These observations, most likely related to fuel ash contributions to the crucible slag, are discussed in section 8.2.5.

- The change in $^{TiO_2}/_{Al_2O_3}$-ratio, shown in Figure 8.13, has a normal distribution around a minor average increase.

- The change in $^{FeO}/_{Al_2O_3}$-ratio, shown in Figure 8.14, has no normal distribution. The scatter plot shows the samples sorted by increasing enrichment. This trend shows an iron enrichment with normal distribution around a low value, with an extended tail of higher enrichment. The low enrichment (normally distributed) occurs in both

body and rim fragments. The tail of eight samples with higher enrichment encompasses mainly body fragments (seven out of eight).
The data in Figure 8.14 probably presents two populations: one ($\pm^{38}/_{46}$ samples, 83% of population) normally distributed around a very low iron enrichment (mean: 1.6%, std. dev.: 11.4%), and one group ($\pm^{8}/_{46}$ samples, 17% of population) more clearly enriched in iron. Though this appears similar to iron enrichment seen in the Pi-Ramesse crucibles, it should be noted that the absolute enrichment is very low by comparison. Like the lime enrichment, iron enrichment seen here is ten times smaller than that witnessed in the Pi-Ramesse crucibles.
Figure 8.15 shows that there is no significant correlation ($R = 0.155$, $p = 0.304$) between CaO- and FeO-increase (the highest FeO enrichment does not coincide with high CaO enrichment and vice-versa). Exclusion of the eight samples with higher iron enrichment does not improve this.

- MnO content is very low (at detection limit), does not show any significant changes, and may be considered absent.

- As_2O_3 content is very low (at detection limit), does not show any significant changes, and may be considered absent.

- CuO content increases to varying degrees. All but one of the crucibles contain either copper-based metal prills or oxides, explaining the CuO-increase in nearly all samples. However, due to the irregular occurrence of prills throughout the slag, their measurement is quite variable: it is sensitive to prills being present in the analysed frame. Figure 8.16 shows the distribution of CuO enrichment: most crucibles have enrichments below 10 wt%, while some have enrichments up to 24 wt%.

- SnO_2 content increases to varying degrees. Its measurement is quite variable: it is sensitive to bronze prills and tin oxide clusters, which occur heterogeneously throughout the crucible slag, being present in the analysed frame. Figure 8.17 shows the distribution of SnO_2 enrichment: half of the samples show enrichments up to 3 wt%, while the other half show enrichments up to 19 wt%. Figure 8.18 shows a scatter plot of CuO vs SnO_2 enrichment, indicating some correlation between both ($R = 0.564$, $p = 0.44 \times 10^{-4}$). The highest CuO enrichment occurs at moderately high SnO_2 enrichment, while the highest SnO_2 enrichment occurs at moderate CuO enrichment.

- PbO content increases to varying degrees. In $\pm^{2}/_{3}$ of all crucibles, no significant lead enrichment is measured. In the remainder of the crucibles, enrichments between 0 and 5 wt% are measured, as shown in Figure 8.19. Figure 8.20 shows a scatter

plot of CuO vs PbO enrichment, indicating low (but significant) correlation between both ($R = 0.434$, $p = 0.261 \times 10^{-3}$). This is due to the better correlation ($R = 0.761$, $p = 0.167 \times 10^{-5}$) between CuO and PbO when PbO is actually present.

- Figure 8.21 shows there is no significant relation between the increase in CuO or PbO with higher Δ^{CaO/Al_2O_3} ($R = 0.121$, $p = 0.421$ and $R = 0.0782$, $p = 0.606$) and a very low correlation between the increase in SnO_2 and Δ^{CaO/Al_2O_3} ($R = 0.326$, $p = 0.0272$).
- Figure 8.22 shows the CuO, SnO_2 and PbO content for body and rim fragments. Though there is no full separation (variable metal content occurs in all fragment types), there is a trend for higher metal content in body rather than rim fragments.

It should be mentioned that with a beam voltage of 20 kV, Pb present in low quantities is not sufficiently excited to be picked up by SEM-EDS[4] and remains below detection limits. Contrary to the Pi-Ramesse case, a number of Gordion crucibles show lead contents exceeding this detection limit, indicating more significant lead contamination of the crucible slag.

As mentioned in section 3.3.6, Cl oxide is not reported by INCA. Sections 8.2.3 and 8.2.4 show that chlorine occurs in some phases within the crucible slag, but especially the dross layer, which means it should be expected as a bulk component there.

Finally, a note should be made on the presence of SO_2. In some slag area analyses, INCA suggests the measurement of sulphur. However, there is a strong overlap between sulphur and lead peaks. In the presence of lead, the measurement of SO_2 is false and usually does not account for more than 0.2-0.5 wt% (effectively below the detection limit). Therefore, it is omitted from the bulk measurements presented in Appendix J.
Significant SO_2, however, occurs in two crucibles. In Gordion-23707, SO_2 is measured at ± 1 wt% of the bulk composition of both ceramic and slag, but not in any particular phase. It seems, therefore, that this presents an overall contamination of the sample. In Gordion-28932 (2), sulphur is not measured in the ceramic, but only in the slag, where it is concentrated in a corrosion layer on the interior slag surface (see Figure K.14c). This is rare, but not entirely uncommon (limited copper sulphide corrosion products occurs in three other samples) and most likely represents post-depositional corrosion (not correlated to the presence of sulphidic prills in the crucible slag).

[4] For lead, Lα_1=10.551 keV & Lβ_1=12.619 keV

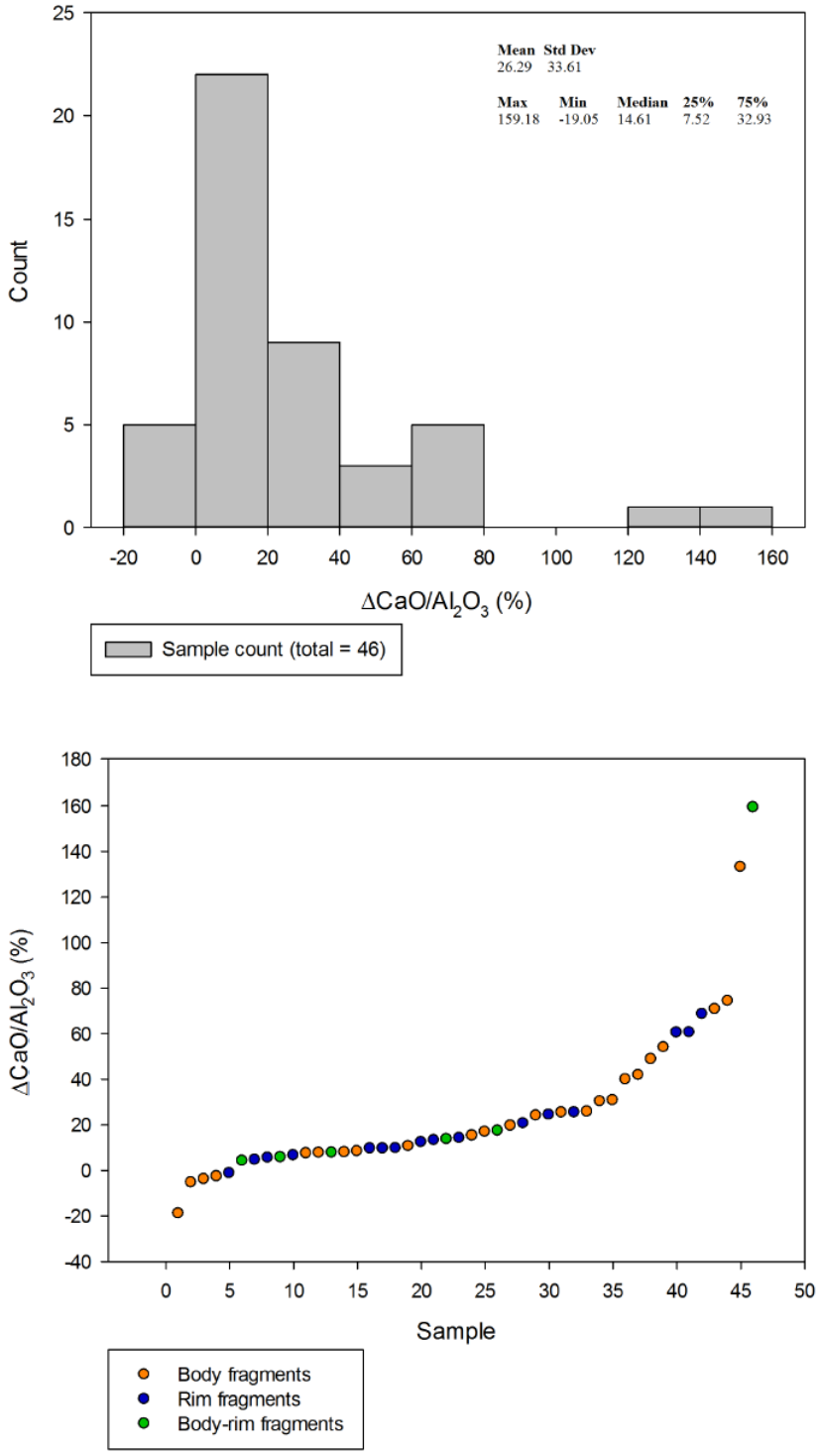

Figure 8.11: Change in the ratio $^{CaO}/_{Al_2O_3}$ between ceramic and slag

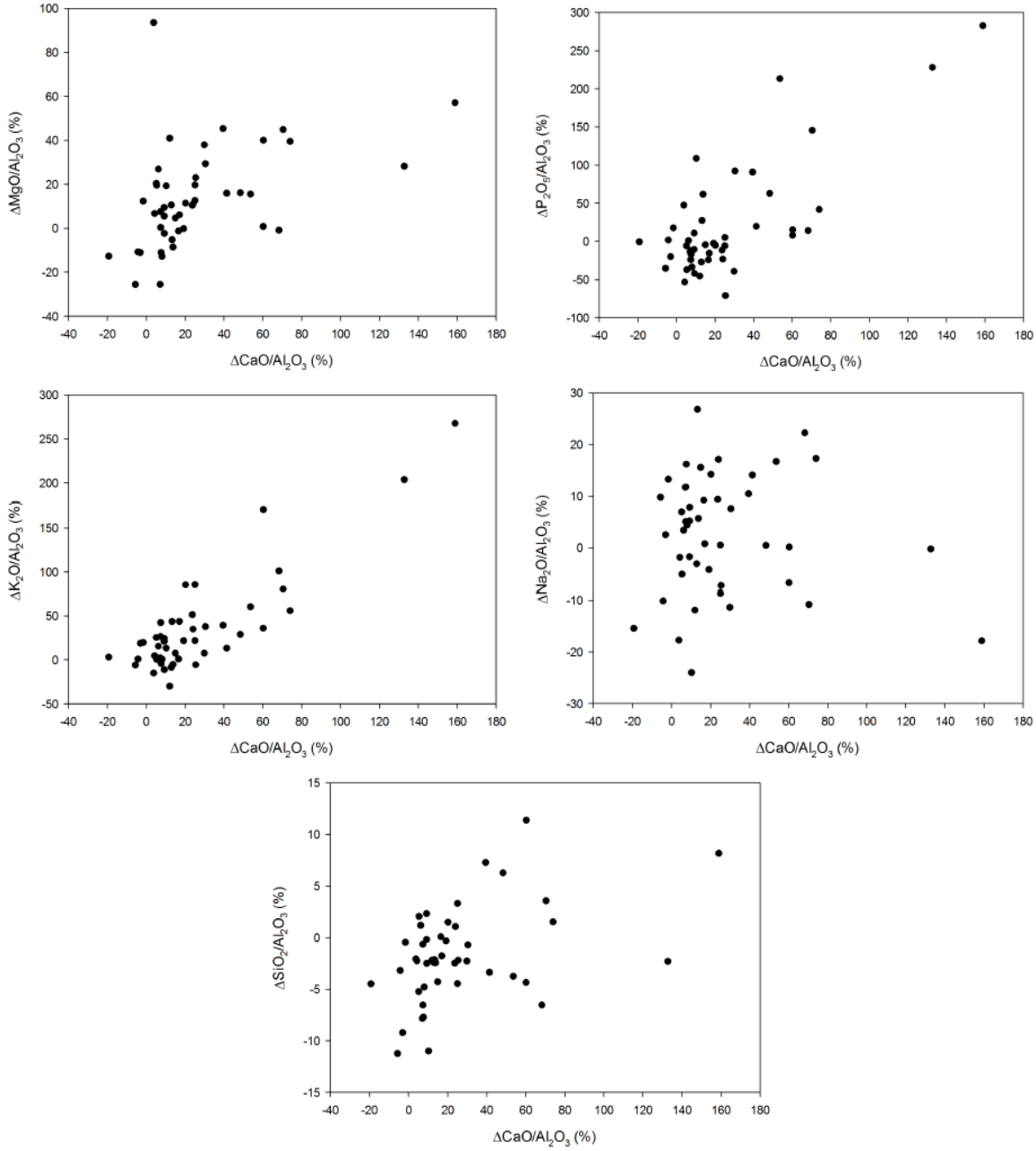

Figure 8.12: Change in the ratio $^{CaO}/_{Al_2O_3}$ vs $^{MgO}/_{Al_2O_3}$, $^{P_2O_5}/_{Al_2O_3}$, $^{K_2O}/_{Al_2O_3}$, $^{Na_2O}/_{Al_2O_3}$ and $^{SiO_2}/_{Al_2O_3}$, between ceramic and slag

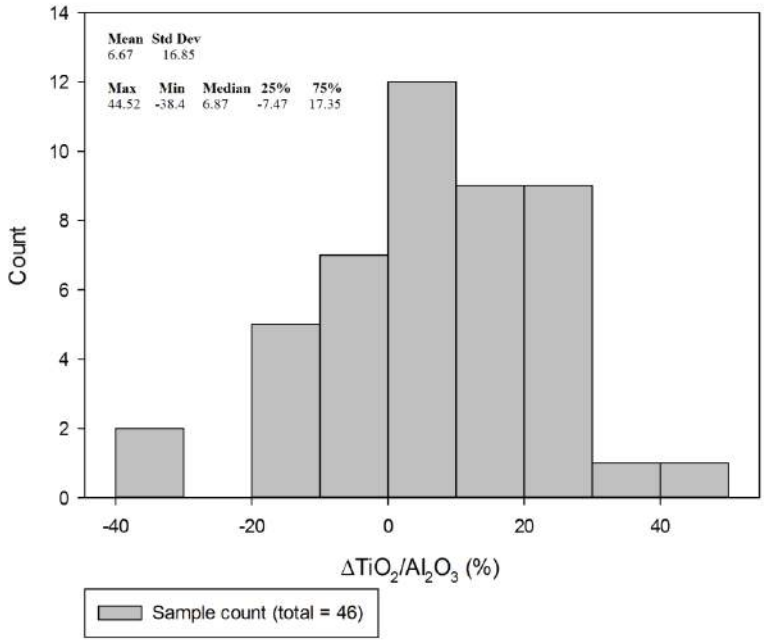

Figure 8.13: Change in the ratio TiO_2/Al_2O_3 between ceramic and slag

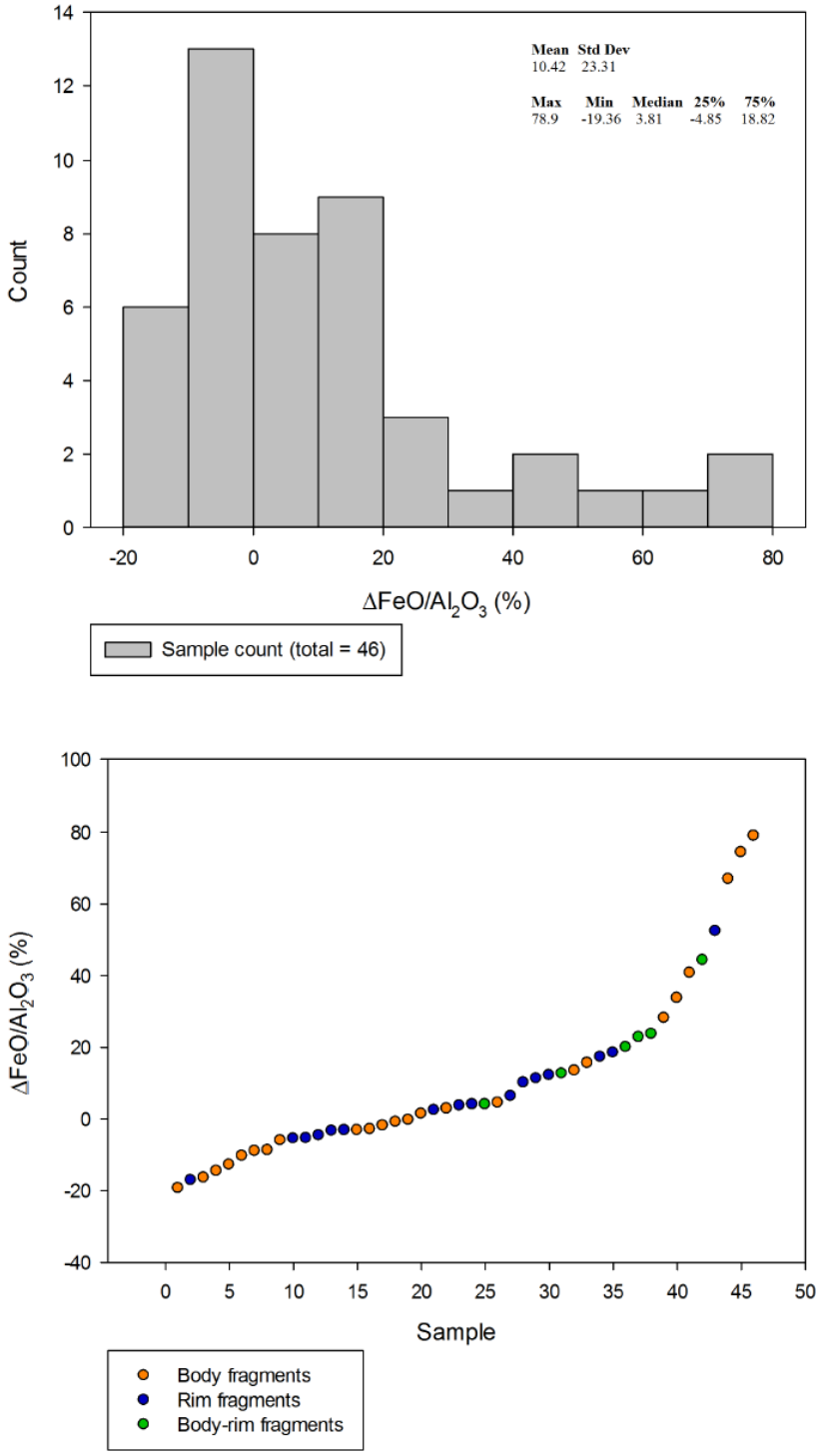

Figure 8.14: Change in the ratio $^{FeO}/_{Al_2O_3}$ between ceramic and slag

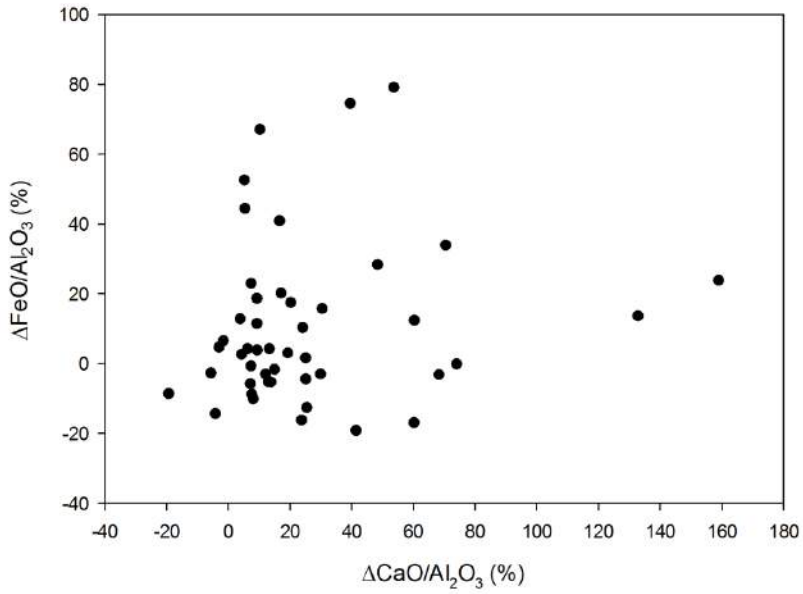

Figure 8.15: Change in the ratio $^{CaO}/_{Al_2O_3}$ vs $^{FeO}/_{Al_2O_3}$ between ceramic and slag

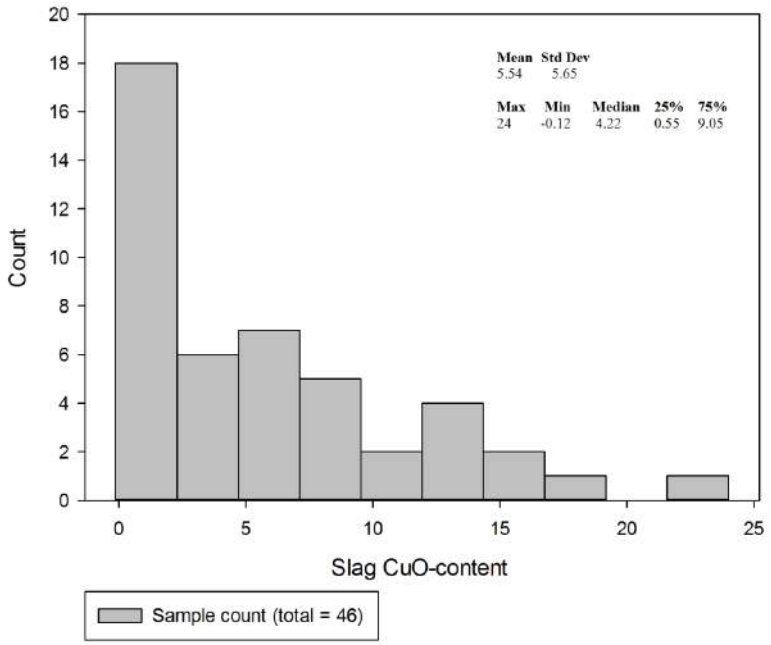

Figure 8.16: Bulk CuO content (in wt%) in slag

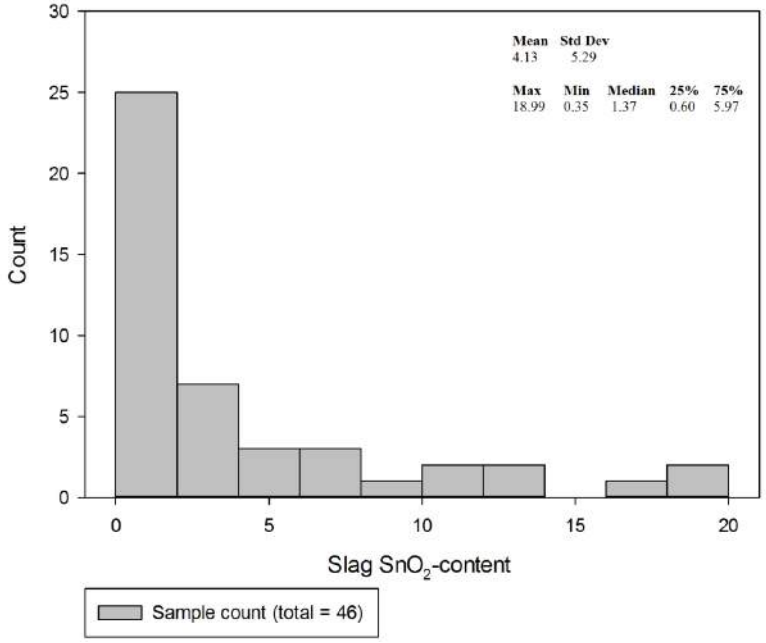

Figure 8.17: Bulk SnO_2 content (in wt%) in slag

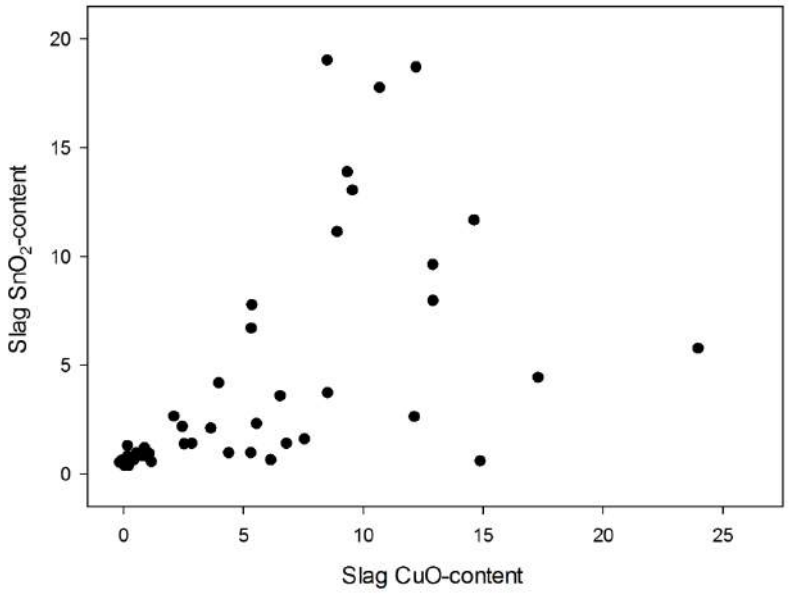

Figure 8.18: Bulk CuO vs SnO_2 content (in wt%) in slag

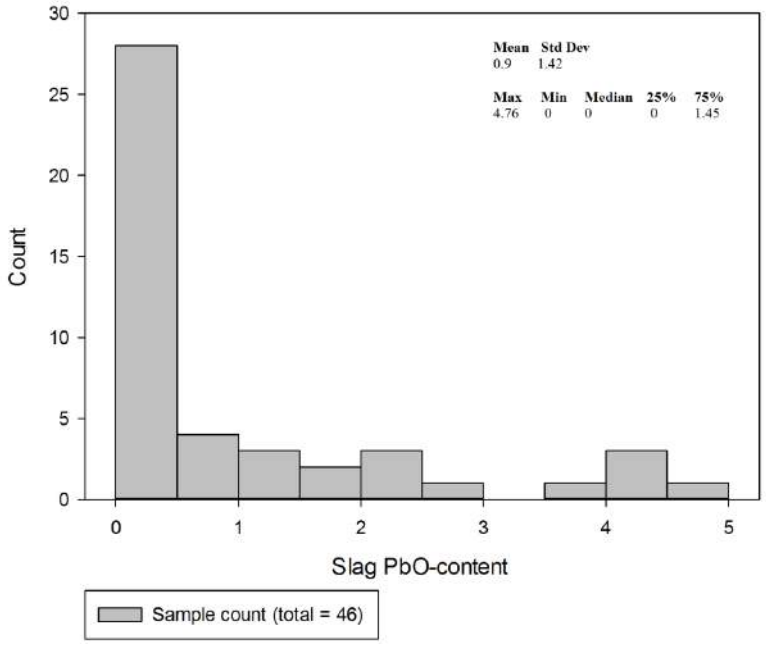

Figure 8.19: Bulk PbO content (in wt%) in slag

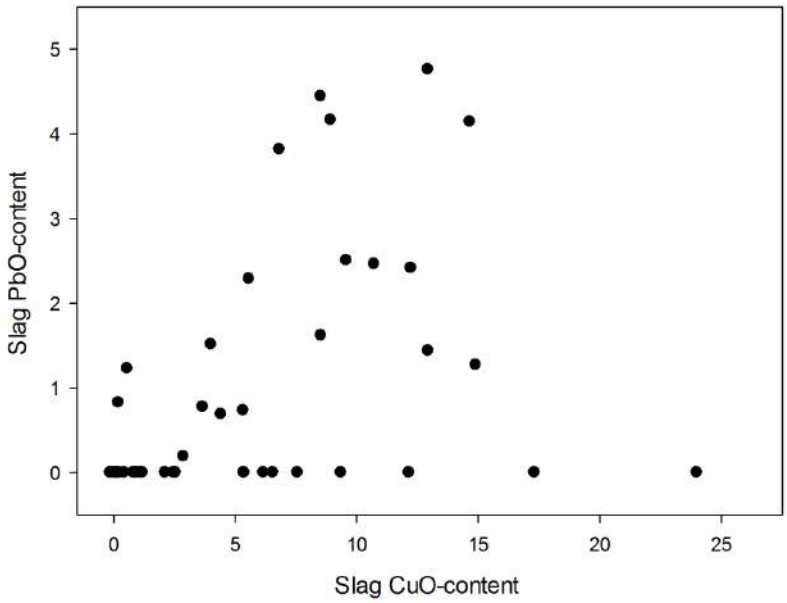

Figure 8.20: Bulk CuO vs PbO content (in wt%) in slag

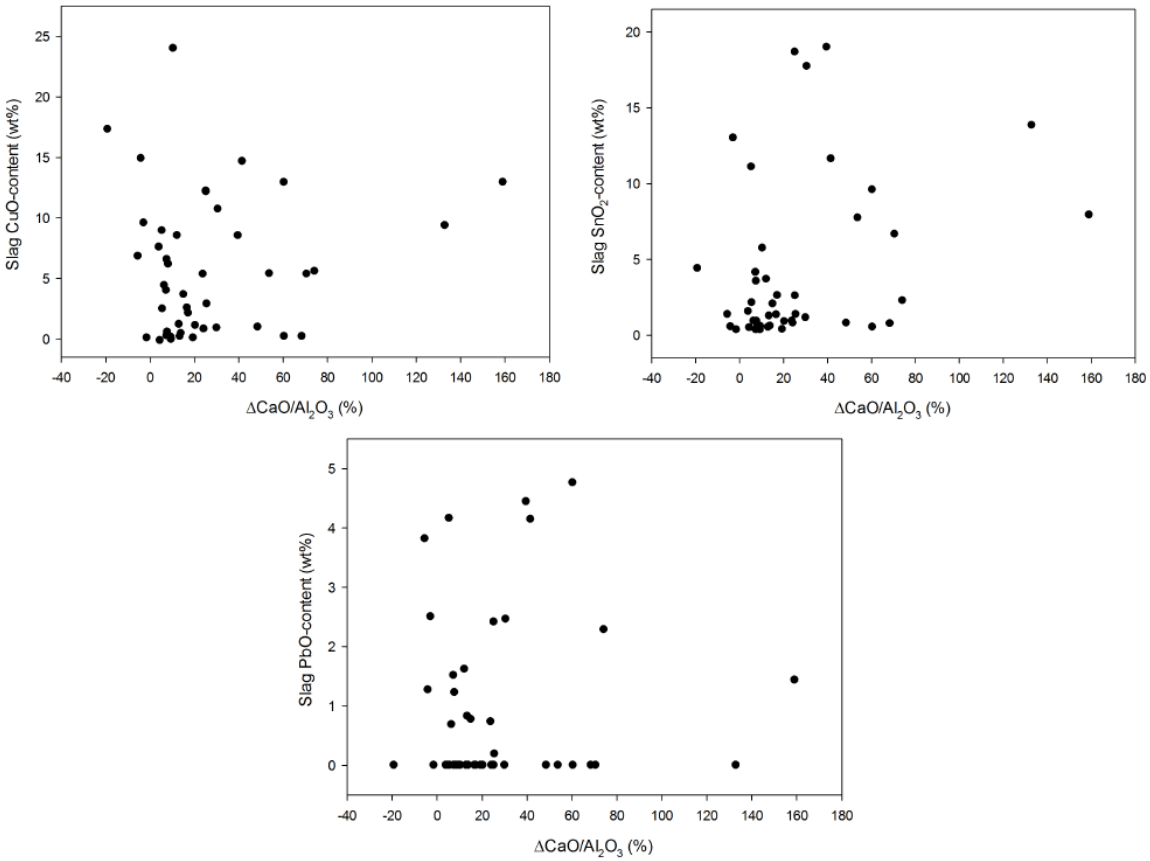

Figure 8.21: Bulk CuO, SnO_2 and PbO content vs Δ^{CaO/Al_2O_3} between ceramic and slag

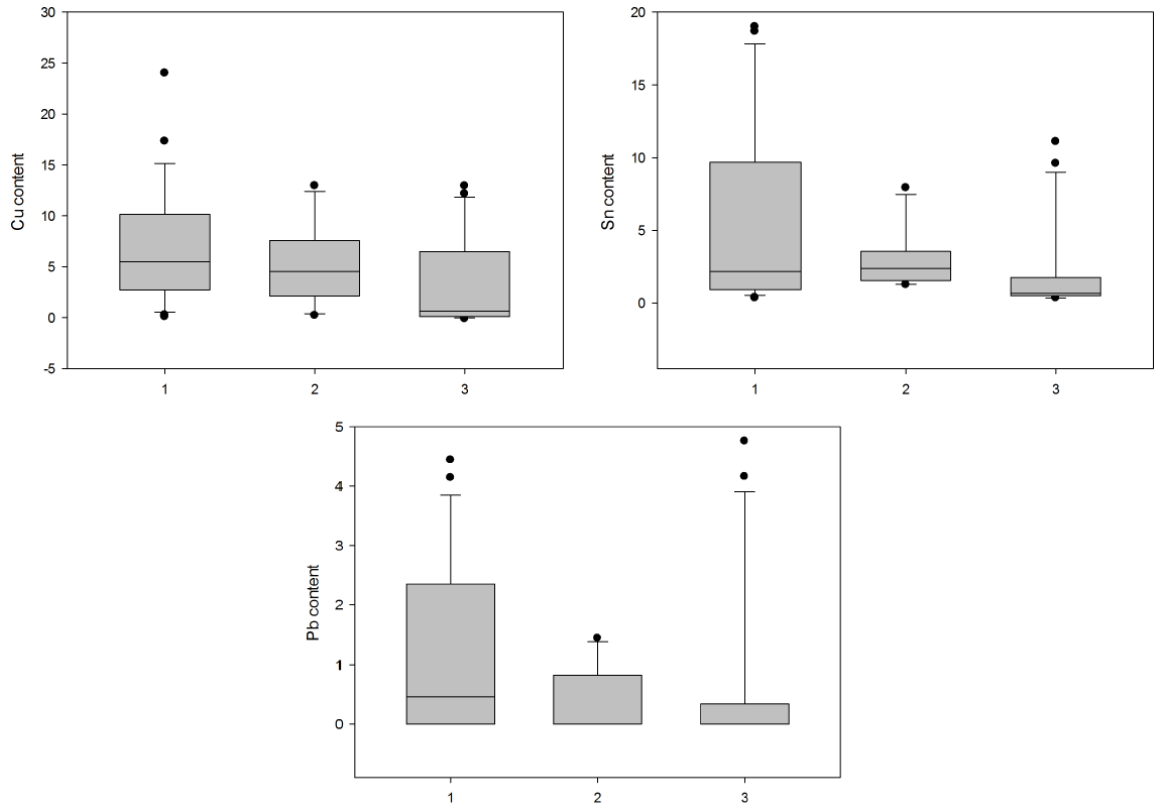

Figure 8.22: Bulk metal content (in wt%) in body (1), body-rim (2) and rim (3) fragments (boxplot[5])

[5]Sigmaplot Version 12: *Boxplots graph data as a box representing statistical values. The boundary of the box closest to zero indicates the 25th percentile, a line within the box marks the median, and the boundary of the box farthest from zero indicates the 75th percentile. Whiskers (error bars) above and below the box indicate the 90th and 10th percentiles.* Individual points are outliers.

8.2.3 Oxide phases in crucible slag

A full list of oxides occurring in the crucible slag has been established, including details such as composition, shape, frequency of occurrence etc. Their varying occurrence is interpreted in section 8.3. The predominant types of oxides are Fe-bearing, Ca-bearing, Cu-bearing, Sn-bearing and Pb-bearing phases, with Ag-rich phases occurring in only two crucibles. Similar to the Pi-Ramesse case study, this overview is given in Appendix K, while diagnostic phases are discussed in more detail throughout the interpretation and discussion below.

8.2.4 Metallic prills

Metallic prills (typically spherical, indicating liquidity during the crucible process) have been recorded in 74% of the crucibles. The majority of these prills are copper-based (ranging from pure copper to (leaded) bronze, incorporating variable amounts of Fe), though some exceptions occur. A complete overview of all measured metallic prills is given in Appendix L, with a summary presented here.

1. *Copper and (leaded) bronze*:

   (a) Pure copper prills occur in a few crucibles, typically surrounded by various oxides (see Figure 8.23).

   (b) (Leaded) tin bronze. Tin content in (leaded) bronze prills varies from 0 to 51.6 wt%, with good representation of low- to intermediate-tin (±0-12 wt% Sn), intermediate- to high-tin (±12-20 wt% Sn) and high-tin (over ±20-25 wt% Sn) bronze. Lead content is generally quite low, varying from 0 to 3.5 wt% (often ±1.5 wt%) without any correlation to tin content. An exception occurs in Gordion-26891: a prill with 31 wt% Pb. Some examples of low- to intermediate-tin (leaded) bronzes are shown in Figure 8.24 and Figures K.3e, K.8d, K.18a, K.20c and K.20d.

   (c) High-tin (leaded) bronze prills have been measured more frequently for Gordion than for Pi-Ramesse crucibles. Prills with >25 wt% Sn occur in 26% of crucibles, with half of them having tin contents >40 wt%. The highest prill tin content (51.5 wt%) occurs in Gordion-23797, with 2.7 wt% Co (no cobalt is measured in any of the other crucibles). It is important to point out here that high-tin prills occur both in reducing and oxidising (accompanied by Cu/Sn/Fe/Pb oxides) crucible slag and dross environments. Some examples are shown in Figures 8.25 and K.3f.

   The various Cn-Sn oxides and silicates mentioned in Appendix K.3 offer highly distorted reflections of these bronze prills.

   (d) Iron content in the (leaded) bronze prills typically varies from zero to 10 wt%. An exception occurs in Gordion-22626, where some small prills contain 37.4 wt% Fe and an elevated zinc content (no zinc is noted in other crucibles).

   (e) Non-metallic prills: copper chloride (CuCl or cuprous chloride) prills occur in some crucibles (Figure 8.26), often in the corrosion/dross layer. In Gordion-23329, a Cu_2S and Pb-Cu-Cl oxide inclusion where noted. Similar Pb-Cu-Cl oxide inclusions are noted in Gordion-26891.

2. *Iron*: A tiny prill of almost pure iron occurs in Gordion-27638, with 90.5 wt% Fe, 7.5 wt% Cu and 2 wt% As.

3. *Silver*: Found in one crucible: Gordion-22529. Almost pure silver prills have been measured (slightly corroded: 4-7.5 wt% Cl), and some copper prills contain 6-10 wt% Ag. In the same crucible, 1.4 at% Ag is noted in Cu-Pb-Cl oxides (oxidised/corroded prills). The crucible slag for Gordion-22529 has a 0.35 wt% bulk increase in Ag_2O, omitted in Appendix J. In Gordion-23329, 3.38 at% Ag occurs in a corroded prill as well, but was not measured in metallic prills. Examples are shown in Figure 8.27.

Nickel is noted in low (< 1 wt%) quantities in (high-tin) bronze prills in two crucibles (Gordion-25568 and -27734 (1)), where 0.5-1.2 at% Ni is present in some of the Cu-Sn oxides and silicates too.
Antimony (0.5-3.5 wt%) occurs in bronze prills in two crucibles (Gordion-22529 and -26891), both associated with elevated PbO content in the bulk crucible slag and in some cases significant lead content in the prills as well.

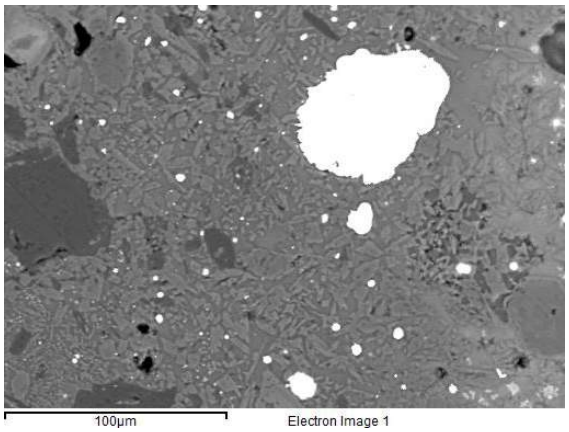

(a) Pure (with < 1 wt% Fe) copper (bright), Gordion-28932 (2)

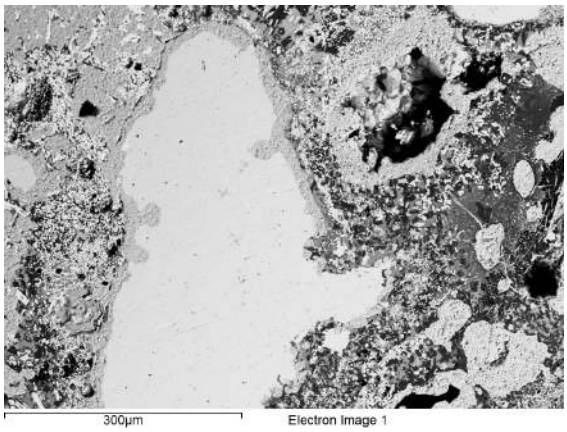

(b) Pure copper (light grey) with various surrounding oxides, Gordion-23128

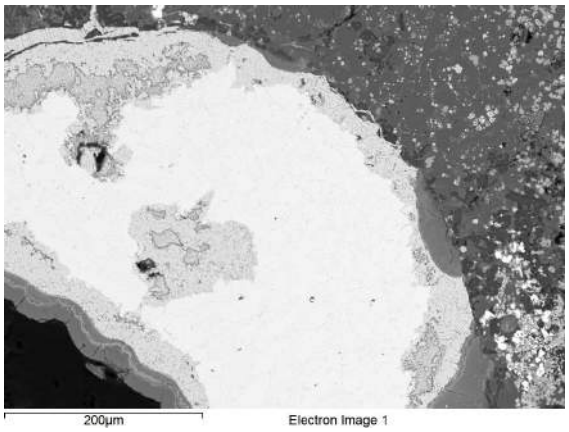

(c) Pure copper (bright) with Cu-Cl oxide corrosion (light grey), Gordion-28236

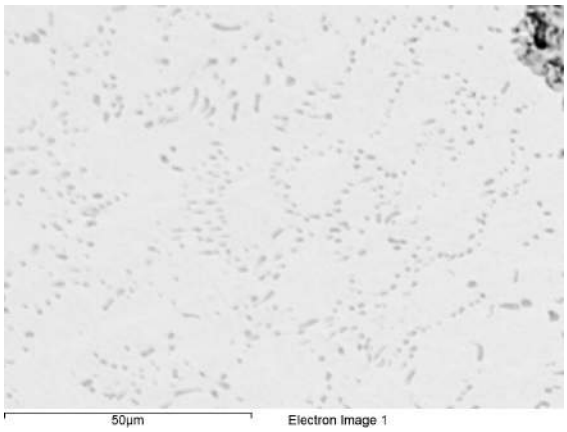

(d) Close-up showing minor copper oxide (light grey) in between pure copper (bright), Gordion-28236

Figure 8.23: Pure copper prills

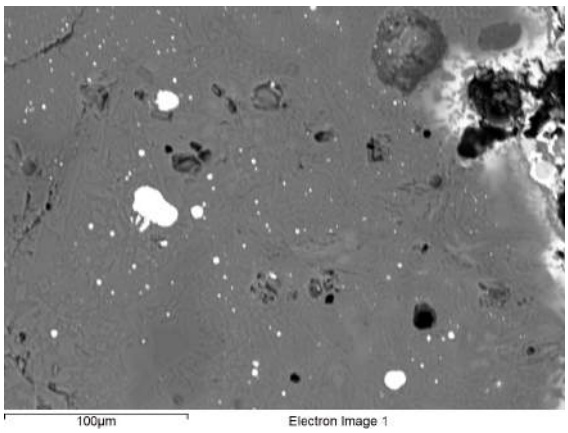

(a) Low-tin, iron-rich (2.9-3.5 wt% Sn, 1.1-1.4 wt% Fe, 1.1-1.6 wt% As) bronze prills, Gordion-28932 (1)

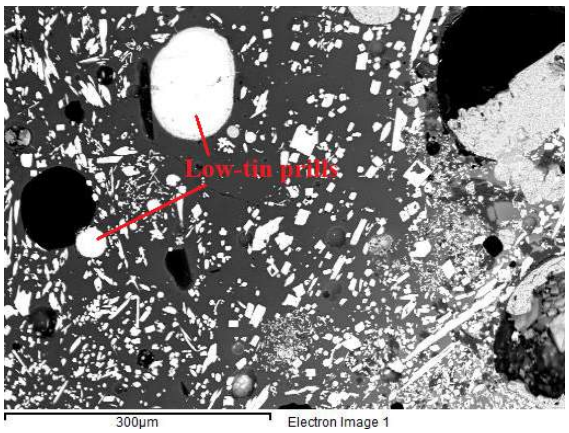

(b) Low-tin leaded bronze prills, abundant tin oxide, Gordion-27640

Figure 8.24: Low-tin bronze prills (bright)

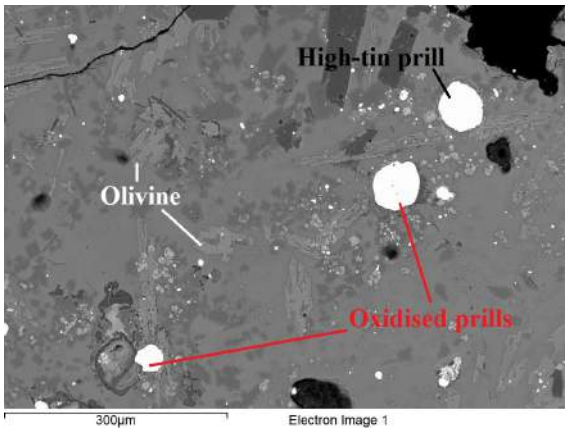

(a) High-tin (leaded) bronze prill (limited Fe) with oxidised prills and olivine, Gordion-22958

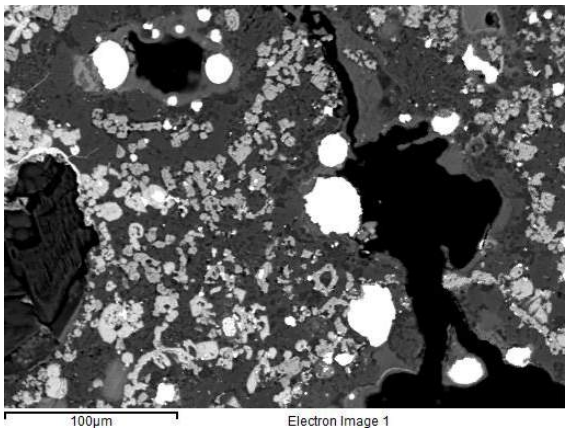

(b) High-tin bronze prills (limited Fe) with spinel and malayaite (both light grey), Gordion-27734 (1)

Figure 8.25: High-tin (leaded) bronze prills (bright)

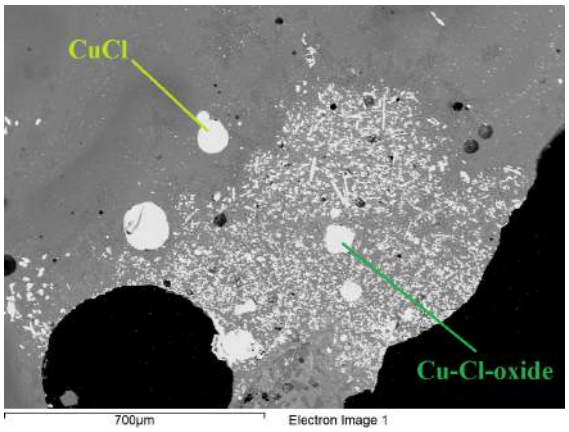

(a) CuCl and Cu_2ClO_2-Cu_2ClO_3, Gordion-27609-S

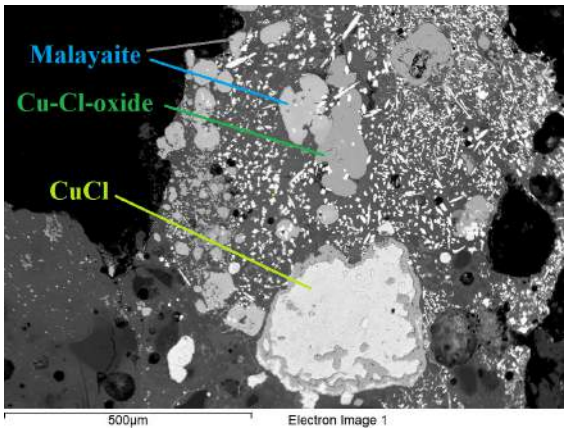

(b) CuCl with Cu_2ClO_2-Cu_2ClO_3 and malayaite, Gordion-23707

Figure 8.26: CuCl prills

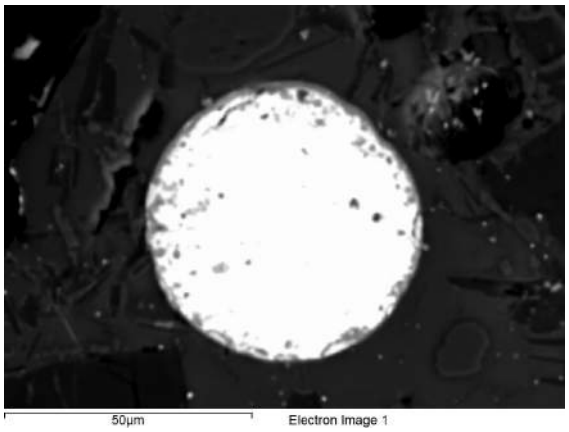

(a) Silver prill (with Cl), Gordion-22529

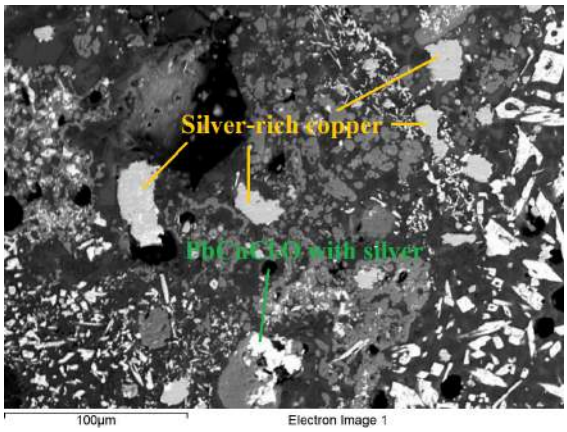

(b) Silver-rich copper and Cu-Pb-Cl oxides, Gordion-22529

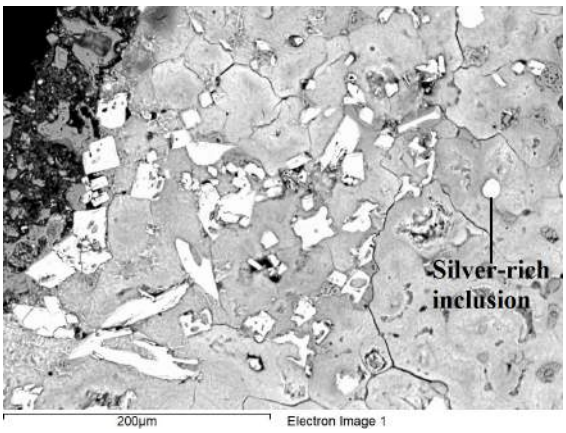

(c) Silver-rich corrosion (of leaded tin-bronze), Gordion-23329

Figure 8.27: Silver(-rich) prills

8.2.5 Charcoal and fuel ash

Contrary to Pi-Ramesse, the Gordion excavations have not yielded any evidence for tuyères or furnace installations in which the crucibles were used. Their heating profile, however, indicates that they were heated from the inside, presumably under a charcoal cover. Evidence in the form of charcoal inclusions in the crucible slag is much scarcer here than for Pi-Ramesse, though an example occurs in Gordion-23797 (Figure K.11), associated with increased lime and magnesia content.

Further evidence can be obtained from the comparison of crucible ceramic and slag, with specific attention to lime, alkali and P_2O_5 content, shown in Figure 8.12. As explained in section 5.2.5, increases in these elements are indicative of a fuel ash contribution to the crucible slag formation. For the Gordion crucible slag, there is a good correlation between increases in lime and magnesia, phosphorus oxide, potash and silica, but not between lime and soda.

The average relative increase in potash ($\pm 40\%$ $\frac{K_2O}{Al_2O_3}$) is similar to that in lime ($\pm 30\%$ $\frac{CaO}{Al_2O_3}$), whereas in the Pi-Ramesse crucibles, the average relative increase in lime is over seven times greater than that in potash ($\pm 330\%$ and $\pm 40\%$ respectively). Furthermore, the ceramic silica content is significantly lower in the Gordion crucibles, which could explain the more pronounced silica fuel ash contribution (though still low compared to magnesia, phosphorus oxide and potash enrichment). While these differences are noteworthy, their cause cannot easily be deduced: charcoal and fuel composition can be highly variable, even within the same species of tree used, depending on which part of the tree (trunk, branch or twigs) is used and what time of year of the wood is cut. Additionally, blowing conditions during firing can influence the varying enrichments of different fuel ash components. This difference can therefore not be easily explained, but makes little difference in terms of the technological interpretation presented here.

From Table K.1, it appears that lime and particularly magnesia are mostly concentrated in the glassy slag matrix, though the content strongly varies. The variation on the potash and phosphorus oxide measurement is too great to confidently suggest the same for these two components, though they are most likely equally concentrated in the glassy matrix.

These findings suggest an important fuel ash contribution to slag formation in the Gordion crucibles, supporting an interpretation that open crucibles were heated under a charcoal cover, very similar to the situation attested in Pi-Ramesse.

8.2.6 Aberrant crucible fragments

Three samples have a ceramic fabric different from the other crucibles, as shown in Figure 8.28. Their bulk composition is different from that of the rest of the assemblage, as shown in Table 8.2.

Two samples were taken from the group of small fragments (Gordion-23707, possibly representing one crucible). These are comprised of a thin (<5 mm) ceramic layer and a glassy slag layer with green corrosion products (<10 mm). The ceramic has a light grey colour with small (<1 mm) red and white inclusions.
One sample was taken from Gordion-28236, which has a grey (centre) to red (exterior) colour (pointing to oxidising conditions outside of the crucible, and more reducing conditions at its interior) and limited inclusions. This fragment shows cracks along its exterior surface, extending deep into the profile. Its fabric feels more brittle than the other crucibles (as does the Gordion-23707 fabric).
These crucible fragments therefore immediately stand out due to their softer fabric and the lack of large rock inclusions.

Microscopic and chemical analysis further verifies their aberrant nature. Gordion-23707 is rich in medium-large (sub-)angular quartz fragments (Figure 8.29a), reflected in an increased bulk silica content, as well as a lowered magnesium, aluminium, titanium and iron oxide content. Additionally, higher potash and lime can be noted.
Gordion-28236 has no large inclusions (though many small-medium sub-rounded to sub-angular quartz fragments) and is more porous than other crucibles, as indicated in Figure 8.29b. This crucible has 'normal' silica content, but is characterised by highly elevated lime content (almost 20 wt%) and somewhat elevated potash content. Conversely, it has lower magnesium, aluminium, titanium and iron oxide content.
In summary, both Gordion-23707 and Gordion-28236 show elevated soda, silica, potash and lime, and lower iron oxide (relative to alumina), compared to other crucibles.

Referring back to the available clay sources for ceramic production (see section 8.1.3), Gordion-28236 was probably made using the more calcareous, marl-derived clay. Gordion-23707 might have been made using the same clay, with the addition of quartz temper. Comparison to fabric descriptions of contemporary domestic ceramics would be interesting to further understand the ceramic recipe used in preparing these aberrant crucibles.

As far as their metallurgical use is concerned, these crucibles do not show aberrant behaviour. The changes in bulk content between ceramic and slag do not vary significantly from the 'normal range' seen in other crucibles (see section 8.2.2), and 'normal' metallic

(a) Small fragments, Gordion-23707 (b) Large fragment, Gordion-28236

Figure 8.28: Aberrant crucible fragments

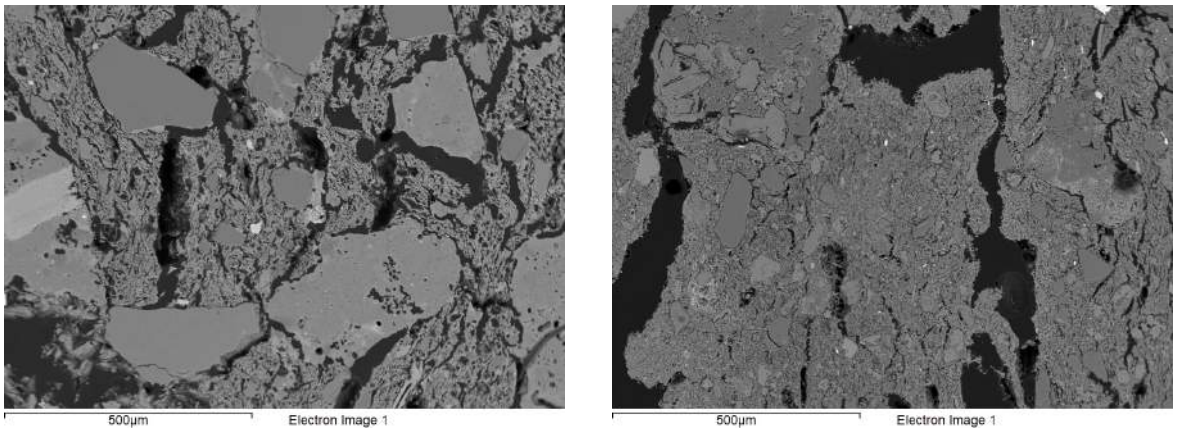

(a) Ceramic fabric, Gordion-23707 (b) Ceramic fabric, Gordion-28236

Figure 8.29: Ceramic fabric Gordion-23707 and -28236

prills are encountered in the crucible slag (see Appendix L). One notable difference is the exceptionally high CuO content in the two Gordion-23707 samples (17.3 and 24 wt%).

8.2.7 Dross

A dross layer (comprising various oxides) sometimes forms and floats on top of the crucible charge during the metallurgical process which, during casting, can be deposited on top of the interior crucible slag. Such a layer therefore does not necessarily cover the entire crucible interior surface, but a rather small area (typically towards the crucible bottom), and could be missed during sampling. Dross layer formation is comparable to that of the 'second slag layer' in Pi-Ramesse crucible 94_560, shown in Figure 5.59, though no primary slag inclusions are requisite: the dross layer is made up mainly of oxidised metal.

	Na_2O	MgO	Al_2O_3	SiO_2	P_2O_5	K_2O	CaO	TiO_2	MnO	FeO
Gordion 23707	2.7	3.0	13	60	0.3	3.6	11.8	0.6	0.1	4.0
Gordion 28236	3.6	2.8	13	49	0.3	3.8	19.8	1.0	0	5.7
Other crucibles	3.0	3.8	18	51	0.5	1.9	10.4	1.6	0.1	9.2

Table 8.2: Average ceramic bulk composition for three aberrant samples (Gordion-23707 and Gordion-28236) and rest of the assemblage (in wt%, normalised to 100%)

	Na_2O	MgO	Al_2O_3	SiO_2	P_2O_5	K_2O	CaO	TiO_2	MnO	FeO	CuO	As_2O_3	SnO_2	PbO
Ceramic	3.0	3.8	18	51	0.5	1.9	10.4	1.6	0.1	9.2	0.1	0.2	0.4	0
Slag	2.8	3.6	16	44	0.5	2.2	11.3	1.5	0.1	8.6	4.8	0.2	4.1	0-2.2
Dross	0.5	1.1	5	14	0.3	0.5	3.7	0.3	0	7.3	35.0	0.1	27.7	4.0

Table 8.3: Average bulk composition of ceramic, slag and dross (in wt%, normalised to 100%)

Dross layers have been noted for 30% of the examined crucible fragments, though almost exclusively on body fragments (out of this 30%, 28% are body fragments). Therefore, out of all the body fragment samples, 50-60% exhibit these dross layers[6]. It is therefore likely (though not necessary) that nearly all crucibles formed such a dross layer, which is represented in only half of the examined body samples as a result of its limited extent and random sampling.

A comparison between the average crucible ceramic, slag and dross[7] composition is given in Table 8.3.

Clearly, this dross is distinct from the crucible slag: it is dominated by copper, tin and lead oxide. The slag contribution is low, as indicated by the limited alumina and silica content. Calculating the ratios of oxides to alumina (omitted here), shows that Na_2O, MgO, SiO_2, P_2O_5, K_2O, CaO and TiO_2 ratios are more or less the same as those in the slag. These oxides therefore represent the crucible slag contribution to dross formation. FeO/Al_2O_3, however, is three times higher for the dross than the slag (1.55 instead of 0.56). This indicates that additional iron is burnt out of the crucible charge into the dross layer, together with copper, tin and lead. In total, the dross is therefore typically made up of $\pm 1/3$ crucible slag and $\pm 2/3$ oxidised metal.

[6] As body fragments make up ±52% of the assemblage (see section 8.3.2), and ±28/52% contain dross, ±54% of the body fragments contain dross, while it has only been noted on ±4% of the rim fragments.)

[7] The dross layer was measured separately for five crucibles; averages here represent five times five measurements.

Section 8.3

Technical interpretation

8.3.1 Interpreting general crucible characteristics

A further interpretation of crucible characteristics (see section 8.1) is given here.

The choice of a mafic rock-derived clay, as discussed in section 8.1.3, has some important consequences for the crucibles' behaviour. While crucible slag is routinely developed in most Pi-Ramesse crucibles, this is not the case in many Gordion crucibles. Typically, the thickness of the slag layer is far more modest, with a more limited bloated zone and less true vitrification. In many crucibles, (large parts of) the interior surfaces are merely burnt, without slag formation occurring (e.g., variable slagging on fragment in Figure 8.1). The variability in slag within a single crucible, assessed by taking multiple samples in a single crucible, is discussed further in section 8.3.8.

Several factors influence the development of crucible slag, one of the most important being the ceramic fabric. More refractory ceramics tend to react less with the crucible charge and remain both chemically and mechanically stable. The chemical composition of the Gordion crucibles is close to that of mafic rocks (basalt-trachyandesite), which have relatively high melting temperatures (Bowen, 1915) that equal or exceed temperatures typically attained during copper or bronze melting. This means that, compared to Pi-Ramesse crucibles that completely bloat at 1200°C, the Gordion crucibles were operating just below or at their thermal stability, and therefore did not disintegrate as extensively.

This lack of crucible slagging limits the possibility of interaction between the crucible and its charge. While the crucible charge could interact with slag in Pi-Ramesse, resulting in increased fuel ash, iron, copper, tin, and sometimes cobalt content, this exchange is limited in the Gordion crucibles. Rather, a dross layer formed in many (if not all) Gordion crucibles, in which significantly more iron, copper, tin and lead oxides are gathered than can be noted in the actual crucible slag. Therefore, sufficient attention should be given to these dross layers to fully appreciate the metallurgical process.

An unfortunate consequence of such dross formation, however, appears to be its increased sensitivity to corrosion. While crucible slag is a glassy product, effectively protecting trapped metallic phases, dross is dominated by metal (oxides), with only limited glassy phase present, and therefore corrodes more readily. Though metallic content is sometimes noted in this dross layer during microscopic inspection (including high-tin prills), it has mostly been corroded post-depositionally. This results in the prevalent green corrosion products shown

in Figure 8.4. The high metal oxide content greatly hinders the identification of metallic phases in the dross layer during SEM(-EDS) analysis, due to their similar greyscale tone.

Contrary to Pi-Ramesse crucibles, none of the Gordion crucibles is bloated or slagged throughout the full wall profile. Crucible wall thickness in Gordion is similar to or slightly lower than in Pi-Ramesse, which is another indication that (presuming similar temperature gradients) the Gordion crucibles have better refractory performance. This performance can be partly attributed to their bulk chemistry, but is further influenced by the presence of voids induced by (perhaps limited) burnt organic temper and around coarse rock fragments. Furthermore, these coarse fragments add mechanical stability to the crucibles. Though further geological information is required, it appears that these rock fragments are residual to the clay, rather than intentionally added. Comparison to other ceramics could indicate the extent to which this fragment-rich clay was selected specifically (rather than fragment-poor clay) for the purpose of crucible making, or simply was the only clay at hand.
During the metallurgical process, these rock fragments remain fairly stable throughout the bloated zone and in less developed slag layers, as shown in Figure K.7. However, in fully developed slag, the rock fragments are dissolved and plagioclase[8] appears to re-crystallise into finer, more elongated shapes, often resulting in a plagioclase-dominated slag with glassy background.

The charcoal and fuel ash evidence indicates that the crucibles were left open, and heated from above with a tuyère (possibly more than one) blowing into the crucible under a charcoal cover. The exact set-up at Gordion is unknown, however. The number of tuyères, the angle at which they blew air into the crucibles, the type of bellows and the shape of the furnace cannot be reconstructed. Most likely, a bowl-type furnace (see Timberlake, 1994) or simple depression in the ground was used, where the crucibles may have sat on a bed of sand or perhaps (non-burning) charcoal if the bowl was clay-lined. Alternatively, more permanent structures may have been present in the so-called 'foundry'. The crucible evidence itself does not offer any further evidence, apart from the fact that the heat was concentrated at the crucibles' interior, while their exterior surface was exposed to far lower temperatures.

The presence of copper and tin (oxides) in nearly all crucibles is indicative of their use for the processing of bronze (and perhaps pure copper in some). The relatively frequent occurrence of lead further points to the processing of leaded bronze, at least in some of the

[8] Klein and Dutrow (2007), Fig. 11.6, p. 253, indicates a melting temperature of (labradorite) plagioclase of ±1300°C.

crucibles. Whether these crucibles were used for remelting or alloying, is further discussed in the following sections.

8.3.2 Rim vs. body fragments, crucible distributions and sample selection

Again, a distinction can be made between rim and body fragments (defined in section 5.4.3). The entire Late Phrygian assemblage is composed of 36 (60%) rim and 24 (40%) body fragments: a total of 60 crucible fragments. Compared to Pi-Ramesse, rim fragments are more strongly represented in the Gordion assemblage. However, many of the rim fragments here contain large portions of the crucible profile.

46 samples have been analysed from the Gordion crucibles, out of which 16 (±35%) are rim fragments, 24 (±52%) are body fragments and 6 (±13%) are body fragments from near rims. As many of the 'rim fragments' contain large portions of the full crucible profile, it was possible to take body-near-rim as well as body samples from 'rim fragments'. For a few crucibles, rim and body samples were taken from the same fragment.
Based on the experience with the Pi-Ramesse crucibles, a stronger representation of body fragments has been selected, while further assessing variability within single crucibles, as discussed in section 8.3.8.

An attempt has been made to achieve a sample distribution that is representative of the actual distribution of crucible fragments for the various contexts. An overview of the selected samples for each context is given in Table 8.4. Individual samples and their respective contexts are presented in Appendix I.

8.3.3 Alloying evidence

As explained in section 5.4.4, high-tin prills (over ±20-25 wt% Sn) give direct evidence for the active alloying of copper (or recycled bronze) with fresh tin (or cassiterite). This reasoning is based on the premise that no circulating bronzes at that time had such high tin contents, and these high-tin prills can therefore not represent recycling. An overview of contemporary, regional bronzes and newly analysed bronze spills from Gordion (section 8.4) indicates that typical bronzes did not have tin contents exceeding ±15 wt%, making this a reasonable assumption. The best explanation for high-tin prills, then, is that they result from the addition of a high-tin, and most likely pure tin, additive to the crucible.
As outlined in section 8.2.4, bronze prills with >25 wt% Sn are found in about a quarter

# fragments	Rim	Body	# samples	Rim	Body	Body-rim	Phase	Operation	Locus	Lot	Context type
5	4	1	3	1	2		0	2	12	17	Balk trimming
2	2		1	1			0	2	33	141	Mixed in excavation
1	1		1	1			0	2	51	149	Pit
3	2	1	1	1			0	2	66	157	Trash
1	1		3	1	1	1	400	2	19	57	Mixed in excavation
5	4	1	2		2		400	2	6	123	Mixed in excavation
2	1	1	1		1		400	7	32	123	?
3	1	2	1		1		400	2	19	154	Mixed in excavation
3	2	1	2			2	410	2	11	16	Trash on surface
1		1	1		1		410.04	1	65	130	Pit
1	1		1			1	420	1	75	149	Ash lense
6	4	2	4	1	3		420	1	82	162	Exterior surface
4	2	2	2		2		420	2	73	177	Lensed trash
2	1	1	2	2			420.01	1	51	129	Pit
1		1	1		1		430	1	18	61	Pits mixed in excavation
2	1	1	2	1	1		430.07	1	18	63	Pit
1	1		1	1			430.08	1	19	64	Pit
3	2	1	2	1	1		435	2	6	118	Exterior surfaces
2	1	1	1			1	440.01	1	34	111	Floor deposit
3		3	1		1		440.03	1	32	96	Pit
1	1		1		1		460	1	98	228	Robber trench
2	1	1	2	1	1		460	1	98	237	Robber trench
1	1		2	1	1		470	1	25	76	Exterior surface
1	1		2	1		1	470.02	1	26	80	Pit
2		2	3		3		620	1	100	213	Pit
2	1	1	3	2	1			1	82	188	?
60	**36**	**24**	**46**	**16**	**24**	**6**					

Table 8.4: Distribution of fragments and samples for different contexts

of all crucibles, while one eighth of all crucibles have prills with tin content exceeding 40 wt%. Therefore, there is abundant evidence to suggest that active tin alloying was taking place at Gordion.
Interestingly, the detection frequency of high-tin prills is much higher than in Pi-Ramesse. This could be incidental, but might point to the higher importance of active alloying at Gordion and lower prevalence of recycling. As discussed earlier, however, this kind of argument *in absentia* is difficult to substantiate.

Contrary to the Pi-Ramesse crucibles, lead occurs in metallic prills in ten of the Gordion crucibles (and more often in surrounding corrosion products). Therefore, the possibility of active lead alloying should be considered. Following an argument similar to that for tin alloying, it could be expected that prills with lead levels greatly exceeding those of common leaded bronzes are indicative of an active alloying process. High-lead prills (>30 wt% Pb), containing antimony (and arsenic), have only been encountered in one crucible (Gordion-26891), which contained several copper-lead oxides and chlorides. Interestingly, these prills show only low tin contents.
It should be kept in mind that lead content is somewhat underestimated by SEM-EDS analysis, especially for metal prills (see section 3.3.5). Nevertheless, the limited occurrence of high or even slightly elevated lead contents in bronze prills, as well as the more limited bulk slag content (bulk $^{PbO}/_{SnO_2} \approx 0-0.5$), seems to indicate that lead was probably

not added separately to the crucible charge and came in with another charge constituent.

The high-lead prills in Gordion-26891 are surrounded by tin oxide and characterised by low tin content, as shown in Figure 8.30. The shape of the tin oxide suggests that it has been burnt out from the bronze. Indeed, tin is expected to oxidise more readily than lead (Ellingham, 1944), which mostly remains in the metal prill until all tin is burnt off. The oxidising context in this particular (tiny!) area of the crucible does not point to active alloying. However, given the heterogeneity seen within single crucibles (see section 8.3.8), it is very well possible that this crucible was used for alloying. Several scenarios are plausible:

- Lead was added to bronze, forming an intermediate high-lead bronze prill, which subsequently partially oxidised in the area shown in Figure 8.30.
- Tin was added to leaded copper, forming a (high-)lead bronze prill which then partially oxidised.
- Tin and lead were added to copper, forming a (high-)lead bronze prill which then partially oxidised.
- Leaded bronze was remelted in this crucible, with oxidising conditions leading to some loss of tin.

Whatever the true scenario may be, either a pure source of lead or lead enriched copper or bronze was added to the crucible. Given the evidence from other crucibles, it seems most likely that a leaded copper was added to this particular crucible. However, the lead content witnessed in this prill is not necessarily representative of the lead content of this added leaded copper.
Finally, it should be noted that this is the only crucible where significant Sb has been noted repeatedly in metal prills (with the exception of the crucible associated with silver, see section 8.3.7). This antimony presence could be related to the lead source.

Taking into account both the evidence from crucible analysis and metal analysis (section 8.4), it can be reasonably assumed that pure tin bronze as well as leaded tin bronze was produced in Gordion. Most likely, lead was not introduced separately into the crucible, but as leaded copper. At levels of ±1-5 wt%, this would have produced a noticeable effect on the bronze's properties, arguing for an intentional selection of lead-rich copper. At low levels (below ±1 wt%), the presence of lead is probably unintentional.

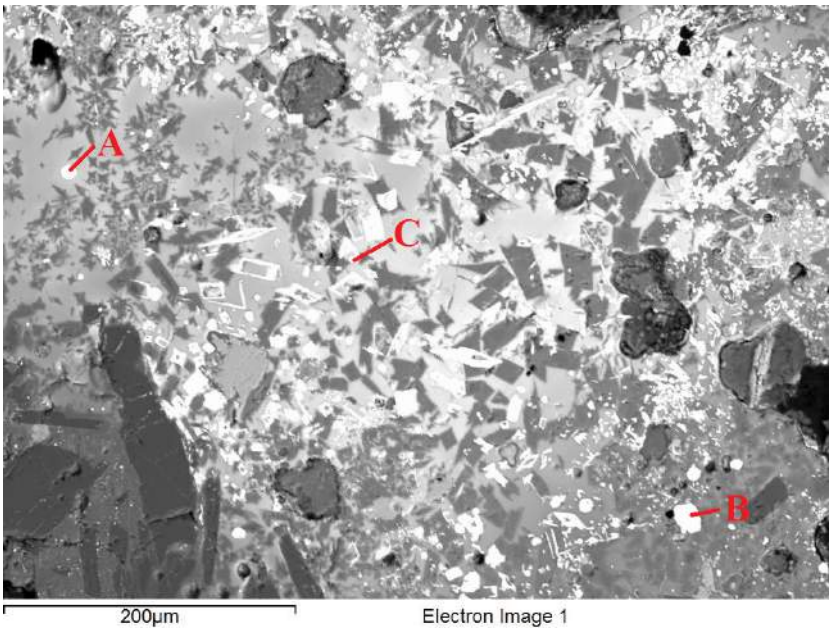

Figure 8.30: Slag with pyroxene (medium-dark grey, angular), plagioclase (dark grey, on bottom left and right), tin oxide (white, angular), and prills (copper with *A*: 0.6 wt% Fe and 2.8 wt% Sb, *B*: 1.5 wt% As, 1.5 wt% Sn, 3.4 wt% Sb and 31 wt% Pb, *C*: 0.7 wt% Sb), Gordion-26891

8.3.4 Sources of tin

There is ample evidence, present in the crucible slag in the form of high-tin prills, to indicate the practice of active alloying at Gordion. These prills do not provide any conclusive evidence as to the used source of tin, which could either be tin metal or ore (cassiterite), to be used in a metal mixing or cementation process respectively (excluding the possibility of co-smelting).
Though tin could have been introduced into crucibles as a component of recycled bronze (scrap), this explanation only suffices for crucibles where no high-tin prills are encountered. When high-tin prills are present, a fresh source of tin is implied (see section 5.4.4).

As in the Pi-Ramesse crucibles, high-temperature SnO_2 crystals are very common in both the crucible slag and dross in Gordion, which do not provide any information on the nature of the alloying process, but could indeed even form during simple recycling and (re-)melting operations (Rademakers and Rehren, 2013).
Therefore, the only possible evidence that can be used to distinguish between alloying pure metals and the cementation process can be found in remnant cassiterite grains, embedded in the crucible slag.

As discussed in Appendix K.4, the evidence for cassiterite use is far from compelling in the

Gordion crucibles. The only (somewhat) convincing examples occur in Gordion-25394, shown in Figure K.19a. Here, the few possible cassiterite clusters are located in the deeper crucible slag, while the overlying dross layer is dominated by newly formed tin oxide crystals. All other clusters witnessed in the crucible slag are either too tiny to confidently build a case for cementation, or are clusters of high-temperature SnO_2 crystals. Though it is possible that clusters of such crystals (e.g., Figures K.18f and K.19d) represent re-crystallised mineral cassiterite grains, their common association with iron and more importantly copper oxides is indicative of a different process. Such clusters are more likely to be the result of complete oxidation/burning of a bronze prill at that particular location, whereby all tin is converted into SnO_2 crystals, iron is burnt into spinel (often incorporating some tin) and finally copper is turned into cuprite. This is discussed in some more detail in Chapter 13.

In conclusion, then, it appears that there is very little direct evidence for the use of cassiterite in a cementation process. However, the absence of residual mineral grains, which are intermediate products, cannot convincingly argue against cassiterite cementation here. Furthermore, the use of more refractory crucibles which form a less developed slag, could work against the trapping of such grains. The consequential development of a dross layer (see section 8.2.7), which floats at the top of the crucible charge, might be a further reason prohibiting the preservation of mineral grains: the dross layers are dominated by high-temperature oxide products, due to their exposure to more oxidising conditions (CuO and SnO_2 make up $^2/_3$ of the bulk content). Such an environment is in stark contrast to the 'desired' setting for preservation of residual mineral grains (reducing areas, cut off from further participation in the alloying process).
Presented with this evidence, the nature of the tin source added in the alloying process must remain unknown: either tin metal or ore could have been added to the crucibles.

8.3.5 Iron enriched crucible slag

As discussed in section 8.2.2, 83% of the examined samples show only minor iron enrichment (+1.6% $\Delta^{FeO}/_{Al_2O_3}$), which does not represent any significant change. The crucible slag in 17% of the samples (most of which are body fragments), however, is further enriched in iron (+30-80% $\Delta^{FeO}/_{Al_2O_3}$). This includes the two 'pure slag' samples (Gordion-23045-S and -27609-S), taken from (exceptionally) thick crucible slag (see section 8.3.8). Though this enrichment is only minor in absolute terms (especially compared to that seen in Pi-Ramesse crucible slag), it differs significantly from the normal population and therefore merits some further attention.

Spinel is found in 33% of all samples, which include seven out of eight significantly enriched samples (and the most highly enriched samples from the 'normal population'). Though a real correlation cannot be determined, bulk iron enrichment appears to coincide with the appearance of iron-rich oxide phases. These are typically associated with iron-rich (±0.5-4 wt% Fe) copper/bronze prills, as shown in Figure K.3, implying copper as the source from which iron is introduced into the crucible slag. This is fully in line with observations made for the Pi-Ramesse crucibles, despite the difference in absolute enrichments.

The different nature of the Gordion crucibles is probably again important in explaining this result. The limited slagging of these crucibles provides little opportunity for iron to be exchanged between the charge and the crucible. The dross layer, however, which forms on top of the charge, is three times more enriched in iron (section 8.2.7). Therefore, any iron burnt out of the crucible charge is expected to be reflected in the crucible slag to a lesser extent. Nonetheless, even when considering the iron enriched dross layer, the iron content of the copper used at Gordion was probably not as significant as that used in a third of the Pi-Ramesse crucibles.

The possibility of some iron being introduced with the tin source (with cassiterite or as 'hard head' with tin, see section 5.4.6) can not be entirely excluded.

Though it is probably reasonable to assume similar redox-conditions for the Gordion and Pi-Ramesse crucibles when comparing the two, this assumption does not necessarily hold. The conditions in Gordion might have been more reducing, preventing excessive oxidation of iron. However, the similarity in CuO and SnO_2 enrichment (around 4-5 wt%) seen in both assemblages as well as the general resemblance between the crucibles suggests that their operation was quite comparable.

8.3.6 Lead enriched crucible slag

In ±2/3 of examined crucible fragments, no lead enrichment is measured in the crucible slag. In the other third, bulk PbO enrichments up to 5 wt% are noted (mainly body fragments). Leaded bronze prills have been noted in 26% of the samples, of which all but two show bulk PbO enrichments. Therefore, leaded bronze prills are not noted in all samples exhibiting bulk PbO enrichment, and vice-versa, but this most likely represents a sampling artefact, introduced by crucible heterogeneity. For bulk enriched samples, PbO is usually a component of the glassy slag phase. Some lead oxides, chloride-oxides and silicates, often incorporating copper are encountered too. The general impression from the various lead

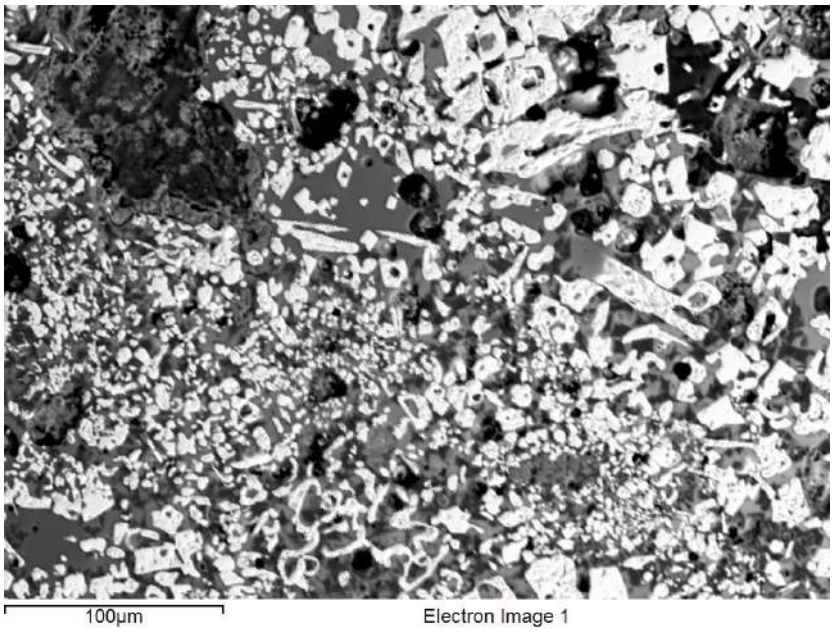

Figure 8.31: Lead-rich glassy phase in area with burnt SnO_2

occurrences in the crucible slag is either its association to copper in a particular oxide, or its dissolution into the glassy slag phase otherwise. Very few pure lead oxides or high-lead phases exist.

Including the observations made in section 8.3.3, the lead appears to be introduced into the crucible slag with the copper. Though lead is usually found dispersed in the copper as metallic droplets, lead sulphate is sometimes encountered (Figure K.22) in association with copper. In dross layers, lead often participates in the formation of various corrosion products.

Contrary to tin, which forms stable SnO_2 crystals upon oxidation from bronze, lead does not seem to produce any characteristic crystals and discreetly disappears into the glassy phase, hindering its identification as a bronze oxidation product. This is illustrated in Figures 8.30 and 8.31, where SnO_2 crystals occur in an area with localised lead-rich glass phase (±19 wt% PbO), indicating a similar source for lead enrichment.

Though the slag analysis by itself does not rule out the possibility that pure lead was added to the crucible, which then subsequently reacted with the crucible slag to form a leaded glass phase, the consideration of all evidence points in the direction of lead being a component of the copper introduced into the crucibles.

As noted in Appendix A, SEM-EDS analysis probably underestimates the actual lead content in the crucible slag. Additionally, the more refractory character of the Gordion crucibles could impede the inclusion of lead into the crucible slag (though the similar copper

and tin enrichments argue against this, as mentioned in section 8.3.5). The general impression that lead was a component in approximately half of the population (half of the body fragments), matches the observations made for Gordion metals (section 8.4): leaded bronze was one out of several alloys produced in Gordion.

8.3.7 Silver

Silver prills have been encountered in one crucible (Gordion-22529), and minor silver has been found in one corroded prill from another crucible (Gordion-23329).

In Gordion-22529, both pure silver prills and silver-copper prills occur. The pure prills are found in the more glassy crucible slag, while the mixed prills occur in the drossy layer, sometimes associated with lead as well. The limited amounts of chloride associated with the silver prills are most likely due to post-depositional corrosion. The bulk Ag_2O content in the slag and dross is ±0.3 and ±0.5-0.8 wt%, respectively. The bulk PbO content in the crucible slag and dross is very high (±5 wt%). Antimony is noted in some of the copper prills in this crucible as well.
This crucible is difficult to interpret, as several scenarios might have produced this outcome:

- It could have first been used for silver melting, which produced the more or less pure silver prills in the crucible slag, without formation of a dross layer. This would have required lower temperatures than those used for melting/alloying bronze. Despite the high lead content, it is unlikely that the crucible was used for a cupellation process[9], as the lead oxide content (litharge) is too low, the crucible itself does not have good cupel characteristics and it does not have an abnormal appearance compared to the rest of the assemblage. Following silver melting, the crucible could then have been used for bronze melting/alloying, whereby some of the silver was taken up by the copper/bronze prills.

- Similarly, the crucible could have been used for bronze melting/alloying first and silver melting later. This appears unlikely, as copper/bronze residue would obviously contaminate the silver, and the silver is embedded deeper in the crucible slag than the copper/bronze.

[9] In cupellation processes, a precious metal (e.g., silver) is molten with excess lead, which under oxidising conditions forms lead oxide (litharge). This litharge incorporates the base metals contaminating the precious metal, thereby purifying it (Bayley, 1996; Bayley *et al.*, 2008).

- A silver-rich or -coated copper/bronze might have been remolten in this crucible, resulting in silver-rich copper/bronze prills and pure silver prills (copper oxidises preferentially to silver).

Though the presence of silver appears remarkable, the actual amount of silver is quite low and most likely points in the direction of a copper contaminant. The occurrence of silver in both the crucible slag and dross furthermore indicates that it was part of a single operation involving bronze. Similarly, the high lead content in both the crucible slag and dross is most likely due to the remelting/alloying of leaded bronze, which fits with the interpretation of the assemblage as a whole, rather than any operation particularly related to silver.
A similar interpretation is most appropriate for the low silver content noted in a corroded prill in Gordion-23329.

It is nonetheless interesting to note that silver-bearing copper was used in one or two crucibles. This probably points to a recycling operation, perhaps of a silver-gilded object (similar to the possible remelting of a gold-gilded object in Pi-Ramesse, section 5.4.11) or silver-bearing coinage. It is difficult to ascertain from this evidence whether the silver content would have actually been noticed by the ancient metallurgists in Gordion.

8.3.8 Variation in crucible slag

The crucible assemblage shows variation in terms of slag composition, mineralogy and metal content, which is due to several interacting factors (Rademakers and Rehren, 2014). These are the same as those outlined in section 5.4.9: variability in the crucible charge composition, the cooling speed of the slag, the redox-conditions and temperature. These again vary through time during the process and depend on the location within a crucible, which can result in varying degrees of slagging throughout a single crucible and between different crucibles.

As the analysis of the Pi-Ramesse crucibles indicated that variation within a single crucible was most likely an important underlying cause for variability seen within a crucible assemblage, multiple samples were taken from four of the Gordion crucibles. The sample selection for these crucibles is shown in Figure 8.32. For three fragments, both a rim and lower body sample were taken. These are Gordion-23045 (the largest fragment in the assemblage), Gordion-27609 and Gordion-27613. For the fourth fragment, Gordion-25394, three samples were taken along the crucible profile. A comparison between the slag bulk

	Na_2O	MgO	Al_2O_3	SiO_2	P_2O_5	K_2O	CaO	TiO_2	MnO	FeO	CuO	As_2O_3	SnO_2	PbO
Gordion-23045: Rim	3.1	4.3	17	50	0.4	2.1	11.6	2.0	0.2	8.4	0.1	0.1	0.4	
Gordion-23045: Body	2.6	4.9	16	47	0.3	1.8	14.4	1.7	0.1	8.7	0.9	0.2	1.2	
Gordion-27609: Rim	2.3	4.4	15	47	0.6	4.3	15.6	1.5	0.1	7.8	0.2	0.1	0.5	
Gordion-27609: Thick slag	2.0	4.1	13	40	1.0	2.8	14.0	1.2	0.2	8.9	5.4	0.2	6.7	
Gordion-27613: Rim	3.1	3.8	17	49	0.5	2.2	11.6	2.0	0.1	9.9	0.1	0.3	0.3	
Gordion-27613: Body	4.1	3.3	18	48	0.6	2.5	10.8	1.6	0.1	8.3	0.2	0.2	1.3	0.8
Gordion-25394: Rim	2.6	4.7	16	47	0.4	2.7	12.7	1.8	0.2	9.5	0.8	0.1	0.8	
Gordion-25394: Body (near rim)	2.6	3.9	17	45	0.4	2.7	11.6	1.5	0.2	10.2	2.1	0.3	2.6	
Gordion-25394: Lower body	1.8	3.4	11	31	0.5	1.8	9.4	0.9	0	8.7	8.5	0.2	19	4.4

Table 8.5: Bulk composition of slag (in wt%, normalised to 100%) for four samples in different locations

	$\Delta\frac{Na_2O}{Al_2O_3}$	$\Delta\frac{MgO}{Al_2O_3}$	$\Delta\frac{SiO_2}{Al_2O_3}$	$\Delta\frac{P_2O_5}{Al_2O_3}$	$\Delta\frac{K_2O}{Al_2O_3}$	$\Delta\frac{CaO}{Al_2O_3}$	$\Delta\frac{TiO_2}{Al_2O_3}$	$\Delta\frac{MnO}{Al_2O_3}$	$\Delta\frac{FeO}{Al_2O_3}$
Gordion-23045: Rim	13	12	-1	17	19	-1	29	60	6
Gordion-23045: Body	-12	38	-2	-40	7	30	9	-20	-3
Gordion-27609: Rim	0	40	11	15	170	61	22	177	12
Gordion-27609: Thick slag	-11	45	4	145	80	71	6	77	34
Gordion-27613: Rim	5	9	0	-11	21	10	35	4	18
Gordion-27613: Body	27	-5	-2	27	43	14	5	223	4
Gordion-25394: Rim	17	11	1	-24	34	24	45	92	10
Gordion-25394: Body (near rim)	1	6	-2	-16	43	17	7	57	20
Gordion-25394: Lower body	10	45	7	90	39	40	1	90	74

Table 8.6: Relative changes (%) between ceramic and slag for four samples in different locations

contents for these samples is given in Table 8.5, while the relative change between ceramic and slag is shown in Table 8.6.

Some differences between samples from a single crucible stand out: in all cases, the copper, tin and lead content (when present) is elevated in body fragments compared to rim fragments. Relative iron enrichment (which is very modest here, compared to the Pi-Ramesse crucibles), when significantly present (>30% $\Delta^{FeO}/_{Al_2O_3}$) as in Gordion-27609 and Gordion-25394, is more outspoken in the body fragments. Differences in fuel ash components are more difficult to discern.
The thickest slag development for these four crucibles is seen in Gordion-27609 and Gordion-25394, whereas Gordion-27613 and Gordion-23045 show more equal and limited slagging. The lower areas of Gordion-27609 and Gordion-25394 are thicker due to the combined presence of crucible slag and dross, which is further reflected in the more significant copper, tin and iron enrichments.

Some more information can be gathered from examining the variability in micro-structure and phases for these samples. For Gordion-25394, several differences in the crucible slag can be noted for the rim, intermediate and lower body samples, shown in Figure 8.33. The rim sample exhibits limited slagging, and most of the interior is simply bloated and vitrified ceramic. A few tiny prills occur further away from the rim (towards the lower body),

Figure 8.32: Multi-sampling of crucible fragments (top: Gordion-27609, middle: Gordion-27613, bottom left: Gordion-23045, bottom right: Gordion-25394)

which are iron- and arsenic-rich bronze (see Appendix L), and the total metal content is low. In the second (intermediate) sample, the slag is more developed (though not everywhere) and more metal prills are present. These are mainly pure copper prills with minor iron content, while the slag contains large amounts of tin oxide, malayaite and copper (chloride) oxides. Finally, the third sample represents the thick crucible slag and dross at the bottom of the fragment, where the ceramic was broken off. Here, the deeper slag layer is similar to the intermediate sample (with iron-rich bronze prills), while the surface layer is more dross-like and dominated by various metal oxides. The base metal content in the second sample is higher than that of the rim fragment, but lower than that measured in the bottom fragment (Table 8.5). However, this is reflective of the high metal oxide content in the dross, rather than the elevated presence of metallic prills. In fact, the large amounts of metal oxides greatly impede the detection of metallic prills in dross during SEM-EDS analysis. Fuel ash contributions and iron contamination of the crucible slag are lower for the rim and intermediate sample than for the bottom sample.

This shows that rim samples generally capture fewer charge constituents than lower body samples, while variable redox-conditions modify the type of evidence found in these body fragments (e.g., variable metal content, different oxide phases etc.).
The location at which a crucible fragment is sampled therefore strongly influences the informative nature of analytical results. A notable feature of the Gordion crucibles in this context is the formation of dross. This typically accumulates at the lower end of the crucible (after casting), which further changes the explanatory value of lower body samples. This issue is revisited in Chapter 13.

On the whole, most crucibles are slagged to a similar extent with fairly limited variation in slag thickness between them, and the lime contributions are far more modest than those seen in Pi-Ramesse. As a result, there is no obvious correlation between more enriched (in iron, copper, tin or lead) crucibles and the degree of slagging here. Nevertheless, some vitrification is a prerequisite to the entrapment of prills and other charge components.

A final note on corrosion products should be made here as well. As mentioned in section 8.3.1, the presence of a dross layer appears to be at least partially responsible for the high amounts of corrosion products on the crucible interior surface (see Figure 8.4): the lack of a protective glassy slag phase increases its sensitivity to corrosion. However, post-depositional conditions have played an important role as well and the metal remains are equally corroded (see section 8.4). The abundance of chloride-dominated corrosion products is indicative of a different post-depositional environment to that of Qantir. The burial below the water table in Qantir restricted oxygen supply, thereby protecting the bronzes

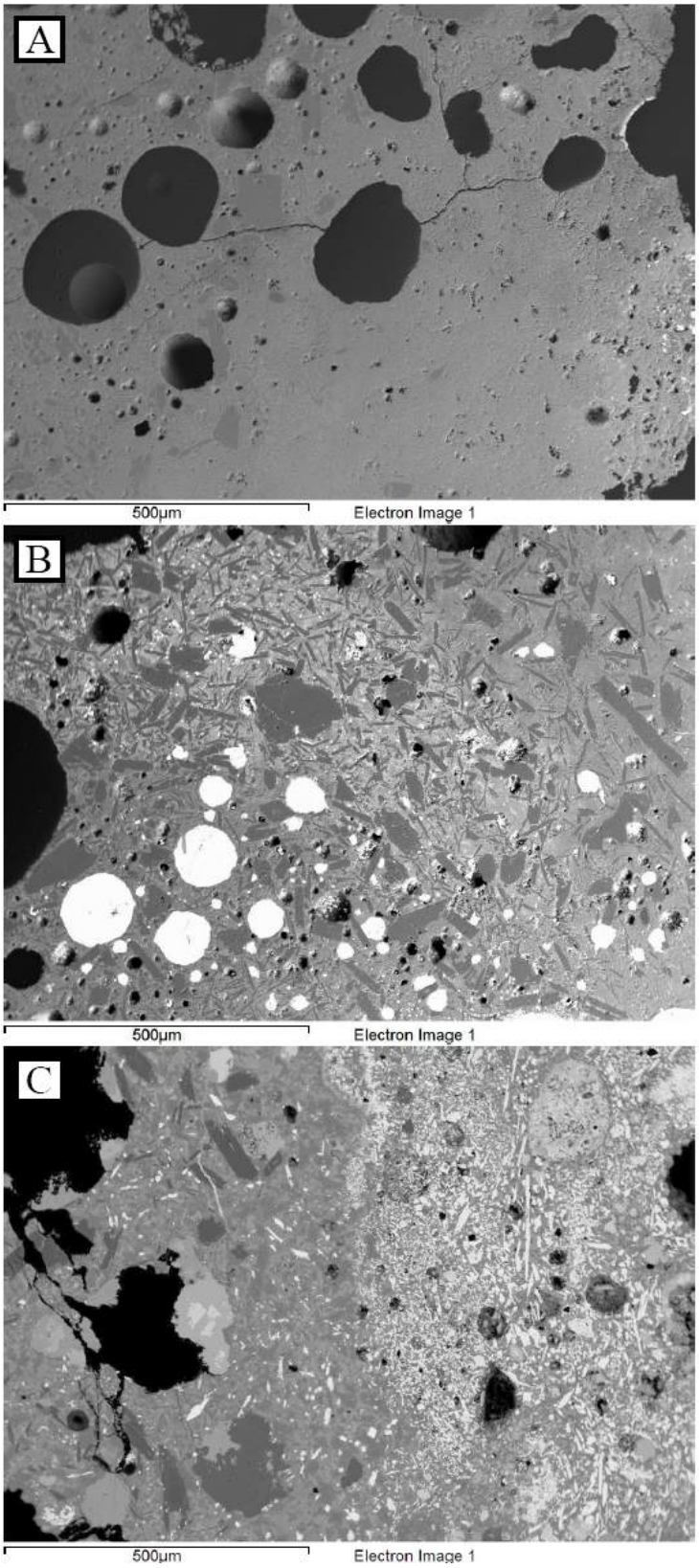

Figure 8.33: Variation in crucible slag for rim (A), intermediate (B) and lower body (C) samples in Gordion 25394

	Na_2O	MgO	Al_2O_3	SiO_2	K_2O	CaO	TiO_2	FeO	CuO	SnO_2
Deeper slag	3.8	3.6	18	50	3.2	10.5	2.1	9.7		
Thin layer	2.0	3.8	17	50	10.7	9.7	1.6	5.0		
Outer slag	2.6	5.2	12	37	4.5	24.0	1.2	7.4	4.0	1.7

Table 8.7: Composition (in wt%, normalised to 100%) of three zones in Gordion-22673-A crucible slag

from corrosion. In Gordion, however, the more variable seasons expose the remains to dry and wet conditions. In salt-bearing soils, this typically leads to 'bronze disease'. Some corrosion may have occurred post-excavation (Mödlinger and Piccardo, 2013). Detailed analysis of corrosion processes belongs to the field of conservation science (see, e.g., Fabrizi, 1988; Figueiredo *et al.*, 2010a; Ingo *et al.*, 2006; McNeil and Little, 1992 and Scott, 1985) and is beyond the scope of this project.

8.3.9 Potassium in Gordion-22673

A type of 'slag layering' occurs in two samples: Gordion-22673-A and B (from two different crucible fragments, which may or may not have belonged to the same crucible, but do not fit together). This layering is shown in Figure 8.34, with the composition of these three areas (for Gordion-22763-A; it is similar for Gordion-22763-B) given in Table 8.7. On the left, the deeper-lying slag (mostly vitrified ceramic) can be seen, dominated by plagioclase. On the right, the slag is dominated by pyroxene (with a drossy layer at the interior crucible surface). In between the plagioclase and pyroxene slag areas, a more porous area can be noted ('thin layer' in Table 8.7).

What is particular about this intermediate layer is its high potash content. This layering effect, however, does not persist from the top to the lower end of the mounted crucible section, and is probably a localised phenomenon, due to a small area of the ceramic being particularly enriched in potash (either a natural clay effect or due to segregation upon heating). Its isolated occurrence does not argue for any technological significance.

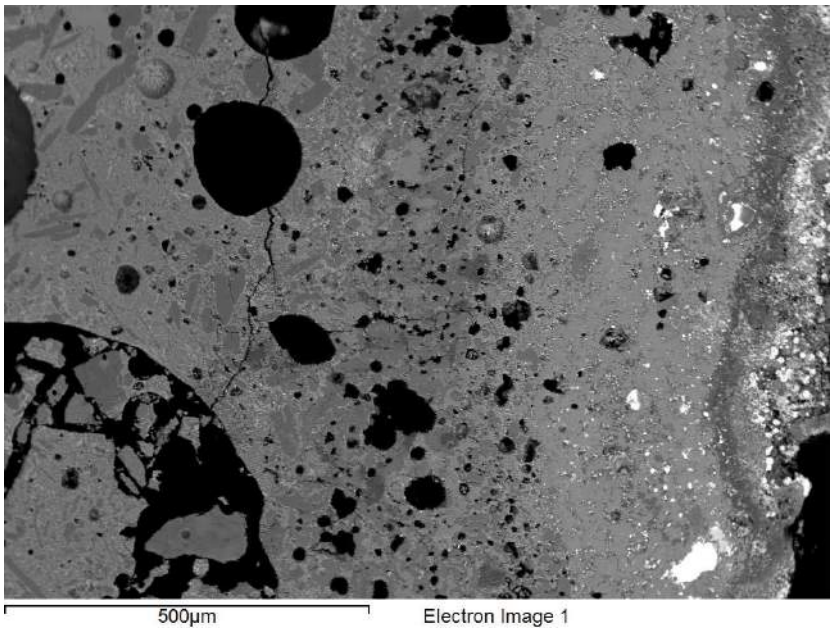

Figure 8.34: Slag layering in Gordion-22673-A

Section 8.4

Metals

A very brief overview of metals analyses conducted for Gordion metal artefacts is given in this section. The full results of the analysis of five metal samples by the author are given in Appendix M.1. These consist of three metal spills, and two cast metal objects, all of which are corroded to some degree. The cast objects were leaded tin bronzes, with approximately 6-7 wt% Sn and 1-2 wt% Pb. Two of the spills have similar compositions, while the third one was probably a pure tin bronze with 10-11 wt% Sn.
The exact assessment of these compositions is impeded by the significant corrosion present on most samples, which consists of various copper-tin-lead oxides and chloride(-oxide)s. One of the cast fragments (Figure 8.35) has a ring-like shape, with a rectangular corner, which roughly matches the size and shape of some of the (tentatively identified) moulds from Gordion (see section 8.5). The other large cast fragment (Figure 8.36) has a less distinct shape, and is characterised by copious amounts of high-temperature SnO_2 crystals (see Figures M.3 and M.4). These indicate highly oxidising conditions, probably during casting.

Some previous analyses of copper-base material from Gordion were undertaken by Pigott *et al.* (1991). These comprise microscopic description of (etched) metal samples and the

Figure 8.35: Gordion-22611: ring-like fragment

Figure 8.36: Gordion-22611: large cast fragment

results of their analysis by PIXE[10] analysis, which are reproduced in Appendix M.2.
There are three main alloys present: low-tin bronze (3.5-6.7 wt% Sn), normal (intermediate) tin bronze (10-15 wt% Sn) and leaded tin bronze (10-16 wt% Sn, 0.7-1.7 wt% Pb). The minimal lead content for considering a sample to be either leaded bronze or 'normal' bronze is quite arbitrary here, especially since all these analyses were performed on corroded samples. Nevertheless, there appear to be samples with negligible as well as significant lead contents, with some samples falling in between. Tin contents, on the other hand, appear to indicate a meaningful differentiation between low- and high-tin bronze. In sample YH 29997, a tin content of 20 wt% is noted. Though this is possible, the heavy corrosion and elevated presence of SnO_2 inclusions probably causes an over-estimation of the actual tin content. In some samples, Pigott *et al.* (1991) have identified SnO_2 laths, which they relate to the intentional alloying of copper with cassiterite mineral in a crucible cementation process. The quality of images supporting this interim report, however, are insufficient to properly assess this suggestion. Given that these crystals are described as laths, and the two samples are spills or casts, it appears most likely that these SnO_2 crystals point to oxidising casting conditions where tin was burnt out of the bronze (see, e.g., Dungworth, 2013), rather than a cementation process. This interpretation is furthermore supported by crucible slag analysis (section 8.3) and the author's analysis of other metal spills (Appendix M.1).

The overall impression from these analyses is that two alloy types were being produced and cast in Gordion: pure tin bronzes and leaded tin bronzes. The pure tin bronzes, which sometimes have minor lead content, can be further subdivided in low- and high-tin bronzes. The (fairly) good separation between these different alloys indicates that they were probably intentionally selected for specific purposes and perhaps subjected to different processes (casting, with or without cold working or annealing). Furthermore, it is possible that alloy preference changed through time. However, the sample size presented here is far too small to assess these questions and relate alloy selection to intended object use with any true confidence.

Section 8.5

Moulds

Within the crucible find bags, some ceramic fragments are not actual crucibles, but rather appear to be mould fragments. Though full analysis and discussion of moulds for bronze

[10] PIXE: Particle Induced X-ray Emission.

Figure 8.37: Two examples of mould fragments (see Figure N.6 as well)

casting is beyond the scope of this PhD project, a brief overview is presented here. Two examples are shown in Figure 8.37, while the complete set of moulds is illustrated in Appendix N.

The fabric for these moulds is similar to that of the Gordion crucibles, based on visual inspection (no further microscopic analysis has been undertaken). The interior surface of the moulds, however, appears to be more fine-grained and smooth. The temperature profile throughout the moulds indicates that they were probably pre-fired (similar to the crucibles, see section 8.1.1), and subsequently exposed to higher temperatures under reducing conditions on the interior, resulting in a grey surface typical for clay moulds (Bayley *et al.*, 2001, p. 16-17, Figures 24 and 26). This exposure is most likely due to the contact of the interior surface with liquid metal, as it was poured into the mould and left to cool there. Contrary to the crucibles, however, no significant slag or dross formation can be noted, and the ceramic did not lose its structure. Though liquid metal would have entered

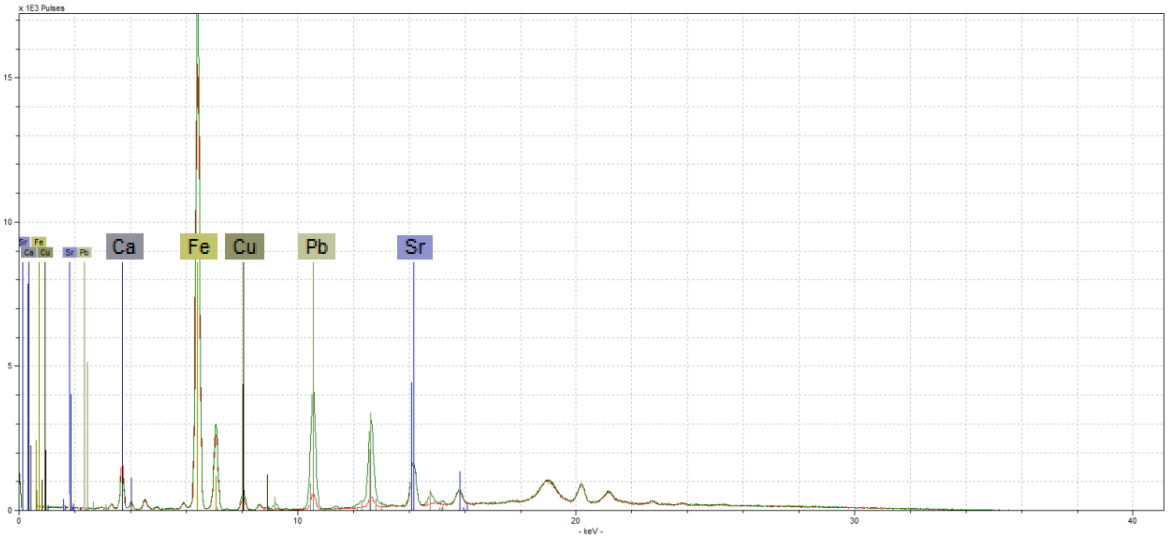

Figure 8.38: Raw handheld XRF spectrum for Gordion mould (exterior surface in red, interior surface in green)

the moulds at approximately the same temperatures as those within the hot crucibles, these temperatures were not sustained in the moulds. The internal temperature would have quickly decreased when the metal was left to cool, in contrast to the prolonged internal heating of the crucibles, explaining the difference in slag formation.
Their similarity in ceramic fabric and firing conditions may suggest that these moulds were made and pre-fired together with the crucibles.

The varied shapes (see Appendix N) are indicative of a variety of objects being cast in Gordion, ranging from small ring-like shapes (Figure 8.35) to elongated, rod-like (?) shapes and perhaps vessels (Figure N.3). Figure N.3 furthermore indicates that in some cases an existing ceramic vessel or shape may have been used as a mould, with the application of a coarser clay (similar to crucible fabric) on the exterior.

Analysis of the exterior and interior surface by handheld XRF indicated a significant increase in lead on the interior surface, as well as a minor increase in copper (Figure 8.38). Crucibles, on the other hand, showed increased tin content on their interior surfaces, in addition to more significant copper increases (Figure 8.39).
This is in line with the expectations for mould surface enrichments, as discussed by Kearns *et al.* (2010): for (leaded) bronzes, lead is very strongly enriched, while only minor copper and very minor tin enrichments can be detected. This skewed enrichment does not allow further evaluation of the relation between alloy selection and object typology.

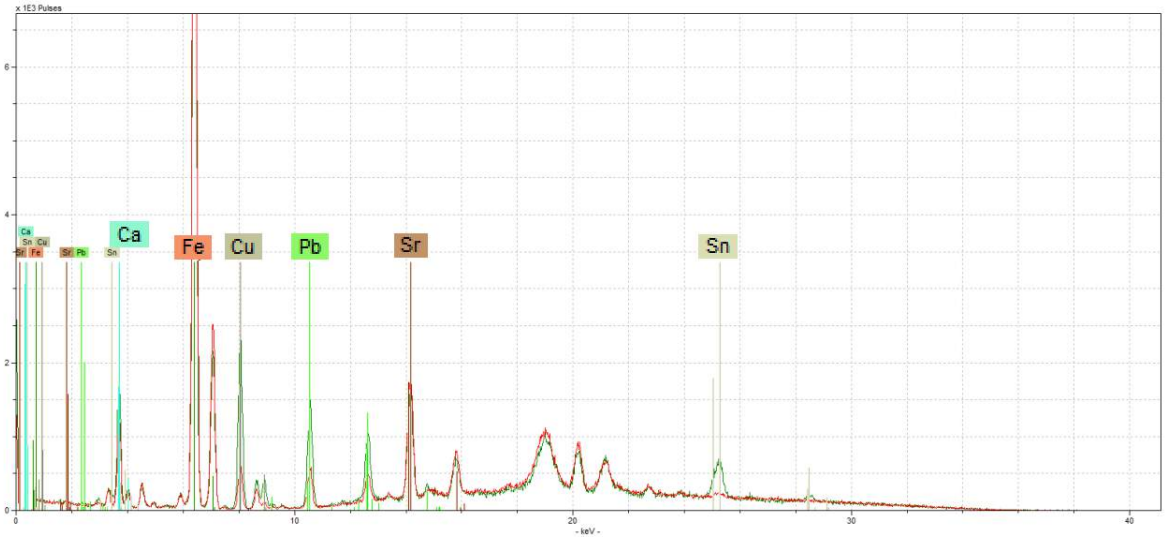

Figure 8.39: Raw handheld XRF spectrum for Gordion crucible (exterior surface in red, interior surface in green)

Note on handheld XRF analysis

The pXRF analysis of these moulds took place in the University of Pennsylvania Museum of Archaeology and Anthropology as a means of sorting through the assemblage for sample selection. This data was obtained using their recently acquired handheld XRF device (Bruker Tracer III SD, S/N: T3S165q, yellow filter[11], 45 seconds live-time), which had not been calibrated for quantitative analysis. Raw spectra were visually inspected to look at presence/absence of elements, in order to assess variability in the assemblage.
No structured assemblage-wide analysis was undertaken for this assemblage.

[11] 'Yellow Filter': "*These settings allow all the x rays from 12 kV to 40kV to reach the sample thus efficiently exciting the elements noted above (Ti to Ag K lines and the W to Bi L lines). There is little or no sensitivity to elements below Ca with these settings*". (Bruker Tracer III SD Manual)

CHAPTER 9

Discussion

This discussion aims to provide a broader perspective to the Gordion crucibles. Not only do they offer the first example of Phrygian crucible technology, but equally an original insight into the types of metal produced within the citadel. This is compared here to the limited available data for (roughly) contemporary metal production, trade and consumption in the region, and used to indicate where further research is needed.

The production of crucibles at Gordion seems to have been a local affair. Similarly to Pi-Ramesse, the metallurgists selected the most appropriate, easily available clay and made minor adjustments (e.g., addition of organic temper) to improve its refractoriness. The crucibles were shaped by hand, suggesting a fast, *ad hoc* production (probably by the metallurgists themselves, rather than specialised potters). That is not to say that the crucibles were a flimsy product: their characteristics were perfectly suited to their intended technological purpose.

Based on the analysis of metals and crucibles from Gordion, it appears that during the Achaemenid/Late Phrygian period, both tin bronzes and leaded tin bronzes were being produced. This was done using either recycled or raw copper, some of which probably had a significant lead content (naturally from the smelting process or intentionally added), together with a fresh source of tin. It is difficult to assess whether tin was added in its metallic form or as cassiterite, due to the nature of slag formation in the Gordion crucibles. Overall, very few indications for a cementation process exist within these crucibles. The extent to which metallic tin would have been available through trade in this region in the Achaemenid Period is not well documented either, however, leaving this issue unresolved for now.

Lead isotope studies have not been performed for either the metals or crucibles from Gordion. For the bronzes and crucibles with elevated lead contents, the lead isotope signatures would be dominated by the lead that was probably added to the bronze, rather than naturally present in the copper. Though such results could be interesting, the rough stratigraphical resolution available for the Gordion crucibles would render an examination of variable metal sourcing within the workshop through time (as attempted for Pi-Ramesse, section 5.5) almost impossible. It is therefore harder to justify the (financial and time) cost associated with such analysis for the Gordion material.

Contrary to the Pi-Ramesse crucibles, the compositional analysis of crucible slag from Gordion does not provide many clues as to the sources of copper used to produce (leaded) bronze there. Most of the copper appear to have been fairly 'clean', pointing to refined (raw or recycled) copper, while more iron-rich copper was introduced into a small portion (±17%) of the crucibles. This iron content appears to have been comparatively lower than that reflected in the Pi-Ramesse crucibles, which should mainly be attributed to a less contaminated copper source (though higher crucibles refractoriness plays a role here too). The presence of lead in $\pm 1/3$ of the crucibles most likely indicates the specific selection of a lead-rich copper source to produce leaded bronze. Recycling of existing (leaded) bronze appears to have been important, though the use of fresh materials, particularly tin (ore), is attested as well. The provenance of this tin cannot be identified based on the results presented here. Tin ore may have been available within the Sakarya basin, in the Phrygian hinterland, as indicated in Gale *et al.* (1985), Figure 2, p. 150, but no further information on the ancient exploitation of this deposit is available.
In summary, a mixture of different technological choices is reflected in the crucible assemblage. Their contextual distribution, however, does not allow any analysis to be made on whether this variable technology reflects a change in time, space or intended purpose of the produced alloy. The variability seen here might well attest the *ad hoc* nature of the workshops, where small batches of metal could have been produced with the material resources at hand (often recycled scrap) to produce fairly small objects. It is at present not possible to provide any further insights into the practical organisation of the metallurgical workshops at Gordion.

Apart from the production of leaded bronze, the presence of various iron slags indicates that iron was both being smelted (primary production) and smithed (secondary process) in Gordion in the same workshop context. Though further analysis and discussion of iron metallurgy at Gordion is beyond the scope of this research, it can be noted that in Gordion, there probably was no clear separation between bronze and iron metallurgists. Though it is hard to unequivocally prove that these were the same people, the contextual proximity

indicates that they were well aware of each other's craft.

Young (1963: 357) described the Phrygians as "*bronze-workers of the first order, familiar with all the techniques of casting, solid or hollow, of hammering bronze vessels by sinking or by raising, and of decorating them repoussé or by chasing*", which Bilgi (2004) attributes to a deep-rooted cultural tradition. Young similarly identified the forms of bronze vessels and fibulae found at Gordion as local Phrygian productions and takes their ready use and adaptation abroad (e.g., in Western Turkey (Lafli and Buora, 2012), the Aegean (Craddock, 1976) and Lydia) as a proxy for the dissemination of Phrygian ideas and influence.
This flow of goods and ideas along the Royal Road during the 8th and 7th century BC (Birmingham, 1961) may have dwindled prior to the Achaemenid (Late Phrygian) period, but was restored by Darius, confirming Gordion in its role as a trade hub.
The available compositional data for Phrygian(-style) objects, however, is too limited to assess the extent to which metal objects, cast in Phrygia, were transported and used abroad.

The quintessential (archaeologically attested) Phrygian metal object is the fibula, which is found in many contemporary contexts of cultures in contact with Phrygia. Muscarella (1967) discusses the variety in Phrygian fibulae from Gordion, as well as their prevalence in foreign sites. More fibulae, as well as bronze belts, are presented by Vassileva (2012). The characteristic fibula typology marks them as domestic products, with production most likely situated in Gordion, though no moulds have been found. Examination of the fibulae indicates that they were most likely cast in 'one-use' on some and 'multiple-use' moulds on other occasions. It appears that both open and closed moulds were used. The brief results presented in section 8.5 are the first attestation of moulds in Gordion, some of which may have been related to the casting of fibulae. The alloys employed in the making of these various fibulae are not specified by Muscarella or Vassileva beyond the generic 'bronze' description. Some were later analysed by the Oxford Research Laboratory for Archaeology and the History of Art for Arthur Steinburg, and mentiond by Craddock (1978): the 8th-7th century Phrygian fibulae from Gordion were made of brass, with ±10% zinc and little tin or lead. This is confirmed by later XRF analysis of other Gordion fibulae and equally true for other Phrygian and East Greek material (though three 'Phrygian fibulae' from northern Greece are made of tin bronze (Craddock, 1976)). This result is quite surprising, as no indications for brass-working, -casting or -processing are found in the metallurgical assemblage presented in this chapter. It could point to a changing preference in copper alloys through time, perhaps related to Achaemenid influence, but equally to the existence of other metallurgical workshop contexts in Gordion (and other Phrygian sites) that have hitherto not been discovered. Clearly, further excavation and analysis of metallurgical production waste is needed to shed more light on this issue.

Analysis of eight Phrygian metal objects from 8th-7th century BC Ankara by Atasoy and Buluç (1982) shows the use of tin (±10%) bronzes, some of which were hammered and annealed. They go on to suggest that metal workshops outside Gordion were probably in existence as well, producing Phrygian-style bronzes.
Overall, the results from metal and crucible analysis presented in this chapter are the first evidence of leaded bronze production in Gordion and Phrygia. The use of this alloy at this time in history, however, is not unusual and similarly attested, for example, in Boğazköy during the Iron Age (Lehner, 2012). The absence of references to (Late) Phrygian leaded bronze in the literature mainly reflects the scarcity of analyses hitherto performed.

There exist a fair amount of publications on Anatolian metals, mostly concerned with the composition (chemical and lead isotopes) of geological deposits and metal artefacts. These studies cover a huge chronological scale, ranging from the Chalcolithic to Islamic times, and are typically focused on the provenance of metals. Some examples (though by no means an exhaustive list) are: Gale *et al.*, 1985; Lehner and Prikhodko, 2010; Lehner *et al.*, 2009; Moorey and Schweizer, 1974; Pernicka *et al.*, 1984; Sayre *et al.*, 1992; Seeliger *et al.*, 1985; Wagner *et al.*, 1985, 1989, 2003 and Yener *et al.*, 1991. These concentrate mainly on copper-related artefacts and mines (evidence for (Early Bronze Age) tin mining in Anatolia has previously been mentioned in section 6.2.3).
The analysis of Phrygian artefacts in particular is mentioned by Hirao *et al.* (1995), who note that most (copper) metals (from Kaman-Kalehöyük) appear to agree with minerals from the Ala and Bolkar Mountains (Taurus). Sayre *et al.* (2001) equally indicate a local origin for most (copper) metals employed within Phrygia/Anatolia, which is not surprising given the abundance of metalliferous deposits in the region. It is possible that tin was similarly acquired from within Anatolia. However, these broad observations cannot be tested for Gordion specifically without further analyses (e.g., lead and tin isotopes, as well as trace element analysis).

There are no published studies of Phrygian crucible metallurgy known to the author. Bossert (2000), for example, discusses Phrygian ceramics in Boğazköy, but mentions no crucibles. de Jesus (1980) presents some drawings of (3rd millennium BC) Trojan crucibles, tuyères and moulds, and a few from Arslantepe and Alishar, which reveal little stylistic resemblance to the Gordion material and were not scientifically analysed. Early Bronze Age examples of internally heated crucibles from Nevalı Çori, used for primary smelting, are shown by Hauptmann *et al.* (1993). The analysis of Phrygian crucibles presented here is the first of its kind, and will serve as a reference for future studies of Phrygian metallurgy. As a consequence, there are no comparisons to be made between the Gordion crucibles and other Phrygian assemblages.

Contemporary crucible metallurgy in Anatolia or Achaemenid Persia is equally poorly represented in the literature. This makes it very difficult to hold a meaningful discussion of technological (ex)changes in the region, both diachronic and between different cultures. Finally, the crucibles themselves point to a local tradition or at least adaptation of crucible manufacture. This is commonly the case for Bronze and Iron Age crucibles, with the exception of very specialised (and chronologically much later) technical ceramics with particular fabrics, such as those used in the production of crucible steel (e.g., Rehren and Papachristou, 2003) or the widely distributed medieval Hessian wares (Martinón-Torres and Rehren, 2009). Typically, crucibles are as indigenous as the local cooking ware, and their typological comparison to examples from distant contexts (in time and space) holds little value. More interesting results can be obtained from the comparison of their metallurgical application and the information about technological choices that are hidden in their fragmented remains. At this point, such comparisons cannot be made.

Part V

Roman Thrace

Felix, qui potuit rerum cognoscere causas

Goscinny and Uderzo, 1997, after Vergilius

CHAPTER 10

Archaeological background

In the final case study presented for this thesis, four assemblages from different sites in Roman Thrace are discussed. Though there is much to be said about the history and archaeology of the eastern Roman provinces, including Thrace, such a discussion would fill several PhD theses. Therefore, a more succinct introduction is given here, focusing on aspects relevant to the interpretation of the crucible remains.

Section 10.1

Roman Thrace

The assemblages discussed in this chapter were excavated at four different sites in modern-day Bulgaria, shown in Figure 10.1. This region was known as Thrace in pre-Roman times and the sites were included in the Roman province of Thracia, though provincial boundaries were re-drawn over time. Serdica became part of Dacia Mediterranea under Diocletian (late third century AD) and Nicopolis ad Istrum was incorporated into Moesia Secunda.

As in most provinces, gradual Romanisation took place following the conquest of these regions, with strong Roman influence visible in the urban development of the sites under discussion (Ivanov and von Bülow, 2008). Local traditions of agriculture and exploitation of other resources (e.g., mining: Dušanić, 2004) were adapted by the conquerors, but new industries were equally introduced (see, e.g., Vagalinski, 2011), resulting in an economic and cultural 'revival' during the second and early third centuries AD (Ivanov, 1983).

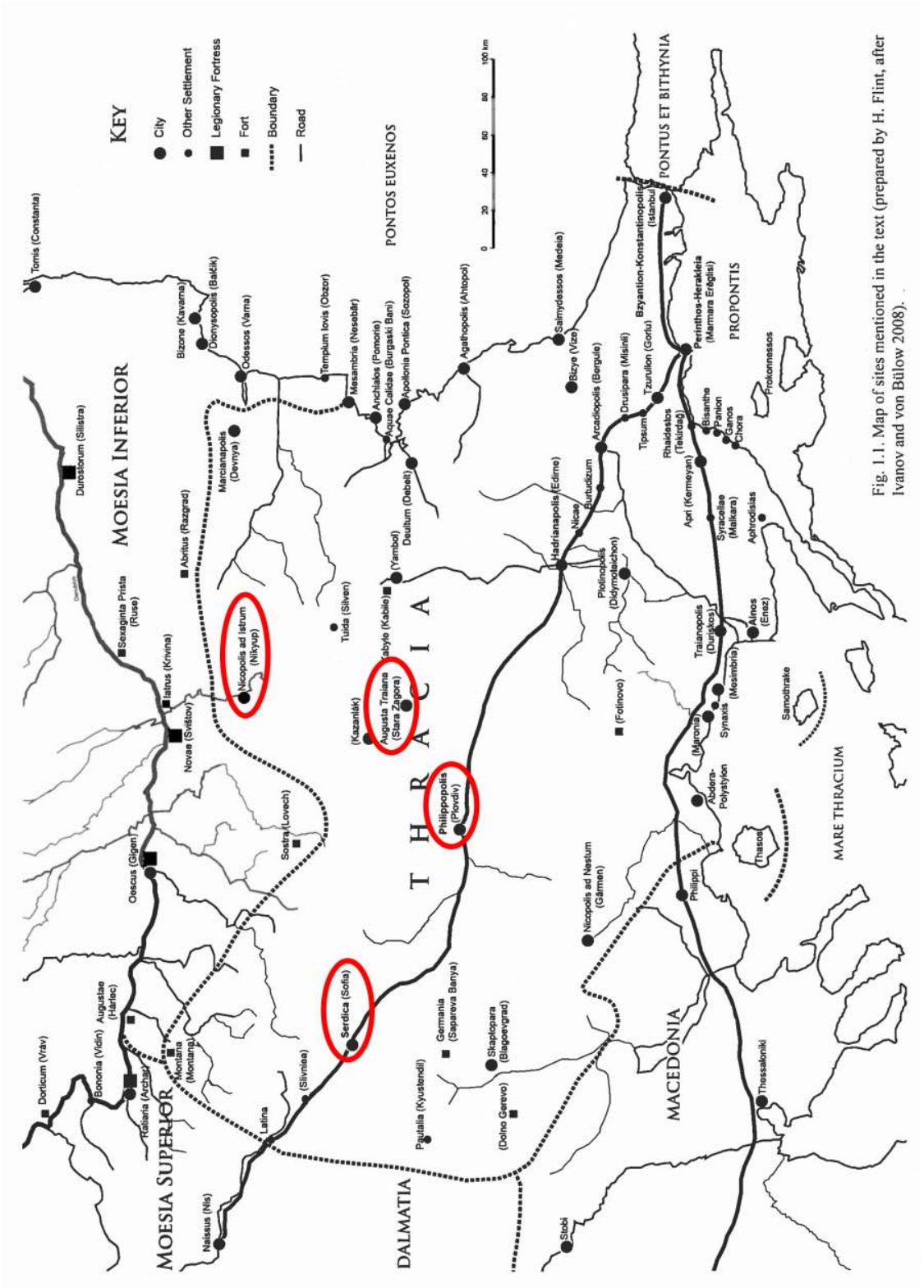

Figure 10.1: Map of Roman Thrace, showing four sites from which assemblages are examined (adapted from Haynes, 2011, p. 6)

Though no legions were stationed in Thracia, the province was well known as a supplier of military troops to the Empire (Haynes, 2011), particularly from the Serdica and Philippopolis regions (Boyanov, 2013).
It is far beyond the scope of this thesis to discuss all the developments that took place in Thracia under Roman rule, and only very basic introduction to each site and known metallurgical activity there is given here. Further details of the particular contexts pertaining to the assemblages under study are given in section 10.2.

Nicopolis ad Istrum (near modern-day Nikyup village) was founded under Trajan (around 110 AD), in memory of his victory over the Dacians (Poulter, 1983, 2002, 2007a; Slokoska, 2002). The town is located at the confluence of the Rositsa and Yantra rivers and built following the classical orthogonal system. Excavations by a British team at Nicopolis (unrelated to crucibles discussed in this chapter) have yielded significant amounts of lead and copper-alloy scrap, mostly concentrated in particular areas close to the late Roman city walls and presumably intended for recycling (Poulter, 2007b), as well as significant evidence for ferrous metallurgy and minor evidence for copper-related metallurgy[1] (Salter, 2007). Nicopolis had its own mint under the Severan dynasty (Ivanov and von Bülow, 2008), though some coins were struck before (Minkova, 2002).
Philippopolis (after Philip II of Macedonia, modern-day Plovdiv) was already an important centre in existence before Roman occupation (Ivanov, 1983), and continued to grow following its incorporation into the province Thracia, eventually becoming its capital (named *Trimontium*) in the early third century AD, with a very intensive mint earlier, under Domitianus until Elagabalus (Ivanov and von Bülow, 2008).
Serdica (modern-day Sofia) was another important settlement long before the arrival of the Romans (Ivanov, 1983; Staddon and Mollov, 2000) and expanded as a *municipium* from the end of the first century AD onwards, with its own mint under Marcus Aurelius until Gallienus (Ivanov and von Bülow, 2008). It finally became the capital of Dacia Mediterranea under Diocletian's reforms, with renewed minting taking place in 303-308 AD (Hendy, 1972).
Stara Zagora (modern-day name) was founded at the start of the second century AD and named *Augusta Traiana*, after its founder Emperor Marcus Ulpius Traianus. It was one of the largest cities of Roman Thrace, second only to Philippopolis, and had its own mint from the mid-second to mid-third century AD (Ivanov and von Bülow, 2008).

[1] Two (?) crucible fragments were recovered in areas K 4508 and P 5021, made of a thin white fabric with the application of a less refractory external clay layer, vitrified during use.

Section 10.2

Assemblage-specific backgrounds

Most of the information presented in this section is based on notes by A. Cholakova, who excavated many of the crucibles discussed here, and Th. Rehren, who accompanied her for sampling these crucibles at several museums in Bulgaria. I am greatly indebted to both for the documentation and preliminary interpretation of this material.
Samples N1, N2, N3, N4 (as well as P9 and S7) come from fragments published by Cholakova (2006). Fragments N5-N6, P6, and StZ1 derive from recent rescue excavations, hitherto unpublished. Excavation reports for fragments P1-P5 (1976), P7-P8 (1987) and S1-S11 (1953-1958) offer no contextual information beyond their rough dating outlined below.

10.2.1 Nicopolis ad Istrum

All the Nicopolis samples belong to the Regional Museum of History, Veliko Tarnovo, and derive from two different locations within the site, comprising three particular contexts: N660 and 0012 are different layers of a single area (Cholakova, 2006) and context 604 (unpublished) is located in an unknown area.

The first context (N660, trench excavated in 2000/2001) is dated to the early second century AD and contained fragments N1-N3. It is a dump deposit[2] comprising pottery, glass and other small parts, of which a considerable amount are metalworking remains and production waste. These remains cannot be linked to any *in situ* production installations. The crucibles from this context are shown in Figure 10.2. N1 is an internally heated, large hemispherical crucible, shaped by hand (finger traces on exterior), with 2-3 cm thick walls. N3 is an externally heated crucible fragment. N2 is something quite different, and has been tentatively described as a type of 'collar', probably belonging to a larger metallurgical structure, with slag adhering to its internal surface.
Clay moulds were found in this context, suggesting the casting of small rings, as well as many pieces of copper-base metal scrap. Finally, the presence of over 25 kg of iron (s)melting slag (both primary tap slag and smithing slag) indicates associated ferrous metallurgy.

The second group was excavated between 1996-2002 and consists of three different crucible fragments (N4-N6), shown in Figure 10.3. N4 is a base fragment of a crucible from

[2] Specifically between pillars V and VI of the civil *basilica*, shown by Cholakova, 2006, Figure 1.

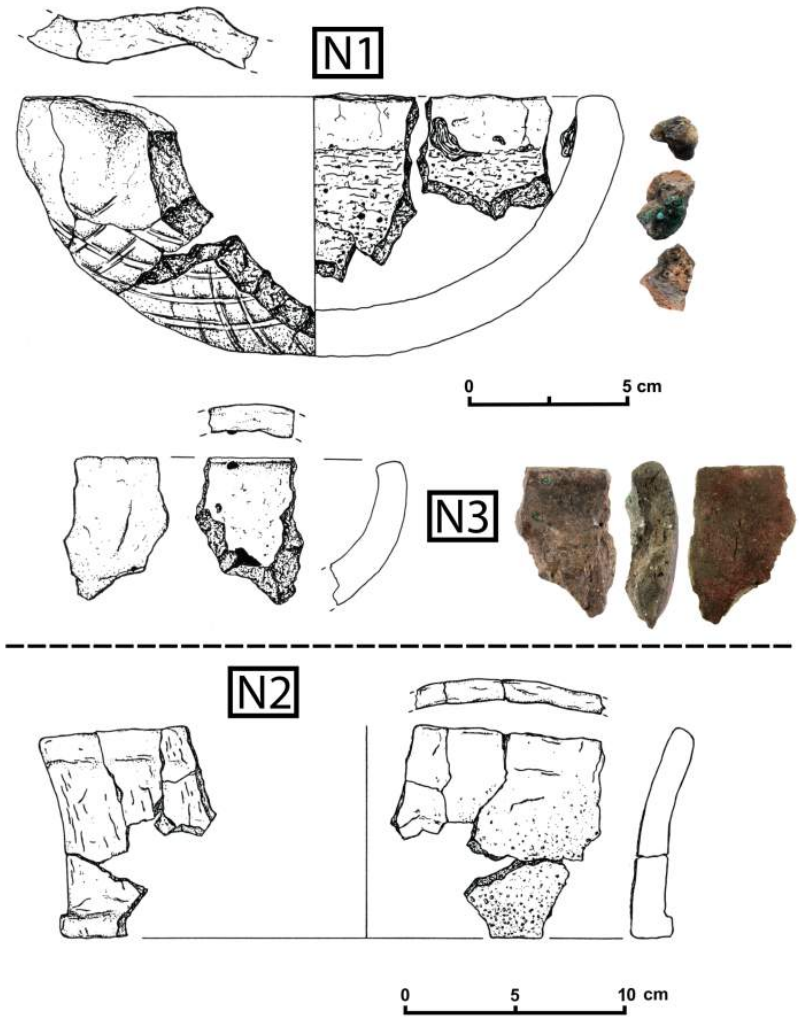

Figure 10.2: Crucible fragments from Nicopolis, context N660

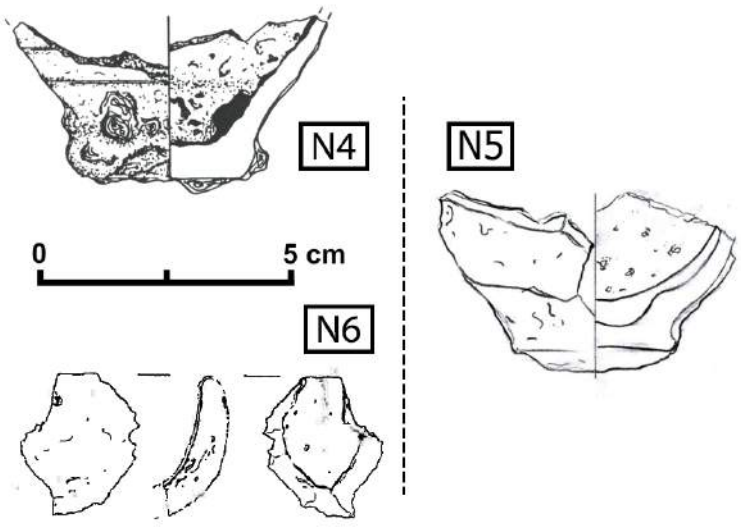

Figure 10.3: Remaining crucible fragments from Nicopolis

Figure 10.4: Crucibles (P1-P5) from second century workshop, Philippopolis

context 0012 (*basilica*, no exact location or date). N5 is a base fragment from a third-fourth century AD context (604). Both N4 and N5 appear to be wheel turned domestic pottery, re-used as crucibles. N6 is an unstratified rim fragment from the same area (604).

10.2.2 Philippopolis

All the Philippopolis samples belong to the Regional Museum of Archaeology, Plovdiv, and derive from four separate contexts.

Samples P1-P5[3] were taken from an assemblage of eight crucibles (Figure 10.4), dated to the second century AD. They were excavated in 1976, and belong to a Roman workshop in Philippopolis, together with copper (alloy) ingots and scrap. All crucibles were handmade with non-refractory, soft clay fabrics and heated on the outside, which resulted in reddish exterior vitrification with charcoal impressions. The insides were all dry with some prills adhering but little dross and no slag present. All samples consist of small dross flakes and fragments, taken from the crucible interior, without crucible ceramic.

Sample P6[4] was taken from a crucible base fragment (no image available) dated to the Late Roman period (fourth-sixth century AD?), excavated in 2005 in a non-workshop, residential context. It is an externally heated, pear-shaped crucible base with heavy external vitrification, charcoal impressions and a reddish glaze. It has a dark fabric with 12-15 mm thick walls, and appears to be wheel-turned.

[3]Museum inventory numbers: P1 = II 403, P2 = II 404, P3 = II 405, P4 = II 409 and P5 = II 410.
[4]Museum inventory number: P6 = NSF 637.

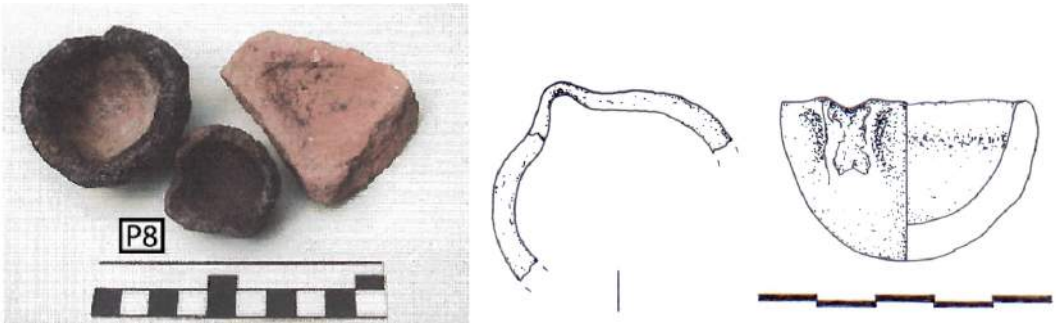

Figure 10.5: Left: crucible P8 (left) with an unsampled gold-processing crucible (centre) and ingot mould (right) from second-third century Roman forum context, Philippopolis. Right: drawing of P8

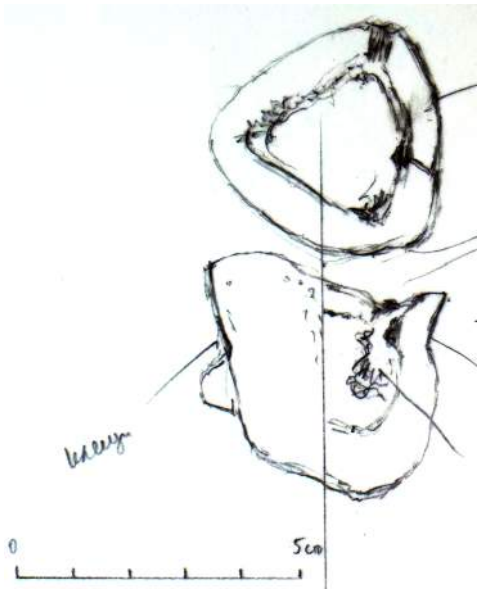

Figure 10.6: Preliminary drawing of crucible P7, Philippopolis

Samples P7-8[5] derive from a second-third century AD context, excavated in 1987, where three crucibles and an ingot mould (?) were found. Two of these crucibles, including P8, are shown in Figure 10.5. From the small, triangular crucible (P8), a wall section was taken. This showed hardly any vitrification (in or out) and has tentatively been linked to silver processing. Dumped in the Roman forum of Philippopolis, there is again no directly related workshop context. Crucible P7 (Figure 10.6) was externally heated and the copper dross on its interior has been sampled.

Finally, sample P9[6] was taken from a group of crucible fragments (Figure 10.7) found in a smithy context (excavated in 2004), dated to the second century AD. In this workshop,

[5]Museum inventory numbers: P7 = II 1039 and P8 = II 2250
[6]Corresponding museum inventory number: P9 = NSF 638

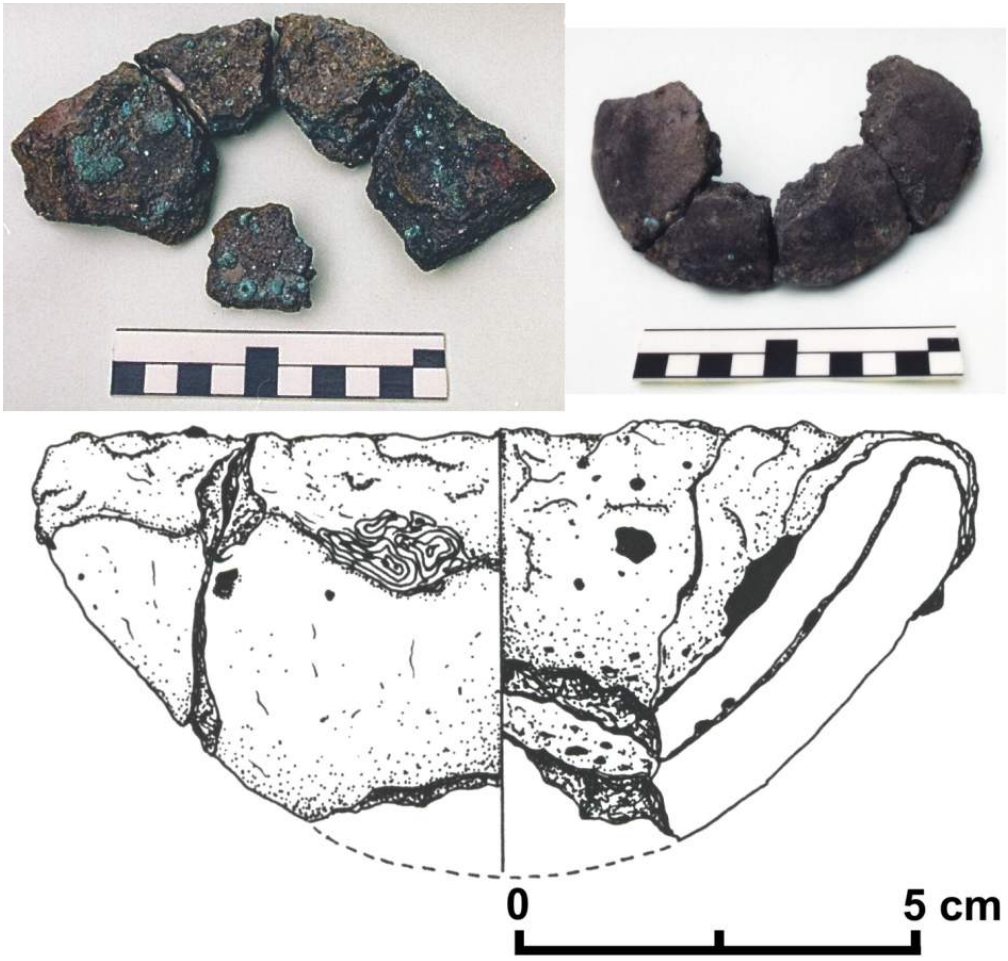

Figure 10.7: Crucible fragments (P9) from second century smithy, Philippopolis

remains of iron-working (slag, hammerscale) and other metal finds were found together with this crucible. It is handmade, heated from above and two layers are macroscopically visible, indicating reuse. It has been suggested that this workshop produced small iron implements with copper alloy parts (e.g., keys or brooches). The crucible remains consist of rim fragments only.

10.2.3 Serdica

All the Serdica samples belong to the Historical Museum of Sofia (ME 'Old Sofia'), and derive from four (tentatively identified) contexts excavated in the 1950's. Excavation reports offer no further information on the nature of these deposits.

Samples S1 and S2[7] were taken from two crucible fragments belonging to a single late Roman (?) context excavated in 1958 (Figure 10.8). Both S1 and S2 are re-used pottery

[7]Museum inventory numbers: S1 = MHS A-1380, S2 = MHS A-1379

(either domestic or storage (amphorae?) fragments), wheel-turned and very thick-walled, with flat bottoms. Though their morphologies are quite different, their stable flat bases, thick walls and size were probably the criterion for their selection. A secondary layer of clay has been applied to the external surface of both crucibles. Due to external heating of the crucibles, this clay has turned black and fully vitrified, while protecting the crucibles' interiors from disintegration.
S1 has a whitish main body and dark outer layer. A sample was taken from the internal black dross/corrosion. The second crucible has a similar white, micaceous body and black internal 'skin'. The interior is very 'dry', with only a few black prills visible in grooves near the bottom, from which a sample was taken (i.e., no ceramic, slag or dross). Both crucibles were tentatively identified as silver-related.

Samples S3 and S4[8] were both excavated from the same large area in 1953, but are not necessarily contextually associated and from unclear stratigraphy.
S3 is a hemisphere-like small vessel, hand-made and thin-walled, with a spout (Figure 10.9). It was intentionally produced as a crucible, and heated from outside. Small cracks in the walls occur. The sample is a rim fragment of this crucible, which has a very fine grey clay fabric with small quartz grains and some fine-medium feldspar. The outer surface is vitrified and the spout contains traces of gold. Gold sparks on the inside appear to indicate a 'watermark' of half the interior height. An olive green glassy slag occurs at the bottom only, with gold prills within, eating into the porous crucible body.
S4 is a sample from a bottom fragment of another purpose-made crucible which has a flat, thick bottom, but is conical inside. With its graphite-dominated fabric, it resembles early modern (17^{th} century?) triangular crucibles. It has $\pm$1 mm exterior vitrification and a very thin interior slag layer (red to blue, green whitish ?). The exterior slag/lining could indicate its fixing on a pedestal during use, but is too heavily burnt for confident interpretation. It probably had a spout.

Sample S5[9] was excavated in 1955 and derives from a tentatively identified late (?) context (and might be related to S4, despite deriving from a different location). It was taken from another flat, thick-bottomed crucible, with a rounded inside (Figure 10.10). It has vitrified 'hotspots' on its exterior, but is otherwise 'dry'. Inside, a thin red slag coat is present, which is somewhat thicker upwards. The sample was taken from an exceptionally thick slag area.

Finally, fragments S6-S11[10] look very similar to each other and are therefore assumed to form a single production debris assemblage of Roman/late Roman date. Though all come

[8]Museum inventory numbers: S3 = MHS A-668 and S4 = MHS A-490
[9]Museum inventory number: S5 = MHS A-1034
[10]S6 = MHS A-676, S7 = MHS A-675, S8-11 = MHS A-677

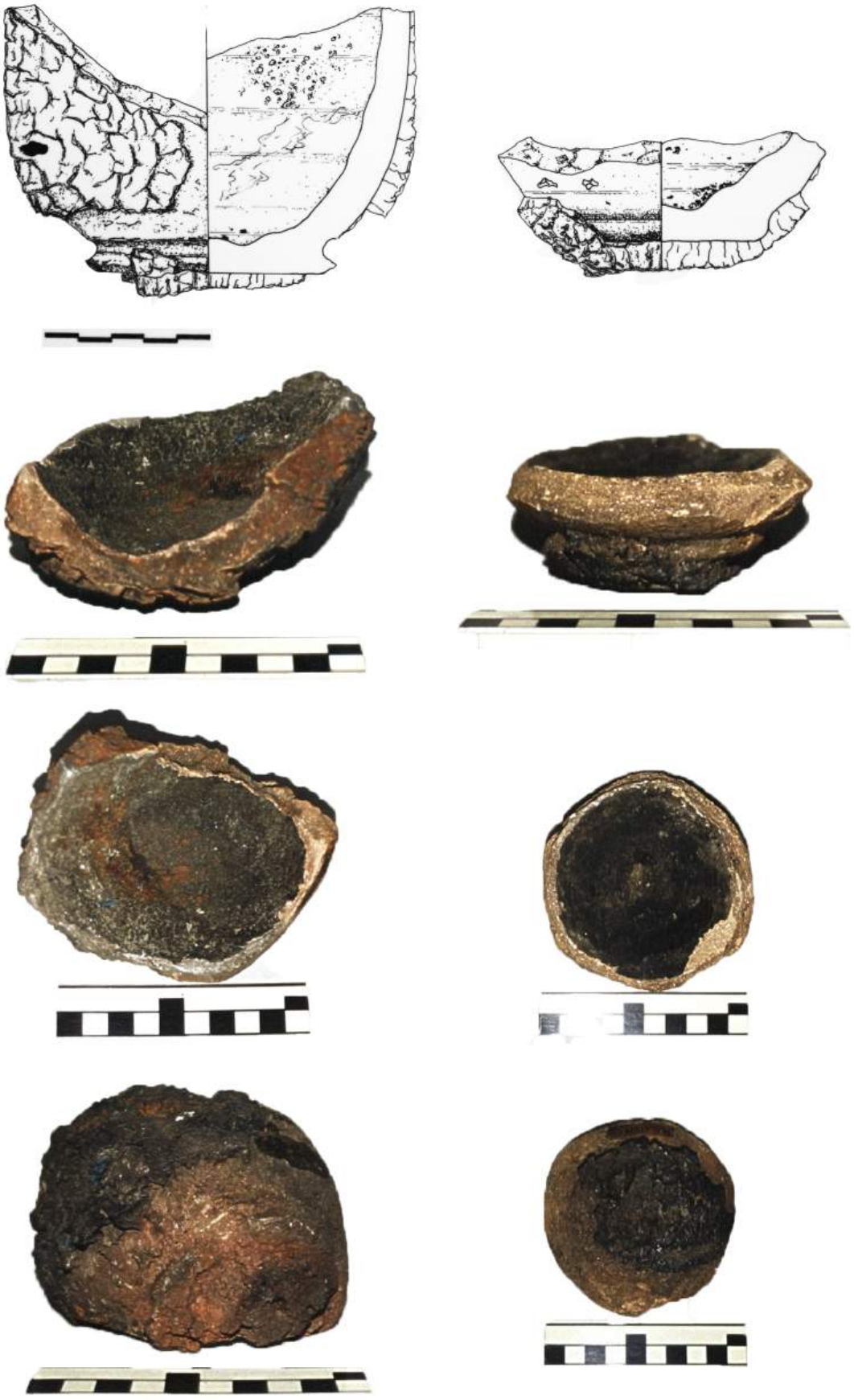

Figure 10.8: Crucible fragments S1-S2 from late Roman Serdica. Left: S1, right: S2

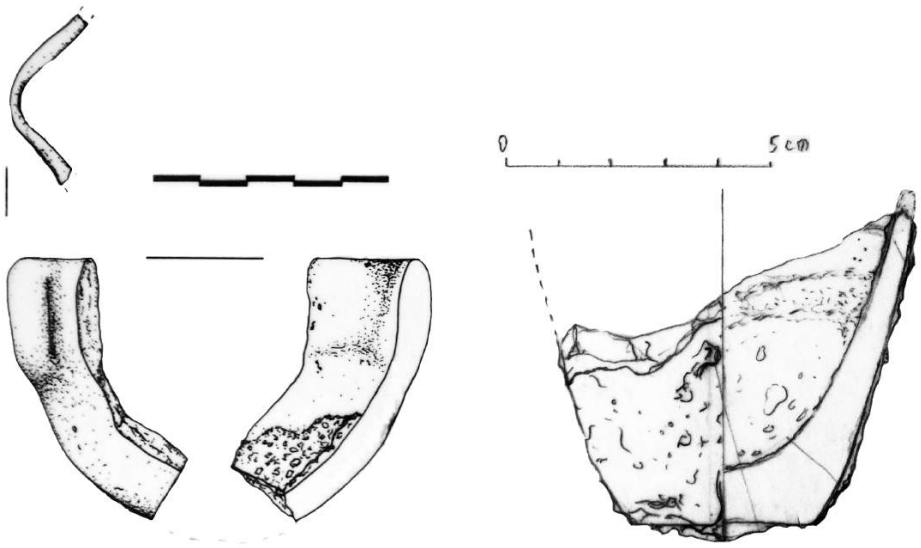

Figure 10.9: Crucible fragments S3-S4, Serdica

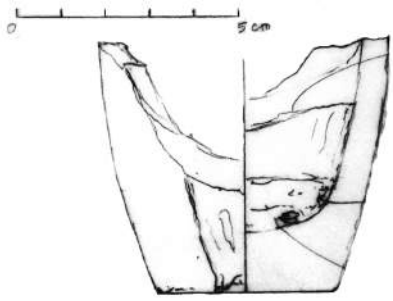

Figure 10.10: Crucible fragment S5 drawing, Serdica

Figure 10.11: Crucible fragments S6 (left) and S7 (middle, right) from Roman or late Roman (?) Serdica

from the same 1953 excavations, the excavated area is too big to assume any relationship between the fragments based on location. Their inferred relation is based on macroscopic similarity, and their consecutive numbering. S6-S11 probably represent at least three or four vessels, possibly more, which all appear fairly large compared to the crucibles from the other sites presented here. All are hand-made, with round bases and cylindrical bodies (?), whitish very hard (refractory) clay, and no evidence for additional layers. For S7, it appears that the vessel had a relatively wide spout for pouring metal. Comparison to general types of local and regional Roman/late Roman pottery indicates an intentional selection of particular clay, not the most commonly used by the local potters.

S6 was taken from a base fragment, for which a thick, irregular, reddish to greenish dross layer is present on the inside with some copper metal trapped inside (Figure 10.11). The outside is ash-glazed, with some copper contamination, but no separate layer is present. S7 (Figure 10.11) is taken from a similar crucible with outside vitrification/corrosion and some drips at the bottom. The inside slag has been sampled, and some dross (less than for S6) is present. 'A-677' consists of five different fragments, shown in Figure 10.12. S8 is a rim fragment, S9-S10 are two base fragments and S11 is a big body fragment. The rim fragment indicates an internal diameter of 8-9 cm. The slag is olive-green and glassy inside, reddish on the outside. Small, flaky samples were taken for S8-S10, while a crucible wall section was available for S11. It is impossible to reconstruct S8-S11 as a single vessel.

Figure 10.12: Crucible fragments S8-S11 from Roman or late Roman (?) Serdica

10.2.4 Stara Zagora

Only one sample from Stara Zagora (Augusta Traiana) was available for study. It belongs to the Regional Museum of History in Stara Zagora.

The sample was taken from a rim fragment of a crucible shown in Figure 10.13, which was excavated in 2006, and belongs to a late Roman (fourth-sixth century AD) context. It has some small green drops of metal in the rim, inner surface and fractures. The walls are lined (repaired?) with as secondary layer of clay, very thick on the rim and even present on (some of?) the interior.

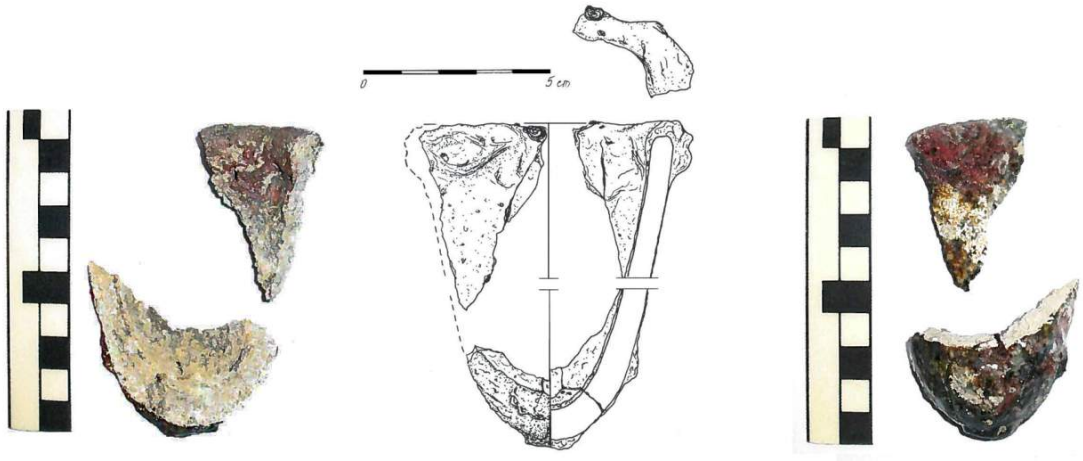

Figure 10.13: Crucible drawing (StZ1) from late Roman Stara Zagora

CHAPTER 11

Analytical results

Section 11.1

Detailed description of crucible ceramic and slag

Contrary to Pi-Ramesse and Gordion (Parts III and IV), this case study does not cover a (macroscopically) homogeneous assemblage. Rather, material from several sites is presented, with visible variability existing within each assemblage. For this reason, each site is discussed separately, with an overview given in section 11.3.
The layout of the following chapters differs further from the previous two, due to the more fragmented nature of the crucible remains. Where Pi-Ramesse and Gordion offered many large fragments for sampling, only a few pieces and flakes from diverse crucibles were available here, all of which were mounted for analysis. Therefore, it does not make sense to discuss general crucible characteristics for each site as for the other case studies. Rather, each sample must be discussed separately. However, the degree of detail described for each sample is limited, as within-crucible variability (Chapter 13) cannot be assessed on the basis of single samples, and the discussion of every occurring slag phase (sections 5.2.3 and 8.2.3) is less informative here.

Bulk compositions for ceramic and slag are presented in Appendix O, while the compositions of metallic prills embedded in crucible slag are given in Appendix P. The terminology used for various copper alloys throughout this chapter is shown schematically in Figure 11.1.
An important difference between these Roman and previously presented assemblages must

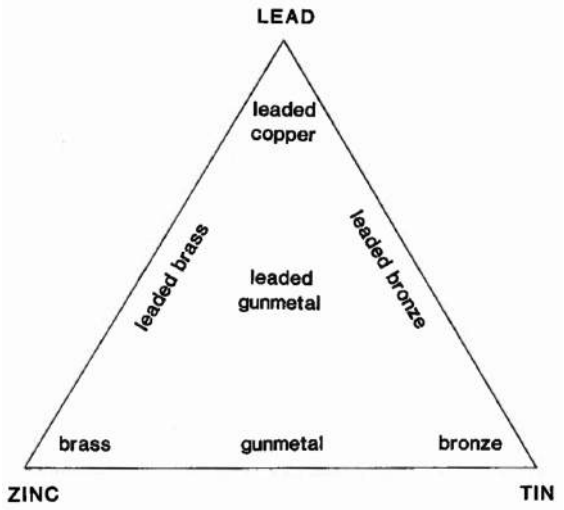

Figure 11.1: Terminology used for various copper alloys (from Bayley, 1998, Figure 1, p.8)

be noted. As slag layers are often quite thin in these crucibles, smaller frame sizes had sometimes to be used to measure their bulk compositions. Therefore, the comparison between ceramic (still measured at 100X) and slag (usually measured at 100X, but 200X where needed) is not always based on the same sample size.

11.1.1 Nicopolis ad Istrum

Three crucible groups (fragments N2, N4-N5 and N1-N3-N6) can be distinguished within the Nicopolis assemblage, based on their ceramic composition and fabric, as shown in Figure 11.2, and are discussed separately below. Figure 11.3 shows the bulk composition of crucible slag, relative to ceramic, for each crucible.

11.1.1.1 Fragment N2

The ceramic fabric of this fragment can be subdivided into an exterior and interior zone (Figure 11.4). For both zones, the ceramic consists of small, angular to sub-rounded quartz grains in a fine grey clay matrix, with elongated pores indicative of burnt out organic temper. In the exterior zone, a more brownish fine clay (without quartz fragments) is interwoven with the grey matrix. This is particularly so for sample N2a, for which the exterior zone composition does not overlap other N2 compositions (Figure 11.3): it has elevated lime and slightly elevated iron content. Furthermore, the exterior zone exhibits some cracks originating from the exterior surface, most likely formed during the metallurgical process. The interior ceramic zone has somewhat higher porosity.

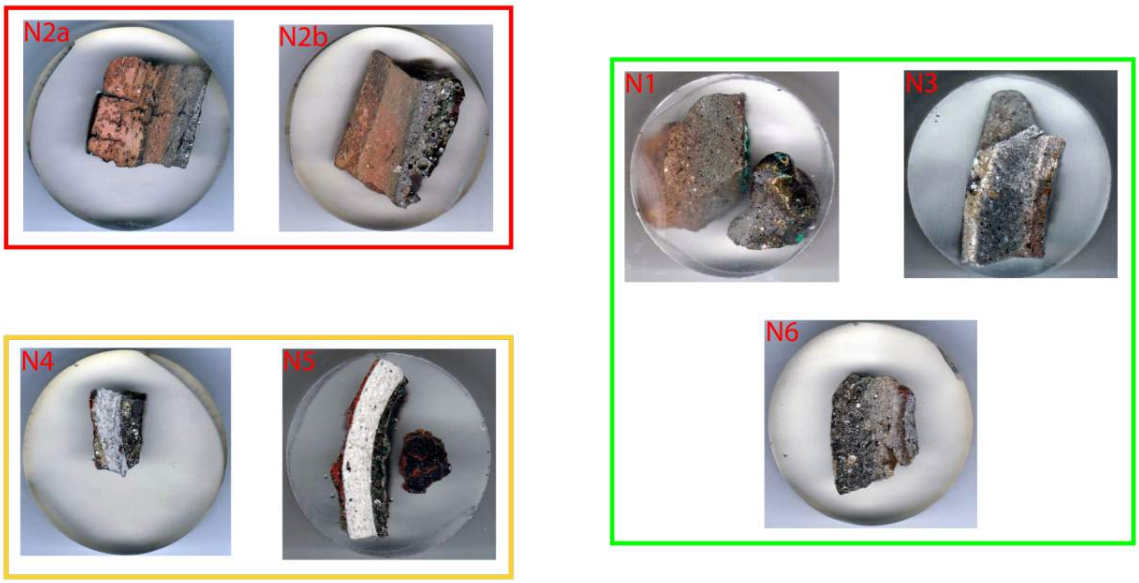

(a) Mounted sections

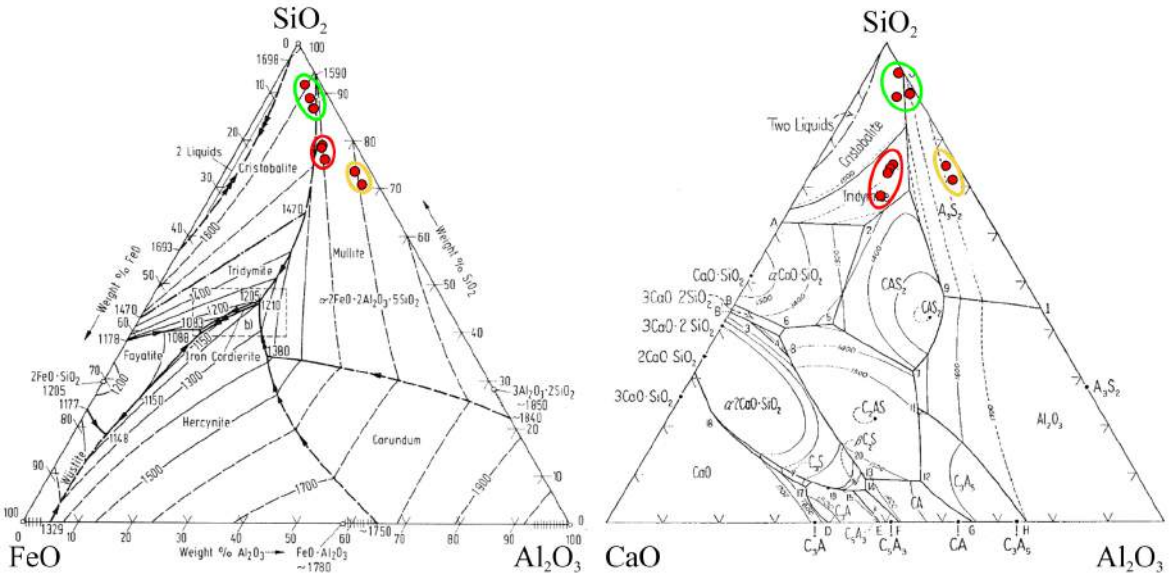

(b) Ternary diagrams showing compositional groups

Figure 11.2: Nicopolis ceramic groups

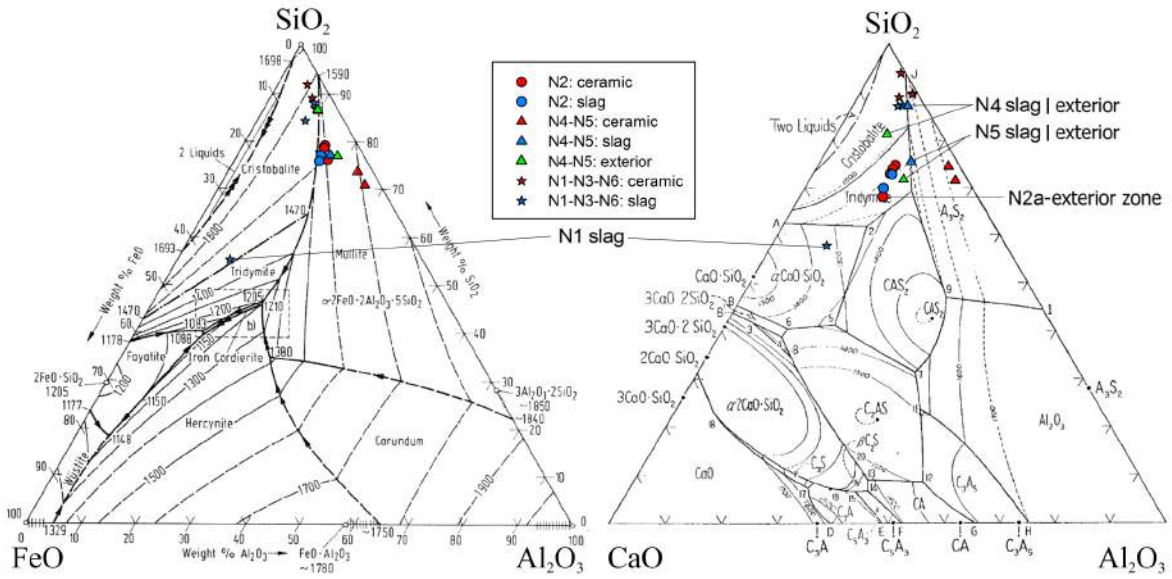

Figure 11.3: Nicopolis bulk compositions of ceramic and slag

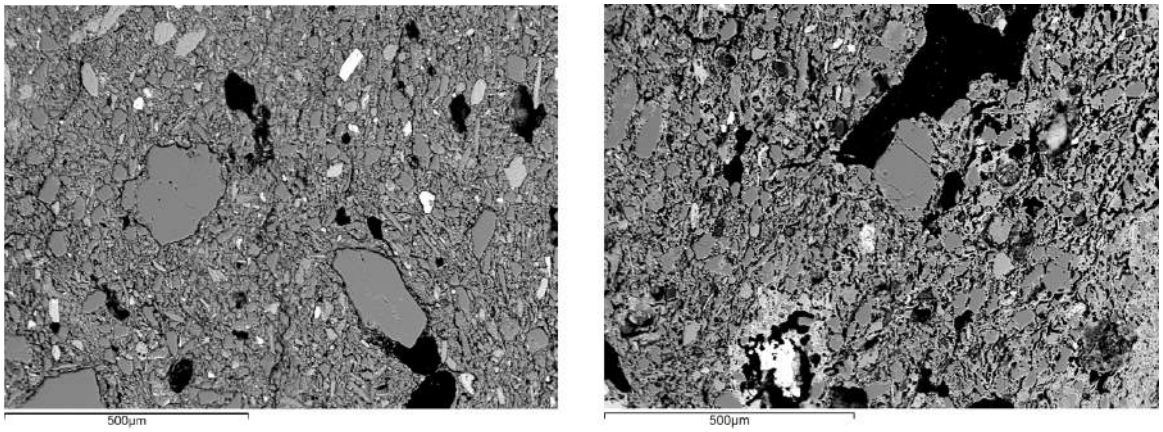

Figure 11.4: N2 ceramic fabric. Left: exterior zone, right: interior zone

The interior slag is not very well developed for sample N2a (Figure 11.5), and no metallic prills occur within the layer. For sample N2b, however, a more glassy slag layer has developed, within which many copper prills occur, all with 1-4 wt% iron and up to ±1 wt% tin or lead, associated with spinel crystals. No significant bulk slag enrichment in metal content can be noted (though minor copper content (0.5 wt% CuO) occurs in both ceramic and slag) and no other significant relative enrichments occur.

11.1.1.2 Fragments N4 and N5

These crucibles are quite thin-walled, made of highly refractory clay (white to light grey). The clay has fully fused, with fractured quartz being the only remaining original mineral

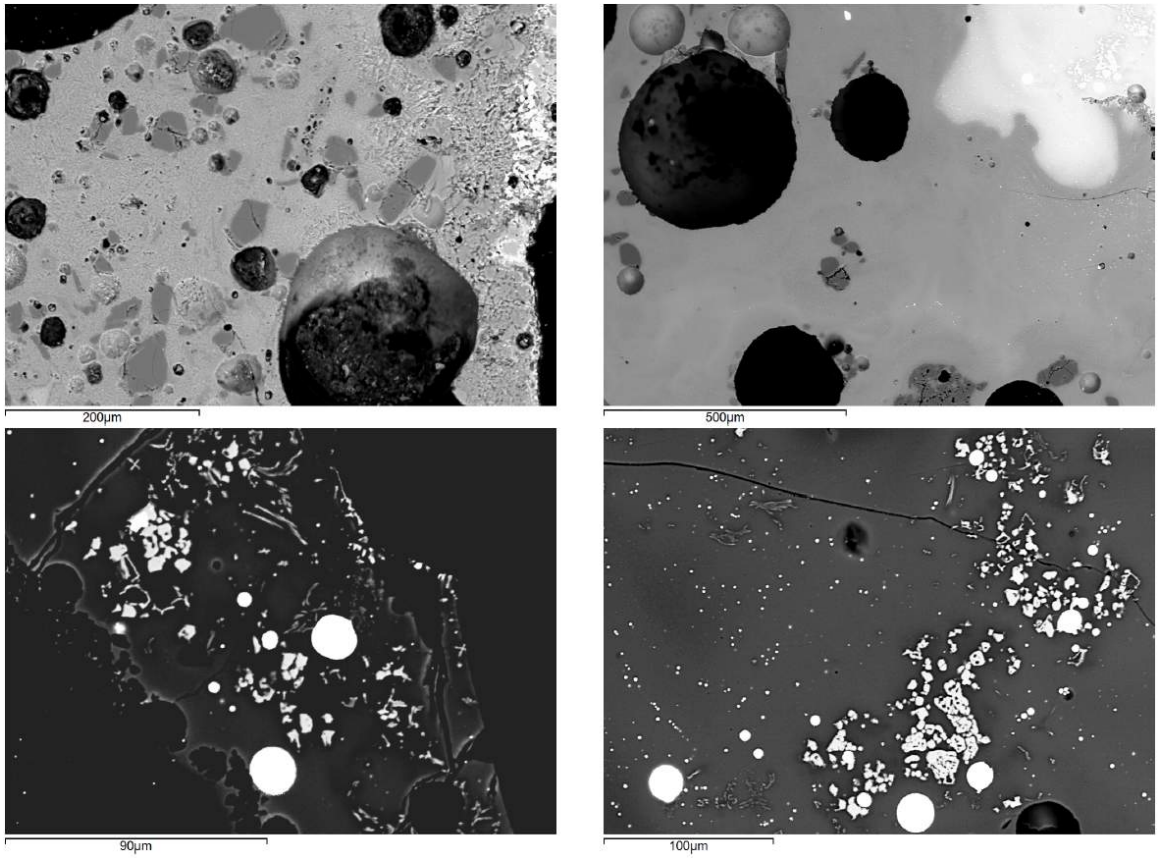

Figure 11.5: N2 slag (N2a: top left, N2b: top right), and prills embedded in N2b (bright, bottom) with spinel (light grey)

(Figure 11.6). N4 remains more porous than N5, which has vitrified almost completely. Both crucibles have a very thin, porous and glassy, reddish exterior layer.

In N4 no internal slag layer has developed, and the interior consists of bloated ceramic with (more) cracked quartz. In N5, a glassy slag layer has developed, as well as a corrosion/dross layer. Finally, a 'slag lump' of N5 was analysed, which consists of fused ceramic with some cracks filled in by glassy slag. These slag zones are illustrated in Figure 11.7.
Both bloated interior (N4) or slag (N5) and exterior vitrified layers show similar relative enrichments in iron ($\Delta^{FeO}/_{Al_2O_3} \approx 200\%$). There is a strong increase in lime for both interior and exterior layers, with more outspoken enrichment on the exterior (Figure 11.3). Lime and magnesia, potash and phosphorus oxide (Figure O.1) seem to increase proportionally[1], suggesting a single enrichment source (fuel ash). Strong soda enrichment exists as well. Lime and iron oxide do not share this proportional relationship.

The bloated interior of N4 does not show significant bulk enrichment in metal content, while a bulk increase in copper, zinc and lead oxide occurs for the interior slag layer in N5 (in the 'slag lump', only minor CuO-enrichment can be noted). Similarly, no metal prills were found embedded in N4, while a few iron-rich leaded bronze prills were found in N5 (and almost pure copper prills in the 'slag lump'). No zinc has been detected in the metal prills. Copper, zinc and lead are present as various (chlorine) oxides in N5, mainly in the corrosion/dross layer (Figure 11.7, bottom right).

11.1.1.3 Fragments N1, N3 and N6

These fragments have a wall thickness of 2-3 cm. N1 has a fine clay matrix, with very abundant, small to medium, sub-rounded quartz grains. N3 has a similarly high quartz content, but its matrix is mostly fused and bloated, with no real ceramic remaining (Figure 11.8). While N6 has a similar bulk composition, its fabric is quite different: it consists of quartz (often fractured closer to the exterior crucible surface) within a glassy phase, with no other clay minerals remaining. Interestingly, on top of the interior slag surface of N6, another ceramic layer is present, which is almost identical to the N1 ceramic in fabric and composition. The porosity in all crucibles is indicative of limited organic temper.

The interior zone of N1 consists of fully recrystallised slag, as shown in Figure 11.9. It exhibits extreme relative enrichment in iron ($\Delta^{FeO}/_{Al_2O_3} \approx 850\%$) and lime content ($\Delta^{CaO}/_{Al_2O_3} \approx 4000\%$), causing the big shift seen in Figure 11.3. There is a similarly strong relative enrichment in soda, potash, phosphorus oxide and magnesia. The slag shows further bulk

[1] Sample is too small for statistical evaluation of this statement.

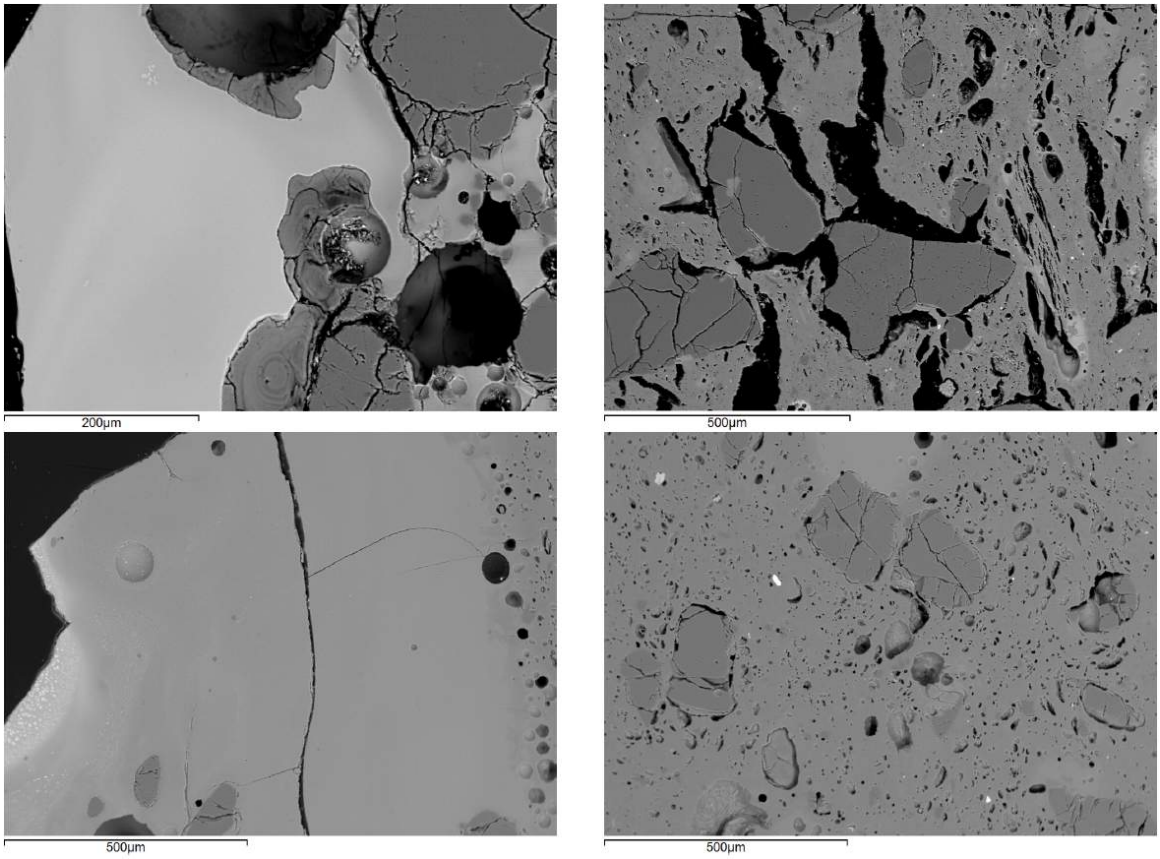

Figure 11.6: N4 (top) and N5 (bottom) vitrified exterior layer (left) and fused ceramic (right)

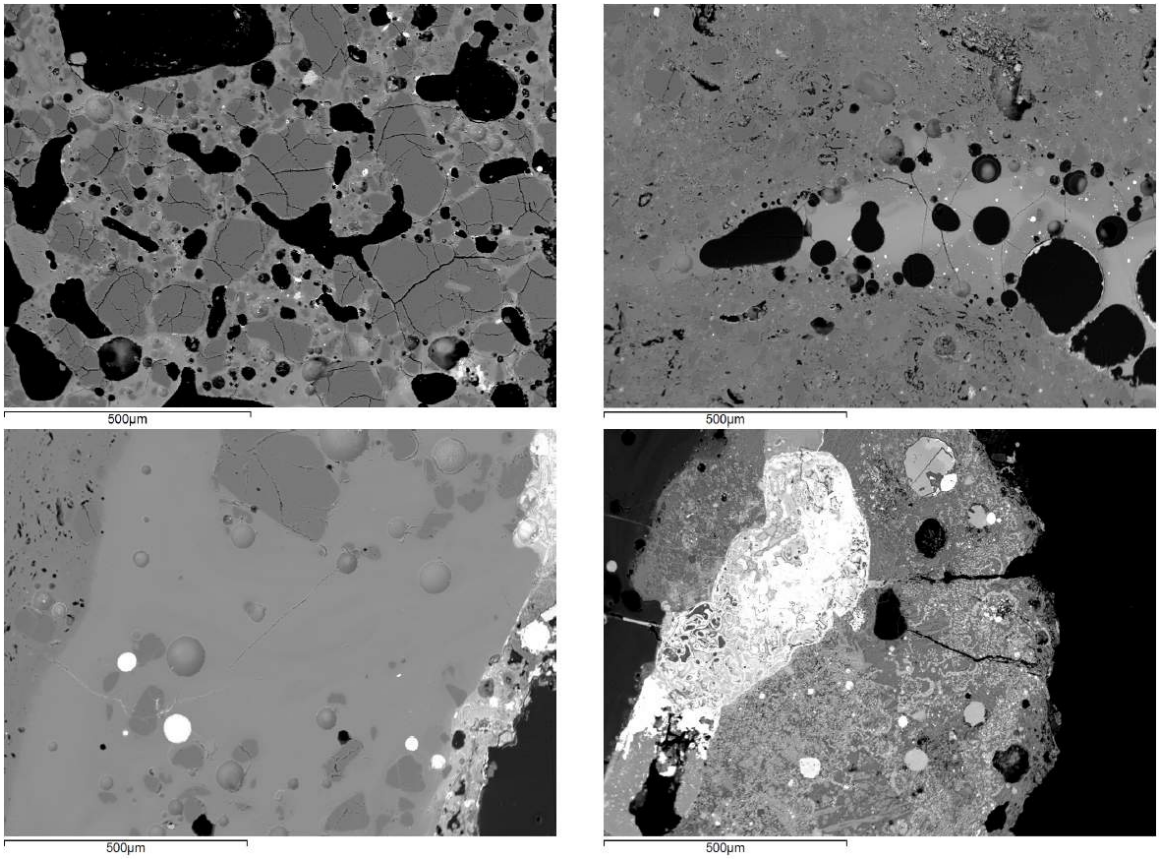

Figure 11.7: Bloated interior of N4 (top left), N5 'slag lump' (top right) and N5 slag and dross layer (bottom left and right)

enrichment in copper, zinc, tin and lead oxide, which is present in the form of malayaite ($Ca(Sn,Fe)(SiO_4)$ with iron substituting for tin), Pb in various states of oxidation (with minor iron substitution) and other Cu-Pb-Zn-Sn-Fe-oxides, some of which appear to have spinel-like structure (Fe_3O_4, with various elements substituting for iron). No metallic prills have been detected.

The slag layer of N3 is not as thickly developed, but consists of a thin glassy layer, in which several metal prills are embedded (Figure 11.10). It shows moderate iron enrichment and is enriched in fuel ash components (lime, soda, phosphorus oxide and magnesia). Strong bulk slag enrichment in copper, tin and zinc oxide can be noted (not in lead oxide). Several high-tin prills occur, typically averaging 30-40 wt% tin (with one prill containing 64 wt% Sn), sometimes accompanied by 1-2 wt% Pb. No zinc is found in the metallic state, but it occurs together with tin and iron in spinel-like crystals (approximately $FeSnZn_{1-2}O_7$-$FeSnZn_{2-3}O_{10}$). Lead is only found in the metallic state.

Finally, the slag layer of N6 (Figure 11.11) does not show any significant changes in bulk composition relative to the ceramic, with the exception of strongly elevated tin and lead content and modestly elevated copper content. This occurs mainly as low-tin (3-4 wt% tin) prills, a high-tin bronze prill (35 wt% tin) and various copper-lead oxides and tin-lead oxides (SnO_2 with up to 5 wt% Pb).

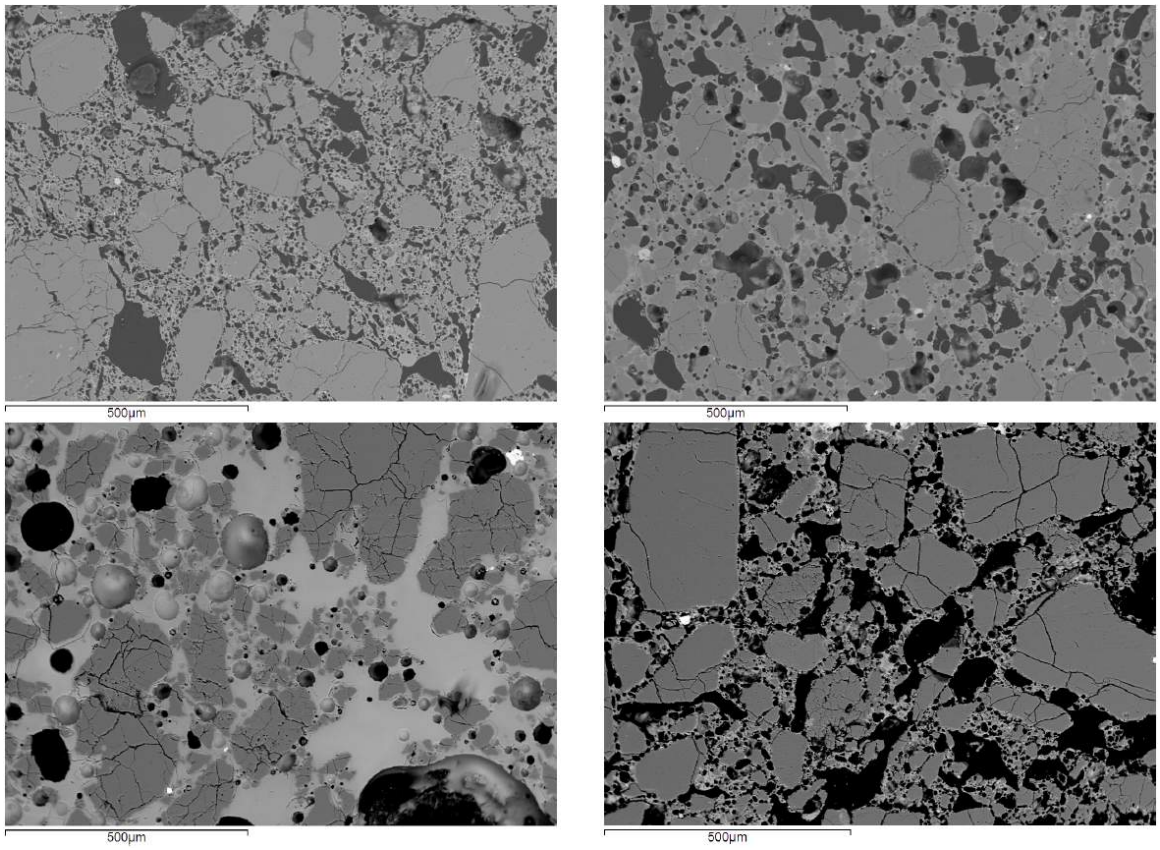

Figure 11.8: Top: N1 (left) and N3 (right) ceramic. Bottom: N6 ceramic (left) and interior ceramic layer (right)

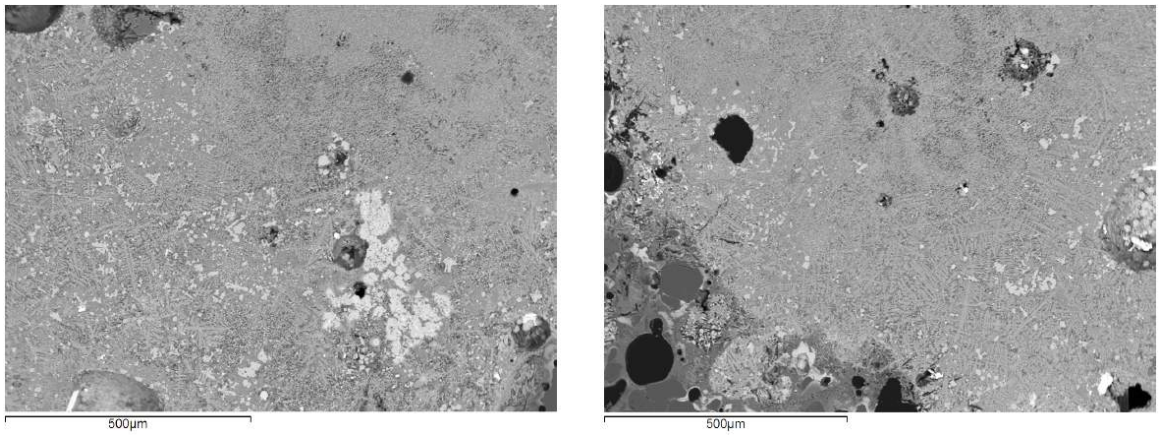

Figure 11.9: N1 slag layer with malayaite (light grey) and spinel-like oxides (medium-light grey)

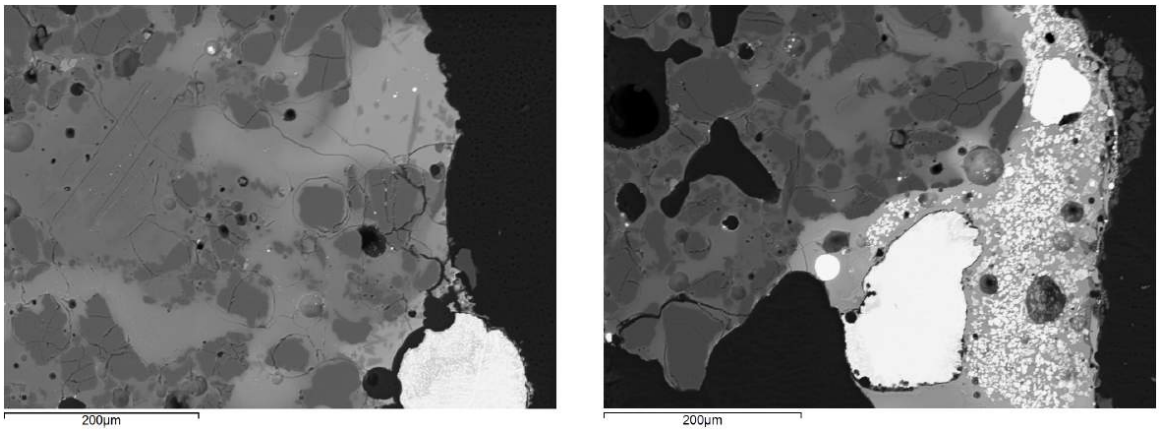

Figure 11.10: N3 slag layer with high-tin prills (bright) and Fe-Sn-Zn oxides (light grey)

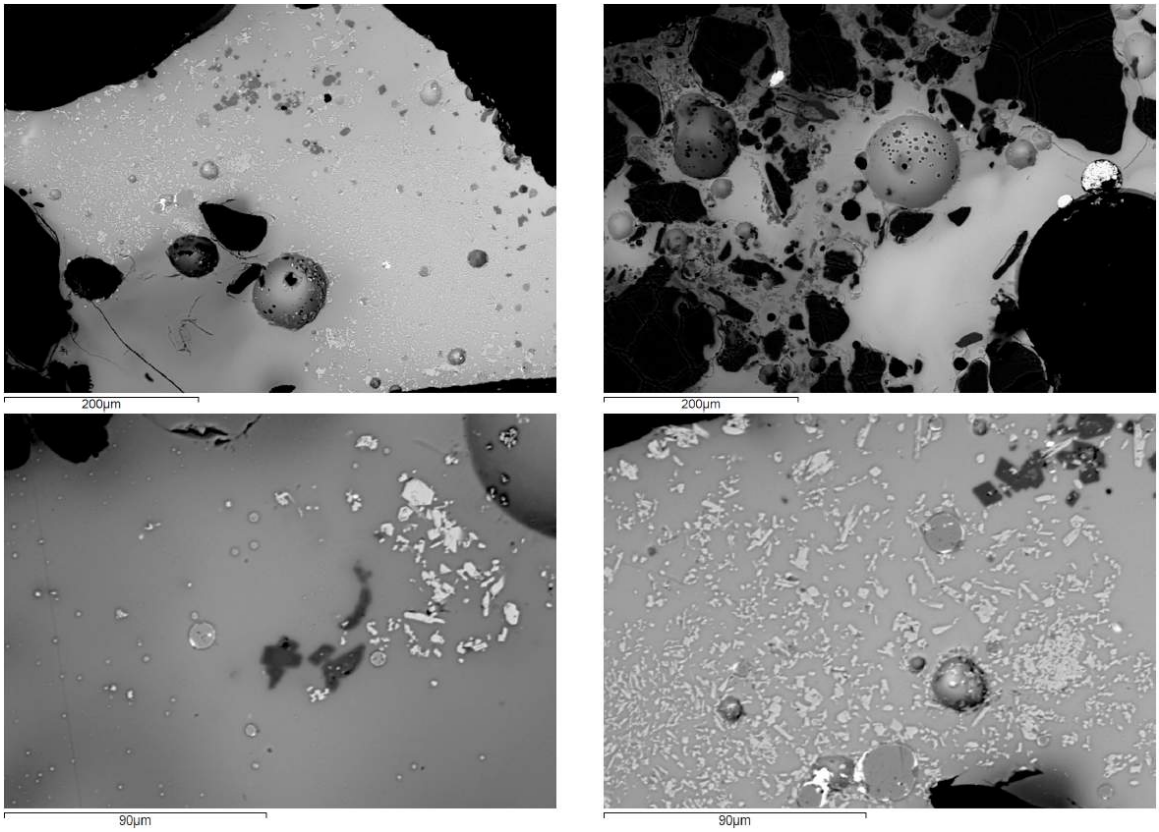

Figure 11.11: N6 slag layer (top) and SnO_2 with elevated lead content (bottom, light grey angular phases)

11.1.2 Philippopolis

Based on the ceramic composition and fabric, three groups of crucibles can be distinguished within the Philippopolis assemblage, as shown in Figure 11.12. The 'dark blue group' (P2-P5) has no preserved ceramic fabric, and is therefore not shown on Figure 11.12b. This grouping is therefore not as convincing as for Nicopolis: the 'red group' consists of two samples taken from the same crucible, while the 'olive group' (stroke outline) is not tightly defined and exhibits macroscopic variation. Hence, the discussion below is organised by context (see section 10.2.2). Ternary diagrams for ceramic and slag compositions are shown in Figure 11.13.

11.1.2.1 Fragments P1-P5

Sample P1 (Figure 11.14) consists of ceramic to vitrified ceramic (it is impossible to measure ceramic and slag separately). Its bulk composition is the closest approximation available to 'ceramic composition' for this group of crucibles (P1-P5). Prills sampled for P1 are pure copper (with lead and zinc oxides) and leaded brass (±6 wt% lead and 4-8 wt% zinc).

For P2-P5, only dross is available for analysis, as reflected in the low bulk alumina and silica content (Appendix O.2.1). Relative to P1, samples P2-P5 show relative increases in lime and phosphorus oxide content and P2-P4 in iron oxide as well. Some examples of this dross are shown in Figures 11.15 and 11.16.

Sample P2 contains many Cu-Sn-Zn-Pb oxides, of highly variable composition (typically $\pm(Cu,Sn,Zn,Pb)_2O_3$). Various low- to high-tin prills occur (Figure 11.16a), with variable lead (up to 4 wt%) and rare antimony (1 wt%).

Sample P3 comprises many corroded prills, with only limited dross available for analysis (2 areas for bulk analysis). Within the dross, one leaded bronze prill (medium/high-tin) with minor antimony occurs.

Sample P4 again contains many (partially) corroded prills with minor dross adhering (Figure 11.16b), though some metallic high-tin (34-36 wt% Sn) prills exist as well. One of these incorporates 0.9 wt% Co, and a bulk dross content of 0.4 wt% CoO can be noted (at detection limit).

Sample P5 has a more developed slag component (higher lime content), within which black angular slag crystals ($\pm Ca_2Si_2ZnO_{7-8}$) and light grey angular crystals ($\pm SnZn_2O_6$) occur (Figure 11.16c). It further contains pure copper prills with cuprite dendrites and undissolved lead droplets (Figure 11.16d).

(a) Mounted sections

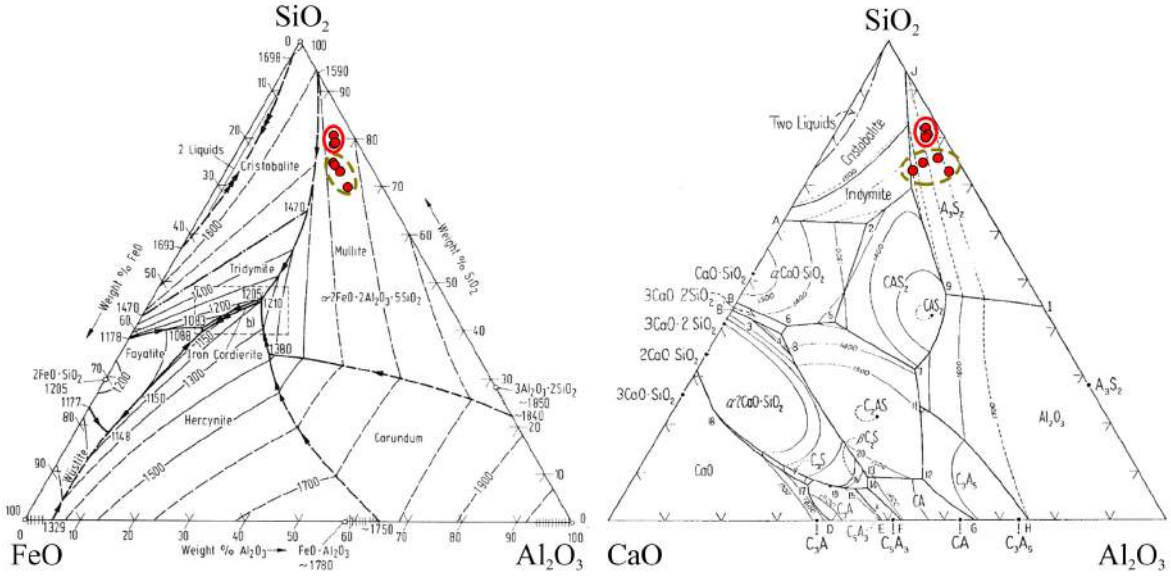

(b) Ternary diagrams showing compositional groups

Figure 11.12: Philippopolis ceramic groups

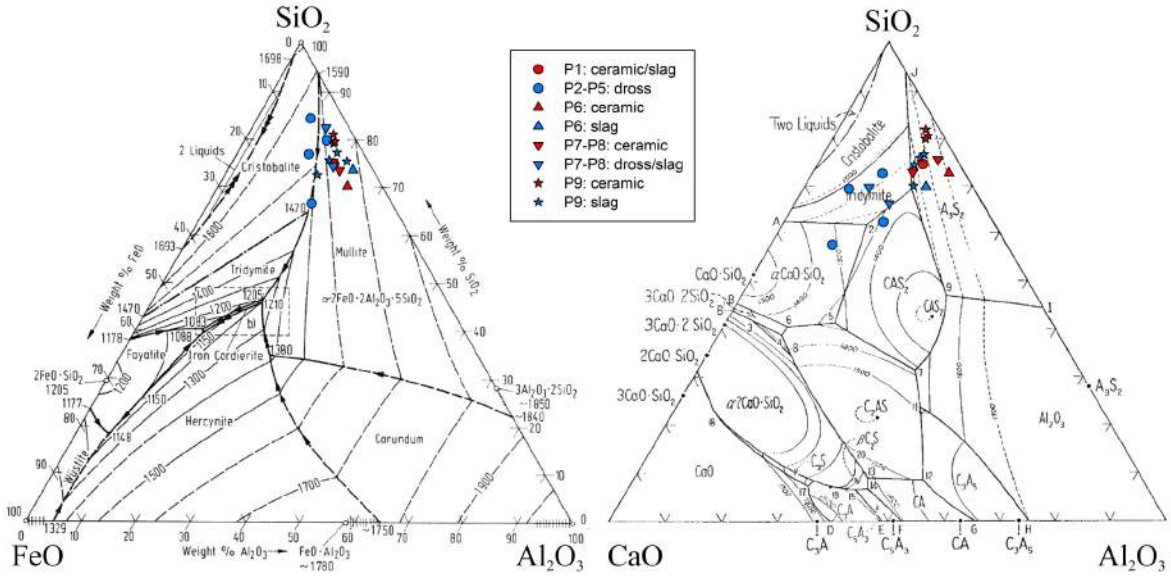

Figure 11.13: Philippopolis bulk compositions of ceramic and slag

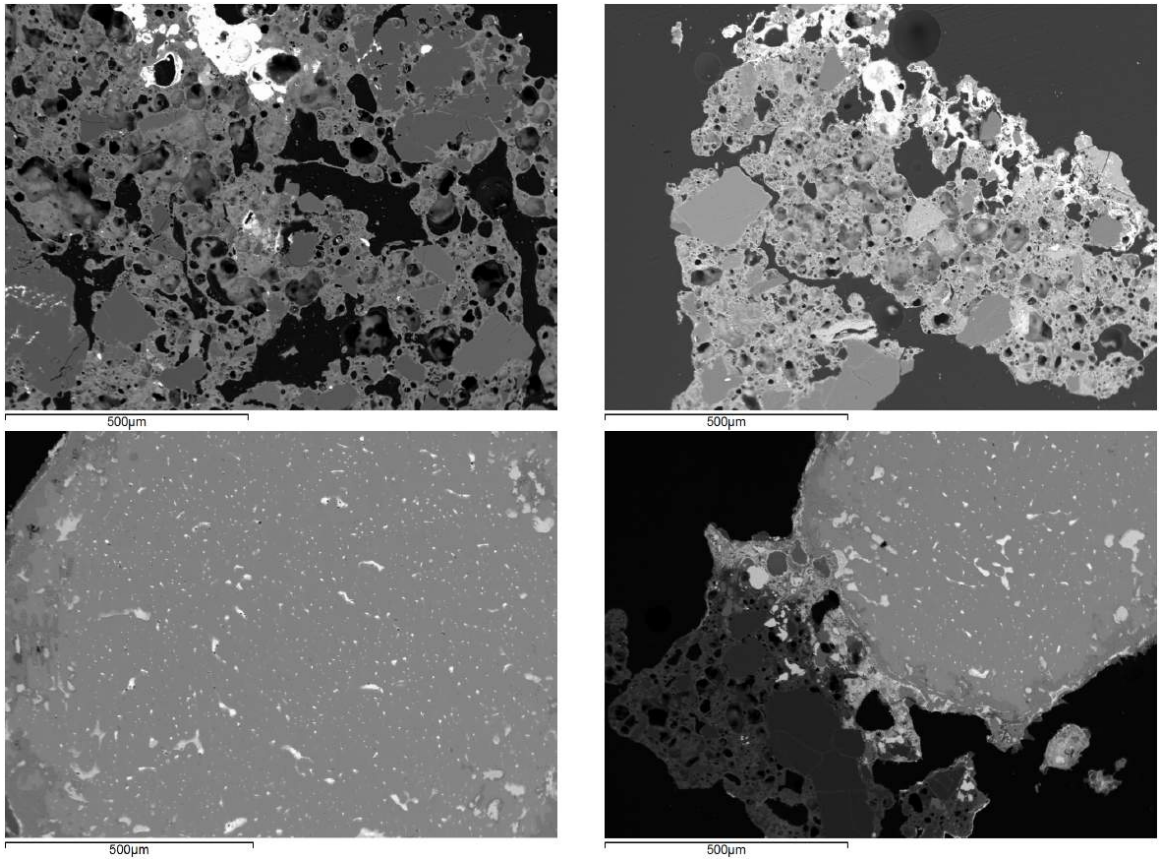

Figure 11.14: Sample P1: (vitrified) ceramic (top) and leaded brass prills (bottom)

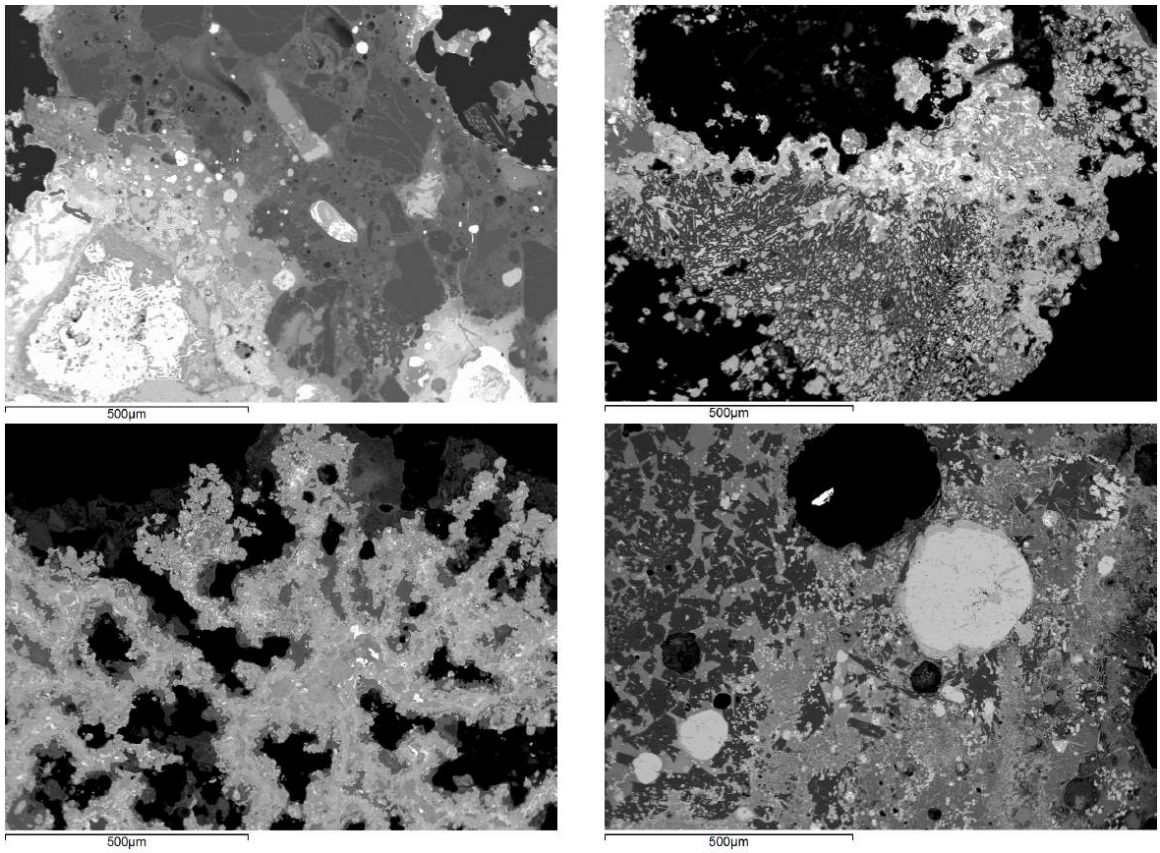

Figure 11.15: Examples of dross from sample P2 (top left), P3 (top right), P4 (bottom left) and P5 (bottom right)

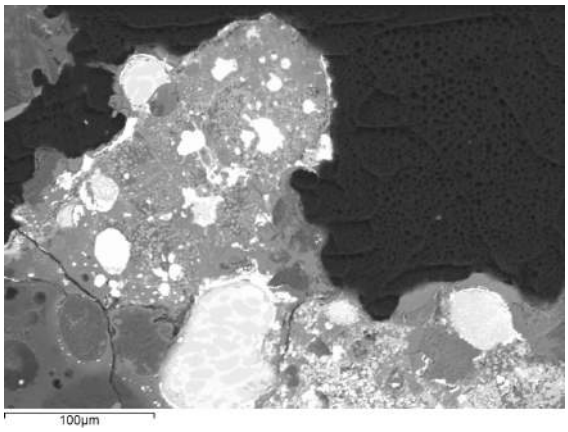

(a) Small prills in P2

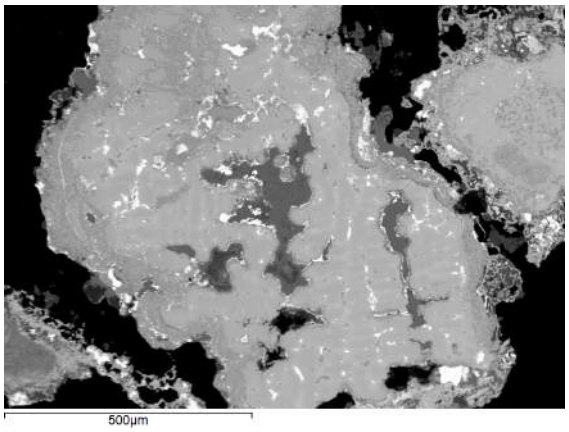

(b) Corroded prills in P4

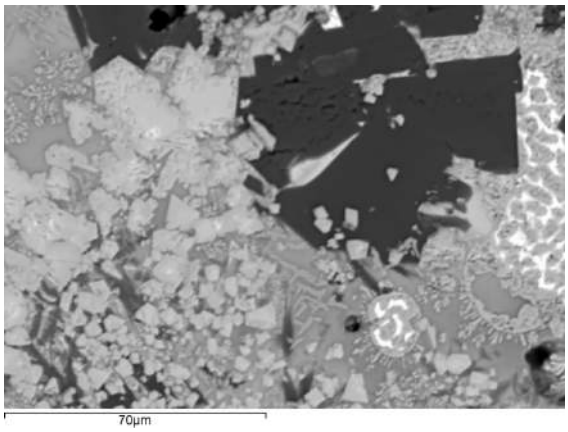

(c) Tin- and zinc-bearing crystals in P5

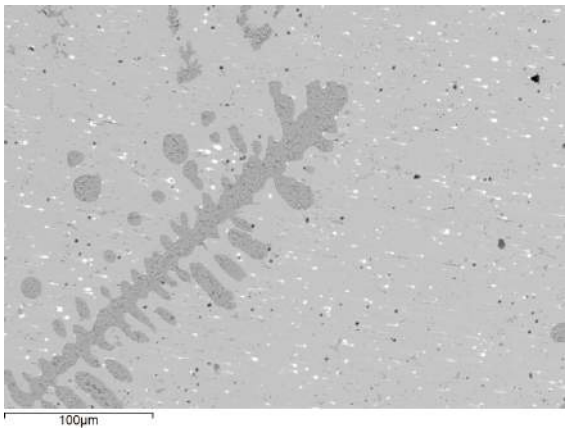

(d) Prill with dendritic cuprite and undissolved lead, P5

Figure 11.16: Dross details in samples P2-P5

11.1.2.2 Fragment P6

The crucible fabric is almost entirely fused, with only some fractured quartz remaining of the original ceramic. An almost pure iron prill was noted within the 'ceramic' area.
The crucible exterior is bloated and fully vitrified in places, and contains almost pure iron prills with 2-4 wt% copper.
The crucible interior is less vitrified than the exterior surface, contains residual fractured quartz, and exhibits various copper oxides, sometimes incorporating lead, which are mostly corroded prills. Very few, tiny metallic slag prills (copper with low tin and high iron content) remain. The various areas are illustrated in Figure 11.17.

11.1.2.3 Fragments P7-P8

Sample P7 (Figure 11.18) consists of dross fragments (though one small 'ceramic' fragment has been analysed). These are composed of various copper oxides (mainly cuprite) and Cu-Sn-Zn-Pb oxides of highly variable composition, with very low 'slag' content (alumina, silica or lime). Within all this corrosion, some metal phase remains, which is all brass (2-8 wt% Zn), surrounded by the Cu-Sn-Zn-Pb oxides.

Sample P8 (Figure 11.19) is a crucible wall cross-section, for which the ceramic, slag, exterior and dross areas have been analysed. The ceramic consists of a fine matrix with small to medium, angular quartz and some elongated porosity, indicative of organic temper.
The exterior surface is slightly bloated, but not vitrified.
The interior slag contains many silver chloride (no true AgCl; mostly limited chlorine) prills and some silver sulphides (Ag_2S), occasionally including minor (<2 wt%) copper or iron, but no metallic silver. Some dross is present as well, with increased calcium, sulphur, silver, tin and lead oxide content and low alumina and silica.

11.1.2.4 Fragment P9

Samples P9a and P9b were taken from the same fragment, shown in Figure 11.20. Two layers of ceramic and slag can be seen superimposed on each other: the primary (interior) sequence and a secondary use sequence.

P9a comprises the top of the rim. Though some remnant primary ceramic and slag remains, the sample contains mainly secondary slag (no ceramic).
The primary slag layer sits in between the primary and secondary bloated ceramic, as shown in Figure 11.21, and is separate from the secondary slag layer with which it fuses

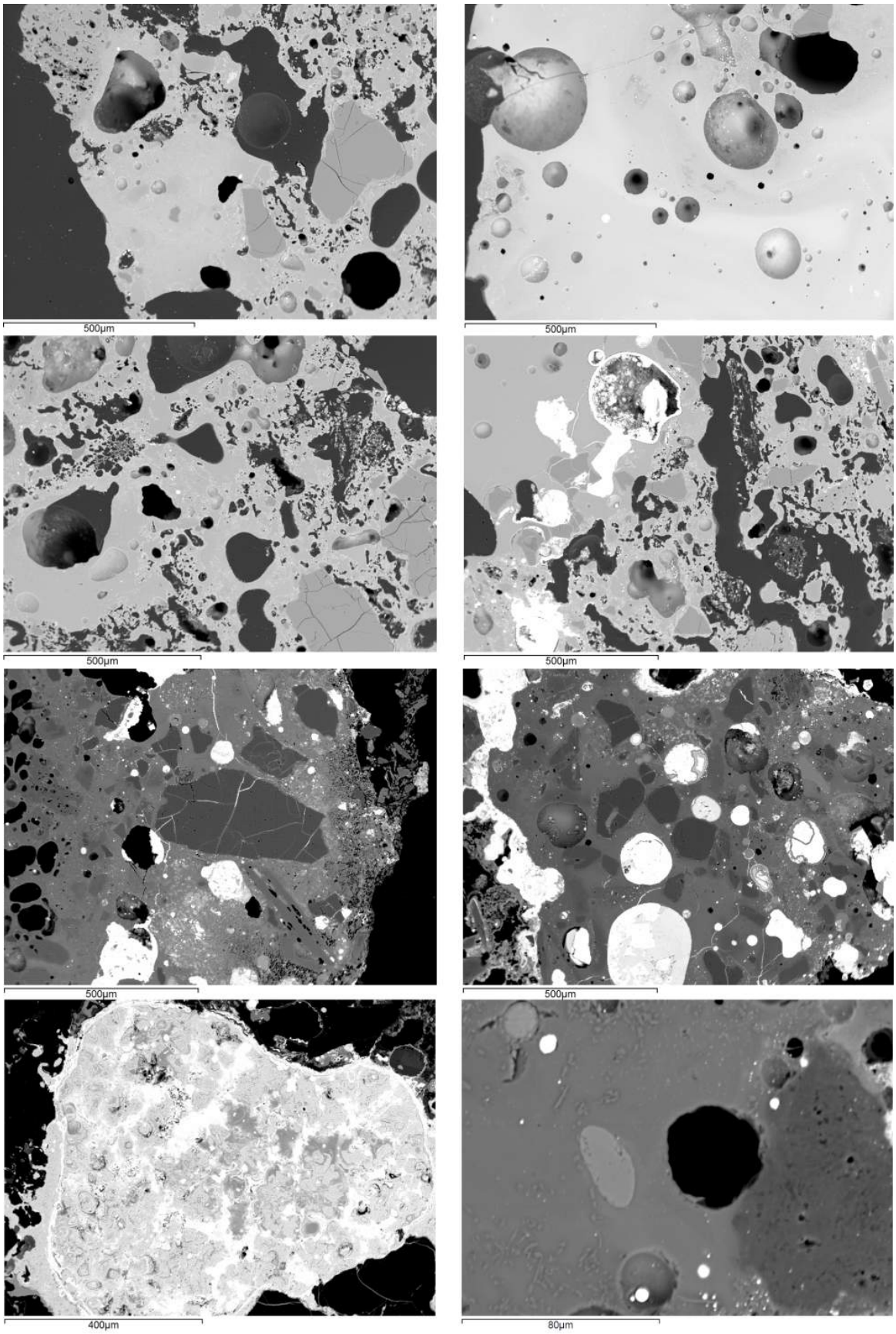

Figure 11.17: Overview of fragment P6. Top: bloated and vitrified external surface, 2^{nd} row: fused crucible fabric, 3^{rd} row: interior slag layer, bottom: interior slag: corroded prills (left) and tiny metallic prills (right)

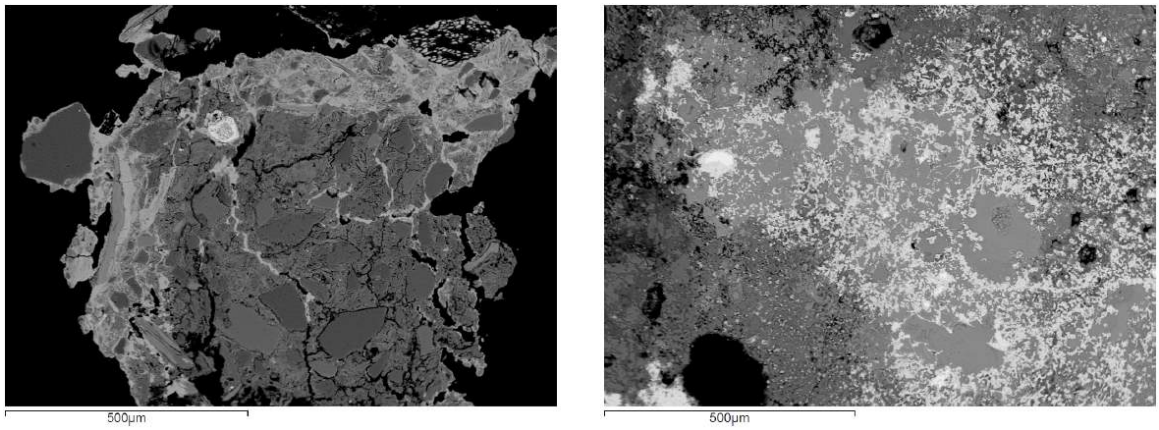

Figure 11.18: Fragment P7 'ceramic' (left) and dross (right)

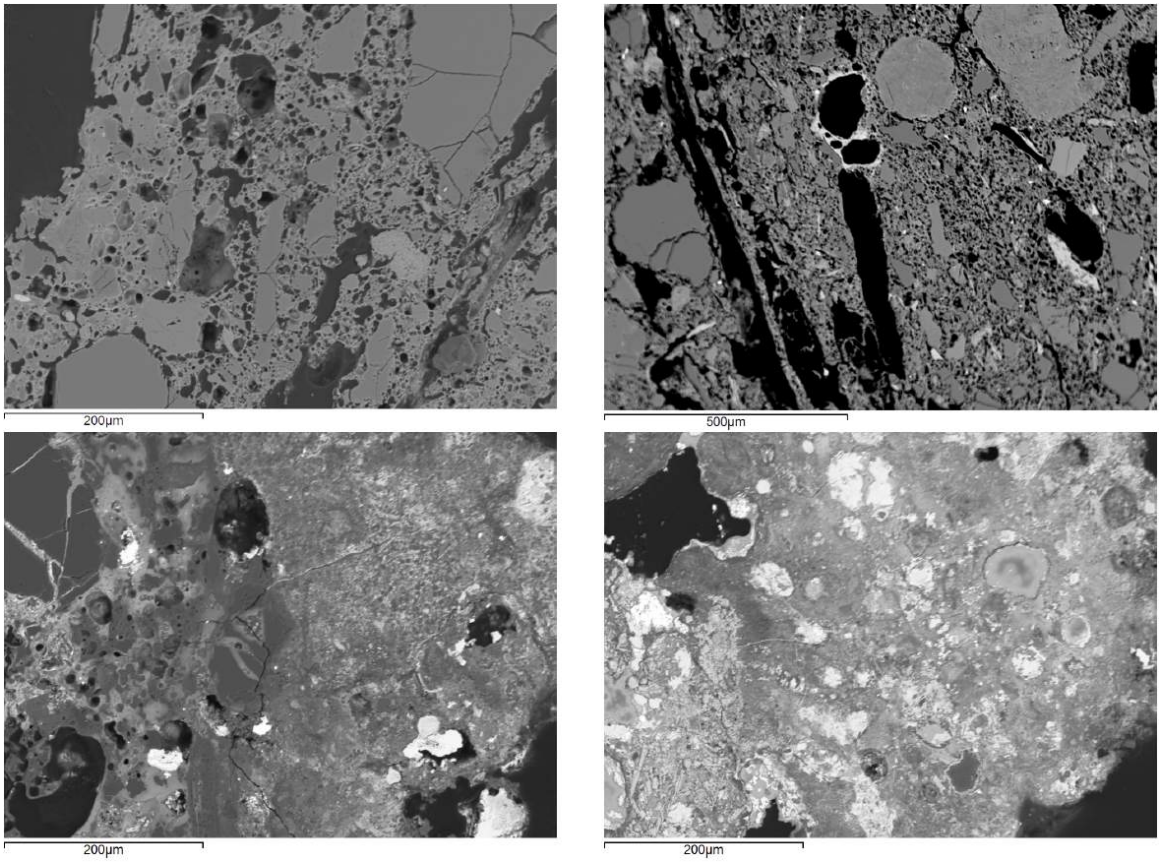

Figure 11.19: Fragment P8 exterior surface (top left), ceramic (top right), slag (bottom left) and dross (bottom right)

Figure 11.20: Fragment P9

only at the top of the crucible rim. It contains mainly pure copper prills and some bronze, with up to 15 wt% Sn. Interesting tin oxide structures occur, some of which might be identified as residual cassiterite (Figure 11.22).
Some tiny prills occur in the thin secondary (surface) slag layer, which are all pure copper (with <1 wt% Fe), and some high-temperature tin oxide crystals are present (Figure 11.23).

P9b better exhibits the two ceramic-slag layers. The ceramic is similar in both layers (and chemically identical, within analytical error), consisting of small to large (sometimes fractured) quartz grains in a porous fine matrix, which is more fused in the secondary layer (Figure 11.24).
The primary (interior) slag (Figure 11.25) contains many leaded bronze prills (1.5-3.5 wt% lead and 11-24 wt% tin, some iron) and some spinel, with up to 10 wt% Zn and 10 wt% Sn. Comparison of the primary slag layer in the two samples shows relatively higher-tin prills occurring lower on the rim.
The secondary (surface) slag layer (Figure 11.26) is again not as well developed: it is thin and contains less and smaller prills. However, many high-temperature tin oxides and various Fe-Cu-Sn-Zn-Pb oxides ($\pm$(Fe,Cu,Sn,Zn,Pb)$_2$O$_3$) occur.

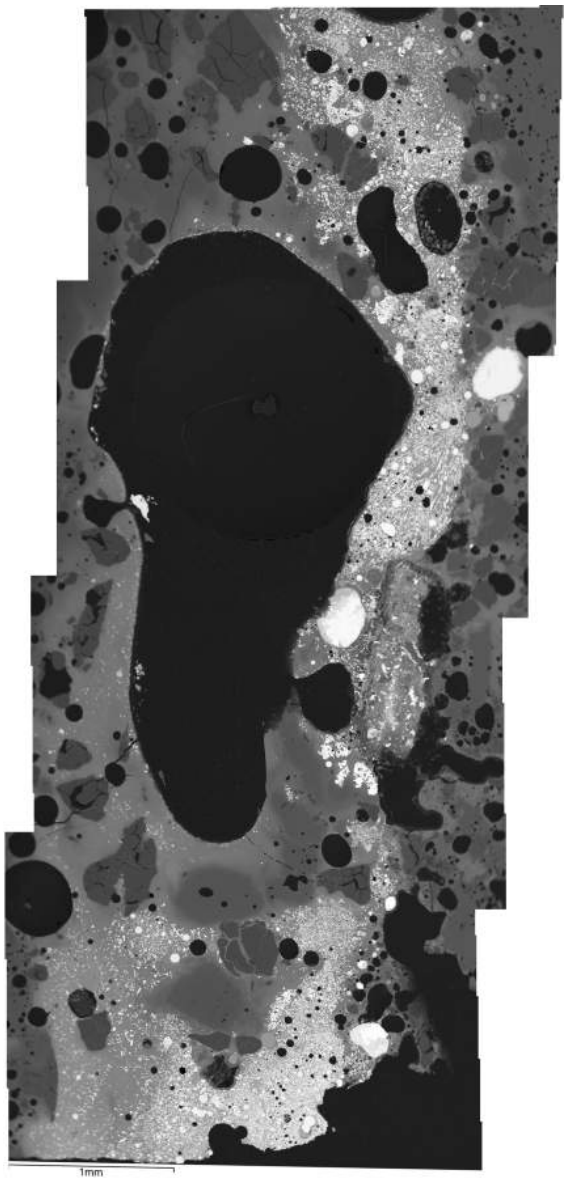

Figure 11.21: Sample P9a: primary slag layer in between two bloated ceramic layers (composite SEM image)

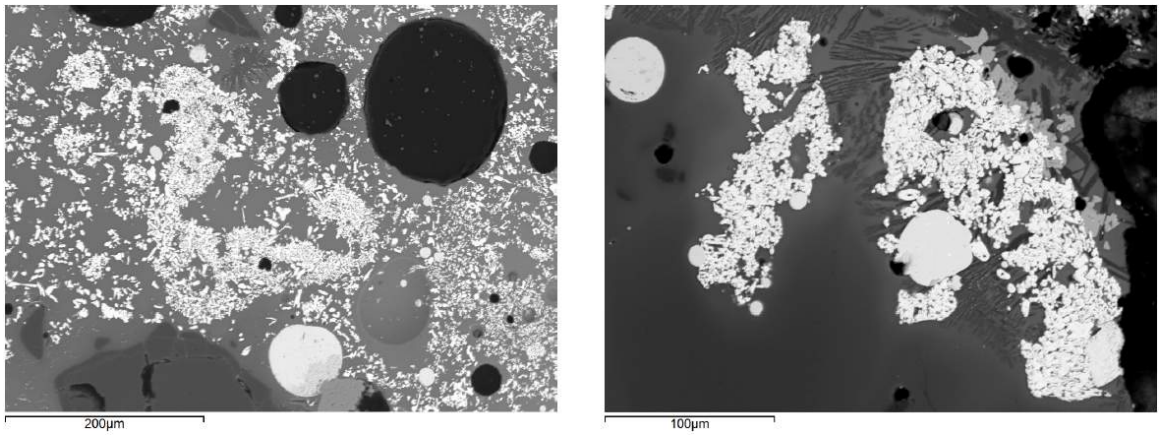

Figure 11.22: Sample P9a: possible residual cassiterite

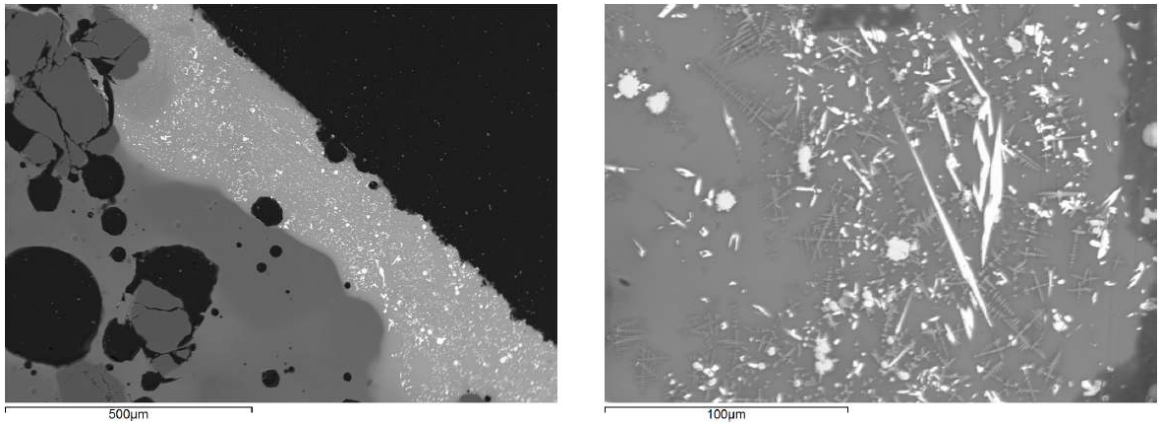

Figure 11.23: Sample P9a: thin secondary slag layer (left) with high-temperature tin oxide crystals (right)

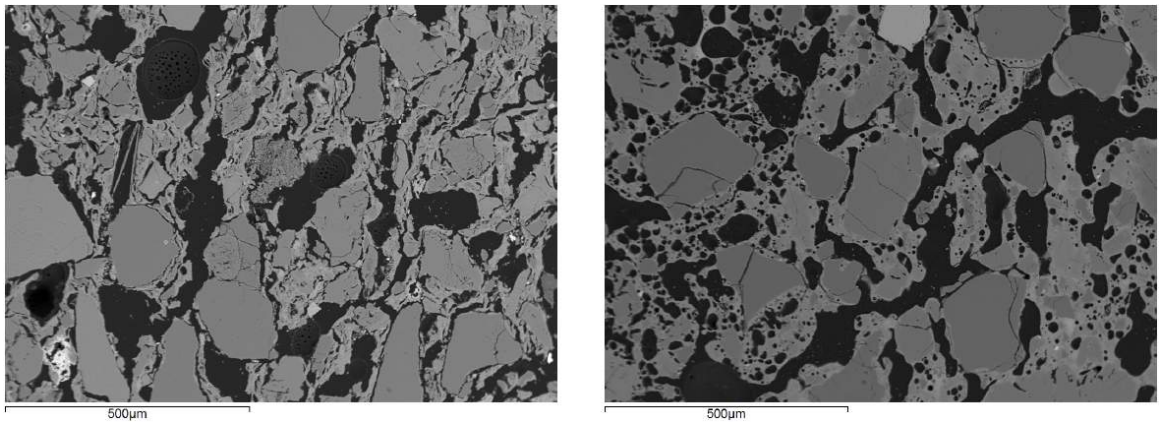

Figure 11.24: Sample P9b: primary (left) and secondary (right) ceramic layers

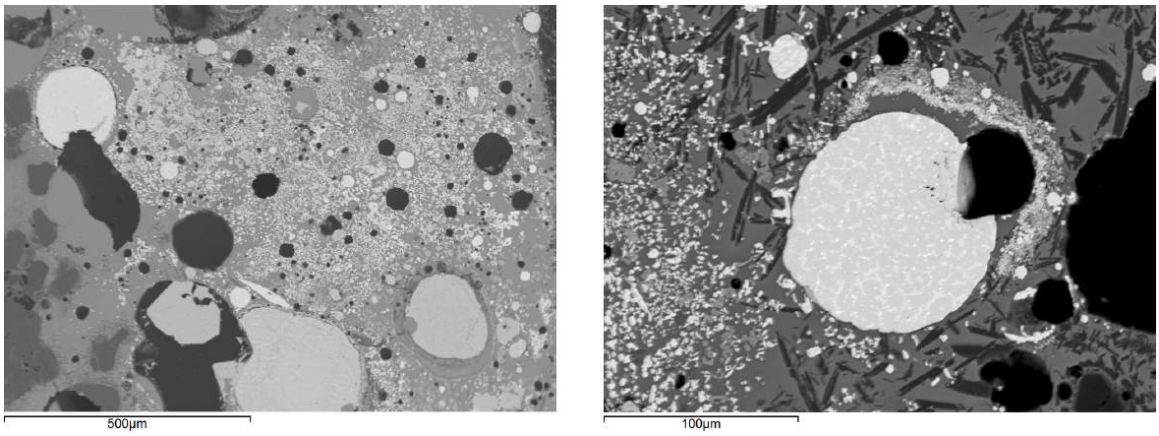

Figure 11.25: Sample P9b: primary slag layer (left) with leaded bronze prills (right)

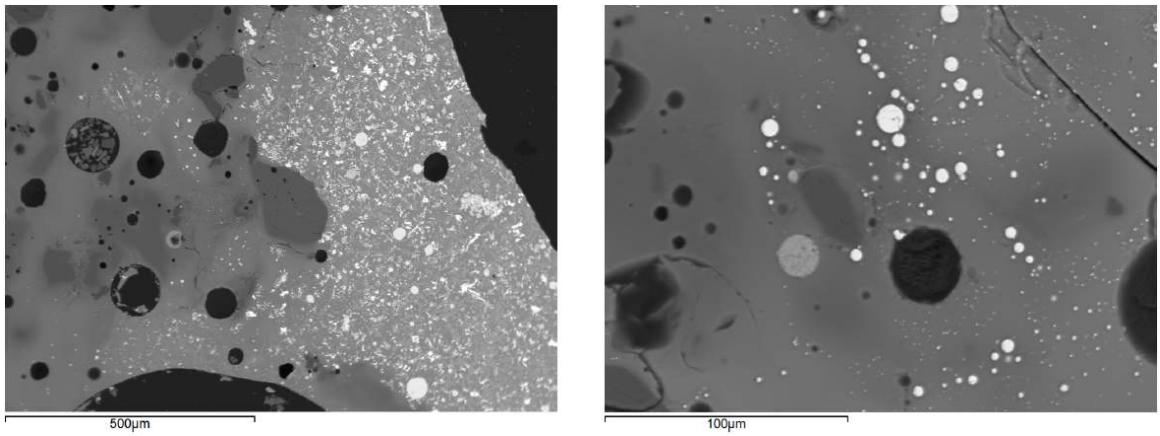

Figure 11.26: Sample P9b: secondary slag layer (left) with small prills (right)

11.1.3 Serdica

Based on the ceramic composition and fabric, four groups of crucibles can be distinguished within the Nicopolis assemblage, as shown in Figure 11.2. The 'dark blue group' (S2 and S8) has no preserved ceramic fabric, and is therefore not shown on Figure 11.12b. This grouping does not follow the contextual segregation of samples (section 10.2.3), which is followed below. The ceramic grouping is noteworthy, however, and is addressed in section 11.2.3. Ternary diagrams for ceramic and slag compositions are shown in Figure 11.28.

11.1.3.1 Fragments S1-S2

Despite not being intentionally sampled (see section 10.2.3), fragments of two different ceramic fabrics (Figure 11.29) occur in sample S1: ceramic A has elongate feldspar/feldspathoid[2] matrix with small-medium angular quartz grains, ilmenite, zircon, monazite ($(Ce, La, Nd)PO_4$) and $(FeS)_2SO_2$. Ceramic B has no elongate feldspar/feldspathoid minerals (though some small grains may occur) and is dominated by small angular quartz grains.
The slag fragments (Figure 11.30) are porous and contain no metallic prills, but many silver sulphides[3]. Their bulk composition shows a modest relative increase in fuel ash and iron oxide. One silver prill with 2.5 wt% copper and a few silver prills with minor cadmium were embedded as well (not within slag).

Sample S2 consists of metal sulphides only: no ceramic, slag or dross was sampled. The sulphides (Figure 11.31) are the same as those described for S2: some pure silver sulphide (Ag_2S), but mainly iron-silver sulphides with variable substitution of silver by copper (up to 31 wt% Cu).

11.1.3.2 Fragments S3-S4

The crucible fabric in S3 (Figure 11.32) is fully fused but remains fairly porous, with no ceramic remaining except the medium, angular, fractured quartz grains and some zircon. The interior surface is bloated, but no true slag has developed. No metallic prills or significant enrichments of any kind (except a relative increase in soda) can be noted.

The crucible fabric in S4 (Figure 11.33) is mainly composed of graphite, interspersed with vitrified ceramic which makes up the bulk composition (SEM-EDS cannot distinguish be-

[2] Feldspar/felspatoid in S1: $\pm(K,Fe,Mg)(Si,Al)_3O_5$ and $\pm(Na,K,P)Si_6Al_5O_{20}$ (not a correct formula; composition (in at%) is: 59.5 O, 0.9 Na, 0.5 Mg, 15 Al, 19 Si, 2.2 P, 2.0 K, 0.3 Ca, 0.1 Ti 0.5 Fe.)

[3] Silver sulphides in S1: $AgFeS_2$, $(Cu,Ag,Fe)S_2$ with Cu/Ag/Fe ≈ 15/1/9, $\pm Ag_4Fe_4(SO_3)_3$ and $\pm(Cu,Ag)Fe_2(SO)_2$ with Cu/Ag ≈ 1/4 - 1/1

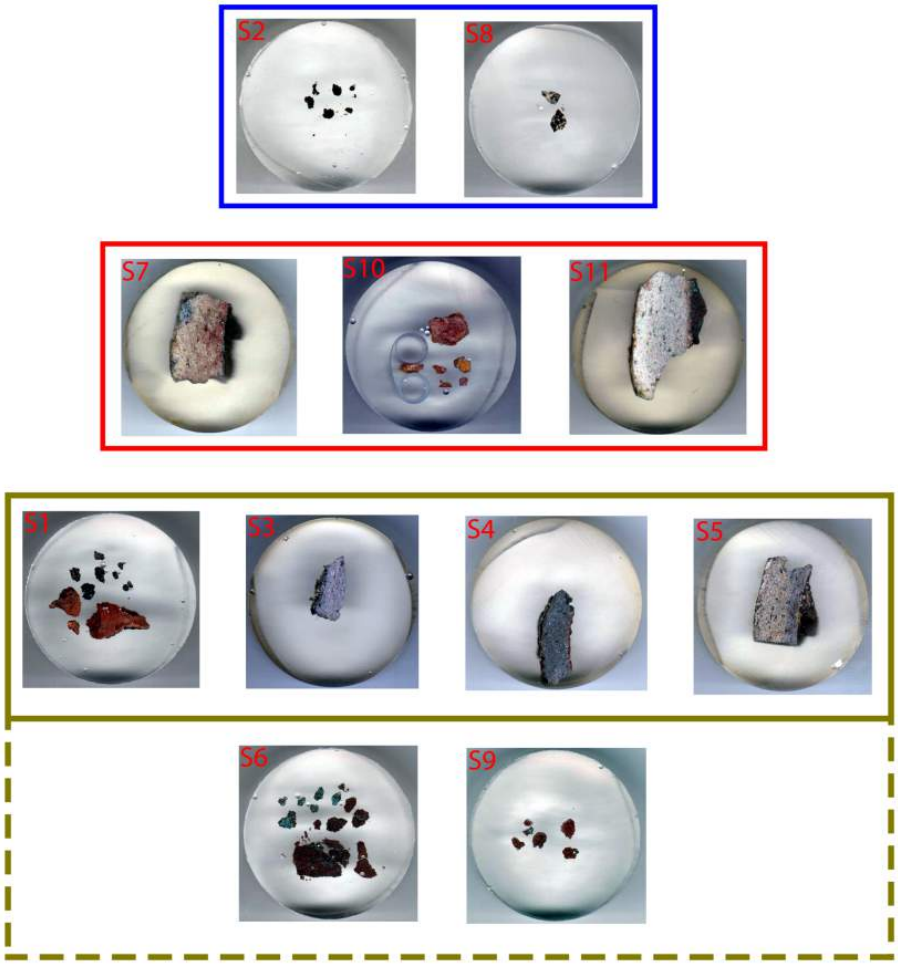

(a) Mounted sections

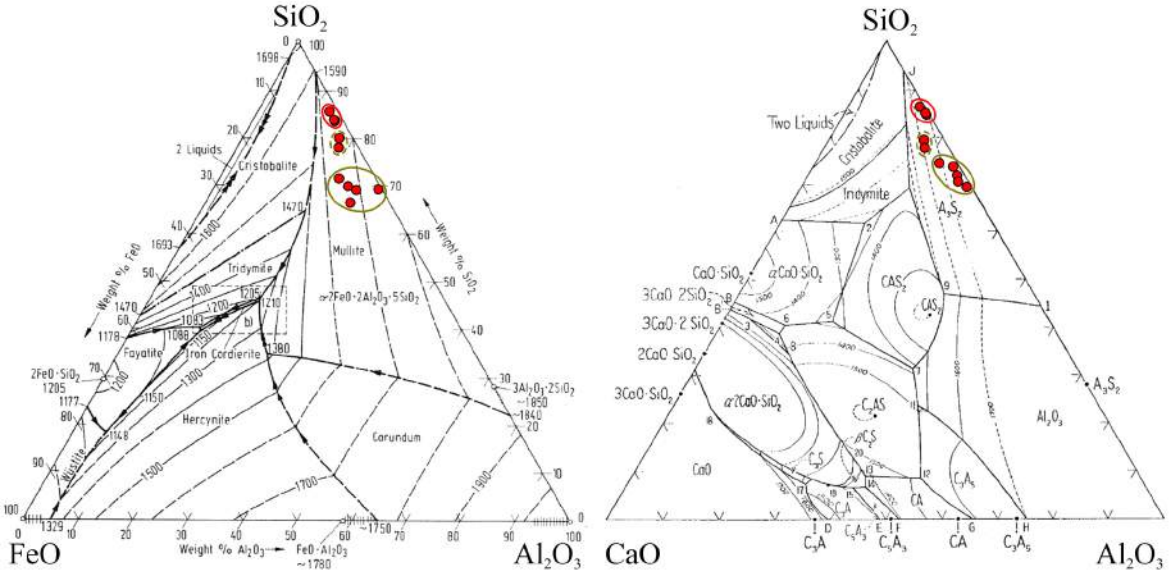

(b) Ternary diagrams showing compositional groups ('blue group' has no preserved ceramic)

Figure 11.27: Serdica ceramic groups

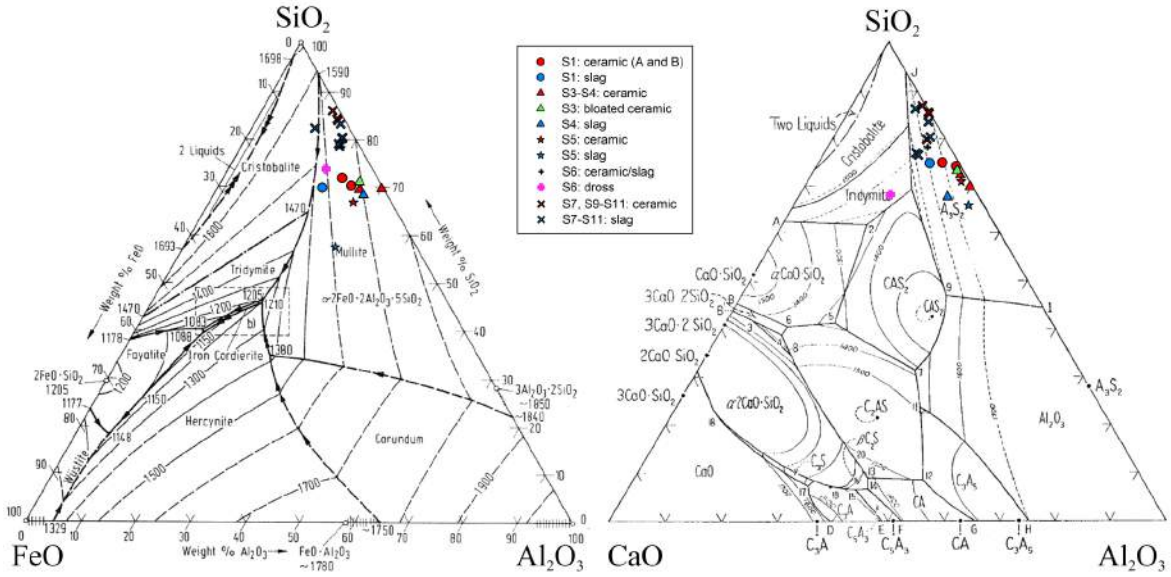

Figure 11.28: Serdica bulk compositions of ceramic and slag

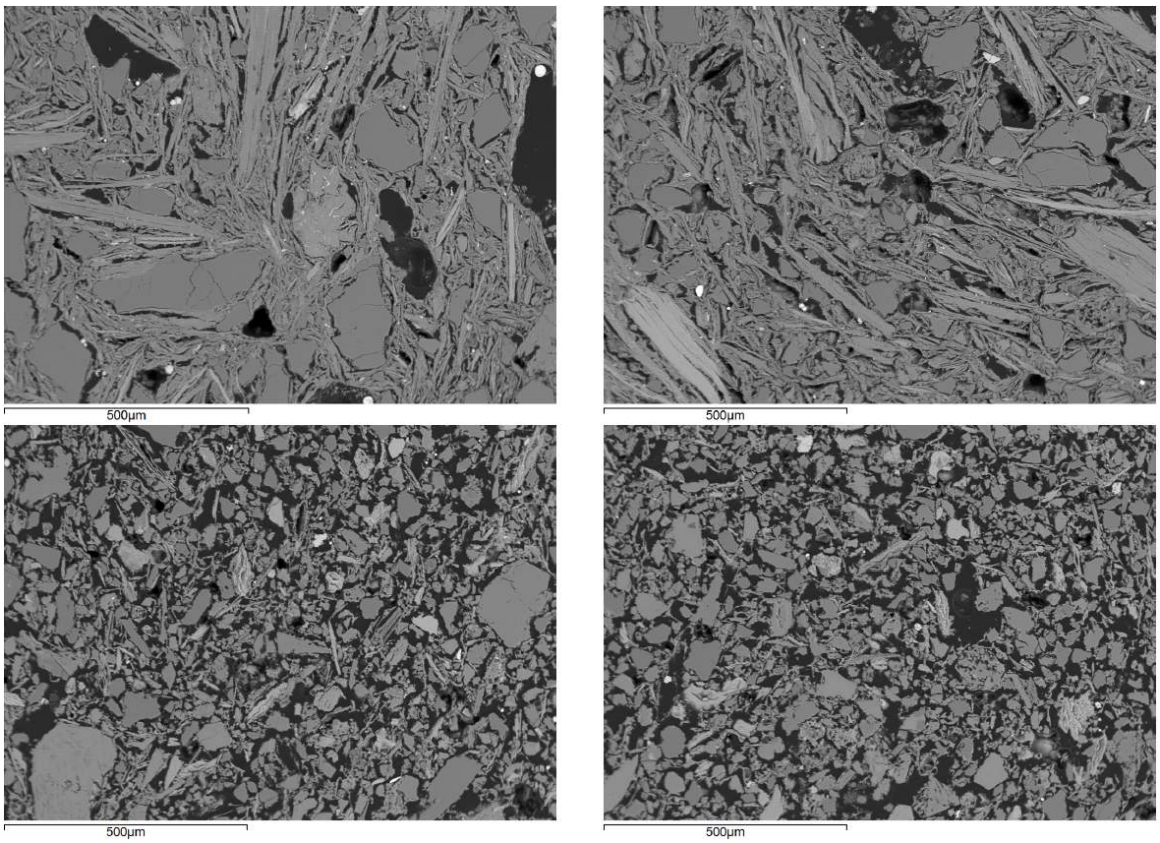

Figure 11.29: S1 ceramic A (top) and B (bottom)

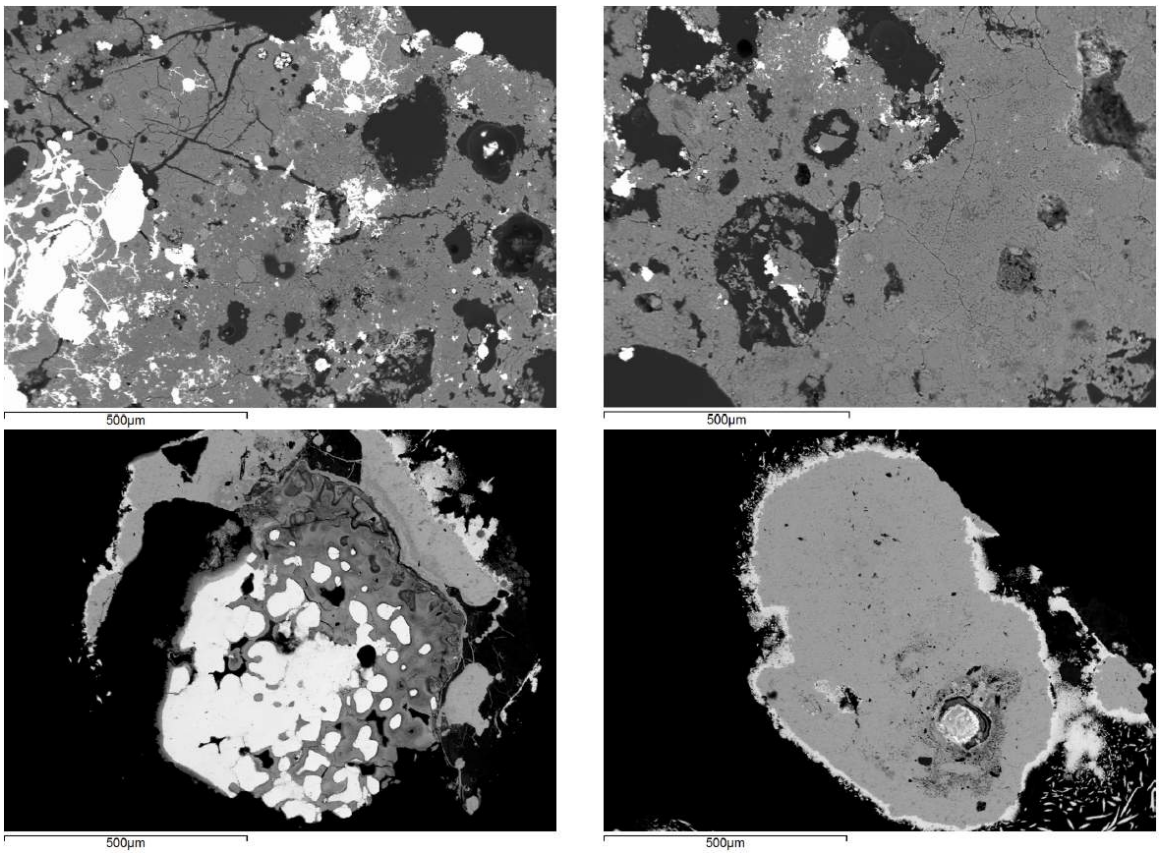

Figure 11.30: S1 slag (top), silver (bottom left) and silver sulphide (bottom right)

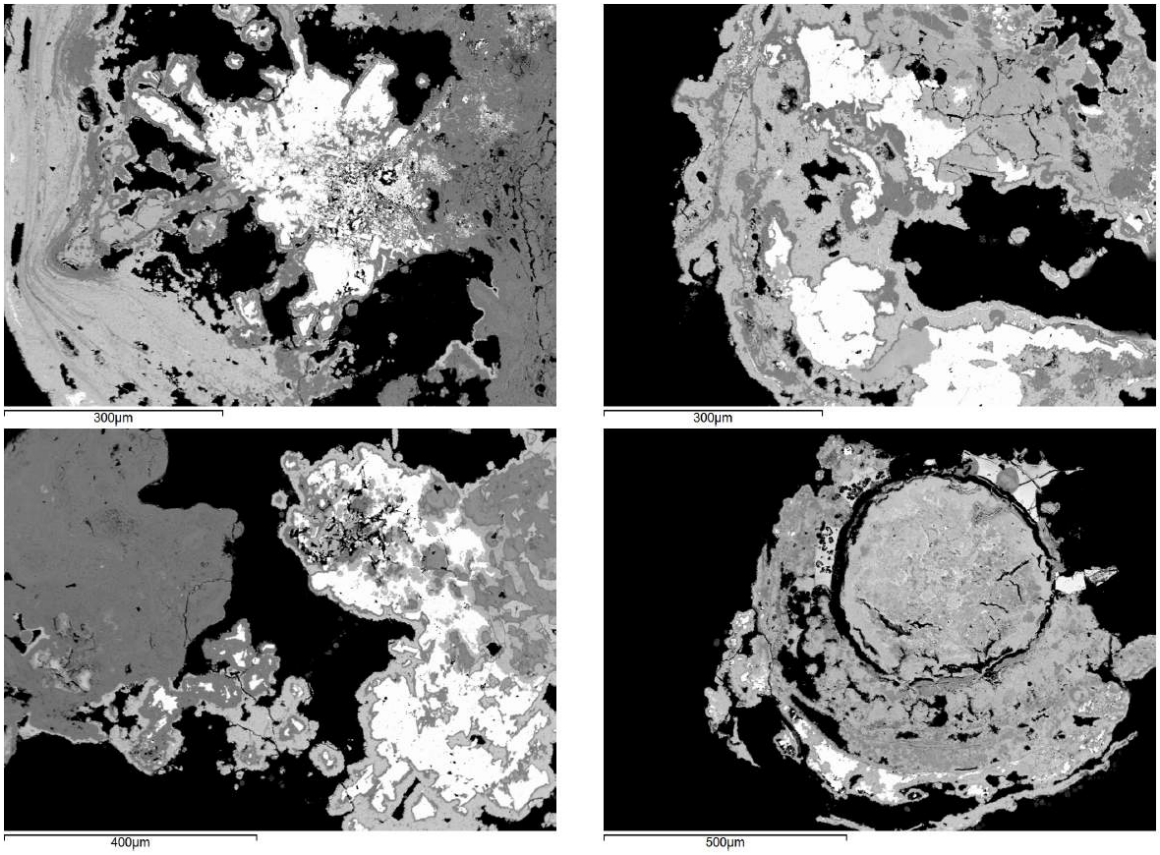

Figure 11.31: S2 silver sulphide (bright) with various iron-silver sulphides (light grey) and iron-copper-silver sulphides (medium grey)

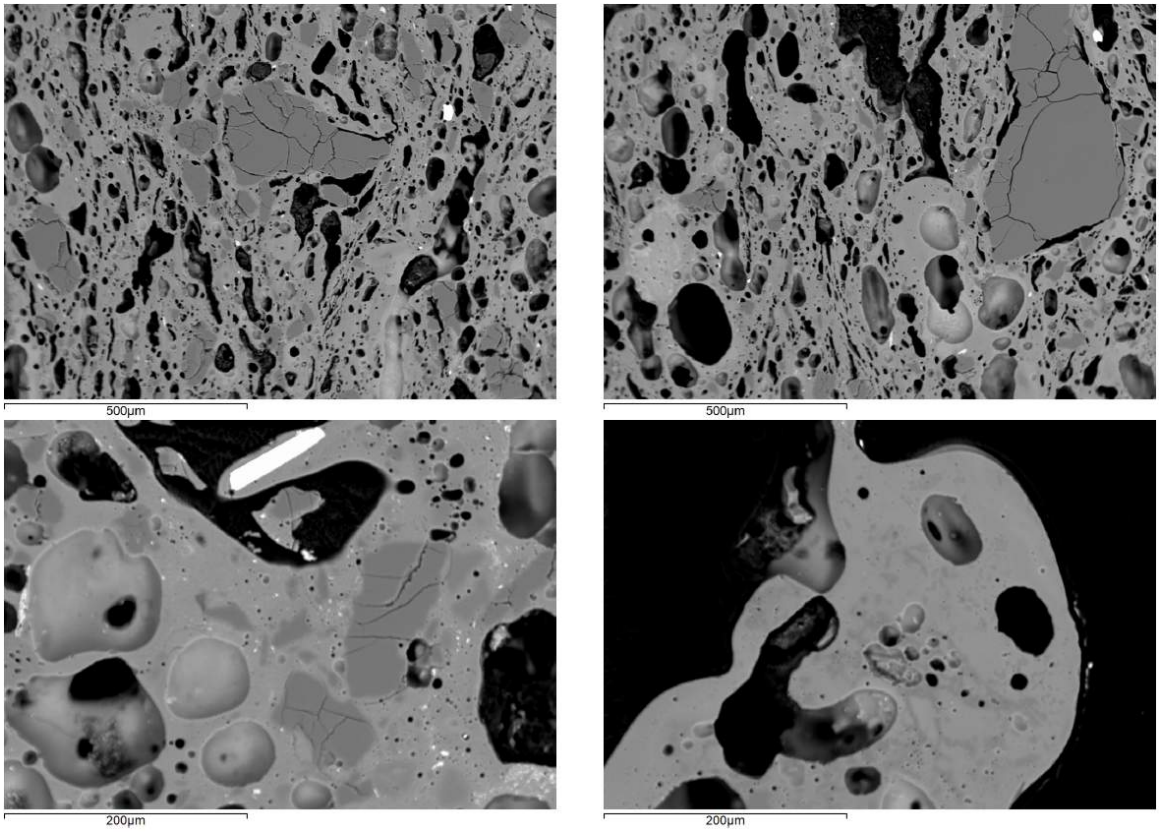

Figure 11.32: S3 ceramic (top) and bloated ceramic (bottom) with zircon (bright)

tween graphite carbon and applied carbon coating).

A thin but fully vitrified slag layer has developed on the crucible interior, which shows strong relative enrichment in fuel ash components and iron oxide ($\Delta^{FeO}/_{Al_2O_3} \approx 1200\%$). Many prills are embedded in the interior slag (Figure 11.34), all of which are copper with varying amounts of arsenic and silver (up to 20 and 13 wt%, respectively). The slag itself, however, is not only enriched in copper, arsenic and silver, but furthermore in zinc and lead (which do not occur in the metallic state). Small areas of dross/corrosion have been noted as well (mainly composed of copper-arsenic-lead oxide).

The exterior surface is extremely enriched in fuel ash components ($\Delta^{CaO}/_{Al_2O_3} \approx 5800\%$) as well as iron oxide ($\Delta^{FeO}/_{Al_2O_3} \approx 3100\%$), and shows modestly increased copper, zinc, arsenic, silver, and lead oxide content. This exterior glaze (Figure 11.35) exhibits various lime- and potash-rich oxide and silicate phases and metal (mainly copper) oxides. Metallic prills on the exterior have similar compositions to the interior slag prills, with the exception of a few gold-bearing (5 wt%) copper-arsenic-silver prills.

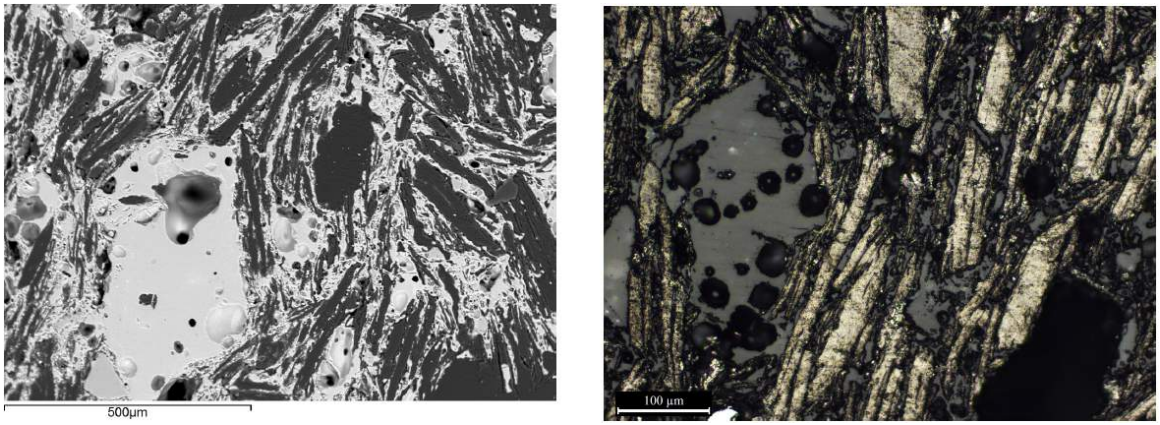

Figure 11.33: S4 ceramic. Graphite temper clearly visible under reflected light microscope (right: bright, yellow; O.M. image)

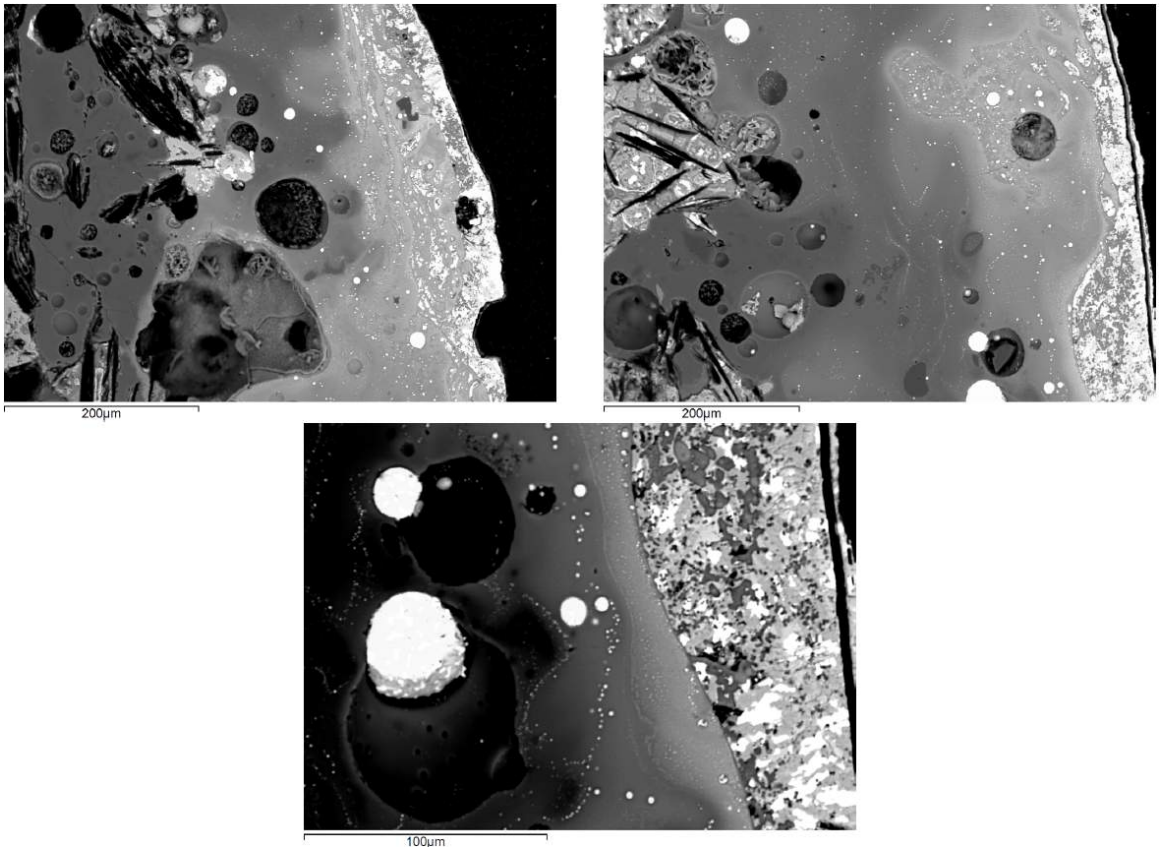

Figure 11.34: S4 interior slag (top) with (multi-phase) prills and limited dross (bottom)

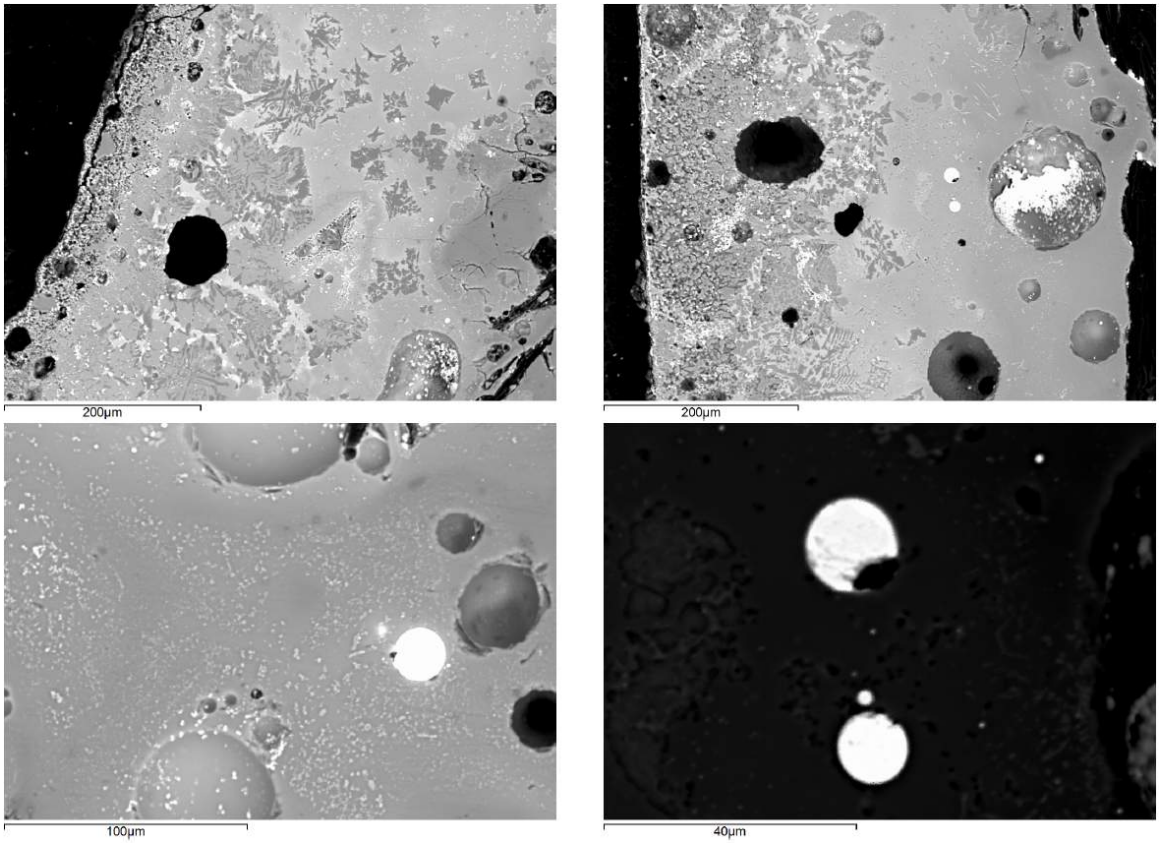

Figure 11.35: S4 exterior glaze (top) with prills (bottom), some gold-bearing (bottom prill, bottom right)

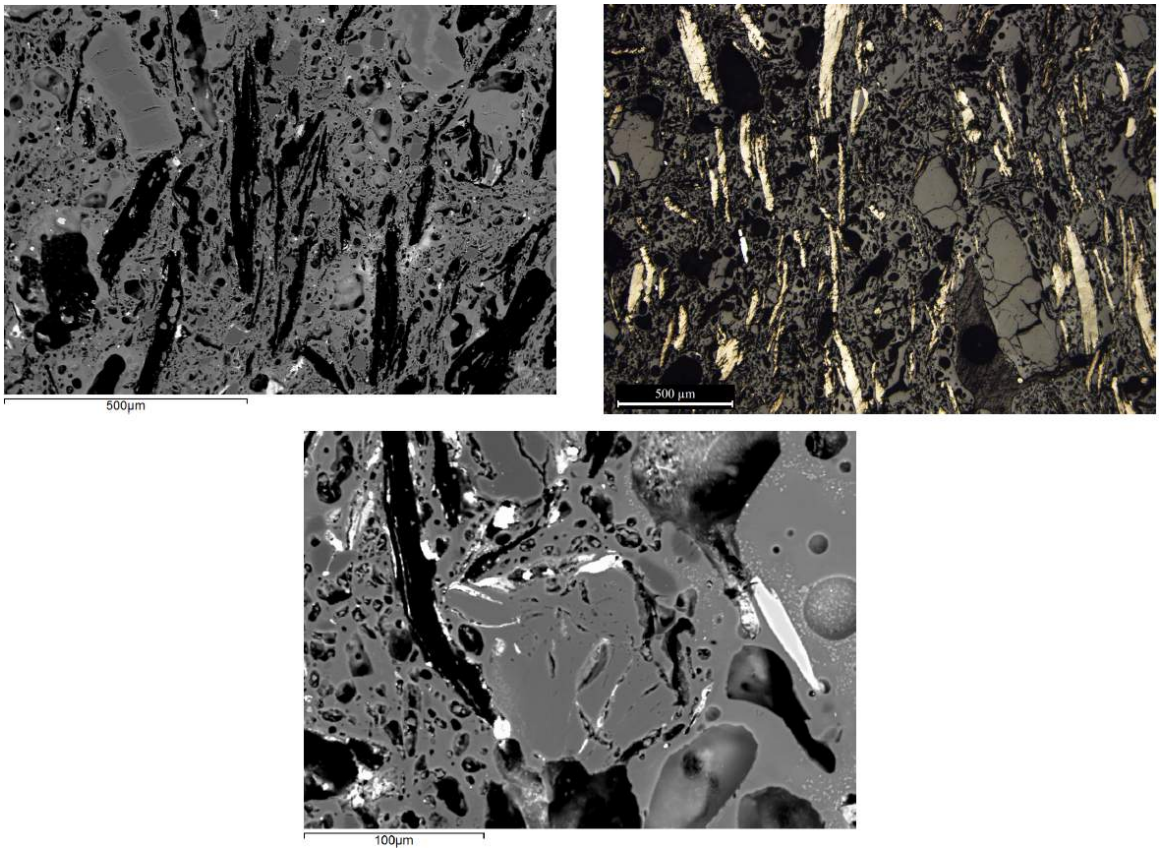

Figure 11.36: S5 ceramic (top) with graphite temper clearly visible under reflected light microscope (top right: bright, yellow; O.M. image) and rutile (elongate, light grey) and silver chloride (bright) (bottom)

11.1.3.3 Fragments S5

The ceramic (Figure 11.36) is highly fused, with limited porosity and graphite temper (though not extensive as in S4), rutile and some silver chloride (intrusion through cracks?).
The interior slag is very peculiar, with minor relative fuel ash and iron oxide enrichment, but very strong enrichment in copper, silver, lead, and, strikingly, bismuth oxide (>20 wt%). This gives the slag an unusual appearance, shown in Figure 11.37, with Bi_2O_3 making up approximately 20-40 wt% of the background matrix. The black crystals are lead- and lime-rich aluminosilicates. Many metallic prills occur, all of which contain >90 wt% silver with varying copper (up to 1 wt%) and/or gold (up to 8 wt%) content, and occasionally minor chlorine (up to 8 wt% Cl, no true AgCl). Bismuth was not detected in the metallic state.
The exterior crucible surface (Figure 11.38) is bloated but not slagged, and shows only minor enrichment in fuel ash components.

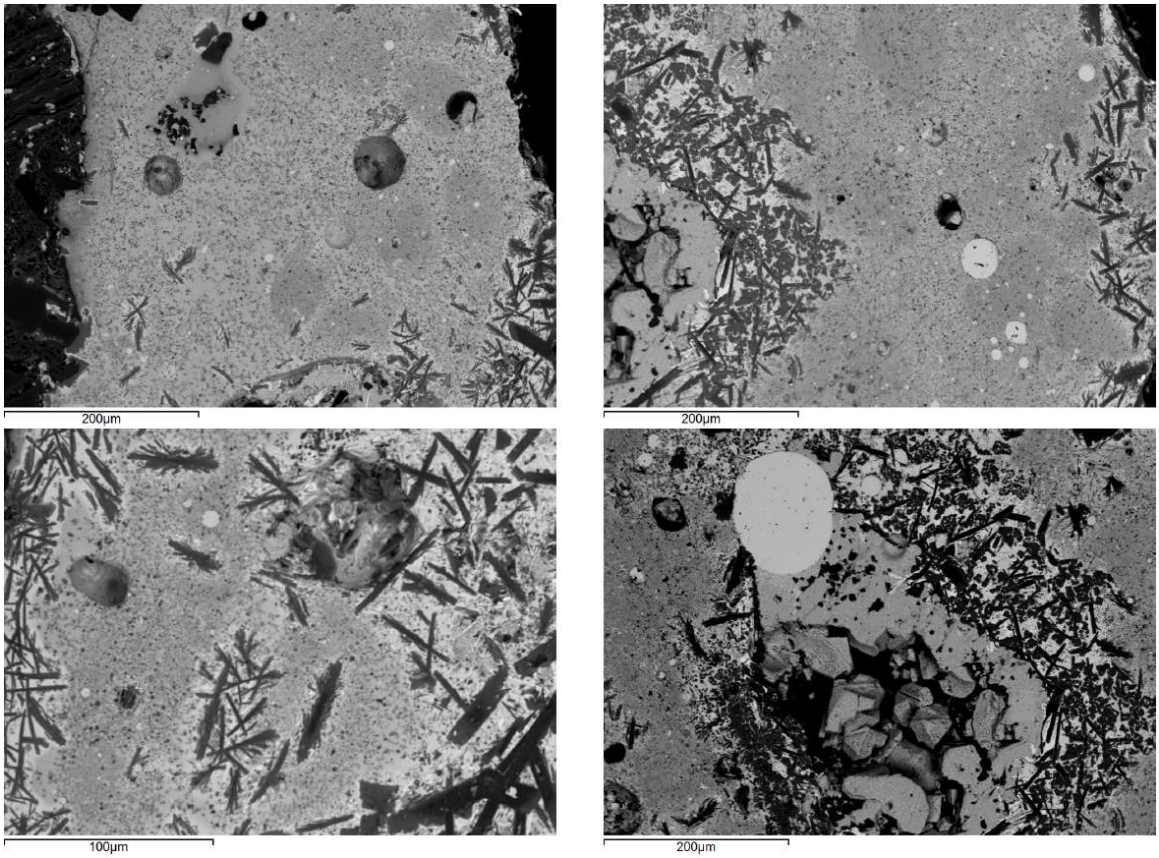

Figure 11.37: S5 interior slag (top) with lead- and lime-rich aluminosilicates (bottom left, black) and some gold-bearing silver prills (bottom right, with adjacent cubic silver chloride crystals)

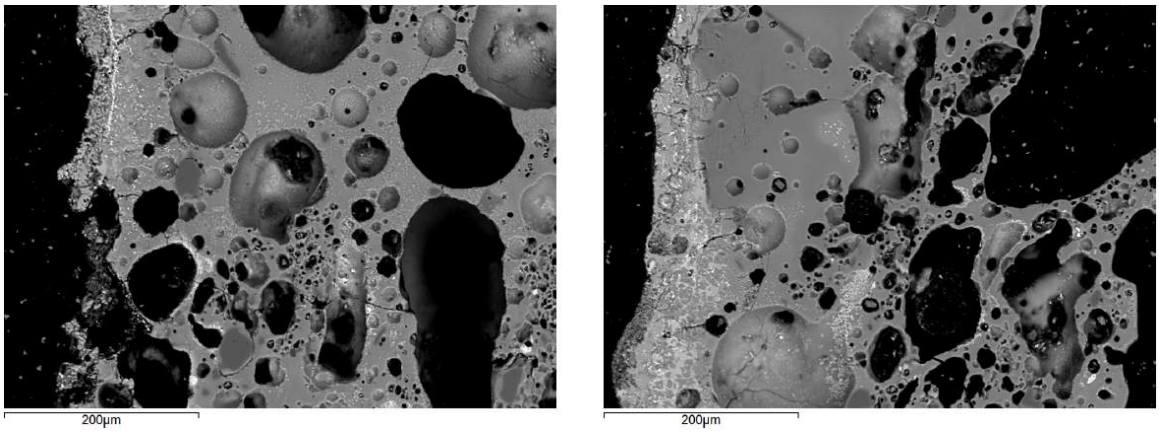

Figure 11.38: S5 bloated exterior

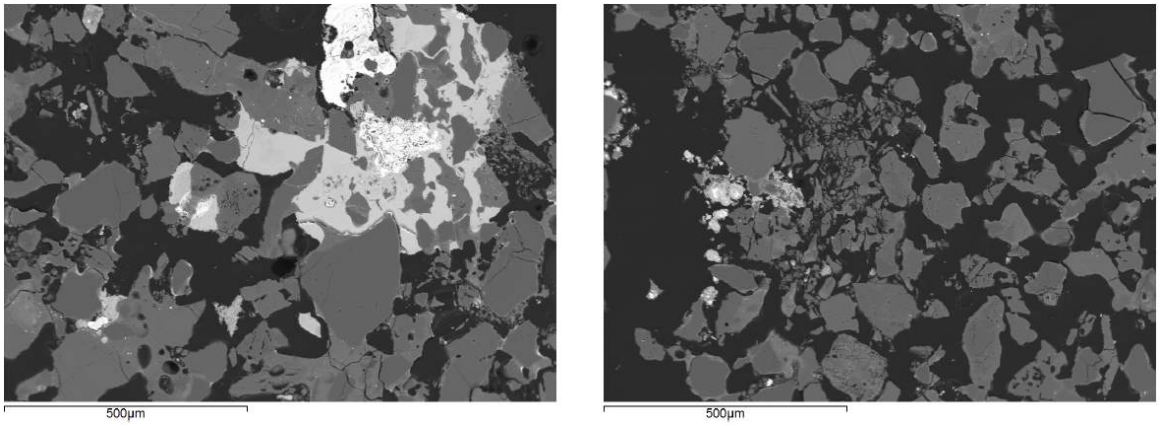

Figure 11.39: S6 (vitrified) ceramic

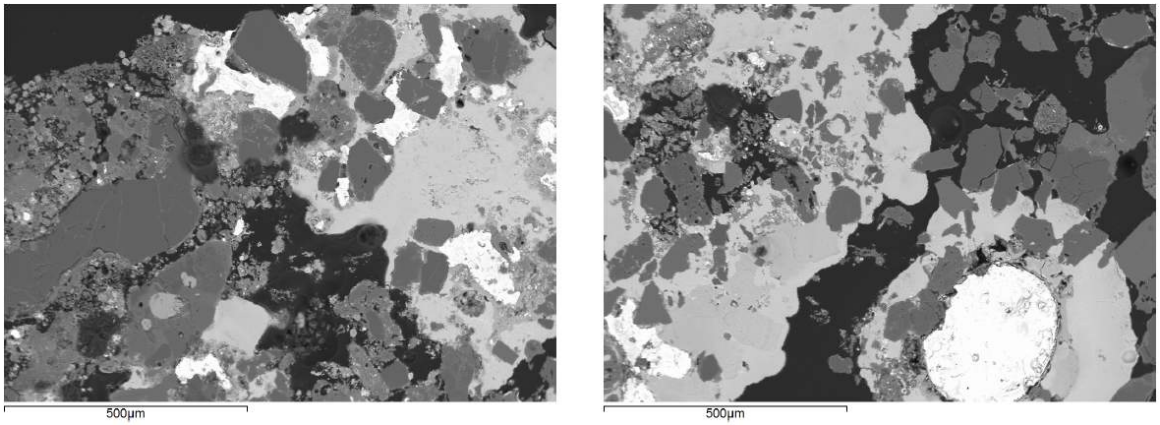

Figure 11.40: S6 dross with copper(-tin) oxides (bright)

11.1.3.4 Fragments S6-S11

Sample S6 has no pure ceramic fragments available, but rather '(vitrified) ceramic' fragments (similar to P1, section 11.1.2.1), shown in Figure 11.39. It is generally dominated by quartz with vitrified areas in between, within which various copper-tin-lead oxides occur. The drossy fragments (Figure 11.40) still contain many quartz fragments, but are relatively enriched in fuel ash components and iron oxide, and full of copper and copper-tin oxides. These drossy fragments cannot be considered fully separate from the (vitrified) ceramic fragments, but are simply closer to the far end of the continuous 'ceramic-slag-dross spectrum'. The distinction here was deemed appropriate, based on the clearly visible differences (Figures 11.39 and 11.40). A few metallic prills have been detected, which are high-tin bronzes (33-35 wt% Sn) with arsenic, antimony, (nickel) and lead.

The fabric of S7 (Figure 11.41) is fused/vitrified throughout, with only fractured quartz and some zircon remaining of the ceramic. Close to the exterior surface, some further vitrification occurs and a few metallic prills can be noted, which are all nickel-bearing

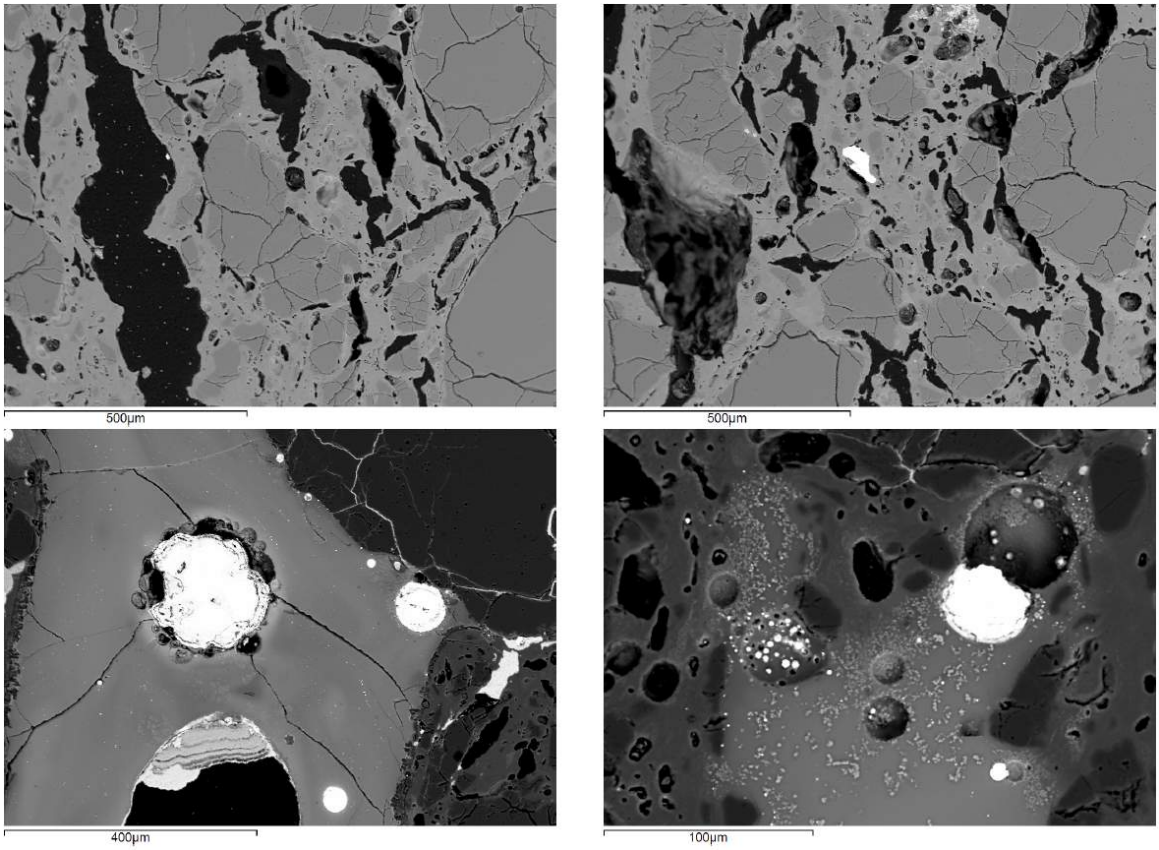

Figure 11.41: S7 ceramic (top) and prills on exterior surface (bottom)

bronzes or gunmetals (±2 wt% Ni, 9-13 wt% Sn and 0-1.5 wt% Zn).
On the crucible interior, a very thin and not well developed slag layer occurs (Figure 11.42), within which copper-tin and copper-lead oxides occur, as well as a few tiny bronze prills with minor iron, arsenic and nickel content. The interior is quite strongly enriched in fuel ash components ($\Delta^{CaO/Al_2O_3} \approx 2700\%$), but not in iron. The exterior shows lower, though fairly significant fuel ash component enrichment ($\Delta^{CaO/Al_2O_3} \approx 800\%$).

S8 consists of slag fragments only, shown in Figure 11.43. These are made up of a lead-rich glassy matrix with minor zinc content and remnant quartz (fractured and with smooth contours) and zircon. Various lead- and potassium-rich aluminosilicates, as well as iron-tin-lead-silicates have crystallised from the slag. No metallic prills could be detected.

S9 (Figure 11.44) consists mainly of ceramic, similar to S6, but without the abundant glassy phase. It is dominated by quartz grains, fused together by vitrified ceramic 'bridges'. A glassy phase occurs in one area, and has been measured separately as 'slag'. Within the fused ceramic 'bridges', tiny prills can be found, which are mainly composed of medium/high-tin gunmetal (17-32 wt% tin) with minor to high (9.5 wt%) iron content, up to 5 wt% zinc and in one occasion 0.8 wt% silver. A pure high-tin bronze prill (35 wt% Sn) occurs as well.

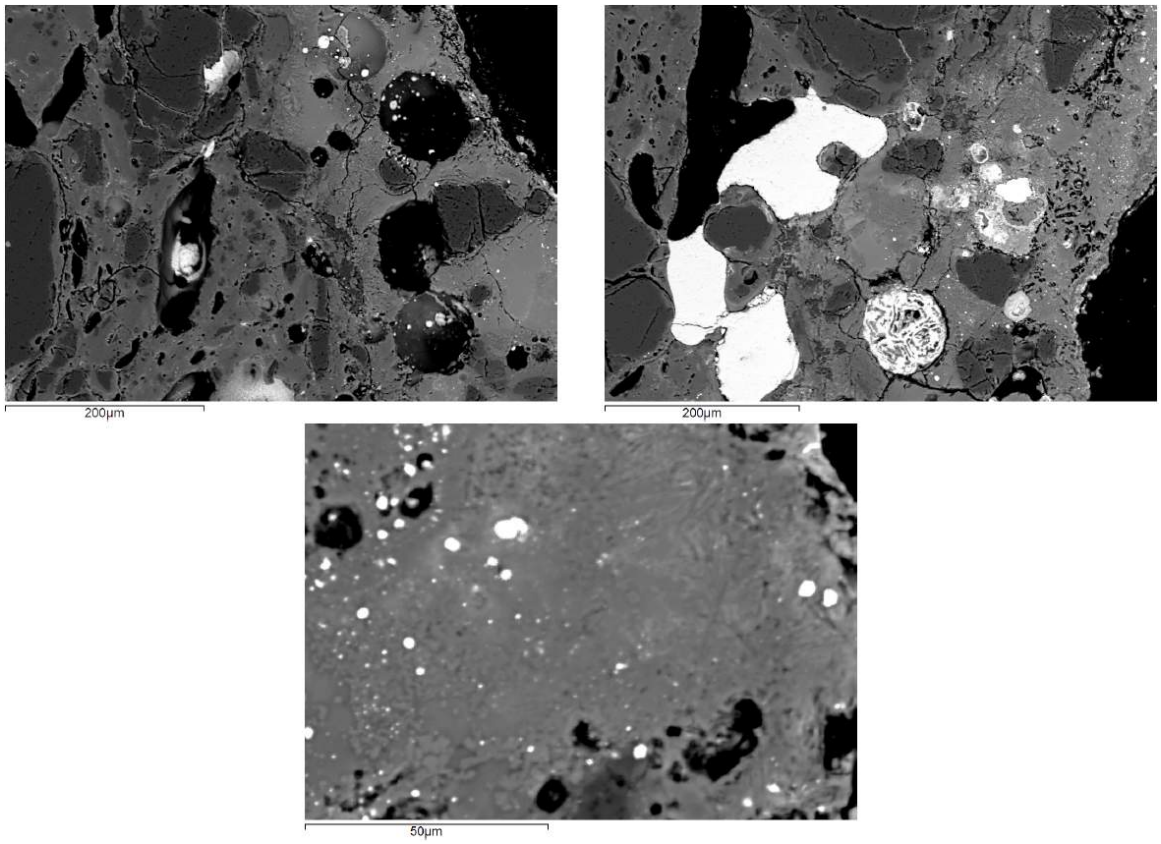

Figure 11.42: S7 slag (top) with copper-tin and copper-lead oxides (bright), and tiny metallic prills (bottom)

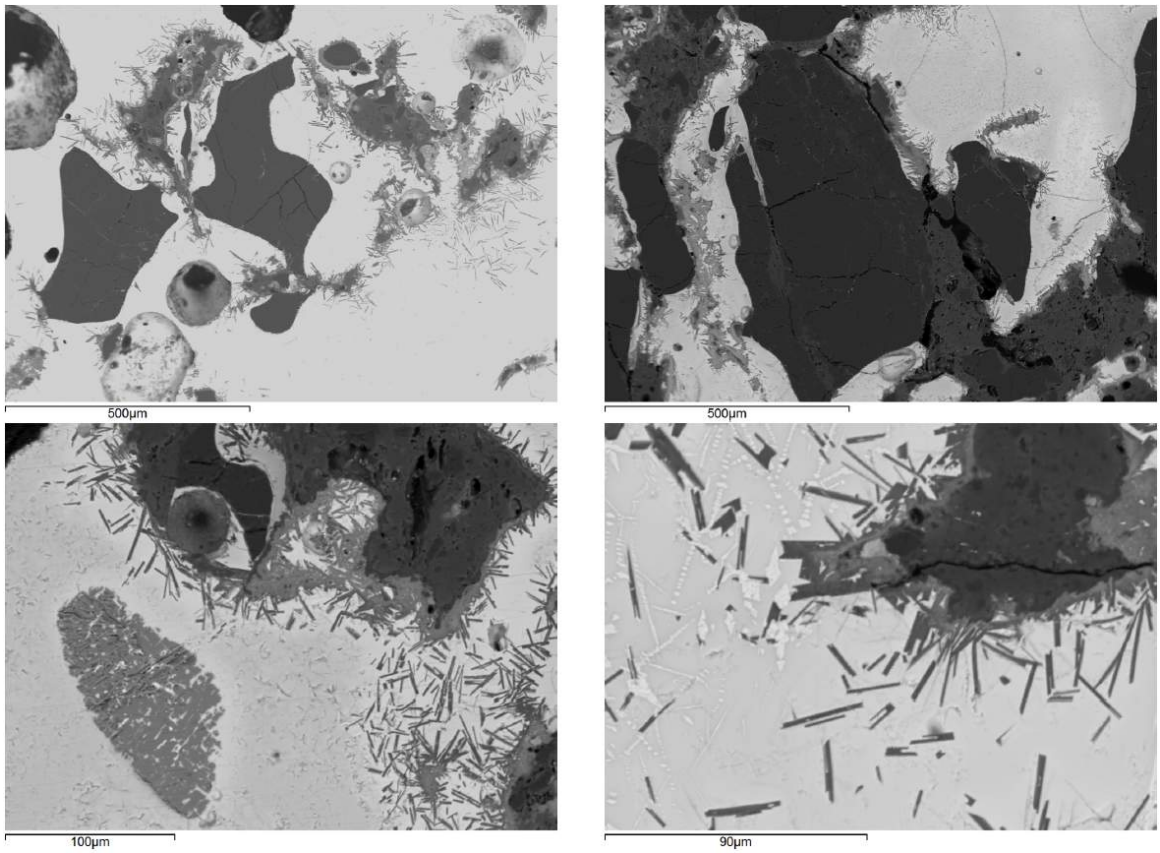

Figure 11.43: S8 slag (top) with (bottom) Pb-K-rich aluminosilicates (dark, elongate) and iron-tin-lead silicates (light grey, angular)

Finally, some high-iron prills should be noted (93-95 wt% iron, 5-7 wt% copper).

S10 (Figure 11.45) consists of fused ceramic with small to large, fractured quartz grains and a 'glazed surface' (probably crucible exterior) of more closely fused ceramic with similar quartz grains. Only one prill (94 wt% iron, 6 wt% copper) was noted on the glazed surface, which is relatively enriched in zinc oxide.

The fabric of S11 (Figure 11.46) is fully fused with medium to large, fractured quartz fragments, zircon and monazite ((Ce, La)PO_4, with 2 wt% Ag) remaining. Its interior surface is not really slagged but slightly bloated, incorporating cuprite and copper-tin-lead oxides, as well as tiny prills (±95 wt% iron, 1-2 wt% copper and 0.5-3.5 wt% tin). The interior is strongly enriched in lime and iron, and particularly in soda ($\Delta^{Na_2O}/_{Al_2O_3} \approx 2600\%$).

11.1.4 Stara Zagora

Only one sample (StZ1) has been analysed from Stara Zagora. Two distinct parts are visible in cross-section, as indicated on Figure 11.47. Part A is the crucible interior, while part B is an external layer, extending over the rim of part A, but not onto the interior surface. However, slag A and B have fused at the transition on the rim, blurring this distinction. At the centre of part A, a limited amount of remnant ceramic fabric occurs, which is almost entirely fused, but contains some remnant fractured quartz grains (Figure 11.48). The chemical difference between these two parts is illustrated in Figure 11.49.
Towards the crucible interior, further bloating and vitrification occurs. Several prills are embedded within this interior slag layer (Figure 11.50), varying in composition between bronze, leaded bronze, leaded copper, brass and gunmetal, sometimes incorporating up to 1.3 wt% iron. Notably, a prill of 93 wt% lead and 7 wt% copper occurs as well. Relative to the remnant ceramic, this interior slag layer is enriched in fuel ash components.
The area of part A closest to part B ('part A - central') is equally characterised by vitrification with residual quartz (Figure 11.51), which is similarly enriched in fuel ash components. Several prills can be noted, ranging mostly from pure copper to leaded copper, with rare low tin or iron content.
Part B (Figure 11.52) consists of vitrified ceramic, more porous (bloated) than part A. There is no distinct boundary between part A (central) and part B, which have fully fused. Part B contains very few (pure copper) prills, which are concentrated on the exterior surface. It is difficult to say if part B is enriched in any particular oxides, as its reference composition is unknown. The difference in silica and alumina relative to part A, as well as high soda, magnesia and potash content, suggests the use of a different clay from part A, and enrich-

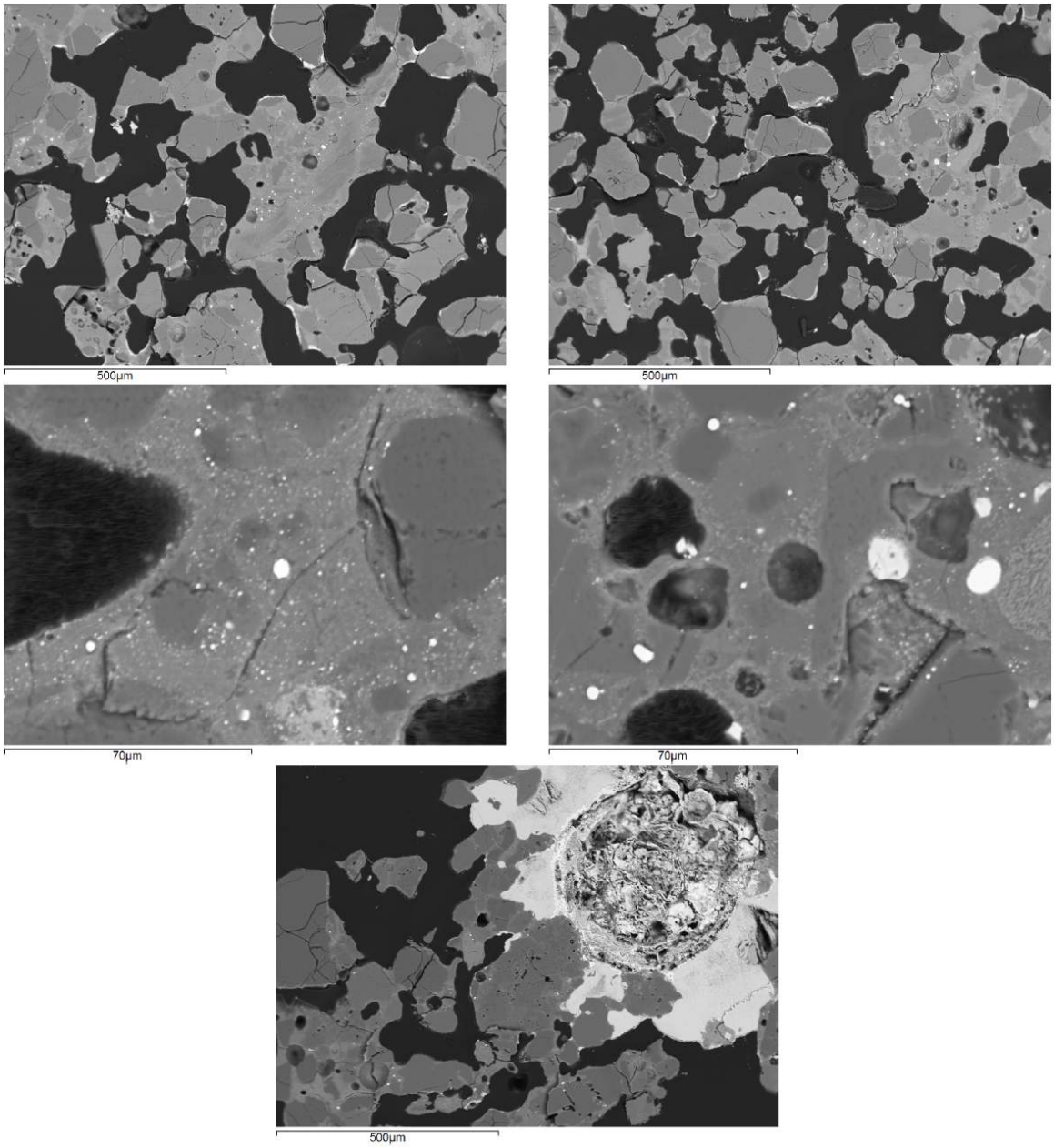

Figure 11.44: S9 ceramic (top) with gunmetal prills (middle left) and iron-rich prills (middle right) within fused ceramic and 'slag' (bottom)

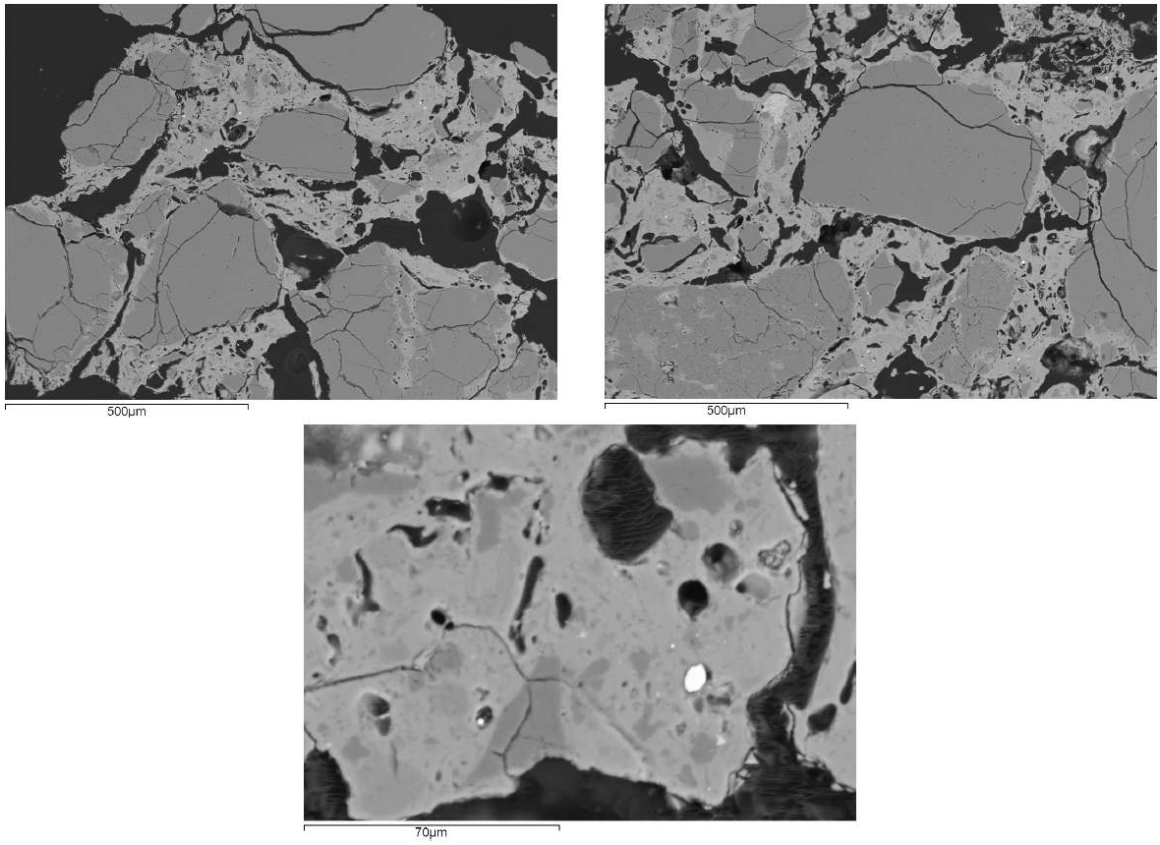

Figure 11.45: S10 ceramic (left) and glazed surface (right) with iron-copper prill (bottom)

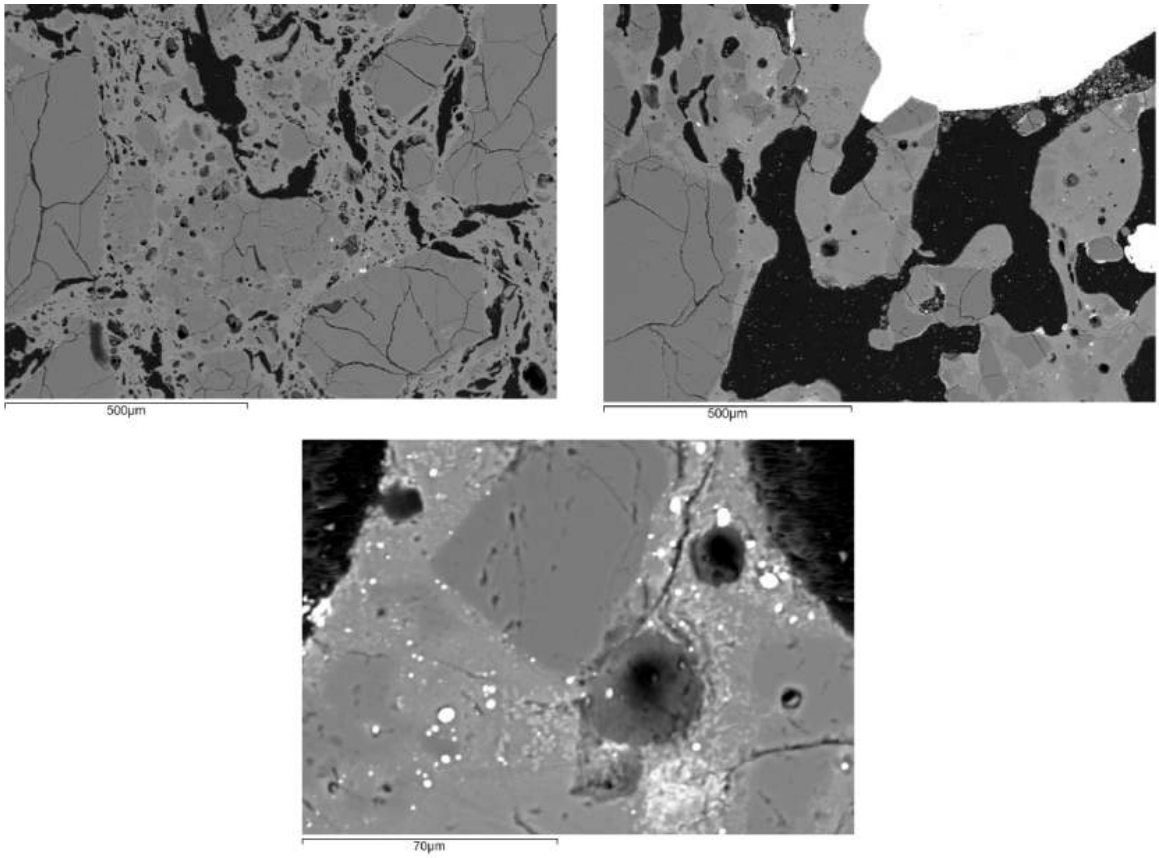

Figure 11.46: S11 ceramic (left) and bloated interior (right) with copper oxides (bright) and iron-copper-tin prills (bottom)

Figure 11.47: Stara Zagora sample zoning (left: view onto interior surface A)

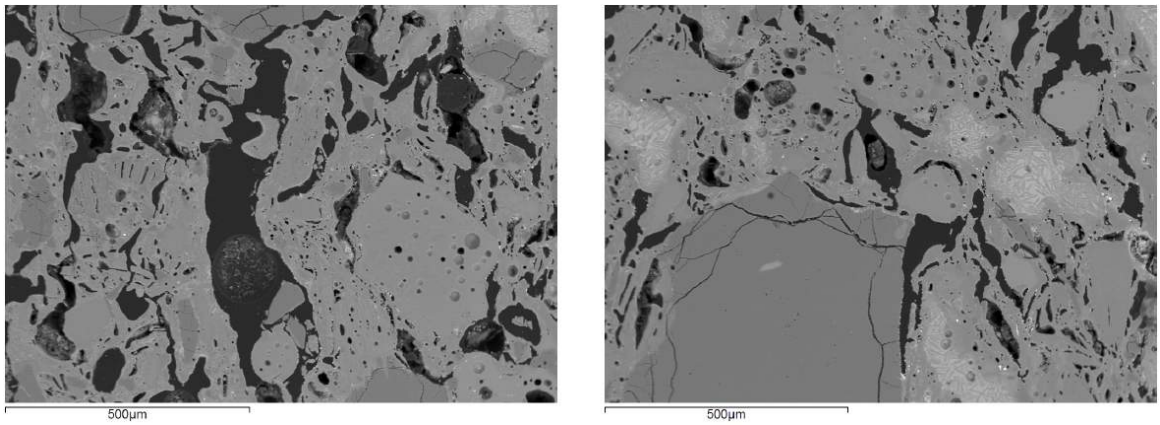

Figure 11.48: StZ1, part A ceramic

ment with fuel ash. Iron oxide enrichment is difficult to assess. At the top of part B (top of the crucible rim) sits a partially corroded prill.

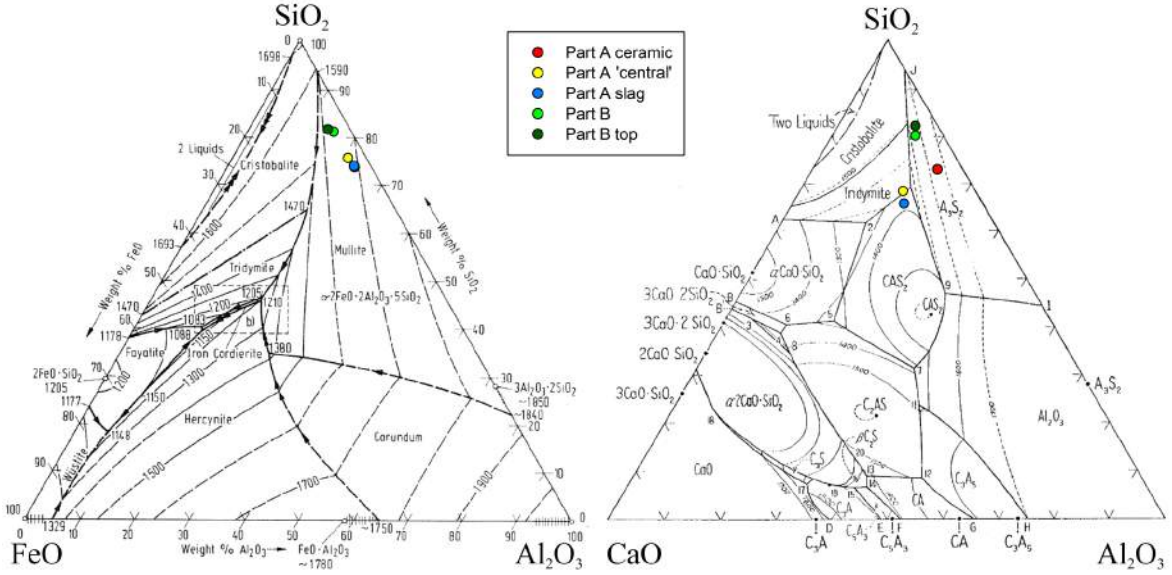

Figure 11.49: Stara Zagora bulk compositions of ceramic and slag

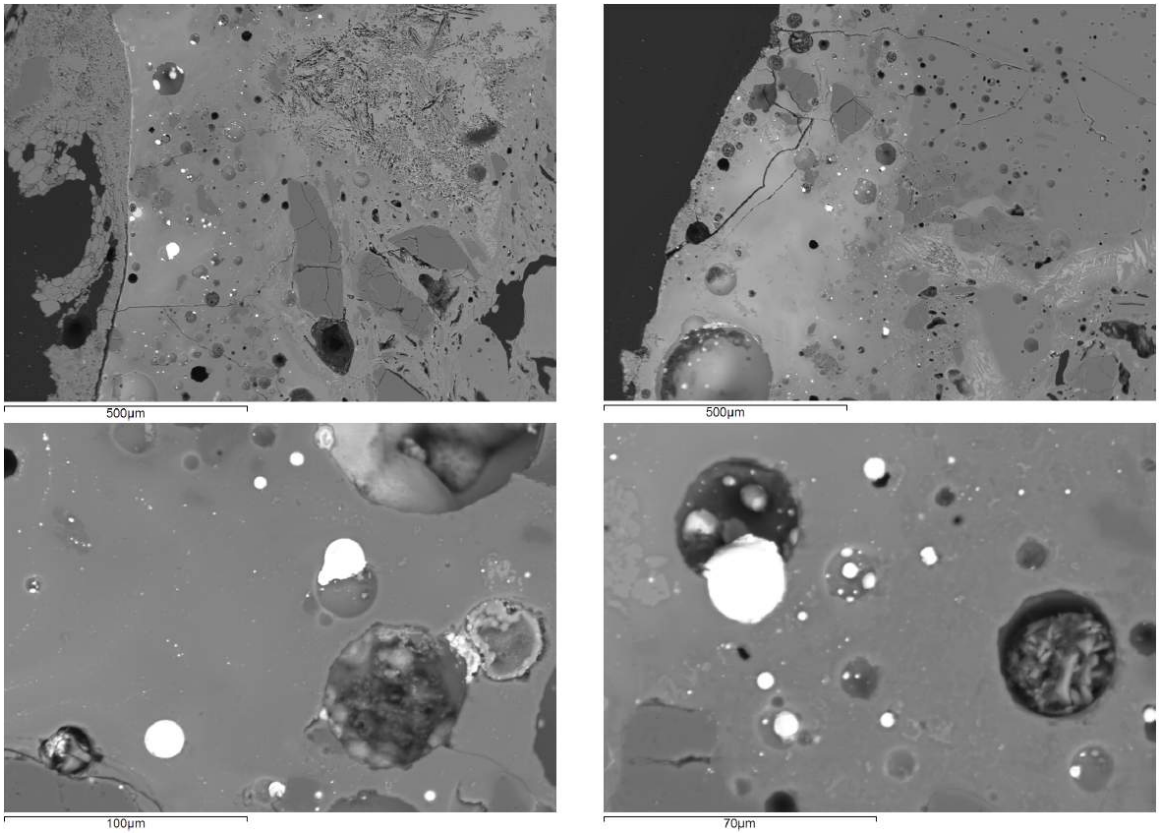

Figure 11.50: StZ1, part A interior slag (top) and embedded prills (bottom)

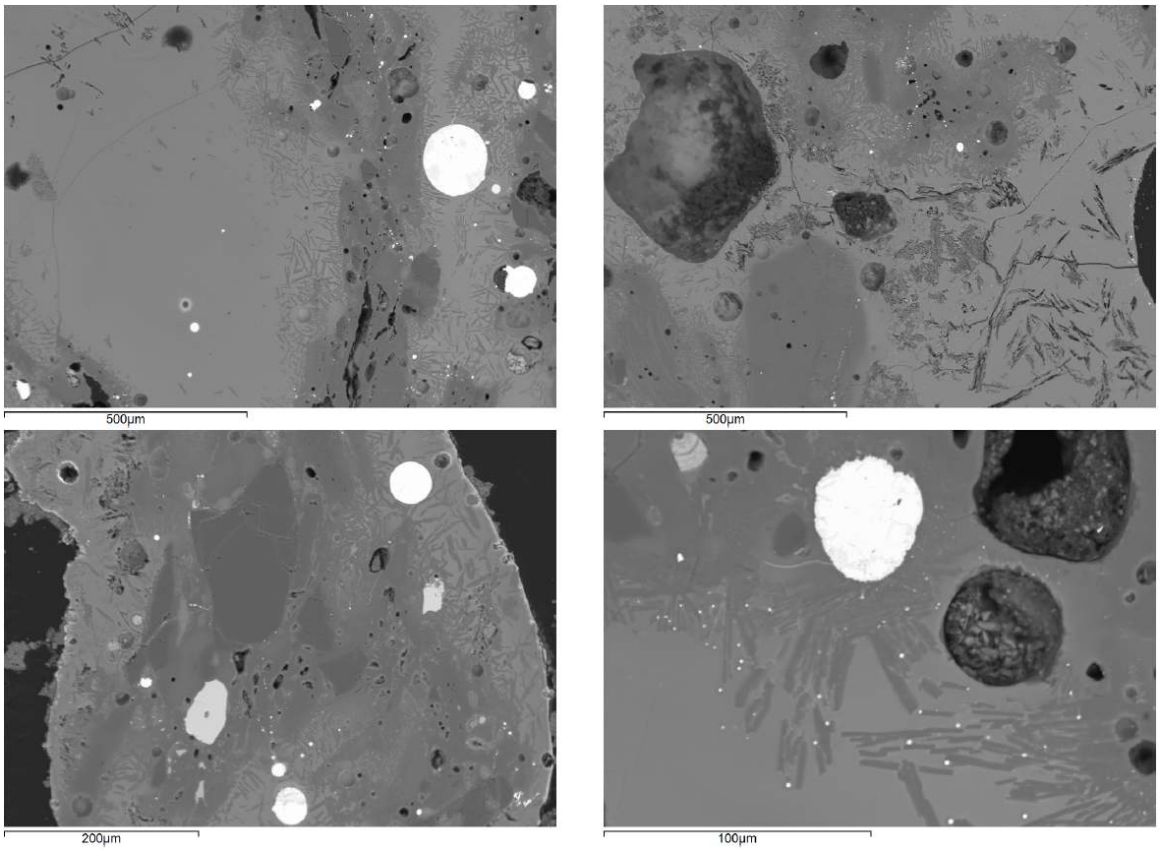

Figure 11.51: StZ1, part A central vitrification (top) and embedded prills (bottom)

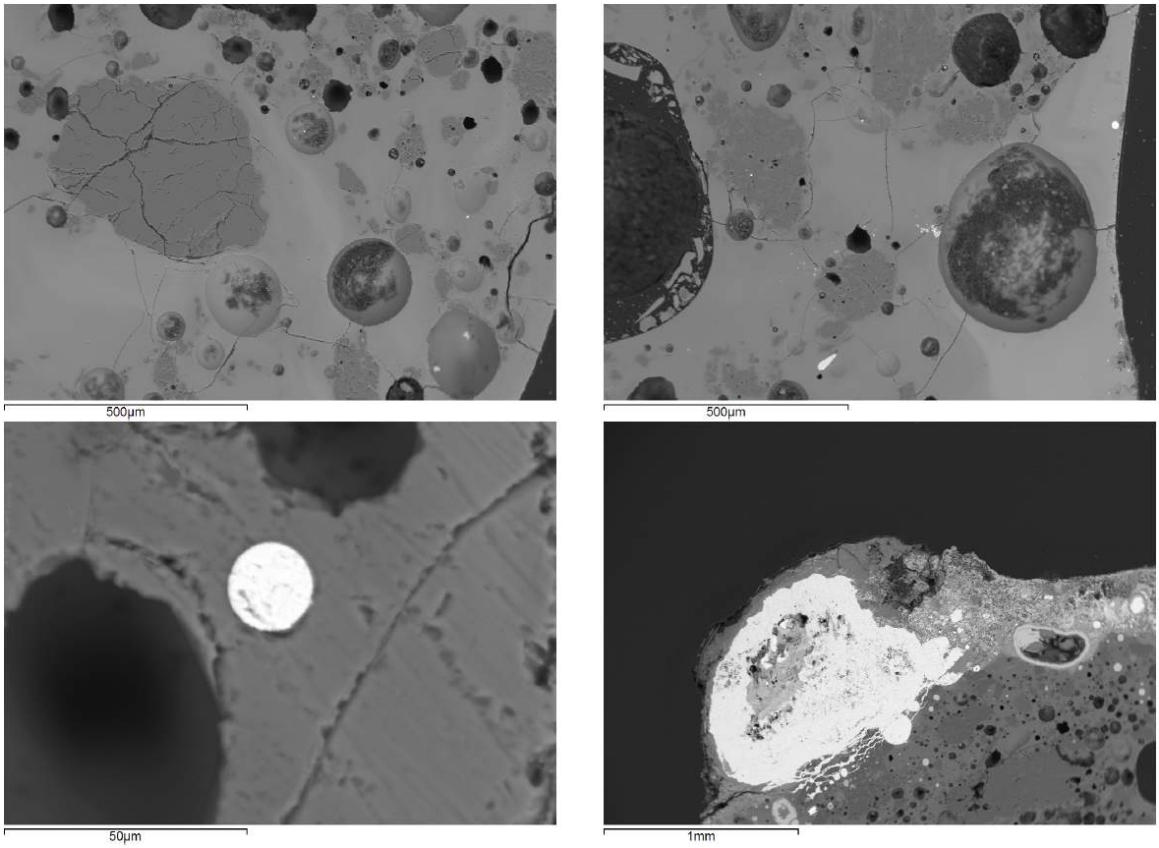

Figure 11.52: StZ1, part B porous glaze (top), embedded prills (bottom left) and corroded prill on crucible rim (bottom right)

Section 11.2

Technical interpretation

The evidence presented by the fragmented remains in this chapter is almost invariably ambiguous. An effort is made in this section to spell out all relevant possible interpretations for each crucible, but in some cases omission are made and only the most likely scenarios are discussed.
Furthermore, the basic assumption is made that all crucibles reflect a single use, or at least use for a single purpose. Only where such interpretations do not fit the evidence are multi-use scenarios elaborated. The interpretative issues of possible reuse are further elaborated in Chapter 13.

11.2.1 Nicopolis ad Istrum

Fragment N2 stands out from the rest of the assemblage on the basis of typology and ceramic fabric. It is not a true crucible, but its relation to metallurgical activity is indicated by the presence of prills in sample N2b. Exposure to high temperatures for a significant time is suggested by the development of a slag layer there, and the inclusion of several prills indicates direct contact with a liquid metal charge while at high temperature. This contact could have been continuous or momentary. The presence of less slagged areas (N2a) on the 'collar', indicates variable conditions, whereby certain areas were exposed to lower temperatures and did not come into contact with liquid metal.
Variability in ceramic composition has been noted, with slightly less refractory clay towards the exterior surface in N2a, but not N2b. While this may point to the application of an outer clay layer, it may equally reflect ceramic heterogeneity.
The open shape and size of the 'collar' suggest that it was a stationary feature of the metallurgical installation. Its diameter of approximately 25 centimetre makes it too wide to act as a casting sprue, and it would be relatively small for a smelting furnace rim. It was perhaps sitting on top of a hearth or crucible employed for copper-based metallurgy, but its exact function is difficult to reconstruct.

Fragments N1 and N3 derive from the same context, and have a similar ceramic fabric, though N3 is more bloated than N1. N6, an unstratified find from a different area (same as N4-N5), has a similar ceramic bulk composition, but very different fabric. All fragments have a similar wall thickness, but the heating profiles are different. While N1 has been internally heated, and has a red-fired exterior surface (reflecting oxidising conditions), both

N3 and N6 were externally heated, resulting in bloating (N3) and vitrification (N6) of the grey-fired exterior surface.

Slag analysis of these crucibles further corroborates their different modes of use. Sample N1 shows extreme enrichments in iron, fuel ash and metal oxides (and lowered alumina and silica contents), in line with enrichments encountered in dross layers. The absence of metallic prills suggests that the sampled area of the crucible reflects highly oxidising conditions, resulting in the burning of its metal content: most likely an iron-contaminated leaded bronze or gunmetal. The high contribution of fuel ash further indicates that the crucible was covered with charcoal for heating. This again illustrates crucible heterogeneity: despite charcoal cover, highly oxidising conditions can prevail for a certain amount of time in a certain crucible area, resulting in (localised) burning of metal.

Crucible N3 has developed only a thin slag layer, within which leaded bronze prills are found, indicating active bronze alloying: up to ±65 wt% tin occurs in these prills. Following similar arguments held for the Gordion crucibles (see section 8.3.3), the source of lead cannot be reconstructed here: it could have entered the charge either as a pure metal, a leaded copper, a tin-lead alloy or, more unlikely, as a lead ore. Zinc could have been involved in this process as well, as suggested by its high oxide content in the slag. However, it does not occur in any of the prills. Probably, it was present as a contaminant in the (leaded) copper that was being alloyed with tin in this crucible, and burnt off into the crucible slag. If (leaded) brass was alloyed with tin to produce leaded gunmetal, higher zinc contents should be expected in the embedded prills. Tin could have been added either as a mineral or metal.

N1 and N3 could be different reflections of the same process (leaded bronze alloying) carried out in different crucible types and under different heating modes, resulting in very different production evidence.

The slag layer of N6 does not show strong contamination, with the exception of bronze prills and various lead-bearing oxides. This strong bulk enrichment in tin and lead suggests the processing of a leaded bronze, whereby the many copper-lead and tin-lead oxides represent oxidising crucible conditions, but the single high-tin (unleaded) bronze prill (35 wt% tin) reflects an area with more reducing conditions. Though this single prill may not appear entirely convincing evidence for the identification of active alloying, it sits well above the average tin content for contemporary bronzes (±10 wt% in tin bronzes, 5 wt% in leaded bronzes, 20 wt% for mirror/bell bronzes (Riederer, 2002b)). The absence of zinc distinguishes this crucible from N1 and N3.

As a final note, the secondary clay layer on top of the slag layer of N6 should be discussed. It has the exact (within analytical error) same composition and fabric as the N1 ceramic.

Though this layer could indicate the preparation of this crucible for secondary use, no metallurgical indicators can be found on its surface, and it was probably never reused.

Crucibles N4 and N5 have both been identified as wheel-turned, re-used domestic pottery. Their ceramic fabrics are more or less identical chemically, with only minor differences in structure and colour due to firing. Both have a thin external vitrified layer, which seems to be the result of ceramic fluxing by fuel ash. This suggests an external heating mode for both crucibles. However, this fuel ash contribution is seen quite strongly in the interior slag as well, which may indicate that the crucibles were left open and perhaps sitting in a charcoal bed, with fuel ash allowed to fall into the crucibles.
Interestingly, the relative increase in iron is equally seen for both the internal slag and external vitrified layer, and does not correlate to the fuel ash increases (see Table 11.1). Taking into account the visible differentiation between the central ceramic areas in N4 and N5 (grey, white), and their external vitrified and internal slag layers (reddish to black), this could suggest the application of a thin (secondary) clay layer (different to the original ceramic) to both internal and external surfaces of these crucibles. This (secondary) clay layer appears to be less refractory than the original ceramic, resulting in more outspoken bloating and vitrification. This has produced a vitrified layer on the exterior crucible surface, and a slag layer on its interior surface, through interaction with the crucible charge. Both the external vitrified layer and the internal slag layer are completely fused with the original, central ceramic, erasing any boundaries visible under the microscope or SEM[4]. An increased lime content in the applied (secondary) clay layer may further explain the increased lime content on both interior and exterior surfaces, relative to the original central ceramic. The relatively higher lime enrichment on the exterior surface can then be attributed to fuel ash, as a result of external heating (with only limited fuel ash entering the crucible). Though the application of such a clay layer to the crucible exterior is not uncommon (e.g., König and Serneels, 2013 and Thornton and Rehren, 2009), its application to the interior is surprising, as it results in a more outspoken interior slag layer than would be the case without this added clay. Furthermore, this increases the likelihood of interaction and trapped prills inside the slag, which could be seen as undesirable.
N4 does not offer any indication of metal contamination, making it impossible to reconstruct its charge. This suggests that the applied clay layer was in fact sufficiently refractory for the process. N5 contains (iron-rich) leaded bronze prills, and the dross layer contains copper, zinc and lead oxides, but no tin. Its exterior vitrified layer[5] is weakly enriched in

[4]Using cross-polarised microscopy, however, a difference in colour can still be seen between the central ceramic area and the external vitrified and internal slag layers respectively.

[5]Though some copper, zinc and lead oxide is present within this exterior vitrified layer, it does not qualify

	Na_2O	MgO	Al_2O_3	SiO_2	P_2O_5	K_2O	CaO	TiO_2	FeO	CuO	ZnO	PbO
N4 ceramic	**0.7**	**0.9**	**22**	**69**	**0.2**	**2.0**	**1.7**	**1.0**	**2.5**	**0.1**		
Std. dev. (5 ms)	0.1	0.1	2	2	0.4	0.1	1.2	0.3	0.1	0.1		
N4 internal slag	**3.4**	**1.0**	**9**	**78**	**0.2**	**2.3**	**2.6**	**0.6**	**3.1**	**0.1**		
Std. dev. (5 ms)	0.7	0.1	1	1	0.1	0.2	0.8	0.1	0.2	0.1		
N4 external layer	**1.8**	**1.6**	**8**	**70**	**1.5**	**5.2**	**8.3**	**0.4**	**2.8**	**0**		
Std. dev. (5 ms)	0.3	0.6	1	5	0.7	1.0	4.5	0.1	0.2	0.1		
N5 ceramic	**0.9**	**0.9**	**24**	**65**	**0.1**	**3.0**	**1.9**	**0.8**	**2.5**	**0.3**	**0**	**0**
Std. dev. (5 ms)	0.2	0.3	3	2	0.1	1.0	1.2	0.1	0.2	0.4	0.2	0.1
N5 internal slag	**2.5**	**0.9**	**14**	**64**	**0.3**	**1.9**	**6.9**	**0.6**	**4.9**	**2.1**	**0.9**	**1.0**
Std. dev. (5 ms)	0.1	0.1	2	6	0.1	0.4	0.6	0.2	2.3	1.6	1.2	1.8
N5 external layer	**1.7**	**1.5**	**14**	**59**	**0.9**	**6.4**	**9.3**	**0.8**	**3.6**	**2.5**	**0.2**	**0.2**
Std. dev. (5 ms)	0.3	0.5	2	3	0.6	1.0	3.0	0.3	0.5	1.4	0.3	0.1

Table 11.1: Bulk composition (in wt%, normalised to 100%) of crucibles N4 and N5 (full data in Appendix O.1)

zinc and lead oxide, but more strongly in copper. This points to the melting of leaded bronze in fairly oxidising conditions (with high lead contamination of the interior slag), with zinc again present as a possible contaminant (similar to N3).
Though no good stratigraphical connection exists for N4 and N5, the apparent application of a relatively iron- and lime-rich clay layer connects these two crucibles from a technological perspective.

Overall, the crucibles from Nicopolis appear to have mainly been used for active alloying of leaded bronze. This was done in a variety of crucibles and under variable heating conditions, resulting in very different metallurgical waste products.
It is interesting to note that no zinc has been encountered in the metallic state within any of these crucibles, but often occurred in an oxidised state on either the crucible interior and/or exterior. This indicates that zinc was not actively added to the crucible charge, but was often present as a contaminant, most likely of (recycled) copper. Due to its easy volatilisation and oxidation relative to other alloy components, even minute levels of zinc in the molten metal can give rise to high enrichments in crucibles (and moulds), as noted by Dungworth (2000a) and Kearns *et al.* (2010). It appears that zinc is a common copper contaminant for Roman copper/bronze, and this issue is further elaborated in section 11.3.
The frequent enrichment of exterior crucible surfaces in metal oxides (copper, tin, lead and zinc) most likely reflects contamination during the casting phase, through spillage and vaporisation.
A discussion of technological variability (e.g., application of an extra clay layer in N4 and N5, but not N3 and N6) across contexts and time for this site cannot reasonably be devel-

as *'slag'*. Rather, a fuel ash glaze was formed, which was then contaminated by spilled metal, dross or fumes, most likely during casting.

oped on the basis of these few samples.

11.2.2 Philippopolis

Samples P1-P5 were all taken from a group of macroscopically identical crucibles, deriving from a single context. No proper ceramic fabric was available for study of these crucibles. Relative to the P1 (vitrified) ceramic (which was taken as the best representative for ceramic composition for the crucible group), the P2-P5 dross shows increased fuel ash content. All four samples show bulk increases in copper, zinc, tin and lead oxide content, averaging to 70 wt% of the dross. The relative proportions of these metal oxides vary, however, with P2 and P3 being most similar, while P4 is most strongly enriched in copper oxide (and metal oxides overall) and P5 is most strongly enriched in zinc oxide.
The likeness between P2 and P3 extends to their prill content, with both showing indications for alloying in the form of high-tin prills, which incorporate lead and sometimes minor antimony. P4 equally exhibits fairly high-tin prills and lead, but no antimony. The presence of minor cobalt may further distinguish P4 from the other crucibles, though it is only present at the EDS detection limit. P5, finally, contains only pure copper prills.
It is again remarkable to find no zinc in the metallic phase in any of these crucibles, while all show bulk enrichment in zinc oxide. It appears therefore, that zinc is volatilised/oxidised from the metal in all of these crucibles, similarly to the Nicopolis crucibles.
Overall, it is possible to suggest an overarching interpretation for crucibles P2-P5, whereby active alloying of leaded bronze can be suggested, using a copper (or tin) source with some iron contamination. Zinc was probably present only as a contaminant in the used copper, and not as an element that was added to the alloy. Lead could have been introduced separately or as part of an existing (copper) alloy. Minor antimony entered the charge, probably together with lead or copper. Tin was added either as a mineral or metal.
A problem with this interpretation is introduced, however, by P1: here, several prills (from the crucible interior) were sampled, which are leaded gunmetal. This suggests that leaded gunmetal, rather than bronze was being produced in these crucibles. The absence of such prills in samples from P2-P5 may be a sampling issue or the result of extreme oxidation in the sampled areas for those crucibles. If an overarching interpretation is to be made, P1-P5 can all be understood as the result of leaded gunmetal production. The importance of a single sample for reaching this conclusion is striking, and is further discussed in section 11.3.

P6 is another externally heated crucible, showing limited fuel ash enrichments and slag formation. The metal oxides point to the processing of leaded bronze. Both interior and

exterior slag are relatively impoverished in iron, which is unusual. Furthermore, pure iron prills occur within the ceramic fabric, and similarly on the exterior surface (with minor copper content). This could point to very reducing heating conditions, whereby iron from the clay is locally reduced to its metallic state. The interaction of such iron with bronze prills on the crucible interior may be a better explanation for their very high iron content (26.5 wt%), rather than the iron being present as a copper contaminant. This last possibility cannot be excluded, however.

The crucible dross (relatively enriched in fuel ash) from P7 again points to the processing of leaded brass or gunmetal. Here, brass prills remain present, while lead and tin have oxidised, as well as some copper and zinc. As zinc is more prone to volatilisation/oxidation than lead and tin (Dungworth, 2000a), its remaining presence in metal prills after the removal of lead and tin strongly indicates that zinc is a major alloy component here. Under highly oxidising conditions, it can be expected that some copper, tin and lead will oxidise before all zinc is oxidised (despite thermodynamics predicting all zinc will burn off first). When zinc-bearing prills (without tin or lead) survive such conditions, it suggests a major presence of that element and only minor tin and lead content. Furthermore, it is worth noting that the bulk lead and tin oxide content in the P7 dross is much lower than that in P2-P5 dross, while its bulk zinc (and copper) oxide content is much higher. This further corroborates the different nature of P7 with respect to P1-P5. P7 is therefore best interpreted as a crucible used for leaded brass melting/alloying.
P8 derives from the same context, but is a different crucible type, used for a different purpose: it is clearly related to the processing of silver. Its interior shows significant fuel ash enrichment, while its exterior does not. The minor dross enrichment in copper and tin and strong enrichment in lead and silver, together with the limited macroscopic evidence for heating, could point to recycling activity: a small amount of debased silver may have been briefly exposed to a concentrated heat source, together with some charcoal, to burn off base metals, which resulted in the loss of minor silver as well. This would constitute the 'assaying' of scrap silver before its reuse, rather than the assaying of silver ore (Bayley and Eckstein, 1997). However, it is equally possible that a small amount of debased silver was simply remelted in this crucible for casting into a new small object, with some base metals being oxidised in the process. The presence of silver chlorides suggests (incomplete) post-depositional corrosion (see Graedel (1992); McNeil and Little (1992) and Rice *et al.* (1981) and 'patina' mentioned by Rehren *et al.* (1996)) of silver prills embedded in the crucible dross.

Crucible P9 is the largest crucible from Philippopolis, and internally heated for the melting of leaded bronze. The tin contents within the metallic prills are too low to assert active

alloying. However, some tin oxide agglomerations could be tentatively identified as residual cassiterite grains, suggesting a cementation process (and thus active alloying). Again, iron and zinc have been burnt off into the crucible slag, and are probably present as copper contaminants. In some areas, copper and lead are oxidised as well. The comparable levels of zinc and tin oxide in the crucible slag, but retention of only tin in metallic prills, is indicative of tin being an actual alloy component, while zinc is merely present as a contaminant.
This crucible has clearly been used twice, with a layer of clay (same clay as original crucible) being applied on top of the slag layer from the first use. While the first use can be tentatively linked to cementation of cassiterite with (leaded) copper, the second layer does not exhibit technological markers to suggest the same. It appears to be more enriched in zinc (though not that strongly), but more importantly, far less enriched in tin and lead. Furthermore, fuel ash enrichments are much higher for the first layer than for the second. This can all be explained by the more limited development of the second slag layer, which therefore trapped fewer charge fragments and contaminants. Most likely, the process conducted during secondary use of this crucible was the same as during the first use: bronze melting/alloying.

Overall, the entire Philoppopolis assemblage consists of externally heated crucibles, with the exception of P8 and P9. The production of (leaded) bronze, leaded brass and leaded gunmetal is attested, as well as small-scale silver melting. Again, zinc plays a difficult role when interpreting these crucibles. For both leaded brass and gunmetal production here, zinc was most likely introduced as a copper contaminant or alloy component, and copper/brass was mixed with lead and/or tin. As such, the 'active alloying' here refers to the addition of lead and/or tin, rather than zinc.
Similar to the Nicopolis case, no meaningful discussion of technological variability through time at this site can be made, given the limited evidence at hand and the rough dating available. It is notable, however, that the later (in a very rough sense) crucibles (P6, P7-P8) appear to be made of more refractory clay than the earlier, second century crucibles.

11.2.3 Serdica

Similar pottery appears to have been selected for reuse as crucibles for S1 and S2. These were probably employed for the same metallurgical purpose. As ceramic fragments were only sampled (accidentally) for S1, these must be taken as representative for both crucible fabrics. The reused domestic vessels were made of 'ceramic A', employing a fairly refractory, micaceous clay, while 'ceramic B' derives from a more sandy clay. It is difficult to say

if 'ceramic B' represents the external clay layer, which was not sampled and in fact completely bloated, or is simply dirt ('a layer of wet clay' was noted in Sofia).
These crucibles were clearly used for silver related metallurgy. Though little metallic silver remains, the few prills, many sulphides and overall dross enrichment reveal the presence of iron, copper and minor cadmium. This abundance of sulphides and their shapes, suggest severe sulphide corrosion of silver that was once present in these crucibles. Though the identification of some iron, copper and cadmium as probable contaminants of that silver is possible, it is difficult to further reconstruct the metallurgical process for which these crucibles were used.
Whether entire vessels (*amphorae*?) or just the bottom fragments (possibly closed on top) were reused as crucibles, cannot be reconstructed from examination of these dross fragments.

The rim sample of crucible S3 is not very illuminating: it simply shows that the rim was somewhat bloated and mildly enriched in fuel ash. No further interpretation beyond that made by macroscopic examination can be made here: the crucible was probably used for the melting or refining of gold. No compositional data for this gold (alloy) can be presented here.

Though copper is the main metal present in crucible S4, it is accompanied by iron, zinc, arsenic, silver and lead. It appears that silver and arsenic are the main alloy elements, with fairly high levels occurring in the metallic state, while zinc and lead are burnt off into the slag and most likely represent contaminants. The fuel ash enrichment is very strong in the crucible interior slag, and even more so in the exterior glaze (see Table 11.2). This indicates exposure to high temperatures mainly on the outside, but on the inside as well, probably through covering the entire, open crucible with charcoal. Alternatively, it could be indicative of reuse of this crucible, switching between internal and external heating.
It is remarkable that no iron oxide crystals were noted in either the external glaze or internal slag, despite their enormous bulk enrichment in iron oxide. This could suggest that, rather than iron entering the slag as a copper contaminant, this enrichment is in fact the result of a (very) thin, iron-rich clay lining being applied to the crucible's surface (inside and outside), which subsequently formed a glaze on the external crucible surface, and a slag layer on its interior. If that is indeed the case, the change in fuel ash components may have to be partially attributed to the different bulk chemistry of the applied clay layer, similar to the suggested interpretation of N4-N5. The far greater iron and fuel ash enrichment of the exterior surface suggests that most of that clay would have been applied to the crucible exterior, where the crucible was heated.
The lesser enrichment of the crucible exterior in copper, zinc, arsenic, silver and lead is

	Na_2O	MgO	Al_2O_3	SiO_2	P_2O_5	SO_3	K_2O	CaO	TiO_2	FeO	CuO	ZnO	As_2O_3	Ag_2O	PbO
S4 ceramic	**5.9**	**0.3**	**25**	**58**		**0.5**	**4.3**	**0.4**	**1.8**	**0.3**	**2.6**	**0.1**	**0.6**	**0**	**0.1**
Std. dev. (5 ms)	0.2	0.2	1	1		0.1	0.1	0.2	0.5	0.2	1.0	0.3	0.6	0.2	0.2
S4 internal slag	**7.5**	**0.6**	**16**	**40**	**1.0**	**0.8**	**2.8**	**3.3**	**0.9**	**2.5**	**13.0**	**1.3**	**6.0**	**0.9**	**3.9**
Std. dev. (5 ms)	0.4	0.3	3	4	0.1	0.4	0.5	0.4	0.2	0.3	4.9	0.3	0.9	1.3	0.8
S4 external glaze	**5.6**	**2.7**	**17**	**38**	**3.9**	**0.2**	**6.0**	**16.1**	**1.4**	**6.6**	**1.8**	**0.1**	**0.4**	**0.1**	**0.3**
Std. dev. (5 ms)	0.6	0.2	1	2	0.2	0.5	0.6	3.2	0.1	0.7	0.9	0.3	0.4	0.1	0.2

Table 11.2: Bulk composition (in wt%, normalised to 100%) of crucible S4 (full data in Appendix O.3)

probably due to contamination of the glaze during casting.
It should further be mentioned that gold was detected in exterior surface prills. Though gold-bearing prills have not been detected on the interior, the abundance of prills there may have led them to be missed during analysis. Alternatively, gold on the interior may have been removed during several cycles of use (with gold being more likely to be used in earlier cycles, when the crucible was still 'clean').
The variability in metals seen in this crucible may indeed not be the reflection of a single operation. If this crucible is an early modern intrusion, it would not be surprising to see the repeated use of a graphite-tempered crucible. Even in Roman times, such high-quality, refractory crucibles are more likely[6] to have been used several times. This obstructs the straightforward reconstruction of activity. While interpretation of single use would suggest the melting or alloying of arsenic- and silver-rich copper, contaminated by zinc and lead, this may seem a bit far-fetched.
Perhaps a better explanation is a first use for melting (aurian) silver, followed by later reuse involving (arsenic-bearing) copper (with minor zinc-iron-lead). During that secondary use, the arsenic-rich copper would have scavenged the remnant silver from the previous operation, to produce the uncommon arsenic-copper-silver alloy prills.
Though interpretations involving more phases of use could be suggested, an overview of the exponentially increasing number of scenarios (and therefore assumptions) involved is omitted here (Thorburn, 1918).

Fragment S5 is similar to S4, though slightly less graphite temper occurs within the ceramic, which is further infiltrated by silver chloride. Contrary to S4, the exterior (and interior) surface is not particularly enriched in fuel ash, indicating a different mode of heating. The 'hotspots' (noted by the samplers in Sofia) probably indicate very localised, external heat sources. The application of a secondary clay lining cannot be suggested here either. Based on prill analysis, this crucible can be clearly linked to silver, with minor copper

[6]These high-quality crucibles are more likely to have been reused several times than less refractory examples, like P1-P5. Nonetheless, reuse should be considered for each crucible under examination.

involved and, notably, significant gold content. This could suggest the processing of an electrum-like alloy or 'aurian silver'. However, enrichments of the interior slag could suggest different scenarios. While the presence of copper, silver, and even some lead would not be surprising (Thompson, 2003), the highly elevated bismuth content is unusual.
The presence of bismuth in aurian silver is explained by Craddock (1995) as a result of smelting silver from jarosite ores (Amorós *et al.*, 1981). This was practised by the Romans in Rio Tinto (Spain) and resulted in raw silver (after cupellation) with significant gold, copper and bismuth content (Craddock, 1995, Fig. 6.7, p. 220). The melting of such raw silver in a crucible under (mildly) oxidising conditions would result in the formation of a dross from the preferred oxidation of bismuth, prior to copper, silver or gold (Ellingham, 1944). It is important to bear in mind that strong slag enrichment in Bi_2O_3 does not necessarily represent high bismuth content in the metal charge. As the relative volumes of slag and melt are unknown, it is difficult to say whether raw silver, rather than silver with minor bismuth content (e.g., common *denarius* coins (Butcher and Ponting, 2005)) were melted in this crucible. As noted earlier, the slag that was sampled for S5 was exceptionally thick, sitting relatively close to the crucible rim. This corroborates its identification as burnt-off contaminants floating on top of the charge, but it remains hard to assess the relative amount of bismuth in the original melt. The presence of lead could indicate its intentional addition with the purpose of silver refining (removal of copper/bismuth), but the use of a graphite crucible and relatively low level of lead argues against cupellation for S5. Lead is therefore probably only present as a contaminant from the earlier smelting and cupellation processes. It should be noted that silver may have been intentionally mixed with gold in particular contexts, as shown for example by Rehren *et al.* (1996), but the combined presence of bismuth, copper and gold suggests that ore geology is responsible for the observations here.

Before continuing the interpretation of crucibles S6-S11, it should be noted that the ceramic compositions of S3-S5 are quite close to those of S1-S2. This could suggest the use of a similar clay, though graphite-tempered in the case of S4 and S5. Even if there might be a large temporal discrepancy between these crucibles, the repeated use of a local clay from the Serdica area for different crucible types might be reflected here.
Though some similarities exist between S4 and S5 (graphite temper, presence of aurian silver), there are notable differences as well (abundance of graphite, application of secondary clay layer, presence/absence of bismuth in silver), which make it difficult to consolidate the tentatively suggested relation between these two crucibles, excavated from different contexts.

Fragments S6-S11 form a single context, with the crucible clay compositions coinciding

(red group, Figure 11.27), and the ceramic of S6 and S9 having a slightly different but comparable composition. This crucible fabric is strongly dominated by fused quartz grains.
S6 appears to have been used for active bronze alloying (fairly high-tin prills), with lead and antimony being important further alloy components. The more humble arsenic and nickel (and minor iron) contents probably represent copper contaminants, originating from the copper ore. Lead and antimony could have entered the charge as separately added alloy components, or as previous alloy components of copper. Tin was most likely added in its pure form (metal or cassiterite). Minor fuel ash contributions in the dross corroborate external heating, as derived by visual examination, but suggest an open crucible.
S7 was probably equally used without a lid, more thoroughly covered in fuel, using a similar iron/arsenic/nickel-rich copper for bronze making. No high-tin prills are present in this crucible to suggest active alloying, however. The similarity to S6, with the exception of lead and antimony in this crucible could suggest that those two metals were added together in S6, possibly as a single alloying component. Furthermore, the analysis of the exterior surface of S7 reveals the presence of zinc (and increased nickel) in prills.
The analysis of sample S8 did not reveal anything conclusive. The high lead content of the slag, with minor zinc and some tin does not contradict its initial interpretation as part of the same operation as S6-S11.
Fragment S9 is more revealing and clearly shows more reducing conditions within that crucible, attested by the reduction of iron. As a result, gunmetal, sometimes with high iron content is preserved in this fragment, while zinc and iron are lost in the prills of other fragments (with the rare exception in S7). The high tin content of the prills again argues for its active addition to the crucible charge.
It appears that for S10, fragments of the interior surface were either not sampled or poorly mounted, and there is again not much to say. The reddish exterior surface is enriched in zinc. The high iron content in the only prill again argues for reducing conditions.
S11 is similarly indicative of reducing conditions, with inconclusive indications for bronze processing.

It is possible to suggest an overall interpretation for S6-S11 at this point. S6 appears to have been used for the production of leaded bronze. Antimony in S6 was most likely introduced together with lead, perhaps mixed up as a single metal (either intentionally or accidentally). For the other crucibles, the addition of lead/antimony to the bronze is not attested. However, the use of a similar copper source, enriched in iron-arsenic-nickel (and possibly zinc) may be seen throughout this group of crucibles, though its reflection in the samples varies. The most reducing conditions are attested in sample S9, where elevated zinc content is accompanied by high iron and tin content, suggesting the active addition

of tin.
It therefore appears that, while leaded bronze was produced in S6, S7-S11 were used for the production of plain bronze. The same source of copper was probably used in all crucibles, though S9 may have had exceptionally high iron and zinc content, indicative of a different raw copper, or possibly the production of gunmetal in that crucible.
Though fragments S8-S11 may not constitute a single crucible, their interpretation as part of a single, larger operation seems most appropriate, rather than suggesting a plethora of possible interpretations for each individual fragment.

Overall, the Serdica crucibles can be subdivided into those used for precious metals (S1-S5) and those for base metal alloys (S6-S11). Domestic pottery was reused for some silver-related process in S1 and S2, while a purpose-made crucible (S3) was most likely involved with gold processing. The graphite-tempered crucibles (S4-S5) present more complicated cases of (aurian) silver processing, with the possible addition of an additional clay layer and multiple phases of use in S4 making interpretation particularly difficult. A different crucible type, mostly made up of quartz sand, was used for the alloying of (leaded) bronze and possibly gunmetal, in a separate context (S6-S11). Similarly to Philippopolis, zinc was probably not added actively to these alloys.

11.2.4 Stara Zagora

The zoning of this crucible suggest two distinct episodes of use. First, the crucible was used without external layer B, and some prills were deposited on its exterior as well as interior surface. For its second (or perhaps 'n^{th}') use, an additional layer was applied to its external surface (covering the exterior prills deposited during previous use). If this layer was applied further over the rim and onto the interior surface, this is no longer visible due to fusing of those layers.
Reconstructing the alloys melted or produced within this crucible is complicated by the issue of double use, whereby the interior crucible slag represents the mixed result of two operations. No structural indications (e.g., two slag layers) exist to differentiate between features of the two operations. The embedded prills suggest the melting of leaded bronze. This could, however, be an alloy resulting from the mixture of metals introduced into the crucible during distinct operations. The presence of an almost pure lead prill suggests the introduction of lead as a pure metal for active alloying.
Prills on the exterior of part A are all leaded copper (with minor tin or iron), and its vitrified surface is more strongly enriched in zinc than the interior. This is evidence for the presence of copper, tin, zinc and lead in the crucible during its first phase of use.

For its second use, the exterior surface (part B) only reveals pure copper prills, and its slag is not particularly enriched in zinc.
It is notable that tin is more or less absent on both exterior surfaces, though present in low quantities in part A.
The most abundantly occurring prills on the crucible interior are bronze and leaded bronze. Zinc occurs only in prills with fairly low tin content or more outspoken iron content, suggesting that zinc, like iron, is therefore again present as a copper contaminant and not as an intended component of the final alloy. The first phase of use, then, could have been the active alloying of copper/bronze with lead to produced leaded bronze, while the second phase consisted of copper or bronze melting, with no indications for active alloying or the presence of lead.
It must be stressed that some aspects of this argument rely on the absence of evidence.

Section 11.3

Overview

One common characteristic of all crucibles investigated in this chapter is their compositional homogeneity: within each crucible, the ceramic fabric shows little variation. However, differences in ceramic fabric exist between the various crucibles. An overview of all crucible ceramic compositions (showing alumina, silica and 'flux components', cfr. Freestone and Tite, 1986) is shown in Figure 11.53.

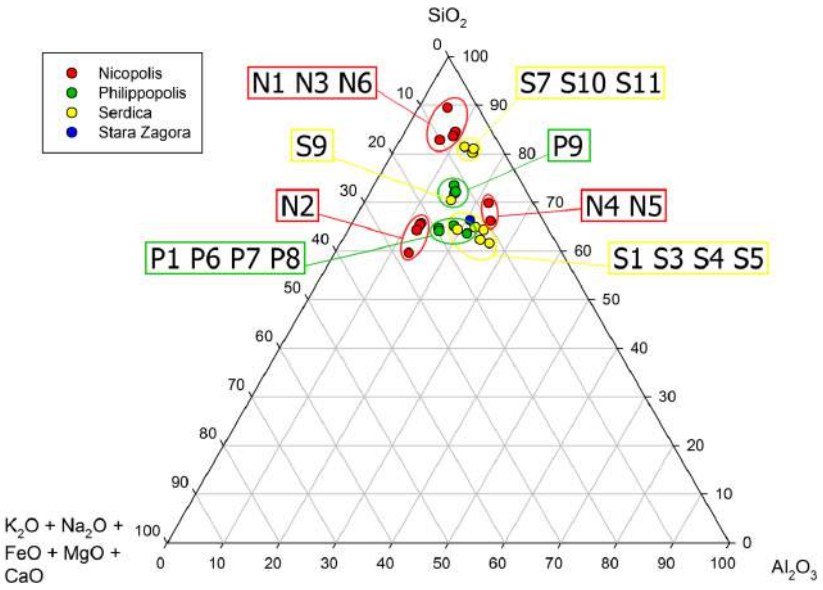

Figure 11.53: Ternary diagram showing all analysed ceramics from Roman Thrace

The most silica-rich crucibles (N1, N3, N6, S7, S10 and S11) were all used for the melting and alloying of leaded and plain bronze. The compositional clustering of these crucibles, as well as the similar type of metallurgy for which they were employed, does not coincide with a single crucible typology, however. Within this group, both external and internal heating modes are attested, which is reflected in the different crucible designs.
The improvised crucibles N4 and N5 (reused pottery with additional clay layer) have similarly low flux components (0-10%), but relatively higher alumina content. Their slag compositions, however, are largely dominated by the application of an additional clay layer, which is similar in composition to N1, N3 and N6. They can again be related to the melting of leaded bronze.

The majority of examined crucibles is richer in flux components (10-20%). A first group here are the Serdica crucibles used for precious metal melting (S1-S5). S1 and S2 were

used for silver-related metallurgy and are not purpose-made crucibles. However, it appears the functionality of these particular domestic vessels was known to the metallurgist who reused them, following application of a protective clay layer. Their compositions are indeed very close to those of the purpose-made crucibles S3 (gold metallurgy) and S4-S5 (graphite-tempered crucibles, employed for silver-related metallurgy). All are characterised by relatively high alumina content. S9, in contrast, has lower alumina content, and was used for melting leaded bronze/gunmetal.
P9 is compositionally very similar to S9, and equally used for the production of leaded bronze, possibly through a cementation process. In this case, however, a very different crucible design was employed for internal heating. Interestingly, crucible P9 has been relined with the same clay and reused for bronze melting a second time.
P1-P5 and P6-P8 are compositionally closer to the precious metal crucibles from Serdica. The first group of crucibles was used for the production of leaded gunmetal (or bronze) and, with their fairly high flux content and rough design, became quite malleable and lost some of their shape in the process.
P7 is closest in composition to this group, and similarly looks a bit bent after its use for leaded brass melting/alloying. It should be noted that this limited (apparent) loss of structural integrity of crucibles P1-P5 and P7 probably did not affect their functionality.
P8, which is relatively closer to S1-S5 in terms of ceramic composition, was used for silver processing, and therefore probably exposed to relatively lower temperatures over a shorter period than crucibles P1-P7, allowing it to fully retain its structure.
P6, applied in the processing of leaded bronze, has the lowest bulk flux components in this crucible group.
Finally, the Stara Zagora crucible, used for active leaded bronze alloying and reused for bronze melting, must be situated in this broad compositional cluster as well.

The crucible with the largest flux component (20-30%) is N2. This is, however, not really a crucible, but should simply be labelled a 'technical ceramic', involved in copper-based metallurgy. This corresponds to the observations made by Freestone and Tite (1986), that furnace materials tend to be slightly less refractory than those employed in the manufacture of crucibles.

It should be noted here that for many crucibles, some difficulty existed in performing a good comparison of ceramic and slag compositions. This was due to the frequent lack of either 'pure' ceramic or slag areas available in the sample (e.g., no ceramic for group P1-P5). Therefore, calculations of variable enrichment in certain components has not always been possible, or not as accurate as those presented for the Pi-Ramesse and Gordion case studies. Furthermore, the information on crucible shapes strongly varies as well. While

some crucibles have remained complete (e.g., P1-P5), most (e.g., S8-S11) are very fragmented and usually only one piece is available for a particular crucible type (provided such types exist), making it very difficult to reconstruct their shapes. Their overall interpretation is therefore further impeded, as crucible shapes and the use of lids vary strongly in Roman times (as opposed to the typical open Bronze Age vessels for bronze melting and alloying) and provide essential clues to identifying their metallurgical purpose.

The very fragmented nature of these assemblages therefore present a strong limitation on their overall interpretation. In fact, as can be seen from the lengthy interpretations in section 11.2, the limited evidence provides less opportunities to build strong interpretations through the comparison of multiple samples and much ambiguity remains.

Despite its small size, the assemblage reveals some significant aspects in the context of this thesis, nonetheless. While the above mentioned limitations are further discussed in Chapter 13, some further general interpretative remarks can be made here.

More than half of the investigated crucibles show bulk enrichment in zinc oxide, which corresponds to ±65% of all crucibles used for copper based metallurgy. However, it appears that in most cases, zinc is present merely as a contaminant, rather than an actually intended alloy component. This distinction is sometimes difficult to make, though. The main factors to distinguish actual brass-making from zinc-contaminated copper or brass melting, are the presence/absence of zinc-bearing metallic prills, the absence/presence of other contaminants, such as iron[7], in those prills and the indications for a reducing atmosphere through the use of a (perforated) lid, which provides the necessary pressure for zinc vapour to enter the copper. Bayley (1984) remarks that relative bulk enrichments of zinc[8] are up to an order of magnitude higher in brass cementation crucibles than in melting crucibles, but such distinctions seem difficult to maintain given variable process conditions. Some examples of (lidded) Roman brass-making crucibles are shown in Rehren and Martinón-Torres, 2008, Figure 9.1, p. 171. In general, Roman brass-making appears to have followed a cementation process, though very rare finds of metallic zinc, which could have been used for pure metal alloying, are known as well (Craddock, 1998; Rehren, 1996b).

In a cementation brass-making process, copper is expected to remain solid while zinc is vaporised inside the crucible. As such, liquid prills could be considered evidence for brass-melting rather than -making. However, it is possible that the same crucibles used for cementation were subsequently used for melting. Such a practice would further elim-

[7] In such cases, however, 'dirty copper' might have been alloyed with zinc, creating a similar outcome.

[8] Measured relative to iron by Bayley, which may be problematic as iron could be present as a copper contaminant.

inate another possible technological marker: the degree of crucible slagging. Where brass-making requires relatively low, very controlled temperatures (Rehren and Martinón-Torres, 2008), resulting in limited crucible slagging (e.g., in Roman Xanten (Rehren, 1999), where crucibles are heated indirectly), the subsequent heating to increased temperatures for brass melting and casting in the same crucible, as seen in Roman Britain (Bayley, 1998), could result in crucible slagging anyway (Craddock and Eckstein, 2003). Obviously, the refractoriness of the ceramics employed in brass-making or -melting influences their slagging in the process and limits the generality of these remarks. Finally, the presence of residual calamine, the zinc ore (in fact smithsonite, $ZnCO_3$) employed in brass cementation, could be a technological marker for the process. However, similar to residual cassiterite in bronze cementation crucibles (see sections 5.4.5 and 8.3.4), this has hitherto not been implemented in any published studies.
Overall, it appears that none of the crucibles presented here were used for an active alloying of zinc (ore) with copper.

The following distinction that must be made, then, is between brass melting and the melting of a copper (alloy) with limited zinc contamination. Making such a distinction is particularly difficult due to the over-representation of zinc as a contaminant in crucibles and moulds, relative to its importance as an actual charge component (Dungworth, 2000a; Kearns *et al.*, 2010). In general, very high zinc oxide content should be expected in slag/dross of crucibles where zinc is present as an alloy component, while more moderate zinc oxide content can be expected when zinc is present on a contaminant level. However, the variability in crucible conditions makes such a distinction untenable. Important zinc content (>4 wt%, see Craddock, 1978) in metallic prills more strongly argues for its presence as a significant alloy component.
For example, crucibles P2-P5 all show strong enrichments of zinc oxide in their dross, together with copper, tin and lead oxide. In a strictly theoretical sense, the presence of metal oxides other than zinc oxide, suggests that all zinc has burnt from the metal charge (high to low Gibbs-free energy: Zn-Sn-Pb-Cu, and high to low volatility: Zn-Pb-Sn-Cu), but this assumes ideal conditions. The absence of zinc in any of the metallic prills may confirm the hypothesis that zinc is only present as a copper contaminant in these crucibles.
However, taking into account crucible P1, which should represent the same process, the occurrence of leaded brass/gunmetal prills, suggests that zinc may have been present at more significant levels. The choice of dross samples for P2-P5 could therefore have prohibited the reconstruction of the crucible charge. Furthermore, it is possible that the sampling of an oxidising crucible fragment (rather than dross) could have resulted in a similar representation: copper/bronze prills from which all zinc has oxidised into the crucible

slag. This illustrates the (uncontrollable) effect of sample selection on crucible interpretation that is introduced by crucible heterogeneity: one sample (P1) can strongly alter the overall interpretation of a group of crucibles (P1-P5), and a single sample will often miss important information ('nugget effect'). For the identification of processes involving zinc, this effect seems to be especially problematic.
It is of course possible that P1 represents a different process from P2-P5, i.e., leaded gunmetal making on the one hand and (contaminated) leaded bronze making on the other hand, but this does not alter the above-mentioned problems faced during analysis. Here, it is best to suggest a single process interpretation that fits the data, rather than multiple possible processes.
P7 appears to represent the dross from a crucible in which leaded brass was melted. It shows very high zinc content, burnt off under oxidising conditions, but significant zinc content remains in the prills. In contrast, all tin and lead are burnt off, despite the remaining zinc content. Therefore, it can be concluded that zinc is a more important alloy component here. In the case of P1-P5, the presence of more important tin and lead can be said to 'push zinc out' of the metallic state. However, it must be emphasised again that different operating conditions, changing in time and location within the crucibles, could have altered the outcome of what may have been the same processes.
Finally, it can be noted that N6, used for leaded bronze alloying, does not show any zinc contamination. Though arguments *in absentio* are dangerous, the presence of various metal oxides and the lack of zinc oxide in crucible slag/dross is fairly compelling to suggest zinc absence in the charge.

A final, more general note on zinc oxide contamination of crucible slag should be made here, which equally applies to other metal oxides (see Appendix G). The actual amounts of zinc oxide in crucible slag or dross, converted to metal zinc, are usually very small relative to the metal charge in the crucible. Slag enrichments of several wt% usually translate to losses in the order or 0.1 wt% or less from the metal charge. Therefore, the zinc contents of preserved metallic prills provide a more reliable tool in assessing the relative importance of zinc in the charge.

The identification of the processes to which the precious metals were subjected is again difficult, based on the limited evidence available. The silver is often strongly corroded by either chlorine or sulphur, each indicative of particular environmental parameters, which are not really of interest for this discussion. Though chlorine and sulphur are known to have been used for the parting of silver and gold (Rehren, 2013), the shapes of the various silver chlorides and sulphides seen in the crucibles discussed here correspond best to corroded silver, rather than those seen in parting vessels (Meeks *et al.*, 1996). The occur-

rence of copper-rich aurian silver, with bismuth and lead-rich slag (S5) therefore probably points to remelting of raw (aurian) silver, rather than attempted gold/silver parting.
Silver, aurian silver and gold were melted in crucibles in Serdica and Philippopolis, though the purpose of these operations cannot be specified much further based on the analyses presented here. The identification of contaminants such as bismuth and lead does reveal some more detail regarding the origin of the silver processed in S5, tentatively linking it to poly-metallic ores. For S3, however, no information is gained beyond that available before analysis.

A note can be made here on the occurrence of almost pure iron prills in several crucibles (P6, S9-S11). These prills point to highly reducing conditions, provoking the reduction of iron oxide from the ceramic to the metallic state. The presence of minor copper in these prills, may suggest that tiny copper prills could act as nuclei for such reduction. It should be further noted that, though such iron prills indeed point to locally reducing conditions, those conditions did not necessarily prevail throughout the crucible. In Pi-Ramesse (sample 86_0749c) and Gordion (samples 22626 and 27638), for example, iron prills have been noted in the context of an open crucible process.

Finally, some comments are required on the practice of crucible reuse and its implications for the interpretations made in this chapter. Direct indications for reuse have been found on all sites, with the exception of Nicopolis. In Philippolis, P9 shows the unmistakable application of a secondary clay layer (identical to primary ceramic fabric) for its second use. In Serdica, S4 does not show any clear structural features revealing reuse, which is in that case suggested by the nature of the metal prills. In Stara Zagora, the crucible was clearly repaired or reinforced for its second use.
It should be remarked here that 'second use' in the above implies a minimum number of uses, suggested by prills or the application secondary clay layers. However, it is possible that these crucibles were used several times before and/or after a secondary clay layer was applied, without leaving any diagnostic evidence. Here, the same reasoning is applied as that applied for all other crucibles: a 'single use perspective' is adopted for interpretation wherever possible.
Overall, it appears that repair and reuse of crucibles is not uncommon in this assemblage. Though not directly attested in Nicopolis, the interior ceramic layer in N6 may be an indication of 'prepared reuse' that was never executed. The positive identification of reuse in several crucibles may provide confidence in the interpretation of other crucibles as single use vessels, but this is no guarantee. Though a single use interpretation is preferable wherever possible, it is easy to imagine that certain crucibles were used for the same purpose several times, resulting in a slag and dross representative of that purpose. For highly

refractory crucibles, it is even easier to envisage the 'overwriting' of evidence through frequent reuse, as little crucible slag is formed and dross is easily removed. In those cases, the slag/dross most likely reveals the most recent metallurgical process executed in those crucibles. All in all, the most likely candidates for such 'invisible reuse' in this assemblage are N4, P8 and S1-S3.

A final aspect of reuse in this assemblage is the adaptation of existing (domestic) pottery for metallurgical purposes, seen in N4-N5 and S1-S2. Such reuse is not expected to influence the interpretation of the actual metallurgical process.

CHAPTER 12

Discussion

From the foregoing discussion, it appears that zinc is quite common as a contaminant in Roman copper based alloys. Though it is beyond the scope of this project to discuss the various alloys produced in Roman times and their application, a few points can be made based on the crucible analysis presented here. Some general overviews of the use of standardised Roman alloys is given by Dungworth (1997), Hook and Craddock (1996), Riederer (2002a,b) and Unglik (1991). Roman brass in particular is discussed by Craddock (1978). Brass was adopted as a popular alloy at the early stages of the empire, in particular for the production of military equipment, but additionally for other purposes such as coinage. In Roman Britain, for example, it appears within a decade following conquest, though mainly in an imperial military setting (Bayley, 1998). Similarly, it was introduced in other newly conquered Roman provinces and reflects a 'typically Roman' metallurgical practice. In Palestine, for example, local inhabitants seem to have preferred their traditional bronze alloys over the imported Roman technology (Ponting, 2002). In North-Africa, it appears that the imported copper and brass may have been locally manipulated and perhaps mixed with local metals (in some cases mined by the Romans themselves (Skaggs *et al.*, 2012)) as it was incorporated into the trans-Saharan metal trade (Fenn *et al.*, 2009).

At any rate, brass production seems to have been largely under imperial control, and the decline in zinc content of copper alloys during the later Roman empire (Rehren and Martinón-Torres, 2008), particularly in brass coinage (where this decline was first noted by Caley (1964)), was most likely a deliberate choice. Brass coins were diluted by the addition of leaded bronze, which parallels the dilution of the silver *denarius* coinage (Dungworth, 1996). A similar transition from brass to leaded bronze is noted in military equipment by

Dungworth and Starley (2009). Bayley (1998) further mentions the deliberate or accidental mixing of brass and bronze scrap as indicated by the inversely proportional relation between tin and zinc in many copper alloys. This was equally observed by (Craddock, 1978), who further noted the lack of tin-zinc correlation for levels of zinc below 4%, which suggests zinc's unintentional presence as scrap at that level.

The contribution that can be made to this picture through the analysis of the crucibles presented in this chapter is perhaps limited, though it shows that Roman metallurgical practice reached Thracia, and can aid future comparisons with imperial centres. It corroborates that zinc was pervasively present in Roman copper alloys, either as a deliberate alloy component or as a contaminant. Zinc's occurrence as a contaminant here may probably be explained by the repeated recycling of brass, rather than reflecting the ore from which copper was smelted. Though it is often difficult to reconstruct the exact alloys that were being produced in these crucibles, many give the impression that various copper scrap may have been recycled and mixed together to form (leaded) brass, bronze or gunmetal. In P9, for example, (leaded) bronze was produced using a zinc-contaminated copper, as in N1 and N3, while leaded bronze was alloyed in N6 using a zinc-free copper.

Within these Thracian workshops, brass then appears to have been available mainly as scrap, as the use of a fresh zinc source is not attested. However, this does not exclude the availability of zinc, which may have been used in hitherto unexamined crucibles. Future case studies may reveal patterns of zinc availability in the Roman provinces, and the degree to which various workshops were reliant on recycling brass. Whether recycling in the crucibles under discussion reflects a conscious choice by the metallurgists to achieve particular mechanical, visual or other properties is impossible to guess. Different metals (pure and alloys) were most likely available, though probably at different costs, allowing them to select the appropriate material for particular purposes. A comparison of these single samples from different contexts and periods does not allow further discussion on this subject.

A few moulds discovered at Nicopolis (Cholakova, 2006), which indicate the production of small rings, are the only objects which may be tentatively related to the metallurgical *chaîne opératoire* to which these crucibles belong. Contrary to the artefact analysis performed by Ponting (2002) for Roman Palestine, these crucibles themselves offer little insight into the social implementation of Roman metallurgy in Thrace. The particular social contexts in which these crucibles were used is unknown, and they can therefore not be used to compare technological choices made in different settings here. Though some information can be gained from the analysis of metal finds from the region, their relation to these particular crucibles cannot be established. No information is available for the fur-

ther working of the metal produced at the contexts under discussion, as no furnaces, tools for cold/hot working, metal objects etc. were available for study. The actual object production techniques beyond the crucible stage, like casting and annealing (Unglik, 1991), can therefore not be discussed here.

It is, however, possible to make some tentative suggestions on the types of object that might have been produced from the various crucibles presented here. In Nicopolis, the larger crucibles are related to (leaded) bronze alloying, and the smaller crucibles to melting/alloying. The use of leaded bronze was preferred to plain bronze for casting (Riederer, 2002a), and the volumes seen here conform to small object casting, like small rings, though somewhat larger objects may have been cast as well. Lead may equally have been alloyed with bronze for the purpose of adding weight at a lower price (Unglik, 1991).

In Philippopolis, both (leaded) bronze/brass/gunmetal and silver were processed. P1-P5 are fairly small crucibles, offering better control of interior conditions, which is important for brass/gunmetal melting and production. This small scale is compensated by their numbers, indicating that perhaps several crucibles were heated at once to produce more significant amounts of leaded brass/gunmetal (through the addition of tin to existing leaded copper/brass). There are no indications (spouts or rim traces) to suggest that liquid metal was poured from these crucibles. The produced metal may have been remelted in a different crucible for casting (either as small batches or by combining metal from several crucibles) or worked as such. P6 and P7 are of a similar size, but used for the melting/alloying of leaded bronze and brass respectively. P9 is quite different, as it appears to have been used for a cassiterite cementation process to produce (leaded) bronze, and is quite a bit larger. It is interesting to note here the difference in size and shape between P6 and P9, both used for leaded bronze metallurgy. This could be indicative of many things, such as simple melting of limited metal (P6) or active alloying of more significant amounts (P9) or perhaps objects of different sizes being intended for casting. The singular occurrence of these crucibles renders such discussions very difficult, if not futile. In fact, if gunmetal prills happened to be missed in this particular sample of P6, its comparison to P9 becomes even more tenuous. P8 stands out as the only crucible used for silver processing, and its spout suggests it may have been used to cast small silver objects.

In Serdica, a particular group of crucibles was used for the alloying of leaded bronze, possibly gunmetal (S6-S11). Though their size is difficult to estimate exactly, they appear to be fairly large and, as a group, suggest the production of more substantial amounts of metal. Of course, it is difficult to establish whether all crucibles were used contemporaneously. The other crucibles, used for precious metal melting, are fairly small. S1-S2 were probably used for simple remelting of silver, and S3 for the remelting of gold. While S3 has a

spout and was clearly used for subsequent casting, this is difficult to establish for S1-S2, which probably did not have a spout as they were not purpose-made crucibles. S4-S5 may have been used for refining of (raw) aurian silver, and subsequent casting. Their similarity to post-medieval crucibles (compare Figure 11.33 and Martinón-Torres and Rehren, 2009, Figure 6, p. 61) suggests they could be late intrusions.
The Stara Zagora crucible was most likely used for the alloying and casting of a relatively modest amount of leaded bronze.

It should be noted that both base metals and precious metals were probably being recycled, melted, alloyed and cast in all of the sites under discussion, without this necessarily being represented in the limited sample investigated here. Furthermore, this would have taken place alongside ferrous metallurgy, as noted by Salter (2007) in Nicopolis. These samples therefore do not allow any further comparison of the different sites in terms of variety and importance of different metallurgical operations, as they are simply not representative at that scale. Furthermore, any link between crucible typology and alloy type cannot be securely established on the basis of these samples. Though preferences for certain crucibles for particular purposes probably existed, it is evident that a range of shapes, sizes and ceramics were used, sometimes in a rather *ad hoc* way, as exemplified by the reused domestic pottery. This reveals a flexibility of the Roman metallurgist, reflected in the crucible remains, which may be partially related to the scale at which they were working. These small, urban workshops would probably have produced a large variety of objects, composed of different metals and alloys, and drew from a range of vessels for particular purposes. However, the most specialised vessels appear to have been reserved for precious metals (e.g., P8 and S4-S5). Nonetheless, the overall high quality of ceramics available in Roman times allowed them to use less specialised vessels, provided with a protective clay layer, if that ceramic was of the right quality. The clustering of clay compositions across crucible typology indicates the recognition of such quality by the ancient craftspeople.
An exhaustive comparison of this assemblage to different crucibles found across the entire Roman Empire would therefore be exciting, but such a gargantuan task is beyond the scope of this thesis. Many such crucibles have been published in various site reports, as well as more crucible-oriented studies (e.g., Bachmann, 1976; Bayley, 1984, 1987; Dungworth, 2001a,b; Dungworth and Bowstead Stallybrass, 2000; Dungworth and Starley, 2009; Horsley, 1997; König and Serneels, 2013; Nicholas, 2003; Rehren, 1999), with a strong bias towards the western Roman provinces. For the majority of these crucibles, analysis was restricted to pXRF. The potential for pXRF, in particular when limited fragments are available for study, as is the case for the assemblages discussed in this chapter, is further discussed

in Chapter 13.

One particular comparison can be made here to Roman crucibles discussed by König and Serneels (2013), who noted the presence of an 'engobe' on most of the crucibles. This appears to be a thin layer of clay on the interior of the crucible, made up of the same material as the exterior protective layer applied to the crucible. Though a strong visual identification of such a layer could not be made for any of the crucibles discussed in this chapter, some similarity may exist to the added clay layer tentatively identified in crucibles N4-N5 and on S4. In both cases, however, an iron-rich clay appears to have been applied, while König and Serneels (2013) note particularly high lime contents, which may be (partially) attributed to fuel ash contributions, as well as the selection of a particular clay. As mentioned before, the application of this iron-rich clay to the crucible interior is quite peculiar, as it does not seem to offer any discernible technical advantage. Perhaps surface unevenness or small cracks in the reused pottery warranted this application, and was intended to avoid any losses (e.g., silver chloride in fragment S5, but not S4). At any rate, it appears that these layers served their purpose and did not result in failure of the crucible process.

The sources of metal available to Roman metallurgists were probably quite varied. Clearly, a well-established Roman trade system for ingots existed, which covered many different metal types (Beagrie, 1985; Hughes, 1980; Kingsley and Raveh, 1994; Klein *et al.*, 2007; Pagès *et al.*, 2011; Parker, 1974; Parker and Price, 1981; Pinarelli *et al.*, 1995; Skaggs *et al.*, 2012; Tisseyre *et al.*, 2008; Trincherini *et al.*, 2009). In this context, it is perhaps interesting to mention the existence of mixed metal ingots. Pewter (tin/lead) ingots with deliberately varied compositions were most probably intended for the easy production of specific alloys (Hughes, 1980). The suggested use of a mixed lead/antimony additive to the S6 crucible may tentatively be related to this practice, but such ingots are yet to be identified in the archaeological record.

Though ingots probably reached Thracia, both precious metals and base metals occurred and were mined in the province as well (Davies, 1935b, 1936; Dušanić, 2004). The evidence for primary iron production in Nicopolis (Salter, 2007), probably points to the smelting of local rather than imported iron ore, and allows the possibility that other local metal ores were being smelted as well. Evidence for such primary metal production has hitherto not been published.

This introduces the question of where the raw (or at least bismuth-contaminated) silver, identified in crucible S5, may have come from. Though some complex silver ore occurrences are known in Thrace (Davies, 1935b), the evidence for raw silver extraction from jarosite ores in Spain, mentioned in section 11.2.3, is perhaps more compelling. This suggests the export of raw silver from the region, which would still require further refining

before its actual use. However, such refining may have taken place in a single process immediately preceding the casting of the desired object, with any dross/slag remaining in the crucible. As such, it would not be surprising to find some remaining bismuth and perhaps minor lead, but especially copper and gold in the resulting silver artefact. Through repeated recycling and remelting, the bismuth, lead and copper content is expected to decrease significantly, though not disappear completely (e.g., *denarius* coins (Butcher and Ponting, 2005)).

Despite Spain being a likely candidate for this silver, the evidence from relatively nearby Sardis should be mentioned here as well. Bismuth and copper are noted there by Meeks (2000) in silver mixed with gold, and furthermore in silver coins (Cowell and Hyne, 2000). However, this much pre-dates the Roman period, during which Sardis was part of the province Lydia rather than Thracia. Another interesting case is a silver coin with high gold content, as well as elemental copper and bismuth inclusions, discussed by Giovannelli *et al.* (2005) who interpret it as unrefined silver smelted from a poly-metallic ore, possibly jarosite. Though from a (6^{th} century BC) Greek, rather than late Roman, context, this type of metal is probably quite close to what should be envisaged as the charge for crucible S5.

Overall, it is interesting to point out the identification of jarosite ores being used for *denarius* minting under Augustus and Tiberius (Butcher and Ponting, 2005), followed by an apparent switch to oxidised ores (lower bismuth), dry ores and galena (which do not produce the same gold/bismuth enrichment, though sometimes one of both occurs) later on[1]. This in turn opens the issue of minting, which has been mentioned already during the introduction to this chapter. Even though the minting of coinage took place at each of the cities discussed in this chapter, the particular contexts under investigation are not clearly linked to any mint. Furthermore, none of the crucibles provide convincing evidence that such a relation should be presumed. Though any of the crucibles could be related to minting (of either bronze, brass or precious metal coinage), each may have equally been used for different purposes. Without further contextual information and related finds such as moulds or blanks, a relation to minting will remain tentative at best.

Nonetheless, some general remarks on coinage in Thracia can be made here. An overview of coin hoards in Bulgaria is given by Paunov and Prokopov (2002), who note that coins were first circulated in Thracia-Moesia just after the start of the first century BC, with *denarii* being particularly introduced for military and strategic reasons, rather than commerce. More general discussion on Roman coinage can be found in, e.g., Bland (2013); Butcher and Ponting (1995, 2005); Carradice and Cowell (1987); Carter (1978); Crawford (1977); Hendy (1972); Klein and von Kaenel (2000); Klein *et al.* (2004) and Reece (1985),

[1]This could be suggestive of an early dating for crucible S5, though the evidence is very conjectural.

and is quite beyond the scope of this thesis. In this context, Butcher and Ponting (2005) note that lead isotope analysis of silver mostly reflects the lead used in the silver refining process, rather than the original silver ore. Any attempts at relating silver objects to their ores through lead isotope analysis (Baron *et al.*, 2011), is therefore particularly difficult. The widespread use of lead in brass and bronze, compounded by the regular recycling and debasement of coins, renders the use of lead isotopes for provenance studies in a Roman context very complicated, and mostly relevant for the study of lead sources (e.g., Bode *et al.*, 2009; Boni *et al.*, 2000; Durali-Müller *et al.*, 2007; Kuleff *et al.*, 2006; Pinarelli *et al.*, 1995; Skaggs *et al.*, 2012), though attempts have been made for copper using a combined analytical approach (e.g., Klein *et al.*, 2007). Ponting *et al.* (2003) suggest that, rather than reconstructing ore sources, particular mints or workshops may be reflected in the lead isotopes, though further analysis is needed to determine the applicability of this hypothesis. Where only limited sampling for crucibles is possible, technological reconstruction is more likely (though definitely not guaranteed) to succeed than metal provenancing. Nonetheless, the identification of particular chemical/mineralogical markers (like bismuth in the case of silver) can provide some clues here.

Bronze vessels from Roman Thrace are discussed by Nenova-Merdjanova (1997, 2002a,b, 2011), who furthermore suggests that approximately half of all these were imported from abroad (mainly Italy, Egypt and Syria), while the rest was produced in Thrace. These imports were apparently mainly luxury products, intended for consumption by the local nobility, while the local production furnished vessels for the less wealthy, and was not organised on an industrial scale. Similarly, it appears that functional workshops for the repair of military items were set up *ad hoc*, for example in military camps, while mass production took place in centralised *fabricae*. Of interest here, perhaps, is the location chosen for these smaller scale workshops, both private and military. As noted by Dungworth and Starley (2009), workshops in military encampments (in that case fairly sizeable) are typically located close to the ramparts. This is paralleled in Xanten, where the private workshops are found in the craft quarter, close to the walls (insula 39, Rehren and Kraus, 1999), as well as Nicopolis ad Istrum. Poulter (2007b) suggests this may be related to the better control of fire hazards.

The crucibles discussed in this chapter can most likely be situated in such a context of small, urban workshops, geared towards producing and repairing a variety of rather small objects for local consumption and following a more adaptive, *ad hoc* approach than what could be expected in the more industrialised *fabricae*.

In conclusion, it must be noted that the fragmented nature of these crucibles is largely responsible for spawning a rather exasperating (and perhaps tedious) interpretation and

discussion. Where many samples were available to study the metallurgical process executed in a homogeneous group of crucibles in the two preceding case studies, this assemblage is made up almost completely of unique crucibles. In the few cases were several similar crucibles were available (e.g., P1-P5 and S6-S11), the combined information deduced from these fragments typically allowed more meaningful discussions than possible on the basis of single samples. The issues introduced by limited samples are further aggravated by the complexity and variety of Roman metallurgy, where mixing and recycling of old and new metal appears not to have been uncommon. Restricted contextual information further limits the scope for broader discussion of these results. These issues are further examined in a broader methodological discussion in Chapter 13.

Nonetheless, the reconstructions offered in this chapter present some of the most detailed elaborations of metallurgical practice in eastern Roman provincial cities currently available. As such, their examination stands as an important basis of comparison for future metallurgical studies in the region. Despite interpretative difficulties discussed here, these crucibles shed light on the alloys worked within these urban workshops, and raise questions on provincial metal production (organisation) that may be addressed by future research.

Part VI

Discussion

At work here is that powerful WYSIATI[2] rule. You cannot help dealing with the limited information you have as if it were all there is to know. You build the best possible story from the information available to you, and if it is a good story, you believe it. Paradoxically, it is easier to construct a coherent story when you know little, when there are fewer pieces to fit into the puzzle. Our comforting conviction that the world makes sense rests on a secure foundation: our almost unlimited ability to ignore our ignorance.

Kahneman, 2012

[2] WYSIATI: What you see is all there is.

CHAPTER 13

Methodological issues for crucible metallurgy studies

The outcome of ancient crucible studies depends on many factors, some of which are within the researcher's control, while others are not. Crucible slag variability, first noted in this thesis for the Pi-Ramesse assemblage (section 5.4.9) is discussed in more detail here, distinguishing between the variability witnessed within crucibles (section 13.1) and throughout crucible assemblages (section 13.2). These two forms of variability have hitherto not been discussed in the literature, but are shown to impact greatly on the interpretation of analytical data. In fact, with the exception of work by Humphris *et al.* (2009) on iron smelting slag, the methodological implications of variability in ancient production remains for archaeometallurgical studies has barely received any attention.

In section 13.3, the methodological options to cope with such variability are discussed, and an agenda for 'best practice' in crucible studies is outlined. Bayley *et al.* (2001), Bayley and Rehren (2007), Martinón-Torres and Rehren (2014), Rehren (2003) and Tite *et al.* (1985) provide a general framework for the analysis of ancient metallurgical crucibles. This chapter offers a more detailed discussion of sampling, analysis and interpretation issues.

Section 13.1

Within-crucible variability

Previous studies have not considered the variability that may exist within crucible assemblages. As this section demonstrates, the first type of variability that can be identified within crucible assemblages is the variation that occurs within crucibles themselves. The analysis of a single crucible sample does not necessarily capture this variability, and some of the differences seen between samples from different crucibles can often be attributed to variability of the same process. The main factors influencing this within-crucible variability and its characteristics are discussed in this section.

Several process parameters may vary strongly during metallurgical crucible processes. The most important are redox-conditions, temperature and the distribution of charge constituents. The first two are strongly related to changing oxygen supply within the crucible, which in turn is controlled by tuyère placement, continuity in bellowing action and charcoal cover. This oxygen supply is a dynamic factor, producing hotter and cooler regions within a crucible, and more oxidising or reducing conditions in different areas, as shown in Figure 13.1. These zones may change rapidly through time, and as crucibles go through several stages in their use, such as pre-firing, charging, melting/smelting, casting, cooling and reuse.

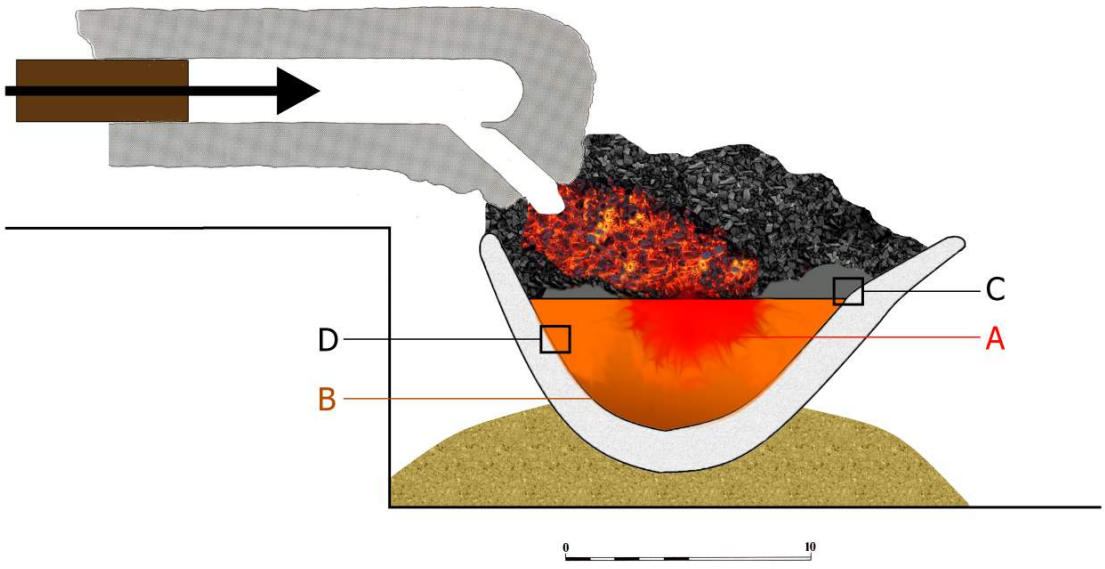

Figure 13.1: Schematic representation of heterogeneous crucible conditions at a particular point in time, with hotter (A) and cooler (B) regions and more oxidising (C) and reducing (D) conditions

Most information on the metallurgical process is contained in the crucible slag forming through the melting of the inner surface of the crucible. The degree of this melting is a function of the composition and refractoriness of the ceramic, which is usually constant across the crucible fabric. Despite this compositional homogeneity of the ceramic, vitrification and slag formation may vary strongly within crucibles. This changing rate of ceramic disintegration stems mainly from variability in process parameters throughout the crucible. The degree to which the ceramic vitrifies and melts in turn influences the amounts of charge constituents that can be encapsulated, such as charcoal/fuel ash, ore fragments, metal prills and metal oxides, which transform vitrified ceramic into crucible slag. None of these charge constituents are necessarily present in every particular area of the crucible, even though they may occur in one area.
In oxidising areas of the crucible, some of the metal in the charge can oxidise. In the case of copper, contaminants such as iron, cobalt, nickel and arsenic or alloying elements such as tin, lead and zinc are burnt off before the copper itself oxidises (Ellingham, 1944; Dungworth, 2000a; Kearns *et al.*, 2010). If this happens in an area with a sufficiently developed liquid slag layer, the metal oxides can be incorporated into that slag layer and provide highly distorted information on the nature of the original metal melted in a crucible. Under more reducing conditions, metal prills can be trapped nearly unaltered in the slag, reflecting the original metal composition more adequately. The relative proportions of molten ceramic, fuel ash, metal oxides and metal inclusions in the crucible slag can vary highly from one part of the crucible to the next, and over very short distances. When no slag is formed, some of these metal oxides typically gather on top of the molten charge as a dross layer. Similarly, slag inclusions (silicate-based waste) will typically float on top of the charge and mix with any dross (oxide-based waste) formed, as illustrated in section 5.4.10. At the casting stage, the dross layer may be removed by the metallurgist, or deposited on the crucible interior.

Some examples from the three case studies discussed in this thesis can be used to illustrate this variable slag formation. A crucible fragment from Pi-Ramesse, shown in Figure 13.2 (and earlier in Figure 5.7), is slagged along its entire profile. The slag layer is fairly regular and thin closer to the rim (top) and its reddish surface is quite flat. Lower down, however, the slag thickness increases and is more variable, and the dark grey slag exhibits a more irregular surface with visibly corroded copper-based prills. Analysis by pXRF shows that closer to the rim, the slag is mainly enriched with lime (with limited copper enrichment), while the slag in the body part of the sherd (measured only 3 cm away) is enriched in iron, copper, tin and cobalt. Though this particular sherd could not be sampled in Egypt, the rim and lower body areas are represented by similar samples analysed by SEM-EDS, such

Figure 13.2: Pi-Ramesse crucible fragment 88_1374,0001, showing macroscopic differentiation between rim (top) and lower body (bottom)

as 87_0849a,04 and 87_0762 respectively. Microscopic inspection of those samples reveals the slag at the rim area to be mainly composed of vitrified ceramic, fluxed by fuel ash and with only minor copper content. The slag forming at the lower body, in contrast, is strongly enriched in copper and tin, as well as iron and cobalt. This iron and cobalt occur as spinel (see Appendix D.5) in the crucible slag, and originate from the preferential oxidation of raw copper. Differences in redox-conditions and material presence produced these different slag enrichment in the two zones and resulted in their different macroscopic appearance. An important observation here is that the Pi-Ramesse assemblage contains many fragments that consist only of either the upper rim area or the lower body area, and therefore do not allow the comparison of both zones within one sherd. Considered in isolation, analysis of the rim in Figure 13.2 only reveals fuel ash contributions and the limited presence of copper (not bronze), and does not allow interpretation beyond 'copper-related metallurgy'. The lower body tells a different story: it points to 'bronze-related metallurgy', with the use of iron and cobalt contaminated copper.

A second example from Pi-Ramesse is shown in Figure 13.3, where two samples have been taken from a small rim fragment. They show a similarly poor type of crucible slag as seen in the previous example near the rim, composed almost exclusively of vitrified ceramic. However, tiny embedded metal prills were noted in both samples. For the top sample, all prills were composed of almost pure copper, with up to 1 wt% iron. In the bottom sample,

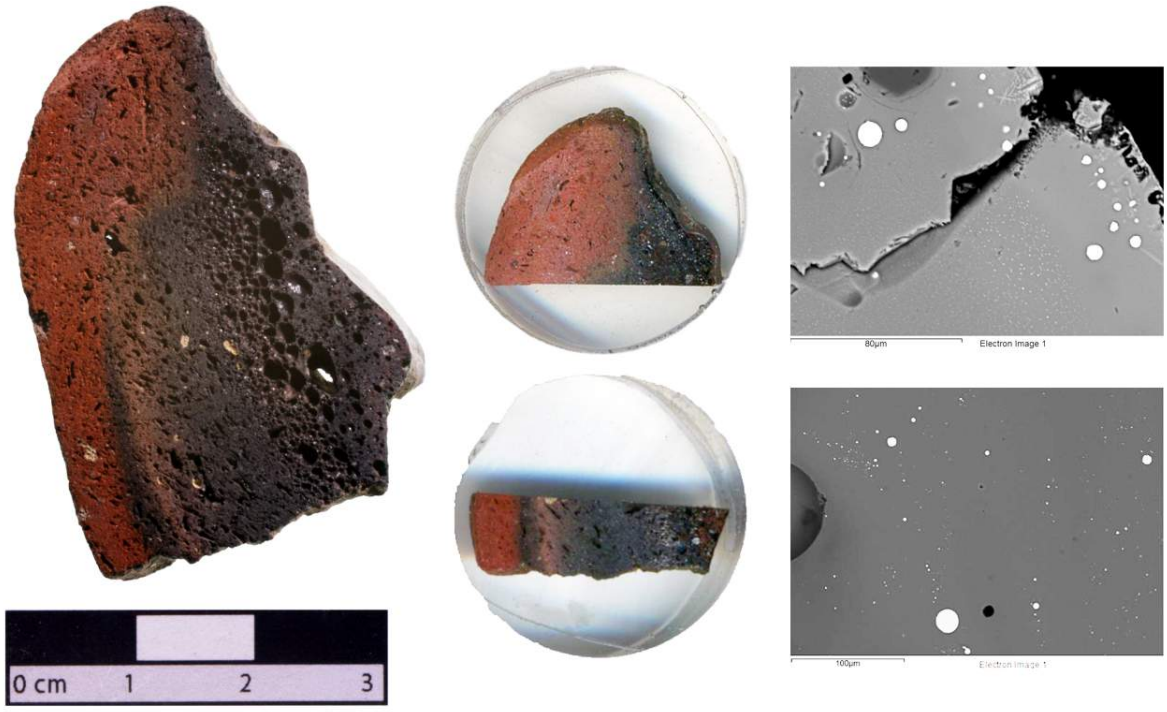

Figure 13.3: Small Pi-Ramesse rim fragment (left), from which two samples (83_1149b - 1 and 2) were cut and mounted (middle). Prills in both samples are shown on the right

all prills had a radically different composition, averaging around ±30 wt% copper, 40 wt% nickel, 15 wt% cobalt and 15 wt% iron. Despite being taken only two centimetres apart, these samples present varying evidence of what must have been the same process and, viewed in isolation, would again lead to divergent interpretations.

Upon noting this variability in the Pi-Ramesse assemblage, the analysis of several samples from single fragments of the Gordion crucibles was undertaken, as detailed in section 8.3.8. The variability seen in Gordion-25394 is summarised in Figure 13.4. The rim sample (A) exhibits limited slagging, and most of the interior is simply vitrified ceramic. A few tiny prills occur further away from the rim (towards the lower body), which are iron- and arsenic-rich bronze, but the bulk slag metal content is low (Table 13.1). In the intermediate sample (B), the slag is more developed (though not everywhere) and more metal prills are present. These are mainly pure copper prills with minor iron content, while the slag contains large amounts of tin oxide, malayaite and copper (chloride) oxides. Finally, the lower body sample (C) presents the thick crucible slag at the bottom of the fragment. Here, two layers exist: the deeper slag layer is similar to sample B (with iron-rich bronze prills), while a dross layer is deposited on its surface, which is dominated by various metal oxides (including lead oxide). The bulk slag metal content in sample B is higher than that of sample A, but lower than that measured in sample C (Table 13.1), which is reflective of

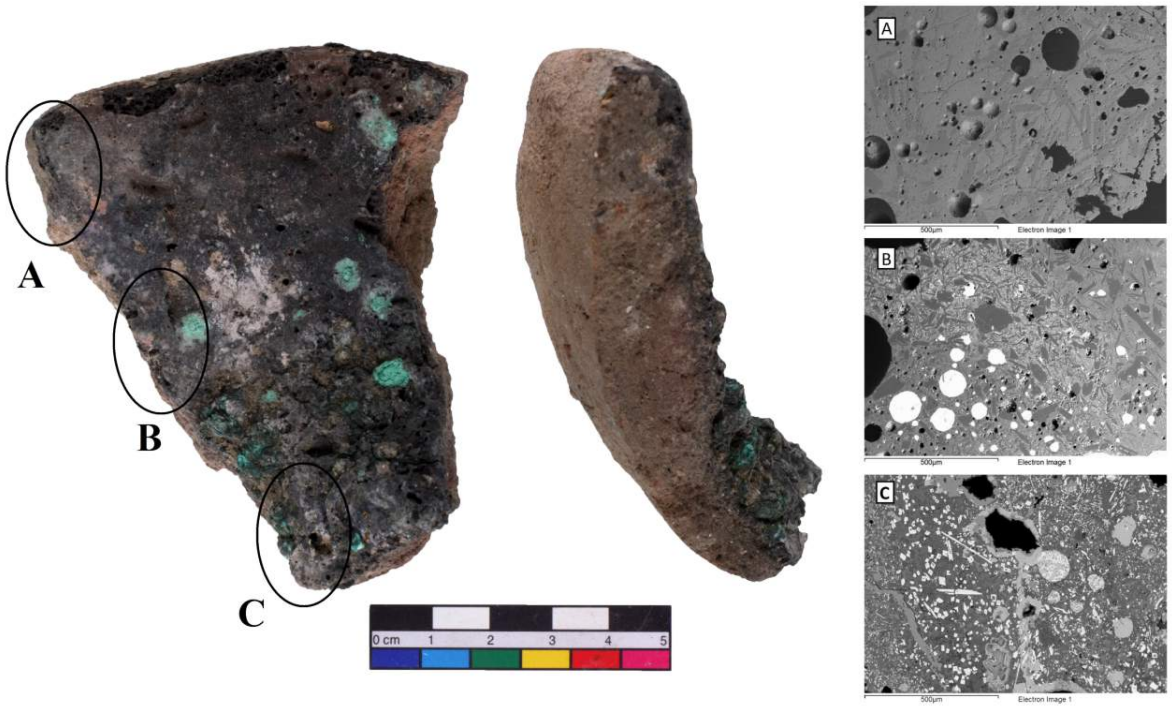

Figure 13.4: Gordion crucible fragment from which three samples were taken (left), with representative images of the three areas (right)

	CuO	SnO_2	PbO
Sample A	0.8	0.8	0
Sample B	2.1	2.6	0
Sample C	8.5	19.0	4.4

Table 13.1: Bulk slag metal content for Gordion-25394 (in wt% (following normalisation to 100%), other oxides omitted)

the high metal oxide content in the dross, rather than the elevated presence of metallic prills. Though these dross layers can be helpful in identifying alloy types melted in a crucible, metallic prills rather than metal oxides are required to assess better the actual alloy composition. Fuel ash contributions and iron contamination of the crucible slag are lower for samples A and B than for sample C.

It should be emphasised, however, that such variability is not seen in every crucible, as exemplified by Gordion-23045 and Gordion-27613 (see section 8.3.8). Overall, it appears that high variability is to be expected though, especially when the crucible interior is slagged throughout. As discussed above, this degree of slagging is related to oxygen supply, temperature and charge distribution, as well as the refractoriness of the crucible. Even when no variability is macroscopically apparent, it should be assumed *a priori*.

For the crucible assemblage from Roman Thrace, it has not been possible to evaluate within-crucible variability. Due to sampling limitations, only single fragments were available for study, which often consisted of no more than a few dross scrapings. Furthermore, the crucibles showed far greater variety in terms of both their ceramic fabric and their metallurgical use. Finally, complementary data from the analysis of interior surfaces by pXRF was not available. It is obvious that such conditions present problems in evaluating the representativeness of a single sample for a particular crucible process. When only dross samples are available, metal prills are usually absent, making it difficult to reconstruct the original alloy. However, this matter may often not be resolved by increased sampling: some crucibles are simply very 'dry', meaning little or no crucible slag has developed. This situation often occurs in more refractory (and thus often historically later) crucibles, particularly when process temperatures were not extremely high. For such processes, the evidence is scarce by default. Though some dross may develop, this is not always the case and when it does, it is not always preserved in the crucible.
Nonetheless, if the Philippopolis crucibles P1-P5, which all have a similar crucible fabric and design, can be taken as representative for a single process, their within-process variability can be discussed through comparison of the five samples. As mentioned in section 11.3, it appears that the involvement of zinc in an oxidising metallurgical process hinders straightforward interpretation. Its over-representation in crucible slag makes it difficult to reconstruct its actual importance in the charge. Zinc's volatility further impedes the preservation of zinc-rich prills, which limits the likelihood of their detection during analysis, particularly in dross layers. The hit-or-miss nature of such evidence is further discussed in section 13.3, and appears particularly important for more refractory crucibles, where limited slag develops and therefore fewer technological markers are trapped.

At this point, some examples of more refractory crucibles may be discussed, drawing from examples beyond the crucibles presented in this thesis. Steel production crucibles are typically made of a highly refractory ceramic which interacts very little with the charge. Examples from Uzbekistan are shown by Martinón-Torres and Rehren (2014) in Figure 6.7, p. 115, Rehren and Papachristou (2003) in Figure 2, p. 398, and Bayley and Rehren (2007) in Figure 10, p. 52. In such processes, a steel ingot forms at the bottom of the crucible, with a layer of slag floating on top of it. After use, the crucible is broken to remove the steel ingot, resulting in many fragments of fairly 'clean' ceramic, as well as a larger fragment to which the slag layer is attached. The analysis of such 'crucible slag' is more akin to primary smelting slag analysis than crucible slag analysis discussed in this thesis, as the ceramic does not partake in its formation. The crucibles themselves tend to maintain very 'dry' interior surfaces, while the exterior surface typically develops a vitrified layer through ex-

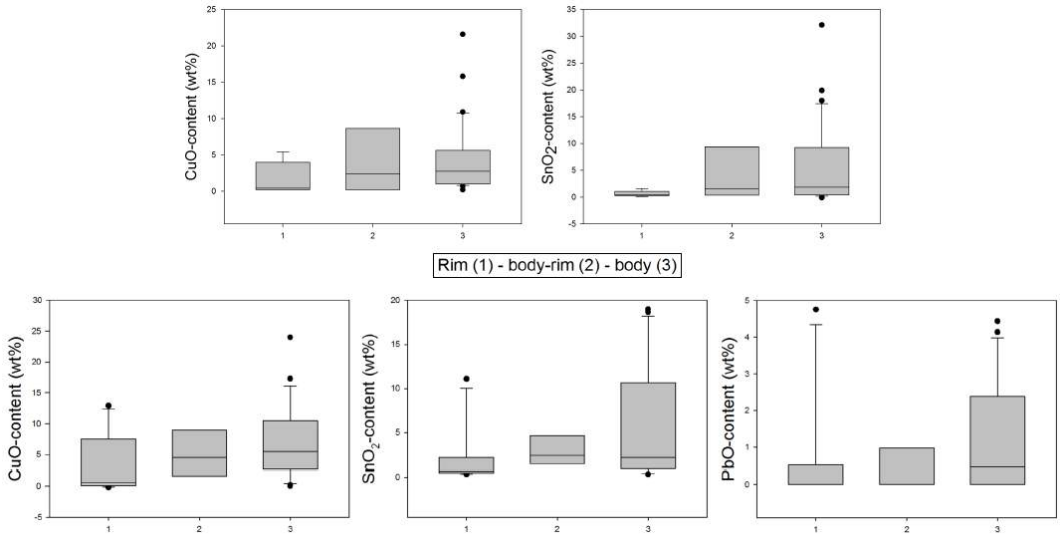

Figure 13.5: Boxplot of bulk copper, tin and lead oxide content in 49 Pi-Ramesse (top - 9 rim, 6 body-rim and 34 body samples) and 46 Gordion crucible samples (bottom - 16 rim, 6 body-rim and 24 body samples)

ternal heating.
Another example of refractory ceramics can be found in medieval Austrian scorifiers, which are shallow ceramic dishes used for various oxidising metallurgical reactions. Examples are shown by Martinón-Torres and Rehren (2014) in Figure 6.11, p. 117 and Mongiatti (2010) in Figure 5.6, p. 116, where the *regulus* of metal settling at the bottom of the crucible can be seen, leaving a negative imprint on the slag after its removal. This crucible slag is in fact mainly dross, as limited reaction usually takes place with the actual ceramic. For such crucibles, some of the crucible slag/dross has been removed by mechanically breaking out the settled metal, resulting in a skewed representation of the original process in the archaeological remains.
A similar example of refractory crucibles from 19^{th} century London, showing a *regulus* and limited vitrification in particular areas is discussed by Dungworth (2010, 2012b).

Returning to the Pi-Ramesse and Gordion assemblages, some more general observations concerning body and rim fragments can be made. When comparing the copper, tin and lead content in all analysed rim and body samples (where 'body-rim' means body samples taken near the crucible rim, as opposed to lower body samples), a trend becomes evident: body fragments are generally more highly enriched in metal (oxides) than rim fragments, as illustrated in Figure 13.5. However, this trend is by no means a strict rule, and high variability exists. The highest lead oxide content within Gordion crucibles, for example, is measured in a rim fragment.

These observations confirm that slag of rim fragments often consists of vitrified ceramic, fluxed by fuel ash, and is generally less informative than lower body slag, which was in contact with the crucible charge[1]. For these body fragments, the variable temperature, redox-conditions and distribution of charge components modify the type of evidence available (e.g., metal content, different oxide phases). When sampling a crucible fragment, the chosen location will therefore strongly influence the informative nature of analytical results, and complete disclosure of the crucible process is rarely obtained from a single sample. Post-depositional effects such as differential corrosion and fracturing can further bias the representativeness of a fragment for understanding ancient metallurgical processes.

Section 13.2

Assemblage-wide variability

Two main types of variability can be expected within crucible assemblages. The first is due to the variability inherent to the crucible process, as discussed in section 13.1. The second type is introduced by the variable technological choices ancient craftspeople made, which are sometimes reflected in the crucible slag. This involves the variation in techniques, as well as variation in raw materials used in the metallurgical process. Here archaeologists can address questions such as: did ancient metallurgists stick to one 'recipe' or draw from several technological options? Were raw materials from several sources used? Is there any variation in these choices through time or various production contexts? Obviously, such questions have higher archaeological significance than the detailed understanding of process variability, described above, which probably played a minor role for the ancient metallurgist.

The example of plain bronze production is used to discuss the concept of assemblage-wide variability. The main techniques of choice are:

1. Alloying of two fresh metals (copper and tin)
2. Cementation (copper metal with tin ore)
3. Co-smelting (copper and tin ore)
4. Recycling (possibly involving addition of fresh metal (or tin ore))

[1] It is interesting to contrast this with typological studies of ceramics in general, where rim fragments are typically considered more diagnostic than body fragments.

Their differentiation in actual archaeological finds has received relatively little attention in archaeometallurgical studies (however see Pigott *et al.*, 2003; Rovira, 2007), but has been discussed in greater detail for Pi-Ramesse (Rademakers *et al.*, in press) and Gordion in Chapters 6 and 9. In addition to choices of technique, variability due to the use of different raw materials can be expected as well. Here, the identification of materials from different sources (geologically, economically, culturally) does not necessarily represent a deliberate choice by the metallurgist. Finally, though variability in techniques and materials can occur across an assemblage, this is obviously not always necessarily the case.

The main problem for identification of technological variation lies in the nature of the available evidence. This can be illustrated by the typical process indicators as preserved in crucible slag that allow identifying different bronze production techniques. Active alloying, as opposed to the mere recycling of existing bronze, can lead to the production of high-tin prills with δ-, ϵ- and/or η-phase bronze. Though these prills allow exclusion of 'technique 4' from the list above (i.e., recycling), they offer no distinction between 'techniques 1-3'. During cementation and co-smelting ('techniques 2-3'), however, it is possible for mineral grains from the ore to be trapped in the crucible slag and excluded from further participation in the metallurgical process. As such, residual mineral grains can allow the differentiation of 'techniques 2-3' from '1 and 4'.
The problem here is that these phases are not the intended end products of the metallurgical operation: high-tin prills and residual ore are the result of processes not reaching completion (in a particular crucible area). Under 'ideal conditions', these process indicators are not preserved in crucible slag at the end of the operation, and they cannot always be expected to be found in a crucible sample taken for analysis. Furthermore, many slag phases are ambiguous and inconclusive towards identifying technological choices. Low-tin prills, for example, could indicate the production of a low-tin bronze, but equally result from the recycling (and partial burning) of medium-tin bronze. Similarly, acicular, high-temperature tin oxide crystals can be formed in a crucible following any production technique (Dungworth, 2000b and Rademakers and Farci, in preparation). This is discussed further in section 13.4.

Recognising variability in the use of raw material is equally difficult. For the case of (raw) copper added to a crucible, a general distinction can be made between 'clean' and 'contaminated' copper. 'Contaminated copper' is typically raw copper which has not been refined after the primary smelting stage. Depending on the type of ore that was smelted, contaminated copper can contain elements such as iron, cobalt, nickel, arsenic, tin or lead that were reduced during smelting and incorporated in the copper. Alternatively, raw copper could be contaminated by remnant primary smelting slag, when poor separation was

achieved during the smelting process (Hauptmann *et al.*, 2002) or when slag was intentionally added to copper ingots, in an attempt at cheating when trading the copper. Most contaminants oxidise preferentially to copper and will burn off into the crucible slag first. Enrichment of the crucible slag in these oxides, therefore, can be used as an indicator for the use of different raw materials across a crucible assemblage. Furthermore, it offers the possibility to broadly relate crucibles to final artefact chemistry.
However, while a distinction can sometimes be made between 'clean' and 'contaminated' raw materials used in different crucibles, it is important to remember that contaminants are only oxidised into the crucible slag under oxidising conditions. These environments are not necessarily present in every crucible (area) and, as a result, the relevant metal oxides are not present in each sample taken from a crucible.

Therefore, the absence of certain process indicators, technical or material, is often not sufficient to exclude certain technological choices from the interpretation of an assemblage. Due to the inherent process variability witnessed within each crucible, the absence of evidence can usually not be taken as the evidence for absence. Only when the researcher has investigated sufficiently large sample numbers can more confidence in an overall interpretation be achieved. Defining 'sufficiently large sample numbers', however, is not an easy task. This depends both on the process-inherent (i.e., within-crucible) variability, and the *a priori* unknown variability in technology and material use present within the assemblage. As discussed further in section 13.3, visual inspection of the assemblage and the application of pXRF can provide some measure of this variability and inform sampling strategies. Overall, conservativeness with regards to generalising interpretations is most appropriate. The quote from Kahneman (2012) at the start of this discussion (page 417) mirrors this idea that there is often more (to crucibles) than what we see (in our samples), and we must actively acknowledge our unavoidable ignorance of certain facts when making broad interpretations.

The effect of within-crucible variability on the assessment of assemblage-wide variability is illustrated by looking at the changes in bulk chemistry between crucible ceramic and slag for the Pi-Ramesse crucibles (Figure 5.5). As discussed in section 5.2.2, all samples show enrichment in lime (and other fuel ash components), but this enrichment ranges from low to high. As all crucibles were presumably placed under a similar charcoal cover during operation, this range of enrichment reflects the within-crucible variability of fuel ash contribution. However, the possibility of aberrant practice, employing exceptionally little or large charcoal cover, cannot be teased out from such a pattern. Only when such aberrant practice occurs frequently (at which point it is no longer aberrant), would a shift in distribution of fuel ash enrichments become visible (e.g., bi-modal distribution). As

such, the heterogeneous nature of the crucible process tends to hide aberrant or rare occurrences of technological variability within the assemblage.
In two thirds of the Pi-Ramesse crucible fragments, no slag enrichment in iron can be noted, whereas one third exhibits varying degrees of iron enrichment. This enrichment is most likely due to the use of 'contaminated (raw) copper', and the spread from low to high enrichment is a result of within-crucible variability as well as variable iron content in the raw copper. Therefore, some of the crucibles without notable iron enrichment could similarly have contained 'contaminated copper', for which iron was not oxidised into the crucible slag in the sampled part of the crucible.
Figure 5.6 shows the same ternary diagrams, distinguishing between rim and body crucible fragments. Corroborating the remarks made in section 13.1, some differences can be noted between rim and lower body fragments. Higher lime slag enrichments typically occur for body fragments, though some rim fragments show moderate to high enrichments, too. This reflects a fairly equal distribution of fuel ash throughout the crucibles, though somewhat higher uptake in the more slagged lower body fragments, reflected in a bi-modal distribution of lime enrichment (see Figure 5.10).
Slag enrichment in iron, on the contrary, occurs almost exclusively for body fragments and is low for the rim fragments where it occurs. This reflects one of the primary factors for within-crucible variation: the spatial distribution of charge constituents. Closer to the crucible rim, less or no copper is available to exchange contaminants with the crucible slag. An important consequence of this (perhaps elementary) observation is that the deduced importance of 'contaminated' raw copper use is skewed for the full assemblage, and should be based only on the analysis of body fragments. For Pi-Ramesse, this means that in reality about half of the crucibles show iron enrichments, indicative of the use of 'contaminated' copper (out of which ±15% are additionally contaminated with cobalt/nickel, indicating a different raw material).

In contrast to the Pi-Ramesse crucibles, strong variability in bulk composition is not witnessed in the Gordion crucibles, as illustrated in Figure 8.7. One the one hand, this reflects the more refractory nature of these crucibles, which do not interact as strongly with the charge. On the other hand, it appears that the metal charge is fairly 'clean', compared to that in Pi-Ramesse. Though this result may appear less exciting than the bulk compositional variability seen in Pi-Ramesse, it is equally interesting in its own right. As mentioned above, variability in material use is not to be expected in every assemblage and its absence equally informative for broader archaeological interpretation.
Assessment of the complete range of analytical results, however, shows that technological variability did exist within the Gordion assemblage: it appears that both plain and leaded

bronze were being alloyed. The more refractory nature of the crucibles limited slag formation, which in turn limited the trapping of technological markers. Therefore, the importance of cassiterite for alloying through cementation is more difficult to ascertain for this case. As discussed in section 13.1, within-crucible variability does exist for the Gordion crucibles, and is reflected most strongly in the prill compositions.

For the Thracian crucibles, it is not possible to discuss assemblage-wide variability in terms of metallurgical technology: very few crucibles were used for the same purpose, only limited samples were available and these derived from a variety of contexts (ranging greatly in both time and space). Rather than opening an assemblage-wide discussion, each fragment necessitates an isolated case study, which is difficult to relate technologically to fragments used for other processes. Within-crucible variability could not be assessed either, and as only single crucibles were usually present to reconstruct a particular process, variability in technology and material use for that particular process is not attested. Though a discussion of variability in ceramic technology is possible (see section 11.3), it must be emphasised that this does not reflect variability within a particular context, and therefore differs significantly from discussions of Pi-Ramesse and Gordion. Finally, it should be remembered that the more refractory nature of these Roman crucibles limits the range of evidence available for analysis in general, and increased sampling would not necessarily provide further information on assemblage-wide variability.

As a final note, it should be mentioned that variability in the crucible ceramic throughout an assemblage should be examined as well. For the Pi-Ramesse assemblage, this variability appears to be limited to the natural variability present in Nile silt, and possibly the influence of limited sand temper. In Gordion, the natural clay variability appears to be smaller, but a few crucibles are made from a different fabric altogether. In the Thracian assemblage, few crucibles are made from the same fabric. This is a further source of variability that should always be considered in crucible studies, and necessitates the reconstruction of bulk slag enrichments to be assessed through comparison to the ceramic composition of the same crucible. When no crucible ceramic is attached to a slag sample, its interpretative value is therefore always limited: even though technological markers may still be preserved, bulk enrichments cannot be discerned confidently.
Though it is expected (and therefore not discussed in section 13.1) that the ceramic fabric is fairly homogeneous within a crucible both in terms of texture and composition, this may not always be the case. If variability in chemical composition indeed exists throughout the ceramic, this introduces a further possible source of error when comparing ceramic and slag composition for a crucible: the contribution of particular elements to the crucible slag may be under- or overestimated in a single sample. Such effects appear to be limited in

terms of bulk chemistry, but it should be noted that variability in lead isotope composition throughout a crucible ceramic (and slag) may be more problematic, and poses significant issues when interpreting lead isotope composition shifts between ceramic and slag.

Section 13.3

Methodological implications

Sections 13.1 and 13.2 have identified several issues, fundamental to understanding variability within crucible assemblages. The importance of within-crucible variability, superimposed on assemblage-wide variability, has hitherto not been discussed in the literature. Furthermore, their influence on methodological choices, such as sampling and analytical strategies, has not been evaluated. This is investigated further in this section.

The degree to which these issues affect crucible slag formation strongly varies, of course. One of the critical factors influencing the degree of slag formation is crucible refractoriness. Poorly refractory crucibles typically form thick slag layers as their fabric disintegrates at high temperatures. This enables the mechanical trapping of charge fragments (e.g., charcoal, ore and metal fragments) and the incorporation of contaminants into the slag through chemical interaction. In more refractory crucibles, this melting of the ceramic fabric is less pronounced, as for example in the Gordion and Thracia crucibles. An important result of limited slag formation is the absence of an exchange medium for the crucible charge into which contaminants can be burnt off. When iron-rich copper is used, for example, this iron will oxidise and, in the absence of a crucible slag phase, collect as a dross layer on top of the crucible charge together with other metal oxides. Upon casting, such dross layers are either manually removed, or are deposited as a thin layer on top of a limited area of the crucible slag, which is typically enriched in metal oxides several times more strongly than normal crucible slag. It should be noted that these dross layers, due to the absence of a protecting glassy slag phase, are typically more susceptible to post-depositional corrosion or mechanical loss than regular crucible slag. This further illustrates the impact of crucible refractoriness on the evidence available to the archaeological scientist.

In this section, the implications of these unavoidable issues on sampling and analysis strategies are discussed further.
As a first point, the sampling strategy for analysis by optical microscopy and SEM-EDS analysis, which has formed the core of this thesis, can be discussed. This sampling should

follow a thorough visual inspection of the entire assemblage to assess variable slag formation. Ideally, a large number of samples should be taken to assess variability within crucibles and discover variation within the assemblage with confidence. As mentioned earlier, it is difficult to define a general guideline for sample numbers, and every case study requires specific consideration. The use of pXRF in defining minimum sample numbers is discussed further below.

In reality, however, sampling is constrained by limitations in time or budget, export regulations and curatorial considerations, rather than the concerns expressed above. For such cases, the foregoing discussion has shown that selecting lower body fragments for analysis will generally prove to be more informative than rim fragments when reconstructing technology and material use, and thicker, more developed slag is more likely to capture process indicators. This corresponds to what most researchers have probably been doing intuitively for decades: go for the 'juicy'-looking slag. The results presented in this thesis, however, finally provide a more scientific basis to follow those instincts. Nonetheless, it is important to stress that no strict regularity exists and 'juicy' samples might not be as informative as they look. Furthermore, a strong 'nugget effect' exists for technological process indicators: one may capture a particularly informative inclusion in a sample, or miss it by a hair. Finally, it is possible that a single fragment does capture a large amount of the process-inherent variability. Here, thermodynamically incompatible conditions can sometimes be seen occurring in close proximity, highlighting the absence of equilibrium conditions in most crucibles (e.g., Müller *et al.*, 2004), and the importance of kinetics in slag formation. Similar to the firing of ceramics (see Heimann, 1989), the crucible process must be understood as one of micro- or local equilibria, with the entire system (ceramic and charge) never being in complete equilibrium.

Thus, while previous studies may have often discovered essential process indicators through the analysis of promising samples, their representativeness is difficult to establish when no measure of process variability is offered. Of course, this does not render their contribution useless, but the results presented here encourage their critical appraisal.

The use of pXRF, which is becoming increasingly available to archaeologists everywhere, may offer further assistance for an adequately adapted sampling strategy. A few examples from the extensively sampled Pi-Ramesse assemblage illustrate this point. In Figure 13.6, left, the relative change in bulk iron content between crucible ceramic and slag is shown, as measured by SEM-EDS analysis of 49 samples (see Figure 5.14). The largest group of samples (about $^2/_3$, in blue) shows a normal distribution around zero, indicating no iron contamination. The second group (about one third, in purple) shows increased iron content relative to alumina, indicative of the use of an iron-contaminated copper source. Alu-

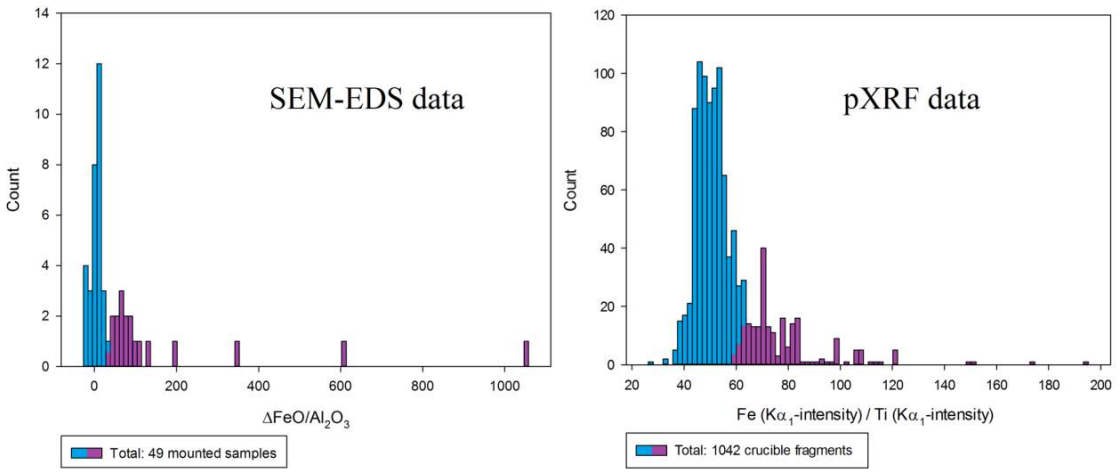

Figure 13.6: Histogram showing relative change in bulk iron content between ceramic and slag measured by SEM-EDS (left, in %) and ratio of iron to titanium in crucible slag measured by pXRF (right), for the Pi-Ramesse assemblage

minium peak intensities are not readily measured by pXRF; hence, a similar ratio (using the iron and titanium Kα_1-intensities measured in crucible slag) has been used for in-the-field analysis, as shown in Figure 13.6, right, based on the analysis of the large Pi-Ramesse sample by pXRF. The same pattern emerges, indicating a large group of 'clean slag' and a smaller group of iron-contaminated slag. Though less clearly defined for the pXRF data, it is much more easily obtained and provides the same assemblage-wide pattern.

Within-crucible variation can equally be investigated using pXRF, as shown by example in Figure 13.7, where the copper and tin content for rim and body fragments is compared. Though increased content in both metals can be noted for both fragment types, the incidence of greater enrichments is significantly higher for body fragments, in similar proportions as noted by SEM-EDS analysis of mounted samples.

These examples show the potential for pXRF in fast qualitative analysis of entire assemblages to pick up overall trends, though its efficacy should be further tested for other assemblages. This has not been possible for the Gordion and Thracia assemblages, as they could not be accessed for such analysis.

As an analytical method in its own right, pXRF has some limitations. It does not provide the same high-resolution data acquired through micro-analysis of mounted sections, and hence cannot possibly furnish the same detailed technological reconstruction. Nonetheless, it is commonly applied for the analysis of crucibles, for example by English Heritage (e.g., Bayley, 1987; Blakelock, 2005; Doonan, 1999b,c; Dungworth, 2001a; Dungworth and Bayley, 1999; Dungworth and Bowstead Stallybrass, 2000; Dungworth and Starley, 2009; Horsley, 1997; Nicholas, 2003; Phelps *et al.*, 2011 and Robbins and Bayley, 1996). While

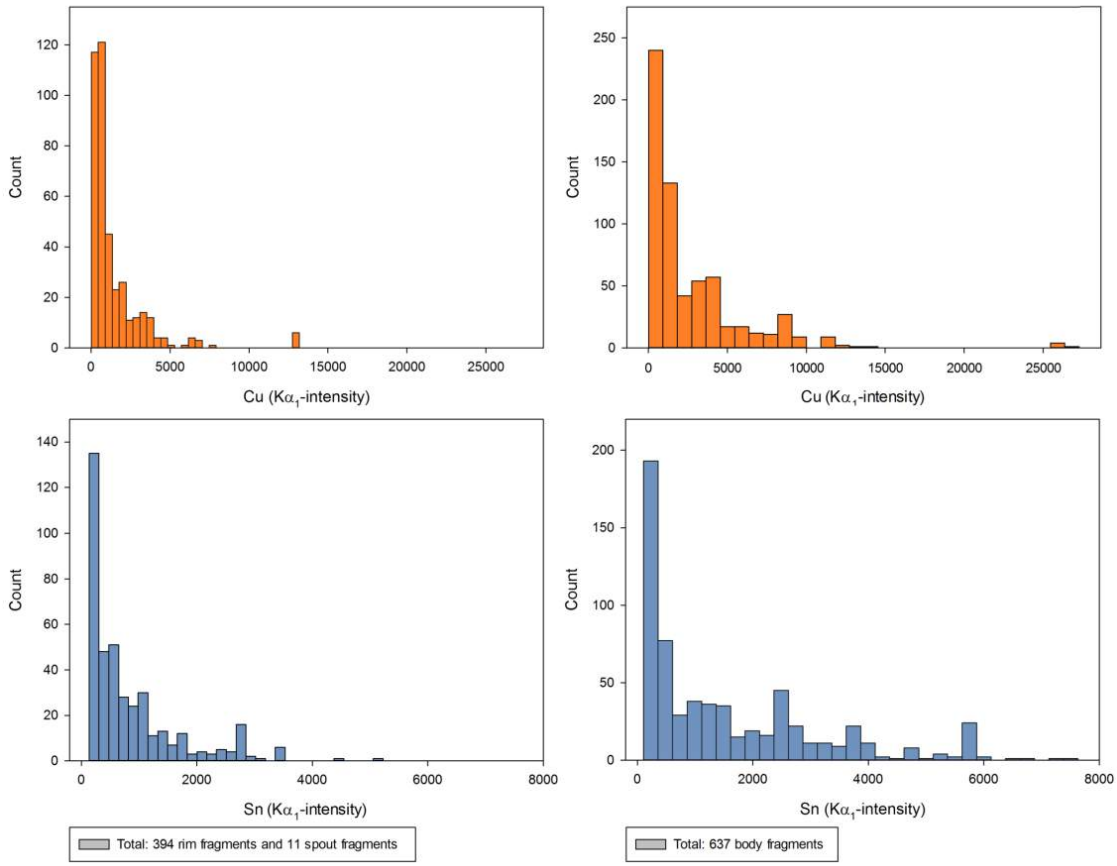

Figure 13.7: Histogram showing copper (top) and tin (bottom) enrichments in rim (left) and body fragments (right), measured by pXRF for the Pi-Ramesse assemblage

this only provides a rough estimation of the alloy molten inside the crucibles, such results can still support meaningful discussion, as long as these limitations are duly recognised (Dungworth, 2000a). As such, the successful use of pXRF for the analysis of crucibles is simply a matter of querying the obtained data appropriately.
Finally, it should be pointed out that pXRF analysis of crucible fragments does not always correspond on a one-to-one basis with SEM-EDS analysis of the same fragment. Here the 'nugget effect' as an extreme example of the heterogeneity of individual crucible fragments can produce different results depending on the relatively small area analysed by the pXRF beam. For this reason, pXRF analysis yields better results as a qualitative screening method applied to entire assemblages, while for individual samples, SEM-EDS analysis provides more reliable data.

It is, however, important to discuss the limitations of analysis by SEM-EDS as well. Though the analysis of mounted samples by optical microscopy and SEM allows a finely detailed understanding of a crucible's micro-structure and the distribution of different phases within

		Na_2O	MgO	Al_2O_3	SiO_2	P_2O_5	SO_2	K_2O	CaO	TiO_2	MnO	FeO	CuO	ZnO	As_2O_3	Ag_2O	SnO_2	PbO	CoO	Bi_2O_3
Pi-Ramesse	Ceramic	17.2	15.0	11.0	5.4	41.6		15.6	17.2	18.4	80.0	11.4								
	Slag	24.3	19.5	16.2	11.1	34.7		24.3	30.7	24.2	84.4	23.2	70.6		108.0		61.7	54.9	72.5	
Gordion	Ceramic	10.9	11.0	4.4	2.2	38.9		12.0	7.8	17.7	161.3	12.7								
	Slag	15.2	16.4	14.5	10.9	39.4	78.0	18.0	16.2	42.4	105.8	18.9	76.7		136.1	104.1	68.3	59.5		
Nicopolis	Ceramic	26.6	18.4	10.8	3.2	67.2		13.0	31.2	27.5		8.5								
	Slag	31.1	15.5	14.1	8.1	39.0		22.2	17.1	29.8		24.8	74.0	78.5			60.2	96.7		
Philippopolis	Ceramic/slag	27.5	27.9	34.1	20.4	79.3		38.7	45.6	44.3		40.2	72.1	63.8		66.2	85.7	65.3		
Serdica	Ceramic	39.4	23.7	8.8	3.6	83.3	48.3	10.1	28.6	30.5		21.6								
	Slag	37.6	32.5	19.3	15.7	23.6	108.9	26.2	39.6	32.8		35.1	92.0	82.9	57.5	104.4	48.6	37.8		49.8
Stara Zagora	All	17.2	21.8	16.9	5.9	53.2		12.6	42.5	30.0		13.1	56.2	65.8						
Average		24.7	20.2	15.0	8.7	50.0	78.4	19.3	27.7	29.8	107.9	20.9	73.6	72.7	100.5	91.5	64.9	62.9	72.5	49.8

Table 13.2: Average coefficient of variation (in %) of all measured oxides for each assemblage

crucible slag, the areas that can be analysed are small relative to the volumes analysed by XRF or NAA, for example. However, SEM-EDS offers far better control over exactly which crucible zone is analysed, compared to crushed and homogenised samples, for which the mechanical separation of ceramic and slag is often difficult to achieve. This trade-off entails increased sensitivity to chemical heterogeneity for measurements of bulk composition by SEM-EDS. It should be clear from the above that such heterogeneity can certainly be an issue for crucible studies. From the data presented in Appendices C, J and O, the coefficient of variation for each oxide measured[2] for each sample can be calculated (omitted here). The average coefficient of variation for each oxide, as measured for each assemblage[3], is presented in Table 13.2. These values give a relative measure of the precision by which these oxides are measured within a particular sample. This value reflects two effects: the analytical precision of the machine (see section 3.3.5) and the heterogeneity of those oxides in samples of each analysed assemblage. While the measurements of oxides in certified reference materials typically deliver a coefficient of variation of 5-10%, much higher variability is measured in the actual samples: 10-30% for the main elements, and even higher for copper oxide and the other alloy constituent oxides. This mostly reflects heterogeneity within the crucible samples, which is not present in the homogenised CRM's. Table 13.2 shows that this variability is more problematic for the crucible slag than the crucible ceramic, and for oxides present in low (at detection limit) quantities like phosphorus, sulphur and manganese oxide. The increased variability measured for copper and its alloy components is due to the highly variable inclusion of prills and corroded metal in the analysed areas.

To limit analytical sensitivity to heterogeneity, five area measurements were taken for each sample and averaged for the ceramic and slag zones respectively. Figure 13.8 shows the results for the Pi-Ramesse assemblage when only one area measurement (randomly selected from the five existing measurements) is used for each sample. The average compositions for such an analysis are presented in Table 13.3. Clearly, the same general trends appear (not reiterated here), despite the severe reduction in area analysed per sample. This is not surprising, however, and reflects the same conclusion reached through the discussion of pXRF results: a rough analysis performed on sufficiently high sample numbers will reveal the broad trends that exist within an assemblage. However, comparison to the full data highlights an important difference: there is a great drop in the precision of these results. While little difference is apparent for the ceramic part (which is quite homogeneous), it is

[2]The coefficient of variation on these measurements is calculated as $\sigma/\bar{x}$ and expressed in %.

[3]The coefficient of variation, calculated for different oxides for each sample, is averaged across each assemblage.

strongly pronounced for the slag part. There, the standard deviation is doubled and sometimes tripled due to the decrease in analysed area. Though the average compositions are not greatly affected, some differences can be noted for calcium, iron, copper and tin oxide. This is not surprising, as these elements are most sensitive to local variation throughout the crucible slag. In summary, the trade-off between analytical speed and precision, which is obvious when comparing pXRF and SEM-EDS analysis, is similarly present when considering the analytical procedure used for a specific technique. Under time constraints, one may prefer to analyse fewer areas for bulk composition using SEM-EDS, at a significant loss of precision and to a lesser extent accuracy, in order to dedicate more time to the identification of particular phases in the crucible slag.

However, such focus on specific phases is perhaps not always warranted. When few crucibles are available for analysis, as for the Thracian crucibles, it makes less sense to compile a complete list of phases as has been done for the Pi-Ramesse and Gordion assemblages. While such a list is useful to understand variability of a process as expressed in a wide range of samples, such an endeavour is unlikely to succeed when only one sample of a unique crucible is available. Therefore, it seems more appropriate to perform a more precise bulk measurement of the crucible areas (i.e., more measurements) and to look at the various slag phases more qualitatively, while dedicating more focus on technological markers. Though it is often difficult to predict what those markers will be prior to analysis, many have been discussed for various metallurgical processes in the course of this thesis and may serve as examples. In general, metallic prills, residual ore fragments and bulk enrichments of slag relative to ceramic provide the key parameters in reconstructing metallurgical technology. When the data processing for a particular sample generates an interpretative hypothesis for which particular technological markers are missing, it is more useful to revisit that sample with this particular hypothesis in mind, rather than analysing all phases during the first examination as a default procedure.

The focus on bulk measurements is especially useful when investigating additional layers of the crucible ceramic, as discussed for the Thracian crucibles N4-N5 and S4. The analytical approach employed throughout this thesis allows an easy and reliable recognition of such added layers, and enables distinction between outer layers that are fuel ash glazes (i.e., the vitrified crucible ceramic, fluxed by fuel ash) and intentionally added, less refractory clay layers (that may have vitrified, possibly with fuel ash contributions). While similar bulk compositional SEM-EDS data for layered crucibles is presented by Thornton and Rehren (2009: Table 1, p. 2704), they omit analytical details of their measurement (i.e., frame size, number of analyses, variation within layers). König and Serneels (2013: Table 2, p. 161) present similar data from XRF-WDS analysis of powder discs from various

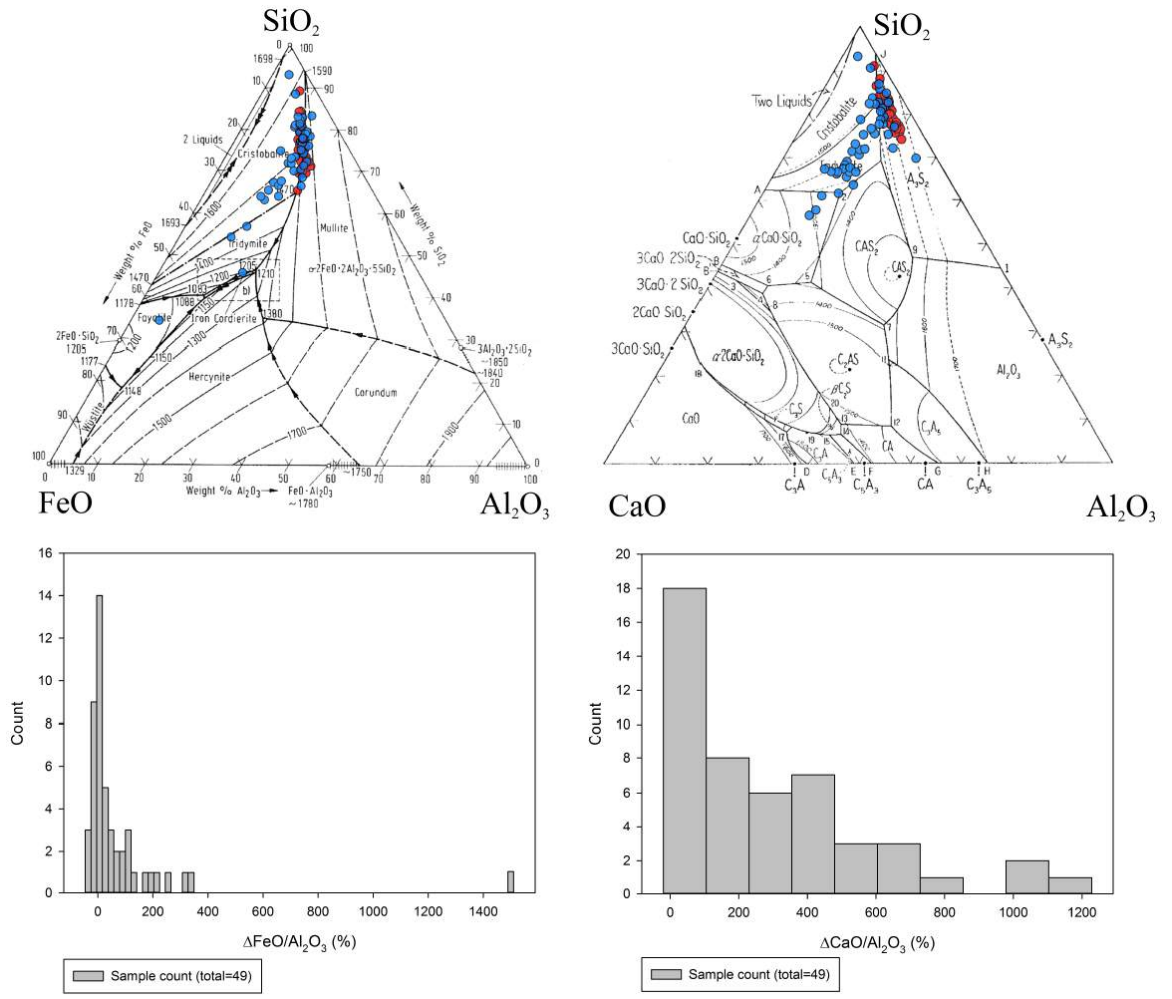

Figure 13.8: Ternary diagrams and histograms for Pi-Ramesse sample compositions, based on randomly chosen single measurements for each sample

crucible layers, but omit details of analyses per crucible fragment and variation within fragments. Though both offer very useful comparative data, future analyses may benefit from such added analytical detail to better represent crucible variability and its possible interpretative limitations.

Further drawbacks of SEM-EDS analysis are the relatively high detection limits for most elements, and the ensuing inability to measure trace elements. Such elements can be valuable for the comparison of trace elements typically measured in the analysis of metal artefacts (often performed by XRF, EPMA, (I)NAA or ICP-techniques, e.g., Butcher and Ponting, 2005; Chen *et al.*, 2009; Guerra *et al.*, 1999; Hancock *et al.*, 1994; Kassianidou, 2003a; Lutz and Pernicka, 1996; Northover and Saghieh, 2002; Rehren and Temme, 1994 and Thornton *et al.*, 2002, though sometimes by SEM-EDS, e.g., Kaufman, 2013; Lehner, 2012; Martinón-Torres *et al.*, 2012 and Park and Gordon, 2007, and increasingly by pXRF

	Na_2O	MgO	Al_2O_3	SiO_2	P_2O_5	K_2O	CaO	TiO_2	MnO	FeO	CuO	As_2O_3	SnO_2
Average (1 area)	**2.1**	**2.2**	**13**	**66**	**0.6**	**1.9**	**3.2**	**1.5**	**0.1**	**8.4**	**0.3**	**0.2**	**0.1**
St.dev. (1 area)	0.6	0.4	2	5	0.4	0.5	0.6	0.4	0.1	1.7	0.9	0.2	0.3
Average (5 areas)	**2.0**	**2.2**	**13**	**66**	**0.6**	**1.9**	**3.2**	**1.5**	**0.1**	**8.3**	**0.6**	**0.2**	**0.2**
St.dev. (5 areas)	0.3	0.3	1	4	0.3	0.3	0.6	0.3	0.1	1.0	0.5	0.2	0.3
Average (1 area)	**2.7**	**2.5**	**10**	**55**	**0.9**	**2.0**	**8.0**	**1.2**	**0.1**	**9.4**	**3.9**	**0.2**	**3.4**
St.dev. (1 area)	1.8	0.8	3	14	0.5	0.9	4.6	0.5	0.1	6.3	6.1	0.2	6.0
Average (5 areas)	**2.8**	**2.5**	**10**	**54**	**1.1**	**1.9**	**9.0**	**1.2**	**0.1**	**8.9**	**4.3**	**0.2**	**4.4**
St.dev. (5 areas)	0.6	0.5	2	6	0.3	0.4	2.6	0.3	0.1	2.2	2.3	0.2	2.4

Table 13.3: Average composition (in wt%, normalised to 100%) for ceramic (top four rows) and slag (bottom four rows) for Pi-Ramesse crucibles, based on random single area measurements for each sample, compared to standard approach (5 area measurements)

as well, e.g., Charalambous *et al.*, 2014; Gouda *et al.*, 2012 and Montero-Ruiz *et al.*, 2003), to those encountered in the crucible slag, to relate better these two material categories. However, it must be stressed that the heterogeneity of crucible slag is expected to impede such efforts regardless of the analytical technique used: the variable enrichment of crucible slag in copper contaminants will rarely reflect the complete trace element pattern of that copper as measured in an artefact.

This warrants the repetition of an issue that has been noted in earlier chapters: the levels of crucible slag enrichment in a particular charge constituent necessarily represent the loss of a certain amount of that constituent from the crucible charge (see Appendix G). When calculated this way, even 'strong slag enrichments' typically do not amount to severe losses of those particular constituents from the charge, given the much smaller volume of crucible slag present, relative to the metal within the crucible. Therefore, it remains difficult to assess the actual abundance of these particular constituents in the crucible charge based on their enrichment in the crucible slag: this is a highly unstable, non-equilibrium exchange process, for which the chemical equations are unknown, the starting products are unknown, the end products are only partially known, and therefore the activity levels for the unknown equation cannot be assessed. Taking the example of Pi-Ramesse, this could mean that the cobalt and iron enriched crucible slags reflect the use of either a copper source with very minor cobalt, of which a lot has burnt off into the crucible slag, or a copper source with more important cobalt content, of which only a minor amount was oxidised[4]. Such considerations reduce the confidence one can obtain in linking certain crucibles to particular metal artefacts: a presence/absence comparison of particular components is most useful here, and can best be used to exclude possible crucible-artefact

[4]The presence of contaminants in prills plays an important role in evaluating their abundance in the original charge. Prills are, however, not always available for analysis in the crucible sample.

associations rather than proving them.

Following this discussion of the advantages and drawbacks of the main techniques used in the analysis of metallurgical crucibles, it is instructive to return to the issue of sampling. It has been argued above that, when no restrictions of time, money, regulations or conservation apply, a selection of thickly slagged crucible fragments for analysis in mounted section is preferable. However, such restrictions usually exist. Though the availability of research time on a scanning electron microscope for archaeological purposes may seem self-evident at certain institutions (*in casu*, the UCL Institute of Archaeology), budget limitations and the need for inter-departmental or inter-university collaborations to access such equipment at many other archaeological research units may prevent extensive use of this technique as presented in this thesis. Furthermore, restrictions on sample export often exclude crucible samples from leaving the excavation site for laboratory analysis in the first place. When (limited) invasive sampling is allowed on site, some further information on micro-structure could be obtained using a portable microscopy set-up (Goren, 2014).

Even when export of samples is possible, however, invasive sampling should not necessarily be the default approach. This choice should be guided by the nature of the crucibles, the freedom the archaeologist has in taking a sample and the particular research questions he or she has in mind. For this issue, it is particularly instructive to consider the Thracian crucibles. In many cases, the crucibles were quite 'dry', and limited crucible slag was available to aid in the reconstruction of metallurgical technology. In particular when a sample is taken from a very 'dry' area of the crucible (which happened equally for some Pi-Ramesse and Gordion crucibles), its interpretative value is limited. Though the study of ceramic technology may be approached through such samples, they should not be made when this is no research aim. If it is, the use of thin sections rather than mounted sections would be preferable. In some cases, restrictions on which area of a crucible could be sampled were applicable. When a crucible is complete, for example, curators tend to be less inclined to allow invasive sampling. When only limited scrapings of crucible slag or dross are available for sampling, it should be contemplated whether or not to take those samples. It has been shown that, particularly when considered in isolation, such samples have only limited informative value: metal prills are rarely preserved and, when present, are often severely oxidised and no comparison between slag and ceramic composition can be made. Under such conditions, technological reconstruction is much impeded, and the analysis by pXRF may often provide similar data. It is appropriate to consider not sampling under such conditions, in particular when limited SEM-time is available, which could be dedicated to the analysis of more promising samples. This is-

sue is further exacerbated when only a single crucible of a particular type or function is retrieved from an archaeological context. A single sample from that crucible is unlikely to reveal the within-crucible variability inherent to its ancient use and the 'nugget effect' limits the validity of any reconstruction based on a single sample, in particular when certain technological markers are noted as 'absent'. If present, however, such markers can of course only be found through detailed analysis in mounted section. Only when such considerations are fully acknowledged in the interpretation of such a single sample, can it be useful. In many cases, however, this will mean that the interpretation cannot be extended beyond that typically obtained through pXRF analysis, in a much faster and cheaper way. In fact, the pXRF analysis of many points on the crucible interior may reveal more of the within-crucible variability than analysis of the mounted sample. In conclusion then, it seems only appropriate to analyse a single mounted sample of a unique crucible when a sufficiently 'juicy' sample can be taken, and ideally its analysis should be complemented by pXRF analysis of the crucible interior and exterior. When the crucible is more or less 'dry', not sampling may often be the best strategy.

A discussion of the application of lead isotope analysis for crucible studies must be brief at this point. With exception of the single Göltepe crucible analysed by Lehner *et al.* (2009), no comparable studies have hitherto been undertaken. The Göltepe example shows widely ranging lead isotope compositions, which are most likely reflective of varying lead isotope composition of the crucible ceramic itself, rather than the metal charged in it, and environmental contamination (mobile lead ions from lead artefacts in the excavation area) may equally be an issue. This has been similarly witnessed for the Pi-Ramesse crucibles, and an investigation of lead content and its isotopic variability in clays is needed in this context. Furthermore, experimental archaeometallurgical studies to elucidate the relative contributions of crucible charge, ceramic and possibly other contributors such as fuel ash are required to interpret such data.

The issue of how lead isotope ratios are influenced during bronze recycling and mixing has been much debated but never resolved. Similar to the analysis of lead isotope measurements for crucibles, these issues could be much better understood through the execution of a range of controlled laboratory experiments.

However, the analysis of lead isotopes within crucible slag can clearly not be equated to that of metals. Their interpretation is far more complex, and it seems that convincing arguments can only be made on the basis of metallic prills embedded in crucible slag at this point. Nonetheless, if this type of analysis is further developed, with the aid of experimental work, it holds the promise of further elucidating certain archaeological questions. In conjunction with trace element chemistry, it may offer a stronger basis to link crucibles to

the final artefacts that were cast from them, thus increasing the detail by which we understand metallurgical activities.

Finally, it should be noted that this thesis has focused entirely on secondary metallurgical crucible processes, with little mention of primary crucible metallurgy. The selection of crucibles from urban context generally implies, from the Late Bronze Age onwards, mainly secondary metallurgical activity. By that time, most primary metal production took place in furnaces (Bayley and Rehren, 2007; Craddock, 1995), reflecting increased production scales and the easier transport of metal produced and cast into ingots (e.g., Ben-Yosef, 2012; Hauptmann *et al.*, 2002; Kassianidou, 2013 and Roman, 1990) at or close to the mines. Particularly in urban environments (from which all assemblages in this thesis derive), then, primary smelting is quite rare. When it does occur, it is usually performed in furnaces rather than crucibles.
However, it should be pointed out that the methodological discussion on the analysis of crucibles presented in this thesis is expected to be equally valid for smelting crucibles. The methodology outlined for the analysis of mounted sections should yield satisfactory results in the identification of primary smelting. It can be expected that the crucible slag will in such cases be more strongly enriched in gangue constituents, such as iron, alumina and silica, and possible flux components, apart from containing residual ore fragments and freshly produced metal prills. As such, it more strongly resembles primary production slag as described in the more extensive literature concerning that subject (see section 1.2) compared to literature available for crucible slag. It is beyond the scope of this discussion to list all the possible markers that could exist for primary smelting (there are probably as many as there are different ores and smelting techniques), but it should be highlighted that the considerations of within-crucible and assemblage-wide variability, presented in sections 13.1 and 13.2, are directly applicable to the study of primary smelting crucibles.

Section 13.4

Technical interpretative issues

One of the issues that has been reiterated several times throughout this thesis is the identification of tin oxide in crucible slag. While the final word has not been spoken on this matter, experiments are under way (Rademakers and Farci, in preparation), which so far support the hypothesis put forth in this thesis: elongated, acicular, columnar tin oxide crystals are all products of high-temperature recrystallisation, with highly variable shapes (see section 5.4.5) representing different degrees and conditions of crystallisation. They

provide no diagnostic evidence for any type of bronze-related metallurgy ('techniques 1-4', section 13.2) and it is therefore advisable to label them as 'tin oxide' rather than 'cassiterite', as this last term leads to confusion in discussions of bronze technology.

This is evident from the literature, where it is often difficult to ascertain whether authors consider the tin oxide they encounter in crucible slag to be residual cassiterite or newly crystallised tin oxide (or simply do not care to differentiate between them), despite earlier efforts by Benvenuti *et al.* (2003); Cooke and Nielsen (1978); Dungworth (2000b); Hofmann and Klein (1966) and Klein and Hauptmann (1999) to address this issue. Some examples of natural cassiterite grains, which could be helpful for identifying residual cassiterite in crucible slag, are shown by Dill (2007); Dill *et al.* (2008); Earl and Özbal (1996); Pirrie *et al.* (2002); Nezafati *et al.* (2009); Salvarredy-Aranguren *et al.* (2008) and Yener *et al.* (1989). Though residual cassiterite in archaeological samples has been identified convincingly by Adriaens (1996); Merideth (1998); Murillo-Barroso *et al.* (2010) and Rovira (2011-2012), these publications[5] do not emphasise the particular attributes that distinguish these residual grains from high-temperature tin oxide crystals. The occurrence of tin oxide crystals is widely noted throughout the archaeometallurgical literature, however. An exhaustive (though probably incomplete) list of publications includes Adriaens (1996); Chirikure *et al.* (2010); Cooke and Nielsen (1978); Crew and Rehren (2002); Denbow and Miller (2007); Dungworth (2000b, 2001b); Eliyahu-Behar *et al.* (2009, 2012); Figueiredo *et al.* (2010b); Frisch and Thiele (1985); Heimann *et al.* (2010); Hofmann and Klein (1966); Klein and Hauptmann (1999); Lackinger *et al.* (2013); Meeks (1990); Miller (2003); Miller and Hall (2008); Murillo-Barroso *et al.* (2010); Renzi *et al.* (2009); Rodriguez Diaz *et al.* (2001); Rovira (2007, 2011-2012); Rovira *et al.* (2009); Schwab (2011); Valério *et al.* (2013); Wayman *et al.* (1988); Yener *et al.* (2003); Yener and Vandiver (1993); Zhou *et al.* (2009) and Zwicker *et al.* (1985). It is beyond the scope of this chapter to discuss each of these occurrences and their interpretations, but in many of these publications, the interpretation of tin oxide as a technological marker remains quite unclear.

It is interesting to note that similar crystals are found to occur in Egyptian Blue (El Goresy *et al.*, 1996; Jaksch *et al.*, 1983) and tin glazes (Bajnóczi *et al.*, 2014; Mason and Tite, 1997). Though it is often unclear what the source of tin is in these processes, some of the crystals (Bajnóczi *et al.*, 2014, Figure 4b, p. 6), appear to be residual cassiterite (surrounded by high-temperature crystals). The others, however, are very similar to those most commonly noted in crucible slag, supporting their interpretation as high-temperature crystallisation of tin oxide in a glassy matrix. It is hoped that the identification of residual cassiterite in the Pi-Ramesse crucibles (Rademakers *et al.*, in press), as part of this PhD research, in con-

[5] Yener and Earl (1994), Figure 8, p. 174 may provide another example, but the images are unclear.

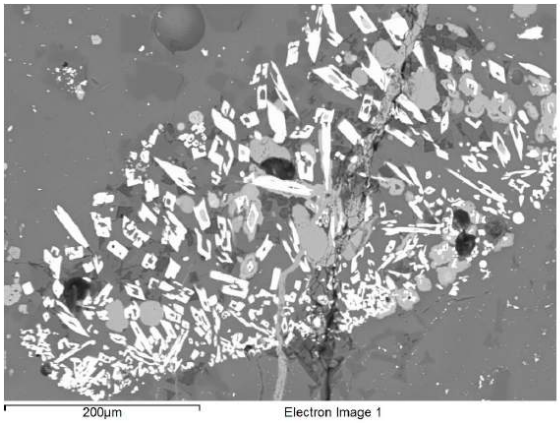

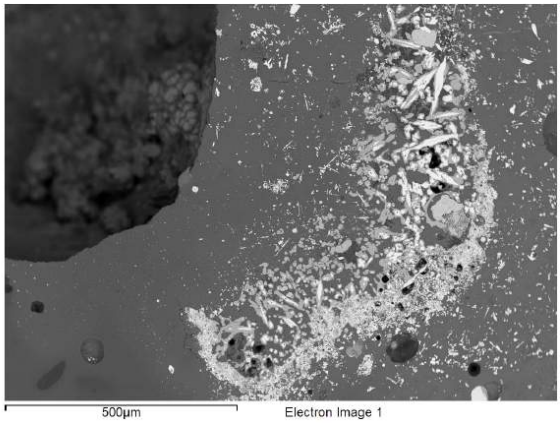

(a) 'Typical' tin oxide (white) clusters with cuprite (light grey) and malayaite (medium grey), sample 87_0762 (left) and 87_0762,0Nv (1) (right)

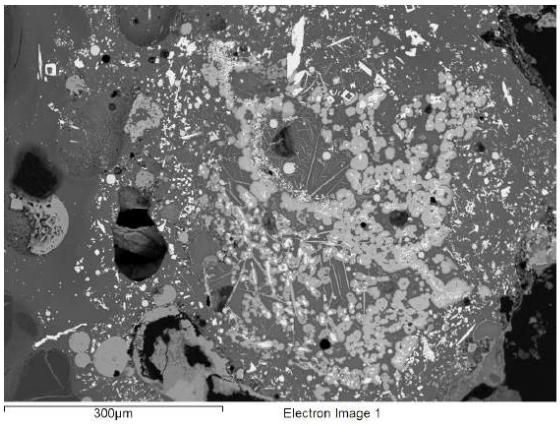

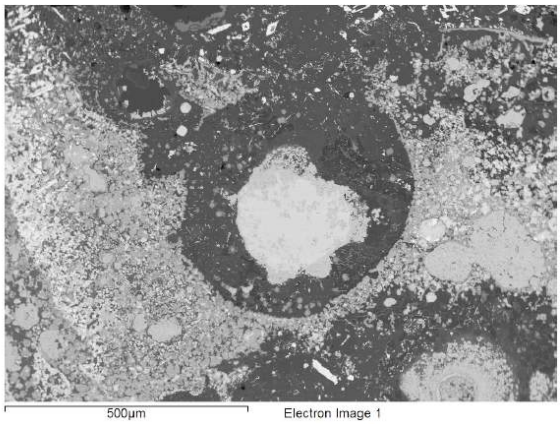

(b) Cluster of tin oxide (white) and malayaite (medium grey), with delafossite (medium grey) (left) and cluster of tin oxide, malayaite and cuprite (light grey) surrounding a partially oxidised copper prill (right), sample 87_0762,0Nv (1)

Figure 13.9: Tin oxide clusters (Pi-Ramesse)

junction with forthcoming experimental studies (Rademakers and Farci, in preparation) will extinguish any remaining confusion surrounding these crystals from the literature.

It is at this point interesting to talk about clusters of various oxides, using tin oxide as a starting point. Such clusters have been noted in Appendix D.4, and are illustrated in Figures D.15b (Pi-Ramesse) and K.18e-K.18f (Gordion). For convenience, a few examples are shown here in Figure 13.9. Being entirely made up of high-temperature tin oxide crystals and commonly associated with other oxides (typically of iron and copper) and (low tin) bronze prills, such clusters are quite distinct from those tentatively identified as residual cassiterite. As suggested in section 8.3.4, these clusters should probably be interpreted as the result of localised bronze burning: under oxidising conditions, a bronze prill burns off some of its tin content (as seen in Figure 5.51), which forms a dense cluster of oxides in

that area. Unlike the rare situation shown in Figure 5.51, the liquid metal often migrates to another location within the crucible (slag) following this burning, while the tin oxide cluster remains immobile. A few metallic prills typically accompany these clusters, however, and in many cases some cuprite and spinel is associated with them. As such, they are fairly easily distinguished from (tentatively identified) residual cassiterite.
Similarly, clusters of iron oxide are often found, as shown in Figures D.2 (Pi-Ramesse) and K.3e (Gordion). These are typically associated with (iron-rich) copper prills, indicative of their formation through localised burning. A comparable clustering of cobalt-rich spinel is shown in Figure D.21, right (Pi-Ramesse).
Some cuprite clusters from a Pi-Ramesse crucible are shown in Figure 13.10, with surrounding delafossite and tin oxide. It may be suggested that such clusters are indicative of complete burning of a copper/bronze prill, and therefore strongly oxidising conditions (unlike post-depositional cuprite formation, e.g., Figure D.12). The same phenomenon therefore seems to give rise to these various oxide clusters: oxidation first burns off the various copper contaminants, in order of reactivity, followed by the ultimate oxidation of copper itself. The final oxide cluster composition then depends on the copper contaminants present in the metal and the duration of the oxidation event.
To emphasise the localised nature of such phenomena, it should be noted that residual cassiterite was equally noted (see Figure D.16a) in a deeper-lying slag area of the same sample (87_0762 (2)) shown in Figure 13.10. Similarly, examples of residual cassiterite have tentatively been identified in Pi-Ramesse sample 87_0762,0Nv (1) (bottom of Figure 5.53) in fairly 'reducing' slag areas, while severely oxidising conditions are attested elsewhere (see Figure 13.9). Considering that these samples are only ±3 cm in diameter, the concentrated nature of this variability becomes even more apparent.
The distinction between newly formed oxide clusters and residual minerals is not always clear, however. The occurrence of a massive magnetite cluster (see Figures D.2c and 13.11, left) with only a few tiny associated prills might represent a 'well-drained' area of extreme iron burning, but the lack of other oxides within the cluster and its size may argue for an interpretation as residual magnetite, which was introduced into the crucible as such. A comparable occurrence in copper smelting slag is shown by Erb-Satullo *et al.* (2014), Figure 6, p. 152. Similarly, a (small) cobalt spinel cluster shown in Figure 13.11, right, is difficult to interpret. Though it appears similar to other cobalt spinel clusters, no macro-prills could be noted nearby, indicating it should probably be interpreted as a residual spinel fragment, perhaps introduced as a contaminant from primary smelting. Contrary to the residual cassiterite fragments, which are sometimes similar in shape, these (cobalt) spinels invariably incorporate ±1 wt% copper in their bulk composition, strengthening

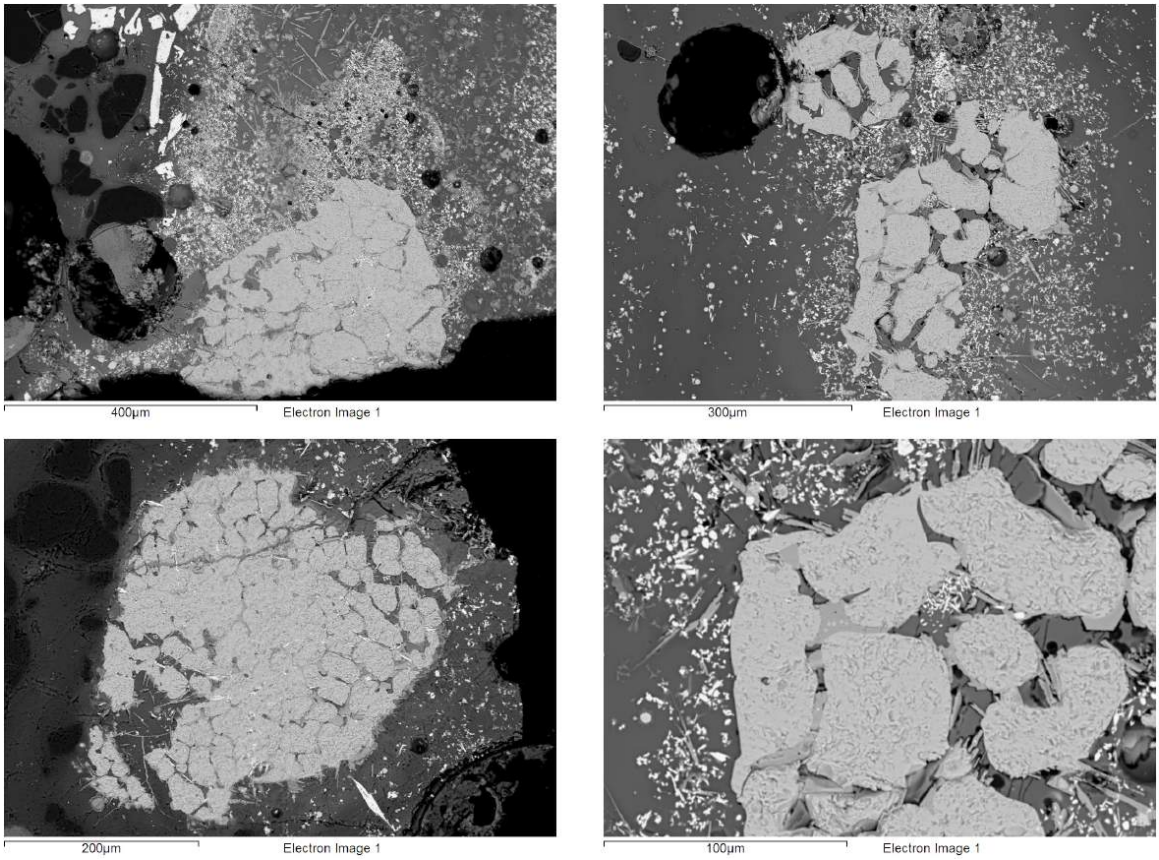

Figure 13.10: Cuprite (light grey) clusters with surrounding delafossite (medium grey) and tin oxide (white). Delafossite can further be noted in between cuprite, Pi-Ramesse sample 87_0762 (2)

their interpretation as copper-related neo-forms. Finally, a residual cassiterite fragment which subsequently re-crystallises completely may not be distinguishable from the clusters discussed above. An example of such a situation may be attested in Murillo-Barroso *et al.*, 2010, Figure 14, p. 1170, and partial reaction could possibly be identified in Figure 5.53, bottom right. Experimental work, by which such shapes are produced under controlled conditions, is needed to further this discussion.
In summary, some clusters pose interpretative difficulties, such as the ambiguous clusters shown in Figure 13.11, but it seems that the majority of oxide clusters encountered during analysis should be interpreted as the products of localised burning.

Next, some remarks on metallic prills should be made. The above discussion has illustrated how prills may be informative technological markers. They supply a better representation of the original metal charge of a crucible than the variable oxidation products reflected in bulk slag and dross compositions, and sometimes prills can provide a strong argument for a particular production process (e.g., high-tin prills argue for active alloy-

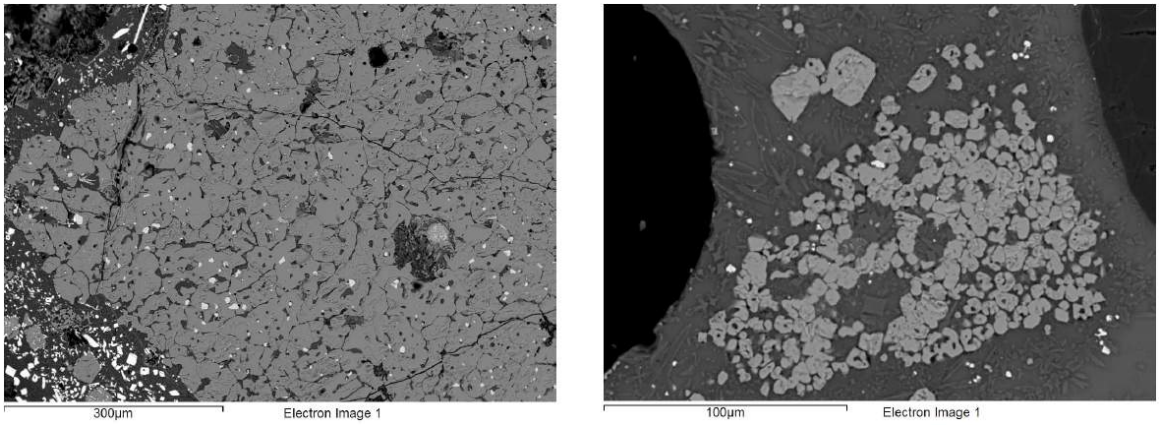

Figure 13.11: Massive magnetite cluster and small cobalt spinel cluster (medium grey), both without associated macro-prills, though tiny prills may be noted (bright specks), Pi-Ramesse samples 87_0634c,04 and 87_0762,0Nv (2)

ing). Nonetheless, their use has limitations as well. Where high contents of a particular element (e.g., tin) in a prill offer a good basis for technological discussion, low contents do not. This reflects the same problem witnessed on a higher scale for crucible analysis in general: the absence of evidence (in crucible slag or prills) does not equate the evidence for absence. Strength comes in numbers here, though such numbers are difficult to define for metal prills. A few dozen prills occurring close together are expected to have similar compositions, and their numbers do not count for much. Only through the analysis of many prills from various areas within a crucible and throughout many crucibles, can some confidence be gained in the absence of certain alloy components or contaminants. It is important here to consider the various locations on which prills are encountered: sitting deeper within the crucible slag, on its interior surface, the crucible rim or even its exterior surface. These environments present significantly different temperature and redox-conditions during the metallurgical process, and different sensitivity to post-depositional corrosion. Prills preserved deeper in the crucible slag are less likely to be affected by post-depositional corrosion, but their early trapping during the crucible process could have prevented their reaction with alloy products added later. Therefore, prills closer to the crucible interior surface may be more reliable for reconstructing the crucible charge. Prills on the exterior surface have typically been more exposed to oxidising conditions (Dungworth, 2001b), resulting in increased loss of alloy components. Though the issue of corrosion plays an important role, particularly for prills embedded in dross layers, this tends to be limited for prills embedded in the crucible slag, making them the most reliable for charge reconstruction. Nevertheless, changing crucible process conditions necessitate a conservative approach when interpreting prills.

These observations further emphasise the problematic nature of analysing highly refractory crucibles: as little slag is usually developed, the adhering prills are less likely to be fully representative of the original crucible charge and should be used with more caution. In this context, it is interesting to note the higher frequency by which high-tin prills were observed in the Gordion crucibles, compared to the Pi-Ramesse crucibles, despite the more limited slagging in the Gordion crucibles. Though this could very well be a sampling bias ('nugget effect'), it may equally indicate the higher importance of active alloying in the Gordion assemblage, with more frequent recycling attested in the Pi-Ramesse assemblage. Similarly, the higher abundance of residual cassiterite (though still relatively low) in the Pi-Ramesse crucibles, compared to the Gordion crucibles, may indicate that cementation was more important in Pi-Ramesse. However, the more limited slag formation would have inhibited cassiterite trapping for the Gordion crucibles, and furthermore, its occurrence and recognition in a sample is really hit-or-miss. As a counter-example, the occurrence of cassiterite in Thracian crucible P9, without the presence of high-tin prills, serves as a reminder that these technological process indicators are intermediate products and their preservation is highly variable: while residual cassiterite points to active alloying, supporting evidence in the form of high-tin prills cannot always be expected within the same sample (or even crucible). Nonetheless, taking into consideration the evidence presented for the Thracian crucibles, it appears that more refractory crucibles generally offer a lower abundance of technological markers.

Finally, the issue of reuse is revisited. As with the attestation of any technique in a crucible, specific indicators are expected to exist for reuse, and their frequent identification throughout an assemblage can be taken as a measure of its importance. The indications for reuse in the three assemblages discussed in this thesis vary. For Pi-Ramesse, only one fragment shows macroscopic evidence of reuse (see section 5.4.2), while no microscopic indications for reuse were identified. The Gordion assemblage shows no indications for crucible reuse at all. For the Thracian assemblage, reuse is more common and attested at each site (see section 11.3).

The primary macroscopic indicator for reuse is the application of a second clay layer on the crucible interior and/or exterior[6]. This appears particularly true for less refractory crucibles, which may be in need of repair after a first use, while more refractory crucibles (e.g., Thracian crucible S4) do not show any macroscopic evidence. Such repair attempts were most likely undertaken to avoid failure during a crucible's second use. The more outspoken slag development in less refractory crucibles, like the Pi-Ramesse ones or Thracian

[6]This does not refer to the application of a (less refractory) clay layer to existing pottery before use (e.g., N4-N5 and S1-S2), which implies 'pottery reuse' rather than 'metallurgical reuse'.

crucible P9, may itself not have concerned ancient metallurgists too much, as their relatively small volume could not present significant contamination to the second charge. Such contemplations are difficult to assess on the basis of fragmented crucible remains. An important observation, however, is that the interior slag produced during secondary use can fuse entirely with the primary crucible slag, though mainly on the lower crucible body. At the crucible rim, a double profile (ceramic-slag-ceramic-slag) is more likely to be preserved. This means that the macroscopic identification of reuse for body fragments could be quite problematic. In particular when no secondary clay layer is applied, macroscopic evidence is most likely absent. The question, then, is whether any microscopic evidence can be found for reuse. While it seems reasonable to suggest that the execution of two different metallurgical processes will produce a final crucible slag which cannot be reconciled with a single use interpretation (e.g., Thracian crucible S4), the reuse of a crucible for the same purpose may remain quite invisible when no secondary clay layer is applied. When a secondary clay layer is applied, its preservation is more likely closer to the crucible rim. The only known examples of crucible reuse in the literature show two layers of slag separated by a clay layer (Evely *et al.*, 2012) or, more dramatically, eight slag layers separated by clay (Mecking and Walter, 2004). When no secondary clay is applied, crucible slag from the first use may simply remelt and charge constituents from the secondary use could then join those of the first use in that slag. The degree to which slag constituents of the first use would mix with those introduced during secondary use is probably limited: most oxides crystallised into a glassy matrix are very stable (e.g., tin oxide: Charles, 1979) and therefore unlikely to react with newly introduced contaminants. As such, any embedded prills most likely reflect a particular operation, rather than the mixed reflection of several uses. This idea does not hold, however, for more refractory crucibles, where prills are not protected by a vitrified slag, and can more freely interact with different crucible charges during consecutive operations. Similarly, crucible dross is more sensitive to homogenisation when a crucible is reused, and as such it is more difficult to filter several processes out from it.

As a general rule for crucible interpretation, then, each crucible slag that can be reasonably explained as representing single crucible use, should be interpreted as such. Only when observations cannot be reconciled as reflecting a single process, should reuse scenarios be elaborated. However, it should be noted that such single use may, in reality, represent multiple uses of that crucible for a single process (e.g., bronze melting). To determine the likelihood of reuse, several factors can be taken into consideration. At Pi-Ramesse, for example, the low cost of production for crucibles, relative to the potentially high cost of crucible failure and associated failure of a large bronze casting, makes crucible reuse

unlikely as a common practice. The single observed occurrence there is most likely just that: an exception. It would, however, be interesting to have experimental data on the effects of reuse on less refractory crucibles (e.g., after how many uses do crucibles fracture, does slag development become excessive etc.), to better assess its reflection in archaeological remains. For later, more refractory crucibles, the same general rule applies, though the likelihood of reuse is increased. As always, the contextual evidence accompanying the crucibles (when available) can provide further confidence in their interpretation.

CHAPTER 14

Site-specific contextualisation: synthesis

The most extensive crucible assemblage and contextual information has been available for study from Pi-Ramesse. For this reason, the largest analytical focus has been given to this assemblage within this PhD project, applying the full range of available methods. As a result, a richer dataset is available to reconstruct the metallurgical activities in the Ramesside capital compared not only to the other two case studies, but any case study hitherto published. The question, then, is what valuable information such an extensive analytical study has yielded and may continue to provide for future studies.

Analysis of the Pi-Ramesse assemblage, featuring a combination of optical microscopy, SEM-EDS, pXRF, (lab-based) XRF, NAA and MC-ICP-MS analysis, has provided the reconstruction of bronze production technology, and illuminated the material sources associated with it. For the first time, the complexity of variable techniques being applied within a single workshop has been elucidated, revealing not only the technical flexibility of the ancient Egyptian craftspeople, but furthermore highlighting the need for increased attention to such variability from archaeological scientists. Never before has any reconstruction of secondary Egyptian metallurgical activity been produced in such detail, and it will serve as a baseline for future crucible studies in ancient Egypt. Furthermore, the identification of potential sources from which these Ramesside workshops obtained their metal, through an integrated approach combining all listed analytical techniques, is the most significant (and only) contribution towards understanding New Kingdom copper provisioning within Egypt to be published since Stos-Gale *et al.*'s 1995 work. In addition to this, the tentative identification of cassiterite within the crucibles not only adds to the technological narrative for the Pi-Ramesse workshops, but widens the perspective on Late Bronze Age tin

provisioning for the eastern Mediterranean polities, suggesting the significant reliance on domestic resources which are less represented in historical sources.

Further contextualisation of these results is particularly difficult, given the lack of comparable studies on (large) crucible assemblages available for Egypt. In fact, no such publications on ancient bronze production exist at all. Discussions on the evolution of bronze production technology within ancient Egypt are therefore excluded. Obviously, such diachronic discussions are necessary to better understand how the workshops in Pi-Ramesse are representative as an expression of ancient Egyptian metallurgy. While the suggestion that some Hittite chariot maintenance probably took place in Pi-Ramesse (Van De Mieroop, 2007) cannot be dismissed, it is quite certain that the workshop activities discussed here are the work of Egyptian craftspeople. It must be stressed, however, that Pi-Ramesse is an extraordinary site. Ramses II is the first pharaoh to initiate building projects on such a large scale (Desroches-Noblecourt, 2007; Kitchen, 1982; Menu, 1999), but even so, the production of such large amounts of bronze presumably did not happen on a regular basis. Bronze production and working on a day-to-day basis almost certainly took place in very different contexts throughout ancient Egypt. The smaller workshops in Pi-Ramesse (QI-B/2 and QIV) are unlikely to be representative of such activity, and the broader focus of past excavations in Egypt on palatial, religious and funerary context may have strongly skewed the available record for archaeometallurgical studies towards 'unusual settings'. To come to terms with broad questions like 'How did the ancient Egyptians produce bronze?', or 'Where did the ancient Egyptians get their metal from?', many more case studies of production waste from various contexts are necessary (Rehren and Pusch, 2012). The recent work at Ayn Soukhna (Abd el Raziq *et al.*, 2011) is a good example, but while it is clear that most urban environments in ancient Egypt are in some way state controlled (see, e.g., Uphill, 2001), evidence from expeditions like those at Ayn Soukhna probably similarly reflect some state involvement. Our currently limited knowledge of the social standing and mobility of high-temperature craftspeople within ancient Egypt obscures our understanding of the contexts in which they worked. At this point, we probably only see them operating in state-commissioned larger projects (see, e.g., Stevens and Eccleston, 2007), while smaller scale activities, perhaps more reflective of their daily activities, are not reflected in our current archaeological record. The excavation of village environments, for example, may shed light on their activities in more informal settings. Through the integration of results from such varied contexts, a more nuanced understanding of metal provisioning and bronze production throughout Egypt's long history may be established.

For now, the Pi-Ramesse case study stands as a first example of how, despite methodological limitations, detailed crucible analysis may reveal differentiated production technology

and material use on a workshops scale. Some ambiguity will always remain, given the variability that cannot be assessed for each individual crucible. Similarly, the ambiguity concerning copper sources would not necessarily disappear through increased sampling, though it is likely to improve the interpretation of lead isotope results. Nonetheless, this research has shown the technological continuity existing between different workshops at Pi-Ramesse, and offered important insights into variable metal supply between them and through time. It further hints at new cross-craft relations with Egyptian Blue, and will hopefully stimulate further investigations of ancient Egyptian mining and metallurgy, of which the current state of research does not reflect its social and economic importance throughout Egypt's long history.

Although a similar number of mounted sections has been studied, the Gordion assemblage itself is far smaller than the Pi-Ramesse one. Compared to Pi-Ramesse, the Gordion crucible remains exhibited lower variability, reflective of their more refractory nature and (probably) the use of 'cleaner' starting materials. This hinders the easy evaluation of production technology: though it has been possible to identify active alloying, a discrimination between cassiterite cementation and pure metal alloying could not be securely made. It has, however, been possible to distinguish between the production of plain and leaded bronze, which has hitherto not been recognised in any other published crucible assemblage in such detail.

Again, no material evidence from Phrygia is available to make a meaningful comparison to this assemblage, and parallels can neither be found in (contemporary) Anatolia and Persia. Therefore, it remains difficult to assess this metallurgical technology in a diachronic perspective at this point. Given that Gordion was under Achaemenid rule during the Late Phrygian period, it is even unclear whether this metallurgical activity reflects Phrygian or Achaemenid technology. At any rate, the crucibles appear to have been made using local ceramic recipes.

The Gordion casting moulds are similarly made of local clay, and represent the first example of such moulds for Phrygia. Late Bronze and Iron Age casting moulds are quite rarely found in the eastern Mediterranean, and this particular assemblage was preserved as a result of their firing before use. Their preservation, coupled to a small assemblage of metal casting waste, has allowed for a more complete reconstruction of the *chaîne opératoire* of (leaded) bronze artefact production. Indeed, the identification of both leaded and unleaded bronze in the metal spills validates and strengthens the interpretation of this distinction within the Gordion crucibles. This illustrates the importance of studying the entire range of material evidence associated with metallurgical activity to better understand the processes, but equally for building confidence in these newly developed interpretative

frameworks for crucible analysis.

Considering the ore sources from which the Gordion metallurgists may have obtained their metal, little evidence has been made available through this research. In retrospect, it would have been interesting to have some lead isotope data for Gordion, as almost none is available for Phrygia, or even (Achaemenid) Persia for that matter. Budget considerations, the acquisition of this crucible assemblage at a later point in the PhD, and the more ambiguous evaluation of lead isotope data for leaded bronze has led to its exclusion from this research, in favour of the Pi-Ramesse assemblage. Nonetheless, information on lead sources during the Iron Age, when leaded bronze becomes far more prevalent throughout the Mediterranean, would be of interest for future research.

A truly contextual understanding of the use of these crucibles will equally remain impossible for now. This, however, is a result of the limited contextual information available for these crucibles, rather than the analytical methodology followed. The discovery of these crucibles in difficult and varied contexts, coupled to the absence of comparable material from other sites, limits the possibilities for linking this activity to a particular socio-economic setting. Each deposit may represent a group of crucibles from a single production event, all related to a single workshop; perhaps the so-called 'foundry'. More likely, several workshops are represented here (through time). Each context may represent a longer period of activity from a particular workshop, while other (contemporary) workshops used different dump locations, presumably closer by their work area. Then again, multiple workshops may have shared dump locations, and many other scenarios may be suggested. Such hypotheses are not testable in the absence of associated workshop environments, and archaeological dating cannot confidently separate the different dump contexts in time. The interesting issues concerned with organisation of production, frequency of activity, scale, and variability in time, are therefore beyond the scope of crucible analysis performed on assemblages from contexts without well-constrained chronology and associated workshops.

These issues similarly affect the assemblage from Roman Thrace, where no associated metal working installations were discovered during excavation of the crucibles. Furthermore, the dating of these crucibles is often problematic, and they tend to be isolated finds. As such, their interpretation as representative of a particular workshop, or even period, is beyond the realms of possibility.

Notwithstanding their currently unsettled contextual interpretation, the analysis of these crucibles again serves several purposes. For example, the identification of their particular metallurgical purpose can be related to their ceramic fabric and typology. The current lack of comparable material should not deter researchers from undertaking such studies:

the identical exercise is performed for other material categories, such as glass and ceramics, where compositional data equally add another dimension to typological studies. The present-day absence of a framework for comparison is hopefully of a transient nature, and the crucibles presented here may one day provide context for another assemblage from the eastern Roman provinces, or have their dating refined through analogy with many similar, well-dated crucibles. Their current isolation may appear discouraging, but confidence in continued crucible research within the eastern Mediterranean offers some consolation. Obviously, the time consuming nature of detailed crucible research may impede immediate progress, but the use of pXRF for fast, qualitative analysis may help in accelerating the establishment of a (somewhat rough) framework for crucible typologies and their associated metallurgical processes. Given the industrial nature of the Roman economy, it may be reasonably expected that general trends in crucible use will appear across wider geographical areas once enough data is assembled, similar to those seen in other ceramic categories. Detailed analysis of thin sections (crucible fabric) and mounted section (metallurgical technology) remains necessary, however, for such a framework to be able to answer more refined questions concerning technological traditions, adaptations and innovations in the Roman provinces through time.

Furthermore, the analysis of these crucibles has identified a range of metals being processed in these different sites. Though it is commonly assumed that a large range of metals were indeed routinely worked in Roman settlements, evidence for this is lacking in the literature, particularly for the eastern Roman provinces. Therefore, the evidence presented here is a first step towards identifying patterns of metal production at different provincial centres. It should be emphasised that many workshops probably existed within a single settlement, and within-site comparisons are a necessary component to such research. Obviously, it would be preferable to select more contextualised material for this purpose, whenever available.

Finally, the analysis of this assemblage has highlighted some methodological difficulties inherently associated with the study of refractory crucibles. Though this does not directly provide information on their particular context, it aids in shaping reasonable expectations on the nature of evidence that can be obtained from such analysis in the future.

In general then, successful, contextualised reconstructions of technology rely on both a considerate analysis of the crucible remains and the availability of detailed contextual information. The various issues related to crucible sampling, analysis and technical interpretation have been thoroughly discussed in Chapter 13. Here, it is important to contemplate what is actually reflected in a crucible. Beyond the identification of technology and material use, both in terms of ceramic and metallurgical technology, what do these cru-

cibles represent? What do they tell us about their users? Are these craftspeople full-time metallurgists? Is it possible to identify the manufacturers of early crucibles as potters or the metallurgists themselves? Are crucibles representative of occasional or daily activities? Over what period of time were they used? Do they reflect a tradition of metalworking, or were they *ad hoc* adaptations? If they are the latter, where and when did the necessary technological insights for their successful manufacture and use develop?

Such questions can clearly not be resolved by considering the results of crucible analysis in isolation. They require the integration of all available information, ranging from the particular context from which they were excavated, to the wider site, region and, eventually, all comparable contexts across the world. A collaborative effort from all archaeologists involved with the site is required to obtain an integrated understanding of the crucible assemblage within its context, and its relationship to other material evidence. Though it is the task of archaeometallurgists to familiarise themselves with the site's material culture and stratigraphy, it is obviously unrealistic for archaeometallurgists to become an authority on every site from which production waste is investigated. It is therefore vital to collaborate closely with excavation directors and other project members, in order to obtain the best results. In particular cases, such as Egypt, visual and written evidence may provide further insights into the social (who?) and cultural (why?) aspects of technology (e.g., Stevens and Eccleston, 2007). In addition, a diachronic, region-wide perspective is needed to address questions of technological development, spread and adaptation. The development of a frame of reference, through the study and, particularly, publication of many more crucible assemblages across the world is urgently needed before such diachronic issues can be tackled.

Furthermore, the integration of theoretical, anthropological and experimental archaeology frameworks of interpretation is necessary to consider many of these problems. Such a background is needed to shape reasonable expectations on what may be inferred from the material evidence in relation to the general questions raised at the start of this paragraph.

Mirroring the technical interpretation of crucible remains, practical guidelines for contextual interpretation of crucible assemblages have not yet been established. An attempt has been made in this thesis to discuss issues such as the number of crucibles one would expect to be associated to a single, large-scale event such as the industrial workshops in Pi-Ramesse, and where on site these may be deposited. Similarly, it should be considered what evidence can be expected from the excavation of a single (smaller scale) workshop which operated for a longer period in time. Obviously, the crucibles related to a decade of daily activity would not have been stored inside such a workshop (unless they were continuously recycled, perhaps as grog temper), but were more likely dumped elsewhere on

site, and are therefore too disconnected archaeologically to securely relate them to their production area. Crucibles preserved within the workshop, on the other hand, are probably representative of only the most recent activity. The majority of activities performed in a particular workshop are therefore often not preserved within it, and this should be kept in mind when interpreting the evidence from it. The availability of both workshop environments and well-dated dump contexts related to them, revealing a diachronic perspective on activities, may rarely be expected from archaeological excavation, in particular when no specific focus on metallurgical activity is given. The successful study of crucible assemblages therefore begins during excavation, where an increased awareness for this material category is key.

Although reconstructions of metallurgical activity should aim to include as much detail as possible on the actions performed during its course, this should not be stretched beyond the available data (contextual and material). For example, the reconstruction of crucibles as vessels for ritually reinforcing social and political world views (Swenson and Warner, 2012) seems to border on what is permissible, especially on the basis of limited metallurgical evidence. The scale of activity represented in crucibles should be taken at face value, and the interpretation of a single crucible, though interesting from a technological perspective (see, e.g., Thornton and Rehren, 2009) and in continuously building a reference framework, cannot be taken as representative for a metallurgical tradition when found in isolation. Given that the methodology for technological reconstruction of crucible metallurgy is still under development, it seems inadvisable to start running before we are steady on our feet. As has been argued throughout this thesis, a much larger sample is needed to confidently asses technological choices, which may or may not be related to changing context, and disentangle them from process-inherent variability.

While technological information can (usually) be obtained from their study, their nature as mobile items, typically discarded after use, renders the contextual attribution of crucibles difficult and often impossible. Therefore, the hopes of providing a truly detailed understanding of what crucibles represent, beyond vessels for metallurgical operation, should be tempered by the detail of their archaeological context, and await further empirical development of methodological and interpretative frameworks. This establishment of reference frameworks is necessary, but it is not the only justification for continued crucible research. The technological information obtained from their study, through the establishment of wider narratives of technological choice, metallurgical development and trade, will eventually lead to a detailed understanding of metallurgical practice on a workshop level. As always, however, for successful reconstructions, good context is everything.

Part VII

Conclusion

Oh let the sun beat down upon my face,
stars to fill my dream
I am a traveler of both time and space,
to be where I have been
To sit with elders of the gentle race,
this world has seldom seen
They talk of days for which they sit and wait,
when all will be revealed

Plant *et al.*, 1975

CHAPTER 15

Conclusions and avenues of future research

This thesis set out to explore the contextualised reconstruction of crucible metallurgy for several eastern Mediterranean sites, and to offer a discussion of methodological issues related to the study of ancient metallurgical crucible assemblages.

For each of these case studies, the first step towards reconstructing metallurgical technology has consisted of a technical description of the crucible remains. This has started from the ceramic fabric of each crucible, which, together with its design, is key to understanding its performance for a particular metallurgical operation. Following this, a more detailed investigation of crucible slag has been undertaken for each sample, as the main source of evidence for reconstructing the raw materials, techniques and process parameters that characterised the metallurgical process. Finally, these results have been interpreted within their particular context to further elucidate their place within the *chaîne opératoire* of bronze production for each particular workshop environment and wider regional setting.

At Pi-Ramesse, several techniques were employed to produce bronze (fresh metals, cementation and recycling), while making use of raw materials from various origins. The surprisingly high proportion of domestic materials such as copper and cassiterite, in addition to imported materials, suggests a well-developed tradition of indigenous bronze production. The shared use of these materials between high-temperature industries, as suggested earlier for glass, may now be tentatively extended to Egyptian Blue production. Bronze production does not vary distinctly from context to context within Pi-Ramesse: the use of similar techniques may reflect widespread tradition or the activity of the same craftspeople within different workshops. In terms of material use, however, it seems that

the industrial workshops relied, at least in part, on different copper sources for their provisioning. This could relate to differential access to material sources within different production contexts, but may equally reflect other factors such as changing availability of particular materials through time.

These results offer the first detailed insight into Egyptian bronze production on a workshop level, illuminating the different steps from workshop preparation to object casting, as well as the broader technology within ancient Egypt, and may serve as a baseline for further research into the subject. Here, the examination of many more crucible assemblages will be key to creating a more refined and differentiated understanding of bronze technology in a variety of social settings, while continued exploration of primary metal mining and smelting, as well as the analysis of final objects are necessary to provide the relevant context within which those results should be interpreted. The core of the Pi-Ramesse assemblage most likely represents an unusual event, lasting only a few weeks, while everyday bronze production, across thousands of years of pharaonic Egyptian history, remains to be explored.

For Gordion, far less variability has been witnessed inside the crucibles. They reflect the production of both bronze and leaded bronze, which entail the same technique but different starting products: copper with tin/cassiterite and leaded copper with tin/cassiterite. This distinction is further supported by the analysis of casting spills. Though further variability may have existed in the used copper sources, all appear to have been relatively pure, making such distinctions invisible for slag analysis without the measurement of lead isotope ratios. An added feature to this assemblage are the moulds, which offer insight into another step of secondary metallurgy. The recovery of these crucibles from various contexts makes it very difficult to address questions of workshop practice, and their isolation on a regional scale prevents comparisons to contemporary activity. As such, they must stand as a first example of Phrygian and/or Achaemenid metal production technology which may be further illuminated through continued study of not only crucible assemblages, but primary smelting as well as consumption contexts.

For Roman Thrace, a much larger range of different crucible fabrics and designs, related to different metallurgical processes, has been discovered. Though too many to list here, each of these crucibles offers a contribution towards understanding provincial Roman metallurgical practice. For example, a variety of crucibles has been employed in the production of (leaded) bronze across different sites. Whether this reflects changing technologies through time, or different solutions to the same problem under different environmental or social settings cannot be evaluated at this point. The main factor inhibiting such discussions is the problematic contextual information accompanying these crucibles. However,

this effect is further exaggerated by the limited comparative material currently available, presenting these crucibles to be more isolated than they actually are. As for the previous two case studies, the continued examination of Roman crucible assemblages from the wider region will much improve their explanatory value. In fact, while their presentation within this thesis may have left more questions unanswered than the other assemblages, the far greater abundance of Roman site excavations (within which metallurgical activity may be expected) holds the promise of developing an interpretative framework for Roman (crucible) metallurgy in a much shorter time. As everywhere, well contextualised crucible evidence will be essential to lending more gravity to its research beyond the metallurgical techniques, towards an integrated understanding of metallurgy across different socio-cultural contexts.

Apart from site-specific contributions, technological markers for particular crucible processes have been elaborated. For example, the identification of residual cassiterite to identify cementation, and the often ambiguous interpretation of its absence, have not been thoroughly explored before. Furthermore, identification of the use of multiple raw copper sources within a single assemblage, through both slag analysis and lead isotope studies, has not been achieved previously. Finally, highlighting the problematic nature of certain crucible slag phases with regards to process identification, such as tin and zinc oxide, offers important contributions towards future crucible studies.

In relation to methodology more generally, three main issues have emerged from the results of these case studies. Firstly, strongly variable slag formation is possible within a single crucible: crucible slag is a palimpsest, reflecting the changing conditions through space and time inside a crucible. This can result in different slag types in various zones of the crucible, with typically strong discrepancy between rim and lower body areas. Such variability has been commonly ignored in previous studies, making it difficult to assess inherent bias and the broader validity of published results.
Secondly, different technological choices made by the ancient craftspeople can exist within the assemblage as a whole. These differences, for example in production techniques, raw materials and crucible design, may in turn reflect underlying socio-cultural factors and more practical issues of material availability and technical knowledge. Not all techniques and raw materials provide diagnostic evidence, however, and some of the technological variation may be hidden by process-inherent variation that is superimposed on it. Therefore, these choices can not always be extricated from the crucible remains, though the methodology laid out in this thesis, summarised below, offers a sound approach to recognising them whenever possible. Evidently, such technological variations do not necessarily exist within every assemblage.

Thirdly, multiple technological pathways must always be considered when assessing crucible remains. On the one hand, a single process can produce a range of crucible slag types due to varying crucible conditions. On the other hand, a range of processes can result in very similar crucible slag types.
These issues affect crucibles to varying degrees, depending on the refractoriness of the crucible and the metallurgical process for which it was employed. However, they present the essential background against which studies should be undertaken, and their consideration advances some more general guidelines for the study of ancient crucible assemblages.

First, a macroscopic investigation of the entire assemblage should be undertaken, focusing on the variability in crucible fabric and design, as well as the degree of external vitrification and internal slagging, to develop an understanding of technological variability within the assemblage.
Whenever possible, at least one sample should be taken from each macroscopically identifiable group within a particular archaeological context, but preferably two or three as a starting point to detect variability within each group. For larger assemblages, where such groups are represented by hundreds or thousands of sherds, rather than a (few) dozen, sample numbers should increase proportionally. When sampling opportunities are limited, the use of pXRF may offer a grip on chemical variability: the analysis of several areas within a single crucible can illuminate within-crucible variability, while population-wide trends may be picked up through analysis of the entire assemblage. Subject to sampling limitations, it is usually more appropriate to sample a lower body fragment for which a fairly substantial slag layer has developed, rather than rim fragments. If this is not possible, it must be considered whether rim samples or dross scrapings offer sufficient promise towards answering the research questions to justify the costs of detailed analysis.
While the issue of representativeness is difficult to scale in absolute terms, the use of pXRF and more detailed analysis of multiple samples typically allows the researcher to build a measure of confidence in assessing variability, both on a crucible and assemblage-wide scale. Though it seems that a complete understanding of process variability is beyond the powers of current research methods, any recognition of it improves the authority of suggested interpretations. When this cannot be established, the identification of particular process markers will always improve process interpretation, though limitations in broader validity of such interpretations must be recognised.
A cross section of a lower body fragment should be mounted in resin for reconstructions of metallurgical techniques and raw material use. The key parameters for such reconstructions on which to focus during analysis are metallic prills and residual ore fragments

embedded in the crucible slag, and bulk chemical enrichments of slag relative to ceramic. For the interpretation of results, it is advisable to attempt reconciliation of all observations as reflections of a single process wherever possible. This applies both to the interpretation of a single sherd, as well as to that of all samples taken across an assemblage. Only when process-inherent variability cannot account for observed variations should differentiation in techniques and raw materials be considered.
In general, a conservative attitude towards broader interpretations is advisable. It is necessary to consider for each assemblage the degree to which process variability may hide evidence for particular techniques, and where particular processes may not leave any diagnostic evidence. Greater sample numbers offer greater confidence for assemblage-wide interpretations, but only the continued examination (and publication) of many crucible assemblages will empirically strengthen interpretation cogency.

Of course, many methodological issues remain to be resolved. Experimental work is vital in this regard, for example to verify the validity of tentatively identified technological markers, such as residual cassiterite, or to elucidate the various lead contributions to crucible slag (and metal) during bronze production. This will increase confidence in the identification of different techniques and raw materials within crucible assemblages. Furthermore, it is crucial to expand the debate on what is reflected exactly in these crucibles. With assemblages varying from isolated sherds to thousands of fragments, it is essential to question continuously the informative value of detailed analysis for a particular context. The greatest strength in examining material culture lies in its comparison to similar materials within different contexts. The case studies presented in this thesis create a foundation for refined methodology and interpretation, which future work across the ancient world can build on. An increased potency of reconstructed technological choices, as well as the broader methodology for their study, will follow from such continued study of crucible assemblages.

Crucibles stand at the cross-roads of metallurgy and ceramic technology, of raw materials trade and the market of consumable objects, and of massive as well as individual production scales. From there, they can play an informative role for each of these contingent spheres of human activity. Their transformational and integrative nature, both from a technological perspective and a more socio-cultural point of view, make crucibles worthy of far more attention than they currently receive.
I hope this thesis may therefore inspire others to jump the many hurdles presented by process variability and to have shown how a considerate methodology for journeys into the crucible may reveal the choices made by ancient craftspeople and their societies.

Bibliography

Abd El-Rahman, Y., Surour, A. A., El Manawi, A. H. W., Rifai, M., Abdel Motelib, A., Ali, W. K., and El Dougdoug, A. M. (2013): Ancient mining and smelting activities in the Wadi Abu Gerida area, central Eastern Desert, Egypt: preliminary results, *Archaeometry*, 55, 1067–1087.

Abd el Raziq, M., Castel, G., Tallet, P., and Fluzin, P. (2011): *Ayn Soukhna II: les Ateliers Métallurgiques du Moyen Empire*, Cairo: Institut français d'archéologie orientale.

Abdallatif, T. F., Mousa, S. E., and Elbassiony, A. (2003): Geophysical investigation for mapping the archaeological features at Qantir, Sharqyia, Egypt, *Archaeological Prospection*, 10, 27–42.

Abdel-Motelib, A., Bode, M., Hartmann, R., Hartung, U., Hauptmann, A., and Pfeiffer, K. (2012): Archaeometallurgical expeditions to the Sinai Peninsula and the Eastern Desert of Egypt (2006, 2008), *Metalla (Bochum)*, 19, 3–59.

Abouzeid, A.-Z. M. and Khalid, A.-A. M. (2011): Mineral industry in Egypt - Part I: metallic mineral commodities, *Natural Resources*, 2, 35–53.

Adamson, D. A., Gasse, F., Street, F. A., and Williams, M. A. J. (1980): Late Quaternary history of the Nile, *Nature*, 288, 50–55.

Adriaens, A. (1996): Elemental composition and microstructure of Early Bronze Age and Medieval tin slags, *Mikrochimica Acta*, 124, 89–98.

Aimers, J. J., Farthing, D. J., and Shugar, A. N. (2012): Handheld XRF analysis of Maya ceramics: a pilot study presenting issues related to quantification and calibration, in A. N. Shugar and J. L. Mass, eds., *Handheld XRF for Art and Archaeology*, Studies in Archaeological Sciences 3, Leuven University Press, pp. 423–448.

Albarède, F., Desaulty, A.-M., and Blichert-Toft, J. (2012): A geological perspective on the use of Pb isotopes in archaeometry, *Archaeometry*, 54, 853–867.

Alimov, K., Boroffka, N., Burjakov, Ju., Cierny, J., Lutz, J., Parzinger, H., Pernicka, E., Ruzanov, V., Shirinov, T., and Weisgerber, G. (1999): Research at Karnab, Uzbekistan. Preliminary notes from the 1997 campaign, *History of Material Culture of Uzbekistan*, 30, 80–87.

Allan, J. W. (1979): *Persian Metal Technology, 700-1300 AD*, London: Ithaca Press for the Faculty of Oriental Studies and the Ashmolean Museum, University of Oxford.

Allen, R. O., Hamroush, H., and Hoffman, M. A. (1989): Archaeological implications of differences in the composition of Nile sediments, in R. O. Allen, ed., *Archaeological Chemistry IV*, Washington: American Chemical Society, pp. 33–56.

Amorós, J. L., Lunar, R., and Tavira, P. (1981): Jarosite: a silver bearing mineral of the gossan of Rio Tinto (Huelva) and la Union (Cartagena, Spain), *Mineralium Deposita*, 16, 205–213.

Angelini, I., Masiero, E., Bianchi, P., and Molin, G. (2009): Crucibles, wastes, and metals from the Terramara settlement of Beneceto (PR, Italy): report of preliminary archaeometric investigation, in *Archaeometallurgy in Europe 2007. Selected Papers of the 2nd International Conference 17.-21. June 2007 in Aquileia*, Milan: Associazione Italiana di Metallurgia, pp. 177–190.

Anguilano, L., Oberrauch, H., Hauser, H., Rehren, Th., and Artiolo, G. (2009): Copper smelting at Fennhals-Kurtatsch, in J.-F. Moreau, R. Auger, J. Chabot, and A. Herzog, eds., *Proceedings of the 36th International Symposium on Archaeometry, Quebec City, Canada, 2-6 May, 2006*, CELAT, Université du Laval, pp. 375–382.

Arnold, D., Bourriau, J. D., and Nordström, H.-Å., eds. (1993): *An Introduction to Ancient Egyptian Pottery*, Mainz: Verlag Philip Von Zabern.

Artioli, G., Angelini, I., Burger, E., Bourgarit, D., and Colpani, F. (2009): Petrographic and chemical investigations of the earliest copper smelting slags in Italy: towards a reconstruction of the beginning of copper metallurgy, in *Archaeometallurgy in Europe 2007. Selected Papers of the 2nd International Conference 17.-21. June 2007 in Aquileia [CD-ROM]*, Milan: Associazione Italiana di Metallurgia.

Aston, D. A., Mommsen, H., Mountjoy, P., Pusch, E. B., and Rehren, Th. (2007): Die in- und ausländischen Werkstoffe der Grabung Qantir in Wort und Bild, in E. B. Pusch and

M. Bietak, eds., *Die Keramik des Grabungsplatzes Q I - Teil 2: Schaber, Scherben und Marken.*, Forschungen in der Ramses-Stadt Band 5, Hildesheim: Gerstenberg Verlag, pp. 509–554.

Atasoy, E. and Buluç, S. (1982): Metallurgical and archaeological examination of Phrygian objects, *Anatolian Studies*, 32, 157–160.

Audouze, F. (2002): Leroi-Gourhan, a philosopher of technique and evolution, *Journal of Archaeological Research*, 10, 277–306.

Avner, U. (2013): Egyptian Timna - reconsidered, *Paper presented at the Timna Park International Conference in memory of Professor Beno Rothenberg. Mining for Copper: Environment, Culture and Copper in Antiquity. 22-25 April 2013, Timna, Israel.*

Bachmann, H.-G. (1976): Crucibles from a Roman settlement in Germany, *Journal of the Historical Metallurgy Society*, 10, 34–35.

Bachmann, H.-G. (1980): Early copper smelting techniques in Sinai and Negev as deduced from slag investigations, in P. T. Craddock, ed., *Scientific Studies in Early Mining and Extractive Metallurgy*, Occasional Paper 20, London: British Museum, pp. 103–134.

Bachmann, H.-G. (1982a): Copper smelting slags from Cyprus: review and classification of analytical data, in J. D. Muhly, R. Maddin, and V. Karageorghis, eds., *Early Metallurgy in Cyprus, 4000-500B.C.*, Nicosia: Pierides Foundation, pp. 143–152.

Bachmann, H.-G. (1982b): *The Identification of Slags from Archaeological Sites*, London: Institute of Archaeology.

Bajnóczi, B., Nagy, G., Tóth, M., Ringer, I., and Ridovics, A. (2014): Archaeometric characterization of 17th-century tin-glazed Anabaptist (Hutterite) faience artefacts from North-East-Hungary, *Journal of Archaeological Science*, 45, 1–14.

Balmuth, M. S. and Tylecote, R. F. (1976): Ancient copper and bronze in Sardinia: excavation and analysis, *Journal of Field Archaeology*, 3, 195–201.

Bamberger, M. (1985): The working conditions of the ancient copper smelting process, in P. T. Craddock and M. J. Hughes, eds., *Furnaces and Smelting Technology in Antiquity*, Occasional Paper 48, London: British Museum, pp. 151–157.

Baron, S., Tămaş, C. G., Cauuet, B., and Munoz, M. (2011): Lead isotope analyses of gold-silver ores from Rosia Montana (Romania): a first step of metal provenance study of

Roman mining activity in Alburnus Maior (Roman Dacia), *Journal of Archaeological Science*, 38, 1090–1100.

Bartelheim, M., Niederschlag, E., and Rehren, Th. (1998): Research into prehistoric metallurgy in the Bohemian/Saxon Erzgebirge, in B. Hänsel, ed., *Mensch und Umwelt in der Bronzezeit Europas. Man and Environment in European Bronze Age*, Kiel: Oetker-Voges Verlag, pp. 225–229.

Bass, G. F. (1967): Cape Gelidonya: a Bronze Age shipwreck, *Transactions of the American Philosophical Society*, 57, 1–177.

Bassiakos, Y. and Catapotis, M. (2006): Reconstruction of the copper smelting process based on the analysis of ore and slag samples, in P. P. Betancourt, ed., *The Chrysokamino Metallurgy Workshop and Its Territory*, Hesperia Supplements 36, The American School of Classical Studies at Athens, pp. 329–353.

Baxter, M. J. (1999): On the multivariate normality of data arising from lead isotope fields, *Journal of Archaeological Science*, 26, 117–124.

Baxter, M. J. and Gale, N. H. (1998): Testing for multivariate normality via univariate tests: a case study using lead isotope ratio data, *Journal of Applied Statistics*, 25, 671–683.

Bayley, J. (1984): Roman brass-making in Britain, *Journal of the Historical Metallurgy Society*, 18, 42–43.

Bayley, J. (1987): *Final Report on the Brooch Analyses and Crucibles from Prestatyn, Clwyd*, Ancient Monuments Laboratory Report 28/87, Historic Buildings and Monuments Commission.

Bayley, J. (1996): Innovation in later medieval urban metalworking, *Historical Metallurgy*, 30, 67–71.

Bayley, J. (1998): The production of brass in antiquity with particular reference to Roman Britain, in P. T. Craddock, ed., *2000 Years of Zinc and Brass*, Occasional Paper 50, London: British Museum, pp. 7–26.

Bayley, J., Crossley, D., and Ponting, M. (2008): *Metals and Metalworking - A Research Framework for Archaeometallurgy*, The Historical Metallurgy Society.

Bayley, J., Dungworth, D., and Paynter, S. (2001): *Centre for Archaeology Guidelines: Archaeometallurgy*, Swindon: English Heritage Publications.

Bayley, J. and Eckstein, K. (1997): Silver refining - production, recycling, assaying, in A. Sinclair, E. Slater, and J. Gowlett, eds., *Archaeological Sciences 1995. Proceedings of a Conference on the Application of Scientific Techniques to the Study of Archaeology, Liverpool, July 1995*, Oxbow Monograph 64, Oxford: Oxbow Books, pp. 107–111.

Bayley, J. and Rehren, Th. (2007): Towards a functional and typological classification of crucibles, in S. La Niece, D. Hook, and P. T. Craddock, eds., *Metals and Mines. Studies in Archaeometallurgy*, London: Archetype Books, pp. 46–55.

Beagrie, N. (1985): Some early tin ingots, ores and slags from Western Europe, *Historical Metallurgy*, 19, 162–168.

Becker, J. S. (2002): State-of-the-art and progress in precise and accurate isotope ratio measurements by ICP-MS and LA-ICP-MS, *Journal of Analytical Atomic Spectrometry*, 17, 1172–1185.

Beeley, P. R. (2001): *Foundry Technology*, Oxford: Butterworth-Heinemann.

Begemann, F., Hauptmann, A., Schmitt-Strecker, S., and Weisgerber, G. (2010): Lead isotope and chemical signature of copper from Oman and its occurrence in Mesopotamia and sites on the Arabian Gulf coast, *Arabian Archaeology and Epigraphy*, 21, 135–169.

Begemann, F., Kallas, K., Schmitt-Strecker, S., and Pernicka, E. (1999): Tracing ancient tin via isotope analyses, in A. Hauptmann, E. Pernicka, Th. Rehren, and Ü. Yalçin, eds., *The Beginnings of Metallurgy*, Bochum: Deutsches Bergbau-Museum, pp. 277–284.

Begemann, F., Schmitt-Strecker, S., Pernicka, E., and Lo Schiavo, F. (2001): Chemical composition and lead isotopy of copper and bronze from Nuragic Sardinia, *European Journal of Archaeology*, 4, 43–85.

Behrendt, S., Mielke, D. P., and Mecking, O. (2012): Die Portable Röntgenfluoreszenzanalyse (P-RFA) in der Keramikforschung: Grundlagen und Potenzial, *Restaurierung und Archäologie*, 5, 93–110.

Beit-Arieh, I. (1985): Serabit el-Khadim: new metallurgical and chronological aspects, *Levant*, 17, 89–116.

Ben-Yosef, E. (2012): A unique casting mould from the new excavations at Timna Site 30 (Israel): evidence of western influence?, in V. Kassianidou and G. Papasavvas, eds., *Eastern Mediterranean Metallurgy and Metalwork in the Second Millennium BC - A Conference in Honour of James D. Muhly, Nicosia, 10th-11th October 2009*, Oxford: Oxbow Books, pp. 188–196.

Ben-Yosef, E. and Levy, T. E. (2014): Tracking technological change in high resolution: an XRF study of Iron Age copper smelting in the Southern Levant, *Poster presented at the 40th International Symposium on Archaeometry, 19-23 May 2014, Los Angeles, USA*.

Ben-Yosef, E., Levy, T. E., Higham, T., Najjar, M., and Tauxe, L. (2010): The beginning of Iron Age copper production in the southern Levant: new evidence from Khirbat al-Jariya, Faynan, Jordan, *Antiquity*, 84, 724–746.

Ben-Yosef, E., Shaar, R., Tauxe, L., and Ron, H. (2012): A new chronological framework for Iron Age copper production at Timna (Israel), *Bulletin of the American Schools of Oriental Research*, 367, 31–71.

Benvenuti, M., Chiarantini, L., Norfini, L., Casini, A., Guideri, S., and Tanelli, G. (2003): The "Etruscan tin": a preliminary contribution from researches at Monte Valerio and Baratti-Populonia (southern Tuscany, Italy), in A. Giumlia-Mair and F. Lo Schiavo, eds., *The Problem of Early Tin. Acts of the XIVth UISPP Congress*, BAR International Series 1199, Oxford: Archaeopress, pp. 55–65.

Bevan, A. (2010): Making and marking relationships: Bronze Age brandings and Mediterranean commodities, in A. Bevan and D. Wengrow, eds., *Cultures of Commodity Branding*, Walnut Creek, US: Left Coast Press, pp. 35–86.

Bietak, M. (1981): *Avaris and Piramesse. Archaeological Exploration in the Eastern Nile Delta*, Oxford: University Press.

Bietak, M. (1996): *Avaris, the Capital of the Hyksos. Recent Excavations at Tell el-Dab'a*, London: British Museum Press.

Bietak, M. and Forstner-Müller, I. (2011): The topography of New Kingdom Avaris and Per-Ramesses, in M. Collier and S. Snape, eds., *Ramesside Studies in Honour of K.A. Kitchen*, Bolton: Rutherford, pp. 23–50.

Bilgi, Ö., ed. (2004): *Anatolia, Cradle of Castings*, Istanbul: Döktaş.

Birmingham, J. M. (1961): The overland route across Anatolia in the eighth and seventh centuries B.C., *Anatolian Studies*, 11, 185–195.

Blakelock, E. (2005): *Qualitative Analysis of the Crucibles from Bloodmoor Hill, Carlton Colville, Suffolk*, Centre for Archaeology Report 22/2005, English Heritage.

Bland, R. (2013): What happened to gold coinage in the 3rd c. A.D.?, *Journal of Roman Archaeology*, 26, 263–280.

Bode, M., Hauptmann, A., and Mezger, K. (2009): Tracing Roman lead sources using lead isotope analyses in conjunction with archaeological and epigraphic evidence - a case study from Augustan/Tiberian Germania, *Archaeological and Anthropological Sciences*, 1, 177–194.

Boni, M., Di Maio, G., Frei, R., and Villa, I. M. (2000): Lead isotopic evidence for a mixed provenance for Roman water pipes from Pompeii, *Archaeometry*, 42, 201–208.

Bonnet, C. (1986): Un atelier de bronziers à Kerma, in M. Krause, ed., *Nubische Studien. Tagungsakten der 5. Internationalen Konferenz der International Society for Nubian Studies, Heidelberg, 22.-25. September 1982*, Mainz: Verlag Philip Von Zabern, pp. 19–22.

Bonnet, C. (2004): *Le Temple Principal de la Ville de Kerma et son Quartier Religieux*, Paris: Editions Errance.

Boroffka, N., Cierny, J., Lutz, J., Parzinger, H., Pernicka, E., and Weisgerber, G. (2002): Bronze Age tin from Central Asia: preliminary notes, in K. Boyle, C. Renfrew, and M. Levine, eds., *Ancient Interactions: East and West in Eurasia*, McDonald Institute Monographs, Cambridge: McDonald Institute for Archaeological Research, pp. 135–159.

Bossert, E.-M. (2000): *Die Keramik phrygischer Zeit von Boğazköy: Funde aus den Grabungskampagnen 1906, 1907, 1911, 1912, 1931-1939 und 1952-1960*, Mainz: Philip von Zabern.

Bourgarit, D. (2007): Chalcolithic copper smelting, in S. La Niece, D. Hook, and P. T. Craddock, eds., *Metals and Mines. Studies in Archaeometallurgy*, London: Archetype Books, pp. 3–14.

Bourriau, J. D., Bellido, A., Bryan, N., and Robinson, V. (2006): Egyptian pottery fabrics: a comparison between NAA groupings and the "Vienna System", in E. Czerny, I. Hein, H. Hunger, D. Melman, and A. Schwab, eds., *Timelines. Studies in Honour of Manfred Bietak, Volume III*, Leuven: Peeters Publishers & Department of Oriental Studies, pp. 261–292.

Bourriau, J. D. and Nicholson, P. T. (1992): Marl clay pottery fabrics of the New Kingdom from Memphis, Saqqara and Amarna, *The Journal of Egyptian Archaeology*, 78, 29–91.

Bourriau, J. D., Smith, L. M. V., and Nicholson, P. T. (2000): *New Kingdom Pottery Fabrics: Nile Clay and Mixed Nile/Marl Clay Fabrics from Memphis and Amarna*, Fourteenth Occasional Publication, London: The Egypt Exploration Society.

Bowen, N. L. (1915): The later stages of the evolution of the igneous rocks, *The Journal of Geology*, 23, 1–91.

Boyanov, I. (2013): Veterans and society in Roman Serdica, *Ancient West and East*, 12, 237–249.

Brauns, M., Schwab, R., Gassmann, G., Wieland, G., and Pernicka, E. (2013): Provenance of Iron Age iron in southern Germany: a new approach, *Journal of Archaeological Science*, 40, 841–849.

Bray, P. J. and Pollard, A. M. (2012): A new interpretative approach to the chemistry of copper-alloy objects: source, recycling and technology, *Antiquity*, 86, 853–867.

Brewer, W. F. and Lambert, B. L. (2001): The theory-ladenness of observation and the theory-ladenness of the rest of the scientific process, *Philosophy of Science*, 68, 176–186.

Brill, R. H., Barnes, I. L., and Adams, B. (1974): Lead isotopes in some ancient Egyptian objects, in A. Bishay, ed., *Recent Advances in Science and Technology of Materials, Band 3 (= The Proceedings of the Second Cairo Solid State Conference Held in Cairo, Egypt, April 21-26, 1973)*, New York: Plenum, pp. 9–27.

Brill, R. H. and Wampler, J. M. (1967): Isotope studies of ancient lead, *American Journal of Archaeology*, 71, 63–77.

Budd, P., Gale, D., Pollard, A. M., Thomas, R. G., and Williams, P. A. (1993): Evaluating lead isotope data: further observations, *Archaeometry*, 35, 241–263.

Budd, P., Haggerty, R., Pollard, A. M., Scaife, B., and Thomas, R. G. (1995a): New heavy isotope studies in archaeology, *Israel Journal of Chemistry*, 35, 125–130.

Budd, P., Pollard, A. M., Scaife, B., and Thomas, R. G. (1995b): Oxhide ingots, recycling and the Mediterranean metals trade, *Journal of Mediterranean Archaeology*, 8, 1–32.

Budd, P., Pollard, A. M., Scaife, B., and Thomas, R. G. (1995c): The possible fractionation of lead isotopes in ancient metallurgical processes, *Archaeometry*, 37, 143–150.

Burger, E., Bourgarit, D., Wattiaux, A., and Fialin, M. (2010): The reconstruction of the first copper-smelting processes in Europe during the 4th and the 3rd millennium BC: where does the oxygen come from?, *Applied Physics A. Materials Science and Processing*, 100, 713–724.

Butcher, K. and Ponting, M. (1995): Rome and the east. Production of Roman provincial silver coinage for Caesarea in Cappadocia under Vespasian, AD 69-79, *Oxford Journal of Archaeology*, 14, 63–77.

Butcher, K. and Ponting, M. (2005): The Roman denarius under the Julio-Claudian emperors: mints, metallurgy and technology, *Oxford Journal of Archaeology*, 24, 163–197.

Caley, E. R. (1964): *Orichalcum and Related Ancient Alloys. Origin, Composition, and Manufacture, with Special Reference to the Coinage of the Roman Empire*, New York: American Numismatic Society.

Carradice, I. and Cowell, M. (1987): The minting of Roman imperial bronze coins for circulation in the east: Vespasian to Trajan, *The Numismatic Chronicle*, 147, 26–50.

Carter, G. F. (1978): Precision in the X-ray fluorescence analysis of sixty-one Augustan quadrantes, *Journal of Archaeological Science*, 5, 293–300.

Castel, G., Mathieu, B., Pouit, G., El Hawari, M., Shaaban, G., Hellal, H., Abdallah, T., and Ossama, A. (1996): Wadi Dara copper mines, in F. A. Esmael, ed., *Proceedings of the First International Conference on Ancient Egyptian Mining and Metallurgy and Conservation of Metallic Artifacts*, Cairo: Ministry of Culture, Supreme Council of Antiquities, pp. 15–31.

Castel, G., Tallet, P., and Fluzin, P. (2008): La métallurgie du cuivre au temps des pharaons, *Archéologia*, 460, 62–71.

Cech, B. and Rehren, Th., eds. (2014): *Early Iron in Europe*, Monographies Instrumentum 50, Montagnac: Editions Monique Mergoil.

Charalambous, A., Kassianidou, V., and Papasavvas, G. (2014): A compositional study of Cypriot bronzes dating to the Early Iron Age using portable X-ray fluorescence spectrometry (pXRF), *Journal of Archaeological Science*, 46, 205–216.

Charles, J. A. (1979): The development of the usage of tin and tin-bronze: some problems, in A. D. Franklin, J. S. Olin, and T. A. Wertime, eds., *The Search for Ancient Tin: a Seminar Organized by Theodore A. Wertime and held at the Smithsonian Institution and the National Bureau of Standards, Washington, D.C., March 14-15, 1977*, Washington, D.C.: Smithsonian Institution Press, pp. 25–32.

Charles, J. A. (1980): The coming of copper and copper-base alloys and iron, in T. A. Wertime and J. D. Muhly, eds., *The Coming of Age of Iron*, New Haven: Yale University Press, pp. 151–181.

Chartier-Raymond, M., Gratien, B., Traunecker, C., and Vinçon, J.-M. (1994): Les site miniers pharaoniques du Sud-Sinai. Quelques notes et observations de terrain, *Cahiers de Recherches de l'Institut de Papyrologie et d'Egyptologie de Lille*, 16, 31–77.

Chen, K., Rehren, Th., Mei, J., and Zhao, C. (2009): Special alloys from remote frontiers of the Shang Kingdom: scientific study of the Hanzhong bronzes from southwest Shaanxi, China, *Journal of Archaeological Science*, 36, 2108–2118.

Chescoe, D. and Goodhew, P. J. (1990): *The Operation of Transmission and Scanning Electron Microscopes*, Oxford: Oxford University Press.

Chiarantini, L., Benvenuti, M., Costagliola, P., Fedi, M. E., Guideri, S., and Romualdi, A. (2009): Copper production at Baratti (Populonia, southern Tuscany) in the early Etruscan period (9th-8th centuries BC), *Journal of Archaeological Science*, 36, 1626–1636.

Childs, S. T. (1991): Style, technology, and iron smelting furnaces in Bantu-speaking Africa, *Journal of Anthropological Archaeology*, 10, 332–359.

Chirikure, S., Heimann, R. B., and Killick, D. (2010): The technology of tin smelting in the Rooiberg Valley, Limpopo Province, South Africa, ca. 1650-1850 CE, *Journal of Archaeological Science*, 37, 1656–1669.

Cholakova, A. (2006): Metalworking in the earliest site period of Nicopolis ad Istrum, *Bulletin of the National Institute of Archaeology*, 39, 163–184.

Cierny, J. and Weisgerber, G. (2003): Bronze Age tin mines in Central Asia, in A. Giumlia-Mair and F. Lo Schiavo, eds., *The Problem of Early Tin. Acts of the XIVth UISPP Congress*, BAR International Series 1199, Oxford: Archaeopress, pp. 23–31.

Clayton, R., Andersson, P., Gale, N. H., Gillis, C., and Whitehouse, M. J. (2002): Precise determination of the isotopic composition of Sn using MC-ICP-MS, *Journal of Analytical Atomic Spectrometry*, 17, 1248–1256.

Coghlan, H. H. (1975): *Notes on the Prehistoric Metallurgy of Copper and Bronze in the Old World (Second Edition)*, Oxford: University Press.

Constantinou, G. (1980): Metallogenesis associated with the Troodos ophiolite, in A. Panayiotou, ed., *Ophiolites. Proceedings of the International Ophiolite Symposium, Cyprus, 1979*, Nicosia: Cyprus Geological Survey Department, pp. 663–674.

Cooke, S. R. B. and Nielsen, B. V. (1978): Slags and other metallurgical products, in G. Jr. Rapp and S. E. Aschenbrenner, eds., *Excavations at Nichoria in Southwest Greece. Vol.1: Site, Environs and Techniques*, Minneapolis: University of Minnesota Press, pp. 182–224.

Cooper, H. K., Duke, M. J. M., Simonetti, A., and Chen, G. (2008): Trace element and Pb isotope provenance analyses of native copper in northwestern North America: results of a recent pilot study using INAA, ICP-MS, and LA-MC-ICP-MS, *Journal of Archaeological Science*, 35, 1732–1747.

Costin, C. L. (1991): Craft specialization: issues in defining, documenting, and explaining the organization of production, *Archaeological Method and Theory*, 3, 1–56.

Cowell, M. R. (1986): The composition of Egyptian copper-based metalwork, in R. A. David, ed., *Science in Egyptology*, Manchester: Manchester University Press, pp. 463–468.

Cowell, M. R. and Hyne, K. (2000): Scientific examination of the Lydian precious metal coinages, in A. Ramage and P. T. Craddock, eds., *King Croesus' Gold. Excavations at Sardis and the History of Gold Refining*, London: British Museum Press, pp. 169–174.

Craddock, P. T. (1976): The composition of the copper alloys used by the Greek, Etruscan and Roman civilizations. 1: The Greeks before the Archaic Period, *Journal of Archaeological Science*, 3, 93–113.

Craddock, P. T. (1978): The composition of the copper alloys used by the Greek, Etruscan and Roman civilizations. 3: The origins and early use of brass, *Journal of Archaeological Science*, 5, 1–16.

Craddock, P. T. (1995): *Early Metal Mining and Production*, Cambridge: Edinburgh University Press.

Craddock, P. T. (1998): Zinc in classical antiquity, in P. T. Craddock, ed., *2000 Years of Zinc and Brass*, Occasional Paper 50, London: British Museum, pp. 1–6.

Craddock, P. T. (2000): From hearth to furnace: evidences for the earliest metal smelting technologies in the eastern Mediterranean, *Paléorient*, 26, 151–165.

Craddock, P. T. (2013): Refractories: ceramics with a purpose, *The Old Potter's Almanack*, 18, 9–20.

Craddock, P. T. and Eckstein, K. (2003): Production of brass in Antiquity by direct reduction, in P. T. Craddock and J. Lang, eds., *Mining and Metal Production. Through the Ages*, London: British Museum Press, pp. 216–230.

Craddock, P. T., La Niece, S., and Hook, D. R. (2003): Evidences for the production, trading and refining of copper in the Gulf of Oman during the third millennium BC, in T. Stöllner, G. Körlin, G. Steffens, and J. Cierny, eds., *Man and Mining (Mensch und Bergbau)*, Der Anschnitt, Beiheft 16, Bochum: Deutsches Bergbau-Museum, pp. 103–112.

Craddock, P. T. and Meeks, N. D. (1987): Iron in ancient copper, *Archaeometry*, 29, 187–204.

Crawford, M. H. (1977): Republican denarii in Romania: the suppression of piracy and the slave-trade, *The Journal of Roman Studies*, 67, 117–124.

Crew, P. and Rehren, Th. (2002): High-temperature workshop residues from Tara - iron, bronze and glass, *Discovery Programme Report*, 6, 83–103.

Cui, J. and Wu, X. (2011): An experimental investigation on lead isotopic fractionation during metallurgical processes, *Archaeometry*, 53, 205–214.

Cumming, G. L. and Richards, J. R. (1975): Ore lead isotope ratios in a continuously changing earth, *Earth and Planetary Science Letters*, 28, 155–171.

Darbyshire, G. and Pizzorno, G. H. (2009): Gordion in history, *Expedition*, 51, 11–22.

Davenport, W. G., King, M., Schlesinger, M. E., and Biswas, A. K. (2002): *Extractive Metallurgy of Copper (4th Edition)*, Oxford: Pergamon.

Davey, C. J. (1985): Crucibles in the Petrie Collection and hieroglyphic ideograms for metal, *Journal of Egyptian Archaeology*, 71, 142–148.

Davey, C. J. and Edwards, W. I. (2007): Crucibles from the Bronze Age of Egypt and Mesopotamia, *Proceedings of the Royal Society of Victoria*, 120, 146–154.

Davies, N. de G. (1935a): *Paintings from the Tomb of Rekh-mi-Re at Thebes*, New York: Plantin Press.

Davies, O. (1935b): *Roman Mines in Europe*, Oxford: Clarendon Press.

Davies, O. (1936): Prehistoric copper mines near Burgas, *Man*, 36, 92–93.

Davis, L. G., Macfarlan, S. J., and Henrickson, C. N. (2012): A PXRF-based chemostratigraphy and provenience system for the Cooper's Ferry site, Idaho, *Journal of Archaeological Science*, 39, 663–671.

Day, P. M., Kiriatzi, E., Tsolakidou, A., and Kilikoglou, V. (1999): Group therapy in Crete: a comparison between analyses by NAA and thin section petrography of Early Minoan pottery, *Journal of Archaeological Science*, 26, 1025–1036.

Dayton, J. E. (1971): The problem of tin in the ancient world, *World Archaeology*, 3, 49–70.

Dayton, J. E. (2003): The problem of tin in the ancient world (part 2), in A. Giumlia-Mair and F. Lo Schiavo, eds., *The Problem of Early Tin. Acts of the XIVth UISPP Congress*, BAR International Series 1199, Oxford: Archaeopress, pp. 165–170.

de Jesus, P. S. (1979): Considerations on the occurrence and exploitation of tin sources in the ancient Near East, in A. D. Franklin, J. S. Olin, and T. A. Wertime, eds., *The Search for Ancient Tin: a Seminar organized by Theodore A. Wertime and held at the Smithsonian Institution and the National Bureau of Standards, Washington, D.C., March 14-15, 1977*, Washington, D.C.: Smithsonian Institution Press, pp. 33–38.

de Jesus, P. S. (1980): *The Development of Prehistoric Mining and Metallurgy in Anatolia. Part I*, BAR International Series 74, Oxford: British Archaeological Reports.

Denbow, J. and Miller, D. (2007): Metal working at Bosutswe, Botswana, *Journal of African Archaeology*, 5, 271–313.

Derham, B., Doonan, R. C. P., Lolos, Y., Sarris, A., and Jones, R. (2013): Integrating geochemical survey, ethnography and organic residue analysis to identify and understand areas of foodstuff processing, in S. Voutsaki and S. M. Valamoti, eds., *Diet, Economy and Society in the Ancient Greek World. Towards a Better Integration of Archaeology and Science. Proceedings of the International Conference held at the Netherlands Institute at Athens on 22-24 March 2010*, Leuven/Paris/Walpole, MA: Peeters, pp. 47–54.

Desroches-Noblecourt, C. (2007): *Ramses II: An Illustrated Biography*, Paris: Flammarion.

Dill, H. G. (2007): Grain morphology of heavy minerals from marine and continental placer deposits, with special reference to Fe-Ti oxides, *Sedimentary Geology*, 198, 1–27.

Dill, H. G., Techmer, A., Weber, B., and Füßl, M. (2008): Mineralogical and chemical distribution patterns of placers and ferricretes in Quaternary sediments in SE Germany: the impact of nature and man on the unroofing of pegmatites, *Journal of Geochemical Exploration*, 96, 1–24.

Dobres, M.-A. (2010): Archaeologies of technology, *Cambridge Journal of Economics*, 34, 103–114.

Doonan, R. C. P. (1994): Sweat, fire and brimstone: pre-treatment of copper ore and the effects on smelting techniques, *Historical Metallurgy*, 28, 84–97.

Doonan, R. C. P. (1999a): Copper production in the eastern Alps during the Bronze Age: technological change and the unintended consequences of social reorganisation, in S. M. M. Young, A. M. Pollard, P. Budd, and R. A. Ixer, eds., *Metals in Antiquity*, BAR S792, Oxford: Archaeopress, pp. 72–77.

Doonan, R. C. P. (1999b): *Metallurgical Debris from Eynsham Abbey, Oxfordshire*, Ancient Monuments Laboratory Report 70/1999, English Heritage.

Doonan, R. C. P. (1999c): *The Mould Fragments and Slag from Huntsman's Quarry, Kemerton*, Ancient Monuments Laboratory Report 71/1999, English Heritage.

Doonan, R. C. P., Klemm, S., Ottaway, B. S., Sperl, G., and Weinek, H. (1996): The east Alpine Bronze Age copper smelting process: evidence from the Ramsau Valley, Eisenerz, Austria, in S. Demirci, A. M. Özer, and G. D. Summers, eds., *Archaeometry 94. The Proceedings of the 29th International Symposium on Archaeometry. Ankara, 9-14 May 1994*, Ankara: TÜBITAK.

Dungworth, D. (1996): Caley's 'zinc decline' reconsidered, *The Numismatic Chronicle*, 156, 228–234.

Dungworth, D. (1997): Roman copper alloys: analysis of artefacts from Northern Britain, *Journal of Archaeological Science*, 24, 901–910.

Dungworth, D. (2000a): A note on the analysis of crucibles and moulds, *Historical Metallurgy*, 34, 83–86.

Dungworth, D. (2000b): Serendipity in the foundry? Tin oxide inclusions in copper and copper alloys as an indicator of production process, *Bulletin of the Metals Museum*, 32, 1–5.

Dungworth, D. (2001a): *Metal Working Debris from Elms Farm, Heybridge, Essex*, Centre for Archaeology Report 69/2001, English Heritage.

Dungworth, D. (2001b): *Metal Working Evidence from Housesteads Roman Fort, Northumberland*, Centre for Archaeology Report 109/2001, English Heritage.

Dungworth, D. (2010): *Wild Court Rookery, City of London. Scientific Examination of Early 19th-century Crucibles*, Research Department Report Series 58-2010, English Heritage.

Dungworth, D. (2012a): Historic window glass. The use of chemical analysis to date manufacture, *Journal of Architectural Conservation*, 18, 7–25.

Dungworth, D. (2012b): Scientific examination of the crucible fragments from Cesspit 1, Appendix to Jeffries, N. and Watson, B. From Saxon Lundenwic to Victorian Rookery: excavations at the City Lit, Keeley Street, London WC2, *Transactions of the London and Middlesex Archaeological Society*, 65, 85–87.

Dungworth, D. (2013): Experimental archaeometallurgy: hypothesis testing, happy accidents and theatrical performances, in D. Dungworth and R. C. P. Doonan, eds., *Accidental and Experimental Archaeometallurgy*, HMS Occasional Publication 7, The Historical Metallurgy Society, pp. 11–16.

Dungworth, D. and Bayley, J. (1999): *Crucibles, moulds and tuyeres from Mucking, Essex*, Ancient Monuments Laboratory Report 72, English Heritage.

Dungworth, D. and Bowstead Stallybrass, H. S. (2000): *Metal Working Evidence from No 1 Poultry, London*, Ancient Monuments Laboratory Report 54/2000, English Heritage.

Dungworth, D., Comeau, B., and Lowerre, A. (2013): *St. Algar's Farm, Selwood, Somerset. Geochemical Survey*, Research Department Report Series 28-2013, English Heritage.

Dungworth, D. and Starley, D. (2009): The metalworking debris, in A. Rushworth, ed., *Housesteads Roman Fort - The Grandest Station*, Swindon: English Heritage, pp. 579–588.

Durali-Müller, S., Brey, G. P., Wigg-Wolf, D., and Lahaye, Y. (2007): Roman lead mining in Germany: its origin and development through time deduced from lead isotope provenance studies, *Journal of Archaeological Science*, 34, 1555–1567.

Durman, A. (1997): Tin in southeastern Europe?, *Opuscula Archaeologica*, 21, 7–14.

Dušanić, S. (2004): Roman mining in Illyricum: historical aspects, in G. Urso, ed., *Dall' Adriatico al Danubio. L'Illyrico nell'étà Greca é Romana. Atti del Convegno Internazionale Cividale del Friuli, 25-27 Settembre 2003*, Pisa, pp. 247–270.

Earl, B. and Özbal, H. (1996): Early Bronze Age tin processing at Kestel/Göltepe, Anatolia, *Archaeometry*, 38, 289–303.

Eaton, E. R. and McKerrel, H. (1976): Near Eastern alloying and some textual evidence for the early use of arsenical copper, *World Archaeology*, 8, 169–191.

Eccleston, M. A. J. and Kemp, B. J. (2008): Metalworking and crucibles, in B. J. Kemp and A. K. Stevens, eds., *Busy Lives at Amarna: Excavations at Grid 12 in the Main City*, London: Egypt Exploration Society.

Eekelers, K., Scott, R., Degryse, P., and Muchez, P. (2014): Comparison between quantitative (ICP-OES) and qualitative (pXRF) data of iron slag from Sagalassos (SW-Turkey), *Poster presented at the 40th International Symposium on Archaeometry, 19-23 May 2014, Los Angeles, USA*.

El Gayar, E.-S. and Jones, M. P. (1989a): Old Kingdom copper smelting artifacts from Buhen in Upper Egypt, *Historical Metallurgy*, 23, 16–24.

El Gayar, E.-S. and Jones, M. P. (1989b): A possible source of copper ore fragments found at the Old Kingdom town of Buhen, *The Journal of Egyptian Archaeology*, 75, 31–40.

El Goresy, A., Schiegl, S., and Weiner, K. L. (1996): A chronological scheme for the technological evolution of copper in ancient Egypt, in F. A. Esmael, ed., *Proceedings of the First International Conference on Ancient Egyptian Mining and Metallurgy and Conservation of Metallic Artifacts*, Cairo: Ministry of Culture, Supreme Council of Antiquities, pp. 215–234.

El Goresy, A., Tera, F., Schlick-Nolte, B., and Pernicka, E. (1998): Chemistry and lead isotopic compositions of glass from a Ramesside workshop at Lisht and Egyptian lead ores: a test for a genetic link and for the source of glass, in C. J. Eyre, ed., *Proceedings of the Seventh International Congress of Egyptologists. Cambridge, 3-9 September 1995*, Orientalia Lovaniensia Analecta 82, Leuven: Peeters, pp. 471–481.

Eliyahu-Behar, A., Regev, L., Shilstein, S., Weiner, S., Shalev, Y., Sharon, I., and Berg, J. (2009): Identifying a Roman casting pit at Tel Dor, Israel: integrating field and laboratory research, *Journal of Field Archaeology*, 34, 135–151.

Eliyahu-Behar, A., Yahalom-Mack, N., Shilstein, S., Zukerman, A., Shafer-Elliott, C., Maeir, A. M., Boaretto, E., Finkelstein, I., and Weiner, S. (2012): Iron and bronze production in Iron Age IIA Philistia: new evidence from Tell es-Safi/Gath, Israel, *Journal of Archaeological Science*, 39, 255–267.

Ellam, R. M. (2010): The graphical presentation of lead isotope data for environmental source apportionment, *Science of the Total Environment*, 408, 3490–3492.

Ellingham, H. J. T. (1944): Reducibility of oxides and sulphides in metallurgical processes, *Journal of the Society of Chemical Industry*, 5, 125–133.

Elliott, T., Zindler, A., and Bourdon, B. (1999): Exploring the kappa conundrum: the role of recycling in the lead isotope evolution of the mantle, *Earth and Planetary Science Letters*, 169, 129–145.

Eniosova, N. and Rehren, Th. (2012): Metal melting crucibles from medieval Novgorod, in M. Brisbane, N. Makarov, and E. Nosov, eds., *The Archaeology of Medieval Novgorod in Context. Studies in Centre/Periphery Relations*, Oxford: Oxbow Books, pp. 210–223.

Erb-Satullo, N. L., Gilmour, B. J. J., and Khakhutaishvili, N. (2014): Late Bronze and Early Iron Age copper smelting technologies in the South Caucasus: the view from ancient Colchis c. 1500-600 BC, *Journal of Archaeological Science*, 49, 147–159.

Evans, R. T. and Tylecote, R. F. (1967): Some vitrified products, *Bulletin of the Historical Metallurgy Group*, 1, 22–23.

Evely, D., Hein, A., and Nodarou, E. (2012): Crucibles from Palaikastro, East Crete: insights into metallurgical technology in the Aegean Late Bronze Age, *Journal of Archaeological Science*, 39, 1821–1836.

Fabrizi, M. (1988): Copper corrosion products: analysis and interpretation, in E. A. Slater and J. O. Tate, eds., *Science and Archaeology. Proceedings of a Conference on the Application of Scientific Techniques to Archaeology, Glasgow, September 1987*, BAR British Series 196, Oxford: BAR, pp. 295–303.

Fang, J.-L. and McDonnell, G. (2011): The colour of copper alloys, *Historical Metallurgy*, 45, 52–61.

Farag, M. (1981): Metallurgy in ancient Egypt - some aspects of techniques and materials, *Metals Museum Bulletin*, 6, 15–30.

Fattovich, R. (2012): Egypt's trade with Punt: new discoveries on the Red Sea coast, *British Museum Studies in Ancient Egypt and Sudan*, 18, 1–59.

Fenn, T. R., Killick, D. J., Chesley, J., Magnavita, S., and Ruiz, J. (2009): Contacts between West Africa and Roman North Africa: archaeometallurgical results from Kissi, north-eastern Burkina Faso, in S. Magnavita, L. Kote, and P. Breunig, eds., *Crossroads/Carrefour Sahel: Cultural and Technological Developments in First Millennium BC/AD West Africa*, Journal of African Archaeology Monograph Series 2, Frankfurt: Africa Magna Verlag, pp. 119–146.

Fields, A. (2011): *The Late Phrygian Citadel at Gordion, Turkey: a Preliminary Study*, Master's thesis, University of Cincinnati, Department of Classics, Cincinnati, OH.

Figueiredo, E., Silva, R. J. C., Braz Fernandes, F. M., and Araújo, M. F. (2010a): Some long term corrosion patterns in archaeological metal artefacts, *Materials Science Forum*, 636-637, 1030–1035.

Figueiredo, E., Silva, R. J. C., Senna-Martinez, J. C., Araújo, M. F., Braz Fernandes, F. M., and Inêz Vaz, J. L. (2010b): Smelting and recycling evidences from the Late Bronze Age habitat site of Baiões (Viseu, Portugal), *Journal of Archaeological Science*, 37, 1623–1634.

Fitzenreiter, M., Loeben, C. E., Raue, D., and Wallenstein, U., eds. (2014): *Gegossene Götter. Metallhandwerk und Massenproduktion im alten Ägypten*, Rahden/Westfalen: Verlag Marie Leidorf GmbH.

Fleming, S. J. (1982): Lead isotope analyses of Late Period Egyptian bronzes, *MASCA Journal*, 2, 65–69.

Fluzin, P., Ploquin, A., and Serneels, V. (2000): Archéométrie des déchets de production sidérurgique. Moyens et méthodes d'identification des différents éléments de la chaîne opératoire directe, *Gallia*, 57, 101–121.

Forster, N., Grave, P., Vickery, N., and Kealhofer, L. (2011): Non-destructive analysis using PXRF: methodology and application to archaeological ceramics, *X-Ray Spectrometry*, 40, 389–398.

Forstner-Müller, I. (2009): Providing a map of Avaris, *Egyptian Archaeology*, 34, 10–13.

Forstner-Müller, I., Herbich, T., Schweitzer, C., and Weissl, M. (2009): Preliminary report on the geophysical survey at Tell el-Dab'a/Qantir in spring 2008, *Ägypten und Levante*, 18, 87–106.

Forstner-Müller, I. and Müller, W. (2007): Neueste Ergebnisse des Magnetometersurveys während der Frühjahrskampagne 2006 in Tell el-Dab'a/Qantir, *Ägypten und Levante*, 16, 79–87.

Foucault, A. and Stanley, D. J. (1989): Late Quaternary paleoclimatic oscillations in East Africa recorded by heavy minerals in the Nile delta, *Nature*, 339, 44–46.

Frahm, E. (2013a): Is obsidian sourcing about geochemistry or archaeology? A reply to Speakman and Shackley, *Journal of Archaeological Science*, 40, 1444–1448.

Frahm, E. (2013b): Validity of "off-the-shelf" handheld portable XRF for sourcing Near Eastern obsidian chip debris, *Journal of Archaeological Science*, 40, 1080–1092.

Frahm, E. and Doonan, R. C. P. (2013): The technological versus methodological revolution of portable XRF in archaeology, *Journal of Archaeological Science*, 40, 1425–1434.

Frahm, E., Schmidt, B. A., Gasparyan, B., Yeritsyan, B., Karapetian, S., Meliksetian, K., and Adler, D. S. (2014): Ten seconds in the field: rapid Armenian obsidian sourcing with portable XRF to inform excavations and surveys, *Journal of Archaeological Science*, 41, 333–348.

Freestone, I. C. (1989): Refractory materials and their procurement, in A. Hauptmann, E. Pernicka, and G. Wagner, eds., *Old World Archaeometallurgy. Der Anschnitt, Beiheft 7*, Bochum: Deutsches Bergbau-Museum, pp. 155–162.

Freestone, I. C., Leslie, K. A., Thirlwall, M., and Goren-Rosen, Y. (2003): Strontium isotopes in the investigation of early glass production: Byzantine and Early Islamic glass from the Near East, *Archaeometry*, 45, 19–32.

Freestone, I. C. and Tite, M. S. (1986): Refractories in the ancient and preindustrial world, in W. D. Kingery and E. Lense, eds., *High-technology Ceramics: Past, Present, and Future. The Nature of Innovation and Change in Ceramic Technology*, Westerville, OH: American Ceramic Society, pp. 35–63.

Frisch, B. and Thiele, W.-R. (1985): Die vorgeschichtliche Bronze- und Eisenmetallurgie von Kamid el-Loz, in B. Frisch, G. Mansfeld, and W.-R. Thiele, eds., *Kamid el-Loz 6. Die Werkstätten der spätbronzezeitlichen Paläste*, Saarbrücker Beiträge zur Altertumskunde, Band 33, Bonn: Habelt, pp. 151–164.

Gale, N. H. (1991): *Bronze Age Trade in the Mediterranean: Papers presented at the Conference held at Rewley House, Oxford, in December 1989*, Jonsered: Åstrom.

Gale, N. H. (1997): The isotopic composition of tin in some ancient metals and the recycling problem in metal provenancing, *Archaeometry*, 39, 71–82.

Gale, N. H. (1999): Lead isotope characterization of the ore deposits of Cyprus and Sardinia and its application to the discovery of the sources of copper for Late Bronze Age oxhide ingots, in S. M. M. Young, A. M. Pollard, P. Budd, and R. A. Ixer, eds., *Metals in Antiquity*, BAR S792, Oxford: Archaeopress, pp. 110–121.

Gale, N. H. (2001): Archaeology, science-based archaeology and the Mediterranean Bronze Age metals trade: a contribution to the debate, *European Journal of Archaeology*, 4, 113–130.

Gale, N. H. (2005): Die Kupferbarren von Uluburun. Teil 2: Bleiisotopenanalysen von Bohrkernen aus den Barren, in Ü. Yalçin, C. Pulak, and R. Slotta, eds., *Das Schiff von Uluburun. Welthandel vor 3000 Jahren*, Bochum: Deutsches Bergbau-Museum, pp. 141–148.

Gale, N. H. (2009): A response to the paper of A. M. Pollard: What a long strange trip it's been: lead isotopes and archaeology, in A. J. Shortland, I. C. Freestone, and Th. Rehren, eds., *From Mine to Microscope. Advances in the Study of Ancient Technology*, Oxford: Oxbow Books, pp. 191–196.

Gale, N. H. (2011): Copper oxhide ingots and lead isotope provenancing, in P. P. Betancourt and S. C. Ferrence, eds., *Metallurgy: Understanding How, Learning Why. Studies in Honor of James D. Muhly*, Philadelphia, PA: INSTAP Academic Press, pp. 213–220.

Gale, N. H., Bachmann, H.-G., Rothenberg, B., Stos-Gale, Z. A., and Tylecote, R. F. (1990): The adventitious production of iron in the smelting of copper, in B. Rothenberg, ed., *The Ancient Metallurgy of Copper: Archaeology-Experiment-Theory. (Researches in the Arabah 1959-84; v. 2)*, London: The Institute for Archaeo-Metallurgical Studies, pp. 182–191.

Gale, N. H., Kayafa, M., and Stos-Gale, Z. A. (2009): Further evidence for Bronze Age production of copper from ores in the Lavrion district, Attica, Greece, in *Archaeometallurgy in Europe 2007. Selected Papers of the 2nd International Conference 17.-21. June 2007 in Aquileia*, Milan: Associazione Italiana di Metallurgia, pp. 158–176.

Gale, N. H. and Stos-Gale, Z. A. (1982): Bronze Age copper sources in the Mediterranean: a new approach, *Science*, 216, 11–19.

Gale, N. H. and Stos-Gale, Z. A. (1995): Comments on 'Oxhide ingots, recycling, and the Mediterranean metals trade', *Journal of Mediterranean Archaeology*, 8, 33–41.

Gale, N. H. and Stos-Gale, Z. A. (2012): The role of the Apliki mine region in the post c. 1400 BC copper production and trade networks in Cyprus and the wider Mediterranean, in V. Kassianidou and G. Papasavvas, eds., *Eastern Mediterranean Metallurgy and Metalwork in the Second Millennium BC - A Conference in Honour of James D. Muhly, Nicosia, 10th-11th October 2009*, Oxford: Oxbow Books, pp. 70–82.

Gale, N. H., Stos-Gale, Z. A., and Gilmore, G. R. (1985): Alloy types and copper sources of Anatolian copper alloy artifacts, *Anatolian Studies*, 35, 143–173.

Gale, N. H., Stos-Gale, Z. A., Maliotis, G., and Annetts, N. (1997): Lead isotope data from the Isotrace Laboratory, Oxford: Archaeometry data base 4, ores from Cyprus, *Archaeometry*, 39, 237–246.

Gale, N. H., Stos-Gale, Z. A., Raduncheva, A., Panayotov, I., Ivanov, I., Lilov, P., and Todorov, T. (2003): Early metallurgy in Bulgaria, in P. T. Craddock and J. Lang, eds., *Mining and Metal Production. Through the Ages*, London: British Museum Press, pp. 122–174.

Galili, E., Gale, N. H., and Rosen, B. (2013): A Late Bronze Age shipwreck with a metal cargo from Hishuley Carmel, Israel, *The International Journal of Nautical Archaeology*, 42, 2–23.

Galili, E., Shmueli, N., and Artzy, M. (1986): Bronze Age ship's cargo of copper and tin, *The International Journal of Nautical Archaeology*, 15, 25–37.

Garland, H. and Bannister, C. O. (1927): *Ancient Egyptian Metallurgy*, London: Charles Griffin & Co.

Garson, M. S. (1977): Younger granites of Egypt and associated mineralization, *Transactions of the Institution of Mining and Metallurgy*, 86, 161.

Garzanti, E., Andò, S., Vezzoli, G., Abdel Megid, A. A., and El Kammar, A. (2006): Petrology of Nile River sands (Ethiopia and Sudan): sediment budgets and erosion patterns, *Earth and Planetary Science Letters*, 252, 327–341.

Gauss, R. K., Bátora, J., Nowaczinski, E., Rassmann, K., and Schukraft, G. (2013): The Early Bronze Age settlement of Fidvár, Vráble (Slovakia): reconstructing prehistoric settlement patterns using portable XRF, *Journal of Archaeological Science*, 40, 2942–2960.

Georgakopoulou, M., Bassiakos, Y., and Philaniotou, O. (2011): Seriphos surfaces: a study of copper slag heaps and copper sources in the context of Early Bronze Age Aegean metal production, *Archaeometry*, 53, 123–145.

Gillis, C., Clayton, R., Pernicka, E., and Gale, N. H. (2003): Tin in the Aegean Bronze Age, in R. Laffineur and K. Foster, eds., *Metron. Measuring the Aegean Bronze Age. Proceedings of the 9th International Aegean Conference, New Haven, Yale University, 18-21 April 2002*, Aegaeum 24, Liege/Austin, pp. 103–110.

Giovannelli, G., Natali, S., Bozzini, B., Siciliano, A., Sarcinelli, G., and Vitale, R. (2005): Microstructural characterization of early western Greek incuse coins, *Archaeometry*, 47, 817–833.

Goldstein, J. I., Newbury, D. E., Joy, D. C., Lyman, C. E., Echlin, P., Lifshin, E., Sawyer, L., and Michael, J. R. (2007): *Scanning Electron Microscopy and X-Ray Microanalysis*, New York and London: Kluwer Academic/ Plenum Publishers.

Goren, Y. (2014): The operation of a portable petrographic thin-section laboratory for field studies, *New York Microscopical Society Newsletter*, September, 1–17.

Goscinny, R. and Uderzo, A. (1997): *Asterix in Corsica*, Paris: Hachette.

Gouda, V. K., Youssef, G. I., and Abdel Ghany, N. A. (2012): Characterization of Egyptian bronze archaeological artifacts, *Surface and Interface Analysis*, 44, 1338–1345.

Goy, J., Le Carlier de Veslud, C., and Degli Esposti, M. (2013): Archaeometallurgical research in the northern Hajjar Mountains (Oman Peninsula) during the Iron Age (1200-300 BCE), *Poster presented at the Timna Park International Conference in memory of Professor Beno Rothenberg. Mining for Copper: Environment, Culture and Copper in Antiquity. 22-25 April 2013, Timna, Israel.*

Graedel, T. E. (1992): Corrosion mechanisms for silver exposed to the atmosphere, *Journal of the Electrochemical Society*, 139, 1963–1970.

Grant, M. R. (1999): The sourcing of southern African tin artefacts, *Journal of Archaeological Science*, 26, 1111–1117.

Grave, P., Kealhofer, L., and Marsh, B. (2005): Ceramic compositional analysis and the Phrygian sanctuary at Dümrek, in L. Kealhofer, ed., *The Archaeology of Midas and the Phrygians: Recent Work at Gordion*, Philadelphia, PA: University of Pennsylvania Museum of Archaeology and Anthropology, pp. 149–160.

Grave, P., Kealhofer, L., Marsh, B., Sams, K., Voigt, M., and DeVries, K. (2009): Ceramic production and provenience at Gordion, Central Anatolia, *Journal of Archaeological Science*, 36, 2162–2176.

Guerra, M. F. (2004): The circulation of South American precious metals in Brazil at the end of the 17th century, *Journal of Archaeological Science*, 31, 1225–1236.

Guerra, M. F., Sarthre, C.-O., Gondonneau, A., and Barrandon, J.-N. (1999): Precious metals and provenance enquiries using LA-ICP-MS, *Journal of Archaeological Science*, 26, 1101–1110.

Hall, F. P. and Insley, H. (1933): A compilation of phase-rule diagrams of interest to the ceramist and silicate technologist, *Journal of the American Ceramic Society*, 16, 463–567.

Hall, M. C. (1995): Comments on 'Oxhide ingots, recycling, and the Mediterranean metals trade', *Journal of Mediterranean Archaeology*, 8, 42–44.

Hall, M. C. and Steadman, S. R. (1991): Tin and Anatolia - another look, *Journal of Mediterranean Archaeology*, 4, 217–234.

Hamza, M. (1930): Excavations of the Department of Antiquities at Qantir (Faqus District), *Annales du Service des Antiquités*, 30, 31–68.

Hancock, R. G. V., Millet, N. B., and Mills, A. J. (1986): A rapid INAA method to characterize Egyptian ceramics, *Journal of Archaeological Science*, 13, 107–117.

Hancock, R. G. V., Pavlish, L. A., Farquhar, R. M., Julig, P. J., and Fox, W. A. (1994): Chemical seriation of northeastern North American archaeological sites using copper artifacts, in D. Scott and P. Meyers, eds., *Archaeometry of Pre-Columbian Sites and Artifacts. Proceedings of a Symposium organized by the UCLA Institute of Archaeology and the Getty Conservation Institute, Los Angeles, California, March 23-27, 1992*, Los Angeles, CA: The Getty Conservation Institute, pp. 255–265.

Hauptmann, A. (2007): *The Archaeometallurgy of Copper - Evidence from Faynan, Jordan*, Springer.

Hauptmann, A. (2014): The investigation of archaeometallurgical slag, in B. W. Roberts and C. P. Thornton, eds., *Archaeometallurgy in Global Perspective*, Springer, pp. 91–105.

Hauptmann, A., Begemann, F., Heitkemper, E., Pernicka, E., and Schmitt-Strecker, S. (1992): Early copper produced at Feinan, Wadi Araba, Jordan: the composition of ores and copper, *Archeomaterials*, 6, 1–33.

Hauptmann, A., Lutz, J., Pernicka, E., and Yalçin, Ü. (1993): Zur Technologie der Frühesten Kupferverhüttung im Östlichen Mittelmeerraum, in M. Frangipane, H. Hauptmann, M. Liverani, P. Matthiae, and M. Mellink, eds., *Between the Rivers and Over the Mountains. Archaeologica Anatolica et Mesopotamica. Alba Palmieri Dedicata*, Rome: Dipartimento di Scienze Storiche Archeologiche e Antropologiche dell'Antichità. Università di Roma La Sapienza, pp. 541–572.

Hauptmann, A., Maddin, R., and Prange, M. (2002): On the structure and composition of copper and tin ingots excavated from the shipwreck of Uluburun, *Bulletin of the American Schools of Oriental Research*, 328, 1–30.

Hauptmann, A., Rehren, Th., and Schmitt-Strecker, S. (2003): Early Bronze Age copper metallurgy at Shahr-i Sokhta (Iran), reconsidered, in T. Stöllner, G. Körlin, G. Steffens, and J. Cierny, eds., *Man and Mining (Mensch und Bergbau)*, Der Anschnitt, Beiheft 16, Bochum: Deutsches Bergbau-Museum, pp. 197–213.

Hauptmann, A., Weisgerber, G., and Bachmann, H.-G. (1988): Early copper metallurgy in Oman, in R. Maddin, ed., *The Beginning of the Use of Metals and Alloys*, Cambridge, MA: MIT Press.

Haustein, M., Gillis, C., and Pernicka, E. (2010): Tin isotopy - a new method for solving old questions, *Archaeometry*, 52, 816–832.

Hayes, W. C. (1937): *Glazed Tiles from a Palace of Ramesses II at Kantir*, New York: The Metropolitan Museum of Art.

Haynes, I. P. (2011): Early Roman Thrace, in I. P. Haynes, ed., *Early Roman Thrace. New Evidence from Bulgaria*, JRA Supplementary Series 82, Portsmouth, Rhode Island, pp. 6–14.

Heimann, R. B. (1989): Assessing the technology of ancient pottery: the use of ceramic phase diagrams, *Archeomaterials*, 3, 123–148.

Heimann, R. B., Chirikure, S., and Killick, D. (2010): Mineralogical study of precolonial (1650-1850 CE) tin smelting slags from Rooiberg, Limpopo Province, South Africa, *European Journal of Mineralogy*, 22, 751–761.

Hein, A., Karatasios, I., Müller, N. S., and Kilikoglou, V. (2013): Heat transfer properties of pyrotechnical ceramics used in ancient metallurgy, *Thermochimica Acta*, 573, 87–94.

Hein, A. and Kilikoglou, V. (2007): Modeling of thermal behavior of ancient metallurgical ceramics, *Journal of the American Ceramic Society*, 90, 878–884.

Hein, A. and Kilikoglou, V. (2011): Technological aspects of Bronze Age metallurgical ceramics in the eastern Mediterranean, in P. P. Betancourt and S. C. Ferrence, eds., *Metallurgy: Understanding How, Learning Why. Studies in Honor of James D. Muhly*, Philadelphia, PA: INSTAP Academic Press, pp. 181–187.

Hein, A., Kilikoglou, V., and Kassianidou, V. (2007): Chemical and mineralogical examination of metallurgical ceramics from a Late Bronze Age copper smelting site in Cyprus, *Journal of Archaeological Science*, 34, 141–154.

Hein, A., Müller, N. S., Day, P. M., and Kilikoglou, V. (2008): Thermal conductivity of archaeological ceramics: the effect of inclusions, porosity and firing temperature, *Thermochimica Acta*, 480, 35–42.

Helwing, B. (2009): Rethinking the tin mountains: patterns of usage and circulation of tin in greater Iran from the 4th to the 1st millennium BC, *Turkiye Bilimler Akademisi Arkeoloji Dergisi (TUBA-AR). Turkish Academy of Sciences Journal of Archaeology*, 12, 209–221.

Hemingway, E. (1927): The Undefeated, in *Men Without Women*, New York: Charles Scribner's Sons.

Hendy, M. (1972): Mint and fiscal administration under Diocletian, his colleagues, and his successiors, A. D. 305-24, *The Journal of Roman Studies*, 62, 75–82.

Henrickson, R. C. (1994): Continuity and discontinuity in the ceramic tradition at Gordion during the Iron Age, in D. French and A. Çilingiroğlu, eds., *Anatolian Iron Ages 3. The Proceedings of the Third Anatolian Iron Ages Colloquium Held at Van, 6-12 August 1990*, British Institute of Archaeology at Ankara, Monograph 16, London: British Institute of Archaeology at Ankara, pp. 95–129.

Henrickson, R. C. (2005): The local potter's craft at Phrygian Gordion, in L. Kealhofer, ed., *The Archaeology of Midas and the Phrygians: Recent Work at Gordion*, Philadelphia, PA: University of Pennsylvania Museum of Archaeology and Anthropology, pp. 124–135.

Henrickson, R. C. and Blackman, M. J. (1996): Large-scale production of pottery at Gordion: a comparison of the Late Bronze and Early Phrygian industries, *Paléorient*, 22, 67–87.

Herbert, E. W. (1984): *Red Gold of Africa: Copper in Precolonial History and Culture*, Madison: University of Wisconsin Press.

Herbert, F. (1965): *Dune*, New York: Chilton Books.

Herold, A. (1998): Gegossen - Geschmiedet - Tordiert. Zur Herstellung van bronzenen Trensen in der Ramses-Stadt Piramesse/Ägypten, *Metalla (Bochum)*, 5, 3–21.

Herrmann, C. (1957): *Formen für Ägyptische Fayencen aus Qantir: Katalog der Sammlung des Franciscan Biblical Museum, Jerusalem und zweier Privatsammlungen*, Fribourg: Academic Press.

Hikade, T. (1998): Economic aspects of the New Kingdom: the expeditions to the copper mines of the Sinai, *Bulletin of the Australian Centre for Egyptology*, 9, 43–52.

Hikade, T. (2006): Expeditions to the Wadi Hammamat during the New Kingdom, *The Journal of Egyptian Archaeology*, 92, 153–168.

Hikade, T. (2007): Crossing the frontier into the desert: Egyptian expeditions to the Sinai Peninsula, *Ancient West and East*, 6, 1–22.

Hirao, Y., Enomoto, J., and Tachikawa, H. (1995): Lead isotope ratios of copper, zinc and lead minerals in Turkey in relation to the provenance study of artefacts, in H. I. H. Prince Takahito Mikasa, ed., *Essays on Ancient Anatolia and its surrounding civilisations*, Wiesbaden: Harrassowitz Verlag, pp. 89–114.

Hodgkinson, A. K. (2007): The final phase of Per-Ramesses: the history of the city in light of its natural environment, in M. Cannata, ed., *Current Research in Egyptology 2006: Proceedings of the Seventh Annual Symposium, Which Took Place at the University of Oxford, April 2006*, Oxford: Oxbow, pp. 99–115.

Hofmann, W. and Klein, M. (1966): Beitrag zur Kenntnis des Dreistoffsystems Kupfer-Zinn-Sauerstoff, *Zeitschrift für Metallkunde*, 83, 421–441.

Hook, D. R. and Craddock, P. T. (1996): Appendix. The scientific analysis of the copper-alloy lamps: aspects of classical alloying practices, in D. M. Bailey, ed., *Catalogue of Lamps in the British Museum*, London: British Museum Press, pp. 144–163.

Horne, L. (1982): Fuel for the metal worker - the role of charcoal and charcoal production in ancient metallurgy, *Expedition*, 25, 6–13.

Horsley, T. (1997): *Roman and Medieval Crucible Sherds from London*, Ancient Monuments Laboratory Report 8/97, English Heritage.

Hughes, M. J. (1980): The analysis of Roman tin and pewter ingots, in W. A. Oddy, ed., *Aspects of early metallurgy*, Occasional Paper 17, London: British Museum, pp. 41–50.

Humphris, J., Martinón-Torres, M., Rehren, Th., and Reid, A. (2009): Variability in single smelting episodes - a pilot study using iron slag from Uganda, *Journal of Archaeological Science*, 36, 359–369.

Humphris, J. and Rehren, Th., eds. (2013): *The World of Iron*, London: Archetype Publications.

Hunt, A. (2013): Development of quartz cathodoluminescence for the geological grouping of archaeological ceramics: firing effects and data analysis, *Journal of Archaeological Science*, 40, 2902–2912.

Hunt, A. and Speakman, R. J. (2014): Protocol for the analysis of archaeological ceramics and sediments by pXRF, *Poster presented at the 79th Annual Meeting of the Society for American Archaeology, April 23-27 2014, Austin, Texas*.

Iles, L. and Martinón-Torres, M. (2009): Pastoralist iron production on the Laikipia Plateau, Kenya: wider implications for archaeometallurgical studies, *Journal of Archaeological Science*, 36, 2314–2326.

Ineson, P. R. (1989): *Introduction to Practical Ore Microscopy*, Harlow: Longman Scientific and Technical.

Ingo, G. M., De Caro, T., Riccucci, C., Angelini, E., Grassini, S., Balbi, S., Bernardini, P., Salvi, D., Bousselmi, I., Çilingiroğlu, A., Gener, M., Gouda, V. K., al Jarrah, O., Khosroff, S., Mahdjoub, Z., al Saad, Z., el Saddik, W., and Vassiliou, P. (2006): Large scale investigation of chemical composition, structure and corrosion mechanism of bronze archeological artefacts from Mediterranean basin, *Applied Physics A*, 83, 513–520.

Ivanov, R. T. and von Bülow, G. (2008): *Thracia: eine römische Provinz auf der Balkanhalbinsel*, Zaberns Bildbände zur Archäologie. Sonderbände der Antiken Welt. Orbis provinciarum, Mainz: Verlag Philip von Zabern.

Ivanov, T. (1983): The Roman cities of Moesia and Thrace (modern Bulgaria), in A. G. Poulter, ed., *Ancient Bulgaria. Papers presented to the International Symposium on the Ancient History and Archaeology of Bulgaria, University of Nottingham, 1981*, Nottingham: Department of Classical and Archaeological Studies, pp. 129–154.

Jackson, C. M. (2005): Glassmaking in Bronze-Age Egypt, *Science*, 308, 1750–1752.

Jaksch, H., Seipel, W., Weiner, K. L., and El Goresy, A. (1983): Egyptian blue - cuprorivaite: a window to ancient Egyptian technology, *Naturwissenschaften*, 70, 525–535.

James, T. G. H. (1972): Gold technology in ancient Egypt. Mastery of metal working methods, *Gold Bulletin*, 5, 38–42.

Jefferson, T. (1785): *Letter to Peter Carr. August 19, 1785*.

Johnson, M. (2010): *Archaeological Theory: An Introduction (2nd Edition)*, Wiley-Blackwell.

Jones, A. (2004): Archaeometry and materiality: materials-based analysis in theory and practice, *Archaeometry*, 46, 327–338.

Jung, R., Mehofer, M., and Pernicka, E. (2011): Metal exchange in Italy from the Middle to the Final Bronze Age (14th-11th century BCE), in P. P. Betancourt and S. C. Ferrence, eds., *Metallurgy: Understanding How, Learning Why. Studies in Honor of James D. Muhly*, Philadelphia, PA: INSTAP Academic Press, pp. 231–248.

Kaczmarczyk, A. (1986): The source of cobalt in ancient Egyptian pigments, in J. S. Olin and M. J. Blackman, eds., *Proceedings of the 24th International Archaeometry Symposium*, Washington, D.C.: Smithsonian Institution Press, pp. 369–376.

Kahneman, D. (2012): *Thinking, Fast and Slow*, London: Penguin.

Kallfass, M. and Hörz, G. (1989): Metallographic investigations on archaeological tin bronzes of Late Egyptian and Bronze Period, *Practical Metallography*, 26, 105–121.

Karageorghis, V. and Kassianidou, V. (1999): Metalworking and recycling in Late Bronze Age Cyprus - the evidence from Kition, *Oxford Journal of Archaeology*, 18, 171–188.

Kassianidou, V. (2003a): Archaeometallurgical procedures, in M. Given and A. B. Knapp, eds., *The Sydney Cyprus Survey Project. Social Approaches to Regional Archaeological Survey*, Monumenta Archaeologica 21, Los Angeles, CA: UCLA Cotsen Institute of Archaeology, pp. 44–48.

Kassianidou, V. (2003b): The trade of tin and the island of copper, in A. Giumlia-Mair and F. Lo Schiavo, eds., *The Problem of Early Tin. Acts of the XIVth UISPP Congress*, BAR International Series 1199, Oxford: Archaeopress, pp. 109–119.

Kassianidou, V. (2009): Oxhide ingots in Cyprus, in F. Lo Schiavo, J. D. Muhly, R. Maddin, and A. Giumlia-Mair, eds., *Oxhide Ingots in the Central Mediterranean*, A. G. Leventis Foundation and CNR Instituto di Studi sulle Civiltà dell'Egeo e del Vicino Oriente, pp. 41–81.

Kassianidou, V. (2013): The production and trade of Cypriot copper in the Late Bronze Age. An analysis of the evidence, *Pasiphae*, 7, 133–146.

Katona, I., Bourgarit, D., Thomas, N., and Bouquillon, A. (2007): From furnace to casting moulds: an exceptional 14th century copper-metallurgy workshop studied in the light

of refractory ceramic materials, in S. Y. Waksman, ed., *Archaeometric and Archaeological Approaches to Ceramics: Papers Presented at EMAC '05, 8th European Meeting on Ancient Ceramics, Lyon 2005*, BAR International Series 1691, Oxford: Archaeopress, pp. 161–167.

Kaufman, B. (2013): Copper alloys from the 'Enot Shuni cemetery and the origins of bronze metallurgy in the EB IV - MB II Levant, *Archaeometry*, 55, 663–690.

Kealhofer, L., ed. (2005): *The Archaeology of Midas and the Phrygians: Recent Work at Gordion*, Philadelphia, PA: University of Pennsylvania Museum of Archaeology and Anthropology.

Kearns, T., Martinón-Torres, M., and Rehren, Th. (2010): Metal to mould: alloy identification in experimental casting moulds using XRF, *Historical Metallurgy*, 44, 48–58.

Kilikoglou, V., Vekinis, G., and Maniatis, Y. (1995): Toughening of ceramic earthenwares by quartz inclusions: an ancient art revisited, *Acta Metallurgica et Materialia*, 43, 2959–2965.

Kilikoglou, V., Vekinis, G., Maniatis, Y., and Day, P. M. (1998): Mechanical performance of quartz-tempered ceramics: part I, strength and toughness, *Archaeometry*, 40, 261–279.

Killick, D. (2009): Cairo to Cape: the spread of metallurgy through eastern and southern Africa, *Journal of World Prehistory*, 22, 399–414.

Killick, D. and Fenn, T. (2012): Archaeometallurgy: the study of preindustrial mining and metallurgy, *Annual Review of Anthropology*, 41, 559–575.

Kingsley, S. A. and Raveh, K. (1994): Stamped lead ingots from the coast of Israel, *The International Journal of Nautical Archaeology*, 23, 119–128.

Kipling, R. (1899): *From Sea to Sea: Letters of Travel*, New York: Doubleday and McClure.

Kitchen, K. A. (1982): *Pharaoh Triumphant: the Life and Times of Ramesses II King of Egypt*, Warminster: Aris & Phillips.

Klein, C. and Dutrow, B. (2007): *Manual of Mineral Science (23rd edition)*, Wiley.

Klein, S. and Hauptmann, A. (1999): Iron Age leaded tin bronzes from Khirbet edh-Dharih, Jordan, *Journal of Archaeological Science*, 26, 1075–1082.

Klein, S., Lahaye, Y., Brey, G. P., and Von Kaenel, H.-M. (2004): The early Roman Imperial Aes coinage II: tracing the copper sources by analysis of lead and copper isotopes - copper coins of Augustus and Tiberius, *Archaeometry*, 46, 469–480.

Klein, S., Rico, C., Lahaye, Y., von Kaenel, H. M., Domergue, C., and Brey, G. P. (2007): Copper ingots form the western Mediterranean Sea: chemical characterisation and provenance studies through lead- and copper isotope analyses, *Journal of Roman Archaeology*, 20, 202–221.

Klein, S. and von Kaenel, H.-M. (2000): The early Roman Imperial aes coinage: metal analysis and numismatic studies. Part 1, *Schweizerische Numismatische Rundschau*, 79, 53–106.

Klemm, R. and Klemm, D. (2013): *Gold and Gold Mining in Ancient Egypt and Nubia. Geoarchaeology of the Ancient Gold Mining Sites in the Egyptian and Sudanese Eastern Deserts*, Berlin: Springer.

Knapp, A. B. (2000): Archaeology, science-based archaeology and the Mediterranean Bronze Age metals trade, *European Journal of Archaeology*, 3, 31–56.

Knapp, A. B. (2011): Cyprus, copper, and Alashiya, in P. P. Betancourt and S. C. Ferrence, eds., *Metallurgy: Understanding How, Learning Why. Studies in Honor of James D. Muhly*, Philadelphia, PA: INSTAP Academic Press, pp. 249–254.

Knapp, A. B., Kassianidou, V., and Donnelly, M. (2001): Copper smelting in Late Bronze Age Cyprus: the excavations at Politiko Phorades, *Near Eastern Archaeology*, 64, 204–210.

König, D. and Serneels, V. (2013): Roman double-layered crucibles from Autun/France: a petrological and geochemical approach, *Journal of Archaeological Science*, 40, 156–165.

Kramers, J. D. and Tolstikhin, I. N. (1997): Two terrestrial lead isotope paradoxes, forward transport modelling, core formation and the history of the continental crust, *Chemical Geology*, 139, 75–110.

Krismer, M., Töchterle, U., Goldenberg, G., Tropper, P., and Vavtar, F. (2013): Mineralogical and petrological investigations of Early Bronze Age copper-smelting remains from the Kiechlberg (Tyrol, Austria), *Archaeometry*, 55, 923–945.

Krom, M. D., Stanley, D. J., Cliff, R. A., and Woodward, J. C. (2002): Nile River sediment fluctuations over the past 7000 yr and their key role in sapropel development, *Geology*, 30, 71–74.

Kuleff, I., Iliev, I., Pernicka, E., and Gergova, D. (2006): Chemical and lead isotope compositions of lead artefacts from ancient Thracia (Bulgaria), *Journal of Cultural Heritage*, 7, 244–256.

Lackinger, A., Comendador, B., Figueiredo, E., Araújo, M. F., Silva, R., and Rovira, S. (2013): Copper plus tin plus people. Public co-smelting experimentation in northwestern Iberia, *Poster presented at the 7th Experimental Archaeology Conference, Cardiff (UK) Amgueddfa Cymru - St Fagans National History Museum (WLS), January 2013*.

Lafli, E. and Buora, M. (2012): Fibulae in the Museum of Ödemis (Western Turkey), *Oriental Archive*, 80, 1–18.

Le Bas, M. J., Le Maitre, R. W., Streckeisen, A., and Zanettin, B. (1986): A chemical classification of volcanic rocks based on the total alkali-silica diagram, *Journal of Petrology*, 27, 745–750.

Leese, M. N. (1992): Evaluating lead isotope data: comments on E. V. Sayre, K. A. Yener, E. C. Joel and I. L. Barnes, 'Statistical evaluation of the presently accumulated lead isotope data from Anatolia and surrounding regions', Archaeometry, 34 (1) (1992), 73-105, and reply. Comments... II, *Archaeometry*, 34, 318–322.

Lehner, J. W. (2012): A preliminary report on the microstructure and microanalysis of metal from Boğazköy, *Archaologischer Anzeiger*, 2011, 57–64.

Lehner, J. W. and Prikhodko, S. (2010): Microstructure and microanalysis of metal artifacts from Kerkenes Dağ, Central Turkey, ca. 600 BC, *Microscopy and Microanalysis*, 16, 1244–1245.

Lehner, J. W., Yener, K. A., and Burton, J. (2009): Lead isotope analysis and chemical characterization of metallic residues of an Early Bronze Age crucible from Göltepe using ICP-MS, *Turkiye Bilimler Akademisi Arkeoloji Dergisi (TUBA-AR). Turkish Academy of Sciences Journal of Archaeology*, 12, 165–174.

Lemonnier, P. (1993): Introduction, in P. Lemonnier, ed., *Technological Choices: Transformations in Material Cultures Since the Neolithic*, London: Routledge, pp. 1–35.

Lemonnier, P. and Pfaffenberger, B. (1989): Towards an anthropology of technology, *Man*, 24 (New Series), 526–527.

Leroi-Gourhan, A. (1964): *La Geste et la Parole I - Technique et Langage*, Paris: Albin Michel.

Leroi-Gourhan, A. (1965): *La Geste et la Parole II - La Mémoire et les Rythmes*, Paris: Albin Michel.

Levy, T. E., Adams, R. B., Hauptmann, A., Prange, M., Schmitt-Strecker, S., and Najjar, M. (2002): Early Bronze Age metallurgy: a newly discovered copper manufactory in southern Jordan, *Antiquity*, 76, 425–437.

Levy, T. E., Ben-Yosef, E., and Najjar, M. (2012): New perspectives on Iron Age copper production and society in the Faynan Region, Jordan, in V. Kassianidou and G. Papasavvas, eds., *Eastern Mediterranean Metallurgy and Metalwork in the Second Millennium BC - A Conference in Honour of James D. Muhly, Nicosia, 10th-11th October 2009*, Oxford: Oxbow Books, pp. 197–214.

Li, X. J., Martinón-Torres, M., Meeks, N. D., Xia, Y., and Zhao, K. (2011): Inscriptions, filing, grinding and polishing marks on the bronze weapons frin the Qin Terracotta Army in China, *Journal of Archaeological Science*, 38, 492–501.

Ling, J., Hjärthner-Holdar, E., Grandin, L., Billström, K., and Persson, P.-O. (2013): Moving metals or indigenous mining? Provenancing Scandinavian Bronze Age artefacts by lead isotopes and trace elements, *Journal of Archaeological Science*, 40, 291–304.

Ling, J., Stos-Gale, Z. A., Grandin, L., Billström, K., Hjärthner-Holdar, E., and Persson, P.-O. (2014): Moving metals II: provenancing Scandinavian Bronze Age artefacts by lead isotope and elemental analyses, *Journal of Archaeological Science*, 41, 106–132.

Lo Schiavo, F. (2012): Cyprus and Sardinia, beyond the oxhide ingots, in V. Kassianidou and G. Papasavvas, eds., *Eastern Mediterranean Metallurgy and Metalwork in the Second Millennium BC - A Conference in Honour of James D. Muhly, Nicosia, 10th-11th October 2009*, Oxford: Oxbow Books, pp. 142–150.

Lo Schiavo, F., Sorge, E., Cucuzza, N., Gale, N. H., and Stos-Gale, Z. A. (2013): An oxhide ingot fragment from Piazzale dei Sacelli, Ayia Triada (Crete) to the National Archaeological Museum, Florence, in G. Graziadio, R. Guglielmino, V. Lenuzza, and S. Vitale, eds., *Studies in Mediterranean Archaeology for Mario Benzi*, BAR International Series 2460, Oxford: Archaeopress, pp. 49–60.

Lucas, A. (1962): *Ancient Egyptian Materials and Industries*, London: Edward Arnold.

Lutz, J. and Pernicka, E. (1996): Energy dispersive X-ray fluorescence analysis of ancient copper alloys: empirical values for precision and accuracy, *Archaeometry*, 38, 313–323.

Lyman, R. L. (2012): A historical sketch on the concepts of archaeological association, context, and provenience, *Journal of Archaeological Method and Theory*, 19, 207–240.

MacKenzie, W. S. and Guilford, C. (1980): *Atlas of Rock Forming Minerals in Thin Section*, London: Longman.

Maldonado, B. and Rehren, Th. (2009): Early copper smelting at Itziparátzico, Mexico, *Journal of Archaeological Science*, 36, 1998–2006.

Manasse, A., Mellini, M., and Viti, C. (2001): The copper slags of the Capattoli Valley, Campiglia Marittima, Italy, *European Journal of Mineralogy*, 13, 949–960.

Mangou, H. and Ioannou, P. V. (2000): Studies of the Late Bronze Age copper-based ingots found in Greece, *The Annual of the British School at Athens*, 95, 207–217.

Manzo, A. (2012): From the sea to the deserts and back: new research in eastern Sudan, *British Museum Studies in Ancient Egypt and Sudan*, 18, 75–106.

Marsh, B. (2000): *Geomorphology of the Gordion Regional Survey*, Unpublished report dated September 12, 2000, Gordion archive, Philadelphia, PA: University of Pennsylvania Museum of Archaeology and Anthropology.

Marsh, B. (2005): Physical geography, land use, and human impact at Gordion, in L. Kealhofer, ed., *The Archaeology of Midas and the Phrygians: Recent Work at Gordion*, Philadelphia, PA: University of Pennsylvania Museum of Archaeology and Anthropology, pp. 161–171.

Martinón-Torres, M., Freestone, I. C., Hunt, A., and Rehren, Th. (2008): Mass-produced mullite crucibles in medieval Europe: manufacture and material properties, *Journal of the American Ceramic Society*, 91, 2071–2074.

Martinón-Torres, M. and Rehren, Th. (2009): Post-medieval crucible production and distribution: a study of materials and materialities, *Archaeometry*, 51, 49–74.

Martinón-Torres, M. and Rehren, Th. (2014): Technical ceramics, in B. W. Roberts and C. P. Thornton, eds., *Archaeometallurgy in Global Perspective*, Springer, pp. 107–131.

Martinón-Torres, M., Rehren, Th., and Freestone, I. C. (2006): Mullite and the mystery of Hessian wares, *Nature*, 444, 437–438.

Martinón-Torres, M., Rojas, R. V., Cooper, J., and Rehren, Th. (2007): Metals, microanalysis and meaning: a study of metal objects excavated from the indigenous cemetery of El Chorro de Maíta, Cuba, *Journal of Archaeological Science*, 34, 194–204.

Martinón-Torres, M., Valcárcel Rojas, R., Sáenz Samper, J., and Guerra, M. F. (2012): Metallic encounters in Cuba: the technology, exchange and meaning of metals before and after Columbus, *Journal of Anthropological Archaeology*, 31, 439–454.

Masioli, E., Vidale, M., Artioli, D., Bianchetti, P., Guida, G., Sidoti, G., Di Pilato, S., and Salvatori, S. (2006): Copper-melting crucibles from the surface of Altyn-Depe, Turkmenistan (ca 2500-2000 BC), *Paléorient*, 32, 157–174.

Mason, R. B. and Tite, M. S. (1997): The beginnings of tin-opacification of pottery glazes, *Archaeometry*, 39, 41–58.

Mass, J. L., Wypyski, M. T., and Stone, R. E. (2002): Malkata and Lisht glassmaking technologies: towards a specific link between second millennium BC metallurgists and glassmakers, *Archaeometry*, 44, 67–82.

McNeil, M. B. and Little, B. J. (1992): Corrosion mechanisms for copper and silver objects in near-surface environments, *Journal of the American Institute for Conservation*, 31, 355–366.

Mödlinger, M. and Piccardo, P. (2013): Corrosion on prehistoric Cu-Sn-alloys: the influence of artificial environment and storage, *Applied Physics A: Materials Science & Processing*, 113, 1069–1080.

Mecking, O. and Walter, D. (2004): Gussformen und Tiegel aus zwei Siedlungen der Urnenfelderzeit im nördlichen Thüringen, *Alt-Thüringen*, 37, 53–67.

Meeks, D. (2003): Locating Punt, in D. O'Connor and S. Quirke, eds., *Mysterious Lands*, London: UCL Press, pp. 53–80.

Meeks, N. D. (1990): The examination of a sample from a copper ingot found off Plymouth, Devon, *The International Journal of Nautical Archaeology*, 19, 153–156.

Meeks, N. D. (2000): Scanning electron microscopy of the refractory remains and the gold, in A. Ramage and P. T. Craddock, eds., *King Croesus' Gold. Excavations at Sardis and the History of Gold Refining*, London: British Museum Press, pp. 99–156.

Meeks, N. D., Craddock, P. T., Hook, D. R., Middleton, A. P., Geçkinli, A., and Ramage, A. (1996): The scientific study of the refractory remains and gold particles from the Lydian gold refinery at Sardis, in A. Demirci, Ş. Özer and G. Summers, eds., *Archaeometry 94. The Proceedings of the 29th International Symposium on Archaeometry, Ankara 9-14, May 1994*, Ankara: Tübitak, pp. 461–482.

Mellink, M. J. (1956): Archaeology in Asia Minor, *American Journal of Archaeology*, 60, 369–384.

Menu, B. (1999): *Ramesses the Great: Warrior and Builder*, London: Thames & Hudson.

Merideth, C. (1998): *An Archaeometallurgical Survey for Ancient Tin Mines and Smelting Sites in Spain and Portugal*, BAR International Series B714, Oxford: Archaeopress.

Merkel, J. F. (1990): Experimental reconstruction of Bronze Age copper smelting based on archaeological evidence from Timna, in B. Rothenberg, ed., *The Ancient Metallurgy of Copper: Archaeology-Experiment-Theory. (Researches in the Arabah 1959-84; v. 2)*, London: The Institute for Archaeo-Metallurgical Studies, pp. 78–122.

Merkel, S. and Rehren, Th. (2007): Parting layers, ash trays, and Ramesside glass-making: an experimental study, in E. B. Pusch and Th. Rehren, eds., *Hochtemperatur-Technologie in der Ramses-Stadt - Rubinglas für den Pharao*, Forschungen in der Ramses-Stadt Band 6, Hildesheim: Gerstenberg Verlag, pp. 201–221.

Miller, D. (2003): Archaeological bronze processing in Botswana, in *Proceedings of the Microscopy Society of Southern Africa 33*, Microscopy Society of Southern Africa, p. 18.

Miller, D. and Hall, S. (2008): Rooiberg revisited - the analysis of tin and copper smelting debris, *Historical Metallurgy*, 42, 23–38.

Miller, H. M.-L. (2007): *Archaeological Approaches to Technology*, Amsterdan; London: Elsevier/Academic Press.

Minkova, M. (2002): Some remarks on the circulation and the coinage of Nicopolis ad Istrum in light of specimens from the Historical Museum in Stara Zagora, in L. Slokoska, R. T. Ivanov, and V. Dinchev, eds., *The Roman and Late Roman City. The International Conference, Veliko Turnovo, 26-30 July 2000*, Sofia: Prof. Marin Drinov Academic Publishing House, pp. 128–132.

Misra, M. K., Ragland, K. W., and Baker, A. J. (1993): Wood ash composition as a function of furnace temperature, *Biomass and Bioenergy*, 4, 103–116.

Müller, N. S., Kilikoglou, V., Day, P. M., and Vekinis, G. (2010): The influence of temper shape on the mechanical properties of archaeological ceramics, *Journal of the European Ceramic Society*, 30, 2457–2465.

Müller, R., Rehren, Th., and Rovira, S. (2004): Almizaraque and the early copper metallurgy of southeast Spain: new data, *Madrider Mitteilungen*, 45, 33–56.

Molofsky, L. J., Killick, D., Ducea, M. N., Macovei, M., Chesley, J. T., Ruiz, J., Thibodeau, A., and Popescu, G. C. (2014): A novel approach to lead isotope provenance studies of tin and bronze: applications to South African, Botswanan and Romanian artifacts, *Journal of Archaeological Science*, 50, 440–450.

Mongiatti, A. (2010): *Assaying and Smelting Noble Metals in Sixteenth-century Austria: a Comparative Analytical Study*, Ph.D. thesis, University College London.

Montero-Ruiz, I., Rovira, S., Delibes, G., Fernández-Manzano, J., Fernández-Posse, M. D., Herrán, J. I., Martín, C., and Maicas, R. (2003): High leaded bronze in the Late Bronze Age metallurgy of the Iberian Peninsula, in *Archaeometallurgy in Europe. International Conference 24.-26. September 2003 Milan, Italy. Proceedings Vol. 1*, Milan: Associazione Italiana di Metallurgia, pp. 39–46.

Moorey, P. R. S. and Schweizer, F. (1974): Copper and copper alloys in ancient Turkey: some new analyses, *Archaeometry*, 16, 112–115.

Muan, A. (1957): Phase equilibria at liquidus temperatures in the system iron oxide-Al_2O_3-SiO_2 in air atmosphere, *Journal of the American Ceramic Society*, 40, 121–133.

Muhly, J. D. (1977): The copper ox-hide ingots and the Bronze Age metal trade, *Iraq*, 39, 73–82.

Muhly, J. D. (1979): New evidence for sources of and trade in Bronze Age tin, in A. D. Franklin, J. S. Olin, and T. A. Wertime, eds., *The Search for Ancient Tin: a Seminar organized by Theodore A. Wertime and held at the Smithsonian Institution and the National Bureau of Standards, Washington, D.C., March 14-15, 1977*, Washington, D.C.: Smithsonian Institution Press, pp. 43–48.

Muhly, J. D. (1985): Sources of tin and the beginnings of bronze metallurgy, *American Journal of Archaeology*, 89, 275–291.

Muhly, J. D. (1995): Lead isotope analysis and the archaeologist, *Journal of Mediterranean Archaeology*, 8, 54–58.

Muhly, J. D. (1999): Copper and bronze in Cyprus and the eastern Mediterranean, in V. C. Pigott, ed., *The Archaeometallurgy of the Asian Old World*, Philadelphia, PA: University of Pennsylvania Museum of Archaeology and Anthropology, pp. 15–25.

Muhly, J. D. (2003): Trade in metals in the Late Bronze Age and the Iron Age, in N. Chr. Stampolidis and V. Karageorggis, eds., *Sea Routes... Interconnections in the Mediterranean 16th - 6th c. BC. Proceedings of the International Symposium held at Rethymnon,*

Crete, September 29th - October 2nd, 2002, Athens: The University of Crete and the A.G. Leventis Foundation, pp. 141–150.

Muhly, J. D. (2009): Oxhide ingots in the Aegean and Egypt, in F. Lo Schiavo, J. D. Muhly, R. Maddin, and A. Giumlia-Mair, eds., *Oxhide Ingots in the Central Mediterranean*, Rome: A.G. Leventis Foundation. CNR - Instituto di Studi sulle Civiltà dell'Egeo e del Vicino Oriente, pp. 17–39.

Murillo-Barroso, M., Pryce, T. O., Bellina, B., and Martinón-Torres, M. (2010): Khao Sam Kaeo - an archaeometallurgical crossroads for trans-asiatic technological traditions, *Journal of Archaeological Science*, 37, 1761–1772.

Muscarella, O. W. (1967): *Phrygian Fibulae from Gordion*, Colt Archaeological Institute, London and Beccles: William Clowes and Sons, Limited.

Nenova-Merdjanova, R. (1997): Roman precious bronze vessels from Moesia and Thracia, *Archaeologia Bulgarica*, 1, 30–37.

Nenova-Merdjanova, R. (2002a): Bronze production of Pautalia, in L. Slokoska, R. T. Ivanov, and V. Dinchev, eds., *The Roman and Late Roman City. The International Conference, Veliko Turnovo, 26-30 July 2000*, Sofia: Prof. Marin Drinov Academic Publishing House, pp. 378–382.

Nenova-Merdjanova, R. (2002b): Tradition and inventiveness. On the local production of bronze vessels in the Roman province Thracia, in A. Giumlia-Mair, ed., *I Bronzi Antichi: Produzione e tecnologia. Atti del XV Congresso Internazionale sui Bronzi Antichi, organizzato dall' Università di Udine, sede di Gorizia, Grado-Aquileia, 22-26 maggio 2001*, Monographies Instrumentum 21, Montagnac: Editions Monique Mergoil, pp. 591–599.

Nenova-Merdjanova, R. (2011): Production and consumption of bronzework in Roman Thrace, in I. P. Haynes, ed., *Early Roman Thrace. New Evidence from Bulgaria*, JRA Supplementary Series 82, Portsmouth, Rhode Island, pp. 115–134.

Nezafati, N., Pernicka, E., and Momenzadeh, M. (2006): Ancient tin: old question and a new answer, *Antiquity Project Gallery*, 80.

Nezafati, N., Pernicka, E., and Momenzadeh, M. (2009): Introduction of the Deh Hosein ancient tin-copper mine, western Iran: evidence from geology, archaeology, geochemistry and lead isotope data, *Turkiye Bilimler Akademisi Arkeoloji Dergisi (TUBA-AR). Turkish Academy of Sciences Journal of Archaeology*, 12, 223–236.

Nezafati, N., Pernicka, E., and Momenzadeh, M. (2011): Early tin-copper ore from Iran, a possible clue for the enigma of Bronze Age tin, in Ü. Yalçin, ed., *Anatolian Metal V*, Bochum: Deutsches Bergbau-Museum, pp. 211–230.

Nibbi, A. (1976): Tin from the Eastern Desert, *Göttinger Miszellen*, 19, 49–50.

Nicholas, M. (2003): *Roman Crucibles, Hearth Lining and Alag from Usk, Monmouthshire, South Wales*, Centre for Archaeology Report 35/2003, English Heritage.

Nickel, D., Haustein, M., Lampke, T., and Pernicka, E. (2012): Identification of forgeries by measuring tin isotopes in corroded bronze objects, *Archaeometry*, 54, 167–174.

Niederschlag, E., Pernicka, E., Seifert, Th., and Bartelheim, M. (2003): The determination of lead isotope ratios by multiple collector ICP-MS: a case study of Early Bronze Age artefacts and their possible relation with ore deposits of the Erzgebirge, *Archaeometry*, 45, 61–100.

Nocete, F., Queipo, G., Sáez, R., Nieto, J. M., Inácio, N., Bayona, M. R., Peramo, A., Vargas, J. M., Cruz-Auñón, R., Gil-Ibarguchi, J. I., and Santos, J. F. (2008): The smelting quarter of Valencina de la Concepción (Seville, Spain): the specialised copper industry in a political centre of the Guadalquivir Valley during the third millennium BC (2750-2500 BC), *Journal of Archaeological Science*, 35, 717–732.

Northover, J. P. and Gillis, C. (1999): Questions in the analysis of ancient tin, in S. M. M. Young, A. M. Pollard, P. Budd, and R. A. Ixer, eds., *Metals in Antiquity*, BAR S792, Oxford: Archaeopress, pp. 78–85.

Northover, J. P. and Saghieh, M. B. (2002): Copper alloy metalwork from the 5th-th century levels in Beirut, Lebanon, in A. Giumlia-Mair, ed., *I Bronzi Antichi: Produzione e tecnologia. Atti del XV Congresso Internazionale sui Bronzi Antichi, organizzato dall' Università di Udine, sede di Gorizia, Grado-Aquileia, 22-26 maggio 2001*, Monographies Instrumentum 21, Montagnac: Editions Monique Mergoil, pp. 630–633.

Nowell, G., Clayton, R., Gale, N. H., and Stos-Gale, Z. A. (2002): Sources of tin - is isotopic evidence likely to help?, in E. Bartelheim, M. Pernicka and R. Krause, eds., *Anfänge der Metallurgie in der Alten Welt / The Beginnings of Metallurgy in the Old World*, Forschungen zur Archäometrie und Altertumswissenschaft 1, Rahden/Westfalen: Verlag Marie Leidorf GmbH, pp. 291–302.

Ogden, J. (2000): Metals, in P. T. Nicholson and I. Shaw, eds., *Ancient Egyptian Materials and Technology*, Cambridge: Cambridge University Press, pp. 148–176.

Ottaway, B. S. (2001): Innovation, production and specialization in early prehistoric copper metallurgy, *European Journal of Archaeology 2001 4: 87*, 4, 87–112.

Oxtoby, D. W., Freeman, W. A., and Block, T. F. (2003): *Chemistry: Science of Change*, Thomson - Brooks/Cole.

Pagès, G., Dillmann, P., Fluzin, P., and Long, L. (2011): A study of the Roman iron bars of Saintes-Maries-de-la-Mer (Bouches-du-Rhône, France). A proposal for a comprehensive metallographic approach, *Journal of Archaeological Science*, 38, 1234–1252.

Papadopoulou, D. N., Zachariadis, G. A., Anthemidis, A. N., Tsirliganis, N. C., and Stratis, J. A. (2006): Development and optimisation of a portable micro-XRF method for in situ multi-element analysis of ancient ceramics, *Talanta*, 68, 1692–1699.

Park, J.-S. and Gordon, R. B. (2007): Traditions and transitions in Korean bronze technology, *Journal of Archaeological Science*, 34, 1991–2002.

Parker, A. J. (1974): Lead ingots from a Roman ship at Ses Salines, Majorca, *The International Journal of Nautical Archaeology*, 3, 147–150.

Parker, A. J. and Price, J. (1981): Spanish exports of the Claudian Period: the significance of the Port Vendres II wreck reconsidered, *The International Journal of Nautical Archaeology*, 10, 221–228.

Parzinger, H. and Boroffka, N., eds. (2003): *Das Zinn der Bronzezeit in Mittelasien I: Die siedlungsarchäologischen Forschungen im Umfeld der Zinnlagerstätten*, Archäologie in Iran und Turan, Band 5. Deutsches Archäologisches Institut, Eurasien-Abteilung, Aussenstelle Teheran, Mainz: Verlag Philipp von Zabern.

Paunov, E. I. and Prokopov, I. S. (2002): *An Inventory of Roman Republican Coin Hoards and Coins from Bulgaria*, Glaux. Collana di Studi e Ricerche di Numismatica 15, Milan: Edizioni Ennerre S.r.l.

Peacock, D. P. S. (1982): *Pottery in the Roman world: an Ethnoarchaeological Approach*, London: Longman.

Pelleg, J., Baram, J., and Oren, E. (1979): An investigation of bronze artifacts from the North Sinai coast and the Nile Delta region, *Metallography*, 12, 313–324.

Penhallurick, R. D. (1986): *Tin in Antiquity: Its Mining and Trade Throughout the Ancient World with Particular Reference to Cornwall*, London: Institute of Metals.

Pernicka, E. (1995): Crisis or catharsis in lead isotope analysis?, *Journal of Mediterranean Archaeology*, 8, 59–64.

Pernicka, E. (1999): Trace element fingerprinting of ancient copper: a guide to technology or provenance?, in S. M. M. Young, A. M. Pollard, P. Budd, and R. A. Ixer, eds., *Metals in Antiquity*, BAR S792, Oxford: Archaeopress, pp. 163–171.

Pernicka, E. (2014): Provenance determination of archaeological metal objects, in B. W. Roberts and C. P. Thornton, eds., *Archaeometallurgy in Global Perspective*, Springer, pp. 239–268.

Pernicka, E., Begemann, F., Schmitt-Strecker, S., and Grimanis, A. P. (1990): On the composition and provenance of metal artefacts from Poliochni on Lemnos, *Oxford Journal of Archaeology*, 9, 263–298.

Pernicka, E., Seeliger, T. C., Wagner, G. A., Begemann, F., Schmitt-Strecker, S., Eibner, C., Öztunali, Ö., and Baranyi, I. (1984): Archäometallurgische Untersuchungen in Nordwest-anatolien, *Jahrbuch des Römisch-Germanischen Zentralmuseums Mainz*, 31, 533–599.

Pernicka, E., Wagner, G. A., Muhly, J. D., and Öztunali, Ö. (1992): Comment on the discussion of ancient tin sources in Anatolia, *Journal of Mediterranean Archaeology*, 5, 91–98.

Peterson, S. E. (2009): *Thin-section Petrography of Ceramic Materials*, Philadelphia, PA: INSTAP Academic Press.

Pfaffenberger, B. (1988): Fetishised objects and humanised nature: towards an anthropology of technology, *Man*, 23 (New Series), 236–252.

Pfaffenberger, B. (1992): Social anthropology of technology, *Annual Review of Anthropology*, 21, 491–516.

Phelps, M., Paynter, S., and Dungworth, D. (2011): *Downside Mill, Cobham, Surrey. Analysis of the Metalworking Remains*, Research Department Report Series 43-2011, English Heritage.

Philip, G. (2007): *Tell El-Dab'a XV, Metalwork and Metalworking Evidence of the Late Middle Kingdom and The Second Intermediate Period*, Wien: Verlag der Osterreichischen Akademie der Wissenschaften.

Philip, G., Clogg, P. W., and Dungworth, D. (2003): Copper metallurgy in the Jordan valley from the third to the first millennia BC: chemical, metallographic and lead isotope analyses of artefacts from Pella, *Levant*, 35, 71–100.

Photos, E. and Salter, C. J. (1986): A reappraisal of phase characterization in slags, in J. S. Olin and M. J. Blackman, eds., *Proceedings of the 24th International Archaeometry Symposium*, Washington, D.C.: Smithsonian Institution Press, pp. 259–265.

Pierce, C., Adams, K. R., and Stewart, J. D. (1998): Determining the fuel constituents of ancient hearth ash via ICP-AES analysis, *Journal of Archaeological Science*, 25, 493–503.

Pigott, V. C. (2011): Sources of tin and the tin trade in Southwest Asia: recent research and its relevance to current understanding, in P. P. Betancourt and S. C. Ferrence, eds., *Metallurgy: Understanding How, Learning Why. Studies in Honor of James D. Muhly*, Philadelphia, PA: INSTAP Academic Press, pp. 273–291.

Pigott, V. C. (2012): On ancient tin and tin-bronze in the Asian Old World: further comments, in V. Kassianidou and G. Papasavvas, eds., *Eastern Mediterranean Metallurgy and Metalwork in the Second Millennium BC - A Conference in Honour of James D. Muhly, Nicosia, 10th-11th October 2009*, Oxford: Oxbow Books, pp. 222–236.

Pigott, V. C., Fleming, S. J., and Darby, C. (1991): *Preliminary Research on Copper-Base Material at Gordion: Metallographic and Compositional Analyses*, MASCA Archaeometallurgy Interim Report, University of Pennsylvania Museum of Archaeology and Anthropology.

Pigott, V. C., Rogers, H. C., and Nash, S. K. (2003): Archaeometallurgical investigations at Malyan: the evidence for tin-bronze in the Kaftari Phase, in N. F. Miller and K. Abdi, eds., *Yeki Bud, Yeki Nabud: Essays on the Archaeology of Iran in Honor of William M. Sumner*, Los Angeles: Cotsen Institute of Archaeology at UCLA, in association with the American Institute of Iranian Studies and the University of Pennsylvania Museum of Archaeology and Anthropology, pp. 161–176.

Pinarelli, L. (2004): Lead isotope characterisation of copper ingots from Sardinia (Italy): inferences on their origins, *Bulletin of the Geological Society of Greece*, 36, 1173–1180.

Pinarelli, L., Salvi, D., and Ferrera, G. (1995): The source of ancient Roman lead, as deduced from lead isotopes: the ingots from the Mal di Ventre wreck (western Sardinia, Italy), *Science and Technology for Cultural Heritage*, 4, 79–86.

Pirrie, D., Power, M. R., Wheeler, P. D., Cundy, A., Bridges, C., and Davey, G. (2002): Geochemical signature of historical mining: Fowey Estuary, Cornwall, UK, *Journal of Geochemical Exploration*, 76, 31–43.

Plant, R., Page, J., Bonham, J., and Jones, J. P. (1975): Kashmir, in *Physical Graffiti*, London: Swan Song.

Pollard, A. M. (2009): What a long, strange trip it's been: lead isotopes and archaeology, in A. J. Shortland, I. C. Freestone, and Th. Rehren, eds., *From Mine to Microscope. Advances in the Study of Ancient Technology*, Oxford: Oxbow Books, pp. 181–189.

Pollard, A. M. (2011): Isotopes and impact: a cautionary tale, *Antiquity*, 85, 631–638.

Pollard, A. M., Batt, C. M, Stern, B., and Young, S. M. M. (2007): *Analytical Chemistry in Archaeology*, Cambridge: Cambridge University Press.

Pollard, A. M., Bray, P. J., and Gosden, C. (2014): Is there something missing in scientific provenance studies of prehistoric artefacts?, *Antiquity*, 88, 625–631.

Ponting, M. (2002): Keeping up with the Romans? Romanisation and copper alloys in First Revolt Palestine, *Institute of Archaeo-Metallurgical Studies*, 22, 3–6.

Ponting, M., Evans, J. A., and Pashley, V. (2003): Fingerprinting of Roman mints using laser-ablation MC-ICP-MS lead isotope analysis, *Archaeometry*, 45, 591–597.

Poulter, A. G. (1983): Town and country in Moesia Inferior, in A. G. Poulter, ed., *Ancient Bulgaria. Papers presented to the International Symposium on the Ancient History and Archaeology of Bulgaria, University of Nottingham, 1981*, Nottingham: Department of Classical and Archaeological Studies, pp. 74–118.

Poulter, A. G. (2002): From city to fortress and from town to country: 15 years of Anglo-Bulgarian collaboration, in L. Slokoska, R. T. Ivanov, and V. Dinchev, eds., *The Roman and Late Roman City. The International Conference, Veliko Turnovo, 26-30 July 2000*, Sofia: Prof. Marin Drinov Academic Publishing House, pp. 14–29.

Poulter, A. G. (2007a): Introduction, in A. G. Poulter, ed., *Nicopolis ad Istrum. A Late Roman and Early Byzantine City. The Finds and the Biological Remains*, Oxford: Oxbow Books, pp. 1–14.

Poulter, A. G. (2007b): The metalwork, in A. G. Poulter, ed., *Nicopolis ad Istrum. A Late Roman and Early Byzantine City. The Finds and the Biological Remains*, Oxford: Oxbow Books, pp. 15–64.

Prell, S. (2011): *Einblicke in die Werkstätten der Residenz - Die Stein- und Metallwerkzeuge des Grabungsplatzes Q I*, Forschungen in der Ramses-Stadt Band 8, Hildesheim: Gerstenberg Verlag.

Pryce, T. O., Bassiakos, Y., Catapotis, M., and Doonan, R. C. P. (2007): 'De Caerimoniae' technological choices in copper-smelting furnace design at Early Bronze Age Chrysokamino, Crete, *Archaeometry*, 49, 543–557.

Pryce, T. O., Brauns, M., Chang, N., Pernicka, E., Pollard, A. M., Ramsey, C., Rehren, Th., Souksavatdy, V., and Sayavongkhamdy, T. (2011): Isotopic and technological variation in prehistoric Southeast Asian primary copper production, *Journal of Archaeological Science*, 38, 3309–3322.

Pryce, T. O., Pigott, V. C., Martinón-Torres, M., and Rehren, Th. (2010): Prehistoric copper production and technological reproduction in the Khao Wong Prachan Valley of Central Thailand, *Archaeological and Anthropological Sciences*, 2, 237–264.

Pulak, C. (1997): The Uluburun shipwreck, in S. Swiny, R. L. Hohlfelder, and H. W. Swiny, eds., *Res Maritimae: Cyprus and the Eastern Mediterranean from Prehistory to Late Antiquity: Proceedings of the Second International Symposium "Cities on the Sea", Nicosia, Cyprus, October 18-22, 1994*, Scholars Press, pp. 233–262.

Pulak, C. (2000): The copper and tin ingots from the Late Bronze Age shipwreck at Uluburun, in Ü. Yalçin, ed., *Anatolian Metal I. Der Anschnitt, Beiheft 13*, Bochum: Deutsches Bergbau-Museum, pp. 137–157.

Pulak, C. and Bass, G. F. (1997): Uluburun, in E. Meyers, ed., *The Oxford Encyclopedia of Archaeology in the Near East*, New York and Oxford: Oxford University Press, pp. 266–268.

Pusch, E. B. (1990): Metallverarbeitende Werkstätten der frühen Ramessidenzeit in Qantir-Piramesse/Nord - Ein Zwischenbericht, *Ägypten und Levante*, 1, 75–113.

Pusch, E. B. (1991): Recent work at northern Piramesse - results of excavations by the Pelizaeus-Museum, Hildesheim, at Qantir, in E. Bleiberg and R. Freed, eds., *Fragments of a Shattered Visage: The Proceedings of the International Symposium of Ramesses the Great*, Memphis: Memphis State University, pp. 199–220.

Pusch, E. B. (1993): Pi-Ramesse-geliebt-von-Amun, Hauptquartier Deiner Streitwagen. Ägypter und Hethiter in der Delta-Residenz der Ramessiden, in A. Eggebrecht, ed.,

Pelizaeus-Museum Hildesheim. Die Ägyptische Sammlung, Mainz: Verlag Philip von Zabern, pp. 126–143.

Pusch, E. B. (1994): Divergierende Verfahren der Metallverarbeitung in Theben und Qantir? Bemerkungen zur Konstruktion und Technik, *Ägypten und Levante*, 4, 145–170.

Pusch, E. B. (1998/99): Auf dem Wege zu einem Stadtplan der Ramses-Stadt. Ergebnisse der Hildesheimer Grabung Qantir aus dem Herbst 1998, *Hildesheimer Jahrbuch*, 70/71, 473–478.

Pusch, E. B. (1999a): Goldschmiedewerkstatt oder vergoldeter Fußboden?, *Ägypten und Levante*, 9, 121–133.

Pusch, E. B. (1999b): Towards a map of Piramesse, *Egyptian Archaeology*, 14, 13–15.

Pusch, E. B. (2000): Doors - statues - musical instruments? Large scale bronze production and casting at the delta residence of the Ramessides, Egypt, in R. Eichmann, E. Hickmann, and I. Laufs, eds., *Musikarchäologie früher Metallzeiten; Vorträge des 1. Symposiums der International Study Group on Music Archaeology im Kloster Michaelstein, 18.-24. März 1998*, Studien zur Musikarchäologie 2; Orient-Archäologie 7, Leidorf, pp. 219–232.

Pusch, E. B., Becker, H., and Fassbinder, J. (1999): Wohnen und Leben: oder: weitere Schnitte zum einem Stadtplan der Ramses-Stadt, *Ägypten und Levante*, 9, 155–170.

Pusch, E. B. and Herold, A. (1999): Qantir/Pi-Ramesses, in K. Bard, ed., *Encyclopedia of the Archaeology of Ancient Egypt*, London: Routledge, pp. 647–649.

Pusch, E. B. and Rehren, Th. (2007): *Hochtemperatur-Technologie in der Ramses-Stadt - Rubinglas für den Pharao*, Forschungen in der Ramses-Stadt Band 6, Hildesheim: Gerstenberg Verlag.

Quinn, P. S., ed. (2009): *Interpreting Silent Artefacts: Petrographic Approaches to Archaeological Ceramics*, Oxford: Archaeopress.

Rademakers, F. W. and Rehren, Th. (2013): Tin oxide in crucible slag. From slag crystals to technological choices in bronze production, *Poster presented at the Historical Metallurgy Society 50th Anniversary Conference, 14-16 June 2013, London, UK*.

Rademakers, F. W. and Rehren, Th. (2014): Heterogeneity in the crucible. Some methodological issues for reconstructing ancient crucible metallurgy, *Poster presented at the 40th International Symposium on Archaeometry, 19-23 May 2014, Los Angeles, USA*.

Rademakers, F. W., Rehren, Th., and Pusch, E. B. (in press): Bronze production in Pi-Ramesse: alloying technology and material use, in E. Ben-Yosef and Y. Goren, eds., *Mining for Copper: Essays in Honor of Professor Beno Rothenberg*, Tel Aviv: Institute of Archaeology of Tel Aviv.

Rapp, G. Jr. (1979): Trace elements as a guide to the geographical source of tin ore: smelting experiments, in A. D. Franklin, J. S. Olin, and T. A. Wertime, eds., *The Search for Ancient Tin: a Seminar organized by Theodore A. Wertime and held at the Smithsonian Institution and the National Bureau of Standards, Washington, D.C., March 14-15, 1977*, Washington, D.C.: Smithsonian Institution Press, pp. 59–63.

Rapp, G. Jr., Russel, R., and Zhichun, J. (1999): Using neutron activation analysis to source ancient tin (cassiterite), in S. M. Young, A. M. Pollard, P. Budd, and R. A. Ixer, eds., *Metals in Antiquity*, BAR S792, Oxford: Archaeopress, pp. 153–162.

Redmount, C. A. and Morgenstein, M. E. (1996): Major and trace element analysis of modern Egyptian pottery, *Journal of Archaeological Science*, 23, 741–762.

Reece, R. (1985): The chemical analysis of Roman coins: past and future, in P. Phillips, ed., *The Archaeologist and the Laboratory*, London: Council for British Archaeology, pp. 60–62.

Reedy, T. J. and Reedy, C. L. (1992): Evaluating lead isotope data: comments on E. V. Sayre, K. A. Yener, E. C. Joel and I. L. Barnes, 'Statistical evaluation of the presently accumulated lead isotope data from Anatolia and surrounding regions', Archaeometry, 34 (1) (1992), 73-105, and reply. Comments... IV, *Archaeometry*, 34, 327–329.

Rehren, Th. (1996a): High temperature industries in the Late Bronze Age capital Piramesse-(Qantir): I - bronze and blass production and processing, in F. A. Esmael, ed., *Proceedings of the First International Conference on Ancient Egyptian Mining and Metallurgy and Conservation of Metallic Artifacts*, Cairo: Ministry of Culture, Supreme Council of Antiquities, pp. 101–119.

Rehren, Th. (1996b): A Roman zinc tablet from Bern, Switzerland: reconstruction of the manufacture, in A. Demirci, Ş. Özer and G. Summers, eds., *Archaeometry 94. The Proceedings of the 29th International Symposium on Archaeometry, Ankara 9-14, May 1994*, Ankara: Tübitak, pp. 35–45.

Rehren, Th. (1997a): Die Rolle des Kohlenstoffs in der prähistorischen Metallurgie, *Stahl und Eisen*, 117, 87–92.

Rehren, Th. (1997b): Ramesside glass-colouring crucibles, *Archaeometry*, 39, 355–368.

Rehren, Th. (1999): Small size, large scale: Roman brass production in Germania Inferior, *Journal of Archaeological Science*, 26, 1083–1087.

Rehren, Th. (2000): Archaeometallurgy - an island?, *Antiquity*, 74, 964–967.

Rehren, Th. (2001): Aspects of the production of cobalt-blue glass in Egypt, *Archaeometry*, 43, 483–489.

Rehren, Th. (2003): Crucibles as reaction vessels in ancient metallurgy, in P. T. Craddock and J. Lang, eds., *Mining and Metal Production. Through the Ages*, London: British Museum Press, pp. 207–215.

Rehren, Th. (2009): From mine to microbe - the Neolithic copper melting crucibles from Switzerland, in A. J. Shortland, I. C. Freestone, and Th. Rehren, eds., *From Mine to Microscope. Advances in the Study of Ancient Technology*, Oxford: Oxbow Books, pp. 155–162.

Rehren, Th. (2013): Metallurgy, Greece and Rome, in R. S. Bagnall, K. Brodersen, C. B. Champion, A. Erskine, and S. R. Huebner, eds., *The Encyclopedia of Ancient History*, Blackwell Publishing.

Rehren, Th. (2014): One minute interview, *The Crucible. Historical Metallurgy Society News*, 87, 10–11.

Rehren, Th., Charlton, M., Chirikure, S., Humphris, J., Ige, A., and Veldhuijzen, H. (2007): Decisions set in slag - the human factor in African iron smelting, in S. La Niece, D. Hook, and P. T. Craddock, eds., *Metals and Mines. Studies in Archaeometallurgy*, London: Archetype Books, pp. 211–218.

Rehren, Th., Hess, K., and Philip, G. (1996): Auriferous silver in western Asia: ore or alloy?, *Historical Metallurgy*, 30, 1–10.

Rehren, Th. and Kraus, K. (1999): Cupel and crucible: the refining of debased silver in the Colonia Ulpia Traiana, Xanten, *Journal of Roman Archaeology*, 12, 263–272.

Rehren, Th. and Martinón-Torres, M. (2008): Naturam ars imitata: European brassmaking between craft and science, in M. Martinón-Torres and Th. Rehren, eds., *Archaeology, History and Science. Integrating Approaches to Ancient Materials*, Walnut Creek, CA: Left Coast Press, pp. 167–188.

Rehren, Th. and Papachristou, O. (2003): Similar like white and black: a comparison of steel-making crucibles from Central Asia and the Indian subcontinent, in T. Stöllner, G. Körlin, G. Steffens, and J. Cierny, eds., *Man and Mining (Mensch und Bergbau)*, Der Anschnitt, Beiheft 16, Bochum: Deutsches Bergbau-Museum, pp. 393–404.

Rehren, Th. and Pernicka, E. (2008): Coins, artefacts and isotopes - archaeometallurgy and archaeometry, *Archaeometry*, 50, 232–248.

Rehren, Th. and Pernicka, E. (2014): First data on the nature and origin of the metalwork from Tell el-Farkha, in A. Maczynska, ed., *The Nile Delta as a Centre of Cultural Interactions between Upper Egypt and the Southern Levant in the 4th Millennium BC*, Studies in African Archaeology 13, Poznan, pp. 237–252.

Rehren, Th. and Pusch, E. B. (1997): New Kingdom glass-melting crucibles from Qantir-Piramesses, *Journal of Egyptian Archaeology*, 83, 127–141.

Rehren, Th. and Pusch, E. B. (1999): Glass and glass making at Qantir-Piramesses and beyond, *Ägypten und Levante*, 9, 171–179.

Rehren, Th. and Pusch, E. B. (2005): Late Bronze Age glass production at Qantir-Piramesses, Egypt, *Science*, 308, 1756–1758.

Rehren, Th. and Pusch, E. B. (2012): Alloying and resource management in New Kingdom Egypt: the bronze industry at Qantir - Pi-Ramesse and its relationship to Egyptian copper sources, in V. Kassianidou and G. Papasavvas, eds., *Eastern Mediterranean Metallurgy and Metalwork in the Second Millennium BC - A Conference in Honour of James D. Muhly, Nicosia, 10th-11th October 2009*, Oxford: Oxbow Books, pp. 215–221.

Rehren, Th., Pusch, E. B., and Herold, A. (1998): Glass coloring works within a copper-centered industrial complex in Late Bronze Age Egypt, in P. McCray and W. D. Kingery, eds., *The Prehistory and History of Glassmaking Technology (Ceramics and Civilization Vol. 8)*, The American Ceramic Society, pp. 227–250.

Rehren, Th., Pusch, E. B., and Herold, A. (2001): Qantir-Piramesses and the organisation of the Egyptian glass industry, in A. J. Shortland, ed., *The Social Context of Technological Change. Egypt and the Near East, 1650-1550 BC*, Oxford: Oxbow Books, pp. 223–238.

Rehren, Th. and Temme, M. (1994): Pre-Columbian gold processing at Putushio, south Ecuador: the archaeometallurgical evidence, in D. Scott and P. Meyers, eds., *Archaeometry of Pre-Columbian Sites and Artifacts. Proceedings of a Symposium organized by the*

UCLA Institute of Archaeology and the Getty Conservation Institute, Los Angeles, California, March 23-27, 1992, Los Angeles, CA: The Getty Conservation Institute, pp. 267–284.

Renfrew, C. and Bahn, P. (2012): *Archaeology: Theories, Methods and Practice (6th Edition)*, New York: Thames & Hudson.

Renzi, M., Hauptmann, A., and Rovira, S. (2009): Phoenician metallurgical production at SE-Spain, in *Archaeometallurgy in Europe 2007. Selected Papers of the 2nd International Conference 17.-21. June 2007 in Aquileia [CD-ROM]*, Milan: Associazione Italiana di Metallurgia.

Rice, D. W., Peterson, P., Rigby, E. B., Phipps, P. B. P., Cappell, R. J., and Tremoureux, R. (1981): Atmospheric corrosion of copper and silver, *Journal of the Electrochemical Society*, 128, 275–284.

Riederer, J. (2002a): Die Metallanalyse der römischen Statuetten des Römisch-Germanischen Museums in Köln, in A. Giumlia-Mair, ed., *I Bronzi Antichi: Produzione e tecnologia. Atti del XV Congresso Internazionale sui Bronzi Antichi, organizzato dall' Università di Udine, sede di Gorizia, Grado-Aquileia, 22-26 maggio 2001*, Monographies Instrumentum 21, Montagnac: Editions Monique Mergoil, pp. 292–300.

Riederer, J. (2002b): The use of standardised copper alloys in Roman metal technology, in A. Giumlia-Mair, ed., *I Bronzi Antichi: Produzione e tecnologia. Atti del XV Congresso Internazionale sui Bronzi Antichi, organizzato dall' Università di Udine, sede di Gorizia, Grado-Aquileia, 22-26 maggio 2001*, Monographies Instrumentum 21, Montagnac: Editions Monique Mergoil, pp. 284–291.

Robbins, K. and Bayley, J. (1996): *Coin Pellet Mould and Crucible Fragments from Old Sleaford, Lincolnshire*, Ancient Monuments Laboratory Report 69/1996, English Heritage.

Rodriguez, E. C. and Hastorf, C. A. (2013): Calculating ceramic vessel volume: an assessment of methods, *Antiquity*, 87, 1182–1190.

Rodriguez Diaz, A., Pavon Soldevila, I., Merideth, C., and Tresserras, J. J. I. (2001): *El Cerro de San Cristobal, Logrosan, Extremadura, Spain. The Archaeometallurgical Excavation of a Late Bronze Age Tin-Mining and Metalworking Site. First Excavation Season 1998*, BAR international series 922, Oxford: Archaeopress.

Rohl, B. and Needham, S. (1998): *The Circulation of Metal in the British Bronze Age: the Application of Lead Isotope Analysis*, Occasional Paper 102, London: British Museum.

Roman, I. (1990): Copper ingots, in B. Rothenberg, ed., *The Ancient Metallurgy of Copper: Archaeology-Experiment-Theory. (Researches in the Arabah 1959-84; v. 2)*, London: The Institute for Archaeo-Metallurgical Studies, pp. 176–181.

Rose, C. B. and Darbyshire, G., eds. (2012): *The New Chronology of Iron Age Gordion*, Philadelphia, PA: University of Pennsylvania Museum of Archaeology and Anthropology.

Rosenqvist, T. (1974): *Principles of Extractive Metallurgy*, New York: MacGraw-Hill.

Rostoker, W., Pigott, V. C., and Dvorak, J. R. (1989): Direct reduction to copper metal by oxide-sulfide mineral interaction, *Archeomaterials*, 3, 69–87.

Rothe, R. and Rapp, G. Jr. (1995): Trace-element analyses of Egyptian Eastern Desert tin and its importance to Egyptian archaeology, in A. A. A. Hussein, M. Miele, and S. Riad, eds., *Proceedings of the Egyptian-Italian Seminar on the Geosciences and Archaeology in the Mediterranean Countries*, Special Publication 70, Cairo: Geological Survey of Egypt, pp. 229–244.

Rothe, R. D. and Miller, W. K. (1999): More inscriptions from the southern Eastern Desert, *Journal of the American Research Center in Egypt*, 36, 87–101.

Rothe, R. D., Miller, W. K., and Rapp, G. R. (2008): *Pharaonic Inscriptions from the Southern Eastern Desert of Egypt*, Winona Lake, IN: Eisenbrauns.

Rothe, R. D., Rapp, G. Jr., and Miller, W. K. (1996): New hieroglyphic evidence for pharaonic activity in the Eastern Desert of Egypt, *Journal of the American Research Center in Egypt*, 33, 77–104.

Rothenberg, B. (1987): Pharaonic copper mines in South Sinai, *Institute of Archaeo-Metallurgical Studies*, 10-11, 1–7.

Rothenberg, B. (1988): *The Egyptian Mining Temple at Timna*, London: The Institute for Archaeo-Metallurgical Studies.

Rothenberg, B., ed. (1990): *The Ancient Metallurgy of Copper: Archaeology-Experiment-Theory. (Researches in the Arabah 1959-84; v. 2)*, London: The Institute for Archaeo-Metallurgical Studies.

Rothenberg, B. (2003): Egyptian chariots, Midianites from Hijaz/Midian (Northwest Arabia) and Amalekites from the Negev in the Timna Mines, *Institute of Archaeo-Metallurgical Studies*, 23, 9–14.

Rothenberg, B., Shaw, C. T., Hassan, F. A., and Hussein, A. A. A. (1998): Reconnaissance survey of ancient mining and metallurgy in the Mersa Alam region Eastern Desert of Egypt, *Institute of Archaeo-Metallurgical Studies*, 20, 4–9.

Roux, V. (2003): Ceramic standardization and intensity of production: quantifying degrees of specialization, *American Antiquity*, 68, 768–782.

Rovira, S. (2002): Early slags and smelting by-products of copper metallurgy in Spain, in E. Bartelheim, M. Pernicka and R. Krause, eds., *Anfänge der Metallurgie in der Alten Welt / The Beginnings of Metallurgy in the Old World*, Forschungen zur Archäometrie und Altertumswissenschaft 1, Rahden/Westfalen: Verlag Marie Leidorf GmbH, pp. 83–98.

Rovira, S. (2007): La producción de bronces en la prehistoria, in J. Molera, J. Farjas, P. Roura, and T. Pradell, eds., *Avances En Arqueometría. Actas Del VI Congreso Ibérico De Arqueometría 2005*, Girona: Universidad de Girona, pp. 21–35.

Rovira, S. (2011-2012): Arqueometalurgia experimental en el departamento de Prehistoria y Arqueología de la U.A.M., *Cuadernos de Prehistoria y Arqueología Universidad Autónoma de Madrid*, 37-38, 105–120.

Rovira, S. and Montero-Ruiz, I. (2003): Natural tin-bronze alloy in Iberian Peninsula metallurgy: potentiality and reality, in A. Giumlia-Mair and F. Lo Schiavo, eds., *The Problem of Early Tin. Acts of the XIVth UISPP Congress*, BAR International Series 1199, Oxford: Archaeopress, pp. 15–22.

Rovira, S., Montero-Ruiz, I., and Renzi, M. (2009): Experimental co-smelting to copper-tin alloys, in T. L. Kienlin and B. W. Roberts, eds., *Metals and Societies. Studies in Honour of Barbara S. Ottaway*, Universitätsforschungen zur prähistorischen Archäologie, Band 169, Bonn: Habelt, pp. 407–414.

Ryndina, N., Indenbaum, G., and Kolosova, V. (1999): Copper production from polymetallic sulphide ores in the northeastern Balkan Eneolithic culture, *Journal of Archaeological Science*, 26, 1059–1068.

Sabet, A. H., Tsogoev, V. B., Shibanin, S. P., El-Kadi, M.B., and Awad, S. (1976): The placer tin-deposits of Igla, Abu Dabbab and Nuweibi, *Annals of the Geological Survey of Egypt*, 4, 169–180.

Sahlén, D. (2013): Selected with care? - the technology of crucibles in late prehistoric Scotland. A petrographic and chemical assessment, *Journal of Archaeological Science*, 40, 4207–4221.

Said, R. (1990): *The Geology of Egypt*, Elsevier.

Salter, C. (2007): The metallurgical debris, in A. G. Poulter, ed., *Nicopolis ad Istrum. A Late Roman and Early Byzantine City. The Finds and the Biological Remains*, Oxford: Oxbow Books, pp. 298–305.

Salvarredy-Aranguren, M. M., Probst, A., Roulet, M., and Isaure, M.-P. (2008): Contamination of surface waters by mining wastes in the Milluni Valley (Cordillera Real, Bolivia): mineralogical and hydrological influences, *Applied Geochemistry*, 23, 1299–1324.

Sams, G. K. (1979): Imports at Gordion. Lydian and Persian periods, *Expedition*, 21, 6–17.

Sapir-Hen, L. and Ben-Yosef, E. (2014): The socioeconomic status of Iron Age metalworkers: animal economy in the 'Slaves' Hill', Timna, Israel, *Antiquity*, 88, 775–790.

Sayre, E. V., Joel, E. C., Blackman, M. J., Yener, K. A., and Özbal, H. (2001): Stable lead isotope studies of Black Sea Anatolian ore sources and related Bronze Age and Phrygian artefacts from nearby archaeological sites. Appendix: new Central Taurus ore data, *Archaeometry*, 43, 77–115.

Sayre, E. V., Yener, K. A., and Joel, E. C. (1992): Statistical evaluation of the presently accumulated lead isotope data from Anatolia and surrounding regions, *Archaeometry*, 34, 73–105.

Scheel, B. (1985): Studien zum Metallhandwerk in Alten Ägypten I. Handlungen und Beischriften in den Bildprogrammen der Gräber des Alten Reiches, *Studien zur Altägyptischen Kultur*, 12, 117–177.

Scheel, B. (1986): Studien zum Metallhandwerk in Alten Ägypten II. Handlungen und Beischriften in den Bildprogrammen der Gräber des Mittleren Reiches, *Studien zur Altägyptischen Kultur*, 13, 181–205.

Scheel, B. (1987): Studien zum Metallhandwerk in Alten Ägypten III. Handlungen und Beischriften in den Bildprogrammen der Gräber des Neuen Reiches und der Spätzeit, *Studien zur Altägyptischen Kultur*, 14, 247–264.

Scheel, B. (1988): Fundobjecte eines Ptolemäerzeitlichen Metallverarbeitungsstätte in Theben und Verlgeichsfunde anderer Vorderorientalischer Ausgrabungsplätze, *Studien zur Altägyptischen Kultur*, 15, 243–254.

Scheel, B. (1989): *Egyptian Metalworking and Tools*, Shire.

Schneider, G. and Zimmer, G. (1984): Technische Keramik aus antiken Bronzegußwerkstätten in Olympia und Athen, *Berliner Beiträge zur Archäometrie*, 9, 17–60.

Schreiner, M., Heimann, R. B., and Pernicka, E. (2003): Mineralogical and geochemical investigations into prehistoric smelting slags from Tepe Sialk, Central Iran, in *Archaeometallurgy in Europe. International Conference 24.-26. September 2003 Milan, Italy. Proceedings Vol. 1*, Milan: Associazione Italiana di Metallurgia, pp. 487–496.

Schwab, R. (2011): Kupferlegierungen und Kupferverarbeitung im Oppidum auf dem Martberg, *Berichte zur Archäologie an Mittelrhein und Mosel*, 17, 267–285.

Scott, D. A. (1985): Periodic corrosion phenomena in bronze antiquities, *Studies in Conservation*, 30, 49–57.

Scott, D. A. (1991): *Metallography and Microstructure of Ancient and Historic Metals*, The J. Paul Getty Trust.

Scott, D. A. (2012): *Gold and Platinum Metallurgy of Ancient Colombia and Ecuador*, Ancient Metals: Microstructure and Metallurgy, Volume II, Conservation Science Press.

Scott, D. A. (2013): *Iron and Steel*, Ancient Metals: Microstructure and Metallurgy, Volume IV, Conservation Science Press.

Scott, D. A. and Seeley, N. J. (1983): The examination of a pre-hispanic gold chisel from Columbia, *Journal of Archaeological Science*, 10, 153–163.

Seeliger, T. C., Pernicka, E., Wagner, G. A., Begemann, F., Schmitt-Strecker, S., Eibner, C., Öztunali, Ö., and Baranyi, I. (1985): Archaeometallurgische Untersuchungen in Nord- und Ostanatolien, *Jahrbuch des Römisch-Germanischen Zentralmuseums Mainz*, 32, 597–659.

Severin, T., Rehren, Th., and Schleicher, H. (2011): Early metal smelting in Aksum, Ethiopia: copper or iron?, *European Journal of Mineralogy*, 23, 981–992.

Shackley, M. S. (2011): An introduction to X-Ray Fluorescence (XRF) analysis in archaeology, in M. S. Shackley, ed., *X-Ray Fluorescence Spectrometry (XRF) in Geoarchaeology*, Springer Science, pp. 7–44.

Sharp, W. E. and Mittwede, S. K. (1994): Was Kestel really the source of tin for ancient bronze?, *Geoarchaeology: An International Journal*, 9, 155–158.

Shaw, C. T. and Durucan, Ş. (2008): A study of mining methods and ventilation during the Egyptian period at the mines of Timna, in Ü. Yalçin, H. Özbal, and A. G. Paşamehmetoğlu, eds., *Ancient Mining in Turkey and the Eastern Mediterranean*, Ankara: Atilim University, pp. 435–464.

Shaw, I. (1994): Pharaonic quarrying and mining: settlement and procurement in Egypt's marginal regions, *Antiquity*, 68, 108–119.

Shaw, I. (1998): Exploiting the desert frontier. The logistics and politics of ancient Egyptian mining expeditions, in A. B. Knapp, V. C. Pigott, and E. W. Herbert, eds., *Social Approaches to an Industrial Past*, London and New York: Routledge, pp. 242–258.

Sherratt, S. (1998): Sea peoples and the economic structure of the late second millennium in the eastern Mediterranean, in T. K. Dothan, S. Gitin, A. Mazar, and E. Stern, eds., *Mediterranean Peoples in Transition: Thirteenth to Early Tenth Centuries BCE : in Honor of Professor Trude Dothan*, Israel Exploration Society, pp. 292–313.

Sherratt, S. (2000): Circulation of metals and the end of the Bronze Age in the eastern Mediterranean, in C. F. E. Pare, ed., *Metals Make the World Go Round. The Supply and Circulation of Metals in Bronze Age Europe*, Oxford: Oxbow Books, pp. 82–95.

Sherratt, S. (2003): The Mediterranean economy: "globalization" at the end of the second millennium BCE, in W. G. Dever and S. Gitin, eds., *Symbiosis, Symbolism, and the Power of the Past. Canaan, Ancient Israel, and Their Neighbors from the Late Bronze Age through Roman Palaestina. Proceedings of the Centennial Symposium, W.F. Albright Institute of Archaeological Research and American Schools of Oriental Research, Jerusalem, May 29-31, 2000*, Winona Lake, IN: Eisenbrauns, pp. 37–62.

Shortland, A. J. (2006): Application of lead isotope analysis to a wide range of Late Bronze Age Egyptian materials, *Archaeometry*, 48, 657–669.

Shortland, A. J., Tite, M. S., and Ewart, I. (2006): Ancient exploitation and use of cobalt alums from the Western Oases of Egypt, *Archaeometry*, 45, 153–168.

Shugar, A. (2009): Peaking your interest: an introductory explanation of how to interpret XRF data, *WAAC Newsletter*, 31, 8–10.

Shugar, A. N. (2013): Portable X-ray fluorescence and archaeology: limitations of the instrument and suggested methods to achieve desired results, in R. A. Armitage and J. H. Burton, eds., *Archaeological Chemistry VIII*, Washington, DC: American Chemical Society, pp. 173–193.

Sillar, B. and Tite, M. S. (2000): The challenge of 'technological choices' for materials science approaches in archaeology, *Archaeometry*, 42, 2–20.

Skaggs, S., Norman, N., Garrison, E., Coleman, D., and Bouhlel, S. (2012): Local mining or lead importation in the Roman province of Africa Proconsularis? Lead isotope analysis of curse tablets from Roman Carthage, Tunisia, *Journal of Archaeological Science*, 39, 970–983.

Skarpelis, N. (2003): Potential tin sources in the Aegean, in A. Giumlia-Mair and F. Lo Schiavo, eds., *The Problem of Early Tin. Acts of the XIVth UISPP Congress*, BAR International Series 1199, Oxford: Archaeopress, pp. 159–164.

Slokoska, L. (2002): A century of archaeological excavations in Nicopolis ad Istrum, in L. Slokoska, R. T. Ivanov, and V. Dinchev, eds., *The Roman and Late Roman City. The International Conference, Veliko Turnovo, 26-30 July 2000*, Sofia: Prof. Marin Drinov Academic Publishing House, pp. 9–13.

Smirniou, M. and Rehren, Th. (2011): Direct evidence of primary glass production in Late Bronze Age Amarna, Egypt, *Archaeometry*, 53, 58–80.

Smirniou, M. and Rehren, Th. (2013): Shades of blue - cobalt-copper coloured blue glass from New Kingdom Egypt and the Mycenaean world: a matter of production or colourant source?, *Journal of Archaeological Science*, 40, 4731–4743.

Speakman, R. J. and Shackley, M. S. (2013): Silo science and portable XRF in archaeology: a response to Frahm, *Journal of Archaeological Science*, 40, 1435–1443.

Stacey, J. S. and Kramers, J. D. (1975): Approximation of terrestrial lead isotope evolution by a two-stage model, *Earth and Planetary Science Letters*, 26, 207–221.

Staddon, C. and Mollov, B. (2000): City profile: Sofia, Bulgaria, *Cities*, 17, 379–387.

Stanley, D. J., Sheng, H., and Pan, Y. (1988): Heavy minerals and provenance of Late Quaternary sands, eastern Nile delta, *Journal of African Earth Sciences*, 7, 735–741.

Stevens, A. and Eccleston, M. A. J. (2007): Craft production and technology, in T. Wilkinson, ed., *The Egyptian World*, London: Routledge, pp. 146–159.

Stos, Z. A. (2009): Across the wine dark seas... sailor tinkers and royal cargoes in the Late Bronze Age eastern Mediterranean, in A. J. Shortland, I. C. Freestone, and Th. Rehren, eds., *From Mine to Microscope. Advances in the Study of Ancient Technology*, Oxford: Oxbow Books, pp. 163–180.

Stos, Z. A. and Gale, N. H. (2006): Lead isotope and chemical analyses of slags from Chrysokamino, in P. P. Betancourt, ed., *The Chrysokamino Metallurgy Workshop and Its Territory*, Hesperia Supplements 36, The American School of Classical Studies at Athens, pp. 229–319.

Stos-Gale, Z. A. (2011): "Biscuits with ears": a search for the origin of the earliest oxhide ingots, in P. P. Betancourt and S. C. Ferrence, eds., *Metallurgy: Understanding How, Learning Why. Studies in Honor of James D. Muhly*, Philadelphia, PA: INSTAP Academic Press, pp. 221–229.

Stos-Gale, Z. A. and Gale, N. H. (2009): Metal provenancing using isotopes and the Oxford archaeological lead isotope database (OXALID), *Archaeological and Anthropological Sciences*, 1, 195–213.

Stos-Gale, Z. A. and Gale, N. H. (2010): Bronze Age metal artefacts found on Cyprus - metal from Anatolia and the western Mediterranean, *Trabajos de Prehistoria*, 67, 389–403.

Stos-Gale, Z. A., Gale, N. H., and Houghton, J. (1995): The origins of Egyptian copper: lead-isotope analysis of metals from el-Amarna, in V. W. Davies and L. Schofield, eds., *Egypt, the Aegean and the Levant: Interconnections in the Second Millennium BC*, London: British Museum Press, pp. 127–135.

Stos-Gale, Z. A., Maliotis, G., Gale, N.H., and Annetts, N. (1997): Lead isotope characteristics of the Cyprus copper ore deposits applied to provenance studies of copper oxhide ingots, *Archaeometry*, 39, 83–123.

Swenson, E. R. and Warner, J. P. (2012): Crucibles of power: forging copper and forging subjects at the Moche ceremonial center of Huaca Colorada, Peru, *Journal of Anthropological Archaeology*, 31, 314–333.

Tallet, P. (2012): Ayn Sukhna and Wadi el-Jarf: two newly discovered pharaonic harbours on the Suez Gulf, *British Museum Studies in Ancient Egypt and Sudan*, 18, 147–168.

Tallet, P., Castel, G., and Fluzin, P. (2011): Metallurgical sites of south Sinai (Egypt) in the pharaonic era: new discoveries, *Paléorient*, 37, 79–89.

Taylor, J. W. (1982): A Nigerian tin trade in antiquity?, *Oxford Journal of Archaeology*, 1, 317–324.

Taylor, J. W. (1983): Erzgebirge tin: a closer look, *Oxford Journal of Archaeology*, 2, 295–298.

Thompson, C. M. (2003): Sealed silver in Iron Age Cisjordan and the 'invention' of coinage, *Oxford Journal of Archaeology*, 22, 67–107.

Thompson, C. M. (2006): Slag analysis by wavelength dispersive spectrometry, in P. P. Betancourt, ed., *The Chrysokamino Metallurgy Workshop and Its Territory*, Hesperia Supplements 36, The American School of Classical Studies at Athens, pp. 325–328.

Thorburn, W. M. (1918): The myth of Occam's Razor, *Mind*, 27, 345–353.

Thornton, C. P., Lamberg-Karlovsky, C. C., Liezers, M., and Young, S. M. M. (2002): On pins and needles: tracing the evolution of copper-base alloying at Tepe Yahya, Iran, via ICP-MS analysis of common-place items, *Journal of Archaeological Science*, 29, 1451–1460.

Thornton, C. P. and Rehren, Th. (2009): A truly refractory crucible from fourth millennium Tepe Hissar, northeast Iran, *Journal of Archaeological Science*, 36, 2700–2712.

Timberlake, S. (1994): An experimental tin smelt at Flag Fen, *Historical Metallurgy*, 28, 121–128.

Tisseyre, P., Tusa, S., Cairns, W. R. L., Selvaggio Battacin, F., Barbante, C., Ciriminna, R., and Pagliaro, M. (2008): The lead ingots of Capo Passero: Roman global Mediterranean trade, *Oxford Journal of Archaeology*, 27, 315–323.

Tite, M. S. (1996): In defence of lead isotope analysis, *Antiquity*, 70, 959–962.

Tite, M. S., Freestone, I. C., Meeks, N. D., and Bimson, M. (1982): The use of scanning electron microscopy in the technological analysis of ancient ceramics, in J. S. Olin and A. D. Franklin, eds., *Archaeological Ceramics*, Washington, D.C.: Smithsonian Institution Press, pp. 109–120.

Tite, M. S., Freestone, I. C., Meeks, N. D., and Craddock, P. T. (1985): The examination of refractory ceramics from metal-production and metalworking sites, in P. Phillips, ed., *The Archaeologist and the Laboratory*, London: Council for British Archaeology, pp. 50–55.

Tite, M. S., Kilikoglou, V., and Vekinis, G. (2001): Strength, toughness and thermal shock resistance of ancient ceramics and their influence on technological choice, *Archaeometry*, 43, 301–324.

Tite, M. S. and Shortland, A. J. (2003): Production technology for copper- and cobalt-blue vitreous materials from the New Kingdom site of Amarna - a reappraisal, *Archaeometry*, 45, 285–312.

Trincherini, P. R., Domergue, C., Manteca, I., Nesta, A., and Quarati, P. (2009): The identification of lead ingots from the Roman mines of Cartagena (Murcia, Spain): the role of lead isotope analysis, *Journal of Roman Archaeology*, 22, 123–145.

Troalen, L. G., Tate, J., and Guerra, M. F. (2014): Goldwork in ancient Egypt: workshop practices at Qurneh in the 2nd Intermediate Period, *Journal of Archaeological Science*, 50, 219–226.

Tylecote, R. F. (1979): Early tin ingots and tinstone from Western Europe and the Mediterranean, in A. D. Franklin, J. S. Olin, and T. A. Wertime, eds., *The Search for Ancient Tin: a Seminar organized by Theodore A. Wertime and held at the Smithsonian Institution and the National Bureau of Standards, Washington, D.C., March 14-15, 1977*, Washington, D.C.: Smithsonian Institution Press, pp. 49–52.

Tylecote, R. F. (1982a): The Late Bronze Age: copper and bronze metallurgy at Enkomi and Kition, in J. D. Muhly, R. Maddin, and V. Karageorghis, eds., *Early Metallurgy in Cyprus, 4000-500 BC*, Nicosia: Pierides Foundation, pp. 81–103.

Tylecote, R. F. (1982b): Metallurgical crucibles and crucible slags, in J. S. Olin and A. D. Franklin, eds., *Archaeological Ceramics*, Washington, D.C.: Smithsonian Institution Press, pp. 231–243.

Tylecote, R. F. (1986): *The Prehistory of Metallurgy in the British Isles. 2nd edition.*, London: The Institute of Metals.

Tylecote, R. F. and Bachmann, H.-G. (1990): Metallographic notes on some ingots from the Arabah and Sinai, in B. Rothenberg, ed., *The Ancient Metallurgy of Copper: Archaeology-Experiment-Theory. (Researches in the Arabah 1959-84; v. 2)*, London: The Institute for Archaeo-Metallurgical Studies, pp. 74–77.

Tylecote, R. F., Ghaznavi, H. A., and Boydell, P. J. (1977): Partitioning of trace elements between the ores, fluxes, slags and metal during the smelting of copper, *Journal of Archaeological Science*, 4, 305–333.

Tylecote, R. F., Photos, E., and Earl, B. (1989): The composition of tin slags from the South-West of England, *World Archaeology*, 20, 434–445.

Unglik, H. (1991): Structure, composition, and technology of Late Roman copper alloy artifacts from the Canadian excavations at Carthage, *Archeomaterials*, 5, 91–110.

Uphill, E. P. (2001): *Egyptian Towns and Cities*, Shire.

Vagalinski, L. F. (2011): Light industry in Roman Thrace: the case of lime production, in I. P. Haynes, ed., *Early Roman Thrace. New Evidence from Bulgaria*, JRA Supplementary Series 82, Portsmouth, Rhode Island, pp. 41–58.

Valério, P., Monge Soares, A. M., Silva, R. J. C., Araújo, M. F., Rebelo, P., Neto, N., Santos, R., and Fontes, T. (2013): Bronze production in southwestern Iberian Peninsula: the Late Bronze Age metallurgical workshop from Entre Águas 5 (Portugal), *Journal of Archaeological Science*, 40, 439–451.

Valério, P., Silva, R. J. C., Araújo, M. F., Monge Soares, A. M., and Braz Fernandes, F. M. (2010): Microstructural signatures of bronze archaeological artifacts from the southwestern Iberian Peninsula, *Materials Science Forum*, 636-637, 597–604.

Van De Mieroop, M. (2007): *The Eastern Mediterranean in the Age of Ramesses II*, Oxford: Blackwell Publishing.

Vassileva, M. (2012): Early bronze fibulae and belts from the Gordion citadel mound, in C. B. Rose, ed., *The Archaeology of Phrygian Gordion, Royal City of Midas*, Philadelphia, PA: University of Pennsylvania Museum of Archaeology and Anthropology, pp. 111–126.

VDEh, Verein Deutscher Eisenhüttenleute, ed. (1995): *Slag Atlas. 2nd Edition*, Düsseldorf: Verlag Stahleisen.

Vergilius, P. (2009): *Georgics*, Oxford: Oxford University Press.

Voigt, M. M. (2012): Human and animal sacrifice at Galatian Gordion: the uses of ritual in a multiethnic community, in A. Porter and G. Schwartz, eds., *Sacred Killing: the Archaeology of Sacrifice in the Ancient Near East*, Winona Lake, Indiana: Eisenbrauns, pp. 235–288.

Voigt, M. M. and Young, T. C. Jr. (1999): From Phrygian capital to Achaemenid entrepot: Middle and Late Phrygian Gordion, *Iranica Antiqua*, 34, 191–241.

Vollmer, R. (1977): Terrestrial lead isotope evolution and formation time of the Earth's core, *Nature*, 270, 144–147.

Wagner, G. A., Begemann, F., Eibner, C., Lutz, J., Öztunali, Ö., Pernicka, E., and Schmitt-Strecker, S. (1989): Archäometallurgischer Untersuchungen an Rohstoffquellen des frühen Kupfers Ostanatoliens, *Jahrbuch des Römisch-Germanischen Zentralmuseums Mainz*, 36, 637–686.

Wagner, G. A., Pernicka, E., Seeliger, T. C., Öztunali, Ö., Baranyi, I., Begemann, F., and Schmitt-Strecker, S. (1985): Geologische Untersuchungen zur Fruhen Metallurgie in NW-Anatolien, *Bulletin of the Mineral and Exploration Institute of Turkey*, 100-101, 45–81.

Wagner, G. A., Wagner, I., Öztunali, Ö., Schmitt-Strecker, S., and Begemann, F. (2003): Archäometallurgischer Bericht über Feldforschung in Anatolien und bleiisotopische Studien an Erzen und Schlacken, in T. Stöllner, G. Körlin, G. Steffens, and J. Cierny, eds., *Man and Mining (Mensch und Bergbau)*, Der Anschnitt, Beiheft 16, Bochum: Deutsches Bergbau-Museum, pp. 475–494.

Warburton, D. A. (2010): The Egyptian economy: sources, models and history, in A. Hudecz and M. Petrik, eds., *Commerce and Economy in Ancient Egypt. Proceedings of the Third International Congress for Young Egyptologists 25-27 September 2009, Budapest*, BAR S2131, Oxford: Archaeopress, pp. 71–79.

Watt, I. M. (1997): *The Principles and Practice of Electron Microscopy*, Cambridge: Cambridge University Press.

Watterson, B. (1992): *Calvin and Hobbes*, Universal Press Syndicate.

Wayman, M. L., Gualtieri, M., and Konzuk, R. A. (1988): Bronze metallurgy at Roccagloriosa, in R. M. Farquhar, R. G. V. Hancock, and L. A. Pavlish, eds., *Proceedings of the 26th International Archaeometry Symposium, Toronto*, Toronto: The Archaeometry Laboratory, pp. 128–132.

Wayman, M. L., Smith, R. R., Hickey, C. G., and Duke, M. J. M. (1985): The analysis of copper artifacts of the Copper Inuit, *Journal of Archaeological Science*, 12, 367–375.

Wedepohl, K. H. and Simon, K. (2010): The chemical composition of medieval wood ash glass from Central Europe, *Chemie der Erde*, 70, 89–97.

Wedepohl, K. H., Simon, K., and Kronz, A. (2011): Data on 61 chemical elements for the characterization of three major glass compositions in late antiquity and the Middle Ages, *Archaeometry*, 53, 81–102.

Weeks, L. (2003): *Early Metallurgy of the Persian Gulf*, American School of Prehistoric Research Monograph Series 2, Boston/Leiden: Brill Academic Publishers, Inc.

Wertime, T. A. (1979): The search for ancient tin: the geographic and historic boundaries, in A. D. Franklin, J. S. Olin, and T. A. Wertime, eds., *The Search for Ancient Tin: a Seminar organized by Theodore A. Wertime and held at the Smithsonian Institution and the*

National Bureau of Standards, Washington, D.C., March 14-15, 1977, Washington, D.C.: Smithsonian Institution Press, pp. 1–6.

Wilkinson, R. H. (1994): *Symbol and Magic in Egyptian Art*, London: Thames and Hudson.

Wood, N. (2009): Some implications of the use of wood ash in Chinese stoneware glazes, in A. J. Shortland, I. C. Freestone, and Th. Rehren, eds., *From Mine to Microscope. Advances in the Study of Ancient Technology*, Oxford: Oxbow Books, pp. 51–60.

Yahalom-Mack, N., Galili, E., Segal, I., Eliyahu-Behar, A., Boaretto, E., Shilstein, S., and Finkelstein, I. (2014): New insights into Levantine copper trade: analysis of ingots from the Bronze and Iron Ages in Israel, *Journal of Archaeological Science*, 45, 159–177.

Yalçin, Ü., Pulak, C., and Slotta, R., eds. (2005): *Das Schiff von Uluburun. Welthandel vor 3000 Jahren*, Bochum: Deutsches Bergbau-Museum.

Yamazaki, E., Nakai, S., Sahoo, Y., Yokoyama, T., Mifune, H., Saito, T., Chen, J., Takagi, N., Hokanishi, N., and Yasuda, A. (2014): Feasibility studies of Sn isotope composition for provenancing ancient bronzes, *Journal of Archaeological Science*, 52, 458–467.

Yener, K. A. (2000): *The Domestication of Metals: The Rise of Complex Metal Industries in Anatolia*, Leiden: Brill.

Yener, K. A. (2009): Strategic industries and tin in the ancient Near East: Anatolia updated, *Turkiye Bilimler Akademisi Arkeoloji Dergisi (TUBA-AR). Turkish Academy of Sciences Journal of Archaeology*, 12, 143–154.

Yener, K. A., Adriaens, A., Earl, B., and Özbal, H. (2003): Analysis of metalliferous residues, crucible fragments, experimental smelts, and ores from Kestel tin mine and the tin processing site of Göltepe, Turkey, in P. T. Craddock and J. Lang, eds., *Mining and Metal Production. Through the Ages*, London: British Museum Press, pp. 181–197.

Yener, K. A. and Earl, B. (1994): Replication experiments of tin using crucibles, Göltepe 1992, *Arkeometri Sonuçlari Toplantisi*, 9, 163–176.

Yener, K. A., Sayre, E. V., Joel, E. C., Özbal, H., Barnes, I. L., and Brill, R. H. (1991): Stable lead isotope studies of Central Taurus ore sources and related artifacts from eastern Mediterranean Chalcolithic and Bronze Age sites, *Journal of Archaeological Science*, 18, 541–577.

Yener, K. A. and Vandiver, P. B. (1993): Tin processing at Göltepe, an Early Bronze Age site in Anatolia, *American Journal of Archaeology*, 97, 207–238.

Yener, K. A., Özbal, H., Kaptan, E., Pehlivan, A. N., and Goodway, M. (1989): Kestel: an Early Bronze Age source of tin ore in the Taurus Mountains, Turkey, *Science*, 224, 200–203.

Yi, W., Budd, P., McGill, R. A. R., Young, S. M. M., Halliday, A. N., Haggerty, R., Scaife, B., and Pollard, A. M. (1999): Tin isotope studies of experimental and prehistoric bronzes, in A. Hauptmann, E. Pernicka, Th. Rehren, and Ü. Yalçin, eds., *The Beginnings of Metallurgy*, Bochum: Deutsches Bergbau-Museum, pp. 285–290.

Young, R. S. (1958): Bronzes from Gordion's Royal Tomb, *Archaeology*, 11, 227–231.

Young, R. S. (1963): Gordion on the Royal Road, *Proceedings of the American Philosophical Society*, 107, 348–364.

Zhou, W., Chen, J., Lei, X., Xu, T., Chong, J., and Wang, Z. (2009): Three Western Zhou bronze foundry sites in the Zhouyuan area, Shaanxi province, China, in J. Mei and Th. Rehren, eds., *Metallurgy and Civilisation. Eurasia and Beyond*, London: Archetype Publications, pp. 62–72.

Zori, C., Tropper, P., and Scott, D. (2013): Copper production in late prehispanic northern Chile, *Journal of Archaeological Science*, 40, 1165–1175.

Zwicker, U. (1982): Bronze Age metallurgy at Ambelikou-Aletri and arsenical copper in a crucible from Episcopi-Phaneromeni, in J. D. Muhly, R. Maddin, and V. Karageorghis, eds., *Early Metallurgy in Cyprus, 4000-500 BC*, Nicosia: Pierides Foundation, pp. 63–68.

Zwicker, U. (1984): Metallographische und analytische Untersuchungen an Proben aus den Grabungen der Bronzegießerei in der Phidias-Werkstatt von Olympia und Versuche zum Schmelzen von Bronze in flachen Tiegeln, *Berliner Beiträge zur Archeometrie*, 9, 61–94.

Zwicker, U., Constantinou, G., Buchholz, H. G., and Karageorghis, V. (1981): Investigation on ore, flux and crucible slag from prehistoric copper smelting at Ambelikou, Cyprus, *Revue d'Archéométrie. Bulletin de Liaison du Groupe des Méthodes Physiques et Chimiques de l'Archéologie Rennes. Actes du XX Symposium International d'Archéométrie, Paris 26-29 mars 1980*, 3, 331–340.

Zwicker, U. and Goudarzloo, F. (1979): Investigation on the distribution of metallic elements in copper slag, copper matte and copper and comparison with samples from prehistoric smelting places, in *Proceedings of the 18th International Symposium on Archaeometry and Archaeological Prospection, Bonn, 14-17 March 1978*, Archaeo-Physika Band 10, Köln: Rheinland-Verlag GmbH, pp. 360–375.

Zwicker, U., Greiner, H., Hoffman, K.-H., and Reithinger, M. (1985): Smelting, refining and alloying of copper and copper alloys in crucible furnaces during prehistoric up to Roman times, in P. T. Craddock and M. J. Hughes, eds., *Furnaces and Smelting Technology in Antiquity*, Occasional Paper 48, London: British Museum, pp. 103–115.

Zwicker, U., Grembler, E., and Rollig, H. (1977): Investigations of copper-slags from Cyprus (second report), *Report of the Department of Antiquities Cyprus*, 310–316.

Zwicker, U., Virdis, P., and Ceruti, M. L. (1980): Investigations on copper ore, prehistoric copper slag and copper ingots from Sardinia, in P. T. Craddock, ed., *Scientific Studies in Early Mining and Extractive Metallurgy*, Occasional Paper 20, London: British Museum, pp. 135–163.

Methodology Appendices

APPENDIX A

SEM-EDS analysis of CRM

A number of certified reference materials have been analysed by SEM-EDS (area analysis at 800X, all other machine settings as discussed in section 3.3.4) to assess accuracy and precision. Two basalts, a clay and a burnt refractory have been tested as comparative materials for the crucibles' ceramic fabric. Metal CRM's have been analysed to compare to metallic phases in the crucible slag. Glass standards have been tested as a comparative material for the crucible slag.

Section A.1

Basalt

The results for the analysis of two basalt reference materials (fused to glasses, mounted in resin, ground and polished) are presented in Tables A.1 and A.2. Both basalts are provided by the United States Geological Survey.

For both reference materials, the measurement precision is very good (coefficient of variation below 10% for all oxides, below 5% for most), as is the accuracy (relative error below 10% for all oxides, below 5% for most).
Low levels of phosphorus and manganese oxide are not measured.

Oxide compositions in wt%

	Na_2O	MgO	Al_2O_3	SiO_2	K_2O	CaO	TiO_2	FeO	Total
Measurement 1	2.17	7.03	13.11	50.06	0.54	11.51	2.64	11.15	98.21
Measurement 2	2.34	7.19	12.71	49.63	0.52	11.79	2.90	11.38	98.46
Measurement 3	2.35	7.37	13.01	50.52	0.57	11.51	2.90	10.95	99.16
Measurement 4	2.26	7.33	12.83	50.02	0.54	11.52	2.93	11.41	98.84
Measurement 5	2.73	7.28	13.06	51.07	0.48	11.78	2.73	11.17	100.31
Measurement 6	2.41	7.78	13.09	51.09	0.53	11.42	2.81	11.18	100.30
Average normalised data	**2.41**	**7.11**	**13.10**	**50.94**	**0.54**	**11.72**	**2.85**	**11.34**	**100**
Standard deviation	0.17	0.20	0.15	0.23	0.03	0.19	0.12	0.22	0
Coefficient of variation (%)	**7.25**	**2.80**	**1.18**	**0.46**	**5.86**	**1.64**	**4.20**	**1.96**	**0**
Reference values	2.22	7.23	13.50	49.90	0.52	11.40	2.73	11.07	98.57
Normalised reference values	**2.25**	**7.33**	**13.70**	**50.62**	**0.53**	**11.57**	**2.77**	**11.23**	**100**
Absolute error	-0.16	0.23	0.60	-0.31	-0.01	-0.16	-0.08	-0.11	
Relative error (%)	**-6.89**	**3.10**	**4.35**	**-0.62**	**-1.65**	**-1.38**	**-2.96**	**-0.96**	

Table A.1: BHVO-2: Basalt, Hawaiian Volcanic Observatory. *Not measured: 0.27 wt% P_2O_5, 0.17 wt% MnO and trace elements (F, V, Cr, Cu, Zn, Sr, Zr, Ba)*

Oxide compositions in wt%

	Na_2O	MgO	Al_2O_3	SiO_2	K_2O	CaO	TiO_2	FeO	Total
Measurement 1	3.28	3.66	12.91	55.27	1.79	7.30	2.32	12.54	99.07
Measurement 2	3.25	3.85	13.04	55.50	1.87	7.13	2.32	12.61	99.56
Measurement 3	3.21	3.43	12.84	54.67	1.89	7.30	2.50	12.54	98.37
Measurement 4	3.14	3.69	12.72	55.16	1.71	7.32	2.24	12.43	98.41
Measurement 5	3.32	3.81	13.02	55.06	1.77	7.33	2.20	12.75	99.28
Measurement 6	3.56	3.77	12.72	55.75	1.70	7.15	2.43	12.15	99.24
Average normalised data	**3.33**	**3.59**	**13.02**	**55.88**	**1.81**	**7.34**	**2.37**	**12.65**	**100**
Standard deviation	0.14	0.13	0.11	0.28	0.08	0.12	0.12	0.21	0
Coefficient of variation (%)	**4.20**	**3.72**	**0.86**	**0.49**	**4.30**	**1.59**	**4.98**	**1.64**	**0**
Reference values	3.16	3.59	13.50	54.10	1.79	7.12	2.26	12.42	97.94
Normalised reference values	**3.23**	**3.67**	**13.78**	**55.24**	**1.83**	**7.27**	**2.31**	**12.68**	**100**
Absolute error	-0.11	0.08	0.76	-0.64	0.02	-0.07	-0.06	0.02	
Relative error (%)	**-3.36**	**2.14**	**5.53**	**-1.16**	**0.93**	**-1.03**	**-2.49**	**0.19**	

Table A.2: BCR-2: Basalt, Columbia River, Oregon. *Not measured: 0.35 wt% P_2O_5, 0.20 wt% MnO and trace elements (F, V, Cr, Cu, Zn, Sr, Zr, Mo, Ba)*

Section A.2

Clay and ceramic

The results for the analysis of one clay and one burnt refractory reference material (pressed powder discs, no resin, not polished) are presented in Tables A.3 and A.4 respectively. The clay is provided by the China National Analysis Centre, while the burnt refractory is provided by the National Institute of Standards and Technology.

For both, the measurement precision is quite good (coefficient of variation below 10%), with the exception of TiO_2 (below 15%) in the clay and MgO in the burnt refractory. The accuracy, however, is quite problematic. For the clay, measurement of MgO, Al_2O_3, K_2O, CaO, TiO_2 and FeO differ more than 10% from the reference values. For the burnt refractory, results are better, though measurement of FeO differs strongly from the reference values.
Low levels of sodium, phosphorus, sulphur, calcium and manganese oxide, and chlorine, lithium and strontium are not measured.

These poor results are quite surprising (in light of the good results for all other reference materials) and probably reflect the use of powder samples for analysis (which results in low totals: ±82.6% and ±86.3% respectively). For the clay, there appears to be a dilution effect: lowered silica (6 wt%) could give rise to enrichment in most other oxides. For both cases, however, there appears to be a significant overestimation of iron content.

Oxide compositions in wt%

	Na_2O	MgO	Al_2O_3	SiO_2	K_2O	CaO	TiO_2	FeO	Total
Measurement 1	1.53	2.15	13.77	53.66	2.62	3.19	0.71	5.18	82.82
Measurement 2	1.62	2.09	13.24	53.29	2.65	3.36	0.70	4.92	81.87
Measurement 3	1.38	2.37	13.53	53.34	2.73	3.55	0.67	5.32	82.90
Measurement 4	1.54	2.12	13.17	53.09	2.58	3.29	0.47	5.17	81.43
Measurement 5	1.64	2.16	14.15	54.21	2.62	3.16	0.60	4.59	83.12
Measurement 6	1.52	2.13	13.59	53.38	2.68	3.58	0.62	4.82	82.34
Measurement 7	1.46	2.23	13.97	53.68	2.74	3.49	0.70	5.37	83.64
Average of normalised data	**1.85**	**2.64**	**16.51**	**64.81**	**3.22**	**4.08**	**0.77**	**6.12**	**100**
Standard deviation	0.11	0.10	0.31	0.41	0.06	0.21	0.10	0.34	0
Coefficient of variation (%)	**6.11**	**3.90**	**1.86**	**0.63**	**1.87**	**5.04**	**13.32**	**5.56**	**0**
Reference values	1.81	1.84	13.28	66.64	2.50	3.23	0.66	4.17	94.13
Normalised reference values	**1.92**	**1.95**	**14.11**	**70.80**	**2.66**	**3.43**	**0.70**	**4.43**	**100**
Absolute error	0.07	-0.68	-2.40	5.99	-0.57	-0.65	-0.07	-1.69	
Relative error (%)	**3.86**	**-34.91**	**-17.01**	**8.46**	**-21.40**	**-19.03**	**-10.23**	**-38.08**	

Table A.3: Clay DC60105 (China National Analysis Centre). *Not measured: 0.11 wt% P_2O_5, 0.03 wt% SO_3, 0.09 wt% MnO and 0.01 wt% Cl*

Oxide compositions in wt%

	MgO	Al_2O_3	SiO_2	K_2O	TiO_2	FeO	Total
Measurement 1	0.44	32.08	47.32	1.26	1.92	1.85	84.88
Measurement 2	0.29	32.23	47.96	1.30	2.18	1.78	85.73

Oxide compositions in wt%

	MgO	Al_2O_3	SiO_2	K_2O	TiO_2	FeO	Total
Measurement 3	0.50	33.08	49.18	1.22	2.06	1.66	87.70
Measurement 4	0.38	32.96	49.08	1.11	1.74	1.55	86.82
Measurement 5	0.41	33.05	48.71	1.29	2.00	1.42	86.89
Measurement 6	0.50	32.91	47.69	1.20	1.76	1.65	85.71
Average of normalised data	**0.49**	**37.92**	**56.00**	**1.43**	**2.25**	**1.92**	**100**
Standard deviation	0.09	0.28	0.31	0.09	0.20	0.19	0
Coefficient of variation (%)	**19.17**	**0.75**	**0.55**	**6.07**	**8.66**	**10.06**	**0**
Reference values	0.52	38.70	54.90	1.33	2.03	1.44	98.92
Normalised reference values	**0.53**	**39.12**	**55.50**	**1.34**	**2.05**	**1.46**	**100**
Absolute error	0.04	1.20	-0.50	-0.08	-0.20	-0.46	
Relative error (%)	**7.42**	**3.08**	**-0.91**	**-5.99**	**-9.80**	**-31.69**	

Table A.4: NIST 76a: Burnt Refractory. *Not measured: 0.07 wt% Na_2O, 0.12 wt% P_2O_5, 0.22 wt% CaO, 0.02 wt% Li and 0.03 wt% Sr*

Section A.3

Metal

Four metal CRM's (mounted in resin, ground and polished) have been analysed. As no pure tin-bronze reference materials were available, a group of (leaded) bronzes and brass was used. This matches some of the prills measured in the Gordion and Roman samples, but not those of Pi-Ramesse (mostly unleaded bronze). No cobalt-bearing copper alloys, similar to prills encountered in some Pi-Ramesse crucibles, and no silver-rich alloys, matching the composition of some Gordion prills, were available either. The results for the analysis of the four metal reference materials are presented in Tables A.5, A.6, A.7 and A.8. All samples are provided by the Bureau of Analysed Samples.

The measurements of CURM 42.23-2 (brass) show fairly good precision (coefficient of variation below 10% for all major elements, though high for iron and lead, present at low levels) and good accuracy (relative error below 5% for all elements, except for lead, present at low levels). This indicates that low levels of lead (in brass) are difficult to measure and low levels of iron (in brass) are measured, but not precisely.
Low levels of phosphorus, sulphur, nickel, arsenic, antimony, aluminium, silicon, manganese and bismuth are not measured.

The (15!) measurements of CURM 50.01-4 (leaded bronze) show good precision (coefficient of variation below 10%) for copper, tin and nickel, but poor precision for zinc and lead (present at significant levels), iron, arsenic and antimony (present at lower levels) and phosphorus and sulphur (light elements, present at low levels). The accuracy is slightly better, with copper, iron, nickel and zinc at acceptable levels, while tin, antimony, lead, arsenic, phosphorus and sulphur show poor accuracy.

Looking at these 15 measurements in more detail, it becomes clear that lead is the main problem influencing these measurements: the lead, which forms an undissolved phase in the bronze, has a tendency to be pulled out of the sample surface during polishing, lowering the overall lead content of the sample. This gives rise to a low precision in the measurements (as some areas of analysis contain lead phases while lead has been removed in others) and an average underestimation (±30%) of the lead content. Tin, the other main alloy component, is measured more precisely, but consistently overestimated (±13%, which is not entirely unacceptable).
Low levels of aluminium, silicon, manganese and bismuth are not measured.

The measurements of CURM 50.04-4 (leaded bronze) show good precision (coefficient of variation below 10%) for copper and tin, but poor precision for lead (the other main alloy constituent), arsenic and antimony (present at low levels), nickel (present at significant levels, precision is not entirely unacceptable (coefficient of variation below 15%)) and sulphur (light element, present at low levels). The accuracy is equally poor, with copper (and arsenic) showing relative errors below 10%, while lead is again underestimated by ±30%, tin is overestimated by ±12%, antimony and nickel are ±15% off and sulphur is far off.
These results correspond to those seen for CURM 50.01-4: the lowering effect of polishing on lead content and the overestimation of tin content.
Low levels of phosphorus, iron, zinc, aluminium, silicon, manganese and bismuth are not measured.

The measurements of CURM 71.32.4 (leaded gunmetal) show good precision for copper, zinc and tin (coefficient of variation below 5-10%), but poor precision for lead (similar to the previous cases), nickel (though below 15%, not entirely unacceptable), iron and arsenic (present at low levels). Accuracy is slightly better here, with relative errors below 10% for copper, nickel, zinc and tin, below 15% for iron and arsenic and the (by now) typical underestimation of ±30% for lead.
Low levels of phosphorus, sulphur, antimony, aluminium, silicon, manganese, bismuth, chromium and silver are not measured.

In conclusion, it appears that lead has a strong influence on the measurement of bronzes and brasses. Lead is not measured precisely and it is consistently underestimated. Furthermore, it appears to impact the measurement of tin: though it is measured precisely, the accuracy of its measurement seems to be lowered by the presence of lead (though not to entirely unacceptable levels). A comparison of results for CURM 42.23-2 and 71.32.4 (low lead) to CURM 50.01-4 and 50.04-4 (high lead) supports this idea.
Iron and nickel can be measured fairly accurately at levels down to ±0.5 wt%, though not

always with great precision. Arsenic can similarly be measured at levels down to ±0.5 wt%, though with more problematic precision. For zinc and antimony, levels below ±0.6-0.7 wt% are not detected, while higher levels were detected with poor to fair precision. Light elements like sulphur and phosphorus present more difficulty when present at low levels. All in all, it appears that a detection limit of ±0.5 wt% seems to apply for most elements present in copper. The accuracy of the measurement is quite good, though care must be taken when significant amounts of lead are present.

Elemental compositions in wt%

	Fe	Cu	Zn	Sn	Pb	Total
Measurement 1	0.25	73.96	21.97	1.56	0.01	97.75
Measurement 2	0.39	74.00	22.07	1.67	0.29	98.43
Measurement 3	0.24	74.65	21.35	1.39	0.33	97.97
Measurement 4	0.47	74.24	21.37	1.56	0.41	98.05
Measurement 5	0.35	73.79	21.18	1.83	0.13	97.28
Measurement 6	0.37	73.69	21.68	1.72	0.72	98.17
Measurement 7	0.27	73.73	21.27	1.86	0.59	97.71
Measurement 8	0.40	74.31	20.83	1.46	0.13	97.12
Measurement 9	0.26	73.98	22.21	1.90	0.56	98.91
Measurement 10	0.36	74.50	21.25	1.80	0.61	98.51
Measurement 11	0.33	73.71	21.03	1.59	1.19	97.85
Measurement 12	0.32	73.93	21.08	1.63	0.74	97.71
Average normalised data	**0.34**	**75.59**	**21.89**	**1.70**	**0.48**	**100**
Standard deviation	0.07	0.48	0.38	0.16	0.34	0
Coefficient of variation (%)	**21.06**	**0.63**	**1.73**	**9.64**	**69.98**	**0**
Reference values	0.35	74.36	22.13	1.63	0.58	99.99
Normalised reference values	**0.35**	**74.37**	**22.13**	**1.63**	**0.58**	**100**
Absolute error	0.01	-1.22	0.24	-0.07	0.09	
Relative error (%)	**3.96**	**-1.64**	**1.10**	**-4.18**	**16.10**	

Table A.5: CURM 42.23-2: Admiralty Brass. *Not measured: 0.13 wt% P, 0.05 wt% S, 0.17 wt% Ni, 0.17 wt% As, 0.36 wt% Sb, 0.01 wt% Al, 0.02 wt% Si, 0.02 wt% Mn and 0.03 wt% Bi*

Elemental compositions in wt%

	P	S	Fe	Ni	Cu	Zn	As	Sn	Sb	Pb	Total
Measurement 1	0.16	0.17	0.25	2.24	78.67	1.38	0.24	10.59	0.76	6.53	100.99
Measurement 2	0.28	0.22	0.19	2.47	77.77	1.19	0.39	11.29	0.37	6.66	100.84
Measurement 3	0.13	0.14	0.37	2.60	78.53	1.00	0.11	11.37	0.49	6.61	101.35
Measurement 4	0.14	0.18	0.18	2.51	79.37	0.95	0.34	10.70	0.55	6.96	101.88
Measurement 5	0.31	0.20	0.33	2.81	76.89	1.02	0.35	11.06	0.91	8.33	102.22
Measurement 6	0.17	0.11	0.23	2.63	77.46	1.04	0.14	11.50	0.33	6.85	100.47
Measurement 7	0.23	0.33	0.27	2.14	80.00	1.21	0.38	10.98	0.81	5.06	101.41
Measurement 8	0.21	0.36	0.02	2.22	77.54	1.50	0.31	10.97	0.35	6.09	99.58
Measurement 9	0.17	0.10	0.14	2.73	77.85	1.23	0.72	11.24	0.70	5.86	100.74
Measurement 10	0.16	0.21	0.41	2.54	78.05	1.00	0.19	11.19	0.55	6.48	100.78
Measurement 11	-0.01	0.11	0.21	2.47	83.23	1.48	0.42	9.36	0.01	2.51	99.80
Measurement 12	0.01	0.15	0.23	2.21	75.18	1.47	0.10	10.72	0.40	10.65	101.12
Measurement 13	0.09	0.12	0.05	2.34	73.03	1.35	0.45	10.74	0.16	12.37	100.70
Measurement 14	0.10	0.04	0.18	2.34	70.11	1.52	0.37	9.90	0.36	17.01	101.92
Measurement 15	0.09	1.36	0.25	2.24	70.05	2.00	0.10	10.91	0.75	13.17	100.92
Average normalised data	**0.15**	**0.25**	**0.22**	**2.41**	**76.18**	**1.28**	**0.31**	**10.73**	**0.49**	**7.99**	**100**
Standard deviation	0.09	0.32	0.10	0.20	3.71	0.28	0.17	0.56	0.25	3.63	0
Coefficient of variation (%)	**58.91**	**125.31**	**47.46**	**8.33**	**4.87**	**22.03**	**54.64**	**5.21**	**50.25**	**45.49**	**0**
Reference values	0.11	0.11	0.24	2.24	74.08	1.17	0.22	9.45	0.59	11.74	100.04
Normalised reference values	**0.11**	**0.11**	**0.24**	**2.24**	**74.05**	**1.17**	**0.22**	**9.45**	**0.59**	**11.74**	**100**
Absolute error	-0.04	-0.14	0.02	-0.17	-2.10	-0.11	-0.09	-1.28	0.10	3.75	
Relative error (%)	**-31.56**	**-123.01**	**9.47**	**-7.50**	**-2.83**	**-9.23**	**-39.09**	**-13.54**	**16.27**	**31.96**	

Table A.6: CURM 50.01-4: Leaded Bronze. *Not measured: 0.02 wt% Al, 0.01 wt% Si, 0.02 wt% Mn and 0.03 wt% Bi*

Elemental compositions in wt%

	S	Ni	Cu	As	Sn	Sb	Pb	Total
Measurement 1	0.41	1.41	78.25	0.09	13.26	0.48	6.03	99.93
Measurement 2	0.31	1.43	77.89	0.29	12.96	0.17	6.70	99.75
Measurement 3	0.26	1.28	79.29	-0.04	12.88	0.59	5.38	99.64
Measurement 4	0.35	1.33	77.43	-0.06	13.36	0.88	6.82	100.11
Measurement 5	0.08	1.07	78.35	0.16	12.57	0.15	6.18	98.54
Measurement 6	-0.07	1.24	80.12	0.23	12.17	0.59	5.67	99.95
Measurement 7	0.37	1.49	78.14	0.02	11.76	0.61	7.68	100.08
Measurement 8	0.31	1.06	78.65	-0.10	12.78	0.19	5.58	98.45
Measurement 9	0.32	1.33	76.36	0.09	13.02	0.36	7.55	99.02
Measurement 10	0.26	1.03	77.7	0.05	12.78	0.31	6.49	98.61
Measurement 11	0.32	1.34	81.13	0.04	11.90	0.41	4.28	99.43
Measurement 12	0.29	1.07	76.03	0.01	11.44	0.38	11.12	100.33
Average normalised data	**0.27**	**1.26**	**78.68**	**0.07**	**12.64**	**0.43**	**6.65**	**100**
Standard deviation	0.13	0.16	1.57	0.12	0.64	0.22	1.68	0
Coefficient of variation (%)	**49.95**	**12.59**	**1.99**	**178.85**	**5.10**	**50.36**	**25.30**	**0**
Reference values	0.14	1.10	76.11	0.06	11.30	0.50	9.94	100.10
Normalised reference values	**0.14**	**1.10**	**76.04**	**0.06**	**11.29**	**0.50**	**9.93**	**100**
Absolute error	-0.13	-0.16	-2.65	-0.01	-1.35	0.07	3.28	
Relative error (%)	**-91.25**	**-14.73**	**-3.48**	**-9.83**	**-11.96**	**14.25**	**33.01**	

Table A.7: CURM 50.04-4: Leaded Bronze. *Not measured: 0.03 wt% P, 0.10 wt% Fe, 0.66 wt% Zn, 0.01 wt% Al, 0.01 wt% Si, 0.03 wt% Mn and 0.10 wt% Bi*

Elemental compositions in wt%

	Fe	Ni	Cu	Zn	As	Sn	Pb	Total
Measurement 1	0.33	0.66	80.19	6.19	0.18	6.57	3.67	97.81
Measurement 2	0.55	0.82	80.88	6.43	0.04	6.96	3.20	98.89
Measurement 3	0.44	0.70	82.34	6.77	0.14	7.16	3.06	100.60
Measurement 4	0.45	0.68	82.85	7.01	0.13	7.03	1.66	99.81
Measurement 5	0.41	0.67	81.10	6.78	0.16	7.06	3.06	99.24
Measurement 6	0.36	0.85	78.68	5.81	0.22	6.86	6.01	98.79
Measurement 7	0.13	0.74	80.99	6.18	0.49	7.64	3.09	99.26
Measurement 8	0.37	0.68	81.48	6.40	0.11	7.12	3.13	99.30
Measurement 9	0.34	0.87	81.92	6.82	0.33	6.41	2.03	98.74
Measurement 10	0.53	0.70	82.47	6.68	0.18	7.08	2.05	99.69
Measurement 11	0.38	0.87	81.58	6.44	0.51	6.66	2.30	98.74
Measurement 12	0.39	0.94	80.93	5.98	0.14	7.07	3.46	98.90
Average normalised data	**0.39**	**0.77**	**81.98**	**6.51**	**0.22**	**7.03**	**3.09**	**100**
Standard deviation	0.11	0.10	0.89	0.35	0.15	0.30	1.14	0
Coefficient of variation (%)	**27.37**	**13.27**	**1.09**	**5.36**	**66.47**	**4.23**	**36.89**	**0**
Reference values	0.35	0.70	80.48	6.52	0.25	6.46	4.43	99.87
Normalised reference values	**0.35**	**0.70**	**80.59**	**6.53**	**0.25**	**6.47**	**4.44**	**100**
Absolute error	-0.04	-0.07	-1.40	0.02	0.03	-0.56	1.35	
Relative error (%)	**-12.23**	**-9.86**	**-1.73**	**0.26**	**11.12**	**-8.68**	**30.34**	

Table A.8: CURM 71.32.4: Leaded Gunmetal. *Not measured: 0.02 wt% P, 0.08 wt% S, 0.26 wt% Sb, 0.12 wt% Al, 0.02 wt% Si, 0.05 wt% Mn, 0.05 wt% Bi, 0.05 wt% Cr and 0.03 wt% Ag*

Section A.4

Glass

Three glass reference materials were analysed (mounted in resin, ground and polished). The results of these measurements are given in Tables A.9, A.10 and A.11. The first sample was provided by the National Institute of Standards and Technology, while the other two were provided by the Corning Museum of Glass. No bismuth-bearing glasses, as a comparative for crucible S5 (section 11.1.3.3), were available for analysis.

The measurements for all three samples show very good precision (coefficient of variation below 10% for most oxides) and accuracy (relative error below 10% for most oxides), with some exceptions detailed below.

For the NIST 1412 glass, the only exception is Na_2O, which shows slightly lower accuracy (still below 15% relative error).
Low levels of FeO are not measured. Reported high levels (4.5 wt%) of extremely light oxides Li_2O and B_2O_3 are not measured.

For the Corning B glass, the measurement of MnO, FeO and Cl (all present at relatively low levels) and MgO and SO_3 (light oxides, present at relatively low levels) shows lowered precision. The accuracy, however, is quite good. Only low levels of SO_3 and FeO are not measured accurately (relative error of ±20%), while Al_2O_3 and CuO show relative errors below 15%, which are not entirely unacceptable. 0.9 wt% TiO_2 is measured quite poorly, both in terms of precision and accuracy.
Low levels of V_2O_5, CoO, NiO, ZnO, SrO, SnO_2, Sb_2O_5, BaO and PbO are not measured.

For the Corning D glass, the measurement of Na_2O shows slightly lower precision (still below 15% coefficient of variation). The measurement of SO_3 (light element), TiO_2, MnO, FeO, CuO and Cl (all present at relatively low levels) shows poor precision. Accuracy is poor for Na_2O, SO_3, TiO_2 and Cl.
Low levels of ZnO, SnO_2, Sb_2O_3, BaO, PbO, CoO, NiO and SrO were not measured.

In conclusion, the measurements of these glass samples show very good precision and accuracy for all oxides present at levels down to 0.5 wt%, sometimes lower. TiO_2, Sb_2O_3 and PbO form an exception and appear to have a higher detection limit (±0.7-1 wt%). Measurements of light oxides, such as SO_3 and Na_2O, have lowered precision.

Oxide compositions in wt%

	Na_2O	MgO	Al_2O_3	SiO_2	K_2O	CaO	ZnO	SrO	CdO	BaO	PbO	Total
Measurement 1	5.36	4.63	6.93	41.69	3.55	4.51	4.44	3.63	4.67	4.55	4.60	89.35
Measurement 2	5.37	4.29	7.22	43.03	4.03	4.47	4.30	4.47	4.43	4.70	4.45	90.76

Oxide compositions in wt%

	Na_2O	MgO	Al_2O_3	SiO_2	K_2O	CaO	ZnO	SrO	CdO	BaO	PbO	Total
Measurement 3	5.08	4.59	7.36	42.83	3.80	4.87	5.15	4.47	4.75	4.63	4.85	92.39
Measurement 4	5.58	4.37	7.28	43.09	4.14	4.56	4.63	3.95	4.56	4.76	4.74	91.66
Measurement 5	5.44	4.60	7.11	41.74	4.53	4.56	4.38	4.54	4.28	4.92	4.44	90.52
Measurement 6	5.41	4.58	7.29	43.36	3.98	4.52	4.69	4.34	4.24	4.76	4.50	91.65
Measurement 7	4.95	4.48	6.84	42.99	4.00	4.71	4.22	4.65	4.57	5.00	4.41	90.83
Measurement 8	4.96	4.68	7.39	42.91	4.48	4.56	4.51	4.17	4.56	5.01	4.69	91.93
Measurement 9	5.39	4.66	7.31	42.78	4.16	4.56	4.34	4.57	4.81	4.91	4.65	92.15
Average normalised data	**5.79**	**4.98**	**7.88**	**46.81**	**4.46**	**5.03**	**4.95**	**4.72**	**4.98**	**5.26**	**5.03**	**100**
Standard deviation	0.27	0.15	0.15	0.47	0.33	0.12	0.28	0.35	0.21	0.17	0.14	0
Coefficient of variation (%)	**4.61**	**2.99**	**1.95**	**1.01**	**7.28**	**2.43**	**5.74**	**7.46**	**4.19**	**3.29**	**2.83**	**0**
Reference values	4.69	4.69	7.52	42.38	4.14	4.53	4.48	4.55	4.38	4.67	4.40	90.46
Normalised reference values	**5.18**	**5.18**	**8.31**	**46.85**	**4.58**	**5.01**	**4.95**	**5.03**	**4.84**	**5.16**	**4.86**	**100**
Absolute error	-0.60	0.21	0.43	0.04	0.11	-0.02	0	0.31	-0.14	-0.10	-0.17	
Relative error (%)	**-11.63**	**3.99**	**5.17**	**0.08**	**2.48**	**-0.47**	**0.05**	**6.12**	**-2.81**	**-1.93**	**-3.43**	

Table A.9: NIST 1412: Multi-Component Glass. *Not measured: 0.03 wt% FeO, 4.50 wt% Li_2O and 4.53 wt% B_2O_3*

Oxide compositions in wt%

	Na_2O	MgO	Al_2O_3	SiO_2	P_2O_5	SO_3	K_2O	CaO	TiO_2	MnO	FeO	CuO	**Cl*	Total
Measurement 1	17.16	1.06	3.84	62.30	0.95	0.64	1.04	9.01	0.10	0.13	0.48	3.06	*0.26*	99.74
Measurement 2	17.47	0.70	4.05	62.34	0.98	0.88	0.99	8.74	0.01	0.45	0.22	3.04	*0.14*	99.86
Measurement 3	16.81	0.97	3.72	63.02	0.85	0.58	1.20	8.86	0.01	0.43	0.19	3.10	*0.27*	99.73
Measurement 4	16.78	0.99	3.89	63.11	0.78	0.58	1.08	8.94	0.15	0.21	0.39	2.95	*0.16*	99.84
Measurement 5	17.08	1.13	4.04	62.75	0.87	0.39	1.06	8.57	0.07	0.32	0.32	3.23	*0.16*	99.83
Measurement 6	17.35	0.90	4.04	62.76	0.81	0.66	0.97	8.95	0.06	0.12	0.35	2.77	*0.26*	99.74
Measurement 7	17.20	1.02	3.68	62.65	0.75	0.71	1.18	8.93	0.10	0.18	0.36	3.03	*0.22*	99.78
Measurement 8	17.21	0.94	3.84	62.66	0.93	0.71	1.09	9.10	0.06	0.14	0.52	2.57	*0.22*	99.78
Average of normalised data	**17.13**	**0.96**	**3.89**	**62.70**	**0.87**	**0.64**	**1.08**	**8.89**	**0.07**	**0.25**	**0.35**	**2.97**	***0.21***	**100.01**
Standard deviation	0.24	0.13	0.15	0.29	0.08	0.14	0.08	0.17	0.05	0.14	0.11	0.21	*0.05*	0.01
Coefficient of variation (%)	**1.40**	**13.26**	**3.73**	**0.46**	**9.42**	**21.73**	**7.60**	**1.86**	**67.78**	**54.37**	**32.29**	**6.96**	***24.46***	**0.01**
Reference values	17.00	1.03	4.36	61.55	0.82	0.54	1.00	8.56	0.89	0.25	0.31	2.66	*0.20*	100.59
Normalised reference values	**16.90**	**1.02**	**4.33**	**61.19**	**0.82**	**0.54**	**0.99**	**8.51**	**0.88**	**0.25**	**0.30**	**2.64**		**100**
Absolute error	-0.23	0.06	0.45	-1.50	-0.05	-0.11	-0.08	-0.38	0.82	0	-0.05	-0.32	*-0.01*	
Relative error (%)	**-0.01**	**0.06**	**0.10**	**-0.02**	**-0.06**	**-0.20**	**-0.08**	**-0.04**	**0.92**	**0**	**-0.17**	**-0.12**	***-5.62***	

Table A.10: Corning B: Soda-Lime-Silica Glass. *(Cl in wt%) *Not measured: 0.04 wt% V_2O_5, 0.05 wt% CoO, 0.10 wt% NiO, 0.19 wt% ZnO, 0.02 wt% SrO, 0.04 wt% SnO_2, 0.46 wt% Sb_2O_5, 0.12 wt% BaO and 0.61 wt% PbO*

Oxide compositions in wt%

	Na_2O	MgO	Al_2O_3	SiO_2	P_2O_5	SO_3	K_2O	CaO	TiO_2	MnO	FeO	CuO	**Cl*	Total
Measurement 1	1.55	3.85	4.83	54.75	4.23	0.27	11.55	15.23	0.51	0.52	0.28	0.46	*0.20*	98.04
Measurement 2	1.38	3.92	4.66	55.93	4.18	0.20	11.27	14.57	0.58	0.63	0.47	0.52	*0.18*	98.32
Measurement 3	1.71	3.84	4.78	53.85	4.11	0.31	11.27	14.94	0.64	0.48	0.53	0.40	*0.16*	96.87
Measurement 4	1.47	3.96	4.71	54.96	4.12	0.53	11.71	14.89	0.35	0.36	0.46	0.47	*0.18*	98.00
Measurement 5	1.34	3.84	4.86	54.83	3.93	0.40	11.34	14.86	0.44	0.41	0.49	0.22	*0.11*	96.97
Measurement 6	1.37	3.93	4.69	54.85	4.01	0.23	11.38	14.63	0.59	0.50	0.40	0.32	*0.17*	96.91
Measurement 7	1.22	4.01	4.59	55.28	3.74	0.38	11.32	14.82	0.60	0.61	0.57	0.38	*0.21*	97.52
Measurement 8	1.08	3.81	4.44	54.91	3.98	0.28	11.50	14.77	0.56	0.74	0.51	0.22	*0.12*	96.81
Average normalised data	**1.43**	**3.99**	**4.81**	**56.27**	**4.14**	**0.34**	**11.70**	**15.21**	**0.55**	**0.55**	**0.48**	**0.38**	***0.17***	**99.83**
Standard deviation	0.20	0.06	0.14	0.47	0.15	0.11	0.16	0.22	0.10	0.13	0.09	0.11	*0.04*	0.04
Coefficient of variation (%)	**13.72**	**1.60**	**2.92**	**0.84**	**3.70**	**32.22**	**1.35**	**1.43**	**18.10**	**23.00**	**19.13**	**30.08**	***21.31***	**0.04**
Reference values	1.20	3.94	5.30	55.24	3.93	0.30	11.30	14.80	0.38	0.55	0.48	0.38	*0.40*	100.10
Normalised reference values	**1.20**	**3.94**	**5.29**	**55.18**	**3.93**	**0.30**	**11.29**	**14.79**	**0.38**	**0.55**	**0.48**	**0.38**		**100**
Absolute error	-0.23	-0.05	0.48	-1.09	-0.21	-0.04	-0.41	-0.42	-0.17	0	0	0	*-0.17*	
Relative error (%)	**-18.97**	**-1.37**	**9.11**	**-1.97**	**-5.39**	**-12.20**	**-3.65**	**-2.86**	**-44.22**	**0.81**	**0.94**	**-0.43**	***-41.56***	

Table A.11: Corning D: Potash Glass. *(Cl in wt%) *Not measured: 0.10 wt% ZnO, 0.10 wt% SnO_2, 0.97 wt% Sb_2O_3, 0.51 wt% BaO, 0.48 wt% PbO, 0.02 wt% CoO, 0.06 wt% NiO and 0.06 wt% SrO*

Section A.5

Summary

In summary, the detection limit (i.e., the minimal concentration[1] for which an element or oxide can be accurately measured) for SEM-EDS analysis, using the JEOL 8600 Superprobe, equipped with an Oxford Instruments EDS attachment, appears to be ±0.5 wt%, with the exception of a few elements/oxides which have detection limits of ±1 wt%.
The measurement precision is generally high (coefficient of variation below 10%), though sometimes lower for elements/oxides present at low levels and for light elements/oxides. The accuracy is similarly good, typically showing a relative error of less than 10% when compared to certified reference values.
The presence of lead in metal can be problematic due to polishing effects, leading to poor precision and accuracy (consistent underestimation of ±30%) in its measurement and a lowered accuracy of the measurement of other alloy constituents, such as tin.

[1] Actually mass fractions, expressed in wt%, are used here rather than concentrations (measure relative to volume).

Pi-Ramesse Appendices

APPENDIX B

Sample details

The table below presents contextual details for the forty-nine samples analysed by optical microscopy and SEM-EDS. "PQ" refers to *Planquadrate*, which is the excavation square (see, e.g., Figure 4.7). "Strat" refers to building levels from Table 4.1, while "Context" refers to the primary, secondary, tertiary and unclear (?) excavation context, as assessed by the excavator. Having evaluated the stratigraphical allocation of each individual find, Dr. Pusch is fairly confident of the building levels in column "Strat". Given the particularly high incidence of tertiary find contexts for the industrial area, and bearing in mind considerations presented in section 4.4, many (if not all) of the B/2 fragments from the industrial area likely belong to the industrial phase B/3.

Area	Sample	PQ	Strat	Context	Sample type
QI multifunctional workshops	82_0223b,01 - 10.1.12	QI-d/3	B/1-B/2	Tert	Rim
QI multifunctional workshops	82_298b,01 - 21.3.2012	QI-d/3	B/2a	Tert?	Rim
QI multifunctional workshops	83_0542b,01 - 21.3.2012	QI-e/1	B/2a	Sec	Rim
QI multifunctional workshops	83_0597l,01 - 21.3.2012	QI-e/1	B/1-B/2	Tert	Body
QI multifunctional workshops	83_1149b - 12.11.2012 (1)	QI-d/02.03	B/3	?	Rim
QI multifunctional workshops	83_1149b - 12.11.2012 (2)	QI-d/02.03	B/3	?	Body-rim, below (1)
QI multifunctional workshops	84_0030c,01 - 10.1.2012	QI-e/02.03	B/3	?	Body-rim
QI multifunctional workshops	84_0106c - 12.11.2012	QI-d/4.5	B/3	Sec	Body
QI industrial area	84_0749, - 10.1.12	QI-a/3	B/3	Tert	Body-rim
QI industrial area	84_1189b,0 - 12.11.2012	QI-b/3	B/1	Tert	Body-rim
QI multifunctional workshops	84_1232, - 12.11.2012	QI-f/02.03	B/3	?	Body-rim
QI multifunctional workshops	86_0208b - 12.11.2012	QI-b/10	B/3b	?	Rim
QI industrial area	86_0471b,01 - 19.1.2006	QI-ax/3	B/2a	?	Body
QI industrial area	86_0749c - 19.1.2006	QI-ax/4.5	B/3	?	Body
QI multifunctional workshops	86_0792b,04 - 12.11.2012	QI-d/4.5	B/3	Sec/tert	Body
QI industrial area	87_0423b - 19.1.2006	QI-ax/3-4.5	B/3	?	Body
QI industrial area	87_0634c,04 - 12.11.2012	QI-b/5	B/3b	Sec	Body

Area	Sample	PQ	Strat	Context	Sample type
QI industrial area	87_0725c,1-20 - 12.11.2012	QI-a/3.4	B/2a	?	Body
QI industrial area	87_0726,68-78b - 19.1.2006	QI-a/3.4	B/2a	Sec	Body
QI industrial area	87_0726c,2-60a - 19.1.2006	QI-a/3.4	B/2a	Sec	Body
QI industrial area	87_0762, - 21.3.2012	QI-a/3	B/2a	Tert	Body
QI industrial area	87_0762, - 22.3.2013 (1)	QI-a/3	B/2a	Tert	Body
QI industrial area	87_0762, - 22.3.2013 (2)	QI-a/3	B/2a	Tert	Body
QI industrial area	87_0762,0Nv - 21.2.2012	QI-a/3	B/2a	Tert	Body
QI industrial area	87_0762,0Nv - 22.3.2013 (1)	QI-a/3	B/2a	Tert	Body
QI industrial area	87_0762,0Nv - 22.3.2013 (2)	QI-a/3	B/2a	Tert	Body
QI industrial area	87_0773,04 - 12.11.2012	QI-a/3	B/3	Tert	Rim
QI industrial area	87_0791,01-88 - 12.11.2012	QI-a/3.4	B/2a	Tert	Body
QI industrial area	87_0849a,04 - 21.3.2012	QI-a/3	B/3	Tert	Body
QI industrial area	87_0884,01-56b - 19.1.2006	QI-a/3	B/2a	Tert	Body
QI industrial area	87_0884,01-56c - 19.1.2006	QI-a/3	B/2a	Tert	Body
QI industrial area	87_0897a,01-45 - 12.11.2012 (1)	QI-a/3	B/2a	Tert	Body
QI industrial area	87_0897a,01-45 - 12.11.2012 (2)	QI-a/3	B/2a	Tert	Body
QI industrial area	87_0942g,03 - 12.11.2012	QI-a/3	B/3	Tert	Body
QIV workshop	92_0606 - 12.11.2012	QIV-i/27	?	?	Body
QIV workshop	92_0645b - 21.3.2012	QIV-i/28	Ba	Sec/tert	Body
QIV workshop	94_0239,01 - 21.3.2012	QIV-j.k/28.29	Bb	Tert	Body
QIV workshop	94_0560 - 10.01.12	QIV-j.l/27.28	Ba/b?	Prim?	Body
QIV workshop	94_0775,01 - 12.11.2012	QIV-j.k/28	Ba?	Tert	Body
QIV workshop	94_842 - 21.2.2012	QIV-h.i/31.32	Ba	Sec/tert	Body-rim
QIV workshop	97_0631E,01 - 12.11.2012	QIV-S-Schn	Bc	Prim	Body-rim
QIV workshop	97_0631E,04 - 12.11.2012	QIV-S-Schn	Bc	Prim	Body
QIV workshop	97_0632D,01 - 10.1.12	QIV-S-Schn	Bc	Prim	Body
QIV workshop	97_0675,02 - 12.11.2012	QIV-g/28	Bc/Bd?	Prim/sec	Rim
QIV workshop	97_0690,02 - 21.2.2012	QIV-S-Schn	Bc/2	?	Body
QIV workshop	97_0690,02- - 21.2.2012	QIV-S-Schn	Bc/2	?	Body
QIV workshop	97_1176 - 12.11.2012	QIV-h/28	Bc?	?	Body
QIV workshop	98_0387,03 - 21.3.2012	QIV-j/28	Bb?	Tert	Body
QIV workshop	98_1325 - 12.11.2012	QIV-h/28	Bd/Be?	Prim/sec	Rim

APPENDIX C

Bulk Compositions

In this appendix, the bulk composition of both the crucible ceramic and the crucible slag are given in the first two tables. The final three tables show the ratios of elements to Al_2O_3, for ceramic, slag and the change between them respectively.

Average ceramic composition. All results in wt%, normalised to 100%.

Sample	Na_2O	MgO	Al_2O_3	SiO_2	P_2O_5	K_2O	CaO	TiO_2	MnO	FeO	CuO	As_2O_3	SnO_2
82_0223b,01 - 10.1.12	**3.7**	**1.8**	**12**	**67**	**0.6**	**1.7**	**3.2**	**1.4**	**0.1**	**7.0**	**0.2**	**0.2**	**0.3**
Std. dev. (5 ms)	0.9	0.3	2	5	0.1	0.4	0.7	0.4	0.1	1.0	0.2	0.3	0.4
Min.	2.5	1.4	11	62	0.4	1.3	2.4	1.0	0	5.7	0	0	0
Max.	5.1	2.1	15	74	0.7	2.1	4.1	1.9	0.2	8.1	0.5	0.7	0.7
82_298b,01 - 21.3.2012	**2.1**	**2.2**	**13**	**67**	**0.6**	**1.6**	**3.4**	**1.3**	**0.1**	**7.9**	**0**	**0.1**	**0.3**
Std. dev. (5 ms)	0.2	0.2	1	1	0.8	0.1	0.5	0.2	0.1	0.4	0.1	0.2	0.1
Min.	1.7	2.0	11	65	0.1	1.5	2.8	1.1	0	7.4	0	0	0.2
Max.	2.4	2.4	15	69	2.1	1.8	4.2	1.6	0.2	8.4	0.2	0.4	0.5
83_0542b,01 - 21.3.2012	**2.3**	**2.5**	**12**	**67**	**0.8**	**1.7**	**4.0**	**1.6**	**0.1**	**7.6**	**0.1**	**0.2**	**0.1**
Std. dev. (4 ms)	0.4	0.3	1	3	0.3	0.2	0.7	0.1	0	0.5	0.1	0.4	0.2
Min.	1.9	2.3	11	64	0.5	1.5	2.9	1.4	0	7.1	0	0	0
Max.	2.8	2.8	14	71	1.1	1.9	4.4	1.7	0.1	8.3	0.3	0.5	0.3
83_0597b,01 - 21.3.2012	**2.2**	**2.7**	**16**	**60**	**0.3**	**1.5**	**3.8**	**1.9**	**0.2**	**10.7**	**0**	**0.4**	**0.2**
Std. dev. (4 ms)	0.2	0.1	0	1	0.2	0	0.5	0.3	0.1	0.4	0.2	0.2	0.2
Min.	1.9	2.5	16	59	0	1.5	3.4	1.6	0.2	10.4	0	0.1	0
Max.	2.3	2.9	17	61	0.6	1.6	4.4	2.2	0.3	11.3	0.1	0.6	0.4
83_1149b - 12.11.2012 (1)	**2.0**	**2.3**	**13**	**67**	**0.5**	**1.6**	**3.1**	**1.4**	**0**	**8.4**	**0**	**0.3**	**0.2**
Std. dev. (4 ms)	0.1	0.4	2	6	0.1	0.3	0.7	0.2	0.1	1.2	0.1	0.2	0.5
Min.	1.9	1.8	10	63	0.3	1.3	2.1	1.2	0	6.6	0	0	0
Max.	2.1	2.7	15	75	0.6	2.0	3.5	1.5	0.1	9.3	0.1	0.4	0.9
83_1149b - 12.11.2012 (2)	**3.5**	**2.6**	**14**	**63**	**0.4**	**1.6**	**3.4**	**1.7**	**0.2**	**9.1**	**0**	**0.1**	**0**
Std. dev. (4 ms)	0.2	0	0	1	0.1	0.1	0.5	0.2	0.1	0.5	0.2	0.2	0.2
Min.	3.3	2.5	13	62	0.3	1.4	2.8	1.4	0	8.4	0	0	0
Max.	3.8	2.6	15	64	0.6	1.7	4.1	1.9	0.3	9.7	0.3	0.4	0.2
84_0030c,01 - 10.1.2012	**1.9**	**2.7**	**12**	**64**	**0.7**	**2.1**	**4.3**	**2.0**	**0.1**	**9.0**	**0.1**	**0**	**0.5**
Std. dev. (3 ms)	0.3	0.9	1	3	0.1	0.2	1.1	0.7	0	0.9	0.2	0.2	0.2
Min.	1.6	1.9	12	61	0.6	2.0	3.6	1.2	0.1	7.9	0	0	0.2
Max.	2.1	3.7	13	67	0.7	2.3	5.5	2.5	0.1	9.6	0.3	0.3	0.7
84_0106c - 12.11.2012	**1.6**	**2.0**	**14**	**68**	**0.5**	**1.6**	**2.7**	**1.4**	**0.1**	**8.4**	**0.1**	**0.2**	**0**
Std. dev. (4 ms)	0.3	0.5	2	5	0	0.4	0.4	0.2	0.1	0.9	0.1	0.3	0.3
Min.	1.3	1.5	11	62	0.5	1.2	2.2	1.1	0	7.7	0	0	0
Max.	1.9	2.7	17	72	0.6	2.1	3.2	1.5	0.2	9.8	0.3	0.5	0.3
84_0749, - 10.01.12	**2.5**	**2.7**	**16**	**62**	**0.4**	**1.7**	**2.9**	**1.6**	**0.1**	**9.6**	**0.1**	**0.2**	**0.4**
Std. dev. (9 ms)	0	0.2	1	1	0.1	0.1	0.2	0	0.1	0.2	0.3	0.1	0.1

Average ceramic composition. All results in wt%, normalised to 100%.

Sample	Na_2O	MgO	Al_2O_3	SiO_2	P_2O_5	K_2O	CaO	TiO_2	MnO	FeO	CuO	As_2O_3	SnO_2
Min.	1.7	1.7	12	61	0.2	1.3	2.8	1.6	0	8.0	0	0	0
Max.	5.1	2.9	16	66	0.6	2.3	4.4	2.0	0.9	10.0	0.5	0.4	0.5
84_1189b,0 - 12.11.2012	**1.9**	**2.6**	**13**	**66**	**0.6**	**1.7**	**3.7**	**1.5**	**0.2**	**8.1**	**0**	**0.1**	**0.5**
Std. dev. (5 ms)	0.2	0.3	1	1	0.2	0.2	0.2	0.1	0.1	0.6	0.2	0.1	0.4
Min.	1.6	2.3	12	64	0.4	1.5	3.4	1.4	0.2	7.2	0	0	0
Max.	2.1	3.1	14	67	0.8	2.2	4.0	1.6	0.3	8.9	0.2	0.3	1.0
84_1232, - 12.11.2012	**1.3**	**1.8**	**11**	**72**	**0.4**	**1.4**	**2.9**	**1.2**	**0.3**	**7.5**	**0**	**0.3**	**0.1**
Std. dev. (4 ms)	0.3	0.2	2	3	0.2	0.1	0.5	0.1	0.2	0.7	0.2	0.2	0.2
Min.	1.0	1.6	10	67	0.2	1.2	2.4	1.1	0.1	7.0	0	0	0
Max.	1.8	2.0	14	75	0.6	1.5	3.4	1.3	0.5	8.6	0.3	0.5	0.3
86_0208b - 12.11.2012	**1.7**	**1.9**	**10**	**72**	**0.3**	**1.8**	**3.0**	**1.3**	**0.1**	**6.8**	**0**	**0.1**	**0.1**
Std. dev. (4 ms)	0.2	0.4	2	4	0.1	0.3	0.5	0.2	0.1	0.9	0.1	0.3	0.1
Min.	1.5	1.5	8	70	0.3	1.5	2.2	1.1	0	5.6	0	0	0
Max.	2.1	2.4	12	78	0.5	2.3	3.3	1.5	0.2	7.4	0.1	0.4	0.2
86_0471b,01 - 19.1.2006	**1.5**	**2.0**	**13**	**68**	**0.6**	**1.9**	**2.5**	**1.4**	**0.1**	**8.8**	**0**	**0.1**	**0.1**
Std. dev. (5 ms)	0.2	0.3	1	2	0.1	0.4	0.1	0.2	0.1	1.2	0.1	0.1	0.4
Min.	1.3	1.6	12	64	0.4	1.6	2.4	1.2	0	7.7	0	0	0
Max.	1.8	2.4	15	70	0.7	2.5	2.7	1.8	0.3	10.8	0.1	0.3	0.5
86_0749c - 19.1.2006	**1.9**	**2.0**	**13**	**65**	**1.1**	**1.9**	**3.1**	**1.4**	**0.1**	**9.3**	**0**	**0.4**	**0.1**
Std. dev. (4 ms)	0.3	0.5	2	8	1.1	0.4	1.2	0.2	0.2	1.9	0.2	0.2	0.3
Min.	1.6	1.4	11	56	0.4	1.3	2.2	1.2	0	7.1	0	0.1	0
Max.	2.2	2.5	16	74	2.7	2.3	4.7	1.6	0.5	11.0	0.3	0.6	0.4
86_0792b,04 - 12.11.2012	**2.3**	**2.5**	**15**	**64**	**0.2**	**1.7**	**3.3**	**1.6**	**0.1**	**9.1**	**0.2**	**0.3**	**0.3**
Std. dev. (5 ms)	0.3	0.4	1	1	0.2	0.2	0.1	0.2	0.1	0.4	0.2	0.1	0.3
Min.	2.0	2.1	14	62	0	1.5	3.2	1.4	0	8.7	0	0.1	0.1
Max.	2.6	3	16	65	0.4	2.0	3.4	1.9	0.2	9.7	0.4	0.5	0.8
87_0423b - 19.1.2006	**2.8**	**0.8**	**7**	**83**	**0.3**	**1.1**	**1.8**	**0.7**	**0.1**	**3.0**	**0.1**	**0**	**0**
Std. dev. (4 ms)	0.5	0.2	1	1	0.3	0.3	0.5	0.2	0.1	0.5	0.2	0.2	0.1
Min.	2.1	0.5	6	82	0	0.7	1.3	0.5	0	2.5	0	0	0
Max.	3.1	0.9	7	84	0.7	1.3	2.3	0.9	0.1	3.6	0.3	0.1	0.2
87_0634c,04 - 12.11.2012	**1.7**	**2.0**	**14**	**66**	**0.7**	**1.8**	**3.2**	**1.5**	**0.1**	**8.3**	**0.2**	**0.3**	**0.2**
Std. dev. (4 ms)	0.4	0.1	1	3	0	0.2	0.3	0.1	0	0.7	0.2	0.2	0.2
Min.	1.2	1.9	13	62	0.7	1.7	2.9	1.3	0	7.9	0	0.1	0
Max.	2.2	2.2	16	68	0.7	2.1	3.6	1.6	0.1	9.4	0.4	0.6	0.5
87_0725c,1-20 - 12.11.2012	**2.2**	**1.9**	**13**	**68**	**0.8**	**2.3**	**3.0**	**1.3**	**0.2**	**7.6**	**0.1**	**0.1**	**0**
Std. dev. (5 ms)	0.4	0.4	2	5	0.2	0.4	0.6	0.3	0.1	1.1	0.1	0.2	0.4
Min.	1.8	1.3	10	62	0.5	1.8	2.3	0.8	0.1	6.5	0	0	0
Max.	2.7	2.5	16	74	1.1	2.7	3.9	1.7	0.3	9.3	0.3	0.4	0.5
87_0726,68-78b - 19.1.2006	**1.5**	**2.1**	**11**	**57**	**0.3**	**1.3**	**3.0**	**2.2**	**0.1**	**8.5**	**13.1**	**0.1**	**0.3**
Std. dev. (5 ms)	0.4	0.3	2	4	0.3	0.4	0.4	0.9	0.1	2.2	9.5	0.1	0.3
Min.	1.0	1.6	8	53	0	0.8	2.3	0.9	0	5.1	2.5	0	0
Max.	1.9	2.5	14	62	0.7	1.7	3.3	3.1	0.3	11.1	25.3	0.1	0.6
87_0726c,2-60a - 19.1.2006	**2.0**	**2.5**	**14**	**64**	**0.6**	**1.5**	**3.9**	**1.6**	**0.2**	**9.1**	**0**	**0.1**	**0.1**
Std. dev. (3 ms)	0.3	0.3	1	1	0.2	0.1	0.2	0.2	0	0.5	0.1	0.3	0.1
Min.	1.7	2.2	13	63	0.4	1.4	3.8	1.3	0.1	8.6	0	0	0
Max.	2.3	2.7	15	65	0.9	1.7	4.1	1.8	0.2	9.6	0.1	0.4	0.2
87_0762, - 21.3.2012	**1.7**	**2.3**	**14**	**65**	**0.4**	**1.7**	**3.0**	**1.5**	**0.3**	**9.5**	**0.5**	**0**	**0.3**
Std. dev. (5 ms)	0.2	0.3	1	2	0.3	0.4	0.5	0.1	0.1	0.9	0.3	0.3	0.4
Min.	1.5	1.9	12	63	0.1	1.4	2.3	1.3	0.1	8.3	0.2	0	0
Max.	2.0	2.6	14	69	0.7	2.3	3.5	1.6	0.4	10.6	0.8	0.2	0.8
87_0762, - 22.3.2013 (1)	**2.1**	**2.0**	**12**	**67**	**1.8**	**2.3**	**4.1**	**1.3**	**0.1**	**7.0**	**0**	**0.2**	**0.2**
Std. dev. (5 ms)	0.4	0.4	1	5	0.9	0.4	1.3	0.3	0.2	0.8	0.2	0.1	0.3
Min.	1.6	1.4	11	59	1.2	1.8	3.1	1.0	0	6.2	0	0	0
Max.	2.7	2.3	14	71	3.3	2.7	6.3	1.8	0.3	8.0	0.4	0.3	0.7
87_0762, - 22.3.2013 (2)	**1.5**	**2.1**	**14**	**66**	**0.5**	**1.6**	**3.4**	**1.8**	**0.1**	**8.7**	**0.1**	**0.3**	**0.3**
Std. dev. (5 ms)	0.2	0.2	1	2	0.4	0.1	0.5	0.3	0.1	0.7	0.2	0.1	0.4
Min.	1.2	1.9	12	63	0.3	1.5	2.7	1.4	0	7.8	0	0.2	0
Max.	1.7	2.4	15	68	1.3	1.7	3.9	2.2	0.2	9.7	0.4	0.5	0.9
87_0762,0Nv - 21.2.2012	**2.2**	**2.3**	**12**	**68**	**0.9**	**2.1**	**3.3**	**1.4**	**0.1**	**7.6**	**0**	**0.1**	**0.1**
Std. dev. (5 ms)	0.1	0.4	1	3	0.1	0.3	0.5	0.4	0.1	0.8	0.1	0.3	0.2
Min.	2.0	2.0	11	64	0.8	1.8	2.5	1.0	0	6.5	0	0	0
Max.	2.4	2.8	13	71	1.1	2.5	3.9	1.9	0.2	8.5	0	0.5	0.3
87_0762,0Nv - 22.3.2013 (1)	**2.3**	**2.2**	**13**	**64**	**0.6**	**2.4**	**3.0**	**1.8**	**0.2**	**9.3**	**0.3**	**0**	**0.3**
Std. dev. (5 ms)	0.5	0.3	2	3	0.2	0.5	0.3	0.8	0.1	0.5	0.2	0.2	0.1
Min.	1.9	1.8	12	60	0.4	2.0	2.6	1.1	0	8.6	0.1	0	0.1
Max.	3.0	2.7	16	68	0.9	3.3	3.5	2.7	0.3	9.9	0.5	0.3	0.4
87_0762,0Nv - 22.3.2013 (2)	**1.5**	**2.0**	**12**	**68**	**0.4**	**1.6**	**2.8**	**1.4**	**0.2**	**9.7**	**0**	**0.2**	**0.3**
Std. dev. (5 ms)	0.3	0.3	2	5	0.2	0.4	0.3	0.3	0.1	1.6	0.2	0.2	0.4
Min.	1.3	1.4	10	61	0.2	1.1	2.4	1.1	0.1	7.4	0	0	0

Average ceramic composition. All results in wt%, normalised to 100%.

Sample	Na_2O	MgO	Al_2O_3	SiO_2	P_2O_5	K_2O	CaO	TiO_2	MnO	FeO	CuO	As_2O_3	SnO_2
Max.	2.0	2.2	15	74	0.7	2.3	3.2	1.9	0.3	11.6	0.4	0.3	0.7
87_0773,04 - 12.11.2012	**1.4**	**2.2**	**12**	**70**	**0.3**	**1.4**	**2.7**	**1.4**	**0.2**	**7.9**	**0.1**	**0.1**	**0.2**
Std. dev. (4 ms)	0.2	0.4	1	4	0.1	0.4	0.3	0.2	0.1	0.8	0.1	0.2	0.4
Min.	1.2	1.9	11	65	0.3	1.0	2.3	1.1	0.2	7.1	0	0	0
Max.	1.6	2.7	14	73	0.4	2.0	3.0	1.6	0.3	8.9	0.2	0.3	0.7
87_0791,01-88 - 12.11.2012	**1.8**	**2.2**	**14**	**64**	**0.6**	**1.9**	**3.4**	**1.7**	**0.1**	**9.6**	**0.1**	**0.2**	**0.2**
Std. dev. (5 ms)	0.3	0.3	2	4	0.1	0.2	0.4	0.2	0.1	1.1	0.1	0.2	0.3
Min.	1.3	1.8	11	59	0.4	1.6	2.8	1.4	0	7.9	0	0	0
Max.	2.0	2.6	16	70	0.8	2.1	4.0	1.9	0.2	10.9	0.3	0.4	0.6
87_0849a,04 - 21.3.2012	**1.8**	**2.7**	**15**	**62**	**0.3**	**1.5**	**4.2**	**2.1**	**0.2**	**10.2**	**0.1**	**0.2**	**0.1**
Std. dev. (5 ms)	0.2	0.2	1	3	0.1	0.1	0.8	0.3	0.1	0.8	0.1	0.1	0.2
Min.	1.6	2.5	14	57	0.1	1.4	3.3	1.8	0.1	9.2	0.1	0	0
Max.	2.0	3.0	17	65	0.5	1.7	5.1	2.5	0.3	11.3	0.2	0.4	0.3
87_0884,01-56b - 19.1.2006	**2.6**	**2.5**	**14**	**55**	**0.5**	**2.3**	**4.6**	**1.6**	**0.1**	**11.1**	**3.9**	**0.4**	**1.0**
Std. dev. (6 ms)	0.7	0.2	2	5	0.1	0.3	2.0	0.2	0.1	1.0	3.3	0.2	1.5
Min.	1.3	2.4	12	49	0.4	2.0	3.1	1.3	0	10.2	1.2	0.1	0.2
Max.	3.2	3.8	16	59	0.6	3.2	8.1	1.9	0.3	14.8	8.3	0.7	3.7
87_0884,01-56c - 19.1.2006	**1.9**	**3.3**	**15**	**50**	**0.5**	**2.6**	**3.3**	**1.8**	**0.2**	**14.7**	**5.6**	**0.1**	**0.7**
Std. dev. (3 ms)	0.3	1.0	2	10	0	0.6	0.4	0.3	0.1	4.9	4.6	0.2	0.5
Min.	1.6	2.7	13	42	0.4	1.9	2.9	1.5	0.2	10.4	0.2	0	0.2
Max.	2.2	4.5	16	61	0.5	3.1	3.6	2.0	0.3	20.0	8.3	0.3	1.2
87_0897a,01-45 - 12.11.2012 (1)	**2.6**	**2.5**	**13**	**66**	**0.6**	**1.8**	**3.7**	**1.4**	**0.1**	**7.6**	**0.2**	**0.1**	**0.4**
Std. dev. (4 ms)	0.7	0.3	2	5	0.1	0.6	0.2	0.2	0.1	1.0	0.1	0.3	0.3
Min.	1.9	2.2	10	61	0.4	1.3	3.4	1.3	0	6.6	0.1	0	0
Max.	3.4	2.8	15	72	0.7	2.4	3.9	1.7	0.3	8.9	0.2	0.4	0.7
87_0897a,01-45 - 12.11.2012 (2)	**2.6**	**2.5**	**13**	**66**	**0.6**	**1.8**	**3.7**	**1.4**	**0.1**	**7.6**	**0.2**	**0.1**	**0.4**
Std. dev. (4 ms)	0.7	0.3	2	5	0.1	0.6	0.2	0.2	0.1	1.0	0.1	0.3	0.3
Min.	1.9	2.2	10	61	0.4	1.3	3.4	1.3	0	6.6	0.1	0	0
Max.	3.4	2.8	15	72	0.7	2.4	3.9	1.7	0.3	8.9	0.2	0.4	0.7
87_0942g,03 - 12.11.2012	**1.5**	**2.3**	**13**	**68**	**0.4**	**1.4**	**3.1**	**1.7**	**0.1**	**8.1**	**0.3**	**0.1**	**0.2**
Std. dev. (5 ms)	0.3	0.2	1	3	0.2	0.1	0.2	0.5	0.1	0.8	0.1	0.1	0.1
Min.	1.1	2.0	11	65	0.1	1.2	2.7	1.2	0	7.2	0.1	0	0.1
Max.	1.9	2.5	14	72	0.6	1.4	3.3	2.4	0.2	8.8	0.4	0.2	0.4
92_0606 - 12.11.2012	**1.7**	**1.2**	**9**	**76**	**0.8**	**2.1**	**2.7**	**0.8**	**0**	**4.9**	**0**	**0.1**	**0.1**
Std. dev. (4 ms)	0.4	0.2	1	3	0.1	0.3	0.4	0.2	0.1	0.8	0.2	0.2	0.3
Min.	1.2	0.9	8	72	0.6	1.8	2.3	0.5	0	3.8	0	0	0
Max.	2.0	1.4	11	80	0.9	2.5	3.1	0.9	0.2	5.8	0.3	0.3	0.5
92_0645b - 21.3.2012	**2.4**	**2.1**	**14**	**65**	**1.2**	**2.6**	**3.1**	**1.3**	**0.1**	**7.8**	**0.1**	**0.1**	**0.4**
Std. dev. (4 ms)	0.4	0.3	1	3	0.3	0.2	0.4	0.3	0.1	1.0	0.1	0.2	0.4
Min.	2.1	1.8	12	62	0.9	2.5	2.7	0.9	0.1	6.9	0	0	0
Max.	2.9	2.4	15	68	1.7	2.9	3.5	1.6	0.2	8.8	0.3	0.2	0.8
94_0239,01 - 21.3.2012	**2.2**	**1.9**	**13**	**67**	**0.8**	**2.4**	**2.8**	**1.2**	**0.2**	**7.9**	**0.1**	**0.1**	**0.3**
Std. dev. (4 ms)	0.6	0.4	2	6	0.3	0.4	0.5	0.3	0	1.3	0.1	0.1	0.3
Min.	1.4	1.3	10	62	0.4	1.9	2.3	0.8	0.1	6.3	0	0	0
Max.	2.7	2.3	15	75	1.0	2.8	3.4	1.4	0.2	9.2	0.2	0.3	0.6
94_0560 - 10.1.12	**1.6**	**2.0**	**12**	**69**	**0.4**	**1.7**	**3.3**	**1.3**	**0.2**	**8.0**	**0**	**0.3**	**0.2**
Std. dev. (4 ms)	0	0.4	2	4	0.2	0.2	0.8	0.2	0	1.1	0.3	0.1	0.2
Min.	1.5	1.4	10	64	0.2	1.5	2.4	1.2	0.1	6.5	0	0.1	0
Max.	1.6	2.4	15	74	0.6	1.9	4.2	1.6	0.2	8.9	0.2	0.4	0.3
94_0775,01 - 12.11.2012	**1.7**	**2.6**	**16**	**63**	**0.4**	**1.6**	**4.1**	**1.6**	**0.1**	**9.2**	**0**	**0.1**	**0.2**
Std. dev. (5 ms)	0.2	0.3	0	1	0.2	0.2	0.3	0.2	0.1	0.6	0.2	0.5	0.3
Min.	1.4	2.3	15	62	0.1	1.4	3.7	1.4	0	8.3	0	0	0
Max.	1.9	3.0	16	64	0.7	1.8	4.3	1.8	0.3	9.9	0.2	0.6	0.5
94_842 - 21.2.2012	**1.6**	**1.2**	**9**	**79**	**0.5**	**1.3**	**1.9**	**0.9**	**0**	**4.7**	**0**	**0.2**	**0.2**
Std. dev. (4 ms)	0.4	0.3	1	3	0.4	0.2	0.5	0.3	0.1	0.6	0.1	0.1	0.3
Min.	1.3	0.9	7	76	0.1	0.9	1.4	0.8	0	4.0	0	0.1	0
Max.	2.3	1.5	9	83	1.1	1.4	2.6	1.4	0.2	5.5	0.2	0.3	0.5
97_0631E,01 - 12.11.2012	**1.9**	**1.7**	**12**	**70**	**0.5**	**2.3**	**2.7**	**1.1**	**0.1**	**7.1**	**0.2**	**0.1**	**0**
Std. dev. (5 ms)	0.5	0.4	2	5	0.2	0.6	0.6	0.2	0.1	0.8	0.2	0.2	0.3
Min.	1.1	1.3	9	65	0.2	1.5	2.1	0.9	0	5.9	0	0	0
Max.	2.4	2.3	14	78	0.7	3.2	3.4	1.3	0.3	8.0	0.5	0.3	0.1
97_0631E,04 - 12.11.2012	**1.8**	**1.5**	**10**	**74**	**0.6**	**2.1**	**2.3**	**0.8**	**0.1**	**6.0**	**0.2**	**0.1**	**0.3**
Std. dev. (5 ms)	0.4	0.2	1	2	0.1	0.4	0.2	0.2	0.2	0.8	0.2	0.2	0.3
Min.	1.2	1.3	9	71	0.5	1.7	2.1	0.5	0	4.8	0	0	0
Max.	2.3	1.7	12	76	0.8	2.7	2.6	1.0	0.3	7.0	0.4	0.3	0.5
97_0632D,01 - 10.1.12	**1.8**	**2.3**	**15**	**63**	**1.2**	**2.0**	**3.4**	**1.4**	**0.1**	**9.0**	**0.4**	**0.1**	**0**
Std. dev. (5 ms)	0.4	0.2	1	3	1.6	0.3	1.6	0.2	0.2	0.5	0.2	0.3	0.4
Min.	1.3	2.1	14	58	0.4	1.7	2.7	1.2	0	8.7	0.3	0	0
Max.	2.4	2.5	17	66	4.0	2.4	6.3	1.8	0.3	9.8	0.8	0.3	0.4

Average ceramic composition. All results in wt%, normalised to 100%.

Sample	Na_2O	MgO	Al_2O_3	SiO_2	P_2O_5	K_2O	CaO	TiO_2	MnO	FeO	CuO	As_2O_3	SnO_2
97_0675,02 - 12.11.2012	**1.6**	**1.9**	**12**	**70**	**1.0**	**2.1**	**3.0**	**1.2**	**0.1**	**7.1**	**0.1**	**0.2**	**0.1**
Std. dev. (5 ms)	0.4	0.2	2	4	0.2	0.3	0.2	0.3	0.1	0.9	0.2	0.2	0.3
Min.	1.2	1.7	10	65	0.8	1.7	2.8	0.7	0	6.3	0	0	0
Max.	2.0	2.2	15	74	1.3	2.5	3.2	1.4	0.2	8.4	0.4	0.4	0.5
97_0690,02 - 21.2.2012	**2.2**	**1.7**	**12**	**67**	**1.0**	**2.2**	**3.8**	**1.3**	**0.1**	**7.6**	**0.1**	**0.4**	**0**
Std. dev. (4 ms)	0.6	0.2	2	7	0.4	0.5	2.5	0.4	0.1	1.5	0.2	0.1	0.3
Min.	1.3	1.5	9	60	0.4	1.6	1.9	0.9	0	5.5	0	0.2	0
Max.	2.6	2.1	13	77	1.4	2.8	7.5	1.6	0.2	8.7	0.2	0.5	0.3
97_0690,02- - 21.2.2012	**2.2**	**2.1**	**13**	**66**	**1.1**	**3.1**	**2.8**	**1.2**	**0.2**	**7.9**	**0.3**	**0.3**	**0**
Std. dev. (4 ms)	0.3	0.3	1	3	0.3	0.3	0.7	0.3	0.1	0.7	0.4	0.3	0.4
Min.	1.8	1.8	12	62	0.8	2.6	2.0	0.9	0.1	7.1	0	0	0
Max.	2.5	2.4	15	69	1.4	3.4	3.5	1.5	0.3	8.6	0.9	0.6	0.2
97_1176 - 12.11.2012	**1.9**	**2.2**	**15**	**64**	**0.5**	**2.0**	**2.9**	**1.7**	**0.2**	**9.4**	**0.1**	**0.2**	**0.2**
Std. dev. (5 ms)	0.4	0.2	1	3	0.2	0.2	0.4	0.1	0.1	0.7	0.1	0.2	0.1
Min.	1.4	1.9	13	62	0.2	1.7	2.3	1.5	0.1	8.6	0	0	0
Max.	2.5	2.5	16	68	0.7	2.2	3.2	1.8	0.3	10.3	0.3	0.4	0.3
98_0387,03 - 21.3.2012	**2.2**	**2.4**	**14**	**64**	**0.6**	**1.9**	**3.4**	**1.6**	**0.2**	**8.6**	**0**	**0.4**	**0.3**
Std. dev. (5 ms)	0.4	0.2	1	3	0.3	0.2	0.3	0.2	0.1	0.7	0.1	0.2	0.3
Min.	1.8	2.2	13	62	0.3	1.6	3.1	1.5	0.1	7.5	0	0.1	0
Max.	2.8	2.7	15	68	1.0	2.2	3.8	1.9	0.3	9.4	0.2	0.7	0.7
98_1325 - 12.11.2012	**1.1**	**2.0**	**14**	**67**	**0.3**	**1.6**	**2.9**	**1.5**	**0**	**9.6**	**0**	**0.4**	**0**
Std. dev. (3 ms)	0.2	0.5	2	4	0	0.1	0.5	0.3	0.1	1.3	0.2	0.4	0.3
Min.	1.0	1.7	12	62	0.3	1.5	2.4	1.3	0	8.4	0	0	0
Max.	1.4	2.6	16	71	0.4	1.7	3.5	1.9	0.1	10.9	0.1	0.8	0.2

Average Ceramic Composition	***2.0***	***2.2***	***13***	***66***	***0.6***	***1.9***	***3.2***	***1.5***	***0.1***	***8.3***	***0.6***	***0.2***	***0.2***

Average slag composition. All results in wt%, normalised to 100%.

Sample	Na_2O	MgO	Al_2O_3	SiO_2	P_2O_5	K_2O	CaO	TiO_2	MnO	FeO	CuO	As_2O_3	SnO_2	PbO	CoO
82_0223b,01 - 10.1.12	**2.9**	**1.3**	**4**	**77**	**0.5**	**1.0**	**6.0**	**1.0**	**0**	**3.5**	**1.4**	**0.2**	**0.9**	**0.2**	
Std. dev. (5 ms)	0.9	0.3	2	5	0.1	0.4	0.7	0.4	0.1	1.0	0.2	0.3	0.4	0	
Min.	1.9	0.7	3	66	0.2	0.5	3.3	0.4	0	2.0	0.4	0	0.2	0	
Max.	4.2	2.1	7	84	0.9	1.3	11.3	2.2	0.2	5.7	3.6	0.5	1.6	1.2	
82_298b,01 - 21.3.2012	**9.0**	**2.4**	**11**	**57**	**0.9**	**1.3**	**9.4**	**1.4**	**0.2**	**6.4**	**0.2**	**0.1**	**0.6**		
Std. dev. (5 ms)	0.9	0.3	1	4	0.2	0.2	3.1	0.1	0.1	1.3	0.1	0.1	0.4		
Min.	7.8	2.0	10	51	0.7	1.1	5.6	1.2	0.1	5.1	0	0	0.1		
Max.	10.1	2.7	12	62	1.2	1.5	12.5	1.5	0.3	8.5	0.3	0.3	1.1		
83_0542b,01 - 21.3.2012	**3.2**	**2.7**	**12**	**62**	**0.7**	**2.4**	**5.8**	**1.6**	**0.1**	**7.9**	**0.4**	**0.3**	**1.2**		
Std. dev. (4 ms)	0.5	0.3	1	1	0.2	0.4	0.9	0.5	0.1	0.8	0.3	0.3	1.4		
Min.	2.8	2.3	10	60	0.5	1.8	5.2	1.2	0.1	7.0	0.2	0	0.3		
Max.	3.9	3.0	13	63	0.9	2.7	7.2	2.3	0.2	8.8	0.8	0.6	3.3		
83_0597b,01 - 21.3.2012	**2.7**	**3.2**	**8**	**47**	**1.9**	**2.4**	**15**	**0.9**	**0.2**	**8.5**	**2.7**	**0.2**	**6.7**	**0.7**	
Std. dev. (4 ms)	1.3	0.2	1	3	0.3	0.3	1.6	0.2	0.1	0.9	1.3	0.3	1.9	0.3	
Min.	1.6	3.1	7	42	1.6	2.0	12.9	0.7	0.1	7.9	1.5	0	4.8	0.5	
Max.	4.0	3.4	10	50	2.2	2.7	16.7	1.2	0.3	9.9	4.2	0.5	8.6	1.1	
83_1149b - 12.11.2012 (1)	**2.1**	**3.2**	**12**	**55**	**1.0**	**2.2**	**11.0**	**1.5**	**0.1**	**8.7**	**2.8**	**0.1**	**0.3**		
Std. dev. (4 ms)	0.2	0.8	1	6	0.6	0.3	6.1	0.3	0.1	1.3	3.0	0.2	0.2		
Min.	1.9	2.3	11	49	0.4	1.9	3.9	1.2	0	7.0	0.6	0	0.1		
Max.	2.3	4.1	13	61	1.6	2.5	16.8	1.9	0.3	10.1	7.3	0.2	0.6		
83_1149b - 12.11.2012 (2)	**2.0**	**2.6**	**14**	**61**	**0.5**	**1.8**	**5.4**	**1.9**	**0.2**	**10.4**	**0.4**	**0.4**	**0.2**		
Std. dev. (4 ms)	0.3	0.2	1	3	0.2	0.3	1.0	0.2	0.1	1.9	0.2	0.2	0.2		
Min.	1.7	2.3	13	57	0.3	1.6	4.3	1.6	0.1	8.7	0.2	0.3	0.1		
Max.	2.3	2.9	15	64	0.7	2.2	6.7	2.2	0.3	13.1	0.6	0.6	0.5		
84_0030c,01 - 10.1.2012	**1.3**	**2.2**	**9**	**56**	**0.7**	**1.7**	**6.6**	**1.3**	**0.1**	**7.1**	**4.4**	**0.1**	**8.8**		
Std. dev. (3 ms)	0.3	0.4	2	11	0.1	0.3	0.9	0.4	0.1	2.2	1.7	0.1	12.7		
Min.	1.0	1.9	7	45	0.5	1.4	5.5	0.8	0	5.8	2.5	0	1.5		
Max.	1.6	2.7	12	66	0.8	2.0	7.2	1.5	0.1	9.7	5.8	0.3	23.5		
84_0106c - 12.11.2012	**1.6**	**3.0**	**16**	**53**	**1.1**	**1.9**	**3.5**	**1.5**	**0.2**	**15.4**	**2.0**	**0.2**	**0.4**		
Std. dev. (4 ms)	0.7	0.8	2	10	0.7	0.5	0.9	0.4	0.1	10.8	1.4	0.2	0.2		
Min.	0.8	2.2	13	38	0.4	1.4	2.1	1.1	0	6.6	0.5	0	0.1		
Max.	2.1	4.1	18	61	1.9	2.4	4.1	2.1	0.2	31.1	3.8	0.3	0.6		
84_0749, - 10.1.12	**4.1**	**2.6**	**14**	**61**	**0.4**	**2.2**	**4.6**	**1.8**	**0.1**	**9.0**	**0.2**	**0.2**	**0.3**		
Std. dev. (9 ms)	1.1	0.3	1	3	0.2	0.3	0.9	0.3	0.1	0.9	0.1	0.3	0.3		
Min.	2.5	2.1	12	58	0.2	1.7	3.4	1.5	0	7.7	0	0	0		
Max.	6.3	3.1	15	65	0.8	2.8	6.1	2.3	0.3	9.8	0.4	0.7	0.7		
84_1189b,0 - 12.11.2012	**2.2**	**2.5**	**12**	**65**	**0.4**	**2.0**	**5.3**	**1.8**	**0.2**	**7.8**	**0.2**	**0.1**	**0.4**		
Std. dev. (5 ms)	0.2	0.5	1	4	0.3	0.3	1.3	0.2	0.1	0.6	0.2	0.1	0.5		
Min.	1.9	2.0	11	61	0.2	1.6	3.9	1.5	0.1	7.1	0	0	0		
Max.	2.4	3.0	13	69	0.8	2.3	6.8	2.1	0.2	8.5	0.4	0.3	1.1		
84_1232, - 12.11.2012	**2.7**	**2.0**	**9**	**66**	**0.9**	**2.6**	**6.4**	**1.2**	**0.1**	**6.3**	**0.4**	**0.2**	**2.3**		
Std. dev. (4 ms)	0.6	0.3	1	4	0.4	0.3	2.9	0.3	0.1	1.5	0.3	0.1	2.3		
Min.	2.0	1.5	8	62	0.4	2.3	2.6	0.9	0	5.0	0.1	0.1	0.6		
Max.	3.5	2.3	9	72	1.3	2.8	8.7	1.5	0.1	7.7	0.8	0.3	5.7		
86_0208b - 12.11.2012	**2.4**	**2.4**	**11**	**60**	**1.8**	**2.9**	**10.9**	**1.3**	**0.1**	**7.0**	**0.2**	**0.1**	**0.5**		
Std. dev. (4 ms)	0.3	0.7	1	12	1.7	0.3	8.5	0.3	0.1	1.5	0.3	0.1	0.2		
Min.	2.1	1.5	9	48	0.3	2.4	3.5	1.0	0	5.1	0	0	0.1		
Max.	2.8	3.2	12	73	3.9	3.2	20	1.6	0.1	8.3	0.6	0.3	0.6		
86_0471b,01 - 19.1.2006	**2.1**	**2.0**	**10**	**69**	**0.7**	**2.5**	**6.0**	**1.3**	**0.2**	**4.9**	**0.9**	**0.3**	**0.4**		
Std. dev. (5 ms)	0.3	0.2	1	2	0.2	0.2	1.8	0.2	0.1	0.5	1.5	0.2	0.3		
Min.	1.8	1.8	9	66	0.5	2.2	4.5	1.1	0	4.5	0	0	0.1		
Max.	2.7	2.3	13	71	0.9	2.8	9.1	1.6	0.3	5.6	3.7	0.4	0.9		
86_0749c - 19.1.2006	**1.7**	**2.6**	**12**	**60**	**1.1**	**2.4**	**11.4**	**1.4**	**0.1**	**6.6**	**0.8**	**0.1**	**0.4**		
Std. dev. (4 ms)	0.4	0.9	2	8	0.4	0.5	6.6	0.2	0.1	1.2	0.7	0.2	0.1		
Min.	1.4	1.7	9	53	0.7	1.7	5.7	1.1	0	4.9	0.3	0	0.3		
Max.	2.3	3.7	14	70	1.5	2.8	18.3	1.7	0.2	7.5	1.8	0.4	0.6		
86_0792b,04 - 12.11.2012	**2.1**	**2.9**	**13**	**58**	**0.5**	**2.6**	**5.3**	**1.7**	**0.2**	**9.1**	**4.1**	**0.3**	**0.5**		
Std. dev. (5 ms)	0.1	0.2	1	3	0.2	1.0	1.5	0.2	0.1	1.5	1.6	0.2	0.2		
Min.	2.0	2.5	12	54	0.3	1.8	3.8	1.5	0.1	7.6	2.6	0	0.2		
Max.	2.3	3.1	14	63	0.8	4.3	6.9	2.1	0.3	11.2	6.5	0.4	0.9		
87_0423b - 19.1.2006	**8.7**	**2.8**	**8**	**65**	**0.3**	**1.5**	**4.0**	**1.0**	**0**	**4.8**	**3.7**	**0.1**	**0.2**		
Std. dev. (4 ms)	2.2	1.2	1	2	0.2	0.3	0.7	0.2	0.1	1.1	3.1	0.1	0		
Min.	5.9	1.8	7	63	0	1.1	3.0	0.8	0	4.0	0.7	0	0		
Max.	11.1	4.5	8	67	0.5	1.8	4.8	1.2	0.2	6.5	8.0	0.3	0.5		
87_0634c,04 - 12.11.2012	**1.6**	**2.0**	**7**	**38**	**1.1**	**1.8**	**10.0**	**0.7**	**0.1**	**11.7**	**6.0**	**0.2**	**19.9**		
Std. dev. (4 ms)	0.5	0.7	1	4	0.2	0.3	3.0	0.2	0.1	5.0	1.4	0.2	3.7		
Min.	1.2	1.4	6	32	0.9	1.4	8.3	0.5	0	5.8	4.0	0	16.8		
Max.	2.3	2.8	9	42	1.3	2.1	14.5	0.9	0.1	17.1	7.2	0.3	24.5		
87_0725c,1-20 - 12.11.2012	**3.0**	**3.3**	**12**	**47**	**2.3**	**1.6**	**15.3**	**1.4**	**0.3**	**12.7**	**0.2**	**0.2**	**0.6**		

Average slag composition. All results in wt%, normalised to 100%.

Sample	Na_2O	MgO	Al_2O_3	SiO_2	P_2O_5	K_2O	CaO	TiO_2	MnO	FeO	CuO	As_2O_3	SnO_2	PbO	CoO
Std. dev. (5 ms)	0.5	0.7	2	3	0.6	0.6	4.8	0.5	0.1	4.9	0.2	0.2	0.2		
Min.	2.6	2.4	10	45	1.7	1.1	10.9	0.7	0.2	9.8	0	0	0.4		
Max.	3.6	3.9	13	51	3.1	2.4	19.6	1.8	0.5	20.0	0.5	0.4	0.8		
87_0726,68-78b - 19.1.2006	**1.2**	**2.4**	**4**	**26**	**0.9**	**1.2**	**9.0**	**0.5**	**0.1**	**14.3**	**21.6**	**0.5**	**18.0**		
Std. dev. (5 ms)	0.6	0.7	1	4	0.3	0.4	2.8	0.1	0.1	4.2	4.8	0.3	6.1		
Min.	0.2	1.4	3	22	0.4	0.5	4.7	0.3	0	7.0	16.8	0.2	11.8		
Max.	1.8	3.0	5	33	1.2	1.6	12.2	0.6	0.2	17.9	27.9	1.0	25.9		
87_0726c,2-60a - 19.1.2006	**6.1**	**3.0**	**9**	**46**	**1.3**	**1.6**	**16.6**	**1.1**	**0.1**	**7.3**	**2.8**	**0.3**	**4.6**		
Std. dev. (3 ms)	1.0	0.5	2	9	0.2	0.7	4.4	0.3	0.1	1.4	4.4	0.2	4.2		
Min.	5.0	2.5	7	36	1.1	1.1	11.5	0.7	0	5.8	0.2	0.1	1.4		
Max.	7.0	3.5	11	55	1.5	2.3	19.4	1.3	0.2	8.1	7.9	0.4	9.4		
87_0762, - 21.3.2012	**5.0**	**3.1**	**9**	**46**	**1.5**	**1.9**	**13.1**	**1.0**	**0.1**	**11.8**	**2.1**	**0.1**	**3.7**		**1.7**
Std. dev. (5 ms)	1.4	0.4	1	7	0.3	0.3	2.5	0.1	0.1	4.8	1.0	0.1	4.0		2.0
Min.	3.1	2.8	7	39	1.1	1.6	10.5	0.9	0	8.8	1.0	0	0.7		0.6
Max.	6.5	3.7	11	53	1.9	2.4	16.9	1.2	0.2	20.3	3.5	0.3	10.2		5.2
87_0762, - 22.3.2013 (1)	**2.3**	**1.7**	**10**	**68**	**0.4**	**2.0**	**7.3**	**1.3**	**0.1**	**5.8**	**1.1**	**0**	**0**		
Std. dev. (5 ms)	0.5	0.4	2	6	0.1	0.6	3.3	0.2	0.1	1.0	0.9	0.1	0.2		
Min.	1.6	1.3	7	62	0.3	1.2	4.5	1.0	0	4.5	0.3	0	0		
Max.	3.0	2.3	12	75	0.6	2.7	12.1	1.7	0.2	7.0	2.4	0.2	0.2		
87_0762, - 22.3.2013 (2)	**4.7**	**2.7**	**7**	**32**	**1.2**	**1.3**	**11.2**	**0.6**	**0.2**	**6.0**	**15.8**	**0.4**	**16.4**	**1.4**	
Std. dev. (5 ms)	0.6	0.3	1	4	0.2	0.3	2.8	0.2	0.1	1.3	7.4	0.2	7.1	0.4	
Min.	4.1	2.5	6	26	0.9	0.9	8.5	0.3	0	4.8	5.6	0.1	11.6	1.0	
Max.	5.3	3.3	8	37	1.5	1.7	15.9	0.9	0.3	8.2	24.6	0.6	28.8	2.0	
87_0762,0Nv - 21.2.2012	**3.8**	**2.9**	**11**	**57**	**1.3**	**2.6**	**8.3**	**1.3**	**0.1**	**7.0**	**3.8**	**0.2**	**0.7**		
Std. dev. (5 ms)	1.2	0.7	2	11	0.3	0.5	4.4	0.3	0.1	1.4	8.0	0.2	0.6		
Min.	2.6	2.0	9	42	1.0	1.9	4.2	0.8	0	5.3	0	0	0.2		
Max.	5.5	3.9	13	69	1.7	3.1	14.1	1.7	0.3	8.6	18.1	0.4	1.4		
87_0762,0Nv - 22.3.2013 (1)	**4.3**	**2.7**	**8**	**49**	**1.3**	**2.0**	**9.8**	**0.9**	**0.2**	**6.2**	**5.2**	**0.2**	**9.5**	**0.7**	
Std. dev. (5 ms)	0.9	0.6	2	14	0.7	0.7	5.5	0.2	0.2	0.6	5.9	0.3	6.6	0.5	
Min.	3.1	2.2	5	27	0.8	1.0	5.5	0.6	0	5.3	1.3	0	2.0	0.17	
Max.	5.4	3.4	10	66	2.5	2.7	18.9	1.1	0.3	7.0	15.5	0.5	16.3	1.51	
87_0762,0Nv - 22.3.2013 (2)	**2.3**	**2.3**	**10**	**58**	**1.0**	**2.9**	**7.9**	**1.4**	**0.2**	**8.6**	**3.2**	**0**	**3.0**		
Std. dev. (5 ms)	0.4	0.4	2	13	0.4	0.6	5.0	0.7	0.1	3.4	3.5	0.3	4.4		
Min.	1.8	1.9	6	34	0.5	1.7	3.3	0.7	0	4.8	0.3	0	0.5		
Max.	2.8	2.8	12	70	1.5	3.3	16.3	2.2	0.3	13.3	9.8	0.5	11.5		
87_0773,04 - 12.11.2012	**1.8**	**2.2**	**13**	**67**	**0.4**	**1.9**	**4.0**	**1.5**	**0.2**	**8.1**	**0.2**	**0.1**	**0.1**		
Std. dev. (4 ms)	0.6	0.5	3	6	0.1	0.5	0.9	0.4	0.2	1.8	0.2	0.1	0.2		
Min.	1.0	1.6	8	61	0.3	1.3	3.3	1.0	0.1	5.9	0	0	0		
Max.	2.2	2.7	15	74	0.7	2.4	5.2	1.9	0.4	10.1	0.4	0.2	0.4		
87_0791,01-88 - 12.11.2012	**1.5**	**3.1**	**10**	**48**	**1.2**	**2.8**	**12.8**	**1.2**	**0.1**	**12.9**	**1.7**	**0.3**	**3.6**		**1.4**
Std. dev. (5 ms)	0.1	0.3	1	4	0.1	0.2	0.8	0.1	0.1	2.6	0.3	0.2	1.7		0.6
Min.	1.3	2.7	9	43	1.1	2.6	11.5	1.0	0	9.8	1.3	0.1	1.7		0.6
Max.	1.6	3.5	11	54	1.3	3.1	13.8	1.3	0.3	16.3	2.1	0.5	6.3		2.0
87_0849a,04 - 21.3.2012	**1.4**	**3.6**	**13**	**53**	**0.7**	**1.9**	**13.7**	**1.9**	**0.1**	**8.8**	**0.7**	**0.1**	**0.5**		
Std. dev. (5 ms)	0.2	0.3	1	2	0	0.1	1.2	0.1	0.1	0.9	0.2	0.1	0.1		
Min.	1.2	3.2	13	50	0.6	1.7	12.2	1.8	0	7.6	0.4	0	0.4		
Max.	1.6	3.9	15	56	0.8	2.0	15.4	2.0	0.2	9.7	0.9	0.2	0.7		
87_0884,01-56b - 19.1.2006	**1.9**	**3.1**	**8**	**34**	**1.5**	**1.2**	**15.5**	**0.8**	**0.1**	**13.3**	**10.9**	**0.5**	**6.8**		**2.1**
Std. dev. (6 ms)	1.1	1.1	2	5	0.9	0.8	1.7	0.2	0.2	3.8	6.8	0.5	6.0		1.5
Min.	0.3	2.0	5	27	0.5	0.4	14.0	0.5	0	7.8	4.1	0	1.5		0.8
Max.	3.3	5.1	10	40	3.1	2.3	17.8	1.2	0.5	19.4	20.4	1.1	17.9		4.4
87_0884,01-56c - 19.1.2006	**2.0**	**3.5**	**8**	**36**	**1.5**	**1.3**	**19.5**	**0.8**	**0.1**	**12.5**	**5.1**	**0**	**9.2**		**1.4**
Std. dev. (3 ms)	0.5	0.2	1	1	0.5	0.7	2.6	0.1	0.1	1.1	2.2	0.1	5.3		0.1
Min.	1.6	3.3	7	34	1.1	0.4	16.6	0.7	0.1	11.4	2.9	0	3.3		1.2
Max.	2.5	3.7	8	36	2.1	1.7	21.6	0.9	0.2	13.7	7.2	0.2	13.5		1.5
87_0897a,01-45 - 12.11.2012 (1)	**5.0**	**2.5**	**10**	**53**	**1.0**	**2.0**	**9.4**	**1.7**	**0.1**	**12.9**	**0.9**	**0.1**	**1.2**		
Std. dev. (4 ms)	0.1	0.2	2	6	0.3	0.4	3.9	1.2	0.2	3.1	0.4	0.1	1.0		
Min.	4.9	2.3	8	47	0.6	1.5	4.2	1.0	0	9.1	0.5	0	0		
Max.	5.2	2.8	13	58	1.4	2.5	13.5	3.5	0.3	15.5	1.4	0.2	2.2		
87_0897a,01-45 - 12.11.2012 (2)	**2.0**	**3.5**	**9**	**37**	**1.1**	**0.8**	**16.8**	**1.0**	**0.1**	**8.9**	**10.2**	**0.2**	**8.2**		**1.6**
Std. dev. (3 ms)	0.9	0.2	0	2	0.1	0.4	2.1	0	0.1	0.8	0.2	0.2	4.0		1.0
Min.	1.1	3.3	9	35	1.0	0.5	14.4	0.9	0	8.0	10.0	0	5.8		0.6
Max.	2.7	3.7	9	38	1.3	1.2	18.3	1.0	0.2	9.5	10.5	0.4	12.9		2.4
87_0942g,03 - 12.11.2012	**1.7**	**2.5**	**12**	**64**	**0.6**	**1.9**	**5.8**	**1.6**	**0.2**	**8.4**	**1.0**	**0.1**	**0.3**		
Std. dev. (5 ms)	0.2	0.5	1	6	0.1	0.2	2.0	0.3	0.1	2.0	1.8	0.3	0.1		
Min.	1.3	1.9	10	57	0.4	1.7	3.6	1.4	0.1	6.3	0.1	0	0.1		
Max.	1.9	3.1	13	72	0.7	2.1	8.3	2.2	0.4	11.2	4.2	0.6	0.4		
92_0606 - 12.11.2012	**1.9**	**1.4**	**8**	**73**	**0.8**	**2.7**	**2.5**	**1.0**	**0.1**	**4.4**	**3.3**	**0.1**	**0**		**0.3**
Std. dev. (4 ms)	0.6	0.3	2	7	0.3	1.1	1.0	0.1	0.1	0.8	4.2	0.2	0.2		0.4

Average slag composition. All results in wt%, normalised to 100%.

Sample	Na_2O	MgO	Al_2O_3	SiO_2	P_2O_5	K_2O	CaO	TiO_2	MnO	FeO	CuO	As_2O_3	SnO_2	PbO	CoO
Min.	1.4	1.0	6	64	0.5	1.9	1.7	0.8	0	3.5	0.3	0	0		0
Max.	2.8	1.6	11	80	1.1	4.2	3.8	1.1	0.2	5.4	9.3	0.4	0.1		0.9
92_0645b - 21.3.2012	**1.9**	**2.4**	**11**	**60**	**2.1**	**3.9**	**8.3**	**1.1**	**0.1**	**6.2**	**1.6**	**0.2**	**1.0**		
Std. dev. (4 ms)	0.2	0.5	2	7	0.4	0.7	2.5	0.1	0	1.1	0.4	0.1	0.6		
Min.	1.8	1.6	9	53	1.5	3.2	4.7	0.9	0	4.7	1.2	0.1	0.3		
Max.	2.2	2.8	13	69	2.5	4.8	10.1	1.3	0.1	7.1	2.1	0.4	1.7		
94_0239,01 - 21.3.2012	**6.7**	**2.3**	**5**	**31**	**2.6**	**0.9**	**9.7**	**0.5**	**0.2**	**20.7**	**6.3**	**0.2**	**13.9**		
Std. dev. (4 ms)	2.3	0.4	1	3	0.7	0.2	1.2	0.1	0.1	5.1	3.0	0.2	4.8		
Min.	4.4	1.9	4	28	1.7	0.7	8.6	0.4	0.1	13.3	3.5	0	7.0		
Max.	9.5	2.6	7	35	3.1	1.1	11.1	0.6	0.2	24.8	9.4	0.3	18.1		
94_0560 - 10.1.12 - 1^{st} layer	**1.6**	**2.0**	**12**	**68**	**0.4**	**1.7**	**3.0**	**1.4**	**0.2**	**7.9**	**1.3**	**0**	**0.1**	**0.1**	
Std. dev. (4 ms)	0	0.4	2	4	0.2	0.2	0.8	0.2	0	1.1	0.3	0.1	0.2	0.2	
Min.	1.0	2.0	9	66	0.3	1.5	2.5	1.2	0.1	6.4	0.3	0	0	0.1	
Max.	1.9	2.2	13	73	0.5	1.9	3.5	1.5	0.3	8.9	3.5	0.1	0.2	0.2	
94_0560 - 10.1.12 - 2^{nd} layer	**1.6**	**1.6**	**5**	**27**	**1.4**	**1.0**	**8.6**	**0.4**	**0.4**	**35.3**	**8.3**	**0.3**	**10.2**	**0.8**	
Std. dev. (4 ms)	0.3	0.2	1	3.0	0.2	0.2	1.2	0.1	0.2	5.9	1.7	0.3	6.3	0.3	
Min.	1.0	1.1	4	21	1.1	0.6	7.2	0.3	0.1	24.9	3.4	0	0.4	0.2	
Max.	1.9	2.1	6	32	1.7	1.2	10.0	0.6	0.7	43.2	11.7	0.5	22.1	1.5	
94_0775,01 - 12.11.2012	**3.1**	**2.6**	**12**	**53**	**0.7**	**1.8**	**8.5**	**1.6**	**0.1**	**12.1**	**1.3**	**0.2**	**2.4**		
Std. dev. (5 ms)	1.2	0.5	2	6	0.3	0.3	3.4	0.4	0.1	4.0	1.4	0.2	1.1		
Min.	1.9	1.8	10	48	0.2	1.5	4.2	1.3	0	6.0	0.3	0	0.6		
Max.	4.8	3.1	16	63	1.0	2.2	12.9	2.3	0.2	16.5	3.4	0.4	3.3		
94_842 - 21.2.2012	**1.4**	**2.1**	**8**	**62**	**0.9**	**2.0**	**7.5**	**1.1**	**0.2**	**5.7**	**7.4**	**0.2**	**0.7**		
Std. dev. (4 ms)	0.2	0.5	1	7	0.4	0.4	1.9	0.1	0.1	1.4	1.9	0.3	0.2		
Min.	1.1	1.4	7	56	0.5	1.6	4.7	1.0	0.1	4.0	5.8	0	0.5		
Max.	1.6	2.6	10	73	1.3	2.5	9.2	1.2	0.3	7.1	9.8	0.6	0.9		
97_0631E,01 - 12.11.2012	**2.1**	**2.2**	**9**	**47**	**0.9**	**2.2**	**7.2**	**0.8**	**0.1**	**4.5**	**12.3**	**0.2**	**11.1**	**0.4**	
Std. dev. (5 ms)	0.4	0.6	4	18	0.2	0.7	3.7	0.3	0.1	1.6	8.5	0.1	12.1	0.5	
Min.	1.7	1.8	5	25	0.5	1.4	4.4	0.4	0	3.0	2.5	0.1	0.4	0	
Max.	2.5	3.2	15	65	1.1	3.2	12.9	1.1	0.2	6.6	20.1	0.3	25.4	1.0	
97_0631E,04 - 12.11.2012	**5.9**	**1.9**	**4**	**29**	**1.2**	**0.7**	**8.8**	**0.4**	**0**	**4.6**	**10.6**	**0.1**	**32.1**	**0.9**	
Std. dev. (5 ms)	1.5	0.5	1	4	0.1	0.1	2.2	0.2	0.1	1.2	4.3	0.1	6.5	0.6	
Min.	3.8	1.2	3	23	1.0	0.6	6.0	0.3	0	3.3	6.8	0	21.4	0.3	
Max.	8.0	2.5	4	35	1.3	0.9	10.8	0.8	0.1	6.0	15.8	0.3	38.1	1.72	
97_0632D,01 - 10.1.12	**0.7**	**1.2**	**7**	**61**	**0.4**	**0.8**	**1.8**	**0.4**	**0.2**	**3.4**	**21.6**	**0**	**1.3**		
Std. dev. (5 ms)	0.5	0.4	2	6	0.5	0.4	0.4	0.2	0.2	1.0	7.3	0.2	0.2		
Min.	0.1	0.5	5	54	0	0.5	1.4	0.3	0	2.4	0.7	0	1.1		
Max.	3.1	1.9	9	68	1.2	3.5	8.1	0.8	0.4	7.0	29.7	0.2	3.7		
97_0675,02 - 12.11.2012	**1.4**	**1.8**	**10**	**68**	**0.7**	**1.8**	**2.7**	**1.3**	**0.2**	**5.9**	**5.4**	**0.1**	**0.4**		
Std. dev. (5 ms)	0.9	0.6	3	6	0.2	1.2	1.0	0.5	0.1	2.6	6.7	0.1	0.4		
Min.	0.6	1.0	6	61	0.4	0.6	1.8	0.5	0.1	3.0	0	0	0		
Max.	2.6	2.4	14	75	1.0	3.4	4.5	2.1	0.4	9.3	16.0	0.3	1.0		
97_0690,02 - 21.2.2012	**1.8**	**1.8**	**9**	**68**	**1.2**	**2.5**	**4.7**	**1.1**	**0.1**	**6.6**	**1.0**	**0.2**	**1.3**		
Std. dev. (4 ms)	0.7	0.9	3	10	0.4	0.6	2.0	0.4	0.1	2.0	0.2	0.2	0.6		
Min.	1.2	1.0	6	55	0.8	1.9	2.2	0.7	0	4.0	0.8	0	0.6		
Max.	2.7	3.0	13	79	1.7	3.2	7.2	1.6	0.3	8.9	1.2	0.4	2.1		
97_0690,02- - 21.2.2012	**2.4**	**2.1**	**11**	**62**	**1.1**	**2.8**	**4.8**	**1.4**	**0.1**	**6.3**	**5.5**	**0.3**	**0.2**		
Std. dev. (4 ms)	0.3	0.4	1	3	0.4	0.4	2.8	1.2	0.1	1.7	3.9	0.1	0.3		
Min.	2.0	1.6	10	59	0.7	2.4	2.7	0.7	0	4.4	1.2	0.2	0		
Max.	2.7	2.6	13	67	1.7	3.4	9.6	3.4	0.2	9.1	10.6	0.4	0.5		
97_1176 - 12.11.2012	**1.5**	**3.0**	**13**	**60**	**0.5**	**1.6**	**7.9**	**1.8**	**0.1**	**9.3**	**0.8**	**0.1**	**1.1**		
Std. dev. (5 ms)	0.2	0.4	2	5	0.3	0.3	2.7	0.3	0.1	1.7	0.7	0.2	0.5		
Min.	1.4	2.4	10	53	0.2	1.2	4.4	1.5	0	6.9	0.2	0	0.5		
Max.	1.7	3.4	15	66	0.9	2.0	11.3	2.2	0.3	11.5	1.8	0.4	1.7		
98_0387,03 - 21.3.2012	**2.2**	**3.3**	**13**	**56**	**1.1**	**2.6**	**11.0**	**1.6**	**0.1**	**8.3**	**1.0**	**0.1**	**0.3**		
Std. dev. (5 ms)	0.5	0.5	1	7	0.6	0.2	6.2	0.1	0.1	0.4	0.5	0.2	0.3		
Min.	1.7	2.8	11	47	0.4	2.4	4.4	1.4	0	7.9	0.6	0	0		
Max.	2.8	3.9	14	63	1.8	2.9	18.3	1.7	0.2	8.9	1.9	0.4	0.8		
98_1325 - 12.11.2012	**0.7**	**4.1**	**10**	**41**	**2.5**	**0.9**	**22.6**	**1.4**	**0.3**	**8.8**	**5.2**	**0.7**	**1.6**		
Std. dev. (1 ms)	0	0	0	0	0	0	0	0	0	0	0	0	0		
Min.	0.7	4.1	10	41	2.5	0.9	22.6	1.4	0.3	8.8	5.2	0.7	1.6		
Max.	0.7	4.1	10	41	2.5	0.9	22.6	1.4	0.3	8.8	5.2	0.7	1.6		
Average Slag Composition	***2.8***	***2.5***	***10***	***54***	***1.1***	***1.9***	***9***	***1.2***	***0.1***	***8.9***	***4.3***	***0.2***	***4.4***	**/**	**/**

Ceramic. Ratio of oxides to Al_2O_3, metals removed.

Sample	$\frac{Na_2O}{Al_2O_3}$	$\frac{MgO}{Al_2O_3}$	$\frac{SiO_2}{Al_2O_3}$	$\frac{P_2O_5}{Al_2O_3}$	$\frac{K_2O}{Al_2O_3}$	$\frac{CaO}{Al_2O_3}$	$\frac{TiO_2}{Al_2O_3}$	$\frac{MnO}{Al_2O_3}$	$\frac{FeO}{Al_2O_3}$
82_0223b,01 - 10.1.12	0.31	0.15	5.58	0.05	0.14	0.27	0.12	0.01	0.58
82_298b,01 - 21.3.2012	0.16	0.17	5.15	0.05	0.12	0.26	0.10	0.01	0.61
83_0542b,01 - 21.3.2012	0.19	0.21	5.58	0.07	0.14	0.33	0.13	0.01	0.63
83_0597b,01 - 21.3.2012	0.14	0.17	3.75	0.02	0.09	0.24	0.12	0.01	0.67
83_1149b - 12.11.2012 (1)	0.15	0.18	5.15	0.04	0.12	0.24	0.11	0	0.65
83_1149b - 12.11.2012 (2)	0.25	0.19	4.50	0.03	0.11	0.24	0.12	0.01	0.65
84_0030c,01 - 10.1.2012	0.16	0.23	5.33	0.06	0.18	0.36	0.17	0.01	0.75
84_0106c - 12.11.2012	0.11	0.14	4.86	0.04	0.11	0.19	0.10	0.01	0.60
84_0749, - 10.1.12	0.16	0.17	3.88	0.03	0.11	0.18	0.10	0.01	0.60
84_1189b,0 - 12.11.2012	0.15	0.20	5.08	0.05	0.13	0.28	0.12	0.02	0.62
84_1232, - 12.11.2012	0.12	0.16	6.55	0.04	0.13	0.26	0.11	0.03	0.68
86_0208b - 12.11.2012	0.17	0.19	7.20	0.03	0.18	0.30	0.13	0.01	0.68
86_0471b,01 - 19.1.2006	0.12	0.15	5.23	0.05	0.15	0.19	0.11	0.01	0.68
86_0749c - 19.1.2006	0.15	0.15	5.00	0.08	0.15	0.24	0.11	0.01	0.72
86_0792b,04 - 12.11.2012	0.15	0.17	4.27	0.01	0.11	0.22	0.11	0.01	0.61
87_0423b - 19.1.2006	0.40	0.11	11.86	0.04	0.16	0.26	0.10	0.01	0.43
87_0634c,04 - 12.11.2012	0.12	0.14	4.71	0.05	0.13	0.23	0.11	0.01	0.59
87_0725c,1-20 - 12.11.2012	0.17	0.15	5.23	0.06	0.18	0.23	0.10	0.02	0.58
87_0726,68-78b - 19.1.2006	0.14	0.19	5.18	0.03	0.12	0.27	0.20	0.01	0.77
87_0726c,2-60a - 19.1.2006	0.14	0.18	4.57	0.04	0.11	0.28	0.11	0.01	0.65
87_0762, - 21.3.2012	0.12	0.16	4.64	0.03	0.12	0.21	0.11	0.02	0.68
87_0762, - 22.3.2013 (1)	0.18	0.17	5.58	0.15	0.19	0.34	0.11	0.01	0.58
87_0762, - 22.3.2013 (2)	0.11	0.15	4.71	0.04	0.11	0.24	0.13	0.01	0.62
87_0762,0Nv - 21.2.2012	0.18	0.19	5.67	0.08	0.18	0.28	0.12	0.01	0.63
87_0762,0Nv - 22.3.2013 (1)	0.18	0.17	4.92	0.05	0.18	0.23	0.14	0.02	0.72
87_0762,0Nv - 22.3.2013 (2)	0.13	0.17	5.67	0.03	0.13	0.23	0.12	0.02	0.81
87_0773,04 - 12.11.2012	0.12	0.18	5.83	0.03	0.12	0.23	0.12	0.02	0.66
87_0791,01-88 - 12.11.2012	0.13	0.16	4.57	0.04	0.14	0.24	0.12	0.01	0.69
87_0849a,04 - 21.3.2012	0.12	0.18	4.13	0.02	0.10	0.28	0.14	0.01	0.68
87_0884,01-56b - 19.1.2006	0.19	0.18	3.93	0.04	0.16	0.33	0.11	0.01	0.79
87_0884,01-56c - 19.1.2006	0.13	0.22	3.33	0.03	0.17	0.22	0.12	0.01	0.98
87_0897a,01-45 - 12.11.2012 (1)	0.20	0.19	5.08	0.05	0.14	0.28	0.11	0.01	0.58
87_0897a,01-45 - 12.11.2012 (2)	0.20	0.19	5.08	0.05	0.14	0.28	0.11	0.01	0.58
87_0942g,03 - 12.11.2012	0.12	0.18	5.23	0.03	0.11	0.24	0.13	0.01	0.62
92_0606 - 12.11.2012	0.19	0.13	8.44	0.09	0.23	0.30	0.09	0	0.54
92_0645b - 21.3.2012	0.17	0.15	4.64	0.09	0.19	0.22	0.09	0.01	0.56
94_0239,01 - 21.3.2012	0.17	0.15	5.15	0.06	0.18	0.22	0.09	0.02	0.61
94_0560 - 10.1.12	0.13	0.17	5.75	0.03	0.14	0.28	0.11	0.02	0.67
94_0775,01 - 12.11.2012	0.11	0.16	3.94	0.03	0.10	0.26	0.10	0.01	0.58
94_842 - 21.2.2012	0.18	0.13	8.78	0.06	0.14	0.21	0.10	0	0.52
97_0631E,01 - 12.11.2012	0.16	0.14	5.83	0.04	0.19	0.23	0.09	0.01	0.59
97_0631E,04 - 12.11.2012	0.18	0.15	7.40	0.06	0.21	0.23	0.08	0.01	0.60
97_0632D,01 - 10.1.12	0.12	0.15	4.20	0.08	0.13	0.23	0.09	0.01	0.60
97_0675,02 - 12.11.2012	0.13	0.16	5.83	0.08	0.18	0.25	0.10	0.01	0.59
97_0690,02 - 21.2.2012	0.18	0.14	5.58	0.08	0.18	0.32	0.11	0.01	0.63
97_0690,02- - 21.2.2012	0.17	0.16	5.08	0.08	0.24	0.22	0.09	0.02	0.61
97_1176 - 12.11.2012	0.13	0.15	4.27	0.03	0.13	0.19	0.11	0.01	0.63
98_0387,03 - 21.3.2012	0.16	0.17	4.57	0.04	0.14	0.24	0.11	0.01	0.61
98_1325 - 12.11.2012	0.08	0.14	4.79	0.02	0.11	0.21	0.11	0	0.69
Average	***0.16***	***0.17***	***5.33***	***0.05***	***0.15***	***0.25***	***0.11***	***0.01***	***0.64***

Slag. Ratio of oxides to Al_2O_3, metals removed.

Sample	$\frac{Na_2O}{Al_2O_3}$	$\frac{MgO}{Al_2O_3}$	$\frac{SiO_2}{Al_2O_3}$	$\frac{P_2O_5}{Al_2O_3}$	$\frac{K_2O}{Al_2O_3}$	$\frac{CaO}{Al_2O_3}$	$\frac{TiO_2}{Al_2O_3}$	$\frac{MnO}{Al_2O_3}$	$\frac{FeO}{Al_2O_3}$
82_0223b,01 - 10.1.12	0.75	0.33	19.75	0.13	0.25	1.55	0.25	0	0.90
82_298b,01 - 21.3.2012	0.83	0.22	5.27	0.08	0.12	0.86	0.13	0.02	0.59
83_0542b,01 - 21.3.2012	0.28	0.23	5.25	0.06	0.20	0.49	0.13	0.01	0.67
83_0597b,01 - 21.3.2012	0.33	0.40	5.78	0.23	0.30	1.86	0.11	0.02	1.06
83_1149b - 12.11.2012 (1)	0.18	0.28	4.75	0.08	0.19	0.95	0.13	0.01	0.75
83_1149b - 12.11.2012 (2)	0.14	0.19	4.36	0.04	0.13	0.39	0.14	0.01	0.74
84_0030c,01 - 10.1.2012	0.15	0.26	6.50	0.08	0.20	0.77	0.15	0.01	0.83
84_0106c - 12.11.2012	0.10	0.19	3.44	0.07	0.13	0.23	0.09	0.01	0.99
84_0749, - 10.1.12	0.29	0.19	4.36	0.03	0.16	0.33	0.13	0.01	0.64
84_1189b,0 - 12.11.2012	0.18	0.21	5.50	0.03	0.17	0.44	0.15	0.02	0.66
84_1232, - 12.11.2012	0.31	0.23	7.56	0.10	0.30	0.73	0.13	0.01	0.72
86_0208b - 12.11.2012	0.22	0.22	5.45	0.16	0.26	0.99	0.12	0.01	0.64
86_0471b,01 - 19.1.2006	0.21	0.20	7.00	0.07	0.25	0.61	0.13	0.02	0.50
86_0749c - 19.1.2006	0.14	0.22	5.00	0.09	0.20	0.96	0.12	0.01	0.55
86_0792b,04 - 12.11.2012	0.16	0.21	4.36	0.04	0.19	0.40	0.13	0.01	0.68
87_0423b - 19.1.2006	1.14	0.36	8.50	0.04	0.20	0.53	0.13	0	0.63
87_0634c,04 - 12.11.2012	0.24	0.30	5.67	0.17	0.27	1.50	0.10	0.01	1.76
87_0725c,1-20 - 12.11.2012	0.25	0.28	4.00	0.19	0.13	1.29	0.12	0.03	1.07
87_0726,68-78b - 19.1.2006	0.29	0.57	6.29	0.21	0.29	2.16	0.11	0.03	3.43
87_0726c,2-60a - 19.1.2006	0.66	0.33	5.00	0.14	0.17	1.80	0.12	0.01	0.79
87_0762, - 21.3.2012	0.54	0.34	5.00	0.16	0.21	1.42	0.11	0.01	1.28
87_0762, - 22.3.2013 (1)	0.23	0.17	6.90	0.04	0.20	0.74	0.13	0.01	0.59
87_0762, - 22.3.2013 (2)	0.70	0.40	4.80	0.18	0.19	1.67	0.09	0.03	0.90
87_0762,0Nv - 21.2.2012	0.33	0.25	5.00	0.12	0.23	0.73	0.12	0.01	0.61
87_0762,0Nv - 22.3.2013 (1)	0.57	0.36	6.44	0.17	0.27	1.29	0.12	0.02	0.81
87_0762,0Nv - 22.3.2013 (2)	0.22	0.22	5.55	0.10	0.28	0.76	0.14	0.02	0.83
87_0773,04 - 12.11.2012	0.14	0.17	5.15	0.03	0.15	0.31	0.12	0.02	0.62
87_0791,01-88 - 12.11.2012	0.15	0.30	4.64	0.12	0.27	1.25	0.12	0.01	1.25
87_0849a,04 - 21.3.2012	0.11	0.28	4.15	0.05	0.15	1.08	0.15	0.01	0.69
87_0884,01-56b - 19.1.2006	0.24	0.39	4.30	0.19	0.15	1.95	0.10	0.01	1.68
87_0884,01-56c - 19.1.2006	0.26	0.46	4.67	0.20	0.17	2.54	0.10	0.01	1.63
87_0897a,01-45 - 12.11.2012 (1)	0.51	0.26	5.40	0.10	0.20	0.96	0.17	0.01	1.32
87_0897a,01-45 - 12.11.2012 (2)	0.23	0.40	4.18	0.13	0.09	1.90	0.11	0.01	1.01
87_0942g,03 - 12.11.2012	0.14	0.21	5.42	0.05	0.16	0.49	0.13	0.02	0.71
92_0606 - 12.11.2012	0.25	0.19	9.50	0.10	0.35	0.33	0.13	0.01	0.58
92_0645b - 21.3.2012	0.18	0.23	5.64	0.20	0.36	0.78	0.10	0.01	0.58
94_0239,01 - 21.3.2012	1.40	0.48	6.50	0.55	0.18	2.03	0.10	0.05	4.33
94_0560 - 10.1.12 - 1^{st} layer	0.14	0.18	5.87	0.04	0.15	0.26	0.12	0.02	0.68
94_0560 - 10.1.12 - 2^{nd} layer	0.37	0.38	6.20	0.33	0.23	2.09	0.09	0.08	8.40
94_0775,01 - 12.11.2012	0.25	0.21	4.23	0.05	0.15	0.68	0.13	0.01	0.98
94_842 - 21.2.2012	0.17	0.26	7.56	0.11	0.24	0.92	0.13	0.02	0.70
97_0631E,01 - 12.11.2012	0.23	0.24	5.17	0.10	0.24	0.79	0.09	0.01	0.49
97_0631E,04 - 12.11.2012	1.49	0.49	7.29	0.30	0.17	2.23	0.10	0	1.16
97_0632D,01 - 10.1.12	0.10	0.18	8.78	0.06	0.11	0.26	0.06	0.03	0.49
97_0675,02 - 12.11.2012	0.14	0.17	6.55	0.06	0.17	0.26	0.13	0.02	0.57
97_0690,02 - 21.2.2012	0.21	0.21	7.78	0.13	0.29	0.54	0.12	0.01	0.76
97_0690,02- - 21.2.2012	0.22	0.18	5.50	0.10	0.25	0.43	0.13	0.01	0.56
97_1176 - 12.11.2012	0.12	0.23	4.69	0.04	0.12	0.62	0.14	0.01	0.72
98_0387,03 - 21.3.2012	0.17	0.25	4.31	0.08	0.20	0.85	0.12	0.01	0.65
98_1325 - 12.11.2012	0.07	0.40	4.00	0.25	0.09	2.23	0.14	0.03	0.86
Average	***0.34***	***0.28***	***5.90***	***0.13***	***0.20***	***1.06***	***0.12***	***0.01***	***1.10***

Change (in %) in ratio of oxides to Al_2O_3 between ceramic and slag, metals removed.

Sample	$\frac{Na_2O}{Al_2O_3}$	$\frac{MgO}{Al_2O_3}$	$\frac{SiO_2}{Al_2O_3}$	$\frac{P_2O_5}{Al_2O_3}$	$\frac{K_2O}{Al_2O_3}$	$\frac{CaO}{Al_2O_3}$	$\frac{TiO_2}{Al_2O_3}$	$\frac{MnO}{Al_2O_3}$	$\frac{FeO}{Al_2O_3}$
82_0223b,01 - 10.1.12	142	120	254	160	79	474	108	-100	55
82_298b,01 - 21.3.2012	419	29	2	60	0	231	30	100	-3
83_0542b,01 - 21.3.2012	47	10	-6	-14	43	48	0	0	6
83_0597b,01 - 21.3.2012	136	135	54	1050	233	675	-8	100	58
83_1149b - 12.11.2012 (1)	20	56	-8	100	58	296	18	∞	15
83_1149b - 12.11.2012 (2)	-44	0	-3	33	18	63	17	0	14
84_0030c,01 - 10.1.2012	-6	13	22	33	11	114	-12	0	11
84_0106c - 12.11.2012	-9	36	-29	75	18	21	-10	0	65
84_0749, - 10.1.12	81	12	12	0	45	83	30	0	7
84_1189b,0 - 12.11.2012	20	5	8	-40	31	57	25	0	6
84_1232, - 12.11.2012	158	44	15	150	131	181	18	-67	6
86_0208b - 12.11.2012	29	16	-241	433	44	230	-8	0	-6
86_0471b,01 - 19.1.2006	75	33	34	40	67	221	18	100	-26
86_0749c - 19.1.2006	-7	47	0	13	33	300	9	0	-24
86_0792b,04 - 12.11.2012	7	24	2	300	73	82	18	0	11
87_0423b - 19.1.2006	185	227	-28	0	25	104	30	-100	47
87_0634c,04 - 12.11.2012	100	114	20	240	108	552	-9	0	198
87_0725c,1-20 - 12.11.2012	47	87	-24	217	-28	461	20	50	84
87_0726,68-78b - 19.1.2006	107	200	21	600	142	700	-45	200	345
87_0726c,2-60a - 19.1.2006	371	83	9	250	55	543	9	0	22
87_0762, - 21.3.2012	350	113	8	433	75	576	0	-50	88
87_0762, - 22.3.2013 (1)	28	0	24	-73	5	118	18	0	2
87_0762, - 22.3.2013 (2)	536	167	2	350	73	596	-31	200	45
87_0762,0Nv - 21.2.2012	83	32	-12	50	28	161	0	0	-3
87_0762,0Nv - 22.3.2013 (1)	217	112	31	240	50	461	-14	0	13
87_0762,0Nv - 22.3.2013 (2)	69	29	-2	233	115	230	17	0	2
87_0773,04 - 12.11.2012	17	-6	-12	0	25	35	0	0	-6
87_0791,01-88 - 12.11.2012	15	88	2	200	93	421	0	0	81
87_0849a,04 - 21.3.2012	-8	56	0	150	50	286	7	0	1
87_0884,01-56b - 19.1.2006	26	117	9	375	-6	491	-9	0	113
87_0884,01-56c - 19.1.2006	100	109	40	567	0	1055	-17	0	66
87_0897a,01-45 - 12.11.2012 (1)	155	37	6	100	43	243	55	0	128
87_0897a,01-45 - 12.11.2012 (2)	15	111	-18	160	-36	579	0	0	74
87_0942g,03 - 12.11.2012	17	17	4	67	45	104	0	100	15
92_0606 - 12.11.2012	32	46	13	11	52	10	44	∞	7
92_0645b - 21.3.2012	6	53	22	122	89	255	11	0	4
94_0239,01 - 21.3.2012	724	220	26	817	0	823	11	150	610
94_0560 - 10.1.12 - 1^{st} layer	7	9	3	16	4	-3	8	40	3
94_0560 - 10.1.12 - 2^{nd} layer	184	127	8	860	56	676	-19	460	1171
94_0775,01 - 12.11.2012	127	31	7	67	50	162	30	0	69
94_842 - 21.2.2012	-6	100	-14	83	71	338	30	∞	35
97_0631E,01 - 12.11.2012	44	71	-11	150	26	243	0	0	-17
97_0631E,04 - 12.11.2012	728	227	-1	400	-19	870	25	-100	93
97_0632D,01 - 10.1.12	-17	20	109	-25	-15	13	-33	200	-18
97_0675,02 - 12.11.2012	8	6	12	-25	-6	4	30	100	-3
97_0690,02 - 21.2.2012	17	50	39	63	61	69	9	0	21
97_0690,02- - 21.2.2012	29	13	8	25	4	95	44	-50	-8
97_1176 - 12.11.2012	-8	53	10	33	-8	226	27	0	14
98_0387,03 - 21.3.2012	6	47	-6	100	43	254	9	0	7
98_1325 - 12.11.2012	-13	186	-16	1150	-18	962	27	∞	25
Average change	***112***	***73***	***13***	***215***	***44***	***328***	***11***	***19***	***70***

APPENDIX D

Oxide phases in crucible slag

A full list of oxides occurring in the crucible slag has been established, including details such as composition, shape, frequency of occurrence etc. Their varying occurrence is interpreted in section 5.4. The main oxides that occur are Fe-bearing, Ca-bearing, Cu-bearing, Sn-bearing and Co-bearing phases.
Terminology for the different oxides in the crucible slag is adapted from mineralogy (e.g., Klein and Dutrow, 2007). However, it should be emphasised that this terminology is used on the basis of compositional correspondence or similarity to natural minerals. Most slag crystals are formed during the high-temperature process, and are therefore essentially different from naturally occurring minerals. The importance of this distinction is especially crucial for the case of tin oxide and cassiterite, as argued in section 5.4.5.

Section D.1

Fe-bearing oxides

Most of the oxides in the crucible slag contain some FeO and it is an important component of the glassy slag phase. Here, the Fe-based oxides are examined.

1. *Olivine*: This phase (olivine group: fayalite (Fe_2SiO_4) - forsterite (Mg_2SiO_4)) occurs in only two of the analysed samples (94_0560 and 94_0775,01). The morphology is different in each case. In sample 94_0560 (Figure D.1, top), the composition of these crystals is approximately fayalitic: $(Fe,Mg)_2SiO_4$, with $Mg/Fe \approx 1/8$. They are often interspersed with spinel, as shown in Figure D.1b. In sample 94_0775,01, the olivine

phase occurs more as dendrites interspersed between diopside-hedenbergite, as shown in Figure D.1c. In some cases spinels are present, as shown in Figure D.1d. In sample 94_0775,01, the composition is intermediate between fayalite and forsterite: $(Fe,Mg)_2SiO_4$, with $^{Mg}/_{Fe} \approx 1$.

2. *Spinel*: By definition XY_2O_4, with the minerals $MgAl_2O_4$ (*spinel*) and Fe_3O_4 (*magnetite*) as typical examples. Magnetite occurs in noteworthy amounts in eight samples (+ seven samples in which a Co-rich magnetite phase occurs, see section D.5). Examples of magnetite are shown in Figure D.2. It usually occurs agglomerated in certain areas of the sample, often in association with other oxides (SnO_2, malayaite, delafossite). Its composition is typically 33-42 at% Fe, 57 at% O and variable amounts of Al (often around 4 at%), Mg (often around 2 at%), and lower Ti, Si, Ca and Sn (though up to 8 wt% Sn in one sample). This is close to magnetite composition, with some Fe^{2+} being replaced by Mg^{2+} and Ca^{2+} and Fe^{3+} by Al^{3+}, Si^{4+}, Sn^{4+} and Ti^{4+}.

3. *Delafossite*: The nominal composition ($CuFeO_2$) does not occur. Crystals of approximate delafossite composition occur in six samples, though only significantly in two, shown in Figure D.3. In the first example, laths of $Cu_2Fe(Mg,Si,Ca,Al,Ti,Sn)O_4$ (delafossite with about half of the Fe replaced) occur; in the second example, the laths are approximately $Cu(Fe,Mg,Sn)O_2$ (with $^{Mg}/_{Fe} \approx {}^{Sn}/_{Fe} \approx {}^{1}/_{10}$).

4. *Diopside-hedenbergite*: see section D.2.

5. *Ilmenite*: Ilmenite ($FeTiO_3$) is present in the ceramic fabric of all samples. It often occurs in the slag, though not abundantly, and usually concentrated near the bloated transition zone rather than the truly slagged area, as shown in Figure D.4a. An example of ilmenite occurring more dispersed in the slag is shown in Figure D.4b.

Figure D.5 shows ternary diagrams indicating which samples contain Fe-bearing oxides. Generally, these are the samples with a more iron enriched slag.

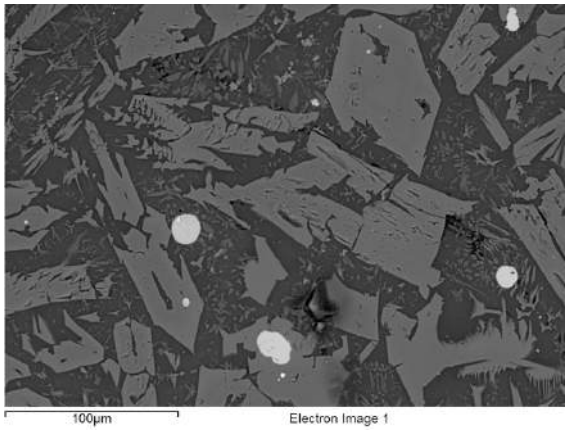

(a) Fayalite

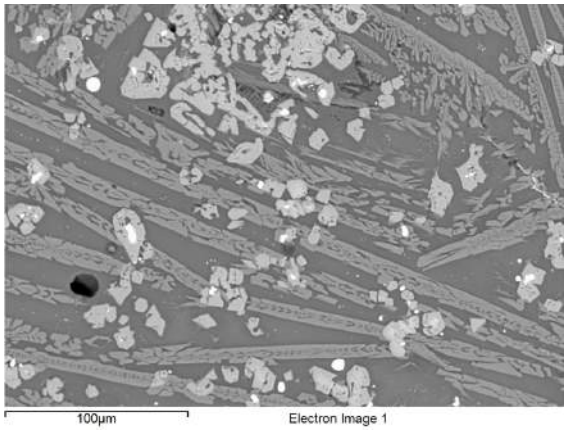

(b) Lath-shaped fayalite with (lighter) spinel

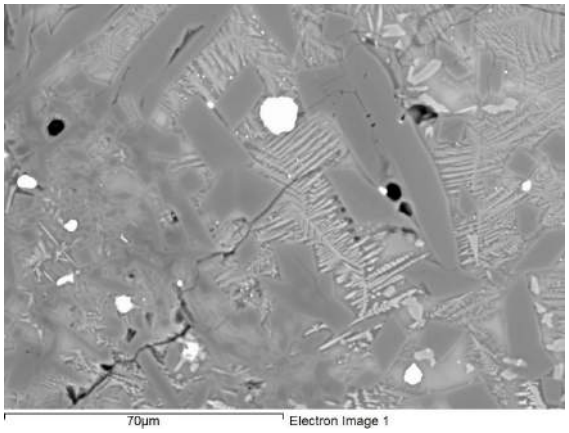

(c) Fayalite-forsterite dendrites (light grey) in between diopside-hedenbergite (dark grey) with high-tin prill (white)

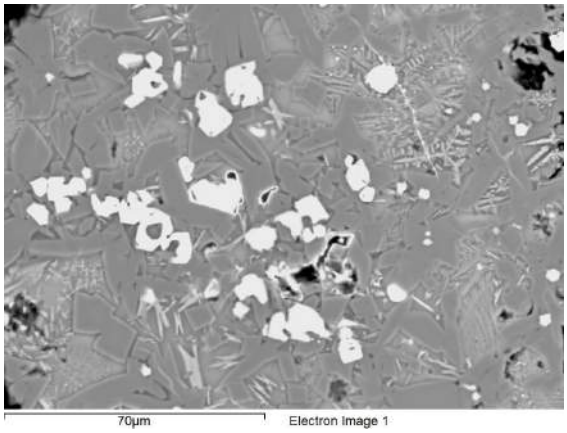

(d) Fayalite-forsterite dendrites (light grey) in between diopside-hedenbergite (dark grey) with (lighter) spinel

Figure D.1: Fayalite in sample 94_560 (top) and sample 94_0775,01 (bottom)

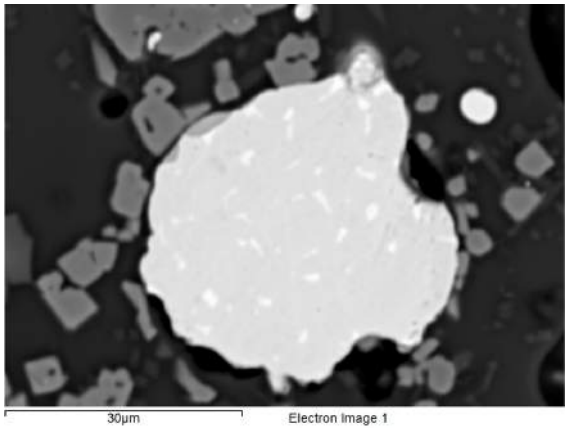

(a) Magnetite in sample 87_0726,68- 78b, surrounding a high-tin bronze prill

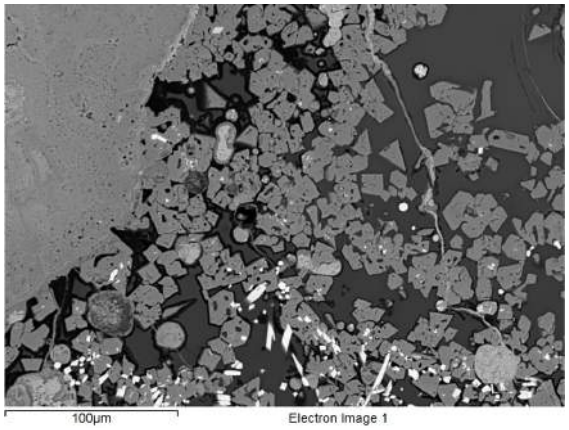

(b) Magnetite in sample 94_0560, next to a (corroded) bronze prill (top left)

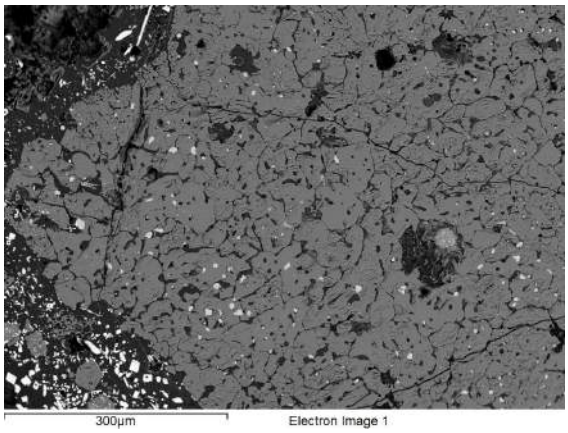

(c) Magnetite agglomeration in sample 87_0634c,04 with interspersed Fe-rich copper metal droplets (bright grey) and surrounding SnO_2 (white)

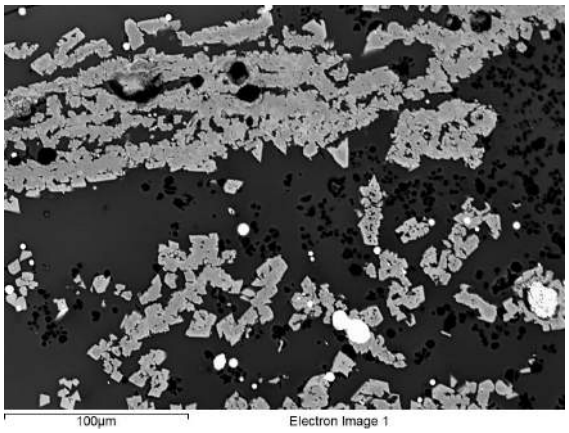

(d) Chain of magnetite with high-tin (+Pb) prills in sample 94_0239,01

Figure D.2: Magnetite

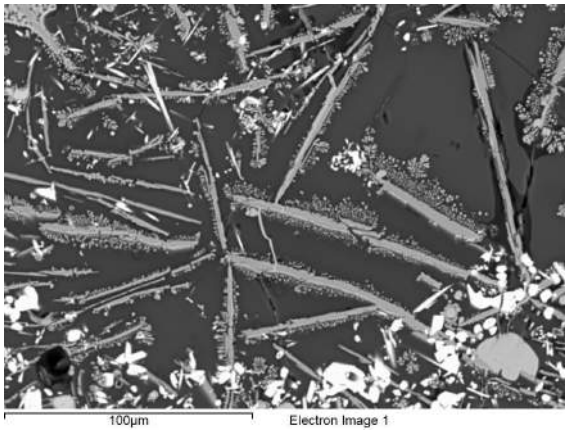

(a) 'Delafossite' laths in sample 87_0726,68- 78b

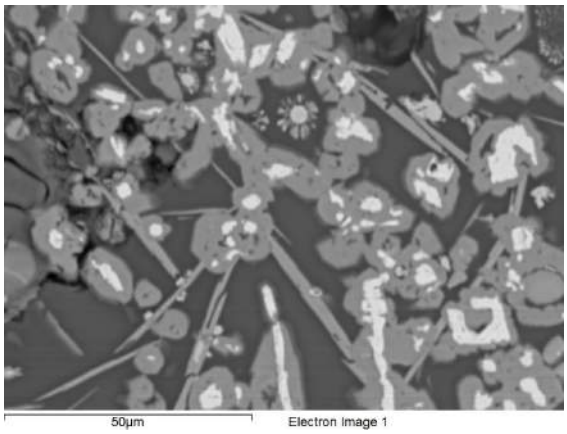

(b) 'Delafossite' laths (light grey) in between SnO_2 (white) and malayite (light grey, slightly darker) in sample 87_0762,0Nv (1)

Figure D.3: 'Delafossite'

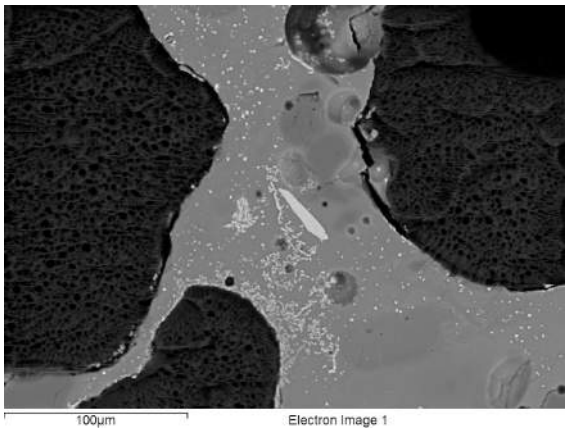

(a) Ilmenite (light grey) occurring in the bloated transition zone, sample 87_0762,0Nv

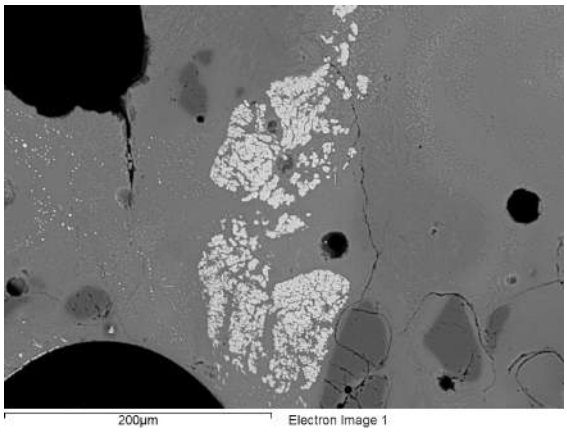

(b) Ilmenite (light grey) occurring more dispersed in the slag area, sample 84_1232

Figure D.4: Ilmenite

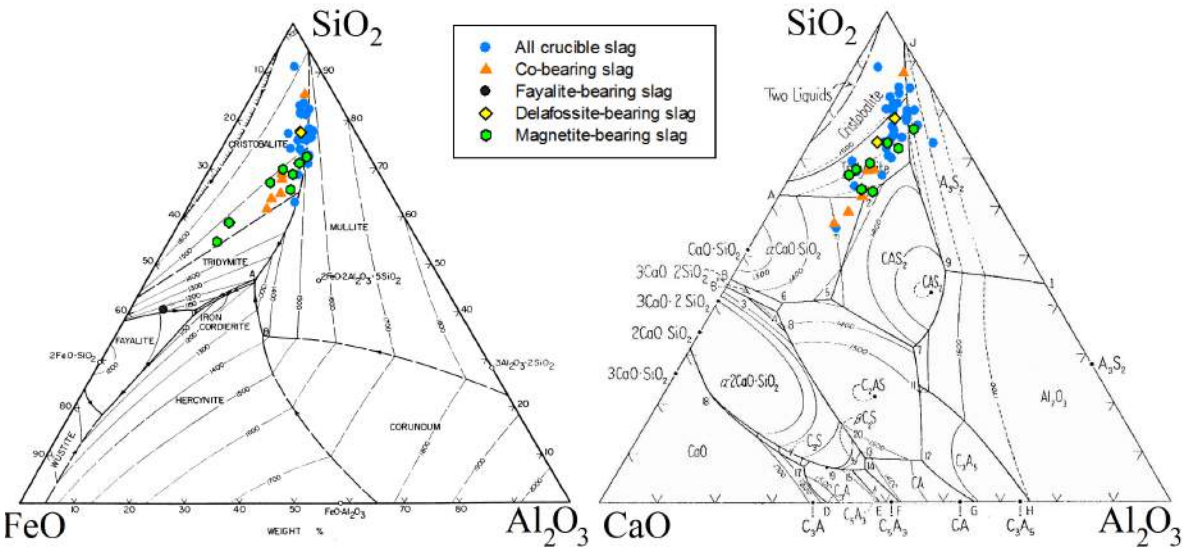

Figure D.5: Ternary diagrams showing samples with Fe-bearing phases

Section D.2

Ca-bearing oxides

CaO is present in most of the crucible slag. It occurs in both the glassy phase and a few crystallised oxides, discussed below.

1. *Diopside-hedenbergite*: Diopside has a nominal $MgCaSi_2O_6$ composition and forms a complete solid solution with hedenbergite, $FeCaSi_2O_6$. Occurrences here usually have intermediate compositions (variable Mg and Fe), with some Al substituting for Si (forming $(Mg,Fe)Ca(Si,Al)_2O_6$). In some cases, Ca^{2+} is partially replaced (up to 50%) by Mg^{2+}/Fe^{2+}. Fe^{2+} and Mg^{2+} are sometimes replaced by a few wt% Na^{2+}. Examples are shown in Figure D.7. In some samples, a few crystals or clusters of crystals are formed in an isolated area of the slag (e.g., Figures D.7a-D.7b). In other samples, the entire matrix is dominated by these crystals (e.g., Figures D.7c-D.7d). Figure D.7e shows an example of Co-bearing (±1 wt%) diopside-hedenbergite. Figure D.7f shows a matrix in which the diopside-hedenbergite crystals seem to have merged. Note that these oxides often show zoning, indicating changing composition during crystal growth.

2. *Plagioclase*: A number of samples have crystals of approximate plagioclase (labradorite-bytownite) composition. This is equivalent to ±70% anorthite ($CaAl_2SiO_8$) and ±30% albite ($NaAlSi_3O_8$). Some examples are shown in Figure D.8. As Figure D.9 shows,

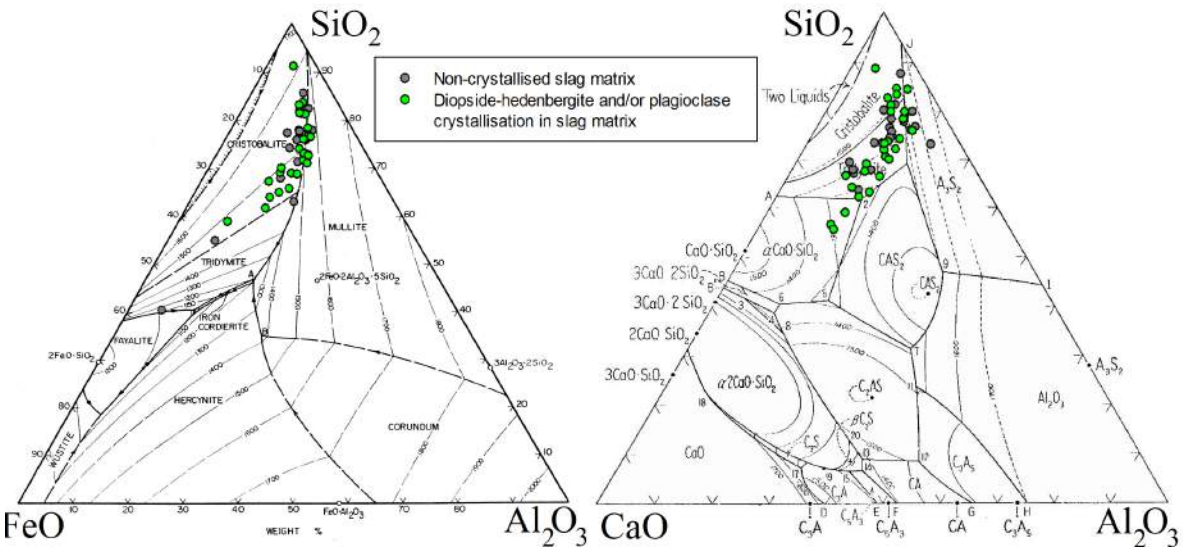

Figure D.6: Ternary diagrams showing samples with Ca-bearing phases

this plagioclase often occurs in association with diopside-hedenbergite (but less frequently).

3. *Malayaite*: see section D.4.

Figure D.6 shows ternary diagrams indicating which samples contain Ca-bearing oxides. These occur both for samples with high and lower lime enrichment.

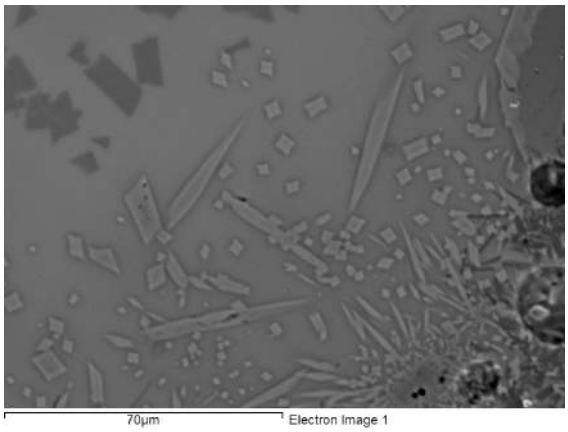

(a) Diopside-hedenbergite cluster in sample 83_1149b (1)

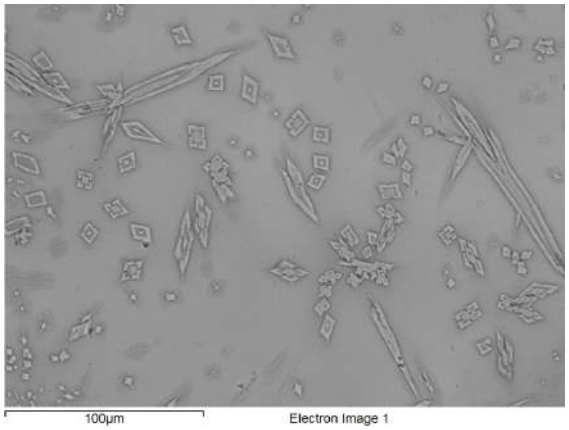

(b) Diopside-hedenbergite cluster in sample 84_1232

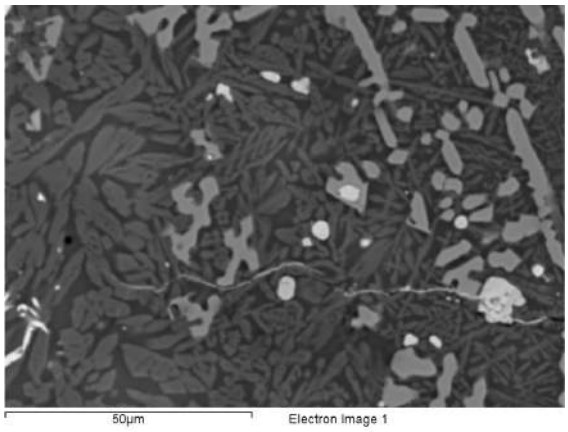

(c) Diopside-hedenbergite (medium-grey) matrix in sample 87_0884,01-56b (with Co-rich spinel, light grey)

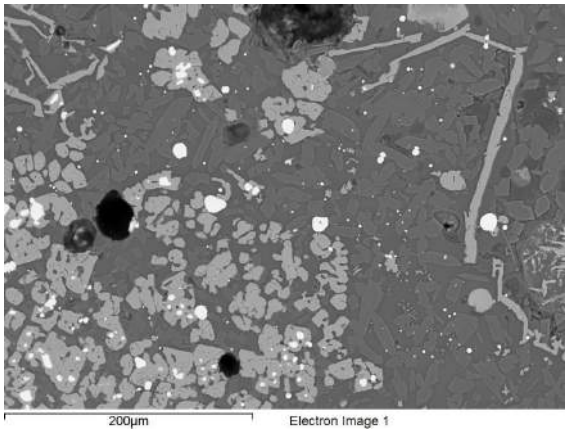

(d) Diopside-hedenbergite (medium-grey) matrix in sample 87_0762, (with Co-rich spinel, light grey)

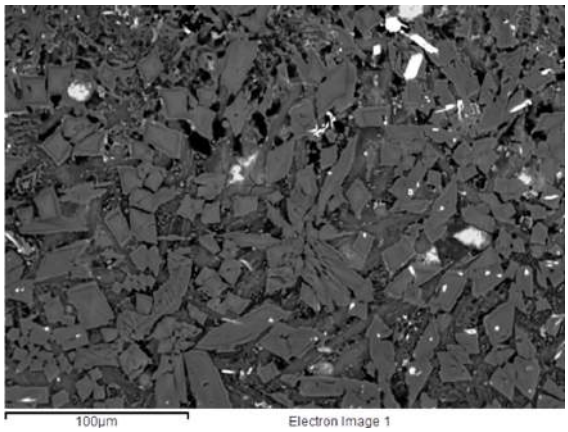

(e) Co-bearing diopside-hedenbergite matrix in sample 87_0897a,01-45 (2)

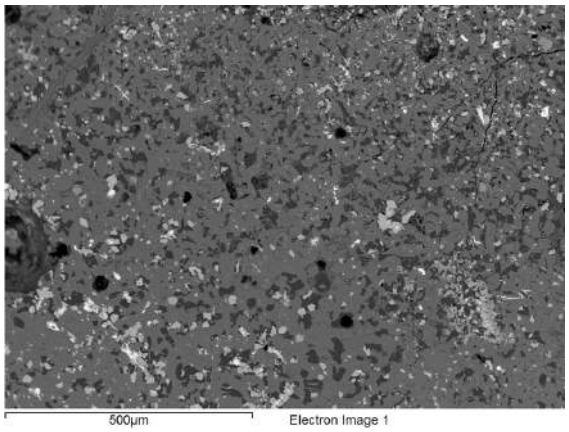

(f) Diopside-hedenbergite matrix in sample 87_0884,01-56c

Figure D.7: Diopside-hedenbergite

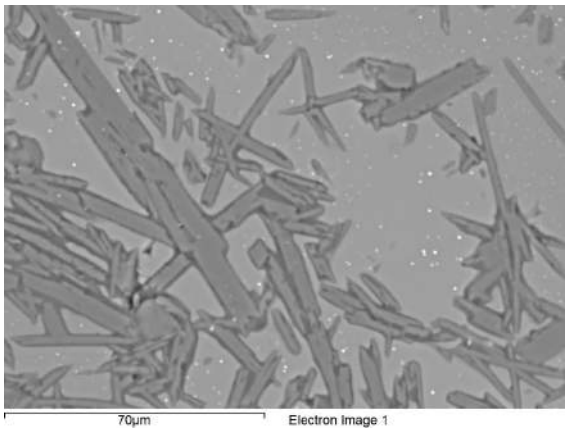

(a) Plagioclase crystals in sample 86_0749c

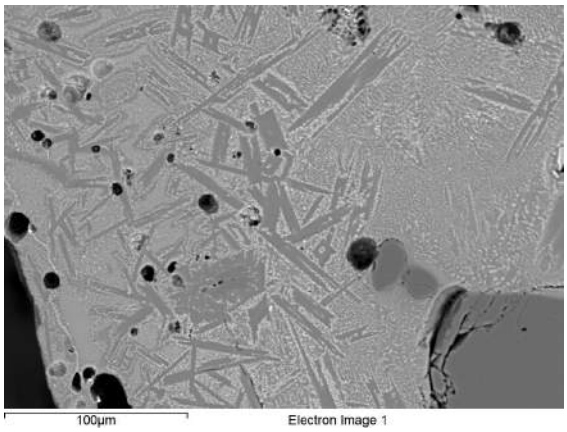

(b) Plagioclase crystals in sample 87_0849a,04

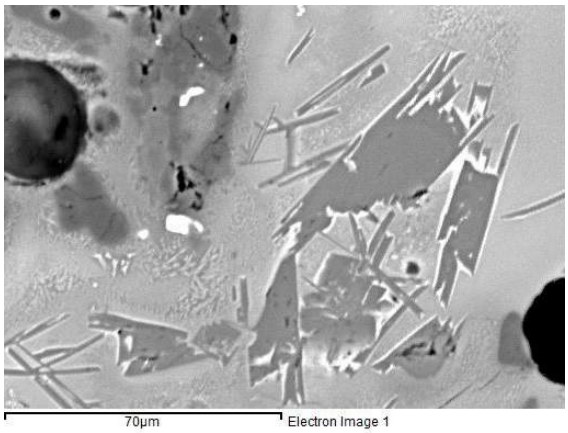

(c) Plagioclase crystals in sample 87_0897a,01-45 (1)

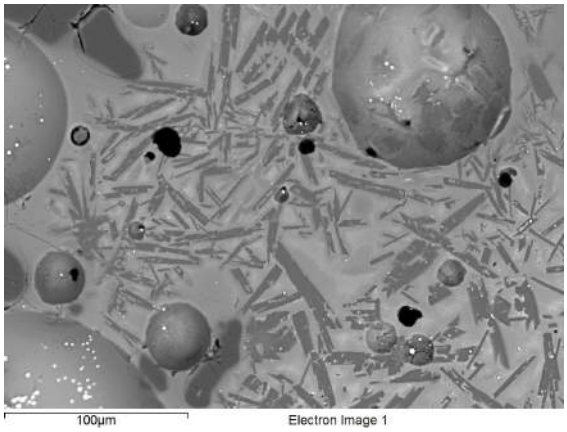

(d) Plagioclase crystals in sample 94_0775,01

Figure D.8: Plagioclase

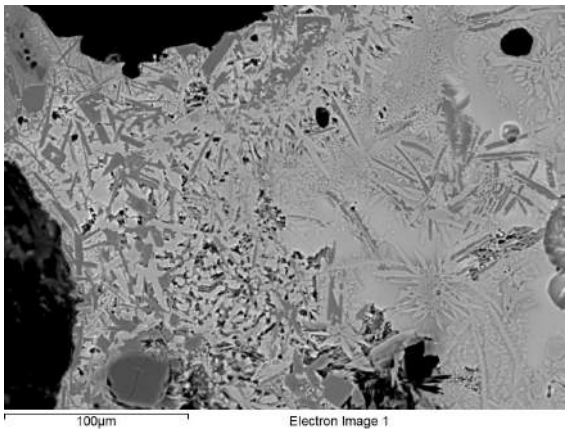

(a) Sample 87_0725c,1-20

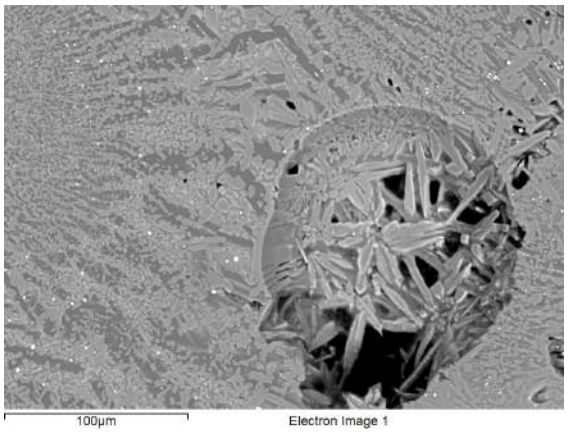

(b) Sample 98_0387,03

Figure D.9: Plagioclase crystals (dark grey) occurring together with diopside-hedenbergite (light grey)

Section D.3

Cu-bearing oxides

Most of the copper in the crucibles occurs in metallic prills (see section 5.2.4). Besides that, it occurs in a number of oxide phases.

1. *Delafossite*: See section D.1.

2. *Cuprite*: Surrounding metallic prills, an oxidised layer is often formed, which is usually a mixture of mostly Cu_2O with some CuO and sometimes Cu_2ClO_{2-3}. These oxide layers appear to form mostly around pure Cu prills, indicating other elements (Fe, Sn, As, Co), when present, burn out before the copper oxidises, as shown in Figure D.10a. In some cases though, a few wt% Sn/As remains (e.g., Figures D.10b-D.10c), while in others entire prills are oxidised into cuprite (e.g., Figure D.10d). Figure D.10e shows how pores and cracks are sometimes filled with cuprite (most likely formed post-depositionally). In pores, cuprite can form (geode-like) cubic crystals as shown in Figure D.11. Probably, these pore structures are related to gas bubbles in the crucible slag. Figure D.12 shows a bronze prill, in which preferential corrosion of part of the alloy has taken place (see section 5.2.4). The alteration products (greenish in PPL, reddish in XPL) are typically Cu-oxide with variable stoichiometry and widely ranging Sn content, and a lower Si, Cl, Fe and As content.

3. *Cu-silicates*: Sample 87_0726,68- 78b has Cu-silicate 'bubbles' occurring in pores, with an approximate composition of $Cu_3Si_4O_9$ (and low Ca, Mg & Al), shown in Figure D.13. These images show that these are actually (corrosion-related) hydrated phases which disintegrate in the SEM-chamber's vacuum. Another occurrence of Cu-silicate, with a (very) approximate composition of Cu_4SiO_4 (with low Fe & Ca), takes a 'sun-like' shape (spherical core with dendritic growth away from the centre) and is dispersed between SnO_2 laths (see Figure D.15a).

Figure D.14 shows ternary diagrams indicating which samples are enriched in bulk CuO content.

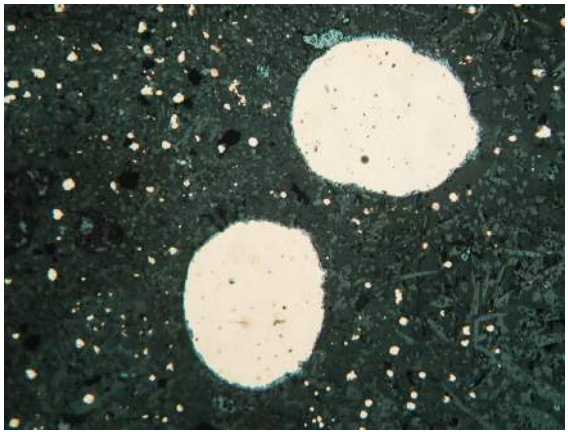

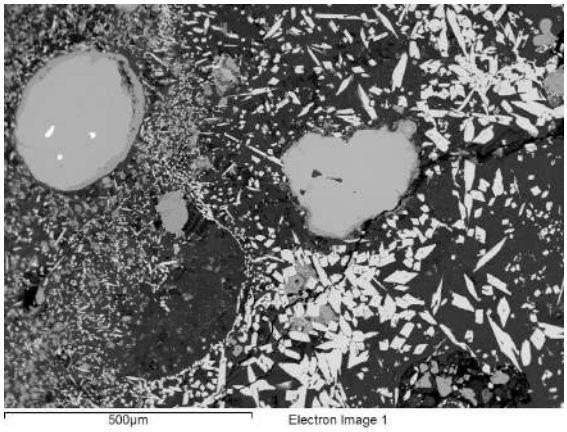

(a) Two examples of pure Cu prills with cuprite edge, surrounded by SnO_2, in sample 87_0726c,2-60a (left: O.M. image, 200X, w.o.i. ±1mm)

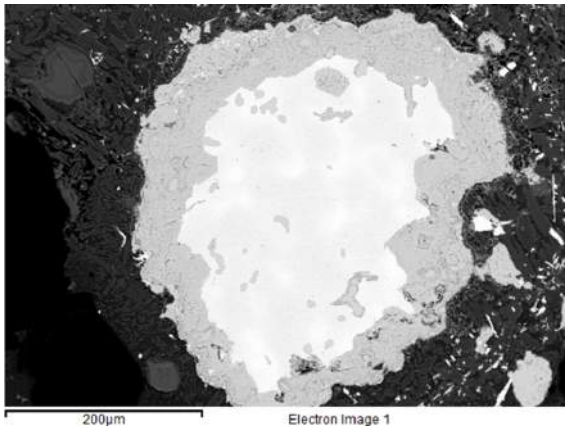

(b) Cuprite surrounding prill with a few wt% Sn and As remaining, sample 87_0897a,01-45 (2)

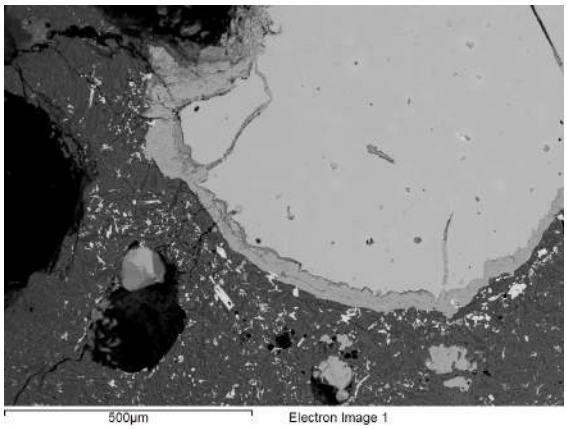

(c) Cuprite surrounding prill with a few wt% Sn and As remaining, sample 87_0884,01-56c

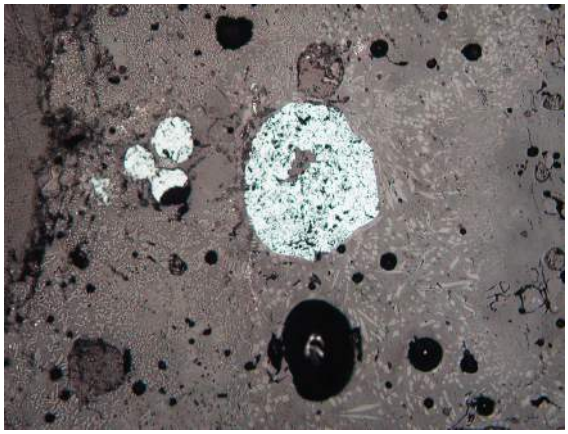

(d) Fully oxidised prill surrounded by SnO_2, sample 87_0726c,2-60a (O.M. image, 100X, w.o.i. ±2mm)

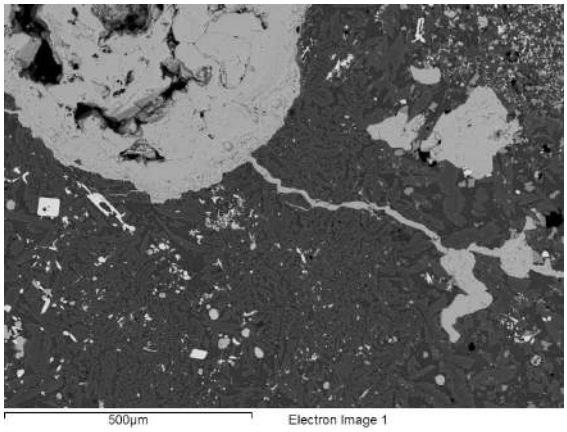

(e) Fully oxidised prill with cuprite 'leaking' into slag, sample 87_0884,01-56c

Figure D.10: Copper-oxides

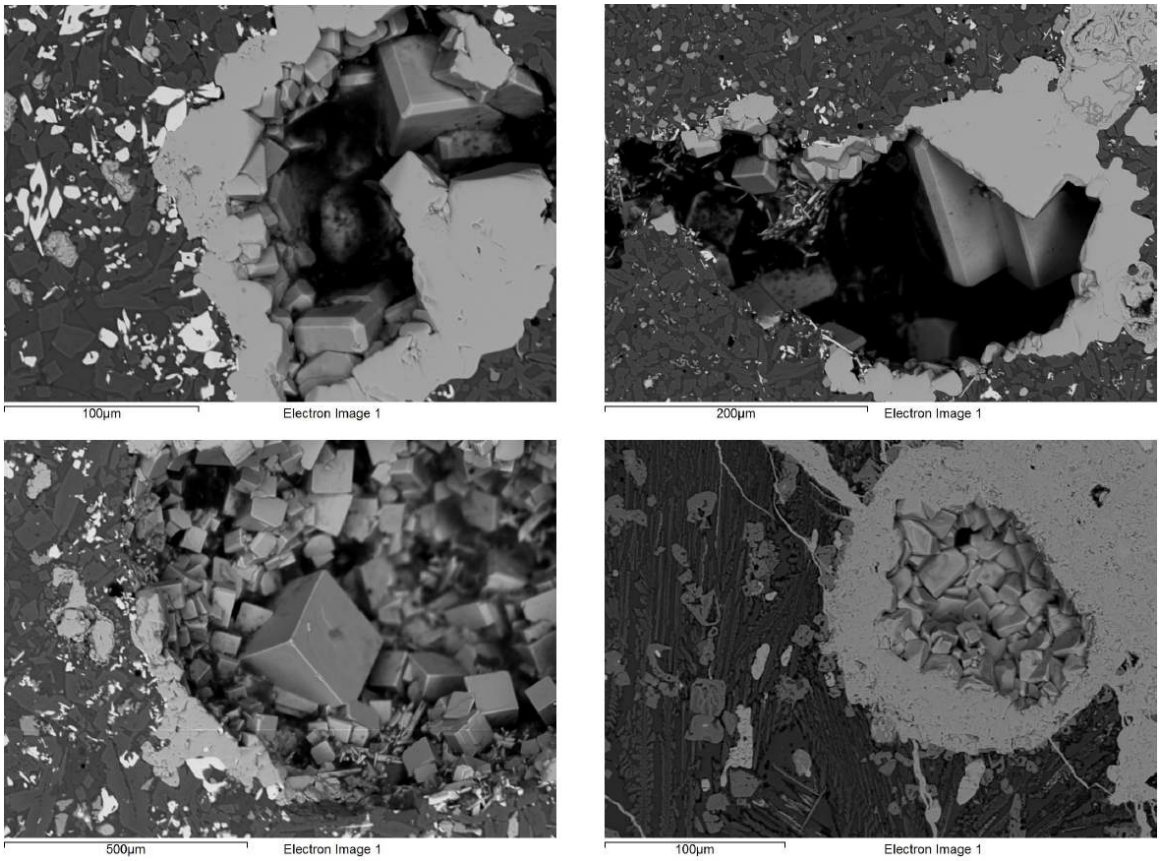

Figure D.11: Cuprite in pores in the crucible slag, samples 87_0884,01-56b, 87_0884,01-56c and 94_0560

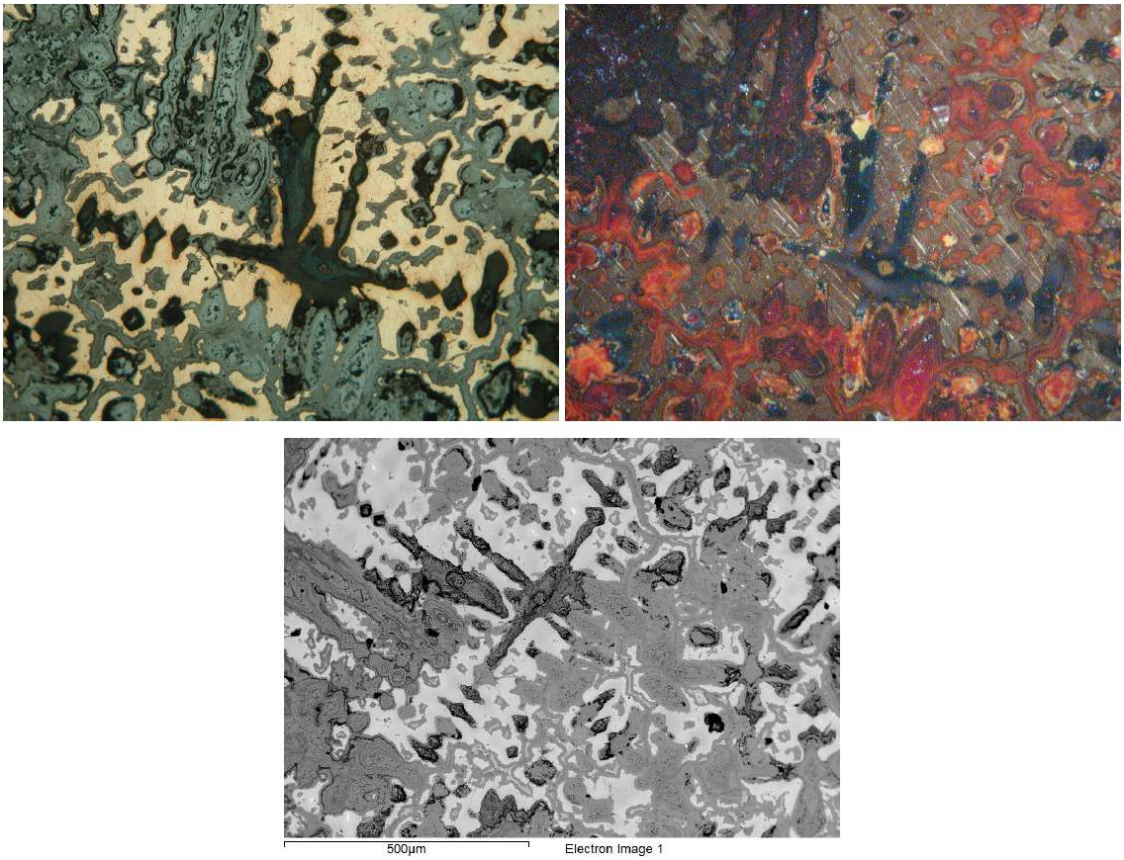

Figure D.12: Corroded bronze prill, sample 86_0471b,01 (top: O.M. image, 200X, w.o.i. ±1mm - left: PPL, right: XPL)

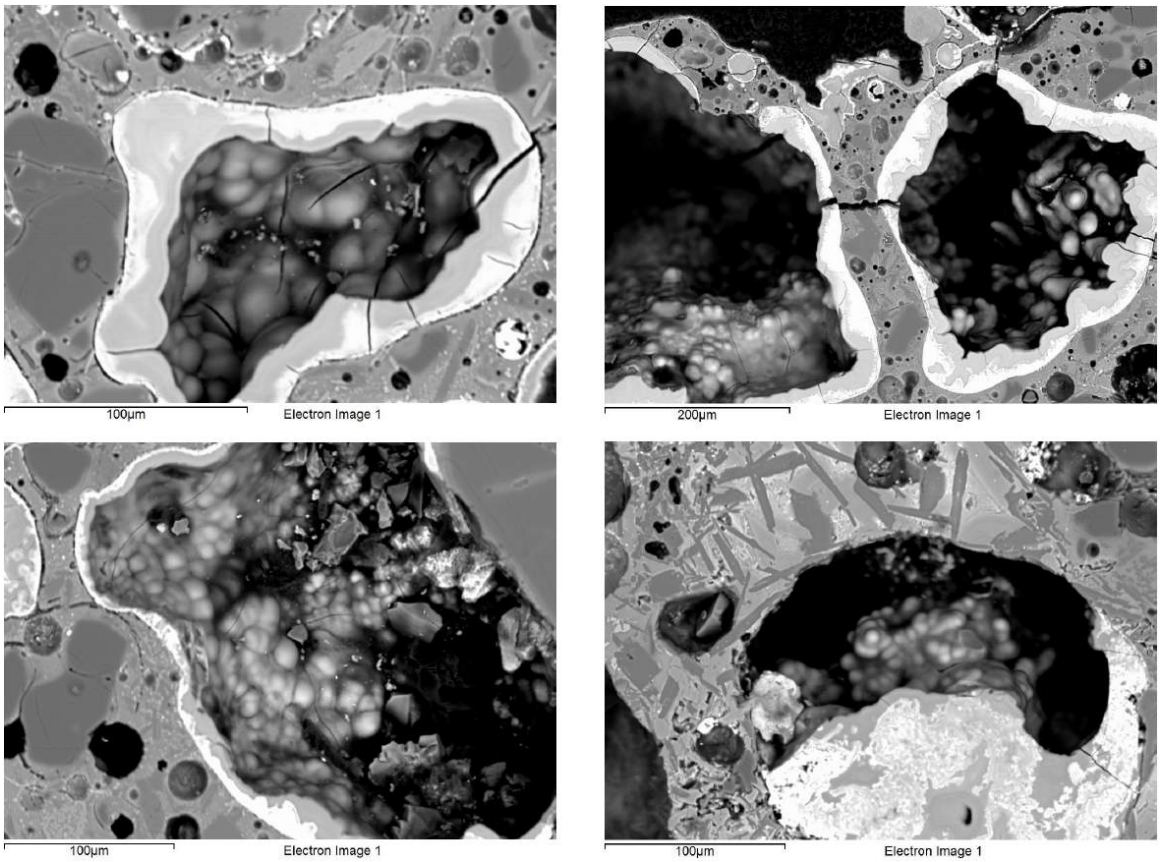

Figure D.13: Cu-silicate 'bubbles' in pores in the crucible slag of sample 87_0726,68- 78b

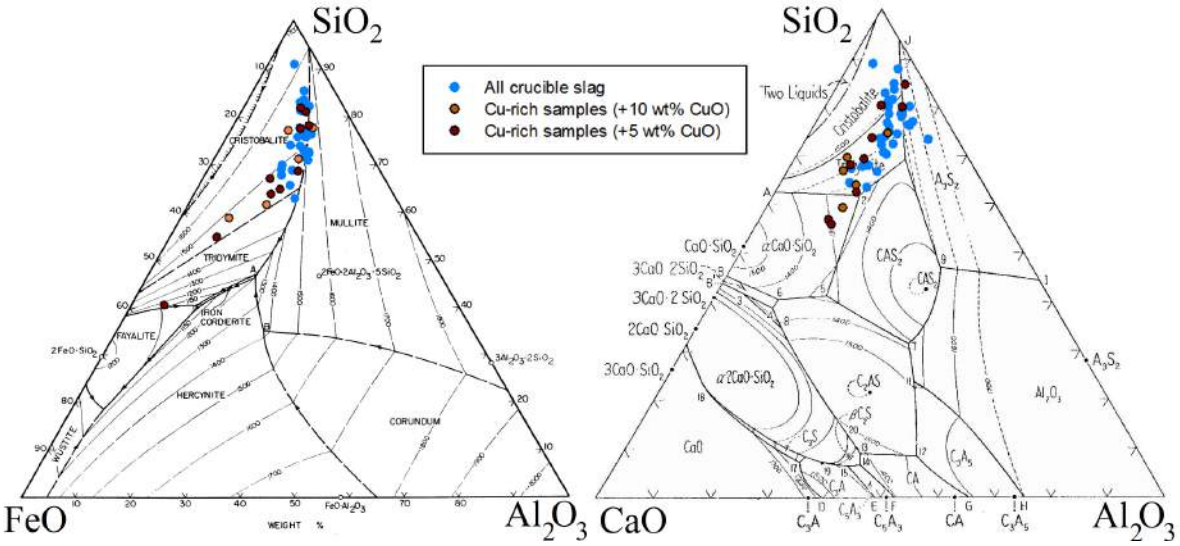

Figure D.14: Ternary diagrams showing samples enriched in CuO (+5 and +10 wt% CuO)

Section D.4

Sn-bearing oxides

When present, tin occurs either in the metallic phase as bronze constituent (no pure tin metal) or in two different oxides in the slag.

1. *Tin oxide*: The first one, shown in Figure D.15, has a composition of SnO_2 (compositionally identical to mineral cassiterite). Very often, these oxides occur in clusters spread throughout the crucible slag, often in association with Cu-phases, and are absent in other areas (e.g., Figure D.15b). There exists large variability in the shapes of these oxides, illustrated in Figures D.15a-D.15f. The cores of the SnO_2 crystals are often filled with copper, as shown in close-up in Figure D.15f. All of these observations are important with respect to the interpretation of these crystals as newly formed, secondary tin oxide (see section 5.4.5).
   There are a few occurrences of SnO_2 which differ strongly from the examples shown in Figure D.15, and could be residual mineral cassiterite (see section 5.4.5). Some examples are given in Figure D.16.

2. *Malayaite*: The second Sn-bearing phase, shown in Figure D.17, has a composition which approximately matches malayaite ($CaSnO(SiO_4)$), and is probably formed by interaction of SnO_2 with the lime-rich slag. These phases are typically subhedral to anhedral, grey, and slightly less bright than magnetite, and often have a pure SnO_2 core.

Figure D.18 shows ternary diagrams indicating which samples are enriched in bulk SnO_2 content. Figure D.19 shows a ternary diagram indicating which samples contain Sn-bearing oxides. As SnO_2 tends to occur abundantly when it does occur, the SnO_2-rich (bulk content) samples mainly correspond to those with Sn-bearing phases.

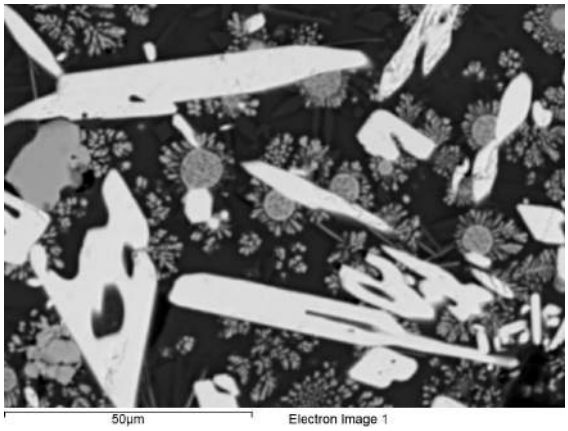

(a) SnO_2 (light grey), copper-silicates in background, sample 87_0726,68-78b

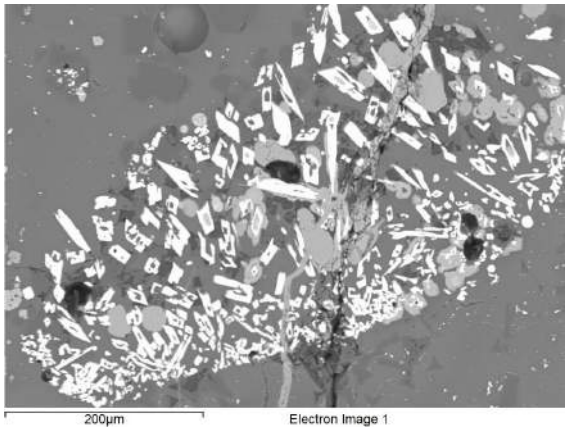

(b) SnO_2 (white), typical aggregation, sample 87_0762

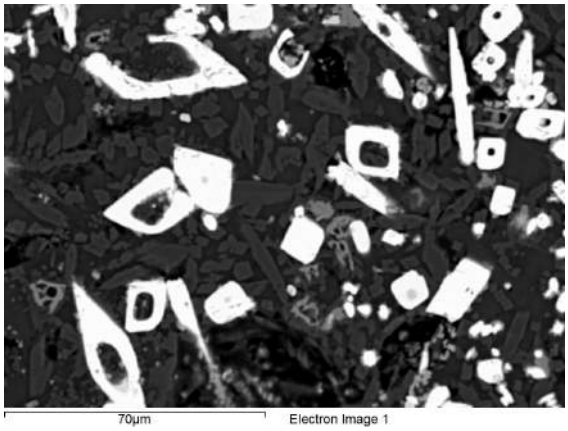

(c) Variable shape of SnO_2 (white), sample 87_0634c,04

(d) Variable shape of SnO_2 (light grey), sample 87_0634c,04

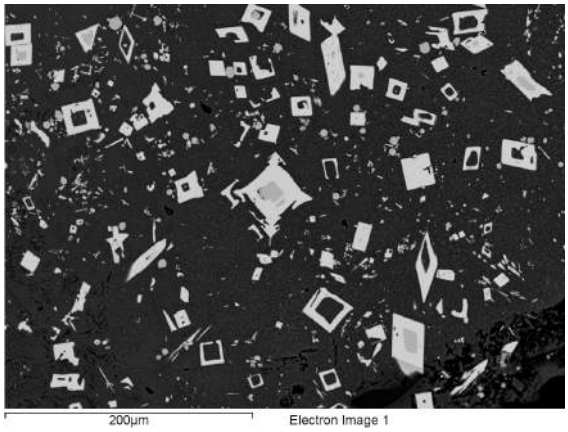

(e) Variable shape of SnO_2 (light grey), sample 87_0634c,04

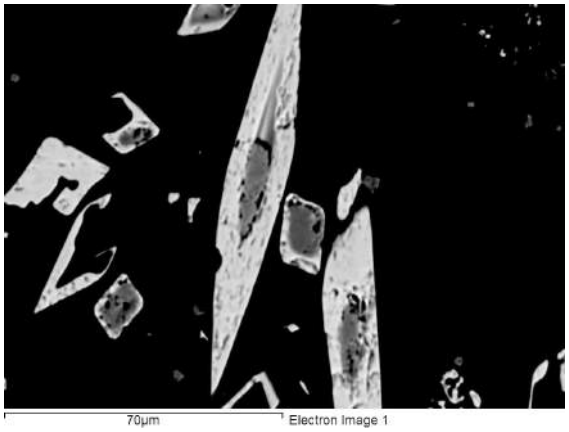

(f) Copper (medium grey) in core of SnO_2 (light grey), sample 84_0030c,01

Figure D.15: SnO_2 phases

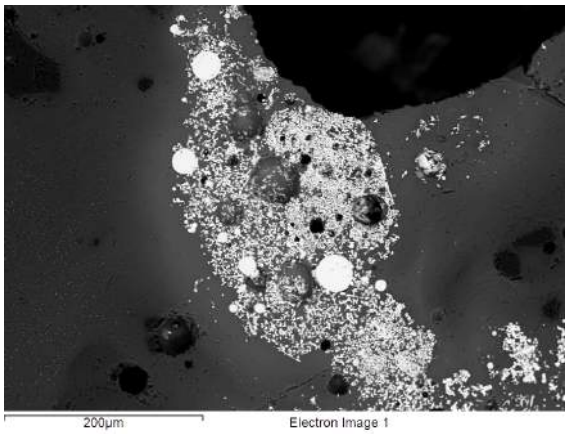

(a) Sample 87_0762 (2)

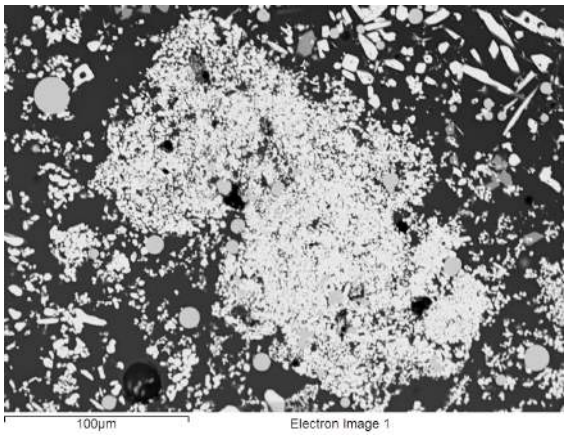

(b) Sample 97_0631E,01

Figure D.16: SnO_2 with distinct different morphology

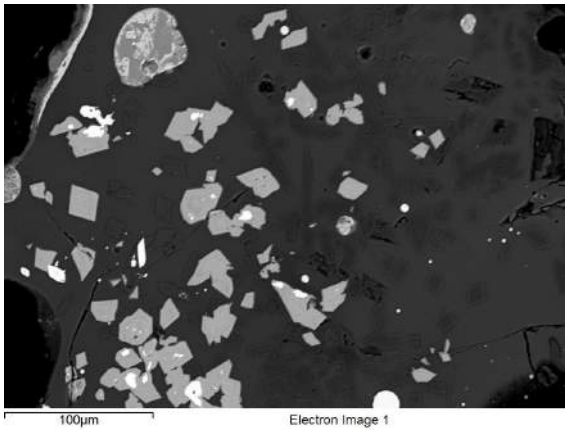

(a) Sample 83_0597b,01

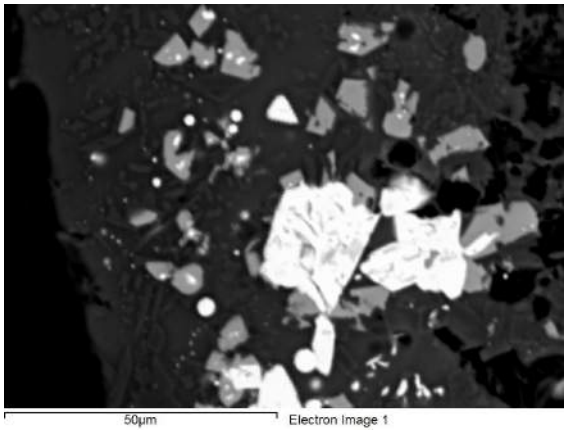

(b) Sample 84_1232

Figure D.17: 'Malayaite' (light grey) with SnO_2 (white)

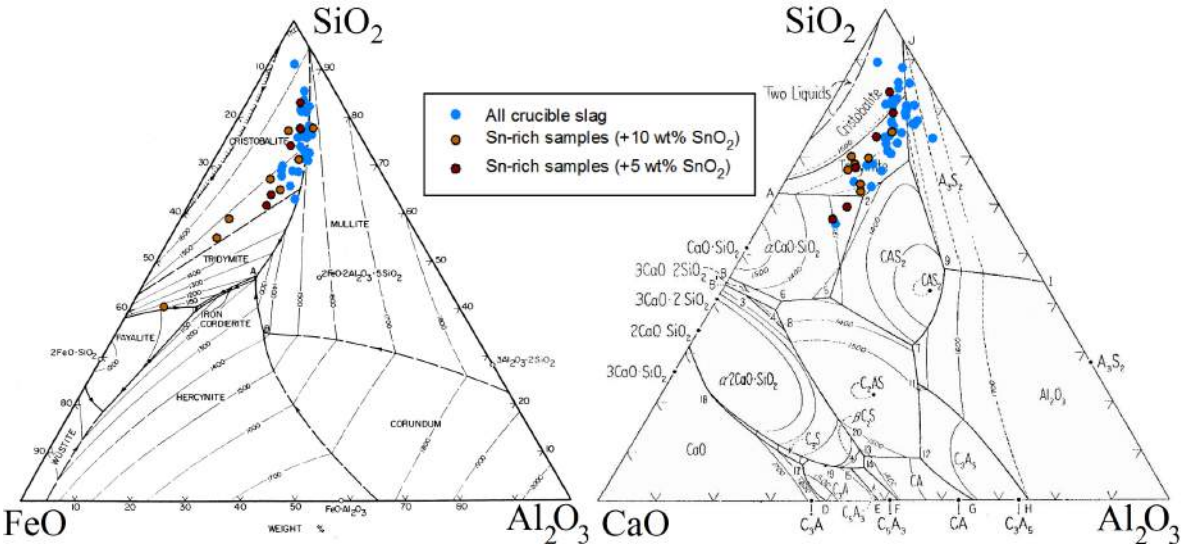

Figure D.18: Ternary diagrams showing samples enriched in SnO_2 (+5 and +10 wt% SnO_2)

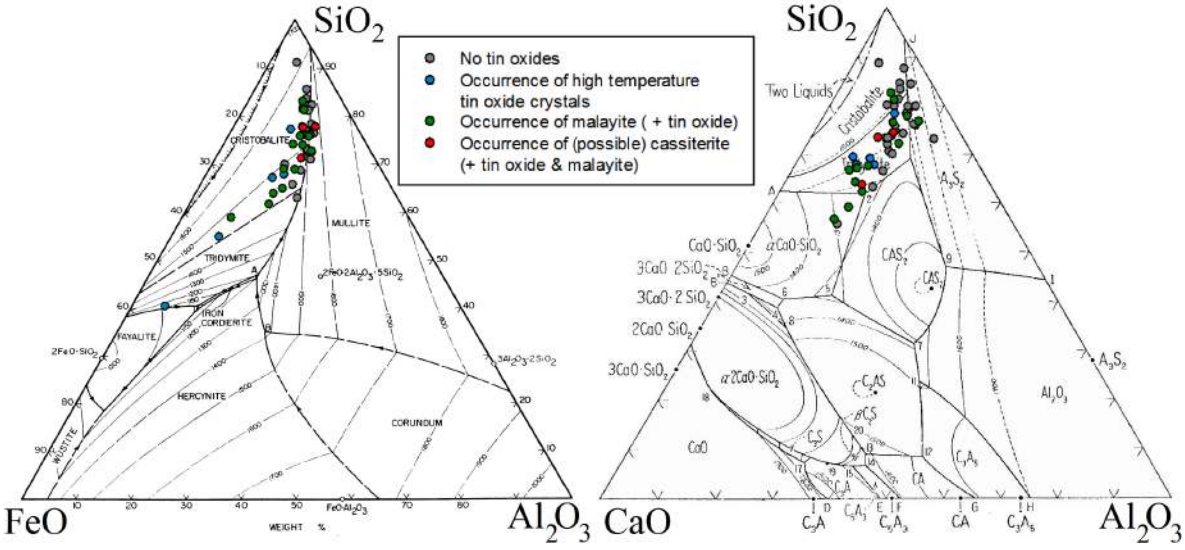

Figure D.19: Ternary diagrams showing samples with Sn-bearing oxides

Section D.5

Co-bearing oxides

Six samples show noticeable amounts (0.3-2.1 wt% of bulk composition) of CoO in the slag phase. Upon closer examination, this cobalt appears to consistently be present in a phase with somewhat variable composition from approximately $Fe_6Co_2AlO_{11}$ to $Fe_5Co(Si,Al)O_9$. This phase appears similar to spinel, where Co replaces some of the Fe (or Al?) (Co commonly has oxidation states 2+ or 3+). The formula could then be $(Fe,Co)(Fe,Al)_2O_4$, with typically up to 6 wt% Co. As shown in Figure D.20a, it can have a typical spinel-like shape, but it equally appears in dendritic and skeletal structures, as shown in Figures D.20b-D.20c, against a background of diopside-hedenbergite. It occurs in the six samples enriched in Co, and in one which does not show bulk increase in CoO content.

Co is present in copper prills (up to 24 wt%) in nine samples (the total number of samples showing presence of cobalt in any form). As Figures D.20c and D.21 show, it appears that the Co-spinel is formed by the oxidation of Fe- and Co-rich copper prills.

It is important to note here that some of the Co-spinel has low Ni contents. A number of Co-rich copper prills has significant Ni content (up to 46 wt%, see section 5.2.4).

Figure D.22 shows ternary diagrams indicating which samples contain Co-bearing oxides. In five out of six, the cobalt enrichment is paired with an iron enrichment of the crucible slag. The sixth sample (92_0606) shows the lowest CoO enrichment (0.3 wt%) and limited iron enrichment.

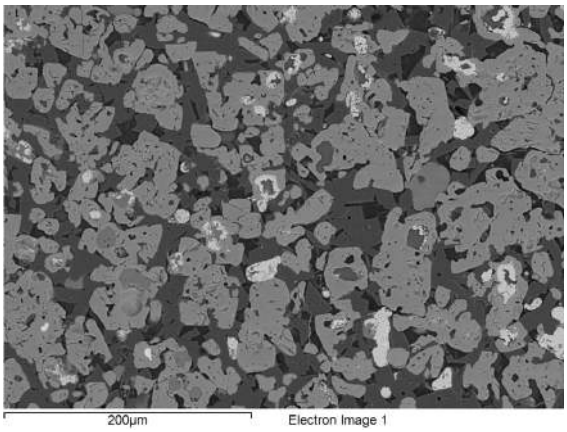

(a) Sample 87_0762, similar to spinel structure.

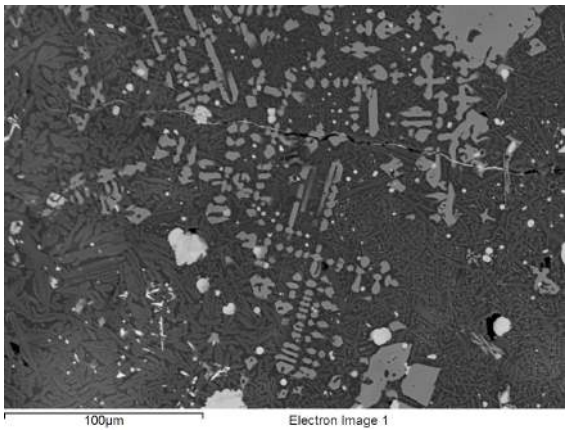

(b) Sample 87_0884,01-56b, with dendritic structure. Diopside-hedenbergite in matrix.

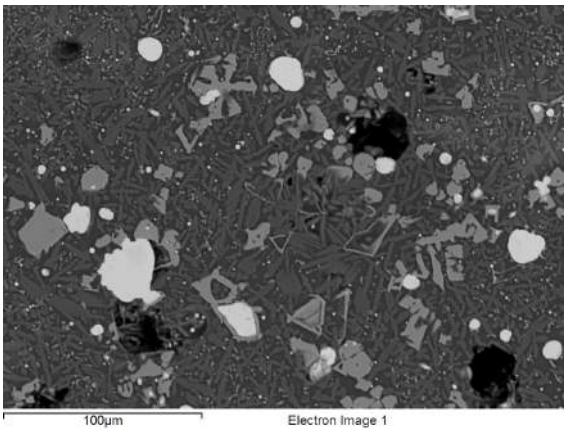

(c) Sample 87_0884,01-56b, with skeletal structure. Diopside-hedenbergite in matrix.

Figure D.20: Co-rich phases

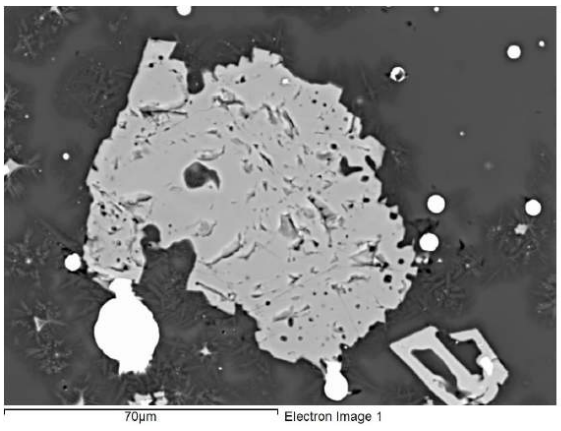

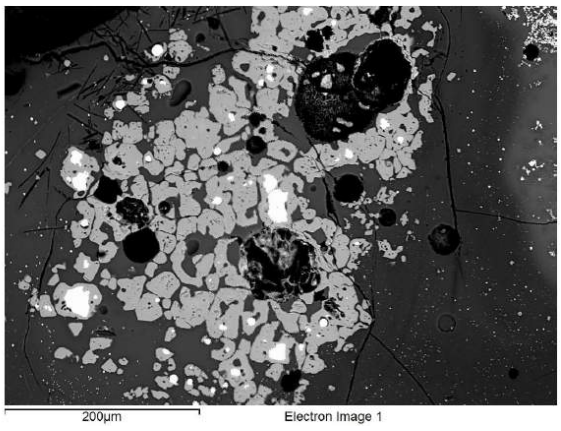

Figure D.21: Co-spinel oxidising into crucible slag from Fe- and Co-rich copper prills, sample 87_0791,01-88

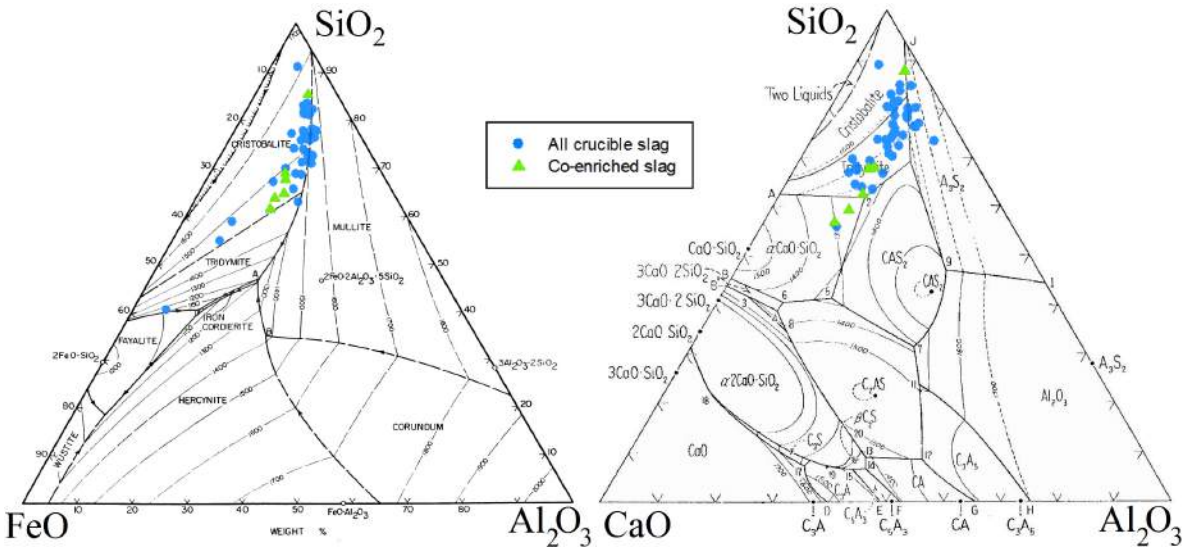

Figure D.22: Ternary diagrams showing samples with Co-bearing phases

Section D.6

Zircon

There are ten samples in which zircon ($ZrSiO_4$) has been detected in the crucible slag (though it could easily have been missed in others). In all cases, zircon occurs as a single, isolated crystal. Some examples are shown in Figure D.23 (Figure D.23c: possibly metamict[1] structure). There is one recorded example of zircon occurring within the ceramic fabric, as shown in Figure D.24. Zircon commonly occurs as an accessory mineral in igneous rocks, particulary in granite, granodiorite, syenite, monzonite and nepheline syenite. It is often an accessory mineral in sediments, due to its chemical stability (Klein and Dutrow, 2007), and is not uncommon in Nile clay fabrics (Bourriau *et al.*, 2000). Most likely this zircon derives from the ceramic (i.e., the Nile Silt), where it is sometimes noted, though it might have come into the crucible slag as an accessory mineral with cassiterite (which often derives from igneous host rocks) as well.

Figure D.25 shows ternary diagrams indicating which samples contain zircon in the slag area.

[1]Metamictisation: natural degradation of a mineral's crystal structure into amorphous structure. Uranium and thorium can cause metamictisation of zircon due to radiation (Klein and Dutrow, 2007).

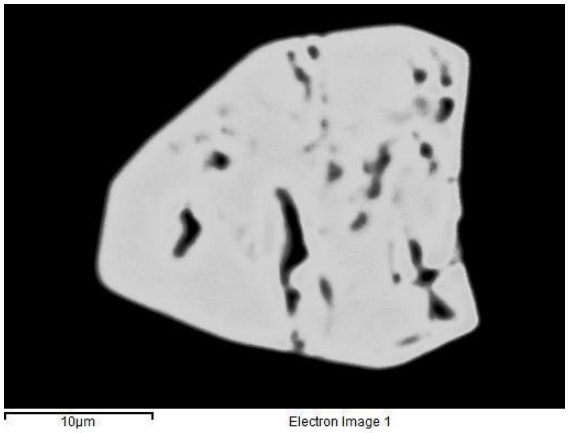

(a) Sample 83_1149b (2)

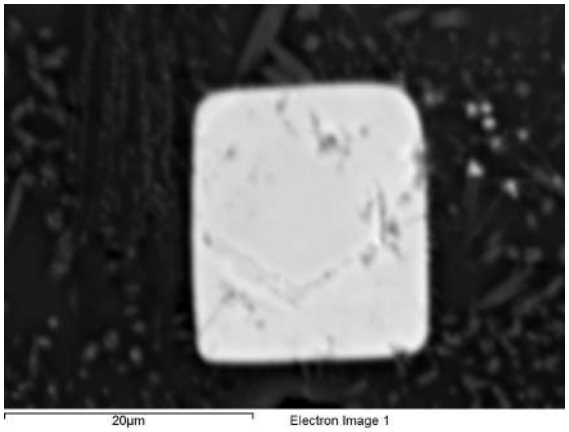

(b) Sample 84_1232

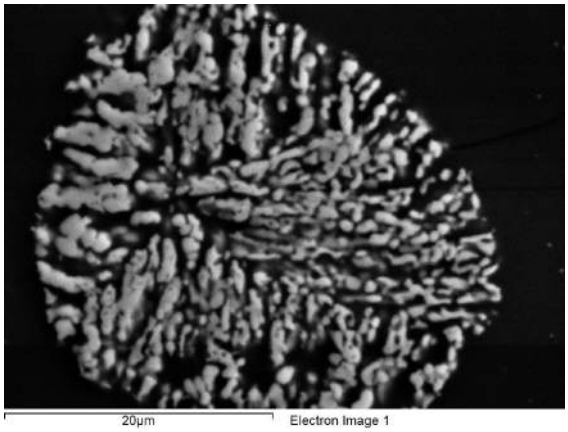

(c) Sample 86_0749c

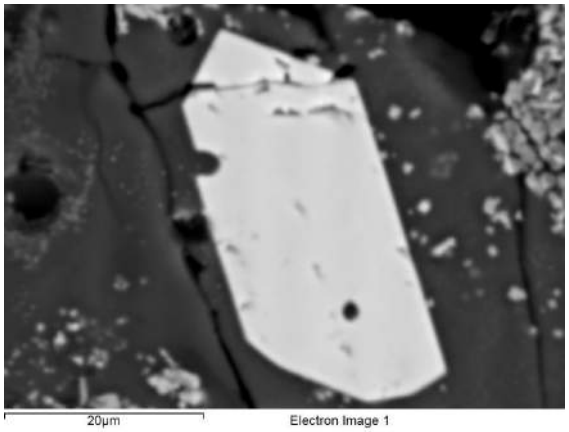

(d) Sample 87_0762,0Nv

Figure D.23: Zircon

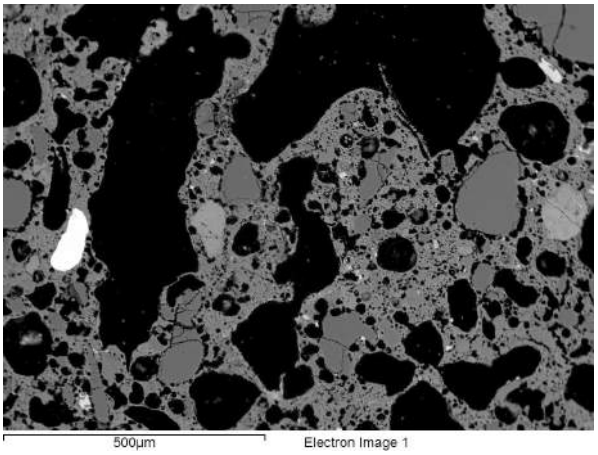

Figure D.24: Zircon (bright, left) in ceramic fabric, sample 87_0762 (1)

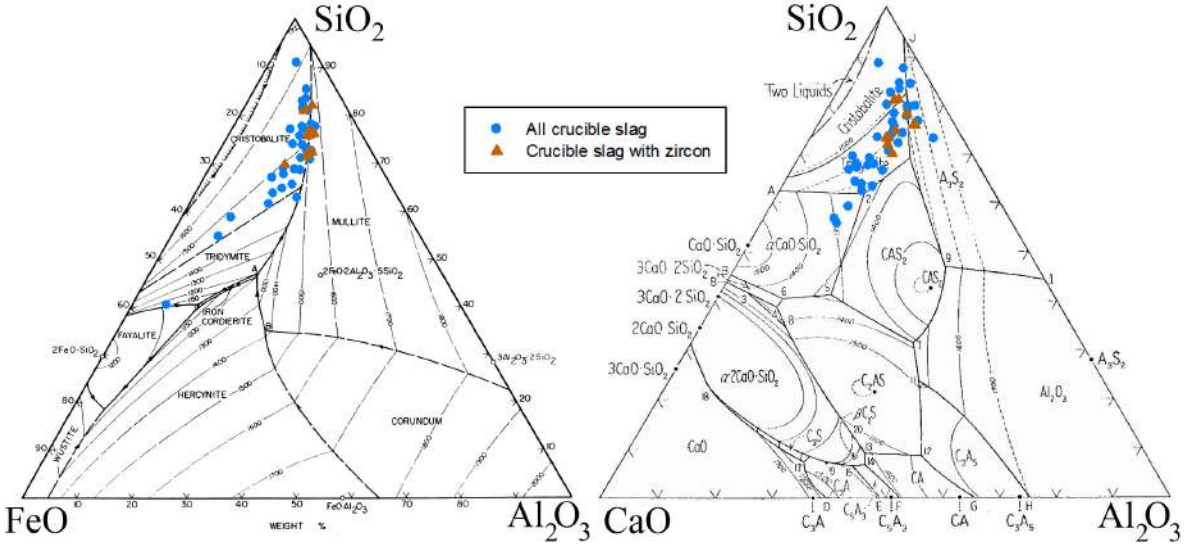

Figure D.25: Ternary diagrams showing samples with zircon in crucible slag

APPENDIX E

Composition of metallic prills

Oxidised prills are omitted. Where an abundance of *1+* is noted, this refers to one measured prill, but probably more of similar composition present in the crucible slag. *Micro* refers to tiny prills dispersed throughout the crucible slag, which are too small to measure.

Composition of metallic prills in crucible slag (in wt%)

Sample	Abundance	Cu	Sn	Fe	As	Co	Ni	Pb	S
82_0223b,01 - 10.1.12	1+	100							
82_298b,01 - 21.3.2012	Micro								
83_0542b,01 - 21.3.2012	Micro								
83_0597b,01 - 21.3.2012	1+	91.9	7.3	0.8					
83_1149b - 12.11.2012 (1)	4	98.5-99		1-1.5					
	1	91.1			1.4		6.1		1.4
	Micro								
83_1149b - 12.11.2012 (2)	7	30-65	0-2	5-20		6-24	26-46		
	Micro								
84_0030c,01 - 10.1.2012	Multi	100							
84_0106c - 12.11.2012	/								
84_0749, - 10.1.12	Multi	95-100	0-5						
	2	96-96.8			3.2-4				
	1	95.1-95.4	4.6-4.9						
84_1189b,0 - 12.11.2012	Micro								
84_1232, - 12.11.2012	1+	99		1					
86_0208b - 12.11.2012	Micro								
86_0471b,01 - 19.1.2006	1+	89	11						
	Micro								
86_0749c - 19.1.2006	1+	98.5			1.5				
	1 (3 phase)	10	tr	87	1.5		tr		
	⟶ *phases:*	*7.3*		*89*	*2.8*		*0.5*		
		93.3	*1*	*7*	*1*				
		68.4		*8.3*					*24.5*
	Micro								
	Gold	*(30 at% Cu and 70 at% Au)*							
86_0792b,04 - 12.11.2012	Multi	100							
	Multi	97.25-99.5		0-2			0.5-0.8		
87_0423b - 19.1.2006	1+	98.4			1.6				
	Micro								
	Cu_2S	x							x
	$Fe_{1-2}S_2O$	x							x
87_0634c,04 - 12.11.2012	Multi	95-100		0-5					
	Multi	96-98	2-4						
	1	92.7	4.3	0.6	1.6				0.8

Composition of metallic prills in crucible slag (in wt%)

Sample	Abundance	Cu	Sn	Fe	As	Co	Ni	Pb	S
87_0725c,1-20 - 12.11.2012	/								
87_0726,68-78b - 19.1.2006	1	82.1	15.2	1.5	1.2				
	1	81.5	17.5	1					
	1	81.8	16.4	0.8	1				
		↪ *16.4 Sn: small areas of 25-28 Sn in 15-15.8 Sn matrix*							
	1	75.9	22.1	2					
	Micro								
87_0726c,2-60a - 19.1.2006	Multi	100							
	Multi	96-97	3-4						
	1	97.8			2.2				
	1	100						x	
87_0762, - 21.3.2012	Multi	95		1.5-2.4	1.8	0.8-1.1			
	Multi	90-91	9-10					x	
87_0762, - 22.3.2013 (1)	/								
87_0762, - 22.3.2013 (2)	Multi	100							
	Multi	92-95	5-8						
	1+	98.8		1.2					
	Micro								
87_0762,0Nv - 21.2.2012	Cu_2S	x							x
	Micro								
87_0762,0Nv - 22.3.2013 (1)	Multi	100							
	Multi	98-100			0-2				
	1+	86.3	11.3		2.4				
	2	71-72	28-29						
		↪ *28-29 Sn: δ-phase in α + δ interdendritic*							
87_0762,0Nv - 22.3.2013 (2)	Multi	99		1					
	1+	98			2				
87_0773,04 - 12.11.2012	/								
87_0791,01-88 - 12.11.2012	1	96	2.4-2.5		1.5-1.6				
	Multi	84.3-95.5	3-7	1-6	0-1.7	0.5-1			
87_0849a,04 - 21.3.2012	Micro								
87_0884,01-56b - 19.1.2006	Multi	100 (?)							
	Multi	84-94	6.3-16		0-2.3				
	Multi	95.8		1.5	2	0.6-0.7			
87_0884,01-56c - 19.1.2006	Multi	100							
	1+	95.3	1.2		3.5				
87_0897a,01-45 - 12.11.2012 (1)	1	69	13.1	2.7	17.2				
	1	81.6	14.4	4.3					
	1	68.3	22.1	4.1	4.4	1.1			
	1	80.2	15.2	4.6					
	1	76.1		3.1					20.8
	1	62.8	33.1	1.7	0.9	0.6	0.9		
87_0897a,01-45 - 12.11.2012 (2)	Multi	85-96		1.5-3.1	1.7-7.5	0.5-1.1	0-0.6		0-2.8
87_0942g,03 - 12.11.2012	Multi	94-97		1.4-1.7	1.5-4.4				
92_0606 - 12.11.2012	Multi	98.6-99		1-1.4					
	Multi	96-98		1.1-1.9		1-1.9			
92_0645b - 21.3.2012	1+	96	2.5		1.5				
	Micro								
94_0239,01 - 21.3.2012	1	69.9	23.6	1.8	1.2			3.5	
	1	70.7	26.7	1.6	1				
	1	68	30	2					
	1	65.3	31.7	3					
	1	83.6	13.4	3					
	1	91.9	6.2	1.9					
	1	94.1	3.2	2.7					
94_0560 - 10.1.12 (Fayalite)	Multi Cu_2S	x		1.8-3.6					x
	1+	91.6	5.1	0.9	1.1			1.3	
		↪ *Prill has Cu_2S edge (2.5 Fe)*							
	1+		9.5	0.6	1			0.4	
94_0560 - 10.1.12 (Magnetite)	3+	80-87	10.6-15.7	1.6-4.3	0.5-1				
	1+	90	6.5	1	1.8		0.7		
		↪ *Prill has Cu_2S edge (2 Fe)*							
94_0775,01 - 12.11.2012	1	58.7	39.8	1.5					
	1	38.4	59.6	2					
	1	54.8	43.1	2.1					
	1: tiny, 2 phase	*35.2*	*60*	*2.2*		*2.6*			
		57	*41*	*2*					
	Micro								
94_842 - 21.2.2012	Multi	100	*(some with Cu_2O edges)*						
	1+	98.5			1.5				
	Micro								

Composition of metallic prills in crucible slag (in wt%)

Sample	Abundance	Cu	Sn	Fe	As	Co	Ni	Pb	S
97_0631E,01 - 12.11.2012	Multi	100	*(some with Cu_2O edges)*						
	Multi	97.9	1.5	0.6					
97_0631E,04 - 12.11.2012	Multi	100	*(Sn burning out, cuprite formation only after)*						
	Multi	Bronze							
	1	66	34						
97_0632D,01 - 10.1.12	1 (2 phase)	80	20						
	⟶ *phases:*	*67.1*	*32.9*						
		83.7	*15.4*		*0.9*				
	Multi	*Unmeasured (multi-phase) prills*							
	Micro								
97_0675,02 - 12.11.2012	/								
97_0690,02 - 21.2.2012	Multi	60	39	1					
	1 (2 phase)	51	48	0.3		0.6			
	⟶ *phases:*	*60*	*40*						
		40	*60*						
	1: tiny, 3 phase	17.3	7.6	28	2.3	44.3			
	⟶ *phases:*	*10*	*4*	*32*	*3*	*51*			
		83	*17*						
		71	*29*						
	Micro								
97_0690,02- - 21.2.2012	Micro								
97_1176 - 12.11.2012	Multi	*Unmeasured (multi-phase) prills*							
	Multi (2 phase)	*12*		*25*		*63*			
		85.3	*8*	*1.4*	*1*	*4.3*			
	Multi	69-71	26.7-29.5	1.1-1.2	1-1.2				
	Micro								
98_0387,03 - 21.3.2012	Multi	100	*(some with Cu_2O edges)*						
	Micro								
98_1325 - 12.11.2012	/								

APPENDIX F

Lead isotope data

Lead isotope analysis has been performed at the Curt-Engelhorn-Centre (CEZ) and Oxford Isotrace (ISO) laboratories. Raw data of lead isotope analysis performed on metal samples (CEZ and ISO), as well as chemical analysis of these metal samples (XRF and NAA by CEZ, XRF only by ISO) are presented in the tables below. This is followed by lead isotope data for crucible samples (CEZ), without chemical data. Finally, some additional plots showing correlations between various copper constituents are offered.

Sample	Lab	PQ	Strat	Type	$^{208}Pb/^{206}Pb$ mean	$^{208}Pb/^{206}Pb$ 2σ	$^{207}Pb/^{206}Pb$ mean	$^{207}Pb/^{206}Pb$ 2σ	$^{208}Pb/^{204}Pb$ mean	$^{208}Pb/^{204}Pb$ 2σ
87_0897a,01-45 (2)	CEZ	QI-a/3	B/2a	Prill	2.07130	0.0002	0.83982	0.00004	38.4500	0.004
97_0390,02-	CEZ	QIV-S-Schn	Bc/2	Prill	2.07270	0.0001	0.84112	0.00005	38.3930	0.01
1985_0027c - Mep96/004	CEZ	QI-b/5	B/3a	Fragment	2.05980	0.0001	0.83038	0.00001	38.9010	0.001
1984_1162,0001 - MeP96/056	CEZ	QI-c/4.5	B/3b?	Fragment with metal core	2.08590	0.0001	0.84958	0.00002	38.3640	0.001
1984_1162,0002 - MeP96/057	CEZ	QI-c/4.5	B/3b?	Fragment with metal core	2.05950	0.0001	0.83034	0.00001	38.9070	0.002
1985_0152 - MeP96/064	CEZ	QI-c/3	B/2b	Powder, corrosion	2.05980	0.0001	0.83060	0.00001	38.8890	0.001
1983_0196 - MeP96/055	CEZ	QI-c/4.5	B/2a	Powder, corrosion	2.06500	0.0001	0.83368	0.00001	38.8490	0.001
1985_0205,0001-0003 - MeP96/063	CEZ	QI-c/4.5	B/2b	Fragment with metal core	2.08500	0.0001	0.85250	0.00001	38.0770	0.001
1984_1498b - MeP96/003	CEZ	QI-c/3	B/2b	Powder, corrosion	2.05820	0.0001	0.82928	0.00001	38.9160	0.001
1988_1211 - MeP96/058	CEZ	QIV-d/28	?	Powder, corrosion	2.11080	0.0001	0.86583	0.00001	38.1560	0.001
1992_0240 - MeP96/060	CEZ	QIV-i.j/26	?	Fragment with metal core	2.11740	0.0001	0.86877	0.00001	38.0860	0.001
1985_0046c - MeP08/055	CEZ	QI-b/5	B/3a	Fragment, corrosion	2.05760	0.0001	0.82938	0.00001	38.8940	0.001
1987_0507,0002 - MeP08/082	CEZ	QI-b/5	B/3b	Fragment, corrosion	2.06030	0.0001	0.83066	0.00001	38.9020	0.002
1987_1633 - MeP08/098	CEZ	QI-b.c/3	B/3a	Fragment, corrosion	2.05650	0.0003	0.82990	0.00001	38.8440	0.007
1987_1670,0008 - MeP08/099	CEZ	QI-b/3	B/2b	Fragment, corrosion	2.05960	0.0001	0.82997	0.00001	38.9260	0.001
1992_0905,0002 - MeP08/117	CEZ	QIV-j/27	?	Fragment, corrosion	2.06200	0.0001	0.83239	0.00001	38.7530	0.001
1997_0575,0005 - MeP08/143	CEZ	QIV-S-Schn	?	Fragment, corrosion	2.11720	0.0001	0.87013	0.00001	38.0770	0.001
1984_1411	ISO	QI-d/3	B/2a	Casting debris	2.06083	n.a	0.83121	n.a	38.9064	n.a
1982_0219b,0002 - MeP 85/03	ISO	QI-d/3	B/2a	Gilded?	2.07498	n.a	0.83934	n.a	38.7793	n.a
1986_0280a - MeP 87/01	ISO	QI-b/9	B/2b	Wheel hub	2.05835	n.a	0.82864	n.a	38.9975	n.a
1984_1381 - MeP 87/14	ISO	QI-f/02.03	B/2	Round rod	2.07461	n.a	0.84035	n.a	38.8678	n.a
1986_0720 - MeP 87/19	ISO	QI-c/4.5	B/3	Dagger	2.08087	n.a	0.84375	n.a	38.6209	n.a
1987_0140 - MeP 87/25	ISO	QI-ax/4.5	B/3b	Rod	2.06052	n.a	0.83052	n.a	38.9376	n.a
1986_0909 - MeP 87/30	ISO	QI-c/4.5	B/3	Casting waste	2.06822	n.a	0.83583	n.a	38.8031	n.a
1987_0512,0002 - MeP 87/39	ISO	QI-b/5	B/3b	Spearhead	2.10477	n.a	0.86185	n.a	38.2441	n.a
1987_0803,0004 - MeP 87/45	ISO	QI-a/3	B/2a	Oxhide ingot fragment	2.07394	n.a	0.84124	n.a	38.4239	n.a

Table F.1: Copper (alloy) samples with context and lead isotope ratios

Sample	PQ	Strat	Type	Cu	Mn	Fe	Co	Ni	Zn	As	Se	Ag	Sn	Sb	Te	Pb	Bi
				%	%	%	%	%	%	%	%	%	%	%	%	%	%
1985_0027c -MeP96/004	QI-b/5	B/3a	Fragment	85	< 0.01	0.12	0.01	0.04	< 0.1	0.78	0.02	0.021	13.7	0.067	0.015	0.54	< 0.01
1984_1162,0001 -MeP96/056	QI-c/4.5	B/3b?	Fragment with metal core	100	< 0.01	0.21	< 0.01	< 0.01	< 0.1	0.01	0.04	0.021	< 0.005	< 0.005	0.023	< 0.01	0.02
1984_1162,0002 -MeP96/057	QI-c/4.5	B/3b?	Fragment with metal core	87	< 0.01	0.34	< 0.01	0.04	< 0.1	0.53	< 0.01	0.022	11.5	0.034	< 0.005	0.57	< 0.01
1985_0152 -MeP96/064	QI-c/3	B/2b	Powder, corrosion	88	< 0.01	0.95	0.03	0.02	< 0.1	0.27	< 0.01	0.011	10.3	0.019	< 0.005	0.32	< 0.01
1983_0196 -MeP96/055	QI-c/4.5	B/2a	Powder, corrosion	83	< 0.01	1.08	0.02	0.03	< 0.1	0.85	0.01	0.101	13.6	0.115	0.008	0.85	< 0.01
1985_0205,0001 -0003 -MeP96/063	QI-c/4.5	B/2b	Fragment with metal core	95	< 0.01	4.4	0.06	< 0.01	< 0.1	0.10	0.01	< 0.002	< 0.005	0.005	0.007	< 0.01	< 0.01
1984_1498b -MeP96/003	QI-c/3	B/2b	Powder, corrosion	85	0.01	3.1	0.02	0.02	< 0.1	0.56	< 0.01	0.013	11.1	0.046	0.005	0.08	< 0.01
1988_1211 -MeP96/058	QIV-d/28	?	Powder, corrosion	84	< 0.01	0.43	0.03	0.04	< 0.1	0.59	< 0.01	0.014	12.5	0.070	< 0.005	1.93	< 0.01
1992_0240 -MeP96/060	QIV-ij/26	?	Fragment with metal core	82	< 0.01	0.25	0.02	0.03	< 0.1	0.22	< 0.01	0.012	16.0	0.019	< 0.005	1.70	< 0.01
1985_0046c -MeP08/055	QI-b/5	B/3a	Fragment with metal core	93	< 0.01	0.34	0.01	0.02	< 0.1	0.47	< 0.01	0.003	5.2	0.017	< 0.005	0.48	< 0.01
1987_0507,0002 -MeP08/082	QI-b/5	B/3b	Fragment, corrosion	92	0.01	0.65	< 0.01	0.02	< 0.1	0.53	< 0.01	0.006	6.5	0.030	0.008	0.46	< 0.01
1987_1633 -MeP08/098	QI-b.c/3	B/3a	Fragment, corrosion	90	< 0.01	0.35	< 0.01	0.03	< 0.1	0.77	< 0.01	0.005	7.6	0.043	0.006	0.78	< 0.01
1987_1670,0008 -MeP08/099	QI-b/3	B/2b	Fragment, corrosion	90	< 0.01	0.84	< 0.01	0.03	< 0.1	0.58	< 0.01	0.006	7.2	0.054	0.006	1.10	0.01
1992_0905,0002 -MeP08/117	QIV-j/27	?	Fragment, corrosion	88	< 0.01	0.55	< 0.01	0.02	< 0.1	0.31	< 0.01	0.003	10.8	0.021	0.010	0.02	< 0.01
1997_0575,0005 -MeP08/143	QIV-S-Schn	?	Fragment, corrosion	87	< 0.01	0.13	< 0.01	0.02	< 0.1	0.42	< 0.01	0.016	9.8	0.051	0.011	2.04	< 0.01

Table F.2: XRF data for CEZ copper (alloy) samples

Sample	PQ	Strat	Type	Cu	σ	Fe	σ	Co	σ	Ni	σ	Zn	σ	As	σ
				%		%		ppm		ppm		ppm		ppm	
1985_0027c -Mep96/004	QI-b/5	B/3a	Fragment	73.2	2.3	0.11	26	103	5	288	8	32	17	6310	2
1984_1162,0001 -MeP96/056	QI-c/4.5	B/3b?	Fragment with metal core	98.3	2.3	0.04	45	5.7	7.6	54	37	35	18	151	2
1984_1162,0002 -MeP96/057	QI-c/4.5	B/3b?	Fragment with metal core	75.9	2.3	0.24	26	106	5	350	11	112	10	4020	2
1985_0152 -MeP96/064	QI-c/3	B/2b	Powder, corrosion	59.1	2.3	1.28	21	630	5	247	11	61	12	1484	2
1985_0205,0001-0003 -MeP96/063	QI-c/4.5	B/2b	Fragment with metal core	83.1	2.3	7.50	21	620	5	340	21	263	8	944	2
1988_1211 -MeP96/058	QIV-d/28	?	Powder, corrosion	64.3	2.3	0.18	24	211	5	280	7	18	23	2830	2
1992_0240 -MeP96/060	QIV-i.j/26	?	Fragment with metal core	69.5	2.3	0.17	25	169	5	266	8	130	5	1749	2

Sample	PQ	Strat	Type	Se	σ	Ag	σ	Sn	σ	Sb	σ	Te	σ	Au	σ
				ppm		ppm		%		ppm		ppm		ppm	
1985_0027c -Mep96/004	QI-b/5	B/3a	Fragment	82.4	2.9	223	1	13.1	1.7	392	1.4	83.0	9.5	198	2
1984_1162,0001 -MeP96/056	QI-c/4.5	B/3b?	Fragment with metal core	418	2	299	1	<0,026		4	3.4	319	5	8.7	3
1984_1162,0002 -MeP96/057	QI-c/4.5	B/3b?	Fragment with metal core	48.8	5.2	183	2	10.3	1.7	306	1.4	56.0	20.2	172	2.4
1985_0152 -MeP96/064	QI-c/3	B/2b	Powder, corrosion	37.6	3.6	96	1.6	11.1	1.7	184	1.4	30.0	19.3	87.6	2
1985_0205,0001-0003 -MeP96/063	QI-c/4.5	B/2b	Fragment with metal core	96.6	2.9	7.0	12.6	<0,013		21.5	1.9	62.0	17.6	2.0	4.0
1988_1211 -MeP96/058	QIV-d/28	?	Powder, corrosion	36.5	3.2	124	1	8.4	1.7	553	1.4	46.0	11.1	80.3	2.4
1992_0240 -MeP96/060	QIV-i.j/26	?	Fragment with metal core	8.8	10.4	104	1	13.6	1.7	137	1.4	< 16		35.6	2.4

Table F.3: NAA data for CEZ copper (alloy) samples

Sample	PQ	Strat	Type	Cu	Fe	Sn	Pb	As	Ag	Au
				%	%	%	%	%	%	%
84_1411	QI-d/3	B/2a	Casting debris	92.00	<0.1	7.0	0.40	<0.2	<0.1	<0.2
1982_0219b,0002 - MeP 85/03	QI-d/3	B/2a	Gilded?	94.00	<0.1	6.0	0.80	<0.2	<0.1	0.2
1986_0280a - MeP 87/01	QI-b/9	B/2b	Wheel hub	79.00	<0.1	21.0	0.20	0.2	<0.1	<0.2
1984_1381 - MeP 87/14	QI-f/02.03	B/2	Round rod	89.00	<0.1	5.0	5.00	<0.2	<0.1	<0.2
1986_0720 - MeP 87/19	QI-c/4.5	B/3	Dagger	89.00	<0.1	10.0	0.20	<0.2	<0.1	<0.2
1987_0140 - MeP 87/25	QI-ax/4.5	B/3b	Rod	88.00	<0.1	12.0	0.30	<0.2	<0.1	<0.2
1986_0909 - MeP 87/30	QI-c/4.5	B/3	Casting waste	99.00	<0.1	<0.2	<0.1	<0.2	<0.1	<0.2
1987_0512,0002 - MeP 87/39	QI-b/5	B/3b	Spearhead	84.00	<0.1	15.0	0.30	<0.2	<0.1	<0.2
1987_0803,0004 - MeP 87/45	QI-a/3	B/2a	Oxhide ingot fragment	99.00	<0.1	<0.2	<0.1	0.2	<0.1	<0.2

Table F.4: XRF data for ISO copper (alloy) samples

Sample	PQ	Strat	Type	^{208}Pb/^{206}Pb mean	^{208}Pb/^{206}Pb 2σ	^{207}Pb/^{206}Pb mean	^{207}Pb/^{206}Pb 2σ	^{208}Pb/^{204}Pb mean	^{208}Pb/^{204}Pb 2σ
83_0597l,01	QI-e/1	B/1-B/2	Ceramic	0.85869	0.00009	2.0991	0.0002	38.212	0.008
			Slag	0.86223	0.00003	2.1061	0.0001	38.255	0.006
87_0897a,01-45 (2)	QI-a/3	B/2a	Ceramic	0.83540	0.00003	2.0663	0.0001	38.708	0.004
			Slag	0.83347	0.00003	2.0640	0.0001	38.811	0.010
87_0762	QI-a/3	B/2a	Ceramic	0.84314	0.00002	2.0773	0.0002	38.534	0.005
			Slag	0.84444	0.00002	2.0802	0.0001	38.609	0.007
87_0762,0Nv	QI-a/3	B/2a	Ceramic	0.85214	0.00003	2.0888	0.0001	38.342	0.010
			Slag	0.86675	0.00001	2.1121	0.0001	38.149	0.005
83_0542b,01	QI-e/1	B/2a	Ceramic	0.83848	0.00004	2.0718	0.0002	38.691	0.009
			Slag	0.84077	0.00005	2.0760	0.0002	38.695	0.004
87_0942g,03	QI-a/3	B/3	Ceramic	0.84051	0.00005	2.0728	0.0003	38.610	0.005
			Slag	0.85859	0.00001	2.1002	0.0001	38.249	0.001
83_1149b	QI-d/02.03	B/3	Ceramic	0.85551	0.00002	2.0939	0.0001	38.291	0.007
			Slag	0.83785	0.00001	2.0747	0.0001	38.799	0.009
87_0634c,04	QI-b/5	B/3b	Ceramic	0.83106	0.00002	2.0550	0.0002	38.735	0.006
			Slag	0.83015	0.00005	2.0590	0.0002	38.907	0.010
98_0387,03	QIV-j/28	Bb?	Ceramic	0.84879	0.00001	2.0844	0.0001	38.418	0.003
			Slag	0.85282	0.00002	2.0904	0.0001	38.290	0.008
97_0631E,01	QIV-S-Schn	Bc	Ceramic	0.85893	0.00008	2.1005	0.0001	38.273	0.010
			Slag	0.86296	0.00003	2.1068	0.0003	38.213	0.006
97_0631E,04	QIV-S-Schn	Bc	Ceramic	0.86343	0.00003	2.1070	0.0001	38.185	0.008
			Slag	0.86430	0.00003	2.1086	0.0001	38.195	0.005
97_0690,02-	QIV-S-Schn	Bc/2	Ceramic	0.86157	0.00004	2.1040	0.0002	38.215	0.004
			Slag	0.85835	0.00001	2.0991	0.0001	38.223	0.002
87_0726,68-78b	QI-a/3.4	B/2a	Slag	0.84961	0.00003	2.0870	0.0001	38.401	0.007

Table F.5: Crucible samples with context and lead isotope ratios

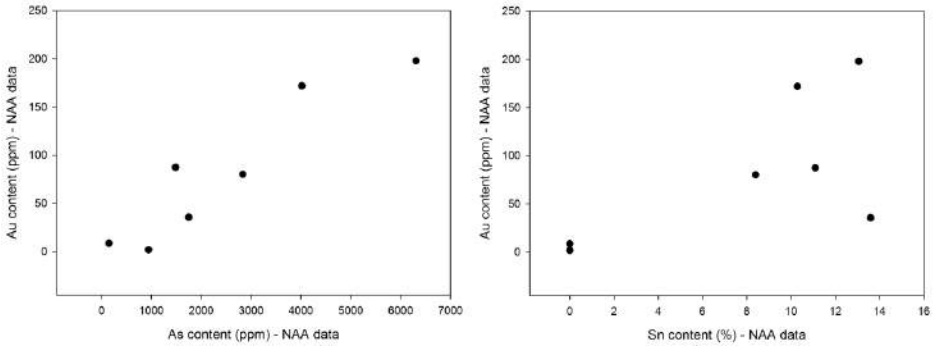

Figure F.1: NAA data: As vs Au content and Sn vs Au content

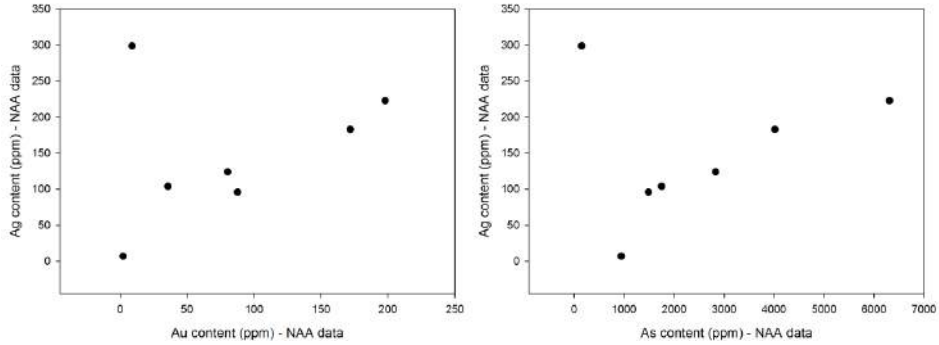

Figure F.2: NAA data: Au vs Ag content and As vs Ag content

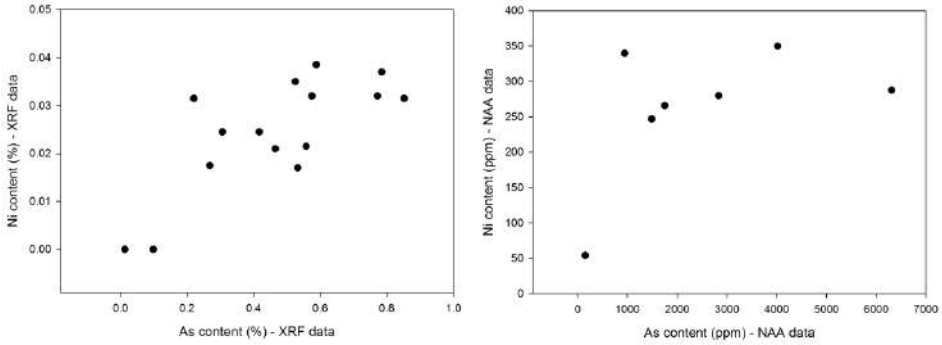

Figure F.3: XRF and NAA data: As vs Ni content

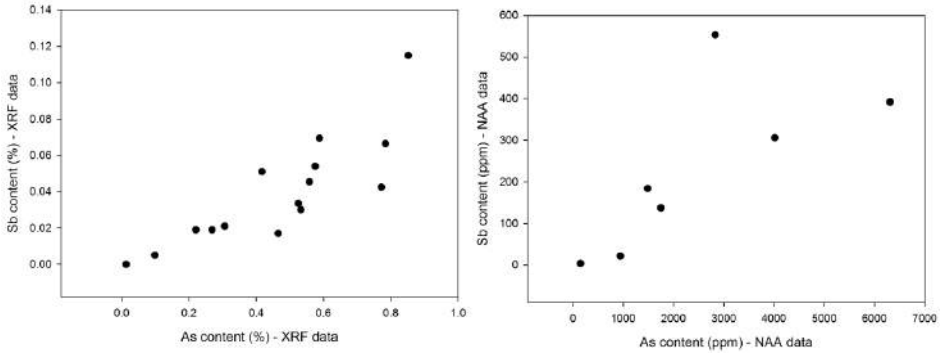

Figure F.4: XRF and NAA data: As vs Sb content

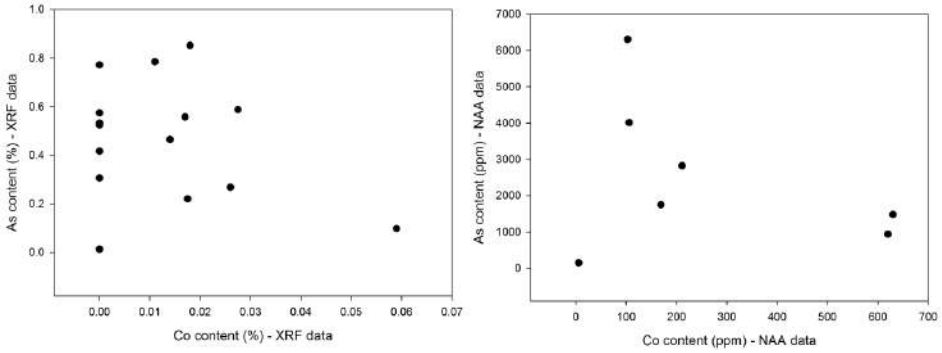

Figure F.5: XRF and NAA data: Co vs As content

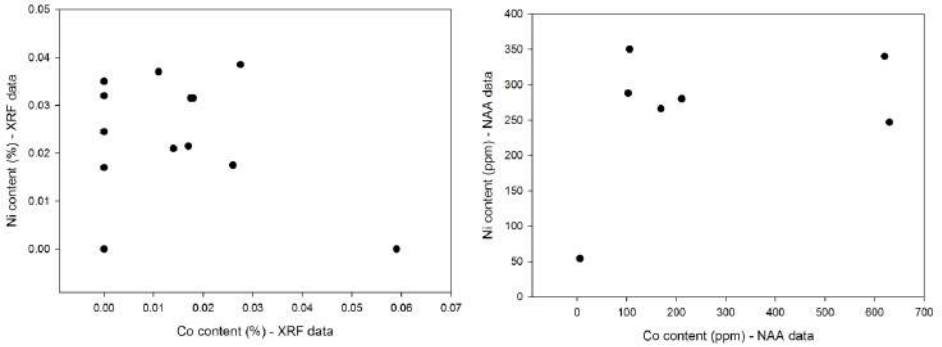

Figure F.6: XRF and NAA data: Co vs Ni content

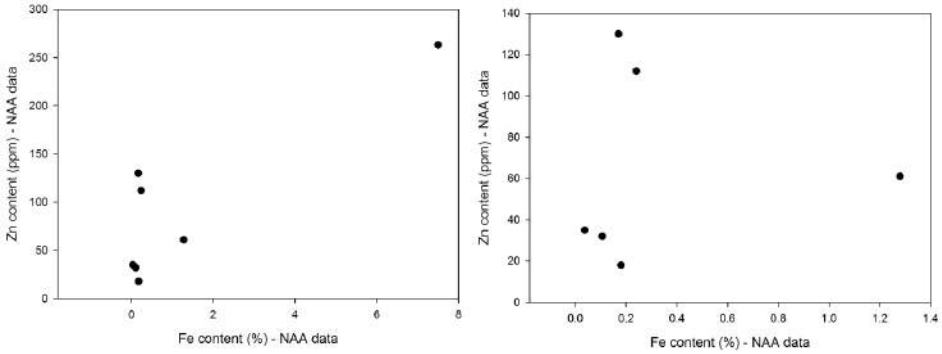

Figure F.7: XRF and NAA data: Fe vs Zn content

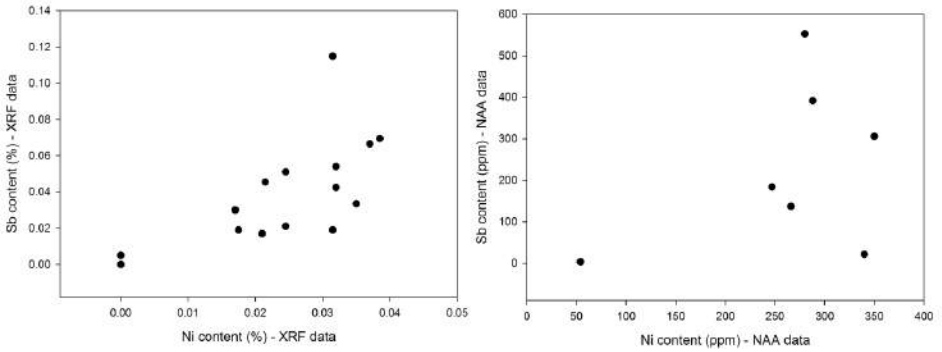

Figure F.8: XRF and NAA data: Ni vs Sb content

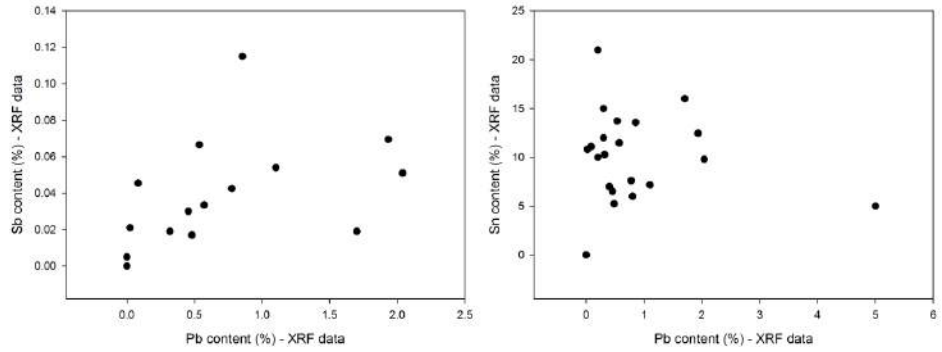

Figure F.9: XRF data: Pb vs Sb content and Pb vs Sn content

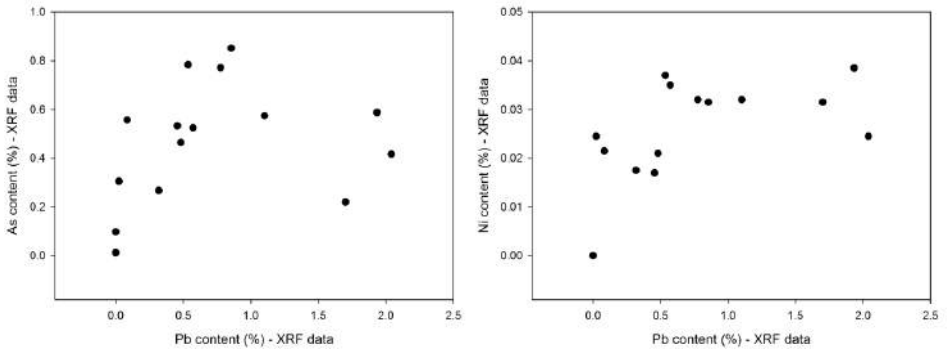

Figure F.10: XRF data: Pb vs As content and Pb vs Ni content

APPENDIX G

Volume Calculations

Section G.1

Crucible dimensions

The crucible dimensions are given in Table G.1:

Exterior	
Length	±19.8 cm
Width	±13.5 cm
Height	±10.4 cm
Bottom diameter	*missing*
Interior	
Length	±18.3 cm
Width	±10.5 cm
Heigth	±7.0 cm
Spout-width	*missing*
Wall thicknesses	
Rim	±1.5 cm
Bottom	±3.5 cm

Table G.1: Crucible dimensions (after Pusch, 1994, Table 4, p. 152)

Assuming that the crucible is approximately half an ellipsoid[1], the inner crucible volume can be calculated as

[1] An elliptical model better approximates the irregular ceramic geometry than a circular model (see Rodriguez and Hastorf, 2013).

$$V_{inner} = \frac{4}{3}\pi abc/2$$

with a, b and c the dimensions (two diameters and height) of the ellipsoid.

For the inner volume, this calculation adds up to $V_{inner} = 352cm^3$ or 352 ml.

This is quite similar to what is published by Pusch (1994), shown in Table G.2:

Volume	
Bottom/rim	±380 ccm
Bottom/spout	±250 ccm
Bottom/spout-0.5cm	±204 ccm
Bottom/spout-1 cm	±158 ccm
Copper weight	
Bottom/rim	±3404.8 g
Bottom/spout	±2240.0 g
Bottom/spout-0.5cm	±1827.8 g
Bottom/spout-1 cm	±1415.7 g

Table G.2: Crucible capacity (after Pusch, 1994, Table 5, p. 160)

In his calculations (unpublished), Pusch approached the crucibles as a combination of a hemisphere and half of a cone:

$$V_{hemisphere} = \frac{4}{3}\pi r^3/2 = \frac{4}{3}\pi 4.8^3/2 = 232cm^3$$

and

$$V_{semicone} = \pi r^2 \frac{h}{3}/2 = \pi 3.6^2 \frac{8}{3}/2 = 16cm^3$$

This sums up to $V = 250cm^3$. A remaining 'unused' volume of $158cm^3$ was then calculated. Added together, this makes $\pm 380cm^3$.

Both calculation methods presented here are approximations. For the sake of convenience, the ellipsoid shape is used for further calculations. As these calculations are aimed at providing a relative assessment of slag volume (and content) to inner crucible volume, the absolute size is less important here.

Section G.2

Approximating cobalt content in copper charge

Based on the cobalt content in the crucible slag, the cobalt content in the copper charge can be approximated, as developed here.

The slag volume (as part of the crucible) can be calculated by assuming a certain thickness of slag layer 't' (equal thickness over entire crucible wall assumed as approximation):

$$V_{slag} = \frac{4}{3}\pi/2((a+t)(b+t)(c+t) - abc)$$

The slag mass, therefore, is:

$$m_{slag} = \rho_{slag} V_{slag} = \rho_{slag}(\frac{2}{3}\pi((a+t)(b+t)(c+t) - abc)$$

The mass of cobalt oxide in the slag is a fraction of this:

$$m_{Co-oxide} = (wt\%CoO) m_{slag} = (wt\%CoO)\rho_{slag}(\frac{2}{3}\pi((a+t)(b+t)(c+t) - abc)$$

The mass of copper charged into the crucible is[2]:

$$m_{copper} = (wt\%Cu-in-bronze) m_{bronze} = (wt\%Cu-in-bronze) V_{inner}\rho_{bronze}$$
$$= (wt\%Cu-in-bronze)(\frac{2}{3}\pi abc)\rho_{bronze}$$

Assuming that the cobalt oxide in the slag derives from the mass of copper charged into the crucible, and no cobalt remains in this copper charge, the original content of cobalt oxide in copper can be approximated as:

$$CoO-content_{original} = \frac{m_{Co-oxide}}{m_{copper}}$$

$$CoO-content_{original} = \frac{(wt\%CoO)\rho_{slag}(\frac{2}{3}\pi((a+t)(b+t)(c+t) - abc))}{(wt\%Cu-in-bronze)(\frac{2}{3}\pi abc)\rho_{bronze}}$$

Assuming:

[2]The density of bronze depends on the tin content (wt%Sn-in-bronze and wt%Cu-in-bronze). As ρ_{copper} = 8.96 g/cm^3 and ρ_{tin} = 7.298 g/cm^3, the density of bronze is usually around 8.5 to 8.9 g/cm^3. For a 10 wt% tin-bronze, ρ_{bronze} = 8.7641 g/cm^3.

- CoO content in slag is 3 wt%
- Cu in bronze content is 90 wt% (i.e., a 10 wt% tin-bronze)
- $\rho_{bronze} = 8.76$ g/cm^3
- $\rho_{slag} = 3$ g/cm^3 (unknown, but should be similar value; see VDEh, 1995)
- a, b and c are (half of) the interior measures from Table G.1.
- t is 0.5 cm

Then the cobalt oxide content originally present in the copper charge is 0.0037 or 0.37 wt%. If this cobalt is present as a metal phase, it would make up 0.29 wt% of the copper charge[3].

Though a number of assumptions and approximations (e.g., crucible shape, slag density and slag layer thickness) are made for this calculation, the result gives an idea of the order of magnitude of the cobalt content in the copper charge: less than 0.5 wt% Co in the copper charge can produce about 3 wt% CoO in the crucible slag. Obviously, the cobalt content in the copper could be higher without leading to stronger enrichment, as long as it was not completely oxidised out. This is a realistic scenario.

A similar conclusion can be made for the slag enrichment in FeO, SnO_2, ZnO and PbO: as the volume of the crucible charge greatly exceeds that of the crucible slag, enrichments of a few wt% (bulk composition) of the slag, do not necessarily represent high metal losses from the charge.

[3]Atomic mass of Co: 58.9332 amu. Atomic mass of O: 15.9994 amu. Wt% Co in CoO: $\frac{58.9332}{58.9332+15.9994} = 78.65$ wt%

Gordion Appendices

APPENDIX H

Notes on Late Phrygian foundry

All the available information on the Late Phrygian foundry, excavated by Young in 1953, was collected by Alison Fields. Her unpublished report is reproduced in full below.

Trench NCT-A3

- *Gordion Notebook 39, p. 113-135*
- *Gordion Notebook 38, p. 125 (possible north extension)*
- *Gordion Notebook 53, p. 59 (final reference; removal of the west wall of the foundry 2 seasons later on June 12-13, 1955, before excavation of Painted House)*

In Notebook 39:
Floor 6 = Floor of foundry
Layer 6/Fill over Floor 6 = Foundry destruction fill

The so-called foundry comprised of two or three rooms on a N-S axis. The southernmost room and the room north of that (which was either the northernmost room or the central room) were excavated in 1953 in Trench NCT-A3; a different excavator digging a dike (NCT-A2-3 dike) just north of these rooms identified a line of three regularly cut stones claiming that it might represent a third room of the foundry to the north (NB 38, p. 125).

The foundry was situated just over the line of the west wall of Building C and thus directly over the Painted House. (The floor of the foundry was ca. 30 cm above the destruction fill of the PH.) The walls of the foundry were constructed of reused stones from Building C that had been turned on end in order to maximize the surface of the stones, creating a sort

of orthostate course (see photographs; Figure H.1*). Rubble was added in the construction above and between these larger stones. The walls were preserved only to a height of about 60 cm. so it is possible that the remaining superstructure was composed of mudbrick. The west wall was the best preserved; only one block was preserved of the south wall; the east wall was mostly robbed out; the northernmost wall is not mentioned (unless you count the three stones from NB 38, p. 125 as the northernmost extent). The interior crosswall is referred to as 'Wall F' and was given measurements: 465 cm long, 110 cm wide).*

*Two features are mentioned in the notebooks: one is a stone-lined pit abutting the internal crosswall ('Wall F') and the west wall. The pit was "filled with pure black burnt sandy substance and pieces of slag iron clunkers, etc..." The second (possible) feature might be represented by a line a stones running E-W and abutting the east wall in the southernmost room. Both of these features can be seen in the sketch in Notebook 39, p. 122 and on the architect's plan I attached to the email (*Figure H.2*). On the architect's plan, the foundry is the structure at the top of the scan. The two rooms mentioned above are easily identifiable; the possible northernmost extension is represented by the small line of three stones to the north (that is, 'notebook north' - or northeast on the architect's plan).*

The building has been identified as a foundry based on the contents of the fill overlying the floor of the building ('Floor 6') and the contents of the pit mentioned above. The excavator notes that it was "covered with burning and slag, pieces of crucibles, arrowheads, bronze, and iron garments" (NB 39, p. 121). Several pits were cut into the floor (locations shown on architect's plan), c. 50 cm in diameter and 40-50 cm deep; all were "filled with some sort of burnt earth, slag, etc, as covered the floor." The northern (or central) room might have had two phases, because the excavator notes that under the floor was a fill c. 10-15 cm thick of heavily burnt earth and ash and a second floor which might be reused from Building C (similar yellow color, NB 39, p. 133).

The dating is not as clear-cut as we would like. I have gone through all of the context pottery I was able to identify in the fill above the floor of the foundry and the fill between the foundry and the Painted House, and I have come to the conclusion that the foundry must have been built at some point at the end of the 5th or early 4th century B.C.E. and was put out of use before the Hellenistic period, perhaps in the first half of the 4th century... so it had a relatively short life. There are no sherds from the fill over the floor dating to the 3rd century, so the argument is one in absentia. In NCT-A3 Bag 1B, which contained fill directly over the floor, there was an Attic bolsal (c. 400), a 5th century Attic askos, and some Achaemenid bowls; bag 1A contained an Attic salt cellar and an oinochoe from the 5th century. Unfortunately the fill between the Painted House and the foundry is inconclusive, as no imported

Figure H.1: View of foundry wall from south-east

pottery has been found here and the local Late Phrygian wares cannot be stylistically dated with any precision. The late Keith DeVries made a note on the context card that the fill is no later than the early 4th century, so it seems that the construction and life span of the foundry was some time around the turn of the 5th-4th centuries, being put out of use before the Hellenistic period, sometime in the mid-4th.

Different descriptions of fill/small finds:

***p. 116**: Immediately over it:*
grey bowl (polish)
4 3-flanged arrowheads (2917 B521)
1 1-flanged arrowhead
triangular strip of bronze 11 cm long
glass frag (blue and white) 2919 G158

***p. 120**: Fill over floor 6*
buff and greyware bowls
black glazed bowl base & rim frag, dated by GRE to 400
smaller bag of fill between floor 4 & 6 - greyware cooking pot ware, Lydion base, buff bowls with orange stripes

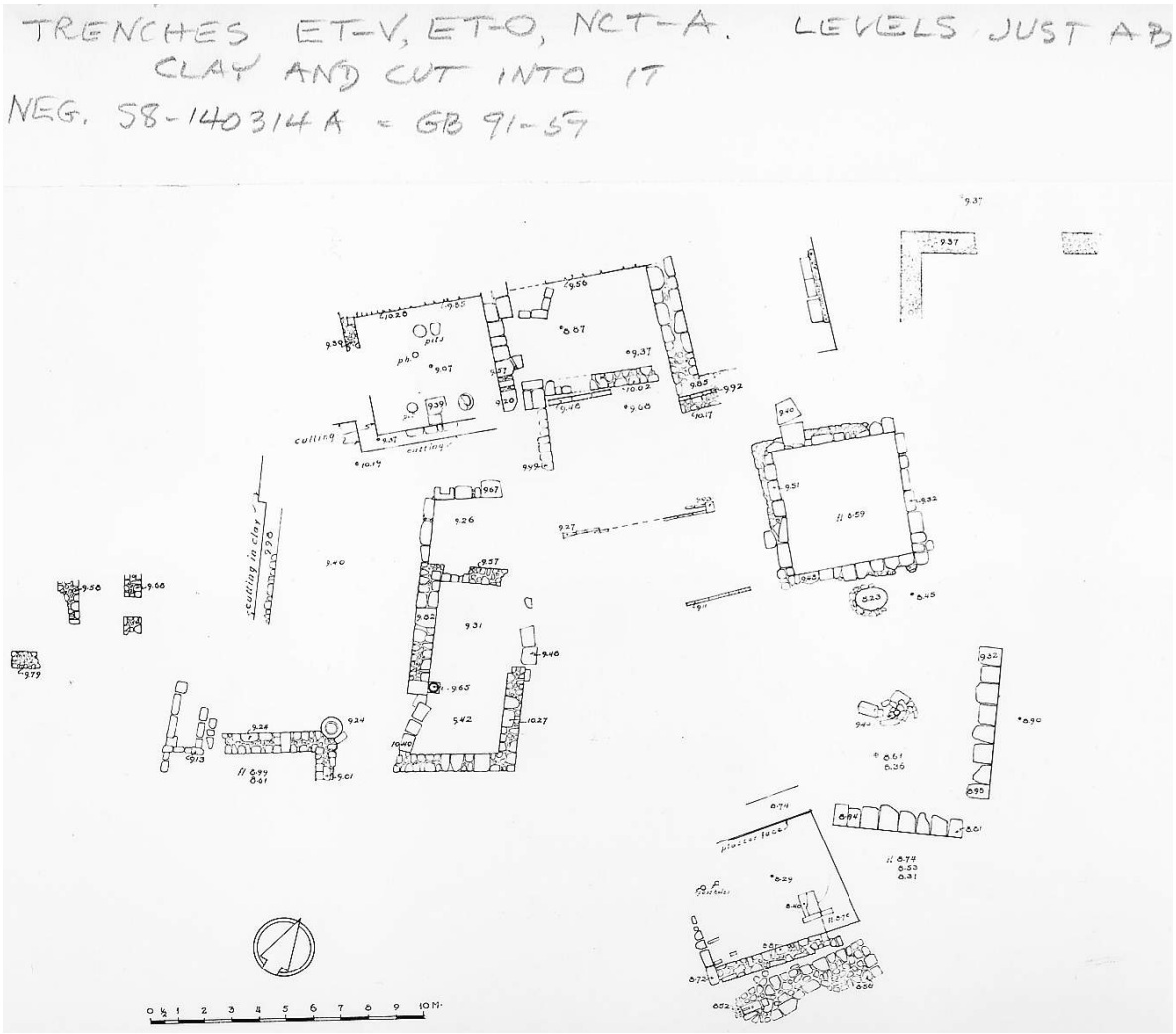

Figure H.2: Architect's plan of foundry area

APPENDIX I

Sample list and overview of excavated contexts

The contexts from which crucibles were excavated are summarised in Table I.1. The different 'operations' are shown in Figure 7.3. Within this, 'phases' denote the time period (Late Phrygian) and different 'loci' and 'lots' have been defined during excavation to identify different layers and material assemblages. This list offers more detailed information for the various (dump) contexts:

A: Deep round, bell-shaped pit in northeast quadrant of trench. Partially cut away by test Loc 61, cuts pit Loc 68. Lot cleared bottom of pit. Hunks of burned dung(?), very loose fill.

B: Removal of wall locus 20. At bottom of foundation trench. Went through bottom, crucible from this new (Late Phrygian) deposit (cf NB II:46), in which several pit tops were visible.

C: Surface along north balk, beneath Loc 77 lot 155; within 'Landfill'. Light grayish-brown silt, compacted but much trash, charcoal, pebbles. Traces of phytoliths. 'Notable' amount of sand, especially to east.

D: Complex of pits associated with lion sculpture; this lot from beneath stones, cut away horizontal strata which are probably matrix–surfaces associated with Wall Locus 76/1989 17.

E: Ash lense at top of Loc 77, L Phrygian land fill. Along north balk, c. 1 m in diameter. Full of charcoal bits, may have had clay edge on one side (indicated by section).

Sample	Phase	Operation	Locus	Lot	Context type	Context description
Gordion 21299 - 15.10.2013	410.04	1	65	130	Pit	A
Gordion 22529 - 13.9.2013	400	2	33	141	Mixed in excavation	B
Gordion 22626 - 15.10.2013	420	1	82	162	Exterior surface	C
Gordion 22673 - 15.1.2014	420	1	82	162	Exterior surface	C
Gordion 22673-A - 15.10.2013	420	1	82	162	Exterior surface	C
Gordion 22673-B - 15.10.2013	420	1	82	162	Exterior surface	C
Gordion 22829 - 15.10.2013	0	2	51	149	Pit	D
Gordion 22958 - 9.4.2013	420	1	75	149	Ash lense	E
Gordion 22999 - 13.9.2013	420	1	100	213	Pit	F
Gordion 23045-A - 15.10.2013		1	82	188	?	?
Gordion 23045-B - 15.10.2013		1	82	188	?	?
Gordion 23045-S - 15.10.2013		1	82	188	?	?
Gordion 23128 - 13.9.2013	0	2	66	157	Trash	G
Gordion 23329 - 9.4.2013	420	2	73	177	Lensed trash	H
Gordion 23329 - 15.1.2014	420	2	73	177	Lensed trash	H
Gordion 23523 - 15.10.2013	460	1	98	237	Robber trench	I
Gordion 23707 - 9.4.2013	430.04	1	100	214	Pit	F
Gordion 23707 - 15.1.2014	430.04	1	100	214	Pit	F
Gordion 23778 - 13.9.2013	460	1	98	237	Robber trench	I
Gordion 23797 - 9.4.2013	460	1	98	228	Robber trench	J
Gordion 25368 - 13.9.2013	0	2	12	17	Balk trimming	K
Gordion 25394 - 9.4.2013	400	2	19	57	Mixed in excavation	L
Gordion 25394_A - 13.9.2013	400	2	19	57	Mixed in excavation	L
Gordion 25394_B - 13.9.2013	400	2	19	57	Mixed in excavation	L
Gordion 25568 - 9.4.2013	410	2	11	16	Trash on surface	M
Gordion 25568 - 15.1.2014	410	2	11	16	Trash on surface	M
Gordion 25569-A - 15.10.2013	0	2	12	17	Balk trimming	K
Gordion 25569-B - 15.10.2013	0	2	12	17	Balk trimming	K
Gordion 26891 - 9.4.2013	435	2	6	118	Exterior surfaces	N
Gordion 27609 - 15.10.2013	470	1	25	76	Exterior surface	O
Gordion 27609-S - 15.10.2013	470	1	25	76	Exterior surface	O
Gordion 27613-A - 13.9.2013	470.02	1	26	80	Pit	P
Gordion 27613-B - 13.9.2013	470.02	1	26	80	Pit	P
Gordion 27629 - 15.10.2013	435	2	6	118	Exterior surfaces	N
Gordion 27634 - 12.11.2013	430.08	1	19	64	Pit	Q
Gordion 27635 (1) - 12.11.2013	430.07	1	18	63	Pit	R
Gordion 27635 (2) - 12.11.2013	430.07	1	18	63	Pit	R
Gordion 27636 - 9.4.2013	430	1	18	61	Pits mixed in excavation	S
Gordion 27638 - 12.11.2013	400	2	6	123	Mixed in excavation	T
Gordion 27640 - 12.11.2013	400	2	6	123	Mixed in excavation	T
Gordion 27734 (1) - 12.11.2013	400	2	19	154	Mixed in excavation	U
Gordion 28218 - 12.11.2013	440.03	1	32	96	Pit	V
Gordion 28236 - 9.04.2013	440.01	1	34	111	Floor deposit	W
Gordion 28877 - 9.04.2013	400	7	32	123	?	X
Gordion 28932 (1) - 12.11.2013	420.01	1	51	129	Pit	Y
Gordion 28932 (2) - 12.11.2013	420.01	1	51	129	Pit	Y

Table I.1: Overview of samples and their respective excavation contexts

F: Pit, completed in 1989 as Op 1 Loc 7; initially dug in 1988 as part of Loc 99. Could be a double pit, but different fill. Lot 213 contained ashy bones, loose silt, charcoal, some pebbles. Lumps of mud brick as well as sherds and bones noted. Cuts into robber trench for Building I.

G: 'Landfill' to northwest of foundation trench locus 20/33, south of lion pit complex. Can't be linked to any section, but cut by pit Locus 65. CK sherds for date.

H: Stripping landfill, southeast quadrant. May include pit tops, but close in date to matrix.

I: Large amorphous trashy area within 'patio'. Large quantity of sherds found in this lot which exposed an oval paved area. Change of texture in area, could have been pit or just variation within dump. Area beneath uppermost clay surfaces, cut away more such surfaces preserved in southeast corner of trench. May be associated with pyrotechnic feature in this area.

J: Dark brown soil, white flecked, next to east balk, just north of patio. Continued in 1989 revealing a pit, Loc 11.2 lot 34 which turned into Loc 12 lot 35. Whole area churned up, this lot probably from pit cut into early robber trench for EW wall of Building I.

K: Trimming east balk, western face. Most of deposit is trash immediately beneath AV.

L: Material on surface associated with cut stone block wall locus 17; between wall and south balk; pit in corner shows up in section. Soft with large pieces of pottery and bone.

M: Trench to east of Wall 17. Dry ashy soil resting on hard yellow surface associated with cut stone wall 17. Metallurgical debris on this yellow surface, [Locus 16].

N: Soft brown soil running along south balk, up against cut stone wall fragment [Locus 17] in southwestern corner of trench. Abundant evidence of metal working including crucible(s), slag, bellows piece or tuyère.

O: Isolated block of material in northern part of operation, left after clearance of pits. Top at same height as remains of cellar wall [Op 1 loc 11]. Brown chunky, presumably 'landfill' above clay?

P: Small oval pit cut in western part of trench to north of Building I:2 extended E-W wall with cobble fill, capped by yellow clay. Pit is dark brown, filled with charcoal.

Q: Large pit near north balk, northeast quadrant. Cut in turn by pit Locus 21. Earlier than 21. At northern end of trench. Soft brown-gray trashy matrix, little charcoal. Discovered at level of cellar top, should be similar in date to Latrine Pit Locus 47.

R: Eastern and deeper pit of 2?(initially mixed in lot 61). Bottoms out on hard clay, 'dance-floor'. Cut from surface of units excavated as Locus 20.1. Capped by 1988 Locus 82, landfill. Along north balk. Lot is from clayey deposit.

S: Two inter-cut pits at northern end of trench, extending into balk. Soft brown matrix, little charcoal or lime. Beneath 1988 Locus 81, above dancefloor surface. Cut from top of Locus 20.1. Lot is from top of pit, soft and ashy.

T: Trash above robbed out wall of Cellar, approximately at level of Wall locus 17. Arrowhead and crucible. Mixture of robber pit, latrine pit, and cellar trash.

U: Surface associated with cut stone wall, locus 17, to south of wall; pit in southwest corner not separately cleared, could also go beneath surface associated with wall locus 17 (435).

V: Pit cut along southern edge of 'patio'. Should have been sealed by upper clay surfaces exposed in 1988. Cut into 'tile fall' layer [locus 34] lying on second paving [locus 71] in this area.

W: Deposit with tile and burning immediately above lower stone paving in 'patio' area, last well-preserved surface in this area, floor drained by tile drain in 'courtyard' of Building I.

X: Notes contradictory. Could be Late Phrygian or foundation levelling mud for north wall Op 2 structure Op 2/7 balk. RCH says Late Phrygian based on pottery.

Y: Large quantities of industrial waste in lower levels of pit, domestic trash above. Same context as 1988 Op 1 Loc 91 [capped by 88 Locus 71]. Cuts pit locus 2.1 1989 [1988 locus 93]. MSR considers pit contemporary with 1989 pits excavated at Loci 23, 30, 7.

APPENDIX J

Bulk Compositions

In this appendix, the bulk composition of both the crucible ceramic and the crucible slag are given in the first two tables. The final three tables show the ratios of elements to Al_2O_3, for ceramic, slag and the change between them respectively.

Average ceramic composition. All results in wt%, normalised to 100%.

Sample	Na_2O	MgO	Al_2O_3	SiO_2	P_2O_5	K_2O	CaO	TiO_2	MnO	FeO	CuO	As_2O_3	SnO_2	PbO
Gordion 21299 - 15.10.2013	**3.2**	**3.5**	**18**	**50**	**0.6**	**1.8**	**10.7**	**1.7**	**0**	**10.7**	**0.1**	**0.2**	**0.1**	**0**
Std. dev. (5 ms)	0.1	0.1	0	1	0.1	0.2	0.3	0.1	0.1	0.3	0.1	0.3	0.2	0.3
Min.	3.1	3.4	17	48	0.4	1.6	10.3	1.6	0	10.4	0	0	0	0
Max.	3.4	3.6	18	50	0.7	2.1	11.1	1.9	0.1	11.1	0.2	0.7	0.4	0.4
Gordion 22529 - 13.9.2013	**2.8**	**3.6**	**17**	**50**	**0.6**	**2.1**	**9.2**	**1.5**	**0.2**	**12.4**	**0**	**0.1**	**0.4**	**0.2**
Std. dev. (5 ms)	0.2	0.3	1	4	0.2	0.3	1.3	0.3	0.2	6.3	0.2	0.3	0.2	0.1
Min.	2.6	3.1	16	43	0.3	1.6	7.2	1.2	0	8.9	0	0	0.1	0.1
Max.	3.2	3.9	18	52	0.9	2.4	10.7	2.0	0.4	23.6	0.2	0.7	0.6	0.3
Gordion 22626 - 15.10.2013	**3.4**	**3.5**	**18**	**52**	**0.4**	**1.8**	**9.1**	**2.0**	**0.2**	**9.0**	**0**	**0.1**	**0.3**	
Std. dev. (5 ms)	0.5	0.5	1	0	0.1	0.3	0.6	0.6	0.1	1.2	0.1	0.2	0.4	
Min.	2.7	2.7	17	51	0.2	1.5	8.3	1.2	0.1	7.4	0	0	0	
Max.	3.9	3.9	20	52	0.6	2.2	9.8	2.6	0.3	10.4	0.2	0.4	0.8	
Gordion 22673 - 15.1.2014	**3.3**	**3.3**	**19**	**52**	**0.6**	**1.6**	**9.2**	**1.7**	**0.1**	**8.6**	**0.1**	**0.2**	**0.4**	**0.2**
Std. dev. (5 ms)	0.2	0.4	1	1	0.1	0.1	0.6	0.4	0.1	0.7	0.2	0.2	0.3	0.2
Min.	3.1	2.8	18	51	0.4	1.4	8.2	1.2	0	7.9	0	0	0.1	0
Max.	3.7	3.9	20	53	0.7	1.8	10.0	2.1	0.3	9.5	0.5	0.4	0.8	0.4
Gordion 22673-A - 15.10.2013	**3.0**	**3.4**	**19**	**51**	**0.6**	**2.0**	**10.4**	**1.6**	**0.3**	**8.6**	**0.1**	**0.1**	**0.4**	
Std. dev. (5 ms)	0.4	0.5	1	1	0.3	0.3	0.8	0.5	0.1	1.4	0.1	0.3	0.5	
Min.	2.6	2.8	18	50	0.2	1.7	9.3	0.8	0.1	6.8	0	0	0	
Max.	3.5	3.9	21	52	1.0	2.4	11.1	2.1	0.4	10.5	0.1	0.5	1.0	
Gordion 22673-B - 15.10.2013	**3.2**	**3.3**	**18**	**52**	**0.6**	**1.8**	**8.6**	**1.8**	**0.1**	**9.1**	**0**	**0.1**	**0.4**	**0.2**
Std. dev. (5 ms)	0.3	0.4	1	2	0.2	0.2	0.6	0.4	0.2	1.0	0.1	0.1	0.3	0.3
Min.	3.0	2.9	17	50	0.3	1.6	7.8	1.5	0	8.0	0	0	0	0
Max.	3.7	3.8	19	56	0.8	2.1	9.5	2.3	0.4	10.3	0	0.2	0.8	0.6
Gordion 22829 - 15.10.2013	**2.8**	**3.6**	**18**	**52**	**0.5**	**2.0**	**9.8**	**1.5**	**0.2**	**8.8**	**0**	**0.2**	**0.6**	
Std. dev. (5 ms)	0.3	0.2	1	2	0.1	0.2	0.5	0.2	0.2	0.7	0.1	0.4	0.4	
Min.	2.5	3.3	17	50	0.4	1.7	9.2	1.3	0	8.0	0	0	0.1	
Max.	3.1	4.0	18	56	0.7	2.2	10.3	1.6	0.3	9.9	0.2	0.9	1.1	
Gordion 22958 - 9.04.2013	**2.8**	**4.1**	**18**	**49**	**0.5**	**1.5**	**13.5**	**1.5**	**0.2**	**8.2**	**0.1**	**0.3**	**0.3**	
Std. dev. (5 ms)	0.5	0.4	1	2	0.2	0.2	1.8	0.2	0.1	0.9	0.2	0.2	0.3	
Min.	2.3	3.6	17	46	0.2	1.3	12.2	1.4	0.1	7.2	0	0.1	0	
Max.	3.4	4.5	19	51	0.6	1.8	16.3	1.7	0.4	9.1	0.3	0.6	0.7	
Gordion 22999 - 13.9.2013	**3.1**	**3.5**	**18**	**51**	**0.5**	**1.8**	**10.1**	**2.0**	**0.2**	**8.8**	**0**	**0.3**	**0.3**	**0.2**
Std. dev. (5 ms)	0.3	0.2	1	1	0.2	0.1	0.6	0.5	0.1	1.5	0.3	0.4	0.4	0.2

Average ceramic composition. All results in wt%, normalised to 100%.

Sample	Na_2O	MgO	Al_2O_3	SiO_2	P_2O_5	K_2O	CaO	TiO_2	MnO	FeO	CuO	As_2O_3	SnO_2	PbO
Min.	2.7	3.3	17	50	0.3	1.6	9.1	1.5	0	7.6	0	0	0	0
Max.	3.6	3.8	19	53	0.9	2.0	10.7	2.8	0.3	11.2	0.2	0.7	0.7	0.3
Gordion 23045-A - 15.10.2013	**2.8**	**3.9**	**18**	**51**	**0.4**	**1.8**	**12.0**	**1.6**	**0.1**	**8.1**	**0**	**0**	**0.3**	
Std. dev. (5 ms)	0.2	0.3	0	0	0.1	0.4	0.8	0.2	0.1	0.5	0.1	0.2	0.4	
Min.	2.7	3.3	16	49	0.2	1.8	10.2	1.6	0	7.1	0	0	0	
Max.	3.6	4.8	18	51	0.7	2.6	12.5	2.3	0.4	9.3	0.2	0.5	0.8	
Gordion 23045-B - 15.10.2013	**3.0**	**3.7**	**17**	**50**	**0.6**	**1.8**	**11.6**	**1.6**	**0.2**	**9.4**	**0**	**0.3**	**0.3**	
Std. dev. (5 ms)	0.5	0.5	0	1	0.2	0.2	1.0	0.2	0.1	1.5	0.2	0.1	0.3	
Min.	2.7	2.8	17	49	0.4	1.5	10.5	1.5	0.1	7.9	0	0.1	0	
Max.	3.9	4.2	18	51	0.8	2.0	13.1	1.9	0.3	11.8	0.2	0.4	0.6	
Gordion 23045-S - 15.10.2013														
(0 ms)														
Gordion 23128 - 13.9.2013														
(0 ms)														
Gordion 23329 - 9.4.2013	**3.3**	**3.4**	**18**	**51**	**0.5**	**1.9**	**8.8**	**1.7**	**0.2**	**9.7**	**0.1**	**0.4**	**0.4**	**0.1**
Std. dev. (5 ms)	0.3	0.5	1	1	0.1	0.2	0.6	0.1	0.1	1.1	0.1	0.2	0.3	0.1
Min.	2.9	2.6	17	51	0.4	1.7	7.9	1.6	0.1	8.8	0	0.2	0.2	0
Max.	3.6	4.0	20	52	0.7	2.3	9.5	1.9	0.3	11.5	0.3	0.7	0.9	0.2
Gordion 23329 - 15.1.2014	**3.0**	**3.7**	**18**	**51**	**0.6**	**2.1**	**9.6**	**1.5**	**0.1**	**10.0**	**0.1**	**0**	**0.3**	**0.1**
Std. dev. (5 ms)	0.3	0.2	1	2	0.2	0.2	0.5	0.2	0.1	1.8	0.1	0.3	0.2	0.2
Min.	2.7	3.5	17	49	0.4	1.7	9.0	1.3	0	8.2	0	0	0	0
Max.	3.3	3.9	19	53	0.8	2.2	10.2	1.8	0.2	12.9	0.3	0.3	0.4	0.4
Gordion 23523 - 15.10.2013	**3.1**	**3.8**	**18**	**51**	**0.4**	**2.0**	**9.7**	**1.5**	**0.1**	**9.8**	**0**	**0.3**	**0.3**	
Std. dev. (5 ms)	0.2	0.2	1	1	0.2	0.3	0.8	0.2	0.1	0.7	0.1	0.2	0.4	
Min.	2.8	3.5	17	50	0.2	1.7	9.1	1.3	0	8.6	0	0.1	0	
Max.	3.4	4.2	19	52	0.6	2.4	11.0	1.6	0.2	10.4	0	0.5	1.0	
Gordion 23707 - 9.4.2013	***2.7***	***3.1***	***13***	***59***	***0.3***	***3.8***	***11.9***	***0.6***	***0.1***	***4.2***	***0.1***	***0.1***	***0.6***	
Std. dev. (5 ms)	0.4	0.6	1	3	0.3	0.4	2.3	0.1	0.1	0.9	0.2	0.3	0.2	
Min.	2.4	2.1	12	57	0	3.3	8.1	0.3	0	3.2	0	0	0.3	
Max.	3.2	3.8	14	65	0.7	4.4	14.1	0.7	0.3	5.5	0.3	0.4	0.8	
Gordion 23707 - 15.1.2014	***2.7***	***2.9***	***12***	***62***	***0.2***	***3.5***	***11.7***	***0.6***	***0.1***	***3.9***	***0***	***0.1***	***0.4***	
Std. dev. (5 ms)	0.3	0.6	1	2	0	0.7	1.7	0.3	0.1	0.3	0.2	0.3	0.2	
Min.	2.4	2.3	12	59	0.2	2.5	9.5	0.4	0	3.5	0	0	0.1	
Max.	3.2	3.7	14	64	0.3	4.2	13.8	1.0	0.3	4.3	0.2	0.5	0.6	
Gordion 23778 - 13.9.2013	**3.0**	**3.7**	**17**	**51**	**0.6**	**2.1**	**9.2**	**1.5**	**0.1**	**9.9**	**0.1**	**0.2**	**0.5**	**0.3**
Std. dev. (5 ms)	0.2	0.3	1	2	0.3	0.1	0.4	0.2	0.1	2.0	0.2	0.3	0.1	0.2
Min.	2.8	3.3	16	49	0.3	2.0	9.0	1.3	0	8.8	0	0	0.3	0.1
Max.	3.2	4.0	18	54	1.1	2.2	10.0	1.7	0.3	13.5	0.5	0.7	0.7	0.4
Gordion 23797 - 9.4.2013	**3.0**	**3.8**	**17**	**51**	**0.8**	**1.9**	**10.7**	**1.3**	**0**	**9.8**	**0.1**	**0.3**	**0.3**	**0.2**
Std. dev. (5 ms)	0.3	0.7	1	2	0.2	0.4	1.7	0.2	0.1	4.0	0.2	0.4	0.3	0.2
Min.	2.6	2.7	16	47	0.5	1.5	8.4	1.0	0	7.2	0	0	0	0
Max.	3.4	4.6	19	52	1.0	2.6	13.0	1.7	0.2	16.8	0.3	0.9	0.6	0.4
Gordion 25368 - 13.9.2013	**2.6**	**4.0**	**18**	**49**	**0.4**	**2.1**	**10.8**	**1.3**	**0.2**	**10.8**	**0.1**	**0.2**	**0.4**	**0.1**
Std. dev. (5 ms)	0.4	0.1	1	2	0.1	0.2	0.6	0.3	0.1	3.4	0.1	0.1	0.1	0.1
Min.	2.2	3.9	16	46	0.4	1.9	9.8	0.9	0	9.0	0	0.2	0.2	0
Max.	3.0	4.1	18	50	0.6	2.3	11.3	1.6	0.4	16.8	0.2	0.3	0.5	0.3
Gordion 25394 - 9.4.2013	**2.8**	**4.1**	**18**	**49**	**0.4**	**2.2**	**11.6**	**1.6**	**0**	**8.6**	**0.1**	**0.1**	**0.5**	**0.2**
Std. dev. (5 ms)	0.4	0.5	1	1	0.2	0.2	0.6	0.1	0.1	1.3	0.1	0.3	0.2	0.1
Min.	2.3	3.3	17	49	0.3	2.0	11.0	1.5	0	6.7	0	0	0.2	0.1
Max.	3.2	4.5	20	50	0.7	2.6	12.4	1.7	0.2	10.3	0.3	0.5	0.8	0.3
Gordion 25394_A - 13.9.2013	**2.4**	**4.6**	**17**	**50**	**0.6**	**2.1**	**10.9**	**1.4**	**0.1**	**9.3**	**0**	**0.2**	**0.6**	
Std. dev. (5 ms)	0.2	0.3	0	1	0.3	0.3	0.8	0.4	0.1	0.6	0.3	0.3	0.2	
Min.	2.0	4.3	17	50	0.3	1.7	10.1	1.0	0	8.7	0	0	0.3	
Max.	2.7	4.9	18	51	1.0	2.5	12.2	2.0	0.2	10.1	0.5	0.7	0.8	
Gordion 25394_B - 13.9.2013	**2.8**	**4.0**	**18**	**50**	**0.6**	**2.0**	**10.8**	**1.5**	**0.1**	**9.2**	**0**	**0.4**	**0.4**	
Std. dev. (5 ms)	0.3	0.3	1	1	0.3	0.3	0.7	0.2	0.1	1.0	0.1	0.3	0.2	
Min.	2.3	3.6	17	49	0.1	1.6	10.0	1.3	0	8.1	0	0	0.1	
Max.	3.1	4.4	19	51	0.9	2.6	11.7	1.8	0.2	10.4	0.1	0.7	0.6	
Gordion 25568 - 9.4.2013	**3.4**	**3.8**	**19**	**51**	**0.3**	**1.4**	**10.5**	**1.5**	**0.1**	**8.6**	**0**	**0.2**	**0.4**	**0.3**
Std. dev. (5 ms)	0.6	0.4	1	1	0.2	0.2	0.5	0.1	0.1	0.9	0.1	0.3	0.2	0.1
Min.	2.7	3.1	18	50	0	1.1	9.8	1.4	0.1	7.1	0	0	0.2	0.1
Max.	4.1	4.2	21	51	0.6	1.7	11.3	1.6	0.2	9.3	0.2	0.6	0.7	0.4
Gordion 25568 - 15.1.2014	**2.8**	**4.2**	**18**	**51**	**0.4**	**1.4**	**11.4**	**1.5**	**0.1**	**8.7**	**0.1**	**0.4**	**0.1**	
Std. dev. (5 ms)	0.3	0.5	0	1	0.2	0.2	0.5	0.3	0	0.5	0.3	0.3	0.3	
Min.	2.6	3.7	17	50	0.2	1.2	11.0	1.2	0.1	8.0	0	0	0	
Max.	3.2	4.9	18	52	0.6	1.6	11.9	1.9	0.2	9.2	0.6	0.8	0.4	
Gordion 25569-A - 15.10.2013	**2.8**	**4.2**	**18**	**50**	**0.4**	**1.4**	**11.9**	**1.6**	**0.1**	**9.4**	**0.1**	**0.3**	**0.3**	**0.1**
Std. dev. (5 ms)	0.4	0.4	1	1	0.1	0.1	0.7	0.3	0.1	1.2	0.1	0.1	0.4	0.1
Min.	2.2	3.8	17	48	0.2	1.2	11.2	1.3	0	7.5	0	0.2	0	0

Average ceramic composition. All results in wt%, normalised to 100%.

Sample	Na_2O	MgO	Al_2O_3	SiO_2	P_2O_5	K_2O	CaO	TiO_2	MnO	FeO	CuO	As_2O_3	SnO_2	PbO
Max.	3.2	4.7	19	51	0.6	1.5	12.8	1.9	0.2	10.7	0.2	0.5	0.9	0.2
Gordion 25569-B - 15.10.2013	**2.7**	**4.2**	**18**	**50**	**0.4**	**1.8**	**11.3**	**1.7**	**0.1**	**9.1**	**0**	**0.1**	**0.2**	
Std. dev. (5 ms)	0.4	0.3	1	1	0.1	0.1	0.7	0.2	0.1	0.4	0.1	0.2	0.3	
Min.	2.3	3.9	17	50	0.2	1.6	10.2	1.3	0	8.4	0	0	0	
Max.	3.3	4.7	19	51	0.6	2.0	12.1	1.9	0.2	9.4	0.1	0.4	0.5	
Gordion 26891 - 9.4.2013	**3.2**	**3.5**	**18**	**52**	**0.5**	**1.7**	**8.8**	**1.8**	**0.1**	**9.8**	**0.2**	**0.1**	**0.4**	**0.2**
Std. dev. (5 ms)	0.3	0.3	1	1	0.2	0.2	0.4	0.3	0.1	0.6	0.2	0.2	0.4	0.2
Min.	2.8	3.3	17	51	0.2	1.5	8.3	1.5	0	9.3	0	0	0	0
Max.	3.7	4.0	19	54	0.7	2.0	9.4	2.2	0.3	10.5	0.4	0.3	1.1	0.5
Gordion 27609 - 15.10.2013	**2.8**	**3.8**	**18**	**51**	**0.6**	**1.9**	**11.6**	**1.4**	**0.1**	**8.3**	**0.1**	**0.2**	**0.2**	
Std. dev. (5 ms)	0.3	0.3	0	1	0.2	0.1	0.6	0.2	0.1	0.4	0.1	0.3	0.2	
Min.	2.6	3.3	18	50	0.3	1.8	11.1	1.2	0	7.9	0	0	0	
Max.	3.2	4.1	19	51	0.9	2.1	12.7	1.6	0.1	9.0	0.3	0.6	0.4	
Gordion 27609-S - 15.10.2013														
(0 ms)														
Gordion 27613_A 13.9.2013	**3.1**	**3.6**	**18**	**51**	**0.6**	**1.9**	**11.0**	**1.5**	**0.1**	**8.7**	**0**	**0.4**	**0.3**	
Std. dev. (5 ms)	0.6	0.2	1	1	0.2	0.1	1.3	0.4	0.2	0.8	0.2	0.3	0.3	
Min.	2.5	3.4	17	50	0.4	1.8	9.4	1.2	0	7.8	0	0	0	
Max.	4.0	3.8	19	52	0.9	2.0	12.9	2.1	0.2	9.7	0.2	0.8	0.7	
Gordion 27613_B - 13.9.2013	**3.3**	**3.6**	**18**	**51**	**0.5**	**1.8**	**9.9**	**1.6**	**0**	**8.3**	**0**	**0.4**	**0.4**	**0.2**
Std. dev. (5 ms)	0.2	0.4	0	1	0.1	0.3	0.7	0.2	0.1	0.9	0.2	0.3	0.4	0.1
Min.	3.1	3.3	18	51	0.4	1.6	8.8	1.4	0	7.3	0	0	0	0.1
Max.	3.5	4.2	19	53	0.7	2.4	10.7	1.9	0.1	9.5	0.2	0.7	1	0.3
Gordion 27629 - 15.10.2013	**3.4**	**3.5**	**18**	**50**	**1.0**	**1.9**	**10.8**	**1.6**	**0.1**	**9.3**	**0**	**0.2**	**0.3**	
Std. dev. (5 ms)	0.4	0.5	1	1	0.6	0.2	0.8	0.2	0.2	0.4	0.1	0.4	0.2	
Min.	2.8	2.9	17	49	0.5	1.6	9.9	1.3	0	8.8	0	0	0.1	
Max.	3.8	4.0	19	51	1.9	2.1	12.0	1.9	0.4	9.8	0	0.9	0.4	
Gordion 27634 - 12.11.2013	**2.5**	**4.9**	**17**	**51**	**0.5**	**2.4**	**11.9**	**1.5**	**0.1**	**7.7**	**0**	**0.2**	**0.6**	
Std. dev. (5 ms)	0.4	1.1	1	1	0.2	0.5	1.2	0.1	0.2	0.5	0.3	0.1	0.1	
Min.	1.8	4.1	16	49	0.4	1.9	10.6	1.4	0	7.1	0	0	0.4	
Max.	3.0	6.7	19	52	0.8	3.2	13.7	1.6	0.3	8.2	0.1	0.4	0.7	
Gordion 27635 (1) - 12.11.2013	**3.4**	**3.8**	**18**	**51**	**0.5**	**2.1**	**10.3**	**1.8**	**0.1**	**9.0**	**0.2**	**0.2**	**0.1**	
Std. dev. (5 ms)	0.3	0.4	0	1	0.3	0.2	0.3	0.4	0.2	0.5	0.2	0.3	0.4	
Min.	3.0	3.5	18	49	0.2	1.9	9.9	1.3	0	8.3	0	0	0	
Max.	3.7	4.2	19	52	0.8	2.3	10.8	2.5	0.3	9.6	0.3	0.5	0.6	
Gordion 27635 (2) - 12.11.2013	**3.3**	**3.4**	**19**	**50**	**0.7**	**1.5**	**10.1**	**1.4**	**0.2**	**9.6**	**0.4**	**0.2**	**0.3**	**0**
Std. dev. (5 ms)	0.5	0.5	1	1	0.3	0.2	0.7	0.3	0.1	1.3	0.7	0.2	0.3	0.1
Min.	2.7	2.8	17	49	0.4	1.3	9.2	1.0	0.1	8.2	0	0	0	0
Max.	3.9	4.1	19	52	1.2	1.8	11.0	1.8	0.3	11.1	1.6	0.5	0.6	0
Gordion 27636 - 9.4.2013	**3.1**	**3.7**	**18**	**51**	**0.6**	**2.0**	**9.7**	**1.6**	**0.1**	**9.1**	**0.1**	**0.2**	**0.4**	
Std. dev. (5 ms)	0.3	0.4	1	1	0.2	0.2	0.2	0.2	0.1	0.6	0.2	0.3	0.4	
Min.	2.7	3.0	18	51	0.2	1.8	9.5	1.4	0	8.3	0	0	0	
Max.	3.5	4.2	20	52	0.9	2.3	10.1	2.0	0.2	9.7	0.3	0.5	0.9	
Gordion 27638 - 12.11.2013	**3.3**	**3.7**	**18**	**51**	**0.6**	**2.3**	**9.9**	**1.7**	**0.1**	**8.7**	**0.1**	**0.2**	**0.2**	
Std. dev. (5 ms)	0.2	0.3	0	0	0.1	0.1	0.8	0.3	0.1	0.5	0.1	0	0.3	
Min.	3.0	3.4	18	50	0.4	2.2	9.2	1.5	0.1	7.9	0	0.2	0	
Max.	3.5	4.3	19	51	0.7	2.4	10.9	2.1	0.2	9.2	0.2	0.3	0.5	
Gordion 27640 - 12.11.2013	**2.9**	**3.7**	**18**	**50**	**0.5**	**2.1**	**10.1**	**1.7**	**0.2**	**10.2**	**0.2**	**0.2**	**0.6**	**0.2**
Std. dev. (5 ms)	0.3	0.4	0	0	0.1	0.2	0.7	0.2	0.1	0.7	0.1	0.4	0.1	0.3
Min.	2.4	3.1	17	49	0.5	1.9	9.0	1.5	0.1	9.3	0	0	0.5	0
Max.	3.2	4.0	18	50	0.7	2.3	11.0	2.1	0.3	10.9	0.4	0.6	0.7	0.5
Gordion 27734 (1) - 12.11.2013	**3.2**	**3.7**	**18**	**52**	**0.4**	**1.9**	**9.2**	**2.1**	**0.1**	**9.8**	**0**	**0.2**	**0.2**	
Std. dev. (5 ms)	0.2	0.5	1	2	0.2	0.3	0.5	1.2	0.1	1.3	0.2	0.1	0.3	
Min.	3.0	2.9	17	49	0.3	1.7	8.7	1.3	0	8.4	0	0.1	0	
Max.	3.4	4.2	19	54	0.6	2.3	10.0	4.1	0.2	11.0	0.2	0.3	0.6	
Gordion 28218 - 12.11.2013	**3.0**	**3.5**	**18**	**52**	**0.4**	**1.8**	**9.2**	**1.6**	**0.1**	**9.6**	**0.1**	**0.3**	**0.3**	
Std. dev. (5 ms)	0.4	0.4	1	2	0.1	0.1	0.7	0.2	0.1	1.4	0.1	0.1	0.1	
Min.	2.6	3.1	18	50	0.2	1.6	8.5	1.4	0	8.1	0	0.2	0.1	
Max.	3.5	4.0	19	54	0.6	1.9	10.4	1.8	0.2	11.3	0.2	0.4	0.5	
Gordion 28236 - 9.4.2013	***3.6***	***2.8***	***13***	***49***	***0.3***	***3.8***	***19.8***	***1.0***	***0***	***5.7***	***0***	***0.2***	***0.4***	
Std. dev. (5 ms)	0.7	0.3	1	2	0.2	0.2	3.4	0.1	0.1	1.3	0.3	0.2	0.2	
Min.	2.5	2.5	11	46	0	3.6	15.6	0.8	0	4.1	0	0	0.2	
Max.	4.2	3.1	14	51	0.5	4.1	25.0	1.1	0.2	7.3	0.2	0.5	0.7	
Gordion 28877 - 9.4.2013	**3.7**	**3.3**	**19**	**52**	**0.6**	**1.7**	**9.1**	**1.6**	**0**	**8.8**	**0.1**	**0.2**	**0.3**	
Std. dev. (5 ms)	0.2	0.6	1	0	0.1	0.2	0.3	0.3	0.1	1.0	0.2	0.2	0.3	
Min.	3.4	2.8	18	51	0.4	1.5	8.7	1.1	0	8.0	0	0	0	
Max.	4.0	4.1	20	52	0.7	2.0	9.5	1.9	0.2	10.0	0.5	0.5	0.8	
Gordion 28932 (1) - 12.11.2013	**3.2**	**3.8**	**18**	**50**	**0.7**	**2.5**	**10.9**	**1.4**	**0.1**	**9.2**	**0**	**0.2**	**0.4**	
Std. dev. (5 ms)	0.4	0.7	1	1	0.2	0.4	2.1	0.1	0.1	1.1	0.1	0.4	0.2	

Average ceramic composition. All results in wt%, normalised to 100%.

Sample	Na_2O	MgO	Al_2O_3	SiO_2	P_2O_5	K_2O	CaO	TiO_2	MnO	FeO	CuO	As_2O_3	SnO_2	PbO
Min.	2.6	2.8	17	49	0.5	2.1	7.5	1.2	0	8.3	0	0	0.1	
Max.	3.7	4.4	18	51	1.0	3.0	12.6	1.6	0.2	11.1	0.2	0.9	0.7	
Gordion 28932 (2) - 12.11.2013	**3.1**	**4.3**	**17**	**49**	**0.6**	**2.6**	**11.2**	**1.6**	**0.1**	**8.9**	**0.1**	**0.1**	**0.6**	
Std. dev. (5 ms)	0.3	0.5	1	0	0.1	0.3	0.8	0.3	0.1	0.7	0.1	0.2	0.1	
Min.	2.8	3.8	16	49	0.4	2.3	9.9	1.4	0	8.0	0.1	0	0.5	
Max.	3.6	5.0	19	50	0.8	2.9	12.2	2.1	0.2	9.8	0.2	0.4	0.7	
Average Ceramic Composition	***3.0***	***3.8***	***18***	***51***	***0.5***	***1.9***	***10.4***	***1.6***	***0.1***	***9.2***	***0.1***	***0.2***	***0.4***	

Average slag composition. All results in wt%, normalised to 100%.

Sample	Na_2O	MgO	Al_2O_3	SiO_2	P_2O_5	K_2O	CaO	TiO_2	MnO	FeO	CuO	As_2O_3	SnO_2	PbO
Gordion 21299 - 15.10.2013	**3.2**	**3.6**	**16**	**45**	**0.4**	**2.6**	**12.2**	**1.4**	**0**	**8.3**	**5.3**	**0.2**	**0.9**	**0.7**
Std. dev. (5 ms)	0.8	0.8	2	4	0.2	0.3	2.3	0.1	0.1	0.7	5.8	0.3	0.4	0.6
Min.	2.4	2.6	14	40	0.2	2.3	9.9	1.3	0	7.1	0.1	0	0.5	0.3
Max.	4.3	4.6	20	49	0.7	3.1	15.5	1.6	0.2	8.8	13.0	0.7	1.4	1.7
Gordion 22529 - 13.9.2013	**1.9**	**2.6**	**12**	**34**	**0.5**	**2.1**	**10.5**	**1.0**	**0.1**	**7.3**	**13.0**	**0.3**	**9.9**	**5.0**
Std. dev. (5 ms)	0.4	0.4	3	7	0.1	0.5	1.1	0.3	0.1	1.0	5.0	0.2	5.6	1.7
Min.	1.5	2.3	9	24	0.4	1.7	8.9	0.6	0	5.6	5.2	0	1.7	2.8
Max.	2.5	3.1	16	44	0.5	2.9	11.5	1.4	0.2	8.4	18.0	0.5	17.2	7.4
Gordion 22626 - 15.10.2013	**3.0**	**3.5**	**16**	**49**	**0.6**	**2.0**	**12.0**	**1.7**	**0.1**	**10.2**	**1.0**	**0.1**	**0.8**	
Std. dev. (5 ms)	0.3	0.4	1	5	0.5	0.1	2.6	0.3	0.1	1.1	1.5	0.2	0.6	
Min.	2.5	3.1	14	41	0.3	1.9	9.9	1.4	0	8.8	0.1	0	0.2	
Max.	3.3	4.1	18	55	1.4	2.2	16.4	2.0	0.2	11.7	3.6	0.5	1.8	
Gordion 22673 - 15.1.2014	**3.4**	**2.4**	**18**	**44**	**0.3**	**1.4**	**8.3**	**1.6**	**0**	**8.0**	**6.8**	**0.3**	**1.4**	**3.8**
Std. dev. (5 ms)	0.4	0.4	2	4	0.1	0.4	0.8	0.2	0.1	0.8	3.1	0.2	2.2	3.4
Min.	2.8	2.0	15	38	0.2	1.0	7.1	1.2	0	7.1	3.6	0	0.2	1.3
Max.	3.9	2.8	20	48	0.5	2.1	9.0	1.7	0.2	9.3	11.0	0.6	5.2	9.8
Second layer	**1.1**	**1.7**	**7**	**19**	**0.3**	**0.6**	**5.3**	**0.6**	**0**	**8.6**	**21.0**	**0.2**	**29.8**	**5.3**
Std. dev. (5 ms)	0.4	0.2	2	3	0.2	0.1	3.6	0	0.2	2.8	3.5	0.2	6.2	2.3
Min.	0.8	1.5	5	16	0	0.4	2.7	0.6	0	6.2	15.3	0	22.9	3.8
Max.	1.8	1.9	10	24	0.5	0.8	11.5	0.7	0.1	13.0	23.9	0.4	35.7	9.3
Gordion 22673-A - 15.10.2013	**3.1**	**3.5**	**17**	**47**	**0.5**	**3.4**	**11.5**	**1.8**	**0.1**	**9.3**	**1.1**	**0.1**	**0.9**	
Std. dev. (5 ms)	0.4	0.2	1	3	0.1	1.7	1.5	0.2	0.1	1.0	1.3	0.1	0.5	
Min.	2.7	3.3	16	45	0.4	2.1	10.2	1.7	0	8.1	0.1	0	0.3	
Max.	3.8	3.7	19	50	0.6	5.5	13.2	2.0	0.3	10.4	2.8	0.3	1.4	
Gordion 22673-B - 15.10.2013	**3.1**	**3.8**	**15**	**44**	**0.7**	**2.4**	**12.3**	**1.3**	**0.1**	**7.5**	**5.6**	**0.1**	**2.3**	**2.3**
Std. dev. (5 ms)	0.8	1.2	4	6	0.4	0.6	2.9	0.6	0.1	1.5	6.3	0.2	2.2	1.6
Min.	1.6	2.7	8	36	0.4	1.8	8.9	0.5	0.1	5.9	0	0	0.4	0.1
Max.	3.6	5.8	18	51	1.3	2.9	16.1	1.9	0.2	9.6	14.5	0.5	5.8	4.5
Gordion 22829 - 15.10.2013	**3.2**	**3.4**	**17**	**46**	**0.5**	**3.7**	**15.6**	**1.6**	**0.1**	**8.0**	**0.2**	**0.3**	**0.8**	
Std. dev. (5 ms)	0.6	0.5	1	3	0.2	0.8	3.2	0.2	0.1	0.8	0.2	0.1	0.5	
Min.	2.3	2.8	14	43	0.4	2.9	11.2	1.4	0	7.3	0	0.2	0.4	
Max.	3.9	4.1	19	50	0.9	4.8	20.0	1.8	0.3	9.2	0.6	0.5	1.5	
Gordion 22958 - 9.4.2013	**2.4**	**4.4**	**16**	**45**	**0.3**	**1.4**	**12.9**	**1.7**	**0.1**	**10.7**	**2.5**	**0.1**	**2.1**	
Std. dev. (5 ms)	0.3	0.5	1	4	0.2	0.1	0.8	0.3	0.1	1.0	4.1	0.2	2.3	
Min.	2.0	3.7	14	38	0.1	1.3	11.6	1.2	0	9.5	0.5	0	0.7	
Max.	2.9	5.0	17	48	0.6	1.5	13.7	2.0	0.3	12.0	9.8	0.3	6.2	
Gordion 22999 - 13.9.2013	**2.6**	**2.5**	**14**	**37**	**0.3**	**1.7**	**7.8**	**1.3**	**0**	**7.3**	**9.6**	**0.2**	**13**	**2.5**
Std. dev. (5 ms)	0.2	0.4	1	4	0.2	0.3	1.4	0.3	0.1	1.1	6.3	0.3	10.6	0.4
Min.	2.3	2.1	12	32	0.1	1.3	6.2	1.0	0	5.8	1.0	0	4.5	1.9
Max.	2.9	3.0	15	42	0.5	2.2	9.7	1.8	0.2	8.5	17.5	0.6	31.0	3.0
Gordion 23045-A - 15.10.2013	**3.1**	**4.3**	**17**	**50**	**0.4**	**2.1**	**11.6**	**2.0**	**0.2**	**8.4**	**0.1**	**0.1**	**0.4**	
Std. dev. (5 ms)	0.4	0.6	1	1	0.2	0.3	0.9	0.2	0.1	0.9	0.1	0.3	0.5	
Min.	2.7	3.3	16	49	0.2	1.8	10.2	1.6	0	7.1	0	0	0	
Max.	3.6	4.8	18	51	0.7	2.6	12.5	2.3	0.4	9.3	0.2	0.5	0.8	
Gordion 23045-B - 15.10.2013	**2.6**	**4.9**	**16**	**47**	**0.3**	**1.8**	**14.4**	**1.7**	**0.1**	**8.7**	**0.9**	**0.2**	**1.2**	
Std. dev. (5 ms)	0.3	0.6	1	2	0.2	0.2	2.5	0.2	0.1	0.9	0.7	0.1	0.4	
Min.	2.2	4.3	14	43	0.1	1.6	12.9	1.5	0	7.5	0.2	0	0.7	
Max.	3.0	5.8	18	49	0.6	2.1	18.7	2.0	0.2	9.6	2.1	0.4	1.7	
Gordion 23045-S - 15.10.2013	**2.4**	**3.3**	**13**	**36**	**0.4**	**1.9**	**8.3**	**1.2**	**0.1**	**9.8**	**8.9**	**0.1**	**11.1**	**4.2**
Std. dev. (5 ms)	0.6	0.2	3	8	0.1	0.4	1.7	0.2	0.1	2.2	6.0	0.3	7.2	3.5
Min.	1.8	3.1	9	26	0.3	1.3	6.3	0.9	0	7.8	2.8	0	1.0	0.8
Max.	3.1	3.6	17	48	0.5	2.4	10.9	1.5	0.2	13.5	15.8	0.7	18.8	9.6
Gordion 23128 - 13.9.2013	**2.3**	**4.5**	**15**	**43**	**0.2**	**1.3**	**10.4**	**1.5**	**0.2**	**7.4**	**8.5**	**0.1**	**3.7**	**1.6**
Std. dev. (5 ms)	0.5	1.1	2	9	0.1	0.3	3	0.3	0.1	2.0	12.0	0.2	4.6	2.3
Min.	1.8	2.8	11	29	0.1	0.7	5.7	1.0	0.1	4.2	0.3	0	0.1	0
Max.	3.0	5.8	18	50	0.4	1.5	13.1	1.8	0.2	9.4	29.2	0.4	9.0	5.4
Gordion 23329 - 9.4.2013	**2.6**	**2.7**	**16**	**43**	**0.5**	**1.7**	**7.4**	**1.4**	**0.1**	**7.3**	**14.9**	**0.3**	**0.6**	**1.3**
Std. dev. (5 ms)	0.1	0.5	0	1	0.3	0.2	0.4	0.2	0.1	1.5	3.9	0.2	0.2	0.3
Min.	2.4	2.2	16	42	0.2	1.4	7.0	1.2	0.1	5.8	9.8	0.1	0.3	1.1
Max.	2.8	3.4	17	45	0.9	1.9	8.1	1.6	0.3	9.5	18.2	0.5	0.8	1.8
Second layer	**1.6**	**2.0**	**10**	**26**	**0.4**	**1.1**	**6.0**	**0.7**	**0**	**7.9**	**14.5**	**0.2**	**25.8**	**3.9**
Std. dev. (5 ms)	0.3	0.4	1	3	0.2	0.2	1.1	0.2	0.1	2.6	4.5	0.2	3.2	0.9
Min.	1.3	1.6	8	22	0.2	0.9	5.0	0.5	0	4.9	10.2	0	21.4	2.9
Max.	2.0	2.5	12	29	0.7	1.4	7.7	0.9	0.1	11.6	21.3	0.4	28.9	4.9
Gordion 23329 - 15.1.2014	**3.2**	**3.6**	**17**	**46**	**0.5**	**2.1**	**10.4**	**1.7**	**0.2**	**9.1**	**3.7**	**0.3**	**2.1**	**0.8**
Std. dev. (5 ms)	0.5	0.8	2	4	0.2	0.2	1.4	0.4	0.2	1.8	3.7	0.2	3.2	0.6
Min.	2.6	2.9	14	39	0.4	1.9	9.2	1.3	0	7.2	0	0.1	0.4	0.1
Max.	3.9	5.0	19	50	0.8	2.3	12.8	2.3	0.5	11.8	9.8	0.7	7.8	1.6
Gordion 23523 - 15.10.2013	**3.3**	**3.4**	**18**	**50**	**0.7**	**1.9**	**11.0**	**1.9**	**0.1**	**9.2**	**0.5**	**0.2**	**0.6**	

Average slag composition. All results in wt%, normalised to 100%.

Sample	Na_2O	MgO	Al_2O_3	SiO_2	P_2O_5	K_2O	CaO	TiO_2	MnO	FeO	CuO	As_2O_3	SnO_2	PbO
Std. dev. (5 ms)	0.4	0.7	1	1	0.3	0.2	1.2	0.1	0.1	0.5	0.6	0.2	0.4	
Min.	2.9	2.5	16	49	0.4	1.6	9.6	1.8	0	8.6	0	0.1	0.2	
Max.	3.8	4.4	19	51	1.1	2.1	12.8	2.0	0.2	9.9	1.3	0.4	1.1	
Gordion 23707 - 9.4.2013	***1.9***	***2.2***	***11***	***47***	***0.2***	***3.2***	***8.1***	***0.4***	***0***	***3.2***	***17.3***	***0.3***	***4.4***	
Std. dev. (5 ms)	0.3	0.5	1	8	0.1	0.8	1.5	0.1	0.1	0.4	7.4	0.1	5.1	
Min.	1.6	1.6	10	37	0.1	2.2	6.2	0.2	0	2.7	9.3	0.1	0.4	
Max.	2.2	2.8	13	57	0.3	3.9	10.3	0.5	0.2	3.7	28.8	0.5	11.0	
Gordion 23707 - 15.1.2014	***1.5***	***2.5***	***9***	***40***	***0.4***	***2.8***	***9.3***	***0.3***	***0***	***4.7***	***24.0***	***0.3***	***5.7***	
Std. dev. (5 ms)	0.4	0.4	2	7	0.1	0.5	2.5	0.2	0.1	2.2	11.3	0.3	4.1	
Min.	0.9	2.1	7	33	0.2	2.2	6.8	0.1	0	2.8	8.8	0	2.9	
Max.	1.9	3.0	11	50	0.5	3.5	12.7	0.5	0.1	8.3	35.5	0.5	12.7	
Gordion 23778 - 13.9.2013	**3.5**	**3.4**	**18**	**49**	**0.5**	**2.1**	**10.2**	**1.6**	**0**	**9.2**	**0.6**	**0.1**	**0.9**	**1.2**
Std. dev. (5 ms)	0.5	0.2	2	2	0.2	0.3	0.4	0.3	0.1	1.5	0.5	0.2	0.3	0.9
Min.	3.1	3.2	16	47	0.3	1.6	9.7	1.2	0	7.3	0	0	0.5	0.2
Max.	4.1	3.8	20	51	0.8	2.3	10.7	1.9	0.2	10.8	1.2	0.3	1.2	2.5
Gordion 23797 - 9.4.2013	**2.0**	**2.8**	**11**	**31**	**0.5**	**2.3**	**8.7**	**1.1**	**0**	**6.5**	**12.2**	**0.1**	**18.7**	**2.4**
Std. dev. (5 ms)	0.8	0.4	3	8	0.1	0.9	2.1	0.4	0.1	1.6	9.4	0.3	12.6	0.5
Min.	1.0	2.3	7	19	0.4	1.4	5.6	0.7	0	4.1	1.9	0	2.6	1.7
Max.	3.1	3.3	15	41	0.6	3.4	11.5	1.7	0.2	8.7	26.9	0.6	30.9	2.9
Gordion 25368 - 13.9.2013	**1.8**	**3.4**	**11**	**32**	**0.6**	**1.9**	**9.2**	**1.0**	**0**	**8.1**	**10.7**	**0.2**	**17.7**	**2.5**
Std. dev. (5 ms)	0.4	0.3	2	4	0.2	0.1	0.7	0.1	0.1	1.5	4.0	0.1	4.7	0.6
Min.	1.3	3.1	9	28	0.4	1.7	8.3	0.9	0	7.0	6.2	0	12.6	2.0
Max.	2.2	3.7	14	38	0.9	2.0	9.7	1.1	0.1	10.8	15.4	0.4	25.0	3.4
Gordion 25394 - 9.4.2013	**1.8**	**3.4**	**11**	**31**	**0.5**	**1.8**	**9.4**	**0.9**	**0**	**8.7**	**8.5**	**0.2**	**19.0**	**4.4**
Std. dev. (5 ms)	0.4	0.3	2	4	0	0.3	0.7	0.3	0.1	0.7	2.7	0.2	4.2	1.0
Min.	1.3	3.2	9	27	0.4	1.4	8.9	0.7	0	7.5	6.8	0	14.1	3.0
Max.	2.1	3.8	13	35	0.5	2.0	10.7	1.2	0.2	9.5	13.2	0.5	23.5	5.6
Gordion 25394_A - 13.9.2013	**2.6**	**4.7**	**16**	**47**	**0.4**	**2.7**	**12.7**	**1.8**	**0.2**	**9.5**	**0.8**	**0.1**	**0.8**	
Std. dev. (5 ms)	0.3	0.5	1	2	0.1	0.5	2.0	0.2	0.1	1.5	1.3	0.2	0.5	
Min.	2.3	4.4	16	44	0.3	1.9	9.3	1.5	0.1	8.5	0	0	0.4	
Max.	2.9	5.6	18	50	0.6	3.3	14.2	2.1	0.2	12.1	3.0	0.3	1.7	
Gordion 25394_B - 13.9.2013	**2.6**	**3.9**	**17**	**45**	**0.4**	**2.7**	**11.6**	**1.5**	**0.2**	**10.2**	**2.1**	**0.3**	**2.6**	
Std. dev. (5 ms)	0.4	0.5	1	2	0.2	0.3	0.7	0.3	0.1	1.3	1.9	0.3	2.2	
Min.	2.2	3.5	15	44	0.2	2.3	10.9	1.1	0.1	8.2	0.1	0	0.4	
Max.	3.1	4.8	18	49	0.7	3.1	12.7	1.9	0.2	11.8	5.0	0.8	5.7	
Gordion 25568 - 9.4.2013	**1.7**	**3.6**	**12**	**33**	**0.8**	**3.1**	**16.4**	**1.0**	**0.2**	**6.4**	**12.9**	**0.1**	**7.9**	**1.4**
Std. dev. (5 ms)	0.4	0.5	2	5	0.4	0.5	3.3	0.2	0.1	1.8	6.8	0.2	2.5	1.2
Min.	1.2	3.2	9	28	0.5	2.8	12.3	0.8	0.1	5.0	4.1	0	3.6	0.4
Max.	2.3	4.4	14	40	1.5	4.0	21.5	1.4	0.4	9.4	19.6	0.3	9.7	3.2
Gordion 25568 - 15.1.2014	**2.8**	**3.8**	**16**	**43**	**0.3**	**1.7**	**11.0**	**1.4**	**0.2**	**9.6**	**6.6**	**0.3**	**3.6**	
Std. dev. (5 ms)	0.5	0.3	2	7	0.1	0.4	1.3	0.3	0.1	2.3	6.4	0.2	3.5	
Min.	1.9	3.4	12	32	0.2	1.2	9.1	1.2	0.1	8.3	0.3	0.1	0.3	
Max.	3.2	4.3	19	50	0.4	2.2	12.5	1.8	0.2	13.7	17.1	0.5	7.7	
Gordion 25569-A - 15.10.2013	**2.7**	**4.9**	**16**	**46**	**0.4**	**1.4**	**11.5**	**1.6**	**0.2**	**9.0**	**4.4**	**0.2**	**0.9**	**0.7**
Std. dev. (5 ms)	0.3	0.7	1	3	0.2	0.3	0.5	0.4	0.1	1.6	4.2	0.2	0.9	0.6
Min.	2.2	3.9	15	42	0.2	1.0	11.2	1.1	0	7.3	0.2	0	0	0.2
Max.	3.0	5.7	18	49	0.6	1.7	12.3	2.2	0.3	10.9	8.9	0.6	2.0	1.7
Gordion 25569-B - 15.10.2013	**2.8**	**4.4**	**18**	**49**	**0.4**	**2.2**	**11.9**	**1.9**	**0.1**	**8.8**	**0.3**	**0.2**	**0.4**	
Std. dev. (5 ms)	0.3	1.0	1	0	0.1	0.2	0.7	0.3	0.1	0.6	0.2	0.3	0.4	
Min.	2.4	3.1	17	49	0.3	1.9	10.8	1.4	0	8.1	0.1	0	0	
Max.	3.2	5.6	20	50	0.5	2.5	12.5	2.2	0.1	9.8	0.5	0.6	0.8	
Gordion 26891 - 9.4.2013	**3.4**	**2.5**	**17**	**46**	**0.4**	**1.7**	**9.0**	**1.6**	**0.1**	**8.8**	**4.0**	**0.1**	**4.1**	**1.5**
Std. dev. (5 ms)	0.5	0.4	2	6	0.1	0.3	1.2	0.3	0.1	0.9	4.1	0.3	5.1	1.6
Min.	2.6	1.9	14	37	0.2	1.3	7.1	1.2	0	7.9	0.1	0	0.2	0.2
Max.	4.0	2.9	19	51	0.6	2.0	10.3	2.0	0.2	9.9	9.9	0.5	12.5	3.7
Gordion 27609 - 15.10.2013	**2.3**	**4.4**	**15**	**47**	**0.6**	**4.3**	**15.6**	**1.5**	**0.1**	**7.8**	**0.2**	**0.1**	**0.5**	
Std. dev. (5 ms)	0.2	0.7	1	1	0.1	0.7	1.9	0.2	0.1	0.6	0.1	0.4	0.2	
Min.	2.0	3.7	14	46	0.4	3.3	14.1	1.2	0	7.0	0.1	0	0.4	
Max.	2.6	5.5	16	49	0.7	5.1	18.4	1.8	0.2	8.5	0.4	0.6	0.9	
Gordion 27609-S - 15.10.2013	**2.0**	**4.1**	**13**	**40**	**1.0**	**2.8**	**14.0**	**1.2**	**0.2**	**8.9**	**5.4**	**0.2**	**6.7**	
Std. dev. (5 ms)	0.5	0.4	2	4	0.9	0.2	2.1	0.2	0.1	1.7	4.5	0.2	2.9	
Min.	1.4	3.6	11	35	0.4	2.5	11.6	1.0	0.1	7.4	2.9	0	3.0	
Max.	2.7	4.5	16	43	2.5	3.0	16.5	1.6	0.2	11.4	13.5	0.4	10.7	
Gordion 27613_A 13.9.2013	**3.1**	**3.8**	**17**	**49**	**0.5**	**2.2**	**11.6**	**2.0**	**0.1**	**9.9**	**0.1**	**0.3**	**0.3**	
Std. dev. (5 ms)	0.3	0.6	1	1	0.2	0.4	1.2	0.1	0.1	1.1	0.2	0.3	0.2	
Min.	2.9	3.3	16	48	0.3	1.7	10.3	1.9	0	8.2	0	0	0.2	
Max.	3.5	4.8	18	49	0.8	2.9	13.6	2.2	0.2	11.1	0.3	0.7	0.7	
Gordion 27613_B - 13.9.2013	**4.1**	**3.3**	**18**	**48**	**0.6**	**2.5**	**10.8**	**1.6**	**0.1**	**8.3**	**0.2**	**0.2**	**1.3**	**0.8**
Std. dev. (5 ms)	0.2	0.3	1	2	0.2	0.2	1.0	0.3	0	1.3	0.1	0.2	0.8	0.9

Average slag composition. All results in wt%, normalised to 100%.

Sample	Na_2O	MgO	Al_2O_3	SiO_2	P_2O_5	K_2O	CaO	TiO_2	MnO	FeO	CuO	As_2O_3	SnO_2	PbO
Min.	3.9	2.9	17	47	0.5	2.2	9.3	1.2	0.1	7.1	0.1	0	0.7	0.2
Max.	4.5	3.7	18	50	0.8	2.8	11.8	2.1	0.2	10.5	0.3	0.6	2.6	2.2
Gordion 27629 - 15.10.2013	**3.4**	**3.8**	**18**	**49**	**0.5**	**2.0**	**11.4**	**1.7**	**0.1**	**9.6**	**0**	**0.2**	**0.5**	
Std. dev. (5 ms)	0.5	1.0	1	1	0.3	0.2	0.9	0.3	0.1	0.8	0.2	0.2	0.3	
Min.	2.9	2.1	17	47	0.1	1.8	10.2	1.4	0	8.4	0	0	0.1	
Max.	4.2	4.9	20	50	1.0	2.1	12.7	2.0	0.2	10.5	0.2	0.5	0.8	
Gordion 27634 - 12.11.2013	**2.7**	**4.8**	**17**	**49**	**0.3**	**2.1**	**13.0**	**1.8**	**0.2**	**8.0**	**0**	**0.1**	**0.6**	
Std. dev. (5 ms)	0.2	0.4	0	1	0.1	0.4	0.7	0.1	0.1	0.3	0.1	0.2	0.4	
Min.	2.5	4.3	17	49	0.2	1.8	11.9	1.7	0.1	7.7	0	0	0.1	
Max.	2.9	5.4	18	50	0.4	2.6	13.8	1.9	0.3	8.5	0.2	0.3	1.2	
Gordion 27635 (1) - 12.11.2013	**3.1**	**3.8**	**17**	**49**	**0.5**	**2.5**	**10.7**	**2.0**	**0.1**	**9.6**	**0.1**	**0.6**	**0.4**	
Std. dev. (5 ms)	0.3	0.5	1	0	0.2	0.4	0.6	0.2	0.1	1.3	0.2	0.4	0.3	
Min.	2.8	3.3	16	49	0.3	1.8	10.1	1.7	0	7.5	0	0.3	0	
Max.	3.5	4.4	19	50	0.6	2.8	11.5	2.2	0.2	10.6	0.4	1.2	0.7	
Gordion 27635 (2) - 12.11.2013	**2.9**	**4.0**	**18**	**47**	**0.2**	**1.4**	**12.1**	**1.7**	**0.1**	**8.0**	**2.9**	**0.3**	**1.4**	**0.2**
Std. dev. (5 ms)	0.3	0.8	1	3	0.1	0.3	1.6	0.4	0.1	0.6	3.4	0.1	2.2	0.5
Min.	2.6	2.8	17	42	0.1	1.0	9.4	1.4	0	7.2	0.5	0.1	0	0
Max.	3.3	4.8	19	49	0.3	1.8	13.3	2.2	0.3	8.7	8.7	0.5	5.3	0.9
Second layer	**0.5**	**1.4**	**4**	**14**	**0.3**	**0.4**	**4.5**	**0.3**	**0**	**14.3**	**24.5**	**0.2**	**32.1**	**3.2**
Std. dev. (3 ms)	0.6	0.8	2	5	0.2	0.3	2.3	0.2	0	7.5	7.1	0.1	5.4	0.9
Min.	0	0.7	2	10	0.1	0.1	2.1	0.1	0	6.8	19.9	0	26.3	2.3
Max.	0.9	2.4	7	19	0.4	0.6	6.8	0.4	0	21.8	32.7	0.3	36.9	4.2
Gordion 27636 - 9.4.2013	**3.1**	**3.3**	**17**	**47**	**0.4**	**1.8**	**10.4**	**1.7**	**0**	**11.7**	**2.6**	**0.2**	**1.3**	
Std. dev. (5 ms)	0.6	0.2	1	2	0.1	0.2	0.6	0.1	0.1	1.9	2.0	0.1	0.8	
Min.	2.2	3.1	15	44	0.3	1.6	9.3	1.6	0	8.8	0.7	0.1	0.3	
Max.	3.7	3.7	18	48	0.5	1.9	11.0	1.8	0.2	13.6	5.4	0.3	2.4	
Gordion 27638 - 12.11.2013	**3.1**	**3.6**	**18**	**49**	**0.6**	**2.8**	**11.6**	**1.7**	**0.1**	**8.7**	**0.1**	**0.3**	**0.4**	
Std. dev. (5 ms)	0.3	0.2	1	1	0.1	0.3	1.1	0.1	0.2	0.8	0.3	0.4	0.1	
Min.	2.6	3.4	17	48	0.5	2.4	10.6	1.6	0	7.6	0	0	0.3	
Max.	3.5	3.8	19	51	0.7	3.2	13.4	1.8	0.3	9.5	0.5	0.6	0.5	
Gordion 27640 - 12.11.2013	**2.3**	**2.9**	**12**	**33**	**0.4**	**1.7**	**9.9**	**1.1**	**0.1**	**5.7**	**14.7**	**0.2**	**11.6**	**4.1**
Std. dev. (5 ms)	0.8	0.6	5	13	0.2	0.4	1.4	0.5	0.1	2.4	9.0	0.3	11.9	1.7
Min.	1.5	2.1	6	17	0.3	1.2	8.6	0.4	0	2.6	7.3	0	2.0	1.9
Max.	3.3	3.5	17	45	0.7	2.0	11.9	1.5	0.2	7.8	28.2	0.5	25.6	5.9
Second layer	**0**	**0.2**	**1**	**4**	**0.3**	**0.3**	**0.6**	**0**	**0**	**0.6**	**73.0**	**0.2**	**16.2**	**4.0**
Std. dev. (5 ms)	0.9	0.2	1	2	0.1	0.1	0.3	0.1	0.2	0.6	15.2	0.4	10.7	0.3
Min.	0	0	0	1	0.2	0.2	0.3	0	0	0	54.2	0	6.8	3.6
Max.	0.5	0.4	2	8	0.4	0.4	0.9	0.2	0.1	1.5	87.2	0.6	28.7	4.2
Gordion 27734 (1) - 12.11.2013	**2.1**	**3.1**	**12**	**33**	**1.0**	**3.8**	**14.0**	**0.9**	**0.1**	**7.2**	**9.4**	**0.1**	**13.8**	
Std. dev. (5 ms)	0.7	0.4	2	6	0.5	0.8	1.9	0.3	0.1	0.8	6.0	0.1	6.7	
Min.	1.3	2.7	9	24	0.3	2.7	12.0	0.5	0	6.5	3.3	0	5.7	
Max.	2.9	3.6	15	41	1.6	4.6	16.9	1.4	0.2	8.2	16.4	0.3	22.9	
Gordion 28218 - 12.11.2013	**2.7**	**3.1**	**14**	**38**	**1.0**	**2.2**	**10.9**	**1.1**	**0.1**	**13.2**	**5.4**	**0.1**	**7.7**	
Std. dev. (5 ms)	0.5	0.1	2	5	0.3	0.3	1.9	0.3	0.1	3.0	3.0	0.1	5.3	
Min.	2.0	2.9	12	33	0.8	1.9	9.2	0.8	0	9.7	0.6	0	2.8	
Max.	3.3	3.2	17	43	1.4	2.5	13.8	1.5	0.2	17.9	8.7	0.2	16.6	
Gordion 28236 - 9.4.2013	***2.6***	***4.9***	***12***	***43***	***0.3***	***2.9***	***18.4***	***1.0***	***0.1***	***5.7***	***7.6***	***0.3***	***1.6***	
Std. dev. (5 ms)	0.3	0.1	2	5	0.1	0.5	3.0	0.3	0.1	1.7	9.4	0.1	1.6	
Min.	2.4	4.7	10	35	0.1	2.1	15.8	0.7	0	3.4	0	0.3	0	
Max.	3.1	5.1	14	48	0.5	3.4	22.6	1.5	0.3	8.2	22.4	0.5	3.8	
Gordion 28877 - 9.4.2013	**3.7**	**2.8**	**18**	**48**	**0.4**	**1.6**	**9.5**	**1.4**	**0.1**	**7.6**	**6.2**	**0.2**	**0.6**	
Std. dev. (5 ms)	0.3	0.4	1	2	0.1	0.2	1.1	0.3	0.1	1.2	3.8	0.1	0.4	
Min.	3.3	2.3	18	45	0.2	1.3	8.3	1.1	0	6.2	2.5	0	0.3	
Max.	4.2	3.1	19	50	0.5	1.9	11.2	1.8	0.2	9.4	11.2	0.3	1.3	
Gordion 28932 (1) - 12.11.2013	**3.0**	**4.1**	**17**	**48**	**0.5**	**2.2**	**12.2**	**1.6**	**0.1**	**8.6**	**1.2**	**0.1**	**0.5**	
Std. dev. (5 ms)	0.4	1.0	2	2	0.1	0.3	1.8	0.2	0	0.6	1.5	0.2	0.3	
Min.	2.3	3.1	15	45	0.3	1.7	10.4	1.4	0.1	7.9	0	0	0.1	
Max.	3.4	5.7	20	50	0.7	2.5	15.1	1.9	0.2	9.2	3.1	0.2	0.8	
Gordion 28932 (2) - 12.11.2013	**2.3**	**4.1**	**14**	**42**	**0.6**	**2.6**	**11.4**	**1.2**	**0.1**	**6.9**	**12.3**	**0.4**	**2.6**	
Std. dev. (5 ms)	0.3	0.2	2	3	0.1	0.3	1.2	0.3	0.1	0.8	4.5	0.2	1.7	
Min.	2.0	4.0	12	37	0.4	2.3	9.9	0.8	0	5.6	7.7	0.2	1.6	
Max.	2.7	4.4	15	44	0.8	2.9	12.9	1.6	0.2	7.7	18.0	0.6	5.7	

Average Slag Composition	***2.8***	***3.6***	***16***	***44***	***0.5***	***2.2***	***11.3***	***1.5***	***0.1***	***8.6***	***4.8***	***0.2***	***4.1***	

Ceramic. Ratio of oxides to Al_2O_3, metals removed.

Sample	$\frac{Na_2O}{Al_2O_3}$	$\frac{MgO}{Al_2O_3}$	$\frac{SiO_2}{Al_2O_3}$	$\frac{P_2O_5}{Al_2O_3}$	$\frac{K_2O}{Al_2O_3}$	$\frac{CaO}{Al_2O_3}$	$\frac{TiO_2}{Al_2O_3}$	$\frac{MnO}{Al_2O_3}$	$\frac{FeO}{Al_2O_3}$
Gordion 21299 - 15.10.2013	0.18	0.20	2.78	0.03	0.10	0.60	0.10	0	0.60
Gordion 22529 - 13.9.2013	0.16	0.21	2.89	0.03	0.12	0.54	0.09	0.01	0.72
Gordion 22626 - 15.10.2013	0.18	0.19	2.79	0.02	0.10	0.49	0.11	0.01	0.49
Gordion 22673 - 15.1.2014	0.17	0.18	2.74	0.03	0.08	0.49	0.09	0	0.46
Gordion 22673-A - 15.10.2013	0.16	0.18	2.69	0.03	0.11	0.55	0.08	0.01	0.46
Gordion 22673-B - 15.10.2013	0.17	0.18	2.86	0.03	0.10	0.47	0.10	0.01	0.50
Gordion 22829 - 15.10.2013	0.16	0.21	2.96	0.03	0.11	0.56	0.08	0.01	0.50
Gordion 22958 - 9.4.2013	0.16	0.23	2.73	0.03	0.09	0.75	0.08	0.01	0.46
Gordion 22999 - 13.9.2013	0.17	0.19	2.81	0.03	0.10	0.56	0.11	0.01	0.48
Gordion 23045-A - 15.10.2013	0.16	0.22	2.88	0.02	0.10	0.68	0.09	0.01	0.45
Gordion 23045-B - 15.10.2013	0.18	0.21	2.91	0.03	0.10	0.67	0.09	0.01	0.54
Gordion 23045-S - 15.10.2013									
Gordion 23128 - 13.9.2013									
Gordion 23329 - 9.4.2013	0.18	0.18	2.76	0.03	0.10	0.48	0.09	0.01	0.53
Gordion 23329 - 15.1.2014	0.17	0.20	2.83	0.03	0.11	0.53	0.08	0.01	0.55
Gordion 23523 - 15.10.2013	0.17	0.21	2.84	0.02	0.11	0.54	0.08	0.01	0.54
Gordion 23707 - 9.4.2013	*0.21*	*0.23*	*4.46*	*0.02*	*0.28*	*0.89*	*0.04*	*0.01*	*0.31*
Gordion 23707 - 15.1.2014	*0.22*	*0.23*	*4.95*	*0.02*	*0.28*	*0.94*	*0.05*	*0.01*	*0.31*
Gordion 23778 - 13.9.2013	0.17	0.21	2.96	0.03	0.12	0.53	0.09	0.01	0.57
Gordion 23797 - 9.4.2013	0.17	0.22	2.93	0.04	0.11	0.62	0.08	0	0.57
Gordion 25368 - 13.9.2013	0.15	0.23	2.78	0.03	0.12	0.61	0.07	0.01	0.61
Gordion 25394 - 9.4.2013	0.15	0.22	2.70	0.02	0.12	0.64	0.09	0	0.47
Gordion 25394_A - 13.9.2013	0.14	0.26	2.89	0.04	0.12	0.63	0.08	0.01	0.53
Gordion 25394_B - 13.9.2013	0.15	0.22	2.80	0.03	0.11	0.60	0.08	0.01	0.51
Gordion 25568 - 9.4.2013	0.18	0.20	2.65	0.02	0.07	0.55	0.08	0.01	0.45
Gordion 25568 - 15.1.2014	0.15	0.24	2.82	0.02	0.08	0.63	0.08	0.01	0.49
Gordion 25569-A - 15.10.2013	0.16	0.24	2.80	0.02	0.08	0.67	0.09	0.01	0.53
Gordion 25569-B - 15.10.2013	0.15	0.23	2.79	0.02	0.10	0.63	0.09	0	0.50
Gordion 26891 - 9.4.2013	0.18	0.19	2.91	0.03	0.10	0.49	0.10	0.01	0.55
Gordion 27609 - 15.10.2013	0.15	0.21	2.76	0.03	0.10	0.63	0.08	0	0.45
Gordion 27609-S - 15.10.2013									
Gordion 27613_A 13.9.2013	0.17	0.20	2.82	0.03	0.11	0.61	0.09	0.01	0.49
Gordion 27613_B - 13.9.2013	0.18	0.20	2.79	0.03	0.10	0.54	0.09	0	0.45
Gordion 27629 - 15.10.2013	0.19	0.19	2.73	0.05	0.10	0.59	0.09	0	0.51
Gordion 27634 - 12.11.2013	0.15	0.29	2.96	0.03	0.14	0.70	0.09	0.01	0.45
Gordion 27635 (1) - 12.11.2013	0.19	0.21	2.80	0.03	0.11	0.57	0.10	0.01	0.50
Gordion 27635 (2) - 12.11.2013	0.18	0.18	2.69	0.04	0.08	0.54	0.08	0.01	0.51
Gordion 27636 - 9.4.2013	0.17	0.20	2.78	0.03	0.11	0.53	0.09	0.01	0.49
Gordion 27638 - 12.11.2013	0.18	0.21	2.80	0.03	0.13	0.55	0.09	0.01	0.48
Gordion 27640 - 12.11.2013	0.16	0.21	2.83	0.03	0.12	0.58	0.10	0.01	0.58
Gordion 27734 (1) - 12.11.2013	0.18	0.21	2.92	0.03	0.11	0.52	0.12	0.01	0.55
Gordion 28218 - 12.11.2013	0.16	0.19	2.79	0.02	0.10	0.50	0.09	0	0.52
Gordion 28236 - 9.4.2013	*0.27*	*0.22*	*3.77*	*0.02*	*0.29*	*1.51*	*0.07*	*0*	*0.43*
Gordion 28877 - 9.4.2013	0.20	0.18	2.71	0.03	0.09	0.48	0.08	0	0.46
Gordion 28932 (1) - 12.11.2013	0.18	0.22	2.87	0.04	0.14	0.62	0.08	0.01	0.53
Gordion 28932 (2) - 12.11.2013	0.18	0.25	2.85	0.04	0.15	0.64	0.09	0	0.51
Average	***0.17***	***0.21***	***2.82***	***0.03***	***0.11***	***0.58***	***0.09***	***0.01***	***0.51***

Slag. Ratio of oxides to Al_2O_3, metals removed.

Sample	$\frac{Na_2O}{Al_2O_3}$	$\frac{MgO}{Al_2O_3}$	$\frac{SiO_2}{Al_2O_3}$	$\frac{P_2O_5}{Al_2O_3}$	$\frac{K_2O}{Al_2O_3}$	$\frac{CaO}{Al_2O_3}$	$\frac{TiO_2}{Al_2O_3}$	$\frac{MnO}{Al_2O_3}$	$\frac{FeO}{Al_2O_3}$
Gordion 21299 - 15.10.2013	0.20	0.22	2.71	0.03	0.16	0.74	0.09	0	0.50
Gordion 22529 - 13.9.2013	0.15	0.21	2.76	0.04	0.16	0.86	0.08	0.01	0.60
Gordion 22626 - 15.10.2013	0.18	0.22	2.97	0.04	0.12	0.73	0.11	0.01	0.63
Gordion 22673 - 15.1.2014	0.19	0.13	2.43	0.02	0.08	0.46	0.09	0	0.44
Gordion 22673-A - 15.10.2013	0.18	0.20	2.73	0.03	0.20	0.66	0.11	0.01	0.53
Gordion 22673-B - 15.10.2013	0.20	0.25	2.90	0.05	0.16	0.82	0.09	0.01	0.50
Gordion 22829 - 15.10.2013	0.19	0.20	2.77	0.03	0.22	0.94	0.10	0.01	0.48
Gordion 22958 - 9.4.2013	0.15	0.27	2.78	0.02	0.09	0.80	0.10	0.01	0.66
Gordion 22999 - 13.9.2013	0.18	0.17	2.55	0.02	0.12	0.54	0.09	0	0.51
Gordion 23045-A - 15.10.2013	0.18	0.25	2.86	0.02	0.12	0.67	0.11	0.01	0.48
Gordion 23045-B - 15.10.2013	0.16	0.30	2.84	0.02	0.11	0.87	0.10	0.01	0.53
Gordion 23045-S - 15.10.2013	0.18	0.25	2.77	0.03	0.15	0.65	0.09	0.01	0.77
Gordion 23128 - 13.9.2013	0.15	0.30	2.86	0.02	0.08	0.69	0.10	0.01	0.49
Gordion 23329 - 9.4.2013	0.16	0.16	2.67	0.03	0.10	0.46	0.09	0.01	0.45
Gordion 23329 - 15.1.2014	0.19	0.21	2.71	0.03	0.12	0.62	0.10	0.01	0.54
Gordion 23523 - 15.10.2013	0.18	0.19	2.77	0.04	0.11	0.61	0.11	0	0.51
Gordion 23707 - 9.4.2013	*0.17*	*0.20*	*4.26*	*0.02*	*0.29*	*0.72*	*0.04*	*0*	*0.29*
Gordion 23707 - 15.1.2014	*0.17*	*0.28*	*4.40*	*0.04*	*0.31*	*1.04*	*0.03*	*0*	*0.52*
Gordion 23778 - 13.9.2013	0.20	0.19	2.73	0.03	0.11	0.57	0.09	0	0.52
Gordion 23797 - 9.4.2013	0.17	0.25	2.80	0.04	0.21	0.78	0.10	0	0.57
Gordion 25368 - 13.9.2013	0.16	0.29	2.76	0.05	0.16	0.80	0.08	0	0.71
Gordion 25394 - 9.4.2013	0.17	0.32	2.90	0.04	0.17	0.89	0.09	0	0.82
Gordion 25394_A - 13.9.2013	0.16	0.29	2.92	0.03	0.16	0.78	0.11	0.01	0.59
Gordion 25394_B - 13.9.2013	0.16	0.24	2.74	0.03	0.16	0.70	0.09	0.01	0.62
Gordion 25568 - 9.4.2013	0.15	0.31	2.86	0.07	0.27	1.42	0.09	0.02	0.55
Gordion 25568 - 15.1.2014	0.17	0.24	2.64	0.02	0.11	0.68	0.09	0.01	0.60
Gordion 25569-A - 15.10.2013	0.16	0.30	2.83	0.02	0.09	0.71	0.10	0.01	0.55
Gordion 25569-B - 15.10.2013	0.16	0.25	2.77	0.02	0.13	0.67	0.10	0	0.50
Gordion 26891 - 9.4.2013	0.20	0.14	2.68	0.02	0.10	0.53	0.09	0.01	0.51
Gordion 27609 - 15.10.2013	0.15	0.29	3.08	0.04	0.28	1.02	0.10	0.01	0.51
Gordion 27609-S - 15.10.2013	0.15	0.31	3.03	0.07	0.21	1.05	0.09	0.01	0.67
Gordion 27613_A 13.9.2013	0.18	0.22	2.82	0.03	0.13	0.67	0.12	0.01	0.57
Gordion 27613_B - 13.9.2013	0.23	0.19	2.73	0.04	0.14	0.61	0.09	0.01	0.47
Gordion 27629 - 15.10.2013	0.18	0.21	2.67	0.02	0.11	0.62	0.09	0.01	0.52
Gordion 27634 - 12.11.2013	0.16	0.28	2.89	0.02	0.12	0.76	0.11	0.01	0.47
Gordion 27635 (1) - 12.11.2013	0.18	0.22	2.87	0.03	0.14	0.62	0.11	0	0.55
Gordion 27635 (2) - 12.11.2013	0.16	0.22	2.63	0.01	0.08	0.68	0.10	0.01	0.45
Gordion 27636 - 9.4.2013	0.18	0.20	2.78	0.02	0.11	0.62	0.10	0	0.7
Gordion 27638 - 12.11.2013	0.17	0.20	2.79	0.03	0.16	0.65	0.09	0.01	0.49
Gordion 27640 - 12.11.2013	0.19	0.24	2.73	0.04	0.14	0.82	0.09	0.01	0.47
Gordion 27734 (1) - 12.11.2013	0.18	0.27	2.86	0.08	0.33	1.22	0.08	0.01	0.63
Gordion 28218 - 12.11.2013	0.19	0.22	2.68	0.07	0.15	0.77	0.08	0.01	0.93
Gordion 28236 - 9.4.2013	*0.22*	*0.42*	*3.69*	*0.03*	*0.25*	*1.58*	*0.08*	*0.01*	*0.49*
Gordion 28877 - 9.4.2013	0.20	0.15	2.58	0.02	0.09	0.52	0.08	0	0.41
Gordion 28932 (1) - 12.11.2013	0.17	0.24	2.79	0.03	0.13	0.70	0.09	0.01	0.50
Gordion 28932 (2) - 12.11.2013	0.16	0.29	2.94	0.04	0.18	0.81	0.09	0.01	0.49
Average	***0.18***	***0.24***	***2.78***	***0.03***	***0.15***	***0.74***	***0.09***	***0.01***	***0.56***

Change (in %) in ratio of oxides to Al_2O_3 between ceramic and slag, metals removed.

Sample	$\frac{Na_2O}{Al_2O_3}$	$\frac{MgO}{Al_2O_3}$	$\frac{SiO_2}{Al_2O_3}$	$\frac{P_2O_5}{Al_2O_3}$	$\frac{K_2O}{Al_2O_3}$	$\frac{CaO}{Al_2O_3}$	$\frac{TiO_2}{Al_2O_3}$	$\frac{MnO}{Al_2O_3}$	$\frac{FeO}{Al_2O_3}$
Gordion 21299 - 15.10.2013	9	10	-3	-12	51	24	-12	198	-16
Gordion 22529 - 13.9.2013	-7	1	-4	7	35	60	-8	-28	-17
Gordion 22626 - 15.10.2013	0	16	6	62	28	49	0	-36	28
Gordion 22673 - 15.1.2014	10	-26	-11	-36	-7	-5	-3	-60	-3
Gordion 22673-A - 15.10.2013	14	11	1	-6	85	20	27	-43	17
Gordion 22673-B - 15.10.2013	17	39	1	41	55	74	-8	54	0
Gordion 22829 - 15.10.2013	22	-1	-7	13	101	69	15	-35	-3
Gordion 22958 - 9.4.2013	-5	19	2	-38	0	6	20	-40	44
Gordion 22999 - 13.9.2013	2	-11	-9	-21	18	-3	-19	-95	4
Gordion 23045-A - 15.10.2013	13	12	-1	17	19	-1	29	60	6
Gordion 23045-B - 15.10.2013	-11	38	-2	-40	7	30	9	-20	-3
Gordion 23045-S - 15.10.2013	7	20	-5	-7	25	5	7	55	52
Gordion 23128 - 13.9.2013	-12	41	-2	-46	-30	12	12	66	-3
Gordion 23329 - 9.4.2013	-10	-11	-3	1	0	-4	-7	-36	-15
Gordion 23329 - 15.1.2014	15	4	-4	-5	7	15	21	60	-2
Gordion 23523 - 15.10.2013	6	-9	-3	61	-6	14	29	-26	-6
Gordion 23707 - 9.4.2013	*-16*	*-13*	*-5*	*-1*	*3*	*-19*	*-9*	*-26*	*-9*
Gordion 23707 - 15.1.2014	*-24*	*19*	*-11*	*108*	*13*	*11*	*-38*	*-69*	*67*
Gordion 23778 - 13.9.2013	16	-11	-8	-17	-5	8	2	-108	-9
Gordion 23797 - 9.4.2013	0	12	-5	-7	85	25	28	-27	1
Gordion 25368 - 13.9.2013	7	29	-1	92	37	31	12	-82	16
Gordion 25394 - 9.4.2013	10	45	7	90	39	40	1	90	74
Gordion 25394_A - 13.9.2013	17	11	1	-24	34	24	45	92	10
Gordion 25394_B - 13.9.2013	1	6	-2	-16	43	17	7	57	20
Gordion 25568 - 9.4.2013	-18	57	8	282	267	159	15	180	24
Gordion 25568 - 15.1.2014	12	0	-7	-25	42	8	4	62	23
Gordion 25569-A - 15.10.2013	3	27	1	0	15	6	7	67	4
Gordion 25569-B - 15.10.2013	5	7	-1	-13	26	8	15	14	-1
Gordion 26891 - 9.4.2013	12	-26	-8	-14	2	7	-5	3	-6
Gordion 27609 - 15.10.2013	0	40	11	15	170	61	22	177	12
Gordion 27609-S - 15.10.2013	-11	45	4	145	80	71	6	77	34
Gordion 27613_A 13.9.2013	5	9	0	-11	21	9	35	4	18
Gordion 27613_B - 13.9.2013	27	-5	-2	27	43	14	5	223	4
Gordion 27629 - 15.10.2013	-2	6	-2	-54	4	5	5	35	2
Gordion 27634 - 12.11.2013	8	-3	-3	-43	-12	10	24	71	4
Gordion 27635 (1) - 12.11.2013	-2	5	2	10	24	9	15	-32	11
Gordion 27635 (2) - 12.11.2013	-7	23	-2	-72	-6	26	25	-20	-13
Gordion 27636 - 9.4.2013	9	-2	0	-25	0	17	16	-45	41
Gordion 27638 - 12.11.2013	-4	0	0	-3	21	19	4	0	3
Gordion 27640 - 12.11.2013	14	16	-3	19	13	42	-12	-23	-19
Gordion 27734 (1) - 12.11.2013	0	28	-2	228	203	133	-32	138	13
Gordion 28218 - 12.11.2013	17	15	-4	213	60	54	-10	93	79
Gordion 28236 - 9.4.2013	*-18*	*93*	*-2*	*47*	*-16*	*4*	*13*	*636*	*13*
Gordion 28877 - 9.4.2013	4	-13	-5	-34	0	8	-10	146	-10
Gordion 28932 (1) - 12.11.2013	-3	10	-2	-28	-9	13	16	35	-5
Gordion 28932 (2) - 12.11.2013	-9	19	3	4	21	25	-9	123	-5
Average change	***4***	***12***	***-1***	***17***	***38***	***29***	***8***	***29***	***9***

APPENDIX K

Oxide phases in crucible slag

A full list of oxides occurring in the crucible slag has been established, which is summarised here. The predominant types of oxides are Fe-bearing, Ca-bearing, Cu-bearing, Sn-bearing and Pb-bearing phases, with Ag-rich phases occurring in only two crucibles. Their varying occurrence is interpreted in section 8.3.
Terminology adapted from mineralogy (as explained in section 5.2.3) is employed. The occurrence of particular phases in certain crucibles is not plotted onto the ternary diagrams, as has been done in Appendix D, because of the tight compositional clustering of crucible slag in these diagrams (Figure 8.7).

Section K.1

Fe-bearing oxides

Most of the oxides in the crucible slag contain some FeO and it is a component of the glassy slag matrix, too. Fe-based oxides are listed here.

1. *Olivine*: Olivine of an intermediate fayalite (Fe_2SiO_4) - forsterite (Mg_2SiO_4) composition (with minor Ca: Fe/Mg/Ca ≈ 14/8/1) is encountered in one crucible (Gordion-22958). These chain-like crystals are shown in Figure K.1.
   Another olivine-like phase has been encountered in two samples (Gordion-25569-B and -28932 (1)), with approximate $(Fe,Mg,Ca,Na,K)_2(Si,Al)O_4$ composition, where Fe/Mg/Ca/Na/K ≈ 71/12.5/8/5/3.5 and Si/Al ≈ 3/1. This corresponds to a fayalite-dominated mixture of the fayalite-forsterite solid solution series, with additional Ca

content (the monticellite ($CaMgSiO_4$) - kirschsteinite ($CaFeSiO_4$) olivine solution series forms very limited solid solution with the fayalite-forsterite series (Klein and Dutrow, 2007, Fig. 19.1, p. 485)) and limited Na and K. The olivine crystals found in these two samples (single occurrence), shown in Figure K.2, appear to be residual mineral fragments rather than oxides formed during the metallurgical process.

2. *Spinel*: Spinel is the most common iron oxide found in these crucibles, with occurrences ranging from almost pure magnetite (Fe_3O_4) to more diluted forms with up to 3.5 at% Sn and 3.5 at% Cu substituting for Fe (typically associated with copper or bronze prills, indicative of their formation through preferential oxidation of iron from these prills). Furthermore, Fe is sometimes substituted by up to 8 at% Mg, 6 at% Al, 3.5 at% Si, 1.3 at% Ca and 1.5 at% Ti. Rare substitutions of 0.8 and 0.4 at% Ni and Co occur together with Cu and Sn. The average spinel composition is approximately $(Fe,Mg,Al)_3O_4$ with $Fe/Mg/Al \approx 11/1/1$. Some examples are shown in Figure K.3.

   Other spinel-like oxides are encountered in three samples. These oxides have a more significant silica content (up to 7 at%), and their structure is quite different from the 'normal' spinel described above, again indicative of a residual rather than newly-formed nature (see Figure K.4).

   Furthermore, a chrome-rich spinel has been noted in two crucibles. These crystals have an average $Cr/Fe/Al/Mg$ ratio $\approx 6/3/3/2$. Some examples are shown in Figure K.5.

   Finally, titanium-rich spinel is noted in many of the crucibles. Its average composition is 23 at% Fe, 11 at% Ti, 3 at% Mg, 1.5 at% Si and 1.5 at% Al, with 60 at% oxygen. Some examples are shown in Figures K.6 and K.2b. As Figure K.6c shows, the 'high-Ti spinel' sometimes exhibits two distinct phases, one relatively enriched in iron, the other relatively enriched in titanium.

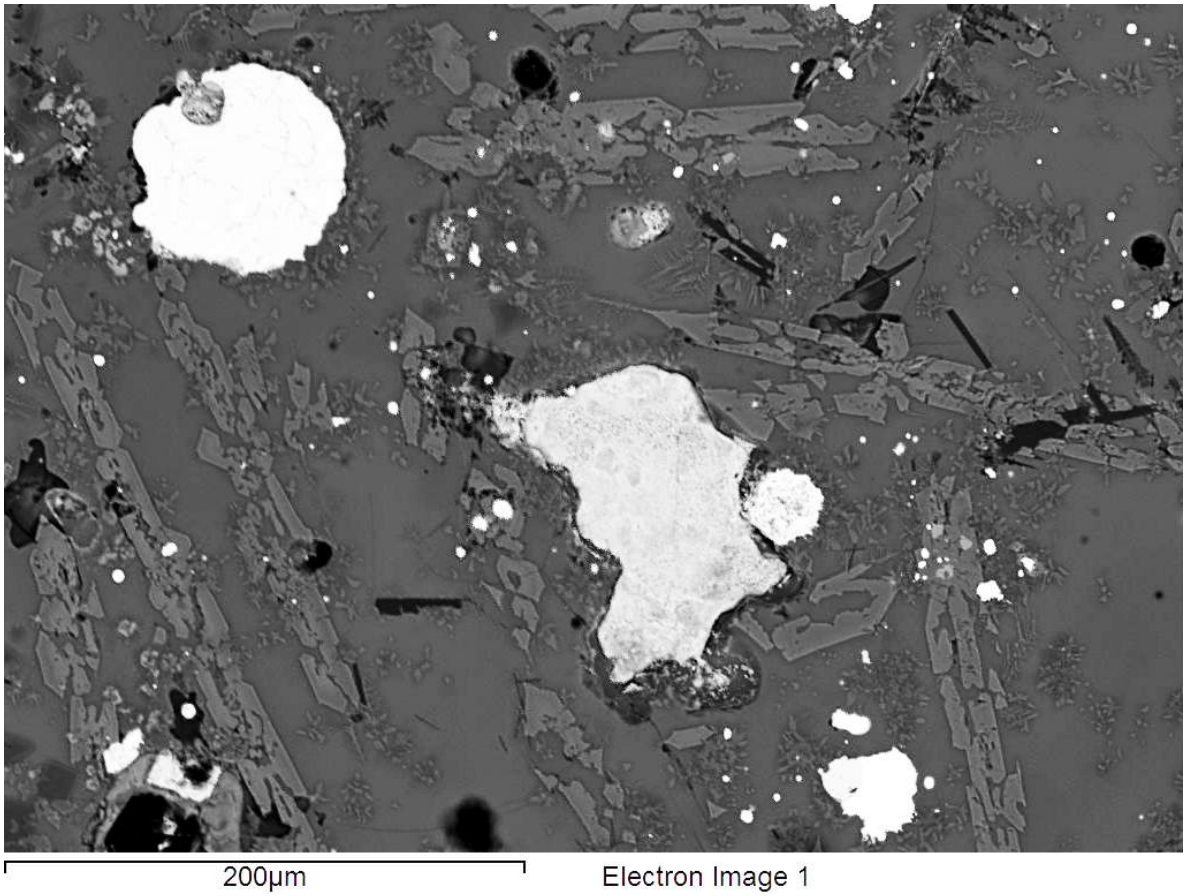

Figure K.1: Olivine (light grey chains) in Gordion-22958

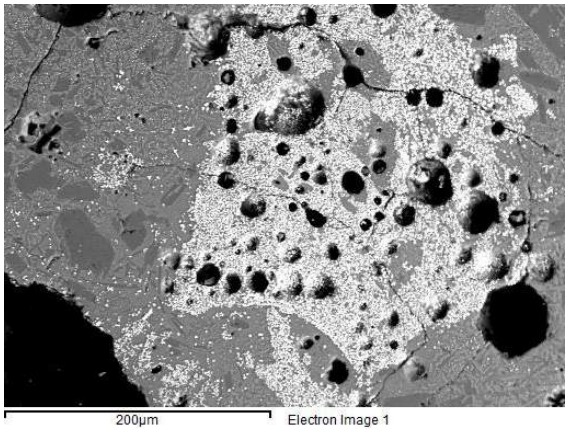

(a) Gordion-25569-B

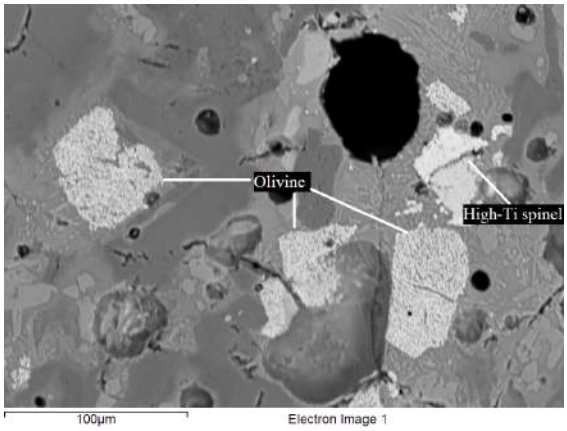

(b) Gordion-28932 (1)

Figure K.2: Olivine-like oxides (bright, angular-shaped, 'dotted')

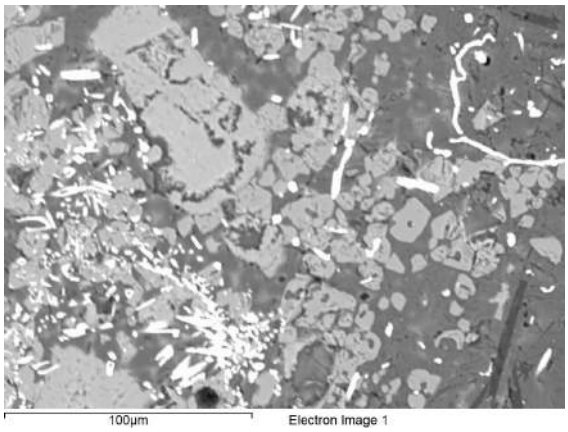

(a) Spinel (light grey), Gordion-22958

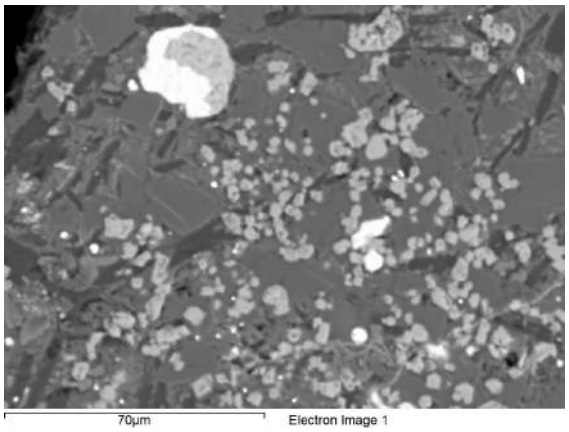

(b) Spinel (light grey), Gordion-25568-A

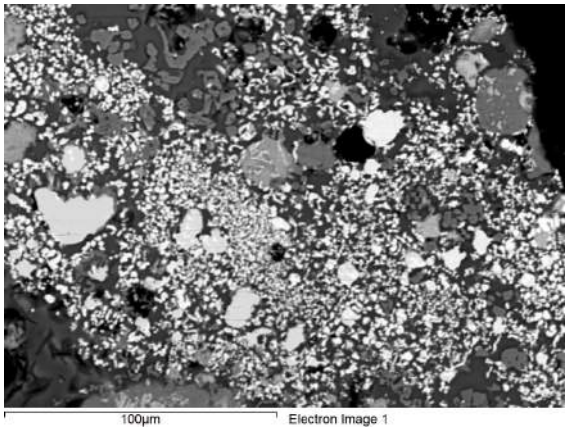

(c) Spinel (medium grey) associated with medium-tin, iron-rich (15-25 wt% Sn, 0.5-0.75 wt% Fe) bronze prills (light grey) and burnt off tin oxide crystals (white), Gordion-27635 (2)

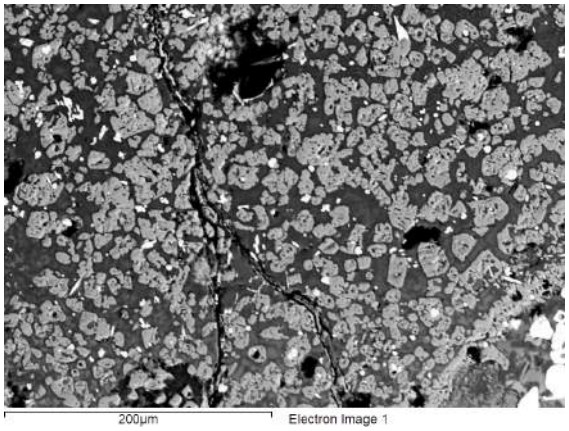

(d) Spinel cluster (medium grey), Gordion-26891

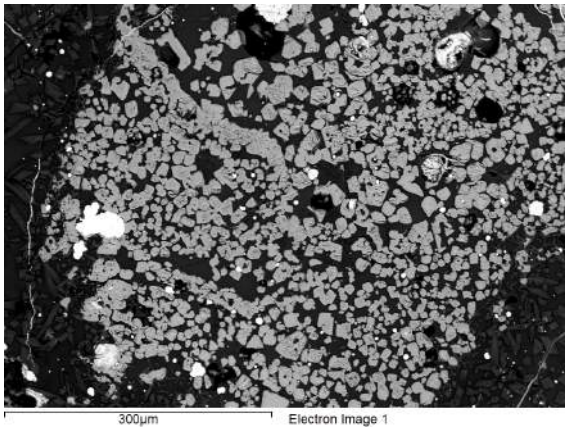

(e) Spinel cluster (medium grey) with iron-rich (7 wt% Sn, 1.3-3.9 wt% Fe) bronze prills, Gordion-27609-S

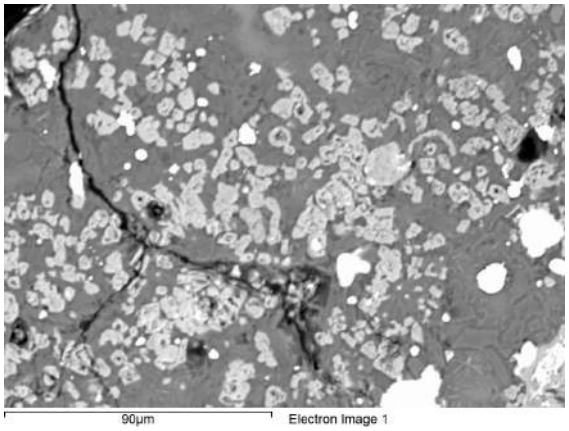

(f) Spinel cluster (light grey) with high-tin, iron-rich leaded (35-39 wt% Sn, 1.1-2.3 wt% Fe, 0-1.6 wt% Pb) bronze prills (white), Gordion-25568-B

Figure K.3: Spinel

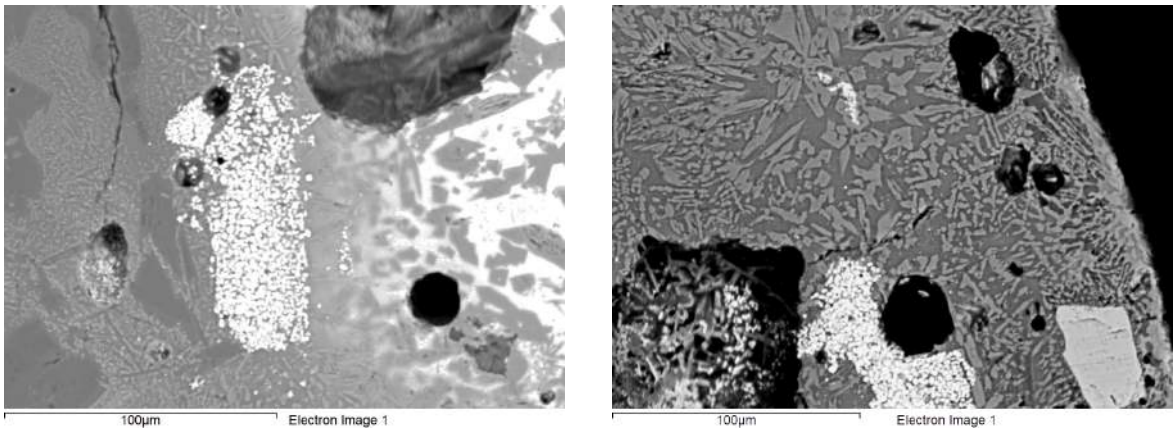

Figure K.4: 'High-silica spinel' (bright, angular-shaped, 'dotted'), Gordion-27635 (1)

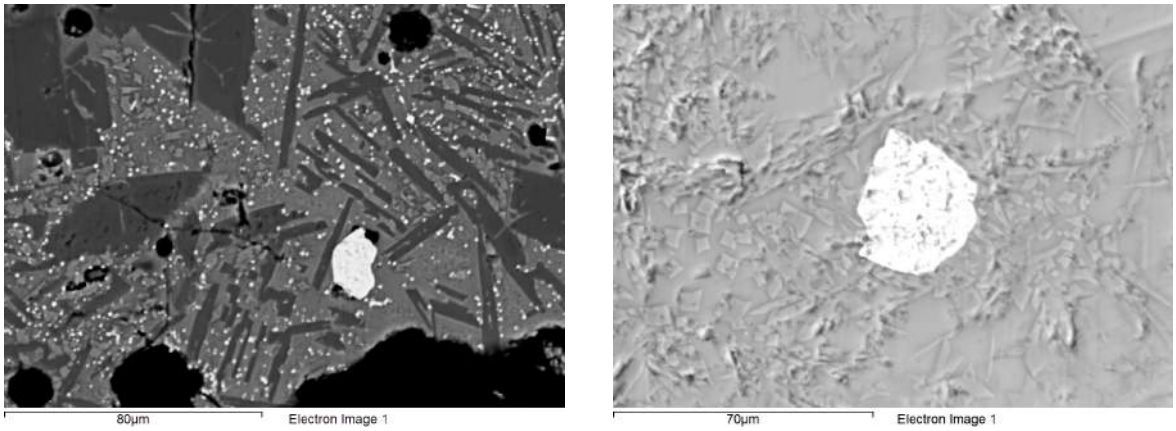

(a) Chrome-rich spinel, Gordion-27635 (1)

(b) Chrome-rich spinel, Gordion-27609

Figure K.5: Chrome-rich spinel (bright)

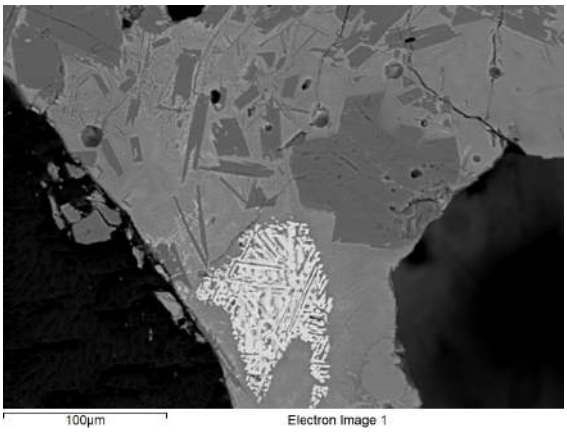

(a) High-Ti spinel, Gordion-27638

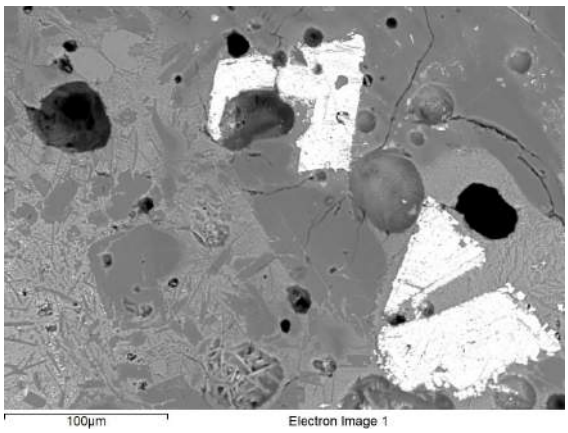

(b) High-Ti spinel, Gordion-27635 (1)

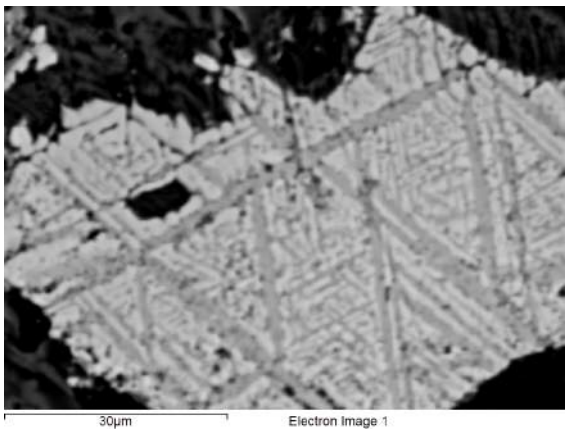

(c) Two phases in high-Ti spinel, Gordion-27635 (1)

Figure K.6: Titanium-rich spinel (bright)

Section K.2

Ca-bearing oxides

Lime is an important component of all crucible slag, as shown in section 8.2.2. It occurs in both the glassy phase and particular oxides, discussed below.

1. *Plagioclase*: A medium grey phase, with approximate labradorite composition, or 65% anorthite ($CaAl_2Si_2O_8$) - 35 % albite ($NaAlSi_3O_8$). These two minerals form a complete solid solution series at elevated temperatures. Typically, 0.2 at% potassium and 0.4 at% Fe are present. This mineral is similar to the plagioclase found in the remnant mafic rock fragments of the crucible ceramic fabric and occurs in nearly all crucibles. It appears that some of the original plagioclase sometimes survives when the slag is not very developed. In better developed, more liquid slag, newly formed plagioclase crystals are formed, which tend to exhibit finer, more elongated shapes. Some examples of plagioclase are shown in Figure K.7 (and Figure K.5a, dark grey).

2. *Pyroxene*: The second important lime-rich phase is pyroxene of approximate augite composition: $(Ca,Na)(Mg,Fe,Ti)(Si,Al)_2O_6$. It is particularly lime-rich, with very low Na content (0.2 at%). The ratios between Mg, Fe and Ti and Si and Al are ±9/5/1 and ±7/2 respectively. Some examples are shown in Figure K.8 and the background of Figures K.4, right (medium grey) and K.5b (light grey).
   A few samples contain a phase similar to this augite, but further enriched in CaO (approximate composition $Ca_2(Fe,Mg,Al)Si_2O_7$), illustrated in Figure K.9.

3. *K-feldspar*: A phase with approximate $KAl_2Si_4O_{12}$-composition occurs in Gordion-22673-B, associated with lead oxides and silicates (see section K.5). This approximates dehydrated muscovite ($KAl_2Si_4O_{10}(OH)_2$) or some form of K-feldspar (e.g., orthoclase $KAlSi_3O_8$, with added alumina and silica). The presence of potassium in Gordion-22763 is discussed further in section 8.3.9.

4. *Anhydrite*: Anhydrous calcium sulphate ($CaSO_4$) has been noted in one crucible (Gordion-28877), in association with Cu_2ClO_2-Cu_2ClO_3 (see section K.3), and is shown in Figure K.10. It occurs at the slag surface and is most likely a (rare) weathering product.

5. *Calcium-magnesium peroxide*: A rare occurrence of calcium-magnesium peroxide ($(Ca,Mg)O_2$, with Ca/Mg≈5) is found in a charcoal inclusion in Gordion-23797, shown in Figure K.11.

	Na_2O	MgO	Al_2O_3	SiO_2	P_2O_5	K_2O	CaO	TiO_2	FeO
Glassy phase	1.8	11.8	12	53	0.2	1.0	13.1	1.9	5.9
St. dev.	1.7	3.9	3	3	0.4	0.9	4.5	0.6	1.5
Ceramic	3.0	3.8	18	51	0.5	1.9	10.4	1.6	9.2

Table K.1: Composition of glassy slag background (11 measurements) in Gordion crucibles, compared to average ceramic composition (Appendix J)

6. *Malayaite*: See section K.4.

Other singular occurrences of crystals with compositions intermediate between pyroxene and plagioclase (not well crystallised from glassy matrix) are not listed here. The 'slag background', or glassy matrix, is a Ca-Mg-Al-(Fe-)silicate, with average composition given in Table K.1. Note the high magnesia and lime content, which is further discussed in section 8.2.5.

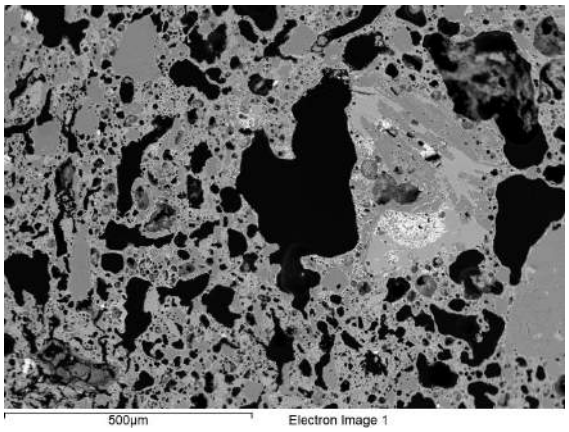

(a) Remnant plagioclase (in rock fragment) in porous transitional zone

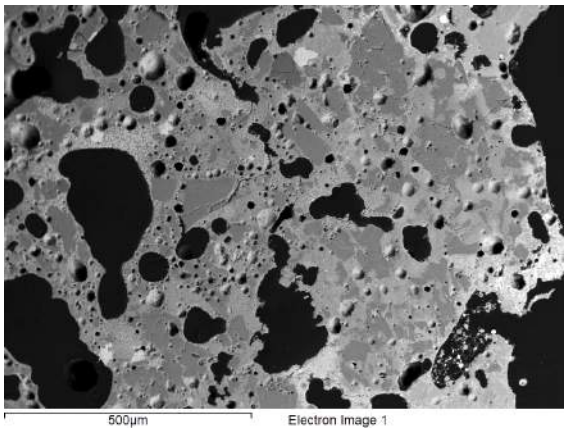

(b) Remnant plagioclase in poorly developed slag

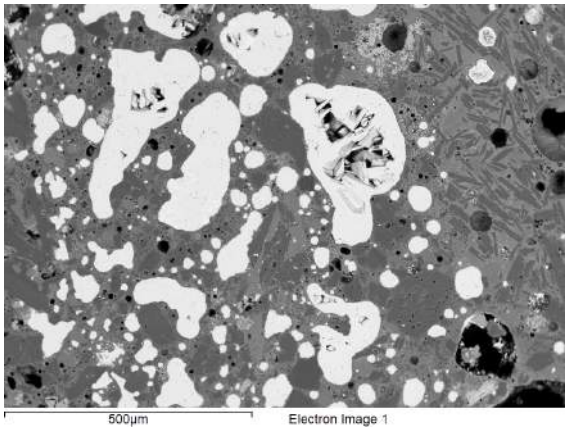

(c) Remnant plagioclase (left) in deeper, less developed slag, and newly formed plagioclase (right) in more developed slag. The bright, rounded phase is Cu-Cl-oxide

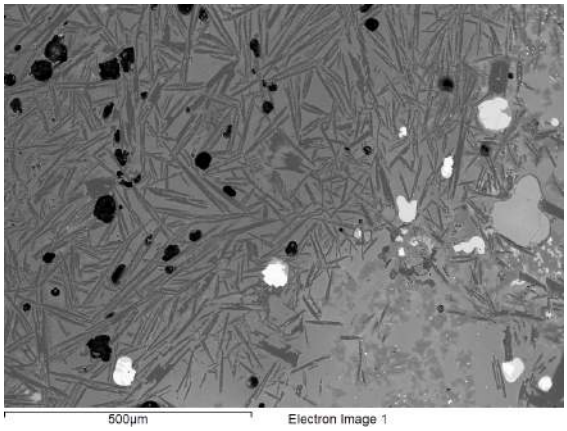

(d) Plagioclase, Gordion-22958

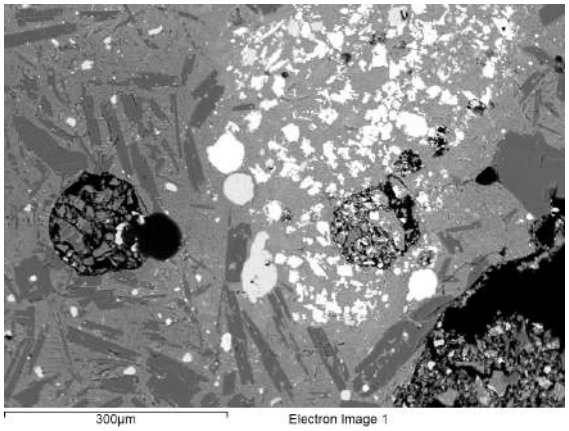

(e) Plagioclase, Gordion-25568

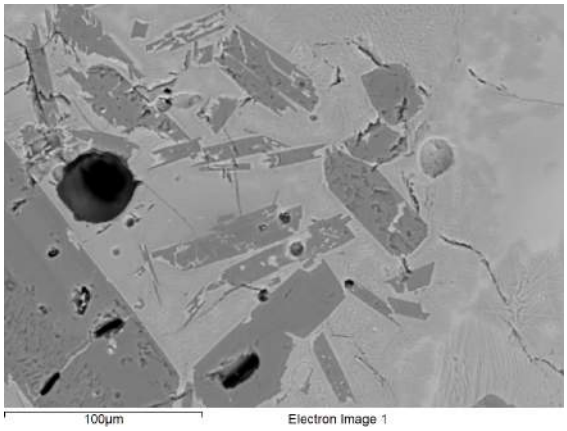

(f) Plagioclase, Gordion-27638

Figure K.7: Plagioclase (dark grey)

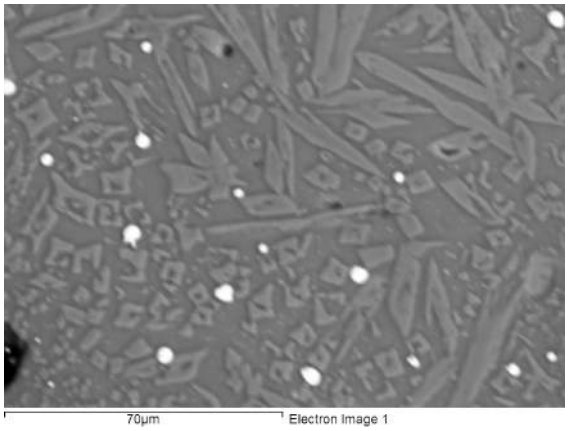

(a) Pyroxene (medium grey), Gordion-23707

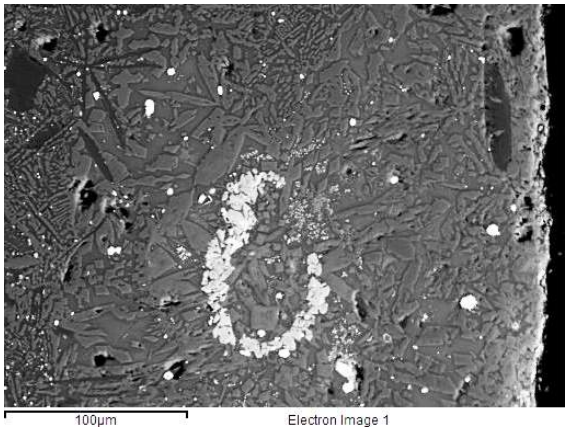

(b) Pyroxene (medium grey) with spinel (light grey), Gordion-25569-B

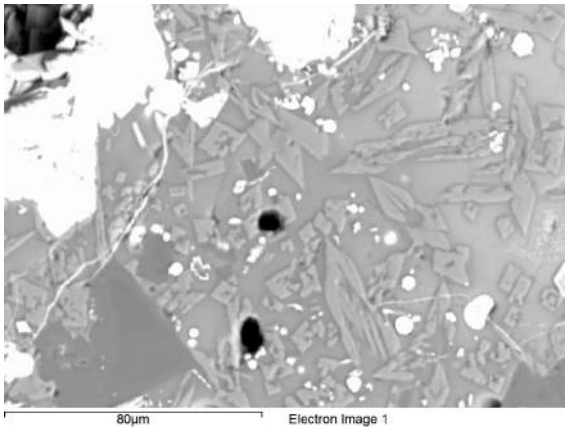

(c) Pyroxene (light grey), Gordion-25394-B

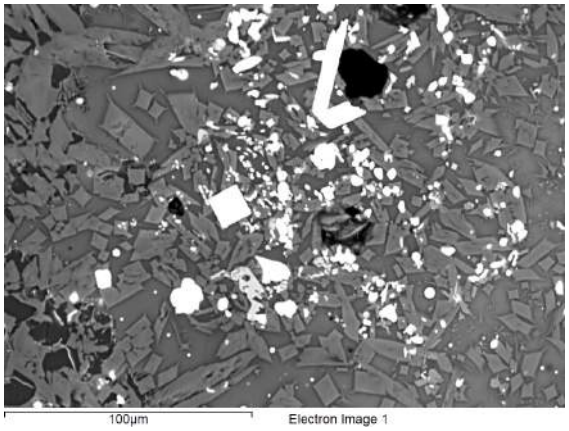

(d) Pyroxene (light grey) with tin oxide (white, angular) and bronze prills (white), Gordion-27609-S

Figure K.8: Pyroxene

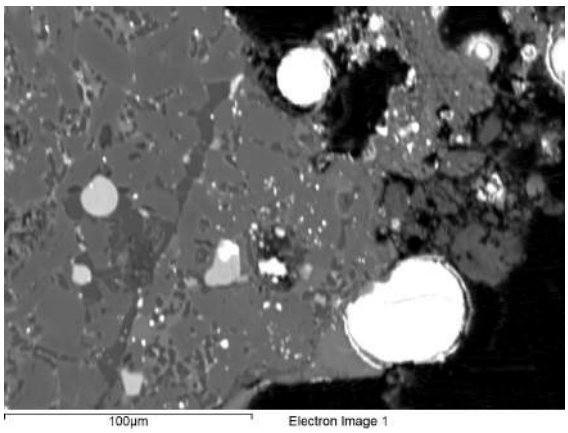

(a) Gordion-21299

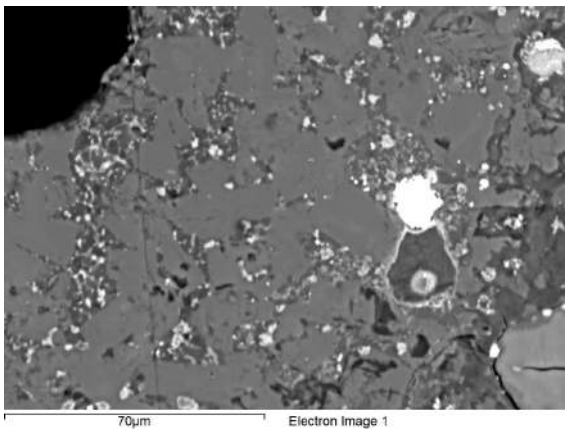

(b) Gordion-22673-A

Figure K.9: High-Ca augite (medium grey)

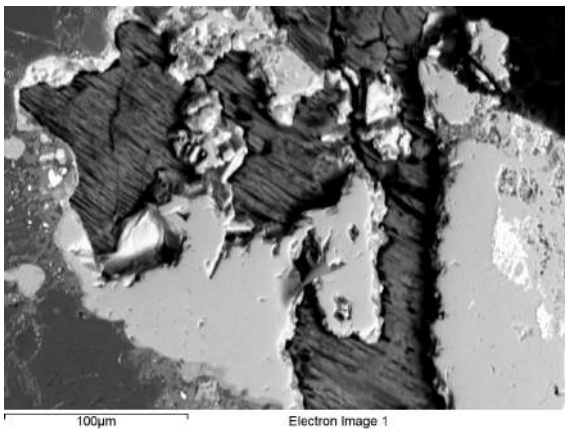

Figure K.10: Anhydrite (dark grey) in between Cu_2ClO_2-Cu_2ClO_3 (light grey) in Gordion-28877

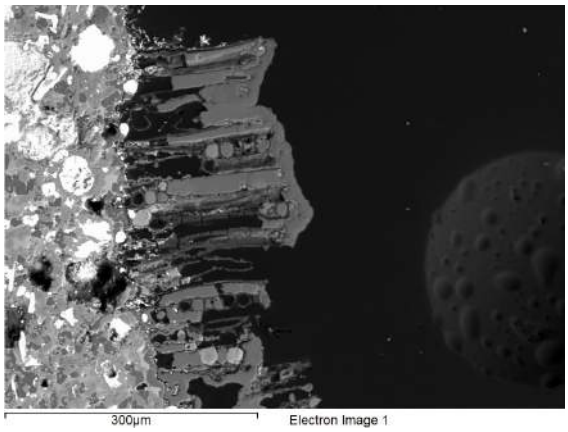

Figure K.11: Ca-Mg-peroxide (dark grey) in charcoal inclusion in Gordion-23797

Section K.3

Cu-bearing oxides

Various copper-bearing oxides occur in the Gordion crucible slag:

1. *Cuprite*: Most crucibles contain some cuprite (Cu_2O), which sometimes includes minor amount of Al, Si, Cl, Ca and Fe. It is however far less abundant than Cu_2ClO_2-Cu_2ClO_3, which occurs in similar quantities to cuprite in the Pi-Ramesse crucibles. Examples are shown in Figure K.12 and tiny cuprite prills (white) can be seen in Figure K.8a.

2. *Cu_2ClO_2-Cu_2ClO_3*: A range of copper-chlorine oxides occur with compositions varying from $\pm Cu_2ClO_2$ to Cu_2ClO_3. In some cases, copper is substituted by up to 6 at% Sn or up to 3.5 at% Si, 3 at% K, 3 at% Ca, 5 at% Fe and/or 1.3 at% Pb. These phases are very abundant and typically present as (post-depositional) corrosion products. They produce the conspicuous green products on the crucible interior. Some examples are shown in Figure K.13 and Figures K.7c. Figure K.14 shows three different occurrences of copper-chlorine oxide in a single sample.
   A few occurrences exist where this copper-chlorine oxide incorporates lead (resulting in $\pm Cu_3Pb_2Cl_3O_2$). Examples are shown in Figure K.15.

3. *Delafossite*: In three crucibles, a phase similar to delafossite ($CuFeO_2$) occurs, with an approximate (Cu,Sn)(Fe,Mg,Al,Si,Ca)O_2 composition (Cu/Sn ≈10, Fe/Si/Mg/Al/Ca ≈ 5/2/1/1/1 and sometimes a few at% Ti or Pb). Some examples are shown in Figure K.16.

4. *Cu-Sn oxides*: A range of copper-tin oxides occur, with highly variable composition. Examples of these bronze oxidation products are shown in Figure K.17.

5. *Cu(-Sn) silicates*: A whole range of copper silicates, copper-tin silicates and copper-tin-iron silicates occurs, the compositions of which are too variable to meaningfully summarise and illustrate. These are products of the variable oxidation of bronze and interaction with the crucible slag.

6. *CuCl*: See section 8.2.4.

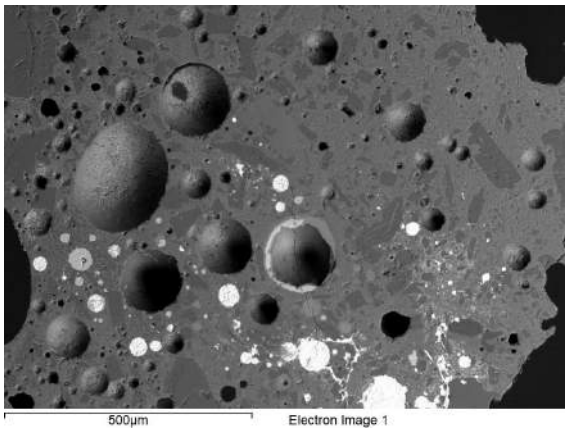

(a) Cuprite prills (bright), Gordion-27636

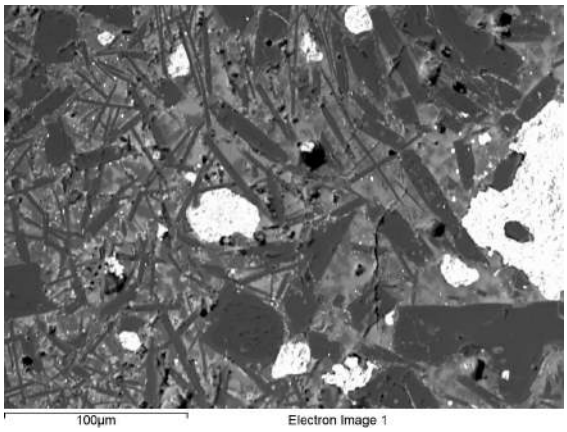

(b) Cuprite prills (bright) in between plagioclase (dark grey), Gordion-23797

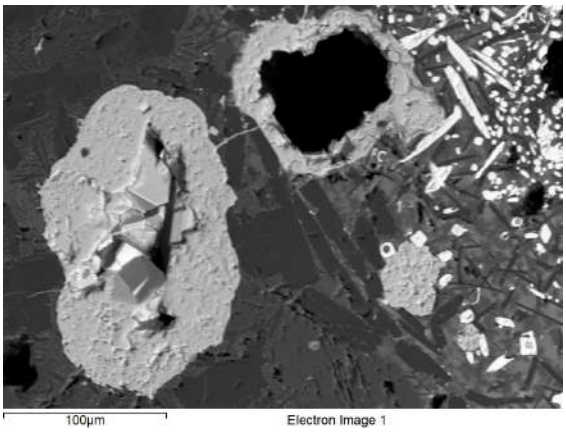

(c) Cuprite (light grey) crystallised in pore, Gordion-23797

Figure K.12: Cuprite

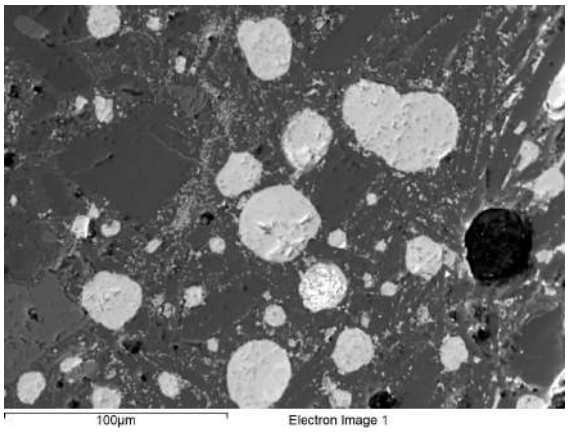

(a) Copper-chlorine oxide prills (light grey) in deeper slag, Gordion-28877

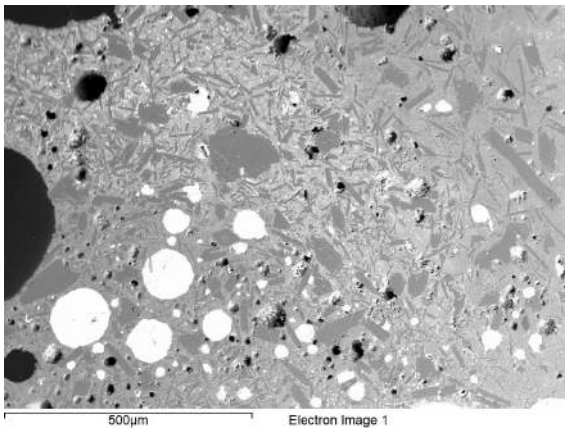

(b) Copper-chlorine oxide prills (bright) in deeper slag, Gordion-25394

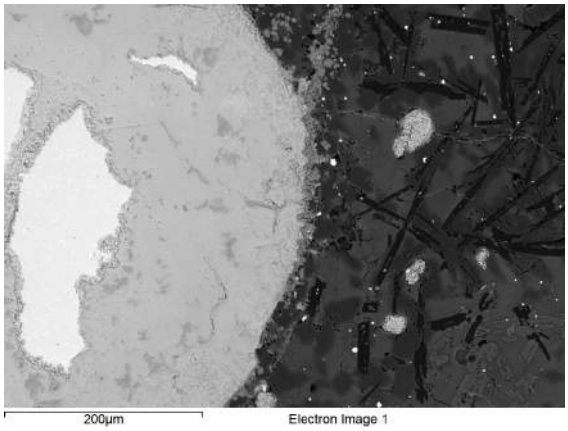

(c) Copper-chlorine oxide corrosion (light grey) around metallic bronze core (bright), Gordion-22958

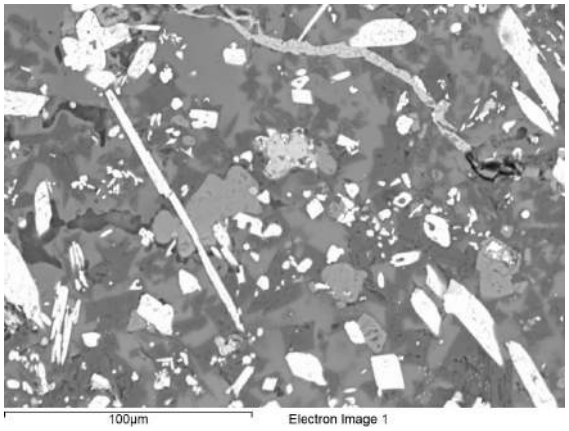

(d) Copper-chlorine oxide (light grey) with tin oxide (white), Gordion-25394

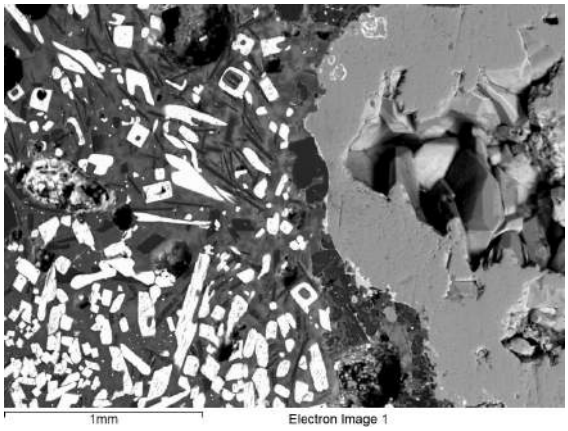

(e) Copper-chlorine oxide crystals (light grey) in pore, with tin oxide (white), Gordion-22999

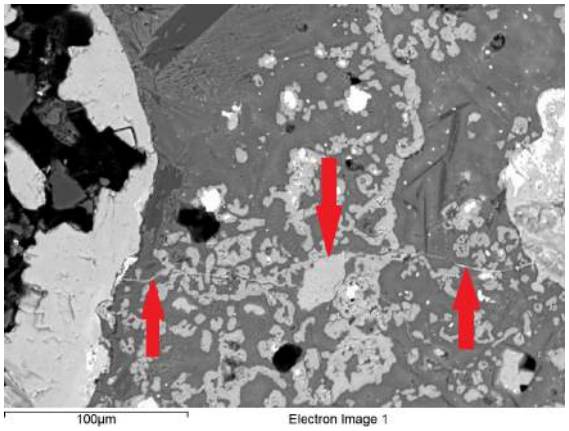

(f) String of copper-chlorine oxide (light grey, arrows) running through slag with spinel (light grey, slightly darker), Gordion-23329

Figure K.13: Cu_2ClO_2-Cu_2ClO_3

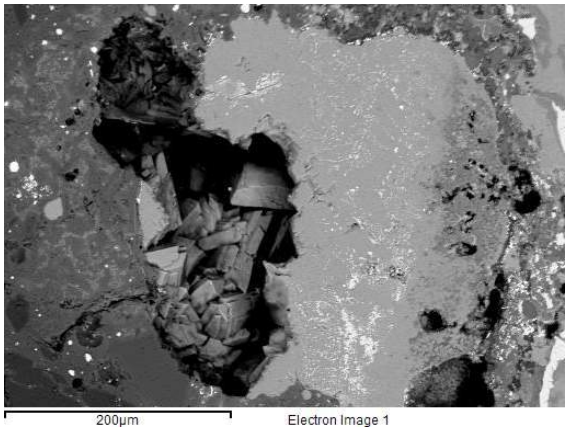

(a) Pore filled with copper-chlorine oxide (light grey)

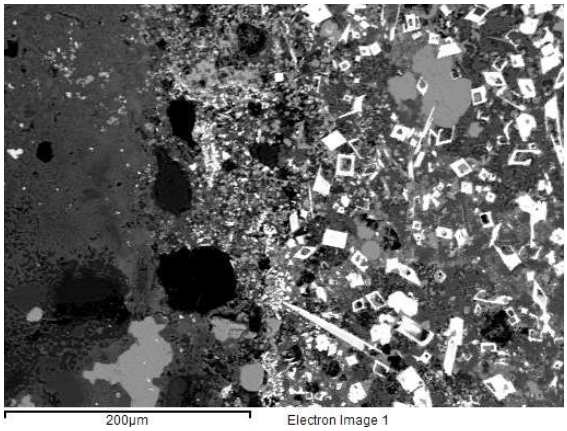

(b) Copper-chlorine oxide (light grey) in between other oxides in dross layer

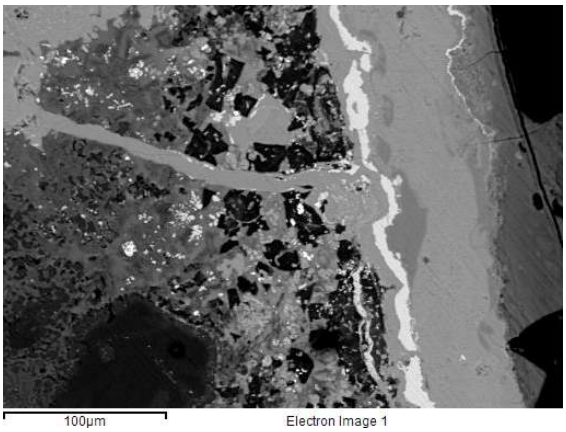

(c) Copper-chlorine oxide (medium-light grey) at interior crucible surface (with thin Cu_2S layer, light grey), running to interior

Figure K.14: Cu_2ClO_2-Cu_2ClO_3 in Gordion-28932 (2)

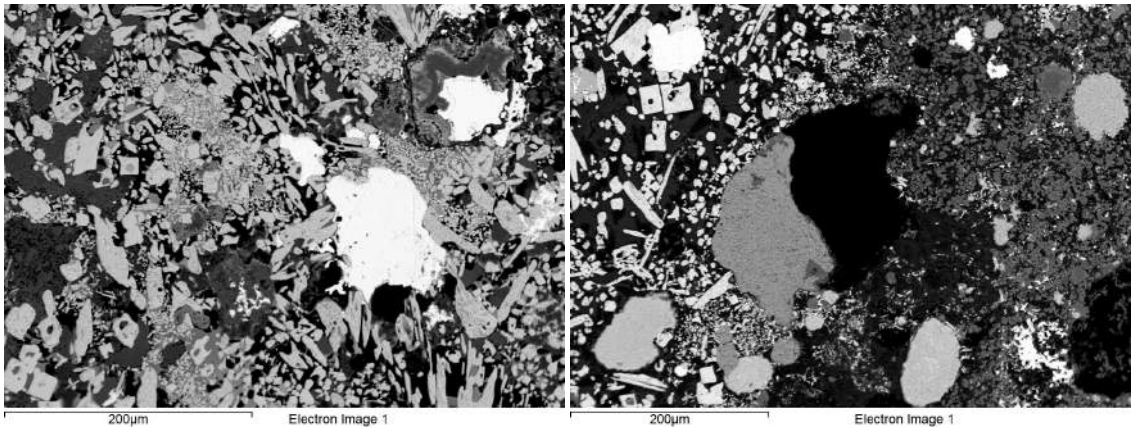

Figure K.15: $Cu_3Pb_2Cl_3O_2$ (white) in dross layer of Gordion-22673 (tin oxide is light grey)

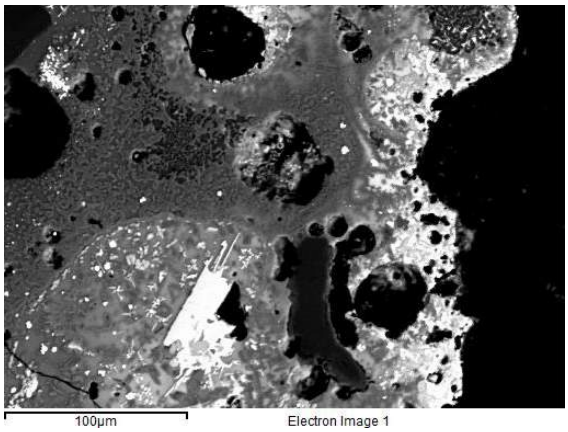

(a) Gordion-22626

(b) Gordion-25569-A

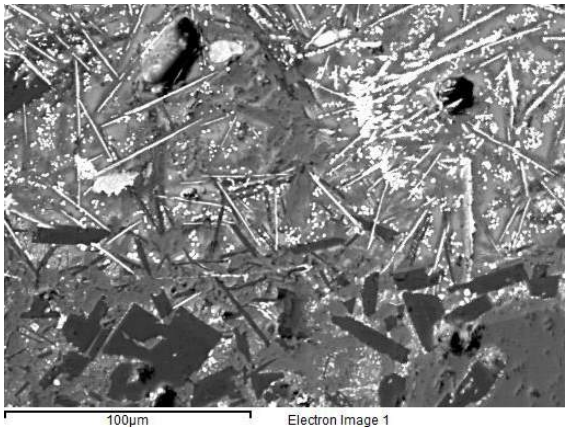

(c) Laths in Gordion-25569-A

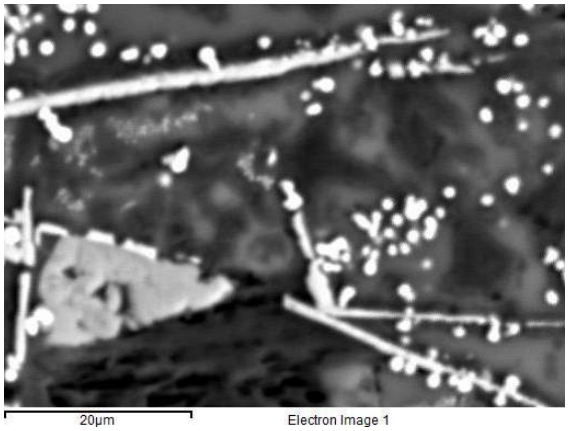

(d) Laths (close), Gordion-25569-A

Figure K.16: Delafossite (white)

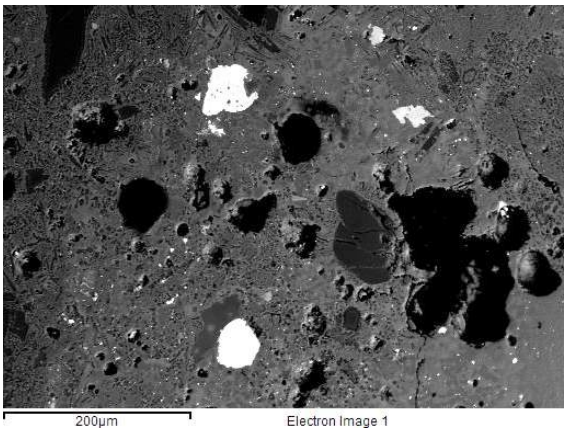

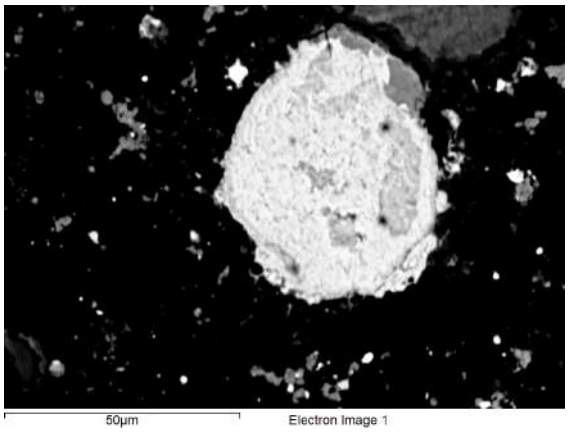

Figure K.17: Variable Cu-Sn oxides in Gordion-22626 and -22673-A

Section K.4

Sn-bearing oxides

The same two tin oxide types noted for Pi-Ramesse crucibles are found in Gordion:

1. *Tin oxide*: SnO_2 crystals occur abundantly in 61% of the analysed Gordion crucibles. The shape of these newly formed crystals shows the same variability as those seen in the Pi-Ramesse crucibles (see sections D.4 and 5.4.5.1 for further discussion), with some examples shown in Figure K.18.
   There are no clear examples of residual mineral cassiterite (see section 5.4.5.2 for examples) in the Gordion crucibles. The few examples showing some resemblance to mineral grains (though not convincing) are shown in Figure K.19. These clusters are mostly re-crystallised, but stand out due to the absence of associated copper-, iron- or other oxides (which point to tin burning out of bronze).

2. *Malayaite*: An oxide similar to malayaite ($CaSnO(SiO_4)$) occurs, though significant substitution occurs, resulting in an approximate $(Ca,Mg)(Sn,Fe)O((Si,Al)O_4)$ composition, with $Ca/Mg \approx 12/1$, $Sn/Fe \approx 7/4$ and $Si/Al \approx 2/1$. It has been noted in 26% of the Gordion crucible samples, typically in association with SnO_2 crystals. Some examples are shown in Figure K.20.

3. *Cu-Sn oxides and silicates*: See section K.3.

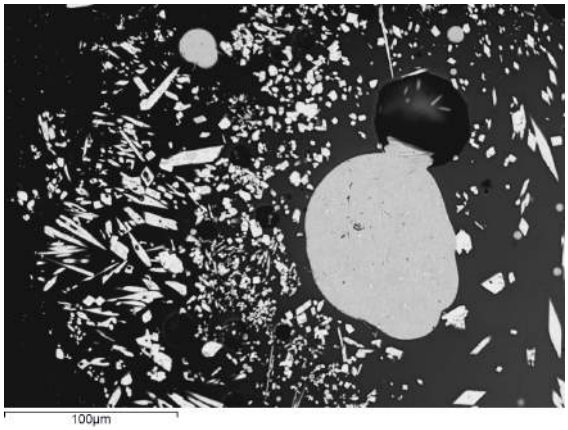

(a) Around (tin-depleted) leaded bronze prill, Gordion-23045-S

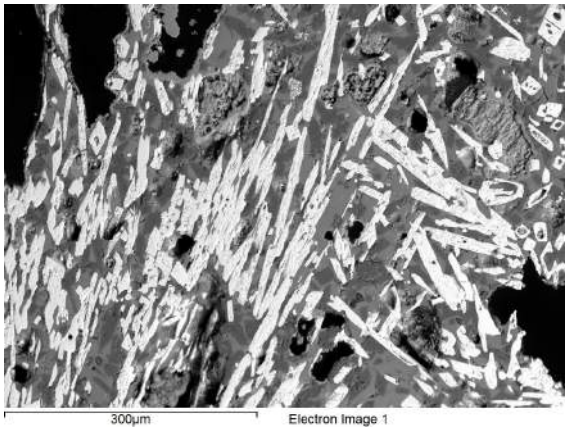

(b) Gordion-23797

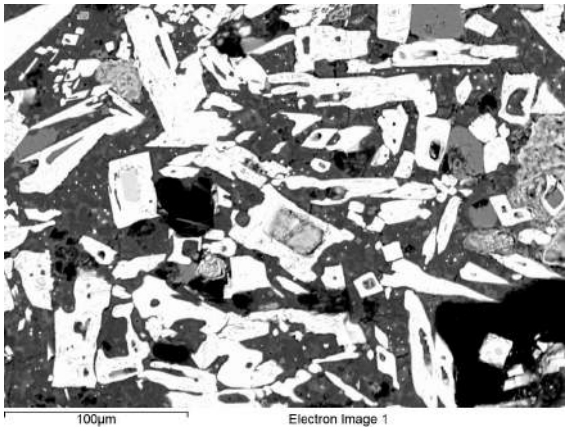

(c) With bronze core, Gordion-23329

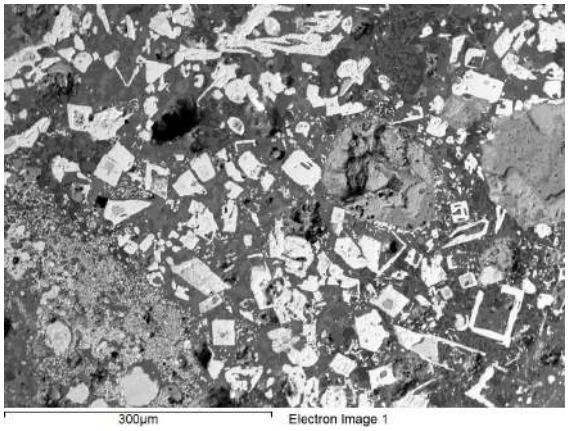

(d) With copper (oxide) in crystal core, Gordion-23797

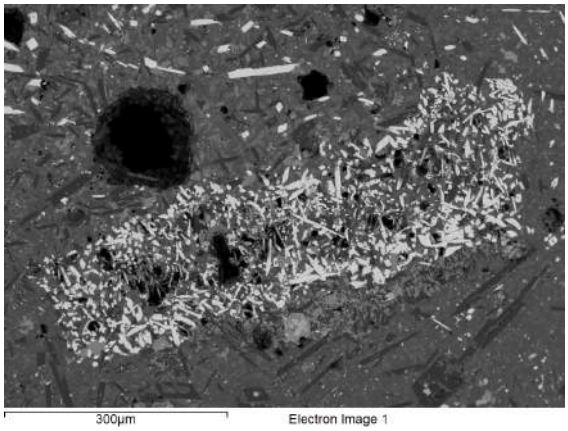

(e) Cluster, Gordion-25394

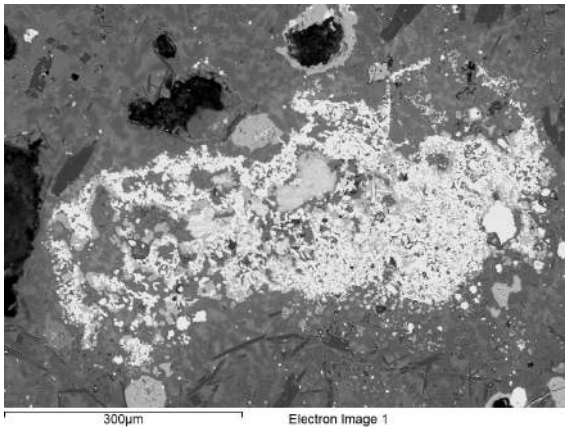

(f) Cluster with Fe- and Cu-oxides, Gordion-22958

Figure K.18: SnO_2 (bright, angular)

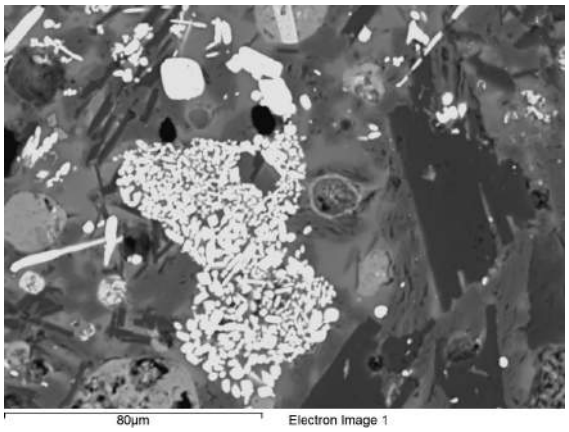

(a) Only good example of possible residual cassiterite, Gordion-25394-C

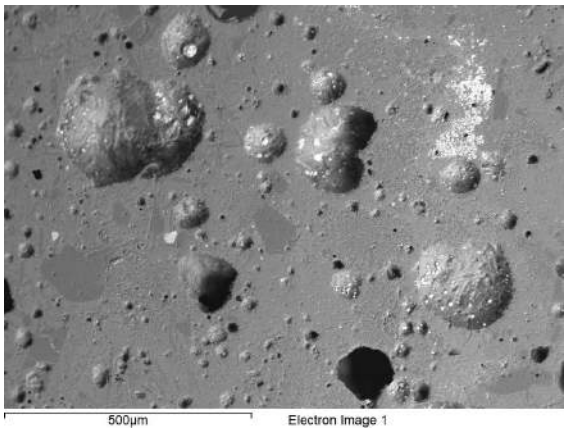

(b) Residual cassiterite (upper right)? Gordion-25394-A

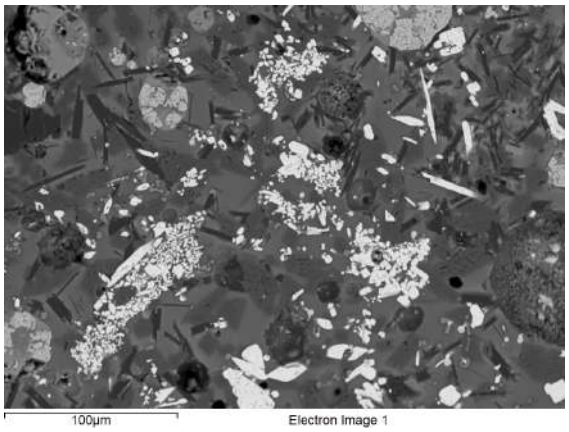

(c) Strongly re-crystallised cassiterite? Gordion-25394-C

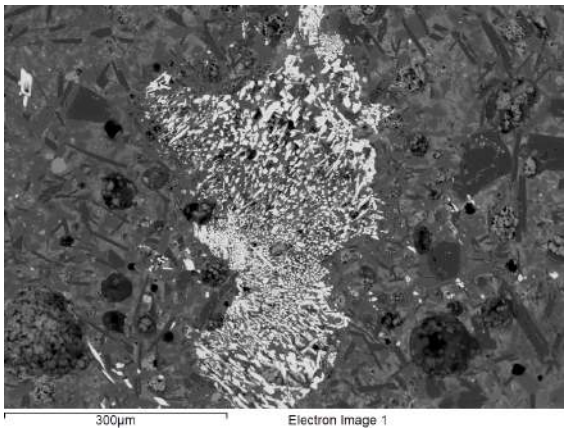

(d) Fully re-crystallised cassiterite? Gordion-25394-C

Figure K.19: Examples of (somewhat) cassiterite-like SnO_2 (bright)

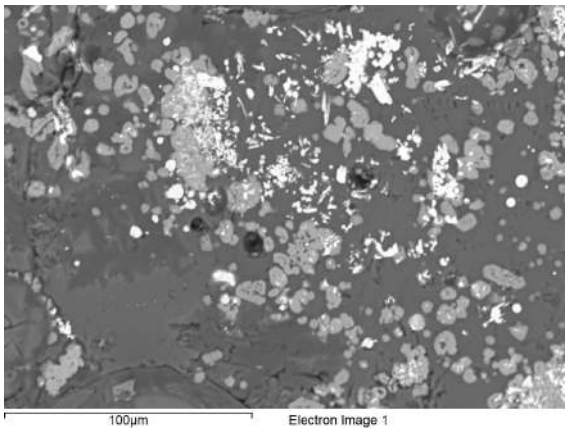

(a) Malayaite (light grey) with SnO_2 (white), Gordion-25568

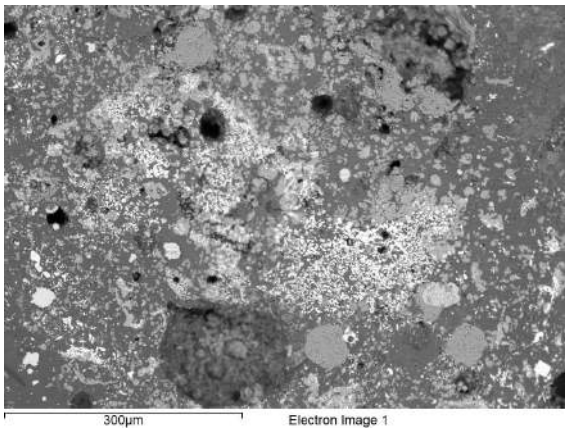

(b) Malayaite (light grey) with SnO_2 (white) and Cu-(Cl-)oxides (light-medium grey), Gordion-25568

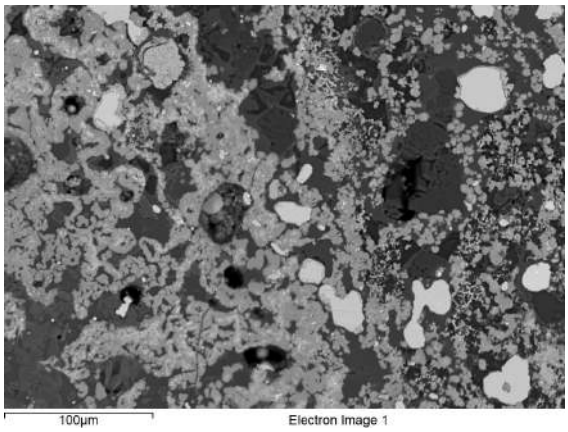

(c) Malayaite (medium grey) with bronze prills (light grey), Gordion-25568

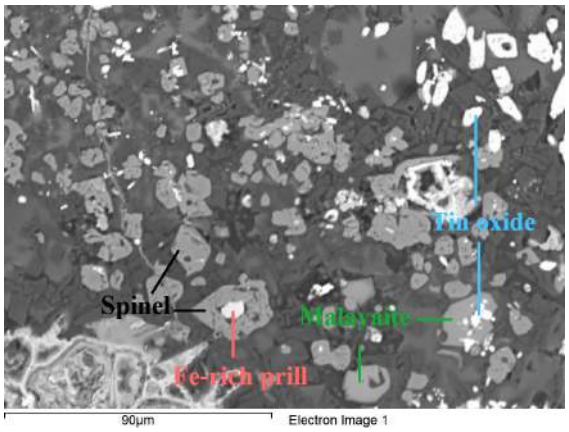

(d) Malayaite with tin oxide and iron-rich prills with spinel, Gordion-25394

Figure K.20: Malayaite

Section K.5

Pb-bearing oxides

Low lead levels occur in some of the copper and tin oxides (section K.3), but several lead-based oxides occur in some crucibles.

1. *Lead oxides and silicates*: Lead oxides and silicates of variable composition ($\pm Pb_3O_4$ and $\pm$(Pb,Cu)(Fe,Al)(Na,Mg,K,Ca)Si_2O_7) were measured in 20% of Gordion crucibles. In a few cases, lead-chlorine oxides ($(Cu,Pb)_3ClO$ - Pb_3ClO_2 and $Pb_2Ca_3(P,Cl)_3O_{11}$) have been noted too. Some examples are shown in Figure K.21.

2. *Lead sulphate*: PbSO4 (with 1-7 at% Cu) has been noted in Gordion 23128 (Figure K.22).

3. *Lead-potassium sulphite/sulphate*: A prill with approximate $PbK_2S_2O_7$ composition (or potassium sulphate K_2SO_4 + lead sulphite $PbSO_3$) has been noted in Gordion-27640, with a Cu_2ClO_3 layer surrounding it, as shown in Figure K.23.

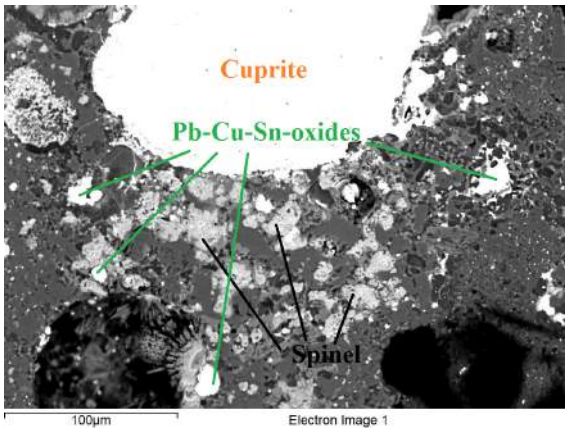

(a) Lead oxides (with copper and tin oxides) surrounding cuprite prill

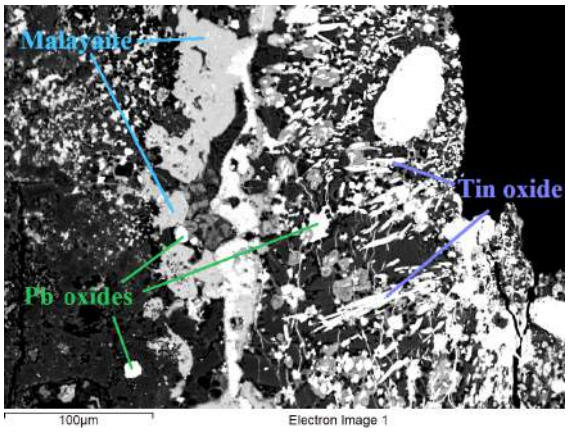

(b) Lead oxides (with copper and tin oxides) in drossy zone

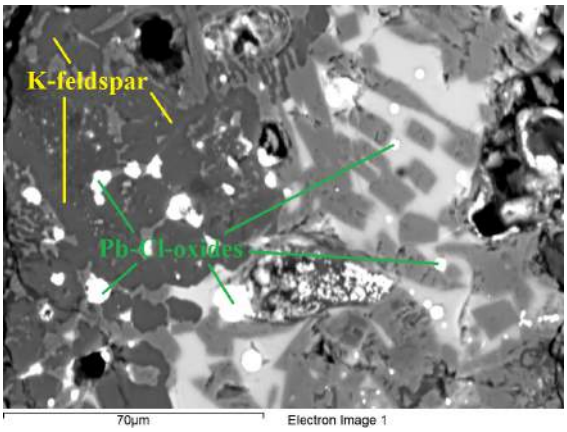

(c) Lead-chlorine oxides with K-feldspar in drossy zone

Figure K.21: Lead oxides in Gordion-22763-B

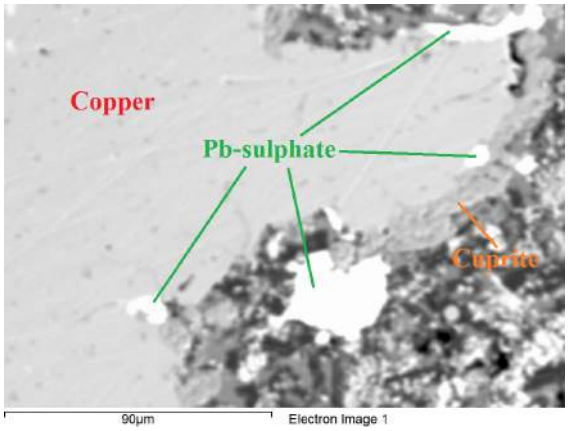

(a) Copper prill with cuprite edge and lead sulphate

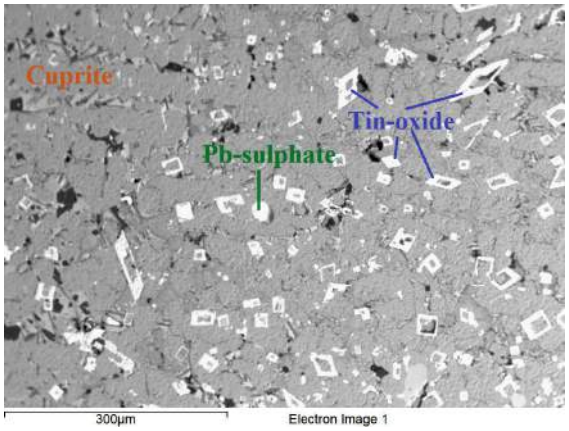

(b) Fully oxidised prill (all cuprite) with lead sulphate prills and tin oxide

Figure K.22: Lead sulphate in Gordion-23128

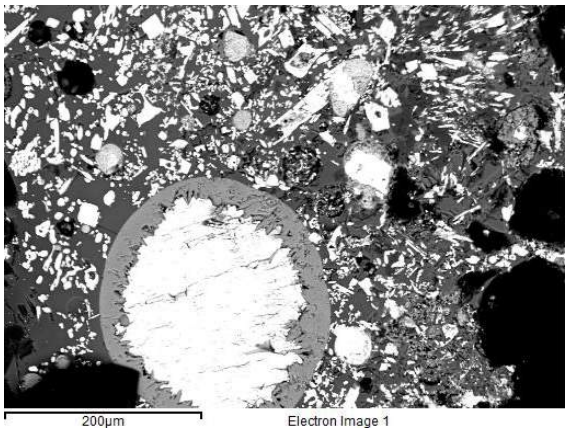

(a) $PbK_2S_2O_7$ (large white prill, lower left) with copper-chlorine oxide rim (light grey) and surrounding SnO_2 (white)

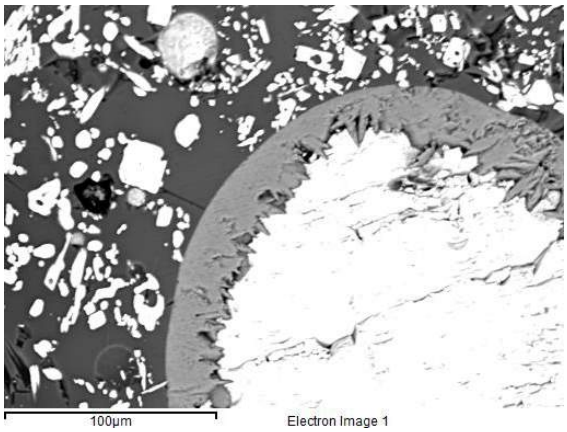

(b) $PbK_2S_2O_7$ with copper-chlorine oxide rim and surrounding SnO_2, close-up

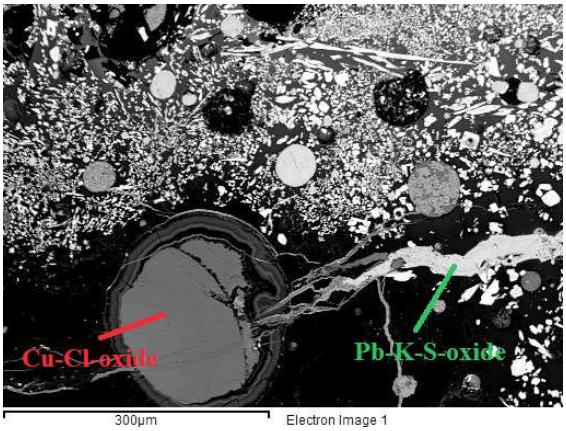

(c) $PbK_2S_2O_7$ crack filling and copper-chlorine oxide

Figure K.23: $PbK_2S_2O_7$ in Gordion-27640

APPENDIX L

Composition of metallic prills

Oxidised prills are omitted. Where an abundance of *1+* is noted, this refers to one measured prill, but probably more of similar composition present in the crucible slag. *Micro* refers to tiny prills dispersed throughout the crucible slag, which are too small to measure.

Composition of metallic prills in crucible slag (in wt%)

Sample	Abundance	Cu	Sn	Fe	As	Sb	Co	Ni	Pb	Ag	Zn	S	Cl
Gordion 21299 - 15.10.2013	/												
Gordion 22529 - 13.9.2013	Multi									95-96			4-5
	Multi	1		0.5						91			7.5
	Multi	95.2	2.7	0.4	0.6	1.1							
	Multi	90-94		0-1						6-10			
Gordion 22626 - 15.10.2013	Multi	99.4		0.6									
	1+ (small, 3 ϕ)	44.6	17	37.4							1		
	→ *phase a*	75.1	13.5	7.3							4.1		
	→ *phase b*	2.6		97.4									
		3.5		96.5									
	→ *phase c*	5.1	1.8	93.1									
	1 (small, 2 ϕ)												
	→ *phase a*	1.9		98.1									
		2.6		97.4									
	→ *phase b*	62.2	30.6	7.2									
		63.6	23.7	10.1							2.7		
Gordion 22673 - 15.1.2014	/												
In corr layer	Multi	70.8	27.7						1.5				
	Multi	63.5	0.5										36
Gordion 22673-A - 15.10.2013	Multi	82-92	7.5-16.5	0.5-1.5									
	1+	73.4	25.1	1.5									
Gordion 22673-B - 15.10.2013	/												
Gordion 22829 - 15.10.2013	/												
Gordion 22958 - 9.4.2013	1+	65.8	32.5	0.6					1.1				
	1+	92.8	7.2										
	Corrosion	*52.2*	*17.3*	*1.5*					*1.9*				*27.1*
	1+	57.2	42.3	0.5									
Gordion 22999 - 13.9.2013	Multi	92-94	6-8										
Gordion 23045-A - 15.10.2013	/												
Gordion 23045-B - 15.10.2013	Multi	81.5-86	10-16	1.1-1.4	1.4-3								
	1+	75.9	20.4	1.4	2.3								
	Multi	62.5-64.5	32.8-33.8	1.5-2.1	1-1.6								
Gordion 23045-S - 15.10.2013	1+ (CuCl)	63.5		0.4									36.2
	1+ ($Cu_5Pb_2O_7$)	31.9							41.6				26.5
	1+	97	1.2						1.8				
	1+	98.1		0.6	1.3								

Composition of metallic prills in crucible slag (in wt%)

Sample	Abundance	Cu	Sn	Fe	As	Sb	Co	Ni	Pb	Ag	Zn	S	Cl
Gordion 23128 - 13.9.2013	Multi	100											
	1+	97	3										
Gordion 23329 - 9.4.2013	Multi	90.7-91.1	5.1-5.7	3.5-4.2									
In corr layer	Multi	97-99	1-3										
Gordion 23329 - 15.1.2014	1	98.1	1.9										
	Inclusion	80.1										19.9	
	Inclusion (ox)	21.5							64.9				10.3
	1+	95.8		1.3	2.9								
	1+	98.8		1.2									
Gordion 23523 - 15.10.2013	/												
Gordion 23707 - 9.4.2013	Multi	97-98		2-3									
In corr layer	/												
Gordion 23707 - 15.1.2014	1+	66.8											33.2
	Multi	96.7-99		1-3.3									
Gordion 23778 - 13.9.2013	Multi	89-91	7.5-9.5	1.5-2									
	Multi	73-74	23-24	1-1.5	1-2				0-0.9				
	Multi	66.7-67.7	30-31	0.7-1					1.3-1.6				
Gordion 23797 - 9.4.2013	1+	57.6	42.4										
	1+	45.8	51.6				2.7						
Gordion 25368 - 13.9.2013	1+	60.5	39.5										
	Pb inclusion	55.2	36.3						8.5				
	Multi	71-74	25-28.5	0.5-0.6									
	1+	93.5	6.1	0.5									
Gordion 25394 - 9.4.2013	1+	88.8	7.9	3.3									
Gordion 25394_A - 13.9.2013	Multi (tiny)	81-83	13-14.6	1.4-1.8	1.1-2.8								
Gordion 25394_B - 13.9.2013	1+	98.7		1.3									
Gordion 25568 - 9.4.2013	1 (large, 3 ϕ)	73.6	22.8		0.1				3.5				
	→ *phase a*	84	16										
	→ *phase b*	67-69	31-33										
	→ *phase c*	55-61	11.5						27.5-33.5				
	Multi	82-89	11-15	0.5-09	0-1.1								
	1+	87.6	7	4.4	1.1								
	1+ *(corr)*	95.5	3.1						1.4				
	Multi	60-74	23-34						0-8				
	Multi	85.5-97.5	2.5-14.5										
	1+	91.8	7.2						1.1				
Gordion 25568 - 15.1.2014	Multi	56-61	35-39	1.1-2.3				0.6-0.9	1.5-1.6				
Gordion 25569-A - 15.10.2013	Multi	99		1									
Gordion 25569-B - 15.10.2013	Multi	92-98.5	0-4	1.5-4									
Gordion 26891 - 9.4.2013	Multi	96.5-99.5		0-0.5		0.5-3							
	1+	90	5.9	4.1									
	1+	62.7	1.5		1.5	3.4			31				
	1	99.1	0.9										
	Pb inclusion	62.1	1.4			0.8			35.7				
	1	99.1	0.9										
	Inclusion	*approximately* $Pb_4Cu_5Cl_4O_6$											
	Corrosion	Cu_2O *corrosion*											
	1	97.4	2.6										
	Inclusion	*approximately* $Pb_6Cu_3Cl_5O_5$											
Gordion 27609 - 15.10-2013	/												
Gordion 27609-S - 15.10.2013	1+ *(CuCl)*	64.2											35.8
	1+	92.8	6.4										0.8
	Multi	88-95	4-11	0-4	0-1								
Gordion 27613_A 13.9.2013	/												
Gordion 27613_B - 13.9.2013	/												
Gordion 27629 - 15.10.2013	/												
Gordion 27634 - 12.11.2013	1 *(in pore)*	2.9	0.7	96.4									
Gordion 27635 (1) - 12.11.2013	/												
Gordion 27635 (2) - 12.11.2013	1+	75	21.6	2					1.4				
	Multi	74-84	15-25	0.5-0.8									
	1+	98.4		1.6									
Gordion 27636 - 9.4.2013	1+	88.1	10.2	1.7									
	1+	91.7	6.9	1.5									
	1+	90.4	7.4	2.2									
Gordion 27638 - 12.11.2013	1+ (tiny)	7.5		90.6	1.9								
		(+ 1-3 wt% Al, Si and Ca)											
Gordion 27640 - 12.11.2013	1+	96.5	3.5										
	1+	94.7	0.7	0.6	3.9								
	Multi	93-95	4-5						1-2				
	Multi	94-95	2.6-3.1		0.8-1.1				1.7				

Composition of metallic prills in crucible slag (in wt%)

Sample	Abundance	Cu	Sn	Fe	As	Sb	Co	Ni	Pb	Ag	Zn	S	Cl
In corr layer	/												
Gordion 27734 (1) - 12.11.2013	1+	97.6	2.4										
	1+	75.4	22.6	1				0.9					
	Multi	62-66	33.5-37	0.4-1.2				0-0.8					
Gordion 28218 - 12.11.2013	1+	92.1	7.1	0.8									
Gordion 28236 - 9.4.2013	1+	100											
		(with Cu-Cl-ox corrosion)											
Gordion 28877 - 9.4.2013	Multi	96-99		1-4									
Gordion 28932 (1) - 12.11.2013	Multi	93-95	3-6.5	0.5-1.4	0-1.6								
	1+	99		1									
	1+	98.7		0.6	0.7								
Gordion 28932 (2) - 12.11.2013	Multi	99-99.6		0.4-1									

APPENDIX M

Metals analysis

Section M.1

Analysis of metal spills and objects

Five samples of corroded metal spills and objects were analysed by the author (one from find bag 25545 and four from 22611, which contains several more corroded pieces). Samples were mounted in resin, ground and polished (procedure as outlined for crucibles, sections 3.2.3 and 3.3.3), and analysed by optical microscopy and SEM-EDS. Detailed discussion of the various corrosion products is beyond the scope of this research. The aim here is to approximate the original alloy composition of the (partially) corroded samples. All compositional results are presented in wt%.

Find bag 25545 contains samples from Operation 1, Locus 7, Lot 14, phase 410.18 (Late Phrygian)[1] and find bag 22611 contains samples from Operation 1, Locus 82, Lot 162, phase 420 (Late Phrygian)[2].

M.1.1 Gordion-25545

This sample of a metal spill is entirely corroded, with only tiny metallic fragments remaining. Some remnant dendritic structure can be seen, indicative of an as cast structure. The

[1] Oval pit, cut above ruins of Building I, east end of trench. Lot took out fine ashy brown soil, charcoal 'stains'. Dark 'greasy' soil, lumps of mud brick; hard yellow clayey lense at bottom.

[2] Description C, Appendix I.

corrosion products are predominantly copper oxides and chloride(-oxide)s, with variable amounts of tin and lead. Minor Fe and Ni are noted in some areas as well. This is illustrated in Figure M.1 and Table M.1. Some of the oxides (e.g., tin oxides, third image) were probably formed at high temperature before post-depositional corrosion of the spill. The exact original composition of this spill is difficult to reconstruct, but it was most likely a leaded tin bronze.

M.1.2 Gordion-22611: ring

This sample appears have been cast into a ring-shaped form with a rectangular edge and subsequently corroded, as shown in Figure 8.35. Some micrographs are shown in Figure M.2, with matching compositions in Table M.2. The ring has a metal core, with both lead-rich and cuprite inclusions, and with various oxide and chloride(-oxide) corrosion products surrounding and penetrating the metal core. Its bulk composition is approximately 90-92 wt% Cu, 6-7 wt% Sn and 1-1.5 wt% Pb.

M.1.3 Gordion-22611: large fragment

This is the largest fragment in find bag 22611, shown in Figure 8.36. Micrographs are shown in Figures M.3 and M.4, with matching compositions in Table M.3.
It is characterised by a metallic core (varying from pure copper to leaded tin bronze with approximately 6-12 wt% Sn and 0-2 wt% Pb) with large amounts of SnO_2 high-temperature crystals, formed during oxidising casting conditions. Image 6, spectrum 3 shows the core of such a tin oxide crystal filled with highly leaded copper.
Surrounding (and in some areas penetrating) this metallic core, various oxide and chloride(-oxide) corrosion products occur. This object probably had a similar original composition to Gordion-22611 ring.

M.1.4 Gordion-22611: medium fragment

Micrographs are shown in Figure M.5, with matching compositions in Table M.4.
This sample is a solid metallic prill with a dendritic, as cast structure, and limited corrosion (chloride and sulphide oxide) on its exterior surface. The prill consists of leaded tin bronze, with an approximate composition of 89-90 wt% Cu, 8-9 wt% Sn and 1.5-2 wt% Pb. The lead is present as insoluble inclusions (Cu-Pb-Cl oxides) in a dendritic tin bronze (tin content varies from 2 to 26 wt% between the dendrite core and outer dendrite layers). This

lead was probably originally present as metallic droplets dispersed throughout the bronze, but preferentially corroded post-depositionally to (Cl-)oxides. Note the minor presence of antimony as well.

M.1.5 Gordion-22611: small fragment

Micrographs are shown in Figure M.6, with matching compositions in Table M.5.
This sample is again a small drop with metal core and corroded exterior. No lead is present in this prill. It appears to be a tin bronze with an approximate tin content of 10-11 wt% Sn, with intergranular corrosion connected to the exterior corrosion layer, comprising copper and copper-tin oxides and chloride(-oxide)s.

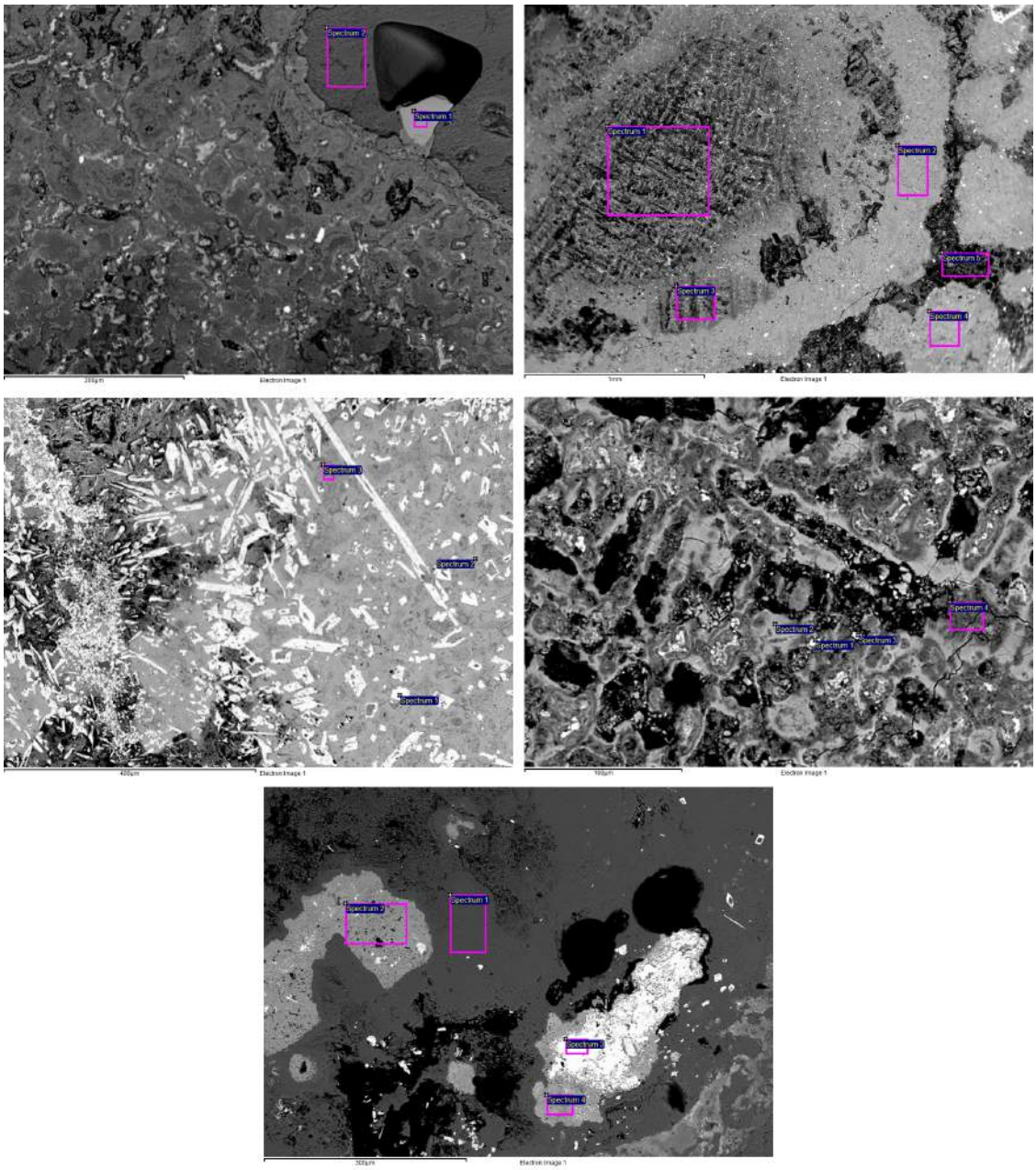

Figure M.1: Gordion-25545

	O	Si	S	Cl	K	Ca	Fe	Ni	Cu	As	Sr	Sn	Pb	Total
Image 1														
Spectrum 1	24.3		13.0		13.4				2.4				46.9	100
Spectrum 2				35.5					64.5					100
Image 2														
Spectrum 1	22.5	4.1		8.3			0.5		33.7	1.1		27.1	2.8	100
Spectrum 2	18.7	047		1.8					62.4	1.1		13.6	1.9	100
Spectrum 3	23.3	2.4		10.1					39.8	1.1		20.4	2.9	100
Spectrum 4	19.5	0.3		1.7					65.9	0.8		11.8		100
Spectrum 5	30.5	2.0	0.3	4.7			0.9		21.5	2.2		35.2	2.8	100
Image 3														
Spectrum 1	28.2								1.4			70.5		100
Spectrum 2	18.6	0.4		0.5					59.3	0.9		18.4	2.0	100
Spectrum 3	15.0			2.4					74.1	0.5		6.8	1.2	100
Image 4														
Spectrum 1	5.6	1.3		0.6				2.1	46.0	0.9		42.3	1.2	100
Spectrum 2	23.9	3.7		2.3			0.9	0.5	12.6	2.1		49.8	4.2	100
Spectrum 3		0.3		0.8				1.9	59.9			37.0		100
Spectrum 4	22.4	0.7		14.9					51.0			9.3	1.7	100
Image 5														
Spectrum 1	20.1			17.8					62.2					100
Spectrum 2	10.2	0.6		0.7					87.5			1.1		100
Spectrum 3	19.5		10.9								1.4		68	100
Spectrum 4	26.7		15.2	0.4	16.5	1.0			2.1		6.1		32.0	100

Table M.1: Compositional analysis Gordion-25545 (in wt%)

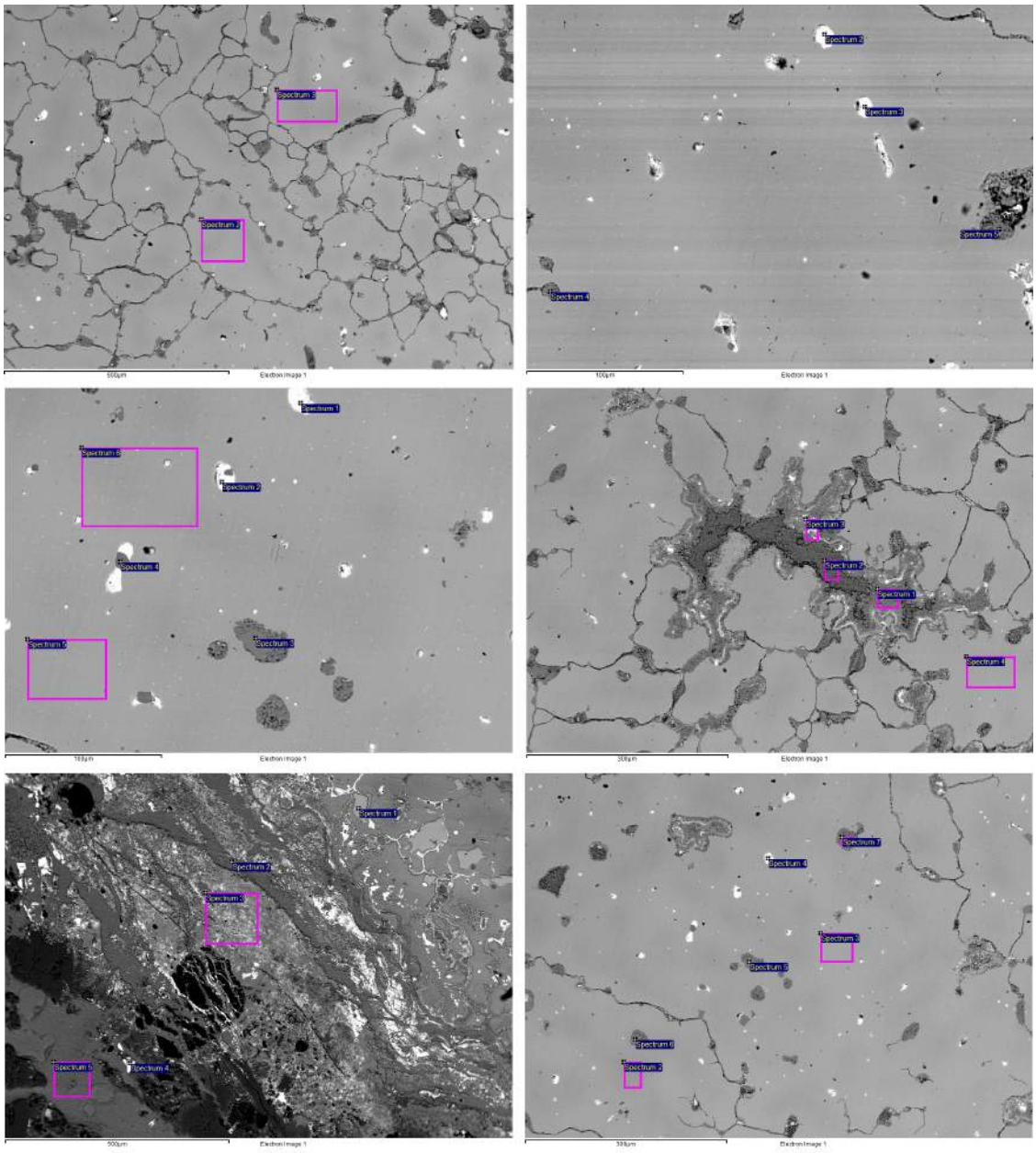

Figure M.2: Gordion-22611: ring

	O	P	S	Cl	Fe	Cu	Mo	Sn	Pb	Total
Image 1										
Frame analysis	1.7			1.3	0.4	89.6		7.1		100
Spectrum 2						92.6		7.4		100
Spectrum 3					0.4	94.2		5.4		100
Image 2										
Frame analysis						92.2		6.3	1.5	100
Spectrum 2				14.5		12.9			72.6	100
Spectrum 3				11.5		8.5			80.0	100
Spectrum 4	10.5					88.7		0.8		100
Spectrum 5	11.6					88.4				100
Image 3										
Spectrum 1				13.7		20.3			66.0	100
Spectrum 2				13.3		15.5			71.2	100
Spectrum 3			20.5			79.5				100
Spectrum 4			22.6		2.9	74.6				100
Spectrum 5						93.8		6.2		100
Spectrum 6					0.4	93.3		6.3		100
Image 4										
Spectrum 1	12.5					84.3		2.2	1.0	100
Spectrum 2				34.3		65.7				100
Spectrum 3	13.3		3.4	0.3		52.0		5.9	25.0	100
Spectrum 4						95.2		4.8		100
Image 5										
Spectrum 1					0.5	92.4		7.2		100
Spectrum 2				32.6		67.4				100
Spectrum 3	11.3	0.6		2.0		70.7	1.7		13.8	100
Spectrum 4	13.8		10.5			5.1			70.6	100
Spectrum 5	2.3			33.6		64.2				100
Image 6										
Frame analysis	2.2			0.6		90.3		6.9		100
Spectrum 2					0.4	96.2		3.4		100
Spectrum 3					0.3	92.7		7.0		100
Spectrum 4				18.2		12.7			76.6	100
Spectrum 5			20.4			79.6				100
Spectrum 6			20.8			79.2				100
Spectrum 7	10.6			0.3		89.1				100

Table M.2: Compositional analysis Gordion-22611: ring (in wt%)

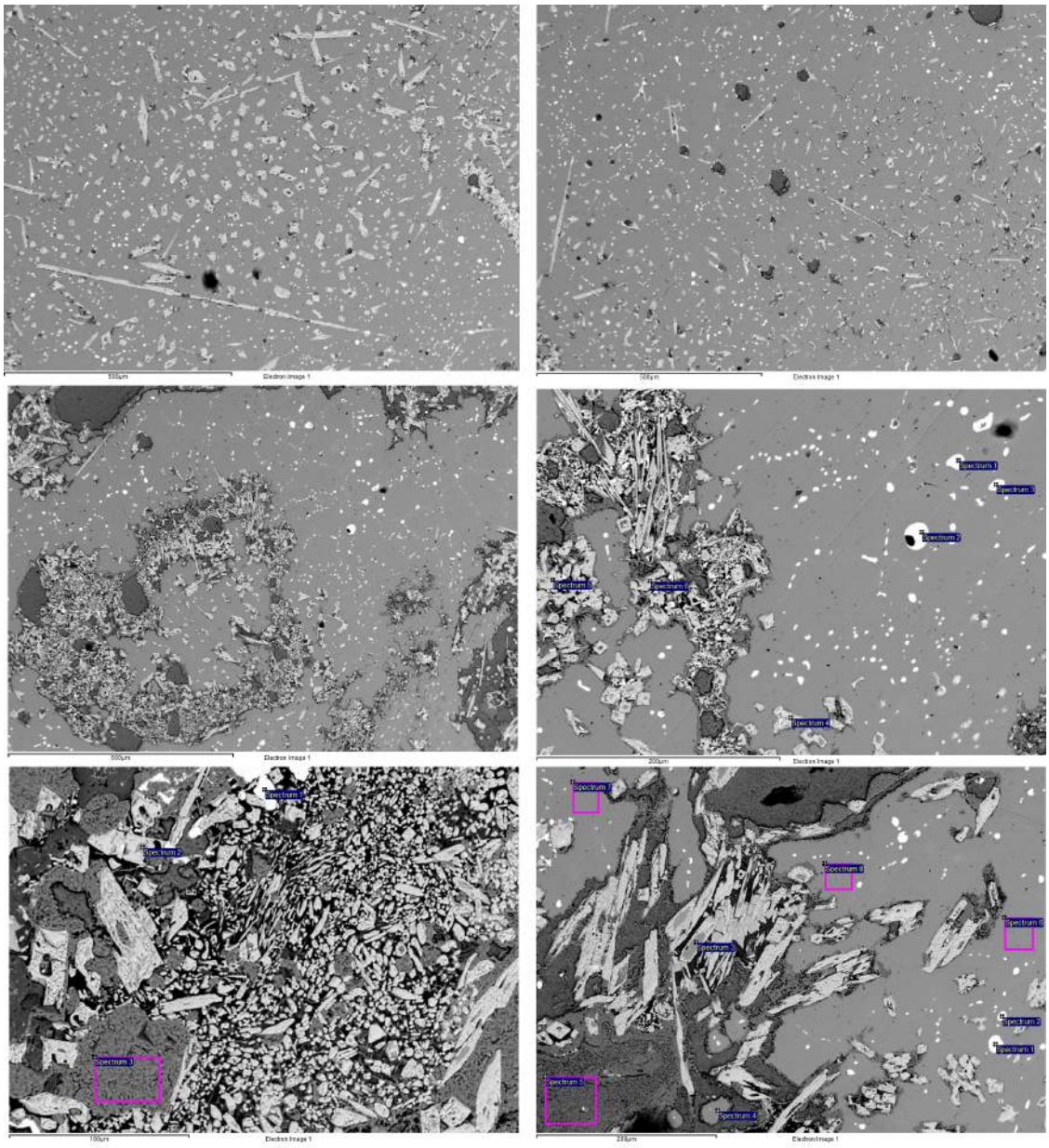

Figure M.3: Gordion-22611: large fragment

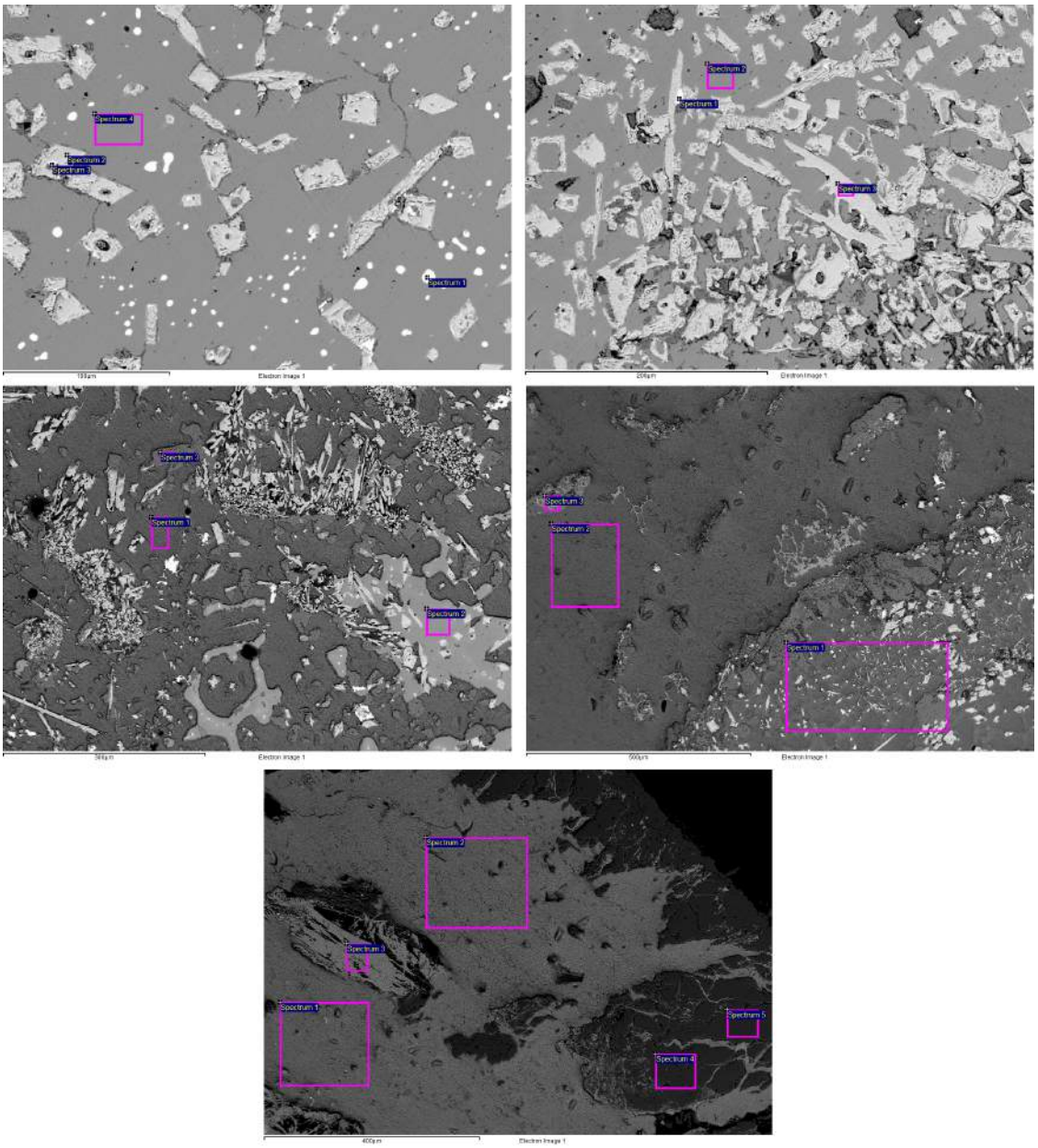

Figure M.4: Gordion-22611: large fragment

	O	Si	S	Cl	Fe	Co	Cu	As	Sn	Sb	Pb	Total
Image 1												
Frame analysis	3.4			0.4			81.3		12.9		2.0	100
Image 2												
Frame analysis	2.0			0.4			89.7		6.3		1.6	100
Image 3												
Frame analysis	5.3	0.6		3.8	0.6		74.9	0.7	12.0		2.3	100
Image 4												
Spectrum 1	8.1						6.8	4.8		6.5	73.8	100
Spectrum 2	8.8						4.0	7.5		3.2	76.5	100
Spectrum 3	5.6						10.5	4.6		3.4	75.8	100
Spectrum 4	26.6						2.4		71.1			100
Spectrum 5	26.7						0.6		72.7			100
Spectrum 6	25.3						1.6		73.1			100
Image 5												
Spectrum 1	14.9		11.1				1.0				73.1	100
Spectrum 2	1.5						92.9		4.0		1.5	100
Spectrum 3	10.4			0.3			89.4					100
Image 6												
Spectrum 1	9.1						5.5	6.0		4.0	75.4	100
Spectrum 2	6.3						21.9	3.9		4.5	63.5	100
Spectrum 3							93.4				6.6	100
Spectrum 4	1.0						99.0					100
Spectrum 5	9.1			6.9			84.0					100
Spectrum 6							100					100
Spectrum 7							100					100
Spectrum 8							100					100
Image 7												
Spectrum 1	11.3						8.5	3.6		14.0	62.6	100
Spectrum 2	26.0						2.0		72.0			100
Spectrum 3	16.6	1.2			4.2	0.9	10.2	1.8	5.3	19.7	39.6	100
Spectrum 4							100					100
Image 8												
Spectrum 1	13.2		7.3				5.0		26.1		48.4	100
Spectrum 2							100					100
Spectrum 3	27.9						1.8		70.3			100
Image 9												
Spectrum 1				34.3			65.7					100
Spectrum 2							100					100
Spectrum 3	9.7			0.3			90.1					100
Image 10												
Spectrum 1	12.0	0.5		20.7			50.3		13.4	1.0	2.2	100
Spectrum 2	3.0			32.5			64.5					100
Spectrum 3	12.1			2.4			72.4		11.4		1.8	100
Image 11												
Spectrum 1	3.2			31.6			65.2					100
Spectrum 2	3.0			32.6			64.4					100
Spectrum 3	10.6	1.0		0.4			87.1		1.0			100
Spectrum 4	22.3			16.1	0.3		61.3					100
Spectrum 5	22.8			17.0			60.2					100

Table M.3: Compositional analysis Gordion-22611: large fragment (in wt%)

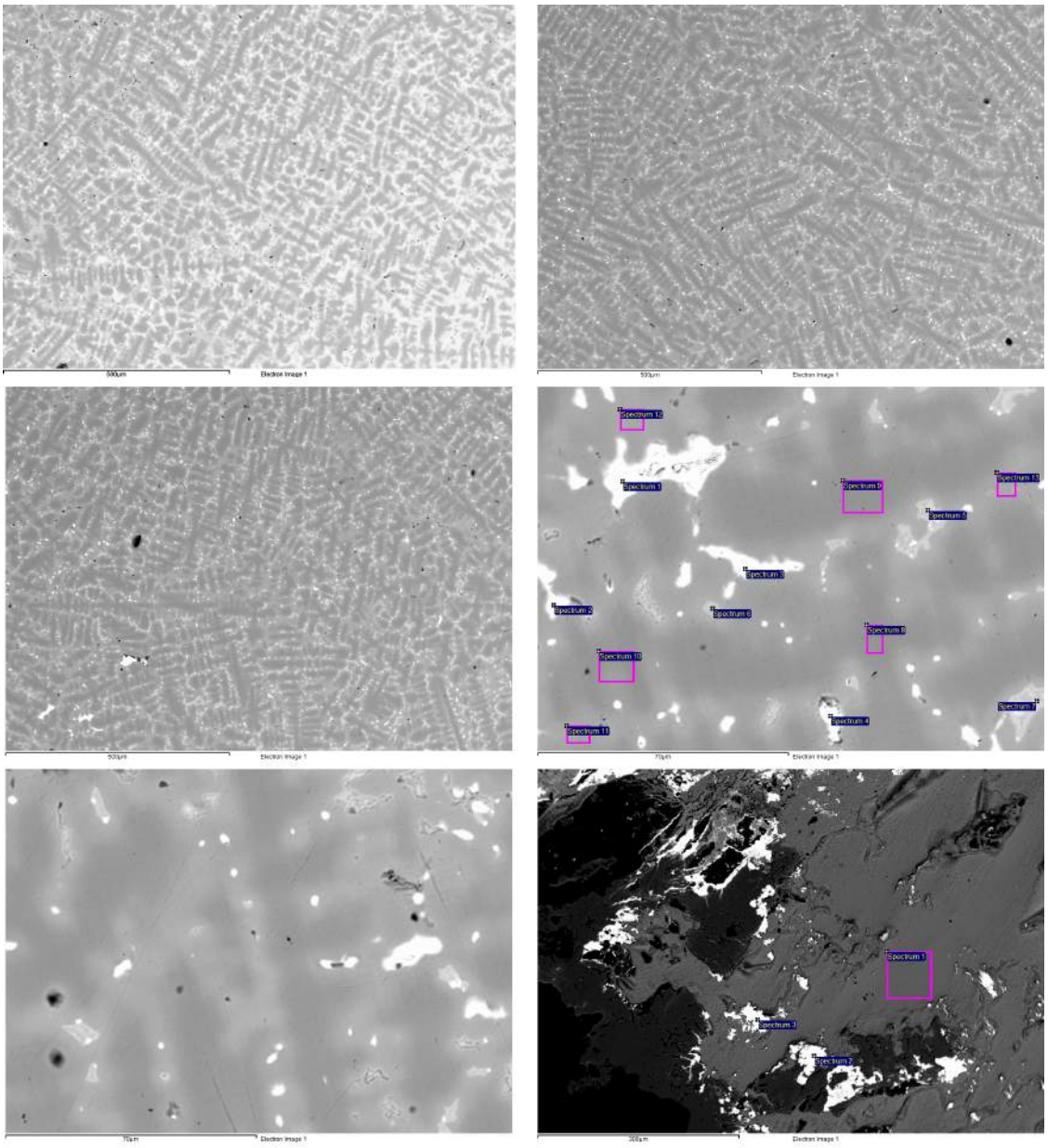

Figure M.5: Gordion-22611: medium fragment

	O	S	Cl	Cu	As	Sr	Sn	Sb	Pb	Total
Image 1										
Frame analysis				89.7			8.4		2.0	100
Image 2										
Frame analysis				90.3			8.2		1.5	100
Image 3										
Frame analysis				89.0			9.0		2.1	100
Image 4										
Spectrum 1	3.8		10.3	29.3			0.8		55.9	100
Spectrum 2			14.7	32.2					53.1	100
Spectrum 3			13.8	29.4			1.0		55.8	100
Spectrum 4	3.1		4.8	20.5			1.8		69.8	100
Spectrum 5				72.6			26.1	1.3		100
Spectrum 6				70.9			27.4	1.7		100
Spectrum 7				74.3	1.0		24.7			100
Spectrum 8				97.8			2.2			100
Spectrum 9				97.5			2.5			100
Spectrum 10				96.2			3.8			100
Spectrum 11				90.2			9.8			100
Spectrum 12				89.1			10.9			100
Spectrum 13				88.1			10.6		1.3	100
Spectrum 14			0.4	88.5			8.0		3.2	100
Image 5										
Spectrum 1				88.0			9.0		3.1	100
Spectrum 2				90.6			8.2		1.2	100
Spectrum 3				90.8			7.9		1.4	100
Spectrum 4				90.4			8.1		1.5	100
Spectrum 5				89.4			8.9		1.6	100
Image 6										
Spectrum 1			35.6	64.4						100
Spectrum 2	16.7	10.7		4.8		1.4			66.5	100
Spectrum 3	15.6	10.7		3.8					69.9	100

Table M.4: Compositional analysis Gordion-22611: medium fragment (in wt%)

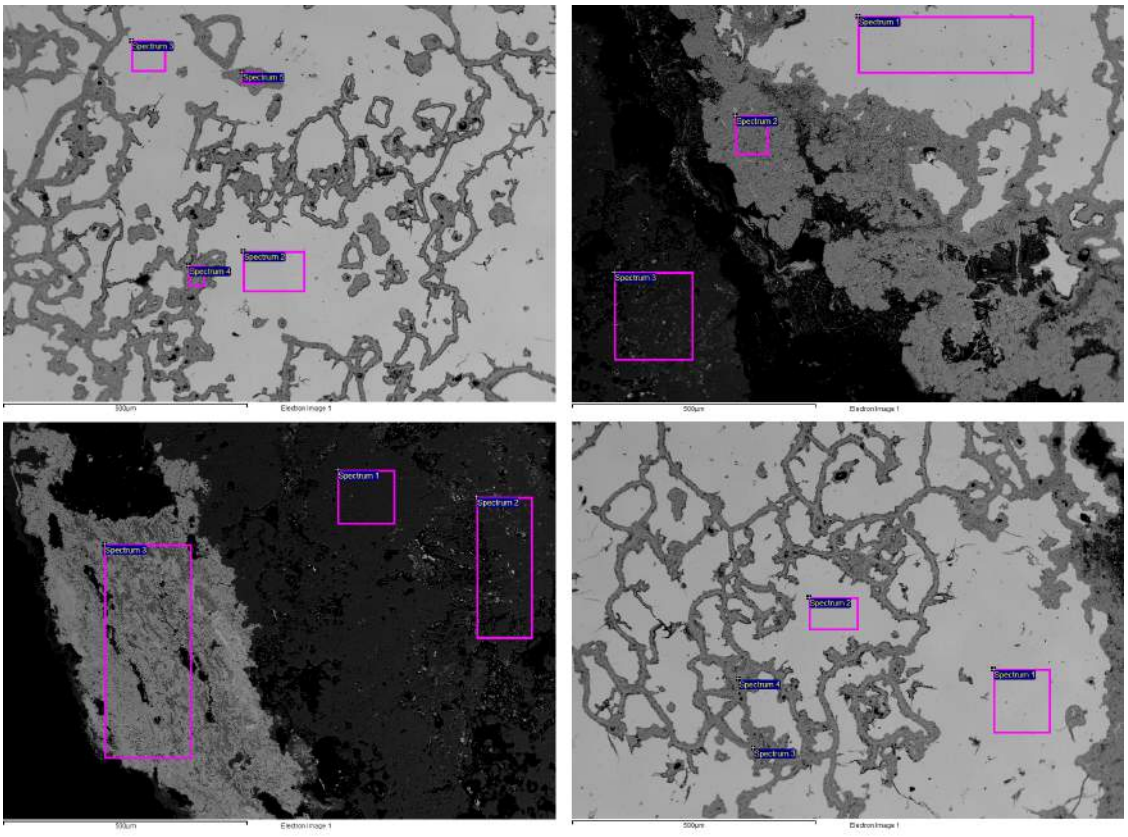

Figure M.6: Gordion-22611: small fragment

	O	Mg	Si	Cl	Fe	Cu	Sn	Total
Image 1								
Frame analysis	7.1	0.5	0.4			77.6	14.4	100
Spectrum 2						90.2	9.8	100
Spectrum 3						89.3	10.7	100
Spectrum 4	24.9	1.0	1.5			41.6	31.0	100
Spectrum 5	12.4					81.2	6.4	100
Image 2								
Spectrum 1						89.6	10.4	100
Spectrum 2	11.8		0.3			82.7	5.2	100
Spectrum 3	21.4		0.9	15.6		55.8	6.3	100
Image 3								
Spectrum 1	22.1			17.5		60.5		100
Spectrum 2	24.1		1.6	14.8		52.9	6.7	100
Spectrum 3	14.3			3.1		76.2	6.4	100
Image 4								
Spectrum 1						89.6	10.4	100
Spectrum 2						89.1	11.0	100
Spectrum 3	13.9		0.3			74.1	11.7	100
Spectrum 4	24.9	0.9	1.2		1.0	20.9	51.1	100

Table M.5: Compositional analysis Gordion-22611: small fragment (in wt%)

Section M.2

MASCA Report

A succinct report on some metal samples from Gordion was prepared by Pigott *et al.* (1991), of which the results are briefly reproduced here. PIXE as well as microscopic analysis of etched sections was undertaken. Contextual data for the samples is given in Table M.6. Results of their analysis are given in Table M.7.

Reference	Artefact	OP	Locus	Lot	Phase	Date	Context
YH 32328	spiral fragment	2	87	317	530	650 - Islamic MP	Good
YH 22882B	amorphous lump/prill	2	66	57	430	650 - Islamic MP	Prime
YH 22882A	folded sheet	2	66	57	430	650 - Islamic - MP	Prime
YH 23257B	amorphous lump/prill	7	21	28	370	400 - Islamic - LP	Prime
YH 30995	nail (or stud)	2	82	257	480	650- Islamic - MP	Good?
YH 23736	triangular lump	1	98	223	430	700 - Islamic	Prime
YH 31915	arrow (spear?) head	12	27	35	540	650 - 500 MP	Good?
YH 29997	rod, circular section	14	39	90	870	Old-Hittite - 700	Prime
YH 23085	rod, flattened	1	94	191	430	700 - Islamic	Good

Table M.6: Contextual data for analysed samples

Reference	Cu	As	Sn	Pb	Cl	Micro-structure
YH 32328	80.2	0.467	15.00	0.689	1.118	cast - cast/annealed - intergranular corrosion
YH 22882B	82.9	0.651	11.05	1.695	2.196	as cast - heavy intergranular corrosion
YH 22882A	79.9	0.127	14.64	0.131	2.513	cold worked/annealed - heavy intergranular corrosion
YH 23257B	93.6	0.108	4.33	0.939	0.048	as cast - solid to Cu-CuO eutectic with SnO_2 laths
YH 30995	95.3	0.148	3.47	0.072	0.004	cold worked - inhomogenous annealing
YH 23736	88.6	0.129	10.20	< 0.025	0.018	as cast, gas pores - corroded dendrites, matte inclusions
YH 31915	79.2	0.052	16.40	1.285	1.972	as cast (rapid cooling), heavily corroded
YH 29997	76.8	0.479	20.03	< 0.031	1.013	as cast - heavy intergranular corrosion, intragranular SnO_2 inclusions
YH 23085	87.1	0.521	6.65	0.039	4.043	too heavily corroded

Table M.7: Results of PIXE analysis and microscopic investigation

APPENDIX N

Moulds

Pictures of tentatively identified moulds, discussed in section 8.5, are shown here, as well as a few drawings.

Full discussion is beyond the scope of this project, but these varied fragments serve as an indicator for the range of shapes that would have been cast in Gordion.

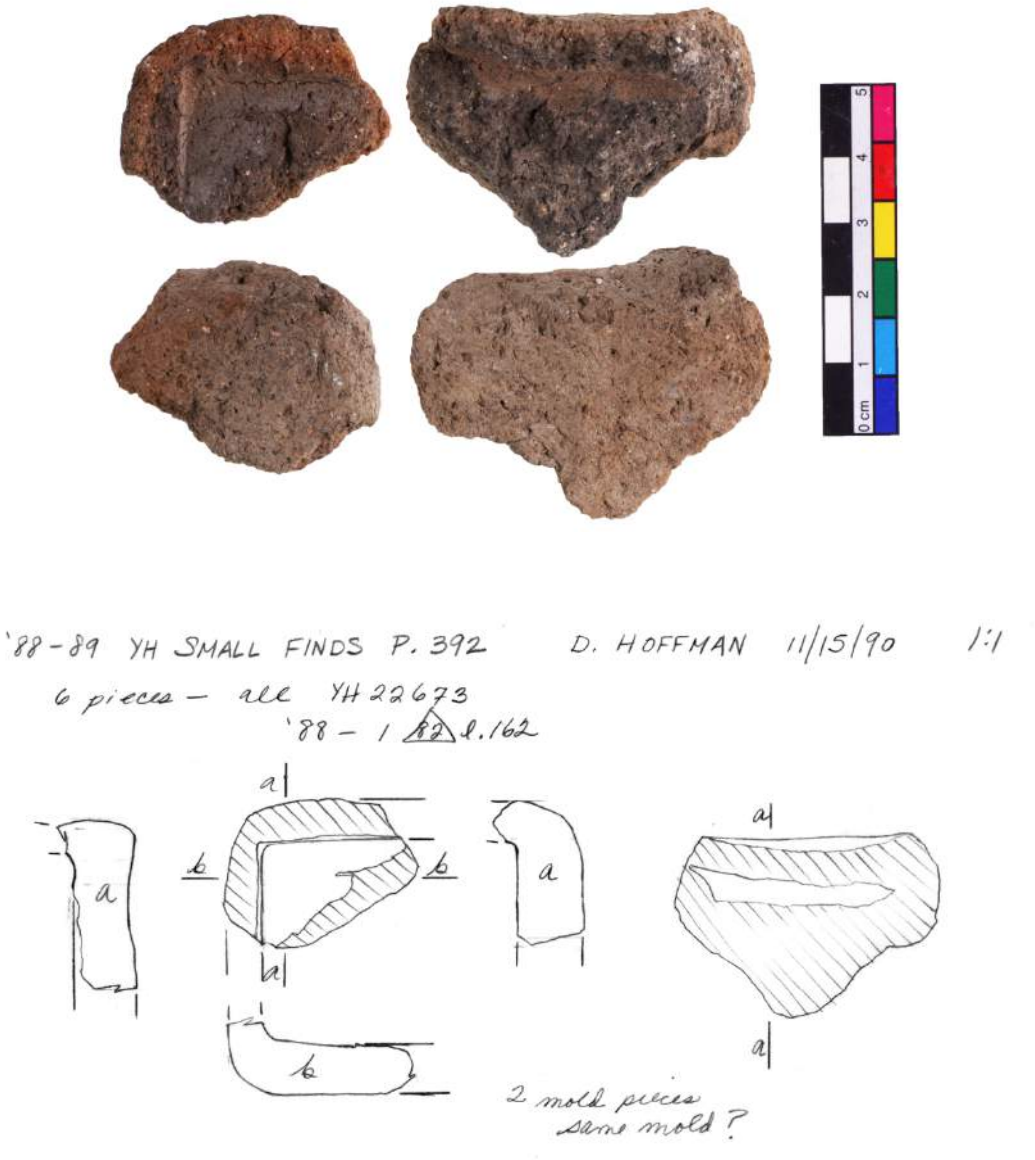

Figure N.1: Two mould fragments with angular shapes

'88-89 YH SMALL FINDS P. 392 D. HOFFMAN 11/15/90 1:1
6 pieces — all YH 22673
'88 – 1 82 l.162

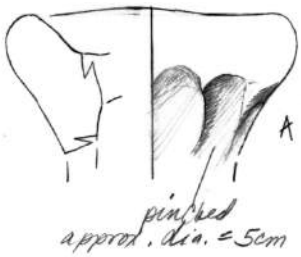

Figure N.2: Possible sprue, through which metal would have been poured into the mould

Figure N.3: Layered mould fragment, possibly indicating use of existing ceramic with additional clay layer

Figure N.4: Three mould fragments for elongated shapes, possibly rods

Figure N.5: Example of ring-shaped moulds

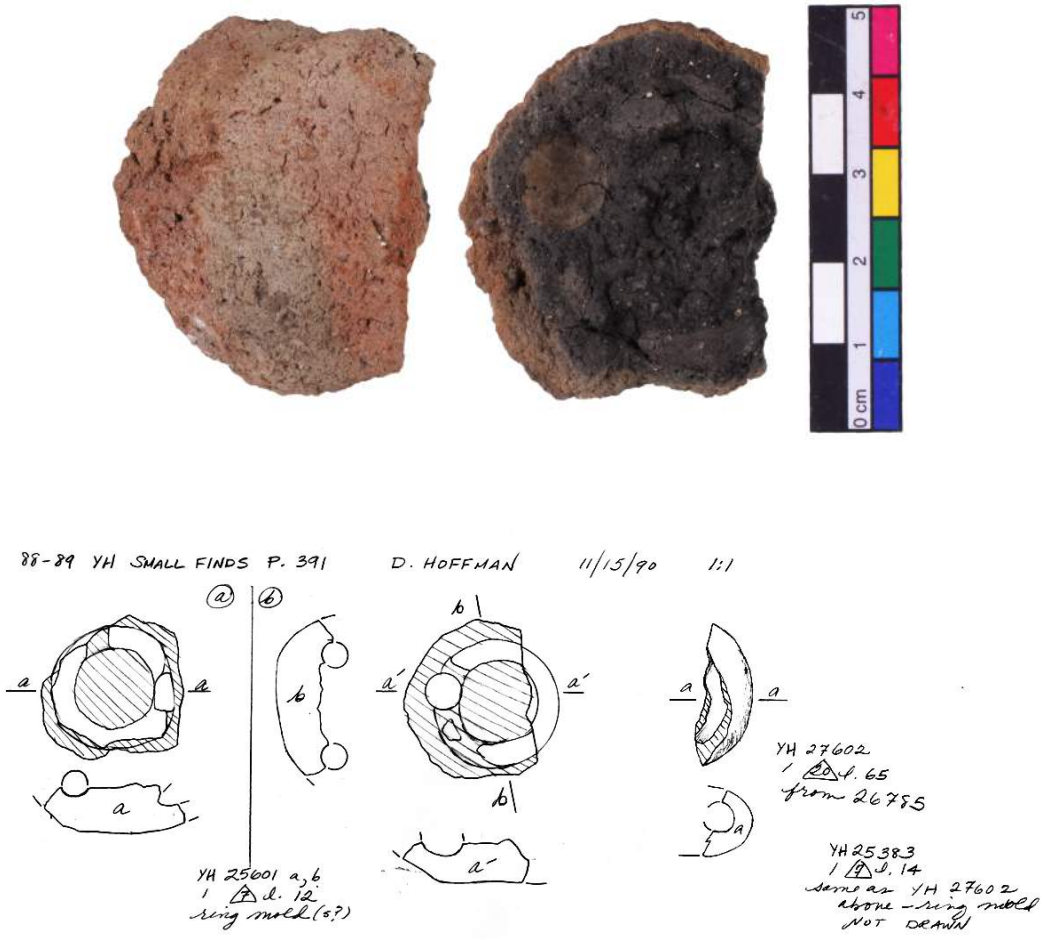

Figure N.6: Example of ring-shaped moulds (see Figure 8.37)

Roman Thrace Appendices

APPENDIX O

Bulk Compositions

In this appendix, compositional data for each of the Roman assemblages is presented. The bulk composition of both crucible ceramic and crucible slag is given in the first two tables, while the final three tables show the ratios of elements to Al_2O_3 for ceramic, slag and the change between them respectively.

Section O.1

Nicopolis bulk compositions

Average ceramic composition. All results in wt%, normalised to 100%.

Sample	Na_2O	MgO	Al_2O_3	SiO_2	P_2O_5	K_2O	CaO	TiO_2	FeO	CuO	ZnO	SnO_2	PbO
N1	**0.1**	**0.8**	**9**	**84**	**0**	**1.4**	**0.7**	**0.7**	**3.5**	**0**	**0**	**0**	**0**
Std. dev. (5 ms)	0.1	0.1	1	1	0.1	0.1	0.2	0.6	0.2	0.1	0.3	0.1	0.1
Min.	0	0.7	8	82	0	1.3	0.5	0.3	3.3	0	0	0	0
Max.	0.3	0.9	10	85	0.1	1.5	1.0	1.7	3.8	0.2	0.3	0	0.2
N2 (1) - A	**1.0**	**3.0**	**13**	**59**	**0.3**	**3.1**	**14.6**	**0.7**	**5.3**	**0.6**			
Std. dev. (5 ms)	0.1	0.1	1	2	0.1	0.2	0.7	0.2	0.3	0.2			
Min.	0.9	2.8	12	56	0.2	2.9	13.6	0.4	4.7	0.3			
Max.	1.2	3.1	13	60	0.5	3.4	15.4	0.8	5.6	0.8			
N2 (1) - B	**1.4**	**2.0**	**12**	**64**	**1.3**	**3.3**	**9.7**	**0.8**	**5.0**	**0.3**			
Std. dev. (5 ms)	0.1	0.2	0	2	0.3	0	0.8	0.1	0.3	0.2			
Min.	1.2	1.8	12	61	0.8	3.2	9.0	0.7	4.7	0			
Max.	1.4	2.3	13	66	1.8	3.3	11.0	0.9	5.3	0.6			
N2 (2) - A	**1.3**	**2.2**	**12**	**64**	**0.9**	**3.1**	**10.6**	**0.7**	**4.7**	**0.4**			
Std. dev. (5 ms)	0.1	0.2	1	1	0.2	0.2	1.3	0.1	0.2	0.2			
Min.	1.1	2.0	11	63	0.6	2.9	9.1	0.6	4.4	0.2			
Max.	1.4	2.5	13	65	1.1	3.4	12.6	0.9	5.0	0.7			
N2 (2) - B	**1.3**	**2.3**	**12**	**63**	**0.8**	**3.0**	**11.4**	**0.7**	**5.0**	**0.3**			
Std. dev. (5 ms)	0.2	0.1	1	1	0.1	0.2	2.0	0.1	0.4	0.2			
Min.	1.0	2.2	12	60	0.6	2.8	10.0	0.7	4.5	0			
Max.	1.4	2.5	13	64	1.0	3.2	14.9	0.9	5.6	0.5			
N3	**0.4**	**0.7**	**9**	**83**	**0.2**	**2.0**	**0.8**	**0.5**	**3.4**	**0.1**	**0**	**0.4**	
Std. dev. (5 ms)	0.2	0.1	1	3	0.2	0.4	0.1	0.1	0.5	0.1	0.1	0.2	

Average ceramic composition. All results in wt%, normalised to 100%.

Sample	Na_2O	MgO	Al_2O_3	SiO_2	P_2O_5	K_2O	CaO	TiO_2	FeO	CuO	ZnO	SnO_2	PbO
Min.	0.3	0.6	7	80	0	1.7	0.7	0.4	2.6	0	0	0	
Max.	0.6	0.8	10	86	0.4	2.5	1.0	0.7	3.9	0.3	0.1	0.6	
N4	**0.7**	**0.9**	**22**	**69**	**0.2**	**2.0**	**1.7**	**1.0**	**2.5**	**0.1**			
Std. dev. (5 ms)	0.1	0.1	2	2	0.4	0.1	1.2	0.3	0.1	0.1			
Min.	0.6	0.7	20	66	0	1.9	0.9	0.6	2.3	0			
Max.	0.7	1.0	24	72	0.9	2.3	3.8	1.4	2.6	0.2			
N4 (exterior)	**1.8**	**1.6**	**8**	**70**	**1.5**	**5.2**	**8.3**	**0.4**	**2.8**	**0**			
Std. dev. (5 ms)	0.3	0.6	1	5	0.7	1.0	4.5	0.1	0.2	0.1			
Min.	1.5	1.0	6	63	0.6	4.1	3.1	0.3	2.5	0			
Max.	2.2	2.4	9	78	2.4	6.6	13.2	0.6	3.0	0.1			
N5	**0.9**	**0.9**	**24**	**65**	**0.1**	**3.0**	**1.9**	**0.8**	**2.5**	**0.3**	**0**		**0**
Std. dev. (5 ms)	0.2	0.3	3	2	0.1	1.0	1.2	0.1	0.2	0.4	0.2		0.1
Min.	0.7	0.5	20	62	0	2.0	0.8	0.7	2.3	0	0		0
Max.	1.2	1.2	27	67	0.2	4.2	3.3	1.0	2.8	1.1	0.2		0.1
N5 (exterior)	**1.7**	**1.5**	**14**	**59**	**0.9**	**6.4**	**9.3**	**0.8**	**3.6**	**2.5**	**0.2**		**0.2**
Std. dev. (5 ms)	0.3	0.5	2	3	0.6	1.0	3.0	0.3	0.5	1.4	0.3		0.1
Min.	1.2	0.8	12	56	0.2	5.2	6.1	0.5	3.1	1.1	0		0
Max.	2.0	1.9	18	62	2.0	7.5	12.5	1.2	4.3	4.5	0.7		0.3
N6	**0.4**	**0.8**	**7**	**83**		**1.5**	**3.1**	**0.4**	**3.2**	**0.1**		**0.3**	**0.2**
Std. dev. (5 ms)	0.1	0.1	1	2		0.2	0.4	0.1	0.4	0.2		0.2	0.3
Min.	0.2	0.7	6	81		1.2	2.4	0.2	2.7	0		0	0
Max.	0.6	1.0	8	86		1.7	3.5	0.5	3.6	0.3		0.6	0.6
N6 (interior ceramic)	**0.3**	**0.5**	**5**	**87**		**1.3**	**0.7**	**0.4**	**2.5**	**0.2**		**0.4**	**1.8**
Std. dev. (5 ms)	0.1	0.2	1	3		0.3	0.4	0.1	0.3	0.2		0.3	2.4
Min.	0.2	0.3	5	82		1.0	0.2	0.3	2.1	0		0	0.2
Max.	0.4	0.7	6	89		1.7	1.3	0.6	2.7	0.5		0.7	6.1

Average slag composition. All results in wt%, normalised to 100%.

Sample	Na_2O	MgO	Al_2O_3	SiO_2	P_2O_5	K_2O	CaO	TiO_2	FeO	CuO	ZnO	SnO_2	PbO
N1	**0.8**	**1.3**	**6**	**35**	**1.9**	**4.0**	**19.4**	**0.3**	**22.1**	**1.5**	**1.0**	**4.2**	**2.5**
Std. dev. (5 ms)	0.2	0.1	1	2	0.5	0.6	2.5	0.1	2.3	0.5	0.2	0.6	1.0
Min.	0.6	1.2	5	33	1.5	3.5	16.4	0.2	19.7	0.8	0.7	3.5	1.1
Max.	1.0	1.5	7	38	2.6	5.0	22.0	0.3	25.1	2.1	1.3	5.0	3.5
N2 (1)	**1.1**	**2.5**	**12**	**61**	**1.2**	**4.6**	**10.8**	**0.8**	**6.0**	**0.5**			
Std. dev. (5 ms)	0.2	0.8	2	5	0.7	0.9	0.7	0.3	1.6	0.2			
Min.	0.9	1.5	9	58	0.5	3.2	9.8	0.5	4.2	0.4			
Max.	1.3	3.6	13	69	2.3	5.3	11.4	1.2	8.6	0.8			
N2 (2)	**1.2**	**3.0**	**12**	**59**	**0.4**	**3.5**	**13.4**	**0.7**	**6.6**	**0.5**			
Std. dev. (5 ms)	0.1	0.3	0	3	0.1	0.5	0.8	0.1	1.8	0.4			
Min.	1.1	2.7	11	56	0.3	3.0	12.2	0.7	4.2	0			
Max.	1.4	3.3	12	63	0.6	4.1	14.0	0.8	8.2	0.9			
N3	**1.0**	**1.0**	**7**	**68**	**0.5**	**2.0**	**3.0**	**0.3**	**5.5**	**2.9**	**3.9**	**5.6**	
Std. dev. (5 ms)	0.3	0.3	1	8	0.3	0.6	0.8	0.1	1.5	3.1	3.2	4.3	
Min.	0.7	0.7	5	57	0.2	1.3	2.2	0.1	3.7	0.5	0.6	1.6	
Max.	1.5	1.3	8	78	0.8	2.6	4.2	0.5	7.2	7.6	8.7	12.9	
N4	**3.4**	**1.0**	**9**	**78**	**0.2**	**2.3**	**2.6**	**0.6**	**3.1**	**0.1**			
Std. dev. (5 ms)	0.7	0.1	1	1	0.1	0.2	0.8	0.1	0.2	0.1			
Min.	2.8	0.9	8	77	0.1	2.0	1.6	0.4	2.8	0			
Max.	4.1	1.2	10	80	0.4	2.7	3.7	0.7	3.4	0.2			
N5	**2.5**	**0.9**	**14**	**64**	**0.3**	**1.9**	**6.9**	**0.6**	**4.9**	**2.1**	**0.9**		**1.0**
Std. dev. (5 ms)	0.1	0.1	2	6	0.1	0.4	0.6	0.2	2.3	1.6	1.2		1.8
Min.	2.3	0.7	13	54	0.2	1.2	6.0	0.4	3.6	0.1	0.3		0
Max.	2.7	1.0	16	67	0.5	2.3	7.7	0.8	8.9	4.5	3.2		4.2
N5 (lump)	**0.7**	**1.6**	**16**	**65**	**0.5**	**3.5**	**3.6**	**1.0**	**6.4**	**0.9**	**0**		**0**
Std. dev. (5 ms)	0.3	0.1	1	1	0.1	0.4	0.9	0.2	1.0	0.9	0.1		0.2
Min.	0.3	1.6	15	63	0.3	3.1	2.6	0.6	5.1	0.1	0		0
Max.	1.2	1.7	17	67	0.7	3.9	4.8	1.1	7.7	2.4	0		0.3
N6	**0.2**	**0.6**	**6**	**63**		**1.9**	**3.4**	**0.4**	**2.4**	**0.9**		**5.8**	**16.1**
Std. dev. (5 ms)	0.2	0.1	2	14		1.1	0.7	0.2	0.9	0.5		5.2	11.3
Min.	0.1	0.4	3	40		1.0	2.3	0.1	1.4	0.4		1.4	4.5
Max.	0.6	0.8	9	74		3.6	4.0	0.6	3.1	1.7		14.6	33.0

Ceramic. Ratio of oxides to Al_2O_3, metals removed.

Sample	$\frac{Na_2O}{Al_2O_3}$	$\frac{MgO}{Al_2O_3}$	$\frac{SiO_2}{Al_2O_3}$	$\frac{P_2O_5}{Al_2O_3}$	$\frac{K_2O}{Al_2O_3}$	$\frac{CaO}{Al_2O_3}$	$\frac{TiO_2}{Al_2O_3}$	$\frac{FeO}{Al_2O_3}$
N1	0.01	0.09	9.33	0	0.16	0.08	0.08	0.39
N2 (1) - A	0.08	0.23	4.54	0.02	0.24	1.12	0.05	0.41
N2 (1) - B	0.12	0.17	5.33	0.11	0.28	0.81	0.07	0.42
N2 (2) - A	0.11	0.18	5.33	0.08	0.26	0.88	0.06	0.39
N2 (2) - B	0.11	0.19	5.25	0.07	0.25	0.95	0.06	0.42
N3	0.04	0.08	9.22	0.02	0.22	0.09	0.06	0.38
N4	0.03	0.04	3.14	0.01	0.09	0.08	0.05	0.11
N4 (exterior)	0.23	0.20	8.75	0.19	0.65	1.04	0.05	0.35
N5	0.04	0.04	2.71	0	0.13	0.08	0.03	0.10
N5 (exterior)	0.12	0.11	4.21	0.06	0.46	0.66	0.06	0.26
N6	0.06	0.11	11.86	0	0.21	0.44	0.06	0.46
N6 (interior ceramic)	0.06	0.10	17.40	0	0.26	0.14	0.08	0.50

Slag. Ratio of oxides to Al_2O_3, metals removed.

Sample	$\frac{Na_2O}{Al_2O_3}$	$\frac{MgO}{Al_2O_3}$	$\frac{SiO_2}{Al_2O_3}$	$\frac{P_2O_5}{Al_2O_3}$	$\frac{K_2O}{Al_2O_3}$	$\frac{CaO}{Al_2O_3}$	$\frac{TiO_2}{Al_2O_3}$	$\frac{FeO}{Al_2O_3}$
N1	0.13	0.22	5.83	0.32	0.67	3.23	0.05	3.68
N2 (1)	0.09	0.21	5.08	0.10	0.38	0.90	0.07	0.50
N2 (2)	0.10	0.25	4.92	0.03	0.29	1.12	0.06	0.55
N3	0.14	0.14	9.71	0.07	0.29	0.43	0.04	0.79
N4	0.38	0.11	8.67	0.02	0.26	0.29	0.07	0.34
N5	0.18	0.06	4.57	0.02	0.14	0.49	0.04	0.35
N5 (lump)	0.04	0.10	4.06	0.03	0.22	0.23	0.06	0.40
N6	0.03	0.10	10.50	0	0.32	0.57	0.07	0.40

Change (in %) in ratio of oxides to Al_2O_3 between ceramic and slag, metals removed.

Sample	$\frac{Na_2O}{Al_2O_3}$	$\frac{MgO}{Al_2O_3}$	$\frac{SiO_2}{Al_2O_3}$	$\frac{P_2O_5}{Al_2O_3}$	$\frac{K_2O}{Al_2O_3}$	$\frac{CaO}{Al_2O_3}$	$\frac{TiO_2}{Al_2O_3}$	$\frac{FeO}{Al_2O_3}$
N1	1100	144	-38	∞	329	4057	-36	847
N2 (1)	-21	25	-5	-8	39	11	0	20
N2 (2)	-8	30	-6	-50	17	18	0	32
N3	221	84	5	221	29	382	-23	108
N4	1087	172	176	144	181	274	47	203
N4 (exterior)	607	389	179	1963	615	1243	10	208
N5	376	71	69	414	9	523	29	236
N5 (lump)	17	167	50	650	75	184	88	284
N5 (exterior)	224	186	56	1443	266	739	71	147
N6	-42	-13	-11	/	48	28	17	-13

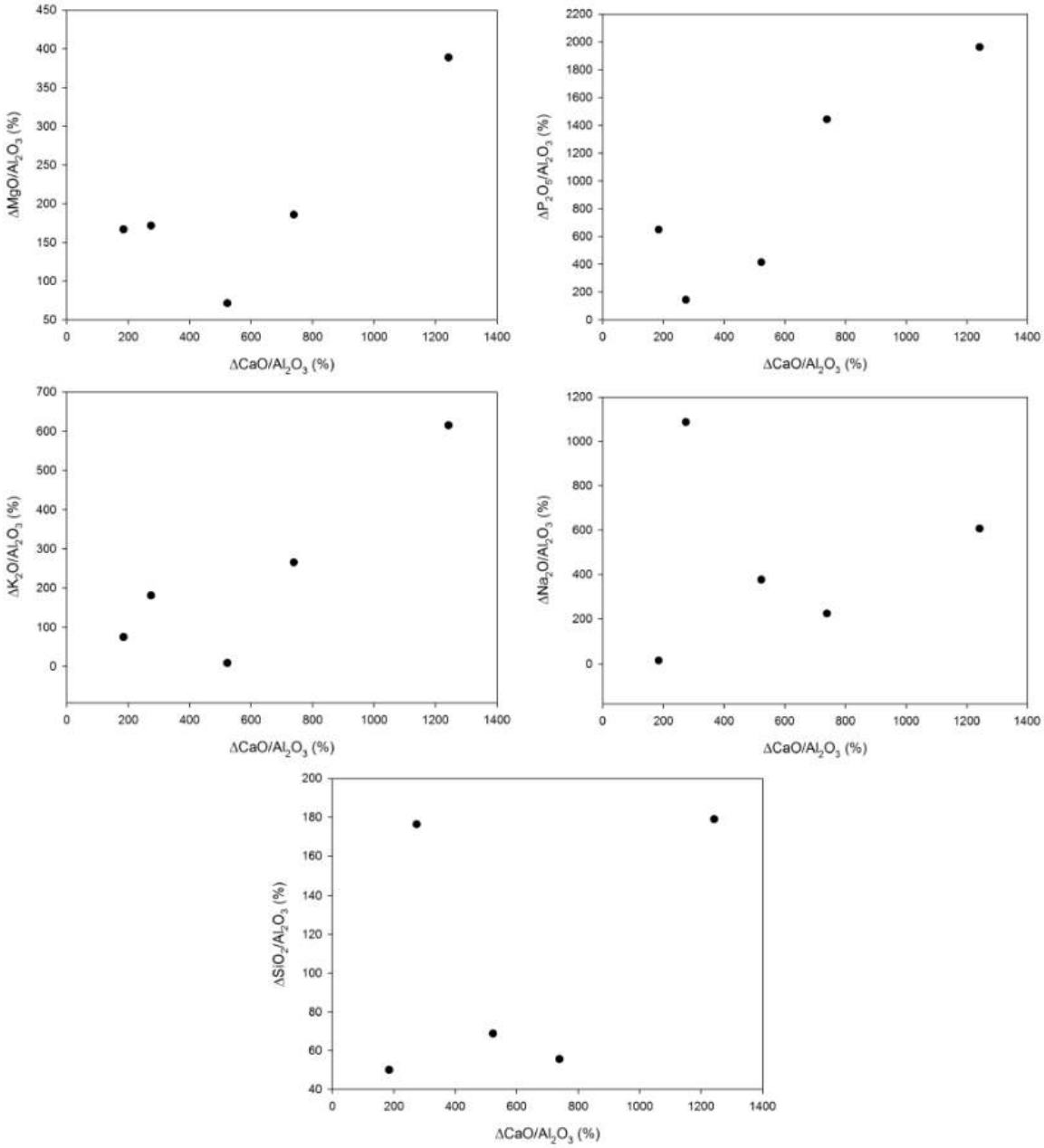

Figure O.1: Change in the ratio CaO/Al_2O_3 vs MgO/Al_2O_3, P_2O_5/Al_2O_3, K_2O/Al_2O_3, Na_2O/Al_2O_3 and SiO_2/Al_2O_3, between ceramic and slag (fragments N4 and N5)

Section O.2

Philippopolis bulk compositions

O.2.1 P1-P5: ceramic/slag

No clear separation between ceramic and slag, see section 11.1.2.1.

0.4 wt% CoO in sample Bul - P4 - 16-01-2014 has been omitted from the tables below.

Average ceramic/slag composition. All results in wt%, normalised to 100%.

Sample	Na_2O	MgO	Al_2O_3	SiO_2	P_2O_5	K_2O	CaO	TiO_2	FeO	CuO	ZnO	SnO_2	PbO
P1	**2.5**	**1.6**	**14**	**55**	**0.6**	**3.3**	**4.7**	**0.6**	**4.7**	**2.3**	**8.1**		**2.7**
Std. dev. (9 ms)	0.8	0.4	3	8	0.4	0.9	8.0	0.2	0.8	0.9	3.3		2.3
Min.	1.7	0.9	8	44	0	1.9	1.5	0.4	3.4	1.2	1.2		0.8
Max.	4.0	2.3	18	71	1.4	4.9	26.1	1.0	6.2	3.8	11.3		8.1
P2	**0.9**	**0.7**	**4**	**14**	**2.6**	**0.8**	**4.4**	**0.1**	**3.1**	**24.7**	**5.5**	**21.2**	**17.9**
Std. dev. (7 ms)	0.8	0.6	3	12	2.7	0.8	1.5	0.2	1.7	9.0	2.9	9.1	5.8
Min.	0	0.1	1	3	0.2	0	2.4	0	0.5	14.3	1.7	9.6	11.4
Max.	2.0	1.7	9	37	6.8	2.2	6.5	0.5	6.0	38.8	10.5	38.6	27.9
P3			**2**	**17**	**4.2**		**5.5**		**1.2**	**25.2**	**7.9**	**21.8**	**14.8**
Std. dev. (2 ms)			2	0	2.8		4.9		0.4	3.5	0.7	18.3	4.2
Min.			0	16	2.2		2.0		1.0	22.7	7.4	8.8	11.8
Max.			4	17	6.2		9.0		1.5	27.6	8.4	34.7	17.7
P4			**1**	**7**	**3.7**		**1.4**		**0.9**	**56.3**	**1.6**	**20.9**	**5.4**
Std. dev. (4 ms)			2	5	3.5		1.7		1.8	15.5	3.1	6.8	1.1
Min.			0	1	0		0		0	36.2	0	14.2	4.1
Max.			4	14	8.3		3.4		3.6	72.8	6.2	29.6	6.5
P5		**1.1**	**4**	**21**	**1.2**	**0.8**	**11.4**		**1.4**	**28.8**	**19.9**	**5.0**	**5.6**
Std. dev. (3 ms)		0.3	1	5	0.6	0.7	4.3		0.5	16.9	4.8	0.9	0.8
Min.		0.8	2	16	0.7	0.2	7.0		1.1	17.6	14.8	4.2	5.0
Max.		1.3	5	26	1.9	1.5	15.5		2.0	48.2	24.3	6.0	6.5

Ceramic/slag. Ratio of oxides to Al_2O_3, metals removed.

Sample	$\frac{Na_2O}{Al_2O_3}$	$\frac{MgO}{Al_2O_3}$	$\frac{SiO_2}{Al_2O_3}$	$\frac{P_2O_5}{Al_2O_3}$	$\frac{K_2O}{Al_2O_3}$	$\frac{CaO}{Al_2O_3}$	$\frac{TiO_2}{Al_2O_3}$	$\frac{FeO}{Al_2O_3}$
P1	0.18	0.11	3.93	0.04	0.24	0.34	0.04	0.34
P2	0.23	0.18	3.50	0.65	0.20	1.10	0.03	0.78
P3			8.50	2.10		2.75		0.60
P4			5.75	3.08		1.17		0.75
P5		0.28	5.25	0.30	0.20	2.85		0.35

O.2.2 P6-P9

2 wt% SO_2 in sample Bul - P8 - 17-02-2014 has been omitted from the tables below.

Average ceramic and slag compositions. All results in wt%, normalised to 100%.

Sample	Na_2O	MgO	Al_2O_3	SiO_2	P_2O_5	K_2O	CaO	TiO_2	FeO	CuO	ZnO	Ag_2O	SnO_2	PbO
P6 (ceramic)	**1.2**	**0.8**	**21**	**62**	**1.1**	**4.7**	**2.2**	**0.3**	**5.6**	**0.2**			**0.3**	**0**
Std. dev. (5 ms)	0.2	0.1	3	5	0.4	0.9	0.4	0.2	2.6	0.2			0.4	0.2
Min.	1.0	0.7	16	58	0.6	3.7	1.8	0.2	4.0	0			0	0
Max.	1.6	1.0	24	71	1.6	6.1	2.8	0.6	10.0	0.5			0.8	0.2
P6 (interior)	**2.6**	**1.4**	**16**	**51**	**1.1**	**3.6**	**6.0**	**0.3**	**2.5**	**12.5**			**1.1**	**2.3**
Std. dev. (5 ms)	0.6	0.5	4	5	0.3	1.1	1.6	0.1	0.7	6.0			0.5	1.1
Min.	1.9	0.7	11	44	0.5	2.0	4.2	0.2	1.4	4.9			0.4	0.9

Average ceramic and slag compositions. All results in wt%, normalised to 100%.

Sample	Na_2O	MgO	Al_2O_3	SiO_2	P_2O_5	K_2O	CaO	TiO_2	FeO	CuO	ZnO	Ag_2O	SnO_2	PbO
Max.	3.4	2.2	21	55	1.3	5.0	7.6	0.4	3.3	20.2			1.9	3.7
P6 (exterior)	**1.2**	**1.2**	**22**	**56**	**1.7**	**5.9**	**6.6**	**0.5**	**4.1**	**0.3**			**0.3**	**0.1**
Std. dev. (2 ms)	0.5	0.5	2	7	1.2	0.3	5.4	0.2	0.6	0.3			0.3	0.3
Min.	0.6	0.6	20	47	0.6	5.5	2.2	0.2	3.4	0			0	0
Max.	1.6	1.8	24	62	3.2	6.3	14.3	0.7	4.7	0.7			0.6	0.4
P7 (ceramic)		**1.4**	**12**	**47**	**11.1**	**2.9**	**5.8**		**4.0**	**4.1**	**11.6**		**0.3**	**0**
Std. dev. (1 ms)		0	0	0	0	0	0		0	0	0		0	0
Min.		1.4	12	47	11.1	2.9	5.8		4.0	4.1	11.6		0.3	0
Max.		1.4	12	47	11.1	2.9	5.8		4.0	4.1	11.6		0.3	0
P7 (dross)		**0.4**	**1**	**6**	**2.4**	**0.1**	**1.6**		**0.3**	**49.7**	**35.3**		**2.0**	**0.9**
Std. dev. (6 ms)		0.2	1	4	3.5	0.1	1.3		0.3	13.8	12.4		3.8	1.1
Min.		0.2	0	1	0	0	0.3		0	24.1	18.4		0	0.1
Max.		0.8	2	13	9.2	0.3	3.7		0.6	62.9	49.5		9.8	3.0
P8 (ceramic)	**2.4**	**1.9**	**18**	**64**	**0.3**	**3.8**	**2.7**	**0.7**	**5.3**	**0**		**0**	**0**	**0**
Std. dev. (5 ms)	0.3	0.1	0	0	0.1	1.0	0.1	0.1	0.4	0.1		0.2	0.2	0.2
Min.	2.0	1.7	18	64	0.1	3.1	2.5	0.6	4.8	0		0	0	0
Max.	2.6	2.0	19	65	0.4	5.5	2.8	0.9	5.9	0.2		0.3	0.3	0.2
P8 (slag)	**3.5**	**1.5**	**12**	**46**	**3.9**	**3.5**	**7.1**	**0.6**	**3.8**	**0.9**		**7.1**	**0.3**	**8.2**
Std. dev. (4 ms)	0.7	0.6	3	4	1.0	1.0	1.1	0.3	1.3	0.8		2.3	0.9	3.7
Min.	2.6	0.8	10	41	2.5	2.2	5.6	0.4	2.8	0.1		4.1	0	2.7
Max.	4.1	2.1	15	50	5.0	4.6	8.2	1.0	5.4	1.7		9.1	1.4	10.7
P8 (exterior)	**2.2**	**2.2**	**18**	**64**	**0.3**	**3.5**	**2.4**	**0.8**	**6.0**	**0**		**0.1**	**0.4**	**0.3**
Std. dev. (3 ms)	0.1	0.3	2	5	0.2	0.5	0.4	0.1	1.3	0.1		0.1	0.2	0.2
Min.	2.1	1.8	15	61	0.1	3.0	2.0	0.7	4.8	0		0	0.1	0.2
Max.	2.3	2.5	19	70	0.5	4.1	2.7	0.8	7.4	0.1		0.2	0.6	0.5
P9a (ceramic A)	**2.4**	**1.1**	**14**	**72**	**0.1**	**3.4**	**2.0**	**0.5**	**3.1**	**0.1**	**0.1**		**0.5**	**0.2**
Std. dev. (2 ms)	0.3	0.4	1	5	0.2	1.7	0.3	0	0.2	0.1	0.1		0.5	0
Min.	2.2	0.9	13	69	0	2.3	1.7	0.5	3.0	0	0.1		0.2	0.2
Max.	2.6	1.4	15	76	0.3	4.6	2.2	0.5	3.3	0.2	0.2		0.8	0.2
P9a (slag A)	**2.7**	**0.6**	**12**	**43**	**1.4**	**2.5**	**6.4**	**0.3**	**2.2**	**10.5**	**1.1**		**13.6**	**4.0**
Std. dev. (2 ms)	1.1	0	1	3	1.0	0.1	3.9	0.1	0.8	6.3	0.9		4.3	2.5
Min.	2.0	0.6	11	41	0.7	2.4	3.6	0.2	1.6	6.0	0.5		10.6	2.2
Max.	3.5	0.7	12	45	2.1	2.6	9.1	0.4	2.7	14.9	1.8		16.7	5.8
P9a (slag B)	**3.1**	**0.8**	**14**	**59**	**0.2**	**3.8**	**4.0**	**0.4**	**3.6**	**4.4**	**3.5**		**2.6**	**0.6**
Std. dev. (5 ms)	0.4	0.2	1	4	0.3	1.5	0.4	0.1	1.3	2.3	1.9		1.0	0.3
Min.	2.5	0.5	13	54	0	2.6	3.6	0.2	1.6	2.4	1.7		1.7	0.4
Max.	3.5	1.0	16	64	0.6	6.4	4.4	0.6	5.4	7.7	6.8		4.0	1.1
P9b (ceramic A)	**2.5**	**0.9**	**15**	**71**	**0.2**	**3.3**	**2.2**	**0.6**	**3.9**	**0.1**	**0**		**0.4**	**0**
Std. dev. (5 ms)	0.8	0.2	2	3	0.2	1.2	0.5	0.3	0.9	0.2	0.2		0.4	0.1
Min.	1.6	0.7	12	68	0	1.8	1.6	0.4	3.1	0	0		0	0
Max.	3.8	1.2	18	74	0.5	5.1	2.9	1.2	5.4	0.3	0.2		1.0	0.2
P9b (slag A)	**2.8**	**1.0**	**8**	**34**	**0.9**	**1.4**	**3.7**	**0.3**	**5.0**	**17.0**	**7.6**		**11.8**	**6.5**
Std. dev. (5 ms)	1.0	0.2	2	10	0.5	0.5	0.6	0.1	2.0	9.5	5.3		6.4	2.9
Min.	1.7	0.6	6	27	0.4	0.8	3.0	0.1	2.9	6.5	3.3		6.9	3.8
Max.	4.0	1.2	11	50	1.6	2.1	4.5	0.4	7.5	26.8	15.8		21.2	9.7
P9b (ceramic B)	**2.5**	**0.9**	**15**	**71**	**0.3**	**2.6**	**2.9**	**0.5**	**3.5**	**0.2**	**0.3**		**0.4**	**0.1**
Std. dev. (5 ms)	0.6	0.1	2	5	0.2	0.7	0.8	0.2	0.4	0.4	0.2		0.4	0.1
Min.	1.4	0.8	11	66	0.1	1.9	1.8	0.3	3.0	0	0.1		0	0
Max.	3.0	1.0	17	79	0.7	3.5	3.8	0.9	3.8	0.8	0.7		0.9	0.2
P9b (slag B)	**3.3**	**0.9**	**11**	**47**	**0.4**	**2.2**	**3.9**	**0.3**	**4.3**	**10.6**	**9.2**		**5.2**	**1.6**
Std. dev. (5 ms)	0.5	0.2	2	7	0.3	0.6	0.7	0.1	0.7	1.8	3.5		1.9	0.4
Min.	2.8	0.7	9	36	0.1	1.5	3.3	0.2	3.7	8.4	7.2		3.1	1.3
Max.	3.8	1.2	13	54	1.0	3.1	5.1	0.4	5.4	13.0	15.2		7.8	2.2

Ceramic and slag. Ratio of oxides to Al_2O_3, metals removed.

Sample	$\frac{Na_2O}{Al_2O_3}$	$\frac{MgO}{Al_2O_3}$	$\frac{SiO_2}{Al_2O_3}$	$\frac{P_2O_5}{Al_2O_3}$	$\frac{K_2O}{Al_2O_3}$	$\frac{CaO}{Al_2O_3}$	$\frac{TiO_2}{Al_2O_3}$	$\frac{FeO}{Al_2O_3}$
P6 (ceramic)	0.06	0.04	2.95	0.05	0.22	0.10	0.01	0.27
P6 (interior)	0.16	0.09	3.19	0.07	0.23	0.38	0.02	0.16
P6 (exterior)	0.05	0.05	2.55	0.08	0.27	0.30	0.02	0.19
P7 (ceramic)		0.12	4.06	0.96	0.25	0.50		0.35
P7 (dross)		0.40	6.00	2.40	0.10	1.60		0.30
P8 (ceramic)	0.13	0.11	3.56	0.02	0.21	0.15	0.04	0.29
P8 (slag)	0.29	0.13	3.83	0.33	0.29	0.59	0.05	0.32
P8 (exterior)	0.12	0.12	3.56	0.02	0.19	0.13	0.04	0.33
P9a (ceramic A)	0.17	0.08	5.14	0.01	0.24	0.14	0.04	0.22
P9a (slag A)	0.23	0.05	3.58	0.12	0.21	0.53	0.03	0.18

Ceramic and slag. Ratio of oxides to Al_2O_3, metals removed.

Sample	$\frac{Na_2O}{Al_2O_3}$	$\frac{MgO}{Al_2O_3}$	$\frac{SiO_2}{Al_2O_3}$	$\frac{P_2O_5}{Al_2O_3}$	$\frac{K_2O}{Al_2O_3}$	$\frac{CaO}{Al_2O_3}$	$\frac{TiO_2}{Al_2O_3}$	$\frac{FeO}{Al_2O_3}$
P9a (slag B)	0.22	0.06	4.21	0.01	0.27	0.29	0.03	0.26
P9b (ceramic A)	0.17	0.06	4.73	0.01	0.22	0.15	0.04	0.26
P9b (slag A)	0.35	0.13	4.25	0.11	0.18	0.46	0.04	0.63
P9b (ceramic B)	0.17	0.06	4.73	0.02	0.17	0.19	0.03	0.23
P9b (slag B)	0.30	0.08	4.27	0.04	0.20	0.35	0.03	0.39

Change (in %) in ratio of oxides to Al_2O_3 between ceramic and slag, metals removed.

Sample	$\frac{Na_2O}{Al_2O_3}$	$\frac{MgO}{Al_2O_3}$	$\frac{SiO_2}{Al_2O_3}$	$\frac{P_2O_5}{Al_2O_3}$	$\frac{K_2O}{Al_2O_3}$	$\frac{CaO}{Al_2O_3}$	$\frac{TiO_2}{Al_2O_3}$	$\frac{FeO}{Al_2O_3}$
P6	184	130	8	31	1	258	31	-41
P6 (exterior)	-5	30	-16	32	17	65	37	-43
P7 (dross)		237	48	151	-59	218		-13
P8	119	18	8	1850	38	294	29	8
P8 (exterior)	-8	16	0	0	-8	-11	14	13
P9a (slag A)	31	-36	-30	1533	-14	273	-30	-17
P9b (slag A)	110	108	-10	744	-20	215	-6	140
P9b (slag B)	80	36	-10	82	15	83	-18	68

Section O.3

Serdica bulk compositions

Average ceramic composition. All results in wt%, normalised to 100%.

Sample	Na_2O	MgO	Al_2O_3	SiO_2	P_2O_5	SO_3	K_2O	CaO	TiO_2	FeO	CuO	ZnO	As_2O_3	Ag_2O	SnO_2	PbO
S1 (A)	**1.0**	**1.5**	**22**	**64**		**0.4**	**4.3**	**0.7**	**1.1**	**5.1**						
Std. dev. (4 ms)	0.3	0.2	2	2		0.4	0.4	0.2	0.2	1.2						
Min.	0.7	1.2	20	61		0.1	3.8	0.4	0.9	3.4						
Max.	1.3	1.7	24	66		0.9	4.6	0.8	1.3	6.2						
S1 (B)	**1.9**	**2.3**	**19**	**63**		**0.8**	**3.5**	**2.5**	**0.9**	**5.6**						
Std. dev. (2 ms)	0.1	0	0	1		0.2	0.1	0.1	0.1	0.2						
Min.	1.8	2.3	19	63		0.7	3.5	2.4	0.8	5.4						
Max.	2.0	2.3	19	64		0.9	3.6	2.6	1.0	5.7						
S3	**1.2**	**1.3**	**24**	**64**			**4.0**	**0.9**	**1.1**	**4.1**						
Std. dev. (5 ms)	0.3	0.2	1	2			0.2	0.2	0.2	0.2						
Min.	0.9	1.1	22	62			3.8	0.7	0.9	3.8						
Max.	1.6	1.6	25	66			4.3	1.3	1.3	4.3						
S4	**5.9**	**0.3**	**25**	**58**		**0.5**	**4.3**	**0.4**	**1.8**	**0.3**	**2.6**	**0.1**	**0.6**	**0**		**0.1**
Std. dev. (5 ms)	0.2	0.2	1	1		0.1	0.1	0.2	0.5	0.2	1.0	0.3	0.6	0.2		0.2
Min.	5.7	0	24	56		0.5	4.2	0.3	1.4	0.1	1.8	0	0.1	0		0
Max.	6.1	0.6	27	59		0.7	4.4	0.7	2.6	0.6	4.3	0.4	1.6	0.3		0.3
S5	**1.2**	**1.0**	**24**	**61**			**3.1**	**1.3**	**1.3**	**6.3**	**0.1**			**0.4**		**0.2**
Std. dev. (4 ms)	0.2	0.2	1	1			0.7	0.2	0.1	0.5	0.1			1.0		0.2
Min.	1.0	0.8	23	60			2.5	1.1	1.1	5.7	0			0		0
Max.	1.4	1.2	25	62			3.9	1.5	1.4	6.7	0.1			1.9		0.5
S6 (vitr. ceramic)	**3.2**	**1.1**	**15**	**64**	**0.6**		**4.8**	**3.3**		**2.6**	**3.8**				**1.2**	**0.7**
Std. dev. (8 ms)	0.6	0.2	1	6	0.4		0.8	0.6		0.8	4.7				0.8	0.5
Min.	2.4	0.7	13	53	0.1		3.8	2.4		1.4	0.1				0.1	0.2
Max.	4.1	1.3	16	70	1.2		6.5	4.4		3.5	12.8				2.4	1.3
S7	**0.2**	**0.6**	**14**	**79**	**0**		**3.4**	**0.2**	**0.2**	**1.1**	**0.2**	**0.4**				
Std. dev. (4 ms)	0.1	0.1	1	1	0.1		0.2	0	0.2	0.1	0.2	0.2				
Min.	0.1	0.5	14	79	0		3.2	0.2	0	1.0	0	0.1				
Max.	0.4	0.7	15	80	0.1		3.5	0.2	0.4	1.3	0.5	0.6				
S9	**4.2**	**1.1**	**15**	**69**	**0.4**		**4.0**	**2.9**		**1.8**	**1.6**				**0.5**	
Std. dev. (6 ms)	0.5	0.2	1	3	0.4		0.3	0.9		0.2	1.6				0.6	
Min.	3.7	0.7	13	66	0		3.7	2.3		1.6	0.6				0	
Max.	5.1	1.3	16	72	0.9		4.3	4.6		2.1	4.8				1.4	
S10	**0.9**	**0.5**	**12**	**80**			**3.3**	**0.6**		**1.0**	**0.2**	**1.2**				
Std. dev. (6 ms)	0.3	0.2	3	4			0.4	0.4		0.4	0.2	0.4				
Min.	0.5	0.4	9	74			2.9	0.1		0.5	0	0.6				
Max.	1.3	0.8	17	84			3.8	1.4		1.4	0.4	1.5				
S11	**0.1**	**0.7**	**14**	**81**			**2.9**	**0.2**		**1.1**	**0**					
Std. dev. (4 ms)	0.2	0.2	3	4			0.5	0.1		0.2	0.1					
Min.	0	0.5	11	76			2.5	0.1		0.9	0					
Max.	0.3	0.9	17	84			3.5	0.3		1.4	0.2					

Average slag composition. All results in wt%, normalised to 100%.

Sample	Na_2O	MgO	Al_2O_3	SiO_2	P_2O_5	SO_3	K_2O	CaO	TiO_2	FeO	CuO	ZnO	As_2O_3	Ag_2O	SnO_2	PbO
S1	**2.3**	**2.0**	**15**	**55**	**0.7**	**6.8**	**2.4**	**3.9**	**0.7**	**8.7**				**3.1**		
Std. dev. (4 ms)	1.2	0.4	3	5	0.3	4.7	0.6	2.3	0.2	2.0				4.1		
Min.	1.0	1.8	12	48	0.4	3.5	1.5	2.5	0.5	6.8				0.7		
Max.	4.0	2.5	18	59	1.0	13.4	2.8	7.4	0.9	11.4				9.3		
S3 (bloated)	**9.1**	**1.1**	**21**	**59**		**0.6**	**4.0**	**0.9**	**0.9**	**3.0**						
Std. dev. (5 ms)	2.2	0.4	3	4		0.4	0.4	0.3	0.1	0.9						
Min.	6.9	0.7	18	53		0.2	3.4	0.5	0.8	1.9						
Max.	12.7	1.5	24	65		1.2	4.6	1.3	1.0	3.9						
S4	**7.5**	**0.6**	**16**	**40**	**1.0**	**0.8**	**2.8**	**3.3**	**0.9**	**2.5**	**13.0**	**1.3**	**6.0**	**0.9**		**3.9**
Std. dev. (5 ms)	0.4	0.3	3	4	0.1	0.4	0.5	0.4	0.2	0.3	4.9	0.3	0.9	1.3		0.8
Min.	7.0	0.2	12	35	0.8	0.4	2.2	2.9	0.7	1.9	8.4	0.9	4.6	0.2		3.0
Max.	8.0	0.8	18	44	1.1	1.4	3.2	3.8	1.2	2.8	19.4	1.7	6.9	3.3		5.0
S4 (exterior)	**5.6**	**2.7**	**17**	**38**	**3.9**	**0.2**	**6.0**	**16.1**	**1.4**	**6.6**	**1.8**	**0.1**	**0.4**	**0.1**		**0.3**
Std. dev. (5 ms)	0.6	0.2	1	2	0.2	0.5	0.6	3.2	0.1	0.7	0.9	0.3	0.4	0.1		0.2
Min.	5.0	2.5	16	36	3.7	0	5.4	10.8	1.3	5.9	0.7	0	0	0		0
Max.	6.5	3.1	17	40	4.2	0.7	6.9	19.1	1.5	7.7	2.9	0.5	0.9	0.2		0.5

Average slag composition. All results in wt%, normalised to 100%.

Sample	Na_2O	MgO	Al_2O_3	SiO_2	P_2O_5	K_2O	CaO	TiO_2	FeO	CuO	ZnO	Ag_2O	SnO_2	PbO	Bi_2O_3
S5	**0.3**	**1.5**	**13**	**27**		**1.2**	**1.1**	**0.5**	**7.0**	**8.0**		**13.5**		**5.0**	**22.5**
Std. dev. (5 ms)	0.3	0.5	3	12		0.9	0.7	0.3	3.6	3.3		5.5		0.5	11.2
Min.	0	1.0	9	13		0.3	0.2	0.2	4.1	3.6		7.7		4.4	13.7
Max.	0.5	2.1	17	37		2.6	2.1	0.8	13.3	12.4		20.2		5.6	41.4
S5 (exterior)	**1.5**	**1.7**	**22**	**57**		**8.2**	**2.2**	**1.0**	**6.1**						
Std. dev. (5 ms)	0.1	0.9	2	4		1.9	1.0	0.4	2.4						
Min.	1.4	0.8	19	52		6.6	1.0	0.4	2.9						
Max.	1.6	3.2	24	62		11.1	3.8	1.4	9.4						
S6 (corrosion/dross)	**1.1**	**1.2**	**7**	**29**	**3.0**	**1.8**	**6.7**		**3.3**	**32.2**			**11.1**	**3.1**	
Std. dev. (6 ms)	1.0	0.4	3	13	1.2	1.1	3.5		2.3	9.7			5.4	1.4	
Min.	0	0.8	1	8	1.2		0.2	1.7	0.8	24.8			5.6	2.2	
Max.	2.1	1.9	10	39	4.4	3.1	11.4		7.1	50.5			18.7	6.0	
S7	**1.6**	**1.6**	**14**	**64**	**1.0**	**3.8**	**5.6**	**0.3**	**1.8**	**4.4**	**1.6**				
Std. dev. (5 ms)	0.6	0.3	4	4	0.2	1.2	1.3	0.1	0.6	4.0	0.4				
Min.	0.9	1.2	8	58	0.6	2.3	3.6	0.1	1.3	1.1	1.0				
Max.	2.3	2.0	20	69	1.2	4.9	6.7	0.4	2.4	9.0	2.0				
S7 (exterior)	**0.6**	**0.9**	**16**	**72**	**0.6**	**3.8**	**2.0**	**0.1**	**1.1**	**0.8**	**2.7**				
Std. dev. (1 ms)	0	0	0	0	0	0	0	0	0	0	0				
Min.	0.6	0.9	16	72	0.6	3.8	2.0	0.1	1.1	0.8	2.7				
Max.	0.6	0.9	16	72	0.6	3.8	2.0	0.1	1.1	0.8	2.7				
S8	**0.7**	**0.4**	**7**	**50**		**2.0**	**1.3**	**0.5**	**3.7**		**0.7**			**33.9**	
Std. dev. (5 ms)	0.2	0.2	2	16		0.3	0.5	0.3	1.6		0.4			15.9	
Min.	0.4	0.2	5	29		1.6	0.7	0.2	1.8		0.3			14.7	
Max.	0.8	0.6	10	68		2.4	2.0	0.9	5.8		1.2			51.7	
S9	**3.4**	**1.2**	**12**	**51**	**1.1**	**1.9**	**4.4**		**2.3**	**17.1**			**5.5**		
Std. dev. (1 ms)	0	0	0	0	0	0	0		0	0			0		
Min.	3.4	1.2	12	51	1.1	1.9	4.4		2.3	17.1			5.5		
Max.	3.4	1.2	12	51	1.1	1.9	4.4		2.3	17.1			5.5		
S10 (glazed)	**1.8**	**0.7**	**14**	**74**		**4.4**	**1.1**		**0.9**	**0.1**	**2.2**				
Std. dev. (4 ms)	0.3	0.2	2	3		0.5	0.5		0.3	0.3	0.2				
Min.	1.3	0.4	13	71		3.6	0.5		0.7	0	1.9				
Max.	2.0	0.9	17	77		4.9	1.6		1.4	0.4	2.3				
S11	**2.9**	**1.1**	**15**	**68**		**3.8**	**2.1**		**3.0**	**5.0**					
Std. dev. (5 ms)	1.2	0.3	1	2		0.3	0.9		1.2	4.7					
Min.	1.5	0.7	14	64		3.2	1.1		1.5	0.4					
Max.	4.4	1.5	16	70		4.1	3.4		4.2	11.4					

Sulphur has been omitted from the 'ratio tables' below.

Ceramic. Ratio of oxides to Al_2O_3, metals removed.

Sample	$\frac{Na_2O}{Al_2O_3}$	$\frac{MgO}{Al_2O_3}$	$\frac{SiO_2}{Al_2O_3}$	$\frac{P_2O_5}{Al_2O_3}$	$\frac{K_2O}{Al_2O_3}$	$\frac{CaO}{Al_2O_3}$	$\frac{TiO_2}{Al_2O_3}$	$\frac{FeO}{Al_2O_3}$
S1 (A)	0.05	0.07	2.91	0	0.20	0.03	0.05	0.23
S1 (B)	0.10	0.12	3.32	0	0.18	0.13	0.05	0.29
S3	0.05	0.05	2.67	0	0.17	0.04	0.05	0.17
S4	0.24	0.01	2.32	0	0.17	0.02	0.07	0.01
S5	0.05	0.04	2.54	0	0.13	0.05	0.05	0.26
S6 (vitr. ceramic)	0.21	0.07	4.27	0.04	0.32	0.22	0	0.17
S7	0.01	0.04	5.64	0	0.24	0.01	0.01	0.08
S9	0.28	0.07	4.60	0.03	0.27	0.19	0	0.12
S10	0.08	0.04	6.67	0	0.28	0.05	0	0.08
S11	0.01	0.05	5.79	0	0.21	0.01	0	0.08

Slag. Ratio of oxides to Al_2O_3, metals removed.

Sample	$\frac{Na_2O}{Al_2O_3}$	$\frac{MgO}{Al_2O_3}$	$\frac{SiO_2}{Al_2O_3}$	$\frac{P_2O_5}{Al_2O_3}$	$\frac{K_2O}{Al_2O_3}$	$\frac{CaO}{Al_2O_3}$	$\frac{TiO_2}{Al_2O_3}$	$\frac{FeO}{Al_2O_3}$
S1	0.15	0.13	3.67	0.05	0.16	0.26	0.05	0.58
S3 (bloated)	0.43	0.05	2.81	0	0.19	0.04	0.04	0.14
S4	0.47	0.04	2.50	0.06	0.18	0.21	0.06	0.16
S4 (exterior)	0.33	0.16	2.24	0.23	0.35	0.95	0.08	0.39
S5	0.02	0.12	2.08	0	0.09	0.08	0.04	0.54
S5 (exterior)	0.07	0.08	2.59	0	0.37	0.10	0.05	0.28
S6 (dross)	0.16	0.17	4.14	0.43	0.26	0.96	0	0.47
S7	0.11	0.11	4.57	0.07	0.27	0.40	0.02	0.13
S7 (exterior)	0.04	0.06	4.62	0.04	0.25	0.13	0	0.07
S8	0.10	0.06	7.14	0	0.29	0.19	0.07	0.53

Slag. Ratio of oxides to Al_2O_3, metals removed.

Sample	$\frac{Na_2O}{Al_2O_3}$	$\frac{MgO}{Al_2O_3}$	$\frac{SiO_2}{Al_2O_3}$	$\frac{P_2O_5}{Al_2O_3}$	$\frac{K_2O}{Al_2O_3}$	$\frac{CaO}{Al_2O_3}$	$\frac{TiO_2}{Al_2O_3}$	$\frac{FeO}{Al_2O_3}$
S9	0.29	0.10	4.38	0.09	0.16	0.37	0	0.20
S10 (glazed)	0.13	0.05	5.29	0	0.31	0.08	0	0.06
S11	0.19	0.07	4.53	0	0.25	0.14	0	0.20

Change (in %) in ratio of oxides to Al_2O_3 between ceramic and slag, metals removed.

Sample	$\frac{Na_2O}{Al_2O_3}$	$\frac{MgO}{Al_2O_3}$	$\frac{SiO_2}{Al_2O_3}$	$\frac{P_2O_5}{Al_2O_3}$	$\frac{K_2O}{Al_2O_3}$	$\frac{CaO}{Al_2O_3}$	$\frac{TiO_2}{Al_2O_3}$	$\frac{FeO}{Al_2O_3}$
S1 (rel. to A)	53	10	11	∞	-13	98	-1	97
S1 (rel. to B)	237	96	26	∞	-18	717	-7	150
S3 (bloated)	767	-3	5	/	14	14	-6	-16
S4	99	213	8	∞	2	1189	-22	1202
S4 (exterior)	40	1224	-4	∞	105	5819	14	3135
S5	-54	177	-18	/	-29	56	-29	105
S5 (exterior)	36	85	2	/	189	85	-16	6
S6 (dross)	-26	134	-3	971	-20	335	/	172
S7	700	167	-19	∞	12	2700	50	64
S7 (exterior)	170	36	-18	∞	2	811	-74	-10
S9	3	40	-5	252	-40	92	/	66
S10 (glazed)	13	5	529	/	31	8	/	6
S11	2607	47	-22	/	22	880	/	155

Section O.4

Stara Zagora bulk compositions

Average compositions. All results in wt%, normalised to 100%.

Sample	Na_2O	MgO	Al_2O_3	SiO_2	P_2O_5	K_2O	CaO	TiO_2	FeO	CuO	ZnO
Part A - interior slag	**3.7**	**1.1**	**16**	**58**	**0.7**	**3.8**	**10.8**	**0.4**	**2.5**	**1.0**	**2.2**
Std. dev. (5 ms)	1.7	0.3	4	5	0.2	0.7	5.8	0.1	0.4	0.7	1.0
Min.	1.8	0.8	10	53	0.4	3.0	3.8	0.3	2.0	0	1.1
Max.	5.6	1.5	20	62	1.0	5.0	15.7	0.6	2.9	1.8	3.2
Part A - remnant ceramic	**2.3**	**0.7**	**20**	**64**	**0.3**	**3.2**	**3.7**	**0.4**	**2.6**	**1.0**	**2.0**
Std. dev. (3 ms)	0.2	0.2	4	2	0.1	0.3	2.0	0.1	0.4	0.2	0.6
Min.	2.1	0.5	16	61	0.2	2.9	2.1	0.4	2.2	0.9	1.5
Max.	2.5	0.9	23	65	0.5	3.5	6.0	0.5	3.0	1.2	2.6
Part A - central vitr.	**2.1**	**0.9**	**17**	**55**	**0.8**	**3.8**	**11.6**	**0.5**	**2.2**	**2.8**	**2.8**
Std. dev. (5 ms)	0.2	0.2	4	5	0.3	0.8	3.1	0.2	0.3	1.5	1.5
Min.	1.9	0.6	10	51	0.5	2.8	7.4	0.3	1.8	1.4	1.0
Max.	2.4	1.0	21	62	1.1	4.9	15.2	0.9	2.7	5.2	4.8
Part B - glaze	**3.2**	**1.3**	**13**	**68**	**0.3**	**5.9**	**4.0**	**0.5**	**2.6**	**0.9**	**0.1**
Std. dev. (5 ms)	0.4	0.3	1	5	0.2	0.7	1.7	0.1	0.3	0.6	0.1
Min.	2.7	1.1	12	64	0.1	5.0	1.6	0.4	2.2	0.2	0
Max.	3.8	1.8	15	73	0.5	6.8	6.1	0.6	3.0	1.4	0.2
Part B - top	**4.2**	**1.3**	**12**	**69**	**0.2**	**4.3**	**3.1**	**0.5**	**3.3**	**1.7**	**0.1**
Std. dev. (3 ms)	0.4	0.1	1	1	0.2	0.1	1.1	0.2	0.3	1.2	0.1
Min.	3.8	1.2	11	67	0	4.3	2.0	0.4	3.0	1.0	0
Max.	4.6	1.4	13	70	0.3	4.4	4.1	0.7	3.6	3.0	0.3

Ceramic and slag. Ratio of oxides to Al_2O_3, metals removed.

Sample	$\frac{Na_2O}{Al_2O_3}$	$\frac{MgO}{Al_2O_3}$	$\frac{SiO_2}{Al_2O_3}$	$\frac{P_2O_5}{Al_2O_3}$	$\frac{K_2O}{Al_2O_3}$	$\frac{CaO}{Al_2O_3}$	$\frac{TiO_2}{Al_2O_3}$	$\frac{FeO}{Al_2O_3}$
Part A - interior slag	0.23	0.07	3.63	0.04	0.24	0.68	0.03	0.16
Part A - remnant ceramic	0.12	0.04	3.20	0.02	0.16	0.19	0.02	0.13
Part A - central vitr.	0.12	0.05	3.24	0.05	0.22	0.68	0.03	0.13
Part B - glaze	0.25	0.10	5.23	0.02	0.45	0.31	0.04	0.20
Part B - top	0.35	0.11	5.75	0.02	0.36	0.26	0.04	0.28

Changes relative to zone A remnant ceramic (%)

Part A - interior slag	101	96	13	192	48	265	25	20
Part A - central vitr.	7	51	1	214	40	269	47	0
Part B - glaze	114	186	63	54	184	66	92	54
Part B - top	204	210	80	11	124	40	108	112

APPENDIX P

Composition of metallic prills

Oxidised prills are omitted. Where an abundance of *1+* is noted, this refers to one measured prill, but probably more of similar composition present in the crucible slag. *Micro* refers to tiny prills dispersed throughout the crucible slag, which are too small to measure.

Section P.1

Nicopolis metallic prills

Composition of metallic prills in crucible slag (in wt%)

Sample	Abundance	Cu	Sn	Fe	Pb	S
N1	/					
N2 (1)	/					
N2 (2)	Multi	96.3-98.9		1.1-3.7		
	Multi	96.5-97.5	0.7-1.1	1.78-2.4		
	Multi	94.5-97.2		2.3-3.6	0-1.2	0.5-0.8
N3	Multi	60.9-66.6	33.4-39.1			
	1+	35.1	64.4	0.5		
	Multi	58.1-70.8	27.5-40.8		1.1-1.7	
N4	/					
N5	1+	86.9	8.8	2.9	1.4	
	Lump, 1+	99.6		0.4		
N6	Multi	95.8-97.2	2.8-4.2			
	1+	65.1	34.9			

Section P.2

Philippopolis metallic prills

One prill omitted for P4: 61.5 wt% Cu, 36.0 wt% Sn, 0.9 wt% Co and 1.6 wt% Pb.

Composition of metallic prills in crucible slag (in wt%)

Sample	Abundance	Cu	Sn	Fe	As	Sb	Ni	Pb	Ag	Zn	P	S	Cl
P1	Multi	100											
	Multi	85.5-89.6	0-1.0	0-0.4	0-0.2			5.5-6.5		4.4-7.8			
P2	1+	85.1	14.9										
	Multi	54.2-62.6	36.1-41.6					1.2-4.2					
	Multi	77.0-95.9	2.4-19.6					1.4-3.4					
	1+	97.2	1.5			1.3							
P3	1+	76.2	18.8			1.8		3.2					
	Corroded, multi	*90.9-98.3*	*1.7-9.1*										
P4	1+	64.3	34.3					1.4					
	Corroded, multi	*85.8-97.5*	*2.5-14.2*										
P5	Multi	100											
P6	1+	70.5	3.0	26.5									
	Ceramic			*100*									
	Exterior, multi	*1.8-4.2*		*86.2-95.5*							*0.3-12.0*		
	1+	*2.0*		*87.2*			*0.9*				*10.0*		
P7	Multi	91.7-98.3								1.7-8.3			
P8	Multi								90.3-95.4				4.6-9.7
	1+	1.9							97.9				0.2
	1+								77.7		0.9	9.7	4.9
	Multi			1.1-5.1					69.5-83.5		0.5-2.9	1.6-4.5	13.4-18.1
	1+			1.1					94.8		0.4		3.7
	1+			1.9					82.9		0.8	14.4	
	1+								86.5			13.5	
P9a	Multi	100.0											
	Multi	85.2-99.2	0.8-14.8										
	Secondary slag, multi	*99.1*		*0.9*									
P9b	Multi	76.9-86.8	11.1-21.0					1.7-3.1					
	Multi	73.3-73.5	22.3-24.4	0.7-0.8				1.5-3.5					
	1+	77.9		0.5								21.6	
	Secondary slag - Multi	99.4-99.5		0.5-0.6									

Section P.3

Serdica metallic prills

Composition of metallic prills in crucible slag (in wt%)

Sample	Abundance	Cu	Sn	Fe	As	Sb	Ni	Pb	Au	Ag	Cd	Zn	S	Cl
S1	1+	2.5								97.5				
	Multi	1.4-1.6								95.2	3.1-3.3			
	1+	1.2		24.1						44.6	2.5		27.6	
	1+			23.4						49.5			27.0	
	1+			10.2					5.0	71.6			12.7	0.5
S2	/													
S3	/													
S4	Multi	81.8-89.8		0.4-0.7	3.2-9.3					2.8-12.6				
	1+	89.9			6.0					4.1				
	1+	67.1			20.2					12.7				
	Partially corr.	*89.3-89.9*			*5.9-6.6*					*3.5-4.8*				
		20.8-38.0			*0.3-1.4*					*60.678.9*				
	Partially corr.	*89.5*		*0.5*	*5.1*					*5.0*				
		28.9			*1.3*					*69.8*				
		17.8								*82.2*				
	Exterior, multi	*84.1-84.5*		*0.5-0.6*	*6.4-6.6*				*5.0-5.3*	*3.4-3.6*				
	Multi	*90.0-92.0*		*0.5-0.7*	*3.4-5.2*					*2.6-5.2*				
	1+	*97.1*		*1.3*						*1.6*				
	1+	*88.9*			*5.9*					*5.1*				
S5	1+	1.3							7.6	90.9				0.2
	Multi	0.8-1.1							1.7-5.0	93.9-97.4				
	Multi	1.0-1.2								98.8-99.0				
	Multi								5.4-8.0	92.0-94.6				
	Multi									92.3-94.1				5.9-7.7
	Partially corr.	*0.9-1.1*								*98.9-99.1*				
										91.6				*8.4*
S6	1+	58.8	33.0		1.2	4.5		2.5						
	1+	58.1	34.9		1.2	4.5	1.2							
S7	1+	91.3	6.1	0.5	1.4		0.7							
	Exterior, 1+	*83.6*	*12.7*	*0.4*			*2.2*					*1.1*		
	1+	*87.5*	*9.3*				*1.6*					*1.6*		
	Multi	*87.3-87.4*	*11.0*				*1.6-1.7*							
S8	/													
S9	1+	76.8	17.0	0.4						0.8		5.0		
	Multi	66.1-66.2	20.6-31.7	0.5-9.4								1.5-3.8		
	1+	63.5	35.4	1.1										
	Multi	5.3-7.2		92.8-94.7										
S10	1+	5.8		94.2										
S11	Multi	1.2-2.0	0.6-3.4	95.3-97.4										

Section P.4

Stara Zagora metallic prills

Composition of metallic prills in crucible slag (in wt%)

Sample	Abundance	Cu	Sn	Fe	Pb	Zn
STZ1						
Part A - interior	1+	88.3	7.4	0.6	3.7	
	1+	90.9	6.1	1.3		1.7
	1+	97.7	0.7			1.6
	Multi	71.9-85.0	10.4-19.6		4.6-8.5	
	Multi	88.9-91.3	8.3-10.4	0.4-0.7		
	1+	7.2			92.8	
Part A - central	Multi	100.0				
	Multi	96.1-98.7			1.3-3.9	
	1+	97.4	0.9		1.7	
	1+	99.7		0.3		
Part B	1+	100				
	1+	99.6		0.4		